

REPORT DOCUMENTATION PAGE

Form Approved
OMB No. 0704-0188

Public reporting burden for this collection of information is estimated to average 1 hour per response, including the time for reviewing instructions, searching existing data sources, gathering and maintaining the data needed, and completing and reviewing the collection of information. Send comments regarding this burden estimate or any other aspect of this collection of information, including suggestions for reducing this burden, to Washington Headquarters Services, Directorate for Information Operations and Reports, 1215 Jefferson Davis Highway, Suite 1204, Arlington, VA 22202-4302, and to the Office of Management and Budget, Paperwork Reduction Project (0704-0188), Washington, DC 20503.

1. AGENCY USE ONLY (Leave blank)

2. REPORT DATE
25 April 2004

3. REPORT TYPE AND DATES COVERED
Final Report, 1 October 2003 – 30 September 2004

4. TITLE AND SUBTITLE
D/B/F 04: FINAL REPORT OF THE AIAA STUDENT AIRCRAFT DESIGN, BUILD & FLY COMPETITION
Vol. 1

5. FUNDING NUMBERS
G: N00014-98-1-0493
PR: 97PR04749-00

6. AUTHORS
By Gregory Page, Chris Bovias, and the student participants of D/B/F 2004.
Compiled by Stephen Brock, AIAA Student Programs

7. PERFORMING ORGANIZATION NAME(S) AND ADDRESS(ES)
American Institute of Aeronautics and Astronautics
ATTN: AIAA Foundation
1801 Alexander Bell Dr., Ste 500
Reston, VA 20191-4344

8. PERFORMING ORGANIZATION
REPORT NUMBER
2004DBF7630

9. SPONSORING/MONITORING AGENCY NAME(S) AND ADDRESS(ES)
Office of Naval Research
800 North Quincy St (ONR 351)
Arlington, VA 22217-5660
Cessna Aircraft Company
7751 E. Pawnee
Wichita, KS 67207

10. SPONSORING/MONITORING AGENCY
REPORT NUMBER

11. SUPPLEMENTARY NOTES

BEST AVAILABLE COPY

20040621 046

12a. DISTRIBUTION/AVAILABILITY STATEMENT
APPROVED FOR PUBLIC RELEASE

12b. DISTRIBUTION CODE

13. ABSTRACT (Maximum 200 words)

This report is made up of the combined reports of 37 separate teams of students who entered the 2004 Design, Build & Fly Competition. The objectives of the Design, Build & Fly Competition were to have students teams design, build and fly unmanned remote control electric aircraft designed for two specific missions: a ferry mission and a fire bomber mission. A "fly-off" took place on the Cessna Air Field in Wichita, KS, in April 2004. Winners of the contest: 1st place, Oklahoma State University; 2nd, Oklahoma State University; 3rd, University of Illinois at Urbana-Champaign. Cessna, the Office of Naval Research and the AIAA Foundation supported the Design, Build & Fly Competition.

14. SUBJECT TERMS

Unmanned / Remote / Control / RC / Aircraft / Student / Design / Build / Fly / AIAA

15. NUMBER OF PAGES

1837

16. PRICE CODE

17. SECURITY CLASSIFICATION OF
REPORT

18. SECURITY CLASSIFICATION OF
THIS PAGE

19. SECURITY CLASSIFICATION OF
ABSTRACT

20. LIMITATION OF ABSTRACT
SAR

INSTRUCTIONS FOR COMPLETING SF 298

The Report Documentation (RDP) is used in announcing and cataloging reports. It is important that this information be consistent with the rest of the report, particularly the cover and title page. Instructions for filling each block of the form follow. It is important to ***stay within the lines to meet optical scanning requirements.***

Block 1. Agency Use Only (*Leave blank*).

Block 2. Report Date. Full publication date including day, month, and year, if available (e.g., 1 Jan 88). Must cite at least the year.

Block 3. Type of Report and Dates Covered. State whether report is interim, final, etc. If applicable, enter inclusive report dates (e.g., 10 Jul 87 - 30 Jun 88).

Block 4. Title and Subtitle. A title is taken from the part of the report that provides the most meaningful and complete information. When a report is prepared in more than one volume, repeat the primary title, add volume number, and include subtitle for the specific volume. On classified documents enter the title classification in parentheses.

Block 5. Funding Numbers. To include contract and grant numbers; may include program element number(s), project number(s), task number(s), and work unit number(s). Use the following labels:

C - Contract	PR - Project
G - Grant	TA - Task
PE - Program Element	WU - Work Unit Accession No.

Block 6. Author(s). Name(s) of person(s) responsible for writing the report, performing the research, or credited with the content of the report. If editor or compiler, this should follow the name(s).

Block 7. Performing Organization Name(s) and Address(es). Self-explanatory.

Block 8. Performing Organization Report Number. Enter the unique alphanumeric report number(s) assigned by the organization performing the report.

Block 9. Sponsoring/Monitoring Agency Name(s) and Address(es). Self-explanatory.

Block 10. Sponsoring/Monitoring Agency Report Number. (*If known*)

Block 11. Supplementary Notes. Enter information not included elsewhere such as: Prepared in cooperation with . . . ; Trans. of . . . ; To be published in When a report is revised, include a statement whether the new report supersedes or supplements the older report.

Block 12a. Distribution/Availability Statement.

Denotes public availability or limitations. Cite any availability to the public. Enter additional limitations or special markings in all capitals (e.g., NOFORN, REL, ITAR).

DOD - See DoDD 5230, "Distribution Statements on Technical Documents"
DOE - See authorities.
NASA - See Handbook NHB 2200.2.
NTIS - Leave blank.

Block 12b. Distribution Code.

DOD - Leave blank.
DOE - Enter DOE distribution categories from the Standard Distribution for Unclassified Scientific and Technical Reports.
NASA - Leave blank.
NTIS - Leave blank.

Block 13. Abstract. Include a brief (*Maximum 200 words*) factual summary of the most significant information contained in the report.

Block 14. Subject Terms. Keywords or phrases identifying major subjects in the report.

Block 15. Number of Pages. Enter the total number of pages.

Block 16. Price Code. Enter appropriate price code (*NTIS only*).

Blocks 17. - 19. Security Classifications. Self-explanatory. Enter U.S. Security Classification in accordance with U.S. Security Regulations (i.e., UNCLASSIFIED). If form contains classified information, stamp classification on the top and bottom of the page.

Block 20. Limitation of Abstract. This block must be completed to assign a limitation to the abstract. Enter either UL (unlimited) or SAR (same as report). An entry in this block is necessary if the abstract is to be limited. If blank, the abstract is assumed to be unlimited.

2003-2004 Design, Build, Fly Competition

Place: Wichita, KS—Cessna Airfield

Ranking by Total Score

Order Within this Document

Position	University	Entry Name	Paper Score	RAC	Flight Score	Total Score
1	Oklahoma State University	OSU Black	94.9	6.74	12.1	170.46
2	Oklahoma State University	OSU Orange	80.53	6.71	11.95	143.49
3	University of Southern California	Scquirt	84.85	8.62	10.07	99.13
4	University of Illinois Urbana/Champaign	Fiberglass Overcast	93.65	9.51	9.73	95.82
5	Cal Poly San Luis Obispo	Moist	91.5	7.84	7.98	93.08
6	La Sapienza Rome	Galileo V	90.8	9.04	4.18	42.02
7	Queen's University	Squirt	86.05	6.57	3.11	40.65
8	Virginia Tech	Turbulence Syndrome	88.25	15.4	4.76	27.3
9	University of Florida	Swamp Stuka	62.23	12.56	5.41	26.83
10	Western Michigan University	Yeager - Bomber	70	20.27	5.42	18.72
11	Mississippi State University	Phyxius	88.1	9.5	1.88	17.41
12	University of California Los Angeles	ENGInuity-IGI	64	15.45	1.73	7.17
13	Clarkson University	Kamikazes	90	17.21	1.22	6.38
14	Georgia Institute of Technology	Buzzweiser	92.5	7.21	0.36	4.64
15	Cal Poly Pomona	Paani Hawaii Jahaz	76.05	16.26	0.66	3.1
16	University of California San Diego	Rain of Terror	91	9.74	0.24	2.21
17	Washington State University	Spirit of Procrastination	85.5	8.72	0.17	1.71
18	Case Western Reserve University	Flying Nemo	80.7	12.3	0.22	1.45
19	West Virginia University	Right Flyer	54.5	13.9	0.27	1.05
20	Columbia University	The Leaking Lion	67	15.8	0.24	1.03
21	University of Central Florida	Poseidon's Fury	87.25	12.55	0.11	0.8
22	*La Sapienza Rome	Michelangelo	84.45	15.04	0	0.01
26	*West Virginia University	Sting Ray	33.5	15.82	0	0
37	†West Point	Knight Wings	43.85	100	0	0
36	°University at Buffalo	MAX DRAG	59	100	0	0
24	*University of Texas Arlington	Volantis	63.87	17.5	0	0
35	°University of Colorado	Water Buffalo	64.75	100	0	0
34	†United States Military Academy	Boombatz Grandioso	65.15	100	0	0
25	*University of Arizona	Aircat 2004	68	18.99	0	0
33	†Miami University	Swoop-a-Loop	68.45	100	0	0
32	°University at Buffalo	Buffalo Bomber	76	100	0	0
23	*Istanbul Technical University	ATA-5	77.68	17.87	0	0
31	°Cal Poly Pomona	Death from Above	78.8	100	0	0
30	°University of California Los Angeles	Aquanaut	79.5	100	0	0
29	†Middle East Technical University	Anatolian-Craft	83	100	0	0
28	°City College of New York/CUNY	Rhino	87	100	0	0
27	†University of Texas Austin	121.5	88.5	100	0	0

2003-2004 Design, Build, Fly Competition

Place: Wichita, KS—Cessna Airfield

Ranking by Paper Score

Position	University	Entry Name	Paper Score	RAC	Flight Score	Total Score
1	Oklahoma State University	OSU Black	94.9	6.74	12.1	170.46
4	University of Illinois Urbana/Champaign	Fiberglass Overcast	93.65	9.51	9.73	95.82
14	Georgia Institute of Technology	Buzzweiser	92.5	7.21	0.36	4.64
5	Cal Poly San Luis Obispo	Moist	91.5	7.84	7.98	93.08
16	University of California San Diego	Rain of Terror	91	9.74	0.24	2.21
6	La Sapienza Rome	Galileo V	90.8	9.04	4.18	42.02
13	Clarkson University	Kamikazes	90	17.21	1.22	6.38
27	†University of Texas Austin	121.5	88.5	100	0	0
8	Virginia Tech	Turbulence Syndrome	88.25	15.4	4.76	27.3
11	Mississippi State University	Phyxius	88.1	9.5	1.88	17.41
21	University of Central Florida	Poseidon's Fury	87.25	12.55	0.11	0.8
28	°City College of New York/CUNY	Rhino	87	100	0	0
7	Queen's University	Squirt	86.05	6.57	3.11	40.65
17	Washington State University	Spirit of Procrastination	85.5	8.72	0.17	1.71
3	University of Southern California	Scquirt	84.85	8.62	10.07	99.13
22	*La Sapienza Rome	Michelangelo	84.45	15.04	0	0.01
29	†Middle East Technical University	Anatolian-Craft	83	100	0	0
18	Case Western Reserve University	Flying Nemo	80.7	12.3	0.22	1.45
2	Oklahoma State University	OSU Orange	80.53	6.71	11.95	143.49
30	°University of California Los Angeles	Aquanaut	79.5	100	0	0
31	°Cal Poly Pomona	Death from Above	78.8	100	0	0
23	*Istanbul Technical University	ATA-5	77.68	17.87	0	0
15	Cal Poly Pomona	Paani Hawaii Jahaz	76.05	16.26	0.66	3.1
32	°University at Buffalo	Buffalo Bomber	76	100	0	0
10	Western Michigan University	Yeager - Bomber	70	20.27	5.42	18.72
33	†Miami University	Swoop-a-Loop	68.45	100	0	0
25	*University of Arizona	Aircat 2004	68	18.99	0	0
20	Columbia University	The Leaking Lion	67	15.8	0.24	1.03
34	†United States Military Academy	Boombatz Grandioso	65.15	100	0	0
35	°University of Colorado	Water Buffalo	64.75	100	0	0
12	University of California Los Angeles	ENGINEuity-IGI	64	15.45	1.73	7.17
24	*University of Texas Arlington	Volantis	63.87	17.5	0	0
9	University of Florida	Swamp Stuka	62.23	12.56	5.41	26.83
36	°University at Buffalo	MAX DRAG	59	100	0	0
19	West Virginia University	Right Flyer	54.5	13.9	0.27	1.05
37	†West Point	Knight Wings	43.85	100	0	0
26	*West Virginia University	Sting Ray	33.5	15.82	0	0

CESSNA / STUDENT ONR / DESIGN / BUILD / FLY COMPETITION

An AIAA Student Activity

The 2004 Cessna/ONR Student Design/Build/Fly competition was held at the Cessna East Field facility in Wichita Kansas over the weekend of 23-25 April. Twenty six teams from the United States, Canada, Italy and Turkey attended the fly-off portion of the contest. Of the 26 teams attending the fly-off competition, 21 made at least one successful scoring flight attempt, with many teams completing the maximum allowed 5 flights during the two days of competition. A portion of Saturday was consumed by rain, which seems to be a DBF tradition, but Sunday provided perfect flying weather.

The design objective for this years competition was to create an airplane that would fit in a 2 x 4 x 1 foot shipping container and could complete a fire bomber mission and a ferry mission in the minimum amount of time. Each mission was assigned it's own Degree of Difficulty multiplier factor. The total score for each team is comprised of their flight performance on their best single flight of each mission type, their score on a written report documenting their aircraft design and selection, and a "Rated Aircraft Cost" representing the complexity and manufacturing costs of their design.

New to the competition this year, the Design Engineering Technical Committee sponsored prizes for the top five teams in the form of copies of their Aerospace Design Engineering Guide handbook. This additional support, above and beyond their participation as one of the administering Technical Committees, is greatly appreciated.

The final results showed a close battle between the two teams from Oklahoma State University, with Team Black the final victor. The University of Illinois team placed third. This is only the second time in the contest history the team with the highest paper score, 94.9, has also won the overall competition (Utah State University also had top paper and won the 2000 competition).

The final positions and scores for all of the competing teams are listed in the table below.

More details on the 2004 competition objectives and rules can be found at the contest web site at <http://www.ae.uiuc.edu/aiaadbf>.

Position	University	Entry Name	Paper Score	RAC	Bomber Score	Ferry Score	Flight Score	Total Score
1	Oklahoma State University	OSU Black	94.90	6.74	11.73	0.37	12.10	170.46
2	Oklahoma State University	OSU Orange	80.53	6.71	11.66	0.29	11.95	143.49
3	University of Southern California	Scquirt	84.85	8.62	10.07	0.00	10.07	99.13
4	University of Illinois Urbana/Champaign	Fiberglass Overcast	93.65	9.51	9.39	0.34	9.73	95.82
4	University of Southern California	Scquirt	84.85	8.62	10.07	0.00	10.07	99.13
5	Cal Poly San Luis Obispo	Moist	91.50	7.84	7.53	0.44	7.98	93.08
6	La Sapienza Rome	Galileo V	90.80	9.04	3.87	0.31	4.18	42.02
7	Queen's University	Squirt	86.05	6.57	2.74	0.37	3.11	40.65
8	Virginia Tech	Turbulence Syndrome	88.25	15.40	4.58	0.18	4.76	27.30
9	University of Florida	Swamp Stuka	62.23	12.56	5.20	0.21	5.41	26.83
10	Western Michigan University	Yeager - Bomber	70.00	20.27	5.21	0.22	5.42	18.72
11	Mississippi State University	Phyxius	88.10	9.50	1.50	0.38	1.88	17.41
12	University of California Los Angeles	ENGINuity-IGI	64.00	15.45	1.43	0.30	1.73	7.17

13	Clarkson University	Kamikazes	90.00	17.21	0.98	0.24	1.22	6.38
14	Georgia Institute of Technology	Buzzweiser	92.50	7.21	0.00	0.36	0.36	4.64
15	Cal Poly Pomona	Paani Hawaii Jahaz	76.05	16.26	0.47	0.20	0.66	3.10
16	University of California San Diego	Rain of Terror	91.00	9.74	0.00	0.24	0.24	2.21
17	Washington State University	Spirit of Procrastination	85.50	8.72	0.00	0.17	0.17	1.71
18	Case Western Reserve University	Flying Nemo	80.70	12.30	0.00	0.22	0.22	1.45
19	West Virginia University	Right Flyer	54.50	13.90	0.00	0.27	0.27	1.05
20	Columbia University	The Leaking Lion	67.00	15.80	0.00	0.24	0.24	1.03
21	University of Central Florida	Poseidon's Fury	87.25	12.55	0.00	0.11	0.11	0.80
22	*La Sapienza Rome	Michelangelo	84.45	15.04	0.00	0.00	0.00	0.01
23	*Istanbul Technical University	ATA-5	77.68	17.87	0.00	0.00	0.00	0.00
24	*University of Texas Arlington	Volantis	63.87	17.50	0.00	0.00	0.00	0.00
25	*University of Arizona	Aircat 2004	68.00	18.99	0.00	0.00	0.00	0.00
26	*West Virginia University	Sting Ray	33.50	15.82	0.00	0.00	0.00	0.00
27	†University of Texas Austin	121.5	88.50	100.00	0.00	0.00	0.00	0.00
28	°City College of New York/CUNY	Rhino	87.00	100.00	0.00	0.00	0.00	0.00
29	†Middle East Technical University	Anatolian-Craft	83.00	100.00	0.00	0.00	0.00	0.00
30	*University of California Los Angeles	Aquanaut	79.50	100.00	0.00	0.00	0.00	0.00
31	°Cal Poly Pomona	Death from Above	78.80	100.00	0.00	0.00	0.00	0.00
32	°University at Buffalo	Buffalo Bomber	76.00	100.00	0.00	0.00	0.00	0.00
33	†Miami University	Swoop-a-Loop	68.45	100.00	0.00	0.00	0.00	0.00
34	†United States Military Academy	Boombatz Grandioso	65.15	100.00	0.00	0.00	0.00	0.00
35	°University of Colorado	Water Buffalo	64.75	100.00	0.00	0.00	0.00	0.00
36	°University at Buffalo	MAX DRAG	59.00	100.00	0.00	0.00	0.00	0.00
37	†West Point	Knight Wings	43.85	100.00	0.00	0.00	0.00	0.00

†Not present at the Fly-off

*Present at Fly-off, but did not complete a successful flight

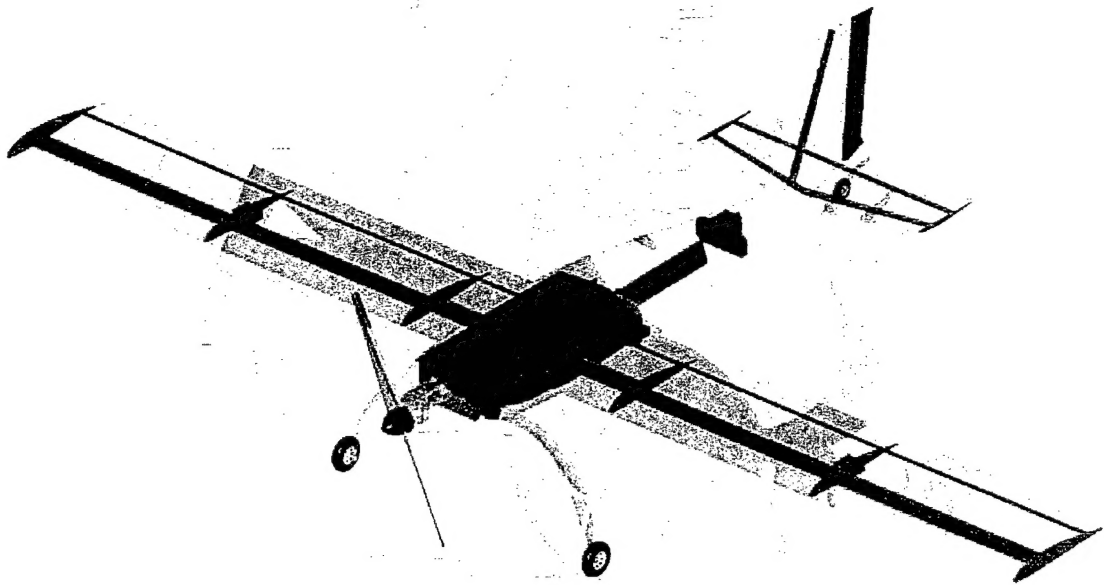
°Present at Fly-off, but did not complete Tech Inspection

The success of the competition required the efforts of many individuals. Our first thanks goes to the judges who assisted in the operation, technical inspections and scoring of the flight competition; and to the many judges who evaluated and scored the teams written proposal reports. Thanks also go to the Applied Aerodynamics, Aircraft Design, Design Engineering, and Flight Test Technical committees of the AIAA who organized and manage the competition, and the AIAA Foundation for their administrative support. Thanks are also due to the competition's corporate supporters, the Cessna Aircraft Company and the Office of Naval Research. A special thanks goes to Cessna for hosting this year's event and providing access to their facilities for both hanger space and the flying field.

Overall the 2004 Cessna/ONR Student Design/Build/Fly competition marked another very successful event, allowing the participating students to mix a highly enlightening educational experience with a good dose of fun. Congratulations to all the teams who participated for your great enthusiasm and achievement.

See you next year - Greg Page: Contest Administrator

***2003 / 2004 AIAA Foundation
Cessna / ONR Student Design-Build-Fly
Competition***



***"Black Stallion"*
Oklahoma State Black Team
Design Report**

March 9, 2004

**Oklahoma State University
School of Mechanical and Aerospace Engineering
Stillwater, Oklahoma**

Table of Contents

1.0 Executive Summary	1
1.1 Design Development	1
1.2 Design Alternatives	2
1.3 Highlights	2
2.0 Management Summary	3
2.1 Team Architecture	3
2.2 Technical Groups	4
2.3 Scheduling	5
3.0 Conceptual Design	6
3.1 Mission Requirements	6
3.2 Alternative Configurations	8
3.2.1 Aircraft Type	8
3.2.2 Empennage	9
3.2.3 Payload	11
3.2.4 Landing Gear	15
3.2.5 Propulsion System	16
3.2.6 Structural Concepts	17
3.3 Conclusions	20
4.0 Preliminary Design	21
4.1 Design Parameters and Sizing Trades Summary	21
4.2 Refined Mission Modeling and Optimization Analysis	22
4.2.1 Mission Profile Optimization Analysis Program	22
4.2.2 Propulsion System Analysis Program	24
4.3 Optimization	26
4.3.1 Mission Profile Program Results	26
4.3.2 Propulsion Program Results	29
4.4 Analysis Methods and Sizing	31
4.4.1 Aerodynamic Group	31
4.4.2 Structures Analysis	33
4.4.3 Payload System Analysis	36
4.4.4 Propulsion Group	38
4.5 Final Aircraft and Predicted performance	39
4.5.1 Aircraft Configuration	39
4.5.2 Predicted Performance	40
4.5.3 Aerodynamic Coefficients and Stability and Control Derivatives	40
5.0 Detail Design	42

5.1 Component Selection and System Architecture	42
5.1.1 Propulsion System.....	43
5.1.2 Structures System	43
5.1.4 Payload System	45
5.2 Final RAC Calculation	46
5.2.2 Drawing Package	46
6.0 Manufacturing Plan	52
6.1 Processes Investigated and FOM Screening Process.....	52
6.2 Component Manufacturing.....	53
6.2.1 Fuselage and Empennage	53
6.2.2 Wing	54
6.2.3 Landing Gear	54
6.3 Analytic Methods	55
6.3.1 Cost.....	55
6.3.2 Skills.....	55
6.3.3 Schedule.....	56
7.0 Testing Plan.....	57
7.1 Test Objective and Schedule	57
7.2 Flight Testing Checklists.....	57
7.3 Testing Results and Lessons Learned	59
References.....	60

1.0 Executive Summary

The methodology used to design and construct Oklahoma State University Black Team's entry in the 2003/2004 Cessna/ONR student Design/Build/Fly competition is outlined in this report. Two predefined missions, the Fire Bomber and Ferry, must be completed with an optimized aircraft. An overall contest score is computed from the written report score, total flight score, and the rated aircraft cost of the design.

1.1 Design Development

At the beginning of the conceptual design phase, aircraft approximations and figures of merit (FOM) were developed from the mission requirements of both the Fire Bomber Mission (FBM) and the Ferry Mission (FM). Scrutinizing all aspects of the competition, these FOMs and design approximations were used to determine the most critical mission and most important design parameters which would dictate the design of the plane. Later in the conceptual phase, these critical design parameters were investigated within the propulsion, aerodynamic, and structural areas of the aircraft. Numerous plane configurations were produced from different combinations of these design parameters. A comprehensive computer code was developed to analyze the mission profiles and provide sensitivity studies of the figures of merit used for screening. The sensitivity analysis enabled candidate configurations that exhibited the greatest scoring potential. Scoring potential trends illustrated the importance of the fire bomber mission over the ferry mission and showed that small adjustments in payload had significant affect on the total score. Also, the analysis showed possible optimal regions in battery weight, and wing area.

In the preliminary design phase, more detailed analysis and experimental testing was performed. The computer model was updated to analyze a chosen aircraft configuration's mission profile computing flight times, airspeeds, rated aircraft cost, and total scores. Iterations were done in the program to find the optimal airfoil, wing area, wing span, number of battery cells, and motor/batter/propeller combinations. These tests verified many of the figures of merit found in the conceptual design phase and uncovered other major design parameters such as pit times and take-off distance. Several payload systems involving loading and un-loading water were analyzed and tested to find the best way to create head pressure. Two superior payload designs for un-loading the payload emerged: a tank which pivoted down from the fuselage and a fixed tank with a boom that swung down from the fuselage. A gravity and pump feed systems were investigated and tested. Trade-offs between mission effectiveness and rated aircraft cost where justified.

During the detailed design phase, finite element analysis, flight simulation programs, dynamic stability analysis and physical experiments were run to finalize component selection and systems architecture concluded in the preliminary design phase. All aircraft dimensions, control systems, structure, and propulsion system were among the components finalized in this phase. Weight improvements were made through continuous refinement of the molded construction method. Additional analysis and testing

aided in power plant selection and performance prediction. Construction drawings were finalized to ensure proper and timely construction. The final result was a well designed and constructed aircraft, which will score well in the competition.

1.2 Design Alternatives

Many aerodynamic, structural, and propulsion configurations were considered and evaluated. The main empennage configurations considered were the conventional tail, V-tail, and canard configurations. A conventional tail was chosen based on stability and construction concerns. Several different airfoil types were considered: high lift airfoil, low drag airfoil and a balanced airfoil. High lift airfoils were eliminated due to high drag possibilities, while low drag airfoils were eliminated due to takeoff concerns. An airfoil that was a compromise between low drag and high lift was chosen. Non-retractable tail dragger landing gear was selected over other possible landing gear designs. With payload being a liquid, the affect of the shift on the pitch and roll axes are serious concerns. Since a shift in CG in the lateral direction is more controllable than in the longitudinal, fuselage was designed to be as wide as possible so that the reservoir could be as short as possible. Also, possible internal geometries that would allow the payload to only shift forward were carefully thought through and considered for possible final configurations. These reservoir considerations were the driving factors of the design of the fuselage. Initially the fuselage was designed to be a lifting body, but evolved into a tear drop shape in light of the payload system requirements. The onboard payload system using the retractable boom was selected while a pump fed ground based system was implemented. A mold based composite construction process was chosen for all aircraft components due to its favorable strength to weight ratio. Graupner motors were selected by the propulsion team due to their superior efficiency. Gearbox and propeller combinations were narrowed for testing.

1.3 Highlights

In order to reduce the number of design parameters, the two missions were analyzed to show the importance of each. Simple mathematical calculation based on the score equations were computed. The contribution of the ferry mission was insignificant, less than 5%. Therefore, design efforts were directed toward optimizing an aircraft for the fire bomber mission.

The optimization program was modified to model the fire bomber mission profile. Through much iteration key aircraft component sizes were selected. Testing, decision matrices, and other analysis confirmed the optimization program's parameters. The program limited the aspect ratio to 8 and a head wing of 10 mph. These design parameters were chosen for stability concerns and increased scoring potential possibilities, respectively. The optimization program helped optimize the battery selection, battery count, airfoil selection, and wing area. In addition, the program allowed for the mission times, speeds, climb rates, and power usage to be predicted.

A static stability analysis showed the optimal placement of the tail surfaces on the aircraft. Placement of the tail could be relatively close to the wing. This would allow for a one-piece fuselage that could fit in the 4 foot long box. Strength and ease of construction are both achieved with the one-piece fuselage.

An extensive analysis was performed to determine the optimal placement of the center of gravity. The worst case shifting of the reservoir's center of gravity forward and aft was found. This enabled the changes in the trim angle of attack for a given elevator deflection to be determined. An aft shift of the center of gravity has a more adverse effect than a forward shift. The farthest forward the center of gravity can be placed the less change it causes for the trim alpha. This analysis predicted the best theoretical center of gravity position and established a tolerance range. Flight testing will be used as the final criteria for the best center of gravity position.

The pump fed ground based payload system evolved into an integrated backpack that would allow one crew member to load all water onto the aircraft. This backpack used two bilge pumps, one small battery, and two quick connects for the bottles. For the onboard payload system, a conformal tank was constructed and connected to a retractable boom via a piece of flexible tubing that doubled as a pinch valve.

The first step in the manufacturing process consisted of cutting and finishing exact plugs of the aircraft's body. The plugs were used to create re-usable molds. Each plug was cut out of foam sheet insulation, and then covered with a thin layer of fiberglass for surface preparation. After the surface had been filled and sanded to a paint quality surface, the plug was fitted into a molding board, which provided a flat surface along the centerline of the part. One half of the mold was laid-up on top of the parting surface and allowed to cure. The second half of the mold was constructed after the parting board was removed, in order to mate together with the first half of the mold. Once the mold was created, the parts were laid up using a balsa core sandwich with fiberglass panels. The mold construction was time-consuming but it enabled exact replicas to be made any part of the aircraft.

Prototype testing served as a valuable tool towards the design of the aircraft. Most importantly, the prototype allowed the propulsion team to find the absolute optimal configuration, while the structures group was able to reduce structural weight through repetitive testing of wing and fuselage laminates.

2.0 Management Summary

Undergraduates and graduates in Mechanical and Aerospace Engineering comprised the design team. To ensure the delivery of a quality aircraft on time, a comprehensive management plan was implemented.

2.1 Team Architecture

In order to maximize the productivity of our team members and ensure a competitive aircraft, the Black Team was divided into three technical groups: propulsion, structures, and aerodynamics/stability and control. Each of the three groups had a lead engineer and specialists who were responsible for the

components of the group. To ensure a good line of communication among the technical groups, a chief engineer headed the team. The chief engineer was responsible for overall team direction, communication among the technical groups, and assurance of the availability of necessary items for aircraft construction. Each group lead engineer was responsible for guiding the group in completion of objectives set forth by the chief engineer and the team as a whole. This hierarchical structure allowed a smooth progression of all the aircraft's design and construction phases, while allowing all aspects of the project to be considered. An organizational breakdown can be seen in Figure 2.1.

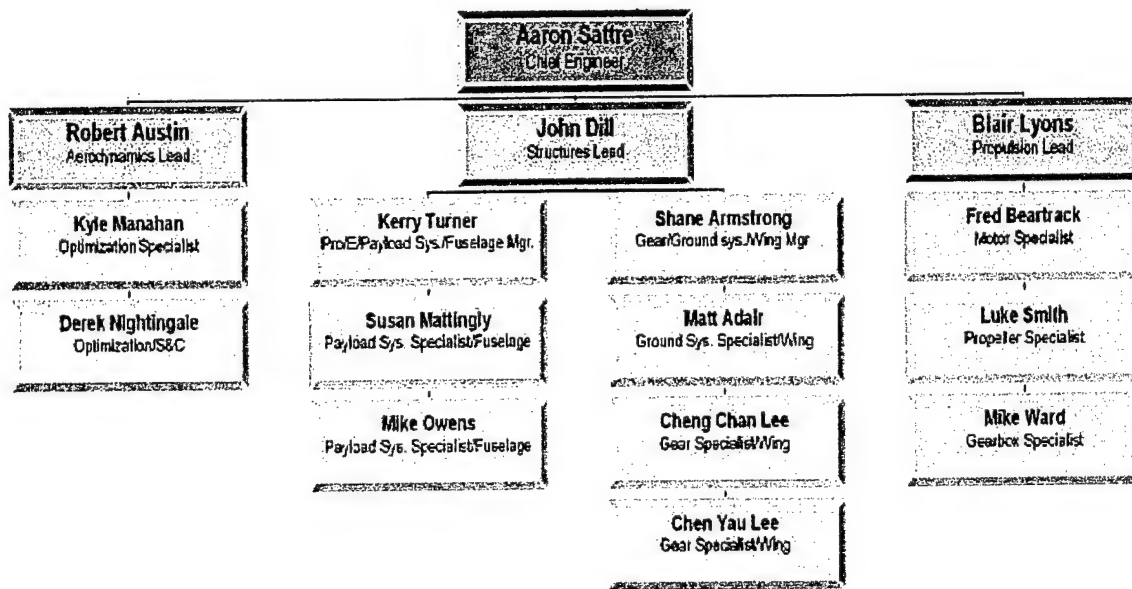


Figure 2.1: Organizational Breakdown of Team

2.2 Technical Groups

In the end, the aircraft's final configuration and design was a result of the combined efforts of all three technical groups. Each group had a system to develop, and all the systems had to be integrated. Therefore, each component depended on, or drove the design, of another component. Such a structure allowed all members of the team to input ideas on each of the aircraft's systems and overall design. The responsibilities of each of the three technical groups, as well as individual assignments, can be seen in Figure 1 and are described in detail in the subsequent discussion.

The primary function of this group was to take the aircraft configuration and do all necessary aerodynamic design. Initially, the aerodynamics task was to oversee the optimization of the aircraft's design through the use of mathematical models. In addition, they were also responsible for assuring the aircraft's design fell within the scope of the contest rules. Preliminary sizing of the aircraft was completed by the aerodynamics group by using optimization results to confirm that contest objectives were met in

the most efficient manner. The aerodynamics team focused on the stability and control aspects of the aircraft, yielding wing and tail sizes, and the appropriate airfoils for each. Another responsibility of the team was to determine the control and actuator sizing. Finally, a prototype was constructed to determine if the design was adequate. Prototype test data was used by the aerodynamics group to refine the design before the final aircraft was constructed.

Responsibilities of the propulsion team involved finding the optimal propulsion system for the aircraft. This task included designing and testing multiple battery, motor, gearbox, and propeller combinations that produced the predicted required thrust. After becoming familiar with the radio-controlled electric propulsion, an optimization program was used to find a reasonable number of combinations for live testing on a dynamometer. Several combinations of propulsion systems were narrowed down using this ground based testing. The group tested the remaining possible combinations on the prototype aircraft. Prototype testing allowed the team to refine the propulsion system and find the configuration which produced the optimal solution for the team's aircraft. The group also investigated tractor versus pusher propellers and placement of the system on the aircraft.

The structures group was responsible for the aircraft's structural design and construction; this entailed fabrication of all aircraft parts and necessary tooling, in addition to successfully integrating all systems. Members of this group were broken into two subgroups in order to accomplish all the goals. One group was responsible for payload system implementation and fuselage and empennage construction while the other was responsible for land based payload systems, landing gear design and test, and wing construction and test. All members of the structures group were involved in the consideration of construction methods, payload handling, and structural analysis and design. During the aircraft's design phase, this group served as the final authority on the feasibility of structurally implementing any designs brought forth by all team members. In addition to implementing the aircraft and systems, this group was responsible for all final construction drawings. The group used the prototype aircraft for structural, construction, and payload system tests.

2.3 Scheduling

The complete design and construction of the aircraft took place over a 3½ month time span. This schedule was accelerated and could not be accomplished without adequate planning and time management. A Gantt chart of the process was built based upon milestones set forth at the beginning of the project. Each phase was dependent upon another phase of the process; therefore the chart had to be explicitly followed to ensure successful completion of all necessary tasks. However, the design was adaptable until the final design freeze. For simplicity, the design report was developed concurrently with each phase of the design process. Figure 2.2 presents the design process to be followed by the team.

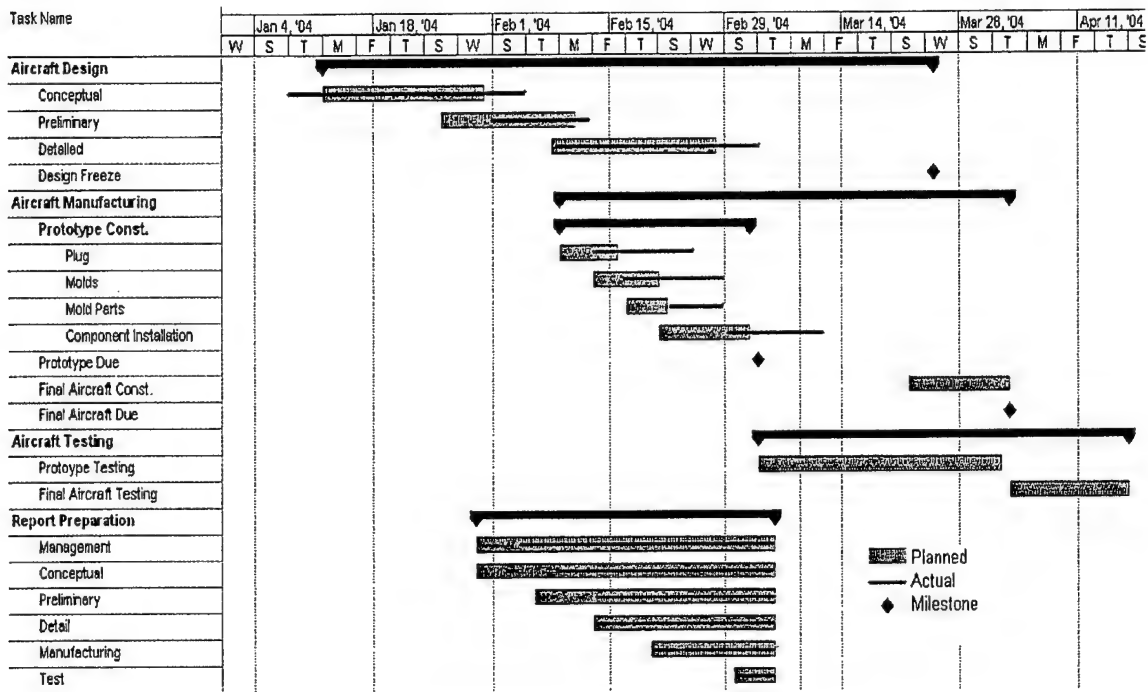


Figure 2.2: Milestone Chart of Design Process

3.0 Conceptual Design

During the conceptual design phase, the team aimed at choosing an aircraft configuration to optimize for performing each mission through an explicit Figure of Merit (FOM) screening process. Multiple tail, gear, and payload configurations were narrowed using the same process.

3.1 Mission Requirements

The purpose of this contest was to design and construct an aircraft that would complete all missions in an efficient manner. The fire bomber mission (FBM) requires an aircraft capable of containing and expelling a payload of up to four liters of water, while the ferry mission (FM) requires the same aircraft to fly the same mission profile without payload. The final aircraft design will complete each mission efficiently while having an optimal rated aircraft cost.

The total flight score for this contest was determined using a weighted function that combined the scores from both missions. It was crucial to determine the importance of each mission during the conceptual design phase. The FBM flight score is a function of 2 times the water weight divided by the total flight time, while the FM flight score is a function of the inverse of the flight time. An initial analysis determined the percentage of each mission's effect on the overall score. The purpose of this analysis was to validate the assumption that the aircraft should be optimized for the fire bomber mission.

Upon inspection of the two mission scores, it can be seen that the FM score will be a small decimal and the FBM score will be a much larger decimal. The total flight score is the summation of the FBM and FM scores. With FBM score being a much larger number than the FM score, it will almost totally control the total flight score. A hypothetical situation was investigated to ensure that this train of thought is correct.

The goal of the design of the aircraft is to maximize the contest score function:

$$\text{Flight Score} = \left(\frac{2 * \text{Payload Weight}}{\text{FBM Time}} + \frac{1}{\text{FM Time}} \right) * \frac{1}{\text{RAC}}$$

- Fire Bomber Mission: This mission requires the aircraft to begin empty. As soon as the payload is loaded, the aircraft can takeoff and after which fly 500 feet before making a 180 degree turn. On the 1000 foot long down wind leg the plane is to expel the payload and perform a 360 degree turn. At the end of the down wind leg the plane will make another 180 turn then land the plane and repeat the process again.
- Ferry Mission: The ferry mission consists of four consecutive laps which include the 360 degree circle with an empty aircraft.

In addition to completing each mission, the aircraft must takeoff in a distance of 150 feet and fit in a 4 by 2 by 1 foot box. The design must also aim at reducing Rated Aircraft Cost (RAC), which is used in calculating the final contest score. RAC is a function of aircraft weight, propulsive power, and manufacturing man hours.

The total flight score for this contest was determined using a weighted function that combined the scores from both missions. It was crucial to determine the importance of each mission during the conceptual design phase. The fire bomber flight score is a function of 2 times the water weight divided by the total flight time, while the ferry flight score is a function of the inverse of the flight time. An initial analysis determined the percentage of each mission's effect on the overall score. The purpose of this analysis was to validate the assumption that the aircraft should be optimized for the fire bomber mission.

Upon inspection of the two mission scores, it can be seen that the FM flight score will be a small decimal and the FBM will be a much larger decimal. The total flight score equals the addition of the FBM flight score and the FM score. With FBM flight be a much larger number than the FM flight, it will almost completely contribute to the total flight score. A hypothetical situation was investigated to ensure that this train of thought is correct.

Once it was determined to design for the fire bomber mission, the mission analysis process took several initial concepts under consideration. Time spent on the ground during the fire bomber mission is a crucial factor in producing an optimal total score. Therefore, delivering the water as fast and efficiently as possible was vital to producing a low mission time and ultimately a high total score.

Structural design of the aircraft had to consider wing loading, durability, and integrity of all components, while the aircraft's aerodynamic design had to produce an aircraft capable of flying in all wind conditions. In addition, the wing had to be large enough to allow the aircraft to take off in the prescribed distance.

3.2 Alternative Configurations

Alternative configurations were formulated for the aircraft type, empennage, payload systems, landing gear, and propulsion system. Configuration possibilities and FOMs were analyzed for each section.

3.2.1 Aircraft Type

When comparing multiple alternatives several assumptions were made: the aircraft could operate with one motor, each alternative would have similar wing lifting efficiency and fuselage length, the maximum allowable payload could be carried, and each alternative would perform at the same design wind speed. More detailed analysis would be necessary if one configuration would not have appeared superior based on the FOMs.

- Conventional: A conventional configuration was used as a baseline for comparing the configurations. The performance characteristics would be easily predicted with ample historical data available.
- Flying Wing: A pure tailless flying wing offered lower RAC due to its lack of a tail and a small fuselage. In addition, a flying wing would offer limited structural weight and drag. However, it had poor handling qualities and would require sophisticated augmentation to perform the optimum mission profile.
- Blended-Wing-Body: The blended-wing-body would have the same handling qualities as a conventional configuration, but less drag due to blended intersections and a more streamlined shape. It could also have a higher RAC due to more fuselage volume.
- Canard: A canard design would allow for the horizontal control surface to not detract from the overall lift of the aircraft. This configuration would have good stall characteristics, but be limited during takeoff. Flexible motor setups would easily be implemented.
- Bi-plane: A bi-plane configuration would be able to produce a large amount of lift with smaller wings, however, RAC penalty is very high for multiple wings. A bi-plane would be very similar to a conventional design with respect to flight characteristics.

The FOMs used to screen the different configurations are listed below and then used in Table 3.1 to rank each configuration.

- Takeoff Distance: Aircraft must lift off in 150 ft or it will not receive a flight score.
- Handling Qualities: An aircraft that is difficult to handle during all legs of the mission will have a low scoring potential. A design with the ability to land in a crosswind, handle center of gravity

movements, and be easily trimmed will be able to fly the optimum profile and have the best possible score.

- **Drag efficiencies:** Configurations should be designed to be fast in order to maximize scoring potential through a reduced mission time. Drag should be minimized in designs to make more efficient use of available power and increase speed potential.
- **Rated Aircraft Cost:** RAC directly affects the contest score. It is very clear that a lower RAC will produce a higher contest score.






						
Figure of Merit	Weighting Factor	Conventional	Flying Wing	Blended-Wing-Body	Canard	Bi-plane
RAC	0.33	2	3	1	2	1
Takeoff Distance	0.27	2	2	2	1	3
Handling Qualities	0.25	3	1	3	2	2
Drag Efficiencies	0.15	2	3	3	2	1
Total	1	2.25	2.23	2.07	1.73	1.79

Table 3.1: Overall Configuration Weighted Decision Matrix

The concept with the best scoring potential is the conventional configuration. The flying wing configuration is a close second, but the aircraft handling qualities make this configuration less desirable. The blended-wing-body's handling qualities and takeoff distances were as good as the conventional, but its RAC score was low due to the sweeping wing and larger fuselage requirements. The conventional design will minimize the fuselage penalty and be as streamlined and as possible. Such a configuration favors a mid-mounted wing. A mid-mounted wing would allow for increased drag efficiencies and moderate stability while allowing for the best fuselage blend. A mid-mounted wing does not interfere with payload ejection as a low-mounted wing would.

3.2.2 Empennage

Empennage alternatives were narrowed down to four possibilities: a conventional tail, a T-tail, a V-tail, and a cruciform tail.

- **Conventional:** A conventional configuration provided reasonable stability characteristics while remaining relatively lightweight. The horizontal stabilizer could also be integrated into fuselage easily.
- **T-Tail:** This tail is heavier than a conventional tail due to the reinforcement necessary to support the horizontal stabilizer. However, it allowed for a smaller horizontal stabilizer since it extended out of the wing wake and propeller wash.

- Cruciform: The cruciform configuration offered a compromise between a T-tail and a conventional tail. It avoided the full weight penalty of the T-tail, while still lifting the horizontal tail and improving its effectiveness.
- V-Tail: A V-tail offered lower RAC penalty and reduced interference drag; however, it introduced stability problems through the adverse roll-yaw coupling of the ruddervators in addition to construction complications.

The FOMs used to screen the different configuration are listed below. The FOMs are then used in Table 3.2 to rank each configuration.

- Weight: The weight of each tail design is counted heavily in the final RAC. To reduce RAC and produce an optimal score the weight must be minimized.
- Construction: The ease of construction for each tail configuration is important to reduce time spent building the aircraft and thus increase the testing time of the aircraft.
- Drag efficiencies: Configurations should be designed to be fast in order to maximize scoring potential through a reduced mission time. Drag should be minimized in designs to make more efficient use of available power and increase speed potential.
- Rated Aircraft Cost: RAC directly affects the contest score. It is very clear that a lower RAC will produce a higher contest score.





					
Figures of Merit	Weighting Factor	Conventional	T-Tail	Cruciform	V-Tail
RAC	0.3	2	2	2	3
Weight	0.2	2	2	3	2
Construction	0.2	3	2	2	2
Drag Efficiencies	0.3	3	2	2	2
Total	1	2.5	2	2.2	2.3

Table 3.2: Tail Configurations Weighted Decision Matrix

Table 3.2 shows the conventional tail performing the best, although a V-tail scored close due to the lower RAC. However, construction complications and increased weight far outweigh the RAC advantage. Therefore, a conventional tail was chosen.

RAC estimates were generated for four aircraft. A conventional aircraft with a conventional and V-tail and a blended-wing-body with a conventional and V-tail. The RAC values were found to be 6.36, 6.31, 6.42, and 6.47, respectively. Although a conventional aircraft with a V-tail has a lower RAC than one with a conventional tail, the disadvantages brought forth by the V-tail far outweigh the RAC advantage.

3.2.3 Payload

An important aspect of the aircraft design were the payload systems, which involved payload containment, evacuation, and loading. Improper water containment could be catastrophic to the aircraft's stability. In order to maximize flight time the plane must not have to slow down during the downwind leg of the FBM. A payload evacuation system must be designed that empties the plane tank as quickly as possible. Another major factor in flight time is pit time, or time spent loading the water onto the plane. Water loading systems must be selected that decrease pit times. On the following pages, multiple possibilities for each system are investigated and FOMs are used to select the superior designs.

Payload containment systems within the aircraft investigated are discussed below.

- Tubing System: Run 24 feet of 1 inch diameter tubing throughout the aircraft. This would drastically reduce dynamic shift of the water. However, the system would be susceptible to static shift in addition to being very complex and heavy.
- Bladder: A bladder would be used to control the payload. Such a device could keep the payload from shifting dynamically or statically. However, the rules prohibit an elastic bladder and a non-elastic bladder wouldn't do a sufficient job of keeping the water from shifting.
- Multiple Reservoirs: Multiple reservoirs with one way valves would control the payload in dynamic and static shift. The reservoirs would be complex and heavy.
- Single Tank: A single tank would be lightweight and simple. Internal baffling could be employed to aide in water containment. This design could be easily adaptable to achieve a high flow rate.

When developing the weighted decision matrix for selecting a final on-board payload concept, the following FOMs were considered. Table 3.3 presents the on-board payload decision matrix.

- CG Placement: The coincidence or proximity of the payload and aircraft centers of gravity directly affects the stability and controllability of the aircraft, and is therefore greatly important when considering alternatives.
- Static Shifting Control: The slow lateral and longitudinal movement of the payload was considered in each of the alternatives. This is important because such a shift would cause unpredictable movement of the payload center of gravity, and cause the aircraft to become unstable and uncontrollable.
- Dynamic Shifting Control: The rapid movement or "sloshing" of payload must be considered because this produces erratic movements, possibly sending the aircraft into a divergent oscillation.
- Reliability and Durability: The system must perform each time it is called upon, because not performing would result in flight score penalties ranging from three to seven minutes. The system must also be durable because of the amount of required flight testing.
- Payload Retention: All water must be expelled from the aircraft. The inability to accomplish this would result in a time penalty and a smaller volume of water being able to be carried on the second sortie of the mission.

Figures of Merit	Weighting Factor	Tubing	Bladder	Multi. Res.	Single
CG	0.25	2	2	3	3
Static shift	0.2	3	3	2	3
Dynamic shift	0.2	3	3	3	2
Reliability	0.2	1	1	2	3
Payload Retention	0.15	1	1	1	3
Total	1	2.05	2.05	2.3	2.8

Table 3.3: Payload Containment Concepts Decision Matrix

Using Table 3.3, the concept that emerged as the most dominant of the alternatives is the single reservoir concept. A single reservoir allows for better placement and control of the payload center of gravity, which ideally coincides with the empty aircraft's CG. Control of the dynamic payload shift is achieved with a baffling system inside of the tank. This baffling system will be further investigated during preliminary design. A tank without proper baffling could cause catastrophic effects to the plane in flight due to dynamic or static shifting.

Payload evacuation systems investigated to expel water from the aircraft are discussed below.

- **Nozzle:** A nozzle could be used to provide the optimum exit flow by capitalizing on the low pressure region created at the aft section of the aircraft. One difficulty with this concept was that the flow would become turbulent as soon as the water was released, possibly reducing the effectiveness of the nozzle design.
- **Pivoting Tank:** The entire tank containing the payload would pivot. Such a tank would allow for a smaller fuselage and sufficient head pressure would be gained. However, the rotational inertia produced by the swinging tank could have adverse effects.
- **Boom:** A boom would retract from the bottom of the aircraft. The valve and boom actuation could be done with a single servo. Since the boom is empty until it is in place, inertial effects would be minimal.

When developing the weighted decision matrix for selecting a payload expulsion system for the payload, the following FOMs were considered. Table 3.4 summarizes the decision.

- **Payload Evacuation Rate:** Payload can only be expelled on the downwind leg. If the aircraft must slow down for this, the mission time will be increased, resulting in a lower score.
- **Inertia effects:** If the payload shifts, its momentum could easily overcome the plane, causing the plane to diverge. With the payload weight being more than the projected plane weight, a small but sudden shift would likely cause a catastrophic failure.

- **CG changes:** The static margin must not be pushed to the point where the airplane becomes neutrally stable or the aircraft's behavior cannot be predicted. In order to prevent this, the payload evacuation cannot force the CG aft more than three quarters of an inch.
- **Drag:** The drag created by the water evacuation must be minimal, in order to keep the plane from becoming unstable during the evacuation. A large drag force created by an object in the flow field or spraying water into the stream in an adverse way might cause a moment which would force the plane into a pitch.


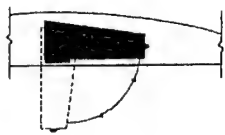
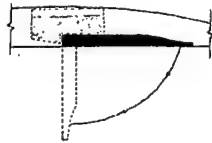
				
Figure of Merit	Weighting Factor	Nozzle	Pivoting Tank	Boom
Evacuation rate	0.35	1	2	3
Inertia effects	0.3	3	1	2
CG changes	0.2	3	1	3
Drag	0.15	3	1	2
Total	1	2.3	1.35	2.55

Table 3.4: Expulsion Payload Concept Decision Matrix

From Table 3.4, the optimal configuration is chosen to be a boom. The boom minimizes the center of gravity shift, while eliminating the adverse inertial effects inherent in the pivoting tank concept. Using the boom also provides the most head pressure, resulting in the fastest evacuation times, and reducing the time for which static payload shifting is an issue.

Water Loading significantly affects the overall flight score through the "pit" time that it takes to load and reload the payload onto the aircraft. The following ground based payload concepts were generated to minimize water loading time. All concepts are presented in Figure 3.1 and described below.

- **Gravity Feed System:** The first consideration for loading the payload onto the plane was a gravity feed. An initial belief was that roughly a six-foot-tall device could hold the two bottles of water and allow gravity to accelerate the loading process. This is a relatively simple device that would provide ease of construction while remaining cost effective.
- **Single Pump System:** This concept consists of a single pump for both bottles. A manifold would be used to connect tubes from each bottle to the pump intake. The total flow would be discharged through one exit which allows for the use of only one loading orifice on the fuselage.

- **Dual Pump System:** This system would assign a pump to each bottle, thus doubling the flow rate. Utilizing two loading ports, one for each pump, the time to load the water could ideally be reduced by half. Although the addition of another pump would be costly, the benefits of saving time in the pits would drastically improve the flight score.

FOM's used to screen the alternatives are discussed below and used to complete the decision matrix shown in Table 3.5.

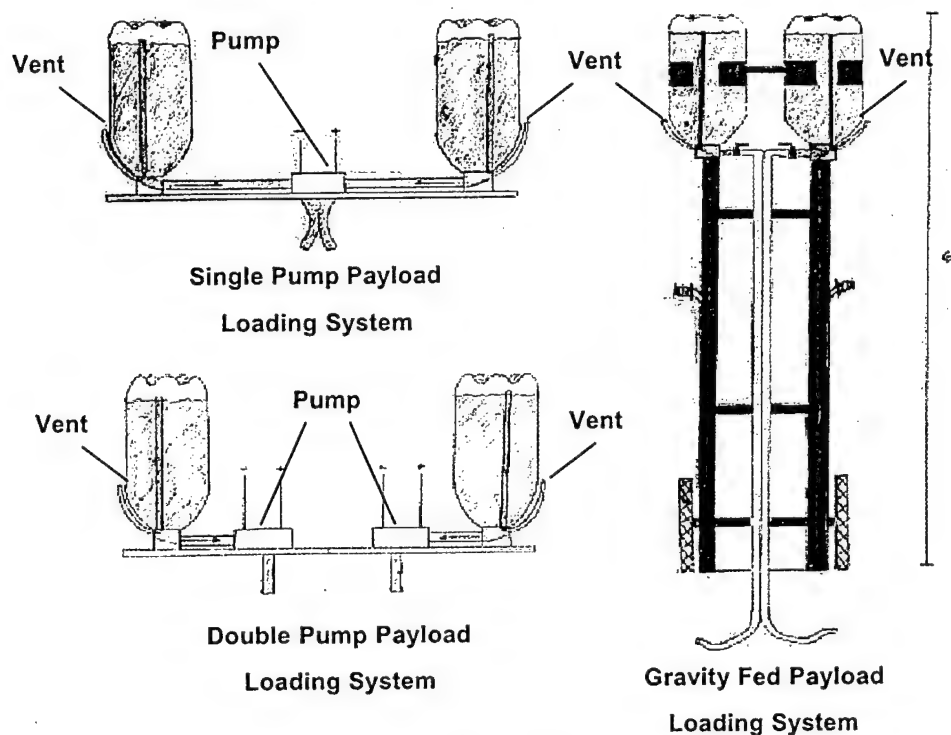


Figure 3.1: Water Loading Concepts

- **Expulsion Rate:** The flight score is based upon the total mission time, including the time required to load and reload the payload onto the aircraft. Therefore it is imperative to have the quickest possible loading rates in order to increase the flight score.
- **Reliability:** A system failure will result in a flight score of zero for that attempt. Mild failures causing excessive spillage will also result in time penalties and reduced flight scores.
- **Mobility:** The ground crew for loading and reloading the aircraft may consist of only three persons, and they must be able to move the apparatus from the staging area to the aircraft and load it as quickly as possible in order to maximize the flight score.
- **Simplicity and Ease of Operation:** The system must be straightforward and easy to operate in order to reduce preparation and loading times for each sortie.

Figure of Merit	Weighting Factor	Gravity Feed	Single Pump	Dual Pump
Expulsion Rate	0.35	1	2	3
Reliability	0.3	3	2	2
Mobility	0.2	1	2	2
Simplicity	0.15	3	2	1
Total	1	1.9	2	2.2

Table 3.5: Water Loading Concept Decision Matrix

Because the loading and reloading of payload have such a profound effect on the total flight score, it becomes necessary to minimize the time required to do such. The dual pump system is slightly more costly and cumbersome, but because the flow rates are doubled and the actual time required to load the water is halved, the benefits prevail over the drawbacks without question. Utilizing two self-contained pumps will undoubtedly increase the flight score and ultimately the overall team score.

3.2.4 Landing Gear

Many configurations of aircraft landing gear exist, the most feasible options are described below.

- Tricycle gear with bow-type main gear: Such a setup provides adequate ground stability. Using a bow would transfer all of the landing loadings to one point in the fuselage, thus only requiring minimal reinforcement.
- Tricycle gear with independent main gear: Independent struts must be built very strong and aircraft integration must be reinforced greatly, but more freedom is given in gear placement.
- Tail Dragger with Bow-type Main Gear: Tail draggers make use of mains and a small tail wheel. The lack of a large nose wheel will reduce drag and weight. A bow for the mains would give the same advantages mentioned above.
- Tail Dragger with Independent Main Gear: This setup has all characteristics as listed in the tail dragger configuration listed above. All problems associated with independent mains are still present.

The most compatible landing gear alternative was selected using the following FOMs to compare the designs:

- Landing performance: Landing gear would be rendered useless if the plane could not land properly. The gear must allow the aircraft to be stable on the ground shortly after touchdown.
- Weight: Minimum weight is desired in order to reduce Rated Aircraft Cost and maximize aircraft performance.
- Pilot preference: The pilot felt more comfortable landing and taking off if the landing gear was designed similar to what they were accustomed to using.

- **Stability:** The landing gear must be capable of creating a stable support for the aircraft while it is stationary or moving on the ground. Without stability, the aircraft could topple forward and damage, if not, destroy the propeller.

Figure of Merit	Weighting Factor	Tricycle		Tail Dragger	
		Bow	Independent	Bow	Independent
Landing Performance	0.35	3	3	3	3
Weight	0.3	2	1	3	2
Pilot Preference	0.2	2	2	3	3
Stability	0.15	3	3	1	1
Total	1	2.5	2.2	2.7	2.4

Table 3.6: Landing Gear Evaluation

Table 3.6 indicates a tail dragger with bow type mains is the most viable alternative. Although this design presents some stability issues, the weight advantage and pilot preference make it the most attractive.

3.2.5 Propulsion System

Propulsion system configurations consisting of various motor and battery combinations were investigated. Each configuration is discussed below.

- **Double Stack:** A Double Stack configuration will provide the most amount of power. The weight of the entire system will be higher due to the multiple motors and battery packs. This extra weight significantly counts against the RAC.
- **Double Stack/Shared Pack:** The Double Stack/ Shared Pack configuration utilizes a single battery pack to power two motors, thus providing power similar to the Double Stack configuration while saving weight and battery cells.
- **Single Stack:** The Single Stack configuration minimizes RAC because it uses only one motor and one battery. This system must be properly designed to provide the required power for the aircraft to fly the mission profiles.
- **Single Stack/Two Packs:** This concept is identical to the Single Stack except that the battery pack is broken up into two smaller packs. Smaller packs will provide for more battery placement options.

These alternatives were compared against the FOMs below to determine the best choice for the battery/motor configuration. Results of this comparison are presented in Table 3.7.

- **RAC:** The propulsion system has a large effect on RAC, therefore it must be minimized.

- **Power Produced:** The power produced directly effects aircraft performance. Without ample power, the aircraft will fail in its ultimate mission.
- **Weight:** Weight is important because total propulsion system and battery weight are heavily penalized in the RAC.
- **Efficiency:** The ability to produce required performance with the lowest number of batteries for both aircraft performance and RAC.

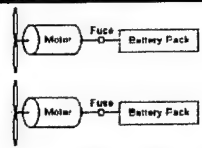
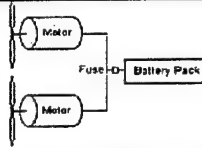
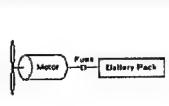
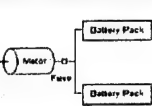
					
Figures of Merit	Weighting Factor	Double Stack	Double/Shared Pack	Single Stack	Single/Two Packs
RAC	0.35	1	2	3	3
Power Produced	0.3	3	3	1	2
Weight	0.25	1	1	3	2
Efficiency	0.1	1	2	1	2
Total	1	1.6	2.05	2.2	2.35

Table 3.7: Battery/Motor Configuration Decision Matrix

Based on Table 3.7, the single stack/two pack configuration is the best choice for this competition. RAC will be minimized as this is one of the lightest configurations. Using two smaller battery packs will allow the team to place the batteries in the fuselage more easily without sacrificing power. One motor should provide the plane with sufficient power to complete the mission in the desired time.

3.2.6 Structural Concepts

Different structural methods were examined and evaluated.

Fuselage Structure

- **Keelson:** Building up the fuselage off of a main keelson has potential to produce an overall strong and stiff aircraft, but does not allow for the most desirable shapes and curves for aerodynamic concerns.
- **Stringers:** A stringer based fuselage allows for more aerodynamic shaping by blending stiff, shaped stringers around a series of bulkheads, creating a more aerodynamic fuselage with smoother cross section transitions.
- **Monocoque:** A monocoque, or reinforced skin fuselage can produce strong and stiff aircraft through the use of stiff and lightweight composite sandwich structures. The most common way to carry out this technique is through the building of molds, allowing the exact outer shape to be controlled by the mold shape.

The FOMs were selected to evaluate the performance of each method. Evaluation results are presented in Table 3.8.

- **Strength/Weight Ratio:** The emphasis on weight in the RAC calculations dictates that any structural design chosen must be lightweight, in order to maximize scoring potential.
- **Reproducibility:** In the event that an aircraft malfunctions or is damaged, it will be necessary to either rebuild or repair, so each method is evaluated on how easily the plane can be fixed or be reproduced.
- **Connection Interface:** In order to minimize losses, methods were evaluated on their junction characteristics because of the unnecessary drag that can be produced at intersections.
- **Dimensionality/Surface Finish:** The plane must be as streamlined as possible in order to eliminate drag, so a FOM was chosen to grade each method on surface smoothness and shaping capabilities of each method.
- **Construction Ease:** An investigation was conducted into the difficulty of each method, and a decision was made based on the audited team skills.




				
Figures of Merit	Weighting Factor	Keelson	Stringers	Monocoque
Strength/Weight Ratio	0.25	2	2	3
Reproducibility	0.25	1	1	3
Connection Interface	0.15	1	2	3
Dimensionality/Surface	0.2	1	2	3
Construction Ease	0.15	2	2	1
Total	1	1.4	1.75	2.7

Table 3.8: Fuselage Construction Evaluation

From Table 3.8., the best choice to provide the desired high strength, light-weight, and streamlined aircraft fuselage was the monocoque skin method. This method has the potential for substantial savings in final aircraft weight, which will reduced the required power, shrink the wing size, and result in a higher performance score and higher total scores.

Wing/Empennage Structure

- **Foam Core:** The first method investigated was foam core composite construction. A CNC foam cutting machine was available, so cutting precise pieces was possible. With proper composite

material considerations, sufficient strength for the mission would be easily possible to achieve. The major drawback to this method is the weight of the internal foam core. It is also fairly easy to create replacement parts, with the exception of the foam core surface preparation process.

- **Built-Up Construction:** Built up construction consists of building a balsa frame and applying Monokote covering to it in order to create the aircraft skin. It was considered mainly because of the advantage that it is extremely lightweight, and fairly simple to build. Another positive aspect of built up construction is that many times, minor damage to the aircraft can be repaired locally. The method is fairly precise due to the use of part templates, which allow for some precision in making the sections of the plane, but in the event of severe failure, a broken part nearly always has to begin from scratch.
- **Monocoque:** For monocoque construction, the external skin is used as most or all of the structure. Internal structure is generally intended for maintaining shape and providing additional stiffness. This design is particularly desirable for wing structure due to the nature of the tension/compression skin pairs formed by the wing lower and upper skins.

The following is a descriptive list of the FOMs used to evaluate each structural technique for wing/empennage construction. The resulting decision is presented Table 3.9.

- **Strength/Weight Ratio:** The wing is likely the largest structure on the aircraft, requiring it to be as lightweight as possible and still carry the required loads.
- **Bending Strength:** The lift force on the wings will impart a bending moment, meaning the most likely failure mode of the wings will be in buckling.
- **Reproducibility:** Wings are likely to be damaged in the event of a crash during flight testing, so the ease of repair to a damaged wing is evaluated, as well as the ease of reproducing a new wing.



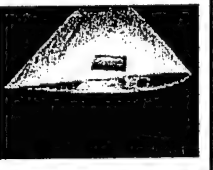
				
Figures of Merit	Weighting Factor	Foam Core	Built Up	Monocoque
Strength/Weight	0.4	1	2	3
Bending Strength	0.3	2	2	3
Reproducibility	0.3	1	1	3
Total	1	1.3	1.7	3

Table 3.9: Wing/Empennage Construction Decision Matrix

The monocoque method of providing structure within the skins is again chosen for the wing and empennage surfaces. The combination of a superior strength/weight ratio and the relatively easy reproduction of monocoque structure were the deciding factor in choosing it as the best alternative.

Payload System Structure

The payload system construction method was chosen to be a fiberglass lay-up, with some reinforcement to aid in carrying the spar loading. A monocoque type container will be constructed, so that it will not need internal structure to carry the water, with some stringers internal to the skin for additional stiffness. The monocoque construction required a foam plug with exact dimension be created.

3.3 Conclusions

Many combinations of aircraft type, empennage, payload systems, landing gear, propulsion systems, structural configurations to choose from, the decision matrices, the RAC calculations, and sensitivity studies narrowed down the possibilities to one final conceptual design. The design proving to be the best was the conventional fuselage with a conventional tail, shown in Figure 3.2. This concept showed the most promise for handling qualities and mission performance without compromising RAC. The on-board payload system that best suited this design was the single reservoir with baffling. A boom attachment on the tank would add the necessary head pressure to expel all of the water during the downwind leg. The superior propulsion system was a single motor powered by a split battery pack. The entire design was to be built with a monocoque design, which minimized weight while providing the necessary strength. Tail dragger landing gear with bow-type main gear was chosen and fits well on the aircraft's design.

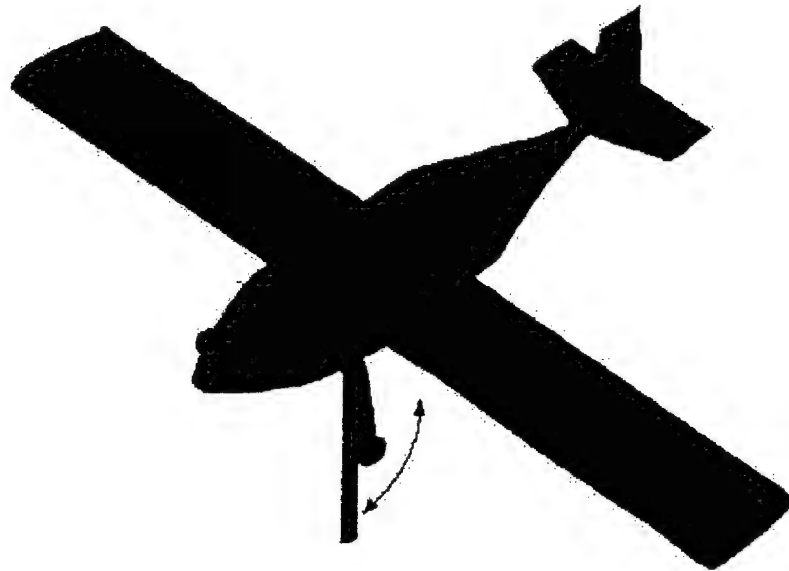


Figure 3.2: Final Conceptual Configuration

4.0 Preliminary Design

The chosen configuration from the conceptual design phase was separated into three groups: aerodynamic, structural, and propulsion groups. Critical design parameters were selected and studied within each group. FOMs were used to find appropriate sizes for many of the design parameters. The mission model program from the conceptual design phase was modeled more accurately and a propulsion performance program was created. These programs optimized the most important design parameters, while the remainder of the design parameters were subsequently analyzed and sized.

4.1 Design Parameters and Sizing Trades Summary

Critical design parameters were selected within each design group. The aerodynamic group investigated wing area, airfoil, wingspan, and fuselage and empennage size, while the structures group investigated payload amount and boom length. The propulsion group investigated motor selection, battery selection and number of cells, propeller pitch and size, and takeoff and cruise power. Many other design parameters existed, but these have the largest effect on RAC, total score, and performance.

- Wing Area: Wing area is crucial for take-off with a short runway. Data found during conceptual design showed the conceptual configuration lifting off at 150 feet with the smallest possible wing area. This trend increases the scoring potential but causes major concerns during take-off. High wing loading allows for faster cruise velocities but longer take-off distances.
- Wingspan: Wingspan has a major effect on wing efficiency and RAC. RAC is minimized for given wing areas as the aspect ratio is lowered, but high aspect ratio wings become more efficient. Also, RAC is minimized with a rectangular wing making elliptical and tapered wings highly penalized. Therefore an RAC/efficiency tradeoff must be made. Construction, fit-in-box, and the ability to pass the wing tip loading test were other considerations.
- Airfoil: Airfoil selection is important because of its direct affect on take-off and cruise. Three low speed airfoils were chosen based on historical data for further analysis: a high lift airfoil, a low drag airfoil, and a more balanced airfoil. The airfoils were evaluated to test the affect each had on the overall score. The high lift airfoil performed well during takeoff due to its high lift coefficient, but its large drag possibilities during cruise was a concern, while the low drag airfoil performed well during cruise due to its low drag coefficients, but its low lift coefficients were a concern during takeoff. The balanced airfoil performed well in both cruise and takeoff situations. More detailed mission models were needed to find the optimal airfoil.
- Fuselage length & Empennage Size: It was desired for the entire plane length to be less than 4 feet long so that it could fit in the box. A one piece fuselage and empennage would benefit the structural integrity and weight of the plane. The empennage size must be sufficient to stabilize the aircraft. As overall aircraft length increases the RAC increases. Drag decreases as the fuselage length increases and empennage size decreases. A compromise must be made to minimize both RAC and drag.

-
- **Battery Selection and Number of Cells:** Battery weight has the most effect on RAC. The capacity of the batteries had to be sufficient to perform the mission profile while minimizing the amount of unspent energy. A lower capacity battery would require more cells, thus increasing voltage and RPM. A high capacity battery would complete the mission using fewer cells, thus decreasing voltage and RPM. Minimizing the number of batteries would lower the weight of the system, thus decreasing the RAC.
 - **Propeller Pitch and Size:** Propeller pitch and size impacts the amount of thrust produced a propeller with a high pitch to diameter ratio would be more efficient at higher airspeeds than a low pitch to diameter ratio propeller. The propeller selection had to be based on a trade-off between takeoff and flight performance.
 - **Takeoff & Cruise Power:** Takeoff and cruise power must be optimized to increase the scoring potential of the aircraft. The power generated at takeoff would account for the majority of the available energy from the propulsion system. The remaining amount of energy would be consumed during cruise. The thrust at take-off must not create a current over 40 amps or use too much energy from the batteries causing an insufficient amount of power for cruise. Gear ratios and propeller sizes may be changes to better suit take-off situations or cruise situations.

4.2 Refined Mission Modeling and Optimization Analysis

A mission profile analysis program and propulsion system analysis program were created to optimization the most important design parameters.

4.2.1 Mission Profile Optimization Analysis Program

A mission analysis performance program was written to assist in analyzing each phase of the mission profile to determine the overall result. The program analyzed the entire FBM as best as possible utilizing techniques found in Nelson (1998). The program consists of mathematical models for aerodynamic characteristics, propulsive efficiency, and the weight of a proposed aircraft. The program was written such that various aircraft configurations could be compared quickly and efficiently utilizing aerodynamic modeling characteristics, such as wind speed, taper ratio, sweep angle, and flaps. Once the flight characteristics of the candidate configurations were determined, the performance characteristics for each phase were calculated:

- Time and power required to takeoff within the 150 foot limit.
- Time and power required to climb at a satisfactory rate.
- Time, distance, and g-loading during turning were calculated from weight and stall characteristics.
- Time and distance required during payload evacuation.
- Time and power required during cruise velocities.
- Time and distance required to slow down from cruise velocity to stopping.

The individual components of the mission profile for each configuration were then combined and compared. The overall values from each configuration measured were the times, distances, and energy consumed. The RAC was then calculated and the final flight score was determined from the equation provided by the contest rules.

Certain limitations were placed upon the modeling method used to reduce the number of possibilities. The most important constraint was the aspect ratio. Based on historical data from previous Oklahoma State University configurations a limit of 8 was implemented. A limit of 8 was chosen because, historically, aircraft with an AR higher than 8 were found more difficult to control. Another assumption employed was that the payload would be completely released after completing the 360° turn. Therefore the aircraft was assumed to be carrying the full payload before 360° turn, no payload after the turn, and partial payload while performing the turn. Therefore, it is crucial that the final configuration is able to evacuate all payload during the downwind leg of the mission. The final limitation implemented was a battery usage of 100%. This constraint was utilized to determine the fewest number of battery cells that would produce a useful final score. These limitations kept the predicted performance models within reason.

- Weight model: The weight model was reconstructed to better represent a plane built using monocoque construction. This model was based on historical data and varied structural weight as a function of wing area and estimated structural weight for the fuselage and empennage. The model was made slightly conservative to provide a margin of safety and checked against historical data.
- Drag model: The drag model was reconstructed for the conceptual design according to the drag build-up method found in Raymer (1999). The method gave a close estimate of drag without having exact dimensions. The drag model also included the drag polar for the chosen airfoil and estimated parasite drag for the plane. Proper Reynolds numbers were used for both cruise and take off.
- Propulsion Model: The propulsion model was refined using historical data from a single motor configuration. The new model was reconstructed to remain conservative, yet represent the propulsive system better than the conceptual model.
- Rated Aircraft Cost Model: RAC was updated to better represent the features chosen in the conceptual design.

These models were placed in the program along with the parameters the sensitivity studies showed as optimal. The values included a wind speed of 10 mph and an altitude of 50 feet. The program was adapted so that the aircraft was optimized for overall score. Figure 4.1 below shows the method used for determining optimal configurations within the program.

Sensitivity Studies

Sensitivity studies were done on the critical variables in the mission profile program. These studies analyzed each variables effect on the overall scoring potential of a configuration. Results of these

sensitivity studies identified the major contributing factors involved in the design requirements. The conceptual design candidate concepts were more easily judged based on the studies' conclusions. The variables studied were time on the ground (or pit time), wind, wing taper and sweep, the use of flaps, and altitude.

- Time on the ground: Flight time is a direct multiplier in the overall score and therefore crucial to minimize. Pit time, or time on the ground loading the payload, is a critical part of the total flight time. As flight time decreases, minimizing pit time becomes the best way to maximize the overall score. Large score improvements were a result of shorter pit times.
- Wind Velocity: Wind sensitivity test were necessary because of the unpredictable wind conditions. Designing for higher wind speed is a risk. With higher wind, less wing area is necessary for lift off, which improves the overall score. If the wind is below the design criteria, the plane may not be able to lift off in the necessary distance causing an overall score of zero. The sensitivity analysis determined the risk/pay-off levels involved in designing for different wind speeds. Results show designing for a 10 mph wind has relatively low risk due to the traditional windy conditions at the competition.
- Flaps: Flapped airfoils were tested to determine the resulting flight characteristics and scoring potential. Flaps may be able to decrease wing area due to better lift off capabilities causing the weight of a configuration to decrease. However, flaps have an adverse effect on RAC.
- Wing Taper and Sweep: Both wing taper and sweep have adverse effects on RAC causing a design's scoring potential to decrease. Any performance advantages gained from using wing taper and/or sweep would be negated because of RAC. Therefore no wing sweep was considered and a taper ratio of one was used.
- Altitude: The cruise altitude makes large differences in power required from the motor. The lower the plane can fly the less energy it uses to get to that altitude. The plane must fly at a safe altitude, but must not fly so high that it uses too much energy. Historical data for R/C planes showed that an altitude of 50 feet is common.

4.2.2 Propulsion System Analysis Program

Although the propulsion model included in the mission analysis program predicted a fairly accurate overall flight profile, it was not detailed enough to design the complete propulsion system. A separate propulsion analysis program preformed a more detail analysis on the number of batteries, types of batteries, propeller diameter and pitch, and gear ratio for the take-off leg of the mission.

- Battery Model: Manufacturer's data on different types of available batteries were utilized in the propulsion model to predict their performance. Along with different types of batteries, the number, capacities of the cells, and overall efficiency of the battery packs were modeled to produce more realistic performance characteristics.

- **Propeller Model:** Varying types of propellers were also tested within the propulsion program. Propellers of different diameters and pitches were modeled to determine the thrust, torque, and angular velocities produced. This resulted in a range of optimal propeller sizes to be used during each mission.
- **Gear ratio:** Different gear ratios were also employed within the propulsion program. The energy consumed by each ratio along with the resulting thrust and energy consumed were evaluated. These tests were performed within the contest constraint of 40 amps. This limitation ensured that the fuse would not be blown during flight.

Many different propulsion configurations were analyzed using the propulsion optimization program that simulated the mission profile. Although the program is very useful in determining the trends associated with changing a given component, the final propulsion system will be determined through numerous static and dynamic tests. Figure 4.1 below shows the method used for determining optimal configurations within the program.

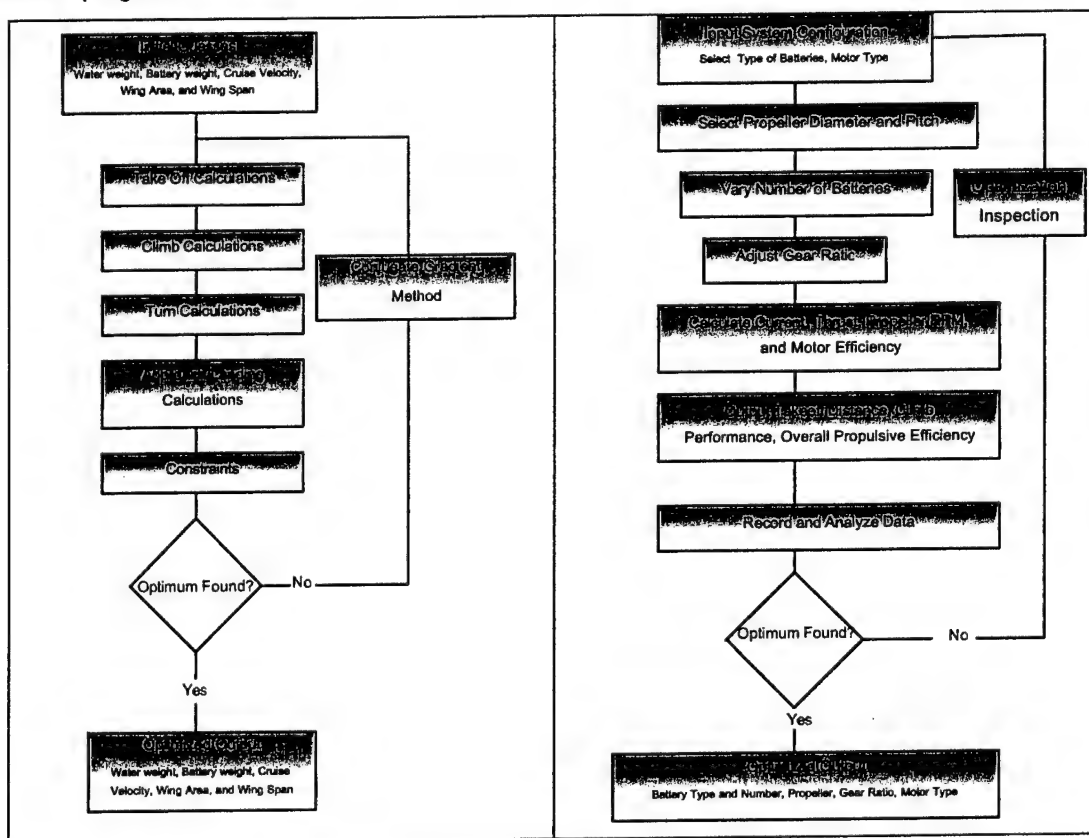


Figure 4.1: Block Diagrams for the Mission Profile and Propulsion Optimization Program

4.3 Optimization

With a base line configuration determined, the optimization program was refined to more accurately model the chosen design.

4.3.1 Mission Profile Program Results

The water weight, wing airfoil, wing area, wing span, and cruise velocity were derived from the mission model optimization program. Overall score was the major driving factor in selecting the best program outputs. The best results allowed lift off in just less than 150 feet and using nearly all of the available energy from the batteries. Performance considerations and stability and control effects not included in the optimization code were another deciding factor. Explained below are the mission profile optimization results.

Water Weight

It was found the maximum amount of payload should be carried. Overall score dropped considerably as payload weight dropped, due to the fact that payload weight affected the single flight score for the FBM significantly.

Wing Airfoil

Using historical data, three low speed airfoil's drag polars were chosen to input into the mission profile optimization program. A high lift airfoil, the Eppler 423; a low drag airfoil, Selig-Donovan (SD) 7032; and a more balanced airfoil, SD7062 were compared. It became clear that the short takeoff distance of 150 feet required an airfoil with a high lift coefficient during take off. The SD7032 was unable to produce scores as high as the other two airfoils. The wing area required for lift off where much larger than the other two airfoils, which increased the RAC considerably. Flaps where added to the SD7032 in an effort to solve this problem but even flapped the airfoil could not produce expectable scores. Therefore the SD 7032 was eliminated as an airfoil choice.

Comparing the scores produced from the E423 and the SD7062, the Eppler prevailed. The SD7062 was then flapped and compared with the E423. The E423 is already a highly cambered wing so the addition of flaps does not create more usable lift due to the large amount of drag created from the flap. The scores produced between the E423 and the flapped SD7062 were to close to be able easily decide. Therefore, other deciding factors were compared.

The deciding factor for airfoil selection was the E423's drag polar. Major concerns with E423 drag potential during cruise made the E423 un-applying. The E423 has a large drag spike near the aircraft's cruise lift coefficient. Therefore the E423 was eliminated as an airfoil choice. Figure 4.2 shows the drag polar and lift curve for the SD7062.

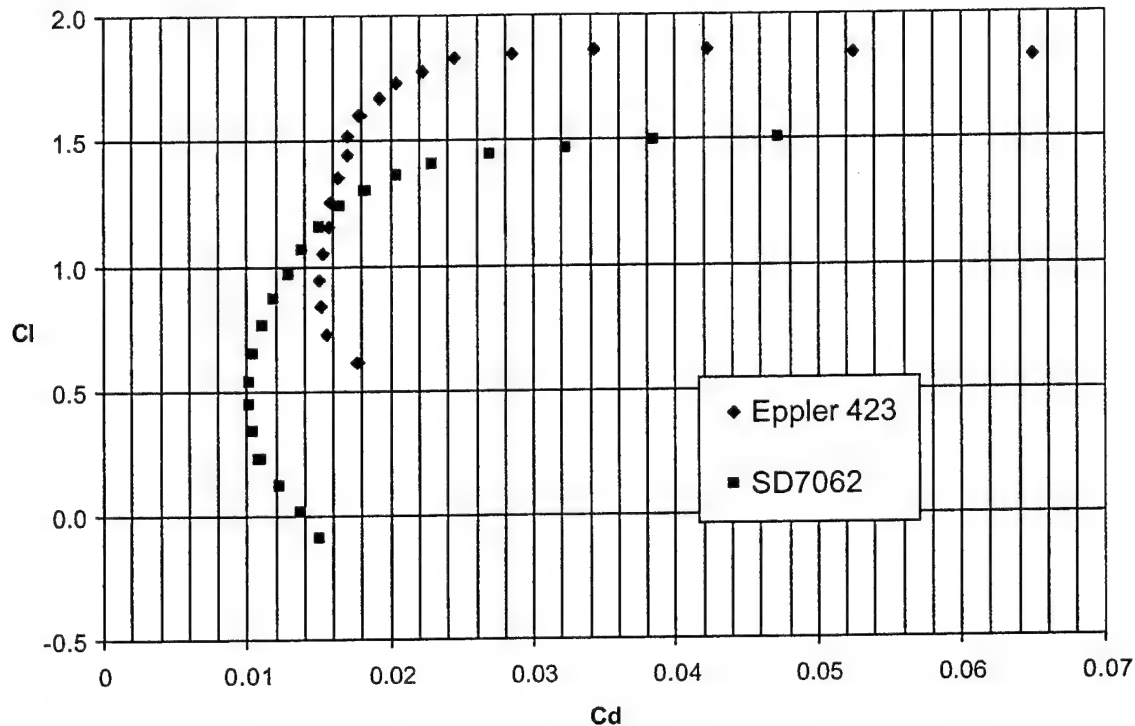


Figure 4.2: Drag Polar and Lift Curve for SD7062 and E423 at a Re of 250,000

Wing Area

The optimization program tended to decrease the wing area as much as possible, since no wing loading constraint was implemented into the program. Concerns with undersized wing areas caused optimal design with larger wing areas to become superior. Therefore the SD7062 was optimized without the use of flaps. Although this increased RAC it provided a margin of safety. The plane could take-off un-flapped in 150 feet with a 10 mph head wind. If the wind were to dip below 10 mph flaps could be deployed and the plane would still be able to take off. Furthermore, flaperons could be used instead of flaps and serve the same purpose without causing a major increase in RAC.

Another constraint not accounted for in the mission optimization program was the decrease in lift due to the disruption of the lift curve over the wing caused by the fuselage. It was assumed the area of the wing covered by the fuselage would be added to the optimized wing area to ensure enough lift is produced. The final range of optimal wing area for the SD7062 was 5.4 to 5.7 square feet.

With the airfoil selected, wing sizing could begin. Two general trends emerged within the optimization code. High scores were found when small wing areas were used with more batteries or large wing areas were used with fewer batteries. The highest scores were found in designs using fewer batteries with smaller wing areas but both configurations had similar scoring potentials. Since the uncertainty range of the optimization code was greater than the scoring range, other deciding factors needed to be examined.

A more detailed study of motor performance during takeoff was necessary in the analysis of the wing. Several optimized combinations were analyzed during takeoff with different propeller sizes, gear box ratios, and batteries. This analysis looked at takeoff distances in different wind conditions, current through the cut-off fuse, and power used during takeoff. All the configurations were re-optimized with the best propulsion system possible in the preliminary phase. The optimization code and propulsion code double-checked one another to ensure that each configuration could successfully takeoff while still maintaining power efficiency and the proper endurance. The score was also monitored as cruise velocity and battery cells varied. The end result showed a more optimized score with smaller wing areas and larger batteries, but this configuration did not have the performance and takeoff margin of safety desired. Figure 4.3 shows the wing area sizing trends produced by the optimization program. The circle on the graph represents the decision made.

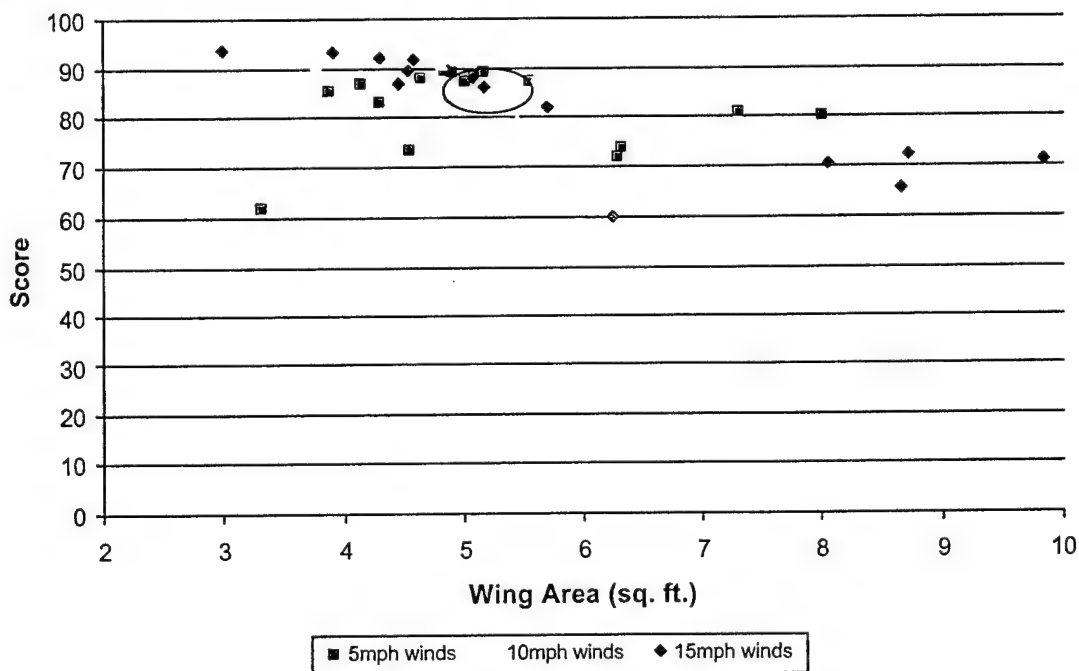


Figure 4.3: Wing Planform Area Optimization Results using an Un-flapped SD7062

Wingspan

Without an aspect ratio limit, the optimization code would drive the aspect ratio too high, which would make the plane nearly uncontrollable. The code includes a maximum aspect ratio constraint of 8 to ensure stability and control is not compromised. As expected the program optimized the wingspan to create an aspect ratio of 8. The range of wingspans considered was 75 to 80 inches.

Cruise Velocity

The optimization program performed a power/speed trade-off to determine the optimal cruise velocity for the design. The energy used at take-off, climb, and cruise must not exceed the batteries capabilities. The program found the optimal power requirements for take-off and cruise, which keep the cruise velocity as high as possible keeping mission times low. Mission time cannot be neglected since it is such a large factor in the scoring function. The optimal cruise velocity that the program outputted ranged from 70 to 80 feet per second.

4.3.2 Propulsion Program Results

The preliminary design phase for the propulsion system involved utilizing a computer program that optimized the motor, gearbox, batteries, and propeller. The program modeled the complete propulsion system throughout the mission profile. The propulsive system components were varied such that the overall propulsion system met or exceeded the aircraft performance requirements estimated for thrust, power, and system efficiency and endurance. This optimization process was an iterative one performed in collaboration with the aerodynamics group. Both groups worked in combination to develop an aircraft model that produced the most desirable score and performance characteristics.

Motor

The propulsion team determined early in the preliminary design phase that Graupner 3300-6 motors would be used. The Graupner motor produced superior results to the Astroflight models. During the optimization process the propeller diameter and pitch, battery cell capacity and number, and gear ratio were held constant, while motor type was varied. Manufacturer provided motor data along with historical test data was varied according to each motor type. The key parameters varied were the voltage constant (Kv) value, internal resistance, and no load current. A direct comparison of the Graupner motors to the Astroflight models can be seen in Figure 4.4 on the following page.

Gearbox and Gear Ratios

An MEC Superbox was used to transmit the power from the motor to the propeller. The pinion and spur gears can be quickly changed to allow gear ratios from 1.18:1 to 3.50:1.

To determine an optimal range of gear ratios, the propeller size, battery type and cell count, and motor were held constant in the optimization program. The gear ratios were then varied and the thrust produced, power required, current drawn, efficiency, and battery endurance were catalogued. The thrust produced and power required from the batteries were matched with the mission profile model requirements for takeoff to obtain realistic results. The current drawn from the batteries was monitored to ensure that the system would not destroy the 40 amp fuse required for safety.

The resulting optimal gear ratios ranged from approximately 1.33 to 2.27. This range provided the most thrust at full throttle while still remaining below the maximum amount of pulled current. At lower gear ratios more thrust is produced at the cost of pulling more current from the batteries.

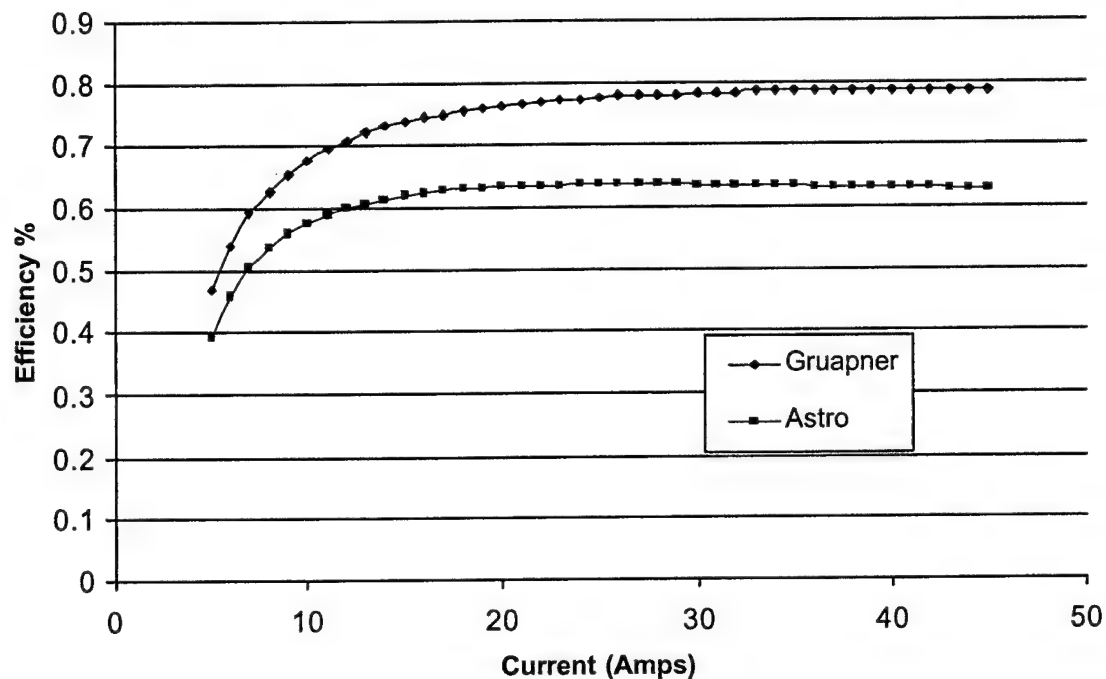


Figure 4.4: Efficiency versus Current for Graupner

Batteries

Battery selection plays a vital role in the optimization of the propulsion system. It is necessary to find the battery which best suit the needs of the propulsion system. The Ni-Cd batteries considered for powering the propulsion system are the CP 1300 SR, SR 1200 Max, SR 900 Max, and SR 2400 Max. Battery information such as the internal resistance, weight, capacity, and capacity to weight ratio can be found in Table 4.1 below.

BATTERY INFORMATION				
Battery Type	R	W	Capacity	Cap/W
CP 1300 SR	0.0065	0.0775	990	12774.19
SR1200 Max	0.004	0.0981	1080	11009.17
SR 900 Max	0.0055	0.083125	810	9744.361
SR 2400 Max	0.0045	0.135	2100	15555.56

Table 4.1: Battery Information

The first major battery selection consideration is weight; every bit of extra weight penalizes the RAC. The next major consideration is the capacity to weight ratio. It is important to get the most power out from the specific battery weight as possible.

All battery types shown in Table 4.1 were tested in the optimization program. The best performers were the CP 1300 SR and the SR 2400. When optimized the CP 1300 SR gave the aircraft a better flight score. It can be noted that the SR 2400 Max has a much greater capacity, but the extra capacity is unnecessary according the optimization program. The CP 1300 SR is much lower in weight, yet still has enough capacity to produce a better flight score. Therefore the CP 1300 SR was chosen as the optimal battery type.

Utilizing the motor selected and the most favorable range of gear ratios the number of battery cells was varied until the thrust and power requirements for the mission profile were met, resulting in an optimal number of cells from 14 to 18 cells.

Propeller

The main design consideration for propeller selection is sizing, propeller pitch and diameter for the best propulsive efficiency, c_p . A larger diameter propeller would be necessary. Another factor to consider is the propeller pitch-to-diameter, p/d , ratio. Propellers with a low p/d ratio have the greatest c_p at lower airspeeds while higher p/d props have a high c_p at higher airspeeds.

Testing various sized propellers in the optimization program resulted in an important conclusion. The optimal propeller size is dependant on whether or not the aircraft has full payload or no payload. For the FBM, the fully loaded aircraft requires a larger propeller. Optimal propeller sizes range from 16" to 20". For the FM, the empty aircraft requires a smaller diameter propeller. Optimal propeller sizes range from 14" to 18" for the FM.

4.4 Analysis Methods and Sizing

All three technical groups employed separate analysis methods to help refine the respective sizing of the aircraft's design.

4.4.1 Aerodynamic Group

Main aircraft component sizing and power and wing loading are discussed below. Issues surrounding sizes of the components are discussed and the optimal sizes are selected. The components covered are fuselage, empennage, and control sizes.

Fuselage Size

In order to fit the entire fuselage in the box, the length was slightly less than 4 feet long. In addition, the cross section was constrained to a 4" X 8" rectangle due to the RAC penalty. A one piece fuselage and empennage would benefit the structural integrity and minimize weight. The fuselage was modeled in

Pro-E and all internal components were placed inside to ensure proper fit. With all the internal components inserted the fuselage was streamlined as much as possible.

Empennage Size

Horizontal and vertical stabilizer's size and airfoil type were determined. The FOMs for the tail included performance and RAC considerations. The tail had two important tasks: produce the necessary pitching moment at takeoff and landing and trim the airplane in cruise.

- Horizontal Stabilizer: If the projected horizontal tail span exceeded a quarter of the wingspan, the tail was classified as a wing by the RAC and penalized. Therefore, the horizontal tail span was limited to a quarter of the wingspan making the span approximately 19.2 inches. An approximate elevator size had to be determined to ensure the elevator would not be an unreasonable portion of the horizontal surface. The elevator was sized by investigating the worst case scenario, landing. If the elevator had enough control power to trim at landing, it would be sufficient for all other flight regimes. Initially, a NACA 0009 was chosen for the horizontal surface. However, it was found that a reasonable elevator size and deflection could not trim the aircraft at C_{Lmax} . Thus a NACA 2412 was selected to give the necessary down force. Using this airfoil, an elevator having 25% area could trim at landing with a deflection of approximately 25° . An elevator deflection of 1° was necessary to trim at cruise conditions. The horizontal stabilizer was tapered for aesthetic reasons, with a root chord of 8.5" and a tip chord of 5.9".
- Vertical Stabilizer: Using historical data a vertical tail volume of 0.09 was chosen. A NACA 0009 airfoil was selected due to its relatively thin thickness. As done for the elevator, the rudder had to be determined to make sure the vertical tail was large enough. Assuming a 7.5 mph cross-wind component, the rudder was sized and found to be an appropriate percentage of the vertical tail. Therefore, the vertical stabilizer did not need to be increased in size. The rudder spans the entire surface and is 30% of the root chord. The vertical stabilizer was swept for aesthetic reasons.

Control Surface Sizes

- Rudder: The rudder was sized to provide adequate yaw control of the airplane. An analysis spreadsheet was developed to determine the necessary size of the rudder to maintain yaw stability in a high crosswind landing. This spreadsheet calculated the weathercock stability coefficient for the aircraft and the maximum sideslip angle. It then determined the necessary rudder deflection to trim the aircraft at a given rudder size. The optimal size was found to be 30 percent of the vertical tail area, or 18.6 square inches. At this size, the rudder deflection required to trim during landing at a maximum pure crosswind of 7.5 mph is 25 degrees, which allows for a slight factor of safety.
- Elevator: Using the procedure developed in the horizontal stabilizer sizing portion, a reasonable elevator size was chosen. An elevator having 25% chord and a maximum deflection of 25° was sufficient to trim the aircraft during the worst case scenario of landing.

- Flaperons:** The flaperon size needs to maximize the efficiency of the wing for takeoff. At this maximum efficiency, it must be able to produce enough lift for takeoff with minimal wind. The flaperons span the entire length of the wing to maximize lift. Several different flapped SD7062 drag polars were investigated. The comparisons are presented in Figure 4.5. It was found that a flap that is 10% of the chord, and flapped 20 degrees produced the optimal lift coefficient. But this flap was not chosen due to concerns with the flex of the skin hinge. Therefore, a flaperon with 15% chord, and 20° deflection was chosen. Flaperons can also be deployed in a way to increase drag, which could be an added benefit when trying to slow the plane down on its decent.

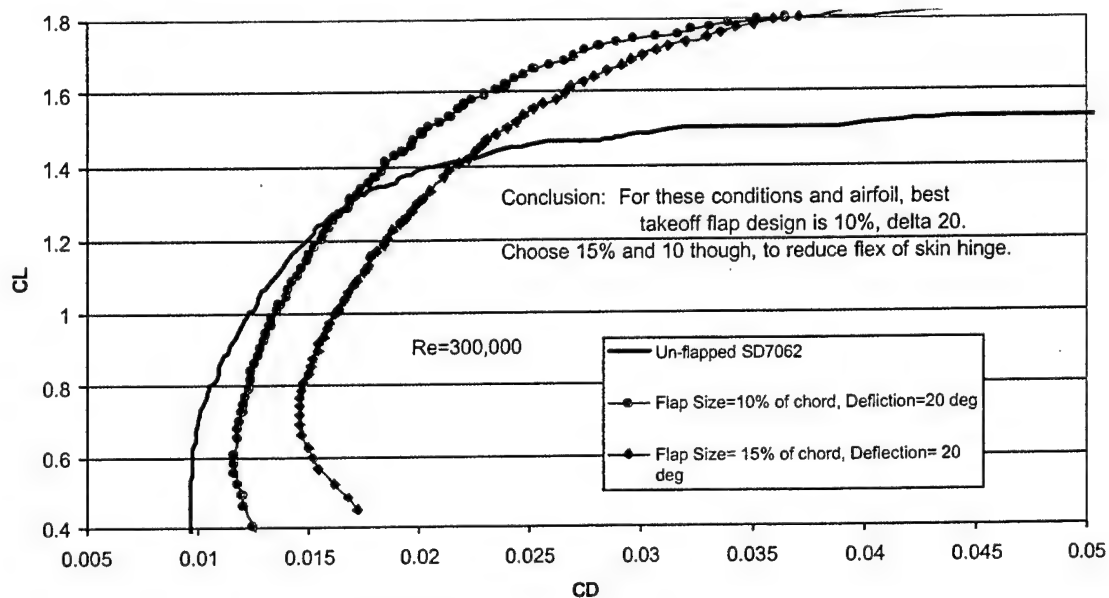


Figure 4.5: Flap Size Determination

Wing and Power Loading

The wing loading for the preliminary configuration was approximately 0.34 oz./in² and the power loading was approximately 52 W/lb. The two loading values were a compromise to achieve the correct mission balance. Higher wing loading allowed the plane to penetrate through the wind better, achieve higher cruise velocities, and be less susceptible to gusty conditions because greater changes in pressure differential are required to disturb the plane. However, high wing loadings are less stable at low speeds. To overcome the wing loading disadvantage, a higher power loading was needed to help overcome takeoff and climb requirements.

4.4.2 Structures Analysis

Finite Element Analysis was used to find stress concentration in major components. The results were then used to determine placement of internal components.

Fuselage

The fuselage was modeled using a Pro/Mechanica finite element analysis. This analysis revealed the areas of the fuselage that would need reinforcement by predicting the overall load distribution. The fuselage was modeled under two load sets: a landing impact of four times normal gravity and a turn that generates four times normal gravity. For the static loading set, the fuselage was fixed at the panel where the gear attaches to the fuselage and at the tail dragger wheel attachment. The loads were then applied to the internal surface of the fuselage at four times their actual weight in order to get a ballpark figure of the stress concentration maximums. Two idealizations were made in order for the analysis to run: the filleted edges were removed to simplifying the geometry and the inner and outer skins were modified into a single shell at the midpoints. These simplifications made it possible to run the simulations and generate the visual distributions in a matter of minutes instead of hours. With a maximum local value of 190 kpsi the most likely place for the fuselage to fail is at the thin tail section in buckling. This visual output of stress and strain concentrations enabled some preliminary decisions to be made about the placement of internal structure. It was apparent that bulkheads were necessary to maintain the structural integrity at the main gear bow connection, aft of the payload holding tank, and at the thin section of the tail.

Wing/Empennage

PRO/Mechanica was also utilized for a finite element analysis of the wing structure. The wing was constrained at the root as a cantilevered beam. Figure 14 illustrates the analysis. Note the dramatic deflections at the wingtip and relatively small values for maximum principal stress. This can be attributed to the strength of the tubular carbon spar. The local high stress region at the wing root indicates that it would fail in the first mode of Euler buckling at that region. A further buckling analysis found the buckling load factor of approximately 1.5, meaning that a load 1.5 times greater than the analysis loading would be required to buckle the wing. The empennage was not modeled as a load carrying member, because it would never see any structural loading. It was assumed that the skin strength would be sufficient with the addition of shear webs to provide the stiffness required to maintain the proper shape.

Landing Gear

It was desired that the main landing gear have a slight airfoil shape to minimize drag. A flat section in the landing gear was required to bend an airfoil shaped core around a corner. The main gear would then have relatively sharp angles compared to a true bow type.

Once a composite sandwich structure was decided on, several material test pieces were constructed to determine the optimum lay up. Initially, two samples were constructed for destructive testing. Each test piece was 14" long and approximately 2" wide. Piece 1 used a 1/8" balsa core and 3 ounce fiberglass with a laminate lay-up of [45, mono-carbon filament tape, 0, 45, 0₄]_s. Piece 2 used a 3/16" core and 3 ounce fiberglass lay-up of [45, mono-carbon filament tape, 0, 45, 0₂]_s. The mono-carbon filament tape was placed near the outside of the lay-up to increase the stiffness of the pieces. Both test pieces

were sanded to a tapered point with a rounded leading edge to approximate an airfoil shape, reducing drag as much as possible.

Both samples were tested in the same manner. One end was rigidly attached to a table, and weights were added at a moment arm of ten inches until the piece failed. From this test, the maximum bending moment and the maximum bending stress were found. The deflection was also measured during the tests to determine if the flex in the landing gear would cause the propeller to hit the ground.

The test piece with the thicker core held more weight and deflected less per pound. The strength of the gear can be increased while decreasing the number of layers by increasing the core thickness. The use of a thicker core to increase strength was important so that the overall weight could be reduced. The most critical part of the landing gear was the elbows due to their high stress concentrations. Two molds were built with an elbow to test how the test pieces react to applied loads. The first test used 1/8" balsa wood core covered with 6 layers of 6-ounce fiberglass. Fiberglass de-lamination occurred at the corner so quantitative data was obtained. The desired amount of stiffness was not produced with this lay-up. The second test used a different lay-up scheme but produced similar results. From these early failures, it was decided that a true bow landing gear mold will be used with a large corner radius, in order to reduce the stress concentrations in the corner.

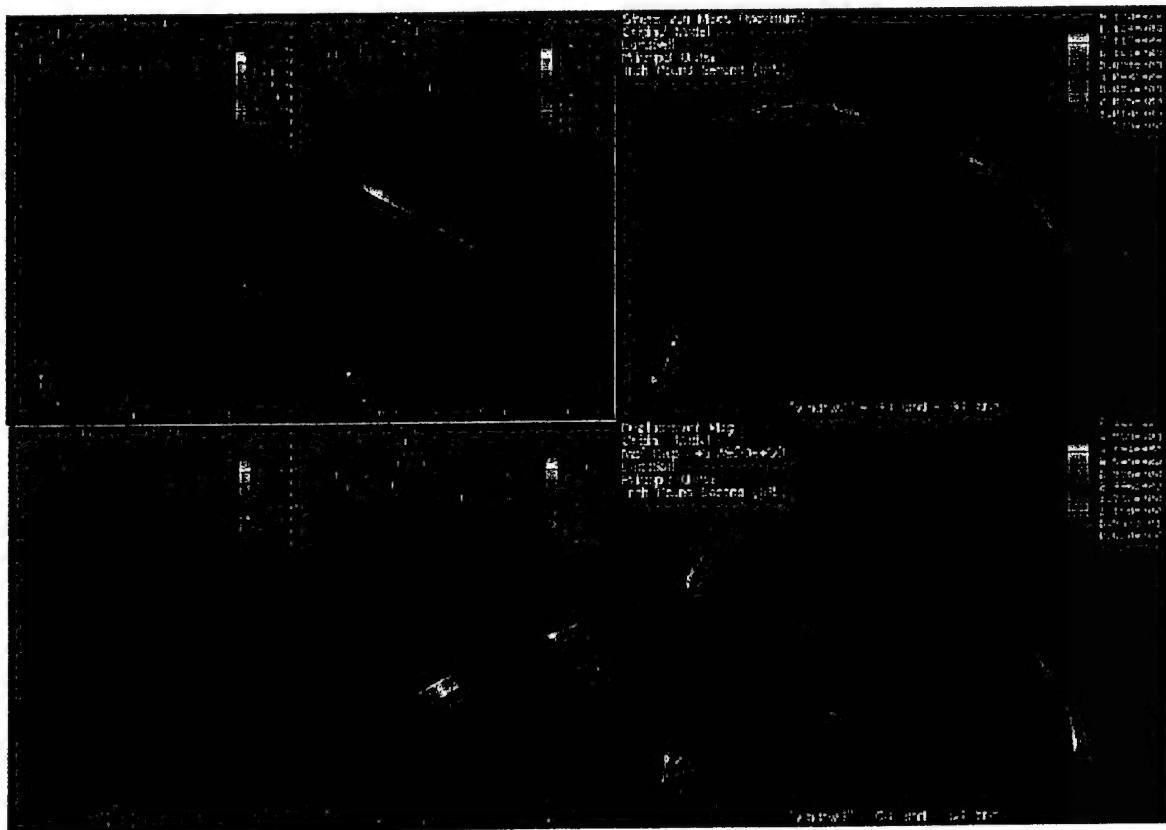


Figure 4.6: Stress and Deflection of Major Structural Components as Predicted by FEA

4.4.3 Payload System Analysis

The payload system required a baffled tank that would carry exactly 4 liters of water and prevent water shifting. The retractable boom was designed to give the best head pressure without causing excess drag of the plane. The boom must ensure no water leaks while retracted. The boom must also be designed to be easily and repeatedly lowered. All these component must be designed in a limited amount of space to allow the fuselage to remain as streamlined as possible.

Tank Sizing

The shape and method of fabrication of the tank was determined. Using the maximum height and width of the inside of the fuselage, an approximate length for the tank was calculated by using a volume slightly greater than four liters. This length along with the maximum fuselage height and width were used to construct a three-dimensional tank in Pro/Engineer. Using Pro/Engineer, the tank was cut and shaped smoothly to fit the inside the fuselage while allowing room for other internal components. The bottom of the tank was change to form a sump to ensure no water could be trapped in the tank. The aft portion of the bottom of the tank was cut to the shape of the boom so that the boom could be flush with the plane. Another design consideration for the tank was the hole through the middle, which allowed the wing's spar to pass through. The tanks final volume was maintained slightly above 4 liters to leave room for baffling.

Baffling

Baffling in the tank was a necessity. Without proper baffling the plane would be uncontrollable. If the water in the tank is free to shift the CG of the plane could change drastically, causing catastrophic results during flight. Listed below are the superior configurations to control the water in the tank.

- Vertical Separation Baffles: Vertical separation baffles were the first solution investigated. They are baffles which only allow travel vertically between parallel horizontal baffles, effectively forming separate compartments. Several orientations of these compartments were investigated, but they generally lacked the desired characteristics, in sloshing or in static settling.
- Horizontal Separation Baffles: Horizontal separation baffles were experimented with, much like those found in an automotive fuel tank. These baffles are usually vertical plates which minimize momentum transfer from compartment to compartment in the tank. Good dynamic movement characteristics are provided, but static shifting characteristics are deficient. Some additional modifications were examined which would assist in the reduction of static shifting, such as one way gates in each baffle allowing static shift toward the plane CG.
- Full Structure Baffles: Several full structure baffles we examined as well, such as a constructed straw box and a honeycomb tank insert. Both tests provided excellent dynamic movement damping, but retained a large amount of water after payload evacuation, due to the baffle's large surface area.

The following FOMs were used to reach a final decision, which is presented by the weight decision matrix in Table 4.2.

- Static Movement: Static movement of the payload is the most serious issue that has to be dealt with in the design. With the small size of the entire aircraft, and the majority of the weight being payload, a shift aft of the payload C.G. of an inch or more could render the aircraft neutrally stable or unstable, and effectively leave the control surfaces useless, resulting in a crash. Also, a neutrally stable aircraft lends itself to pilot induced oscillations (PIO), in which some environmental change or control adjustment sets off an oscillation which cannot be recovered from.
- Dynamic Movement: Dynamic movement of the payload is also a major concern for the design. If the plane has no dynamic damping of the payload movement could trigger a catastrophic PIO.
- Water Retention: The structure must allow for complete payload drainage in order to prevent a penalty to the score. Minimizing surface area not only reduces water retention, but increases the evacuation speed.
- Weight: Weight of this structure must be low for the best score possible.

Figures of Merit	Weighting Factor	Vertical	Full Structure	Horizontal (modified)
Static Shift	0.4	1	2	2
Dynamic Shift	0.2	1	3	3
Water Retention	0.2	3	1	3
Weight	0.2	3	1	3
Total	1	1.8	1.8	2.6

Table 4.2: Baffle System Evaluation

Table 4.2 demonstrates the superior characteristics of the horizontal baffling method. The method of modifying the baffles with one way gates allows for the best payload control. Numerous tests will be performed to produce the optimum baffle and gate sizes and placements. These tests will also ensure no water will be trapped in the tank.

Boom Length

Although the boom is by far the best method for releasing the water, definite challenges that must be considered. The boom must be long enough to provide the necessary head pressure while not creating too much drag.

The tubing that ran from the tank to the end of the nozzle was surgical grade tubing. Surgical tubing provided excellent weight and durability characteristics. The tube diameter from the tank to the end of the boom was 0.75 inches. This allowed for the water to reach the end of the boom faster than smaller tube diameters. The boom was shaped as streamlined as possible around the tube to reduce as much drag as possible. At the end of the boom a 0.5 inch nozzle funneled the water out. A minor pressure drop

from the windward side of the boom to the trailing edge of the boom was utilized by putting the nozzle closer to the trailing edge of the boom and facing it slightly aft.

In order to size the length of the boom a spreadsheet using Bernoulli's equation was created, which calculated drain time. The drain time for 4 liters of water was graphed versus the boom lengths. Optimal drain times are achieved at boom lengths from 16 to 18 inches.

Boom Deployment and Retraction Methods

In order to reliably deploy and retract the boom, a tight-fitting, lightweight method was desired. Initially, the boom was to be mounted onto a ball-type valve to allow for the boom to be deployed by the turning of the valve, simultaneously dropping the boom and starting the payload release. This idea was discarded after some tests were made, which found these valves to be bulky and hard to integrate into the fuselage configuration. The other alternative was a pinch-type valve, relying on passive actuation. When the boom is in the stowed position, the hose is pinched, and forced closed. When the boom is deployed, the pinch-arm is rotated off of the tubing, allowing flow through the boom. The boom is deployed by a hinged arm assembly, attached at the midpoint of the boom. This placement reduces the amount of torque required to extend the boom down by giving a greater mechanical advantage. A test apparatus was built to model the fuselage, and several tests were performed to ensure that the design was reliable. Once satisfactory results were obtained, the construction began with the Bernoulli's calculations from the previous section serving as a basis for component sizing.

4.4.4 Propulsion Group

Once analytical testing with the optimization program was completed during the preliminary design phase, live static testing began. The parameters tested included the gearbox, battery cell count and configuration, and propeller dimensions. Actual performance characteristics provided the most realistic method for optimization of the propulsion system. These tests determined the capacity of the batteries, motor efficiency, thrust, and speed. Temperature was monitored during these tests to determine thermal effects on the system performance.

The final propulsion system was tested using a modified dynamometer. Thrust was calculated using a rope and pulley system, weights, and a Detecto AP-4K 4000 g scale. Current, voltage, and power was recorded at different intervals using an Astro Model 101 Super Whatt Meter.

Performance characteristic curves were created from an optimal configuration. Figure 4.8 shows the voltage, current, thrust output, and revolutions per second versus time for a Graupner 3300-6 with a 20" propeller, gear ratio of 1.72, and 16 CP 1300 battery cells ran at half throttle.

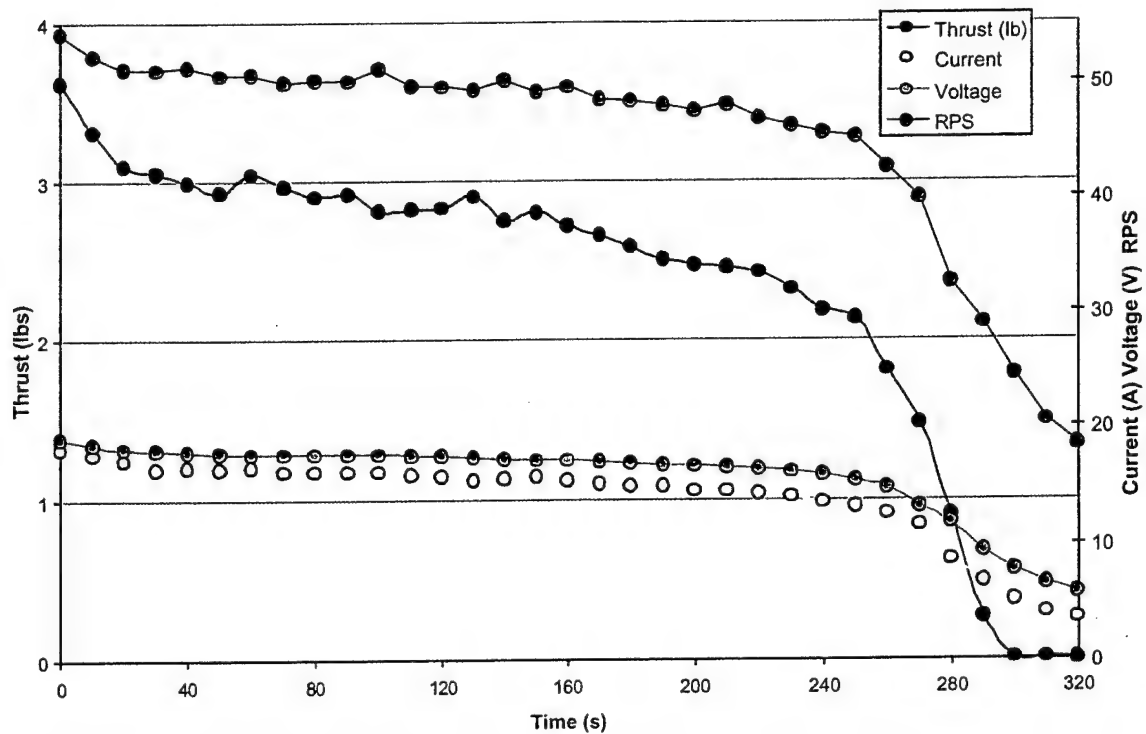


Figure 4.8: Motor/Battery Performance Curve for Graupner 3300-6, 20" Prop., 1.72 gear ratio, and 16 CP 1300 Cells at Half Throttle.

The endurance/performance test shown in Figure 4.8 provides several pieces of information. By integrating the area under the current curve for one battery cycle the total charge in the batteries can be determined. Also the actual internal resistance of the motor can be determined from the no-load voltage of the battery pack and the current pulled.

4.5 Final Aircraft and Predicted performance

At the end of the preliminary phase the optimal ranges for each aircraft component were compiled and compared against one another until a final, optimal configuration was determined. With the final aircraft configuration decided, the predicted performance can be determined. A complete aerodynamic analysis was performed, including a mission simulation, aerodynamic coefficients and derivatives, and static and dynamic stability.

4.5.1 Aircraft Configuration

The final configuration is a conventional aircraft with a mid mounted wing. The fuselage has been streamlined around the interior components creating a low-drag body. The wing was designed with a span of 79.2 inches, a chord of 10.1 inches, and an aspect ratio of 7.8. The wings can vary 17.6 degrees

before scraping the runway. The flaperons extend across the full length of the wing span and occupy 15 percent of the chord.

The tail is of a conventional configuration. The horizontal tail was sized with span of 19.2 inches and a taper ratio of 0.7, keeping it within one quarter the wing span. The vertical tail area was sized to approximately 50 square inches. The rudder and elevator are both sized at 30 percent of the vertical and horizontal tail, respectively. The final propulsion system was a Graupner 3300-6 utilizing 16 CP1300SCR battery cells. For the FBM, an APC 20x13E propeller was chosen.

4.5.2 Predicted Performance

The mission performance of the final aircraft was estimated from the performance code used during optimization. The mission was broken into separate stages for analysis. The results of this analysis can be seen below in Table 4.3.

Mission Components	Time (sec.)	Distance (ft.)	Velocity (ft/sec)
Takeoff (loaded)	5.56	143	41.9
Climb (loaded)	7.3	400	60.47
First Turn (loaded)	10.7	162	Acceleration
Acceleration Leg (loaded)	9.25	674	Acceleration
360 turn (partially loaded)	12.7	0	Acceleration
Cruise Leg (un-loaded)	8.66	326	75
Final Turn (un-loaded)	2	162	Deceleration
Deceleration & landing (un-loaded)	4.56	457	Decelerate to 25.46
Ground time for loading	15	0	-
Total time	75.73	-	-

Table 4.3: Time Spent for One Lap During the FBM, Based on 10 mph Head Wind

From Table 4.3, it can be seen that the takeoff distance was 143 feet going into a 10 mph head wind with no flap deflection. To maintain climb velocity, the plane must accelerate to 60.47 fps. The cruise speed was 75 fps. With all the segment times summed, the total time for one lap is 75.73 seconds. This produces a total FBM time of 136.46 seconds or approximately 2 minutes 16 seconds.

4.5.3 Aerodynamic Coefficients and Stability and Control Derivatives

Table 4.4 provides a listing of all the relevant stability and control derivatives for the cruising portion of the mission. Methods employed for this analysis were taken from Nelson (1998).

$C_{L,\alpha}$	5.12	$C_{m,\delta e}$	-0.89	$C_{n,r}$	-0.066
$C_{X,\alpha}$	0.178	$C_{y,\beta}$	-0.277	$C_{l,r}$	0.059
$C_{m,\alpha}$	-1.35	$C_{n,\beta}$	0.0948	$C_{l,\delta a}$	0.368
$C_{Z,\dot{\alpha}}$	-1.37	$C_{l,\beta}$	0	$C_{n,\delta a}$	-0.024
$C_{m,\dot{\alpha}}$	-3.88	$C_{y,p}$	0	$C_{y,\delta e}$	0.147
$C_{Z,q}$	-3.56	$C_{n,p}$	-0.0342	$C_{n,\delta r}$	-0.049
$C_{m,q}$	-10.07	$C_{l,p}$	-0.853	$C_{l,\delta r}$	0.0072
$C_{Z,\delta e}$	-3.14	$C_{y,r}$	-0.183		

Table 4.4: Stability Derivatives for Cruise (per radian)

The change in position of the water in the tank affects the overall center of gravity of the plane, altering the handling qualities. A computer modeling analysis was used to calculate the worst case movement forward and aft of the initial center of gravity location. Results of this analysis showed that the payload center of gravity shift caused the overall aircraft CG to move 4.78% (in percentage of the wing chord) forward and 10.38% aft of its initial point. Figure 4.9 presents the CG shift graphically. Such shifts are within the capabilities of elevator control as the static margin is never reduced below 9.3%. These shifts also demonstrated the need for tank baffles and valves to help control the static and dynamic shift of the water payload.

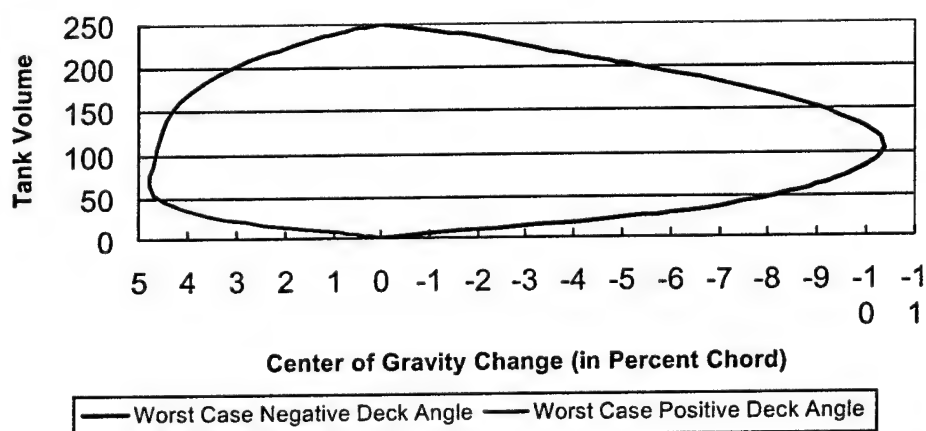


Figure 4.9: Coefficient of Moment Due to Elevator Deflection Versus Alpha and Moment Contributions of Aircraft Components

5.0 Detail Design

The goal of detail design is to finalize the aircraft design and design the methods of construction based on the results from the preliminary phase. Strength and stability requirements were determined and met, while reducing aircraft weight and drag. The final optimization was performed by detailed analysis and design of the plane's aerodynamics, power plant, and structure.

5.1 Component Selection and System Architecture

Table 5.1 presents the final aircraft geometry, weight, systems, and performance configurations.

Geometry	Value	Performance Data	Value
Center of Gravity Location	12 in	C_L max	1.5
Fuselage		L/D max	7.5
Length, (in)	48	Gross Weight Conditions	
Width, (in)	8	Maximum Climb Rate, (fps)	7.5
Height (in)	4	Stall Speed, (fps)	24.3
Wing		Maximum Speed, (fps)	71.65
Airfoil	SD 7062	Take-off Field Length, (ft)	110.2
Span, (in)	79.2	Empty Weight Conditions	
Area, (ft ²)	5.56	Maximum Climb Rate, (fps)	16.5
Aspect Ratio	7.83	Stall Speed, (fps)	16.9
Incidence Angle, (deg.)	0	Maximum Speed, (fps)	80.1
Flaperon Area Per Wing, (in ²)	72	Take-off Field Length, (ft)	76.7
Horizontal Stabilizer		Weight Statement	Value
Airfoil	NACA 2408	Payload, (lb)	8.8
Span, (in)	19.2	Manufacturer's Empty Weight (MEW), (lb)	9
Chord at root, (in)	8.43	Gross Weight, (lb)	17.8
Chord at tip, (in)	5.9	Systems	Details
Volume, (in ³)	0.59	Motor	Graupner 3300-6
Incidence Angle, (deg.)	0	Battery Configuration	16 X CP-1300 SCR
Elevator Area, (in ²)	34.4	Gear Box	MEC Superbox
Vertical Stabilizer		Gear Ratio	1.72:1
Airfoil	NACA 0009	Speed Controller	Astro Flight Model 204
Span, (in)	8.75	Propellor (FBM-nominal)	APC 20x13E
Chord at root, (in)	11.5	Propellor (FM-nominal)	APC 16x12E
Chord at tip, (in)	5.75	Radio	Futaba T8UAP
Volume (in ³)	0.04	Receiver	Futaba FP-R14-8DP
Rudder Area, (in ²)	18.64	Servos	JR DS3421 Premium Digital Servo: Mini

Table 5.1: Final Aircraft Configurations

5.1.1 Propulsion System

The final propulsion configuration can be viewed above in Table 5.1. This configuration required a takeoff thrust of 7.6 pounds and a required power of 684 Watts based the propulsion analysis program. Figure 5.1 below shows a simulated mission profile performed on the dynamometer. The test is based on the power required for each section of the mission profile.

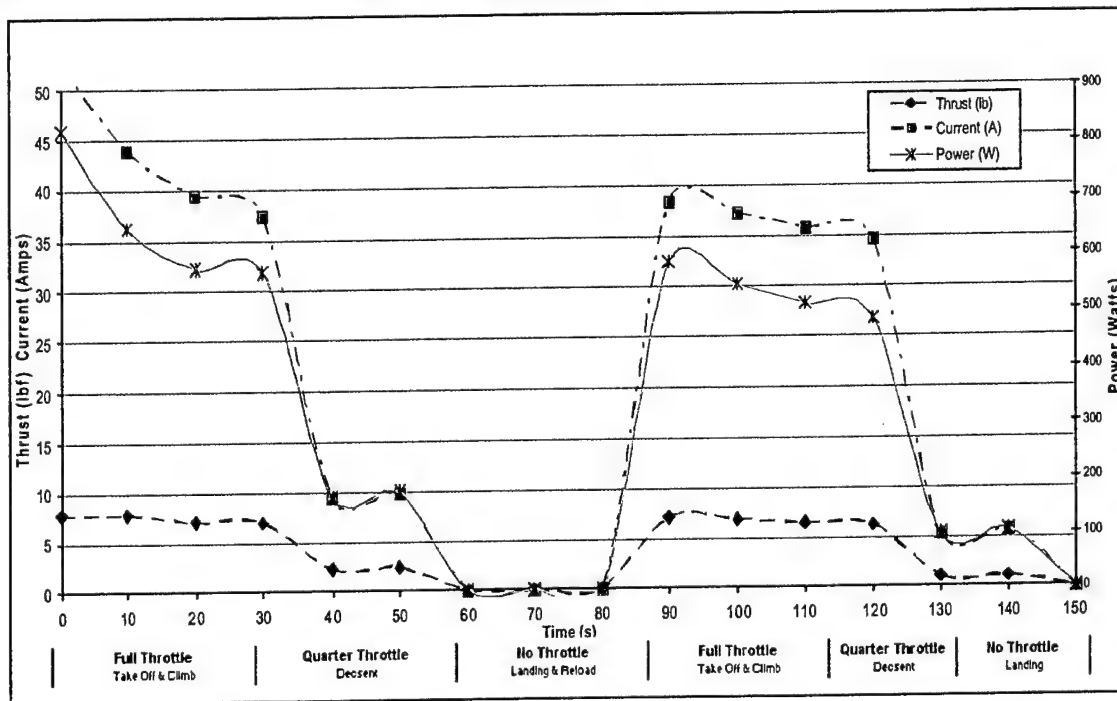


Figure 5.1: Simulated Mission Profile with Thrust, Current, and Power

5.1.2 Structures System

The aircraft's structural design was divided into the following major categories: main wing structure, fuselage, empennage, payload system, and landing gear. The following section will highlight the major components of the aircraft and explain their internal structure. Each of the major components of the structural system can be seen in Figure 5.2.

The internal structure of the wings consists of a standard spar, rib, and shear web configuration. The main spar will be a 0.625" carbon tube 18 inches in length, carrying through the fuselage (including reservoir) and 5 inches into each wing. Ribs will be placed at the root of the wing and at the end of the spar for maximum torsional rigidity. An additional rib will be placed at the end of the wingspan to closeout the wing structure. Shear webs will be placed at approximately 25% and 75% of the chord in order to strengthen the structure in bending. The forward-most shear web will continue the trajectory of the main spar out to the closeout rib. The smaller, aft shear web will enclose the forward edge of the skin-hinged ailerons which run from the middle rib to approximately the close out rib. The aileron servo will be

attached to an intermediate rib in order to place it at the point which will cause the least amount of control surface twist.

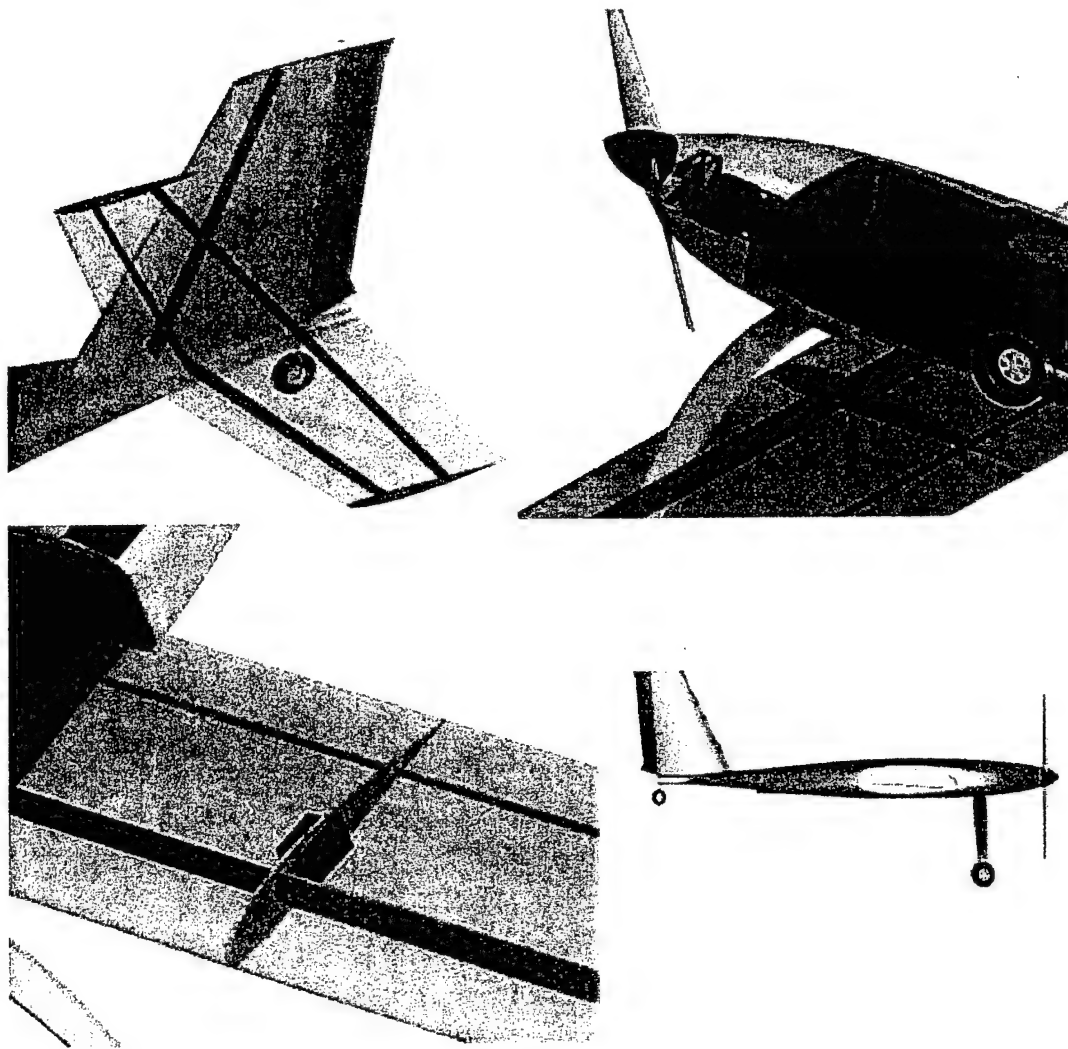


Figure 5.2: Major Structural Structures (Clockwise from Top Left: Empennage, Nose, Wing, and Side View)

Several bulkheads will reinforce the fuselage skins. The nose detail in Figure 5.2 above shows the forward bulkhead. Note that the front reservoir wall is constrained by the bulkhead, allowing the bulkhead to double as structure and a mounting surface. The speed controller is also attached to this bulkhead. Another bulkhead will be used at the rear surface of the tank, coinciding with the trailing edge of the wings, which serves configuration purposes as well as structural purposes. The servo which controls the payload system will be affixed to the aft side of this bulkhead. The final bulkhead will be placed just aft of

the boom opening, protecting the rear internal section of the fuselage. Cutting an opening for the boom in the fuselage dramatically reduces stiffness in that length of the plane. The use of this and the other bulkheads will significantly stiffen the aircraft, and provide torsional rigidity. A firewall bulkhead will also be used to affix the propulsion system at the nose of the plane, but this contributes minimally to the overall stiffness and torsional rigidity of the aircraft.

The empennage structure, Figure 5.2, is similar to that of the other airfoil components of the aircraft. Ribs will be used at the root and closeout of each tail (with the exception of the vertical tail). Two shear webs will be used in each of the components. The vertical tail will also feature a shear web at quarter chord. The elevators and the ailerons will be skin hinged, again using the rear shear web to close the section. The rudder will be hinged on an aluminum torque rod, which will also control the tail dragger wheel.

The landing gear will be constructed via vacuum forming a composite sandwich structure to a tooled mold. The final dimensions of the landing gear are 22" wide at the wheelbase, with a 4" radius in each corner of the bow to reduce stress concentrations and produce a natural shock absorbing effect. The composite sandwich lay-up will consist of 6 layers of 3 ounce fiberglass on each side of a 1/8" balsa core, shaped to a symmetric airfoil. The glass orientations on each side of the core will be [0,Carbon tape,0,45,0,45,0]_s. The carbon tape provides additional stiffness with minimal weight addition.

5.1.4 Payload System

A diagram of the payload mechanism can be seen below in the drawing package. The payload mechanism centers on a pinch-type valve. A length of surgical tubing will be pinched between a small, L-shaped aluminum plate (0.050" thick) and a strengthened, elongated portion of the boom. The plate is affixed to two small balsa support blocks mounted on the lower internal skin of the fuselage. These same blocks support a 0.125" aluminum pin on which the boom will pivot. The mechanism will be actuated by a single rearward servo, which will connect to the boom using a simple two-rod linkage. Because the boom pivots more than 90 degrees for stowing purposes, a good seal in the tubing can be assured.

The reservoir is a softened rectangular tank, approximately 13.75" in length by 7.75" in width by 3" in height. The tank was shaped to conform exactly to the interior volume of the fuselage, with the exception of the recess where the boom retracts. The tank is 250 cubic inches in volume, which contains exactly 4 liters of payload and the volume of the incorporated baffling system. The baffling system will consist of 2 baffles which will completely separate the tank into 3 compartments. Each baffle will have a one-way flapper, only allowing payload flow towards the C.G. in the event of flight attitude changes or rough air during payload evacuation.

The ground loading system for the payload consists of a unit that is capable of discharging 2 two liter bottles through two separate nozzles into the reservoir of the aircraft. The system will utilize a pump for each 2 liter bottle to aid in discharging the water. This entire unit will fit into a back pack structure that one member of the ground crew will wear. The water evacuation should take approximately 4 seconds. The

backpack will consist of two 1100 gallon/minute pumps, with a special activation switch and a 12-volt flight pack to power the system.

The final structures concept was the fit-in-box criteria specified by the contest rules. One selection of the drawing package illustrates how the aircraft will be disassembled and fit inside the box. The main wing will be detached, along with the landing gear, propeller and nose cone. The empennage structure will be able to stay intact while inside the box.

5.2 Final RAC Calculation

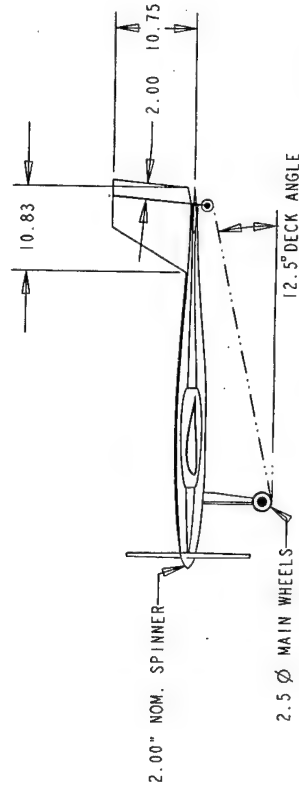
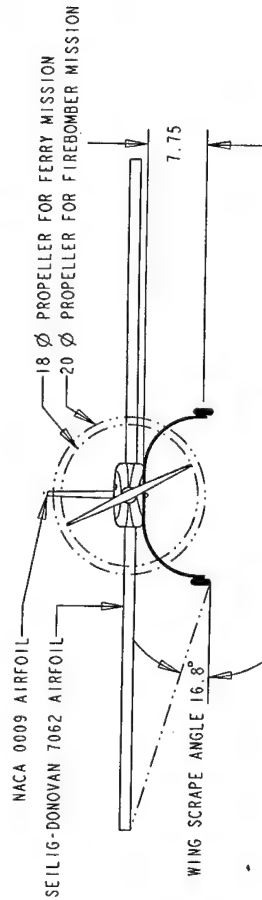
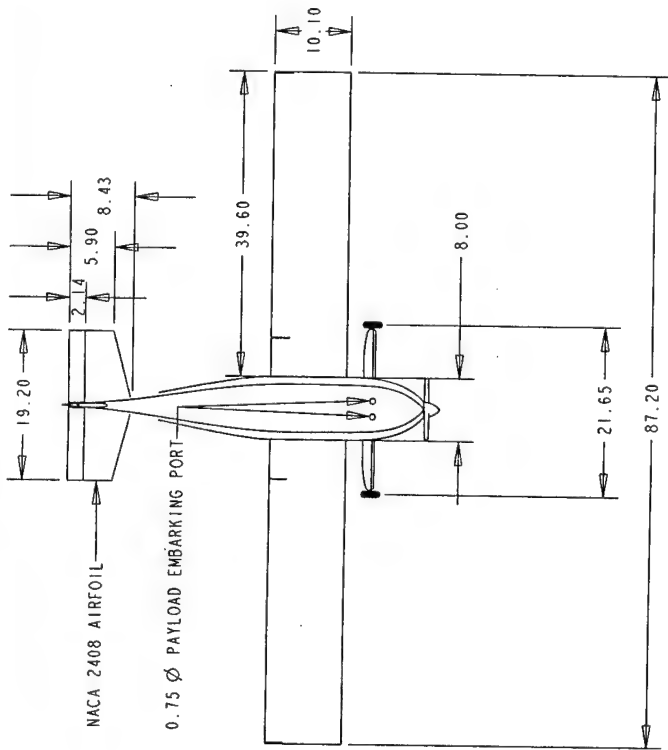
The final predicted RAC of the contest aircraft is presented in Table 5.2.


	Multiplier	Man Hours	Value	Hours	Cost (k\$)
Manufacturers Empty Weight	\$300				
Aircraft Weight			7.5 lbs		2.25
Rated Engine Power	\$1,500				
Battery Weight			1.24 lbs		1.86
Manufacturing Cost	\$20				
Wing Area		10 hrs/ft ²	5.56 ft ²	55.6	
Flaperons		5 hrs	1.5	7.5	
Fuselage		20 hrs/ft ³	0.89 ft ³	17.8	
Vertical Tail		10 hrs/surface	1	10	
Horizontal Tail		10 hrs/surface	1	10	
Servos		5 hrs/servo	5	25	
Total MFHR				125.9	2.52
Total RAC					6.63

Table 5.2: Rated Aircraft Cost for the Final Aircraft Configuration

5.2.2 Drawing Package

The next five pages of the document present the drawing package. Included in this package is a 3-view of the aircraft, component placement, payload system detail, box-fit detail, and an exploded view of all components.



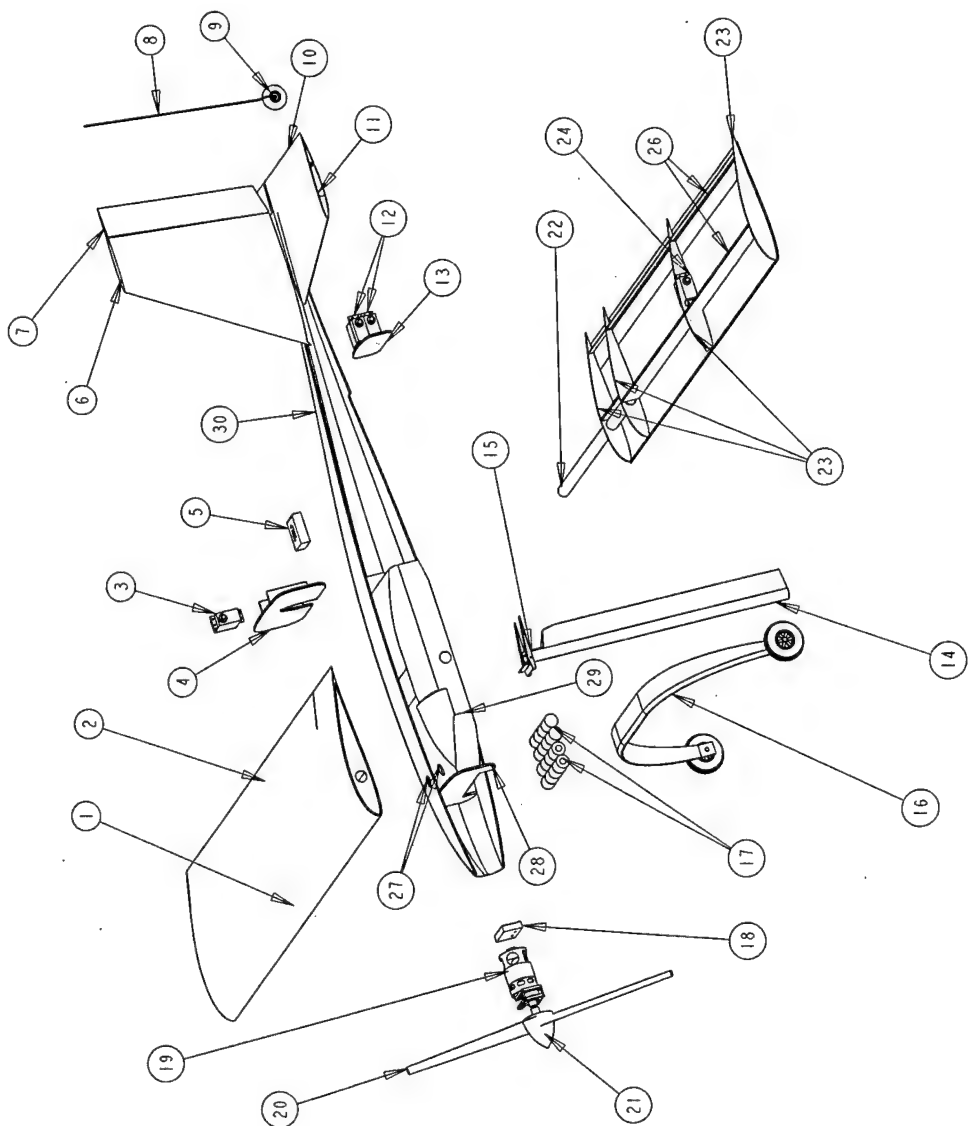
 OKLAHOMA STATE BLACK TEAM 2004	OVERALL DIMENSIONS			
	DIMENSIONS ARE IN INCHES			
	CHIEF ENGINEER	A. SATTRE	FACULTY ADVISOR	DR. A. ARENA
	DRAWN BY	K. TURNER	CONSTRUCTION SUPERVISOR	J. DILL
	SHEET	SCALE	SHEET	
	B	0.0625	1 OF 5	
OKLAHOMA STATE UNIVERSITY MECHANICAL AND AEROSPACE ENGINEERING STILLWATER, OKLAHOMA				

PAYLOAD VALVE DETAIL

PRESSURE PLATE
0.050" AL. SHEET

BOOM SUPPORTS
AL. 6061

PIVOT SHAFT
4-40 THREADED ROD



1: WING ASSEMBLY	KEVLAR REINFORCED
2: SKIN-HINGED FLAP 36" x 2.125"	JRPS342ISA
3: PAYLOAD CONTROL SERVO	0.125" LIGHT-PLY
4: MIDDLE BULKHEAD	NER-6495
5: PCM RECEIVER	
6: VERTICAL STABILIZER	
7: RUDDER	
8: RUDDER / TAILWHEEL CONTROL SHAFT	
9: TAIL WHEEL	
10: SKIN-HINGED ELEVATOR 19.2" x 2.125"	KEVLAR REINFORCED
11: HORIZONTAL STABILIZER CLOSE-OUT RIB	0.125" Balsa
12: EMPENNAGE CONTROL SERVOS	JRPS342ISA
13: REARWARD BULKHEAD	0.125" LIGHT-PLY
14: PAYLOAD EVACUATION BOOM	
15: TANK PINCH-VALVE MECHANISM	
16: MAIN LANDING GEAR ASSEMBLY	2.5" WHEEL
17: PROPULSION BATTERY PACK x2	CP-1300SCR x8
18: MOTOR SPEED CONTROLLER	
19: MOTOR / GEARBOX ASSEMBLY	GRAUPNER 3300-6
20: PROPELLER	
21: 2" NOM. SPINNER	
22: MAIN CARRY-THROUGH SPAR	
23: WING RIB x3	0.125" Balsa
24: CLOSE-OUT RIB	0.125" Balsa
25: FLAPERON CONTROL SERVO	JRPS342ISA
26: WING SHEAR WEB x3	
27: PAYLOAD EMBARKING PORTS	
28: FORWARD BULKHEAD	
29: PAYLOAD RESERVOIR	0.125" LIGHT-PLY
30: MONOCOQUE FUSELAGE	

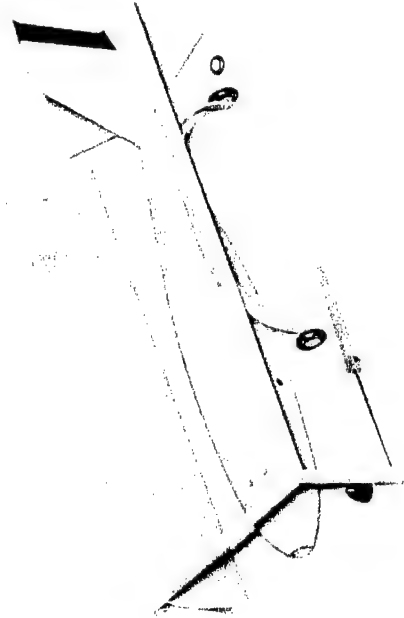
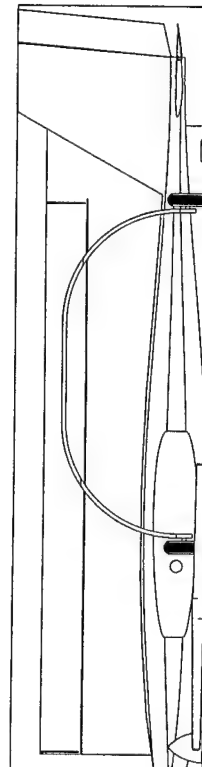
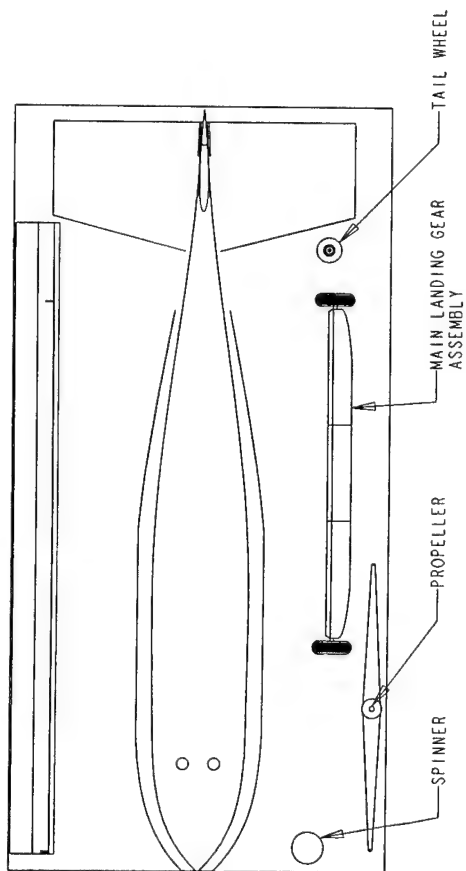
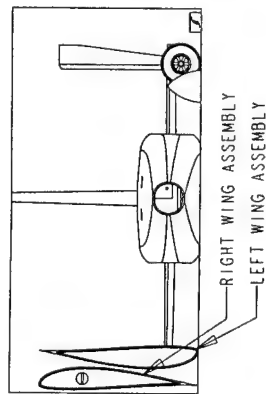



OKLAHOMA STATE
BLACK TEAM 2004

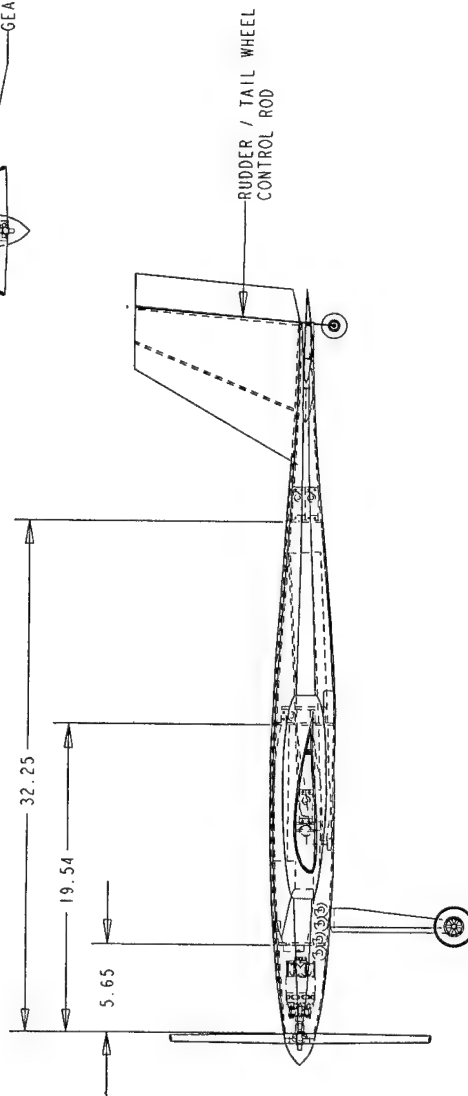
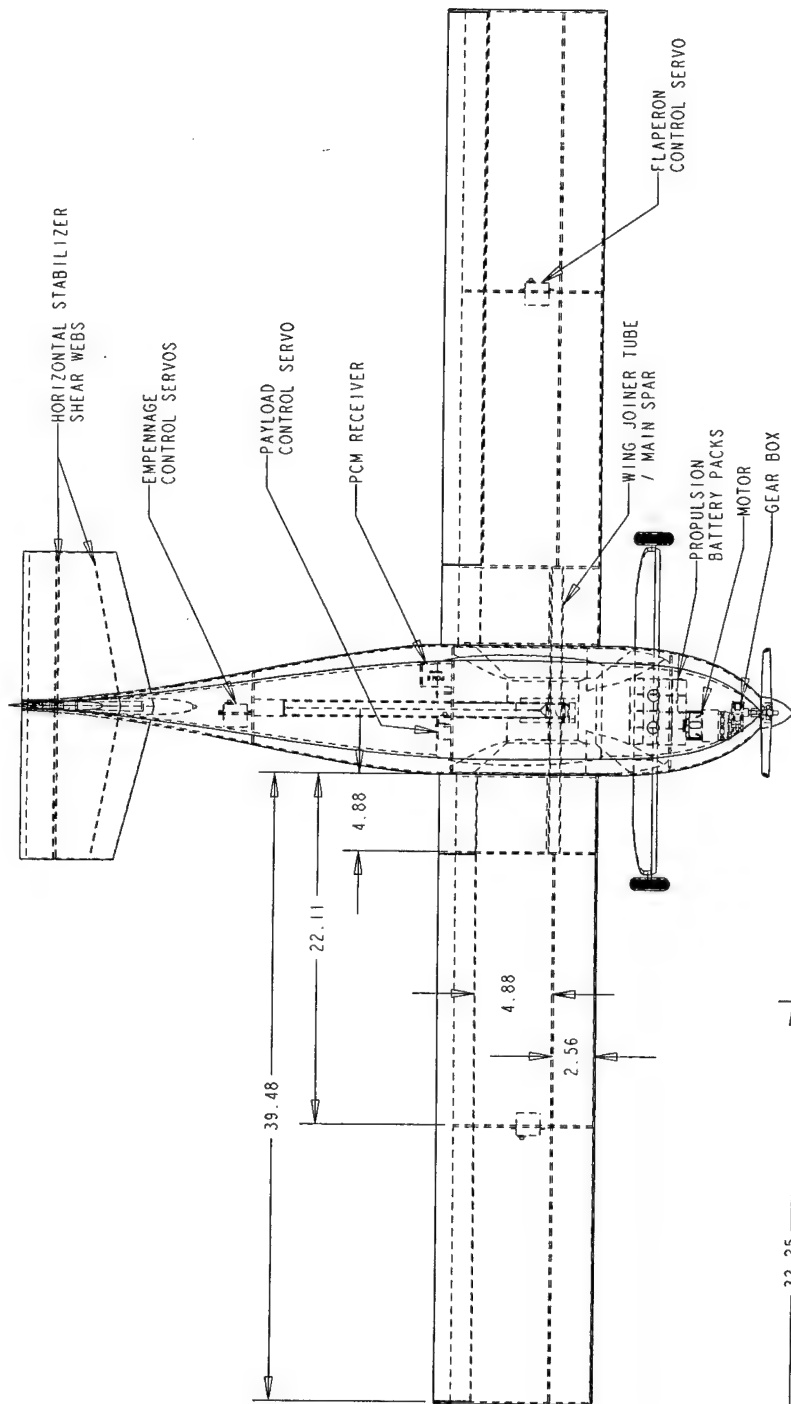
EXPLODED VIEW

CHIEF ENGINEER	A. SATTRE	DIMENSIONS ARE IN INCHES
FACULTY ADVISOR	DR. A. ARENA	
DESIGN BY	K. TURNER	
CONSTRUCTION SUPERVISOR	J. DILL	
SHEET	B	SCALE
	0.125	
		2 OF 5

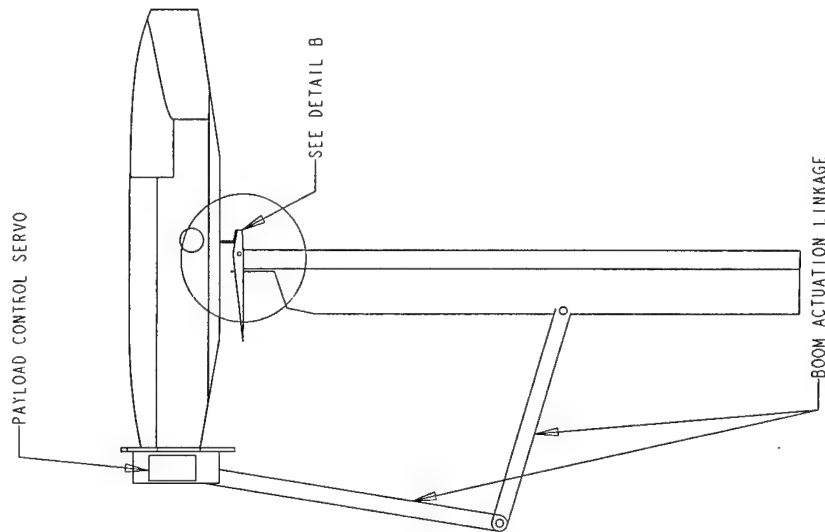
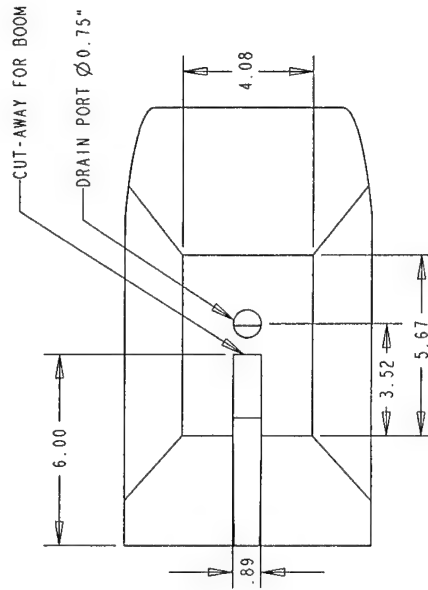
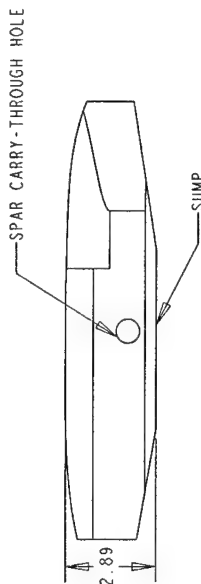
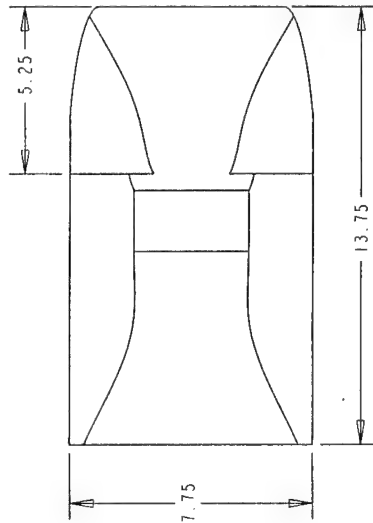
OKLAHOMA STATE UNIVERSITY
DEPARTMENT OF MECHANICAL AND AEROSPACE ENGINEERING
STILLWATER, OKLAHOMA



 OKLAHOMA STATE BLACK TEAM 2004	STOWED CONFIGURATION		
	CHIEF ENGINEER A. SATTRE	DIMENSIONS ARE IN INCHES	
	DESIGNED BY K. TURNER	FACILITY ADVISOR DR. A. ARENA	
		CONSTRUCTION SUPERVISOR J. DILL	
OKLAHOMA STATE UNIVERSITY MECHANICAL AND AEROSPACE ENGINEERING STILLWATER, OKLAHOMA		SHEET B 0.125	3 OF 5

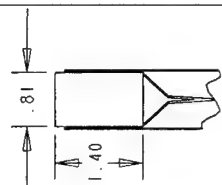


COMPONENT LOCATIONS		DIMENSIONS ARE IN INCHES	
OKLAHOMA STATE UNIVERSITY BLACK TEAM 2004	CHIEF ENGINEER	A. SATTRE	DR. A. ARENA
	CONSTRUCTION SUPERVISOR	K. TURNER	J. DILL
Oklahoma State University School of Mechanical and Aerospace Engineering Stillwater, Oklahoma		SIZE	SHEET
		B	4 OF 5
		SCALE	
		0.125	

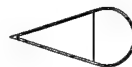


BOOM DETAILS

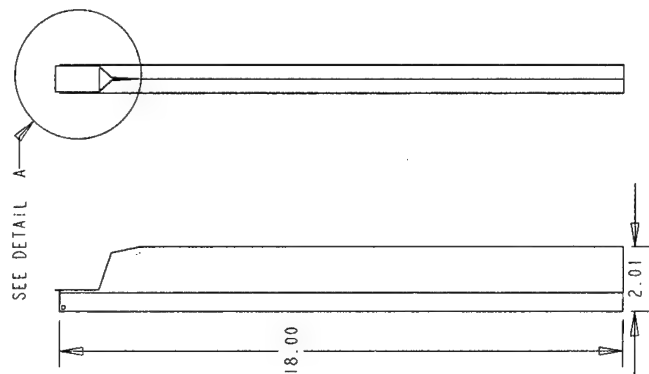
DETAIL A PINCH PLATE



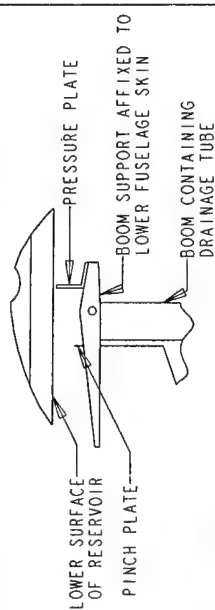
SCALE: 0.500
AERODYNAMIC
PROFILE



SCALE: 0.500



DETAIL B VALVE MECHANISM



SCALE: 0.500

PAYLOAD DETAILS

OKLAHOMA STATE
BLACK TEAM 2004

CHIEF ENGINEER	A. SATTRE	FACULTY ADVISOR	DR. A. ARENA
DRAWN BY	K. TURNER	CONSTRUCTION SUPERVISOR	J. DILL
SIZE	B	SCALE	0.250
SHEET			5 OF 5

OKLAHOMA STATE UNIVERSITY
SCHOOL OF
MECHANICAL AND AEROSPACE ENGINEERING
STILLWATER, OKLAHOMA

6.0 Manufacturing Plan

In this section, manufacturing processes explored and used are discussed. In addition, analytical methods were used to present cost and skill required. A final construction timeline is presented.

6.1 Processes Investigated and FOM Screening Process

As previously discussed, all major structural components will be of monocoque construction. Therefore, only processes available to achieve monocoque construction are considered, and the strengths and weaknesses of each discussed.

- **Lost Foam Mold:** The lost foam method is the easiest of the monocoque methods, because it does not require extensive tooling construction. Once a foam cutout was constructed of each piece, it would be covered in fiberglass, allowed to cure, and then much of the internal foam would be removed. The foam would be removed by cutting tools or by cleaning agents which break down the foam structure, but do not harm the fiberglass. This provides an extremely lightweight structure, but generally lacks the required structural strength unless a significant amount of the foam is left undisturbed.
- **Male Molds:** Building the aircraft components from a series of male molds was one option investigated. To do so, first, an accurate outer image of each part must be constructed and finished to be used as tooling. This requires either skill in woodworking or a reliable way to harden the outer surface of a foam mold that was cut with a CNC foam cutter. The next step would be to lay up the monocoque skins on each side of the mold in either a dry or wet lay-up, cure as necessary, and bond them together. This would provide sufficient strength, but the best surface of the pieces would be on the inside of the structure, requiring finish work on the outside of the aircraft.
- **Female Molds:** Building based off of female molds is the most labor intensive method, frontloading the construction schedule with both of the tasks required of foam filled construction and mold construction. Cutouts must be made of the aircraft components, usually from a CNC foam machine. They must be prepared by coating them with fiberglass then sanding and filling the surface pores as necessary. They are then used to construct female tools by coating them with a thick resin-based coat and a thick lay-up of fiberglass to provide dimensionally stable molds. The advantage to this method is it provides finished parts that have the controlled surface on the outside of the component and, if the mold is correctly made, the part has the desired surface.

The following list presents the figures of merit that are used to create the weighted decision matrix in Table 6.1.

- **Weight:** RAC calculations dictate that any structural design chosen must be lightweight in order to maximize scoring potential. This decision was largely dependent on which method could produce the lightest aircraft structure.

- **Strength:** The strength of the finished part must be sufficient, because once they are bonded it will be difficult to strengthen or stiffen them additionally.
- **Precision:** The outer surface sizing and finish must be on the level of a commercially produced aircraft in order to ensure correct tolerances and reduce drag as much as possible.
- **Repair Process:** The construction method must be either easily repaired or easily repeated, in order to minimize downtime during the flight testing phase.

Figure of Merit	Weighting Factor	Lost Foam	Male Mold	Female Mold
Weight	0.35	3	2	2
Strength	0.25	1	3	3
Precision	0.2	2	2	3
Repair	0.2	2	2	2
Total	1	2.1	2.25	2.45

Table 6.1: Construction Method Weighted Decision Matrix

Using the female molded method of construction will assist in meeting all of the goals of the airplane design. Female molds create a lightweight, strong aircraft which will be easy to repair by creating surplus parts, in addition to having a precise surface. Additionally, it allows the final plane to be constructed quickly. Once the prototype testing is complete, several sets of components can be made for the final plane. Only the best and lightest will be used in competition.

6.2 Component Manufacturing

Detailed descriptions of the process implemented to construct the fuselage, empennage, wing, and landing gear are covered.

6.2.1 Fuselage and Empennage

The fuselage will be constructed of the same skin sandwich panels as the rest of the aircraft. A foam plug of the fuselage was created by first cutting the foam in two dimensions, and then hand sanding to achieve the final shape. After the foam was covered with fiberglass, the horizontal tail was mounted into the correct position on the tail section of the fuselage. This provided several advantages, such as reduction of necessary internal structure, as well as allowing the incidence of the tail to be perfectly fixed in any fuselage piece constructed. The plug was mounted into a parting board cut from plexi-glass, and then coated with a thick gel coating to provide a smooth mold surface. After allowing an appropriate cure time, the gel coat was stiffened with a protective fiberglass shell. This shell also doubled as a parting surface for creating the second mold half. Once the second mold half was created, the parts were allowed to cure for an appropriate time, and then the mold was pulled apart and checked for

imperfections. The mold was dimensionally correct, as well as sufficiently stiff to create a non-warped aircraft part.

After the mold was fully cured, it was seasoned with repeated application of tool wax to allow for the easy release of the finished wing. Each half of the mold was laid-up independently, with one layer of fiberglass against the mold surface, then a core of balsa wood, followed by an internal fiberglass skin to complete the sandwich structure. The internal structure of ribs and spars were then bonded to one of the skins. Next, the final step was to lay a bead of structural epoxy around the edge of one half, then align the pieces perfectly and bolt the molds together for the final bonding process. The vertical empennage surface was created in a separate, smaller mold in order to allow for the rudder to be cut from the molded piece. Once cut, the rudder was hinged by a torque rod to allow for rudder actuation. The torque rod lined up with the tail wheel such that the tail wheel could be actuated simultaneously with the rudder.

6.2.2 Wing

The wing mold was constructed using the same steps as described for the fuselage. Once the mold was complete, a sandwich lay-up of fiberglass and balsa core was used for the skins in order to minimize weight. A balsa core was used to provide the necessary stiffness by increasing the moment of inertia of the material through spreading the two skins farther apart. The weight of the fiberglass used was determined by the loading profile of the wing, which is ideally elliptical. At the highest wing-load regions from the root to the end of the spar, a lay-up of two ounce cloth on each side of a 1/16" balsa core was used. From the end of the spar to 75% of the half span, a lay-up of two ounce cloth on the outside and 1 ounce cloth on the inside was used. From this lay-up to the wing tip, one ounce cloth was used on both sides of the core. A full carry-through 5/8" outer diameter carbon tube was used as the spar of the wing, plugging through the fuselage into each wing at the quarter chord. A nylon bolt was used at 75% chord to hold the wing in place and keep the wing from rotating. Balsa shear webs were used in the span direction to prevent wing deformation. Two ribs were used to anchor the spar with one additional intermediate rib between the spar and the closeout rib. The aileron servo was placed on a mounting rib at half span; this placement was chosen to prevent control surface twisting. All of the internal components were mounted prior to the bonding of the top and bottom wing surfaces.

6.2.3 Landing Gear

The landing gear was constructed using a conventional lay up technique. A male mold was constructed from foam using construction drawings and the CNC foam cutter. This mold was then glassed in order to provide a good surface for part. The landing gear was laid-up according to the strength testing which occurred in the preliminary design phase, which led to an eight layer fiberglass gear piece with mono-carbon fiber tape in the outer layer for additional stiffness. The corner radius on the bow is approximately seven inches. This assembly was laid-up wet and then vacuum bagged to ensure that the part was shaped correctly and minimize de-lamination failure.

6.3 Analytic Methods

Analytic methods were employed to aide in the timely and effective construction of the aircraft. These included cost analysis, required skills matrix, and a construction timeline.

6.3.1 Cost

After choosing a construction method and completing the aircraft design, manufacturing and tooling costs for aircraft construction were determined. Propulsion equipment was found to be the major cost, with tooling and construction materials following closely behind. An itemized breakdown of the final construction cost is shown in Table 6.2.

AIRCRAFT CONSTRUCTION			
ITEM	AMOUNT	UNIT COST	TOTAL COST
Construction			
Foam	5	\$16/Sheet	\$80.00
Tooling/Molded Parts	40	\$20/ft ²	\$800.00
Gear	1	\$20	\$20.00
Flight Control			
Servos	5	\$85	\$425.00
Receiver	1	\$160	\$160.00
Battery	1	\$20	\$20.00
Miscellaneous	N/A	\$50	\$50.00
Propulsion System			
Motor	1	\$385	\$385.00
Batteries	40	\$10/Cell	\$400.00
Speed Controller	1	\$60	\$60.00
Miscellaneous	N/A	\$50	\$50.00
Payload System			
On Board System	1	\$40	\$40.00
Ground System	1	\$125	\$125.00
TOTAL			\$2,615.00

Table 6.2: Estimated Aircraft Manufacturing Cost

6.3.2 Skills

To effectively use structures personnel during aircraft construction, a skills matrix was developed to assign various tasks. This was necessary to ensure personnel had the required competencies to perform a given task, as a poorly constructed component could be detrimental. In the matrix presented in Table 6.3 the columns represent the required skills, while the rows represent the component being constructed. For this matrix, a task requiring little or no skill was given a score of zero, a task requiring moderate skill

was scored one, and a task requiring much skill was scored two. Using the skills matrix, structures personnel were assigned to tasks within their competency.

6.3.3 Schedule

To ensure a timely delivery of the prototype and contest aircraft, a comprehensive construction schedule had to be devised. This schedule, presented in Figure 6.1 was built around predefined milestones and historical time estimates.

	Core Cutting	Fiberglass Layup	Mold/Skin Construction	Control Equipment	Wiring	Modeling
Fuselage/Tail	1	2	2	2	2	2
Wing	1	2	2	2	2	2
Gear	1	1	1	0	0	1
Payload Systems	1	2	2	2	2	2
Propulsion System	0	0	0	1	2	1

Table 6.3: Required Skills Matrix

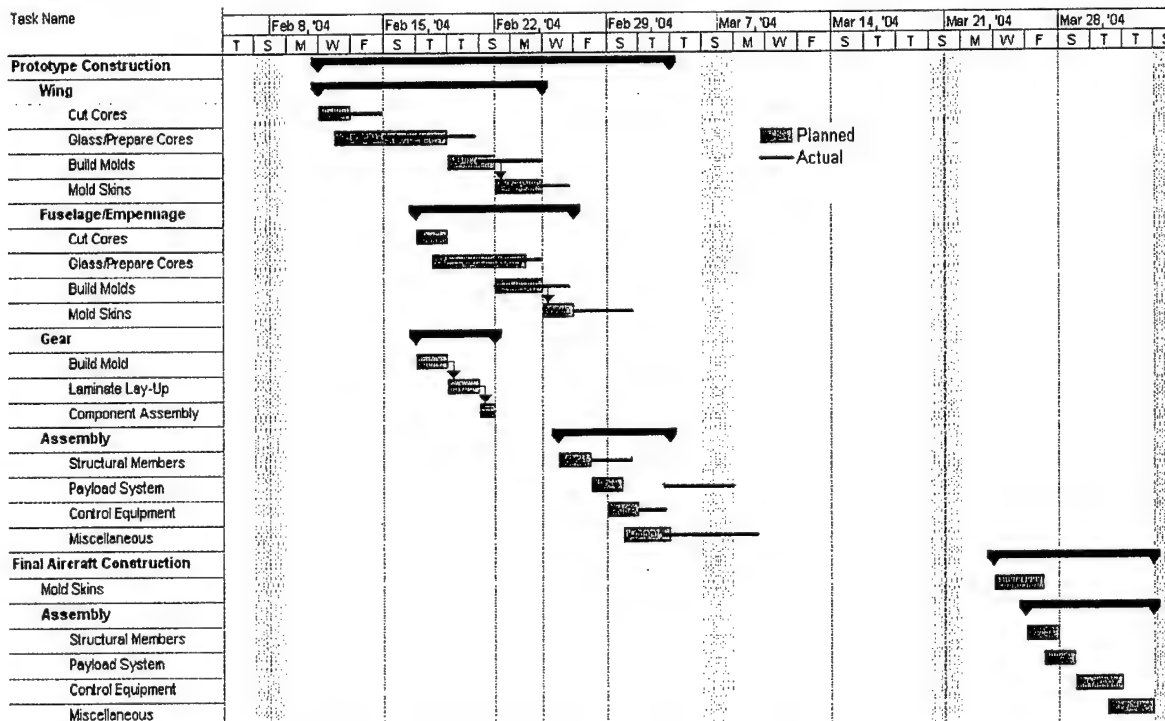


Figure 6.1: Construction Time-line (planned and actual)

7.0 Testing Plan

To validate analytical data and calculations; testing becomes the most important aspect of developing the aircraft's design. New designs can be instantaneously confirmed or invalidated. Due to the importance of testing, a well thought out testing plan must be developed.

7.1 Test Objective and Schedule

Goals were set in order to optimize component design in the payload, propulsion, aircraft structure, and flight testing areas. A detailed schedule was utilized to aide in an effective test procedure. Table 7.1 lists tests preformed, test objectives, and test dates.

Test	Objective	Dates
Payload Stabilization Test	Investigated the effects of dynamic and static movement dampening	1/12 – 2/2
Payload Evacuation Test	Gathered data in order to eject payload as fast as possible	1/12 – 2/16
Motor Test	Collected performance data for motor	1/26 – 2/23
Mold Procedure Test	Allowed for the best construction procedures to be found and practiced	1/12 – 2/9
Wing Structure Test	Determined that wing structure could be undamaged after being lifted by its wingtips	3/22
Final Motor/Battery Test	Optimized the motor and batteries to specific mission requirements	2/23 – 3/3
Ground Crew Test	Optimized for the fastest pit times and allowed the ground crew practice time	3/29 – 4/2
Flight Tests	Fined-tuned aircraft performance and determined usability of stability predictions	3/29 – 4/16

Table 7.1: Test Objectives and Schedule

7.2 Flight Testing Checklists

A thorough and useful execution of flight testing can be accomplished by creating a pre-flight checklist and a flight testing checklist. The pre-flight checklist, seen in Table 7.2 was designed to ensure the plane was airworthy. Structural fatigue or assembly carelessness should be prevented with the use of the pre-flight checklist. The flight test checklist, seen in Table 7.3, was designed to maximize the benefits of flight testing. Specifically in the areas of takeoff, stability and control characteristics, aircraft performance, and competition mission practice.

Ground and takeoff testing will demonstrate aircraft controllability on the ground through rotation velocities and ensure the aircraft will be able to get off the ground in the necessary distance. Different propeller and battery configurations will be tested to ensure the optimal takeoff scenario is reached.

Stability and control characteristics will first be tested with gentle maneuvers in the air. The outcomes of these maneuvers will be a good indication whether or not the analytical data is correct. Next, high speed maneuvers, in addition to stall and tight circle turning, will be used to assess the maneuvering

characteristics of the aircraft. These characteristics will be used to fine tune the aircraft's control system. Such things as vertical and horizontal tail volume, control surface sizing, and control surface deflection will be considered.

Pre-Flight Checklist		
Item	Comments	Complete
Weight and Balance (CG)	CG within operational range	
Motor Mount	Mounting screws tightened, firewall secure	
Control Surfaces		
-Linkages Secure	No endplay	
-Proper Deflection	Check trim points and throw distance	
-Hinge Integrity	Pull on hinge, check for tears	
Landing Gear	Bolts/wheels secure, no delaminations on bow	
Payload System		
-Boom Operational	Full range of motion possible	
-No Water Leaks	Valve, vents, and tank seam	
Structure Sound (Tip Test)	Performed at full gross weight	
Radio Range Test (Including Fail Safe)	Collapsed antennae, motor on and off	

Table 7.2: Pre-Flight Checklist (Used Before Each Flight)

Flight Testing			
Item	Date	Comments or Concerns	Results
Taxi/Ground Handling	3/29		
-Aircraft Tracks Straight			
-Sufficient Maneuvering Control			
First Flight (No Payload)	4/1		
-Sufficient Control in all Axes			
-Aircraft in Control Through all Flight Regimes			
-Stall Characteristics Verified			
-Adequate Control at Takeoff and Landing			
-Boom Operational (Adverse Effects)			
Second Flight (Full Gross Weight)	4/2		
-Repeat First Flight Checklist			
-Adverse CG Effects when Payload Expelled			
-All Water Ejected (Nothing Left in Tank)			
Mission Profile Practice	4/5-4/20		
-Takeoff in Less Than 150 Feet			
-Water Dump Time (FBM only)			
-Landing Distance			
-Pit Time			
-Complete Mission Time			
-Overall Aircraft Control			

Table 7.3: Flight Testing Checklist

Aircraft performance testing will determine the approximate details of the flight. Velocities, takeoff distance, and turning radius will be found and compared to the predicted values. Wingspan, propeller selection, and battery pack configurations will be re-optimized in this stage. In addition to aircraft performance, the payload mechanism will be repeatedly tested and fine tuned for reliability.

With the competition plane optimized, practice for both the pilot and ground crew will be done. Handling and piloting skills are to be refined and perfected through multiple mission simulations.

7.3 Testing Results and Lessons Learned

The series of tests conducted proved to be both, vital and beneficial, to the aircraft's design and operation. Test results were used to refine and strengthen all aspects of the design. Table 7.4 presents a synopsis of results and lessons learned from each of the tests carried out.

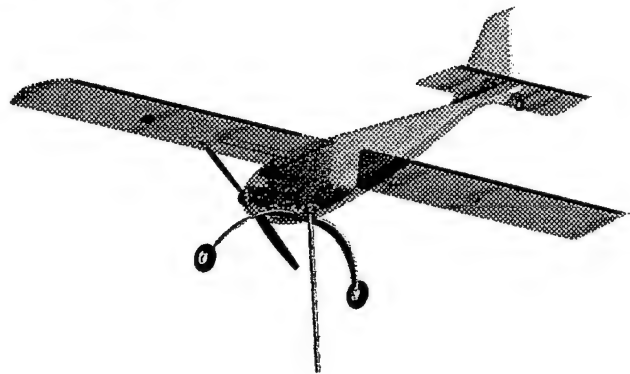
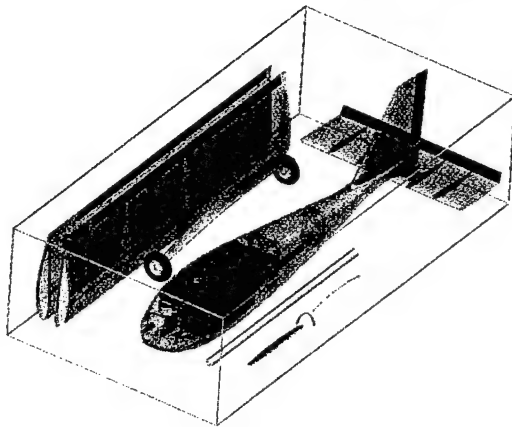
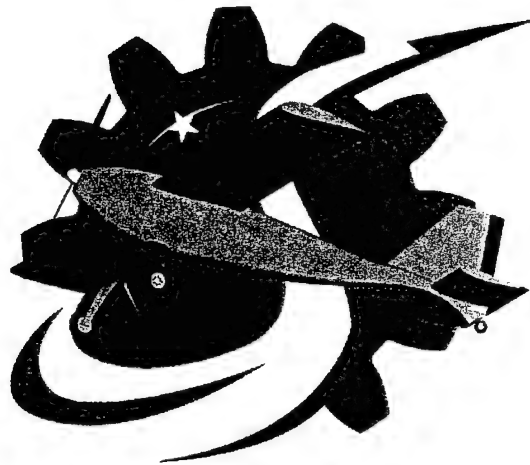
Test	Results and Lessons Learned
Payload Stabilization Test	Baffling greatly reduced dynamic water shift, while one way gates helped reduce the static shift. Payload handling is still a very important design aspect.
Payload Evacuation Test	It was found that it will take approximately 12-15 sec. to expel the water. This should be more than sufficient, no further changes necessary.
Motor Test	Graupner motor at least 20% more efficient than Astro throughout flight regime. 16 battery cells more than sufficient to complete FBM and FM.
Mold Procedure Test	Test molds allowed structures group to refine the molding process. This testing allowed the group to produce nearly flawless, dimensionally sound final molds.
Wing Structure Test	Composite laminate used is sufficient to pass wing tip tests, drove down design of laminate to a total wing weight of 1.5 lbs.
Final Motor and Battery Test	A 20 X 13 and 16 X 12 propeller was chosen for the FMB and FM, respectively. Gear ratios of 1.72 and 1.48 were chosen for the FMB and FM, respectively.
Ground Crew Test	The aircraft can be serviced and returned to flight in approximately 15 sec. Aircraft handling issues need to be investigated to reduce pit time.
Flight Tests	Final aircraft testing has yet to be completed.

Table 7.4: Testing Results and Lessons Learned

References

- Allen, D.H. and W. E. Haisler, *Introduction to Aerospace Structural Analysis*, John Wiley and Sons, New York, 1985.
- Bertin, J. J. and M. L. Smith, *Aerodynamics for Engineers*, 3rd Edition, Prentice Hall, Upper Saddle River, New Jersey, 1998.
- Boucher, R. J., *The Electric Motor Handbook*, Astro Flight, 2003.
- Dieter, G.E., *Engineering Design*, 3rd Edition, McGraw-Hill, Boston, 2000.
- Donald, D., *The Complete Encyclopedia of World Aircraft*, Barnes and Noble Books, New York, 1997.
- Jensen, D. T., *A Drag Prediction Methodology for Low Reynolds Number Flight Vehicles*, Notre Dame, Indiana, 1990.
- Munson, B. R., D. F. Young, and T. H. Okiishi, *Fundamentals of Fluid Mechanics*, 3rd Edition, John Wiley and Sons, New York, 1998.
- Nelson, R. C., *Flight Stability and Automatic Control*, 2nd Edition, McGraw-Hill, Boston, 1998.
- Raymer, D. P., *Aircraft Design: A Conceptual Approach*, 3rd Edition, AIAA, Reston, VA, 1999.
- Shigley, J. E. and C. R. Mischke, *Mechanical Engineering Design*, 6th Edition, McGraw-Hill, Boston, 2001.

Cessna / ONR Student Design Build Fly Competition 2003-2004



SPRAY

Oklahoma State University
Orange Team - 2004 DBF

1	Executive Summary	3
1.1	Conceptual Design	3
1.2	Preliminary Design.....	3
1.3	Detail Design	3
1.4	Manufacturing Plan and Processes.....	4
1.5	Testing Summary.....	4
1.6	Conceptual Design	4
1.7	Preliminary Design.....	4
1.8	Detail Design	4
2	Management Summary	4
2.1	Design Team Composition and Organization.....	5
2.2	Schedule and Planning Summary	6
3	Conceptual Design	8
3.1	Mission Requirements	8
3.2	Mission Analysis	9
3.3	Alternative Configurations and Figures of Merit	10
3.3.1	Aircraft Configuration Concepts and Figures of Merit.....	10
3.3.2	Payload System Concepts and Figures of Merit	12
3.3.3	Landing Gear Configuration Concepts and Figures of Merit	17
3.3.4	Propulsion System Configuration Concepts and Figures of Merit	20
3.3.5	Construction Method Concepts and Figures of Merit	23
3.4	Conceptual Design Results	27
4	Preliminary Design	28
4.1	Major Design Parameters and Sizing Trades.....	28
4.2	Analysis Tools.....	30
4.2.1	Analytical Methods.....	30
4.2.2	Experimental Methods	30
4.3	Aerodynamic Considerations.....	31
4.3.1	Airfoil and Wing Area Considerations	31
4.3.2	Wing Span and Aspect Ratio	33
4.3.3	Tail Volume Analysis.....	33
4.3.4	Aerodynamic Summary.....	35
4.4	Structures Preliminary Design	36
4.4.1	Design Parameters and Trade Studies Investigated	36
4.4.2	Wing Structure Preliminary Design	36
4.4.3	Fuselage Structural Design.....	39
4.4.4	Tail Structural Design.....	40

4.4.5	Landing Gear Structural Design	41
4.5	Payload System Preliminary Design	43
4.5.1	Aircraft CG Movement	44
4.5.2	Payload Tank Shape.....	44
4.5.3	Payload Release Mechanism	44
4.5.4	Payload Ground Handling System.....	44
4.6	Propulsion System Preliminary Design	45
4.6.1	Propulsion System Configuration	45
4.6.2	Motor	46
4.6.3	Battery Number and Size	46
4.6.4	Battery Configuration	46
4.6.5	Propeller and Gearbox Configuration	47
4.6.6	Speed Controller	49
4.6.7	Disarming System Design.....	49
5	Detail Design	49
5.1	Configuration Details	49
5.2	Projected Performance	50
5.3	Structural Details	50
5.3.1	Wing Details	50
5.3.2	Fuselage Details	51
5.3.3	Empennage Details.....	52
5.3.4	Landing Gear Details	52
5.4	Propulsion System Details.....	52
5.4.1	Component Selection.....	52
5.4.2	System Architecture	53
5.5	RAC Calculation/Weight Statement.....	53
5.6	Aircraft Configuration Summary	54
5.7	Drawing Package.....	55
6	Manufacturing Plan and Processes	55
6.1	Manufacturing Process Figures of Merit.....	55
6.2	Process Alternatives	55
6.3	Process Selection	56
6.4	6.3 Manufacturing Plan.....	57
7	Testing Plan.....	57
7.1	Testing Plan.....	57
7.2	Test Cards	57

1 Executive Summary

The following section briefly describes each aspect of the report, and lists the major design issues resolved in each section.

1.1 Conceptual Design

In order to guide the conceptual design process, an initial score sensitivity study was performed to determine the effect of design parameters on the scoring potential of a given aircraft configuration, and the sensitivity of the Total Score and Rated Aircraft Cost to parameters such as aircraft empty weight, propulsion battery weight, payload weight, and Fire Bomber and Ferry mission times. The results showed that a competitive airplane must carry the full weight of payload, and that the Ferry Mission was almost completely negligible in comparison to the Fire Bomber mission in their influence on Total Score. Configurations considered during the conceptual design phase included several non-conventional designs including tailless and hybrid designs. Most of the non-conventional designs were considered because of the possibility they would be able to achieve a lower Rated Aircraft Cost. Conceptual design was also performed for payload handling configurations and construction methods. The final configuration chosen was an aircraft of conventional layout capable of carrying the maximum allowable payload weight. The aircraft was to be equipped with a retractable boom to assist in emptying the payload, and was constructed using a fully monocoque composite sandwich construction.

1.2 Preliminary Design

Computer routines were utilized by both the aero and propulsion groups to perform optimization of design parameters and component capacity and configuration. Major design parameters were varied in the code to determine the sensitivity of total score to each of the parameters, and their optimum ranges. Experimental data was gathered by both the propulsion group and the structures group to aid in the design process. Structural experiments were performed to gather information allowing more optimized composite structures. Tests were performed on propulsion system components to validate the accuracy of the computer models used to predict aircraft performance. Propulsion testing results informed the design team in their selection of system components. Payload concepts were integrated into the aircraft configuration. Initial weight and balance models were refined to allow more accurate analysis of design scoring potential.

1.3 Detail Design

During the Detail Design phase, system architecture and component selection, placement, and mounting methods were finalized, and structural details were decided. Tables are included which describe the aircraft configuration, size and placement of major components, and major system architectures. Estimates of aircraft handling characteristics and performance are also provided, along with a projected contest score.

1.4 Manufacturing Plan and Processes

Several manufacturing processes were considered and evaluated in trying to determine the optimum way to achieve the desired aircraft construction scheme. Processes were evaluated in terms of the quality control obtainable, the cost of implementation as it pertained to both money and scheduling issues, and the overall manufacturing capability they provided. The manufacturing section of the report describes the method by which manufacturing processes were chosen independently for each of the major aircraft sub-assemblies

1.5 Testing Summary

The testing summary describes the areas in which testing data has been gathered and the ways in which it has been used. Lessons learned and ways in which the testing data has been utilized are also included. Plans for future testing of both individual components and aircraft flight testing are described.

1.6 Conceptual Design

An initial score analysis was performed to determine the effect of design parameters on the scoring potential of a given aircraft configuration, and the sensitivity of the Total Score to Rated Aircraft Cost and Flight Score. The results were used to define the design mission objectives and establish the Figures of Merit by which aircraft configuration choices would be made. Multiple configurations were evaluated as to their scoring potential before an optimum design was selected. Conceptual design was also performed for payload handling configurations and construction methods.

1.7 Preliminary Design

A computer routine was utilized to perform optimization of design parameter sizing and airfoil selection. Payload concepts were integrated into the aircraft configuration. Initial weight and balance models were refined to allow more accurate analysis of design scoring potential.

1.8 Detail Design

During the Detail Design phase, system architecture and component selection, placement, and mounting methods were finalized, and structural details were decided.

2 Management Summary

The following section describes the composition of the Orange Team and the manner in which responsibilities were divided among personnel. Project planning, scheduling, and organization information is also included in this section, along with a milestone chart showing the planned and actual completion dates for major tasks and events.

2.1 Design Team Composition and Organization

The Orange Team was comprised of undergraduate students ranging in age and experience from freshmen to seniors in their final semester of undergraduate coursework. Team members drawn from both the Aerospace and Mechanical Engineering disciplines ensured that the team possessed the broad range of design, optimization, and construction capabilities necessary to field a competitive entry in the contest. Key members of the Design Team were divided into three major technical groups:

- Aerodynamics/Stability and Control (Aero/S&C)
- Propulsion
- Structures

Each group was comprised of a Lead Engineer and two or more Technical Specialists. The Structures Group was further divided into three sub-groups specializing in various aspects of the aircraft's physical construction. The Structures sub-groups consisted of the Wing and Empennage group, the Fuselage and Landing Gear Group, and the Payload Group. The Lead Engineers of each group were directly responsible for operations within their technical area, as well as coordinating the overall project with the other Lead Engineers and the Chief Engineer. The Chief Engineer was responsible for managing and directing the entire project as well as maintaining communication between the technical groups. Figure 2.1 shows the hierarchical organization of key Orange Team personnel, including group assignment and sub-group specialization, where appropriate.

The Aerodynamics/Stability and Control group was responsible for the development of models used to predict scoring potential of various designs and design parameter values. Concurrent to their primary role in developing the aircraft configuration, the Aerodynamics group conducted a sensitivity analysis to determine the degree to which score was affected by each design parameter. The results of the analysis were used to establish initial sizing estimates useful in evaluating the practicality of each concept. After the design concept was chosen, the Aerodynamics group was responsible for analysis and optimization of the planform, including airfoil selection, determination of wing span and area, empennage sizing and geometry, and control surface design.

The Structures Group was responsible for development and integration of both the physical structure and systems of the aircraft. Since the design of the aircraft was largely dependent on how it integrated with the payload system, one of the first tasks of the group was to develop a system for handling the payload. The construction method utilized to build the aircraft was also determined by the structures group. The group was also responsible for necessary testing and research to determine the best method for each portion of the aircraft structure, as well as designing the flight control and payload actuation systems.

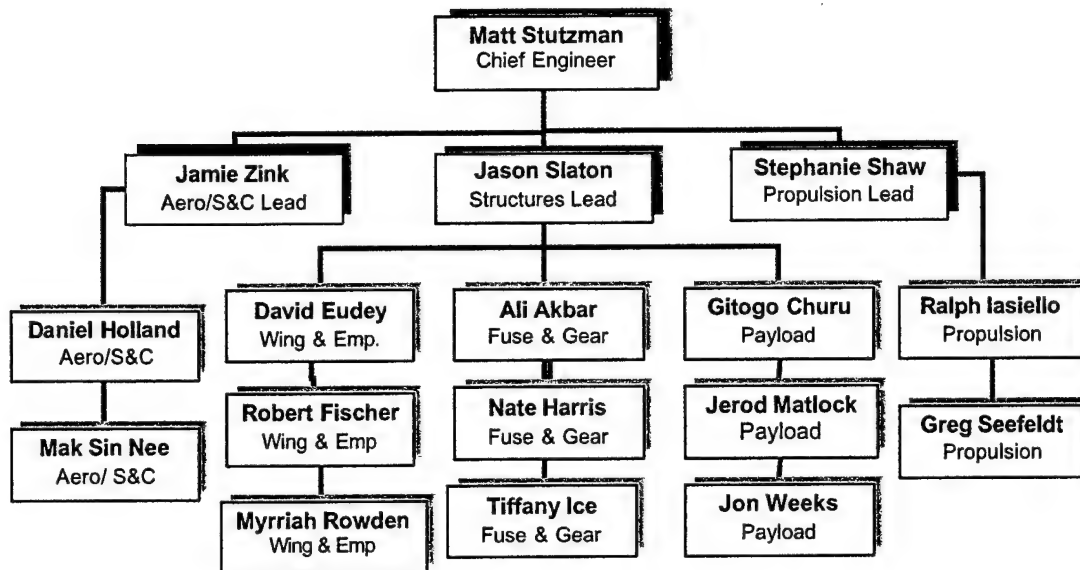


Figure 2.1: Orange Team Organizational Structure

The Propulsion Group focused on determining the best battery/propeller/gearbox combinations for a variety of payload and weather conditions, and developing a scheme in order to obtain maximum efficiency from the available energy in every phase of flight. Much of the Propulsion team's time was spent optimizing the battery pack so that optimal power could be obtained with the lowest weight possible.

2.2 Schedule and Planning Summary

Completing and fielding an entry in the Design/Build/Fly competition necessitated a tight schedule for design, construction, and testing. To ensure that the required tasks were completed in a timely manner, a waterfall chart (Figure 2.2) was created containing projected times for the various aspects of design and manufacturing. The use of this chart along with hard deadlines where required to ensure that the project was completed on time. The following chart shows the major tasks the project was divided into and their projected time frames.

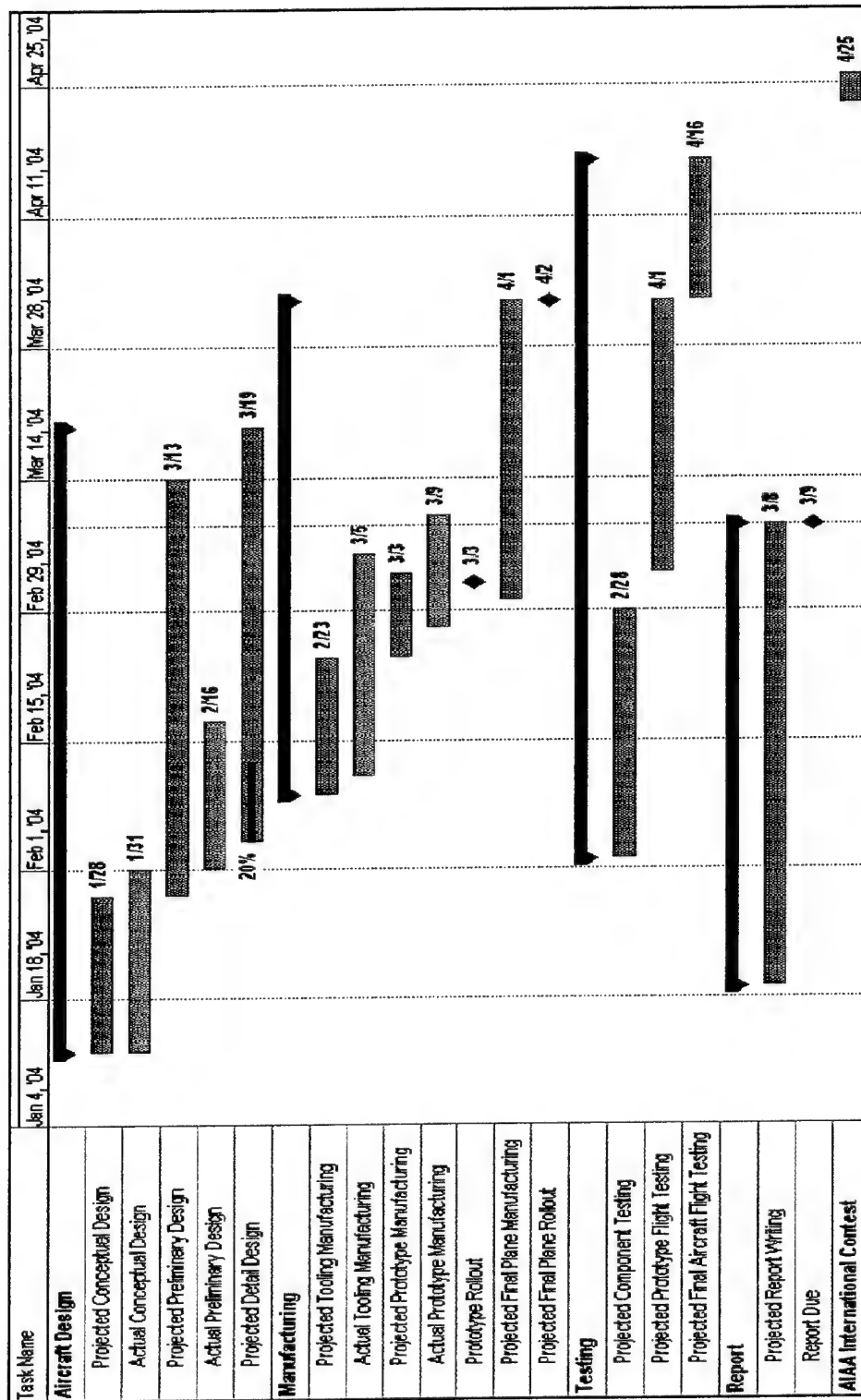


Figure 2.2 : Waterfall Chart with Major Milestones

3 Conceptual Design

The initial step in the design process was to determine the design objectives and the mission for which the aircraft would be optimized. Based on this information, aircraft and system concepts with the possibility of high scoring potential were generated and evaluated. The following section describes the methods by which the design objectives were chosen, the aircraft and component configurations considered, and the resulting overall configuration.

3.1 Mission Requirements

- Secured Storage for Aircraft

The completed aircraft must fit into a storage box that has an interior dimensions of 2-ft wide by 1-ft high by 4-ft long. The aircraft is allowed to have built in folding functions or plug-in joints in order to provide easy access for the entire parts to fit inside the storage box.

- Take-off Limitation

The maximum allowable distance of the runway for take-off for the entire competition is 150 ft. The wheels of the plane must lift off the runway at or before 150 ft from the starting line. If the take-off restriction rule does not meet, flight mission score will result as zero score.

- Fire Bomber Flight Mission

The aircraft is expected to start with empty payload at the beginning of the mission. When the mission started, the teams will load the aircraft with maximum of four 2-liter plastic soda bottles of water. Gravity or pumped loading is allowed to assist the loading as long as it does not pressurize the soda bottles. A time penalty of 1 minute will incur for excessive water spillage during loading.

The aircraft will take-off after loaded with full payload. Once the aircraft reaches the cruise altitude, it will make a U-turn towards the downwind stream. The downwind leg is the only period when the water is allowed to dump from the aircraft payload. The maximum diameter of the dump orifice is limited to 0.5 inch. Therefore, the aircraft needs to slow down in order to have sufficient time to empty the water payload completely before reaching the downwind turn. Late or early dumping will incur a time penalty of 3 minutes per occurrence which including the inadvertent release of water during hard landing. During the cruising period between the upwind and the downwind, the aircraft is also required to make a full 360° turn in the opposite direction of the base. At the downwind turn, the aircraft will make another U-turn and land on the base. Another 3 minutes of time penalty will incur if the water payload of the aircraft is not empty on landing. The aircraft will be reloaded and repeat the similar mission for another lap. If the second lap is not completed, 3 minutes of time penalty will be incurred. The incomplete lap will also count if the 360° turn is not completed. This mission has the difficulty factor of 2.

- Ferry Flight Mission

There will be no water payload for this mission. The aircraft must take-off with no payload and completed all 4 laps before landing on the base. The aircraft is also requiring making a 360° turn for every lap in the

opposite direction of the base between the upwind and the downwind period. The difficulty factor for this mission is 1.

- Cost Effectiveness

The total score of the competition is the multiplication of the written report score and the total flight score which is inversely proportionally to the Rated Aircraft Cost (RAC).

3.2 Mission Analysis

To design an aircraft capable of achieving the maximum score, it was necessary to know which of the design variables had the most impact on the total score. The aircraft with the minimum RAC might not be the optimum design for the competition, and one of the flight missions may contribute more significantly to the total score than the other. To guide the conceptual design process, a sensitivity analysis was performed to determine which design parameters should be emphasized and which should be relegated to secondary or tertiary importance. Based historical data, a reasonable total flight score and RAC for an aircraft capable of performing the mission were established to obtain a baseline for comparison. Major design parameters were then changed nominally from their baseline values and the total score recalculated. The resulting score trends were then plotted versus the design parameters. Figure 3.1, below, shows the sensitivity of the score to several major design parameters.

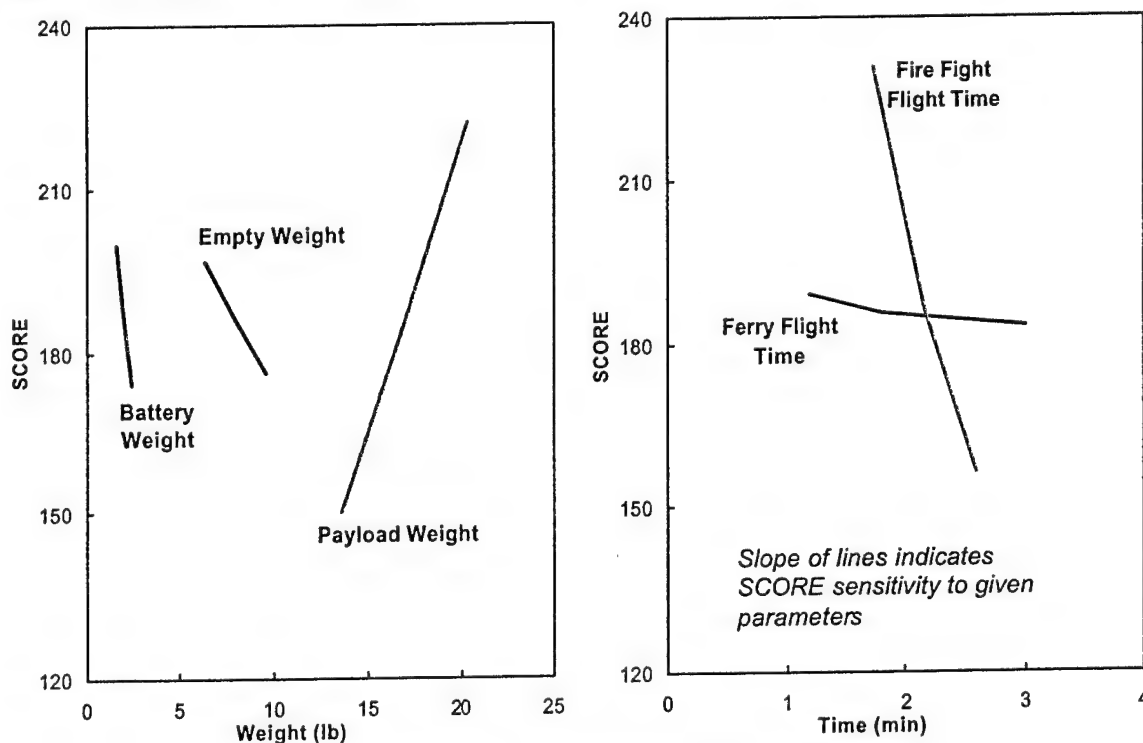


Figure 3.1: Sensitivity Analysis

Note that score has a strong inverse relationship to empty aircraft weight, payload weight and fire bomber mission time, and a strong direct relationship to weight of payload carried. The relationship between ferry mission time and score, however, was very weak. Accordingly, it was decided that the aircraft designed for the contest must carry the full amount of payload while accomplishing the fire bomber mission quickly and efficiently. The aircraft must be as small and light as possible while utilizing the smallest propulsion battery pack consistent with the required performance.

3.3 *Alternative Configurations and Figures of Merit*

For each aspect of the aircraft design, multiple configuration possibilities were considered. Concepts were creatively generated by thinking of ways to maximize score. All ideas were considered initially, and promising alternatives were then evaluated qualitatively and quantitatively based on the Figures of Merit established for each design aspect. The following section discusses many of the design options assessed by the team, and the final choice of each proposed design when evaluated using the previously mentioned Figures of Merit.

3.3.1 Aircraft Configuration Concepts and Figures of Merit

In order to optimize the overall aircraft design, it was necessary to establish a rubric for evaluating competing concepts. The following Figures of Merit were used to compare and quantify each configuration in terms of its scoring potential.

- **Payload System Integration:** The single largest contributor to the flight Score was the weight of payload carried during the fire bomber mission. A competitive aircraft must carry the maximum allowable payload and minimize the pit time between flights. Dumping a liquid payload in flight was considered to be the most significant challenge of the competition. Therefore, the payload system was the most critical aspect of the final aircraft design. As a result, an aircraft configuration that optimized the use of internal volume was required, as well as one that did not exacerbate the negative effects on flight handling caused by water slosh.
- **Takeoff Performance:** A takeoff distance limit of 150 ft. combined with the requirement to lift a relatively heavy payload necessitated an aircraft with a favorable combination of maximum lift coefficient and airframe weight. Inherently stable aircraft configurations with generous control powers and damping coefficients are more easily equipped with high lift devices, and are generally more desirable in this regard than lightly damped aircraft with shorter moment arms and less control authority. In addition, weather conditions at the contest locale required a design that could be reliably flown throughout a wide range of wind speeds and directions.
- **Rated Aircraft Cost:** Sensitivity studies performed showed that at some typical combinations of Flight Score and RAC, an increase in RAC of a given percentage corresponded to a decrease in score of an equal percentage, meaning that the sensitivity of Total Score to RAC was close to -1;. Therefore, a configuration was desired that would incur the lowest RAC consistent with maintaining the required payload and speed capabilities as well as acceptable handling qualities.

- Handling Qualities: The flight score achieved by the aircraft is dependent to a large degree on the ability of the pilot to fly the mission profile. An aircraft with good handling qualities will enable the pilot to devote more attention to accurately flying the profile and less attention to compensating for deficient behavioral tendencies. During the conceptual design phase, handling qualities characteristic to each of the concepts were discussed and factor weighted. Because of the dynamic nature of the liquid payload, an emphasis was placed on configurations that were able to maintain acceptable flying qualities despite a shift in CG location.

Several aircraft configurations were considered because they supported one or more of the Figures of Merit described above. Many of the configurations were considered based largely on a real or perceived savings in RAC. Some of the configurations that initially appeared to hold promise of significantly lowering RAC became much less attractive upon further investigation of the tradeoffs that would have to be performed. It should also be noted that conceptual design for the payload system was performed concurrently and in conjunction with the conceptual design process for the overall aircraft. Because the two processes ran on parallel courses, some of the aircraft configurations considered would not integrate well with the final payload system configuration, but they did support the payload system configurations being considered at the time. The major configurations that were considered are listed below and are shown in Figure 3.2.

- Conventional Configuration: The conventional configuration featuring a single fuselage with a forward lifting wing and aft-mounted tail forms the standard for comparison. It is simple to analyze and optimize since its characteristics are well known and documented. The conventional configuration allows the use of high lift devices due to its longer moment arms and efficient rate damping, but possibly at the expense of a higher RAC due to a longer fuselage length and requirement for a full complement of tail surfaces and servos.
- Bi-wing Conventional: A biplane offers shorter takeoff distance for a given wingspan, but at the expense of more intersection and wetted area drag, and it also incurs a significant RAC penalty. Handling qualities are similar to the conventional configuration.
- Flying Wing Types: A flying wing design might obtain an RAC savings because of its reduction in number of surfaces and shorter fuselage length. However, the wings would probably need to be swept aft to enhance pitch and yaw stability, which would negate the RAC savings. In addition, because of the lack of a horizontal tail, flaps could not be employed on a flying wing, which would limit the attainable lift coefficient and hence require a larger wing with its accompanying increase in RAC. An alternative wing configuration considered was to sweep the wings forward so that their outboard tips would be forward of the CG and could serve as elevators, allowing the use of flaps. This design was rejected early on due to the instability and lack of pitch damping that would occur as a result of the pitch control surfaces being so close to the CG.
- Tailless Lifting Body: The lifting body concept featured a conventional wing blended into a flat, wide fuselage. The aircraft had no horizontal tail, but featured a hinged pitch control surface on

the aft end of the fuselage. Similar in philosophy to the flying wing, the positive attributes of the lifting body configuration are that it would offer a possibly lower RAC due to a shorter fuselage length, along with the RAC savings inherent in a tailless design, although at the expense of handling qualities and stability.

- Inverted V-tail: A hybrid twin boom design was also considered. The design featured short booms protruding aft from the wing on which an inverted V-tail was mounted. The purpose of the configuration was to minimize RAC by decreasing fuselage length, while still achieving enough longitudinal stability and control power to employ high lift devices. It was determined, however, that in order for the V-tail to be effective in its intended function, its span would have to be greater than 25% of the overall wingspan, incurring a dual wing penalty.
- Canard: A lifting canard configuration offers the possibility of reducing the trim drag and downward lift required on a conventional design to counteract the pitching moment produced by the airfoil and the lift of the wing. With the canard, lift needed for stability from the tail (canard) would not take away from the overall lift of the airplane. This design would also possibly allow more room for water storage between the wing and canard. The advantage of a lifting trim surface, however, is somewhat negated by the fact that it is more difficult to incorporate high lift devices. This is due in part to the fact that the lift from the main wing acts further from the aircraft CG, requiring a larger trim surface to counteract the pitching moment introduced by the flaps, which reintroduces the drag that was supposedly saved. In addition, the CG location close to the rear of the aircraft requires excessively large vertical surfaces for yaw control, and both forward and aft motor locations present issues with CG and propeller ground clearance, respectively.

After qualitatively evaluating each of the proposed aircraft configurations, the designs were assigned a ranking of 1, 0, or -1 in accordance with their support for each Figure of Merit when compared with the baseline design (a conventional aircraft configuration). The Figures of Merit were assigned a weighting factor, and a decision matrix was used to determine the optimum aircraft configuration. Table 3.1 on the next page shows the weighting factors used for the Figures of Merit, and the resulting aircraft configuration.

3.3.2 Payload System Concepts and Figures of Merit

Due to the fact that the payload occupied a volume rather than a fixed shape, and also because of the challenge of gradually releasing a liquid payload in flight, payload system integration was one of the primary considerations made while choosing an aircraft configuration. The Figures of Merit selected for evaluating competing payload system concepts are shown below.

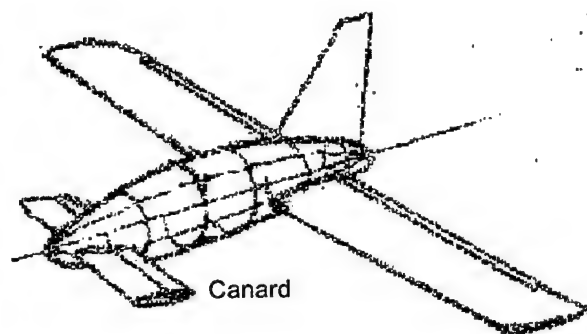
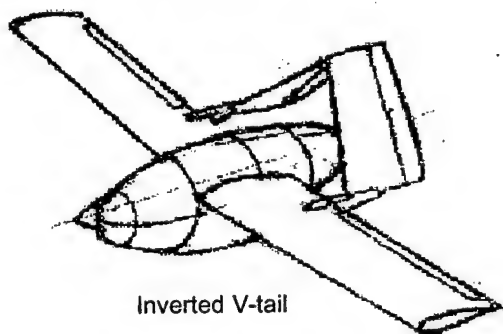
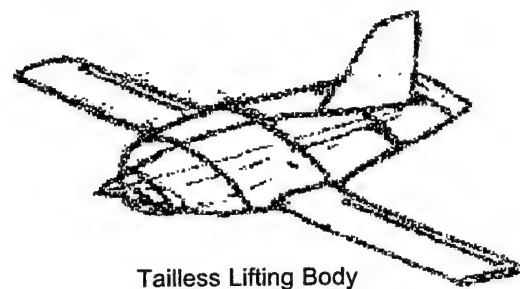
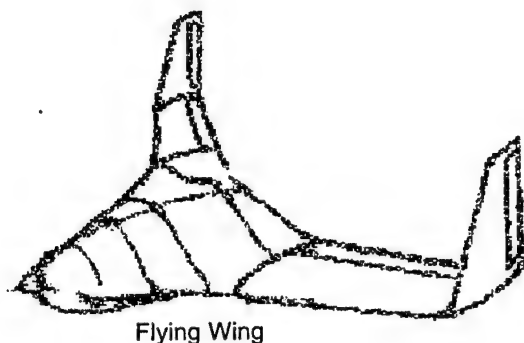


Figure 3.2: Alternative Aircraft Planform Configurations and Rating Results

Table 3.1: Aircraft Configuration Rating Results

Figures of Merit	Weighting Factor	Conventional	Biplane	Flying Wing	Lifting Body	Inverted V-tail	Canard
Payload system integration	0.25	1	1	0	1	1	1
Takeoff performance	0.25	1	1	-1	-1	0	0
Handling qualities	0.20	1	0	0	-1	0	1
Rated Aircraft Cost	0.20	-1	-1	1	1	0	-1
Overall Weighted Score:	-----	0.50	0.30	-0.05	0.00	0.25	0.25

- Discharge Flow Rate: A high volumetric flow rate was required to ensure that the payload was completely discharged on the downwind leg of the course, as the contest rules required. The fluid nozzle exit velocity, and hence the flow rate, is primarily a function of the pressure difference from the inside of the nozzle to the ambient air. Because of the prohibition against pressurizing the

tank to assist in expelling the payload, an alternative method of increasing the pressure difference was required. The contest rules state that the dynamic pressure created by the aircraft flight velocity could be ported to the tank to increase flow rate, but a fluid dynamics analysis using the standard Bernoulli equation showed that the dynamic pressure gain was completely negligible in comparison to what could be obtained by increasing the "head" of the fluid column by even a couple of inches. The results of the Bernoulli analysis can be seen graphically in Figure 3.3, below, which shows the time required to drain a 4-liter reservoir as a function of pressure head when the tank cross sectional area is held constant. The curve showing the time required to drain is highly dependent on pressure head, but unless pressure head is very low, is not strongly dependent on dynamic pressure. Each of the payload systems seriously considered incorporated some mechanism for increasing the pressure head during payload release.

- Volumetric Efficiency: The Rated Aircraft Cost function contains a fuselage volume component, calculated by the product of the fuselage frontal area and its length. It was highly desirable to utilize a payload system that minimized the frontal area required for the reservoir and release mechanism, while preserving the required fuselage volume, in order to minimize the RAC.
- Minimal CG Shift During Payload Release: Because of RAC considerations, the aircraft will be built as small as possible, which implies that the payload will be a large fraction of aircraft gross weight. Any shift in the location of the payload center of gravity could possibly cause a significant shift the total aircraft CG. A reservoir configuration that minimized the amount the CG could shift during payload release was required to preserve the longitudinal stability and pitch trim characteristics of the aircraft.
- Manufacturability: In order to minimize cost and manufacturing time and labor, a design simple in both construction and operation is strongly preferred over a complex one.
- Speed and Ease of Loading: As was shown in the sensitivity analysis, mission time for the Fire Bomber task is one of the single largest determinants of total score. A major contributing factor to mission time will be pit time between sorties. The payload system in the aircraft must be able to be loaded easily and efficiently in order to reduce pit time to the absolute minimum.

Multiple payload system configurations (Figure 3.4) were considered in the conceptual design phase, each with a mechanism for increasing the pressure head of the tank over the duration of payload release. Among the schemes considered was a long, narrow reservoir that pivoted about the aircraft CG during payload release to convert the longitudinal dimension into pressure head. This system had many complications, including the adverse effect on flight qualities cause by a large reservoir protruding into the air stream on the top and bottom of the aircraft, the massive change in mass moments of inertia about the longitudinal and lateral axes, and the moment applied on the aircraft to pivot the mass of the reservoir and payload. During the ensuing discussion, however, a retractable boom was proposed which would utilize a tube of the requisite 0.5" diameter hinged at the bottom of the reservoir. During payload release, the boom would swing downward to increase the pressure head of the tank, and thus the volumetric flow

rate of the payload. The payload systems in the figure below utilize either a retractable boom or a venting system which maintains tank head above the tank level. Each payload system concept is described in the section below the figure.

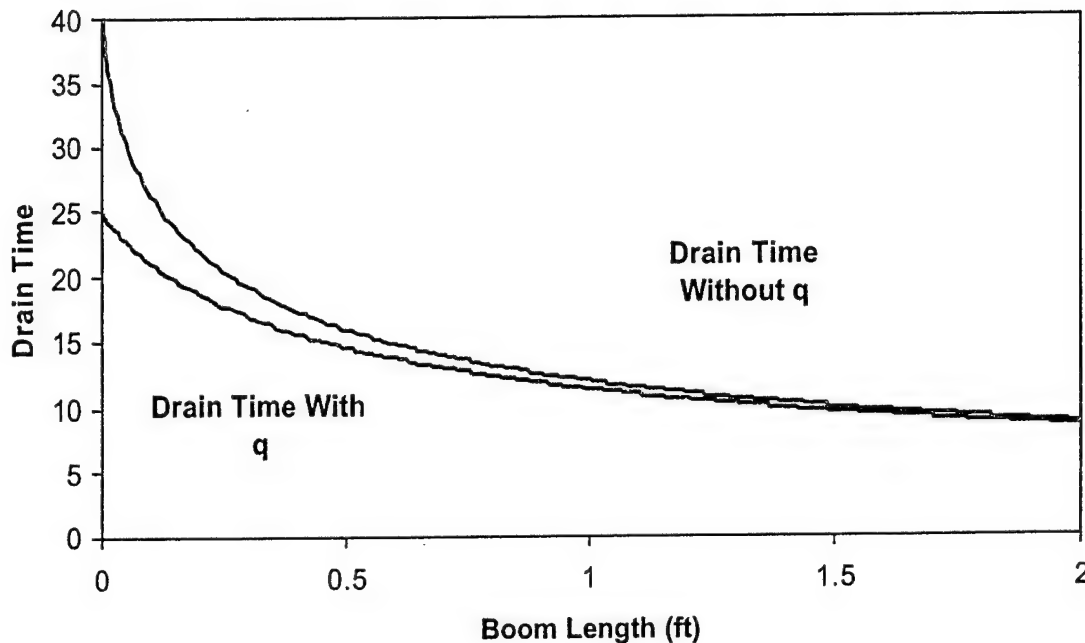


Figure 3.3: Fluid Flow Rate as a Function of Fluid Head and Dynamic Pressure

- Inverted Pyramidal Reservoir with Baffles: An inverted pyramidal tank allows the majority of the volume, and thus weight, to be concentrated at the top of the tank. Depending on the shape of the tank and the slope of the fore and aft tank bulkheads, it may be possible to minimize the CG shift by ensuring that the weight fraction of the payload that can shift significantly is relatively small. The pyramidal reservoir also creates a relatively high head pressure by virtue of its depth. Ease of construction is also an advantage of the pyramidal reservoir. Even complex shapes could easily be created using a foam plug overlaid with fiberglass, then hollowed out using acetone to dissolve the foam. Loading would be easy due to the fact that the tank could be loaded through a single point. The reservoir would require some type of baffling to combat dynamic payload shift due to changes in deck angle.
- Multiple Individual Tanks with Check Valves: To further mitigate water slosh and CG shift from what could be achieved with a single baffled reservoir, multiple tanks could be installed. The tanks would be plumbed together with check valves which only allowed water to flow inward toward the center tank. The multiple tank concept retains the head pressure advantages of the

single tank, but would be slightly more difficult to construct, and also more complicated to load, since multiple ports would be required to fill each compartment.

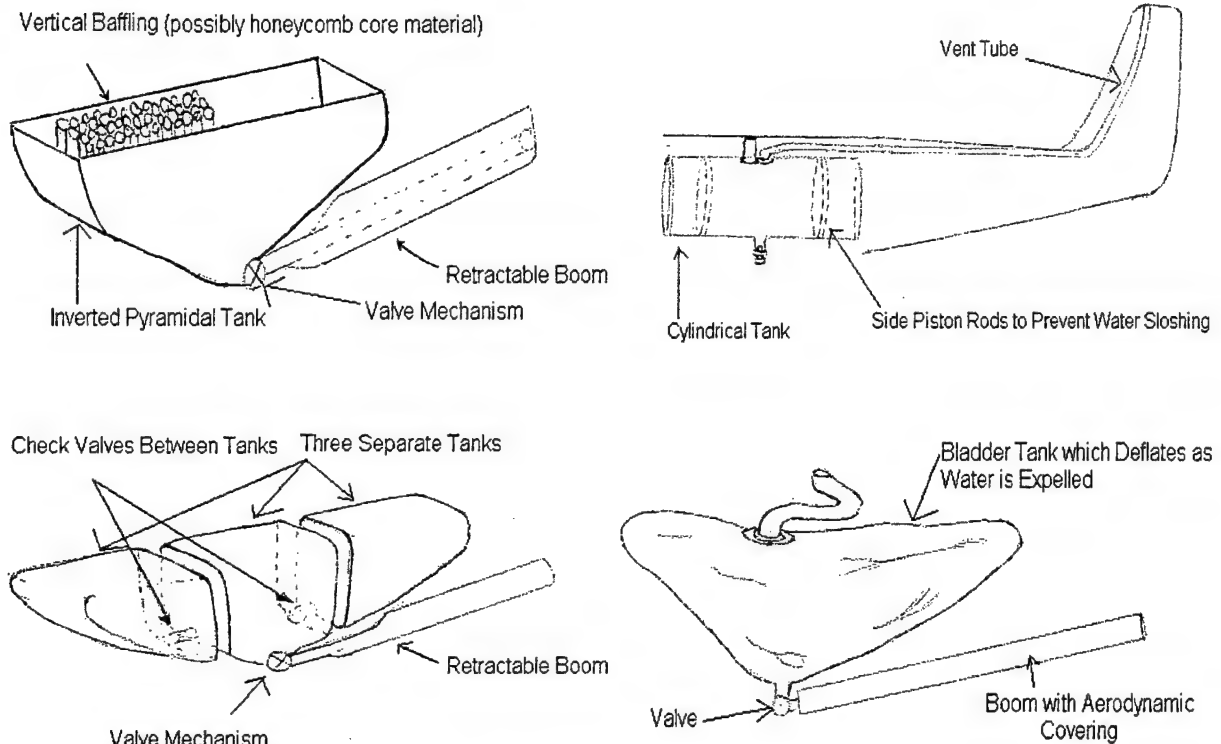


Figure 3.4: Payload System Configuration Concepts

- Variable Volume Cylindrical Reservoir: Another tank concept considered was a long, cylindrical tank equipped with a sealed worm drive running through the center of the tank which operated plungers on each end of the tank. As the payload flowed out of the tank, the worm drive would move the plungers toward the center of the tank, maintaining the tank CG at the original location. The variable volume cylindrical reservoir offers the advantage of minimal CG shift, but at the expense of complexity and weight. A carefully tuned speed would have to be established to collapse the plungers at the same rate that water was flowing from the reservoir, or alternatively, an active control system would have to be designed to regulate the height of water in the cylinder. The cylindrical reservoir also creates some complications with loading; after the payload is released, the plungers would have to be powered back to their expanded position to allow the second sortie's payload to be added. In addition, a cylinder stiff enough to maintain a seal around the plungers would necessarily be heavier than the other concepts.
- Bladder Tank which Deflates as Water is Expelled: A bladder type reservoir offered the advantage of not having to be vented because the tank would collapse as the payload emptied. This also eased manufacture since the tank would expand to fill the available space and did not

have to meet tight shape tolerances. The disadvantage would be that the tank would be hard to restrain, and loading would have to be done through a pressure port. The bladder tank concept was initially conceived with the idea that an elastic bladder might assist with expelling the payload; however, FAQ postings from the contest directors later prohibited elastic bladders.

The nature of the comparisons for the payload systems was such that a numerical decision matrix was not required. The cylindrical reservoir was determined to be non-optimum for several reasons, including the inherent complexity of the variable volume system and the complications associated with loading. In addition, the length of the reservoir would require a longer fuselage which would offset the RAC savings gained from the lower frontal area of the cylindrical reservoir. The bladder tank concept was rejected due to the difficulty of preventing dynamic CG shift (because of a lack of baffling) and also due to the loading complexity. The remaining concepts were considered to be variations on a common theme, and it was decided that the single pyramidal reservoir with a baffling system offered the best compromise of performance, and simplicity. Equipped with a retractable boom, the single reservoir would also provide the highest flow rate of any of the concepts.

3.3.3 Landing Gear Configuration Concepts and Figures of Merit

Proper design of landing gear type and configuration is a key factor in the suitability of the aircraft for its intended mission. Landing gear design holds major implications for aircraft ground handling, structural weight, parasite drag, takeoff and landing performance, and even payload system integration. The optimum landing gear configuration is also dependent on the overall aircraft configuration. Based on these considerations, the Figures of Merit for the Landing Gear system were chosen as follows.

- Compatibility with Aircraft Configuration: As in every other design area, the best landing gear for an aircraft depends on the aircraft. The contest aircraft being designed is highly optimized for its intended mission, so the landing gear system must be well integrated with the rest of the aircraft so as to prevent degradation in utility and performance.
- Weight: As was seen in the mission analysis, empty aircraft weight is a large factor in determining RAC and hence total Score, so a lightweight design is highly desired.
- Drag: Both of the missions in the competition involve a timed course, so speed, and hence drag, should be minimized as much as possible. In addition, lowering drag reduces the amount of power required and hence the battery weight and RAC.
- Ground Handling: The score of the airplane depends on how well the pilot can fly the mission profile, which in turn depends on the aircraft's handling qualities. Ground handling is a major aspect of the operator friendliness of the design.
- Takeoff Performance: Because of the 150 ft. maximum takeoff distance requirement, takeoff is one of the limiting factors when optimizing the aircraft for the mission. A landing gear configuration that offered a better ground stance might make the difference between meeting the 150 ft. requirement or not.

- Ease of Construction: Manufacturability is always a key factor. Proper alignment and strength of the landing gear are important issues that must be able to be accomplished for the design regardless of what is chosen.
- Cost: Material availability and cost are always considerations in any design. The materials used for the landing gear must be available within a reasonable time for a cost that can be met without causing the project budget to be exceeded.

Major landing gear configurations investigated included mostly variations on the common taildragger and tricycle arrangements. Unconventional configurations such as a single main wheel or bicycle type gear with outriggers did not offer any discernible advantages, and thus were eliminated from consideration due to the negative ground handling issues they presented. One of the major considerations in the design of the landing gear was the fact that the aircraft had to fit into the box described in the contest rules. As a result, for most configurations, the landing gear would have to be detached from the aircraft for storage. Because the main wheel location for tricycle landing gear is aft of the CG, and the payload release valve is located roughly on the aircraft CG, tricycle gear configurations must be swept aft from its mounting location to provide clearance for the boom to swing downward from its retracted position. Alternatively, the main gear could be designed as two pieces installed in separate receivers mounted on either side of the fuselage or wing. The section below describes the various configurations considered for the landing gear. Figure 3.5 displays these configurations.

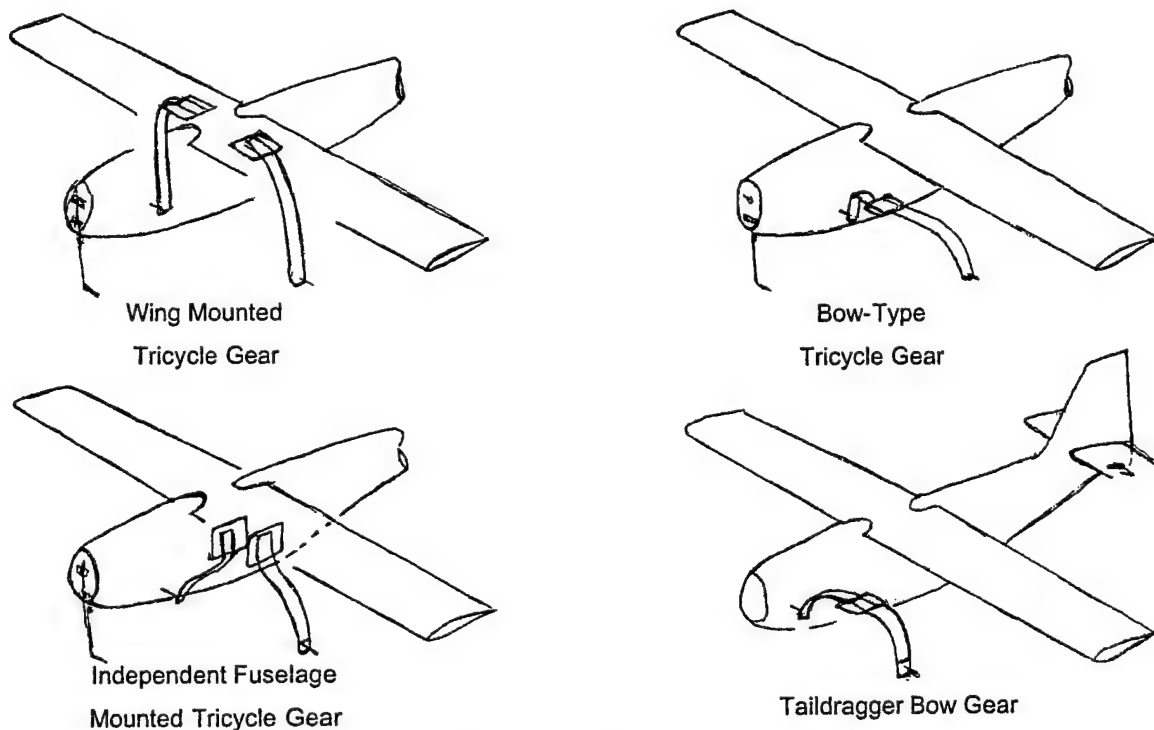


Figure 3.5 Landing Gear Configuration Concepts

- Tricycle Configuration, Bow Gear Swept Aft: The advantages of the tricycle configuration are good ground handling qualities due to the aircraft CG being forward of the main gear contact point, which causes the aircraft to be positively stable on the ground. If the aircraft is landed with a slight crab angle, the aircraft will naturally align itself with the direction of motion. The single piece, bow-type landing gear is simple to build, reliable, and lightweight. Depending on the rake angle, sweeping the bow aft might complicate its manufacture somewhat.
- Tricycle Configuration, Independent Gear Legs Mounted in Fuselage: Because of the need for boom clearance, a design in which the left and right main gear legs were independently mounted in the side of the fuselage was considered. The legs would be mounted in sockets or rails from which they could be removed for storage of the aircraft. The disadvantage would be that the alignment of the two gear legs would be difficult, and the necessity to build two hard points in the fuselage would increase more than the bow type gear.
- Tricycle Configuration, Independent Gear Legs Mounted in Wing: If the landing gear legs were mounted in the wing, they might not need to be removable, since the wing panels must be removable. If the gear legs were permanently mounted they could theoretically be somewhat lighter than if they were removable. The disadvantage with this method is that the gear legs would have to be longer if the aircraft was not a low wing. The required stiffness of the gear legs and hence the weight of the gear would then be increased. Longer gear legs would also be more flexible and possibly have a negative impact on ground handling.
- Taildragger Configuration with Bow-type Gear: The taildragger configuration allows the use of a bow gear without excessive sweep, and employs a single hardpoint installed forward on the fuselage. The lack of a nose gear reduces drag and weight, and the aircraft takeoff performance should be improved, even if only marginally, because the aircraft doesn't have to use the main gear as a fulcrum to raise the nose during rotation. Disadvantages of the taildragger configuration are, of course, that the ground handling qualities are not as good as those of the tricycle gear. Constant corrections must be made to keep the aircraft going in the desired direction on the ground. The bicycle configuration consists of two main wheels, one forward and the other aft of the CG.

Each of the landing gear concepts was qualitatively evaluated and then assigned a numerical ranking based on its support for each of the Figures of Merit. A weighted decision matrix was then created, which showed that the Bow-type Taildragger landing gear was the optimum design for this aircraft. The landing gear decision matrix is shown in Table 3.2, below.

Table 3.2: Landing Gear Decision Matrix

Figures of Merit	Weighting Factor	Taildragger, Bow-type	Tri-Gear, Bow-type	Tri-Gear, Dual Fuselage Mount	Tri-Gear, Wing Mount
Compatibility with Aircraft Configuration	0.2	1	0	-1	0
Weight	0.2	1	-1	0	0
Drag	0.2	1	-1	1	0
Ground Handling	0.1	0	-1	-1	1
Takeoff Performance	0.1	0	0	0	1
Ease of Construction	0.05	0	-1	-1	0
Cost	0.05	0	0	0	0
Overall Weighted Score:	-----	0.60	-0.55	-0.15	0.20

3.3.4 Propulsion System Configuration Concepts and Figures of Merit

The propulsion system accounts for approximately one third of the aircraft's total empty weight. This large percentage of weight has a significant effect on the center of gravity of the aircraft. It is also important to minimize the weight of the propulsion system because of the impact on RAC. Total score is more sensitive to battery weight than to any other single variable, due to the large impact of battery weight on RAC, accounting for a 3% increase in RAC per quarter pound of battery weight in some typical combinations of flight score and aircraft size and complexity. These two parameters, weight and RAC, as well as five others were chosen as the focus of the propulsion system design and were used to evaluate design alternatives. These Figures of Merit, with the relevance of each, are listed below.

- Weight: Battery weight is the highest contributor to RAC. Using an efficient motor and propulsion system can greatly reduce the number of batteries needed to competitively complete the required missions.
- Rated Aircraft Cost: The location and number of the motor(s) and propeller(s) can potentially increase the RAC if the volume of the plane must be increased in order to compensate for the added motor and battery space.
- Ease of Construction: The location of the motor and propeller must allow for reasonable construction for the Structures team in order to minimize errors during fabrication.
- Available Propeller Sizes: The location of the motor should permit maximum flexibility in choosing the most efficient propeller diameter for varying wind conditions.

- **Reliability:** The motor must be located in an area that allows it to run dependably, with enhanced motor cooling.

The location of the motor and propeller plays a significant role in the performance of any RC plane. The following alternatives were considered: pylon mount, tractor, pusher, and wing mount.

Using the before mentioned figures of merit, each of the four alternatives were evaluated for location of the propulsion system in a weighted decision matrix shown in Table 3.3. Since weight and RAC are adversely proportional to Score, they were given the largest priority. Aircraft control and drag were also weighted heavily because of their effect on the size of the aircraft and thus the effect RAC. Ease of construction, propeller sizes, and reliability were not weighted as strongly as the other Figures of Merit because they do not have an immediate effect on Score.

Upon evaluation of the advantages and disadvantages of each design using the decision matrix, the tractor configuration was chosen as the most appropriate for the mission. The frontal mounting allows for greater CG control by displacing the weight of the payload. This also allows for an increased propeller diameter which will generate the thrust needed for zero wind take-offs, and also effectively lowers RAC because less wing area will be required.

Table 3.3: Decision Matrix for Propeller and Motor Placement

Figures of Merit	Weighting Factor	Tractor	Pusher	Wing Mount	Pylon Mount
Weight	0.20	1	1	-1	0
RAC	0.20	1	1	-1	0
Aircraft Control	0.16	1	1	1	0
Drag	0.16	1	1	0	-1
Ease of Construction	0.14	1	1	-1	-1
Available Propeller Sizes	0.08	1	-1	0	1
Reliability	0.06	0	0	1	0
Overall Weighted Score:	-----	0.94	0.78	-0.32	-0.22

Placement of the remaining components of the propulsion system was equally as important as the location of the motor and propeller. Position of each propulsion system component was considered based upon CG control and minimizing power losses. These considerations for each component are as follows:

- **Battery Pack:** The location of the battery pack is vital due to its large contribution to the total aircraft weight. Therefore, the battery pack must be located in the optimum location to maintain CG control. In addition, the battery pack should be located near the motor to reduce the amount of power loss in the wiring. Taking these factors into account, the battery pack will be located in

the front of the plane near the motor. If the decision is made to use two battery packs, they will both be located in the front of the plane.

- **Gearbox:** By using a gearbox, thrust and RPM can be better controlled. Changing the gear ratio ensures that the motor is operating in its most efficient range for the majority of the flight. This saves power and effectively reduces the number of batteries required resulting in a lower RAC score. It is important to choose the best ratio for both the Fire Fight and Ferry Flight missions. Extensive testing during the prototype stage will allow for choosing the most effective gear ratio for the propulsion system. The gearbox will be located directly between the propeller and the motor. The location of the gearbox does not have a significant effect on the RAC score.
- **Speed Controller:** Speed controllers adjust the throttle setting of the motor based on input from the remote control. Finding the right speed control is not the most important part of the propulsion system, but it still must be optimized for a competitive plane. Two speed controllers will be tested during the Preliminary design phase: the AstroFlight 204D and the Jeti JES 60. The speed controller will be placed in the front of the plane near the rest of the propulsion system.
- **Fuse:** To protect the motor from excessive current, the fuse must carry the entire motor current. Because the speed controller is a power transformer, the current in the circuit between the speed controller and the motor is not necessarily the same current in the circuit between the battery and the speed controller. For this reason, the fuse must be placed in the motor circuit between the speed controller and the motor.

- **Motor and Battery Combinations**

Several options for battery and motor configurations were considered: single motor/single battery pack, single motor/dual battery pack, dual motor/single battery pack, and dual motor/dual battery pack. As with all design criteria, weight and RAC were held with highest regard when choosing a design. However, several other Figures of Merit were taken into consideration when choosing a motor/battery combination. These Figures of Merit are listed as follows:

- **Weight:** The motor and battery weight must be kept to a minimum because they will greatly influence both the RAC and the mission times, and thus the overall Score.
- **Rated Aircraft Cost (RAC):** The battery weight has a huge affect on the RAC score – it is included in the Manufacturers Empty Weight and the Rated Engine Power equations. The number of motors is also a factor in the Rated Engine Power equation.
- **Efficiency:** The more efficient a system is the fewer batteries that will be needed. This results in a lower RAC.
- **Thrust Produced:** Enough thrust must be produced for takeoff with a full four liters of payload.
- **CG Control:** The motor and battery combination must allow for effective control of the center of gravity, which affects stability.

- Ease of Construction: The system must be simple enough that it can be constructed in a reasonable amount of time.

Each of these design criteria were taken into account as Figures of Merit when evaluating the above combinations. Weight and RAC were again given highest weighting factor, however, equally important were efficiency and thrust since they also influence Score. CG control and ease of construction were rated lower because they do not directly influence Score. Results from the analysis can be seen below in Table 3.4.

As shown in Table 3.4, a single motor system is the best for the competition. Not only is this the top design for our aircraft, it is also characteristic of the previously chosen tractor design. The optimum design for the motor/battery combination is one battery pack, however, in order to keep the fuselage cross section small, it may be necessary to split the pack into two smaller packs.

Table 3.4: Decision Matrix for Suggested Motor and Battery Combinations

Figures of Merit	Weighting Factor	Single Motor / Single Battery Pack	Single Motor / Dual Battery Pack	Dual Motor / Single Battery Pack	Dual Motor / Dual Battery Pack
Weight	0.19	1	1	-1	-1
RAC	0.19	1	1	-1	-1
Efficiency	0.19	1	0	-1	-1
Thrust Produced	0.19	1	1	1	1
CG Control	0.12	0	1	0	0
Ease of Construction	0.12	1	1	0	0
Overall Weighted Score:		0.86	0.79	-0.37	-0.37

3.3.5 Construction Method Concepts and Figures of Merit

Several primary structural configurations were considered for the aircraft. The goal of the conceptual design phase for structural considerations was to choose a configuration for each aircraft component that would provide the optimum strength to weight ratio and still be within the manufacturing capabilities of the design lab facilities and team members. The Figures of Merit selected for structural configuration were the same for each of the aircraft components, but different weighting factors led to different construction types in some cases. Figures of Merit for the aircraft structural configuration are listed below.

- Strength to Weight Ratio: Aircraft weight was a major contributing factor to Rated Aircraft Cost and was one of the factors to which total Score showed the highest sensitivity. A structural configuration that attained the required strength while minimizing weight was of the highest importance.

- Formability: Aerodynamically optimum shapes contain a multitude of compound curves. The ideal structural configuration would easily allow the formation of complex shapes.
- Manufacturability: Manufacturability relates to both capabilities and time required. A structural configuration that did not require construction of a large amount of jigs and tooling would be more desirable than one that required excessive amounts of time to prepare for construction of the actual aircraft articles.
- Reparability: Damage to the airplanes during testing is inevitable. If the structure can be repaired and used to gain further data, testing can continue instead of waiting for a new article to be constructed.
- Cost: The design team had a limited budget, which meant that the cost of structural configurations had to be considered, especially those involving exotic and expensive materials.

The aircraft was divided into three structural assemblies so that the optimum construction method could be chosen for each assembly. The three assemblies were the Wing, Fuselage, and Empennage. Listed below are the structural configurations considered for each of the three assemblies, and a description of the configuration, along with its advantages and disadvantages.

- Foam Core with Composite Skin: The foam core method is well known and documented, and involves cutting or carving the desired component shape from a block of insulating foam. The foam is then laminated with one or more layers of composite material to obtain the desired strength. This construction provides nearly unlimited formability and good manufacturability. Jigs are mostly constructed of the cradles the foam is cut from, so little time is required to build tooling. Foam core structures are also quite repairable. Broken structures can usually be epoxied together and possibly reinforced with a small amount of additional composite material. The disadvantage of the foam core method is that the weight is higher than with other methods.
- Conventional Built-up Construction: The built-up method also provides a relatively high strength to weight ratio. It involves building an internal structure from light woods such as balsa and poplar plywood, and skinning it with either balsa or a plastic film such as Monokote®. The built-up method is usually semi-monocoque—structures are usually at least partially sheeted, and gain some of their strength from the plastic film covering. Disadvantages to the built-up method are that complex shapes are more difficult to produce, and careful attention is required during construction to maintain alignment and contour accuracy. In addition, the plastic film requires some experience and skill to properly apply, so manufacturability is somewhat less than for the foam core method. Built-up structures can usually be repaired by reattaching broken structural members with adhesive and replacing the plastic film covering.
- Fully Monocoque Composite Skin Construction: The monocoque stressed-skin construction method provides the highest strength to weight ratio of any of the concepts considered. The primary structural members are the skins, constructed of a thin composite sandwich with a core of balsa. The sandwich skin construction maintains the surface contour over large areas due to its

stiffness. Internal structure is drastically reduced, and consists mostly of shear webs used to connect the upper and lower skins, and other localized structure required to join the components together. Occasional fuselage bulkheads are required to mount components and transmit large compressive and torsional loads. The disadvantage of the monocoque construction is that it requires more tooling than the built-up method. Because the internal structure is so sparse, molds of some sort are usually required to construct a monocoque component. If molds are used, the monocoque method provides more formability than the built-up method, but if molds are not used, the skins must be laid up before they are assembled, resulting in less formability than the built-up method. Reparability of fully monocoque structures is also somewhat lower than for built-up structures because of the highly stressed nature of the skins, and also because of the difficulty involved in maintaining alignment while bonding parts with no structural backing.

The different construction techniques were compared for each structural assembly using a decision matrix with weighted figures of merit. Refer to Section 6 of this report for a discussion on the techniques employed to construct each of these structural compositions.

- Wing Construction: In order to perform a preliminary weight comparison, OSU historical data of construction techniques was consulted. The conventional built-up construction method and fully monocoque balsa and composite construction method are empirically the lightest weight. The strength of the monocoque method, however, is significantly superior to the built-up method.

Table 3.5, below, displays the weighted decision matrix used to choose the wing construction scheme. The most important factor in the decision was the strength-to-weight ratio. While the built-up method is light, its strength is significantly less than monocoque construction. Construction with a foam core does not compare to the other two in terms of this factor, though it is easier to manufacture and repair. The built-up method is slightly lower in cost due to the lack of composite materials.

Table 3.5: Wing Construction Method Figures of Merit

Figures of Merit	Weighting Factor	Foam Core w/ Composite Skin	Conventional Built-Up	Fully Monocoque Composite Skin
Strength to Weight Ratio	0.50	-1	0	1
Formability	0.10	1	1	1
Manufacturability	0.20	1	0	0
Reparability	0.15	1	0	0
Cost	0.05	0	1	0
Overall Weighted Score:	-----	-0.15	0.15	0.60

- Fuselage Construction: The fuselage structure is required to meet several conflicting criteria. The fuselage needs to hold the payload and all necessary electronic and mechanical equipment. However, the fuselage must also maintain the lowest drag and lightest weight possible.

Additionally, the fuselage must remain structurally sound because all other components will be anchored to it. Aside from the design of the fuselage shape and dimensions, the construction techniques employed also play a large role in achieving the above requirements.

The fuselage construction methods are evaluated in a decision matrix in Table 3.6. The strength-to-weight ratio was still the most important factor in this decision. However, the ability to construct the complex curves of the fuselage plays a very large role. This task is extremely difficult to perform with the conventional built-up method. The same discussion about the foam core method from the wing construction is still applicable here. The ease of using this technique can not justify the poor strength-to-weight ratio.

Table 3.6: Fuselage Construction Method Decision Matrix

<i>Figures of Merit</i>	Weighting Factor	Foam Core w/ Composite Skin	Conventional Built-Up	Fully Monocoque Composite Skin
Strength to Weight Ratio	0.45	-1	0	1
Formability	0.25	1	-1	1
Manufacturability	0.10	1	0	0
Reparability	0.15	1	0	0
Cost	0.05	0	1	0
Overall Weighted Score:	-----	0.05	-0.20	0.70

- Empennage Construction: Table 3.7, below, explains the rationale behind the construction technique of the empennages using a weighted decision matrix. The horizontal and vertical tails do not require the strength that the wing and fuselage do, as they experience smaller flight loads. Therefore, the overall weight of the built-up method is slightly less than the monocoque composite construction for the devices. Because no complex curves exist in the empennages, formability and manufacturability are not major issues.

The fabrication of the empennage components using the built-up method is easier than dealing with the required molds and composites of the monocoque technique. However, the nature of the vertical stabilizer enabled it to be constructed in the same mold as the fuselage with almost no extra effort. In addition, building both the vertical tail and fuselage pieces together with the monocoque construction method would reduce overall airplane weight by preventing the need for structural reinforcement at their junction. Because the horizontal tail could not be incorporated into the monocoque construction of the fuselage and vertical tail, it would be built separately using the conventional method.

Table 3.7: Empennage Construction Method Decision Matrix

Figures of Merit	Weighting Factor	Foam Core w/ Composite Skin	Conventional Built-Up	Fully Monocoque Composite Skin
Strength to Weight Ratio	0.25	-1	0	1
Formability	0.25	1	1	1
Manufacturability	0.30	1	1	0
Reparability	0.15	1	0	0
Cost	0.05	0	1	0
Overall Weighted Score:	-----	0.45	0.60	0.50

3.4 Conceptual Design Results

Based on the results of the conceptual design phase for each technical group, the final Orange Team aircraft concept was defined. The final aircraft planform configuration chosen was a conventional layout with a single tractor propeller, high-mounted wing and tail-dragger landing gear. A payload system consisting of an inverted pyramidal reservoir would be installed in the aircraft, with a retractable boom to increase water head during payload release. Both handling qualities and attainable lift coefficient were rated at least equal to every other design, as was the compatibility with the payload handling system. The RAC of the design, while not the absolute lowest possible, is the lowest possible among designs that are able to effectively accomplish the other objectives of handling and performance. The aircraft was to be constructed using a monocoque composite and balsa wood structure. The main landing gear was to be of a composite/balsa sandwich bow type construction, which would create low drag and minimum weight effects. The final aircraft was the one found to possess the optimum combination of qualities enumerated in the Figures of Merit. A sketch of the final Orange Team concept aircraft may be seen in Figure 3.6, below.

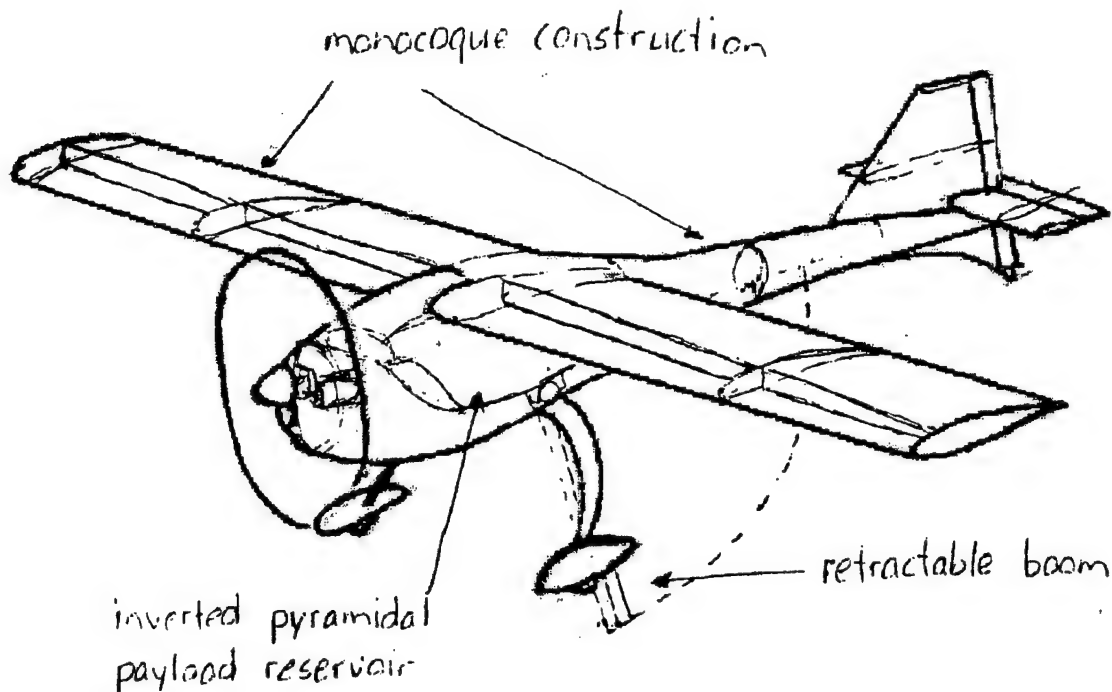


Figure 3.6: Final Aircraft Configuration

4 Preliminary Design

As soon as a final aircraft concept was chosen, the preliminary design process began. During the preliminary design process, the size and configuration of major design parameters were set, structural design schemes and component locations determined, and type, size, and capacity of required components established. Each technical group used unique methods to determine the best way to meet the design goals in their respective area. The following section describes the analytical methods and tools used to optimize the aircraft design in all respects, and the results of the optimization.

4.1 Major Design Parameters and Sizing Trades

Based on the sensitivity analysis performed at the beginning of the conceptual design phase, it was known that several major design parameters were of primary importance in order to optimize the scoring potential of the aircraft. A listing of important design parameters that both directly and indirectly affect the scoring potential of the aircraft are listed in the section below, along with explanations of their importance to the design.

- Wing Area and Aspect Ratio: Required wing area may be one of the single most important design parameters of the optimization. An overly large wing area will increase parasite drag, reducing top speed, and will also increase aircraft empty weight. In addition, a large aircraft that is too lightly loaded may be hard to control in the high winds, and will suffer an unnecessarily high RAC

because of the wing area penalty. Conversely, a wing too small for the intended mission may not be able to achieve the 150 ft. takeoff requirement, resulting in a complete loss of flight score. Scoring potential is not as sensitive to aspect ratio as it is to wing area, but an aspect ratio too low or too high can cause either a loss of aerodynamic efficiency or structural problems and tip stalling tendencies, respectively.

- Fuselage Length: Because the aircraft is required to fit into a four foot long box, fuselage length is a major consideration. A fuselage short enough to fit into the box without disassembly can be built lighter than one requiring a removable joint. In addition, a shorter fuselage length will increase scoring potential by reducing RAC if all other variables are held constant. The tradeoff involved with a shorter fuselage is that it is more difficult to obtain the tail volumes and control powers required for stability and control of the aircraft, especially if the wing utilizes high lift devices, which usually create a strong pitching moment which must be counteracted by the tail surfaces.
- Tail Volumes and Sizing: To a somewhat lesser degree, tail volumes are important in the same manner as the wing area. As indicated in the discussion on fuselage length, tail and control volumes must be large enough to provide the required stability, and control power, but not too large so as to create unnecessary parasite drag. In addition, the horizontal tail span must not exceed 25% of the wing span to avoid being counted as a second wing in the RAC function.
- Number and Type of Batteries: Total scoring potential of the aircraft is more sensitive to the number and type of batteries required and the resulting battery weight than any other design parameter. The number of batteries must be sufficient to achieve the power required for takeoff and the endurance to complete the mission, but remain as light as possible in order to minimize RAC. Choosing a propulsion battery requires an analysis of internal resistance, energy density, sizing and packaging concerns. The energy density of the battery must be carefully matched with the mission.
- Propeller/Gearbox Combinations: As part of the propulsion system, propeller and gearbox combinations are vital to the aircraft being able to meet the performance goals. Optimal propeller/gearbox combinations will allow the aircraft to take off and fly the mission with the most efficiency possible. Efficient combinations will allow the motor and/or the battery pack size to be reduced, which will increase score by decreasing weight and RAC. Tradeoffs involved in propeller and gearbox combinations include trading high cruise speed and efficiency for high static thrust.
- Motor Type: The type of motor selected to power the aircraft is probably the single most important decision of preliminary design as it applies to the propulsion system. The motor's capacity and efficiency will determine the size of the battery pack required, which, as noted above, has the largest sensitivity coefficient on RAC of any design parameter. Motor efficiency is probably the single largest factor in the determination of the optimum motor for the aircraft, but tradeoffs involved include motor weight, cost, obtainable power, and availability.

- Structural Configuration: How well the aircraft structure is designed will determine the strength and weight of the aircraft structure. For composite layups, the weight, number and orientation of plies must be correctly optimized in order to achieve the lightest structure possible consistent with the required strength.

4.2 Analysis Tools

To ensure that each aspect of the design was optimized to the furthest extent possible for the intended mission, a variety of analytical, qualitative, and experimental analysis tools were utilized. The following section provides an overview of the tools used in the optimization, along with a brief description of their use and results.

4.2.1 Analytical Methods

An analysis of aircraft design parameters and their impact on the scoring potential of the aircraft was performed using a computer routine. The program calculated aircraft scoring potential based on a multitude of inputs including component efficiencies and aircraft coefficients as well as major design parameters such as battery weight, payload weight, wing area and wing span. Efficiencies and coefficients were set to the level obtainable with available equipment and design practices and held constant for the optimization, while major design parameters were varied to determine their effect on the total score and the sensitivity of the score to each of the parameters. The program searched for local score maxima after initializing itself from random starting points for the major design parameters. By running the program multiple times and plotting the score outputs versus each of the design variables, trends in scoring potential could be determined.

The Propulsion team utilized a computer routine to determine optimum combinations of gear ratios, battery packs, and propellers. In conjunction with the Aerodynamics/Stability group, the Propulsion group ran simulations under varying wind conditions to predict performance of the aircraft under a variety of aircraft configurations and wind conditions. During the Preliminary Design phase, bench testing began on propulsion system components. The resulting data was used to refine the computer models in order to achieve more accurate simulations.

4.2.2 Experimental Methods

As mentioned in the section on analytical methods, the Propulsion group performed a number of experiments during the preliminary design phase to obtain actual results to compare with the manufacturer's predictions for various components. Efficiencies and thrust profiles were developed for motors, battery packs, and propellers.

The Structures group used a combination of historical and experimental data to perform preliminary design. Before much optimization could be done for the gear ratio and propeller, battery type had to be chosen. Once the type of battery was decided, the minimum number of batteries to provide two fully loaded take-offs in 150 feet could be found. It was essential for RAC to use the minimum number of

batteries possible. Justification for these decisions will be discussed later in the Detail Design portion of the report.

4.3 Aerodynamic Considerations

One of the aspects of preliminary design with the most broad and far reaching implications for the overall design is the configuration and sizing of the aerodynamic surfaces. Choosing appropriate wing and tail sizes and airfoils is crucial to achieving a design capable of performing the desired mission. The following section describes the manner in which the aerodynamic characteristics of the aircraft were determined, and the results of the analysis.

4.3.1 Airfoil and Wing Area Considerations

The Aero Group exhaustively utilized the numerical performance routine to determine the optimum sizes and configurations for each of the major aircraft components. As described in section 4.2.1, above, the code searched for local maxima when it was initialized with a given set of conditions. The input parameters for the optimization code included airfoil lift/drag polars and wind speed. Simulations were run with wind speeds of 5, 10, 20, and 30 miles per hour, to determine the sensitivity of the optimum wing sizes to wind speed. A range of airfoils was also used, from a highly cambered Eppler 423 to a much thinner Selig-Donovan SD7032. Initial results showed that the optimum wing area would not exceed 6 ft^2 . With this knowledge, a stability and control analysis was performed to determine whether acceptable tail volumes could be achieved with a fuselage as short as 4 ft. A 4 ft fuselage was desirable because of the box fit requirement. If the fuselage was required to be longer than 4 ft, a disconnect joint would be required to enable disassembly to fit into the box, which would add complexity and weight. The results of the analysis showed that an acceptable tail volume could be obtained even at the upper ranges of optimum wing areas. This allowed a refinement of the weight model, which resulted in a predicted optimum range of wing areas that was lower than before.

Optimum wing areas predicted by the code ranged from slightly under 5 ft^2 to around 6 ft^2 , depending on the airfoil and wind condition chosen. Outputs from the code showed, however, that the scoring potential of the aircraft, while definitely dependent on the wing area, was not extremely sensitive when close to the optimum. A range of areas existed that would provide performance close to the global maximum. Score calculations were also plotted versus cruise power, wing span, and battery weight, and payload weight. The results of the analysis can be seen in Figure 4.1, below. Score is shown plotted versus wing area, wing span, cruise speed, and battery weight. Program outputs were also taken versus weight of payload weight carried, but plots were not necessary because each high scoring configuration carried the maximum amount of payload. Note that each of the plots demonstrates an optimum area for that parameter, but that a small range of optimum values exist.

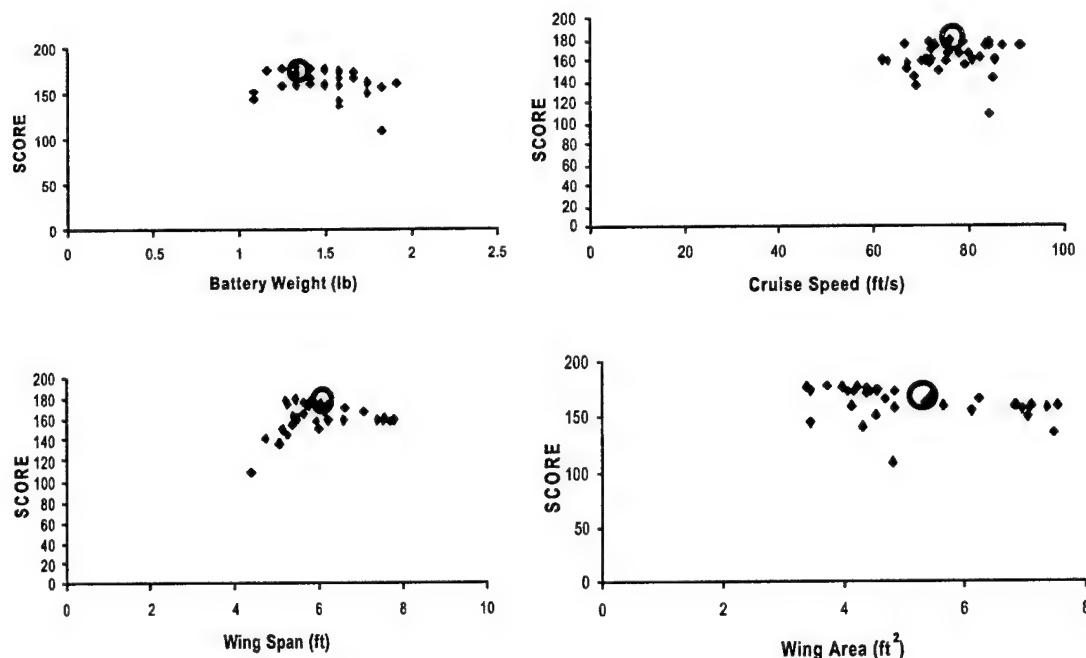


Figure 4.1 Optimization Code Results Run with the SD7062

During the preliminary optimization, the highly cambered Eppler 423 airfoil and the thick SD7062 airfoil seemed to achieve slightly higher scores than the thinner SD7032. The differences were not great enough to determine the optimum airfoil based solely on the merit of the optimization code, but combined with the knowledge that the aircraft would be taking off at a high wing loading during the fire bomber mission led to the elimination of the SD7032 airfoil from consideration. The remaining choices were the SD7062 with or without flaps, and the Eppler 423. The Eppler is designed to operate at high lift coefficients and exhibits a high drag coefficient when operated at a low lift coefficient. In addition, the wind conditions at the contest venue are often gusty during the competition. It was believed that the SD7062 would provide more flexibility than the Eppler in meeting changing weather conditions. In addition, the SD7062 was also more desirable from a manufacturing standpoint because its thick nature and gentle contours make it more easily manufactured than the highly cambered Eppler. In addition, the thickness of the airfoil increased the structural rigidity and strength to weight ratio of the wing as a result. A flapped SD7062 airfoil was chosen for the design. The SD7062 was chosen based on the scoring potential shown in the optimization code, but also because of the Lift/Drag characteristics of the airfoil as predicted by an X-Foil code. Both the flapped and unflapped airfoils exhibit low drag coefficients at their design lift coefficients, and that the drag coefficients do not strong functions of the lift coefficient until they are well above or below the design lift coefficient. The aircraft was optimized for a 10 mile per hour wind, but contingency plans were made so that the aircraft would be able to complete a mission for which there was no wind as well by using different propeller and gearbox combinations. An optimum area of 5.2

ft^2 was chosen for the wing. This area was felt to be slightly conservative while still not handicapping the airplane from its maximum scoring potential.

4.3.2 Wing Span and Aspect Ratio

The optimization program also plotted wingspan, and hence aspect ratios, but wingspan aspect ratio optimization was performed by use of a Prandtl lifting line analysis which showed that the gain in efficiency reached a point of diminishing returns after an aspect ratio of approximately 8 was reached.

The design aspect ratio is based on the consideration of lift distribution and induced drag. The main wing of the aircraft provides most of the lift force to overcome the total weight of the aircraft during the flight mission. Therefore, high lift is needed for this mission especially during take-off with full payload. The induced drag is related to lift coefficient and aspect ratio as shown in the equation:

$$C_{Dv} = \frac{C_L^2}{\pi \cdot AR}$$

From the above equation, it is obvious that the smaller the aspect ratio, the higher is the induced drag. However, if a large aspect ratio is designed to provide large lift coefficient, the wing becomes structurally inefficient and prone to tip stalling. Therefore, the aspect ratio must be optimized to provide the necessary lift coefficient while still keeping a reasonably low induced drag. The parameters are compared with the calculated values for an aspect ratio of 20. Based on the results of the Prandtl lifting line theory, a final aspect ratio of 8 was chosen.

The chosen wing planform was rectangular, mostly because of the nature of the RAC function, which counted wing area as the largest exposed wing chord times the wing span. A rectangular wing planform in the range where the aircraft will be operating would have very little losses, so there was not a reason to use a tapered wing.

4.3.3 Tail Volume Analysis

To obtain a reasonable range of sizes for the horizontal tail, historical data from a variety of sources were reviewed to determine tail volumes characteristic to aircraft with similar types of missions. Although there is no historical data for aircraft of similar size and scale that have similar missions, it was determined that a tail volume of approximately 0.5 should be sufficient to provide the required static stability, even with possible slight shifts in CG during payload release.

As mentioned previously, a key part of the design was the ability to construct the aircraft with a fuselage length of 4 ft. or less. Despite the short moment arm, the required tail volume was achieved with a 4 ft. fuselage and also without violating the 25% horizontal stabilizer rule. (The contest rules state that a horizontal tail with a span greater than 25% is charged as a second wing for RAC purposes).

Based on the pitching moment generated by the wing at cruise, the trim lift coefficient for the tail was calculated. An X-Foil program was used to find a suitable airfoil that would have a low drag when trimmed to the desired lift coefficient. The NACA 2410 was found have the desired characteristics. Using the

moment generated by the tail at cruise, the lift needed to sustain static stability was calculated. The airfoil's graph showed the needed lift coefficient located around zero degrees (after taking into account the downwash effect from the wings).

One of the major issues to be considered in the design analysis was the range over which the aircraft CG could shift as the payload emptied, and the extent to which the shift would affect the flying qualities of the aircraft. Basic stability analysis showed that the static margin was great enough that the worst case CG would not cause the aircraft to become negatively stable. Attention then shifted to the change in trim angle of attack that corresponded with a CG shift. The following graph, Figure 4.2, shows trim alpha plotted versus aircraft CG. Also shown on the graph are the aircraft and tank CG as a function of height of water in the tank.

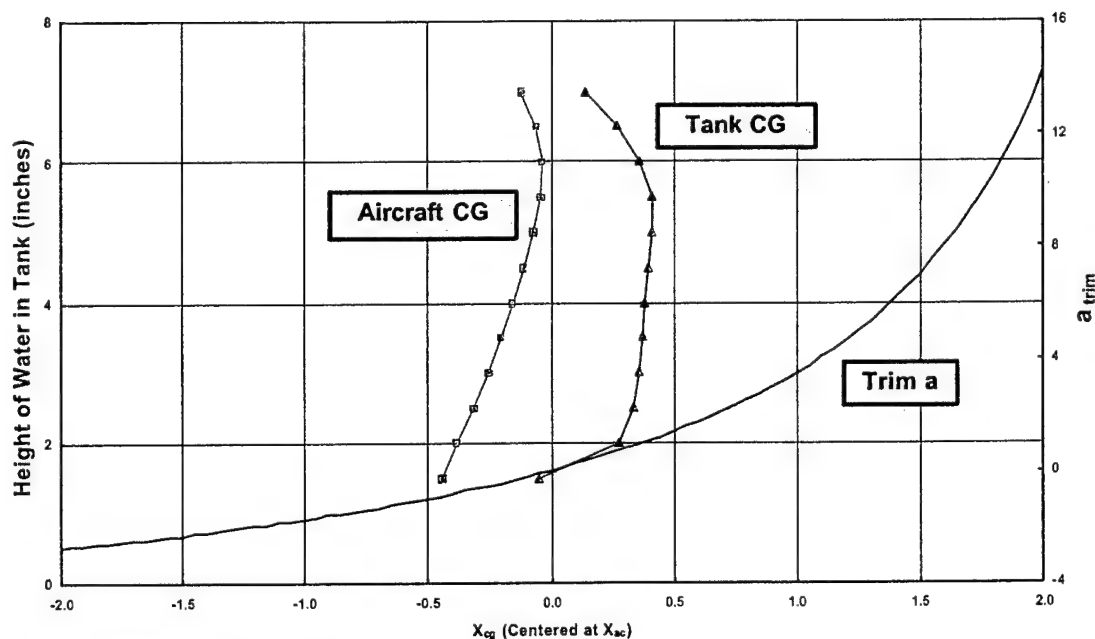


Figure 4.2: Trim alpha as a function of CG, superimposed with CG from Tank Drain Time

- **Vertical Tail Sizing Analysis**

Similar to the horizontal tail, the vertical tail volume was chosen due to historical research and data logs of past airplanes at Oklahoma State University. A tail volume of .05 was decided upon, which corresponded to a vertical tail area of 99 square inches. This tail volume would produce enough stability to maintain a directionally static flight. Reviewing airfoils found in the X-Foil program lead to the decision of using an airfoil that was fairly thin and symmetrical. The optimal airfoil was found to be the NACA 0009. This would allow for the needed static conditions for stability, as well as provide a feasible

thickness for construction ease. The rudder sizing for the plane is based on assumptions made for the side wind and cruise velocity. A program was written which solved for the rudder area needed based on a landing β . The assumption for this case was that the plane would experience a worst case scenario β of 31 degrees. At this β a rudder area of 12" was found to be conservatively sized.

- **Elevator sizing**

To size the elevator, the tail was analyzed under the most extreme circumstance; takeoff with full payload. At this moment in flight, the tail must produce the largest counteracting moment to control the pitch of the airplane. The size of the elevator control surface is dependant on the magnitude of the pitching moment that needs to be balanced by the control. This was done by counteracting the pitching moment at the takeoff angle of attack. An elevator chord ratio of 20% was found to provide sufficient elevator control power to achieve maximum lift coefficient.

4.3.4 Aerodynamic Summary

Table 4.1: Aircraft Parameters

Aircraft Parameters		Wing	
X_{cg} (ft)	0.1667	$Cl_{\alpha w}$ (rad^{-1})	4.666
X_{ac} (ft)	0.2021	AR	7.74
$d\epsilon/d\alpha$	0.371	Cl_{ow}	0.45
$Cm_{\alpha f}$	0.000984	b (ft)	6.45
$Cn_{\beta wf}$	0	S (ft^2)	5.375
CL_{α}	7.922	Cm_{acw}	-8.E-02
CL_o	0.49	C_{bar} (ft)	0.8333
Cd_o	0.045	Vertical Surface	
V_{cruise} (ft/s)	75	$CL_{\alpha v}$	1.527
V_{to} (ft/s)	50	I_v (ft)	2.5
V_l (ft/s)	50	S_v (ft^2)	0.6934
Horizontal Surface		V_v	0.05
S_t (ft^2)	0.8958	S_r (ft^2)	0.06710
$Cl_{\alpha t}$ (rad^{-1})	3.256	Mass Inertias	
V_H	0.5	I_x	4.576
I_t (ft)	2.5	I_y	13.1
τ	0.4	I_z	15.41
Se (ft^2)	0.1875		
b_t (ft)	1.6125		

$C_{m_{\delta e}}$	-0.783
C_t (ft)	0.5556

4.4 Structures Preliminary Design

Each component of the aircraft was conceived and designed with certain figures of merit in mind. The fuselage, wing, tail, and landing gear were evaluated on the following figures of merit.

- Rated Aircraft Cost: Evaluation of each addition's ability to increase performance versus its RAC.
- Weight/Strength: Weight vs. strength analysis and optimization for each component.
- Ease of Construction: The practicality for the part to be produced efficiently and accurately.
- Aerodynamics: The effect each part has on lift, drag, and aircraft stability.
- Ease of Payload Execution: The structural components needed to allow easy loading and unloading of the payload on the ground and in flight.

4.4.1 Design Parameters and Trade Studies Investigated

During preliminary design, several key points were considered for structural analysis. These design parameters were:

- Selection of correct materials for construction
- Investigation of useable combinations of construction materials
- Weights of respective combinations and materials
- Required strengths of fuselage, wing, tail, and landing gear skins
- Landing gear design loads
- Possible reinforcement needs

During structural analysis, each possible combination of balsa and glass layers and thicknesses was investigated. Each combination was analyzed using the above figures of merit and rated according to its strength, weight, and RAC impact. Using this data assisted in meeting the structural and weight restrictions of each major component.

4.4.2 Wing Structure Preliminary Design

Because the wing was designed to attach to either side of the fuselage, each wing was modeled as a cantilever beam anchored at the fuselage and stretching to the respective wingtip. For simplicity, the lift and drag loads were assumed to act evenly along the wingtips in the proper directions. For the buckling analysis, the wing was modeled as an Euler column with one fixed and one free end. Both loads were resolved to a point load and moved closer to the wingtip to increase the bending moment and, thus, created a conservative analysis.

Some test components were built to experiment with different combinations of glass weight, balsa thickness, and resin saturation. The following table 4.2 shows the data obtained from these trials.

Table 4.2: Experimental Wing Characteristics

Construction Tests	Weight [oz]	Area [in²]	W/A [oz/in²]	W/A [lb/ft²]
Test Wing [0.6oz]	3.104	146	0.0213	0.192
Test Wing [2oz]	5.079	146	0.0348	0.311
Test Wing [2oz]	4.762	146	0.0326	0.292
Test Wing [2oz]	4.162	146	0.0285	0.255
Balsa	2.222	146	0.0152	0.137
Main Wing [2oz]	12.134	275	0.0441	0.395

From the testing performed, two ounce fiberglass was found to be the ideal choice for the wing construction. The best composition consisted of 1/16th balsa sandwiched between two layers of two ounce fiberglass.

The above sample components were also used to test various spar and rib configurations. It is assumed that the skin will carry the majority of the stresses with exception to torsional stresses. The internal shear webs will account for the shear stresses and stabilize against torsion.

Pro/Mechanica was employed to perform a finite element analysis on the wing. The results of this modeling are shown below in Figure 4.3. The top left figure is displacement, upper right is strain, and lower left is Von Mises stress. The bottom right shows the convergence of the analysis. All the Pro/Mechanica analysis was performed at a sixth order, but each converged around the fourth series.

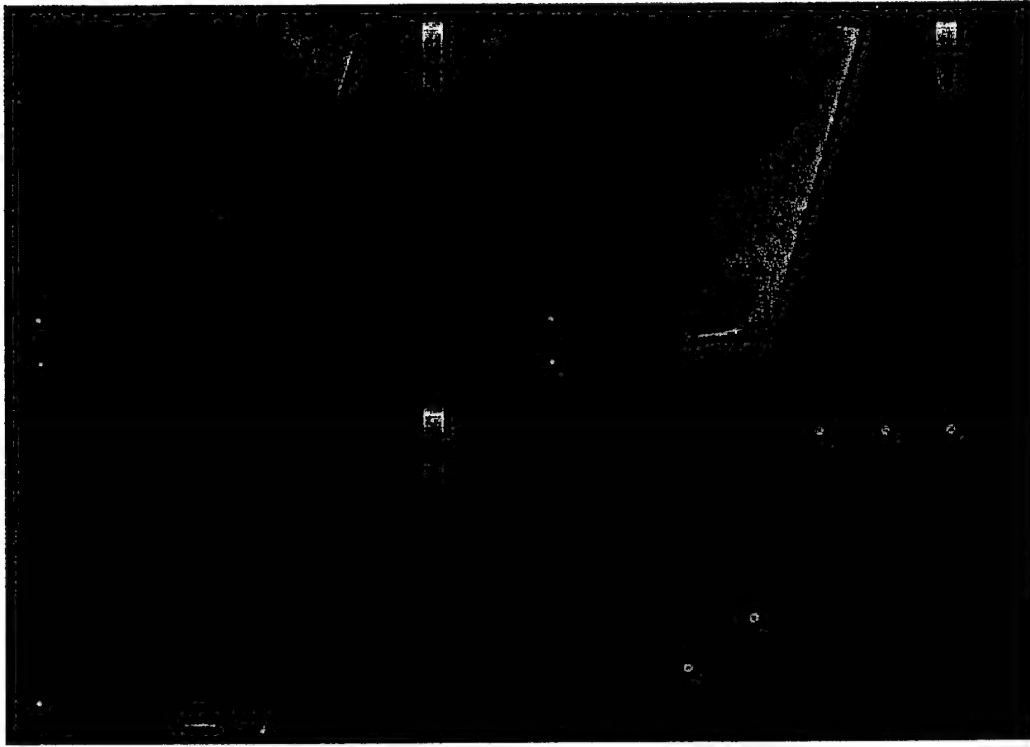


Figure 1.3: Finite Element Analysis for One Wing

One of the test specimens was tested to failure to verify the computational stress analysis. This is shown below in Figure 4.4. The experimental and analytical are consistent. The bottom left experimental picture shows skin buckling at the root. The Von Mises stress concentration from finite element analysis (bottom left picture) also shows this skin buckling at the root edge. The Pro/Mechanica analysis led to a fiberglass make-up that was stronger and thicker at the root and had less material at the tip.

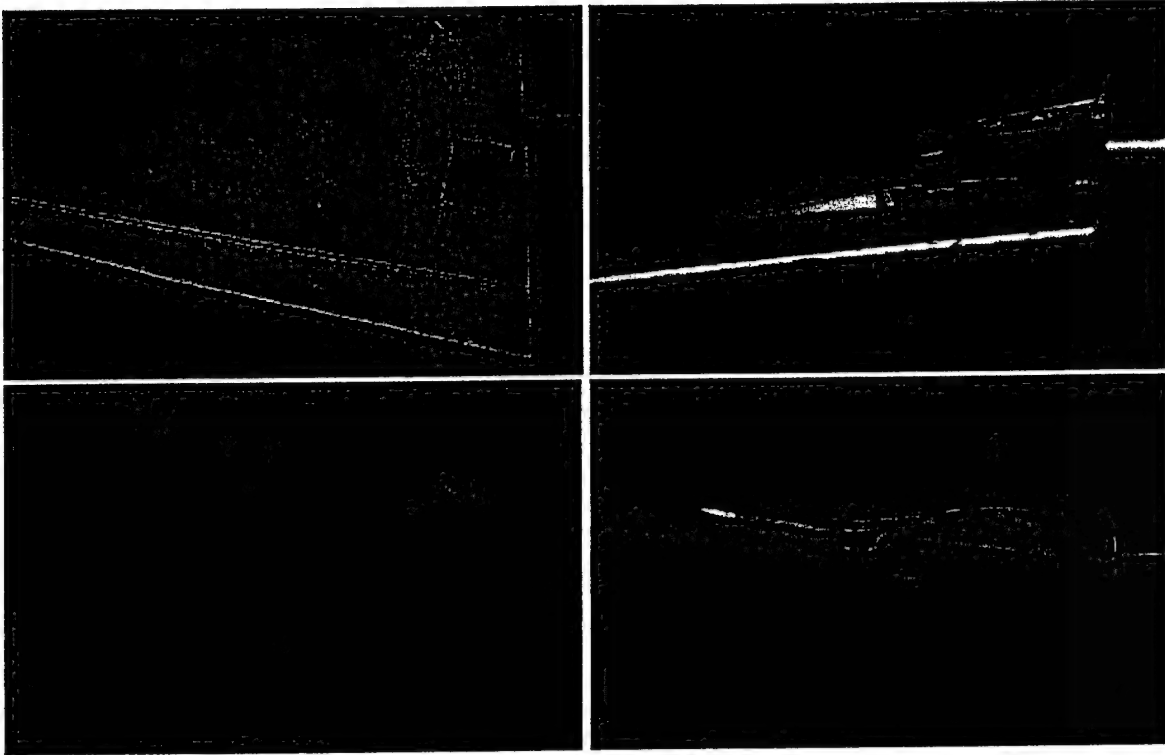


Figure 4.4 Wing Static Tests

4.4.3 Fuselage Structural Design

The fuselage was statically analyzed as a hollow cantilever beam because of the solid mold construction process. Several other simplifications were made in order to perform the analysis. The center of gravity was assumed to be fixed, not allowing for rotation or translation. Dynamic tail forces were not included due to the condition of steady, level flight. The forces applied to the fuselage were modeled as point loads when the aircraft was at full payload capacity. The payload was set at 4 liters of water. Strength comparisons for the fuselage were done with assorted glass and balsa configurations in testing and then optimized for our fuselage. Pro/Mechanica finite element analysis software was used to simulate stresses incurred by the fuselage under a 4-g loading while carrying the maximum payload. This is believed to be the most extreme loading the aircraft will experience in flight.

Due to the payload weight and the method of construction, different areas of the fuselage will carry different loadings. The lower portion will be most influenced by stresses from the payload. The upper portion will carry less loading but will still need to be strong enough to support the anchored wing. In lieu of this, a stronger glass/balsa configuration will be used on the lower fuselage portions while a lighter glass arrangement will be used to construct the upper portions in order to minimize airplane weight.

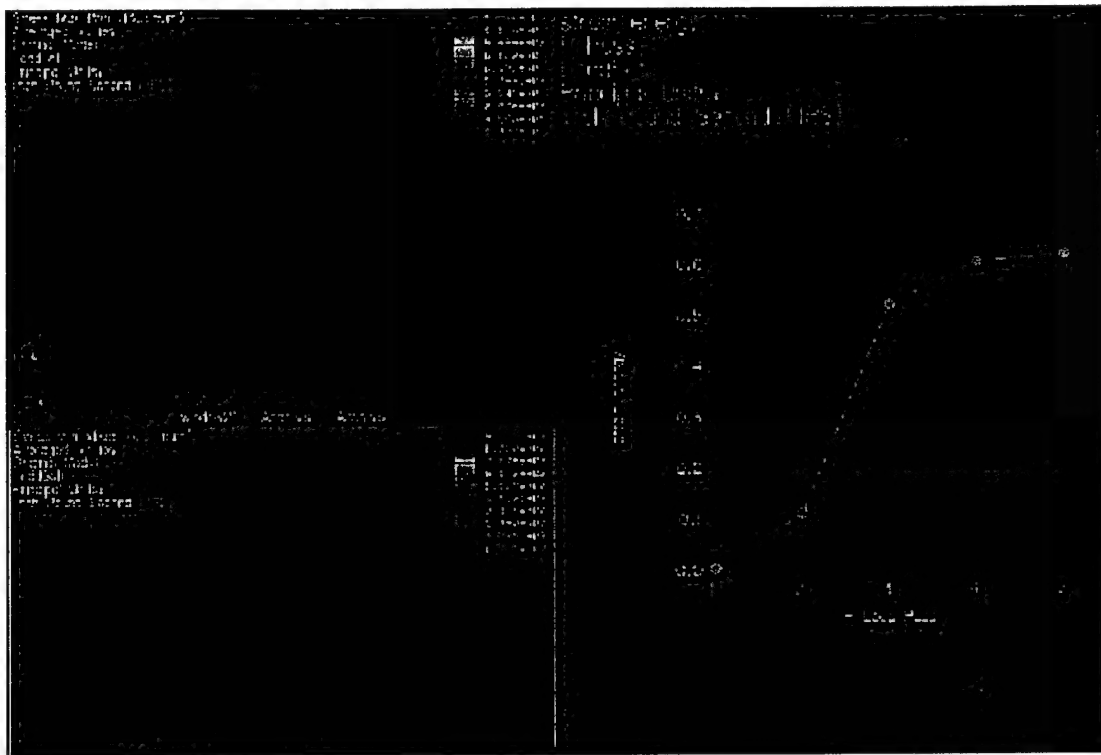


Figure 4.5: Simulation Results for Fuselage Under a 4-g Flight Loading

Finite element analysis was used to estimate the stress distributions resulting from a hard landing. The results may be seen in Figure 4.5. The data obtained from the computational stress analysis was used to better optimize the weight and strength of the individual fuselage areas.

The boom dropping out of the fuselage created some minor design concerns. However, upon further analysis, it was determined that the structure will not lose any critical structural strength due to the boom cutout. It was necessary to place a rubber or semi-stiff plastic brush guard to minimize the airflow into the fuselage from the opening. Figure 4.6 below shows the designed fuselage along with the basic tail structure.

4.4.4 Tail Structural Design

The same analysis was performed for the horizontal tail and vertical stabilizer as the wing analysis. Both the horizontal tail and vertical stabilizer can be treated like a cantilever beam anchored at the fuselage and the same lift and drag assumptions were made. To account for buckling, the tail and stabilizer were then modeled as Euler columns. See Figure 4.7.

Because the bending moment and overall forces will not be as severe on the tail as the wing, the skin will carry most of the load. Due to the reduced loads, it was possible to design a vertical tail without ribs and a horizontal tail composed only of 1/16th balsa.

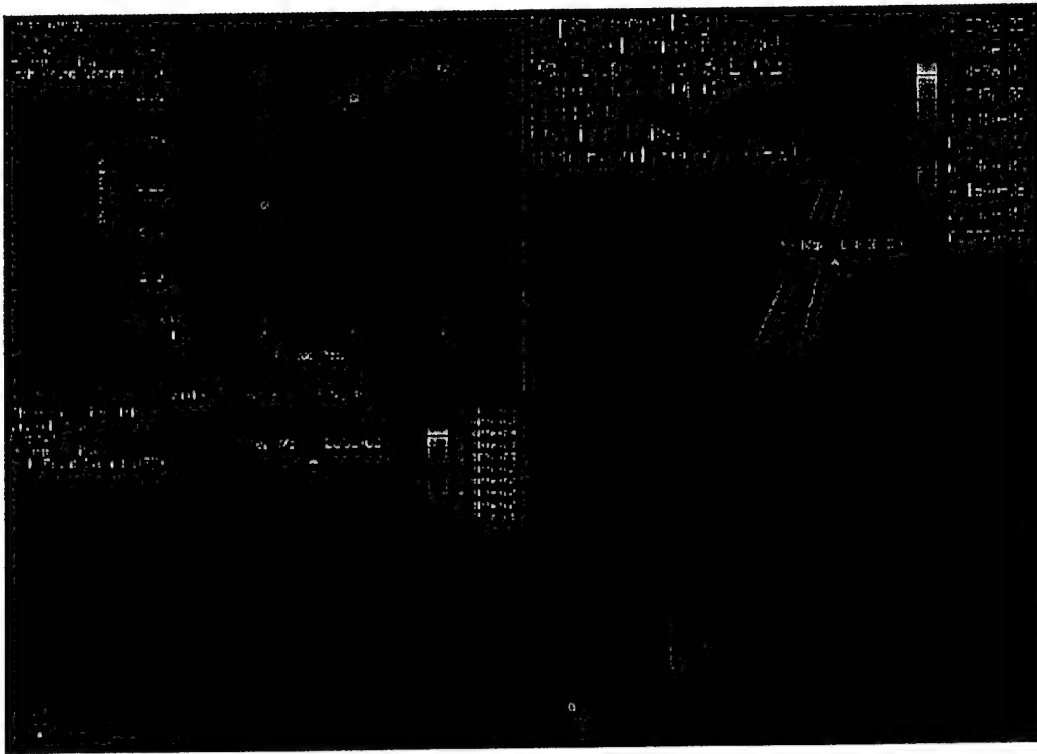


Figure 4.6 : Simulation Results for Fuselage During a 4-g Landing

4.4.5 Landing Gear Structural Design

The tail dragger configuration was chosen for the aircraft. The forward wheels will be located such that a 16-25° angle back from vertical will pass through the forward most and aft most CG points and an angle greater than 25° will pass along the wing plane through the central CG plane to prevent tipping to the left or right. This will prevent the plane from nosing forward or ground looping. The rear wheel was oriented such that it created the greatest lift and propeller clearance while minimizing the aft CG shift of the payload, usually 10-15°.

The preliminary landing gear design sweeps the main gear forward from the CG at an angle of 17.7° and spreads the wheels towards the wings at 42°. When at rest, the plane will sit at a positive angle of attack of 13°.

A Pro/Mechanica model of the landing gear was created to obtain an estimate of the stress and deflection distributions in the landing gear bow. The results of the program are shown in Figure 4.8, in which deflection intensity is examined. Also included in the figure is a picture of a landing gear test specimen. This experiment found the deflection to be in the upper bow area next to the fuselage, which is consistent with the finite element analysis.

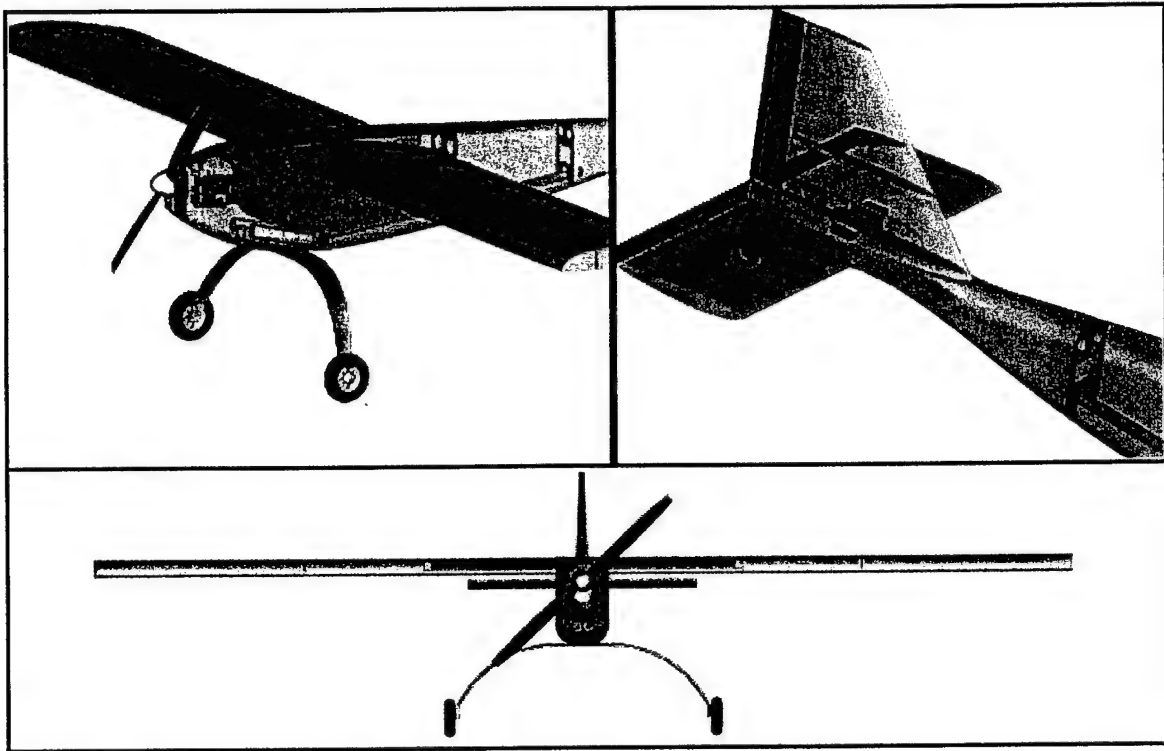


Figure 4.7 Fuselage and Vertical Tail Design

Test gear pieces were constructed and deflection was measured at the failure weight. The plane loaded with water was estimated to weigh a total of 16 pounds. The landing gear was designed with a factor of safety of 1.5, therefore warranting a loading allowance of 24 pounds. An assortment of balsa and fiberglass configurations was used as test specimens. Table 4.3, below, shows the weights of fiberglass, balsa core thicknesses, and carbon fiber mono tape widths used on each test piece. The specimens were built as linear material pieces and were tested at both a 2.5 inch and 10 inch moment arm at various weights up to failure. The final specimen listed was found to meet the weight and loading requirements and represents the gear composition selected.

The landing gear, in a solid spring bow configuration, will be attached to the fuselage using plastic shear bolts to allow disconnection in the event of a crash. A bulkhead will be added inside the fuselage to strengthen the particular attachment area.

The rear landing gear will be streamlined and hidden. The axle and wheel will be built into the base of the tail to reduce drag without inhibiting the aircraft's ability to taxi, takeoff, and land.

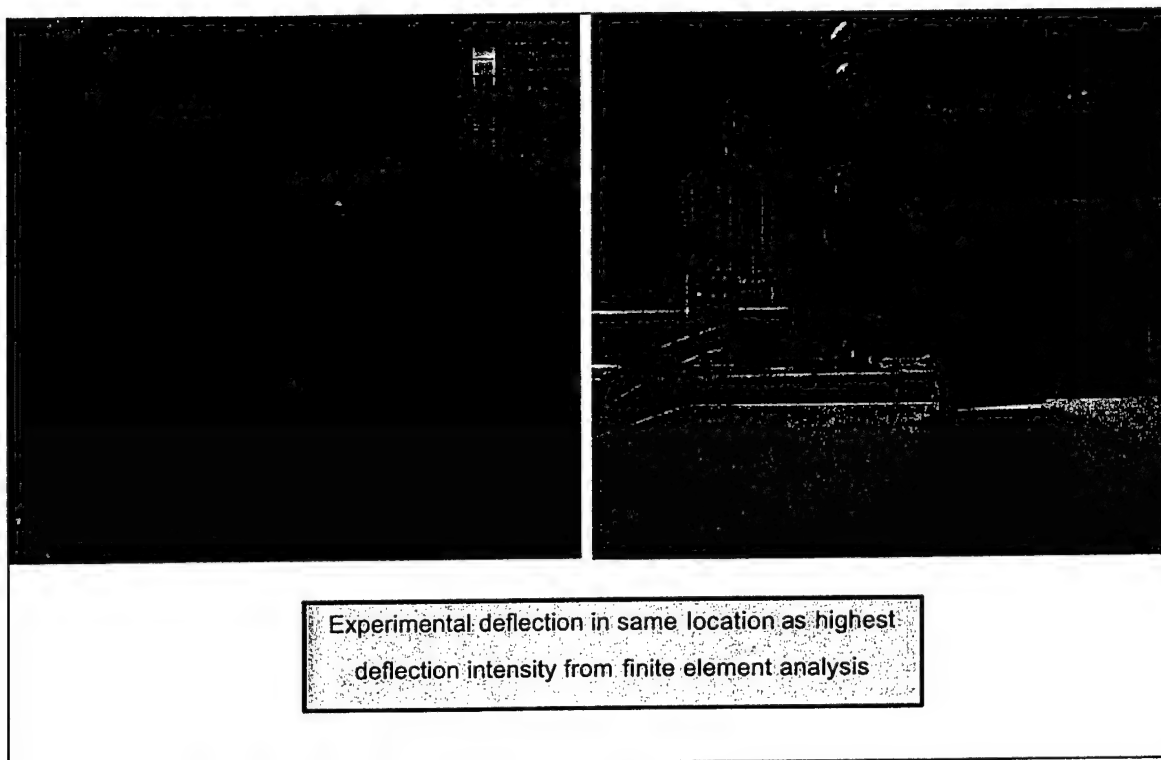


Figure 4.2: Gear Deflection

Table 4.3 Landing Gear Test Specimen Compositions

Glass Wt. [oz]	Glass Fiber Direction	Balsa Core Thickness [in]	Tape Width [in]	Overall Weight [oz]	Failure Wt. [lb] [2.5" Arm]	Deflection [in] [2.5" Arm]	Failure Wt. [lb] [10" Arm]	Deflection [in] [10" Arm]
6	0° [2] 45° [2]	1/4	0.5 [2]	0.92	16.5	1.0	4.8	2.5
3	0° [2] 45° [2]	1/4	0.5 [2]	0.78	9.89	1.0	3.5	2.3
3	0° [4] 45° [2]	1/4	1.0 [2]	1.06	31.5	1.3	7.5	3.5
3	0° [10] 45° [4]	1/8	1.0 [2]	2.15			13.5	3.3
3	0° [6] 45° [4]	3/16	1.0 [2]	2.05			19.1	3.3

4.5 Payload System Preliminary Design

Various aspects of the water payload were investigated, as follows.

1. Problems with changes in the aircraft CG due to water slosh during flight
2. Efficient loading of the plane
3. Efficient water dumping methods

4.5.1 Aircraft CG Movement

As the plane moves, the water in the tank sloshes back and forth causing the center of gravity to shift. Because the payload weighs as much as the unloaded aircraft, any changes in the CG of the payload can potentially destabilize the plane and cause loss of control. To prevent this problem, various designs were investigated by testing different types of baffles and dividers that would restrain the undesirable movement of the water in the tank.

While honeycomb baffling proved very effective, it was discarded as a solution to the water sloshing problem because of its weight, its large volume, and the complexity of making it water-proof. An alternative to honeycomb baffling which was not susceptible to the same issues was designed. Lightweight fiberglass sheets will divide the tank into multiple chambers. A space at the top of the tank will remain un-chambered to allow for a single fill port.

4.5.2 Payload Tank Shape

The water tank is designed to fit in the front quarter of the fuselage with a volume of exactly four liters (245 in³). The shape of the container will be dependent on the geometry of the fuselage and will have a size of approximately 4 by 8 by 12 inches. Glue will bond the tank snugly to the fuselage walls. The tank will taper slightly to a bottom center point, where it will be fitted with the boom valve.

4.5.3 Payload Release Mechanism

A boom was employed to increase the effective head pressure during payload release. While it is true that the longer the boom, the more pressure, there is a point of diminishing return. At this point, the small increase in head does is not worth the increase in boom weight and length. According to the Bernoulli analysis, this length was approximately 18 inches, which was the design decided upon.

The boom was to be attached to the belly of the fuselage. During take off and landing, the boom was to be aligned so that it lies parallel to the fuselage, and then deploys during dumping. A ball valve was designed to open as the boom deployed and close with the boom in the upright position. A servo and gear assembly will actuate this mechanism. A thin fiberglass shell in the shape of an airfoil will cover the boom to minimize drag.

4.5.4 Payload Ground Handling System

The timed extraction of the four liter liquid payload must be accomplished thoroughly and reliably. An inexpensive plunger-type pump made from plumbing hardware was chosen to meet these needs. The loading system will be managed by a two-person team and will load the vessel with a single stroke cycle. Water from the supply tanks will be quickly drawn into the pump chamber with an upward stroke and will be evacuated during the down stroke through a large hose. Check valves will facilitate the intake and exhaust movements during the cycle. At the entry location atop the aircraft, a conical fitting engages a normally-closed flap valve which serves to prevent spillage during flight. Team members will be able to

quickly disconnect the manifold with minimal spillage and will be able to transport the pumping system to the loading area with nominal effort. This concept is shown in Figure 4.9 below.

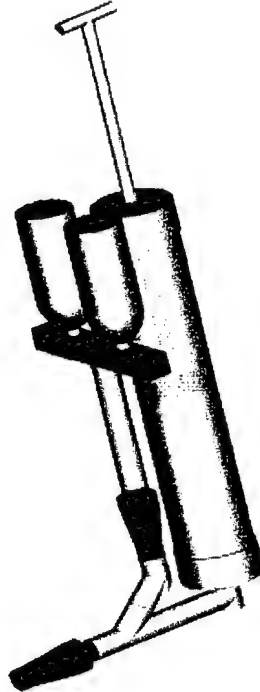


Figure 4.9: Payload Loading System

4.6 Propulsion System Preliminary Design

The propulsion focus during preliminary design was on sizing parameters for the battery packs and propellers. Using an optimization program in conjunction with aerodynamic consideration, optimum power and RAC was found for each wind conditions of 2, 8, 15 and 25 mph winds for take-off.

The program aided in optimizing gear ratio, propeller diameter, pitch to diameter (P/D) ratio, battery size and battery number. By taking into account the weight of the loaded aircraft, parasite drag, and airfoil type, take-off distance could be found by changing the propeller, gear ratio, motor, battery size, and battery number.

4.6.1 Propulsion System Configuration

The propulsion system components needed to be kept as close together as possible in order to minimize power losses. It also needed to be placed in an optimal location for CG control. All parts of the system were located closely to one another, which reduces the amount of power loss in the system. The 40-amp fuse for the quick disarm system was located between the speed controller and motor to avoid overloading the motor.

With the propulsion system components located so closely together, it is crucial to provide a sufficient cooling system. A chin scoop located at the front of the plane just below the nose cone will provide ample cooling for the motor and batteries. A vent will be located behind the nozzle of the water tank allowing for the air to escape.

4.6.2 Motor

Comparison of the AstroFlight Cobalt 40 and Graupner 3300/6 motors proved that although the Cobalt 40 is lighter weight, the efficiency of the Graupner 3300/6 far exceeds that of the AstroFlight motor. This allows for fewer batteries to be used during the competition, which lowers RAC. Not only is the Graupner more efficient, it also creates more thrust than the Cobalt. Thus, the Graupner 3300-6 will be used during the competition.

4.6.3 Battery Number and Size

Battery type was chosen based on several factors. Among the candidates for batteries were Sanyo CP-2400SCR, CP-1300SCR zapped, SR900 Max, and SR650 Max. While each battery provided 1.2 volts, they provided capacities of 2100 milli-amp-hours, 990 mah, 810 mah, and 585 mah, respectively.

Figure 4.10 shows the results of the optimization program for the performance of the propulsion system. These graphs show battery sizing, take-off distance, required thrust, and thrust for various propulsion systems respectively.

Once the size of battery was chosen, the number of batteries needed could be determined. Figure 4.10(b) displays the necessary take-off distance for various wind speeds for 14, 15, or 16 batteries. Because battery weight is so important to the RAC, 16 cells were chosen as the minimum number of cells to power the propulsion system. Though the optimization program shows that 16 cells cannot provide enough power for take-off in 150 feet in the event of no wind, there are options such as lessening payload weight, or overloading the fuse which will provide enough power for take-off in these conditions. Because the Graupner 3300/6 motor can handle upwards of 60 amps, pulling more than 40 amps through the fuse during the few seconds of takeoff exhibits no detrimental repercussions to the motor.

4.6.4 Battery Configuration

The optimum design location of the batteries would have all sixteen together in one pack in order to minimize wire resistance losses. The batteries also needed to be placed as far forward in the fuselage as possible for CG control. It was decided that the batteries would be broken into two smaller packs of eight each due to it not being possible to fit the entire pack in the front of the plane. The two packs will still be placed very close to each other, minimizing loss due to wire resistance.

Endurance and Mission testing were performed on the Sanyo 1300 batteries to ensure that they had enough power to last the two fully loaded take-offs. The second fully loaded take-off was found to be the most critical part of the mission. Results of mission testing can be seen in Figure 4.11. Although not designed to handle more than 30 amps, it was found that the sixteen pack battery would allow for the high

current pulled by the Graupner motor during take-off. Consecutive testing proved that the batteries could withstand multiple runs without any significant loss in capacity.

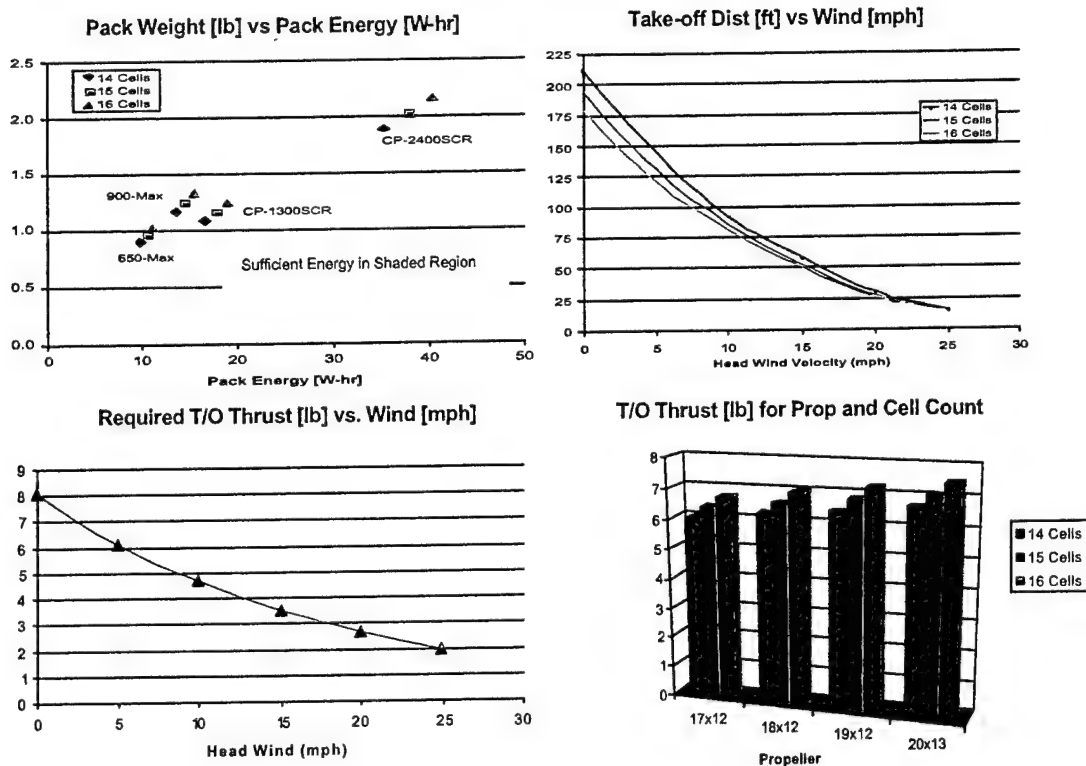


Figure 4.10 : Propulsion System Optimization Results

4.6.5 Propeller and Gearbox Configuration

Several wind and propulsion system scenarios were optimized through simulation programs. Using the program, the propulsion system behavior could be simulated in order to predict the operating conditions for all stages of the flight. Using a flight simulation program a prediction of how the system would perform was created, taking into account all aspects of aircraft weight, aerodynamics, and mission times. Table 4.4 shows several combinations of propulsion system designs to optimize score and efficiency at wind conditions ranging from 2 mph to 25 mph.

Propeller diameter and pitch were optimized using an optimization program. These propellers were then tested on a motor dyno. Initial testing proves that the Bolly 18X12 propeller out performs the APC 18X12 propeller. Therefore, the Bolly propellers will be used during the competition when possible.

Testing between the Motor Electronics Corporation 'Superbox' and the AstroFlight gearbox were conducted based on weight and versatility. The Superbox is much lighter weight and allows multiple gear ratios by allowing the spur gear to be interchanged. A slight modification to the Graupner motor, by way

of a spacer, allowed for the Superbox to be firmly mounted to the motor. It was decided to use the Superbox instead of the AstroFlight because of these advantages over the AstroFlight.

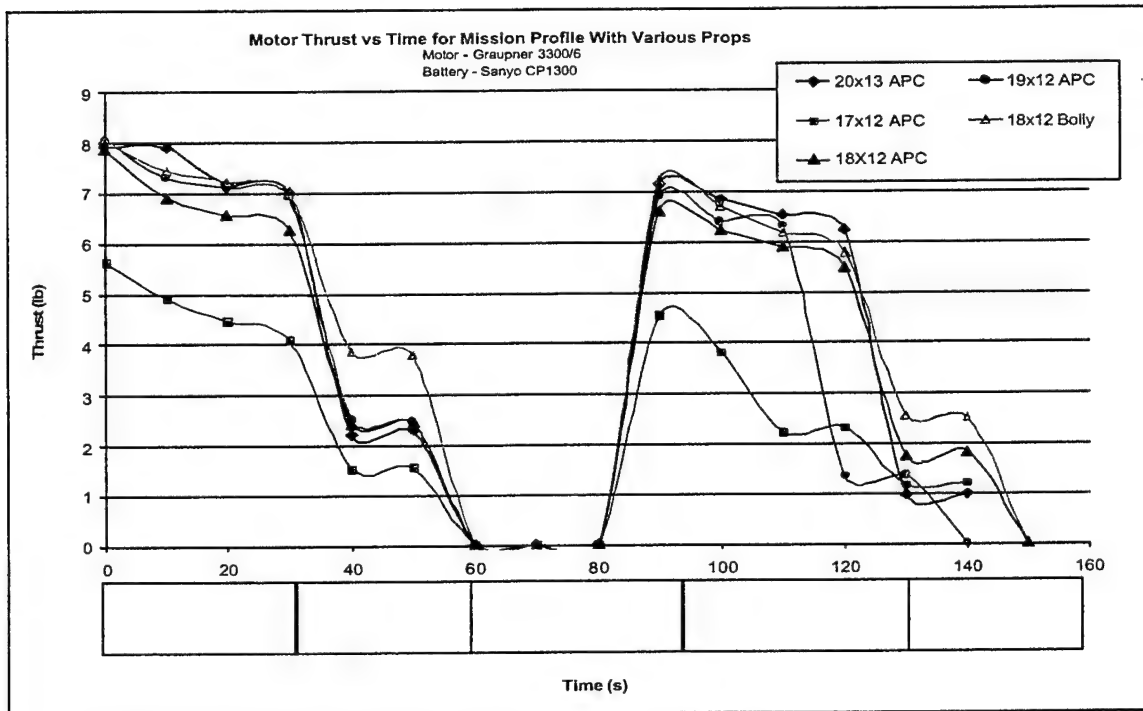


Figure 4.11: Mission Profile Using Optimized Propeller and Gearbox Configurations

These tests show that the following propellers provide enough thrust for both take-offs: APC 20X13E, 19X12E, 18X12E, and Bolly 18X12.

Table 4.4: System Optimization for Various Wind Conditions

Wind Speed (mph)	Battery Number	Propeller Diameter (in)	Propeller Pitch (in)	P/D Ratio	Gear Ratio	Take-off Distance (ft)	Optimum Cruise Velocity (ft/s)
2	16	19	13	.68	1.7	150	78
2	16	18	13	.72	1.5	150	71
8	16	15	13	.87	1.2	138	82
8	16	16	15	.94	1.3	123	81
15	16	15	13	.87	1.8	111	78
15	16	15	14	.93	1.3	75	82
15	16	16	15	.94	1.3	67	81
25	16	15	14	.93	1.3	22	84

25	16	16	15	.94	1.3	18	84
25	16	17	15	.88	1.4	18	84

4.6.6 Speed Controller

After testing of the Jeti JES60 and AstroFlight speed controllers, it was determined that the two were very close in efficiency. Testing was conducted by attaching a thermocouple to the speed controller and measuring temperature change while running a steady current of 40 amps through it. Although the Jeti JES60 is smaller and lighter weight, the motor breaking feature caused difficulties during testing of larger propellers. Turning off the breaking option only allowed for use of half of the radio throttle control. It was decided to use the AstroFlight 204D model because it is more reliable than the Jeti model.

4.6.7 Disarming System Design

The outer housing is 1 ½ inches in diameter and is made of fiberglass. In the center of the circular top is a slot that is only slightly larger than the actual 40 amp fuse. The top surface of the fuse will be flush with the top of the fuse disarming housing as well as the surface of the airplane. The sponge (which acts like a spring) is placed between the plastic circular top and the plastic stationary plate at the upper and lower interface, respectively. The sponge is held into place on the sides by a thin-walled plastic cylinder. Connected to the bottom of the stationary plate are two connectors that will receive the fuse blades when the fuse is inserted. The connectors will be held in by a high strength glue or epoxy. In order to make the insertion of the fuse into the connectors easier, the inlet to each connector has been tapered, which will guide the fuse blades into the connectors. The top of the housing is allowed to move within the cylinder. To insert the fuse, simply place the fuse into the slot and press on the top surface of the fuse until the blades are secure in the connectors. To remove the fuse, press on the circular top being careful not to obstruct the fuse. The top slides past the fuse exposing its sides. The fuse will be gripped with fingers and pulled.

5 Detail Design

After preliminary sizing and component arrangement was complete,

5.1 Configuration Details

Table 5.1: Longitudinal Stability Coefficients Estimation

Longitudinal Stability Coefficients Estimation						
	X-Force Derivatives		Z-Force Derivatives		Pitching Moment Derivatives	
α	C_{x_α}	0.342			C_{m_α}	-1.221
α^*			$C_{z_{\alpha^*}}$	-1.208	$C_{m_{\alpha^*}}$	-3.624
q			C_{z_q}	-3.256	C_{m_q}	-9.768

δ_e			$Cz_{\delta e}$	-0.261	$Cm_{\delta e}$	-0.783
Lateral Stability Coefficients Estimation						
	Y-Force Derivatives		Yawing Moment Derivatives		Rolling Moment Derivatives	
β	Cy_β	-0.252	Cn_β	0.098	Cl_β	-4.666
p	Cy_p	0	Cn_p	-0.061	Cl_r	0.129
r	Cy_r	0.153	Cn_r	-0.059	Cl_δ	0.00721
δ_r	Cy_δ	0.052	Cn_δ	-0.020		

5.2 Projected Performance

Table 5.2: Projected Performance Values of Each Segment of the Fire Bomber Flight

Mission Components For Fire Flight	# Times Performed	Time Spent	Distance	Velocity
Takeoff: Loaded	2	4.43 s	86.52 ft	50.95 ft/s
Climb: Loaded	2	6.25 s		54.47 ft/s
Turn 1: Loaded	2	9.6 s		
Acceleration: Unloading	2	10.09 s	721.13 ft	
360° Turn	2	3.6 s	294.88 ft	
Cruise: Unloaded	2	8.7 s		82 ft/s
Turn 2: Unloaded	2	1.8 s	147.44 ft	
Slow Down: Unloaded	2	5.51 s	359.67 ft	
Ground Time	1	30 s		
TOTAL TIME	—	1.33 min		

The predicted score for the fire mission is given below. This assumes a 100% on report score.

$$Score = \frac{DF \cdot Payload\ Weight}{Time \cdot RAC} = \frac{2 \cdot 17.6}{1.33 \cdot 6.758} = 7.83$$

5.3 Structural Details

5.3.1 Wing Details

• Skin Makeup

For the main wing, the balsa and fiberglass method of monocoque construction was used. The wing was built using 1/16 inch thick competition balsa and fiberglass coating. The glass thickness was transitioned to a lighter ply makeup at approximately 75% of the span from the fuselage. At the inner three-quarters of wingspan, the inner and outer skin of the balsa sandwich was coated with two ounce fiberglass sheets. For the end quarter of the wing span, two layers of 0.6 ounce fiberglass was used to coat the outside balsa surface and 1 layer of 0.6 ounce was used to coat the inside balsa surface.

- **Internal Structure**

The internal structure of each side of the wing consists of three ribs, three shear webs, and the wing-to-fuselage attachment components. The principal shear web is located at approximately quarter-chord and is constructed of 1/16 inch balsa cut along the end-grain. Another web is located just forward of the flaperon hinge, while the third is located just aft of the hinge. The shear webs are used to distribute the loads, add strength, and maintain flexibility of the wing. The inboard rib is made of plywood, while the three internal ribs and closeout rib are made of 1/16 inch balsa.

- **Connection Method**

The wing is attached to the fuselage by a pin that extends outward from the wing into the fuselage. A connecting carbon fiber rod extending from the wing inserts into a tube that spans the fuselage. The rod runs about three inches spanwise into the wing. A plastic fastener on the aft end of the wing is used to further secure the wing into place. This pin is used for anti-rotation and will also function to "snap" the wing into the fuselage. Clear packing tape additionally binds the wing to the fuselage.

- **Flaperon**

The flaperon combines the function of an aileron and a flap. The flaperon was placed at 10% of the chord length and is attached to the wing by a strip of Kevlar sandwiched between layers of fiberglass.

- **Servo Placement and Design for Flaperon**

The flaperon servos are placed on the middle ribs on each of the wing sides. They are located completely inside the wing to eliminate undesirable drag. The servos are accessible through service hatches on the upper surface of the wing.

5.3.2 Fuselage Details

Because of the RAC measuring the maximum points of the fuselage, the optimized fuselage shape was a square or a rectangular shape to maximize the volume. Since the major concern of evacuating the water from the fuselage during flight was maintaining as much head pressure as possible, a rectangular shape with more depth than width was chosen. However, the corners of the fuselage are rounded, and parts are blended to decrease drag and to create a sleeker shape. In determining the size of the fuselage, the housing of all of the components, especially the motor, batteries, and water tank, were of utmost importance. The fuselage shape was determined from the water tank design; thus, the cross-sectional area and, to some extent, the length of the plane were established by the tank. After building the fuselage shape and size around the tank, the fuselage was lengthened to encompass the motor, batteries, boom, and servos. The propulsion items were placed so as to minimize the wire lengths between components as well as to keep the CG of the plane in the front. A chin scoop was decided upon in order to help the cooling of the closely packed propulsion components. A side hinged engine access door is also located on the top of the fuselage to allow an entrance to the engine components.

5.3.3 Empennage Details

- **Horizontal Tail Details**

The horizontal tail is a balsa wood build-up with a Monokote coating to give it a smooth surface. The balsa wood build-up was chosen because of its light weight properties. Because the horizontal tail is not subjected to as high of stresses as the wing and does not have to be as strong and rigid, the mold method using balsa and fiberglass was not needed. This method can be constructed quickly and easily and does not require a fiberglass coating or mold.

The horizontal tail is attached to the plane through a hole in the fuselage. Glue will be used to permanently connect the tail securely into the fuselage cavity. The fuselage will be reinforced with 1/8" balsa doubler around the juncture. The elevator hinge will be a skin Monokote hinge spanning across the length of the horizontal tail. The servo is located in the interior of the horizontal tail to prevent drag.

- **Vertical Tail Details**

The vertical tail will be constructed with the fuselage. It will be constructed during the molding process of the fuselage, but will transition into lighter glass weight. Competition balsa (1/16 inch thickness) will be sandwiched between layers of 0.6 ounce fiberglass. The hinge rotates using flanges; three flanges are located on the top of the rudder and a connecting pin attaches the top and bottom portions of the rudder together. The tail wheel is also located on the bottom of the rudder. Servos for the rudder are completely enclosed in the interior of the back portion of the plane.

5.3.4 Landing Gear Details

Multiple lay-up variations for the landing gear were tested to failure in order to collect data. A solid spring bow landing gear configuration swept forward 30° was decided upon. A mold for the landing gear configuration was created in order to test the specific design with the maximum weight of the plane. Looking at a front view of the plane, the two main front tires will be located 42° from the centerline and at a 17.7° angle from a line drawn through the CG to a line perpendicular to the plane through the wheel. The front tires have a diameter of 2.5 inches and the rear tire's diameter is 1.25 inches.

5.4 Propulsion System Details

The propulsion team performed several tests on the suggested preliminary design concepts. Results of these tests are shown below in the Component Selection section.

5.4.1 Component Selection

Each component of the propulsion system was tested for efficiency, endurance, power, and reliability. The results of these tests are as follows:

Battery Pack

The Sanyo CP-1300SCR battery will be used during the competition. Two eight celled packs, connected with a six inch lead, will be placed in the fuselage under the water tank.

Propeller

Depending on the wind speed, a 20X13E, 19X12E, 18X12E, or Bolly 18X12 will be used for the Fire Bomber mission. Smaller diameter propellers such as a 15.5X13 Bolly or a 16X10 will be used for the Ferry Run, when thrust is not as important as speed.

5.4.2 System Architecture

The general setup for various propulsion systems will consist of the same battery configuration, speed controller, fuse, and motor. The propeller and gearbox can be altered prior to each mission to optimize flight at any wind condition.

Table 5.3: Stability Coefficient Characteristics

Longitudinal Stability Coefficients Estimation						
	X-Force Derivatives		Z-Force Derivatives		Pitching Moment Derivatives	
α	C_{x_α}	0.342			C_{m_α}	-1.221
$\dot{\alpha}$			$C_{z_{\dot{\alpha}}}$	-1.208	$C_{m_{\dot{\alpha}}}$	-3.624
q			C_{z_q}	-3.256	C_{m_q}	-9.768
δ_e			$C_{z_{\delta_e}}$	-0.261	$C_{m_{\delta_e}}$	-0.783
Lateral Stability Coefficients Estimation						
	Y-Force Derivatives		Yawing Moment Derivatives		Rolling Moment Derivatives	
β	C_{y_β}	-0.252	C_{n_β}	0.098	C_{l_β}	-4.666
p	C_{y_p}	0	C_{n_p}	-0.061	C_{l_r}	0.129
r	C_{y_r}	0.153	C_{n_r}	-0.059	$C_{l_{\dot{\delta}}}$	0.00721
δ_r	$C_{y_{\delta_r}}$	0.052	$C_{n_{\delta_r}}$	-0.020		

5.5 RAC Calculation/Weight Statement

Coefficient	Description	Computation	Value	Total
MEW	Manufacturer's Empty Weight	300*Weight	8.2 lb	2460
REP	Rated Engine Power	(1+.25*(# engines-1)) *Total Battery Weight (lbs)	1 Engine 1.24 lb Battery	1860
MFHR	Wings	10 hr/ft ²	10 in Chord 75 in Span	52.08
	Flaperon	5 hr	1.5	7.5

	Fuselage	20 hr/ft ³	43" x 5" x 6.95"	17.295
	Empenage (Vertical)	10 hour	1 Vertical	10
	Empenage (Horizontal)	10 hour	1 Horizontal	10
	Flight Systems	5 hr	5 Servos	25
		Σ WBS hours	20	2437.5
RAC	Rated Aircraft Cost	$(A*MEW+B*REP+C*MFHR)/1000$		6.758

FIGURE 5.2: Rated Aircraft Cost Calculations

5.6 Aircraft Configuration Summary

Given below is a table of all of the final aircraft dimensions.

Table 5.5: Final Plane Parameters

Fuselage		Weight Statement	
Length (ft)	4	Airframe (lb)	7.018
Width (ft)	0.4219	Propulsion System (lb)	2.68
Height (ft)	0.5792	Control System (lb)	0.46
Wing		Payload (lb)	8.8
Area (ft ²)	5.2	Empty Weight (lb)	8.258
Span (ft)	6.45	Gross Weight (lb)	17.058
Aspect Ratio	8	Systems	
Flaperon Area (ft ²)	1.043	Radio	Futaba T8UAP (PCM)
Airfoil	SD7062 with flaps	Servos	[4] JR DS3421SA
Empennage		Speed Controller	AstroFlight 204D
Horizontal Tail Area (ft ²)	0.9375	Battery Type	Sanyo CP-1300SCR
Horizontal Tail Airfoil	NACA 2410	Battery Configuration	18 cells, 2 packs
Vertical Tail Area (ft ²)	0.6736	Motor	Graupner 3300-6
Vertical Tail Airfoil	NACA 0009	Gear Ratio	1.82 : 1
Elevator Area (in ²)	27	Propeller	18x12 Bolly
Rudder Area (in ²)	9.7	Landing Gear	Bow-type Taildragger

5.7 Drawing Package

6 Manufacturing Plan and Processes

The Figures of Merit used dictated the decisions that were made about the manufacturing processes. The Figures of Merit were chosen to help in distinguishing between the various methods of manufacturing available to the team by highlighting the advantages and disadvantages associated with the different techniques. This process allowed the team to select the manufacturing process that was most ideal for our selected aircraft design, time schedule, and skill level. The Figures of Merit chosen are discussed below in more detail. Available processes are evaluated using these criteria and given a weighting factor.

6.1 Manufacturing Process Figures of Merit

- Required Skills: While a design may be feasible in its conceptual phase, it must also be feasible during its manufacture and construction. The manufacturing process must be within the skill level of the team.
- Accuracy and Surface Finish: This criterion is important in the transition from the prototype to the final phase. It will allow the team to replace or improve parts as needed. Each part must be able to be accurately repeated in the event of a part needing to be replacement.
- Cost: The element of cost is a limiting factor in any design. The manufacturing process selected must be financially feasible and appropriate for the given budget. The materials may vary for the different manufacturing techniques, and the cost of these items were considered.
- Fabrication Time: The ability to meet the deadlines of the project is critical to the success of the airplane. The manufacturing process chosen must be able to be completed within the allotted time. This process must provide adequate time for the prototype and final aircraft to be manufactured while still allowing time for testing and improvements.

6.2 Process Alternatives

During the conceptual design phase, a monocoque construction scheme was chosen which utilized a composite/balsa sandwich structure. Different monocoque manufacturing techniques were considered in order to optimize this type of design.

- Conventional Build Up: This process involves the manufacture of the airplane by building up the individual parts by balsa wood and applying layers of fiberglass. This process does not require the building of molds and produces the lightest parts. While this process has a more rapid construction speed than the molded method, it is lacking in repeatability and the ability to keep true to the original airfoil.
- Layup Over Plug: This process involves the construction of the plug using foam and fiberglass. The skins are layed-up over the plug and then removed. This process achieves an accurate inner mold line, but it produces an unfavorable rough outer mold line surface.

- **Full Mold:** Individual molds are constructed and used to build the components by laying sheets of fiber glass and balsa wood into the mold. This method is highly repeatable, produces an accurate airfoil, and creates smooth and accurate outer mold line. The construction of the mold is a time intensive process but gives the part the most strength.

6.3 Process Selection

After evaluating the different manufacturing alternatives based on the selected manufacturing Figures of Merit, the full mold process of manufacturing was chosen for the wing, fuselage, and vertical stabilizer portion of the empennage because it provided the highest repeatability, trueness to original dimensions, and an accurate outer mold line. The method of manufacturing chosen for the horizontal component of the empennage was the built-up method because this section does not require as much strength. The built-up process creates a lighter part while saving time and labor. The landing gear required a curved shape that was lightweight but could also support the applied load. The manufacturing method chosen to meet these requirements was laying up fiberglass and shaped balsa over a curved piece of foam and then utilizing a vacuum bag. This process was selected because it did not require the construction of a mold, which saved time, and provided the curvature needed within tolerable dimensions.

Skills Matrix

The skill matrix below shows the important skills necessary for the completion of the project. The number of team members possessing the identified skills are shown below, as well as the importance of each skill, ranging from 0 to 2, on the manufacturing of the wing, fuselage, empennage, and landing gear.

Table 5.6: Skills Matrix

Skill	# of Team Members	Wing	Fuselage	Empennage	Landing Gear
RAC analysis	3	2	2	2	2
CNC Foam Cutting	3	2	2	2	1
Composite Layups	12	2	2	2	2
Woodworking	6	1	1	1	0
Propulsion System Analysis	4	2	2	1	1
CNC Machining	1	0	1	0	0
Technical Writing	5	2	2	2	2
Conventional Balsa Structures	1	0	0	2	0
Pro Engineer Modeling	3	2	2	2	0

6.4 6.3 Manufacturing Plan

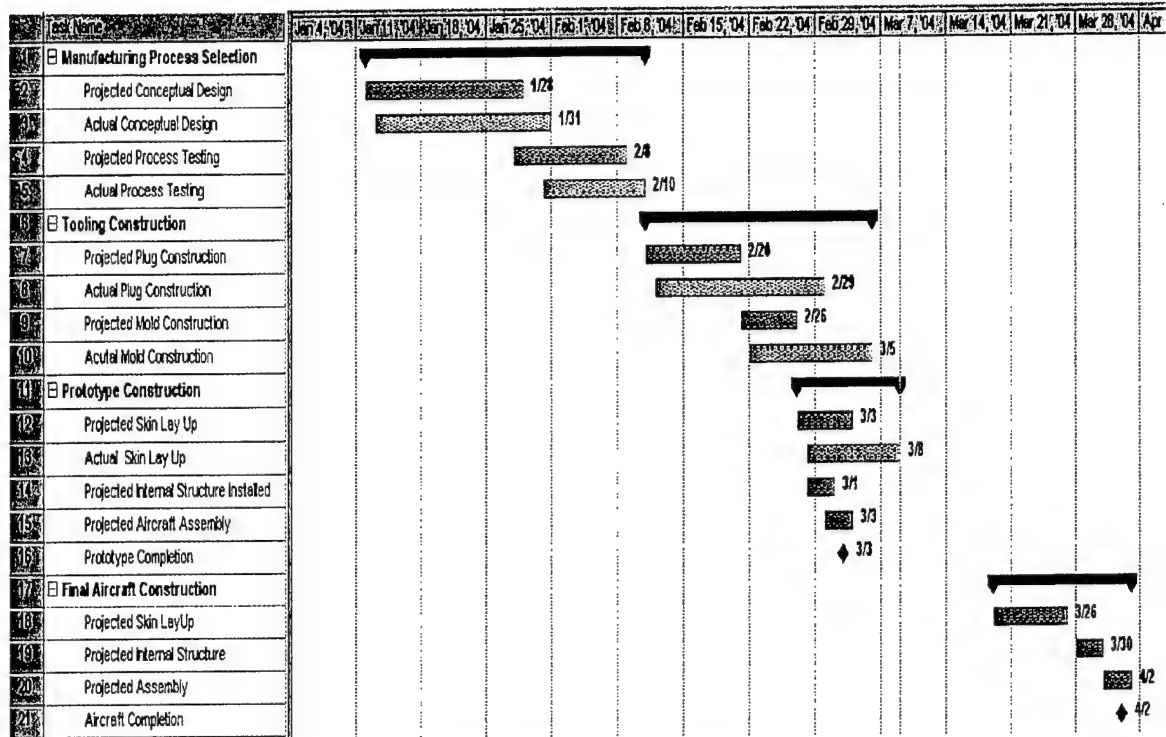


Figure 6.1: Manufacturing Waterfall Timeline

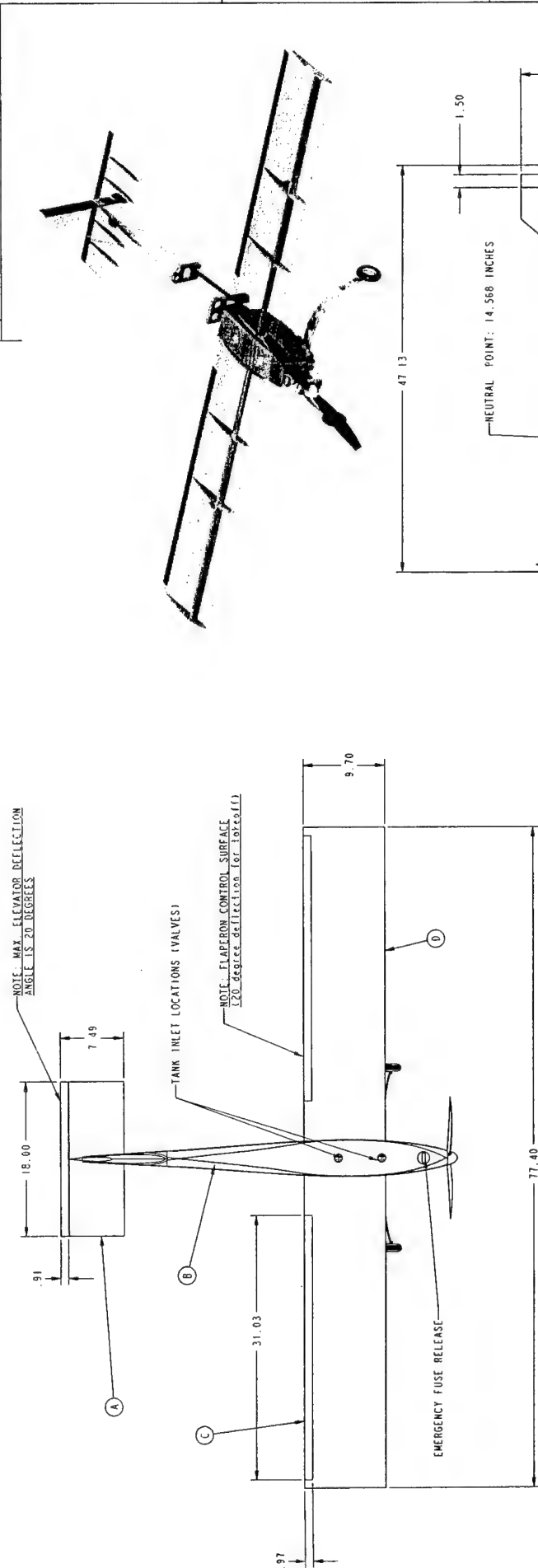
7 Testing Plan

7.1 Testing Plan

Many design tradeoffs can only be verified during actual flight testing. These tests prove or disprove that all aircraft systems are working together correctly as well as working in harmony with the designer's intent. During these tests safety to testing personnel is paramount precautions are taken when ever the aircraft motor is armed. Also in accordance with safety checklists are developed to insure that the aircraft is flight worthy. The test procedures are designed to step up in complexity culminating in the first full-up mission sortie.

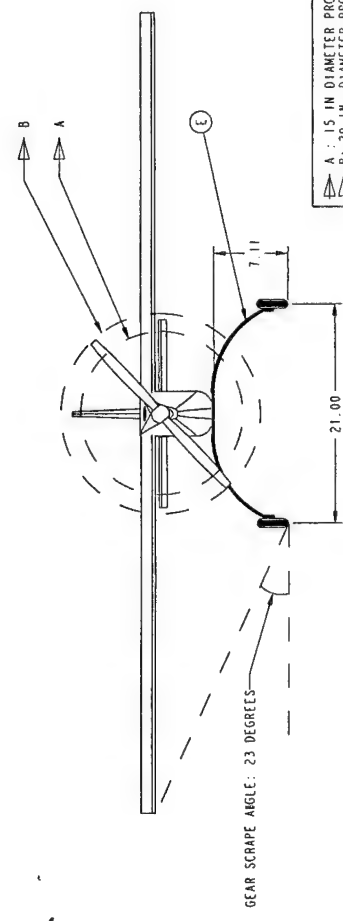
7.2 Test Cards

Individual tests of aircraft systems such as the propulsion system and the major structural components carried out before final assembly. These systems are tested again once they are integrated into the prototype.



PRIMARY COMPONENT LIST	
DESCRIPTION	MATERIAL
A HORIZONTAL TAIL ASSEMBLY	ALUMINUM 6061-T6
B FUSELAGE ASSEMBLY	ALUMINUM 6061-T6
C RIGHT WING ASSEMBLY	ALUMINUM 6061-T6
D LEFT WING ASSEMBLY	ALUMINUM 6061-T6
E MAIN GEAR ASSEMBLY	ALUMINUM 6061-T6

CG LOCATION:
10.75 INCHES LOADED
10.25 INCHES EMPTY



A : 15 IN DIAMETER PROP. FOR FERRY MISSION
B : 20 IN DIAMETER PROP. FOR WATER DROP MISSION
(NOTE: PROPOSED; MAY BE MODIFIED AFTER ADDITIONAL TESTING)

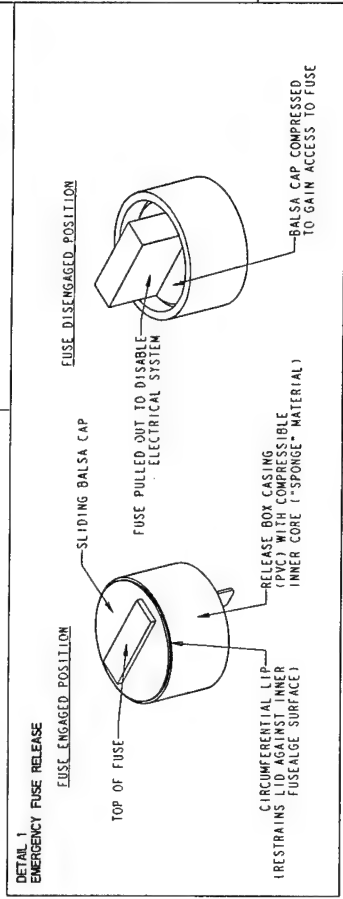


OSPRAY
PROJECT TITLE
TEAM LEAD: M. STUTZMAN
STRUCTURAL LEAD: J. SLATON
DRAWING BY: B. FISCHER
FACULTY ADVISOR: DR. A. ARENA

NOTE: ALL DIMENSIONS ARE GIVEN IN INCHES.
PROP. LENGTH IS NOT TO SCALE.

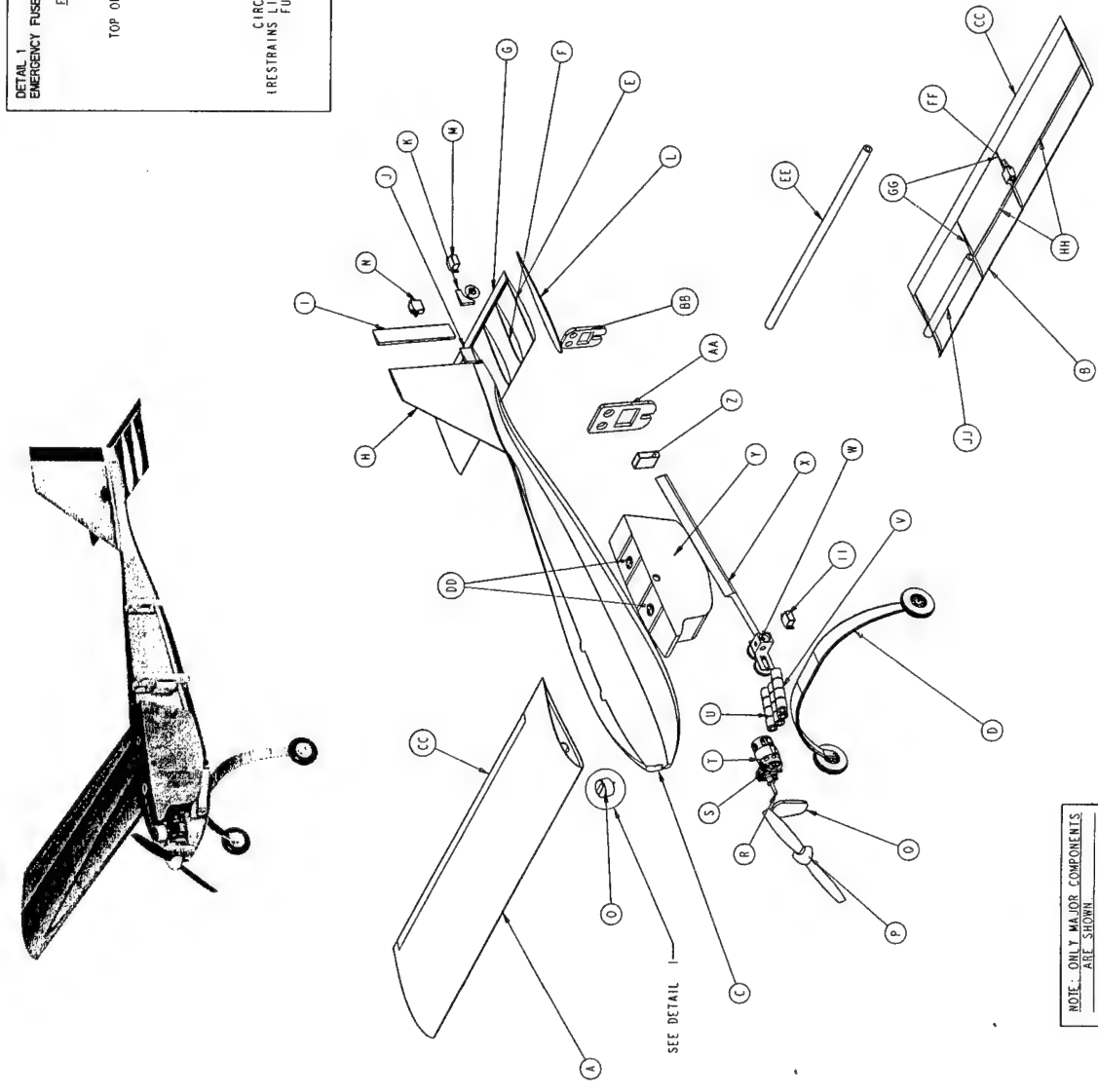
DESIGN REVISION 3
DATE OF APPROVAL: 2-22-04
PAGE 1 OF 5

FLIGHT CONFIGURATION



COMPONENT LIST	DESCRIPTION
A	RIGHT WING ASSEMBLY
B	LEFT WING ASSEMBLY
C	FUSELAGE
D	MAIN GEAR ASSEMBLY
E	HORIZONTAL STABILIZER
F	HORIZONTAL STAB. RIB
G	ELEVATOR
H	VERTICAL STABILIZER
I	RUDDER
J	VERTICAL SUPPORT
K	REAR WHEEL ASSEMBLY
L	VERTICAL STAB. BULKHEAD
M	ELEVATOR SERVO
N	RUDDER SERVO
O	EMERGENCY FUSE
P	PROPELLER AND SPINNER
Q	FORWARD BULKHEAD
R	PROPELLER SHAFT
S	GEAR BOX
T	ENGINE
U	RIGHT SIDE BATTERY PACK
V	LEFT SIDE BATTERY PACK
W	TANK VALVE
X	BOOM

COMPONENT LIST	DESCRIPTION
Y	PAYLOAD TANK
Z	RECEIVER PACK
AA	MID. BULKHEAD
BB	REAR BULKHEAD
CC	FLAPERON
DD	TANK INLET / VALVE
EE	WING PASS-THROUGH SPAR
FF	FLAPERON SERVO
GG	WING RIB
HH	SHEAR WEB
II	BOOM SERVO
JJ	SPAR CONNECTION TUBE



OSPRAY

TEAM LEAD: H. STUTZMAN

DESIGNED BY: J. SLATON

DRAWN BY: R. FISCHER

FACULTY ADVISOR: A. F. H. A.

NOTE: ALL DIMENSIONS ARE GIVEN IN INCHES.

NOTE: ONLY MAJOR COMPONENTS SHOWN.

DESIGN REVISION 3

DATE OF APPROVAL: 2-22-04

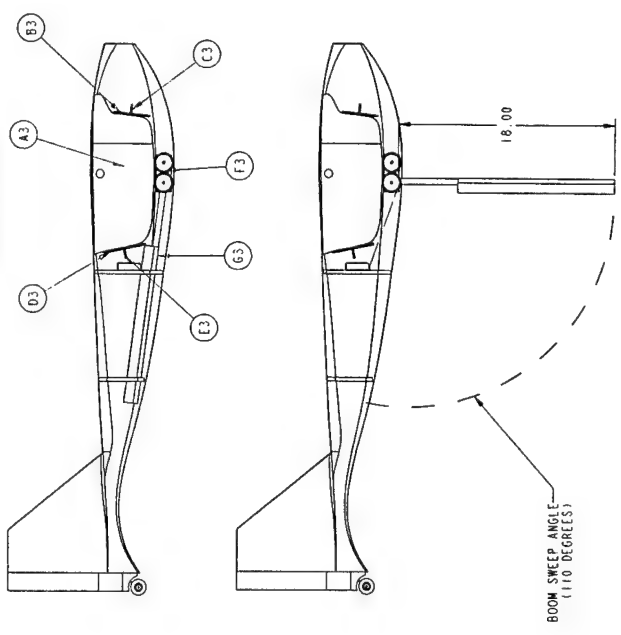
EXPLODED VIEW

OKLAHOMA STATE UNIVERSITY ORANGE TEAM

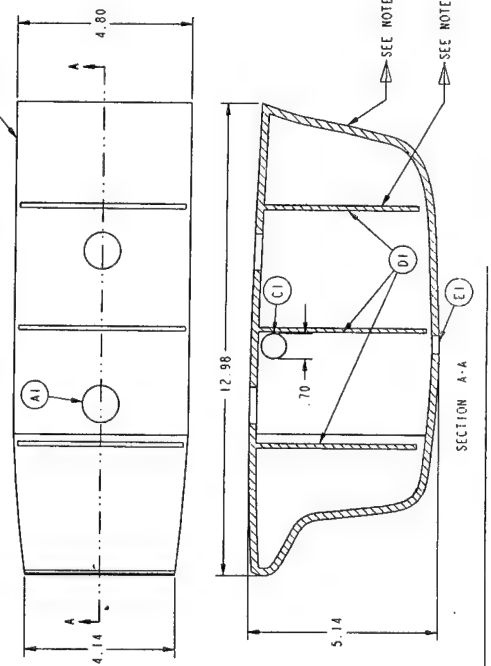
CESSNA DESIGN/BUILD/FLY 2004

NOTE: ONLY MAJOR COMPONENTS ARE SHOWN.

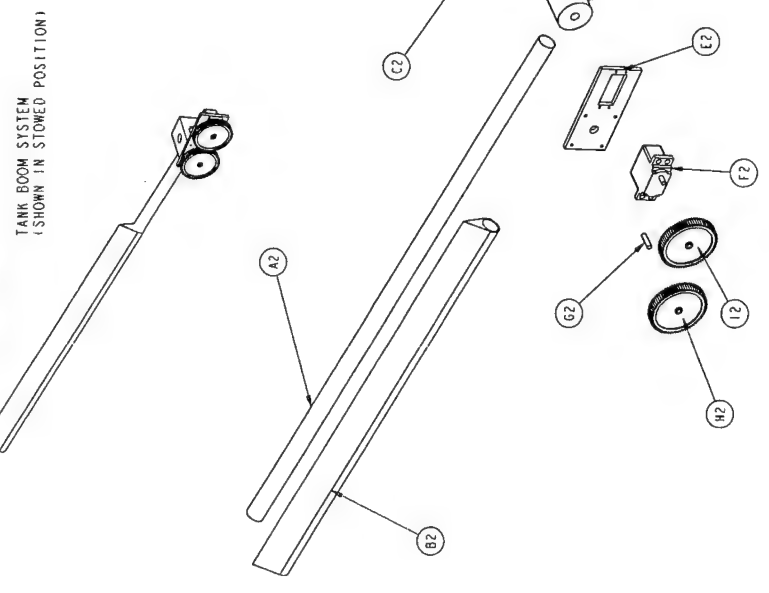
PAYLOAD SYSTEM



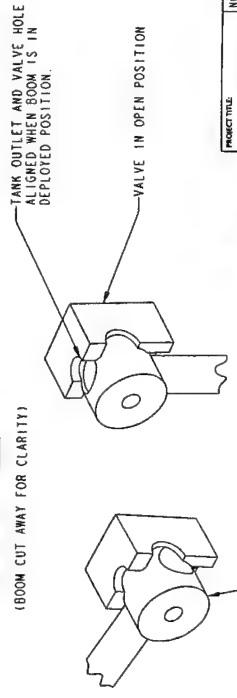
TANK DETAIL



BOOM SYSTEM



BOOM VALVE DETAIL



TANK DETAIL	
DESCRIPTION	MATERIAL
A1 INLET LOCATION	H.D.P.E.
B1 TANK BODY	FIBERGLASS
C1 WING PASS THROUGH SPAR	CARBON FIBER
D1 VERTICAL BAFFLES	FIBERGLASS
E1 TANK OUTLET LOCATION	-----
NOTE 1: TANK BODY CONSISTS OF 3 PLY LAYERS OF FIBERGLASS.	
NOTE 2: VERTICAL BAFFLES CONSIST OF 2 PLY LAYERS OF FIBERGLASS WITH Balsa CORE.	
PLY CONFIGURATION: 1 LAYER OF 2 OZ. Balsa CORE 1 LAYER OF 2 OZ.	

BOOM SYSTEM COMPONENTS	
DESCRIPTION	MATERIAL
A2 BOOM TUBE	LEXAN
B2 BOOM SHEATH	FIBERGLASS
C2 VALVE BODY	NYLON
D2 VALVE CYLINDER	NYLON
E2 SERVO FACE PLATE	1/8" ALUMINUM WITH 2" O.D. GLASS FILLER
F2 SERVO	JR DS 3421
G2 GEAR MOUNTING PIN	NYLON
H2 BOOM GEAR	NYLON
I2 SERVO GEAR	NYLON
NOTE 3: VALVE CYLINDER IS PRESSURE FIT IN VALVE BODY WITH GREASE TO FORM SEAL.	
NOTE 4: VALVE BODY IS MOUNTED DIRECTLY TO TANK OUTLET.	

PAYLOAD SYSTEM COMPONENTS	
DESCRIPTION	MATERIAL
A3 PAYLOAD TANK	FIBERGLASS
B3 TANK FORWARD RESTRAINT	FIBERGLASS
C3 SUPPORT WEB	Balsa
D3 TANK REAR RESTRAINT	FIBERGLASS
E3 SUPPORT WEB	Balsa
F3 BOOM SERVO/VALVE	-----
G3 BOOM	-----
TANK IS MOUNTED FLUSH AGAINST SIDES OF FUSELAGE. FILLER FOAM IS ADDED IN THIS REGION TO FURTHER RESTRAIN TANK.	

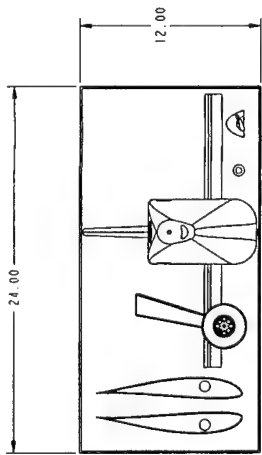
PROJECT TITLE: **OSPRAY**
TEAM LEAD: **JOHN STUTTMAN**
TEAM MEMBER: **J. SLATON**
DRAWING BY: **R. FISCHER**
FACULTY/ADVISOR: **1/2 ARENA**

NOTE: ALL DIMENSIONS ARE GIVEN IN INCHES.
ONLY PAYLOAD COMPONENTS ARE SHOWN.

OKLAHOMA STATE UNIVERSITY ORANGE TEAM
CESSNA DESIGN/BUILD/FLY 2004

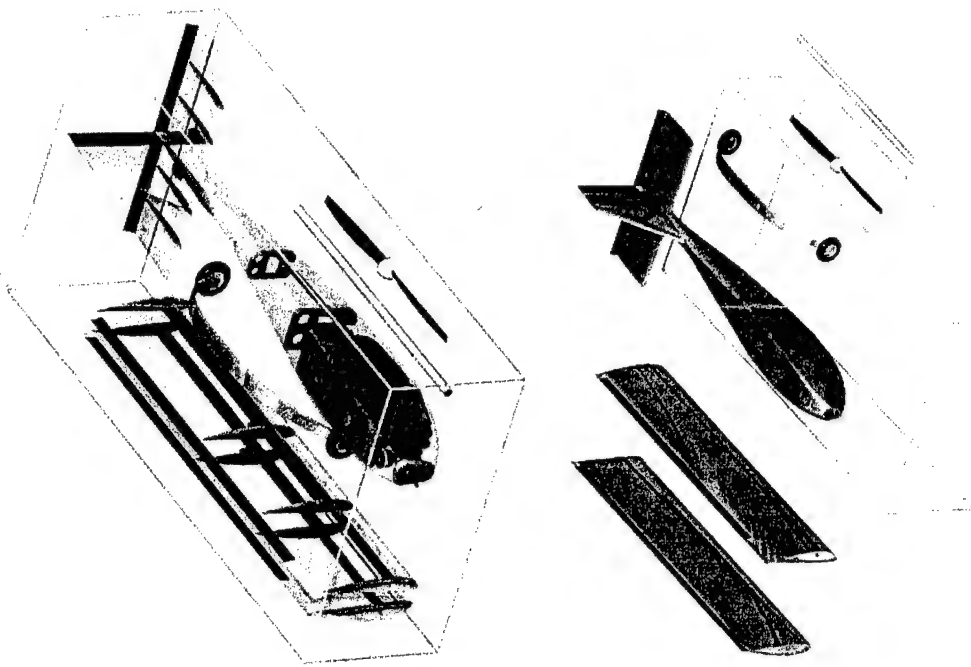
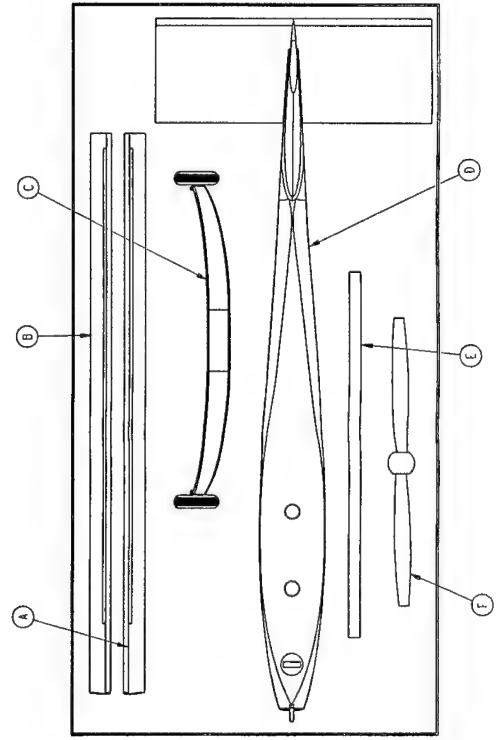
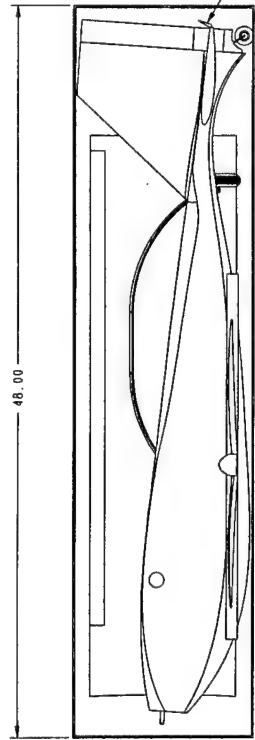
PAYLOAD SYSTEM

DESIGN REVISION 3 C-1
DATE OF APPROVAL: 2-22-04



COMPONENT LIST		
DESCRIPTION		MATERIAL
A LEFT WING ASSEMBLY		FIBERGLASS/BALSA
B RIGHT WING ASSEMBLY		FIBERGLASS/BALSA
C MAIN GEAR ASSEMBLY		FIBERGLASS/ CARBON FIBER
D FUSELAGE ASSEMBLY		FIBERGLASS/BALSA
E WING PASS-THROUGH SPAR		CARBON FIBER
F PROPELLER AND SPINNER		CARBON FIBER/ PLASTIC

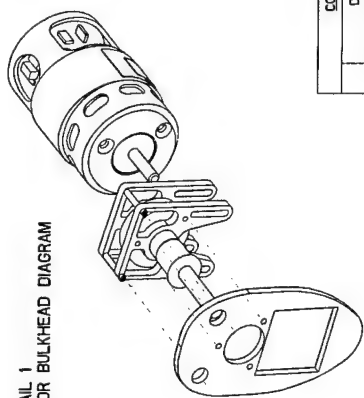
NOTE 1: ELEVATOR DEFLECTED 90 DEGREES FOR STOWED POSITION.



PROJECT TITLE: OSPRAY		NOTE: ALL DIMENSIONS ARE GIVEN IN INCHES.	
TEAM LEAD: M. STUTZMAN	DESIGN REVISION 3	OKLAHOMA STATE UNIVERSITY ORANGE TEAM CESSNA DESIGN/BUILD/FLY 2004	
STRUCTURE LECT: J. SLATON	DATE OF APPROVAL: 2-22-04	SHEET: C-1	
DRAWING: R. FISCHER	PAGE 4 OF 5		
FACULTY ADVISOR: DR. A. APENA			

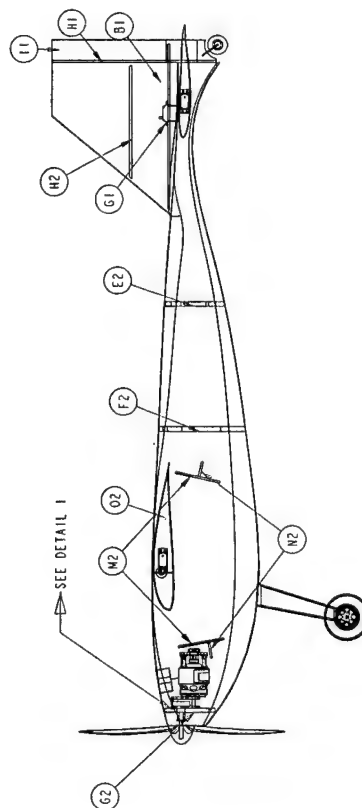
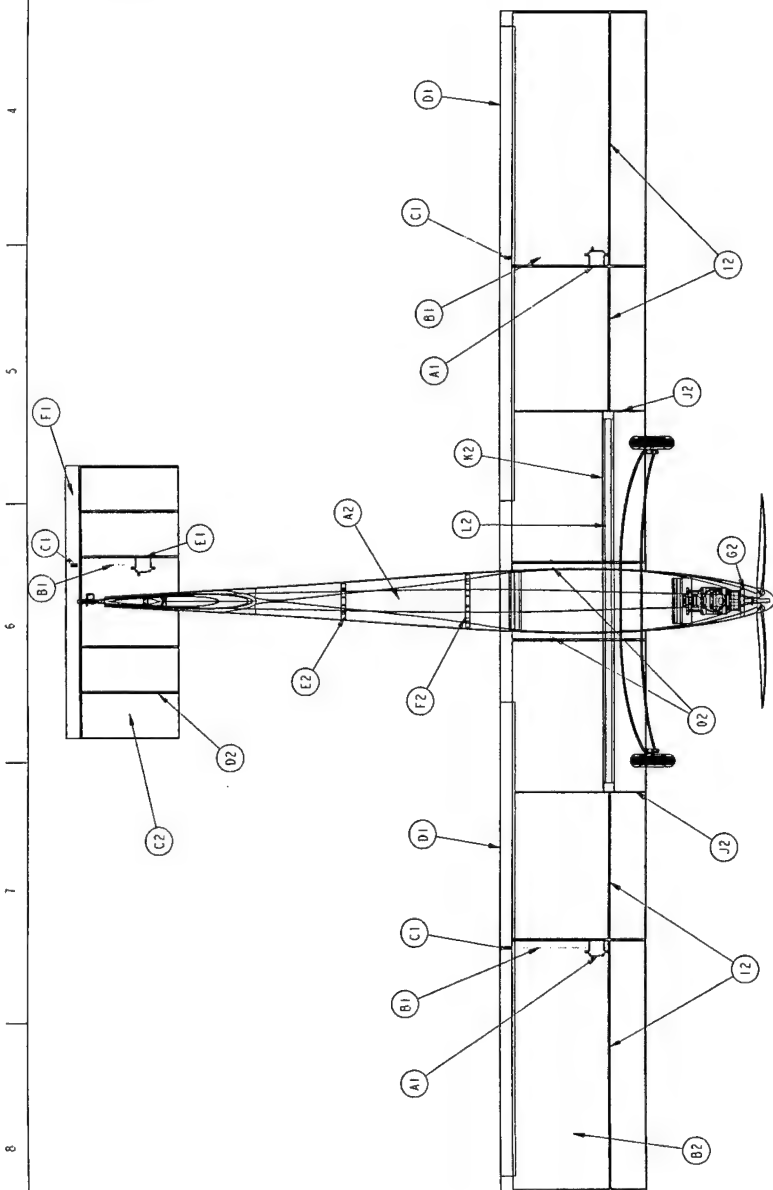
STOWED DIAGRAM

DETAIL 1
MOTOR BULKHEAD DIAGRAM



CONTROL SYSTEM COMPONENTS	
DESCRIPTION	MATERIAL
A1 FLAPERON SERVO	JR DS 3421
B1 CONTROL ROD	WIRE
C1 CONTROL HORN	NYLON
D1 FLAPERON	FIBERGLASS/BALSA
E1 ELEVATOR SERVO	JR DS 3421
F1 ELEVATOR	FIBERGLASS/BALSA
G1 RUDDER SERVO	JR DS 3421
H1 ARROW AND PIN ROD	FIBERGLASS/BALSA
I1 RUDDER	FIBERGLASS/BALSA

STRUCTURAL COMPONENTS	
DESCRIPTION	MATERIAL
A2 FUSELAGE BODY	FIBERGLASS/BALSA
B2 WING SKIN	FIBERGLASS/BALSA
C2 HORIZONTAL STABILIZER	FIBERGLASS/BALSA
D2 FLAPERON	FIBERGLASS/BALSA
E2 AFT BULKHEAD	BALSA
F2 MID. BULKHEAD	BALSA
G2 MOTOR BULKHEAD	BALSA
H2 VERT. STAB. BULKHEAD	BALSA
I2 SHEAR WEB	BALSA
J2 WING RIB	BALSA
K2 SPAR CONNECTION TUBE	CARBON FIBER
L2 WING PASS-THROUGH SPAR	CARBON FIBER
M2 VERTICAL TANK RESTRAINT	BALSA
N2 SUPPORT WEB	BALSA
O2 WING ANTI-ROTATION PIN	P.V.C.



PROJECT TITLE
OSPRAY
TEAM LEAD
H. STUTZMAN
STRUCTURE LEAD
J. SLATON
DRAWN BY
B. FISCHER
FACULTY ADVISOR

NOTE: ALL DIMENSIONS
ARE GIVEN IN INCHES.

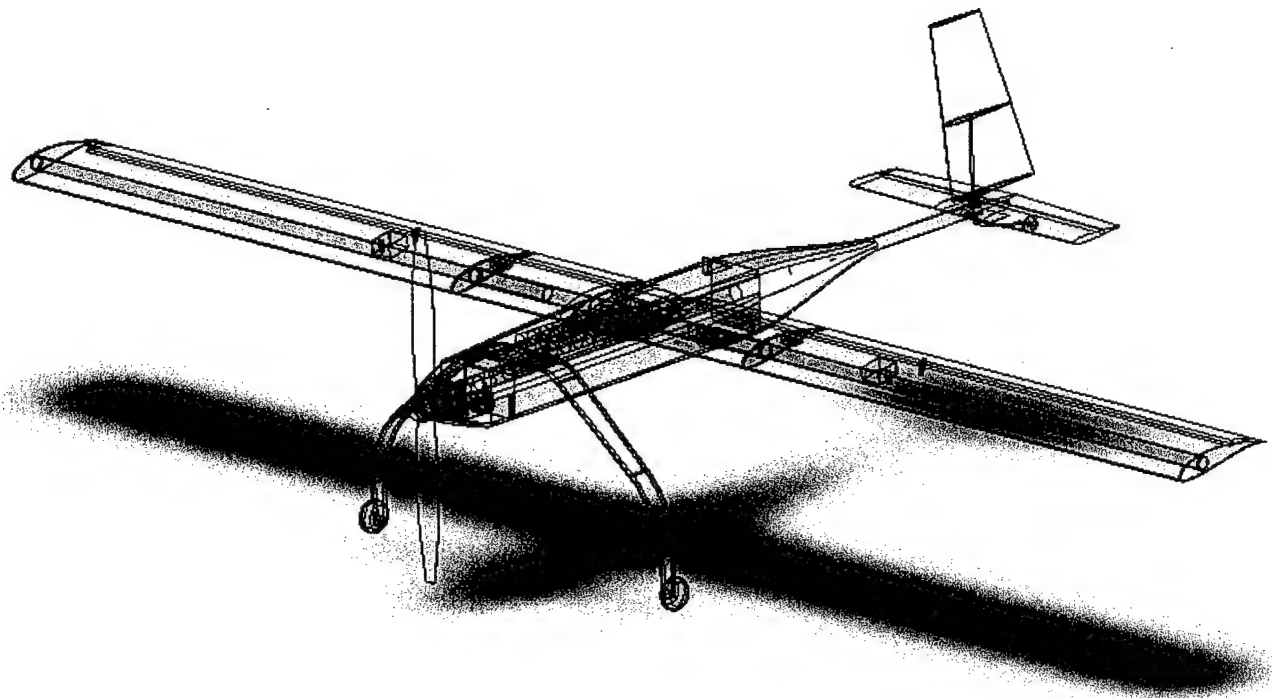
OKLAHOMA STATE UNIVERSITY ORANGE TEAM
CESSNA DESIGN/BUILD/FLY 2004

STRUCTURE AND CONTROL SYSTEM CONFIGURATION

DESIGN REVISION 3	DATE OF APPROVAL
C-1	2-22-04

University of Southern California

SCquirt



AIRCRAFT DESIGN REPORT

2004

TABLE OF CONTENTS

1.0 EXECUTIVE SUMMARY	1
2.0 MANAGEMENT SUMMARY	3
2.1 GENERAL TEAM STRUCTURE	3
2.2 SUBGROUPS AND INDIVIDUAL ASSIGNMENTS	3
2.3 CONFIGURATION AND SCHEDULE CONTROL	6
3.0 CONCEPTUAL DESIGN PHASE	9
3.1 KEY ELEMENTS OF MISSION REQUIREMENTS	9
3.2 ALTERNATE CONFIGURATIONS	10
3.3 FIGURES OF MERIT	11
4.0 PRELIMINARY DESIGN PHASE	13
4.1 MISSION MODEL	13
4.2 DESIGN PARAMETERS AND SIZING TRADES	14
4.2.1 AERODYNAMICS	14
4.2.2 PROPULSION	19
4.2.3 STABILITY AND CONTROL	24
4.2.4 STRUCTURAL SIZING	26
4.2.5 WATER DROP	31
5.0 DETAILED DESIGN PHASE	33
5.1 COMPONENT AND SYSTEMS ARCHITECTURE SELECTION	33
5.2 ESTIMATED MISSION PERFORMANCE	35
5.3 WEIGHT, BALANCE AND RATED AIRCRAFT COST WORKSHEETS	36
5.4 DRAWING PACKAGE	40
6.0 MANUFACTURING PLAN	45
6.1 FIGURES OF MERIT	45
6.2 ANALYTICAL METHODS SELECTING MANUFACTURING PROCESSES	45
6.3 PROCESSES SELECTED FROM COMPONENT MANUFACTURING	46
6.4 MANUFACTURING SCHEDULE	52
7.0 TESTING PLAN	53
7.1 COMPONENT TESTING	53
7.2 FLIGHT TEST OBJECTIVES	59
CONCLUSION	60

1.0 EXECUTIVE SUMMARY:

The University of Southern California Aero Design Team (ADT) has participated in the Cessna ONR AIAA Design/Build/Fly Competition for several years with consistently high results. The nature of the competition is to design, build and fly an electric, radio-controlled aircraft for specific missions outlined in the official rules. For the 2004 competition, two mission profiles were given: *Firefight* and *Ferry*. Each mission had its own difficulty factor and specified tasks. Both missions had to be flown with the same aircraft and the highest flight score of each contributed to the total flight score. The goal of the Aero Design Team was to develop a solid configuration that would most efficiently complete these two missions. To accomplish this goal, the design focus was divided into three sections: Conceptual Design, Preliminary Design, and Detailed Design.

1. Conceptual Design: During this phase, the team focused primarily on satisfying the requirements of the Firefight Mission. Because of the scoring for the two missions, the firefight mission was found to contribute more to the total score than the ferry mission. When considering the propulsion system, fuselage configuration and possible airfoils, the maximum water payload was assumed. Six different conceptual configurations were analyzed according to a set of ten figures of merit. Broad aspects such as tail configuration, wing configuration, fuselage and payload integration, and estimated cost were the main points of debate for each of the conceptual plane designs. The size of the packing box was also taken into consideration. This parameter however, did not carry as much significance as it did last year due to the change in the rules which eliminated the timed assembly.
2. Preliminary Design: During this phase, the main analytical tool was updated and implemented. An Excel Program called "PlaneSizer" was used last year to assist with the sizing of the plane. Originally based on an older code, PlaneSizer was reformatted by current students to improve the iteration process. This program contained a main page, labeled "Frontpage" which compiled all pertinent inputs and summarized all necessary outputs in one single location. Referencing codes on individual pages separated for different portions of plane design, the Frontpage allowed for concise plane sizing in one central location. It was designed to use different libraries established for different parts such as motors or airfoils and was divided into logical subsections with the ability to perform different trade studies. The code performed the iterations part of the design, outputting the plane's sizing and configuration based on the assigned inputs. By using PlaneSizer in the preliminary design portion, the team was able to establish an estimate of the number of cells, the type of batteries, and motor and propeller size that would produce an optimal

propulsion system for the specified flight mission. With the imbedded iterations, PlaneSizer was also able to select an appropriate airfoil and tail configurations that would satisfy the requirements of the given flight mission. PlaneSizer enabled an efficient downselect of plane configurations and sizings and provided a sufficient base from which the team could further analyze before finalizing the design. A number of lab experiments were performed to verify the accuracy of the calculated results. These test were primarily focused on propulsion system optimization and confirming manufacturer's specifications.

3. Detailed Design: During this phase, the team froze the design layout, sized the plane's components and began some preliminary manufacturing of different parts. Sizes and configurations obtained from this stage were based on initial assumptions and parameters that were iterated through the Excel programs. Detailed CAD drawings were made for all the components of the plane to enable a smooth transition into and completion of the building process.

2.0 MANAGEMENT SUMMARY:

2.1 General Team Structure:

The Aero Design Team consisted of approximately twenty undergraduate students organized into subgroups for different disciplines. Cristina Nichitean was the student captain of the team and was responsible for overall team productivity and coordination. She established weekly and monthly agendas, schedules and deadlines. She was responsible for keeping members on assigned tasks, for running meetings and for overseeing the design and construction phases. The rest of the student members were divided into subgroups, each with a designated team captain, a junior or senior with prior team experience. Team captains and the team leader met once a week to divide up tasks, to consolidate design ideas, to brainstorm, and to solve any problems facing the team at the time. Captains then met on an individual basis with their team members to negotiate and complete the designated tasks. In addition, the entire team, students and advisors, met for three hours a week to communicate and discuss the current state of the plane, to update others on the progress of the week prior and to plan ahead. The team was assisted by a faculty advisor, Dr. Ron Blackwelder and several industry advisors from Aerovironment Inc, Raytheon, and Swift Engineering. The advisors served as a resource of experience and supervision and provided several lectures early in the design process for newer team members. They used their expertise to help with design and construction techniques with which the student members were less familiar.

2.2 Subgroups and Individual Assignments:

The team was divided into nine subgroups, each focusing on a specific portion of the plane or flight procedure. Figure 2.2.1 shows the team organization. Each captain was chosen based on team participation, background experience, and interest. To promote learning, underclassmen and new members volunteered to help with each group. Captains were responsible for organizing their group, communicating and coordinating with the rest of the team and ensuring all deadlines and goals were achieved.

The main computational tool used by the team was the Excel program titled "PlaneSizer." This program contained pages for each of the different subcomponents of the plane design. To support this tool, each captain was also responsible for creating and updating an Excel spreadsheet with the appropriate parameters for his or her specific focus. With the help of advisors, the analysis for each spreadsheet was completed and integrated into the main design tool. The development of these work pages was carried further into the three design phases where intense analysis and optimization were performed to obtain the final configuration of the aircraft. Each group was responsible for planning and building the components under the supervision of more experienced team members and industry advisors. The subgroups were defined as follows:

1. Aerodynamics Group: The main responsibility of this group was to choose the most efficient airfoil for the flight objectives and to estimate the total airplane drag. Initial parameters were set and later changed for optimization. To find the total drag, this group needed to calculate the vortex and airfoil drag using independent variables such as plane geometry and published airfoil data. A program called XFOil was used to investigate the benefits of using modified airfoils. Other responsibilities were to determine the efficiency factor "e", C_{Lmax} , $C_{Lcruise}$, flap deflection, and L/D at different flight conditions.
2. Configuration Group: This group had to determine the overall design and architecture of the plane. In the conceptual and preliminary design phases, the configurator had to integrate all design characteristics established during brainstorm sessions and produce drawings of feasible planes at each meeting. He had to insure that the plane remained within given size parameters, could fit in the packaging box, maintain the proper CG location, and could be readily constructed. The configurator used SolidWorks as the 3D CAD program for creating the drawings.
3. Design Report Group: This group gathered all pertinent information and compile notes from each general meeting and captain's meeting. The report writer was responsible for meeting the requirements and guidelines provided in the 2004 rules and presenting the work of the team in a coherent and technical manner. This group assigned deadlines to each captain who needed to provide documentation of testing, manufacturing techniques and necessary data.
4. Flight Test Group: This group was in charge of assigning and accomplishing specific goals for each test flight as well as collecting necessary data. Prior to each test flight, the flight test captain needed to provide test cards which specifically outlined the objects of the coming flight test and he needed to organize the plane components and all necessary equipment to carry out these objectives. After each test flight, this group was responsible for performing further analysis and presenting summary and conclusions to the rest of the team.
5. Payload Deployment Group: To satisfy the FireFight mission parameters in the 2004 rules, a special team was assigned to analyze possible methods of water deployment. Their focus was on tank configuration, system integration within the plane, water loading, and water dropping. They designed and tested a water tank with various nozzles, analyzed exit positions at various speeds, and developed a system to minimize water loading time.
6. Performance Group: This group's main focus was the PlaneSizer spreadsheet. The members had to integrate and update all inputs and outputs to correspond with this

year's flight missions and guidelines. They had to link all subgroup's pages to one common page so that all the inputs and important outputs could be seen after each iteration and kept within assigned limits. Some of the major parameters listed on this page were Take Off Field Length (TOFL), maximum battery weight, current draw and cruise velocity. The performance group was also responsible for optimizing the plane configuration to produce the best flying score possible. Each aircraft system was then sized accordingly and passed down to the individual groups and if proved feasible, drawn up by the configurator.

7. Propulsion Group: This team was responsible for finding the right combination of batteries, motors, propellers and gearboxes to optimize the propulsion system for this year's mission. A library of different manufacturers and specifications was built and integrated within PlaneSizer. Matching these parameters to model the mission for this year was a critical aspect of performance, hence testing of the top choices of each of these components was done to further complete the analysis. In the past it has been found that the motor and battery data published by the manufacturers was inaccurate at the high power levels needed for this competition. This year however, extensive testing was done on both the battery packs and the motors until dependable data was found and a configuration that would allow the plane to complete the missions was established.
8. Stability and Control Group: This group was responsible for analyzing the various tail configurations proposed during the conceptual design. For this year, there was large debate between a V-tail and a conventional T-tail. They had to create a spreadsheet that contained multiple parameters and equations to analyze the different types of tails. Stability and Control (S&C) was also responsible for establishing an appropriate Static Margin, determining hinge lines, servo locations and sizes, moments for each control surface and moments on the entire plane. Two important factors that were taken into consideration for nearly all S&C analysis were the crosswinds present at this year's competition site and the shift in the plane's center of gravity due to the water drop.
9. Structures Group: This group was responsible for sizing the main structural components of the plane. Initial structural analysis was needed to select between a monocoque fuselage design and the chosen design. The structures team was then in charge of sizing wing spars, the backbone of the plane, and the landing gear. This group had to take into account both static and dynamic loadings. They were also responsible for wing and landing gear attachments and for ensuring that all plane components fit into the packaging box specified in the 2004 rules.

2.3 Configuration and Schedule Control

A schedule of important dates and deadlines was created at the beginning of the year so that time management could be easily visualized. For example, each phase of the design process was assigned a definite period of time to allow for sufficient construction and testing. The schedule took into consideration students' school load, allowed for change where needed and had certain processes overlap for efficiency. Figure 2.3.1 shows the final schedule with planned and actual dates.

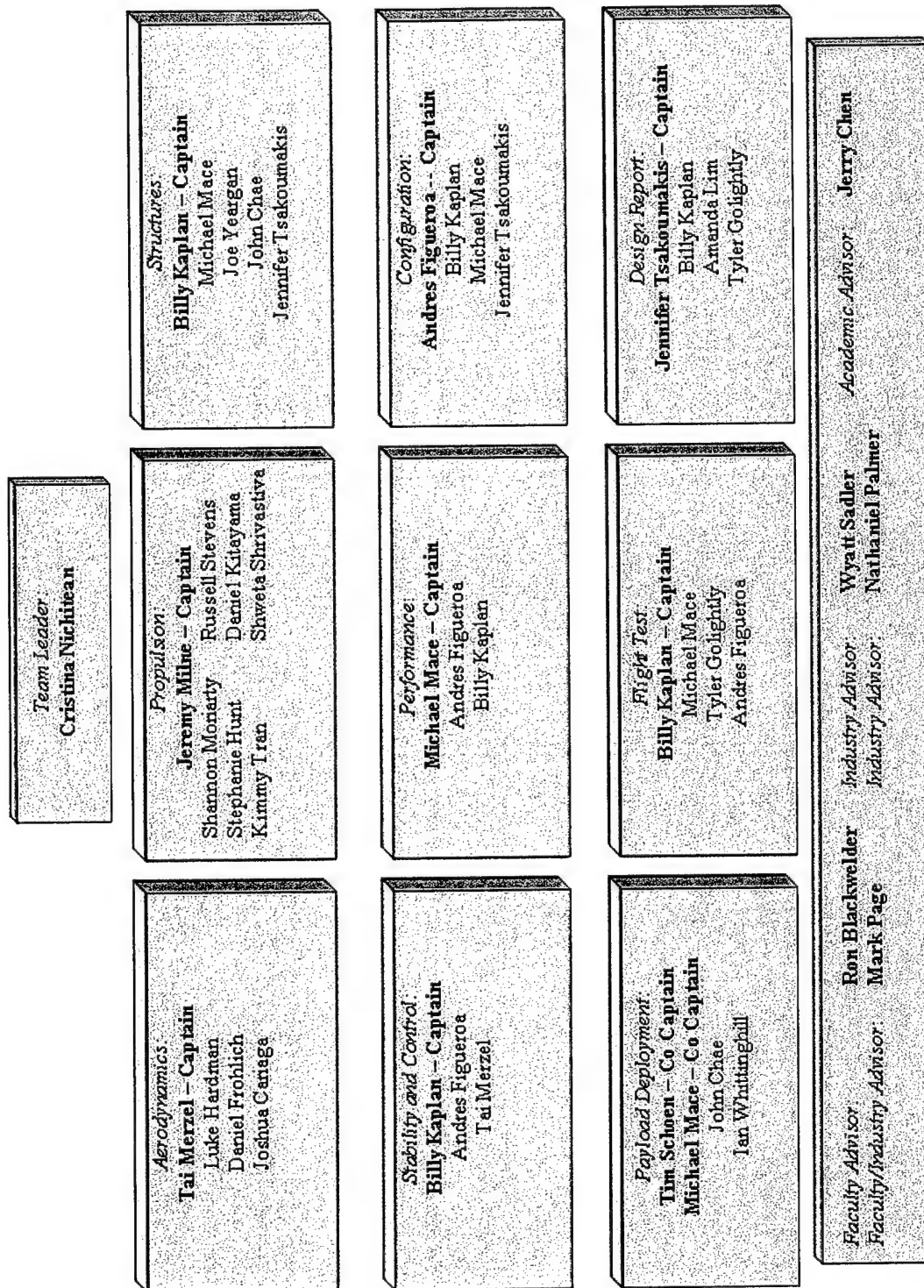


Figure 2.2.1 USC Aero Design Team Structure showing advisors and subgroups.

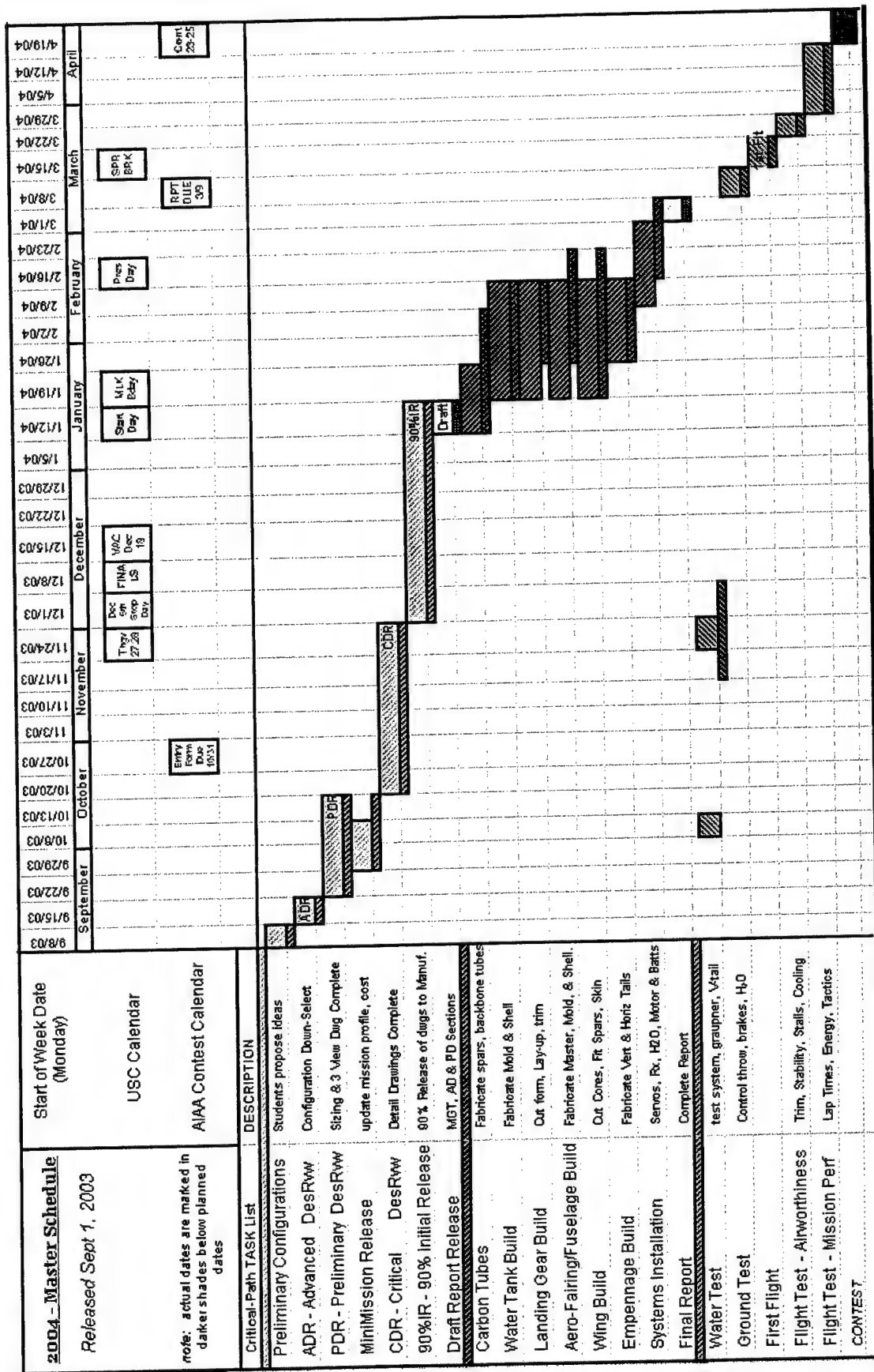


Figure 2.3.1 USC Aero Design Team Schedule 2003/2004

3.0 CONCEPTUAL DESIGN PHASE:

For the 2004 Design/Build/Fly contest, there were two flight missions to accomplish. The *Firefight* mission was designed to be a heavy lift/slow flight mission. It had a difficulty factor of 2.0 and required two water loadings, two water dumps and two landings. Each lap needed to include one 360° turn. The maximum water capacity of the aircraft was four liters and the actual amount carried was factored into the final flight score. The second mission was the *Ferry* mission. It was designed to be a higher speed flight. For this mission the plane had to take off, complete four laps with a 360° turn on each down wind leg, and land. It required no payload and had a difficulty factor of 1.0. As was noted earlier, the driving force behind this year's plane design was meeting the requirements of the *Firefight* mission.

3.1 Key Elements of Mission Requirements

The following conditions were applied to all five configurations under consideration:

1. **Box Constraint:** The contest rules specify that all components of the plane need to fit inside a 4'x2'x1' box. This drove the configuration to be flexible enough to allow for interlocking parts.
2. **Take Off Field Length (TOFL):** The rules require the plane to take off within 150'. As a safety factor, the plane was designed to take off within 75% of the total length. This criterion was determined from flight tests conducted in 2000 and was incorporated into the spreadsheet "PlaneSizer" to calculate the performance and design parameters for an optimum solution to the different missions required this year.
3. **Number of Motors:** Because of the expense that an additional motor would add to the Rated Aircraft Cost, only one motor was assumed for all configurations. From preliminary calculations, one AstroFlight or Graupner motor provided enough power to meet the required TOFL.
4. **Battery Weight:** All configurations had provisions for the maximum 5lb battery weight limited by this year's rules. This condition ensured that each configuration would have sufficient energy to complete each mission.
5. **Water Payload:** All configurations were designed with anticipation of carrying the maximum water capacity of 4 liters. Configurations were selected such that the CG of the water tank would be coincident with the unloaded CG of the plane to minimize the in-flight shift during the FireFight Mission.
6. **Use of Composite Materials:** The high strength-to-weight ratio of composite materials, such as carbon fiber and fiberglass, reduced the weight and provided sufficient strength to withstand the applied loads.

3.2 Alternate Configurations

After an initial brainstorming session, all ideas were compiled into the following five general plane configurations (see figure 3.2.1):

1. Conventional plane with a V-tail: This design was chosen for its simplicity. It was straightforward and familiar to the team members. It would allow for easy water system integration and overall manufacturing. The conventional plane would include two tubes, a main boom and a telescoping tail boom that collapsed into the main boom for packing. The major components attached to the main boom and the tail surfaces attached to the tail boom. This design would provide structural simplicity. The V-tail was chosen to decrease Rated Aircraft Cost.
2. Conventional plane with a conventional tail: This design was chosen for the same reasons as the first plane. A conventional tail was chosen however, despite the added cost. There was debate about the tail construction techniques and about the performance of each configuration in the crosswinds that the plane may encounter at the competition. These points were discussed throughout the entire conceptual design phase and the remainder of the downselect process. Based upon previous experience, the conventional tail was considered to be more crash-worthy than a V-tail. Should the tail be damaged in a hard landing, the 30 minute repair time would be enough to fix a conventional tail where as perfectly realigning the angle of the V-tail could take longer.
3. Biplane with a V-tail: This plane with a V-tail was considered because it would have a low Rated Aircraft Cost (RAC). It would also allow for fairly easy water system integration and with a deeper tank, would possibly allow a faster water dump. However, the manufacturing techniques, the crash worthiness and the assembly process for this plane placed doubt over the possible success of a biplane configuration. With two wings, this plane would be harder to construct and harder to repair.
4. Flying Wing: This configuration was appealing because it did not include a tail. This aspect would provide for easier manufacturing and assembly. Should this configuration be chosen, the team decided it would need a nose gear and downward pointing winglets on the tips of the wing. The landing gear loads would be directed through the wing spar providing stability on a hard landing. A flying wing however would produce poorer flight handling qualities than a plane with a tail due to the crosswind conditions.
5. Blended Wing Body: This configuration was also considered because it has no tail. Without a tail, the blended wing would be easier to manufacture and assemble. However, as with the flying wing, this was a design with which the team has had little experience. With the blended body the hard points and load paths would not be as clearly defined. This configuration would also have a very large sweep angle in the wings which would pose difficulty in making

an angled joiner between the two wing halves. This configuration also has a very low static margin. This would cause difficulty in flight during the Firefight mission due to the CG shift as the water is deployed. Also flight handling would be impaired in crosswinds due to a lack of yaw stability.

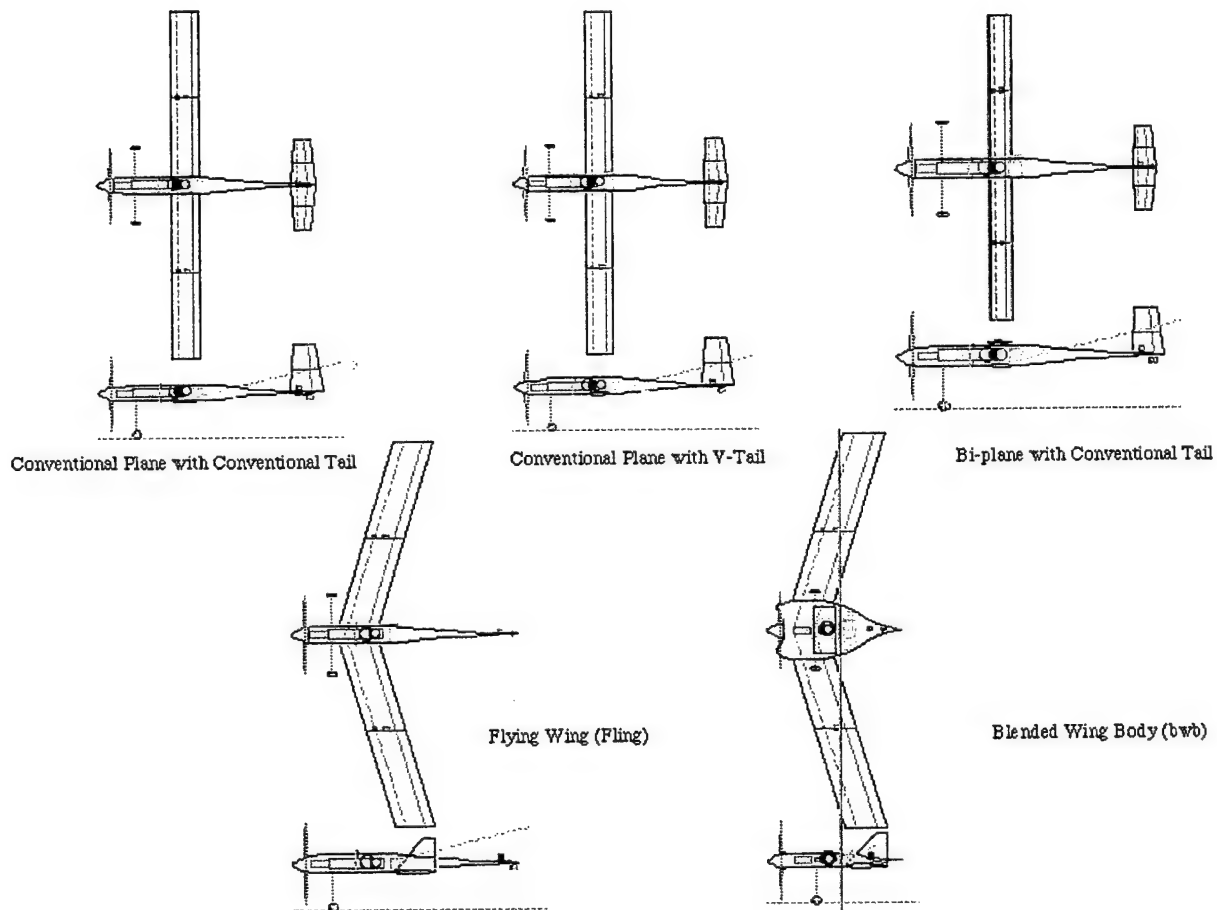


Figure 3.2.1 Conceptual design configurations

3.3 Figures of Merit

Each plane configuration was entered into an Excel program to optimize the two calculated parameters: Drag and Rated Aircraft Cost. The planes were then scored according to 10 Figures of Merit (FOM). First, each FOM was assigned a factor from 1-5 (Column 1 in Table 3.3.1) representing the team's opinion of the relative importance of that FOM in assessing the plane's overall performance in the competition. A factor of 1 was given to a figure that had low importance and a factor of 5 was given to a figure that had high importance. Secondly, for each FOM parameter, each plane configuration was assigned a value from 1-5 representing the quality that configuration would have for the given figure of merit (Columns 3-7 of Table 3.3.1). A value of 1 meant low quality, a value of 5 meant high quality.

The values were then added together and the planes were ranked by total score; the configuration with the highest total score was considered the optimum design. The FOM's were defined as follows:

1. Ease of Manufacturing: This figure of merit was assigned a factor of 1. Manufacturing takes into account the resources and materials available, the techniques required and the feasibility of the team members performing them correctly. With the faculty and industry advisors and experienced team members, it was decided that a plane design should not be heavily influenced by its ability to be manufactured because new construction processes can always be learned.
2. Ease of Assembly: This figure was assigned a factor of 2. It was defined as how readily the plane can fit into the box, how quickly it can be put together from the box and how many components it contains. For this year's contest, assembly time does not contribute to overall flight time so it does not carry much significance for total score. However, it was given a factor of 2 rather than 1 because efficiency at test flights is necessary. The quicker the plane is assembled on the test field the more flights the team can complete before the actual competition.
3. Crash Worthiness: This figure was also assigned a factor of 2. Crash worthiness was defined to include robustness of structure and ease of repair after a crash or hard landing. The teams experience with composite structures has given it confidence that repairs are not that difficult.
4. Structural Simplicity: This figure of merit was assigned a factor of 3. Structural simplicity includes minimizing the number of components and joints as well as incorporating well known load paths.
5. Ground Handling Quality: This figure was also given a factor of 3. Proper steering on the ground prior to take off is essential to minimize mission time. For the FireFight mission, the plane is required to land and refill midway through the mission, so accuracy in landing and stopping is necessary.
6. Experience with Design: This figure was given a factor of 3. Originally this FOM was given a factor of 1, however during the downselect process, the team found that whether or not they had experience with the design was a significant factor in justifying each configuration.
7. Flight Handling Quality: This figure was given a factor of 4. Clearly how the aircraft handles in flight directly affects the overall flight score. Because the competition this year will be held in Wichita, crosswinds will greatly affect plane performance. Stability and control needs to be completely reliable under these conditions.
8. Water System Integration: This figure was also given a factor of 4. The water system is the main part of the FireFight mission and its integration into the structure of the plane and its overall performance is necessary for a good flight score. The team decided that each plane design must allow for a container that would hold four liters of water, must have an access area to expedite the water loading process and provide for quick water dumping.
9. Drag: This figure was given a factor of 5. An Excel model was created to estimate the drag for each of the configurations. Because the drag for all configurations was comparable, this

parameter was normalized to keep small changes in the drag from disproportionately affecting the overall score for each plane.

10. **Rated Aircraft Cost:** This figure was also given a factor of 5. Both of these last two FOM's play directly into the overall flight score. Rated Aircraft Cost is designed to penalize configurations for complex geometry and large size. Minimizing these parameters improves performance and increases the score since the flight score is divided by the RAC factor. Due to the cost equation in this year's rules, a long and narrow fuselage was needed to minimize the RAC.

MF	FOM's	Configurations				
		V conv	Conv	V-bip	Fling	Bwb
1	Ease of Manufacturing	4	4	1	5	5
2	Ease of Assembly	4	3	1	5	5
2	Crash Worthiness	3	4	1	4	5
3	Structural Simplicity	4	4	1	5	4
4	Flight Handling Qualities	4	5	4	2	2
3	Ground Handling Qualities	4	4	4	5	5
4	Water System Integration	5	5	4	5	4
1	Experience with Design	5	5	3	2	1
5	Drag x Cost	2.2	2.1	1.9	2.1	1.8
5	RAC	2.2	2.1	2.4	1.8	1.5
	Total Score	105.0	108.0	76.2	102.2	93.5

Table 3.3.1 Figures of Merit used for downselect process. "Conv" refers to conventional tail configuration. "V-bip" refers to a biplane with a V-tail. "Fling" refers to a flying wing and "Bwb" is a blended wing body.

4.0 PRELIMINARY DESIGN PHASE:

This phase further developed the conceptual design studies by breaking down the different disciplines and analyzing them thoroughly. Five main design subject areas were examined: Aerodynamics, Propulsion, Stability and Control, Structures, and Water Deployment. Parametric models were created for each area and were integrated into the single analytical tool PlaneSizer. Once PlaneSizer was updated for this year's contest, sizing studies were performed, different missions were tested, and the configurations were optimized.

4.1 Mission Model

The goal of the analytical tools used by the USC Aero Design team was to provide simple preliminary calculations. The use of these tools allowed the team to focus on obtaining results rather than

spending time on tedious calculations. As has been cited before, PlaneSizer, was the team's leading mode of analysis. Originally based on an older spreadsheet, PlaneSizer was reconstructed by last year's team and updated for this year's competition. PlaneSizer is a compilation of many Excel Spreadsheets and programs designed to target each major component of plane design and construction. Each team captain was responsible for understanding the current spreadsheet for his design component, updating it to represent this year's parameters, and submitting it to the Performance Group for final inspection and integration. All spreadsheets were then linked together. The result was a complex workbook of different modules categorized by subcomponent and/or task. To facilitate the use of this package, a user friendly "FrontPage" was created to incorporate all the required inputs for the mission profiles as well as the relevant outputs. With all calculations and data on the FrontPage taken from the embedded spreadsheets and pre-established databases, sizing the plane was done easily in a localized fashion. The program ran for several iterations for different variables and produced multiple results that were easily compared. Each sizing iteration began by adjusting the wing area for a target take off field length and then sized the tail for required pitch and yaw stability. Finally, the motor current, voltage, RPMs and thrust were converged to achieve an available rate of climb of 400 fpm. This accounted for the increased lift needed during turns. A cruise velocity could then be calculated from the propulsion parameters and used to analyze mission performance. After the different parameters were put in place, the program ran through the sizing process. The flight time and rated aircraft cost for a given design were combined into a single quantity called "Flight Score". Different designs were compared using this quantity.

4.2 Design Parameters and Sizing Trades

4.2.1 Aerodynamics

The focus of the aerodynamics group was to ensure that the aircraft would meet all of the main constraints of the competition. They had to make sure the plane would make take off field length, provide sufficient lift, and have minimum drag. These were obtained by studies done in three different subdivisions of this group: drag, airfoils, and wings.

1. Drag: To calculate the total airplane drag, vortex and parasite drags were computed using relations derived from *Fluid Dynamic Lift* and *Fluid Dynamic Drag* by S.F Hoerner. The parasite drag coefficient, C_{do} , was found by inserting numbers from *Fluid Dynamic Drag* into the equation

$$C_{do} = (C_{do \text{ fuselage}} + C_{do \text{ wing}} + C_{do \text{ tails}} + C_{do \text{ landing gear}}) K_{\text{excrescence}}$$

where $K_{\text{excrescence}}$ is a multiplier for gaps, vents, and antennas. Airfoil polars were taken from a program called Xfoil. Xfoil is a program developed by Dr. Mark Drela of MIT. It employed a

panel of calculations for the pressure distribution plus a boundary layer model. It then generated plots for lift and drag coefficients as a function of attack angle for a given Reynold's number. Vortex drag due to lift is accompanied by strong wingtip vortices. This influence is minimized by using high aspect ratio wings to separate the vortices. Elliptical span-loading and winglets also reduce vortex drag. But because most wings do not display a perfectly elliptical span-load, an efficiency factor "e" accounts for the discrepancy. The factor "e" is calculated from the following equation:

$$e_o = e_{wing} K_{wing\ viscous}$$

where e_{wing} is the inviscid vortex drag efficiency factor and $K_{wing\ viscous}$ is the multiplier for viscous drag increase due to angle of attack. For an untapered wing, this factor is 0.89. This was the value used in the drag calculations for this year's plane. Other types of drag considered in the aerodynamic model were junction drag, gap drag, base drag, step drag, trim drag, and profile drag. Junction drag was found at the intersection of two aerodynamic bodies such as the wing and the fuselage. Gap drag was taken at the control surface hinge lines. Base drag occurs at the aft part of the fuselage and is eliminated by bringing the tail cone to a point or blade. The step drag is prevented by using flush brackets. Trim drag, which results from download trimming of the tail, can be minimized with a long tail arm and aft CG position. And the profile drag is caused by the two dimensional airfoil type. The total airplane drag could then be calculated as the sum of the parasite drag components and the vortex drag components, using the following equation.

$$C_D = C_{do} + \frac{C_L^2}{\pi e_o AR_w K_{trim} K_{junction} K_{gap} K_{base}}$$

These were all analyzed and the calculations were incorporated into the PlaneSizer spreadsheet. Figure 4.2.1 shows a graph of the total airplane drag as calculated by PlaneSizer.

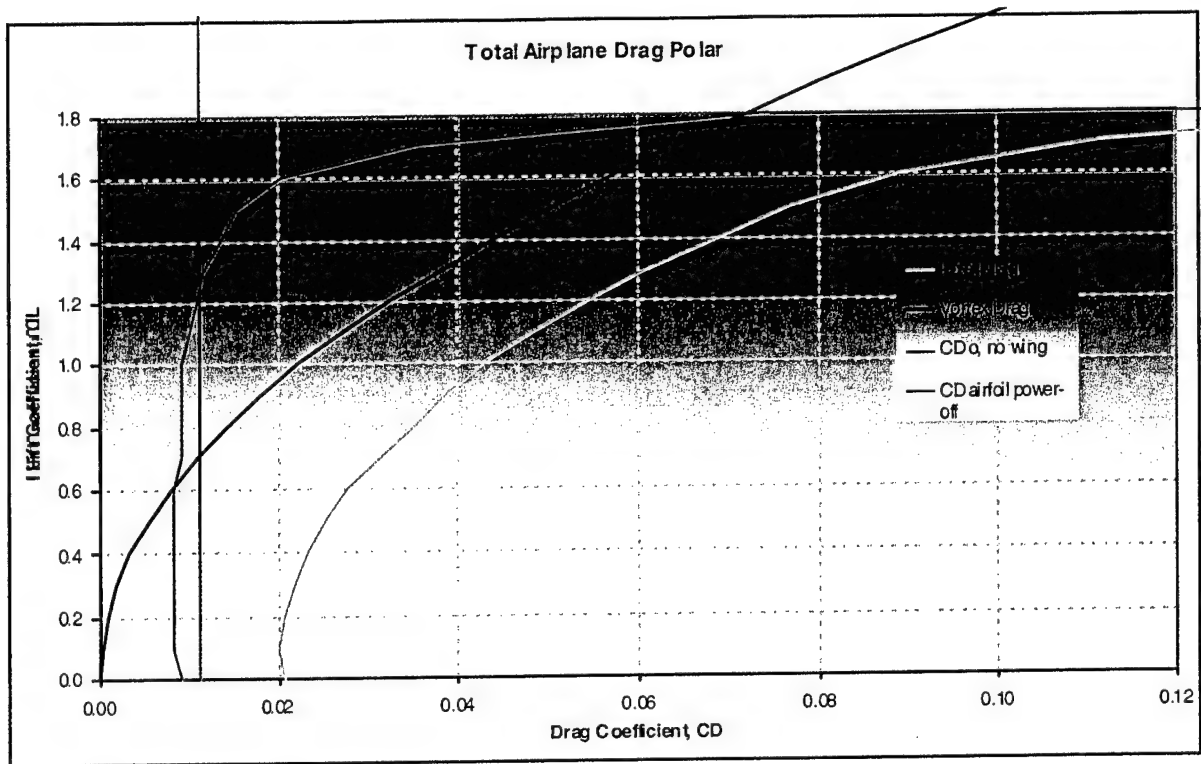


Figure 4.2.1 Example of Total Airplane Drag for the FX-63-137 with 16% increased thickness. Vortex and parasite drag also depicted.

2. Airfoils: The team this year analyzed a variety of airfoil designs that would produce sufficient lift with minimum drag. The chosen airfoil needed to satisfy the following characteristics: high C_{lmax} , low drag at $C_{lcruise}$, acceptable drag on the maneuvers at the approximated C_l , and an appropriate thickness to accommodate wing spar. For example, the LA203-KB, the Eppler 374 and the FX63-137 were specifically tested with Xfoil because they were all airfoils that had a high enough lift coefficient to fulfill the plane needs in this year's FireFight mission. Data on other airfoils, such as the LA203a, SD8020, SD800, RG15, NACA2214, and others with variations in thickness and flaps, was obtained from a library with precalculated data. These airfoils were selected for their high C_{lmax} , their capability to meet take off field length requirements, or their low C_D at cruise velocity. The airfoil chosen was the FX63-137 because it had the lowest drag over the range of lift coefficients anticipated in the contest. The FX was consistently better for both high and low lift coefficients. For structural reasons, a large diameter carbon tube spar was needed to support the wing. Xfoil was used to analyze the airfoils as their thickness was increased from 12% to 16%. Flaps were also added, from 5 degrees up to 10 degrees down to simulate the range that would be used during flight. Figure 4.2.2 shows the total drag polars for different airfoils considered.

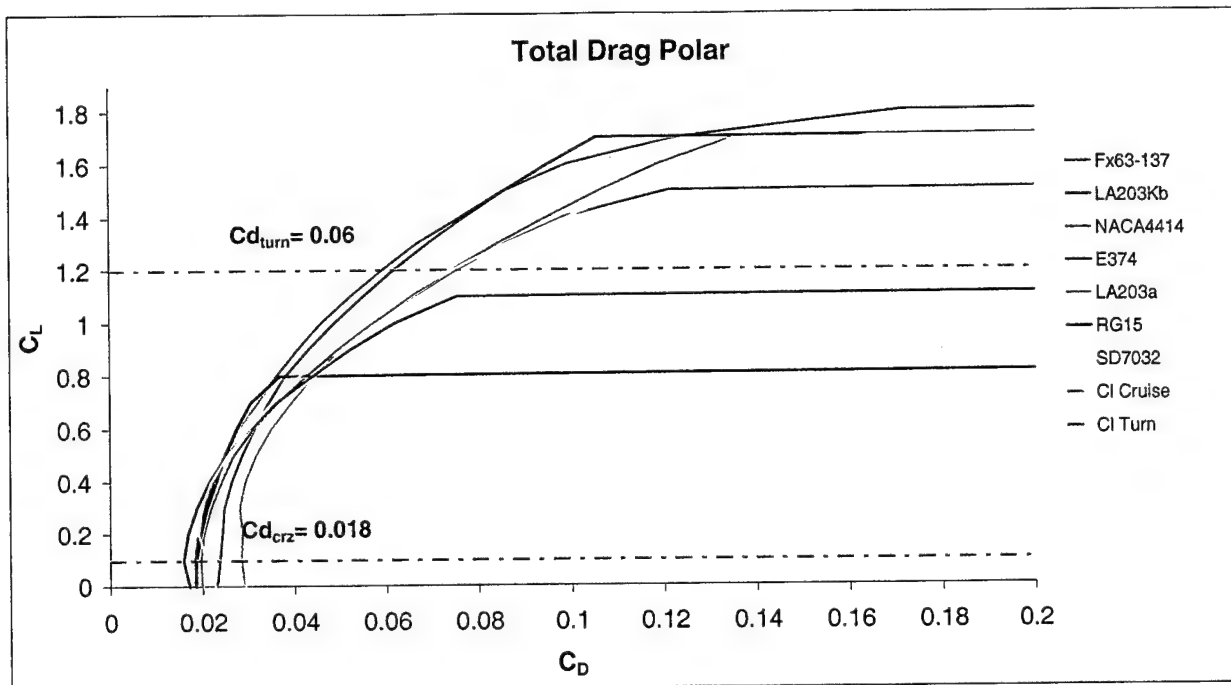


Figure 4.2.2 Graph of C_L v C_D for various airfoils. Dashed lines denote drag coefficients at cruise and turning conditions for the airfoil chosen (Fx63-137)

3. Wing: The two most important parameters for sizing the wing were wingspan and wing area. It was decided to use a non-tapered wing because the increase in difficulty of manufacturing a tapered wing outweighed the slight benefit in drag reduction. Because of the 4'x2'x1' box requirement, it was necessary to have a sectioned wing. In order to minimize weight and complexity, a maximum of two joints in the wing were allowed. This, combined with the box requirement, constrained the wingspan to a maximum of 9 ft. A trade study was performed by varying the wingspan while holding wing area constant and observing the effect on a number of variables such as best flight score, mission time, rated aircraft cost, available/required energy, etc. This study is shown in Figure 4.2.3. It was found that the airplane's performance increased with wingspan up to the limit of 9 ft. However, due to structural limitations in wing spar sizing, it was deemed necessary to reduce the wing span to 8 ft. in order to relieve the bending moment at the center.

The wing also had to have enough area to take off within the required take off field length when filled with 4 liters of water. Takeoff field length was calculated using the following equation.

$$TOFL = \frac{(TOGW)^2 (1.2)^2}{(Takeoff\ Thrust)(1 - MuRoll)(g)C_{Lmax}S_w\rho}$$

This formula was incorporated into the Excel tool PlaneSizer such that wing area was always sized to meet TOFL requirements within a safety factor for a given gross weight, C_{Lmax} and propulsion package. Estimated aerodynamic characteristics for the chosen wing (FX 63-137 with 16% t/c and 8 ft wingspan) are summarized in Table 4.2.1.

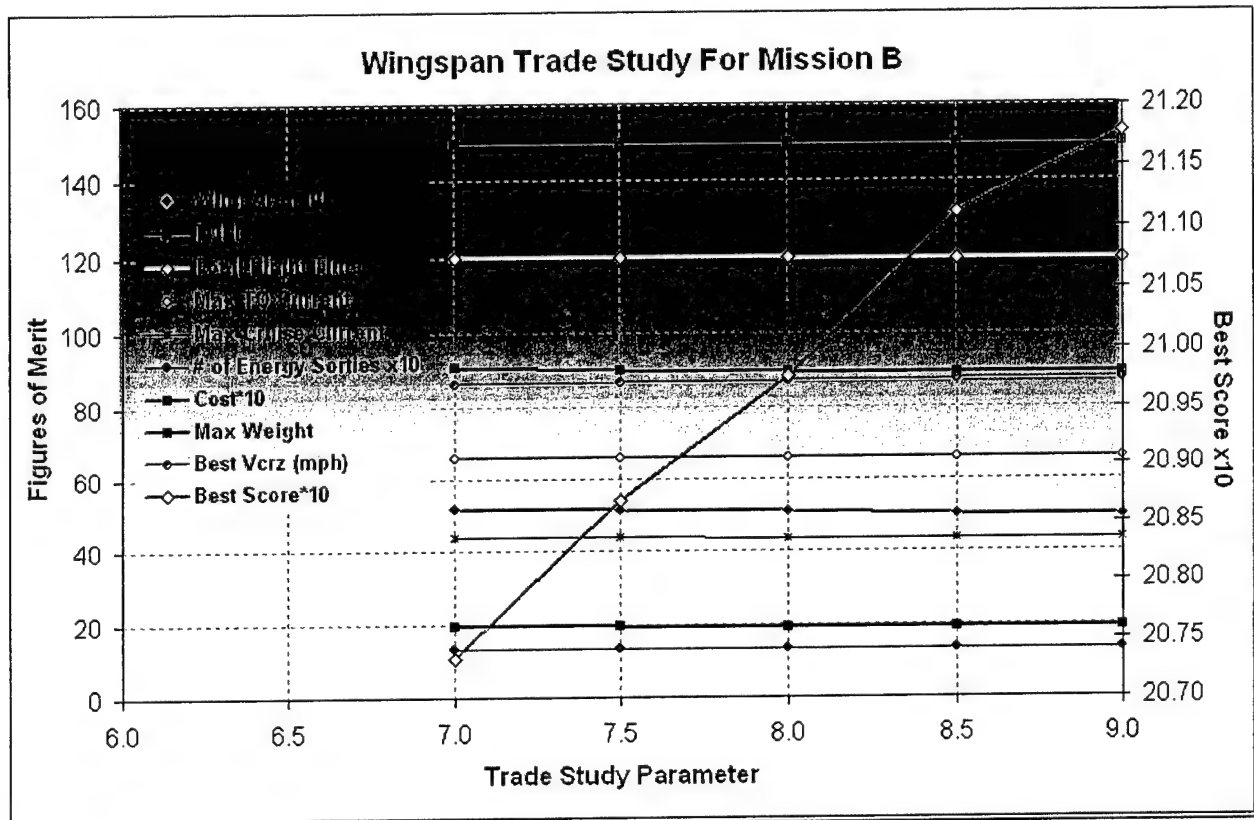


Figure 4.2.3 Trade Study of several Figures of merit vs. Wingspan. Trade Study Parameter is wingspan in dimensions of ft.

Interpolated Drag Values at Cruise				General Aerodynamic Characteristics	
	C_L	C_D	L/D	e	0.94
Heavy Cruise	0.211	0.0236	8.97	C_{Lmax}	1.9
Light Cruise	0.105	0.0237	4.41	t/c	0.16
Airfoil: FX63-137 16% thickness + flap				C_L at V_{cruise}	0.1
				C_L in turns	1.2

Table 4.2.1 Estimated aerodynamic characteristics for Fx 63-137 with 8 ft. span

4.2.2 Propulsion

The most important factor determining aircraft performance and overall score was the propulsion system consisting of the batteries, motors, gearboxes and propellers. Propulsion was analyzed and optimized by PlaneSizer until a final propulsion configuration was obtained. The spreadsheet calculated the total resistance of the circuit by summing the internal resistance of the individual components such as batteries, cables, speed controller, and motor. An initial assumed current was run through the circuit to calculate a voltage drop across each component in the circuit. The voltage across the motor was used to calculate the motor rpm. The propulsion model then took this rpm and computed the torque required for the chosen propeller and a required current was calculated and compared with the initially assumed current. An iteration process altered the assumed current and then repeated the computation until the required current matched the assumed current. In past years, actual propulsion system performance had been inconsistent with predicted performance. Thus extensive testing of each of the components was performed to verify the manufacturer's specifications and the published performance.

1. **Batteries:** According to the contest rules, the battery pack was limited to a five pound maximum weight and a 40 amp maximum current draw. The available energy stored in each cell was needed to provide efficient conversion to kinetic energy. Tests conducted by the team indicated that the advertised energy content of the batteries was not available primarily due to the heavy current draw by the motor. This produced temperature effects resulting in increased resistance in the motor, the controller, and the wiring. The tests suggested that the batteries produced only 60% of the manufacturer's listed storage capacity. The analysis was incorporated into PlaneSizer for a library of Sanyo batteries, including five different types: KR-1400AE, RC-2000, RC-2400, CP-1300, and CP-1700. These types were included because of their accessible data, past performances, and because they satisfied the contest constraint of using over the counter NiCad's. Figures 4.2.4 and 4.2.5 show trade studies for battery type and cell count as was calculated through PlaneSizer. The Cp-1300's were chosen because of their availability and their known performance characteristics from previous years. Cell count was set at 28 cells which gave the proper voltage for take off. The battery life gives the needed energy to complete the mission with the smallest amount of weight.

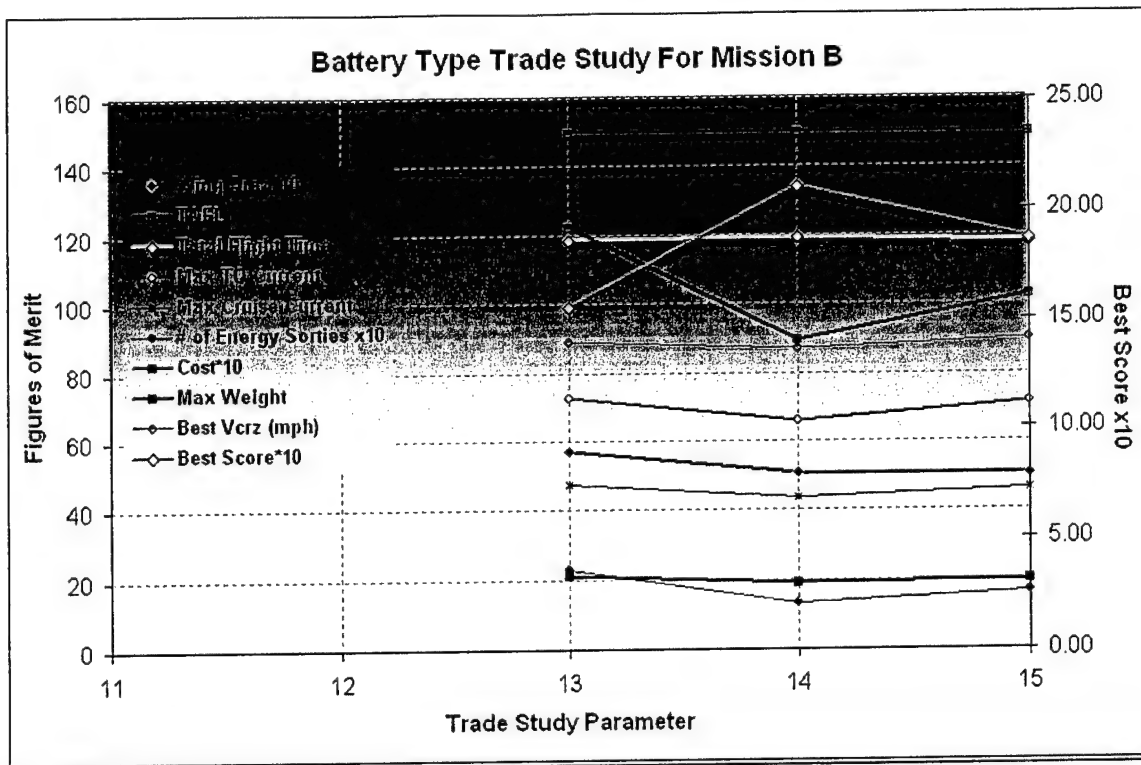


Figure 4.2.4 Trade study of various Figures of Merit vs. Battery type. Trade Study parameter is battery type where 13, 14, and 15 denote RC-2400's, CP-1300's, and CP-1700's respectively

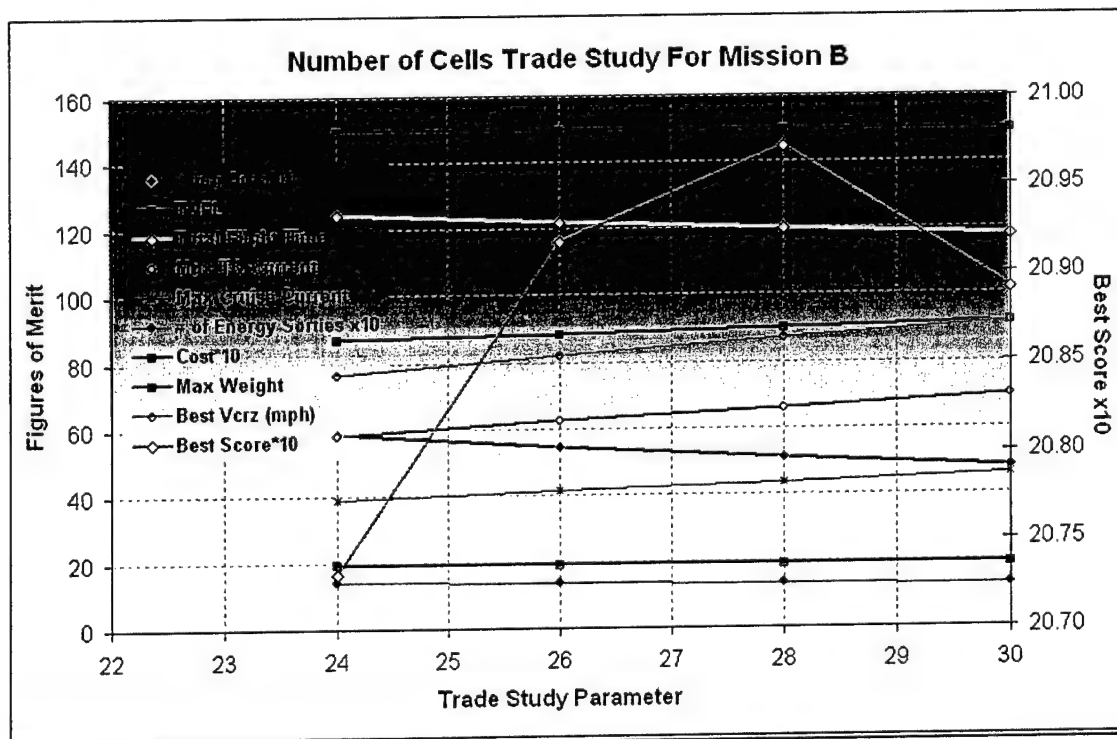


Figure 4.2.5 Trade Study of various Figure of Merit vs. number of cells assuming batteries are CP-1300's. Trade Study Parameter denotes number of battery cells.

During the testing of the battery packs, voltage, current, and duration of pack life were recorded. The objectives of the battery tests were to determine if the actual voltage and battery life matched the predicted values and to verify that the battery packs could perform with as predicted with the chosen motor. For these tests, the battery packs were soldered together in the configuration that was to be used in flight. This caused some difficulty because the batteries were lined up end to end rather than side by side and during the soldering process some batteries were destroyed. A customized soldering iron helped to eliminate this problem. The tests confirmed the expected performances calculated by PlaneSizer and 28 CP-1300 batteries, with approximately 33.6V per pack, were chosen.

2. Motors: According to contest rules, either Graupner or AstroFlight models of brushed electric motors had to be used. A library of motors was constructed in PlaneSizer which included parameters such as torque, speed constant and internal resistance for different motors. These parameters were used to establish efficient battery usage and obtain maximum power provided to the propeller. Three motors were considered for this year's plane; the Graupner 3300, the Graupner 930 and the Colbalt 60. Each motor was tested to determine four characteristic parameters: the speed constant, torque constant, no load current and winding resistance. A student designed and student constructed thrust bench was used for all motor tests as shown in Figure 4.2.6. The tests to study possible non-linearities in the motors failed because the thrust bench was limited to torques less than 1ft-lb. However, the propulsion team was able to determine that the Graupner 930-10 was able to handle the current and voltage needed to produce proper torque at take off and was able to endure the mission at full throttle (with the 28 cell battery pack). Data collected included voltage, current, torque and thrust. Data plots of these values vs. time for a typical test are shown in Figure 4.2.7. The chosen Graupner motor had a higher speed constant, was light and efficient. The other two motors considered were considerably heavier. After tests, it was concluded that the motor behaved as predicted and would handle the power levels required of it. However, it was noted that the motor would be running very close to its ultimate capacity when used during flight missions. A Hall-Effect Sensor was used to measure the RPM.

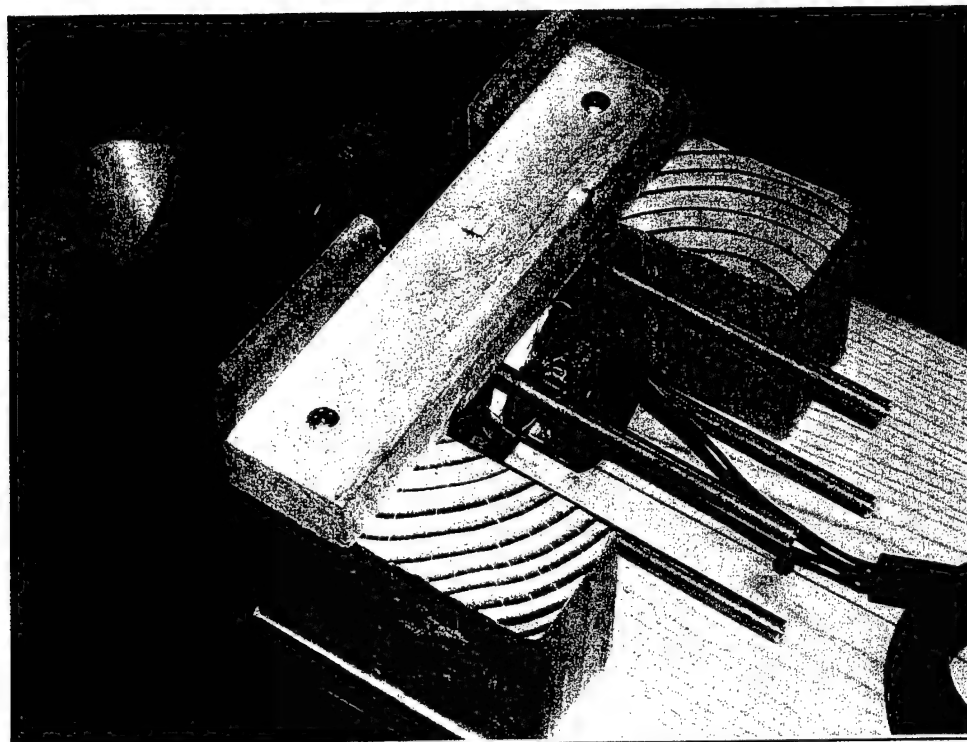


Figure 4.2.6 Thrust bench used to verify analytical propulsion model

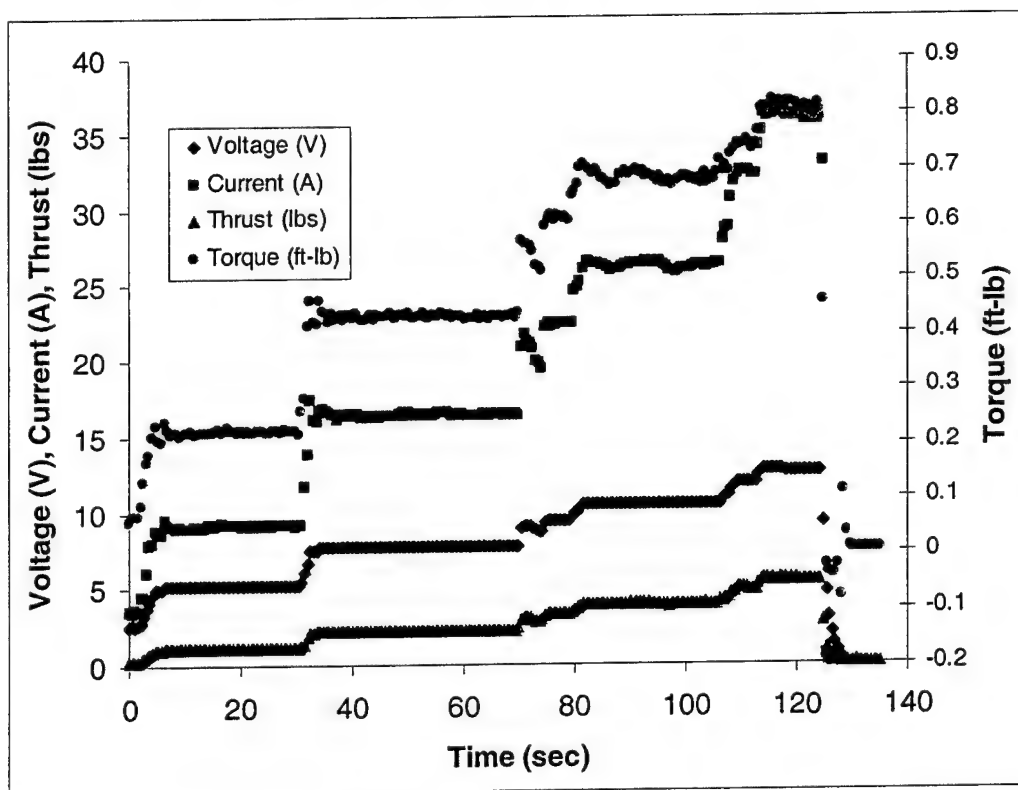


Figure 4.2.7 Time trace of data for Graupner 3300-06 using a power supply and a Bolly carbon 24 x 24 prop

3. Propellers: The propeller diameter and pitch had to be mated properly with the motor and battery pack to ensure the aircraft would meet the take off field length constraint and also to maintain sufficient cruise velocity. Large pitch propellers required more current draw whereas large diameter propellers gave a slower velocity but improved take off field length. Propeller libraries were built and incorporated into PlaneSizer. Trade studies for pitch and diameter were performed as shown in Figures 4.2.8 and 4.2.9. It was found that a 21 in. diameter propeller gave the best flight score without exceeding the 40 amp current limit. The propeller chosen was a wooden Zinger 21-14.
4. Other components: For this year's propulsion model a gear box was necessary. The InnerDemon 3.5:1 was chosen because it allows easy change between gearing ratios. For the speed controller, a Jeti 100 was chosen because it can handle 100A peak current for 30 seconds and 90A current continuously. Fuses were also tested and chosen by the propulsion team. The fuses were tested to see how long they would last at high currents. They were tested at currents greater than takeoff current and for longer than anticipated. The fuses were not a limiting factor in operating current. There was difficulty in providing an accurate measurement of the current and voltage while shorting the battery to the fuse. But by modifying the sensors on the test bench, the team was able to achieve this. The fuses were used throughout propulsion testing to ensure that it would not blow during flight conditions.

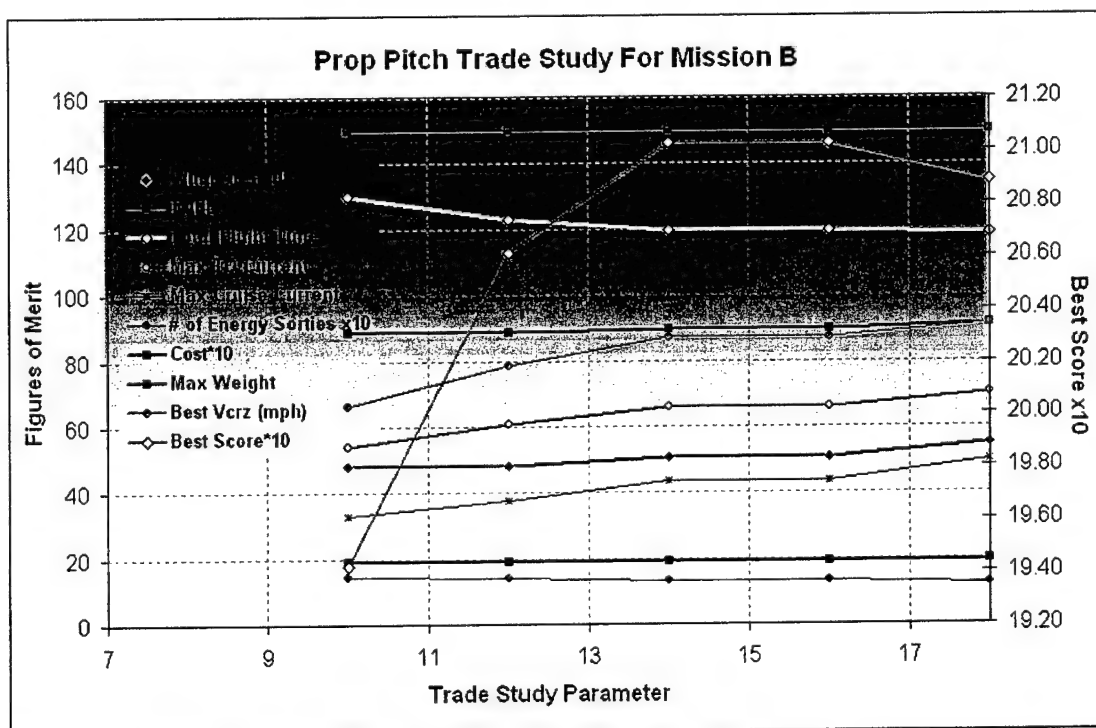


Figure 4.2.8 Trade Study of several Figures of Merit vs. prop pitch. Trade Study Parameter is prop pitch in inches

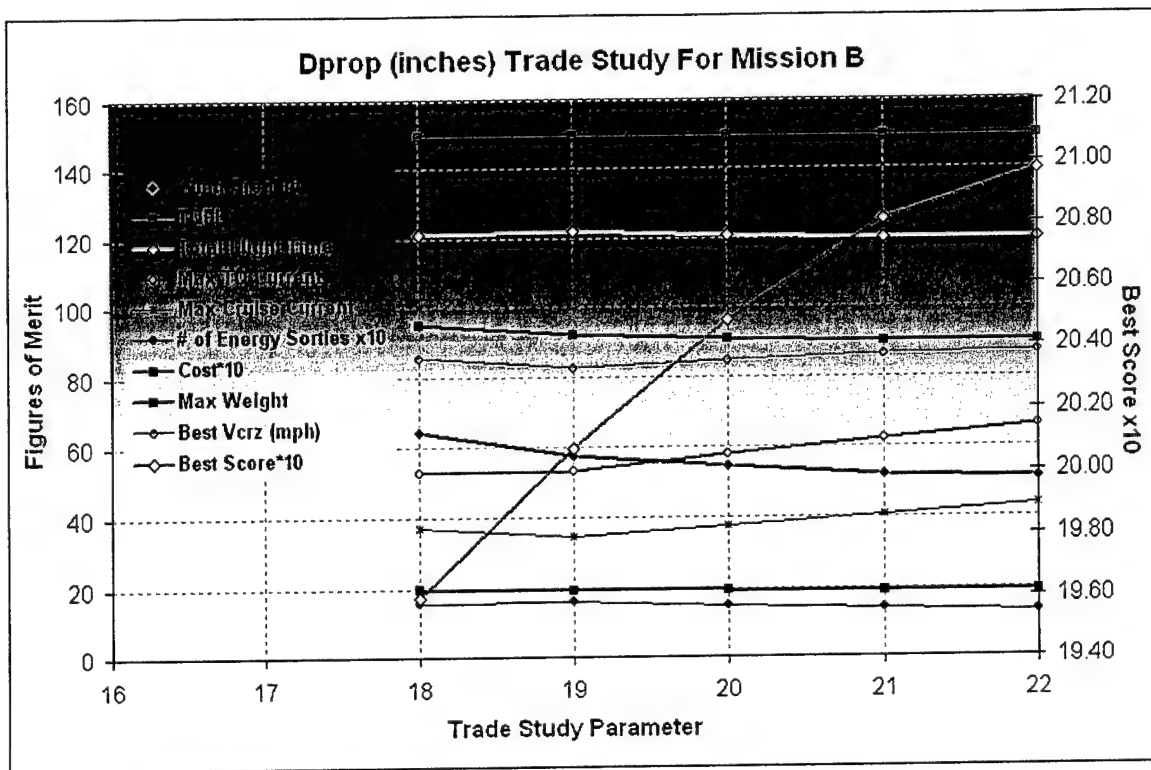


Figure 4.2.9 Trade Study of various Figures of Merit vs. Prop diameter. Trade Study Parameter is prop diameter in inches.

4.2.3 Stability and Control

The goal of the stability and control group was to provide a stable and maneuverable plane with the least tail area to minimize drag. It was decided that a conventional horizontal and vertical tail would be more suited to this year's competition than a V-tail because V-tails have diminished cross wind handling, in return for only a 1% reduction in drag. Crosswinds were a major concern for this year's competition, so the conventional tail was picked over the V-tail. Some issues addressed in designing the tail assembly included the tail lever arm, tail aspect ratios, flutter, sweep, as well as the frequency and damping ratios for the plane. Because the tail design was so closely tied in with other systems on the plane, such as the wing and propulsion system, the tail sizing process had to be performed in parallel with the rest of the aircraft. In PlaneSizer, the tail area was varied during each iteration until the required static margin and directional stability (C_{np}) were satisfied.

1. Static Margin Requirement: The pitch stability was limited by a static margin requirement of 25%. This number was obtained from a test flight in which one of the previous competition's planes center of gravity was shifted away from the c/4 location of the wing until the pilot felt that the plane had insufficient pitch stability to be reliably flown at a competition. By reverse

engineering, it was then determined that the optimal static margin for a DBF plane was approximately 25%. This number was used by PlaneSizer to size the horizontal tail area using a variety of equations from *Aircraft Stability and Control* by Perkins and Hage.

2. *C_{nβ} Requirement*: The directional stability was limited by a $C_{n\beta}$ requirement of 0.0016/degree. This requirement came from another test flight in which a plane with similar geometry to this year's competition plane was used. In this test, sections of the vertical tail were removed incrementally to reduce the vertical tail area for a number of successive flights until the pilot determined that there was insufficient directional stability to perform well in a competition with severe crosswinds. The tail area was then used to calculate a $C_{n\beta}$ of 0.0016. This number was used by PlaneSizer to size the vertical tail area using equations from *Aircraft Stability and Control* by Perkins and Hage.
3. *Flutter Control*: For crosswind handling, it was determined that a full flying vertical tail would provide more control than a conventional tail with a rudder. A major concern with this full flying tail was aerodynamic flutter, which can occur if the center of mass of the tail is behind the hinge line of the tail. The hinge line was placed at the aerodynamic center of the tail to reduce aerodynamic moment loads on the servo. Therefore, in order to keep the center of mass ahead of the hinge line it was necessary to sweep the vertical tail forward. Tests were done to make sure that this forward swept tail would not result in static divergence. This can occur if a change in the $C_{L_{tail}}$ caused a twist in the tail resulting in a significant change in angle of attack. It was determined that with the building methods employed, static divergence was not a major issue. Thus, sweeping the tail forwards was deemed a viable solution to the flutter problem.
4. *Frequency Response and Damping Ratio*: Other important Stability and Control characteristics were the frequency response and the damping ratio for the plane. These parameters would determine how well the plane would return to its initial conditions when perturbed in flight. Ideally, the frequency should be as high as possible, minimizing the time required to return to initial conditions. In reality, frequencies above 1 Hz are deemed acceptable to avoid sluggish handling. The damping ratio specifies how much overshoot the oscillations have and how rapidly the plane will return to its initial conditions. Damping ratios of 70% are considered ideal. Anything above 90% was considered too sluggish, and below 50%, the plane would oscillate excessively. The frequency for SCQuirt was found to be 2.13 Hz and the damping ratio was 57% which fell within the acceptable range.
5. *Stall Characteristics*: Stall characteristics of the aircraft were also analyzed to make sure that, in the event of stall, the plane would behave in a predictable fashion. The tail was designed so that it would stall later than the wing to prevent a loss of control in the event of stall. In addition, an un-tapered wing was selected so that the wing roots would stall earlier

than the tips to prevent sudden rolling and provide an upwash at the tail resulting in a pitch down moment for stall recovery.

4.2.4 Structural Sizing

The main aircraft structural components were the wing spars, the fuselage's "backbone", the tail boom, the landing gear, and joiners to attach them to each other. Robustness, ease of manufacture and reparability were considered in the design of each of these items. Each component was sized to withstand a variety of extreme cases, such as high G turns, hard landings, wing tip hits, etc.

1. Wing Structures: The wing was composed of 3 sections: a middle 2 ft long section permanently affixed to the fuselage and two outer 3 ft. long sections. Several spar designs were considered, such as I-beams, carbon tube spars, live spars with carbon fiber spar caps, C-beams, and square-beams. For ease of assembly and simplicity of design, carbon tube spars were chosen. Each section contained a carbon tube to carry the loads from the wing to the fuselage. The tubes inside the outer wing sections were smaller than the tube in the inner section so that they could slide together during assembly. It was decided to make the tube for the inner section larger because it would be handling more bending loads than the outer sections. This was because the higher moment of inertia from the larger diameter tubes allowed for more toleration of structural loads due to bending. The overlap between the two tubes of 6 in. was sufficient to transfer the shear loads. The major condition for sizing these tubes was a high G turn. To determine the maximum turning loads the plane would generate, a turning envelope was created. This is shown in Figure 4.2.10. It was found that, at cruise velocity, in order to stay within the boundaries of the thrust limit and stall limit it was necessary to set a structural limit of 10 G's. Hence, the wing spars were sized to withstand an unloaded turn at 10 G's with a 1.5 safety factor. The Shear and Bending moment diagrams for a semi-span under this loading condition are displayed in Figures 4.2.11 and 4.2.12 respectively.

Turning Limits for Scquirt Unloaded

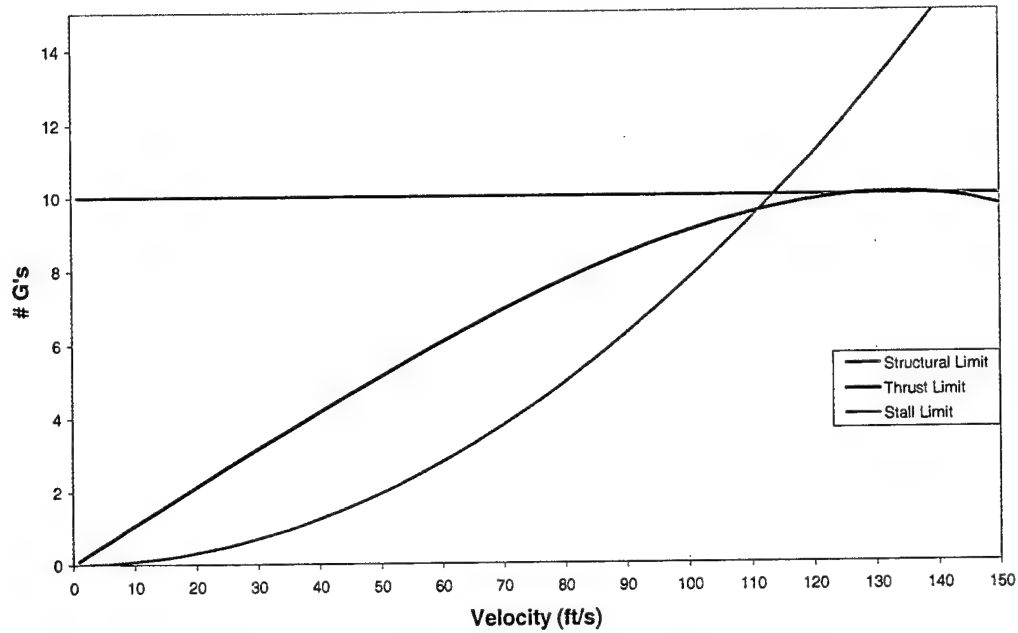


Figure 4.2.10 Turning Envelope for SCquirt (unloaded)

Shear vs. Span with 6 inch joint

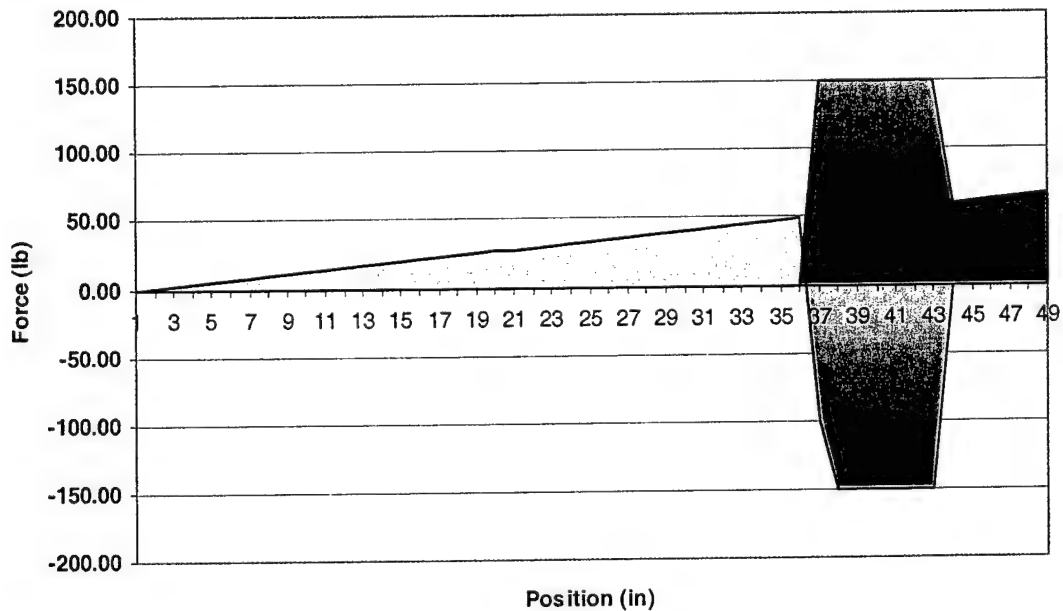


Figure 4.2.11 Shear Loading for semi-span of wing spar in 10G unloaded turn. Red denotes outer wing section, and blue denotes center wing section

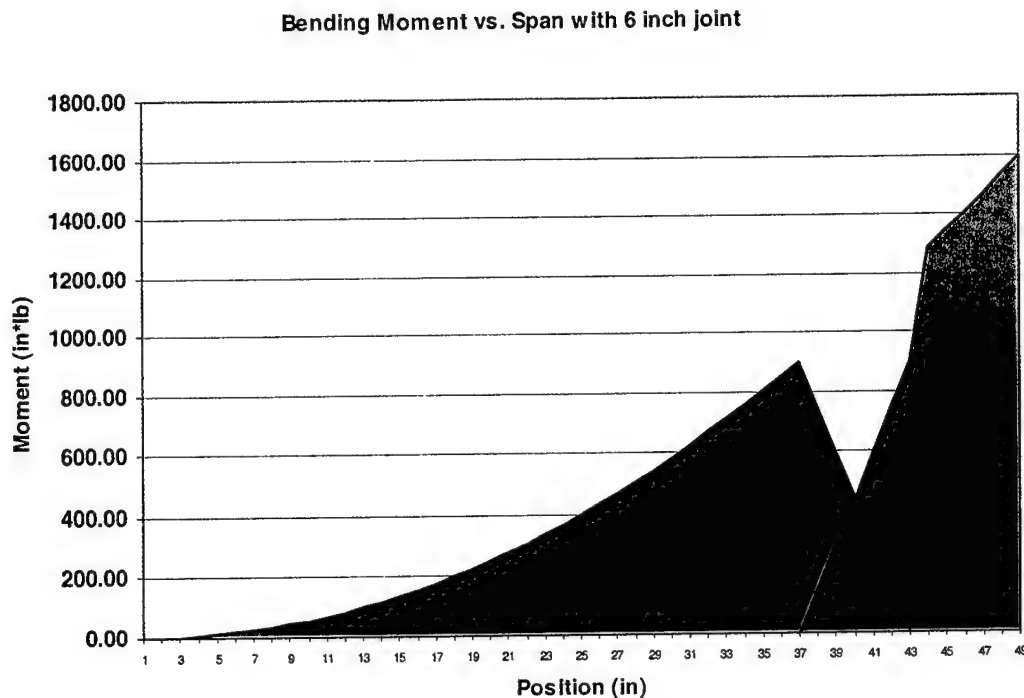


Figure 4.2.12 Shear Loading for semi-span of wing spar in 10G unloaded turn. Red denotes outer wing section, and blue denotes center wing section.

An Excel spreadsheet was created to determine the amount of carbon needed to safely transmit these loads. Other calculations were made to ensure that no skin rupture, shear failure, or core crushing were allowed

2. **Fuselage Structures:** The main structural components of the fuselage were the carbon "backbone" tube and the tail boom. The tail boom had a smaller diameter, so it was able to slide into the backbone during assembly. A 3 in. overlap was left between the two to transfer shear loads. The main condition sizing these structures was a hard landing which would transmit a large load through the landing gear structures. The shear and bending moment diagrams for the backbone and tail boom for this loading case are shown in Figures 4.2.13 and 4.2.14 respectively. The amount of carbon needed was determined using an Excel spreadsheet which calculated the strain energy allowable for a reasonable deflection given a thickness and orientation for the layers of carbon and the values of shear and bending moment from the previous graphs. The layers were bonded at 45° and -45° on the mandrel to withstand the torsional forces on the plane. The backbone was also equipped with carbon caps orientated at 0° for bending strength and hoops orientated at 90° for added stiffness where the motor and tail boom were attached.

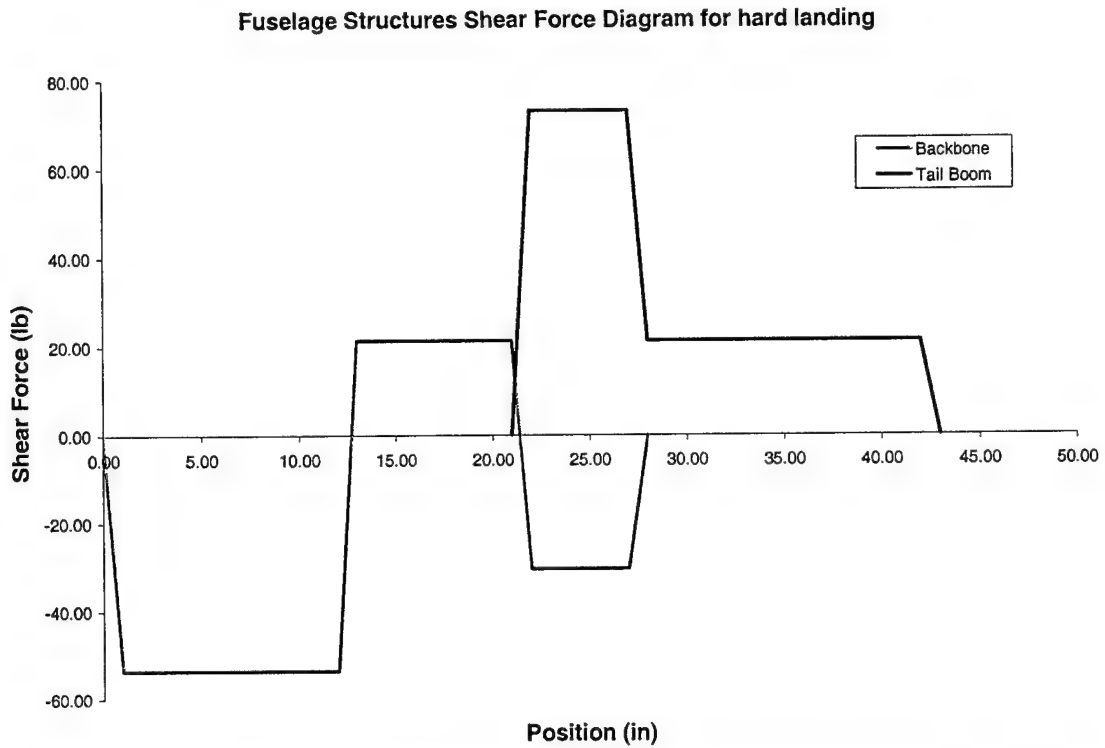


Figure 4.2.13 Shear force diagram for backbone and tail boom during hard landing

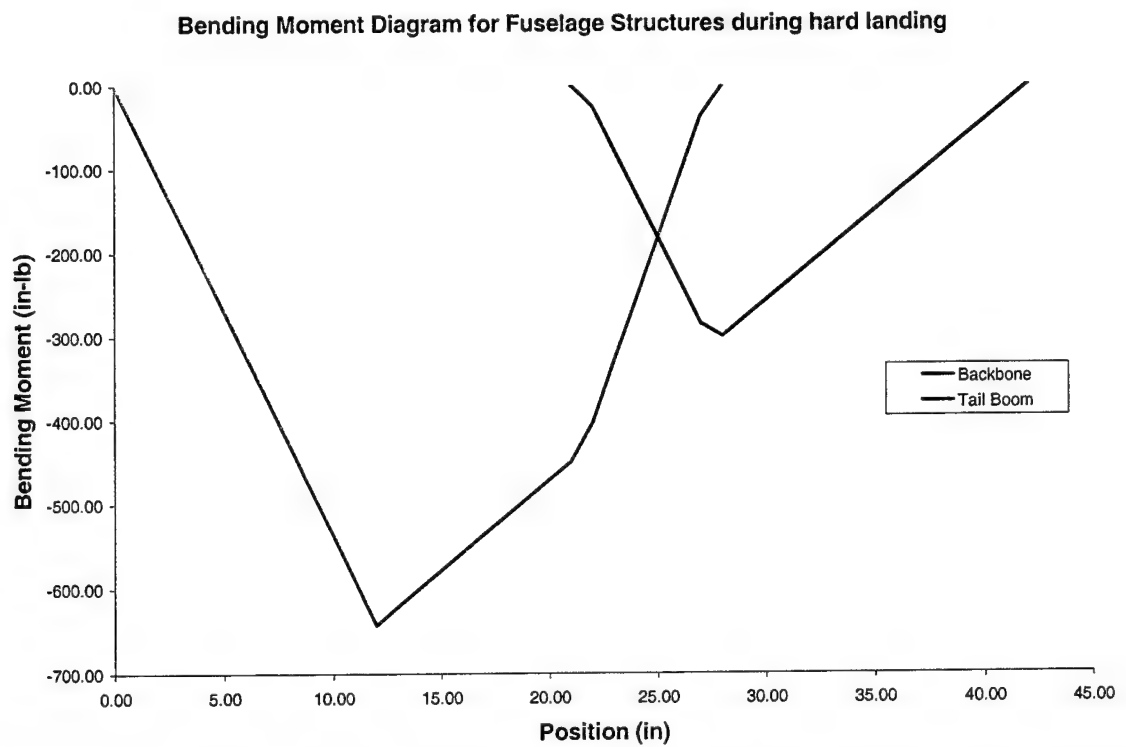


Figure 4.2.14 Bending Moment diagram for backbone and tail boom during hard landing

3. Landing Gear Structures: Two types of landing gear were considered: tricycle gear and tail-dragger gear. The structure necessary to incorporate a nose wheel into the airframe would weigh considerably more than that of a tail wheel. Also, having a tail wheel would allow for the ground steering to be tied into the same servo as the rudder, reducing rated aircraft cost. For these reasons, the tail-dragger configuration was chosen. The main gear (forward wheel struts) were sized to give the propeller sufficient ground clearance while allowing 1.5 in. of vertical deflection during a 5G landing. Structural analysis was done for the chosen geometry, and it was determined that 24 layers of unidirectional prepreg carbon fiber were needed to give the required deflection. The bolts attaching the landing gear to the backbone were sized to shear off if the wheels were brought to a sudden stop while the plane was rolling at speeds in excess of 10 ft/sec to prevent tip over.
4. Wing Spar/Backbone joiner: An advantage to the backbone/tube spar system was the simplicity of joining them together. The design for this joiner entailed two carbon fiber saddles orientated 90° to each other. A picture of one of these joints is shown in Figure 4.2.15. The two saddles were joined together by four nylon bolts that were sized to shear off during a 1G wingtip strike. That is, a 1G aft wingtip loading would shear the nylon bolts so that the wing would easily separate and sustain minimal damage during a crash. The landing gear was joined to the backbone by similar methods.

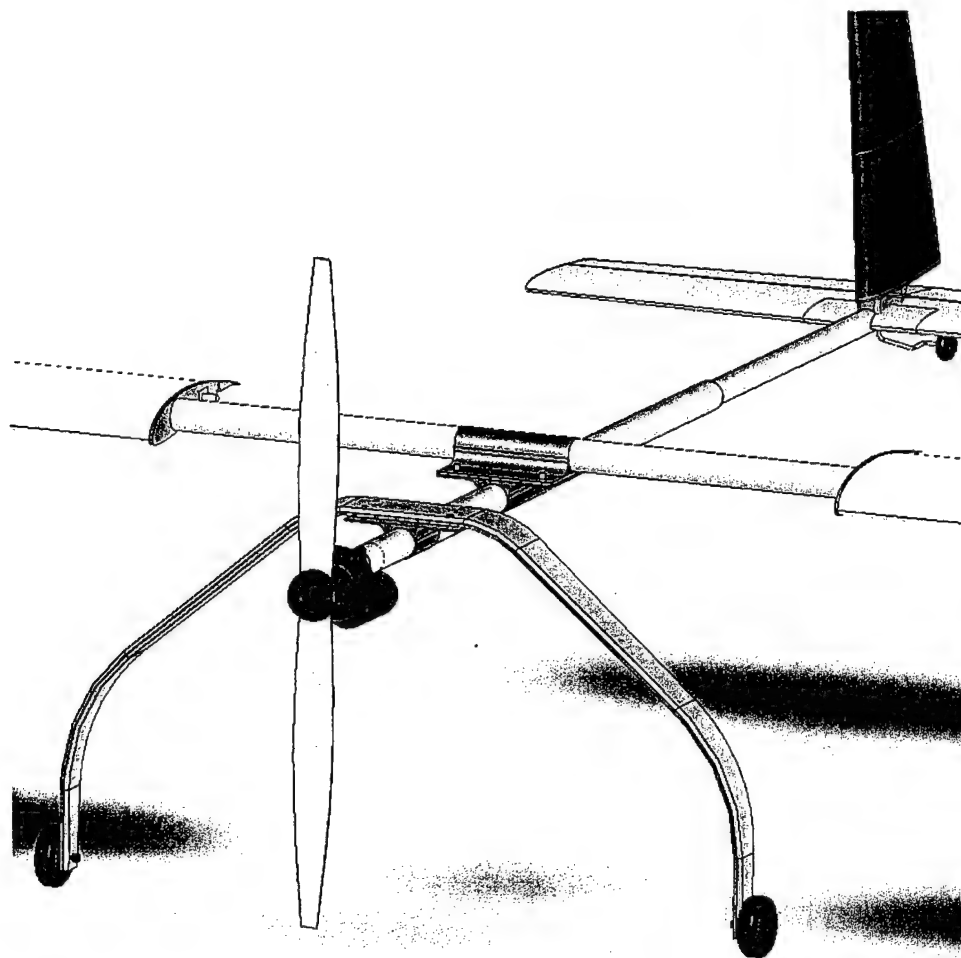


Figure 4.2.15 Joint connecting wing spar and landing gear to backbone

4.2.5 Water Drop:

This year, the rules for the FireFight mission called for four liters of water to be dropped out of the airplane while the plane was in flight. All the water needed to be dumped during the downwind leg of the flight and had to exit out of a half inch diameter hole. One of the major challenges of this requirement was to minimize the time it takes the water to exit in order to accomplish a complete draining of the tank during the downwind leg. It was estimated that a downwind leg takes 17-18 seconds to complete. It was decided that a 15 second drop time was most desirable to give a minimum 2 second safety margin. Preliminary tests showed that draining 4 liters of water out of a half inch diameter hole, unaided, took approximately 25 seconds. The goal of the Payload team was to design a tank and a nozzle to create a configuration that would reduce the drop time by 40%.

The tank design was driven by the airplane geometry. Because the cost equations favored a long narrow fuselage, a simple rectangle box was chosen for a tank design. Having square corners maximized volume and having a long rectangle allowed it to fit inside a narrow fuselage. The maximum height and width of the tank was chosen to be four inches. It was assumed that the tank would be made out of wet lay-up carbon cloth but would offer no structural support.

The nozzle design and location was significant in reducing water drop time. A 3-D model of the nozzle was designed in Solid Works and then machined out of plexiglass for testing. The nozzle needed to be thin to fit under the fuselage and offer limited drag. It also needed to be servo activated and designed with a filleted exit hole. Figure 4.2.16 shows a CAD drawing of the nozzle.

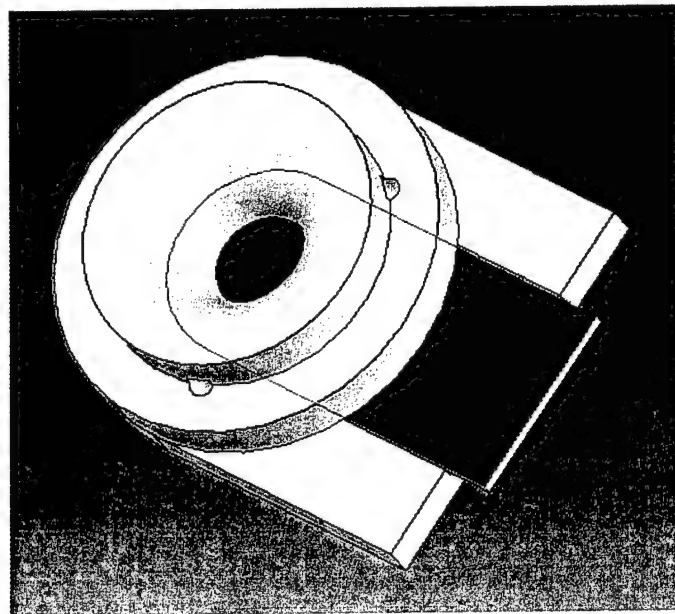


Figure 4.2.16 Knife gate valve and nozzle. The flow would be from upper left to lower right when the knife valve (in green) was opened.

In the preliminary design phase, fluid dynamics, pressure differences, G-loading, and nozzle radius were analyzed and predictions were established. The payload group set up extensive testing to compare theoretical calculations with experimental results. Because the FireFight mission depended so heavily upon the water drop, proper performance was key.

5.0 DETAILED DESIGN PHASE:

This design phase finalized the configuration of the aircraft by refining the analysis performed during the preliminary phase. New assumptions were incorporated within the design that focused on detailed aspects of certain systems. Aircraft components were selected based upon a convergence of analytical results from PlaneSizer and experimentally tested data.

5.1 Component and Systems Architecture Selection

1. **Propulsion System:** The radio used to drive the propulsion system was a Futaba 9CA model. The speed controller used was a Jeti 100. This model was chosen because it can handle 100A peak current for 30 seconds and 90A current continuously. For this year's propulsion model a gear box was necessary. The gear box was InnerDemon 3.5:1. It allows for easy change between gearing ratios. The chosen motor was the Graupner 930-10 with 28 cells of CP-1700 NiCad batteries, and a 21-14 propeller. This system was optimized in PlaneSizer and experimentally verified on the thrust bench as being the best system for this year's aircraft.
2. **Stability and Control:** The empennage consisted of a conventional horizontal and vertical tail assembly. The relevant geometric and aerodynamic properties of these tails are given in Table 5.1.1.

Stability Parameters	Horizontal Tail	Vertical Tail
Tail Area	0.58 ft ²	0.45 ft ²
Tail Span	1.53 ft	0.94 ft
C_{root}	0.42 ft	0.59 ft
C_{tip}	0.34 ft	0.35 ft
Static Margin	25%	---
Directional Stability ($C_{n\beta}$)	---	0.002
Pitch Frequency (at cruise)	2.13 Hz	---
Yaw Frequency (at cruise)	---	1.49 Hz
Pitch Damping Ratio	57%	---

Table 5.1.1 Stability and Control final parameters computed

The wing control surfaces were two full span flaperons. It was determined that flaperons were the best option due to the rated aircraft cost penalty for multiple control surfaces and servos. The drawback to this configuration was the increased stiffness needed over the area of the control surface to guarantee the same deflection angle at both the root and the tip. To

resolve this, the servos were positioned at 40% semi-span to attempt to attain equal loading both inboard and outboard of the servo. The flaperon area was sized to 25% chord and each was driven by a GWS S03N servo rated at 56 oz-in. of torque. This was the lightest servo that satisfied the calculated torque requirement for maximum deflection at cruise velocity plus a 1.3 safety factor. The horizontal tail had an elevator covering 35% of the chord. This was driven by a GWS PARK L mini servo giving 39 oz-in of torque. This servo was sized using the same methods as the wing flaperon servos. The vertical tail was full flying and powered by a GWS S03T servo with 111 oz-in of torque. Extra torque was required because this servo controlled the tail wheel as well as the vertical tail.

The airfoils for both the horizontal and vertical tails were chosen to be symmetric SD8020 at 10% t/c because of their low parasite drag. Much effort was put into assuring that the overall plane CG location stayed constant throughout the water dumping process by carefully positioning the water tank and other components. This assured that the pitch stability remained within the static margin constraint, and made the plane much more reliable to fly. The pitch and yaw frequencies calculated were sufficient to avoid sluggish handling, and the pitch damping ratio, although lower than 70%, was deemed acceptable for test flights.

3. Water Drop: The payload team performed a number of static and dynamic tests, which are further detailed in the testing section. They made multiple prototypes and documented the results from wind tunnel set ups and in flight experiments. The final nozzle configuration was a thin, plexiglass, knife gate valve. It was designed with a discharge coefficient (measure of efficiency of nozzle due to losses from turbulence) of 0.93 and the radius of curvature of the exit hole was equal to the diameter. The custom designed knife gate valve was chosen because commercially available valves were either too heavy or opened too slowly. This gate-valve assembly was able to open quickly and was light enough to be powered by a servo. The final dimensions of the tank were 4"x4"x16" and the tank held the maximum water capacity, 4 liters. A ram air scoop was located at the top of the tank and the nozzle was located on the bottom of the tank near the back. Other possible locations were discussed, such as using a low wing aircraft to utilize the low pressure over the wing to aid the exit flow using the suction pressure from the air passing over the airfoil. However, the aft positioning of the nozzle placed the exiting water away from motor and batteries, and decreased the possibility of water being left in the tank.
4. Landing Gear: Stress analysis was performed on the landing gear, and it was determined that 24 layers of unidirectional carbon were necessary to achieve the required 1.5 in. deflection during a 5G hard landing. Flexibility was set by strut thickness and strength by strut chord. The landing gear was attached to the main backbone using a carbon joint. This joint was designed to be able to slide forward and aft for adjusting the CG location during test flights. The landing gear was affixed to this joint by four 3/8" nylon bolts. These bolts were sized to

shear off in the event that the wheels encountered a rigid object while the plane was rolling in excess of 10 ft/sec to avoid tip over. A steerable tail wheel was attached to the tail boom and controlled by the same servo as the vertical tail.

A pneumatic braking system was installed composed of a pressurized air bottle connected to a servo controlled proportional release valve. The pressure required to activate the brakes was determined by ground testing. The main gear was placed far enough ahead of the CG location to avoid tip over and propeller strikes when the brakes were applied.

5.2 Estimated Mission Performance:

PlaneSizer was used to predict the plane characteristics as well as its flight performance. The different modules built by the group captains calculated the required parameters that allowed for optimization. Final configuration data is tabulated below, including geometry, performance factors and weight statements.

1. **Geometry:** The estimated geometry based upon the aerodynamic calculations is found in Table 5.2.1. The wingspan was set to 8 feet and the control surfaces were sized as 25% of the chord.
2. **Performance Factors:** Table 5.2.2 shows the different velocities for each mission. Table 5.2.3 shows the important flight characteristics such as TOFL, maximum current draw and total energy for different missions. Table 5.2.4 shows the lift and drag coefficients during cruise velocity.

Calculated Geometry	Units	Wing	H.Tail	V.Tail
Total Area Sw, SH, Sv	ft ²	5.06	0.58	0.45
MAC	ft	0.63	0.38	0.48
Y MAC	ft	2.00	0.37	0.43
Projected Span	ft	8.00	1.53	0.94
Root Chord	ft	0.63	0.42	0.59
Tip Chord	ft	0.63	0.34	0.35
Root Incidence	deg	-3.50	1.00	
Tip Incidence	deg	-3.50	1.00	
Fuselage Height, Width, Length(incl spinner)	ft	0.30	0.30	4.92

Table 5.2.1 Main airplane geometry

Parameter	Units	Mission A (heavy)	Mission B1 (heavy)	Mission B2 (light)	Mission B3 (light)	Mission B4 (light)
Vcruise	fps	130.2	125.0	130.2	125.0	130.2
Vstall	fps	34.1	46.4	34.1	46.4	34.1
Vlift-off	fps	40.9	55.7	40.9	55.7	40.9
Vclimb& Ldg	fps	44.3	60.4	44.3	60.4	44.3

Table 5.2.2 In flight velocity breakdown

Parameter	Unit	Mission A (heavy)	Mission B1 (heavy)	Mission B2 (light)	Mission B3 (light)	Mission B4 (light)
TOGW	lbs	10.3	19.1	10.3	19.1	10.3
TOFL (incl safety pad)	ft	39.0	135.0		150.0	
Total Flight Segment Time	sec	106	37	23	37	23
Total Flight Energy	ft-lbs	86682	15025	14460	15025	14460
Max Cruise Current	A	41.6	43.5	41.6	43.5	41.6
Takeoff Thrust	lbs	9.7	9.7		8.7	
Thrust @ Vcrz	lbs	2.8	3.1	2.8	3.1	2.8

Table 5.2.3 Performance characteristics

Parameter	Unit	Mission A (heavy)	Mission B1 (heavy)	Mission B2 (light)	Mission B3 (light)	Mission B4 (light)
CLmax3-D	n.d.	1.53	1.53	1.53	1.53	1.53
CLcruise	n.d.	0.10	0.21	0.10	0.21	0.10
CDcruise	n.d.	0.024	0.024	0.024	0.024	0.024
L/Dcrz	n.d.	4.41	8.97	4.41	8.97	4.41

Table 5.2.4 Aerodynamic characteristics

5.3 Weights, Balance, and Rated Aircraft Cost Worksheets

1. **Rated Aircraft Cost:** The RAC has always been a debilitating factor for USC's aero design team. This year considerable effort was focused on reducing this parameter to be more competitive. By investigating alternatives for different propulsion configurations and structural sizing, the team was able to lower the RAC from 11 last year to 8.95 for this year. The fuselage was designed to be long and narrow and fewer battery cells were used. Table 5.3.1 shows the cost break down for the plane.
2. **Weight Budget:** The predicted weight of the plane was calculated through the model in PlaneSizer using measurements of the aircraft's dimensions from the design and library sheets. The weights and densities of purchased materials were taken from manufacturer's specifications and from lab test data. The lab data was very important because the manufacturer's claimed weights were often inaccurate, especially in composite materials. Lab results were also used to

create data correlations; for example the relation between propeller diameter and propeller weight. Weights for complex shapes were calculated by estimating their volume with simple rectangular approximations and then multiplying by material density. The weight of the outside skin of the wing and the tail was calculated by finding the area of the exposed surfaces and then multiplying by the thickness of the coating material and its density. The spar of the wing was treated as a separate tube and its weight was calculated using its thickness, length and density. The weight build up model is shown in Table 5.3.2 with the break down for the different systems and the Kfudge parameter (weights safety factor). Empty and Heavy Gross weights are given at the bottom of the table.

Cost Table					Total Cost	Rated Cost
Rated Aircraft Cost (AxMEW + BxREP + CxMFHR)/1000	Dims	Manuf. Hrs	Hrs (sub-total)	Cost (sub-total)	\$8,947	8.95
MEW (Manufacturers Empty Weight) (lb.)	10.25		10.25	3076.37		34.4%
REP (Rated Engine Power)	= (1+.25*(#Motors-1))*BattWt		2.26	3390.2		37.9%
# of Engines	1					
Total Battery Weight (lbs)	2.26					
MFHR (Manufacturing Man Hours)			124.03	2480.6		27.7%
WBS1.0 (8hr/ftSpan + 8hr/ftMaxChord + 3 hr/control surface)	# of wings	1	58.1		13.0%	
	Wing Span	8.00				
	Max Wing Chord	0.63				
	# of control surfaces	2				
WBS2.0 (10hr/ft of length)	Fuselage Volume (ft)	0.55	10.9		2.4%	
WBS3.0 (10hr/VertWithRudder + 10hr/horizWithElev)	Number of Vertical Surfaces	0	0.0	Biplane Assumes Inter Plane Struts	4.5%	
	Number of Vertical Tails	1	10.0			
	# of Horizontal Tails	1	10.0			
WBS4.0 (5hr/servo or controller)	# of Servos and Motor Controllers	7	35.0		7.8%	

Fixed Parameters	
A (Manufacturers Empty Weight Multiplier) (\$/lb.)	300
B (Rated Engine Power Multiplier) (\$/Watt)	1500
C (Manufacturing Cost Multiplier) (\$/hour)	20

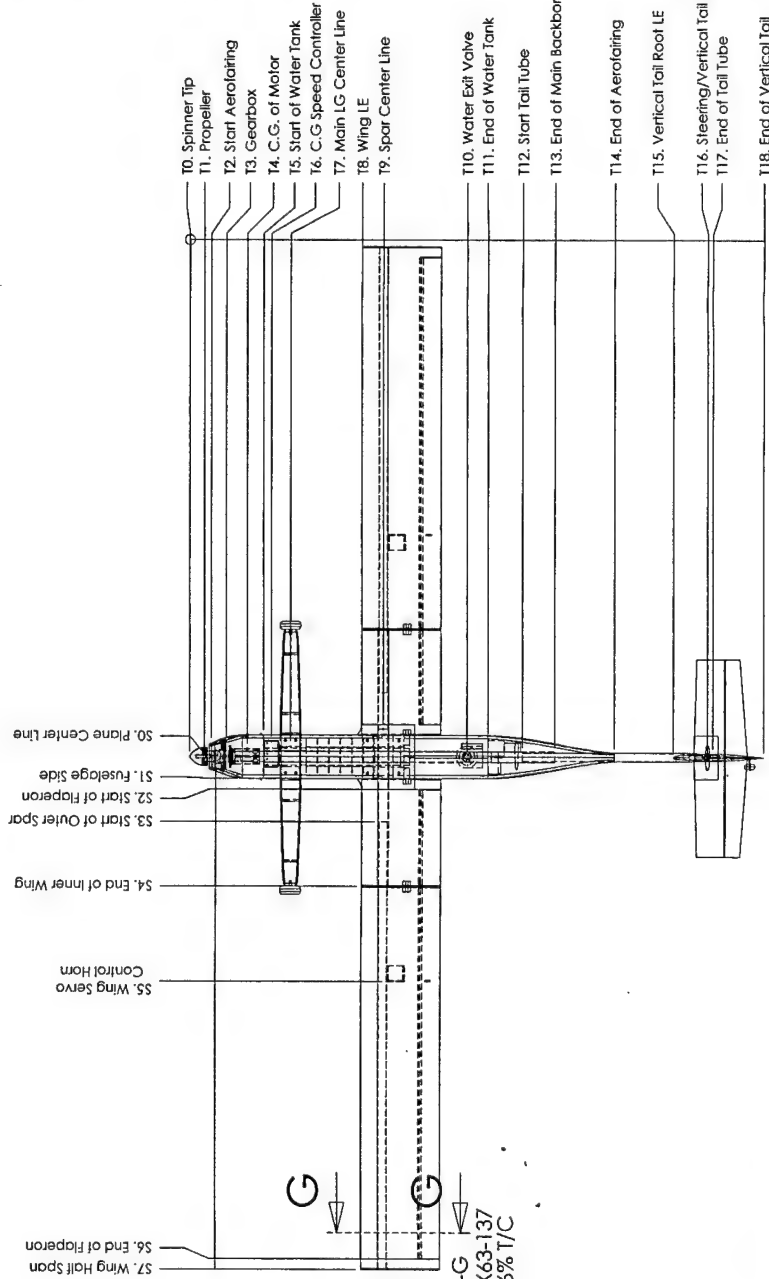
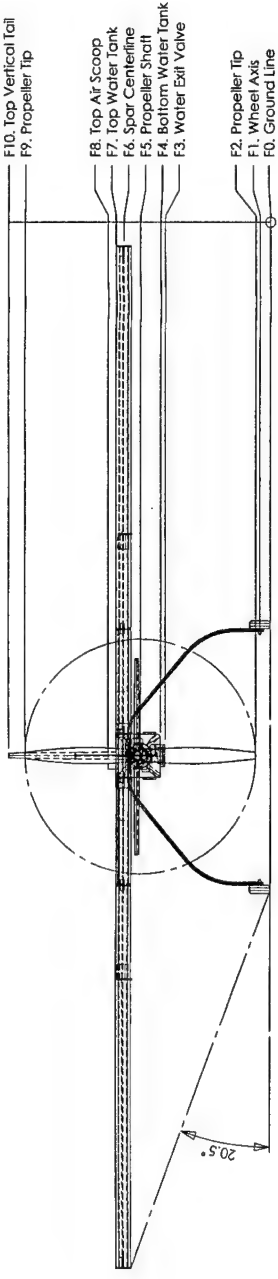
Table 5.3.1 Rated Aircraft Cost calculation and results

System	KFudge	Sub-Component	Weight Breakdown	% of Empty Weight
PROPULSION	1.0	Sub-Total (incl Kfudge))	4.153	40.3%
		Motor(s)	1.069	10.37%
		1 Heatsink	0.138	1.34%
		Battery wt incl. solder & jack	2.260	21.92%
		All Wiring	0.100	0.97%
		1 Speed Controller	0.150	1.45%
		1 Propeller	0.220	2.13%
		1 Spinner & Prop Nut	0.055	0.53%
		1 Motor Mount	0.160	1.56%
WING	1.0	Sub-Total (incl Kfudge))	1.601	15.5%
		Wing Spar	0.035	0.34%
		Wing Core	0.775	7.52%
		Wing Skin	0.790	7.66%
TAIL & Winglets	1.5	Sub-Total (incl Kfudge))	0.395	3.8%
		HTail Skin	0.095	0.92%
		HTail Core	0.025	0.24%
		VTail Skin	0.100	0.97%
		VTail Core	0.044	0.42%
		Winglets	0.000	0.00%
RADIO	1.0	Sub-Total (incl Kfudge))	1.225	11.9%
		Receiver	0.125	1.21%
		Servos	0.600	5.82%
		Battery Pack	0.500	4.85%
LANDING GEAR	1.0	Sub-Total (incl Kfudge))	2.099	20.4%
		Main Gear Struts & Bolts	1.229	11.92%
		Main Wheels	0.290	2.81%
		MG Axle Hardware	0.072	0.70%
		Nose Wheel or Tail Wheel	0.307	2.98%
		Nose Gear Strut & Mount	0.100	0.97%
		Brakes, Tubing, Air Tank	0.100	0.97%
FUSELAGE	1.20	Sub-Total (incl Kfudge))	0.839	8.1%
		Fuselage Skin	0.559	5.42%
		Bulkheads	0.140	1.36%
		Backbone	0	0.00%

Airframe Weight =	4.83	No systems installed
Flying Empty Weight =	10.31	(includes test for actual weight)
Payload Weight (4L water) =	8.82	
Heavy Gross Weight =	19.13	
Light Gross Weight =	10.31	

Table 5.3.2 Weight Breakdown in Lbs.

3. Balance Distribution: The CG for both light and heavy planes was set at the same location for ease of handling and flying. A CG balance sheet was created in PlaneSizer and linked to the configurations sheets. Since the plane was geometrically symmetrical about the center of the plane and the vertical CG location had negligible effects on the handling of the plane, the vertical CG calculations were not performed. The individual components of the plane were then moved fore and aft to position the CG so that it aligned with the desired value at 25% of the wing chord. Since the length of the plane was fixed, the batteries and landing gear placement were the items primarily reconfigured to achieve the desired CG.



Horizontal Tail		Parameter	Unit
Airfoil	SD6020	—	—
Volume	0.505	—	—
Thickness	8%	—	—
Tail Area	0.58	ft ²	—
Chord root	5.09	in	—
Chord tip	4.07	in	—
Span	1.53	ft	—
MAC	4.60	in	—
AR	4	—	—
TR	0.8	—	—
Sweep	3.5	deg	—
Static Margin	25%	—	—
Pitch Frequency (@ Cruise)	2.13	Hz	—
Pitch Damping Ratio (@ Cruise)	47.35%	—	—
Control Surface	35%	—	—
Torque req	20	oz.in	—
Servo max torque @6V	35	oz.in	—

Wing		Parameter	Unit
Airfoil	FX63-137-16%	Thickness	16%
Wing Area	5.06	ft ²	—
Chord	7.59	in	—
Span	8	ft	—
MAC	7.59	in	—
AR	12.05	—	—
TR	1	—	—
Sweep	0	deg	—
Incidence angle	3.4	deg	—
CL max 3-D	1.53	—	—
CL cruise	0.21	—	—
CD cruise	0.02	—	—
ROC	8.97	—	—
L/D cruise	400	—	—
V Liftoff	55.73	fps	—
V cruise	124.96	fps	—
V climb&land	60.37	fps	—
V stall	46.44	fps	—

Component Location Dimensions Relative to T0, S0 and F0

DIM	In	In	DIM	In	In
T0	0.00	0.00	F0	0.00	0.00
T1	1.40	1.40	F1	1.00	1.00
T2	2.05	3.00	F2	1.40	1.40
T3	3.50	6.00	F3	10.04	10.04
T4	5.50	12.00	F4	10.48	10.48
T5	7.05	21.00	F5	13.98	13.98
T6	7.80	47.00	F6	15.48	15.48
T7	9.65	48.00	F7	14.73	14.73
T8	16.48	—	F8	23.40	23.40
T9	18.53	—	F9	24.96	24.96
T10	26.55	—	F10	24.96	24.96
T11	28.55	—			
T12	31.63	—			
T13	34.90	—			
T14	40.55	—			
T15	46.11	—			
T16	48.33	—			
T17	48.83	—			
T18	54.64	—			

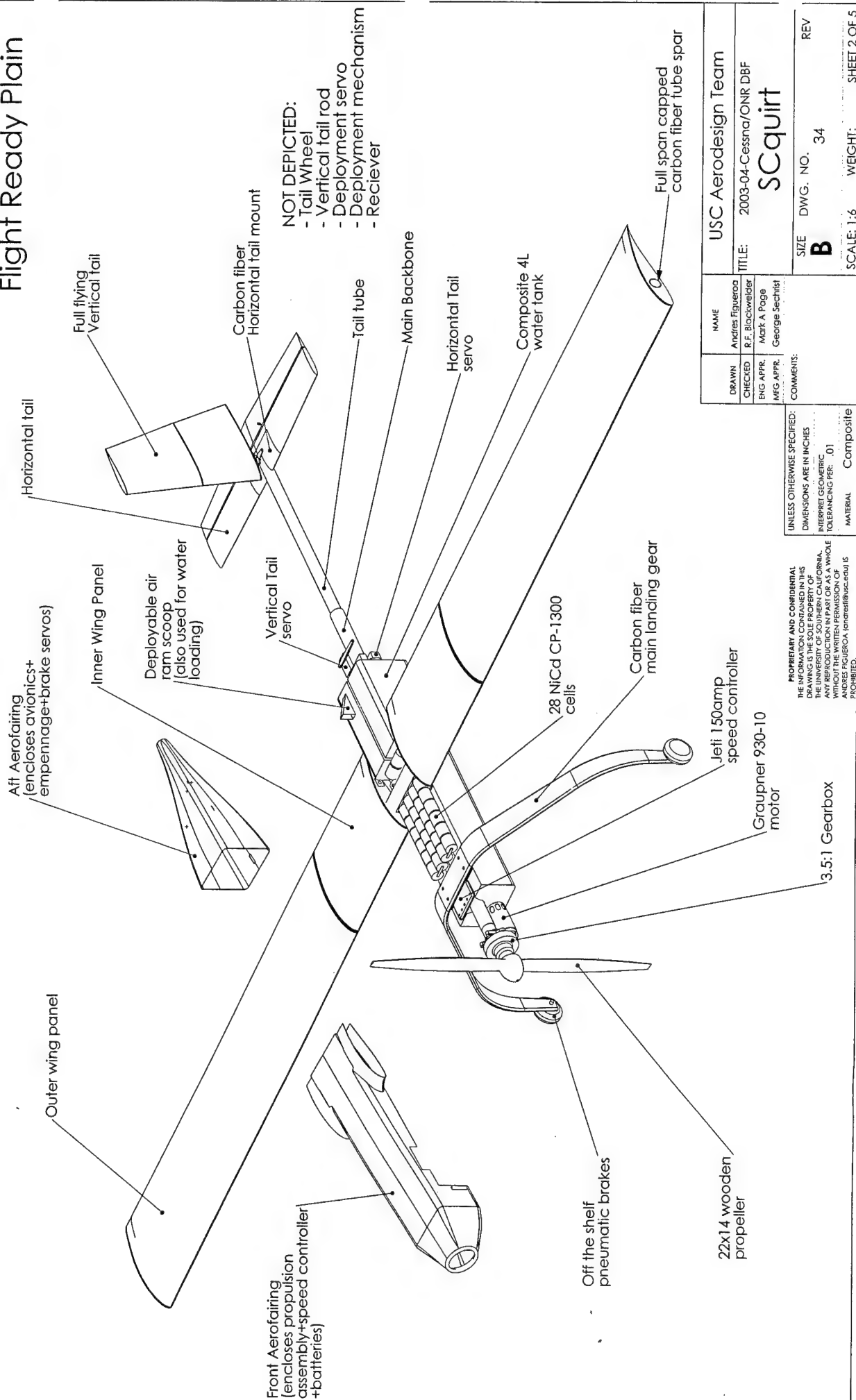
Vertical Tail		Parameter	Unit
Airfoil	SD6020	—	—
Volume	0.030	—	—
Thickness	8%	—	—
Tail Area	0.45	ft ²	—
Chord root	7.08	in	—
Chord tip	4.25	in	—
Span	0.94	ft	—
MAC	5.78	in	—
AR	2	—	—
TR	0.6	—	—
Sweep	-10	deg	—
LV	2.77	ft	—
Chorus	0.0015	—	—
Yaw Frequency (@ Cruise)	1.49	Hz	—
Control Surface	100%	—	—
Torque req	50	oz.in	—
Servo max torque @6V	111	oz.in	—

NAME		USC Aerodesign Team	
DRAWN	Andres Figueroa	TITLE: 2003-04-Cessna/ONR DBF	
CHECKED	R.E. Blockwelder	SCquirt	
ENG APPR.	Mark A Page	SIZE	DWG. NO. 15
MFG APPR.	George Sechrist	B	REV
UNLESS OTHERWISE SPECIFIED: DIMENSIONS ARE IN INCHES INTERPRET GEOMETRIC TOLERANCING PER: 0.01			
MATERIAL	Composite	SCALE: 1:12	WEIGHT: SHEET 1 OF 5

PROPRIETARY AND CONFIDENTIAL
THE INFORMATION CONTAINED IN THIS
DRAWING IS THE SOLE PROPERTY OF
USC AERODESIGN TEAM. NO PART OF
THIS DRAWING IS TO BE REPRODUCED OR
TRANSMITTED IN ANY FORM OR BY ANY
MEANS, ELECTRONIC OR MECHANICAL,
WITHOUT THE WRITTEN PERMISSION OF
ANDRES FIGUEROA. (andresf@usc.edu) IS
PROHIBITED.

G-G
FX63-137
16% T/C

Flight Ready Plain



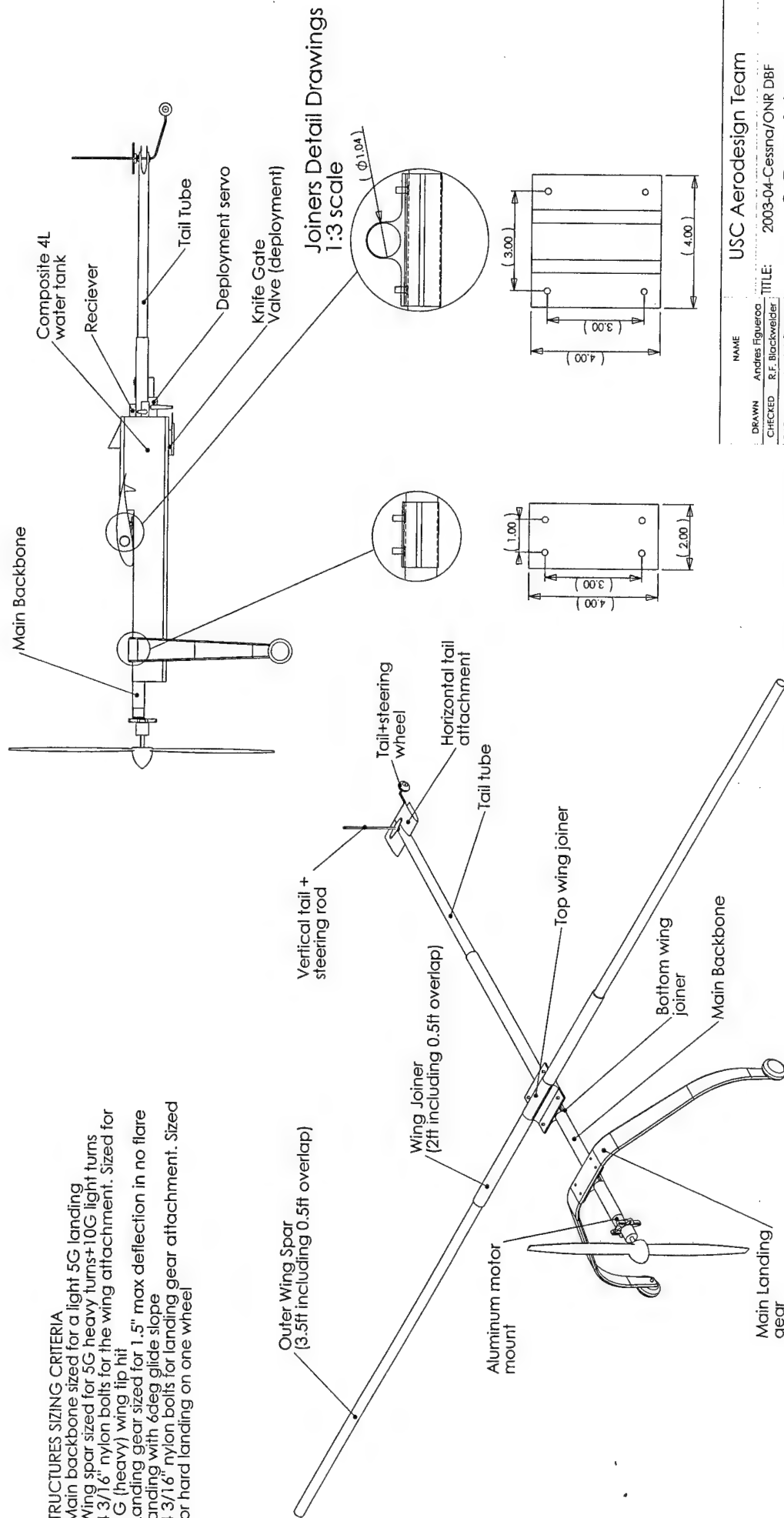
USC Aerodesign Team			
DRAWN	Andres Figueroa	TITLE	2003-04-Cessna/ONR DBF
CHECKED	R.F. Blackwelder	SCquirt	
ENG APPR.	Mark A. Page	SIZE	DWG. NO. 34
MKG APPR.	George Sechlist	REV	
COMMENTS:			
UNLESS OTHERWISE SPECIFIED: DIMENSIONS ARE IN INCHES INTERPRET GEOMETRIC TOLERANCING PER .01			
MATERIAL		Composite	

PROPRIETARY AND CONFIDENTIAL
THE INFORMATION CONTAINED IN THIS
DRAWING IS THE PROPERTY OF USC
AND IS NOT TO BE REPRODUCED IN
ANY MANNER WITHOUT THE WRITTEN
PERMISSION OF USC. (usc.edu) IS
PROHIBITED.

Main Structure Components

STRUCTURES SIZING CRITERIA

- Main backbone sized for a light 5G landing
- Wing spar sized for 5G heavy turns+10G light turns
- 4 3/16" nylon bolts for the wing attachment. Sized for 1G (heavy) wing tip hit
- Landing gear sized for 1.5" max deflection in no flare landing with 6deg glide slope
- 4 3/16" nylon bolts for landing gear attachment. Sized for hard landing on one wheel



USC Aerodesign Team

TITLE: 2003-04-Cessna/ONR DBF

SCquirt

SIZE DWG. NO. 27 REV

SCALE: 1:8 WEIGHT: SHEET 3 OF 5

NAME	Andres Figueroa
DRAWN	R.F. Blackwelder
CHECKED	Mark A. Page
ENG APPR.	George Sechrist
MFG APPR.	

COMMENTS:

UNLESS OTHERWISE SPECIFIED:

THE INFORMATION CONTAINED IN THIS DRAWING IS THE SOLE PROPERTY OF USC AERODESIGN TEAM. NO PART OF THIS DRAWING MAY BE REPRODUCED OR TRANSMITTED IN ANY FORM OR BY ANY MEANS, WITHOUT THE WRITTEN PERMISSION OF USC AERODESIGN TEAM. (usc.aerodesign.com) IS PROHIBITED.

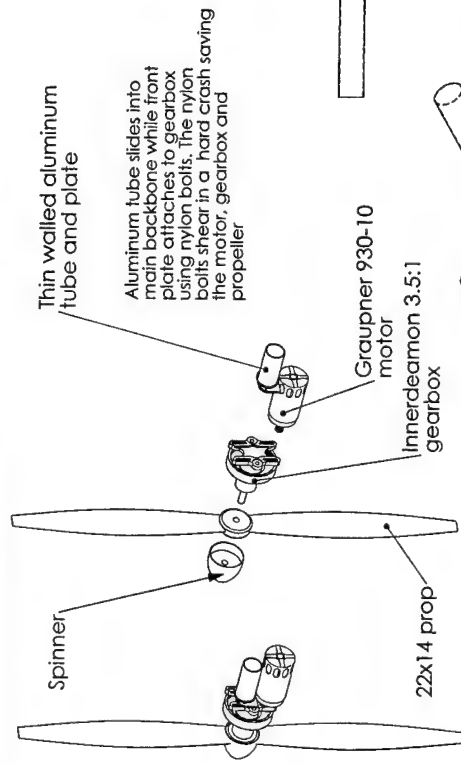
DIMENSIONS ARE IN INCHES

INTERPRET GEOMETRIC

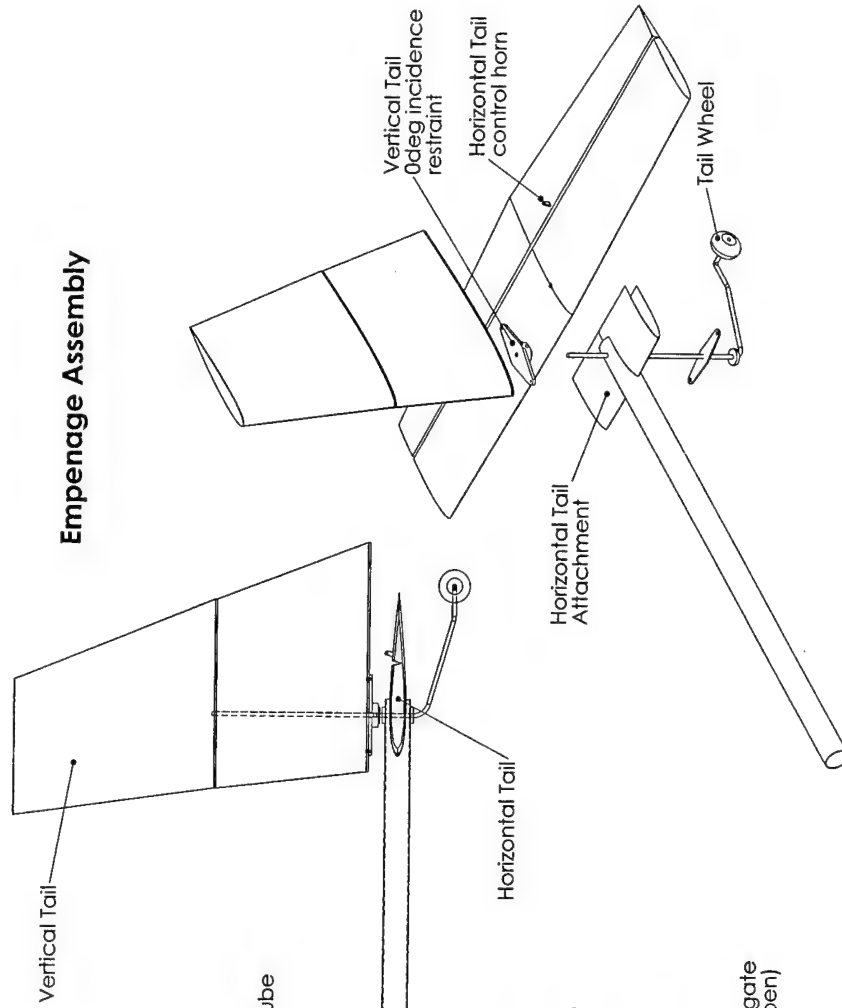
TOLERANCING PER: .01

MATERIAL Composite

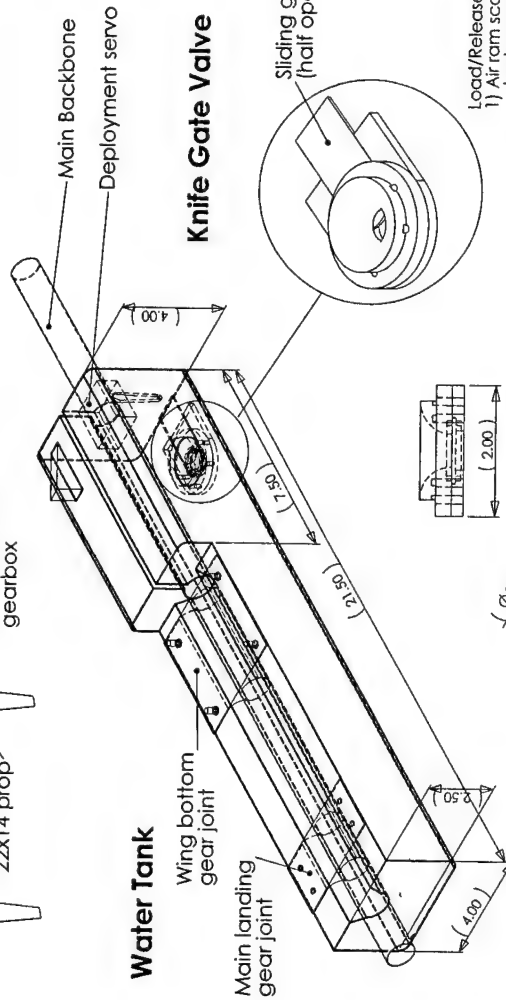
Motor Mount Assembly



Empenage Assembly



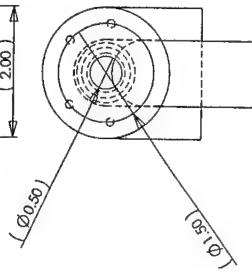
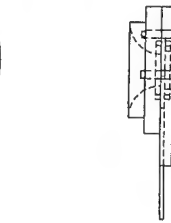
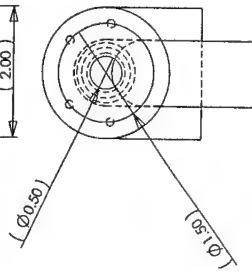
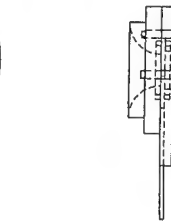
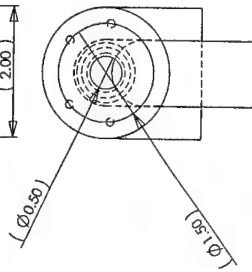
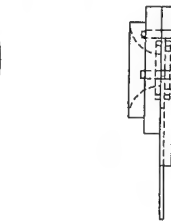
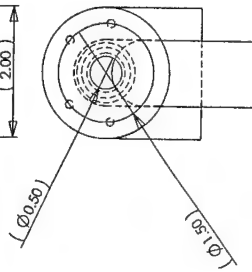
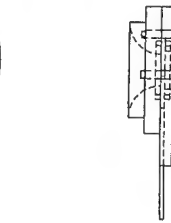
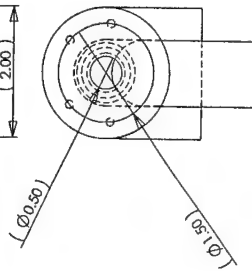
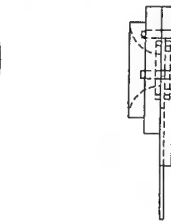
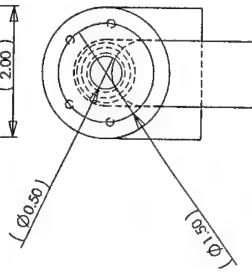
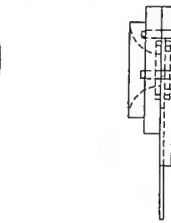
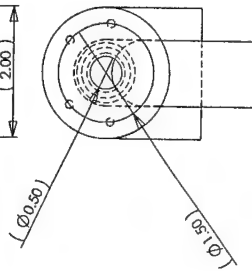
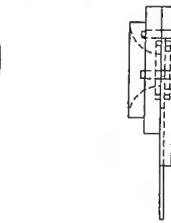
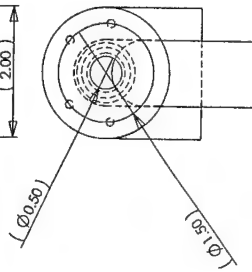
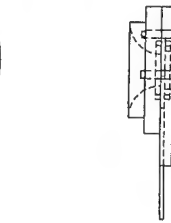
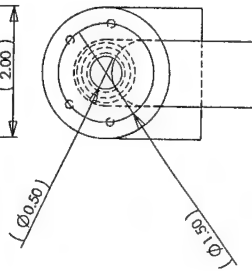
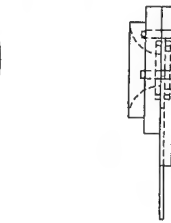
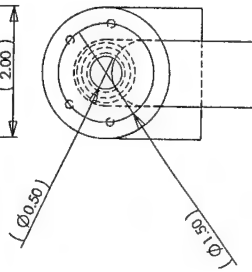
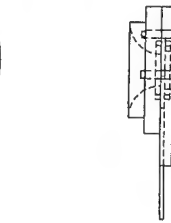
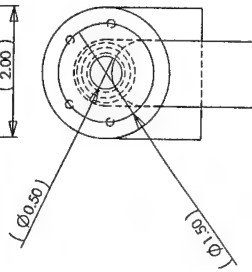
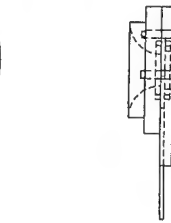
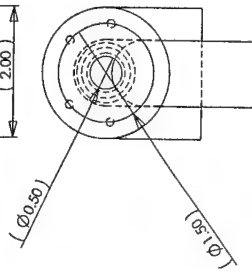
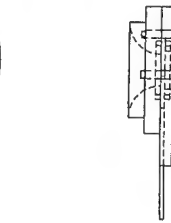
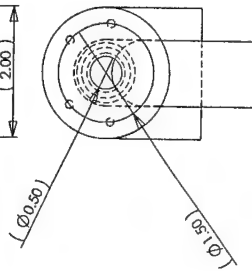
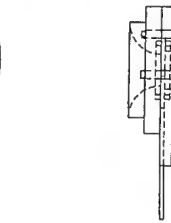
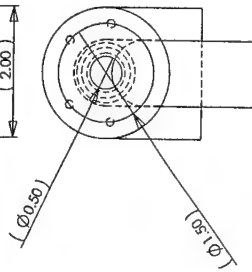
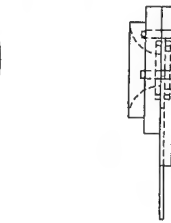
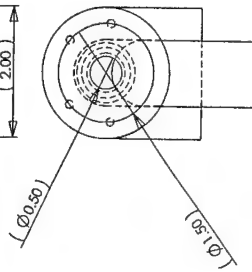
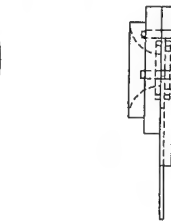
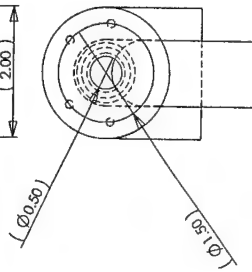
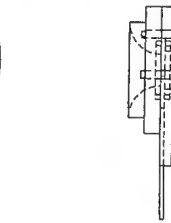
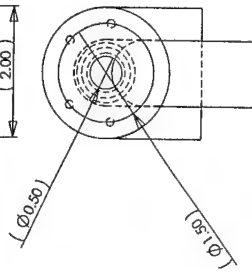
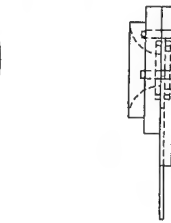
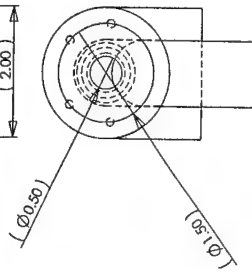
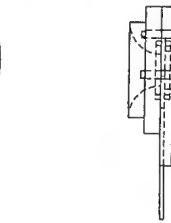
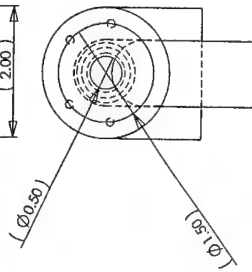
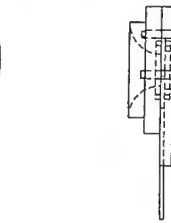
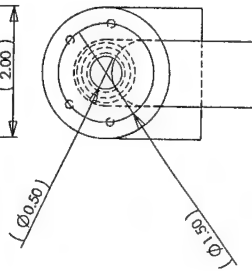
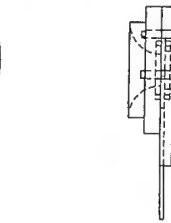
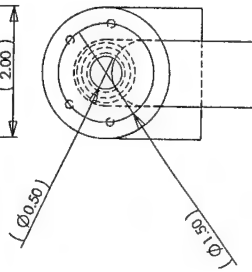
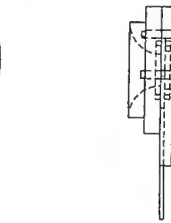
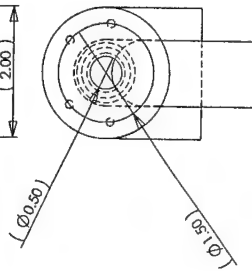
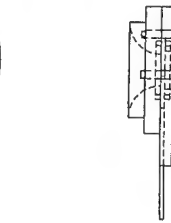
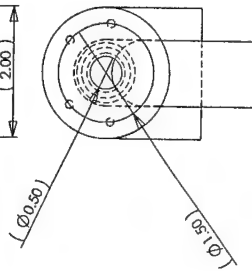
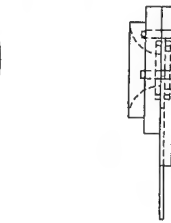
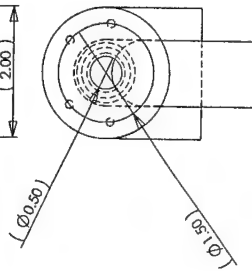
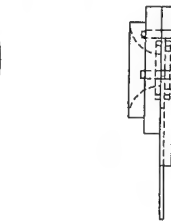
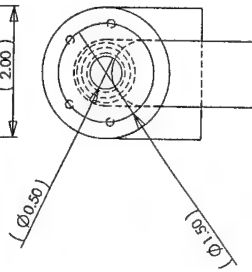
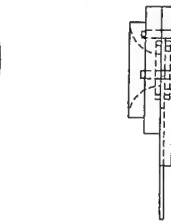
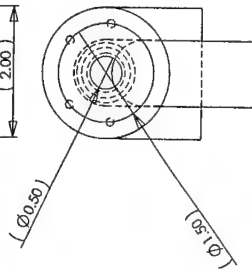
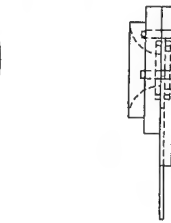
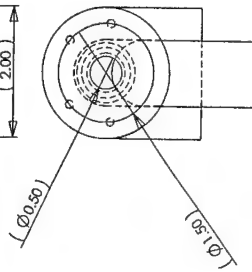
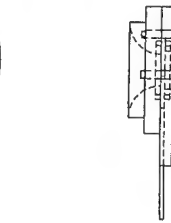
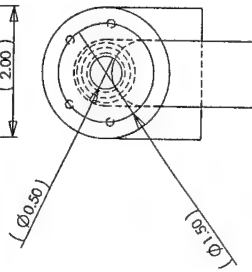
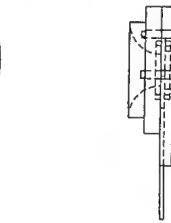
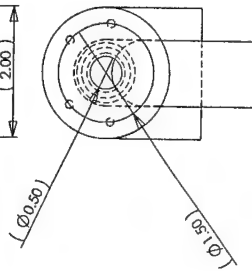
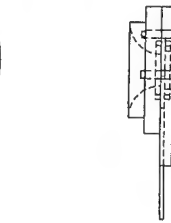
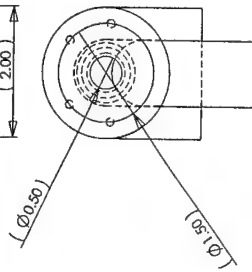
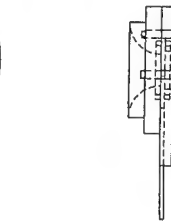
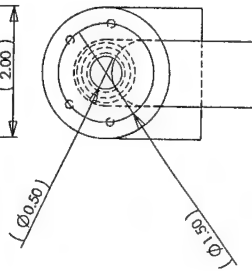
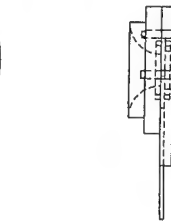
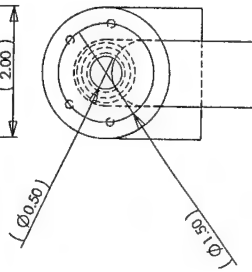
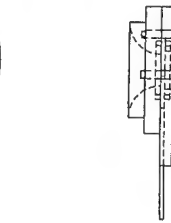
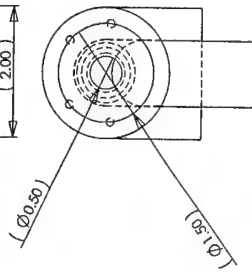
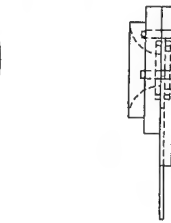
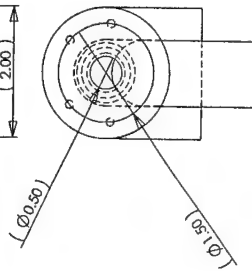
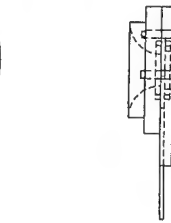
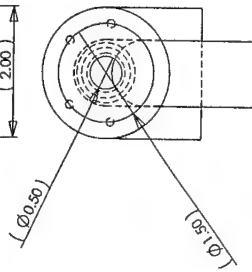
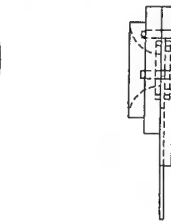
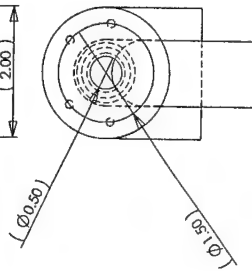
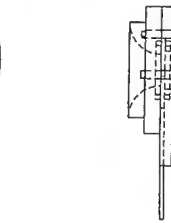
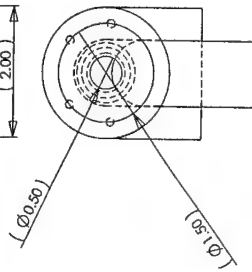
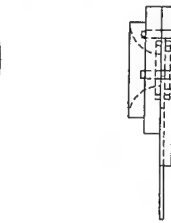
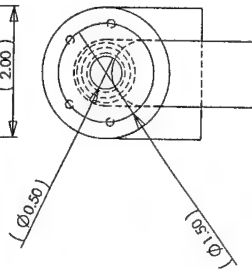
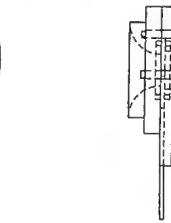
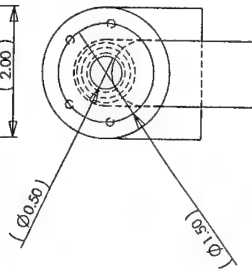
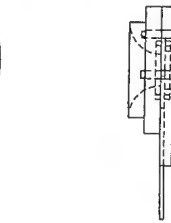
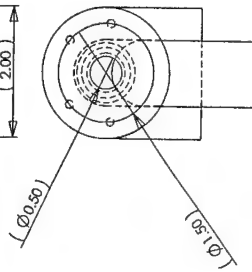
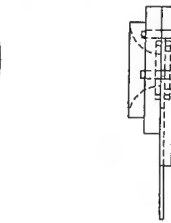
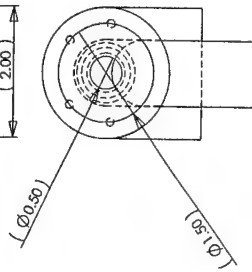
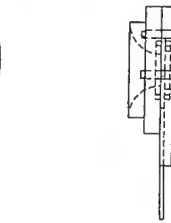
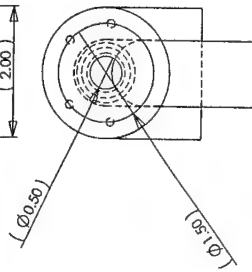
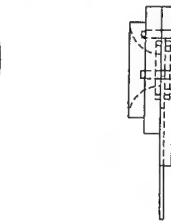
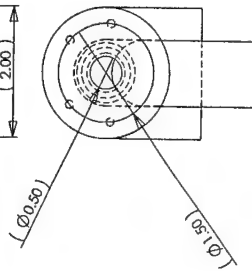
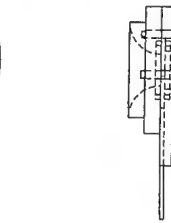
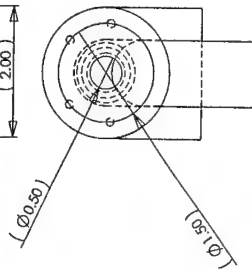
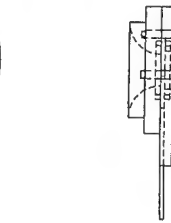
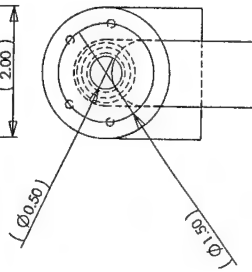
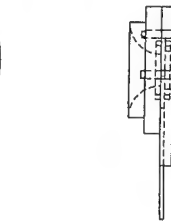
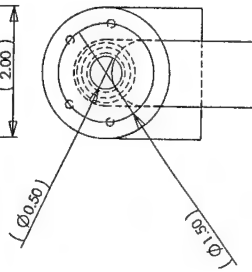
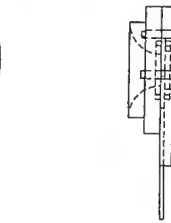
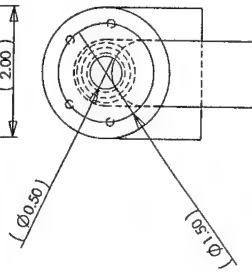
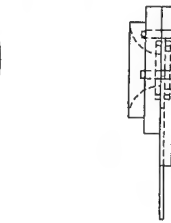
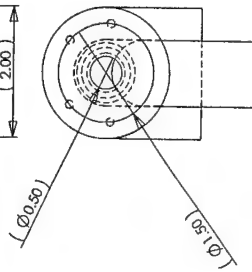
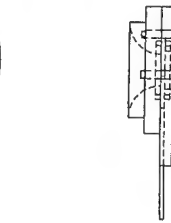
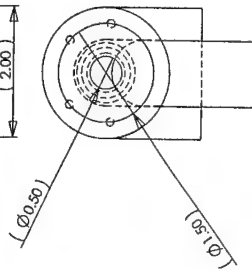
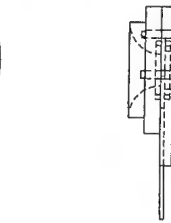
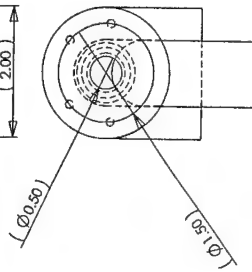
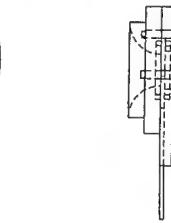
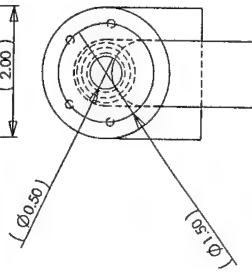
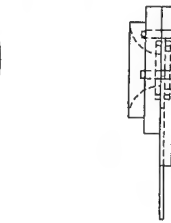
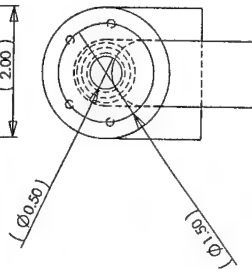
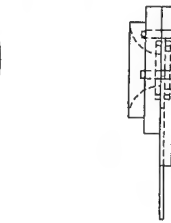
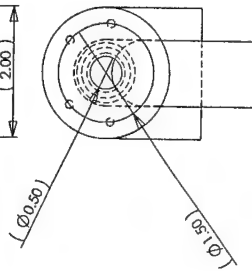
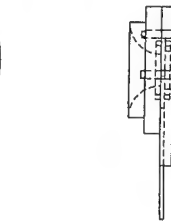
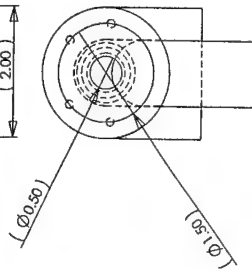
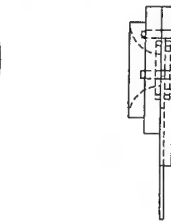
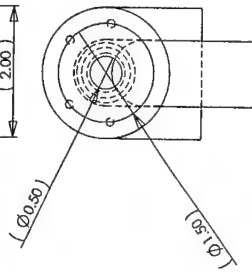
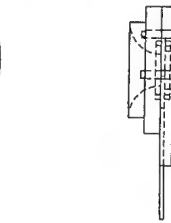
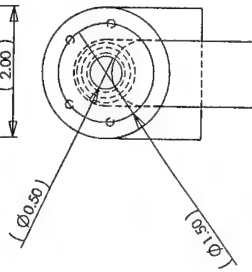
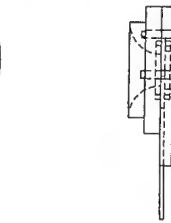
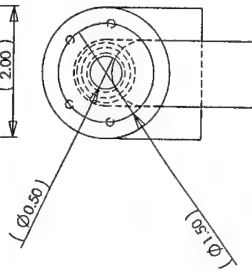
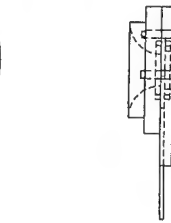
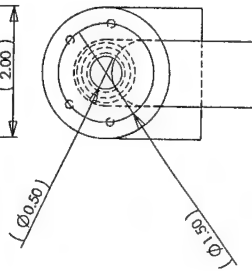
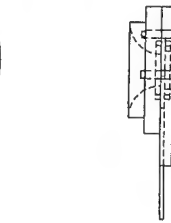
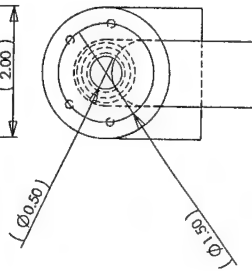
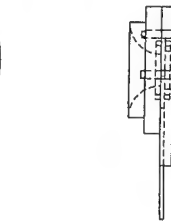
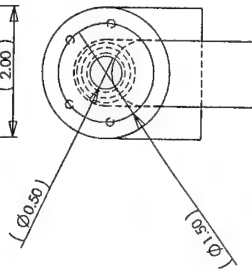
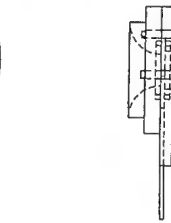
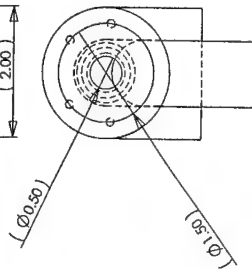
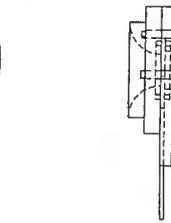
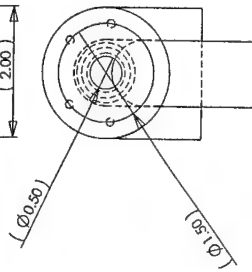
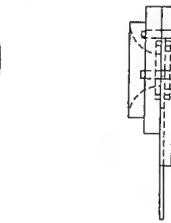
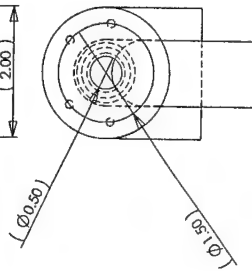
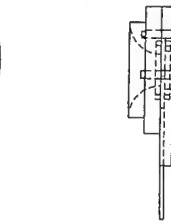
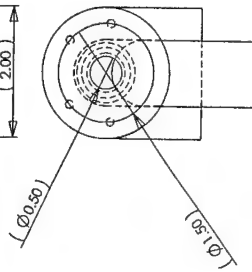
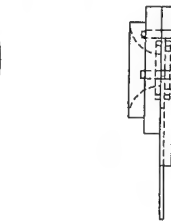
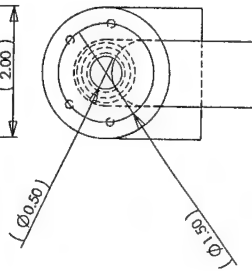
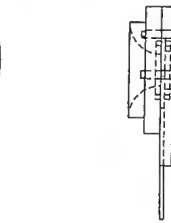
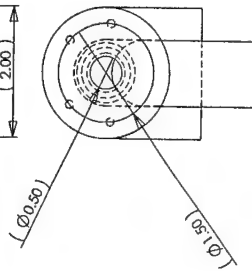
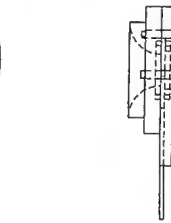
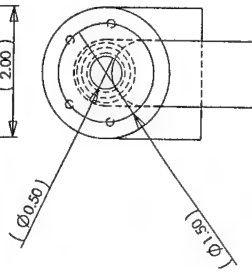
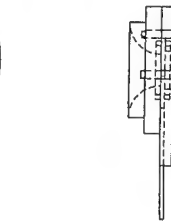
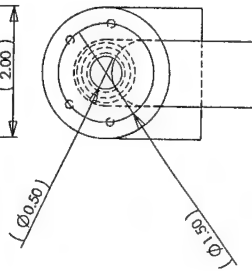
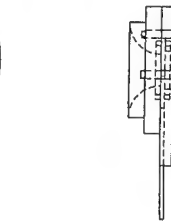
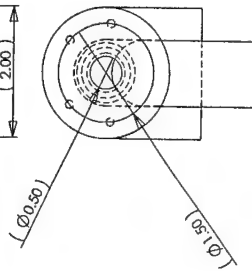
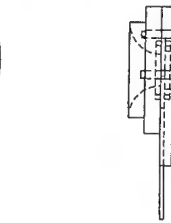
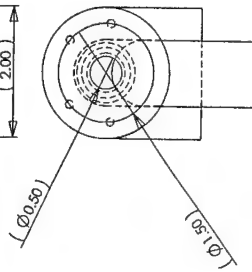
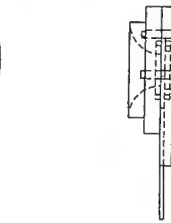
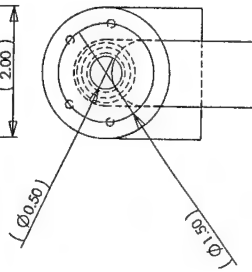
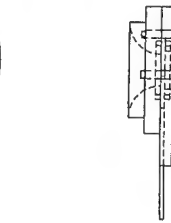
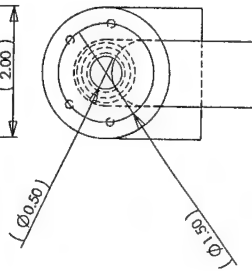
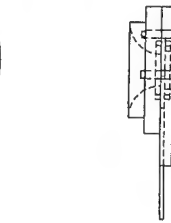
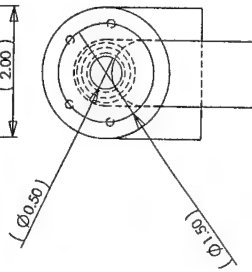
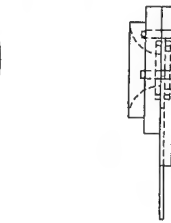
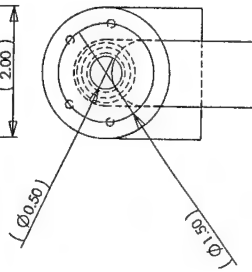
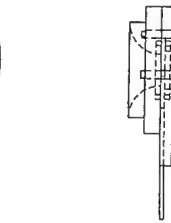
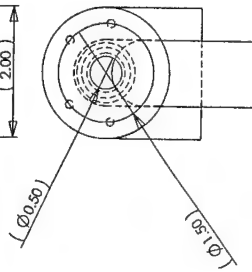
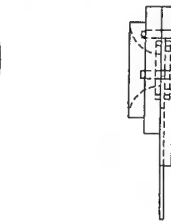
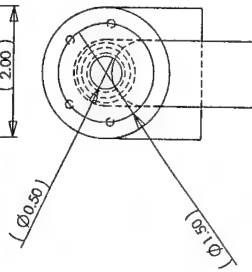
Water Tank



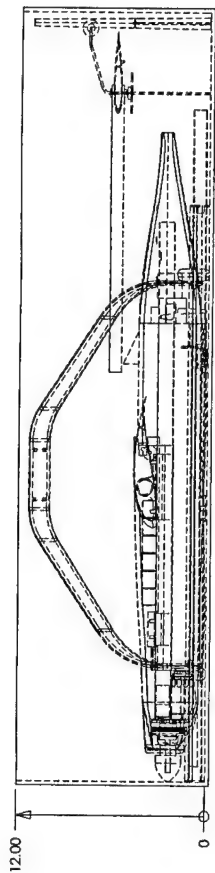
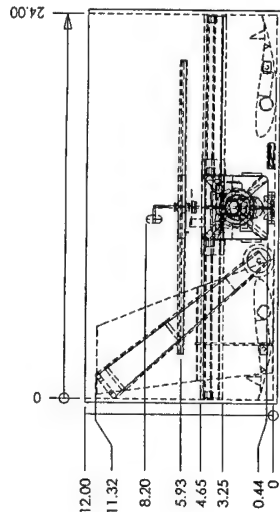
The water tank was fabricated by a wet lay-up technique using 3oz/sq.yd carbon fiber cloth, 0.3oz/sq.yd fiber glass cloth and silkspan for water seal. Notice the "U" shape of the tank necessary to accommodate the main backbone.

Load/Release Procedure

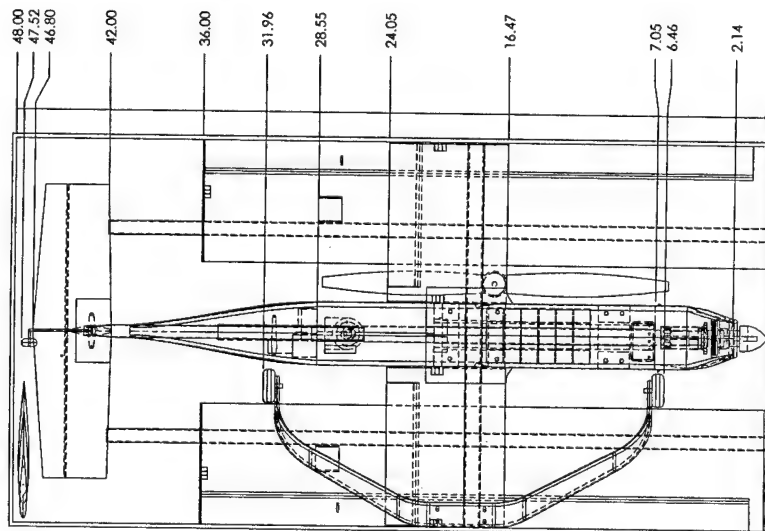
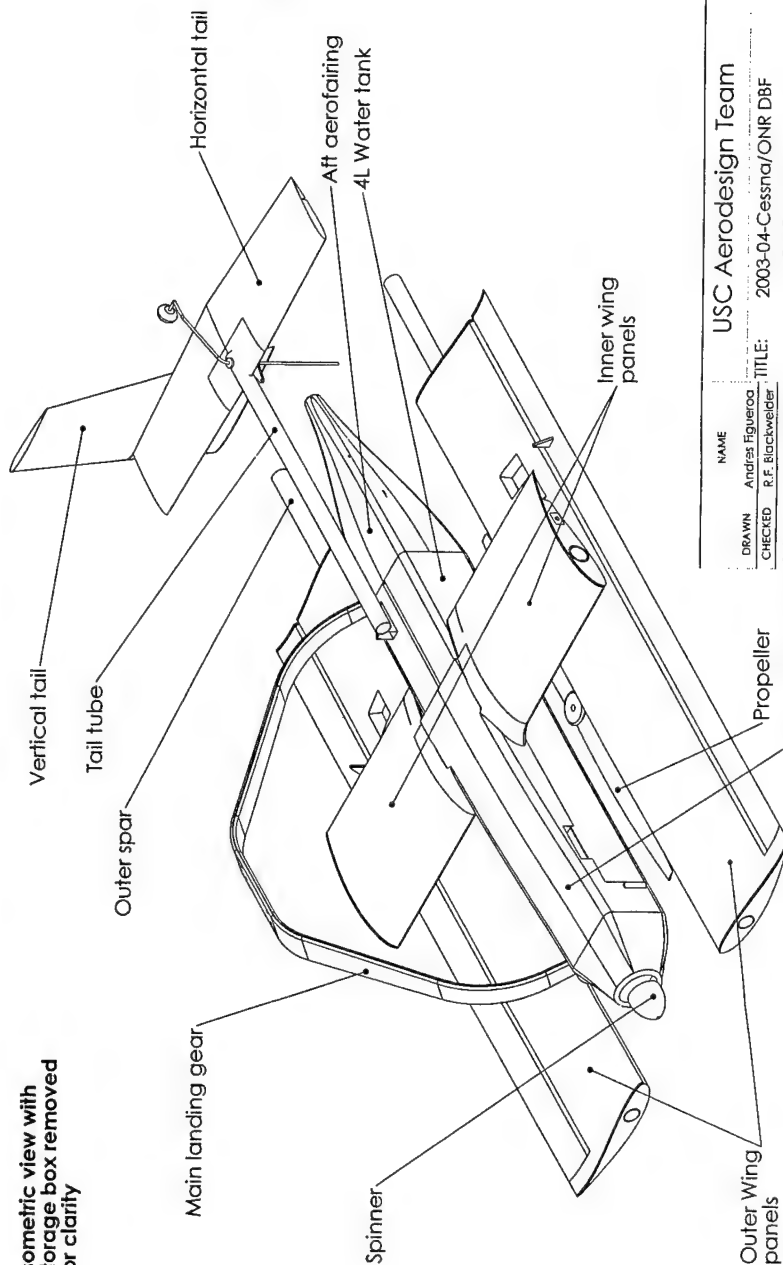
- 1) Air ram scoop is deployed when brakes are applied allowing for water loading on the runway
- 2) Brakes are released before takeoff closing the air scoop
- 3) Deployment servo retrieves sliding gate off to open 1/2" outlet in mid-air
- 4) Deployment servo returns sliding gate to closed position



In Box Storage Configuration



Isometric view with storage box removed for clarity



USC Aerodesign Team

TITLE: 2003-04-Cessna/ONR DBF

SCquirt

SIZE DWG. NO. 53

REV

NAME
DRAWN: Andres Figueroa
CHECKED: R.F. Blackwelder
ENG APPR: Mark A. Page
MFG APPR: George Sechist

COMMENTS:

UNLESS OTHERWISE SPECIFIED:
DIMENSIONS ARE IN INCHES
INTERPRET GEOMETRIC
TOLERANCING PER: .01

PROPRIETARY AND CONFIDENTIAL
THE INFORMATION CONTAINED IN THIS
DRAWING IS THE PROPERTY OF USC
THE UNIVERSITY OF SOUTHERN CALIFORNIA.
ANY REPRODUCTION IN PART OR AS A WHOLE
WITHOUT THE WRITTEN PERMISSION OF
ANDRES FIGUEROA (andresf@usc.edu) IS
PROHIBITED.

MATERIAL Composite

SCALE: 1:8 WEIGHT:

SHEET 5 OF 5

6.0 MANUFACTURING PLAN:

Plans for building and manufacturing of each component were carefully documented. Detailed procedures and lists of required materials were compiled for each part, with material size, weight, and lay-up configuration listed on component drawing. Because increased weight has such a large affect on airplane performance and rated aircraft cost, great care was taken to ensure all parts were made efficiently and free of excess materials. Three figures of merit were applied to the building procedures to ensure optimal manufacturing.

6.1 Figures of Merit

1. Material Availability: Construction time needed to be minimized to allow for a greater period of time for flight testing. Because of this, materials that were readily available were chosen. Standard graphite, fiberglass, balsa wood, and foam were available through Aircraft Spruce and Specialty Company at any time. Nuts, bolts, and fasteners were ordered through McMaster Carr and were always in stock.
2. Material Cost: Historically, the AeroDesign team receives no university funding for their project. Instead, the team has relied on the support of outside donations. Because of this, using materials with relatively low cost was essential. Rolls of carbon fiber prepreg were donated, valuable scraps of materials were carefully saved, and, if possible, parts were student built instead of purchased. All vendors used by the team were chosen not only for having materials immediately available but for also providing materials within the budget range.
3. Required Level of Workmanship: When constructing a component, efficiency is desirable, but the construction skills of team members needed to be considered. The option of using a monocoque fuselage was considered and dismissed for many reasons; for example, a high level of experience and knowledge of composites is required to create such a part. Instead, carbon composite material was used but simpler parts were designed such as tube spars that were easily wrapped and a square fuselage mold that was lined with a wet lay up. The older team members often lead building tasks while new members gained experience.
4. Repeatability and Crashworthiness: All parts were design so that they could be easily and quickly created, repaired, or replaced. Should a part fail during flight testing, the ability to substitute it with a new one in a short amount of time was essential.

6.2 Analytical Methods Used to Select Final Set of Manufacturing Processes

The manufacturing skill of the team members was considered during the design process to ensure that the team had the capability of building this year's plane design. The building skills

of team members were considered ahead of time so it could be determined who would take the lead for each constructed component.

Last year the team received a donation of unidirectional carbon fiber pre-preg. The use of this material was assumed in the design of the structural components. Because many team members gained experience with this material in building last year, the skills, processes and techniques were already understood and were passed on to the newer team members. Tube spars, for example, were first introduced to the team last year. It was estimated that it would take two students about 6 hours to make a tube 40" in length with a 1" diameter. With four spars needing to be built, this was a time consuming process. However, with more experience, the process became more efficient. Using commercially available carbon spars was considered but the specific dimensions and ply orientation needed for structural support could not be matched. The tube analysis and construction proved reliable and efficient based upon last year's plane building and was repeated for this year's construction.

Other components of the plane, such as the wing, landing gear, and fuselage shell, were built with more common methods of construction. Wet lay-ups, female molds and foam cores were used and were easily built based upon experience gained from previous years. This gave an opportunity for these techniques to be taught to new members and allowed for minimal manufacturing time.

6.3 Processes Selected for Component Manufacturing

The manufacturing processes are given for each of the following components.

1. Wing Spar and Backbone: With extensive work and analysis done on shear and moment forces, the backbone and wing spar were both designed to take a maximum crash loading of 5Gs. Tubes were needed for both wing spars, for the main boom and for the backbone of the plane. All were student crafted in the following manner:
 - a. Mandrel Preparation: Thin walled aluminum tubes were purchased with outer diameters matching the required inner diameters for each of the tubes. To prepare these tubes, the ends were de-burred in order for the carbon tubes to slide off easily. Next, the aluminum underwent several rounds of wet sanding with 600, 800 and 1000 grit sand paper. The sanding was performed to remove any scratches that would cause impurities in the carbon lay-up or cause difficulties in removing the final tube. After the sanding the mandrels were cleaned with acetone. From this point on, it was crucial to keep the mandrels clean to prevent contamination and bonding problems. The mandrels were then polished with wax and buffed out lightly with cotton rags. This process of wax polishing was repeated three times. Acetone was then used again to clean the mandrels. They were then brought into the exhaust room where

Freekote44 was applied to the mandrels with a lint cloth until a continuous, smooth wet film was apparent. This process required eye protection, respirators and gloves. The mandrels were then heated for 10 minutes at 150°F with a heat gun. The release agent was then buffed out. This procedure was also repeated three times. After the third time, Miller-Stevenson mold release was sprayed on the mandrels. Protection for eyes, lungs and hands were also needed. The mandrels were then heated again for five minutes and buffed out. This was the final step in preparing the mandrels for the carbon lay up. Great care was taken in handling the mandrels to ensure that the carbon tubes would release properly after they were cured.

- b. Strip Cutting: Dimensions and layout of the prepreg material were calculated and strips were cut ahead of time. All tubes had four layers for 45° and then 0° caps. The width of the 45's needed to be calculated as well as the length to cover the span of the tube.
 - c. Strip Layout: Shear strips were first wrapped on the mandrel. The strips were laid out and stretched by hand so that no bubbles or wrinkles were formed. If any imperfections were present during lay up they would only be magnified with each layer applied, drastically weakening the strength of the tube. After the first layer of shear strips was applied, the tube was then wrapped with a 1" stretch tape with a hand-held tension regulator. This procedure helped eliminate any remaining wrinkles. The wrap was kept on for 10 minutes. After removing the tape the remaining three layers of shear ply was applied, alternating +45° and -45°. After the shear plies were added, another layer of stretch tape was applied and then removed. Caps were then applied to the top and bottom of each tube, covering a portion of 60° each. A heat gun was used to increase the adhesive properties of the caps so they would attach better to the mandrel. Hoops at 90° were added last at the hard points of each tube. This was to strengthen the tubes at the joints to prevent crushing or splitting.
 - d. Curing and Removing: After the tubes were laid up, they were wrapped one more time with stretch tape and placed into an oven to cure at 270°F for approximately six hours. The mandrels were then taken out of the oven and placed in a freezer to allow the aluminum to contract slightly. The carbon tubes were then pulled off, either by hand or with a wrench.
2. Joiners: The plane configuration this year required the wing spars and the backbone to be joined at a 90° angle. The joiner used was designed last year under the guidance of industry advisors and proved successful. The design was repeated and improved slightly this year to help the loads from the wing transmit to the mount through compression. This compression was reacted by the mount and bolts through tension. The bolts then transmitted the loads to

the backbone by compression. As designed, the backbone also supported the shear forces. These joiners were made out of pre-preg carbon fiber. The surface of the main boom was sanded down to create a rough surface onto which the joiners would attach. A block of balsa was formed to fit the curvature of the tube and secured with epoxy and micro balloons. Four layers of carbon were laid flat alternating between 0 and 90. Two layers of carbon at 90° were wrapped over the tubes and attached to the flat pieces. The joints were bagged to an aluminum call plate and cooked at 270°F for 6 hours. The flat ply orientations added strength in the direction of the load path and gave a balanced lay-up. The top plies helps to transmit aft wing tip loads from the spar to the mount. Nylon bolts were used as fasteners and were designed to withstand a 5G turn load and to shear off under a 1G lateral tip load. Figure 6.3.1 shows the joiner lay up.

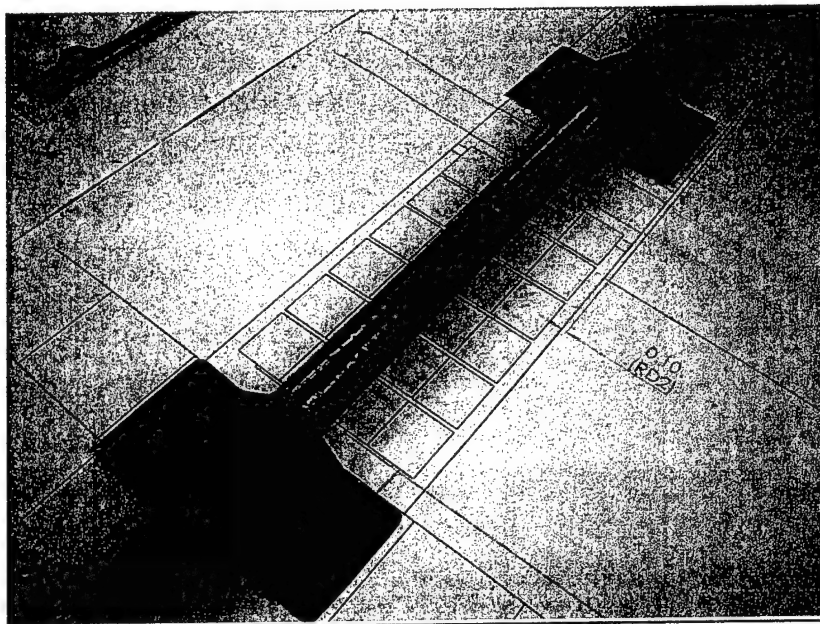


Figure 6.3.1 Joiner lay-up on main backbone tube.

3. Aero-fairings: These were made using a male mold which was hot wired out of foam and sanded. It was covered with clear tape and waxed twice. Carbon strips were taped to the molds to provide rigidity. Two layers of 1.5 oz fiberglass was laid up with reinforced corners. The fairings were bagged with latex and cured.
4. Water Tank: For the water tank, templates were drawn up and the shape of the tank was separated into two sections; the top, essentially being a tank lid, and the bottom, which held the entire volume of water. For the construction of the bottom portion of the tank, a female mold was cut out in tooling foam and covered in monokote. The surface was waxed to act as a release agent so the mold would be reusable. This mold was then covered with two layers

of silk-span, one layer of 3oz fiberglass, and one layer of unidirectional carbon. Bi-directional carbon was used to reinforce the ends of the tank. This tank however, leaked water through sweating. A second tank was made using a male mold. The mold was made with the same tooling foam as the first and this tank had two layers of silk span and one layer of unidirectional carbon. The corners were much cleaner and the part was much lighter than the first version. Figure 6.3.2 shows the bottom of the water tank. It only contained a few point leaks which were eliminated with sealant. Painters plastic spray adhesive was applied to the inside of the tank to make a flexible waterproof liner. The top of the tank was also made from a male mold and constructed with the same lay up schedule as the female molded tank. The top and bottom were sealed together with layers of fiberglass and epoxy with West Systems #410 micro light fairing filler.

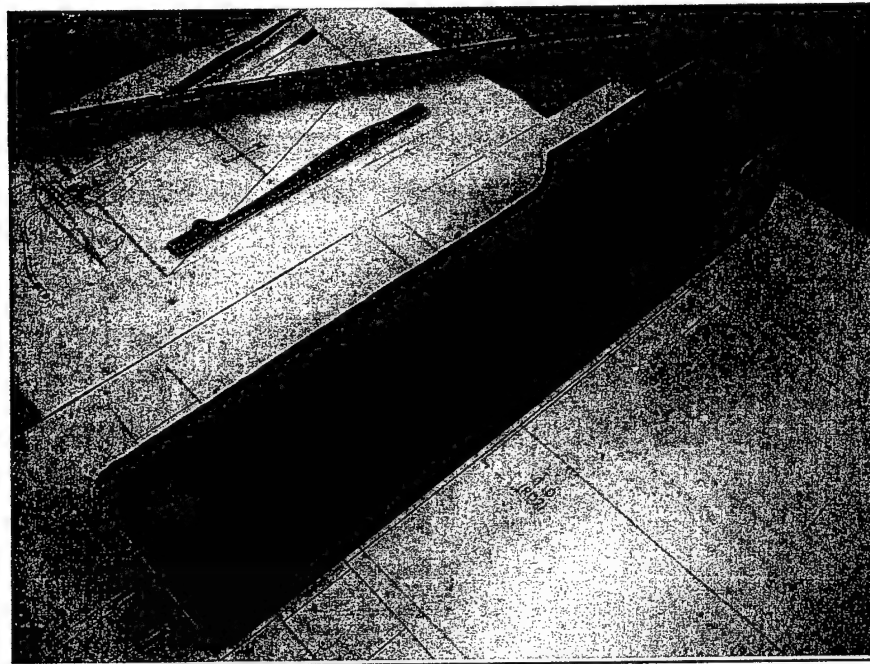


Figure 6.3.2 Bottom half of carbon fiber water tank.

5. Landing Gear: The main gear was made out of pre-preg carbon fiber (see figure 6.3.3). A wooden mold was made out of plywood to fit the drawing templates. An aluminum sheet was placed over this and strips of fibers were laid on top. Twenty seven layers of unidirectional were used with every ninth layer at 90° for shear forces. The gear was then vacuum bagged and cured in an oven at 270°F for six hours. Extra care was taken to prevent delamination at the corners. The tail wheel strut was made with piano wire.

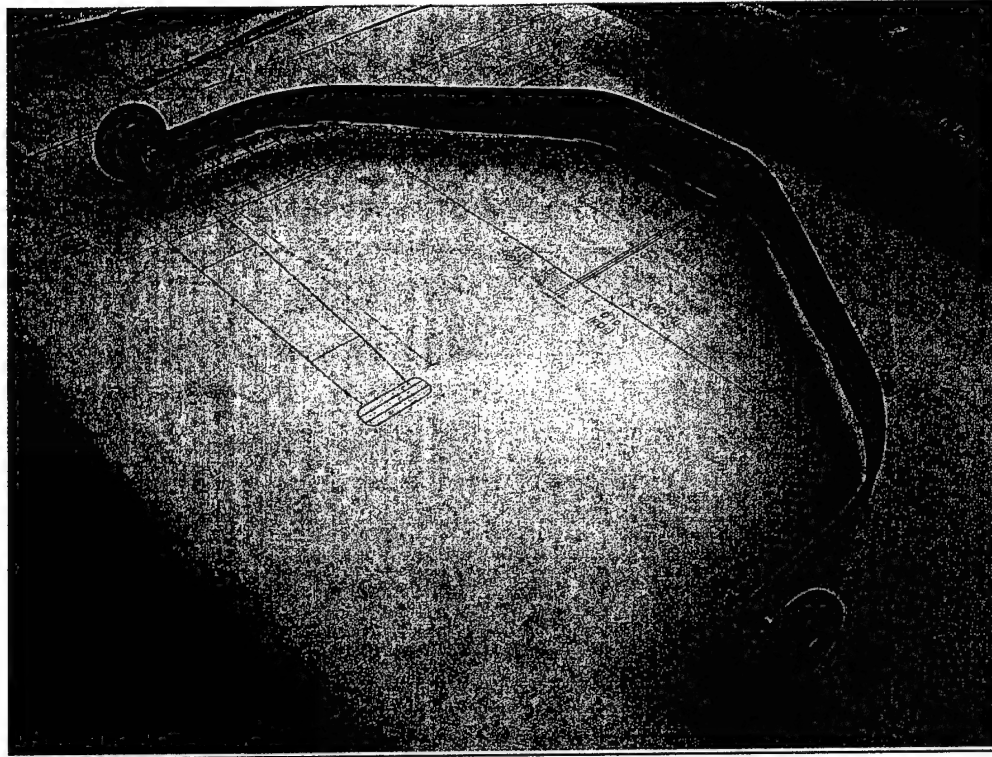


Figure 6.3.3 Picture of finished landing gear.

6. Wing: The wing was constructed out of blue Spyder foam and covered in two layers of 3oz fiberglass. The control surfaces each had a Kevlar hinge. The procedures for wing building were similar to last year's. First the configurator provided actual size drawings of the airfoil. Wooden templates were then made from a laser cutter machine. Ribs were cut from light plywood and the wing cores of the wing were hot wired out of rectangular slabs of foam. Figure 6.3.4 shows the hot wiring process. The cores were then prepared for bagging; first the spar hole was cut and the carbon spars were inserted. A servo wire channel was cut and the ribs were installed. The wings were then covered with two layers of $\pm 45^\circ$ fiberglass. This was chosen to counter the twisting moments of the wing and to reduce any dimpling of the core. The cores were then vacuum bagged separately. Once the epoxy cured, the hinge line was cut and the control surfaces were wrapped again in fiberglass and bagged separately. They were then reattached and servo holes were cut and servos were installed. Figure 6.3.5 shows a completed wing.



Figure 6.3.4 Team members cutting foam cores for wing.

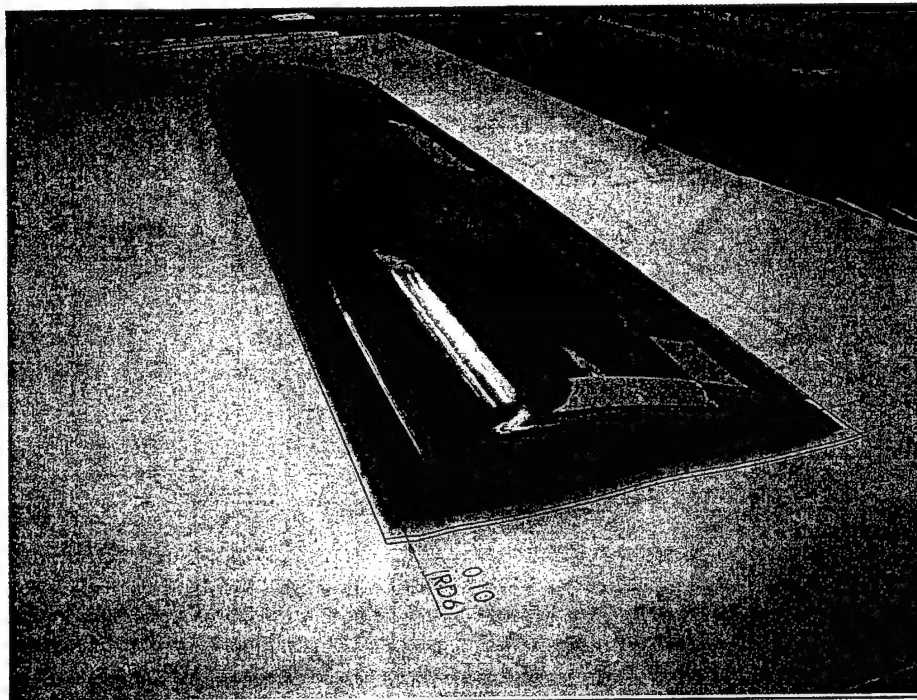


Figure 6.3.5 Picture of completed wing half with carbon spar inserted and covered in fiber glass.

7. Empennage: The building of the tail was divided into two main sets: one for the horizontal tail and one for the vertical tail. A similar process was used for tails as for wings. Drawings and

templates were made and cores were hot wired out of a foam bed with appropriate thickness. For the horizontal and vertical tails, 1.6oz blue foam was used. Ribs for the vertical tail were cut out of light plywood. The vertical tail core was prepared with a channel cut out for a brass tube. A hard point, for the tail wheel wire, and bolting locations were put on the horizontal core. The hinge line was drawn before bagging. The control surface on the horizontal tail was made with a Kevlar live hinge. Each piece was wrapped with one layer of 3oz fiberglass at 45° and carbon caps were laid on top. The pieces were then vacuum bagged separately. Once cured, the hinge line on the horizontal was cut, wing tips were attached, the servo horn hole was cut and the carbon tail wheel attachment was inserted on the vertical portion. Figure 6.3.6 shows a picture of the completed horizontal tail.

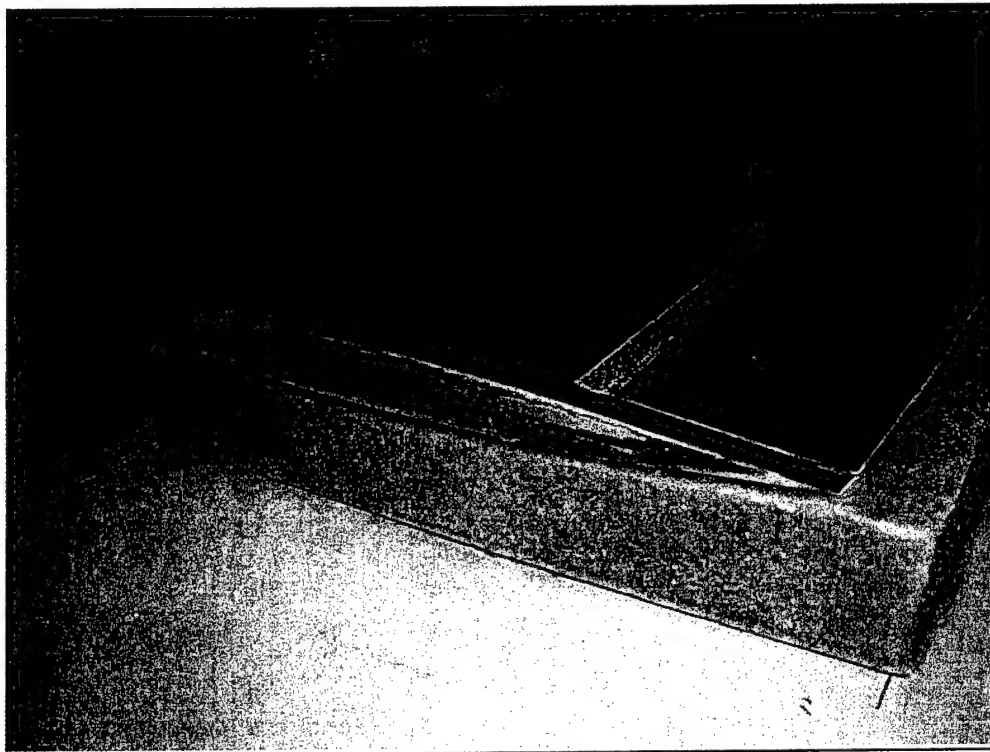


Figure 6.3.6 Completed horizontal tail on foam bed.

6.4 Manufacturing Schedule:

Table 6.4.1 shows the manufacturing schedule. Each part needed to be built was separated and assigned an appropriate allotment of time for component completion.

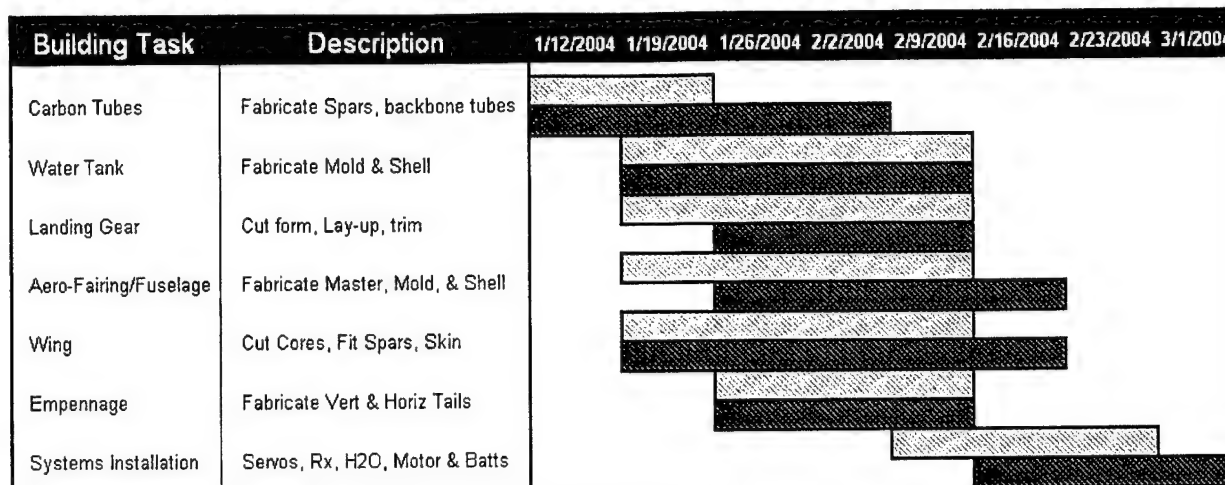


Figure 6.4.1 Detailed building schedule with manufactured parts and dates. Light shaded areas denote planned building, dark shaded areas denote actual building.

7.0 TESTING PLAN:

7.1 Component Testing:

1. Propulsion testing: In past years, manufacturer specifications were unable to be trusted in regards to battery and motor performance. To provide a reliable propulsion system, extensive testing was done on both the motor and battery packs.

- a. Motor Testing: The Graupner 930-10, the Graupner 3300, and the Cobalt 60 were all placed on the thrust bench for testing. The 930-10 was found to be most suitable for this year's plane so more detailed thrust bench testing was conducted for this motor. Figure 7.1.1 shows the motor attached on the thrust bench during one of the tests. The voltage, current, torque, and thrust were all recorded during these tests. The goals of the motor tests were to determine the motor constants and to determine if it would operate at the required power level for the required time.
- b. Battery Testing: Tests were done on battery type and cell number. CP-1300s, 1700s and 2400s were all tested. Batteries were tested for voltage, current and duration of the pack as a whole. The goals of battery testing were to ensure that the voltage and battery life was what was predicted and to verify that they would perform well with the given propeller and motor. For a battery endurance test, the power coefficient was graphed versus the design advance ratio. From this it was possible to find a propeller that would simulate cruise. This prop simulates cruise by drawing less current. The 22x10 prop was used and proved that the CP1300s gave a minimum of 3.5 minutes of power. A test was also performed to document what happens to the

batteries when the motor was briefly pushed up to full throttle. The amps needed to be monitored to ensure it would not blow the motor. Figure 7.1.2 shows the data obtained from this battery test.

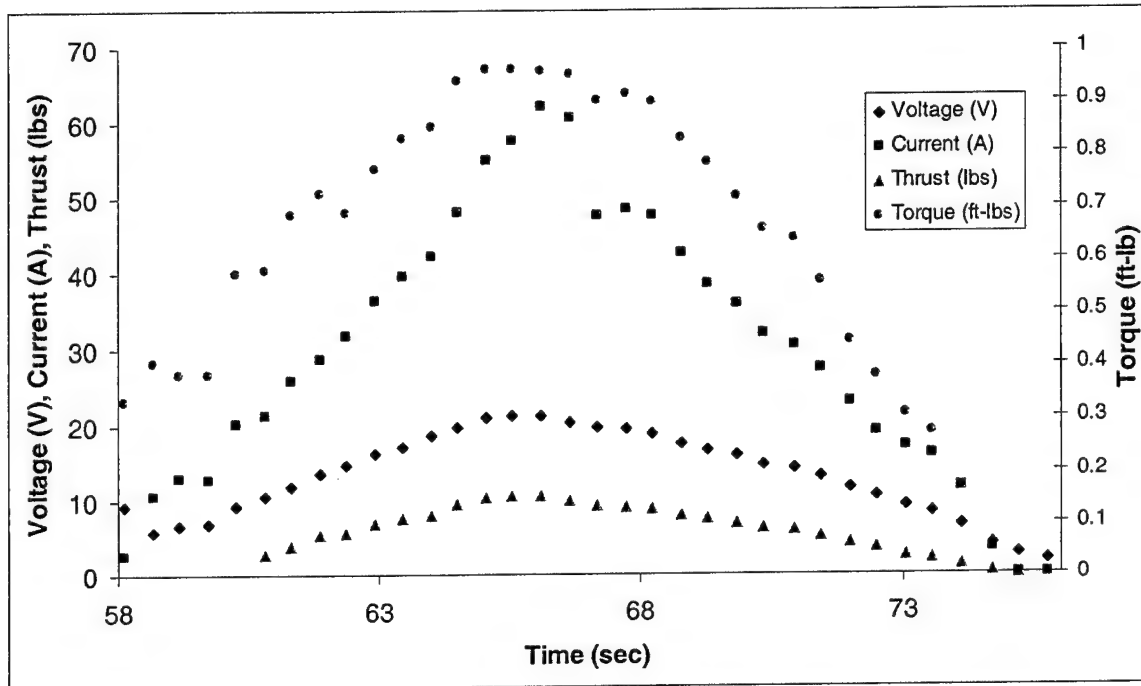


Figure 7.1.1 Time trace of the data for the Graupner 930-10 with the competition prop (zinger 22x14)

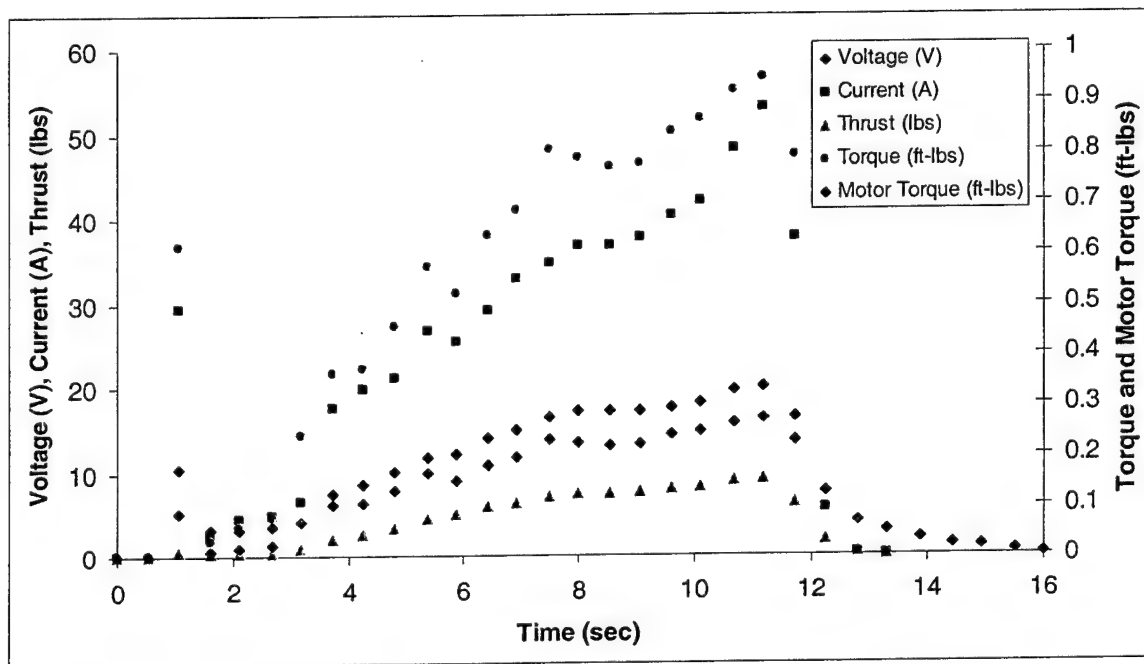


Figure 7.1.2 Time trace for CP 1300's with a 22x14 prop and 3.5 gear ratio.

2. Water Tank: The water tank tests were one of the first tests to be executed. Because the initial water dropping techniques were not dependent upon plane design, they were immediately discussed and analyzed. Water tank testing was divided into two categories: static testing and dynamic testing.
- a. Static Tests: First a plastic tank was constructed. The tank was built 4 inches tall, 4 inches wide and 16 inches long. The tank was sealed using silicone and tubes were built into the top of the tank to allow for pressure readings, refilling, and air inlet. The initial plan called for using pressurized air to create an aerodynamic pressure differential. This plan was deemed impractical due to problems with obtaining a suitable pressure transducer. The air inlet hole was then modified so that it could catch RAM air pressure when the tank was put into a wind tunnel. The tank was placed into the wind tunnel with a 4" hose attached to the end of the nozzle to direct the water out of the tunnel. Because it was not possible to dump water into the free stream air of the wind tunnel (which would be at a lower pressure than room pressure), it was necessary to recreate this lower pressure in the drop zone. This was accomplished by dumping into a four liter beaker that was connected to a tube which had one end perpendicular to the flow in the tunnel, as shown in Figure 7.1.3. This setup was run in the wind tunnel at several different velocities. For each velocity, the pressure in the tank was recorded using a pressure transducer. The air speed was also calculated using a pitot tube and recorded. The valve was manually opened using a servo controller, and the time was taken using a stop watch.

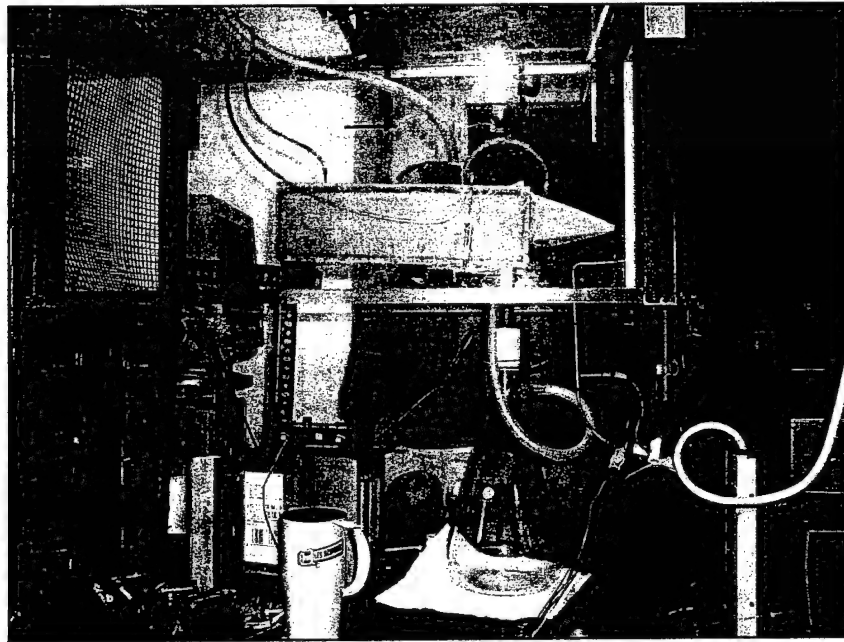


Figure 7.1.3 Wind tunnel set up for static water tank testing

- b. Dynamic Tests: In addition to wind tunnel testing, two tests were performed with a tank in flight. A separate tank was constructed and placed into the cargo bay of last year's competition plane. A ram air scoop was placed above the plane and the exit was perpendicular to the flow below the plane. These two tests were run with the plane flying at about 45 mph. The inlet scoop used for test flights was rather crude; a more refined design would probably result in a higher pressure differential due to fewer losses and thus a reduced drop time. It was noted during the test flights that the flow rate out of the nozzle increased significantly during the turns.
- c. Results: The data taken from the tank in the wind tunnel is shown in the graph in Figure 7.1.4. The graph shows the pressure and the time to empty the tank for each velocity. The results show, as expected, that as the velocity outside the tank is increased, the pressure differential between the inside of the tank and the free stream increases.

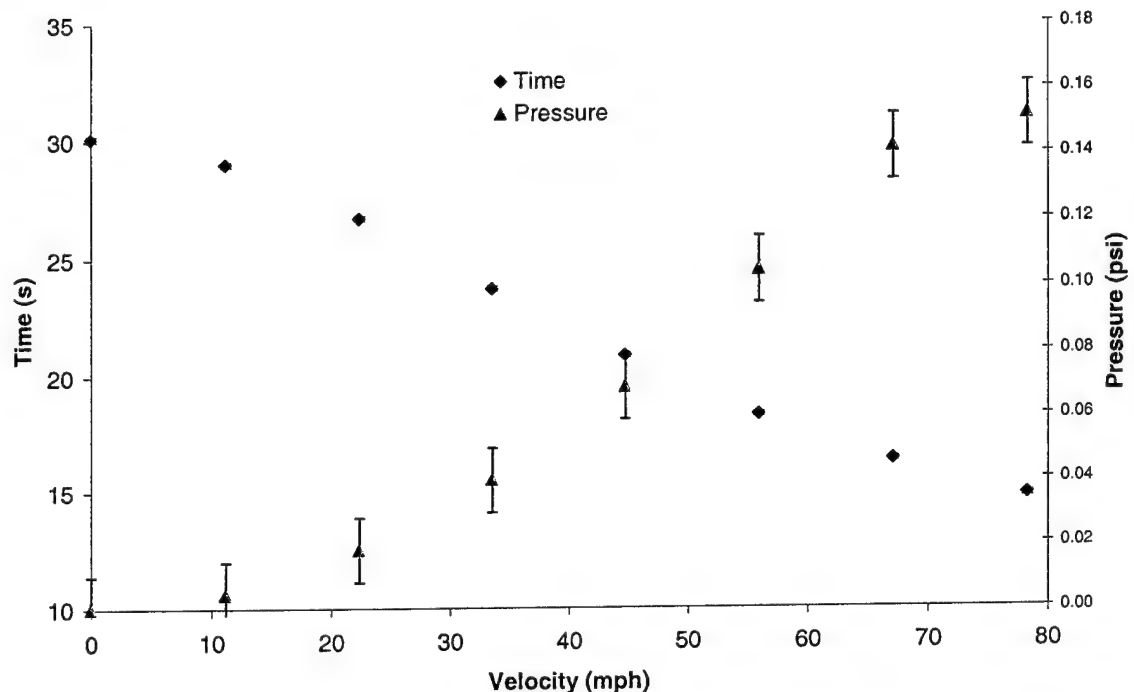


Figure 7.1.4 Graph of pressure and drop time vs. velocity.

The results obtained in the wind tunnel were actually better than predicted. Figure 7.1.5 shows the theoretical drop time (for both the added g-loading and the no g-loading case) and the actual measured drop time vs. pressure. The measured times were less than the theoretical times for the no turn case.

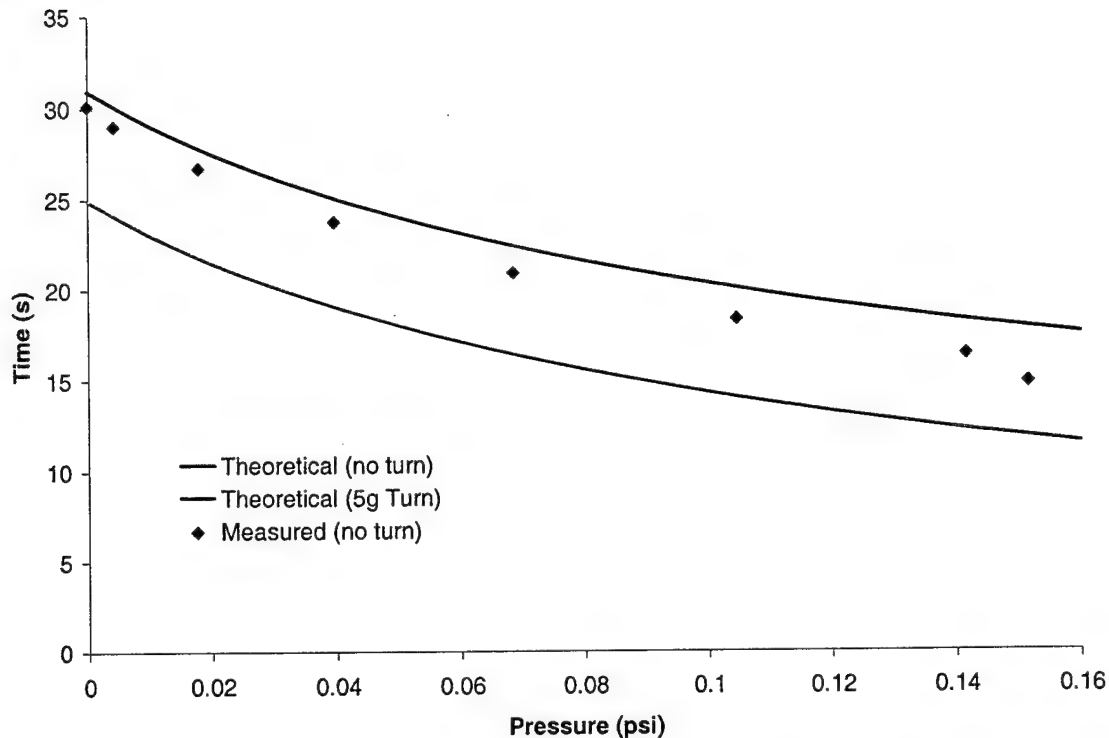


Figure 7.1.5 Theoretical vs. Measured drop times for different pressures.

These results indicate that the competition airplane this year should be able to complete the water drop in under the goal time of 15 seconds.

3. Static Divergence Testing: The full flying vertical tail was swept forward to avoid the possibility of aeroelastic flutter. As a result, there was some concern that the tail would be subject to static divergence. Static divergence occurs if an increase of C_L on the vertical tail as a result of a change in angle of attack causes a significant structural twist in the tail. This twist causes a change in apparent angle of attack, which can cause an even bigger increase in C_L . If this process repeats itself, then the tail could be pushed to the point of structural failure. To analyze this, a tail was taken from a previous competitions airplane. This tail was also swept forward and was built using similar methods to this year's tail. The tail was loaded with weights to simulate the dynamic pressure of a maximum deflection and maximum velocity. The twist in the tail as a result of this loading was negligible. Therefore, it was concluded that static divergence was not a problem given our tail sizes and construction methods.
4. Data Recorder Testing: A new device was purchased this year that allowed the team to collect data while in flight. The USB Flight Data Recorder and Flight Data Recorder Electric

Expander were both manufactured by Eagle Tree Systems. It records the inputs into the servos from the controller and saves the joystick positions in its memory. It has an internal altitude sensor that measures a 1600 foot range, but must be calibrated at ground level at different test sites. A pitot tube measures the stagnation pressure and calculates the dynamic pressure and velocity by comparing that reading with the altimeter's static pressure reading. The electric expander is hooked up to the speed controller and the batteries and measures the voltage and current that passes through them. The RPM sensor works by attaching 2 magnets at a 180 degree difference along a spinning part of the propulsion system and uses a Hall-Effects sensor to determine the RPM from the spinning magnets. The total weight of the recorder, the pitot tube, and the electric expander is .27 pounds. The recorder was located next to the receiver and the pitot tube was attached along the wing, outside the propwash. The electric expander was connected between the speed controller and the batteries. The interface used was provided by the recorder. It records altitude, velocity, receiver battery voltage, and joystick positions. With the addition of the electric expander, it also measures battery voltage, current, watts, amp-hours, and motor RPM. It was ground tested with a Graupner Ultra 3300-6 motor and was verified that the joystick positions work correctly. Figure 7.1.6 and 7.1.7 show outputs from the data recorder. The other recorded data was verified. As of this time, it has yet to be used for in flight tests.

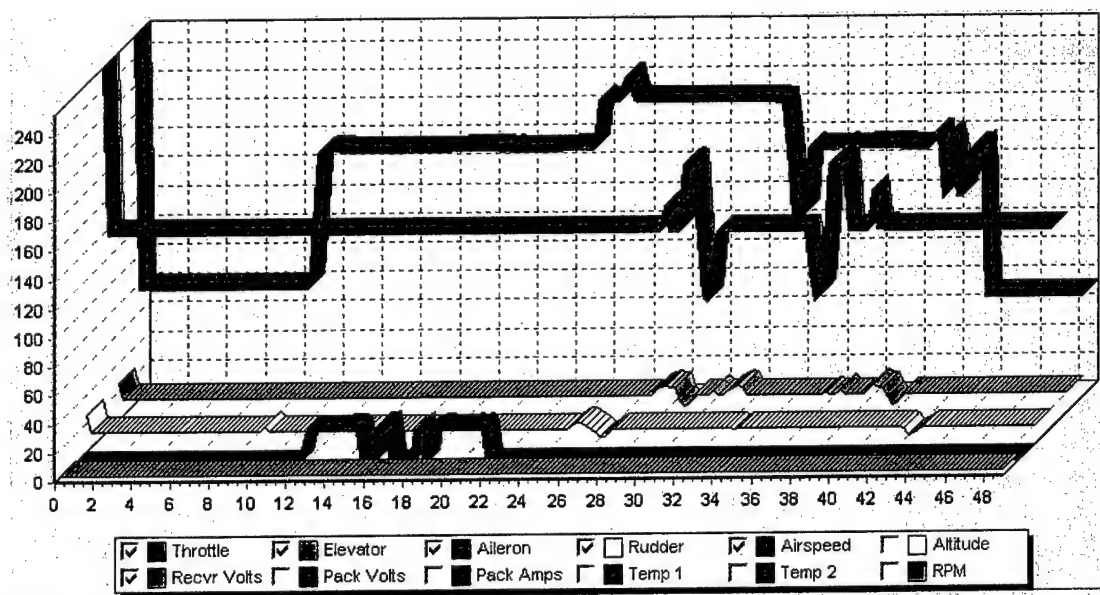


Figure 7.1.6 Flight Data Recorder graph showing joy stick positions and air speed.

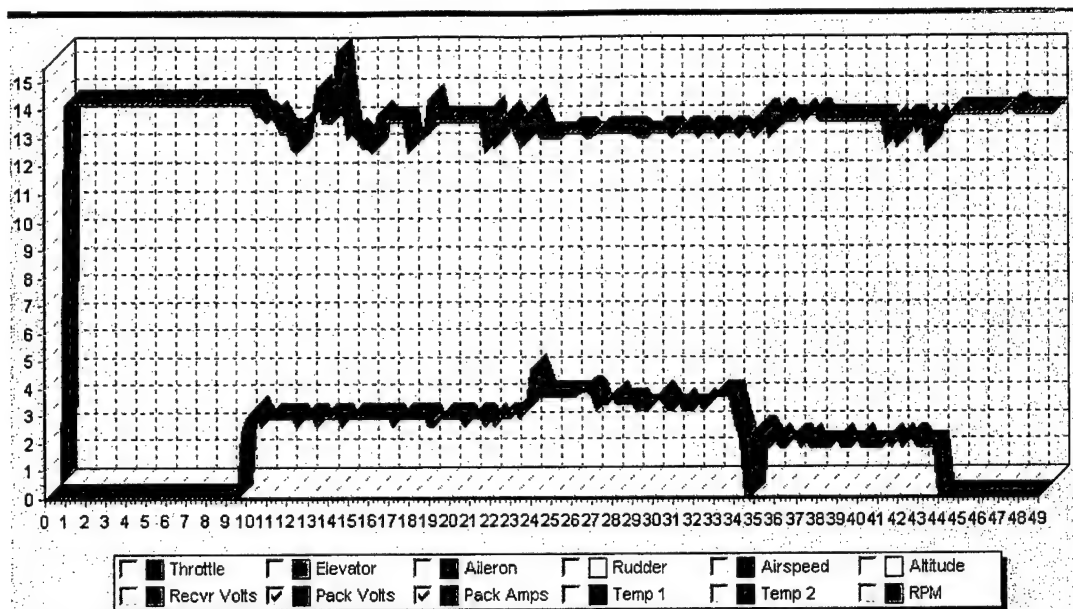


Figure 7.1.7 Flight Data Recorder graph showing voltage and current.

7.2 Flight Test Objectives.

As of report submission date, test flights have not been performed. The first flight is scheduled for March 12. Flight objectives for this first test and all subsequent tests are shown in Table 7.2.1 and 7.2.2.

Flight	Payload?	Primary Objectives	Secondary Objectives
Alpha	No	Determine trim elevator at Vcrz with 0° Flap.	Overall airplane trim and ground handling assessment
Bravo	No	Determine elevator required for stall with 15° Flap	Determine settings for geared flap
Charlie	No	Determine stall characteristics, power on/off	Assess turning performance
Delta	Yes	Analyze overall handling and performance with added weight	Measure cruise Velocity, turning performance

Table 7.2.1 Objectives for first test flight

Further Objectives:

Cruise speed and turning speed
 TOFL requirements
 Alternate prop pitches
 Alternate battery configurations
 Valve system
 Verification of propulsion system with in flight recording system
 Servo loading
 Power off landing

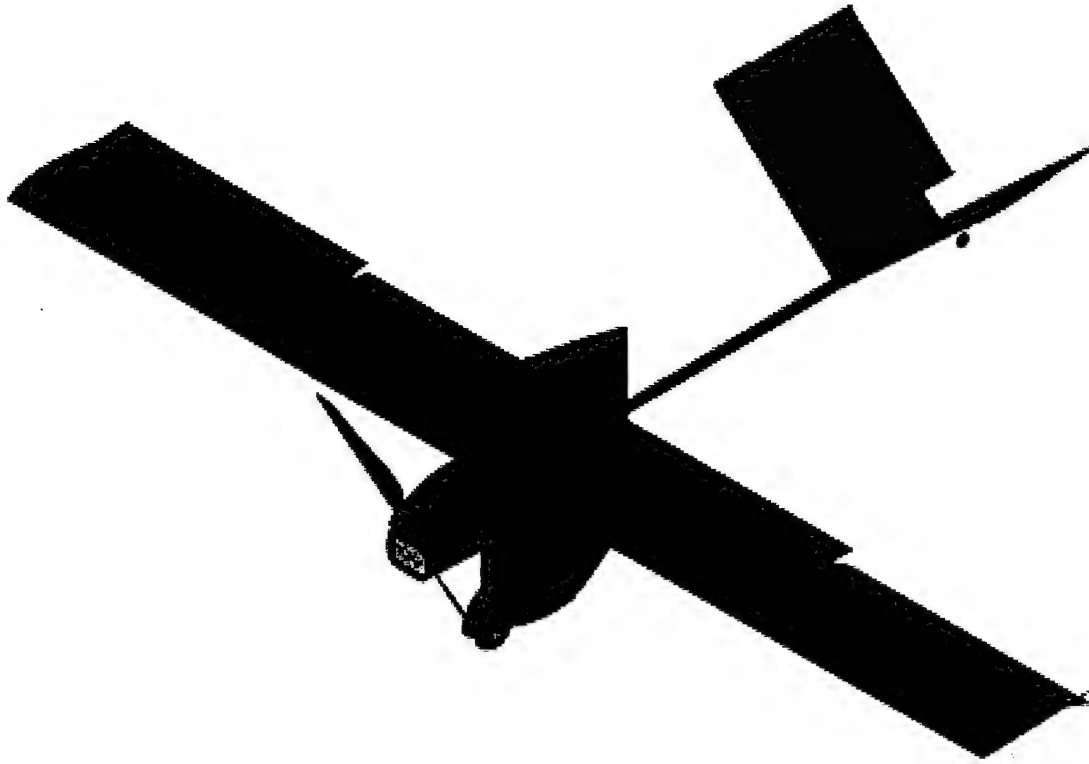
Table 7.2.2 Proposed objectives for subsequent test flights

Conclusion:

The 2003/2004 USC AeroDesign Team made a conscious effort to document the design process for this year's plane. Emphasis was placed on reducing RAC and optimizing the propulsion system. Great strides were made on the experimental front as a significant series of component tests were performed. The team is confident in this year's propulsion model due to the correlation between data acquisition and the theoretical values. The water drop element for this year's flight mission opened a new area of study for the team. A basic understanding of fluid dynamics was gained and demonstrated throughout the water tank testing and building. New techniques in design and manufacturing were explored and incorporated with the techniques on which the team has relied in the past. Under the guidance of a great team leader, the labors of the team were efficient, professional and goal oriented. A sincere and dedicated effort was given by both students and advisors throughout the year. Thanks to all those involved in the success of SCquirt.

Fiberglass Overcast

Final Design Report



AIAA Design Build Fly Competition

Cessna Pawnee East Field

Wichita, Kansas

Submitted by

Department of Aerospace Engineering

University of Illinois Urbana Champaign

March 9, 2004

Table of Contents

1.0 Executive Summary	1
2.0 Management Summary	2
3.0 Conceptual Design	5
3.1 Mission and Design Requirements	5
3.1.1 Fire Bomber Mission	5
3.1.2 Ferry Mission	5
3.1.3 Takeoff Requirement	5
3.1.4 Airplane Storage Requirement	5
3.1.5 Structural Requirements	5
3.1.6 Propulsion System Requirements	5
3.2 Airplane Component Types Considered	6
3.2.1 Wing Types	6
3.2.2 Fuselage Types	6
3.2.3 Empennage Types	7
3.2.4 Landing Gear Types	7
3.2.5 Power System	7
3.3 Rated Airplane Cost and Competition Score Analysis	7
3.4 Possible Airplane Configurations	11
3.5 Figures of Merit	12
3.5.1 Rated Airplane Cost	12
3.5.2 Estimated Mission Performance	12
3.5.3 Stability and Control	15
3.5.4 Ground Handling	16
3.5.5 Water Carriage and Release	16
3.5.6 Manufacturability	16
3.6 Configuration Selection	17
4.0 Preliminary Design	19
4.1 Design Variable Selection	19
4.1.1 Design Parameter Sensitivity Analysis	19
4.1.2 Design Variables	21
4.2 Analysis Methods Used	22
4.2.1 Mission Model	22
4.2.2 MDO code	22
4.2.3 Stability and Control Simulation	22
4.3 Elements of MDO Code	22
4.3.1 Weight Model	23
4.3.2 Aerodynamic Model	24
4.3.3 Tank Draining Model	24
4.3.4 RAC Model	25
4.3.5 Propulsion Model	25
4.3.6 Performance Code	25
4.3.7 Optimization Function	26
4.4 MDO Results	26
4.4.1 General Trends	26
4.4.2 Propulsion System Selection	27
4.4.3 Optimum Design	29
4.4.4 Sensitivity of Design Variables	29
4.5 Stability and Control	29
4.5.1 Static Trim Analysis	30
4.5.2 Dynamic Stability Criteria	30
4.5.3 Dynamic Stability Analysis	30
4.5.4 Empennage and Control Surface Sizing	31
4.5.4.1 Trade Studies	31
4.5.4.2 Empennage Sizing Results	31

4.5.4 Stability and Control Predictions	32
4.6 Preliminary Design Results	33
4.6.1 Component Sizing	33
4.6.2 Airplane Performance Predictions	34
4.6.3 Mission Performance Predictions	35
5.0 Detail Design	37
5.1 Component Selection and Systems Architecture	37
5.1.1 Wing Aerodynamic Design	37
5.1.1.1 Airfoil Selection	37
5.1.1.2 Wing Twist	37
5.1.2 Avionics System	39
5.1.2.1 Servo Selection and Placement and the Tail-Wheel Steering Mechanism	39
5.1.2.2 Telemetry System	39
5.1.2.3 Electronic Speed Control and Radios	39
5.1.3 Propulsion System	39
5.1.4 Structural System	39
5.1.4.1 Fuselage Spine Sizing	40
5.1.4.2 Spar and D-tube Sizing	40
5.1.5 Water Storage and Dump System	40
5.1.6 Landing Gear	41
5.2 Final Airplane Specifications	41
5.3 Drawing Package	44
6.0 Manufacturing Plan	49
6.1 Figures of Merit	49
6.1.1 Strength to Weight Ratio	49
6.1.2 Skill Level Required	49
6.1.3 Actual Cost	50
6.1.4 Time Required	50
6.1.5 Material Availability	50
6.1.6 Component Durability	50
6.2 Investigated Manufacturing Processes	50
6.2.1 Wing	50
6.2.2 Empennage	51
6.2.3 Fuselage	51
6.2.4 Landing Gear	51
6.3 Figure of Merit Analysis Results	51
6.4 Manufacturing Processes	53
6.4.1 Wing Manufacturing Process	53
6.4.2 Empennage Manufacturing Process	54
7.0 Testing	57
7.1 Tank and Nozzle Testing	57
7.2 Propulsion Testing	58
7.3 Flight Testing	59
7.3.1 In-flight Water System Testing	59
7.3.2 Competition Airplane Flight Test Plan	59
8.0 References	60

1.0 Executive Summary

This report describes the design process employed by the University of Illinois Design Build Fly Team to design, build and test the Fiberglass Overcast. The Fiberglass Overcast was designed to compete in the 2003/2004 Cessna/ONR Design Build Fly Competition. It is capable of completing both the Fire Bomber and Ferry missions. However, the airplane was optimized for the Fire Bomber mission because it was found to be the most important in terms of the competition score. The principal requirement of the Fire Bomber mission was to carry and release a water payload. The design process utilized a multidisciplinary design optimization code to fully explore the design space and optimize the configuration. The optimized analysis showed that carrying the maximum amount of water would result in the best total flight score. It was found that, by simply changing the propeller, the airplane optimized for the Fire Bomber mission also could complete the Ferry mission. Ground handling was a critical concern because the airplane had to be refilled during the mission. The speed and accuracy of the landing as well as the refilling process are vital to achieving a high total flight score. Because of this the airplane was, for the most part, built around the system that would store and release the water.

The design process began with a morphological chart that included over 6000 configurations. The Fire Bomber mission was the driving mission in the design of the airplane because it dominated the total flight score. Conceptual design analyses narrowed those options to a simple pod-and-boom type configuration with a V-tail. That configuration efficiently carried the maximum water payload allowed and resulted in a low Rated Airplane Cost (RAC).

Preliminary design sizing resulted in an airplane with a wing area and aspect ratio of 6 ft² and 8.2, respectively, and an estimated weight of approximately 19 pounds. It also estimated the required thrust at 8.5 lb and energy at 720mAh. Detailed stability analyses were conducted to size the empennage and control surfaces.

In detail design, the final components for the airplane were selected and integrated into the design. The S2091 airfoil was chosen for the wing because of its low drag characteristics in the operating range of the airplane. No twist was designed into the wing because efficiency gains were marginal and construction tolerances prohibited manufacturing wings with small amounts of twist. The NACA 0009 airfoil was chosen for the tail surfaces and the NACA 0035 was chosen for the fuselage pod cross section. A mono-wheel landing gear was chosen for simplicity as well as low cost and weight. With a steerable tail wheel, such a landing gear would not compromise the ground handling characteristics. Draining times between 17 and 22 seconds were estimated for the full four liter payload. Measured static draining times, for the full four-liter payload, were on the order of 20 seconds. Flight tests of the system indicated that draining times in flight would be similar to the static values. This time is well within the time to fly the downwind course leg.

2.0 Management Summary

The 2003/2004 team benefited from many experienced members as well as several new members. The season began with the recruitment of several underclassmen, including an electrical engineering student, and a great fund raising effort. The team structure consisted, at the highest level, of a team leader and a chief design engineer. One or both of these team members made all critical decisions. This management strategy had been used in the past and was found to streamline the design, building and writing process by allowing the rapid making and executing of decisions. Other team members were assigned tasks and were put in sub-group leadership roles, as needed, by the team leader and chief design engineer. Table 2.1 shows the design personnel and the tasks they participated in. The following scores indicate the level of contribution to a specific task:

1. Major contributor to completion of the task
2. Contributed to completion of the task
3. Minor contributor to completion of the task

During the first stages of the design process, the team created a schedule for the main elements of the design, testing and construction of the Fiberglass Overcast. Team meetings were held once per week in the early stages of design. The number of meetings increased to two or three towards the end of the design work, with emphasis on work in sub-groups created to more efficiently complete the design, writing and building. The majority of the deadlines were met because of the hard work of the design team. Figure 2.1 shows the milestone chart for the design, construction and testing of the Fiberglass Overcast. The figure shows the planned and actual, or projected if they have not been completed as of the printing of this report, completion dates of the major design elements.

Operations at the team shop were managed in a similar way to the team management strategy. By appointing a chief manufacturing engineer, all decisions were made quickly and executed. The chief manufacturing engineer was intimately involved in all aspects of the construction, materials selection and component selection. The building expertise and manpower was increased significantly by delegating tasks to experienced members who were assigned new members to mentor.

Each aspect of testing was assigned to a different team member and sub-groups were formed to complete the testing. A tank group, flight testing group and propulsion testing group was established. In this way testing of multiple systems was carried out in parallel.

Report writing was aided by writing in parallel with design, testing and manufacturing. This had two advantages. First, the writing was completed earlier and had more time to be edited. And second, the results and procedures were fresh in the mind of the writer. Drawing duties for the report and manufacturing were given to those members most familiar with the drawing software.

Table 2.1 Personnel Assignments

Tasks	Conceptual Design	MDO code	Preliminary Design	Stability and Control	Detail Design	Report Writing	Drawing	Building	Telemetry System	Tank Testing	Propulsion Testing	Flight Testing	Fund Raising
Ed Whalen, Team Leader	1		1		1	1	3	2		1		2	1
Geoff Bower, Chief Design Engineer	1	3	1		1	1	1	1		2	1	2	
Keerti Bhamidipati, Chief Design Engineer			1	1	1	1	1	1	3	1		1	
Jeremy Sebens	1	1	1	2								1	
Chris Lamarre	1		2									2	
Karl Klingebiel	2	1	2		2	2	2	3			1	2	
Vincent Lee		1	2										
Amos Kim	2		1		2	1	2	1				1	
Sean Warrenburg	2		1	1	1	1	1	1		2			
Richard Page, III	3	1											
Ethan Chew	2		1		2		1	1		1		2	
JP Krauss			2		2		3	1	1			1	

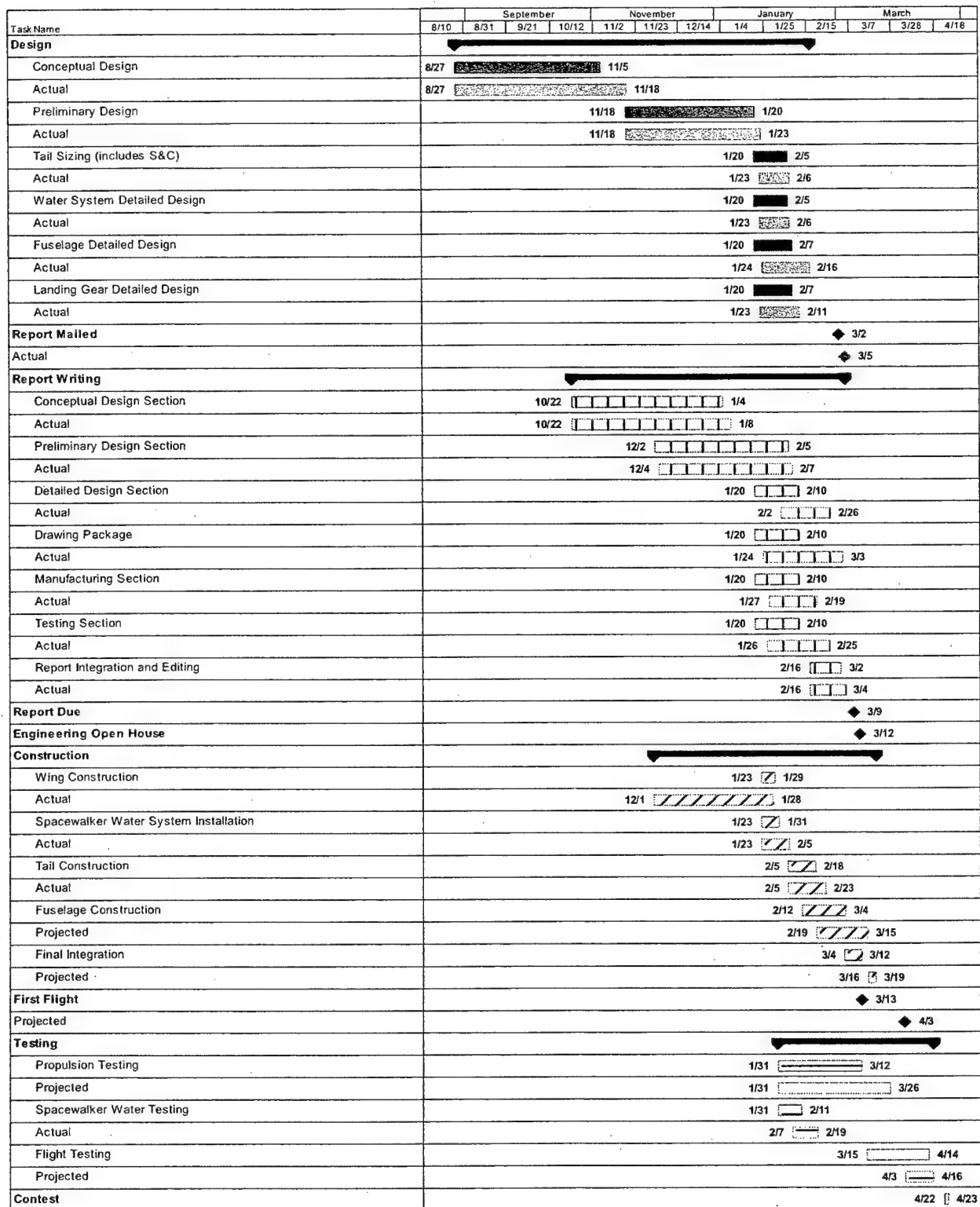


Figure 2.1 Milestone Chart

3.0 Conceptual Design

This section discusses the details of the conceptual design studies for the Fiberglass Overcast. To begin these studies, a morphological chart of possible airplane configurations was developed. Many of these configurations were qualitatively eliminated based on feasibility considerations. The remaining configurations were analyzed based on figures of merit. The relative importance of the two missions was investigated to determine if one was more important with respect to the total flight score. The highest scoring configuration was selected to be refined in the preliminary design.

3.1 Mission and Design Requirements

The 2003/2004 Design Build Fly competition includes two distinct missions; the Fire Bomber mission and the Ferry mission. Each requires the airplane to fly around the closed course shown in the rules.

3.1.1 Fire Bomber Mission

The Fire Bomber mission requires the airplane to release a water payload of up to four liters through a ½-inch diameter orifice while in flight. Two sorties are required. Each sortie has the following required components: fill the airplane water tank, takeoff, accelerate and climb to the upwind turn marker, turn downwind, begin the water dump once past the upwind turn marker, cruise downwind including a 360° turn, terminate the water dump prior to passing the downwind turn marker, turn upwind, descend and land.

3.1.2 Ferry Mission

The Ferry mission requires the airplane to complete one sortie that consists of flying four laps around the competition course without carrying a payload.

3.1.3 Takeoff Requirement

The airplane is required to takeoff in 150 feet or less. The wheels of the airplane must be off the runway in this distance or the flight is scored as a zero.

3.1.4 Airplane Storage Requirement

The airplane is required to completely fit within a 4' x 2' x 1' box. The airplane may be divided into as many subassemblies as are required to fit it in the box.

3.1.5 Structural Requirements

The airplane is subjected to a "tip test" at the competition. This test is the equivalent of a 2.5 g flight load at the root of the wing. The test is conducted by supporting the airplane at maximum gross weight by the wing tips. Both an upright and inverted tests are required.

3.1.6 Propulsion System Requirements

The motors that may be used are limited to the Astroflight™ and Graupner™ families of brushed electric motors. Also, the maximum weight of the propulsion batteries is limited to five pounds. In addition, the batteries are limited to NiCd type and the propeller must be commercially available.

3.2 Airplane Component Types Considered

The first step in selecting a configuration was to create a morphological chart for all of the possible airplane configurations that reasonably could be considered. In order to do this, the airplane configuration was divided into its primary components and possible types for each component were identified. The entire morphological chart is presented as Table 3.1.

Table 3.1 Morphological Chart

Component	Types				
Wing	Monoplane	Biplane	Joined	Ring	Gull
	Tandem	Tri (or greater)-wing		Annular	Channel
Fuselage	Lifting	Conventional	Pod-and-Boom	Multiple	Blended
Empennage	V-tail	T-tail	Conventional	None	Canard
	Cruciform	H-tail	Vertical Only		Inverted V-tail
Landing Gear	Tail Dragger		Bicycle	Monowheel	Tricycle
Propulsion	Pusher		Tractor	Multiple Pusher	Multiple Tractor

3.2.1 Wing Types

There were a large number of possible wing types initially considered, many of which were eliminated for qualitative reasons. Several were eliminated because of the unnecessary structural complexity and manufacturing difficulties associated with them. The ring wing, annular wing, joined wing, channel wing, gull wing and multi-wings beyond a bi-wing were eliminated for this reason. The wing types that were considered further were the monoplane, biplane, and tandem wing. These wing configurations are shown in Fig. 3.1.

3.2.2 Fuselage Types

Initially, six fuselage types were considered. The mission requirements limited the practical application of some fuselage types that were qualitatively eliminated at this stage. An airplane with multiple fuselages was determined to be impractical because only one water orifice is allowed. Running tubing between the fuselages would be heavy and significantly increase the water drain time. The rules prohibit the water payload from being carried in a separate pod. This ruled out an asymmetric design that would carry the water in one fuselage and the airplane systems in another.

The fuselage types considered for further study were separated into three categories. The conventional fuselage category is a fuselage designed to enclose the payload and airplane systems. The pod-and-boom fuselage contains the payload and airplane systems in an aerodynamic pod with the empennage connected through the use of a boom. However for this study, the pod-and-boom type was considered as a subset of the conventional fuselage because of their similarities. A blended fuselage was also considered. This type of fuselage is similar to a conventional fuselage, except that the wing is smoothly blended into the fuselage. Lastly, a lifting fuselage, basically a low aspect ratio wing, was considered. Therefore, the fuselage types considered, as shown in Fig. 3.1, were conventional, blended and lifting.

3.2.3 Empennage Types

A large number of empennage types were considered for the airplane. They were grouped into a number of categories in order to simplify analysis at this point in the design. Conventional, T-tail and cruciform tails were grouped into the conventional category. Both upright and inverted V-tails were considered as a single category. Also considered was a vertical tail only that could be used on a flying wing. A no empennage option was considered, since a flying wing of this type could be used as well. A canard stabilizer was also considered. Finally, H-tails and other multi-tails were considered but eliminated due to Rated Airplane Cost (RAC) concerns. The effect of multiple vertical tails can be achieved with a larger single vertical surface at a lower RAC and it is easier to manufacture one large vertical surface. Sketches of the empennage types considered are shown in Fig. 3.1.

3.2.4 Landing Gear Types

The landing gear types considered were tricycle, tail-dragger, bicycle with tip skids, and mono-wheel with tip skids. These types are shown in Fig. 3.1.

3.2.5 Power System

At this stage the power systems considered concerned the configuration of the motor(s) and propeller(s). A single motor with either a tractor or pusher propeller was considered for further study. Multiple engines and propellers were eliminated since they greatly increase the RAC. The pusher and tractor configurations are shown in Fig. 3.1.

3.3 Rated Airplane Cost and Competition Score Analysis

The RAC is one of the three components of the competition score equation.

$$\text{SCORE} = (\text{Written Report Score} * \text{Total Flight Score}) / \text{Rated Airplane Cost} \quad (3.1)$$

It is evident that for given flight and report scores, the highest competition score will occur with the lowest RAC. The RAC equation and the definitions of its components are outlined below. Each component of the equation was analyzed for variations about a fixed design similar to DBF airplanes from past competitions to gauge the effect on the overall RAC.

$$\text{Rated Airplane Cost, \$ (Thousands)} = (A * \text{MEW} + B * \text{REP} + C * \text{MFHR}) / 1000 \quad (3.2)$$

Where:

- A = \$300 / pound, the Manufacturer's Empty Weight Multiplier,
 - B = \$1500 / pound, the Rated Engine Power Multiplier,
 - C = \$20 / hour, the Manufacturing Cost Multiplier,
 - MEW, the Manufacturer's Empty Weight, is the weight of the airplane and its systems without the payload,
 - REP, the Rated Engine Power, is computed based on the equation
- $$\text{REP} = (1 + .25 * (\# \text{ engines} - 1)) * \text{Total Battery Weight [lbs]} \quad (3.3)$$





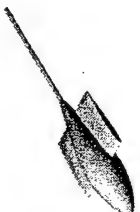
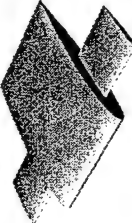
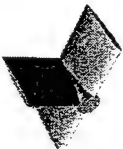








Wing type	 Monoplane	 Biplane	 Tandem
Fuselage type	 Conventional	 Conventional	 Lifting
Tail Type	 Conventional	 Conventional	 Canard
Landing gear type	 Tricycle	 Tail Dragger	 Bicycle with tip skids
Propulsion type	 Tractor	 Pusher	 Monowheel with tip skids

Fig 3.1 Component Types Considered

- MFHR, the Manufacturing Man Hours, is calculated based on the equation

$$\begin{aligned}
 \text{MFHR} = & 10 \text{ hr/ft}^2 * \text{wing span} * \text{maximum wing chord} * \# \text{ of wings} \\
 & + 5 \text{ hr} * \text{Control Surface Multiplier} \\
 & + 20 \text{ hr/ft}^3 * \text{Fuselage Length} * \text{Fuselage Width} * \text{Fuselage Height} \\
 & + 5 \text{ hr} * \# \text{ of vertical surfaces without control} \\
 & + 10 \text{ hr} * \# \text{ of vertical surfaces with control} \\
 & + 10 \text{ hr} * \# \text{ of horizontal surfaces} \\
 & + 5 \text{ hr} * \# \text{ of servos or controllers}
 \end{aligned}
 \tag{3.4}$$

It is clear that for a given size airplane with a constant propulsion system, reducing the empty weight will minimize the RAC. The most important factor in reducing the RAC is the weight of the batteries. The battery weight has the greatest effect in the REP, but it also has a large effect on the empty weight of the airplane. Adding 1 lb of batteries to a given configuration will increase the RAC by about \$2000. Also, from the REP equation it is easy to see that the number of motors has a large effect on the RAC. For each motor added after the first, there is a 25% REP penalty incurred, or an extra \$375 per pound of batteries. The takeoff requirement has been shown to be achievable with only one motor, so multiple motors should not be considered due to their detrimental effect on RAC. Also, if multiple motors are used, the empty weight increases due to added structure and the extra motor(s). Therefore, only one motor was considered for the remainder of the airplane analysis.

The MFHR equation reveals several trends that are important to the overall RAC:

- The wing area and fuselage volume have large effects on the total RAC.
- The aspect ratio of the wing has no effect on the RAC for a given wing area.
- The taper ratio of the wing does have an effect on RAC for a given wing area.
- The number of horizontal and vertical stabilizing surfaces have a moderate effect on the RAC
- The control surface multiplier and number of controllers present have a small effect on the RAC

Clearly, the first point is important due to the large multipliers applied to the wing area and fuselage volume portions of the MFHR equation. Also, it is clear from the wing MFHR terms that the aspect ratio has no effect on the RAC. The three remaining bulleted points required more investigation to determine their effect on the RAC.

Since the RAC is calculated by taking the largest wing chord, not the mean chord, the taper ratio changes the wing MFHR term for a given wing area. This effect can be seen in Fig 3.2. It shows the wing MFHR vs. taper ratio for the baseline configuration wing with constant area and aspect ratio. Tapering of the wing has a noticeable effect on the RAC, so in order to minimize RAC a rectangular wing with optimal twist would be best.

By increasing the number of vertical or horizontal stabilizing surfaces the RAC increases substantially. The cost of adding a vertical stabilizer with control is on the order of \$500 per surface. This cost includes both the weight effect and the cost of the controlling servo. It is cheaper to have only one

vertical surface that is the same size as multiple smaller surfaces to achieve the desired effectiveness. The use of a horizontal stabilizer that is greater than 25% of the wing span has a large effect on the RAC, because above that limit the horizontal tail is counted as a second wing in the cost model. Fig 3.3 shows the effect of varying the horizontal tail span as a fraction of the wing span for a constant wing area. The discontinuity in that figure results from the tail being counted as a wing when its span is greater than 25% of the wing span.

The control surface terms in the MFHR are constant because the number of controllers is essentially fixed for most configurations. This is due to the need for a speed controller, two aileron servos, two empennage servos, and a payload release servo. Some RAC can be saved by using the empennage servos to control ground steering.

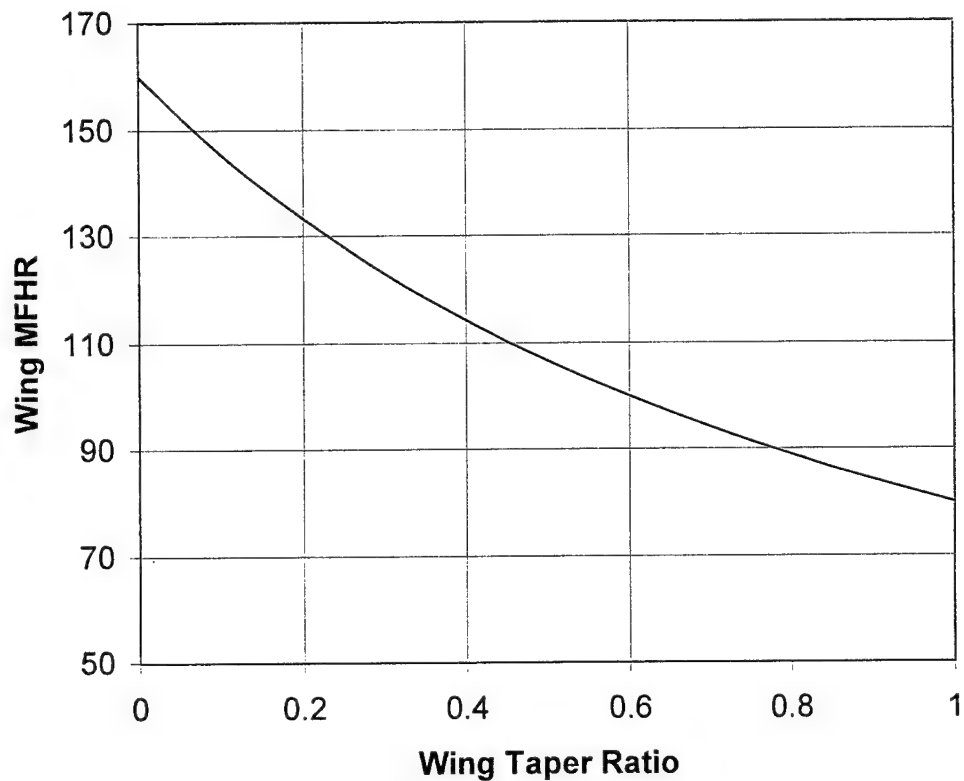


Fig 3.2 Wing MFHR vs. Taper Ratio

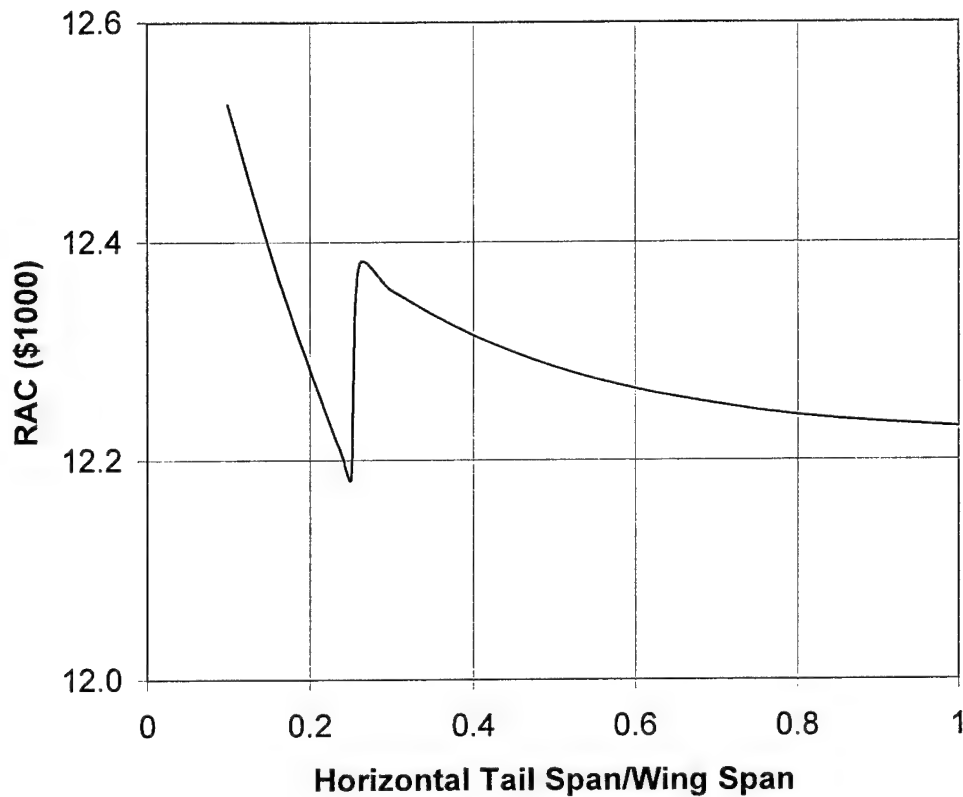


Fig. 3.3 RAC vs. Horizontal Tail Span/Wing Span

3.4 Possible Airplane Configurations

A new morphological chart was created to consider all of the possible airplane configurations that could be assembled from the remaining types for each component. This new chart is shown in Table 3.2. To summarize, there were three wing types, three fuselage types, five empennage types, four landing gear types and two propulsion system types. This resulted in 270 possible airplane configurations to investigate.

Table 3.2 Updated Morphological Chart

Component	Types				
Wing	Monoplane		Biplane		Tandem
Fuselage	Blended		Lifting		Conventional
Empennage	V-tail	Vertical Only	Conventional	None	Canard
Landing Gear	Tricycle		Tail Dragger		Bicycle
Propulsion	Pusher			Tractor	

Each of the possible airplane configurations was examined to determine its feasibility and to identify any major technical problems. The main concerns that led configurations to be eliminated dealt with potential stability problems, takeoff rotation problems and problems associated with effectively releasing the water payload in flight. Based on these considerations, the number of configurations to be

quantitatively evaluated was reduced to eight. These eight configurations, that were analyzed using figures of merit, are shown in Fig. 3.4.

3.5 Figures of Merit

The eight selected airplane configurations were analyzed with a number of quantitative and qualitative figures of merit. The quantitative figures of merit analyzed were RAC and Fire Bomber mission time. The qualitative figures of merit were assigned a score of -1 for poor, 0 for average and 1 for good. These figures of merit included; stability and control, ground handling, water carriage and release, and manufacturability. Based on these figures of merit the best overall airplane configuration to complete the mission was determined. Each figure of merit considered corresponded to one or more of the mission requirements.

3.5.1 Rated Airplane Cost

One of the quantitative figures of merit was the RAC. The competition score for the airplane is computed using this value. The RAC appears in the denominator of the competition score equation. Therefore, it was very important to minimize RAC in order to maximize the competition score. For each of the airplane configurations considered, a RAC was computed and used in determining the best configuration for the mission. A spreadsheet-based weight and RAC model was developed to evaluate each of the configurations. The estimated weights helped to size the configurations and to determine the empty weight contribution to the RAC.

3.5.2 Estimated Mission Performance

The other quantitative figure of merit was the estimated mission performance of each airplane configuration. The amount of water carried, a mission difficulty factor of two and the time required to complete the mission determine the single flight score for the Fire Bomber mission; see Eq. (3.5). A mission difficulty factor of one and the time required to complete the mission determine the single flight score for the Ferry mission; see Eq. (3.6).

$$\text{Fire Bomber Single Flight Score} = \text{Difficulty Factor} * \text{Pounds of Water} / \text{Mission Time} \quad (3.5)$$

$$\text{Ferry Single Flight Score} = \text{Difficulty Factor} / \text{Mission Time} \quad (3.6)$$

The total flight score is determined by the two single flight scores and the RAC as shown in Eq. (3.7).

$$\text{Total Flight Score} = (\text{Fire Bomber Single Flight Score} + \text{Ferry Single Flight Score}) / \text{RAC} \quad (3.7)$$

An analysis was carried out to determine the relative importance of the two missions to the total flight score. For this preliminary analysis, similar flight times were assumed for both missions and the maximum payload was assumed for the Fire Bomber mission. The assumption of approximately equal flight times was justified due to the slower flight speeds and time the airplane spends on the ground in the Fire Bomber mission. The results of this analysis are presented in Table 3.3. Even if the mission time for the Ferry mission was shorter, the difference in Single Flight Scores would be at least an order of magnitude in difference. Furthermore, the importance of the Fire Bomber was so significant that the Ferry mission acted more as a constraint than a mission. That is, the airplane had to complete that mission, but

it was not critical to the overall total flight score. Due to this, only the Fire Bomber mission performance was used as the figure of merit.

Table 3.3 Dominant Mission Analysis

Mission	Difficulty Factor	Payload Weight (lbs.)	Approximate Mission Time (min.)	Single Flight Score
Fire Bomber	2.0	17.6	3.0	11.73
Ferry	1.0	N/A	3.0	0.33

The eight candidate configurations were analyzed using a performance code that integrates the mission flight path to determine flight time. The code also calculates the takeoff distance and the energy required for the mission. The performance code has been developed over the past four years by the UIUC DBF team. The code uses a fourth-order Runge-Kutta scheme to integrate Newton's Second Law of Motion over a prescribed mission. Inputs to the code include: aerodynamics, geometry, weight, motor performance and a mission description. The primary outputs of the code are mission time and energy required.

Some assumptions are made in the code to simplify the calculations. However, it has been found that these assumptions do not seriously affect the accuracy of the code. First, constant altitude turns are assumed. Second, the throttle setting for a given course segment is assumed to operate as if it applied a percentage of the maximum thrust available. Finally, the rolling friction coefficient was empirically determined, for rubber wheels on asphalt, to be 0.1. With these assumptions the accuracy of the code is largely a function of the aerodynamics, motor and weight data.

To perform a meaningful analysis it was necessary to normalize the sizing of each configuration. This was done by sizing each configuration to have a common wing loading and power loading. These values were determined from historical data collected for similar missions at previous DBF competitions. A wing loading of 2.75 lb/ft² and a power loading of 900 [mAh*V/min]/lb were selected from these historical data. The weight of the different configurations was determined based configuration and used in the performance estimate. Since the estimated weights for all of the configurations were similar, selecting a single propulsion system for all of the models would give nearly equal power loadings. The propulsion system from last year's competition yielded a power loading very near the selected value. So, for analysis in the performance code, a geared Astroflight™ 60 motor, spinning an 18 x 18 propeller on 40 Sanyo CP1300 SCR cells was used for all of the configurations. The resulting sizing data are presented in Table 3.4.

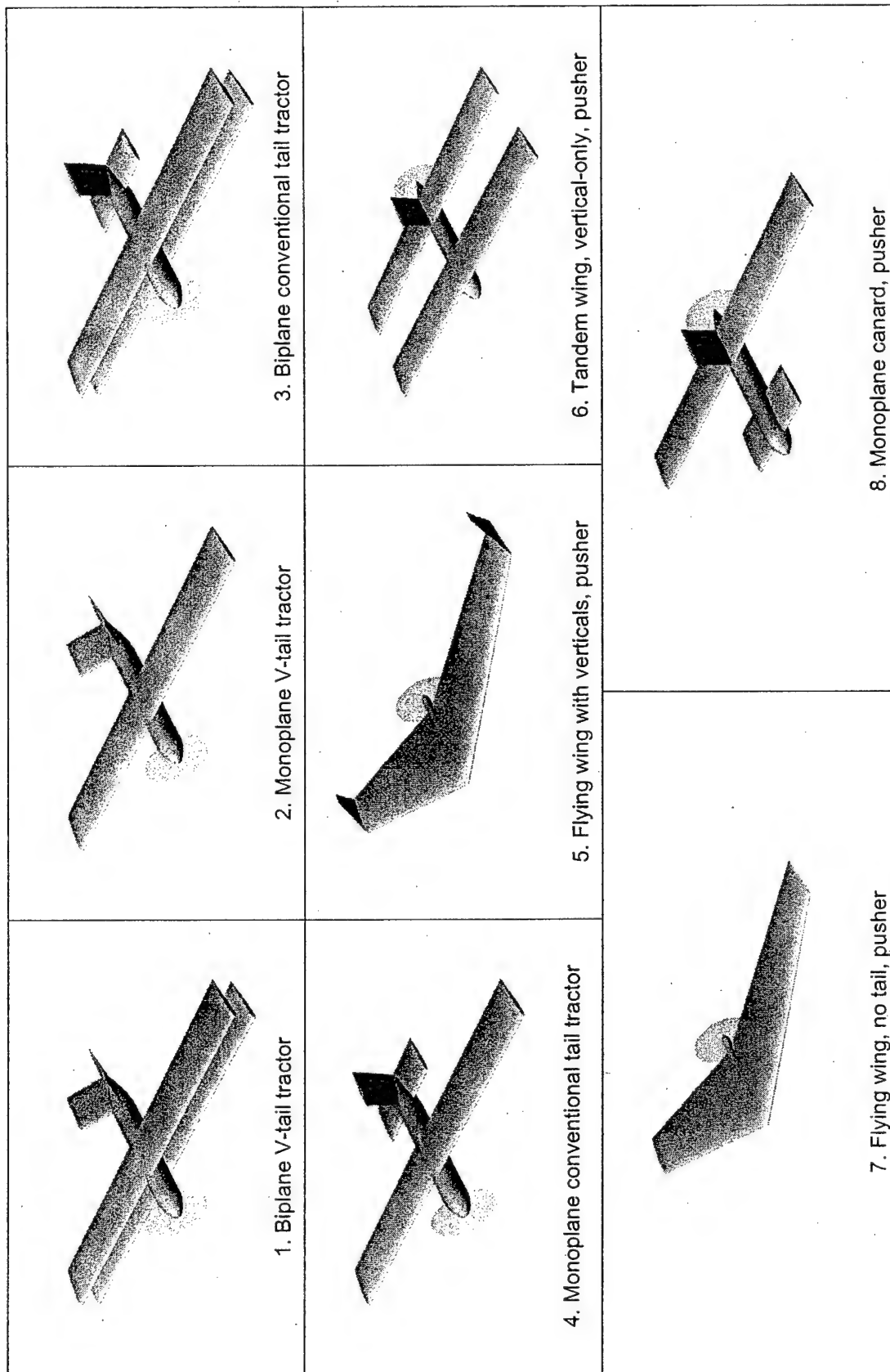


Fig. 3.4 Eight Configurations for Conceptual Design Analysis

Table 3.4 Conceptual Design Configuration Sizing

Configuration	Biplane V-tail tractor	Monoplane V-tail tractor	Biplane conventional tail tractor	Monoplane conventional tail tractor	Flying wing with verticals, pusher	Tandem wing, vertical only, pusher	Flying wing, no tail, pusher	Monoplane canard, pusher
Wing span(ft)	5.20	7.25	5.25	7.32	7.70	5.10	7.65	7.32
Wing chord(ft)	0.65	0.91	0.66	0.92	0.96	0.64	0.96	0.92
Stabilizer span (ft)	1.30	1.81	1.31	1.83	0.00	5.10	0.00	1.83
Stabilizer chord (ft)	0.65	0.91	0.66	0.92	0.00	0.64	0.00	0.92
Fuselage Length (ft)	3.47	4.83	3.50	4.88	1.50	3.40	1.50	4.88
Fuselage Width (ft)	0.33	0.50	0.33	0.50	1.50	0.50	1.50	0.50
Fuselage Height (ft)	1.00	0.50	1.00	0.50	0.25	0.50	0.25	0.50
Weight (lb)	18.62	18.12	18.95	18.45	18.54	18.18	18.28	18.45
RAC (\$1000)	10.0	9.8	10.3	10.1	10.1	9.7	9.3	10.1

3.5.3 Stability and Control

In order to complete the required airplane missions, it was essential that the airplane be both statically stable in all axes and be maneuverable enough to fly the course and withstand any wind conditions present at the contest. A stability and control figure of merit was qualitatively assigned to each configuration considered. The factors that were considered in applying this figure of merit were:

- Capability for robust longitudinal stability including: resistance to sloshing and placing the payload at the airplane center of gravity.
- Inherent lateral and directional stability.
- Adequate pitch control authority without excessive lift penalties.
- Adequate lateral and directional control authority to allow the airplane to takeoff and land in a crosswind.
- Adequate damping in all axes to reduce effects of sloshing and provide good flight qualities.

The scores were assigned as shown in Table 3.5.

Table 3.5 FOM Scores for Stability and Control

Assigned Score	Configuration Characteristic
1	Exhibits positive stability and control characteristics with respect to all criteria
0	Exhibits positive stability and control characteristics with respect to three or four of the criteria
-1	Exhibits positive stability and control characteristics with respect to two or fewer of the criteria

3.5.4 Ground Handling

Another figure of merit that is important to the successful completion of the mission is the ground handling ability of the airplane. For the Fire Bomber mission to be completed quickly, the airplane must be able to land, stop near or taxi back to the starting line, and be refilled with water. To accomplish this, the airplane configuration must have an adequate gear stance, a steerable nose or tail wheel and a method for stopping quickly. In order to fulfill the last requirement, brakes were added to each of the airplane configurations. The braking system was accounted for by adding a controller in the calculation of the RAC. A score was qualitatively assigned to each configuration for its expected ground handling characteristics. The basis for assigning these scores is shown in Table 3.6.

Table 3.6 FOM Scores for Ground Handling

Assigned Score	Configuration Characteristic
1	Nose wheel steering and brakes
0	Tail wheel steering with brakes or Nose wheel steering without brakes
-1	Tail wheel steering without brakes

3.5.5 Water Carriage and Release

The ability for a given airplane configuration to carry and release the water payload for the Fire Bomber mission is an important qualitative figure of merit. In order to successfully complete the Fire Bomber mission with a maximum score it is important that the airplane be able to carry the maximum amount of water and be able to release it as quickly as possible. This can be accomplished by increasing the pressure gradient on the water in the tank and by increasing the physical tank height for a give water volume. From initial observations, it is important that the water tank be tall to facilitate a quick release of the water. Based on this observation, a score was qualitatively assigned to each configuration considered. The scores were assigned as shown in Table 3.7.

Table 3.7 FOM Scores for Water Carriage and Release

Assigned Score	Configuration Characteristic
1	Easily accommodates a tall fuselage
0	Less easily accommodates a tall fuselage
-1	Not able to accommodate a tall fuselage

3.5.6 Manufacturability

For every airplane configuration studied, a qualitative figure of merit was assigned based on its manufacturability. This figure of merit is important to the final score in a number of ways. First, the weight of the airplane plays a major role in the RAC. Next, it is important that all components of the airplane are durable enough to withstand competition and test flying. It is also important that the team have the ability and experience to construct the airplane in a reasonable amount of time. Based on these factors a score

was qualitatively assigned to each of the eight configurations considered. Table 3.8 shows the criteria for assigning these scores.

Table 3.8 FOM Scores for Manufacturability

Assigned Score	Configuration Characteristic
1	Experience building, structurally simple and robust
0	Little or no experience building or structurally complex
-1	Little or no experience building and structurally complex

3.6 Configuration Selection

Table 3.9 presents the final FOM analysis of all eight configurations. The total score was determined from the following relationship:

$$\begin{aligned} \text{Total Score} = & \text{Normalized Flight Score} * 80 + \text{Stability} * 5 \\ & + \text{Ground Handling} * 5 + \text{Water Carriage and Release} * 5 \\ & + \text{Manufacturability} * 5. \end{aligned} \quad (3.7)$$

The Normalized Flight Score was calculated using the following relationship:

$$\text{Normalized Competition Score} = \{1/(\text{RAC} * \text{Performance})\} / \{\text{MAX}[1/(\text{RAC} * \text{Performance})]\}. \quad (3.8)$$

These scoring equations were determined based on the relative importance of the figures of merit. The RAC and mission time are the only figures of merit that are used to directly compute the competition score, therefore they received the highest weighting at a combined 80%. In order to compare the mission time and RAC of the different configurations, a normalized flight score was used. This provided a competition score with a value between zero and one. The four qualitative figures of merit all have an effect on the competition score, but they are not used directly in its computation. These four figures were each weighted to be 5% of the total FOM score.

The monoplane V-tail tractor was found to be the best configuration. The monoplane conventional tail tractor was a close second. The difference in competition score was attributed to the RAC savings of a V-tail compared to that of a conventional tail. The monoplane V-tail tractor configuration was capable of completing the Fire Bomber mission with the highest competition score. It had a low RAC and was among the fastest configurations for the Fire Bomber mission. In addition, the team has much experience with manufacturing monoplane tractor configurations. Furthermore, the conventional configuration exhibits excellent ground handling, as well as easily predictable and adjustable stability and control characteristics. Figure 3.5 is a sketch of the selected conceptual configuration. Preliminary calculations indicated that draining time was a strong function of tank height; because of this the tank needs to be an approximately vertical cylindrical shape in order to minimize draining time. Therefore, a traditional conventional fuselage was not appropriate, fairing the tank to create a pod and boom fuselage resulted in the most aerodynamic fuselage while still providing adequate room for electronics. A faired tank also allowed for taller tanks and therefore, shorter draining times for a given amount of fuselage

drag. Landing gear was considered separately from all other configuration variables. A tail dragger system was selected for the final system because it allows for good ground handling and steering as well as short takeoffs.

Table 3.9 FOM Chart

Configuration	RAC (\$1000)	Performance (min)	Stability & Control	Ground Handling	Water Carriage and Release	Manufacturability	Total FOM Score
Monoplane conventional tail tractor	10.1	2.08	1	1	1	1	94.4
Tandem wing, vertical only, pusher	9.7	2.02	0	1	1	0	89.7
Flying wing, no tail, pusher	9.3	2.10	-1	0	-1	0	70.0
Flying wing with verticals, pusher	10.1	2.11	-1	0	-1	0	63.3
Monoplane canard, pusher	10.1	2.04	0	0	0	1	80.8
Biplane conventional tail tractor	10.3	2.14	1	1	1	0	85.9
Biplane V-tail tractor	10.0	2.12	1	1	1	0	88.7

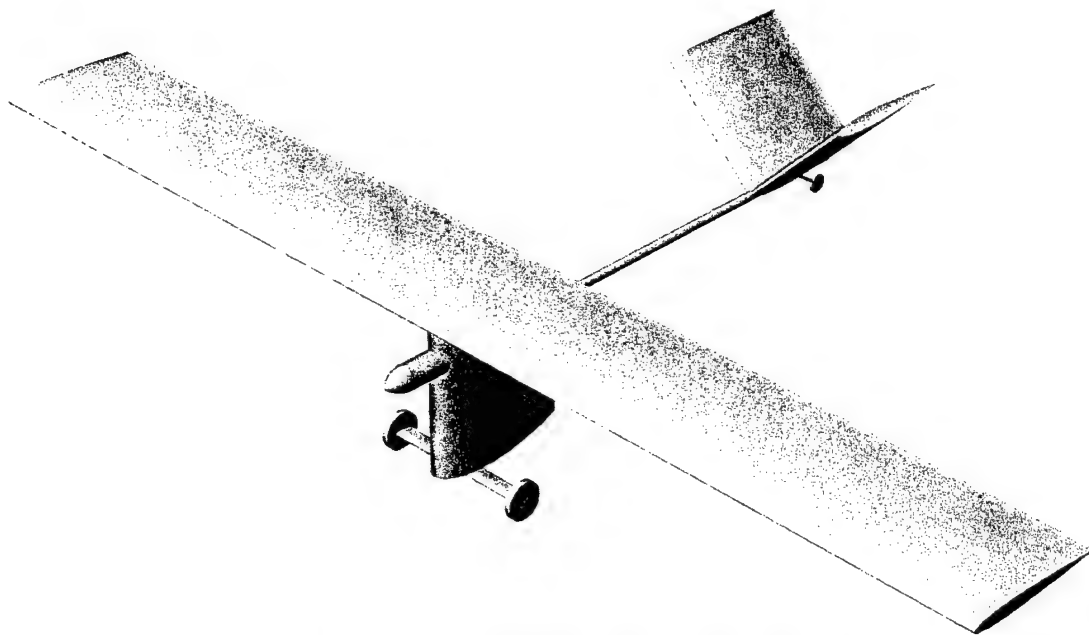


Fig. 3.5 Final Conceptual Design Configuration

4.0 Preliminary Design

The Fiberglass Overcast was designed to complete the Fire Bomber mission in the minimum amount of time at the lowest possible cost. The airplane was also designed to complete the Ferry mission. However, based on the analysis presented in Section 3.5.2, the Ferry mission was not considered critical to the competition score. A multidisciplinary design optimization (MDO) code was developed to analyze the configuration chosen at the end of conceptual design. The MDO code included a detailed performance code that modeled every component of both missions. Critical design parameters were identified and a matrix of these parameters was used to investigate the design space of the airplane. Airplane dimensions, weight, power required and energy required were determined from this analysis.

4.1 Design Variable Selection

Several parameters were investigated in a sensitivity analysis in order to determine their importance to the competition score. Based on these results, design variables were selected for use in the MDO code.

4.1.1 Design Parameter Sensitivity Analysis

A number of primary design parameters were considered. These parameters characterize a given design within the framework of the MDO code. The parameters chosen for the sensitivity analysis were:

- Aspect Ratio – Important aerodynamic parameter for induced drag
- Wing Loading – Important parameter for takeoff analysis and cruise power required
- Parasite Drag – Important parameter for maximum speed and minimum power required
- Oswald Efficiency – Important aerodynamic parameter for induced drag
- Amount of Water Carried – Parameter used in calculating the Fire Bomber single flight score

In order to establish which of these various design parameters should be emphasized in the preliminary design phase, a sensitivity analysis was performed on each of the design parameters, starting from an initial design point. As the current competition has similar weight and energy requirements to the 2003 DBF competition, the UIUC entry for that competition was used as an initial design point. From this point, each of the parameters listed was varied and the sensitivities of the Rated Airplane Cost (RAC), mission time and competition score were evaluated. For this analysis, the Fire Bomber mission was simulated using the performance code to analyze each of these variations. This resulted in mission time and energy results. The RAC was then calculated and combined with the mission time to yield a competition score. Figures 4.1 through 4.3 present the results for competition score, RAC and mission. In those figures, the initial design point had the values of: RAC = \$13550, Mission Time = 112 sec. and Total Score = 0.348.

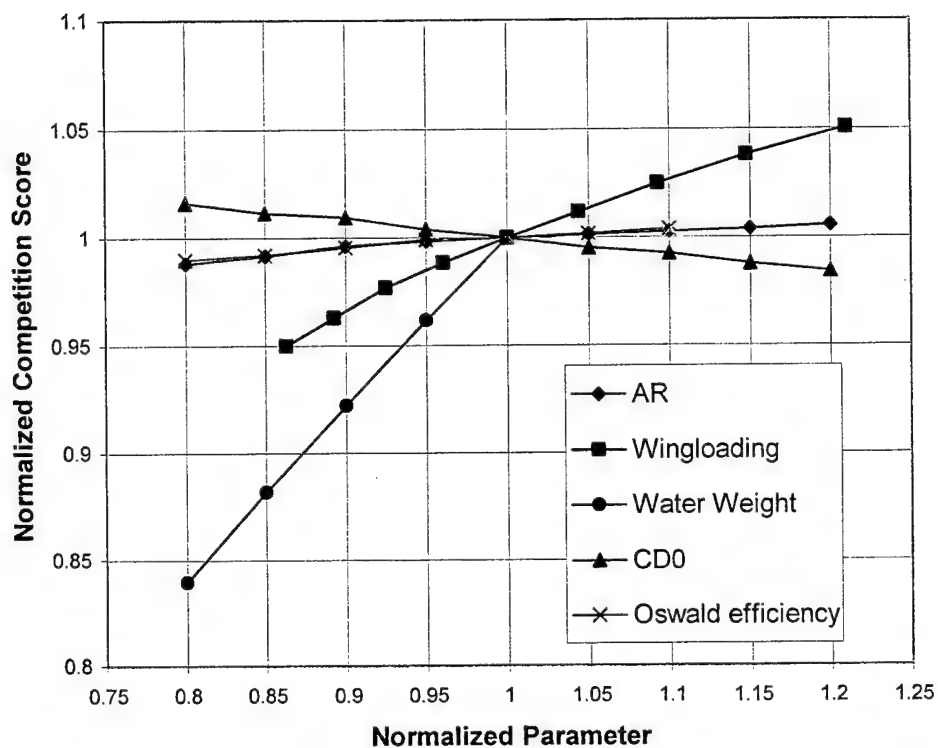


Fig. 4.1 Competition Score Sensitivity

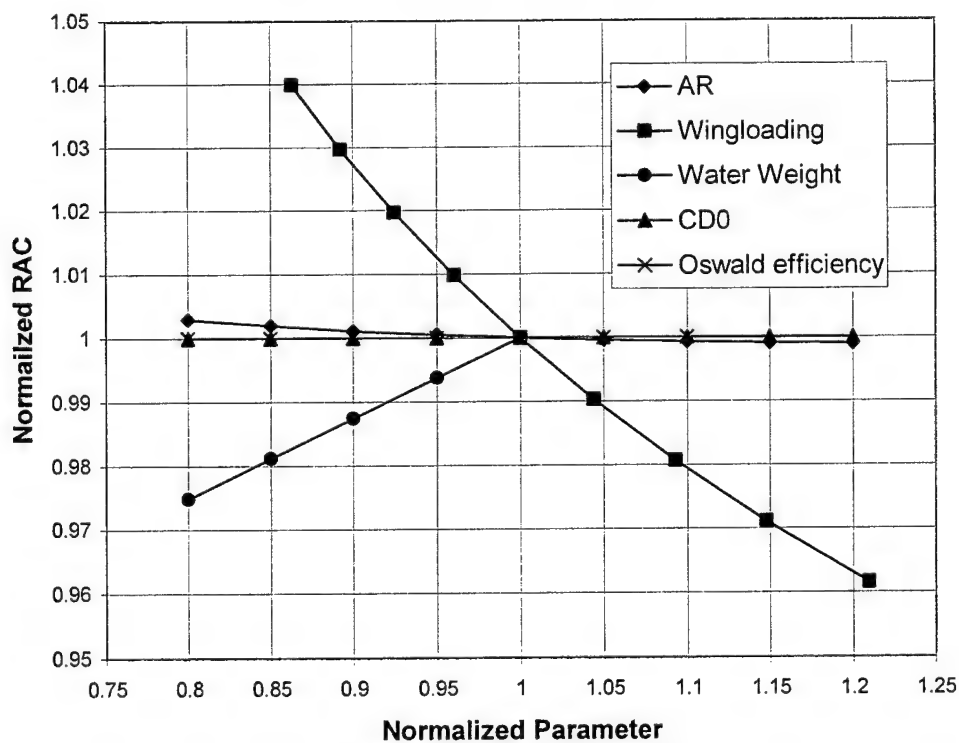


Fig. 4.2 RAC Sensitivity

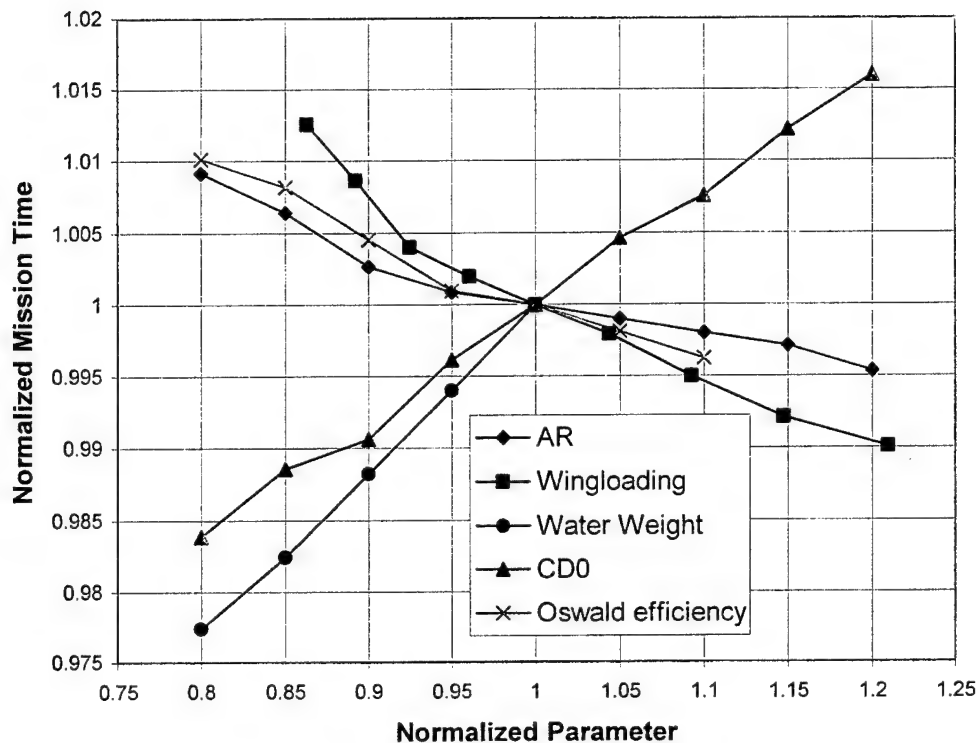


Fig. 4.3 Mission Time Sensitivity

From this analysis (which neglected Reynolds number effects) it was evident that increasing aspect ratio and reducing wing loading would improve competition score. A surprising result was the relative insensitivity of the analysis to parasite drag. This is explained by the fact that the airplane is required to fly at high C_L for the entire Fire Bomber mission. Therefore, induced drag was shown to be far more important than parasite drag. This also explained the improvements with increased AR. The competition score was shown to be very sensitive to the amount of water carried for the Fire Bomber mission. The maximum competition score occurs when the airplane carries the full four liters of water for each sortie.

4.1.2 Design Variables

In order to optimize the airplane using the MDO code, a design vector had to be developed. This design vector was required to describe the airplane with as few design variables as possible. The design parameters from the sensitivity analysis were evaluated and modified. After refinement, the remaining design vector consisted of six continuous variables and one discrete variable. The continuous variables were aspect ratio (AR), wing area (S), fuselage pod height (h_{fuse}), fuselage pod thickness ratio (τ_{fuse}), airplane length (l) and water weight dropped (W_{water}). The discrete variable was the propulsion system (sys_{prop}). This comparatively small set of design variables fully describes an airplane design. Tail and landing gear sizes are dependent upon the various geometric parameters in the vector. The discrete

propulsion system variable describes a complete propulsion system, including number and type of battery cells, motor, gear ratio, propeller diameter, and propeller pitch.

4.2 Analysis Methods Used

There were a few analytic methods used to size the configuration selected in order to maximize the competition score, which is a combination of Mission time and RAC. A performance code developed by previous University of Illinois DBF teams was updated to model the current mission. The MDO code was used to simultaneously investigate tradeoffs of the design variables and maximize competition score. Lastly, a stability and control analysis was performed to refine sizing of the empennage and control surfaces of the optimal design.

4.2.1 Mission Model

The missions modeled by the performance code were selected on the basis of the course outlined in the 2004 DBF rules and a number of assumptions. Both missions begin with the takeoff roll, which is limited to 150 feet before the wheels leave the runway. After climbing to altitude, the first turn is made from the upwind to the downwind leg. For the Fire Bomber mission, water release begins after passing the upwind pylon and continues until empty or until the airplane reaches the downwind pylon. Both missions complete a 360 degree turn on the downwind leg. Both missions then enter a right turn from the downwind leg to the upwind leg. In the case of the Fire Bomber mission, the airplane then descends for landing and is refilled with water. It then takes off again and flies a similar lap. One minute is added to the mission time to account for the time required to land and refuel on the Fire Bomber mission. In the case of the Ferry mission, the airplane continues to fly for 3 more laps that are identical to the first, and then lands. The model used for each mission is summarized in Table 4.1. The first column lists the mission segments, the second and third show the number of times each segment is modeled in a Fire Bomber and Ferry missions respectively.

4.2.2 MDO code

The detailed analysis tools developed for this design were integrated into a single MDO code to investigate the design space. The outputs of that code were the weight and geometric parameters of the airplane as well as the competition score, RAC and mission performance.

4.2.3 Stability and Control Analyses

A stability and control code was developed in MATLABTM.¹ This code input design parameters and output the stability and control characteristics of a given design. The results from the MDO code were analyzed with the stability and control code to properly size the control surfaces and adjust the empennage dimensions output by the MDO code as required.

4.3 Elements of MDO Code

This section describes in more detail the major components of the MDO code.

4.3.1 Weight Model

For the input design vector, the weight model output the weight of every major airplane component and the total weight for the airplane. The weight model was based on a composite building technique.

Table 4.1 Mission Model Segments

Mission Segment	# of segments in Fire Bomber mission	# of segments in Ferry mission	Notes
Takeoff roll	2	1	Less than 150ft
Acceleration and climb out	2	1	From takeoff location to first turn
Level Cruise	0	11	
Level Cruise with water release	4	0	Between upwind and downwind turn markers
180 degree turn	4	8	
360 degree turn	0	4	On downwind leg
360 degree turn with water release	2	0	On downwind leg
Landing approach	2	1	
Ground Roll	2	1	From touchdown until start line
Fill airplane with water	2	0	Assumed 20 seconds

The wing was assumed to be a solid foam core with fiberglass skins and a unidirectional carbon fiber skin spar. The span and area of the wing determined the weight of the wing. The foam weight was based on an estimated volume for the wing, the skin weight was determined by the area of the wing, and the skin spar weight was determined by the span of the wing. Spar size, and hence, weight were determined such that the stresses in the spar were constant for all designs considered.

The empennage weight was determined in the same manner as the wing. The projected span was taken to be 25% of the wing span, and the chord was adjusted to achieve a horizontal tail volume coefficient of 0.5 and a vertical tail volume coefficient of 0.06.

The weight of the propulsion system was determined based on the individual components of the system. The motor weight, gearbox weight and battery cell weight were known *a priori*. An estimate for the propeller weight was obtained based on the diameter.

The weight of the fuselage was estimated by summing the weight of the fuselage skin and underlying structure. First, the fuselage surface area was estimated from the input geometry and then was multiplied by the weight per unit area of the fiberglass skins and a ½ inch foam core. The weight of the underlying structure was calculated on a per unit volume basis.

The estimate for the landing gear weight was obtained by taking into account the wing span, propeller clearance necessary and by assuming it was made of aluminum. The weight of the wheels was also added to this.

Lastly, the weights of the other airplane systems were taken into account. The electronics system weight included the weight of five servos, a speed controller, receiver, wiring and a receiver battery. The control system included the weight of control hinges, horns and pushrods as well as the water release mechanism and the tail wheel steering mechanism.

All of these weights were summed and the weight of the water payload was added. This information was then passed back to the main script of the MDO code for use by the other components.

4.3.2 Aerodynamic Model

The calculation of parasite drag was simplified by the fact that the Fiberglass Overcast is composed almost entirely of airfoil sections. Other components, such as landing gear, were incorporated using established empirical methods². Using the software package XFOIL³, the zero-lift drag coefficients of each section were computed for varying Reynolds numbers. For the fuselage section, the thickness ratio was also computed, assuming symmetrical NACA 4-digit series airfoils. These sectional coefficients were then area-scaled and summed to yield the total parasite drag coefficient.

The induced drag of the wing/tail system was computed using a linear lifting line code. For this analysis, the airplane was assumed to be neutrally stable, and therefore no trim drag was included for varying lift coefficients. The resulting data for induced drag was fit to a cubic polynomial and summed with the parasite drag to yield a drag polar for use in the performance section of the optimization.

4.3.3 Tank Draining Model

An empirical function was developed to estimate the draining time of the water tank as a function of tank height and water volume. Experimental results were used to tune the functions to accurately represent draining time.⁴

$$K = \frac{C_d * A_n}{A_t} \sqrt{2 * g} \quad (4.5)$$

$$h(t) = \left(-\frac{Kt}{2} + \sqrt{h_0} \right)^2 \quad (4.6)$$

The parameter C_d is an empirically determined coefficient called the discharge coefficient that represents the performance of the orifice used. The variables A_n and A_t are the cross sectional areas of the tank and throat, respectively. A detailed discussion of the experiments and their results is presented in the Section 7.1 of this report. Accurately estimating the draining time was critical to the design since the entire payload had to be released on the downwind leg. That constraint set the speed at which the airplane should fly during that leg.

4.3.4 RAC Model

The MDO code used the RAC model described by the 2004 DBF competition rules. The weight component of the RAC model was based on the estimated weights from the Weight Model described in section 4.3.1.

4.3.5 Propulsion Model

The complex relationship between the motor, propeller, gearbox and battery selections and the resulting performance necessitated the use of the entire propulsion system as a discrete input to the MDO code. The following propulsion system components were considered in the analysis:

- All of the Graupner™ Ultra and Astroflight™ series of brushed electric motors
- Carbon folding propellers in the 14 to 20 inch diameter range and with pitches greater than 10 inches
- Gearboxes with ratios of 2.0:1, 2.5:1, 2.73:1 and 3.0:1
- Sanyo™ CP xxxx-SCR batteries in capacities of 1300 mAh, 1700 mAh and 2400 mAh.

These cells have the highest energy density of all NiCd batteries on the market.

Of the thousands of possible combinations of propulsion system components, those meeting minimum performance requirements were selected for use in the optimization. The static performance of each possible combination was estimated using MotoCalc⁵ software and filtered based on estimates of required runtime, thrust, current draw and pitch speed. The values for the filter were determined by a preliminary analysis of the takeoff and cruise portions of the mission. Table 4.2 lists the values for the filter parameters. The filtering of the possible propulsion systems resulted in 58 candidate systems.

Table 4.2 Propulsion Filter Parameters

Filter parameter	Value
Minimum Static thrust	128 oz
Maximum Current draw	40 A
Minimum Run time	150 sec
Minimum Pitch speed	50 mph

The thrust and current draw of each candidate propulsion system were estimated for varying free stream velocities using MotoCalc. These data were then processed using a team-written MATLAB script which uses two 3rd order polynomial curve fits to give current draw as a function of thrust required and airspeed. The result of this processing was an input file for use in the performance code, for each candidate propulsion system.

4.3.6 Performance Code

The performance code described in section 3.5.2 was utilized in the MDO code to determine mission time and energy requirements for the mission.

4.3.7 Optimization Function

The various code components were assembled into an objective function that could evaluate any set of values for the design vector and return a competition score. The flow of the objective function is as follows:

1. Evaluate Weight.
2. Evaluate RAC.
3. Evaluate Drag.
4. Load Propulsion data.
5. Integrate flight path with performance code.
6. Determine if water dump is completed on the downwind leg. If not, reduce throttle on downwind leg and re-integrate. Repeat until dump completes on downwind leg.
7. Determine raw flight score.
8. Determine if airplane takes off in allowed distance. If not, penalize according to

$$p_{TO} = \frac{s_{TO} - s_{allow}}{100ft}$$

9. Determine if airplane completes the mission without exhausting the capacity of the battery pack. If

$$\text{not, penalize according to } p_{cap} = \frac{cap_{required} - cap_{available}}{100mAh}$$

10. Compute final objective function value, according to $f = score - p_{cap} - p_{TO}$.

Penalty methods were incorporated into the objective function to allow a bounded, but unconstrained, optimization method to be used, while allowing the optimizer to seek back into feasible space without restarting.

This objective function was optimized using the MATLAB optimization toolkit. All six continuous design variables were optimized for each propulsion system. By using an "all-else-optimal," rather than "all-else-equal" comparison method, the various propulsion systems, with their sometimes drastically different performance characteristics, could be fairly compared.

4.4 MDO Results

Once the optimization routine was finished, it became possible to make a decision on what propulsion system was to be used, as well as the general sizing of the airplane. In the process of optimizing over 50 propulsion combinations, the optimization code evaluated over 40,000 potential designs. The optimization was started from 3 different initial design points, each chosen as being likely to be feasible, yet substantially different from each other. Doing this helps ensure that any optimum found is global in nature.

4.4.1 General Trends

While optimizing, a few trends surfaced. First, the code tended to converge on moderate aspect ratios (~8) rather quickly. This was interpreted to be a result of the fact that the drag model considered the

tradeoff between increased parasite drag due to smaller Reynolds number and decreased induced drag because of increased aspect ratio. The rapid convergence was surprising since earlier sensitivity studies had shown parasite drag to be relatively unimportant. This phenomenon is most likely a result of the objective function being very well-behaved in this variable. Unsurprisingly, the optimization code immediately converged on a water weight of 8.8 pounds (4 liters). Another rapid convergence was in the area of fuselage thickness ratio. This variable converged to a value around 0.3 for almost all propulsion systems. The rest of the optimization evaluations were essentially spent minimizing the wing area and fuselage length. Additionally, the code spent several cycles converging to a minimum fuselage height that would allow the water to be dumped at full throttle. This resulted in a rather tall, thick fuselage pod.

4.4.2 Propulsion System Selection

The propulsion systems of all the high scoring designs were investigated for any common trends. The flight scores for the resulting 56 propulsion systems are shown in Fig. 4.3. Table 4.3 shows the characteristics of some of the highest scoring propulsion systems. All of the high scoring designs used Graupner 3300-7, Graupner 3300-7H or Graupner 3450-7 motors. It was decided to purchase the Graupner 3300-7H for testing since it slightly out-performed the other two motors. This motor is similar to the 3300-7 except that it is designed to be run at slightly higher voltages and it has an integrated cooling fan. Both of these qualities of the 3300-7H were seen as positives over the 3300-7 since the optimal battery packs were around 30 cells (above the recommended 20V operating voltage for the 3300-7) and because the motor would be run at full throttle for a majority of the flight. It was selected over the 3450-7 primarily on the basis of weight and size of the airplane. The 3300-7H is approximately two-thirds of the weight of the 3450-7. The optimal designs for the 3450-7 motors were typically larger than the optimal designs for the 3300-7. It was decided that a smaller airplane would make storing the airplane in the box easier, reduce actual materials costs and simplify construction.

The flight scores for a given motor, propeller and gearbox tended to increase as cell number was increased, up to the point of about 30 cells. All of the top propulsion systems used propellers that had pitch-to-diameter ratios around 0.7. The gearbox depended primarily on the motor and batteries used.

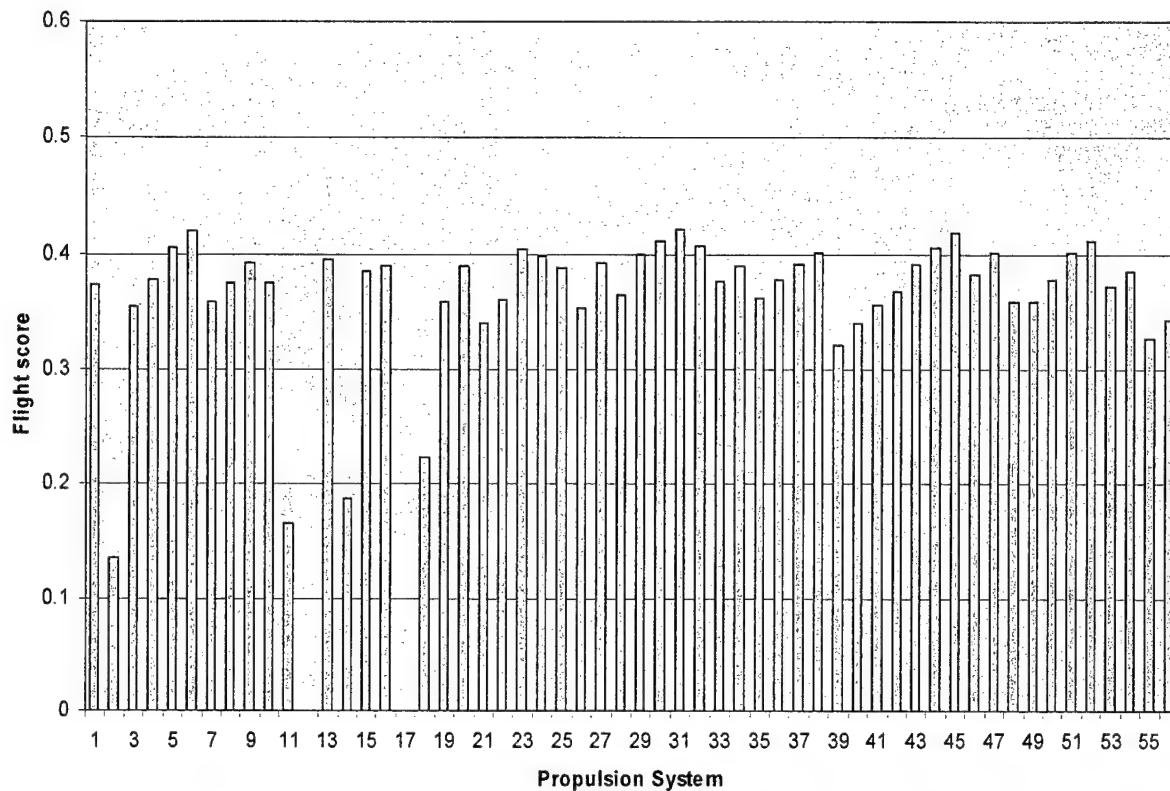


Fig. 4.3 Total Flight Score for each Propulsion System's Optimal Design

Table 4.3 Highest Scoring Propulsion Systems

Propulsion System #	Motor	Battery Type	Propeller	Gearbox
5	Graupner 3300-7H	28 CP-1300	18.5 x 12	3.0:1
6	Graupner 3300-7H	29 CP-1300	18.5 x 12	3.0:1
23	Graupner 3300-7H	21 CP-1700	18.5 x 12	2.0:1
30	Graupner 3300-7	29 CP-1300	18.5 x 12	3.0:1
31	Graupner 3300-7	30 CP-1300	18.5 x 12	3.0:1
32	Graupner 3450-7	25 CP-1300	18.5 x 12	2.0:1
44	Graupner 3450-7	27 CP-1300	20 x 13	2.5:1
45	Graupner 3450-7	28 CP-1300	20 x 13	2.5:1
52	Graupner 3450-7	30 CP-1300	17 x 11	2.0:1

4.4.3 Optimum Design

The optimum design produced by the code used propulsion system 6, with an aspect ratio of 8.36, and a wing area of 5.36 ft^2 . The optimum fuselage height was found to be 1.7 ft, with a pod thickness ratio of 0.36. The optimum airplane length was 4 ft (the lower bound specified for the optimizer). The full 8.8 lb. of water payload was found to be optimum.

This optimum was modified slightly to allow some safety margin, especially in the takeoff requirement, and to give more convenient dimensions for manufacturing. The final selected design uses propulsion system 6, which is a Graupner Ultra 3300-7H with a 3:1 gearing, turning a 18X12.5" RFM carbon folding propeller, and powered by 29 Sanyo CP1300SCR cells. The wing span was set at 7 ft and the wing chord at 10.25 inches. This resulted in a wing area of 6 ft^2 and an aspect ratio of 8.2. Fuselage height was selected to be 18 inches, with a thickness ratio for the fuselage pod of 0.35. Finally, the airplane length was set at 4 ft. These deviations resulted in a predicted competition score decrease of about 3%, but offered a higher degree of confidence in mission success in terms of energy and takeoff distance.

At this time the ability of the airplane to complete the Ferry mission was reevaluated. With the propulsion system selected by the optimization program, the airplane was unable to complete the Ferry mission. Due to this, a 16 x 17 RFM carbon folding propeller was selected for use only in the Ferry mission. This propeller provides sufficient takeoff thrust and run time to complete the Ferry mission as quickly as possible with the same motor, batteries and gearbox as is used for the Fire Bomber mission.

4.4.4 Sensitivity of Design Variables

To check whether the changes to the optimum design had shifted the airplane too far from the optimum, a sensitivity study was performed around the modified optimal design. The results of this study are presented in Fig. 4.4. The normalized score and parameter are normalized by the optimum airplane configuration in order to more clearly see the effects of each variable. Since the gradient of most of the variables was small, the design was considered to be very near optimum. The two variables with strong gradients were wing area and payload weight. Since the design payload weight is the maximum allowed this represents the optimum value of this variable. Decreasing wing area would increase the competition score, but at a risk of entering the infeasible zone since the airplane might fail to takeoff in 150 ft.

4.5 Stability and Control

The longitudinal, lateral and directional stability and control characteristics of the airplane were analyzed using a MATLAB™ code. This was done for the purpose of designing the empennage to provide adequate stability and control for all flight modes. Four separate flight configurations were considered; fully-loaded terminal, fully-loaded cruise, empty cruise, and empty terminal. Terminal flight phases are takeoff and landing. The empennage was sized as conventional horizontal and vertical stabilizing surfaces and then converted to the V-tail configuration.

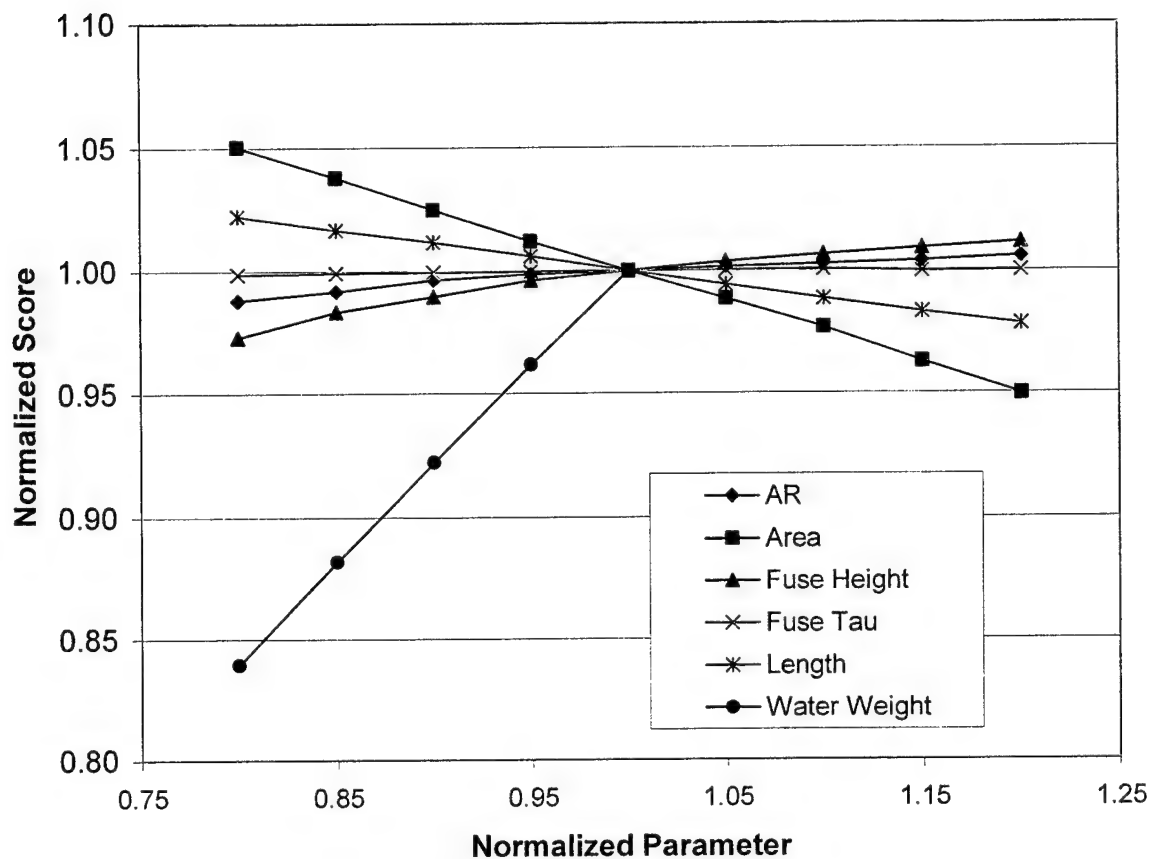


Fig. 4.4 Sensitivity Study of Final Design

4.5.1 Static Trim Analysis

The first step in stability and control analysis is to establish trim deflections during critical portions of flight. The estimated elevator trim during cruise is 2.5 degrees while the deflection required at stall is 9.5 degrees. The rudder and aileron trim for a 20 degree sideslip, an important estimation considering the high winds expected at the competition, was estimated to be 32.2 and 3.1 degrees, respectively.

4.5.2 Dynamic Stability Criteria

Except for the spiral mode, the other dynamic modes need to be convergent and under damped. As an example, the desired values in cruise for each of the modes are shown in Table 4.4 below. These values were taken from Nelson.⁶ Roll mode characteristics were not analyzed since they were deemed unimportant to the mission.

4.5.3 Dynamic Stability Analysis

The optimum design from the MDO code was modified to provide acceptable flight characteristics. The original sizes for the wing and fuselage were preserved, but the empennage surface area and moment arm were modified.

The process used with the MATLABTM stability and control code became an iteration of changing surface area, static margin and the moment arm in order to stabilize each mode. The longitudinal flying

Table 4.4 Desired Dynamic Stability Characteristics for Cruise

Mode	Minimum ζ	Maximum ζ	Minimum time to double amplitude (sec)
Phugoid	0	1	n/a
Short-Period	0.35	1.30	n/a
Dutch-Roll	0.19	1	n/a
Spiral	n/a	n/a	12

qualities are highly dependent on the static margin and empennage moment arm. Increasing the moment arm helps in damping the phugoid and short period modes. However a length constraint for the airplane was set by the dimensions of the box. The static margin was adjusted from 5% to 20% without much effect on the flight qualities. Therefore, the static margin was set to 10%.

The lateral and directional flying qualities also are determined by the tail surface sizing and the length of the moment arm. As the moment arm was increased, the Dutch roll became closer to being critically damped and the time to double amplitude of the spiral mode increased greatly. But again, the moment arm was constrained by the dimensions of the box.

4.5.4 Empennage and Control Surface Sizing

The sizing of the empennage does not depend just on what would produce the best stability and control derivatives. Other things that should be considered are the additional RAC from making the empennage too big or too long, the ability to fit the airplane in the box, the structural issues resulting from the tail being built in multiple pieces, and how difficult it is to build. The control surface sizes were set based on the team's experience.

4.5.4.1 Trade Studies

The larger the horizontal tail was the better the phugoid and short-period modes were. The horizontal tail span was limited to 25% of the wing span in order to avoid it being counted as a wing. For the modified optimum wingspan of 7.0 ft., the maximum projected span of the V-tail is 1.75 ft. Unlike the projected horizontal area, a larger vertical projected area does not yield the best performance. The best performance between the Dutch-roll and spiral modes was achieved with a vertical tail area of 1.1 ft².

4.5.4.2 Empennage Sizing Results

The size of the horizontal and vertical tails was settled at 1.3 ft² and 1.1 ft² respectively. The parameters for the standard tail converted to a V-tail are listed below. The formulas for converting a standard tail to a V-Tail, were taken from Mark Drela's reference on "Quick V-Tail Sizing".⁷

$$A_{v\text{-tail}} = A_{\text{vertical}} + A_{\text{horizontal}} \quad (5.1)$$

$$\text{V-tail Angle} = \text{Arctan}[\text{sqrt}(A_{\text{vertical}} / A_{\text{horizontal}})] \quad (5.2)$$

Table 4.5 Empennage Sizing Results

Surface area of Conventional Horizontal Tail	1.3 ft ²
Surface area of Conventional Vertical Tail	1.1 ft ²
Surface area of V-Tail	2.4 ft ²
Angle of each V-Tail surface from the horizontal	42.6°
Projected Tail Span	1.75 ft
Total Tail Span	2.38 ft
Tail Chord	1.00 ft

4.5.4 Stability and Control Predictions

Tables 4.6 through 4.10 present the results of the stability and control calculations. In those tables all angles are in radians, all rates are in radians/sec and all other parameters are dimensionless.

Table 4.6 Longitudinal Stability Coefficients for Empty Cruise

	X-force derivatives		Z-force derivatives		Pitching moment derivatives	
u	C_{xu}	0.0	C_{zu}	0.0000	C_{mu}	0.0000
α	$C_{x\alpha}$	0.5	$C_{z\alpha}$	6.5000	$C_{m\alpha}$	-0.5865
$\dot{\alpha}$	$C_{x\dot{\alpha}}$	0.0	$C_{z\dot{\alpha}}$	N/A	$C_{m\dot{\alpha}}$	-3.5573
q	C_{xq}	0.0	C_{zq}	N/A	C_{mq}	-9.5459
δ_e	$C_{x\delta_e}$	0.0	$C_{z\delta_e}$	0.3044	$C_{m\delta_e}$	-0.8523

Table 4.7 Longitudinal Stability Coefficients for Full Cruise

	X-force derivatives		Z-force derivatives		Pitching moment derivatives	
u	C_{xu}	0.0	C_{zu}	0.0000	C_{mu}	0.0000
α	$C_{x\alpha}$	0.5	$C_{z\alpha}$	6.5000	$C_{m\alpha}$	-0.5865
$\dot{\alpha}$	$C_{x\dot{\alpha}}$	0.0	$C_{z\dot{\alpha}}$	N/A	$C_{m\dot{\alpha}}$	-3.5573
q	C_{xq}	0.0	C_{zq}	N/A	C_{mq}	-9.5459
δ_e	$C_{x\delta_e}$	0.0	$C_{z\delta_e}$	0.3044	$C_{m\delta_e}$	-0.8523

Table 4.8 Lateral and directional stability coefficients for Empty Cruise

	Y-force derivatives		Yawing moment derivatives		Rolling moment derivatives	
β	$C_{y\beta}$	-0.5570	$C_{n\beta}$	0.1906	$C_{l\beta}$	-0.0004
p	C_{yp}	0.0000	C_{np}	-0.0359	C_{lp}	-0.9015
r	C_{yr}	0.3811	C_{nr}	-0.1302	C_{lr}	0.0990
δ_a	$C_{y\delta_a}$	0.0000	$C_{n\delta_a}$	0.1938	$C_{l\delta_a}$	0.1938
δ_r	$C_{y\delta_r}$	0.2300	$C_{n\delta_r}$	-0.093	$C_{l\delta_r}$	0.0164

Table 4.9 Lateral and directional stability coefficients for Full Cruise

Y-force derivatives			Yawing moment derivatives		Rolling moment derivatives	
β	$C_{y\beta}$	-0.5570	$C_{n\beta}$	0.1906	$C_{l\beta}$	-0.0040
p	C_{yp}	0.0000	C_{np}	-0.0682	C_{lp}	-0.9015
r	C_{yr}	0.3811	C_{nr}	-0.1302	C_{lr}	0.1636
δ_a	$C_{y\delta}$	0.0000	$C_{n\delta a}$	0.0264	$C_{l\delta a}$	0.1938
δ_r	$C_{y\delta r}$	0.2300	$C_{n\delta r}$	-0.0953	$C_{l\delta r}$	0.0164

Table 4.10 Dynamic Stability Characteristics

	ζ	ω_d (rad/sec)	Period (sec)	Time To Double or Half Amplitude (sec)	Handling Quality Level
Short Period					
Fully Loaded Cruise	0.70	7.75	0.81	0.13	1
Empty Cruise	0.86	10.10	0.62	0.08	1
Fully Loaded Terminal	0.68	3.50	1.80	0.29	1
Empty Terminal	0.84	4.49	1.40	0.18	1
Phugoid					
Fully Loaded Cruise	0.04	0.52	12.01	35.72	2
Empty Cruise	0.11	0.46	13.78	13.72	1
Fully Loaded Terminal	-0.05	1.16	5.42	11.93	N/A
Empty Terminal	-0.04	1.02	6.16	17.95	N/A
Spiral					
Fully Loaded Cruise	N/A	N/A	N/A	8.52	3
Empty Cruise	N/A	N/A	N/A	13.80	1
Fully Loaded Terminal	N/A	N/A	N/A	1.08	N/A
Empty Terminal	N/A	N/A	N/A	1.57	N/A
Dutch Roll					
Fully Loaded Cruise	0.21	9.73	0.65	0.34	1
Empty Cruise	0.22	9.67	0.65	0.33	1
Fully Loaded Terminal	0.53	5.83	1.08	0.22	1
Empty Terminal	0.35	4.52	1.39	0.44	1

4.6 Preliminary Design Results

The airplane was sized based on a multi-disciplinary optimization and stability and control analysis. Designing the airplane in this way resulted in maximum performance while maintaining excellent flying qualities.

4.6.1 Component Sizing

Table 4.11 presents the final component sizes for the Fiberglass Overcast.

Table 4.11 Final Component Sizes

Parameter	Value
Wing span	84 in
Wing chord	10.25 in
Aileron span	21 in
Aileron chord	2.5625 in
V-tail span	21 in
V-tail height	9.55 in
Fuselage length	51 in
Fuselage height	16 in
Fuselage width	4.2 in
Tank maximum height	14.5 in
Tank maximum length	5.4 in
Tank maximum width	4.2 in
Motor	Graupner 3300-7H
Gear ratio	3.0 to 1
Propeller diameter	18.5 in
Propeller pitch	12 in
Battery cells	29
Battery pack weight	2.25 lb
Ruddervator span	12 in
Ruddervator chord	3.6 in
Wing Aspect Ratio	8.2
Wing Taper Ratio	1.0
Empennage Aspect Ratio (Horizontal Projection)	1.75
Empennage Taper Ratio	1.0

4.6.2 Airplane Performance Predictions

Various airplane performance parameters were predicted for the airplane in its three main configurations. The first is when the airplane is carrying the full 4 liters of water for the Fire Bomber mission, the second is after the airplane releases its water payload, and the last is for the airplane in the Ferry mission with no payload. The predictions are shown in Table 4.12.

Table 4.12 Airplane Performance Predictions

Parameter	Fire Bomber Loaded	Fire Bomber Unloaded	Ferry
Empty weight	10.0 lb	10.0 lb	10.0 lb
Gross takeoff weight	18.8 lb	10.0 lb	10.0 lb
Takeoff distance	135 ft	N/A	100 ft
Maximum L/D	12	12	12
Cruise L/D	9	9	9
Maximum climb rate	500 ft/min	1500 ft/min	1300 ft/min
Turn radius	36 ft	29 ft	34 ft
$C_{L,max}$	1.3	1.3	1.3
Horizontal tail volume coefficient	0.61	0.61	0.61
Vertical tail volume coefficient	0.07	0.07	0.07
Turn load factor	2.5	4	6
Turn rate	80 deg/s	119 deg/s	136 deg/s
Stall speed	45 ft/s	32 ft/s	32 ft/s
Maximum speed	78 ft/s	83 ft/s	110 ft/s
Cruise speed	71 ft/s	75 ft/s	100 ft/s
Maximum battery current	26.0 A	26.0 A	24.2 A
Static thrust	9.2 lb	9.2 lb	5.0 lb

4.6.3 Mission Performance Predictions

Mission times, takeoff distances and energy requirements were predicted for the airplane in each of the missions for still air and for a 30 mph cross wind, the worst case possible before the contest is delayed. Table 4.11 summarizes the results of these predictions as determined by the performance and takeoff codes.

Table 4.11 Mission Performance Predictions

Mission Parameter	Fire Bomber Mission (No wind)	Fire Bomber Mission (30 mph crosswind)	Ferry Mission (No wind)	Ferry Mission (30 mph crosswind)
Takeoff distance	105 ft	105 ft	33 ft	33 ft
Time to takeoff	4.5 s	4.5 s	2 s	2 s
Time to climb out	7.1 s	7.1 s	9 s	9 s
Time to turn 180 degrees	3.5 s	3.5 s	2.5 s	2.5 s
Time to fly downwind leg	13.2 s	17.8 s	9.5 s	14.3 s
Time to release water payload	18 s	18 s	N/A	N/A
Time to descend and land	3.2 s	3.2 s	2.3 s	2.3 s
Time on the ground	40 s	40 s	N/A	N/A
Time to fly upwind leg	N/A	N/A	9.5 s	14.3 s
Total mission time	130 s	143 s	120 s	157 s
Energy required for takeoff	40 mAh	40 mAh	15 mAh	15 mAh
Energy required for climb out	60 mAh	70 mAh	60 mAh	73 mAh
Energy required to turn 180 degrees	30 mAh	30 mAh	22 mAh	22 mAh
Energy required in downwind leg	110 mAh	145 mAh	88 mAh	90 mAh
Energy required in upwind leg	N/A	N/A	88 mAh	90 mAh
Energy required to descend and land	30 mAh	40 mAh	27 mAh	40 mAh
Energy required for complete mission	720 mAh	830 mAh	1070 mAh	1110 mAh

5.0 Detail Design

At this stage in the design process, the actual airplane components were designed and/or selected and integrated and the required drawings were made using a solid modeling program.

5.1 Component Selection and Systems Architecture

5.1.1 Wing Aerodynamic Design

5.1.1.1 Airfoil Selection

The airplane is required to operate over a large range of angle of attack because of the difference in weight between the two missions as well as the maneuvers required during each mission. Furthermore, because of the takeoff distance constraint, a minimum c_{lmax} of 1.4 was required. A class of airfoils with low drag over a wide range of angles of attack was selected for analysis. Figure 5.1 shows the drag polars for the airfoils considered at a Reynold's number of 350,000.⁸ All of these airfoils have a c_{lmax} between 1.3 and 1.5. The SD7062 has a low minimum drag coefficient and a high c_{lmax} . However the absence of a drag bucket ruled out that airfoil. The FX63-137 has a large drag bucket at low drag coefficient and a very high c_{lmax} . The high thickness ratio of the section (approximately 14%) and the sharp increase in drag at low c_l made it a poor choice for this application. The high thickness would result in a heavier wing and the sharp drag increase was a concern for cruise segments of the missions. The S2091 has the lowest drag in the c_l range that the airplane would be operating in for the greatest amount of time, as predicted by the performance code. In addition, the S2091 is a thin airfoil with a thickness ratio of approximately 10%. The SG6042 is a similar airfoil in terms of thickness and drag characteristics; however the S2091 exhibited slightly lower drag around a c_l of 0.5. The S2091 was ultimately chosen because the airplane was projected to be flying near that lift coefficient and would therefore offer a slight advantage.

5.1.1.2 Wing Twist

The required twist of the wing was studied using LinAir.⁹ A three-element panel was used to model linear twist from the root to the tip. The results of this analysis, in terms of Oswald's efficiency factor, e , are presented in Fig 5.2 and show that the optimal twist for this application was approximately 0.5 degrees of washout. However, by increasing the washout beyond 0.5 degrees the wing experiences a sharp reduction in efficiency. Furthermore, constructing a wing with 0.5 degrees of twist, over approximately 42 inches of span, is very difficult given the team's building tolerances. Therefore zero degrees of twist was chosen with the possibility of using the ailerons to add the small amount of twist required to achieve the optimal efficiency for the wing.

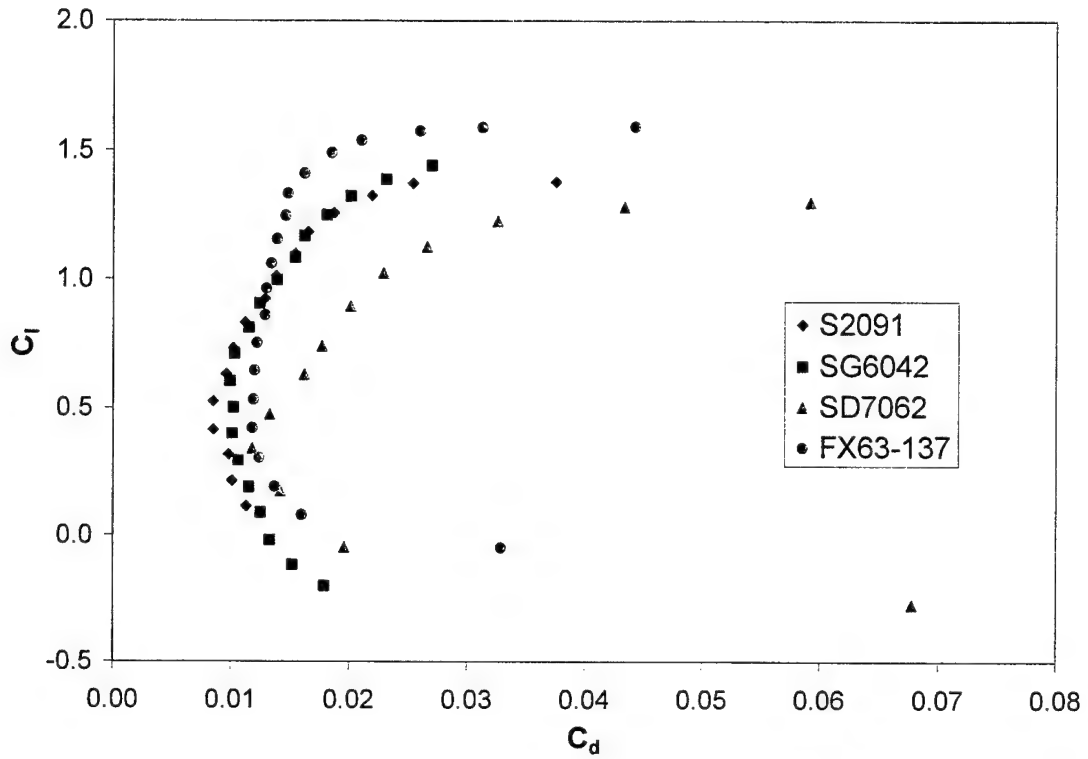


Figure 5.1 Experimental Drag Polars for the Candidate Airfoils

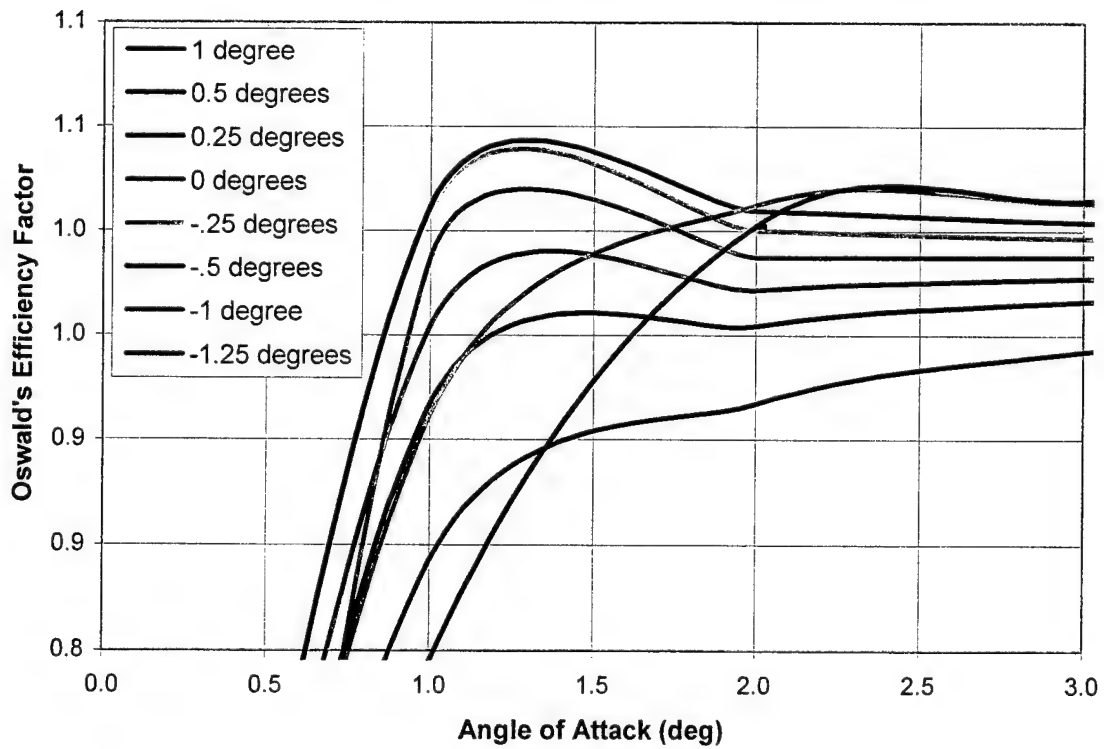


Fig. 5.2 Oswald's Efficiency Factor vs. Angle of Attack with Varying Washout

5.1.2 Avionics System

The components of the avionics system were selected and their positions within the airplane were determined. The avionics system consists of the motor controller, radio receiver, servos and telemetry system.

5.1.2.1 Servo Selection and Placement and the Tail-Wheel Steering Mechanism

The servos for the ailerons were mounted in the rib bays that were centered on the control surfaces. They were placed as close to the control surfaces as possible to keep the pushrods short. The ruddervator servos were placed in the first rib bay from the fuselage centerline in the detachable V-tail surfaces. A pull-pull spring system was set up that allowed the tail wheel to be steered by the ruddervator servos. If both servos move in the same direction as in the case of an elevator input, then there is no net effect on the tail wheel. If the servos move in opposite directions, then the springs turn the tail wheel in the direction of the rudder input. This eliminated the need for an extra tail wheel steering servo and lowered the RAC.

5.1.2.2 Telemetry System

In order to facilitate the quick collection of flight testing data and to monitor system performance during the competition, a telemetry system was developed, tested and integrated into the airplane. The system monitors propeller RPM, battery current, battery voltage, altitude and airspeed. A pitot-static tube is mounted at the tip of the left wing to take airspeed measurements. A magnet is mounted on the prop hub and a sensor is mounted on the firewall to measure RPM. The transmitter antenna and power source are mounted on the rear of the water tank and housed in the airfoil fairing.

5.1.2.3 Electronic Speed Control and Radios

The Electronic Speed Control (ESC), an Astroflight™ 204D, is mounted directly behind the motor in the nose fairing. The receiver and receiver battery are mounted behind the water tank near the telemetry system. The receiver is a Futaba R148DP PCM, and the radio transmitter used is a Futaba 8UHFS. An 750 mAh lithium polymer cell is used to power the receiver. This was selected to save weight over a NiCd receiver pack.

5.1.3 Propulsion System

The propulsion system, selected in preliminary design, was finalized at this stage. This system consisted of a Graupner Ultra 3300-7H, geared 3.0:1, with an 18.5" x 12" folding carbon fiber propeller. The Ferry mission uses the identical power system with a 15.5" x 10" folding carbon fiber propeller. A 50mm diameter Aeronaut spinner and a hub with 52 mm spacing between the blade hinges were selected for their light weight and adjustability.

5.1.4 Structural System

The structure of the Fiberglass Overcast was created to efficiently transfer the primary loads experienced during operation. All of the major components were tied to a carbon fiber spine that ran the length of the fuselage. The spine was sized to provide adequate strength and stiffness with a minimum of

weight. The method for integrating the tank, landing gear and wing joiner tube with the spine were also determined.

5.1.4.1 Fuselage Spine Sizing

A carbon tube that went from the nose of the airplane to the tail of the airplane, was used for the fuselage spine. It was sized so that the maximum angular deflection would not exceed three degrees at the tail in a 5g turn and so that maximum twist would not exceed 5 degrees with both ruddervators fully deflected in opposite directions at cruise speed. The wrapped carbon fiber tube selected was 0.75" diameter with a 0.035" wall thickness. This tube weighed approximately one ounce per foot for a total weight of about four ounces.

5.1.4.2 Spar and D-tube Sizing

The main wing structure was designed by assuming flight loads and by using either a deflection limited criterion or an ultimate failure safety criterion. The main wing spar was designed for a 5g loading with a ultimate safety factor of 2. The carbon fiber spar cap size that satisfied this criterion was 0.5 inches wide by 0.028 inches thick. This spar size also satisfied the upright and inverted tip testing loads required during technical inspection.

To size the carbon fiber D-tube, which handles the wing torsional loads, the moment generated by an aileron deflection of 45 degrees was used. At cruise speed, an aileron deflection of 45 degrees results in approximately 5 ft-lb of torque. Using an ultimate safety factor of 1.5 the carbon fiber D-tube thickness was required to be 0.009", that is approximately 2 layers of woven carbon fiber cloth.

5.1.5 Water Storage and Dump System

The major part of the fuselage is the water tank that occupies the front portion of the NACA 0035 fuselage pod. The cross section of the tank was selected so that the center of gravity of the payload is located at the quarter chord of the fuselage pod. Since the quarter chord is also the center of gravity of the airplane, it ensures that the longitudinal center of gravity does not shift during the dump phase of the Fire Bomber mission. The rear wall of the tank is flat surface that cuts the NACA 0035 at 45% of its chord. The remaining 55% of the NACA 0035 is a fairing that is attached to the rear wall of the tank to complete the fuselage. The tank was designed to be easily faired and tall enough to provide adequate draining pressure. The bottom of the tank was lofted to smoothly transition from the basic tank cross section to the nozzle.

The water release system consists of the venting/filling mechanism, tank, nozzle and release valve. The filling and venting mechanism is simply a pair of doors hinged inside the top of the tank. A float is attached at the end of each door so that when the tank is filled buoyancy keeps the doors closed. When the valve is opened the water will begin to drain and the doors will open to provide venting and capture dynamic pressure from the free stream through a NACA type inlet formed by the doors and short walls formed on the top of the inside of the tank. The doors have an auxiliary latch that keeps them closed when not operating in Fire Bomber mode. The nozzle was chosen based upon experimental data, discussed in Section 7.1, and the walls were designed by revolving a hyperbolic curve about the central

axis. Water is released by a ball valve manufactured using a 3D rapid prototyping machine. The valve is actuated by a servo connected directly to the valve stem. A drawing of the ball valve can be seen in the drawing package in Section 5.3.

5.1.6 Landing Gear

Efficient ground operations can have a significant effect on the mission time and hence the final competition score of the airplane. For this reason, properly designed landing gear was critical to the performance of the airplane. The landing gear must be able to absorb the impact of landing an 18 pound airplane as well provide good maneuverability and stability, and do so with minimal weight.

The unconventional fuselage shape selected for this airplane greatly influenced the landing gear selection. The three main types of landing gear considered were tricycle, taildragger and mono-wheel arrangements. Regardless of configuration, the landing gear must achieve a balance between adequate damping to prevent the airplane from bouncing back into the air upon contact with the runway, and adequate stiffness to prevent the fuselage from contacting the runway.

A tricycle gear arrangement was eliminated from consideration due to the large vertical displacement of the nose of the airplane from the runway and its small volume. This arrangement would require additional structure ahead of the main fuselage and an excessively long nose wheel strut. While the tail dragger arrangement solved this problem, it had other disadvantages. Specifically, the main gear had to be offset laterally from the narrow fuselage to provide stable ground handling. This required the use of a more complex damping system incorporating heavy shock absorbers protruding from the fuselage.

In order to avoid such complexity and weight, a mono-wheel arrangement with wingtip skids was selected. This arrangement allows the main wheel to be faired by the main fuselage, leaving no landing gear structure in the flow besides the tire. Ground handling is achieved through the use of a steerable tail wheel, and aerodynamic control from the rudder. The use of wingtip skids prevents the airplane from tipping over until sufficient aerodynamic control is achieved to keep the wings level. A single Robart Robostrut™ was selected as the shock absorber.

The Robostrut™ was inserted into a 0.5" carbon tube that transfers the landing loads from the landing gear to the fuselage spine. The carbon tube was designed so that the tracking angle of the monowheel can be adjusted, prior to flight, for crosswind landings. This reduces the risk of ground loops that can cause serious structural damage to the airplane.

5.2 Final Airplane Specifications

The final specifications for the airplane are given in the following tables. Table 5.1 shows the specifications for the airplane that will be posted in the teams pit area as required by the contest rules. Table 5.2 is a breakdown of the weight and balance for the airplane. The datum point is located at the projection of the tip of the spinner onto the ground plane. The X direction is positive aft, Z is positive up and Y is positive out the right wing. Table 5.3 is the final RAC computation based on the weight and final dimensions of the design.

Table 5.1 Airplane Specification Sheet

University of Illinois - Fiberglass Overcast	
Geometry	
Span	7.00 ft
Length	4.25 ft
Height	1.50 ft
Wing Area	6.00 ft ²
Wing Aspect Ratio	8.17
Projected Horizontal Area	1.75 ft ²
Projected Vertical Area	0.80 ft ²
Horizontal Stabilizer Volume	4.38 ft ³
Elevator Volume	1.58 ft ³
Vertical Stabilizer Volume	2.00 ft ³
Rudder Volume	0.72 ft ³
Aileron Volume	2.12 ft ³
Wing Airfoil	S2091
Empennage Airfoil	NACA0009
Performance	
C _l max	1.3
L/D max	12
Maximum Rate of Climb	500 ft/min at gross weight 1500 ft/min at empty weight
Stall Speed at Gross Weight	45 ft/s
Stall Speed at Empty Weight	32 ft/s
Maximum Speed	110 ft/s (Ferry mission)
Take-off Field Length Empty Weight	100 ft (Ferry Mission)
Take-off Field Length Gross Weight	135 ft
Weight Statement	
Airframe Weight	5.25 lb
Propulsion System Weight	4.00 lb
Control System Weight	0.50 lb
Payload System Weight	0.25 lb
Payload Weight	8.80 lb
Empty Weight	10.0 lb
Gross Weight	18.8 lb
Systems	
Radio	Futaba 8UHFS
Receiver	Futaba R148DP PCM 72MHz High
Wing Servos	2 - Hitec HS-81S
Empennage Servos	2 - Hobbico CS-12MG
Payload Release Servo	Hitec HS-81S
Battery Configuration	29 Sanyo CP-1300SCR cells, arranged 2 high by 3 wide by 5 deep w/ one corner
Motor	Graupner 3300-7H
Gearbox	Model Motors 3.0:1 Inner Driven
Propellers (nominal)	RFM 18.5x12 folding carbon, RFM 16x17 folding carbon

Table 5.2 Weight and Balance Sheet

Component	Weight (oz)	X C.G. Location	Y C.G. location	Z C.G. location
Wing				
Wing Spar	7.6	12.0	0.0	13.0
Wing Joiner Tube	2.0	12.0	0.0	13.0
Wing D-tube	4.2	10.5	0.0	13.0
Wing Ribs	2.0	14.0	0.0	13.0
Right Aileron	1.7	18.0	31.5	13.0
Left Aileron	1.7	18.0	-31.5	13.0
Wing Servos	2.5	15.0	0.0	13.0
Wing Tip Skids	1.5	12.0	0.0	6.0
Pilot Static Tube	1.0	11.0	42.0	13.0
Empennage				
Empennage Spars	1.7	42.0	0.0	17.0
Empennage Ribs	1.0	44.0	0.0	17.0
Rudder/Vators	0.7	49.0	0.0	17.0
Empennage Servos	2.0	46.0	0.0	14.0
Empennage D-tubes	2.6	40.5	0.0	17.0
Empennage Joiner Tubes	1.0	42.0	0.0	14.0
Drivetrain				
Grapple 3600 ZH	18.9	4.0	0.1	13.5
Model Motors 30:1 Gearbox	2.5	2.0	0.0	13.5
18" 5" x 12" RFM Carbon Folding Propeller	2.3	1.0	0.0	13.5
Aerofair Spinner and hub	0.8	1.0	0.0	13.5
29 CPH 300SCR Cells	36.2	5.0	0.0	10.5
Electronics				
Astroflight 2040 ESC	1.0	7.0	0.0	13.0
Receiver	1.0	15.0	1.0	14.0
Receiver Battery	1.5	15	-1.0	14.0
V-tail Mixer	0.3	17.0	1.0	12.0
Pitch Gyro	1.0	15.0	-1.0	12.0
Water Release Servo	1.0	11.0	0.0	3.5
Landing Gear				
Robart Robostrut	8.0	9.0	0.0	4.0
Main Wheel	2.0	9.0	0.0	1.8
Fuselage Spine	4.0	26.0	0.0	12.0
Payload Equipment				
Water Release Valve	1.5	12.0	0.0	4.0
Water Tank	12.0	11.7	0.0	10.0
Miscellaneous Structures				
Firewall	2.0	2.0	0.0	11.0
Fuselage Bulkhead 1	1.5	5.5	0.0	11.0
Fuselage Bulkhead 2	1.5	9.0	0.0	11.0
Nose Skins	4.0	5.5	0.0	11.5
Water Tank Cap	2.0	11.7	0.0	18.0

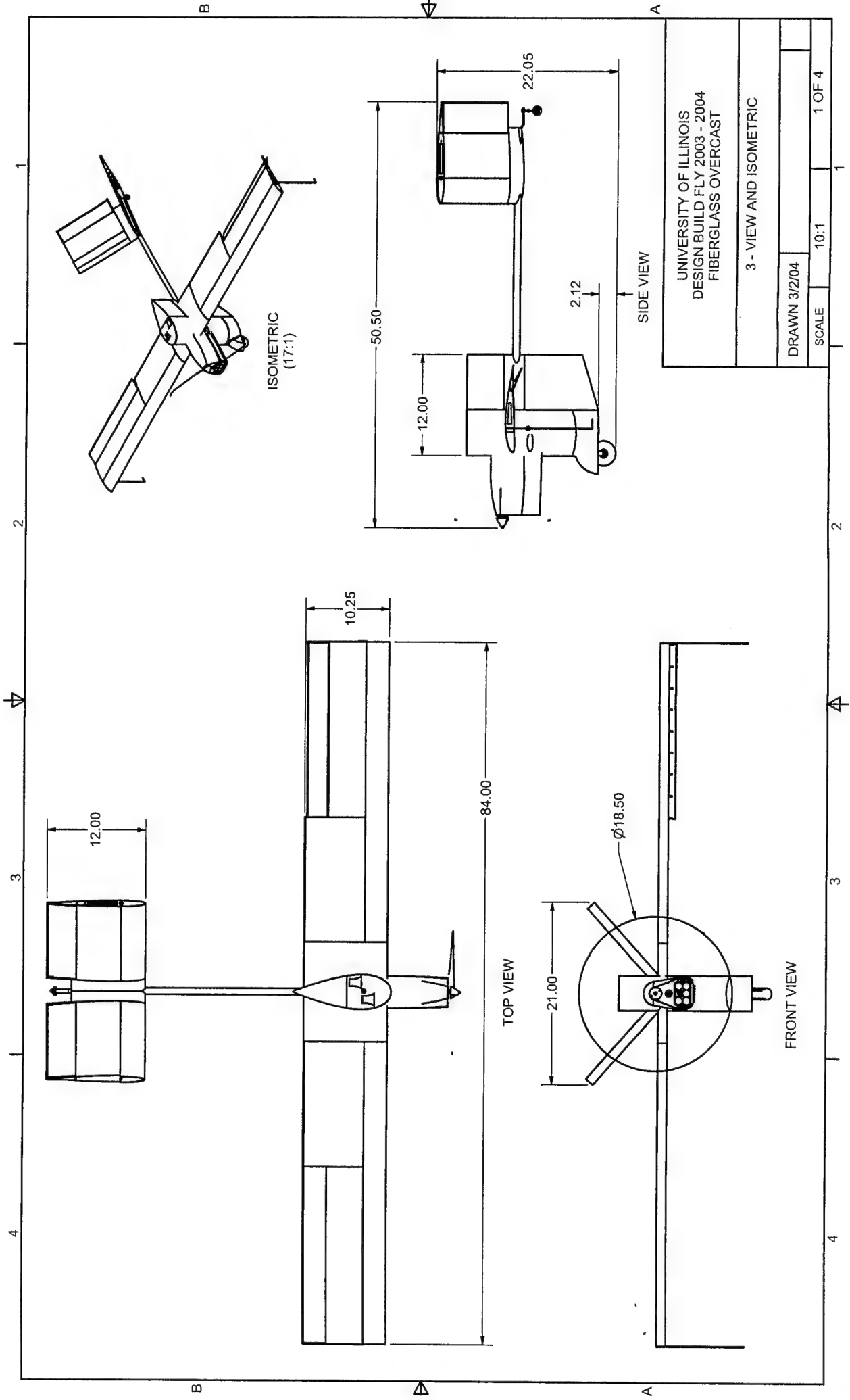
Filling Ports and Inlets	1.0	11.7	0.0	18.0
Wheel Pant/Lower Fuselage	1.0	10.5	0.0	4.0
Fuselage Rear Shell	6.0	18.0	0.0	10.0
Empennage Attachment Block	4.0	44.0	0.0	12.0
Tail Wheel Assembly	2.3	48.0	0.0	10.5
Telemetry				
Telemetry Electronics	6.0	15.0	-1.0	8.0
Payload				
Water Payload	141.1	11.7	0.0	10.0
Total w/o Payload	158.5	12.4	0.2	11.2
Total w/ Payload	299.6	12.1	0.1	10.6

Table 5.3 Rated Airplane Cost

Category	Parameter	Value	Computation	Cost (\$)
MEW	Empty Weight (lb)	10	MEW * 300(\$/lb)	3000
REP	# of Engines	1	[1 + 0.25(# engines-1)] * Total Battery Weight (lb) * 1500 (\$/lb)	3375
	Total Battery Weight (lb)	2.25		
MFHR				(Hrs)
WBS 1.0 Wings	Wing Span (ft)	7	10 hr/ft^2 * Wing Span (ft) * Wing Chord (ft) * # of Wings	59.792
	Wing Chord (ft)	0.854		
	# of Wings	1		
	Control Function Multiplier	1	5 hr * Control Function Multiplier	5
WBS 2.0 Fuselage	Body Length (ft)	4.25	20 hr/ft^3 * Body Length (ft) * Body Width (ft) * Body Height (ft)	44.625
	Body Width (ft)	0.35		
	Body Height (ft)	1.5		
WBS 3.0 Empennage	# of Vertical Surfaces without Control	1	5 hr * # of Vertical Surfaces without Control	5
	# of Vertical Surfaces with Control	0	10 hr * # of Vertical Surfaces with Control	0
	# of Horizontal Surfaces	1	10 hr * # of Horizontal Surfaces	10
WBS 4.0 Flight Systems	# of Servos or Motor Controllers	6	5 hr * # of Servos or Motor Controllers	30
Total MFHR (hr) = Σ[WBS 1.0 Wing (hr) + WBS 2.0 Fuselage (hr) + WBS 3.0 Empennage (hr) + WBS 4.0 Flight Systems (hr)]		154.417	20 (\$/hr) * MFHR (hr)	3088
RAC		[MEW (\$) + REP (\$) + MFHR (\$)] / \$1000		9.463

5.3 Drawing Package

Figures 5.3 through 5.6 are the detailed drawings of the Fiberglass Overcast.



UNIVERSITY OF ILLINOIS DESIGN BUILD FLY 2003 - 2004 FIBERGLASS OVERCAST			
3 - VIEW AND ISOMETRIC			
DRAWN 3/2/04			
SCALE	10:1		1 OF 4

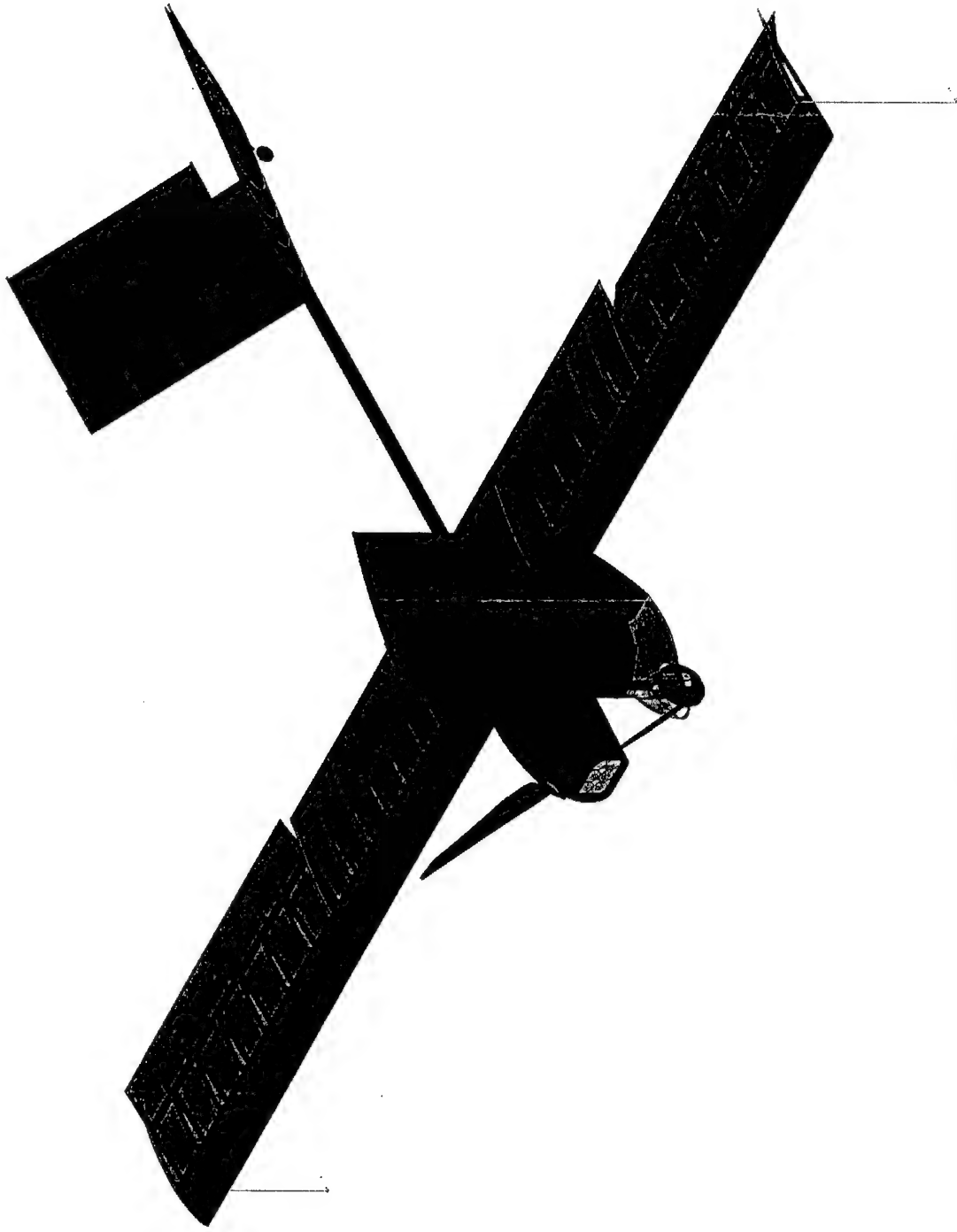
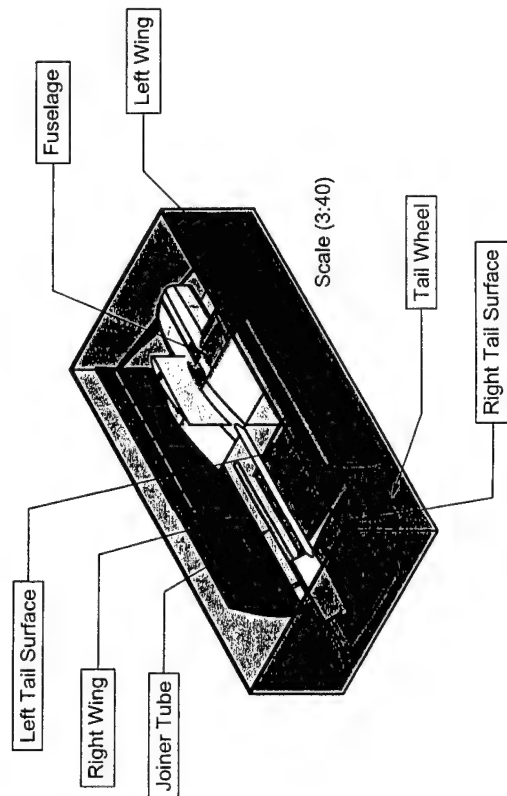
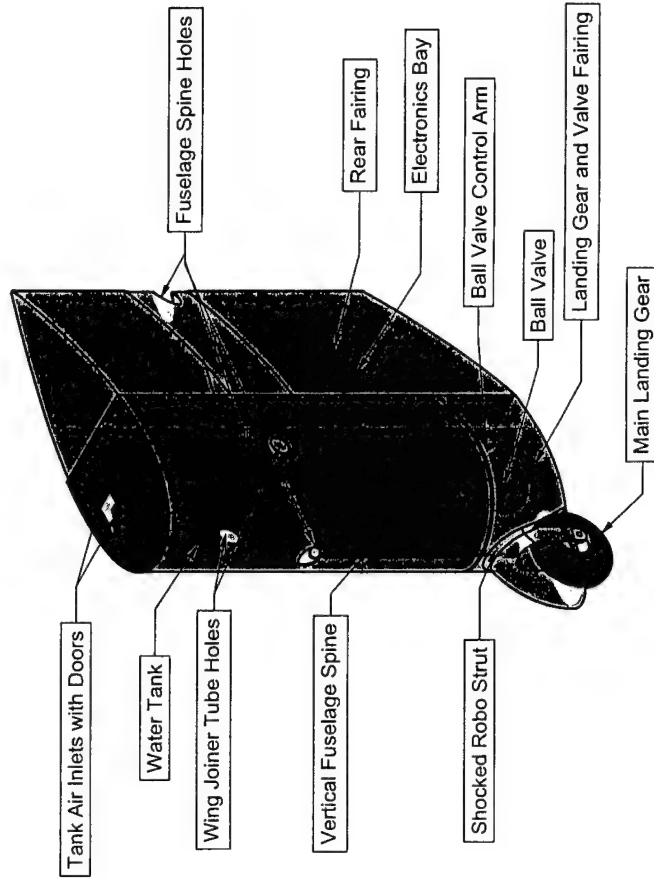
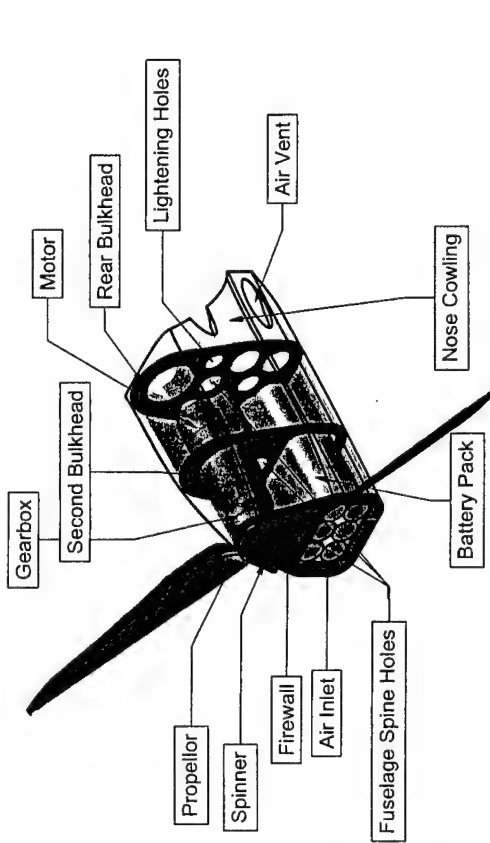


Fig. 5.4 Isometric View of the Fiberglass Overcast

1 2 3 4



DRAWN	3/3/2004	TITLE	Fig. 5.6 - Nose Assembly, Fuselage Pod & Plane in Box
CHECKED		SIZE	B
QA		DWG NO	
MFG		SCALE	1:2
APPROVED		REV	
		SHEET	1 OF 1

1 2 3 4

6.0 Manufacturing Plan

The manufacturing process and material selection were major concerns throughout the design of the airplane. It was important that the airplane be built in a timely manner with affordable materials that the team has experience working with. Keeping the weight as low as possible was also a major concern in choosing the materials and processes for constructing various components. A manufacturing plan was developed to obtain these goals through the use of figures of merit and scheduling.

6.1 Figures of Merit

Figures of merit were used to assist in the selection of materials and manufacturing processes for the various airplane components. The figures of merit were used to eliminate manufacturing processes and materials that are expensive, time consuming and add too much weight. Weight factors were applied to the figures of merit based upon their relative importance to mission performance, construction time and construction quality. The following figures of merit were considered:

6.1.1 Strength to Weight Ratio

One of the primary concerns for the construction of the competition airplane was building at or under the predicted weight. To do this the materials and process selected for each component had to provide adequate strength at as low a weight as possible. Materials and processes with low, average, and high strength to weight ratios received a score of -1, 0, and 1 respectively. This figure of merit had a weight factor of 3 applied to it due to its strong effect on the performance of the airplane.

6.1.2 Skill Level Required

In order to construct a high quality competition airplane, the materials and processes used to construct the components had to be within the skills of the team. A skills matrix for the team is shown in Table 6.1. The number of people that have experience with a given manufacturing technique are shown. If more than 4 people have experience with a given technique it received a score of 1, if 2 or 3 people have experience it received a score of 0, and if only one person or less has experience with a technique it received a score of -1. For each manufacturing process considered, the FOMs for the required building techniques involved in that process are averaged to obtain an overall FOM. Skill level required was given a weight factor of 2 since it influences the construction time and final quality of the airplane.

Table 6.1 Skill Matrix

Skill	Wood Working	Monokote Covering	Foam Hotwiring	CNC Operation	Rapid Prototype Operation	Vacuum Bagging	Lost Foam Composite Construction	RC Modeling Experience	Soldering and Electronics Experience	Metal Working Experience	Mold Making
Number of Personnel with Experience	8	5	5	3	1	5	1	6	5	3	1
FOM Score	1	1	1	0	-1	1	-1	1	1	0	-1

6.1.3 Actual Cost

Another important factor in selecting the materials and manufacturing processes was the actual cost to construct the various components. The team had a limited budget to work with, so it was important to be able to construct the airplane at a reasonable cost. If the manufacturing process or material required little cost it was assigned a score of 1, if the process or material was within our budget, but expensive, a score of 0 was assigned, and if the manufacturing process or material was considered out of our budget a score of -1 was assigned. The actual cost figure of merit was given a weight factor of 1 since it has little impact on the construction time or quality of the finished airplane.

6.1.4 Time Required

The limited time frame for the design and construction of the competition airplane necessitated that the manufacturing processes be efficient and well planned. Due to this constraint, any process that was projected to take less than 20 man-hours received a score of 1. A process that was estimated to take between 20 and 40 man-hours to complete received a score 0, and a process that was projected to take longer than 40 man-hours to complete received a score of -1. This figure of merit was given a weight factor of 2 due because of the limited time available.

6.1.5 Material Availability

Another factor in choosing the manufacturing process for various components was the availability of materials. If the materials were already available to the team with no lead time then a score of 1 was assigned. If the lead time for the materials was on the order of one week then the process received a score of 0. A process that required materials which had an extended acquisition time received a score of -1. Material availability was given a weight factor of 1 because it has little impact on the construction time and quality of the airplane.

6.1.6 Component Durability

The durability of the components resulting from a particular manufacturing process was selected as a final figure of merit. Manufacturing processes that result in durable components received a score of 1, processes that produce components that will wear out beyond the estimated life of the airplane received a score of 0, and processes that result in components with limited life received a score of -1. Component durability was given a weight factor of 2 due to its impact on the survivability of the airplane.

6.2 Investigated Manufacturing Processes

For each major airplane component, a number of manufacturing processes were investigated. The figures of merit detailed above were used to objectively select the materials and manufacturing processes for each component.

6.2.1 Wing

For the wing there were three main manufacturing processes considered. The first was a traditional balsa built up structure with either a spruce or carbon-fiber spar. The open rib and spar structure would then be covered with Monokote™. The next method was bagging composite skins on a foam core. Fiberglass cloth would be used for torsional stiffness and surface finish and unidirectional

carbon fiber cloth would be used for bending stiffness. The last method considered was a hybrid method, utilizing a carbon fiber spar, a leading edge carbon fiber D-tube and a traditional built up structure behind the spar covered with Monokote™.

Another important component of any wing design is the method of joining to the wings to the fuselage. The use of a joiner tube was decided on early in the design for its simplicity and availability. The materials that were considered for the tube were aluminum, carbon fiber and steel.

6.2.2 Empennage

The methods investigated for constructing the empennage surfaces were the same as those investigated for the wing. A method of attaching the empennage to the remainder of the airplane had to be chosen as well. In order for the airplane to fit into the box it was necessary for the empennage surfaces to detach. The methods investigated for this attachment were: having the surfaces slide on either a carbon or aluminum joiner tube in a manner similar to the wings, making the portion of the tail boom with the empennage attached removable, or having a telescoping tailboom.

6.2.3 Fuselage

Several methods were investigated for construction of the main fuselage structure. The first method was a traditional fuselage built up from plywood and balsa, covered with Monokote™. This structure would then hold the water tank and other systems. The next method investigated was lost foam composite construction. With this method, composite skins are laid up over a foam core. Then foam is removed to create space for necessary components. The water tank could be integrated into a structure of this type. The final method investigated consisted of elements from the other two methods. It consisted of a composite primary structure with an integrated tank, and a built up wood structure with a thin composite skin holding the other components.

6.2.4 Landing Gear

There were two primary construction methods considered for the landing gear. One was to obtain or modify a machined aluminum gear. The other was to construct a composite gear from carbon fiber, fiberglass and foam. It was desired to create a strong gear that could handle the high landing loads and also absorb energy for gentler landings.

6.3 Figure of Merit Analysis Results

Table 6.2 shows the numerical figures of merit used to select the manufacturing processes for all of the major airplane components. Based on those results, the following materials and manufacturing methods were selected:

- The hybrid construction method for constructing the wing and empennage surfaces
- A carbon-fiber wing joiner
- The carbon-fiber tube joining method for the empennage surfaces
- The composite skin, built up structure, with an integral water tank, for the fuselage.
- A composite landing gear structure

Details of the construction methods employed are described in Section 6.4. Figure 6.1 shows the manufacturing milestone chart for the competition airplane. The figure shows the planned and actual, or projected if they have not been completed as of the printing of this report, completion dates of the major manufacturing elements.

Table 6.2 Manufacturing Process Figures of Merit

	Figures of Merit	Strength to Weight Ratio	Skill Level Required	Actual Cost	Time Required	Material Availability	Component Durability	
	Weight Factor	3	2	1	2	1	2	
Component	Construction Method							Total Score
Wing	Balsa Structure Covered with Monokote	0	1	1	0	1	-1	2
	Composites Bagged on Foam	0	0	0	1	0	1	4
	Hybrid Method	1	0	0	0	0	1	5
Wing Joiner	Aluminum	0	1	0	0	0	0	2
	Carbon Fiber	1	1	-1	0	0	1	6
	Steel	-1	0	0	0	-1	1	-2
Empennage Surfaces	Balsa Structure Covered with Monokote	0	1	1	0	1	-1	2
	Composites Bagged on Foam	0	0	0	1	0	1	4
	Hybrid Method	1	0	0	0	0	1	5
Empennage Surface Attachment	Carbon Joiner Tubes	1	1	0	1	0	1	9
	Detachable Boom	-1	0	0	1	0	0	-1
	Telescoping Boom	0	-1	0	0	0	0	-2
Fuselage	Wood Structure with Composite Sheeting	1	0	0	0	0	1	5
	Composite Skins on Foam Core	0	1	0	0	1	0	3
	Balsa and Plywood Built Up Covered with Monokote	1	1	1	-1	1	-1	3
Landing Gear	Aluminum	0	1	1	1	0	0	5
	Carbon Fiber Composite	1	0	0	0	1	1	6

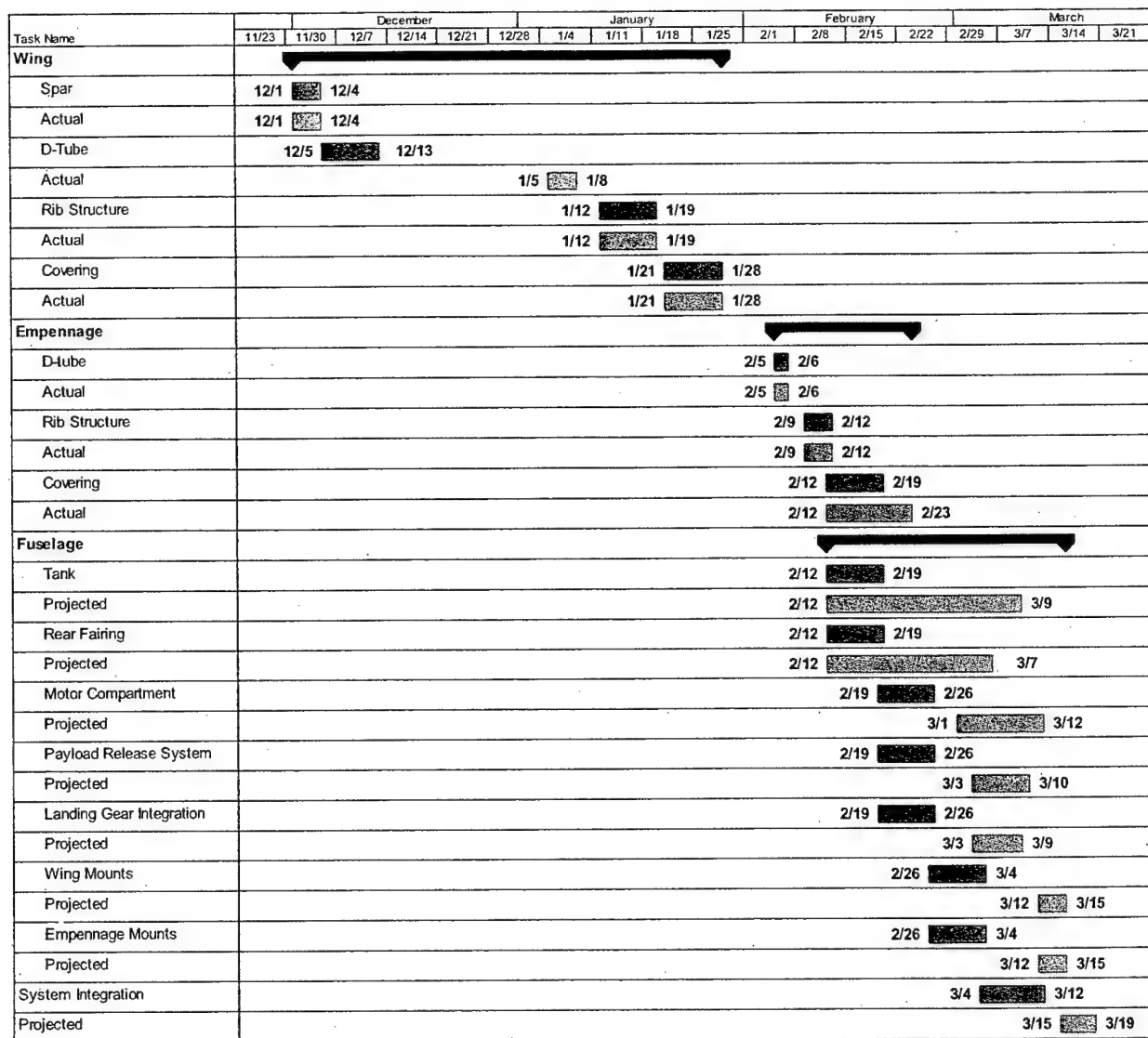


Fig 6.1 Manufacturing Milestone Chart

6.4 Manufacturing Processes

The manufacturing processes selected for building the various airplane components will now be described in more detail. The process involved for construction of each of the major components consisted of many interconnected steps. In order to organize and direct team resources in the most efficient manner, a flow chart of the construction process was created for each component.

6.4.1 Wing Manufacturing Process

The hybrid construction method chosen for the wing involved the following four, main steps. These were: (1) the construction of the spars and the D-tube, (2) the assembly of the spar, the D-tube and the rib structure, (3) applying the carbon rib caps and inserting the control surfaces and servo mounts, and (4) covering the wing.

The spars consisted of 4 main components; the carbon fiber caps, balsa shear web, carbon-fiber joiner tube, and a carbon-fiber sock. First, the contest grade balsa shear webs, with the grain oriented vertically, were glued to each other on a flat surface. They were then bonded to the carbon fiber caps with cyanoacrylate adhesive (CA). At the inboard end of the spar, the joiner tube was tacked into place with CA and the gaps between it and the spar cap were filled with chopped carbon-fiber filler. Next, a one inch diameter carbon-fiber sock was pulled over the spar and epoxy was applied. Lastly, the spar assembly was wrapped in release film and bleeder cloth and vacuum bagged.

To form the carbon-fiber D-tubes a mold was made. A foam block was cut to the leading edge shape of the airfoil with a CNC foam cutter built by the team. The mold was then covered with release film. Two layers of 2.4 oz carbon-fiber cloth, oriented with the fibers $\pm 45^\circ$, were laid on the mold and wetted-out with epoxy. Waxed Mylar, release film and bleeder cloth were then laid over the carbon fiber and the whole assembly was vacuum bagged.

The team had its ribs for the wing and empennage laser cut to save time and materials. The ribs at the tips, inboard end of the aileron and at the root of each panel were made of light plywood. The rest of the ribs were contest grade balsa. First, the leading edge wing ribs were glued to the spars. Then the D-tubes were epoxied in place. The ribs behind the spar then were glued into place. At this time, the aileron ribs were also glued to the carbon-fiber hinge tube. These ribs were then joined to the 0.032 in. x 0.121 in. pultruded carbon-fiber trailing edge and capped with carbon tow applied with CA. Similarly the ribs behind the spar were joined to the trailing edge and capped with carbon-fiber tow that overlapped about 0.5 in. onto the D-tube. The aileron was then installed by aligning the aileron and inserting an inner carbon-fiber hinge tube to hold it in place. By using this carbon-fiber tube hinge method, an essentially gapless control surface can be created.

The remainder of the wing construction consisted of installing servos and covering the wing. Small plywood servo trays were cut out and installed in the rib bay near the center of the aileron. Control arms were inserted into the ailerons and pushrods were installed. The covering material chosen for the wing was transparent Micafilm™. This film is less than half the weight of Monokote™, but more puncture resistant. The wing structure had to first be coated with a thin layer of Balsarite™, and then the Micafilm™ could be ironed on.

6.4.2 Empennage Manufacturing Process

The construction of the empennage was similar to that of the wing. There were, however, some major differences. The spar used was a pultruded carbon tube; the root portion of this was wrapped with Kevlar™ tow so that the tube wouldn't split due to shearing forces from the joiner pin. The D-tube was laid up with one $\pm 45^\circ$ degree layer for torsional stiffness and one 0° - 90° layer for added longitudinal stiffness. For the ruddervators there were no carbon tubes of the proper diameter to construct a gapless hinge as was used in the wing. Instead a 0.125-inch carbon rod was used as a hinge. 1/32-inch balsa was sheeted around the front end of the ruddervators to form what was essentially tube equal in diameter to the

thickness of the empennage at the hinge line; this allowed a nearly gapless hinge to be used. Fig 6.2 shows some pictures of the empennage construction in progress.

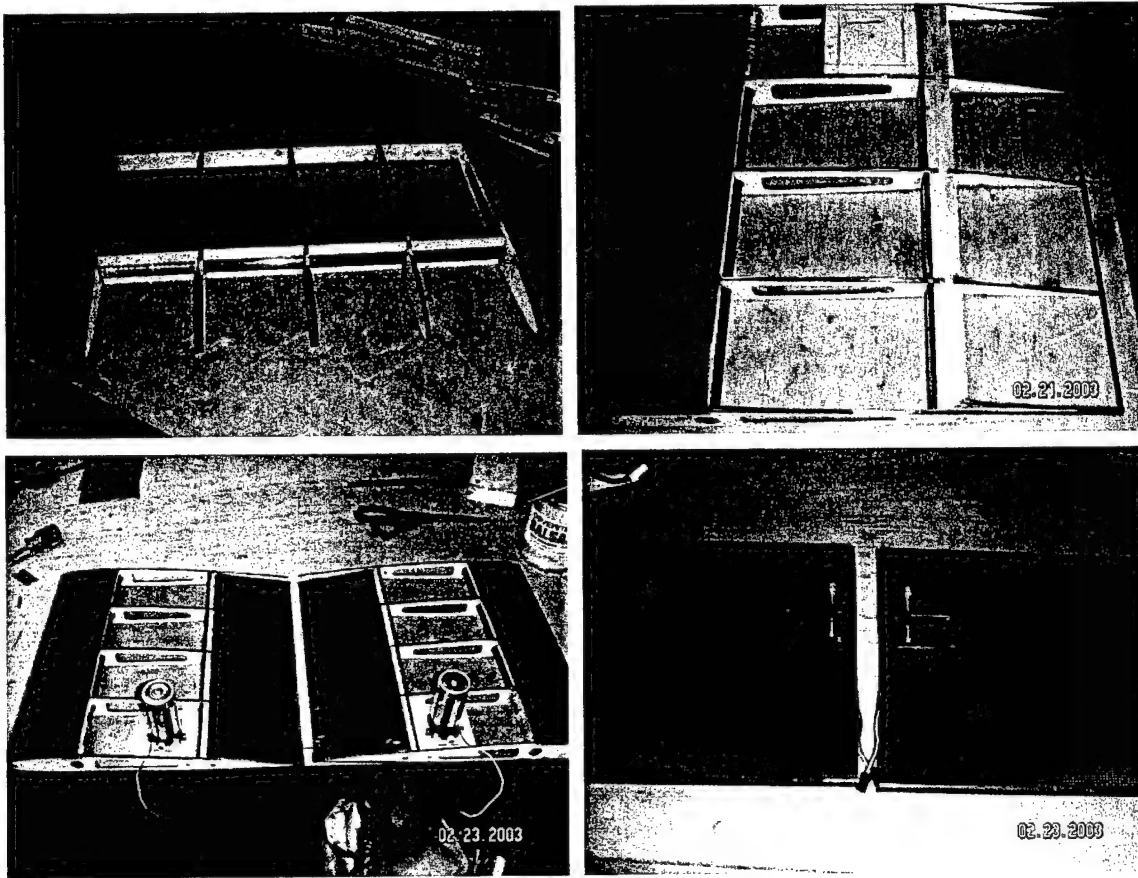


Fig 6.2 Empennage Construction Pictures

6.4.3 Fuselage Manufacturing Process

The fuselage structure is based around the 0.75-inch diameter, wrapped carbon tube that is called the fuselage spine. All of the fuselage components tie into the spine in order to transfer the flight loads throughout the airplane.

The tank shape will be cut first with the CNC foam cutter. This includes cutting holes for the wing joiner tube, the landing gear strut, and for the fuselage spine as well as the taper at the bottom of the tank. Next, the skins and cores for the tank structure will be cut to shape. The tank lay up consists of the following layers; foam blank, 2 layers of 2.4 oz fiberglass, a 1/32" contest grade balsa core, 2 layers of 2.4 oz fiberglass, unidirectional carbon fiber reinforcements and a final layer of 0.5 oz fiberglass. This lay up will then be covered with painted Mylar, release film and bleeder cloth and be vacuum bagged.

After removing the fuselage from the bag, the foam will be removed with a Dremel™ tool and acetone. The spine and joiner tube will then be glued into place. The spine and joiner tube will be lashed together with Kevlar tow to transfer the loads directly from the spine to the wing.

The rear fairing and wing roots will be cut out of foam and two layers of 2.4 oz fiberglass will be applied and the assemblies were vacuum bagged. After curing, the rear fairing will be cut into 3 sections.

The middle one will be permanently attached to the fuselage spine and the tank. The sections above and below will have the foam removed and be made to be removable for access to the radio and telemetry equipment. The wing root sections will be glued to the tank and the joiner tube. The interface between the wing root and the tank will be filleted with epoxy and micro balloons to transfer the loads over a larger surface area.

In front of the tank, the firewall and two other bulkheads will be epoxied to the fuselage spine. The motor will be mounted through the firewall and first bulkhead above the spine. A balsa sheeted battery compartment will be built between the bulkheads below the spine. Using the firewall and bulkheads as templates, the nose fairing will be cut out of foam. Two layers of 2.4 oz fiberglass will then be vacuum bagged over this section. After curing, the foam will be removed with acetone. The nose fairing will fit perfectly over the bulkheads and be faired the nose section into the tank.

The landing gear will be installed next. The carbon fiber tube that the Robart Robostrut™ fits into will have a slit approximately three inches in length cut into it. A washer will be welded to the Robostrut™ at the proper height so that it rests against the bottom of the carbon fiber tube. The orientation of the Robostrut™ can then be adjusted by loosening a hose clamp that is placed around the carbon tube. This allows the main gear to be adjusted to compensate for cross-wind takeoffs and landings.

The payload release servo and nozzle will next be attached to the tank. A fairing that includes a wheel pant for the main wheel and covers the bottom of the fuselage will be vacuum bagged over a foam plug. After curing, the foam will be removed using a solvent. The fairing is removable to allow for access to the main landing gear and the payload release servo.

The remainder of the electronics and wiring will then be installed to complete the systems integration phase. The radio and telemetry gear will be mounted to the flat surface on the back of the tank, with the speed controller and batteries in the nose fairing. The tail wheel assembly will also be attached at this time. Finally, the motor, gearbox and propeller will be installed, completing the Fiberglass Overcast.

7.0 Testing

During the design and construction of the Fiberglass Overcast there were a number of tests that were performed to test various components of the airplane. These tests included static and in-flight water tank dump testing, propulsion testing. The competition airplane has not flown as of the writing of this report, but a testing plan and schedule were developed. The overall testing schedule is presented in Table 7.1.

Table 7.1 Overall Testing Schedule

Task	Start	End
Ground Tank Testing	10/28/03	11/5/03
Propulsion Testing	1/31/04	3/26/04
In-flight Tank Testing	2/7/04	2/19/04
Flight Testing (Competition Airplane)	4/3/04	4/16/04

7.1 Tank and Nozzle Testing

Experiments were conducted to determine the best tank shape and nozzle geometry. The tanks were cut from layers of 2" foam sealed with silicone and the nozzles were made using a 3D rapid prototyping machine. Preliminary drain time estimates were made using empirical relations, as described in section 4.3.3. The results of the analysis showed that, as expected, draining time went down as tank height increased. However, a sharp increase in tank height at very low drain times was observed from empirical data. At those low times, very little decrease in drain time is obtained for large increases in tank height and therefore weight and drag. Tanks with circular cross sections and heights of 10 and 14 inches were chosen from the empirical data for draining four liters of water. A 10 inch tall tank, having an elliptical cross section with a width-to-length ratio of two-to-one (or 2:1), was also tested. The elliptical tank was tested to investigate the influence of wall effects when the tank became narrow. This investigation was of particular concern with respect to the aerodynamic drag produced by the tank. Thinner tanks would produce less drag when properly faired.

Two nozzle geometries with throat diameters of 0.25, 0.375 and 0.5 inches were constructed from hyperbolic curves. All the nozzles had an initial diameter of 4 inches and were created by simply revolving the hyperbolic curve to create a nozzle that was manufactured using a 3D printing machine. Research indicated that the most efficient nozzle may have a smaller throat than the exit, so throats of 0.25, 0.375 and 0.5 inch diameter were tested. All nozzles had the 0.5 inch exit diameter required by the rules.

The elliptical tank shape had little-to-no effect on the draining time when compared to the circular tanks. Furthermore, a tank height between 10 and 14 inches resulted in draining times between 17 and 22 seconds (Table 7.2). An even taller tank would result in lower draining times, but only marginally. The gain in drag and cost, as a result of increased height, outweighs the slight decrease in drain time. Furthermore, the times found were short enough that the water could be comfortably released in the space allotted by the rules. The results presented in the table are the average of three runs.

Experimental data revealed that the hyperbolic nozzles constructed using a curve with a coefficient value, a , of 1 (Eq. 7.1) drained the water in less time than those with a coefficient of 0.5. That was because the

$$y = a * \sqrt{x^2 - 1} \quad (7.1)$$

nozzles with coefficients of one turned the flow from the entrance area to the throat area over a larger distance, resulting in shallower turning angles. In addition, the best performing nozzle had a throat diameter equal to 0.5 inches. Empirical data showed that the addition of gravitational acceleration, beyond 1 g, reduce the drain time by a factor proportional to the square root of the g-loading.

Table 7.2 Results of Tank Draining Experiments

Tank	Hyper1A (s)	Hyper1B (s)	Hyper1C (s)	Hyper05A (s)	Hyper05B (s)	Hyper05C (s)
10" Circular	22	27	69	21	35	76
14" Circular	17	30	60	18	31	71
10" Elliptical	19	30	68	21	33	74

7.2 Propulsion Testing

Given the strong dependence of the airplane design on the MDO results, which were based on propulsion system performance predictions from MotoCalc™, it was necessary to assess the accuracy of these predictions. Propulsion system testing was performed in order to determine the characteristics of the chosen system, and verify that its performance was adequate.

In order to measure the thrust produced by the propulsion system, a thrust stand was constructed. The motor was mounted with its propeller rotation axis horizontal, on a plate supported by low-friction rollers. This plate was constrained to move only along an axis parallel to the propulsion system thrust line. Thrust was measured using an Interface™ MB-25 beam-type load cell secured to the moving plate and linked to the nonmoving thrust stand base.

Due to lack of wind tunnel availability, only static propulsion system testing was performed. All tests used a Graupner™ 3300-7H electric motor mated to a Model Motors™ metal gear, inline gearbox with a 3:1 gear ratio. An RFM™ 18.5 x 12 propeller with folding blades was used in the tests. For these tests, the folding propeller blades were secured in their extended position to avoid contact with thrust stand setup. The motor was powered with a 28 cell pack of Sanyo™ CP-1300SCR batteries and an Astroflight™ 204-D speed control. Battery current and voltage data were recorded by hand with the use of an Astroflight™ Super Whatt-Meter™.

The primary goal of the testing was to verify thrust, current draw and runtime for the selected propulsion system at the maximum power setting. At full power, the system produced up to 9.1 lb of thrust with a 26.1 amp current draw on a fully charged battery pack. As expected with a Ni-Cd battery pack, the initial thrust quickly dropped and settled to a nearly constant thrust of 8.6 lb and 25.5 amp current draw, where it remained through the majority of the battery capacity. In all tests, the thrust and current draw

began to drop rapidly with time after approximately 180 seconds of operation at the full throttle setting. At this point, the tests were terminated since thrust levels would not be sufficient to maintain level flight.

In addition to the continuous full-power data, maximum available thrust after a simulated Fire Bomber mission lap was desired. This was to ensure that the airplane will be capable of completing the second take off required for the Fire Bomber mission. For this test, starting with a fully charged battery pack, the motor was run at full power for 20 seconds. Power was then reduced to 75% throttle and run for 20 seconds to simulate the first lap of the Fire Bomber mission. The motor was then shut off for 60 seconds to simulate water loading. The motor was then set back at full throttle for the second take off. The system produced 8.7 lbs of thrust with a current draw of 25.5 amps following the simulated first lap of the Fire Bomber mission.

The testing indicates that the uninstalled propulsion system performance exceeds that predicted by MotoCalc™. Steady state static thrust was slightly greater than the MotoCalc™ prediction of 8.26 lb. Current draw was significantly lower than the MotoCalc™ prediction of 29.4 amps. Consequently, based on these data, the useful runtime of the actual propulsion system can be estimated to be nearly 45 seconds greater than the MotoCalc™ prediction.

7.3 Flight Testing

7.3.1 In-flight Water System Testing

A Spacewalker™ ARF was purchased to conduct initial flight testing of the water release system and competition propulsion system. A water release system was installed in this airplane. The system included a water tank and drain valve similar to the one to be used on the competition airplane. Results of the test showed that the ball valve operated as expected. However, there was a small leakage problem when the valve was in the closed position. The problem was fixed by increasing the size of the valve, while maintaining a ½ inch exit orifice, so that there would be a more interior surface area to seal the valve when it is closed. It was also observed that water stream leaving the valve immediately broke up into an aerosol spray. The draining times on the ground were found to be comparable to those measured in the air. Therefore, there was no need for any apparatus to eliminate the breakup of the water stream.

7.3.2 Competition Airplane Flight Test Plan

Adequately flight testing the airplane is critical to success at the DBF competition. A schedule was developed (Table 7.3) to identify any unexpected behavior of the airplane, familiarize the pilot with the airplane and practice the competition course. A flight testing checklist was developed to ensure the safety of the airplane and crew during testing. The following items will be checked prior to each flight:

- Structural Integrity – Wing and tail attachment, landing gear rigidity and tip skids secured.
- Control Check – Unpowered “slop” tests on all servos, powered “slop” tests, motion tests on all servos and failsafe operation.
- Batteries – Peak charge flight batteries, check receiver battery voltage, check that batteries are secured, check all connections and insert safety fuse.

- Flight Crew Readiness – Telemetry system check, check ground crew readiness, check pilot readiness and check spotter readiness.

Following each flight, a debriefing session will occur to evaluate the test, record data and identify any changes that need to be made before the next flight.

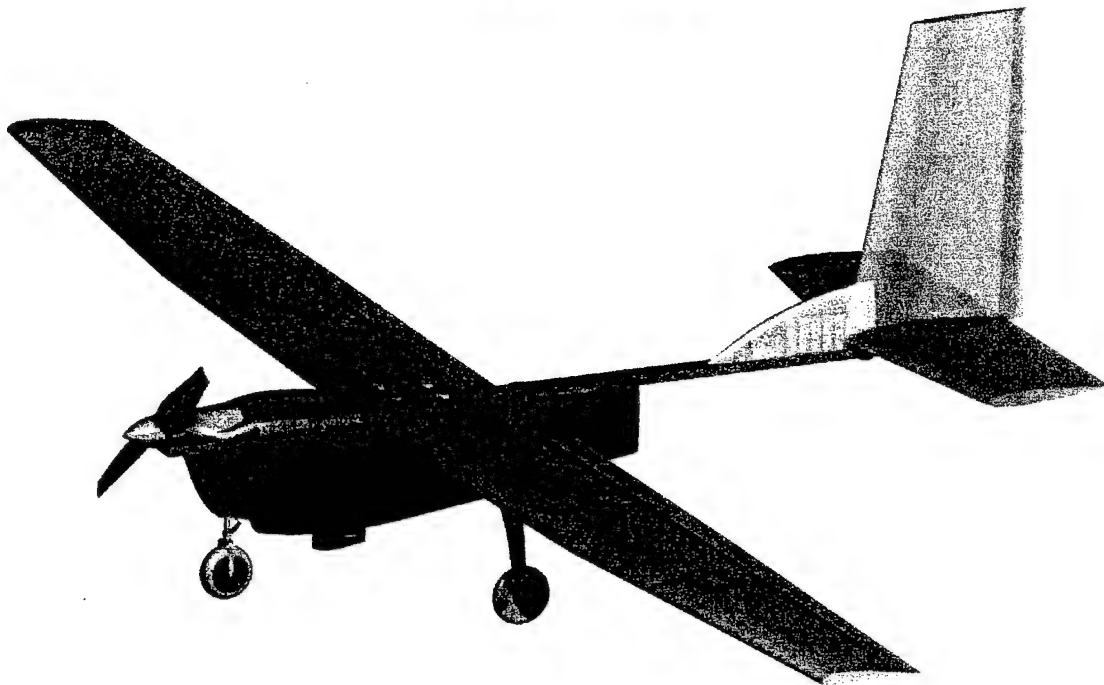
Table 7.3 Flight Testing Schedule

Flight Number	Payload	Maneuvers	Date	Notes
1	No	Systems Checks, Ground Handling and High Speed Taxi	4/3/04	Familiarize pilot with monowheel operations check for proper operation of all electronics and components
2a	No	Pilot familiarization, handling qualities, etc.	4/3/04	Identify any unexpected or unwanted behavior, correct before moving on.
2b	Yes	Pilot familiarization, handling qualities, etc.	4/3/04	Identify any unexpected or unwanted behavior, correct before moving on.
3a	No	Coordinated stalls	4/3/04 and 4/10/04	
3b	Yes	Coordinated stalls	4/3/04 and 4/10/04	
4a	No	Uncoordinated stalls	4/3/04 and 4/10/04	
4b	Yes	Uncoordinated stalls	4/3/04 and 4/10/04	
5	No	Landing Practice	4/3/04 until 4/16/04	As needed to make ground operations for the Fire Bomber as streamlined as possible
6	Yes	Simulated Competition Flights: Fire Bomber Mission	4/3/04 until 4/16/04	Verify energy usage and time estimates. Focus on this mission. Practice refilling procedure (static and during actual flights).
7	No	Simulated Competition Flights: Ferry Mission	4/3/04 until 4/16/04	Verify energy usage and time estimates. Only three flights, at most should be necessary.

8.0 References

- ¹ MATLAB™. Version 6.5, Mathworks Inc., 2002.
- ² Raymer, Daniel P., Airplane Design: A Conceptual Approach, 3rd Edition, American Institute of Aeronautics and Astronautics, Reston, VA, 1999.
- ³ XFOIL. Version 6.94, Mark Drela, 2001.
- ⁴ "Approximate Flow Through an Orifice," <http://www.mcnallyinstitute.com/13-html/13-12.htm>.
- ⁵ Motocalc™. Version 6.03, Capable Computing Inc., 2001.
- ⁶ Nelson, Robert C., Flight Stability and Automatic Control, McGraw Hill, New York, NY, 1986.
- ⁷ Drela, Mark, "Quick V-Tail Sizing," http://www.charlesriverrc.org/articles/design/markdrela_vtailsizing.htm, March, 2000.
- ⁸ NASG Airfoil Database, <http://www.nasg.com/afdb/index-e.phtml>.
- ⁹ LinAir™ for Microsoft Windows. Version 1.4, Desktop Aeronautics Inc., 1996.

'03/'04 AIAA DBF
Cal Poly San Luis Obispo
"Moist"



Theo Coetzee
Francesco Giannini
Yevgeniy (Gene) Gisin
Kevin Lutke
Matt McCue
Eric Naess
Renee Pasman
Kristi Stavros

Table of Contents

1. Executive Summary	1
1.1.1. Conceptual Design Alternatives	1
1.2. Preliminary Design	1
1.2.1. Preliminary Design Alternatives	1
1.2.2. Preliminary Design Results	2
1.3. Detailed Design	2
1.3.1. Detailed Design Alternatives	2
1.3.2. Detailed Design Results	2
1.3.3. Detailed Design Tools	2
2. Management Summary	2
2.1. Design Team Breakdown	2
2.2. Configuration and Schedule Control	4
3. Conceptual Design	5
3.1. Mission Requirements	5
3.1.1. Mission 1: Fire Fight	6
3.1.2. Mission 2: Ferry	6
3.1.3. Takeoff	7
3.1.4. Rated Aircraft Cost	7
3.1.5. Aircraft Storage	7
3.2. Payload Configuration	7
3.3. Airframe Configuration	8
3.3.1. General Configuration	8
3.3.2. Wing Placement	10
3.3.3. Fuselage Configuration	10
3.3.4. Engine Configuration	11
3.3.5. Landing Gear Configuration	11
3.3.6. Empennage Configuration	12
3.4. Materials selection	13
3.5. Conceptual Design Results	13
4. Preliminary Design	14
4.1. Wing Preliminary Design	14
4.1.1. Airfoil/High Lift	14
4.1.2. Aspect Ratio	15
4.1.3. Wing Planform	16
4.1.4. Motor Selection	17
4.1.5. Propeller Pitch and Diameter	19
4.1.6. Battery Pack Sizing	19
4.1.7. Tail Sizing	21
4.1.8. Load Factor Sizing	21
4.2. Analytical Tools	22
4.2.1. Spreadsheet Application	22
4.2.2. Other Simulation Methods	24
4.2.3. Numerical Water Dump Analysis	24
4.2.4. Empirical Water Dump Analysis	25
4.3. Preliminary Design Aircraft Parameters	27
4.3.1. General Characteristics of Optimized Aircraft	27
4.3.2. Aerodynamic and Stability Characteristics of Optimized Aircraft	28
4.3.3. Predicted Mission Performance for Optimized Aircraft	28
4.4. Conclusion	29
5. Detail Design	29
5.1. System Architecture	30
5.1.1. Airfoil Selection	31
5.1.2. Planform Configuration	33
5.1.3. Empennage Configuration	34

5.1.4. Stability and Control	34
5.2. Propulsion System	35
5.2.1. Motor Selection	35
5.2.2. Propeller Sizing	37
5.2.3. Battery Weight and Number of Cells	39
5.3. Structural Configuration	40
5.3.1. Wing Structural Design	40
5.3.2. Wing Joiner Design	41
5.3.3. Wing Structural Verification	42
5.3.4. Wing Weight Buildup	43
5.3.5. Keel Structural Design	44
5.3.6. Main Landing Gear Structural Configuration	44
5.4. Aircraft Performance Characteristics	45
5.5. Water Tank and Release System Design	47
5.6. Aircraft Assembly and Storage	48
5.7. Center of Gravity Calculation	48
5.8. Rated Aircraft Cost	48
5.9. Final Aircraft Configuration	49
5.10. Drawing Package	49
6. Manufacturing Plan	52
6.1. Figures of Merit	52
6.1.1. Availability of Materials and Tools	52
6.1.2. Skill	52
6.1.3. Construction Time	52
6.1.4. Reliability	52
6.1.5. Performance	52
6.1.6. Manufacturing Processes Figure of Merit	53
6.2. Manufacturing processes	53
6.2.1. Keel	53
6.2.2. Wing and Tail Surfaces	54
6.2.3. Water Tank	54
6.2.4. Landing Gear	54
6.3. Manufacturing Plan	54
7. Testing	55
7.1. Testing Objectives	55
7.1.1. Wings and Tail	55
7.1.2. Keel	55
7.1.3. Tank and Nozzle	56
7.2. Flight Tests	56

Table of Figures

Figure 1 – Team architecture, design personnel and their assignment areas	3
Figure 2 – Actual and Planned Project Timeline	5
Figure 3 – Course layout	6
Figure 4 – Candidate Configurations	8
Figure 5 – Airfoil type study	15
Figure 6 – Foam Core Construction Wing – Weight vs. Aspect Ratio	16
Figure 7 – AstroFlight Cobalt 40 and Graupner Ultra 930-6, 16V Input	18
Figure 8 – AstroFlight Cobalt 40 and Graupner Ultra 930-6	18
Figure 9 – Ragone Battery Plot	20
Figure 10 – Maximum Flight Acceleration	22
Figure 11 – Simulation Program Schematic	23
Figure 12 – Estimated Accelerations and Dump Characteristics – No Ram Air Effects	25
Figure 13 – Tank Testing Assemblies and Test Video Sample, Nozzle Close-up Inset	26
Figure 14 – Dump Time vs. Airspeed	26
Figure 15 – Aircraft Configuration Optimized for Peak Score	27
Figure 16 – General Aircraft Configuration	30
Figure 17 – d9g9 airfoil, 0° and 15° flap deflections and original d9 airfoil.	31
Figure 18 – Drag Polar Comparison	32
Figure 19 – Cl vs. Angle of Attack	33
Figure 20 – Modeled Planform, Lift Distribution, Cl Distribution	34
Figure 21 - Aerodynamic Coefficients and Geometry Modeled	35
Figure 22 – Motor Selection vs. Maximum Efficiency - 650 Watts Input	36
Figure 23 – Effects of Gearing on Thrust and Speed	38
Figure 24 – Propeller Efficiency vs. Normalized Speed	38
Figure 25 – Typical NiCd Discharge Rates	39
Figure 26 – Number of Layers vs. Semispan Location	40
Figure 27 – Bending Moment and Normal Stress vs. Semispan	41
Figure 28 – Instrumented Test Panel Undergoing Destructive Testing (Tests 1 and 2)	42
Figure 29 – Destructive Testing of Wing Structure	43
Figure 30 – Meshed Solid Model and Static von Mises Stresses (20G Loading, Maximum Weight)	45
Figure 31 – Power Req'd vs. Power Available, Climb Rates	46
Figure 32 – Drag and Lift/Drag vs. Airspeed	46
Figure 33 – Water Filling and Release Systems	47
Figure 34 – Manufacturing Schedule	55
Figure 35 – Instrumented Aircraft Before Flight Test	57
Figure 36 – Flight Test Performance Data Gathered vs. Predicted	57
Figure 37 – First Flight	58
Figure 38 – Deformed Firewall/Landing Gear Mount	59

Table of Tables

Table 1 – Responsibilities Breakdown	4
Table 2 – Dumping system decision matrix.....	8
Table 3 – Figures of merit for general configurations	10
Table 4 – Figures of merit for wing placement.....	10
Table 5 – Fuselage Length Figures of Merit.....	11
Table 6 – Number of Engines Selection.....	11
Table 7 – Landing gear configuration figures of merit	12
Table 8 – Figures of Merit for Tail Configuration	12
Table 9 – Material Selection.....	13
Table 10 – Wing Planform Design	17
Table 11 – Battery Cell Comparison	20
Table 12 – General Aircraft Characteristics	27
Table 13 – Predicted Aerodynamic/Stability Performance Parameters.....	28
Table 14 – Drag Coefficient Breakdown	28
Table 15 – Predicted Mission Scores.....	28
Table 16 – Mission Performance Breakdown	29
Table 17 – Performance Requirements	29
Table 18 – Airfoil Performance Requirements.....	31
Table 19– Candidate Motors	35
Table 20 – Propulsion Systems Evaluated.....	37
Table 21 – Wing Joiner Geometry Comparison	41
Table 22 – Wing Weight/Spar Cap Thickness Calculations	43
Table 23 – Carbon Fiber Properties	44
Table 24 – Center of Gravity Calculation	48
Table 25 – Rated Aircraft Cost.....	48
Table 26 – Final Configuration	49
Table 27 – Manufacturing Processes and Materials Considered for Construction.....	53
Table 28 – Testing Schedule and Qualifications.....	56

1. Executive Summary

In response to the announcement of the AIAA Design Build Fly 2003/2004 competition, California Polytechnic State University at San Luis Obispo (Cal Poly SLO) assembled a group of aeronautical engineering students to design, build, and fly a radio-controlled aircraft in the Cessna/Office of Naval Research competition. The following report provides an overview of the design, manufacturing, and testing the team went through to arrive at the final configuration.

1.1. Conceptual Design Summary

Cal Poly DBF team began this year's design by evaluating the two different missions to find out how each mission would affect the design of the aircraft. Manufacturing methods and basic aircraft configurations which satisfied the mission profiles were discussed and selected based on data obtained through research, mission performance, and past experience in the DBF competition. Basic tank and nozzle configurations were discussed for further development of the aircraft.

1.1.1. Conceptual Design Alternatives

For configuration of the fuselage/tank, the implementations of a tank that was over the wing, under the wing, and blended into the body of the plane were studied. The ability to deploy the water, and the ease of construction were major factors in feasibility of each configuration. For the wing configuration, the aerodynamics group studied the conventional wing, biplane, canard, flying wing, and blended wing/body. The effects of the tail on the various fuselage/wing configurations were studied to find the effectiveness of each. The conventional tail, cruciform tail, T-tail, V-Tail, and inverted V-Tail were all analyzed. The propulsion group discussed and analyzed the number and type of engines to be used. The structures group studied landing gear and keel placement along with assembly choices.

1.1.2. Conceptual Design Results

Upon analysis the fire fighting mission was found to drive the sizing of the airframe because of the takeoff distance requirement, while the ferry mission was found to size the propulsion system by virtue of being more energy-intensive. Using this information, it was possible to down select on the possible airframes, and propulsion systems. A low tank was chosen for the ease of implementation. To support the tank a high-keel was chosen which led to a high wing for the ease of attaching the wing to the keel and avoiding interference with the tank.

1.2. Preliminary Design

After the basic configuration of the aircraft was finalized, the approximate aircraft size, component placement, landing gear, motors, and control surfaces were decided upon. The aircraft was to have 51 ounces per square foot wing loading, and be powered by a Graupner 930-6 motor operating from the power provided by a 16-cell Sanyo CP-1700SCR battery pack.

1.2.1. Preliminary Design Alternatives

Wing planform alternatives investigated were swept, elliptical, rectangular, tapered, and a modified Schuemann. The optimum aspect ratio was determined from the outputs of the DBF2003 performance simulation program and practical considerations. Tails such as the T-tail, the cruciform tail, and the canard configuration were discarded early since their disadvantages in complexity outweighed any benefits. Propulsion system components were selected to allow the optimum performance in the missions chosen. Motors from Graupner and AstroFlight product lines, different types of NiCd batteries and propellers of various diameter and pitch were compared in order to come up

with the final configuration. Nozzle and tank configurations were discussed to optimize the head of the tank and decrease the exit losses.

1.2.2. Preliminary Design Results

The modified Schuemann wing planform was used in this design because it posed the best compromise between all of the concepts reviewed. After weighing the benefits of the 3 possible tails, the conventional tail empennage was chosen to decrease the aircraft rated cost, provide for maximum control authority and to simplify construction and operation. The size of the selected tail was calculated using tail volume coefficients equations from Raymer¹. The optimal landing gear for the mission was finalized as a non-retractable tricycle configuration with a steering front wheel with brakes. The choice of tank nozzle became important to deploy the water. It was found that a smoothly converging nozzle was needed to decrease the dump time. A blocker to allow the water to exit into freestream air was also implemented.

1.3. Detailed Design

After the basic configuration of the aircraft was laid out, the group developed more detail to the design and was able to perform more analysis of the chosen aircraft components. At this point the materials and manufacture processes were finalized. Finally, solid carbon joiner rods for plug-ins, Velcro, and nylon bolts were chosen for the assembly.

1.3.1. Detailed Design Alternatives

Locations of all secondary components were investigated for aircraft balance requirements. The geometry of the water deployment system was analyzed and improvements on the design were studied.

1.3.2. Detailed Design Results

At the conclusion of the detail design phase all aircraft dimensions, system components, and materials were decided on, aircraft performance and control characteristics determined and manufacturing processes selected. The estimations conducted by the design team predicted an RAC of 7.925, and an ideal final competition score of 45.8, with a flight time of 2.52 minutes for the fire fighter mission and 1.72 for the ferry mission.

1.3.3. Detailed Design Tools

The tools used in the detailed design process were X-foil and the DBF 2003 performance simulation program. A solid model of the aircraft used for visualization and balancing was created in Solid Works 2003. Many of the other estimates and design methods used by the team originated from the experience gained in Cal Poly's previous DBF entries.

2. Management Summary

The Cal Poly design team for the 2004 competition consisted of 8 Aerospace Engineering students. In order to efficiently utilize the skills of each team member, a detailed management plan was devised.

2.1. Design Team Breakdown

To ensure that the design task and work loads were evenly distributed among the team members, the team was divided into four sub-groups; aerodynamics, propulsion, structures, logistics. Project managers were appointed along with a sub-team leader for each category. The project manager was responsible for addressing issues that affected the entire team and drive the team to remain on schedule. The sub-team leaders were responsible for task delegation among their team members. The organizational diagram can be seen in Figure 1.

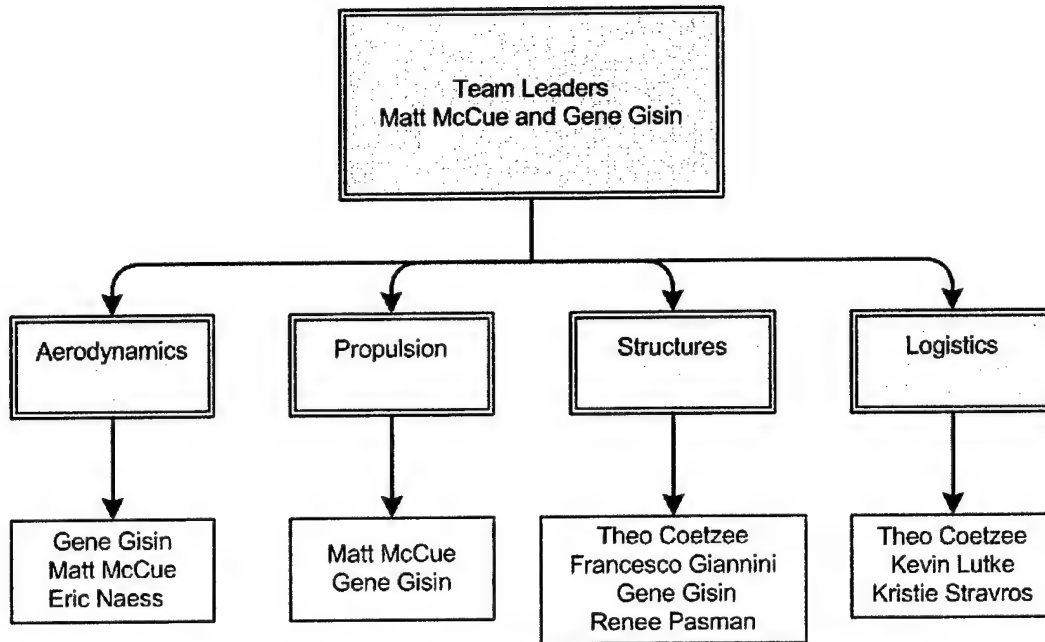


Figure 1 – Team architecture, design personnel and their assignment areas

The aerodynamics team was responsible for creating an aerodynamic model of the aircraft at each flight regime for each feasible configuration to be evaluated. The aerodynamics group was not only responsible for the aircraft performance, but also for stability and controllability of the aircraft. The aerodynamic group worked closely with the propulsion group. The propulsion team was required for generating an optimal battery/motor/propeller combination. This was accomplished with battery and motor characterization to acquire an optimized solution. The structures group was required to analyze the possible structural configurations and construction methods available. Structural testing accompanied with finite element analysis of the major aircraft components were used to determine an optimal structural design point. The logistics team was responsible for generation of an optimal tank configuration. This included the ability to effectively and efficiently load and release the water along with other logistical systems.

Table 1 shows how each team member was involved in the design of the aircraft with a 5 indicating 100% representing full involvement and a 0 representing no involvement.

Table 1 – Responsibilities Breakdown

	Yevgeniy Gisin	Matt McCue	Francesco Giannini	Theo Coetzee	Eric Naess	Renee Pasman	Kevin Lutke	Kristy Stavros
3. Conceptual Design	4	4	4	2	3	1	0	0
3.1 Mission Requirements	4	4	4	2	3	2	1	1
3.2 Payload Configuration	4	4	3	4	3	3	4	4
3.3 Airframe Configuration	4	4	4	3	4	3	2	2
3.3 Material Selection	5	5	5	5	0	0	0	0
4. Preliminary Design	-	-	-	-	-	-	-	-
4.1 Wing Preliminary Design	5	5	0	0	5	0	0	0
4.2 Analytical Research	-	-	-	-	-	-	-	-
4.2.1 Tank Flow Simulation	0	5	0	4	0	0	4	4
4.2.2 Structural Sizing	5	0	4	4	0	5	0	0
4.2.3 Propulsion System Sizing	5	5	0	0	0	0	0	0
4.2.4 Performance and Mission Simulation	5	5	0	0	0	0	0	0
4.3 Aerodynamic and Stability Characteristics	5	5	0	0	5	0	0	0
5. Detailed Design	-	-	-	-	-	-	-	-
5.1 System Architecture	5	5	3	0	0	0	0	0
5.2 Propulsion System	5	5	0	0	0	0	0	0
5.3 Structural Configuration	5	0	5	4	0	4	0	0
5.4 Aircraft Performance Characteristics	5	5	0	0	5	0	0	0
5.5 Water Tank and Release System Design	0	0	4	5	0	0	4	4
5.6 Center of Gravity Calculation	5	0	0	0	0	0	3	3
5.7 Aircraft Assembly and Storage	0	0	5	5	0	5	0	0
6. Manufacturing Plan	-	-	-	-	-	-	-	-
6.1 Figures of Merit	3	3	4	5	0	3	0	0
6.2 Manufacturing Processes	5	5	4	5	0	0	3	4
7. Testing	-	-	-	-	-	-	-	-
7.1 Component Test	5	5	4	4	4	3	1	1
7.2 Flight Test	5	5	4	4	4	3	1	1

2.2. Configuration and Schedule Control

Early in the design process, the team planed out the schedule of the design process, with the expected delivery dates and milestones by which they were to be achieved. The Gantt chart of this schedule can be seen in Figure 2.

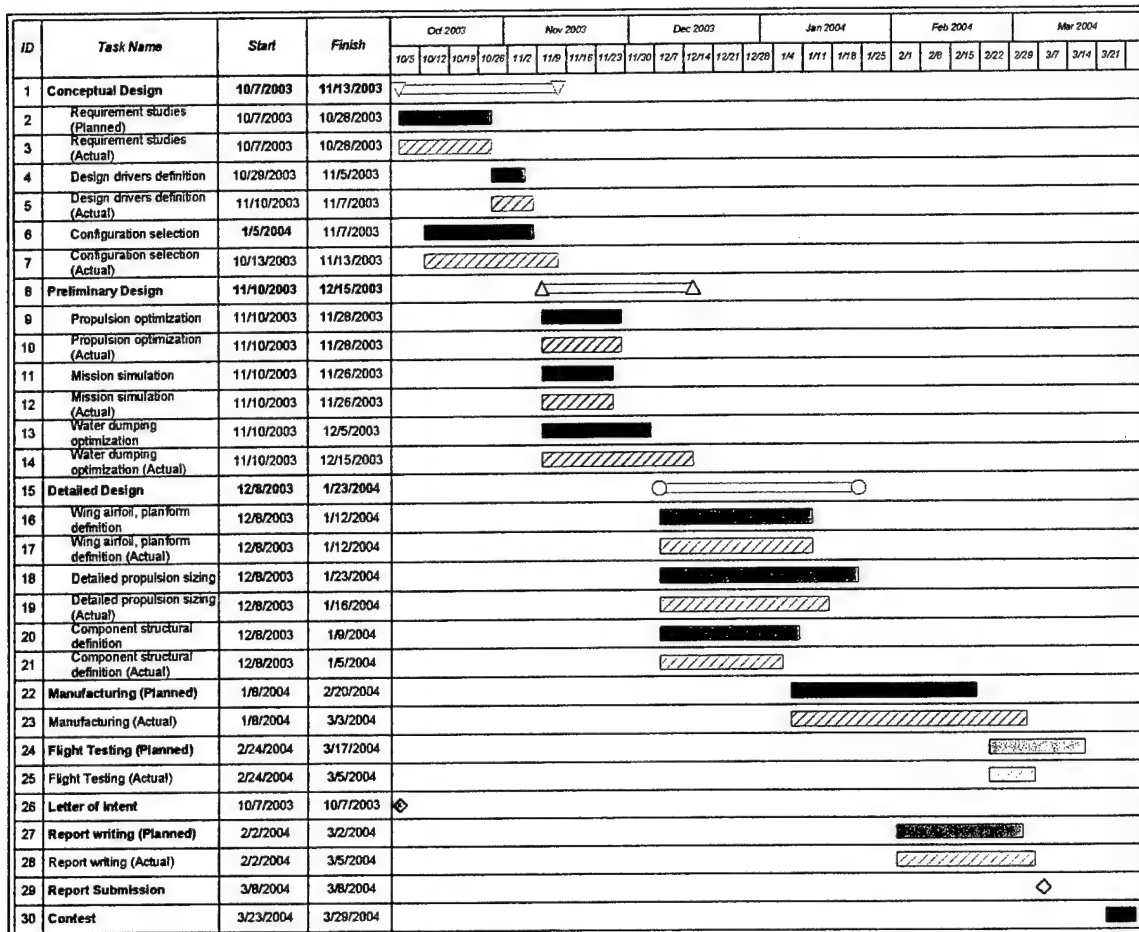


Figure 2 – Actual and Planned Project Timeline

3. Conceptual Design

In the conceptual design phase, the team reviewed the competition requirements, the design drivers, and originated aircraft concepts that might be suitable to the mission. Each one of them was discussed; its merits and flaws were evaluated using figures of merit for the important attributes. At the end of the conceptual design phase, a basic configuration was chosen based on the overall score evinced from the comparison tables and figures of merit.

3.1. Mission Requirements

The competition rules this year require the model aircraft to perform two distinct missions around the course shown in Figure 3. The missions are described below.

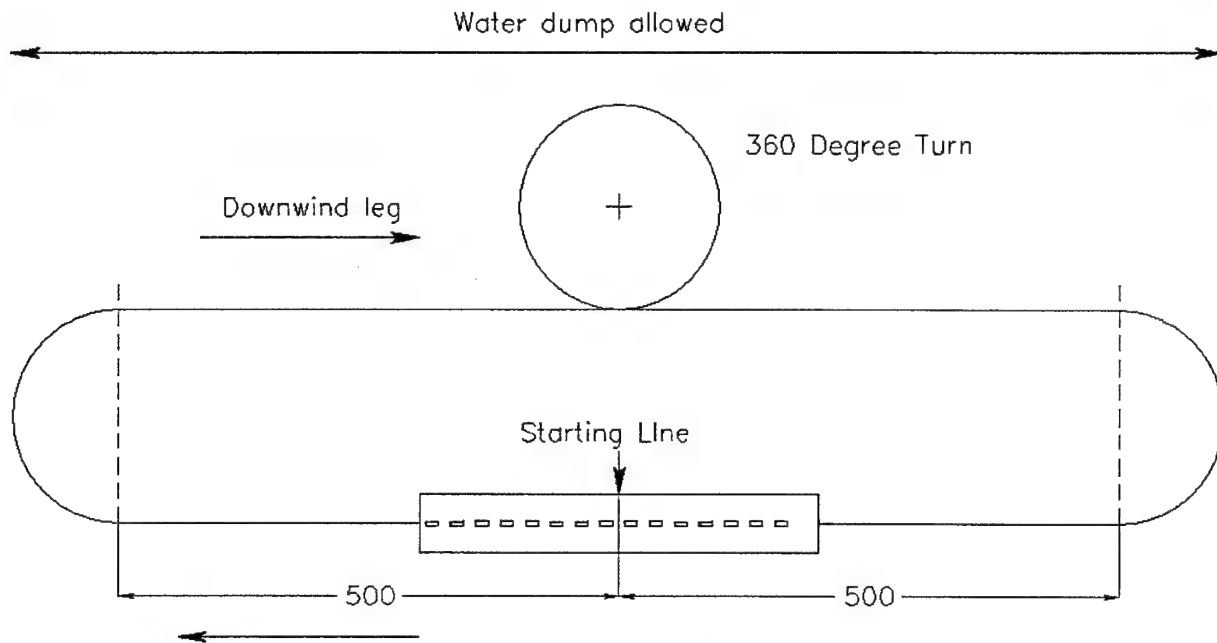


Figure 3 – Course layout

3.1.1. Mission 1: Fire Fight

The mission involves loading the airplane with water, taking off, releasing the load, and landing. Once stopped, the aircraft is reloaded and flies the same mission profile again. On each flight, the aircraft will complete a single 360° turn in the direction opposite of base and final turns on the downwind leg of each lap. The water dump is only allowed during the downwind leg. The flights are timed, with the duration being from the start of the first loading to the full stop following the second landing.

3.1.2. Mission 2: Ferry

During the ferry mission, the aircraft takes off with no water load, flies a 360° turn in the direction opposite of base and final turns on the downwind leg of each lap. The flight consists of four laps, and the time is stopped after the aircraft comes to a complete rest.

The flight scores are calculated differently for the two missions. In the first case, the single flight score is given by

$$Score = \frac{DifficultyFactor * Lbs\ Water}{Mission\ Time}$$

And for the ferry mission

$$Score = \frac{DifficultyFactor}{Mission\ Time}$$

Where the Difficulty Factors are 2 and 1 for the fire fight and ferry mission respectively.

The two flights require conflicting aircraft qualities. Carrying the heavy water payload requires additional frontal area to include the tank and a high lift airfoil section in order to achieve liftoff within the mandatory distance. The competition rules allow the dumping of water only during the downwind leg, which means that the aircraft must fly slowly enough to allow sufficient time for all of the water to drain. On the other hand, the aircraft is relatively light in

the ferry mission, necessitating a lower coefficient of lift on takeoff. Furthermore, the course should be completed as quickly as possible, meaning that the drag of a high-lift section would disadvantageous in those conditions.

3.1.3. Takeoff

The aircraft is subject to an additional constraint. On all missions, takeoffs are performed with liftoff being achieved in 150 feet or less, under the consequence of incurring a time penalty.

3.1.4. Rated Aircraft Cost

The total score in the competition is given by

$$\frac{\text{Written report score} * \text{Total flight score}}{\text{Rated Aircraft Cost}}$$

Where the Rated Aircraft Cost (RAC) is an aircraft cost model that takes into consideration the configuration type, complexity, size, weight and power requirements of the aircraft. It can be seen from the previous formula that the RAC has a powerful effect on total score; obtaining the lowest RAC was a strong design driver.

3.1.5. Aircraft Storage

The aircraft components are designed so that once disassembled, they can all fit inside a 2-ft wide by 1-ft high by 4-ft long box. The assembly is not timed and does not influence flight score. This requirement was considered from the beginning and influenced configuration selection; appropriate structural breaks were planned for in order to minimize the impact of the required additional structure on weight. In this regard, experience gained in the 2002-2003 DBF competition proved invaluable in order to estimate more correctly the impact of joiners on airframe weight, and their implications on overall configuration.

3.2. Payload Configuration

First, the method by which the water would be dumped was established, and only then was an aircraft configuration chosen, based on how well it integrated with the method selected. While the details of the system were yet to be defined at this point, a few constraints on the problem could be drawn. The payload's centroid has to be located very close to the center of gravity of the empty airframe, in order to avoid a change in the static margin, which might have undesirable consequences on the handling characteristics of the aircraft. Additionally, no aircraft part should be in the water spray path, which either precludes some nozzle locations, or affects the aft body shape. From quick initial sizing calculations for aircraft speed, it was determined that between ten and twenty seconds would be required to cover the distance available for the dumping operation; an aircraft with a tank configuration falling outside those bounds would not be competitive. The dumping system should therefore be optimized to allow complete dumping within this timeframe.

The important attributes of a dumping system, in order of importance were reliability, weight, drag and manufacturability. Reliability is paramount, because only a few flight attempts are available and all must count. The weight and drag of the system pose limits to the aircraft's performance and scoring potential. Finally, manufacturability was a concern because changes to the system might be required as a result of flight testing. Rated aircraft cost was not affected by nozzle location or system used and thus was not included in the analysis.

Two actuation mechanisms were considered. The first one uses an internal plunger actuated by a servo to obstruct and clear the passage for the water flow. This installation is aerodynamically clean, but the presence of the plunger partially blocks the water flow at all times, slowing down the emptying process. Furthermore, the system will

necessitate a rubber seal to prevent leakage. The second system uses an external slider plate valve, actuated by an externally mounted servo. This system is exposed to the airflow and will increase drag unless a fairing is provided; however access to the mechanism is excellent, and in the retracted position the slider is out of the way of the water flow. The decision matrix for the dumping system is shown in Table 2.

Table 2 – Dumping system decision matrix

FOM	Manufacturability	Weight	Drag	Reliability	score
Weighting factor	0.1	0.25	0.25	0.4	1
Internal Plunger	2	2	3	1	1.85
External Slider Plate*	3	2	2	3	2.5

* with aerodynamic fairing

3.3. Airframe Configuration

Decision matrices were used to determine the alternatives that best met the mission requirements for each component. Pros and cons were discussed, figures of merit were chosen and a weighting factor was applied to the rating of each component, yielding a final score. For each alternative, the final scores were compared and the highest was chosen.

3.3.1. General Configuration

Configurations considered during this early phase of design included flying wing, canard, biplane, conventional, twin fuselage, and blended wing/lifting body (Figure 4).

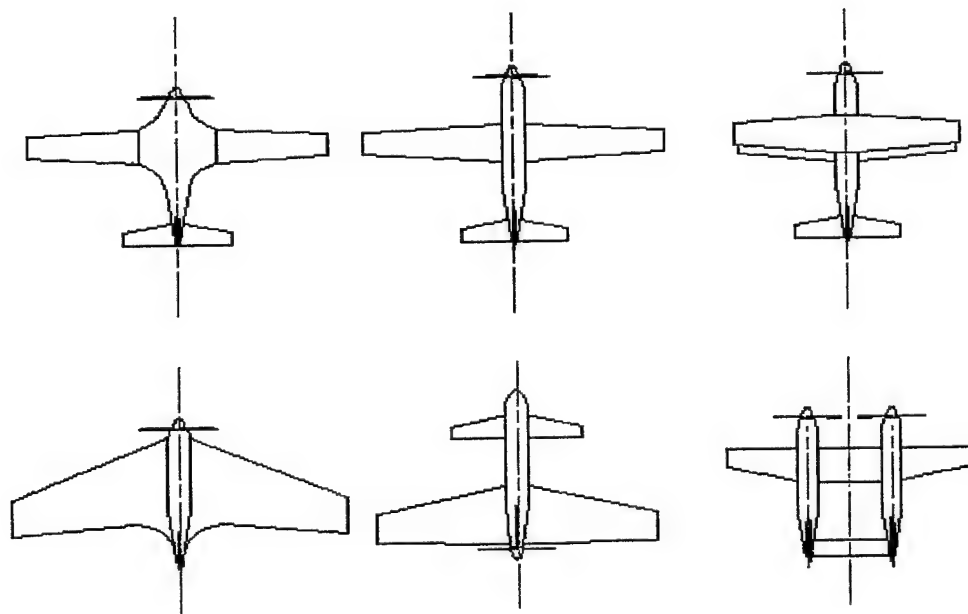


Figure 4 – Candidate Configurations

A flying wing was considered because of the reduction in wetted surface and weight inherent in this configuration. The elimination of tail surfaces also promised a reduction in RAC. However, flying wings require airfoils with reflexed mean camber lines near the trailing edge. This produces a positive pitching moment that obviates the need for a tail. Unfortunately, the maximum trimmable coefficient of lift for that airfoil is adversely affected – therefore

requiring a larger wing to meet the takeoff constraint, negating the benefits of this configuration. The high pitch-down moment created by the flaps upon deployment cannot be offset by the limited trim capabilities of a tailless airplane. Handling problems might also arise during the possible CG shift caused by the dumping of the payload. Under those conditions, an aircraft with more control authority would be desirable.

Biplanes achieve a greater total lift by increasing the wing area and the wing can be made lighter if externally braced, albeit at the expense of drag. The relative closeness of the sets of wings leads to interference drag and a reduction of efficiency. In fact, a monoplane with the same reference area but greater aspect ratio achieves greater efficiency. Since this year's rules place no limit on the wingspan, the biplane configuration presented no real advantages.

The team also investigated the canard configuration. This concept seemed promising because both foreplane and main wing act as lifting surfaces, and a smaller, more compact airframe could be built. On the other hand, the particular lift distribution between the two surfaces requires special consideration. At high angles of attack, the foreplane must stall before the main wing to ensure that an unrecoverable departure does not result. This makes a canard aircraft perform poorly during short takeoff – since the canard is designed to stall before the main wing it prevents the main wing from reaching its maximum lift coefficient. These and other complications involved with fine-tuning this configuration prompted the design group to give the canard configuration a low overall score.

The twin fuselage configuration proves attractive only if a twin-engine solution is chosen. The mass of the fuselages is far from the centerline, which results in high moments of inertia and sluggish lateral handling. The added expense of a second engine makes this arrangement unattractive. Furthermore, the water payload would have to be mounted in two separate tanks in order to avoid rolling moments. It is doubtful that this configuration would fit inside the container, and the second engine adversely affects the RAC.

The blended wing/lifting body configuration was rejected early-on, because of many reasons: at the comparatively low speeds and Reynolds numbers at which the model operates, lifting bodies (basically low-AR wings with a low C_L/C_D) do more harm than good. A blended wing-body would also be much more difficult to manufacture and operate, and presented no advantages in terms of rated aircraft cost over a more conventional configuration.

Finally, a conventional layout was evaluated. While this configuration did not excel in any area, it presented no technical challenges, and its handling characteristics were well understood. The last point was deemed very important, as in previous years the variable wind conditions have played a major effect on the outcome of the competition. It is easy to manufacture, and the design team generally felt that it conformed well to this year's set of rules.

Table 3 shows the results of the team evaluations. Significant figures of merit in the selection of the configuration were ease of manufacture, rated aircraft cost, performance, ease of water release and weight. Rated aircraft cost was rated highest because of its impact on total score, followed by weight, performance, and water dump efficiency, all of which affect the score to a lesser degree. Finally, manufacturability was given a lower coefficient because based on the team's previous years' experience, no more than two airframes were expected to be built.

Table 3 – Figures of merit for general configurations



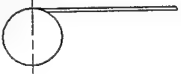
Description	Manufacture	Performance	Rated cost	Weight	Water Dump	score
Weight Factor	0.1	0.2	0.3	0.2	0.2	
Flying Wing	1	1	3	1	2	1.8
Biplane	2	2	2	1	2	1.7
Conventional	3	3	2	2	2	2.3
Canard	3	2	2	2	1	1.9
Blended Wing/Body	1	3	2	2	1	1.9

Based on the results of the configuration matrix, the conventional configuration was deemed the most promising of all, and its study was refined in the preliminary design phase.

3.3.2. Wing Placement

In terms of wing/fuselage arrangement, the wing can be classified in three categories: high wing, mid wing, low wing. Figures of merit include: lateral stability, ease of manufacture, interference drag, payload release, and serviceability. Rated aircraft cost remained unchanged from one configuration to another. Having selected the water dump system, the team proceeded to evaluate the wing placement that hindered operations the least while possessing adequate performance. A mid-wing is desirable from a drag standpoint; a low wing would keep landing gear height small. Figures of merit relative to wing placement were payload deployment, lateral stability, drag, and manufacturability. Table 4 shows the decision matrix used in the downselection.

Table 4 – Figures of merit for wing placement

	Figures of Merit	Manufacturability	Lateral Stability	Payload Deployment	Drag	Score
	Weighting Factor	0.1	0.1	0.4	0.2	1.0
Low Wing		3	2	1	2	1.9
Mid Wing		1	2	0	3	1.1
High Wing		2	3	3	2	2.7

3.3.3. Fuselage Configuration

During the mission, aircraft weight will change as a result of the payload being released. As mentioned before, the center of gravity of the payload was made to coincide with the center of gravity of the airplane to keep the payload from destabilizing the aircraft by shifting the center of gravity location.

An important factor that strongly affected the preliminary design of the fuselage was the length of the container box that the airplane had to fit in. A long fuselage provides a large moment arm for the tail surfaces. However a fuselage length of more than four feet would require a plug-in tail arrangement, which results in a heavier, less rigid

airframe. Because the control surfaces do not have cost assigned to their areas (thus do not affect RAC), it was decided that it would be cheaper and simpler to build an aircraft with a short fuselage and a large empennage to compensate for the short moment arm that would result.

Table 5 – Fuselage Length Figures of Merit

FOM	Construction	Weight	Drag	Complexity	Control	score
Weighting factor	.1	.2	.15	.3	.2	1.0
4ft long body	3	3	2	3	1	2.3
Plug-In Tail Boom	1	1	3	1	3	1.65

The results of the analysis performed on fuselage configuration indicated that overall, the benefits of a one-piece construction would outweigh the disadvantages, and would be preferable to a longer, plug-in fuselage (Table 5).

3.3.4. Engine Configuration

During the conceptual design of the aircraft it was calculated that a single engine operating with the expected battery pack voltage would be able to provide the takeoff power required while not exceeding the 40 ampere limitation dictated by the rules on the engine current. Since large engines are generally more efficient than smaller ones and the stringent takeoff constraint did not drive the design towards the use of multiple engines, a single large engine would be used instead.

Both single motor and twin motor configurations were considered. It was determined universally that for a given power requirement, the single motor solutions outperformed the twins in final score (Table 6). This was caused by the additional cost of having more than one motor and speed controller, because for a given power level, two smaller motors, gearboxes and propellers weigh more than a single (increasing empty weight), and because larger motors generally have higher efficiency. It was decided that unless no single motor of sufficient size was available, the aircraft would not have two motors.

Table 6 – Number of Engines Selection

Description	Weight	Efficiency	Rated cost	score
Weighting Factor	.3	.4	.3	1.0
Single Engine	3	3	3	3.0
Twin Engine	2	2	2	2.0

3.3.5. Landing Gear Configuration

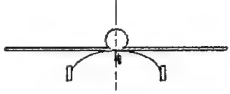
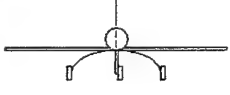
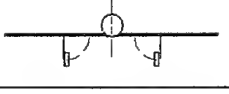
The landing gear design of a propeller driven airplane is governed by two major constraints. The first is to provide adequate clearance between propeller tips and the ground. The second is to permit the plane to rotate on both takeoff and landing so that the wing's angle of attack comes close to the stall angle of its airfoil. At this angle of attack, the wing is near the airfoil's maximum C_L . This permits the aircraft to achieve the lowest allowable landing and takeoff speeds. The configurations considered were realistically limited to taildragger and fixed or retractable tricycle.

A taildragger configuration affords more propeller clearance and low drag. Unfortunately, the tail-dragger gear configuration also exhibits inferior ground handling characteristics compared to those of a tricycle gear setup, namely a propensity for ground looping.

For the reasons above it was decided to build the aircraft with a tricycle landing gear system. While exhibiting higher drag than a taildragger configuration, the tricycle gear makes landings possible at sideslip angles and is generally more forgiving of rough ground handling. The Wichita, KS contest location is fraught with often-switching wind conditions, making the likelihood of having to land in a cross-wind condition very high.

A retractable landing gear eliminates a major source of parasite drag, but adds considerably to the complexity of the aircraft. An additional set of servos would be required, and it is doubtful that typically delicate retractable systems could cope with hard landings. The results of the landing gear evaluation, shown in Table 7 show the superiority of the tricycle arrangement in the context of this year's competition.

Table 7 – Landing gear configuration figures of merit

	Description	Ground handling	Propeller clearance	Manufacturability	Weight	RAC	Score
	Weighting Factor	.3	.2	.1	.1	.3	1.0
	Taildragger	1	2	3	3	2	1.9
	Tricycle	3	2	3	2	2	2.4
	Retractable	3	2	1	1	1	1.8

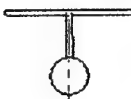


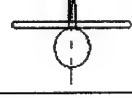
3.3.6. Empennage Configuration

For an airplane in level flight at a steady-state, the sum of the positive and negative pitching moments must be zero. The balancing is achieved in a conventional and canard design by the use of a horizontal tail or foreplane. The horizontal tail's angle of attack, relative to the wing's downwash, should be sufficient to provide lift or most often, down force required to provide equilibrium.

Figures of merit considered for the tail configuration were rated aircraft cost, manufacturability and effectiveness. Because of its larger impact on score, the RAC was given a higher coefficient, than the remaining two categories.

The H-tail configuration was considered as having a set of benefits for the particular mission that this airplane would be designed for. An inverted H-tail has the benefits of not requiring assembly after removal from the storage box. However, the H-tail might cause ground clearance issues and is also more expensive, requiring two servos for control and being counted as two vertical surfaces with control. The outcome of the team deliberations on empennage configuration are shown in Table 8.

Table 8 – Figures of Merit for Tail Configuration

Description	Manufacturability	Effectiveness	RAC	Score
Weighting Factor	0.3	0.3	0.4	1
	2	3	2	2.3
	1	2	3	1.8
	1	2	1	1.1
	3	3	2	2.6

The conventional tail offered the best compromise in overall performance and cost, and was selected for further study.

3.4. Materials selection

The next decision made was the choice of materials and construction methods. These affect the strength, rigidity, durability, reparability and manufacturability of the aircraft.

Three materials and construction methods were considered: conventional buildup of lightweight wood skeleton and Monocote skin, conventional buildup of carbon fiber skeleton and skin, and composite skin with foam core. The figures of merit that were selected for the conceptual material selection were: ease of manufacturing, reparability, and durability. The rated aircraft cost is not explicitly affected by the construction method; however, it is dependent on gross weight, which varies with the different construction techniques.

Table 9 contains the elements of the decision matrix and the figures of merit used in the downselection of materials and construction technique.

Table 9 – Material Selection

Description	Manufacture	Reparability	Durability	RAC	Score
Weighting Factor	0.2	0.3	0.3	0.2	1
Mixed carbon/kevlar with foam core	3	3	2	3	2.7
Wood with Monocote	2	2	2	1	1.8
Molded composite	1	2	2	3	1.9

The data concluded that the mixed carbon/kevlar with foam core had the greatest potential to satisfy the rigidity and durability requirements at the lightest weight possible. Additionally, the foam core allows for accurate construction of the wing airfoil section without major tooling, and is a method the team was familiar with.

3.5. Conceptual Design Results

As a result of the conceptual design stage, a single-engine, one-piece conventional fuselage layout was selected. This configuration, together with a high-set wing and fixed tricycle landing gear, promises trouble free water dumping operations, which was a key concern in this design phase.

4. Preliminary Design

The aircraft's conceptual design stage laid the foundation for the design and specific attributes and characteristics were obtained in the preliminary design phase. The preliminary design phase utilized design trades and parameterization to guide the development of the design to an optimized solution.

The preliminary design stage commenced following the completion of the conceptual configuration. The objective of the preliminary design phase was to determine weight, size, energy required, and other physical characteristics of an optimized configuration that would best satisfy both missions. The aircraft's wing area, wing span, battery requirements, motor and propeller combination, empennage size, and weight of the aircraft were all optimized to increase final score.

4.1. Wing Preliminary Design

The attributes for the wing were each investigated for an optimum airfoil, wing area, aspect ratio, and planform. Trade studies were conducted to determine an optimized solution that would satisfy the mission requirements while minimizing RAC and maximizing score.

4.1.1. Airfoil/High Lift

In sizing the aircraft, many different airfoils were evaluated to find the airfoil and wing configuration that would maximize score and performance. In most aircraft, the airfoil has to be designed to meet two conflicting requirements – one imposed by the takeoff/landing and other by the cruise segment. The airfoil has to provide high lift to meet the takeoff constraint – therefore favoring the choice of a highly-cambered, thick airfoil. At the same time, the airfoil has to be aerodynamically “clean” at the design cruise/dash lift coefficients in order to reduce aircraft drag which is best accomplished by a thin, uncambered airfoil. These different lift requirements were very difficult to meet with any single, commonly used model aircraft wing section. In attempt to achieve both, an adjustable trailing edge camber changing airfoil was investigated. Airfoil selection focused on achieving a good balance between these two requirements.

When conducting preliminary analysis of the mission requirements for the 2004 competition, it was judged that generally, the aircraft would be flown at two distinct speeds. During the “water dump” lap, the aircraft would fly relatively slow, being constrained by the necessity to allow for sufficient time for all of the water to dump. It was believed that because of the fixed time constraints and short flight times during this mission, a large point gain would not be possible to achieve. However, it appeared to be extremely beneficial to perform the ferry mission at the maximum possible speed. In order to back up these preliminary conjectures, a trade study was conducted on the pros and cons of different ways to fly this mission.

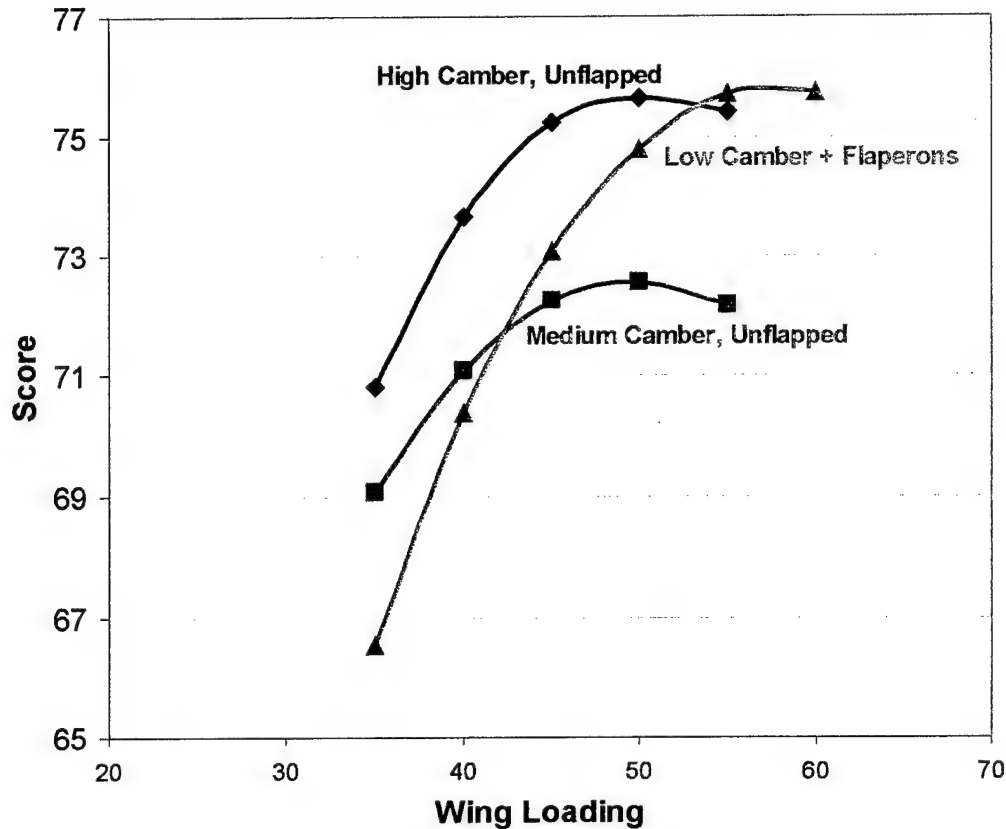


Figure 5 – Airfoil type study

It can be seen from the trade study above, that the medium-camber, unflapped wing would produce the lowest score out of the three configurations attempted. Unable to produce the high CL values, the aircraft of this type would have to have excess power in order to accelerate to a higher takeoff speed in the constraint of the runway. It can be seen that the RAC increase imposed by the flap servo or the drag increase of the high-camber wing are more than negated by the benefits of improved takeoff performance.

The peak scores of configurations with high-camber unflapped and the low-camber, flapped wings can be observed to be very close. When considering the weather likely at the Wichita Kansas fly-off location, a higher wing loading aircraft was desirable because of its lower sensitivity to gusty wind conditions. Therefore, a choice was made to focus on a low-cambered wing with flaperon high-lift devices. The flaperons extend for the inboard 80% of the wingspan and 20% of the chord, and are used for roll and camber control.

4.1.2. Aspect Ratio

For a fixed wing area that is optimized for the mission, the aspect ratio is constrained by the RAC which places a weighing factor on wing span. As the aspect ratio is increased, the volume of the foam cores decrease while the bending moment increases with length, driving the weight of the spar caps to increase. High aspect ratio wings have extremely thin sections that decrease the moment of inertia of structural components, requiring a heavier spar. When considering the construction methods used, the following plot could be derived, and an optimum aspect ratio range found.

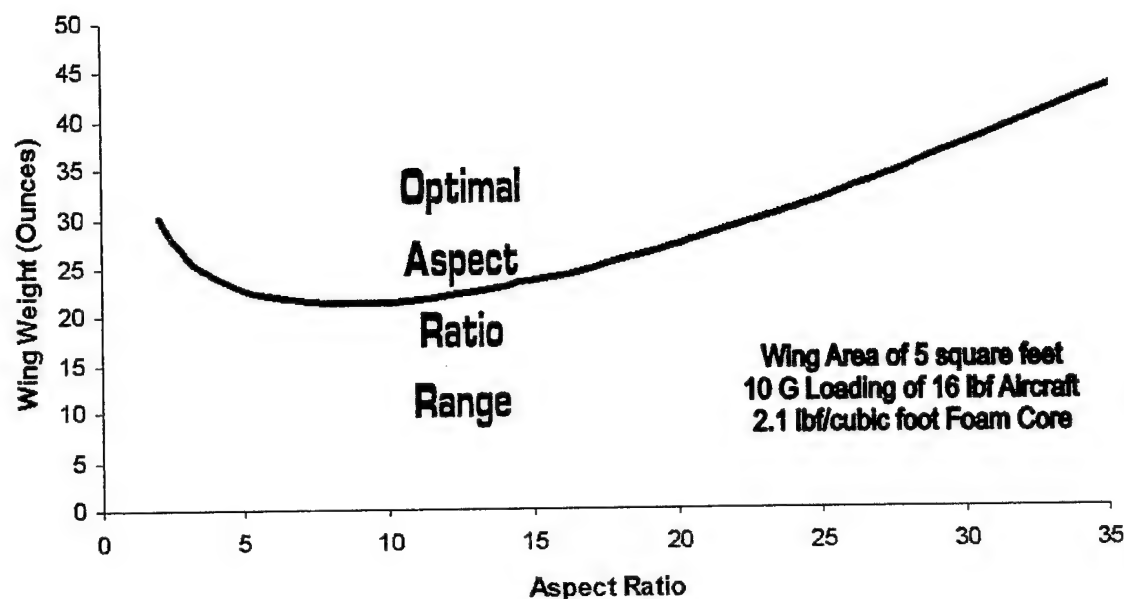


Figure 6 – Foam Core Construction Wing – Weight vs. Aspect Ratio


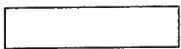


4.1.3. Wing Planform

Planform is the shape of the wing as viewed from above. The wing planform is important in defining the performance of the aircraft. It may be swept, elliptical, straight, tapered, or a combination of both. Swept wings were ruled out immediately because they only offer disadvantages at the expected flight conditions.

- **Elliptical wings:** This is the ideal wing planform. It has the lowest induced angle of attack and induced drag, and stalls evenly across its span. These factors increase for rectangular and tapered wings. Structurally, the elliptical wing is difficult to manufacture, especially using some of the methods likely to be used on this type of an airplane.
- **Rectangular wings:** Rectangular wings are the easiest to design and build. While suffering in comparison with an elliptical wing, it maintains a constant Reynolds number across its span. A tapered wing of the same area could have tip Reynolds numbers in the high drag/ lower lift and stalling-angle range of low Reynolds numbers, leading to premature tip-stalls at low speeds. Structurally, the wing roots need reinforcing, owing both to narrower root chords and higher bending moments that are generated as a result of the center of lift of each wing being farther from the centerline than an elliptical or tapered wing.
- **Tapered wings:** A tapered wing with a tip chord of 40 percent of the root chord closely approximates the ideal elliptical planform both in induced angle of attack and induced drag. For wings of model aircraft, this taper ratio results in narrow tip chords and undesirably low Reynolds numbers at low speeds. Increasing the taper ratio produces larger tip chords. Lift is lost at the tips; the wider the tip chord, the greater the loss. The resulting loss in efficiency isn't great and is the lesser of the two evils. Structurally, the tapered wing has lower root bending moments, and the wider, deeper root chord provides the greatest strength where it's needed most- at the root. A tapered wing can be lighter yet stronger than a rectangular wing of the same area.

- Modified Schuemann wings: This planform has an elliptical leading and trailing edge for 70% percent of the semispan and a sheared wingtip. It comes close to the elliptical wing in efficiency and is more easily produced than an elliptical wing. The rectangular inner portion is wider in chord, which provides a strong root, and bending moments are lower than for a rectangular wing.

Table 10 – Wing Planform Design

	Figures of Merit	Ease of Manufacture	Efficiency	Strength to Weight	Stall	Score
	Weighting Factor	0.3	0.4	0.1	0.2	1
Elliptical		1	3	3	1.5	2.1
Rectangular		3	1	1	3	2
Simply Tapered		2.5	2	2	2.5	2.25
Modified Schuemann		2	2.5	2.5	2.5	2.35

The design team chose the Modified Schuemann wing because it represents the best compromise in terms of performance.

4.1.4. Motor Selection

To ensure a competitive configuration, proper motor selection along with the rest of propulsion system is imperative. The motor selection was based on trades of motor weight, the power produced by the motor, the maximum current draw, which all in some way drive the rated aircraft cost. The power output from the motor into the air is inversely related to the takeoff distance. Electric motors are not ideal and suffer from heating, frictional, and magnetic losses, not to mention the induced losses from the motor controller. Using a second motor halves the total propulsive efficiency of the system and also negatively effects the weight and the RAC. The motor selection will be an optimal trade between propulsive efficiency and cost.

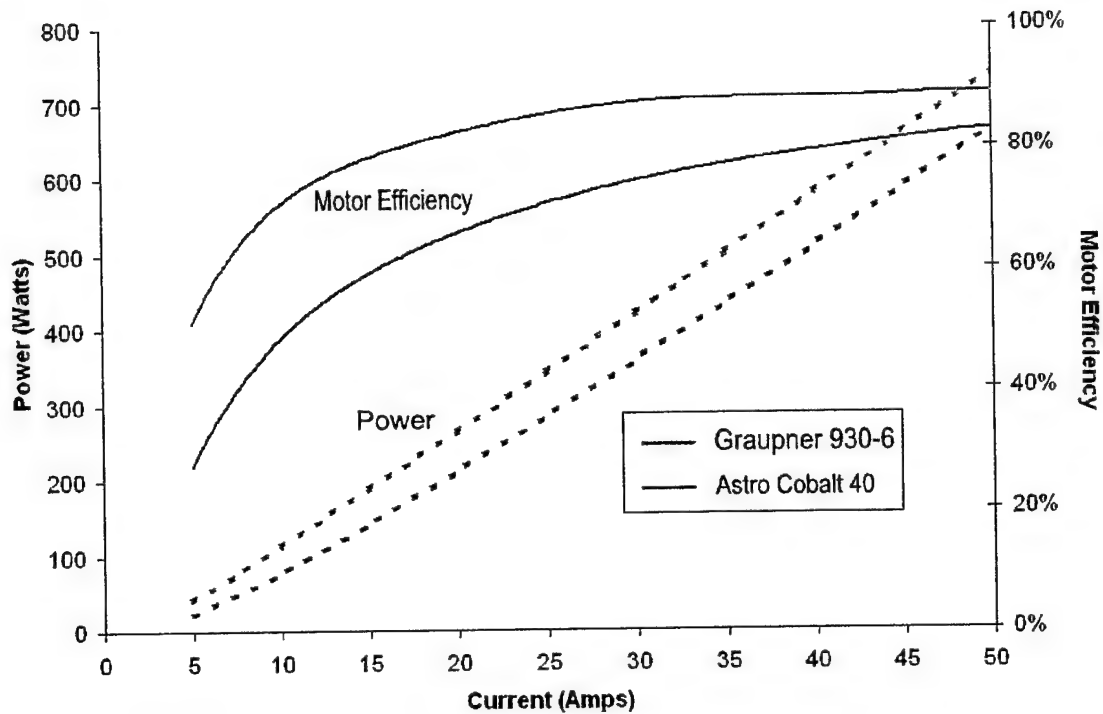


Figure 7 – AstroFlight Cobalt 40 and Graupner Ultra 930-6, 16V Input

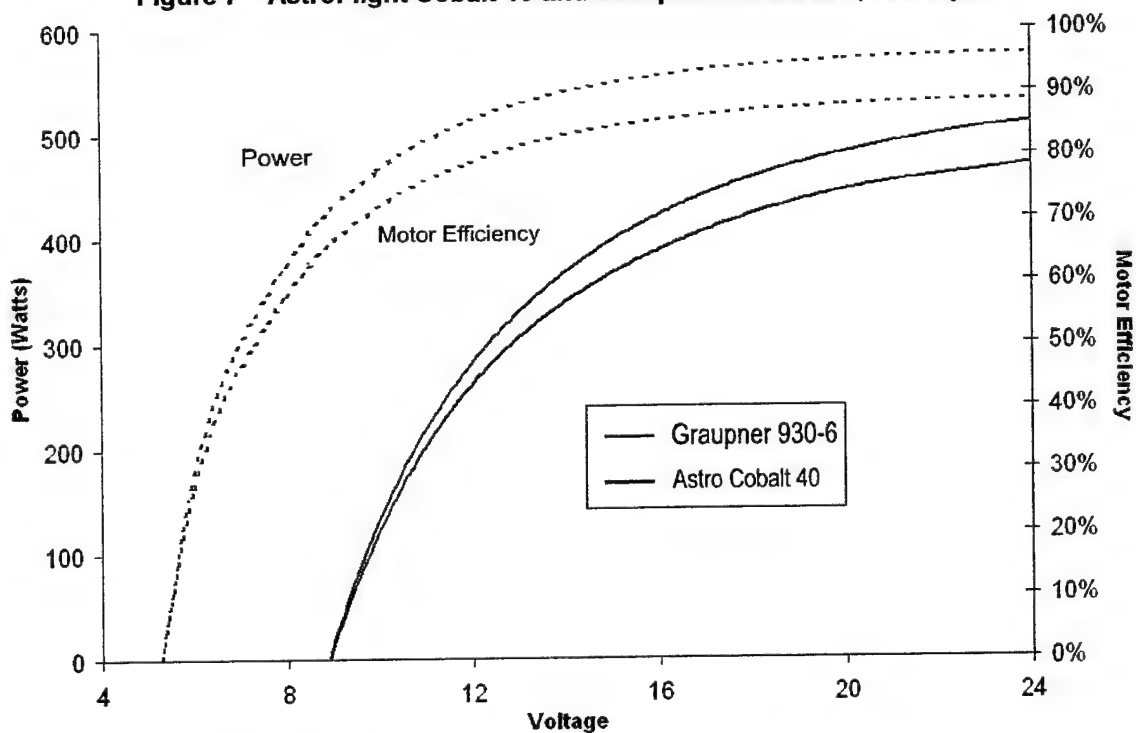


Figure 8 – AstroFlight Cobalt 40 and Graupner Ultra 930-6

After initial sizing, it was determined that the propulsion requirements for each of the missions are constrained differently. The "fire fight" mission is the heavy-lift, slow flying mission which effectively sized the maximum power required to be output from the motor at takeoff. The aircraft required a propulsion system able to run on

approximately 15-16 NiCd cells, and be capable of handling 600-650 watts to attain the necessary takeoff and climb performance.

To evaluate the performance of the motors available for the aircraft, a Visual Basic subroutine modeling electric motors was written. This model uses motor parameters including Kv (RPM/V), idle current, armature resistance, RPM and thermal limits to calculate output power and efficiency for DC motors. This program was used in conjunction with a propeller model and the mission simulation to compare the various motors offered by AstroFlight and Graupner. After testing of sample motors from both AstroFlight and Graupner, it was discovered that the Graupner motor (930-6) tested was more efficient than a comparable size AstroFlight motor (Astro 40). Because of these study results and previous years' experience the team decided to select motors from the Graupner product line.

4.1.5. Propeller Pitch and Diameter

Propeller selection will be a result of maximizing the effectiveness of acceleration of the air at certain airspeeds. Typical momentum characteristics of a propeller show that it is much more efficient to have a large propeller accelerate a fixed mass of air a small amount than to have a small propeller accelerate a fixed mass of air a large amount. Due to the high level of complexity along with the lack of availability of variable pitch propellers at this scale, a trade must be made for an optimum pitch to diameter ratio. A general trend in propeller sizing, selecting the right pitch of a propeller is similar to selecting the right gear in a car transmission. The lower pitch propeller is more effective in translating power from the motor into the air at lower speeds while higher pitch propellers will have higher propeller efficiencies at higher speed. This will be a trade between thrust available at takeoff and top speed desired at dash. The optimal speed of the aircraft for the "Fire Fighter" mission will be constrained by the time required to off load the water payload and the for the "Ferry" mission maximizing flight speed to reduce mission times.

4.1.6. Battery Pack Sizing

The battery pack selection has the most impact on the rated aircraft cost out of all components of the design. The batteries are represented in the RAC twice, first part of the Manufacture Empty Weight then again for Rated Engine Power. The number of cells and the energy capacity size the maximum flight speed, endurance, and takeoff distance. The cell count sizes the voltage and maximum RPM while the capacity constrains the endurance of the aircraft. To attain an optimum RAC, the battery pack must be sized carefully. Each of the missions constrain the energy required differently, the "Fire Fight" heavy-lift mission sizes the cell count for takeoff while the "Ferry" mission fast flight sizes the capacity for the cells. From these two constraints a trade between cell count and capacity can be made.

If possible, the battery pack should be sized for complete discharge by the end of the mission in order to minimize the RAC. For preliminary sizing, the commercially available cells were plotted below in a Ragone plot. This plot provided a qualitative way of comparing how much power and energy a cell would produce at a given discharge times. With the compiled data displayed, it can be seen that the lower capacity cells have lower energy densities and efficiencies at high current discharge rates while the higher capacity cells appear to have higher performance. From this data the pack selection can be better optimized in the detail design phase for lowest RAC while maximizing the flight score.

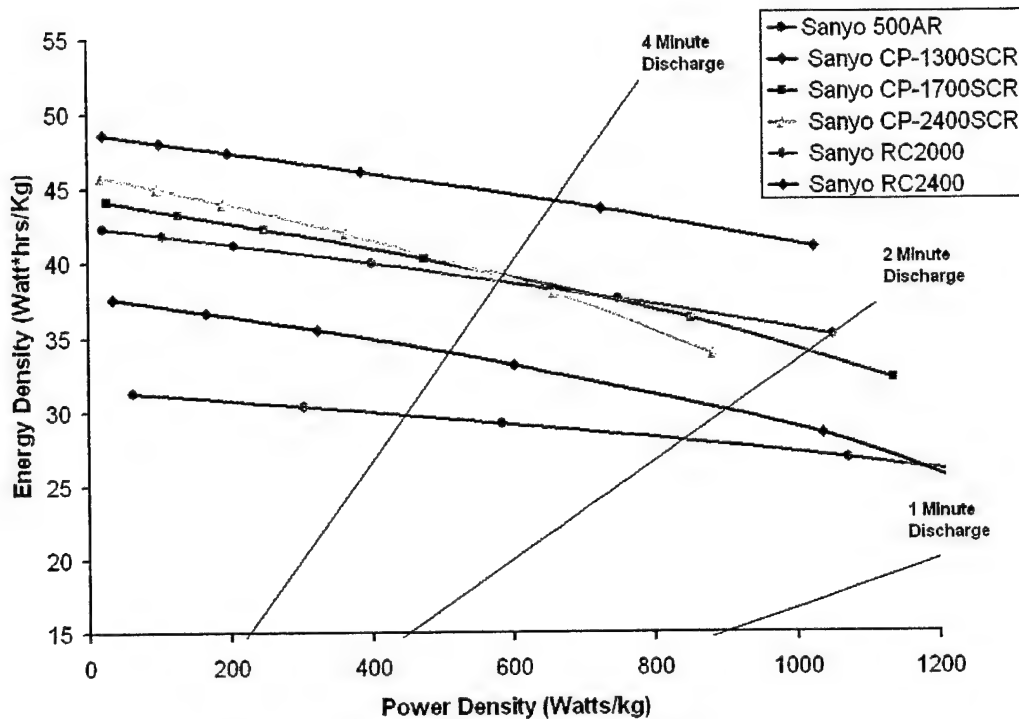


Figure 9 – Ragone Battery Plot

The contest rules specify that the propulsion system must be powered by a nickel cadmium battery pack no more than 80 oz in weight. Numerous types and sizes of NiCd batteries were available. Approximately 30% of the rated aircraft cost of most configurations was due to the battery cost, which is directly related to battery weight. Because of this, battery selection heavily drove the design. Depending on the characteristics and type of NiCd cell used, there are limits to the maximum power and efficiency to the rate of discharge. Research on the characteristics of NiCd cells was conducted to choose the best battery to fulfill both the aircraft's energy and maximum power requirements. The 40amp fuse restriction and the voltage requirements/maximum current capabilities of the available motors were all considered during the search.

Two styles of NiCd cells were investigated in detail, the high capacity Sanyo KR series, and the NiCd cells typically used for electric powered R/C models, the fast charge Sanyo R series. Table 11 shows the characteristics of each cell type.

Table 11 – Battery Cell Comparison

Nicad Cell	mAh	Weight (oz)	mOhm/cell	Amps @ 1.0V	Watts/oz	Watt-hr/oz
KR-1100AAU	1100	0.85	20	10	11.8	1.55
KR-1700AU	1700	1.25	14	14	11.4	1.63
N-1250SCR	1250	1.50	4.5	44	29.6	1.00
RC-2000	2000	2.00	3.8	53	26.3	1.20
RC-2400	2400	2.15	3.6	56	25.8	1.34
CP-2400SCR	2400	2.10	3.6	56	26.5	1.37
CP-1700SCR	1700	1.65	4.5	44	26.9	1.24
CP-1300SCR	1300	1.25	6.5	31	24.6	1.25

The fast charge cells are designed to handle high maximum current and therefore are well suited for typical electric aircraft motors. The specific power density of these cells is on the order of 25 Watts/oz. These cells have a specific energy density of approximately 1.2 Watt-Hours/oz. The new Sanyo "CP" series cells have the highest energy density and excellent power density compared to all of the fast charge cells.

The high capacity KR cells were considered because of their higher energy density (1.6 Watt-hours/oz). The compromises in the cell design that give them the high capacity also hurt the cells' internal resistance – affecting their maximum discharge rate. Therefore, the power density is only half that of the fast charge cells, approximately 11 Watts/oz. Unfortunately, most of the design concepts required nearly 650 Watts of peak power to meet the take off constraint and minimum climb requirement, making the high capacity cells unsuitable. NiCd cells delivering power at their maximum rate do not operate efficiently, significantly reducing their delivered energy.

After deliberation, it was decided to proceed to detail design having chosen the Sanyo CP-xxxxSCR range of cells as the ideal cell type to use.

4.1.7. Tail Sizing

The tail surfaces are sized for allowing adequate static and dynamic stability in pitch and yaw as effectively and efficiently as possible. The horizontal tail width is limited to be 25% the wingspan while the vertical must be able to be fit into the box. Since the RAC increases with the overall aircraft length and weight, a compromise will be made. Due to the historical weather characteristics of Wichita Kansas, large cross-winds are typically present therefore adequate control authority will be required to handle these conditions.

4.1.8. Load Factor Sizing

The competition rules require a "tip test" both right side up and inverted which simulates positive and negative 2.5 G loading. Through previous years experience and this years need for minimized mission times in both heavy-lifting conditions and high speed empty laps, the load requirements are much greater than 2.5 G. Through an accurate weight buildup and mission simulation, the speeds and loads that will be experienced in flight can be estimated for high both high lift and maximum allowable bank angles experienced. These loads will then have a factor of safety designed into them providing a safety margin. This safety margin ultimately increases the structure weight, power required, and in turn the RAC. The predicted load factor value for which the aircraft structure will be sized can be seen in Figure 10.

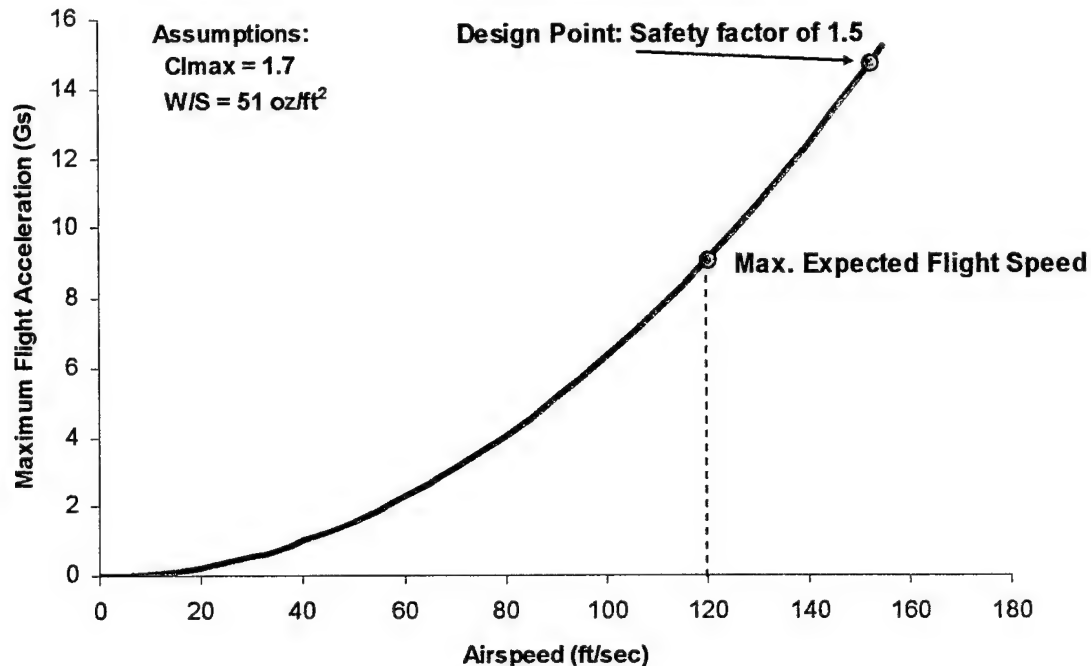


Figure 10 – Maximum Flight Acceleration

4.2. Analytical Tools

Several analytical methods were used in design analysis, including tools used by previous Cal Poly DBF teams, and additions in both Visual Basic and Microsoft Excel.

4.2.1. Spreadsheet Application

Previous years of the DBF competition, the performance design of the airplane was analyzed using an interactive Microsoft Excel based program. Although rudimentary, this program provided good indication of the parameters driving the design but lacked the ability to easily implement and modularize the software. Therefore a new performance design program (DBF03/04) was created from the ground up using the Microsoft Visual Basic programming language. This program used a Microsoft Excel front end similar to that used by the previous version of the design software, but was more powerful and provided a much higher ease of expansion than the previous version. This software simulated the performance of the aircraft through all the stages of the mission, iteratively calculating thrust, drag and other characteristics of the aircraft performance. For example, DBF02 used a simple approximation formula to calculate takeoff distance. DBF03/04 iterated through increments of 0.1 second, calculating thrust, drag, lift, power input to the engine and other parameters in order to output an answer with a higher degree of precision. A particular benefit of this program was noticeable during this year's design process – unlike in previous years, the weight of the aircraft changed during flight. The software was modified to accurately simulate this weight change during flight.

The program estimated the overall performance of the airplane by combining many specific performance calculations and estimation methods.

- **Weight** – This estimate was created from weight/area constants that were obtained from weighing model parts created via different traditional RC-model construction methods.

- **Drag** – A flat-plate drag estimate was created based on CD estimates and experience compiled by the previous year's DBF teams. A drag estimate using skin-friction coefficients following methods out of Shaufele² design text was also created, and the results of two calculations compared.
- **Thrust** –The curve predicting thrust was derived using a combination of two methodologies – using momentum methodology to predict the decline of thrust with increase in forward speed and using static thrust equations from AstroFlight Electric Motor Handbook³.
- **Energy Consumption** – A propulsion system efficiency constant (efficiency in converting electric energy into volts – motor + propeller + drive efficiencies) was used to estimate the amounts of current/energy that will be drawn out of the batteries during the duration of the contest. This was later pooled with the propulsion system selected and designed for and iterated upon to further ensure an accurate prediction.
- **Mission Time** – This parameter was created by adding together the following separate mission segments: Takeoff, Climb, Turns, Water Dump/Cruise, Landing, Refill.
- **Cost** – A cost estimate was easy to create by simply applying the given rules to the airframe parts, the dimensions of which were estimated by the simulation components described above.
- **Mission score** – This result was obtained by using the preceding estimates in the context of the competition rules.

The 4 main variables that were systematically modified in order to achieve the highest possible flight score were Airplane Weight, Wing Loading, Aspect Ratio, Number and Type of Batteries. Other assumptions and initial values were used, but did not vary when trying to select an optimum airplane configuration. The general functioning of the software can be visualized from Figure 11 below.

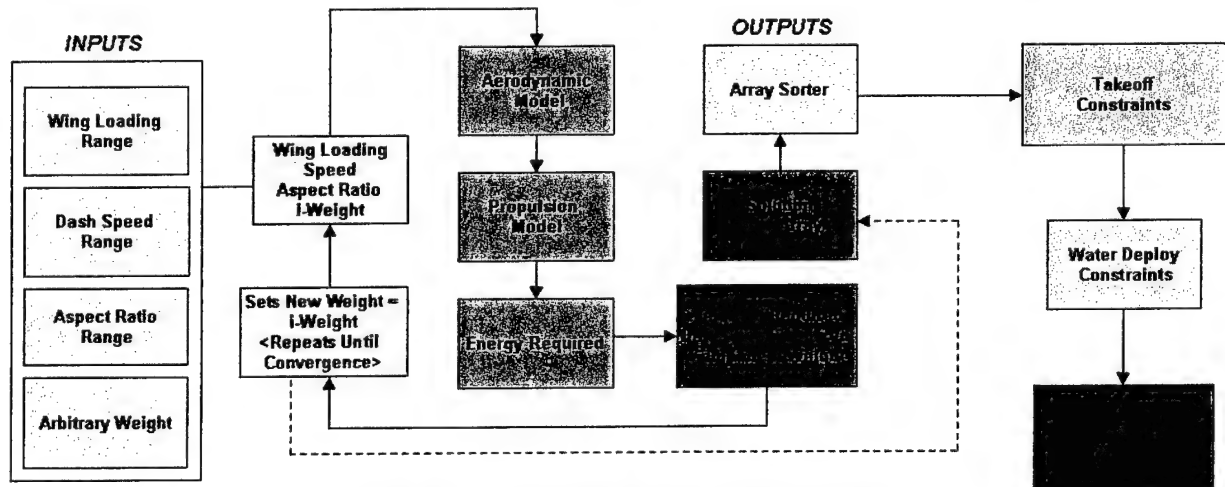


Figure 11 – Simulation Program Schematic

A comprehensive set of data was output to show the performance of the aircraft in the entire mission, allowing educated design choices to be made and new designs to be evaluated. Being written in Visual Basic, the program could be made modular, having different functions and subroutines that would execute the same calculation using data inputs from different sources.

Besides doing performance estimation for the aircraft, the program evaluated many other variables, all of which affected the preliminary design decisions made.

- Estimation of the effects of aspect ratio on weight (because of the varying strength required from the spar cap) and on wing efficiency (induced drag).
- Estimation of wing root bending moment and output of necessary spar cap thickness.
- Estimation of weight breakdown of the aircraft's components based on configuration.
- Effects of wing planform on efficiency
- Aircraft longitudinal static stability
- Wing lift distribution depending on the planform picked

The price breakdown output of the spreadsheet enabled the team to visualize which components of the aircraft were of the most impact on the final score, therefore allowing the optimization process to focus on addressing those significant score drivers.

4.2.2. Other Simulation Methods

Many of the tools used in the design process were created by the team members using Visual Basic or in Microsoft Excel. These programs include an electric motor/ propeller model, an aerodynamic model, a weight estimation spreadsheet, a longitudinal static stability model, takeoff and climb simulation, and a lift distribution spreadsheet. These tools were incorporated into a 03/04 DBF mission simulation model that included a cost model. To check validity, aircraft with known performance from the 99/03 competition years were also run through the simulation successfully.

One tool not developed by the team members was X-foil, written by Mark Drela of the Massachusetts Institute of Technology. After learning to use X-foil, results from low Reynolds number wind tunnel testing performed at University Illinois Urbana Champaign were compared with data produced by X-foil. At the relatively high Reynolds numbers that this aircraft will fly at, the correlation between test data and predicted performance was excellent. Experience gained with these correlations and the good results obtained with the D9 airfoil designed using X-foil and flown during the 02/03 DBF contest gave the team confidence in the design tool.

4.2.3. Numerical Water Dump Analysis

To enable the proper sizing of the aircraft, the time required to off load the water must be predicted. This part of the mission was simulated by conducting several design iterations on a tank system to minimize the time to empty a four liter water tank. A tank similar to that simulated was then constructed to validate the design point.

A simulation using hydrostatic analysis to show the volumetric flow rate and ultimately the time required to dump 4 liters of water from a given tank geometry was created. The analysis also took into account the acceleration acting on the fluid which is known to vary in flight according to turn performance. According to the flight accelerations and tank geometry, the estimated water dump time can be shown below in Figure 12.

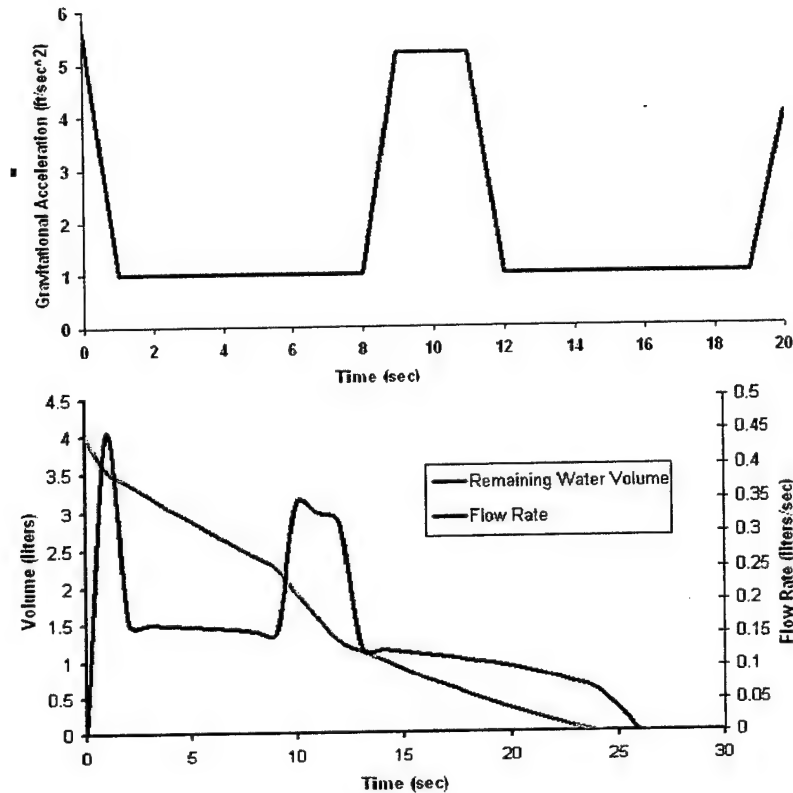


Figure 12 – Estimated Accelerations and Dump Characteristics – No Ram Air Effects

4.2.4. Empirical Water Dump Analysis

After numerical predicting the expected dump time required off-loading the water, it was decided to validate this with a working model. A model tank was attached to the 2003 DBF aircraft *Bareback*, and a servo used to actuate a rudimentary valve and vent. The aircraft was then flown at 40 feet/sec in a flight path similar to that flown in competition. Unlike our predictions, the water took approximately a minute to off-load – twice the time predicted. With further analysis from the flight video, it appeared that the water was atomizing upon exiting the orifice due to the angle of the free stream air hitting the hole. This revealed the need to conduct further testing with a possible flow blocker.

After the first tank iteration it was shown that minimization of exit losses is imperative to maximization of flow rate. From this observation, a nozzle was created by using a .25 inch constant radius router bit to machine a cylindrical piece of Delrin into a nozzle. The nozzle was then attached to the base of the tank and sealed with several layers of resin and glass. A stagnation air pressure port was fitted to the tank to pressurize the tank. Data was then collected at a range of airspeeds of 0 to 70 feet per second. From this data it can be seen that above 40 feet per second of airspeed, the water begins to atomize at the exit of the nozzle, increasing the time required to drain the water payload. After installation of a wind blocker, the data collected showed that water leaving the nozzle into static air decreased the time required for the dump.

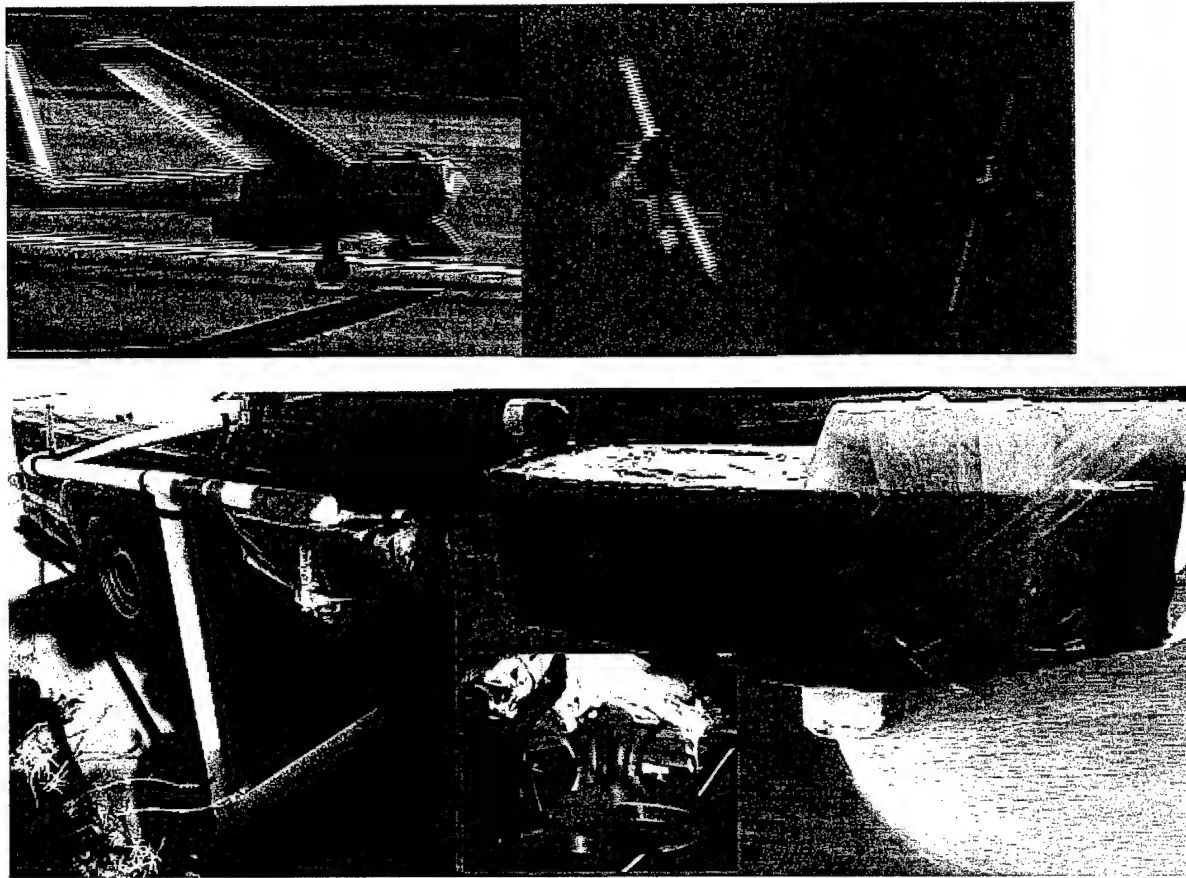


Figure 13 – Tank Testing Assemblies and Test Video Sample, Nozzle Close-up Inset

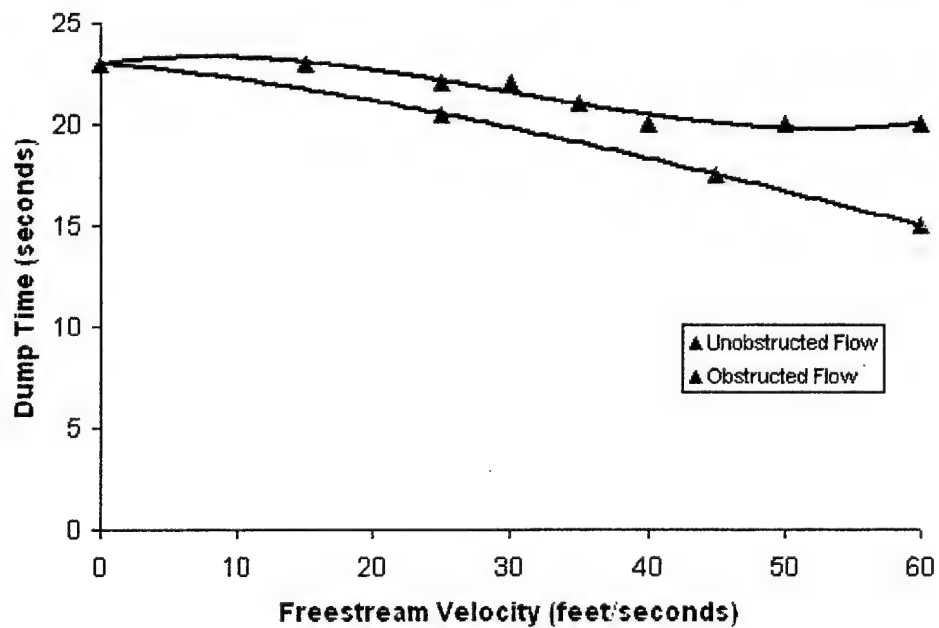


Figure 14 – Dump Time vs. Airspeed

From the data collected from the testing, it was shown that with a freestream velocity around 60 feet per second, the water can be extracted in approximately 15 seconds. Due to the fact that the pressure port is located within the area hit by the propeller blast, the velocity that will be seen by the pressure port will be approximately 1.3 times that of the flight velocity. Observing the "obstructed flow" data points, it was clear that it was necessary to prevent freestream air from hitting the exit orifice of the tank.

4.3. Preliminary Design Aircraft Parameters

Having used the integrated sizing program to perform a trade of maximum score versus heavy mission wing loading, the relationship in Figure 15 was produced.

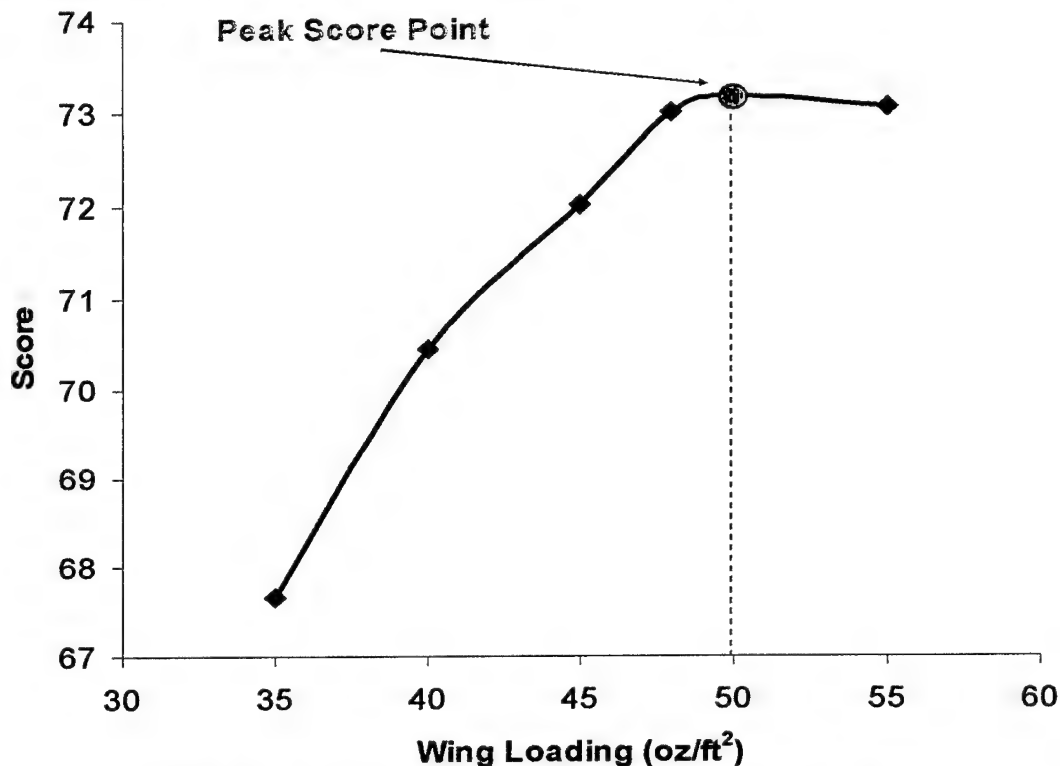


Figure 15 – Aircraft Configuration Optimized for Peak Score

The relationship of maximum score possible with respect to wing loading can be seen to have the shape of a parabolic, with a peak at approximately 50oz/ft². The optimum aircraft configuration parameters defined in preliminary design were obtained for an aircraft of this wing loading. These parameters were later used to define requirements for the component selection performed during detailed design.

4.3.1. General Characteristics of Optimized Aircraft

The following table shows the predicted general aircraft characteristics for an aircraft that has been optimized for the 2004 AIAA Design, Build, Fly Competition converging from the numerous configurations evaluated during the preliminary design phase.

Table 12 – General Aircraft Characteristics

Parameter	Value
Wing Span (ft)	8
Aspect Ratio (-)	12.8

Wing Loading (oz/ft ²)	~50
Wing area (ft ²)	~5
Engine Takeoff Power (watt)	800
Aircraft Empty Weight (lb)	6.2
Aircraft Takeoff Gross Weight (lb)	15

4.3.2. Aerodynamic and Stability Characteristics of Optimized Aircraft

The DBF04 performance model generated a large number of performance characteristics of the configurations satisfying the mission requirements. The aerodynamic/stability performance calculations for the optimized aircraft configuration are shown below in Table 13 and the drag coefficient estimates in Table 14.

Table 13 – Predicted Aerodynamic/Stability Performance Parameters

Performance Parameter	Analytical Value
Maximum Lift Coefficient	1.75
Maximum Lift-to-Drag Ratio (L/D)	15
Takeoff Distance Limitation, ft	150
Aircraft Takeoff Distance Loaded, ft	130
Aircraft Takeoff Distance Empty, ft	80
Static Margin, %	10
Yaw Stability Derivative	0.055

Table 14 – Drag Coefficient Breakdown

Drag Coefficient Breakdown	
Cf_wing (ft ²)	0.045
Cf_tails (ft ²)	0.036
Cf_fuselage (ft ²)	0.013
Cf_gear (ft ²)	0.012
Total flat-plate drag area (ft ²)	0.106
Total drag coefficient, normalized to wing area (-)	0.0198

4.3.3. Predicted Mission Performance for Optimized Aircraft

Table 15 – Predicted Mission Scores

Performance Parameter	Analytical Value
Rated Aircraft Cost, \$1000	7.925
Time of "Fire Fighter" Mission, min	2.52
Time of "Ferry" Mission, min	1.72
Score of "Fire Fighter" Mission	3.181
Score of "Ferry" Mission	0.583

Table 16 – Mission Performance Breakdown

Fire Fighting											
Heavy Portion	Seconds	ft/sec	L/D	Cl	Req'd Watts	power η	Elec. Watts	Volts	Amp	Batt η	kJ
Takeoff	6.1	24			364	0.45	808	16.2	50.0	0.81	6.11
Climb	7.2	59	20.4	0.7	364	0.45	808	16.2	50.0	0.81	7.21
Turn (180)	1.1	89	4.6	1.3	421	0.45	840	16.0	52.6	0.80	1.18
Dumping Water	Seconds	ft/sec	L/D	Cl	Req'd Watts	power η	Elec. Watts	Volts	Amp	Batt η	kJ
Cruising	18.18	55	19.8	0.6	44	0.45	97	19.6	4.9	0.98	1.80
Turn	1.2	55	3.0	2.5	286	0.4	716	16.7	42.8	0.84	1.05
Empty Coming In	Seconds	ft/sec	L/D	Cl	Req'd Watts	power η	Elec. Watts	Volts	Amp	Batt η	kJ
Turn	0.5	55	3.1	1.7	274	0.45	608	17.3	35.1	0.87	0.38
Landing	11.1	55	14.9	0.35	81	0.4	202	19.2	10.5	0.96	0.63
Heavy Cruise Total	45.5										18.36
Empty Mission											
One Lap	Seconds	ft/sec	L/D	Cl	Req'd Watts	power η	Elec. Watts	Volts	Amp	Batt η	kJ
Takeoff	1.5	15			364	0.45	808	16.2	50.0	0.81	1.51
Climb	2.5	36	20.5	0.8	364	0.45	808	16.2	50.0	0.81	2.49
Turns	4.8	120	3.2	0.3	321	0.4	803	16.2	49.6	0.81	4.75
Cruising	10.7	120	3.6	0.07	287	0.45	639	17.1	37.3	0.86	7.99
Landing	6.2	120	3.6	0.1	81	0.4	202	19.2	10.5	0.96	0.63
"Heavy" total	25.7										17.37

4.4. Conclusion

At the end of the preliminary phase, the primary components of the configuration were all sized and placed according to the figures of merit. Based on the scores obtained in the decision matrices, the aerodynamic characteristics of the airplane were defined. The aircraft now utilized a high aspect ratio wing with a modified Schuermann planform, and a low-cambered airfoil. The propulsion system was agreed upon and consisted of a Graupner motor and a battery pack size made up of Sanyo CP-1700SCR cells. The fine-tuning of the less general details of the aircraft was left to be performed during the detailed portion of the design process.

5. Detail Design

Having determined during the basic requirements for the chosen aircraft configuration during the preliminary design process, detailed design of specific components could be undertaken. Detail design focused on finalizing the aerodynamic, propulsive and structural configuration of the aircraft and the payload mechanisms used in it.

Table 17 – Performance Requirements

Engineering Requirement	Required	Goal
Mission Rules		
Gross Weight (lbf)	<55	<16
Takeoff Distance (ft)	<150	140 ~ 150
Flight Time (min)	<10	2~3

Radio Fail Safe Mode	Yes	Yes
Disassembled Dimensions (ft)	4 X 2 X 1	4 X 2 X 1
Rated Aircraft Cost (\$1000)		<8
Strength		
Load Factor Limit (g)	>12	15
Max Design Lift Limit (lbf)	192	240
Max Payload Support Force (lbf)	102	128
Flight Performance		
Maximum Lift Coefficient	1.5	1.8
Maximum Lift-To-Drag Ratio	20	25
Maximum Speed Empty (ft/sec)	100	120
Stability		
Static Margin %	5 ~ 15	10

5.1. System Architecture

With the general configuration of individual aircraft components having been arrived at in the preliminary design section, a suitable way to arrange these within the airframe had to be determined. The main components of the aircraft were: The keel, water tank, main gear and wing/empennage. Because water is quite dense and its shape is inherently flexible, it did not appear to be difficult to design an aerodynamically "clean" aircraft. Water is carried in a streamlined tank which, like the rest of the aircraft components attaches to the load-bearing keel.

It was desirable to locate the water fill location on the rear of the tank – away from electronics and other mission-critical components of the aircraft. This desire led to one of the most distinctive features of the configuration – the asymmetric keel. The tail boom part of the keel locates the vertical tail approximately 2 inches off the span-wise centerline of the aircraft. The space freed up by this keel asymmetry is sufficient to fit the fill orifice of the water tank.

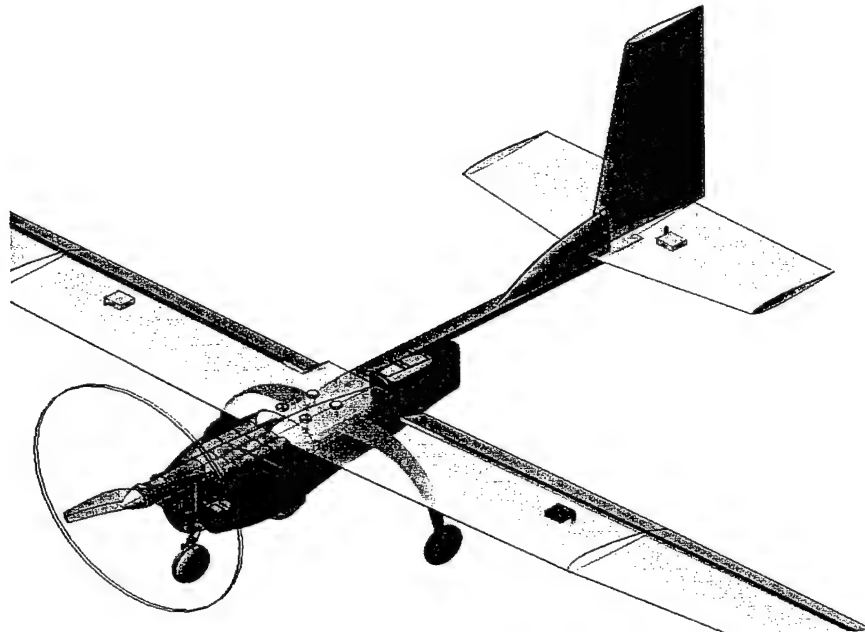


Figure 16 – General Aircraft Configuration

5.1.1. Airfoil Selection

Using the performance simulation program, the requirements of this year's mission were analyzed and basic performance parameters necessary for the airfoil were established. These performance requirements are outlined in Table 18 below.

Table 18 – Airfoil Performance Requirements

Parameter	Value
Maximum C_L	1.7
Design Payload C_L	0.6
Design Dash C_L	0.15
Takeoff Reynolds Number	200,000
Reduced Reynolds Number ($Re(C_L)^{0.5}$)	130,000-210,000

Other non-quantitative parameters required of the airfoil include soft and non-abrupt stall behavior and a shallow drag bucket within the operational C_L range (0.15-0.6), aided by in-flight camber changing.

The design team used the XFOIL software to evaluate the commonly available airfoil sections and perform design of new ones. This software, available for free download from the Massachusetts Institute of Technology is commonly used to investigate the performance of 2-d airfoils in non-compressible air flow. It had been established that the best way to meet the varied requirements of the mission was using a variable-camber airfoil which could function equally well at the low lift coefficients of high-speed flight and at the high-lift conditions of takeoff segment. Using the guidelines of the preliminary design section, a specific airfoil could be chosen for use in *Moist*. After a number of iterations, a moderately cambered airfoil, well-suited for incorporation of flaperons resulted.

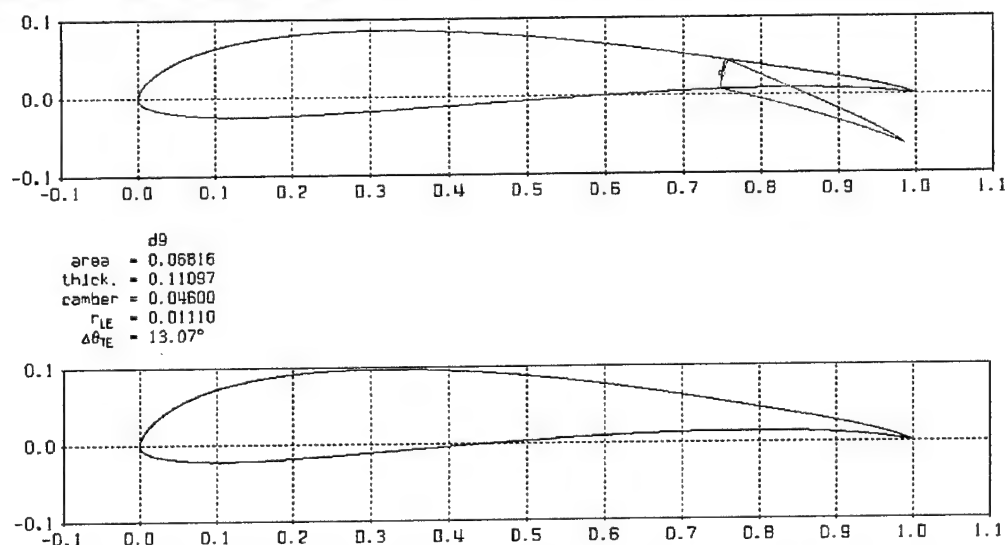


Figure 17 – d9g9 airfoil, 0° and 15° flap deflections and original d9 airfoil.

The airfoil chosen, d9g9, can be seen in Figure 17, with a 0° and a 15° trailing edge flap deflections outlined in black and blue, respectively. The d9g9 is a modification of the d9 airfoil, used on the CalPoly DBF aircraft in the 2003 competition and also displayed in Figure 17. The higher camber and thickness of the original airfoil can be seen in the figure above, with leading edge modifications not as readily visible. By decreasing the camber and thickness of

the baseline d9 airfoil and increasing the radius of the nose, an airfoil with the necessary performance characteristics was created. The performance of the d9g9 can be compared to that of a number of other candidate airfoils in Figure 18 and Figure 19 below, which have all seen use in similar aircraft. The d9 high-lift unflapped airfoil was used on the 2003 Cal Poly DBF aircraft, the JA40 camber-changing airfoil was used on the 2002 Cal Poly DBF aircraft, and the RG15 is an extremely popular competition sailplane airfoil which fit the requirements defined above quite well.

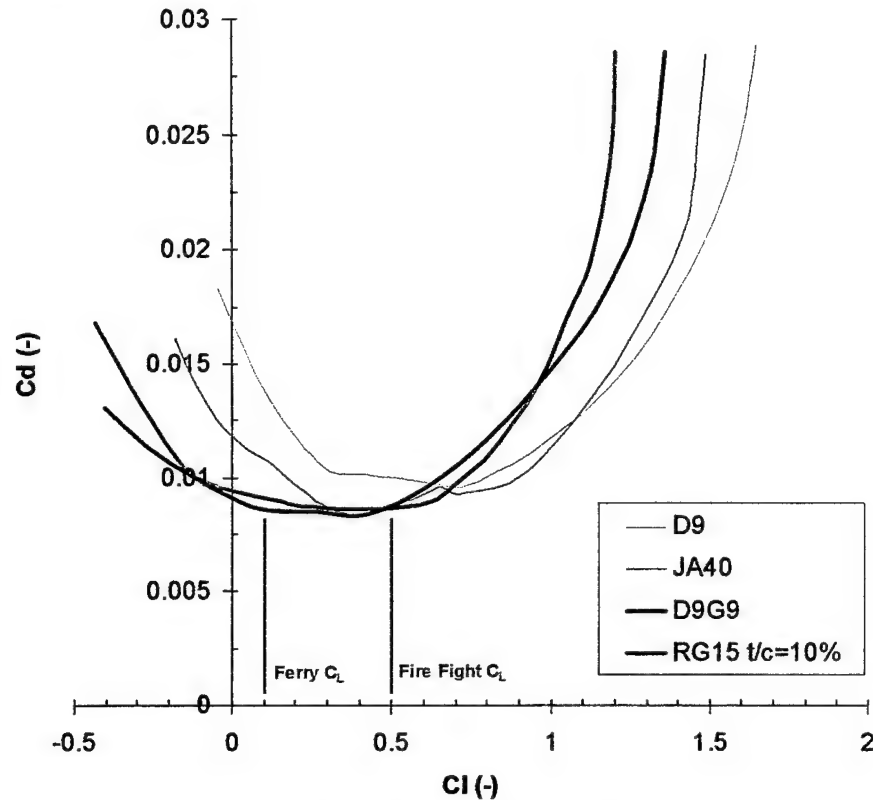


Figure 18 – Drag Polar Comparison

As can be seen from Figure 18, the d9g9 airfoil in its unflapped condition has a lower drag coefficient at the majority of the normal-flight lift coefficients (0.1-0.6 range). The bottom of its drag bucket is close to that of the tried-and-true RG15 airfoil. In the unflapped condition, the d9g9 airfoil exhibits relatively poor high-lift drag characteristics as a result of its low camber and thickness. However, the behavior of the airfoil changes dramatically when a simple flap is deflected by 15%. Refer to Figure 19.

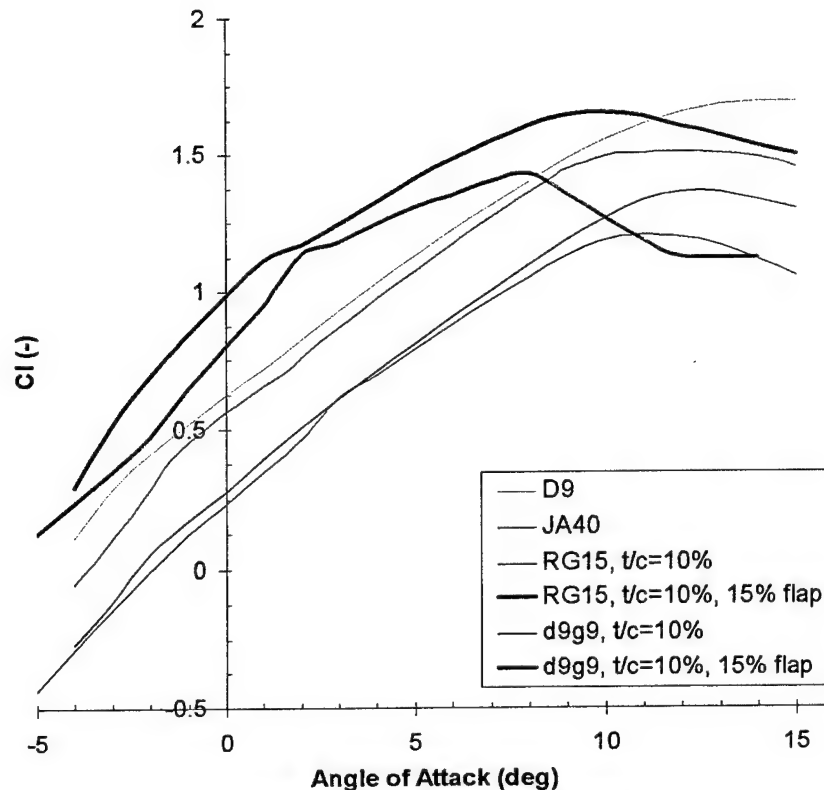


Figure 19 – C_L vs. Angle of Attack

A dramatic difference can be observed in the flapped C_L vs. α behavior of the seemingly similar RG15 and d9g9 airfoils. Due to a lack of curvature on the upper surface, the RG15 airfoil suffers from boundary layer separation forward of the flap. This causes in a sharp stall to occur at a C_L of ≈ 1.4 . On the other hand, being designed specifically for flapped high-lift operation, the d9g9 airfoil not only has a maximum C_L of ~ 1.65 , but also a much milder stall onset. The airfoil thickness chosen was 10%, which is optimal for drag reduction, while still reasonable when considering structural and high-lift requirements.

5.1.2. Planform Configuration

The planform finally selected was a modified Schuermann wing as seen in Figure 20. The wing has elliptical leading and trailing edges for the inner 70% of the span and a sheared wingtip design. This closely approximates the ideal span wise lift distribution, also seen in Figure 20, without incurring the low Reynolds numbers at the tips that can lead to tip-stall. The wing was also designed so that at a given angle of attack, the outer section of the wing would be operating at a C_L value 0.1 lower than that of the root section. This allows the spanwise sections of the wing to fly near peak efficiency while still preventing tip-stall.

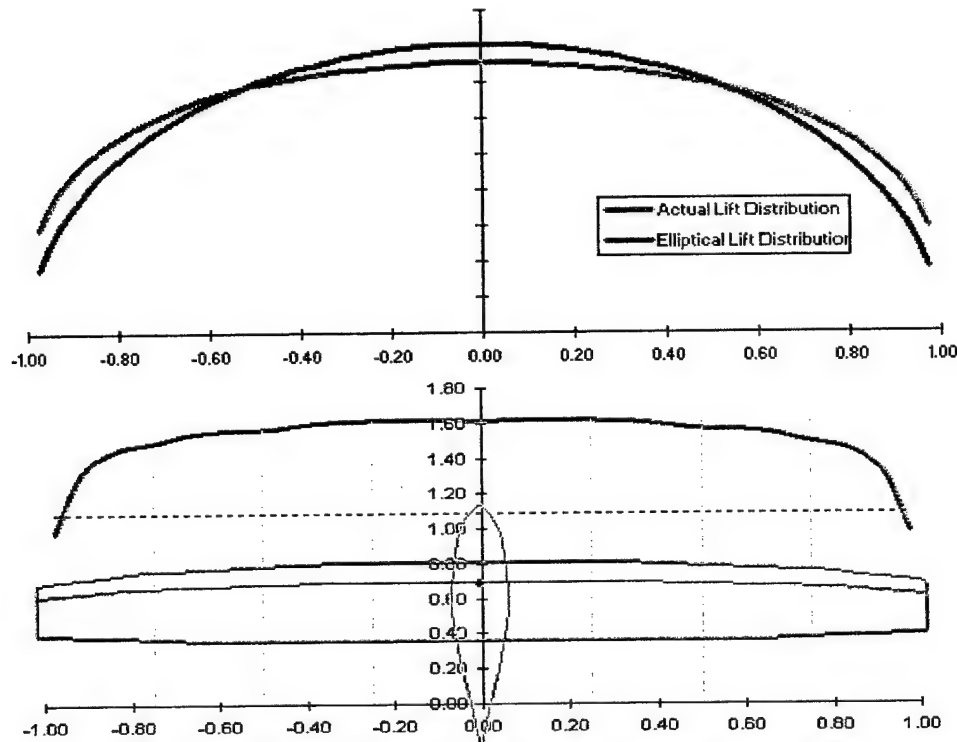


Figure 20 – Modeled Planform, Lift Distribution, Cl Distribution

5.1.3. Empennage Configuration

Vertical and horizontal tail sizes were calculated using tail volume coefficient formulas on page 124 of Aircraft Design¹.

$$S_{VT} = c_{VT} b_W S_W / L_{VT}$$

$$S_{HT} = c_{HT} \bar{C}_W S_W / L_{HT}$$

where L is the moment arm taken to be the length from the tail's quarter chord to the wing's quarter chord. S_W is the wing area, b_W is the wing span, and \bar{C}_W is the wing mean chord. The vertical and horizontal tail volume coefficients are c_{VT} and c_{HT} , respectively. The tail volume coefficients were chosen based on experience gained from the past three Cal Poly DBF aircraft. The handling qualities of these airplanes were very quite satisfactory; therefore the tail volume coefficients chosen to be used on this year's aircraft remained the same. The vertical and horizontal tail volume coefficients of the aircraft are 0.06 and 1.1, respectively.

5.1.4. Stability and Control

The aircraft was modeled in Tornado®, a vortex lattice code designed to output stability derivatives of a general aerodynamic configuration. A simple solution computation for control coefficients was run, and stability derivatives obtained. The stability derivatives output by the program and the geometry used can be seen in Figure 21. The outputs of the program, such as the negative pitching moment coefficient C_m can be seen to point to a stable and controllable aircraft configuration.

TORNADO CALCULATION RESULTS

JID: db04 Downwash matrix condition: 22.2321
 Reference area: 734.4
 Reference chord: 7.7294
 Reference span: 96

Net Wind Forces: (Nm) Net Body Forces: (Nm) Net Body Moments: (Nm)
 L: 83305.5669 Z: 83305.5669 Pitch: -53056.6451
 D: 418.3585 X: -383.7245 Yaw: -9917.2815
 S: -383.7245 Y: 418.3585 Roll: 1602.726

CL 0.20578 CZ 0.20578 Cm -0.016956
 CD 0.0010394 CX 0.0010394 Cn -0.00025518
 CY -0.00094785 CC -0.00094785 Cl 4.1239e-005

STATE:
 alpha: 0 P: 0 Rudder setting [deg]: 0
 beta: 0 Q: 0
 Airspeed: 30 R: 0
 Density: 1.225

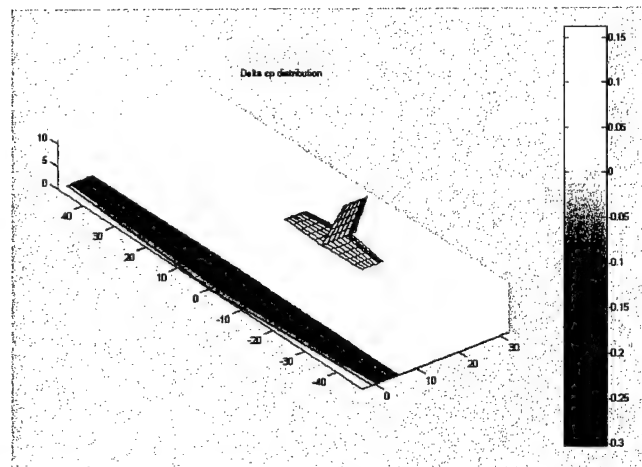


Figure 21 - Aerodynamic Coefficients and Geometry Modeled

5.2. Propulsion System

The propulsion system components had to be analyzed together in order to come up with the best combination of motor, battery pack and propeller.

5.2.1. Motor Selection

The power requirements of the design limited our selection to two motors in the Graupner line: the Graupner 930 and the Graupner 920. Table 19 shows the available winding configurations of the two Graupner motors that were considered. With the battery pack picked from the endurance requirements of the missions flown, the motors were expected to handle 600Watts of electric power input at a voltage of 15 volts that would be provided by a 16 cell CP1700SCR battery pack under load. Generally the motors with lower turn armatures were more efficient at full takeoff power while suffering in efficiency during the relatively low powered cruise. The higher turn motors showed lower efficiency at full power while being much more efficient during cruise. Most of the propulsive energy during the mission is used during cruise so the decision was made to optimize cruise efficiency. Another constraint to consider was the fact that a high-winding motor would not be able to function at the current it is required to operate at during the takeoff segment.

Table 19– Candidate Motors

Motor	Weight (oz)	Max Power (Watts)	RPM/V	Resistance Ohms	Idle Current	Gear
Graupner Ultra 920-4 7V	11.3	480	3298	0.016	3.480	5.1:1
Graupner Ultra 920-5 7V	11.3	500	3422	0.02	3.91	5.1:1
Graupner Ultra 930-6 8V	13	600	1975	0.04	2.0	3.7:1
Graupner Ultra 930-7 10V	13	680	1667	0.0463	2.0	3.7:1
Graupner Ultra 1300-6 12V	12	1200	1511	0.052	5.6	1:1

All of the motors come available with various gear reductions. Although the gear reduction reduces the mechanical efficiency of the motor, the larger, lower disk-loading propeller usually makes up the difference in

efficiency while also providing significantly higher static thrust for takeoff. Another advantage of the high-diameter propeller is that, with the fuselage being approximately 20 square inches in frontal area, a large propeller is needed to avoid thrust loss due to the effects of fuselage interference. The Graupner motors are capable of producing more power using a gear reduction because they can be run at higher voltages. Because of the above reasons and using numerical output of the motor efficiency program (Figure 23, in the end of chapter), the decision was made to use a motor with gear reduction.

The Graupner (Ultra 1300) is capable of running at 1200 watts of input power, but is oversized for this mission. This motor was nonetheless considered in the preliminary motor selection stage as a possible direct-drive solution. The Graupner 920 and 930 motors can operate at power levels up to 800 watts, which is higher than the takeoff power level projected for the aircraft in takeoff. The mission profile calls for short periods at full power for takeoff and climb followed by extended cruise periods well within the normal power limits of both of the Graupner motors. The Graupner 930 motor possesses a comfortable "safety margin" that would allow extra power to be input to the power system in case of the built aircraft having takeoff performance inferior to that of the predictions. The 930 motor is also projected to be very efficient at the cruise level of operation. Since the 920 is lighter, it has a smaller magnet, causing the 920 to not have as much peak torque as the larger 930 and causing poorer high-power takeoff performance. During the takeoff segment, the 920 motor would be operating at very high power levels. The disadvantage of running the motor at such high power levels is premature erosion of the brushes and commutator, and loss of efficiency due to increased resistance and demagnetizing of the permanent magnets.

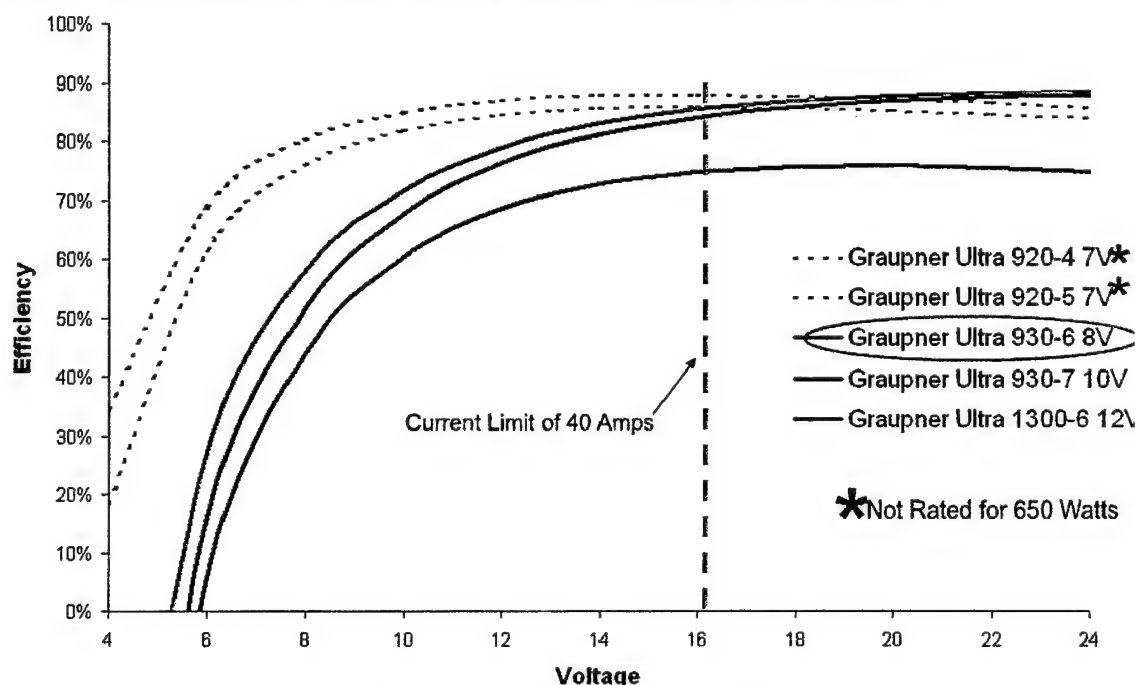


Figure 22 – Motor Selection vs. Maximum Efficiency - 650 Watts Input

After considering all the alternatives, the team decided to use the 930-6 motor because of the safety margin provided and the high efficiency during cruise. This motor choice provides the aircraft with a good power to weight

ratio, high cruise efficiency and improved scoring potential, along with its larger armature spinning causes the 930-6 produce more torque which is needed to use a large diameter propeller.

5.2.2. Propeller Sizing

The propeller performance model indicated propellers 14 to 17 inches in diameter with 10 to 13 inches of pitch would load the selected motor to the required 550-650 watts. The relatively high pitch of the propeller was chosen because of the aircraft's high cruise speed required for reduced mission times. This pitch was a compromise between the advance ratio required for efficient cruise, and for good full throttle takeoff and climb performance. Because of the variation in efficiency and power absorption between different propeller manufacturers, the propeller model was calibrated using data gathered from the motor manufacturer and with testing performed with the Graupner 930-6.

The required static thrust for takeoff was determined from the initial performance code. The static power and the RPM the Graupner 930-6 would operate at were then input into the following equation relating the diameter and pitch of a propeller. The propeller sizes that would accommodate the necessary static power to achieve the takeoff distance were then optimized for cruise efficiency. The highest propeller efficiency was determined using advance ratio theory and normalized propeller speed for an optimized pitch to diameter ratio. The equations used⁴ can be seen below.

$$StaticPower = 1.11 * Diameter^4 * Pitch * RPM^3$$

$$AdvanceRatio = \frac{Velocity}{RPM * Diameter}$$

By implementing a gear reduction, pitch speed can be exchanged for thrust. Gearing only improves propeller efficiency if the direct drive propulsion solution propeller has a pitch speed that is much higher than the actual flight speed of the aircraft. The following plots were generated from the relationship of the thrust, velocity, RPM, to diameter and pitch optimization for a given flight cruise speed. From these relationships, the following motor, propeller, and gearbox combinations were chosen as possible candidates for the aircraft.

Table 20 – Propulsion Systems Evaluated

Motor	Reduction	Propeller	Max. Efficiency	Weight (g)
1300-6	3.71:1	16x13	40	420
1300-6	1:1	10x6	28	340
1300-6	1:1	12x7	29	340
930-6	3.71:1	14x14	55	370
930-6	3.71:1	17x13	55	370
920-5	5.1:1	14x13	50	320
920-6	5.1:1	16x12	50	320

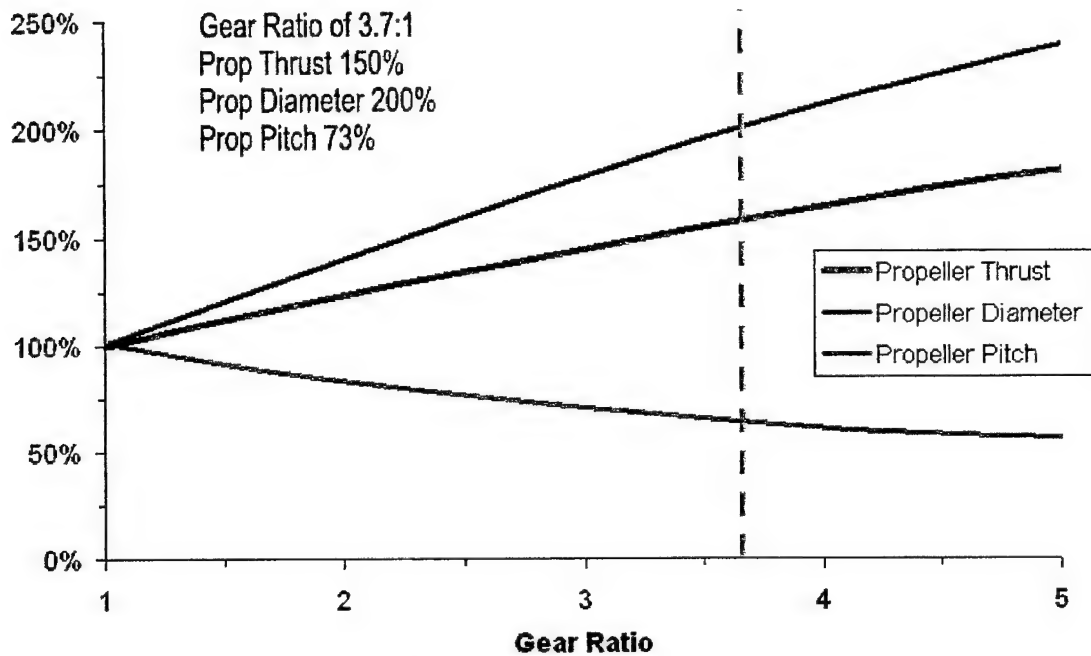


Figure 23 – Effects of Gearing on Thrust and Speed

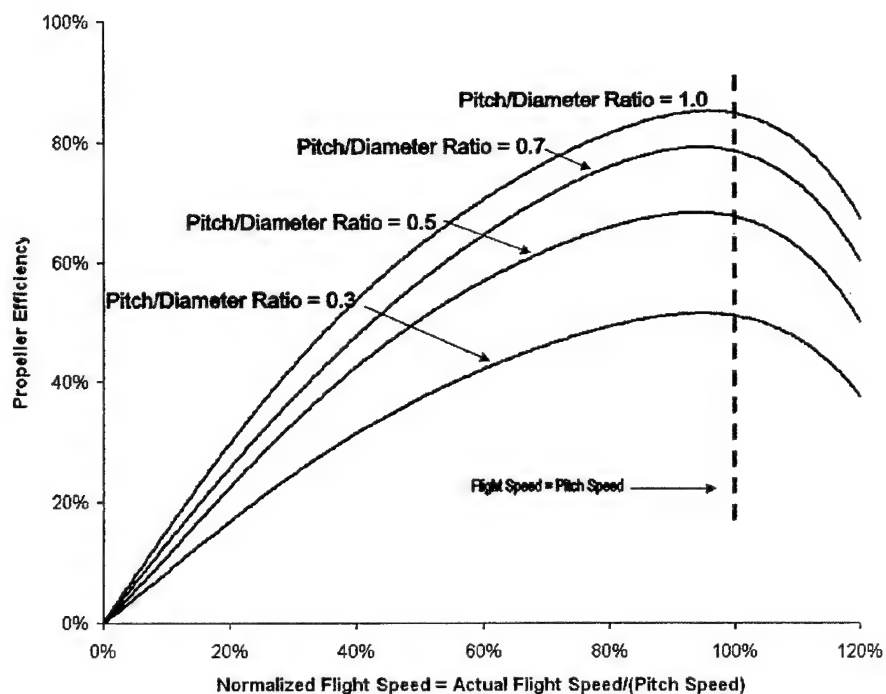


Figure 24 – Propeller Efficiency vs. Normalized Speed

Utilizing a 3.71:1 planetary gearbox and a 17x13 propeller, the Graupner Ultra 930-6 was chosen for the heavy-lift "Fire Fighter" mission and a 14x14 propeller with the same gearbox for the "Ferry" mission. Both of these solutions produce maximum propulsive efficiencies of approximately 55%. For the heavy-lift "Fire Fighter" mission, the

maximum propeller diameter was constrained by the required ground clearance of the aircraft. The 17 inch diameter propeller in consideration was judged as the maximum diameter possible to be installed on the aircraft.

5.2.3. Battery Weight and Number of Cells

Having selected the CP-xxxxSCR range of cells as optimal, a correct cell type had to be picked on the basis of the pack "C rate". Charge or discharge comparison of batteries is done using the term "C" or "C rate". The term "C" is numerically equivalent to the rated capacity of a cell discharged at the "C" rate will expend its minimum capacity in one hour, while taking only 15 minutes if discharged at a rate of 4Cs. The resistance of the cells is extremely important when one considers that the energy lost to the resistance is mainly converted into heat. With the C discharge rate for the 2004 aircraft approaching the value of 15, the team was extremely concerned with the cooling of the battery pack – both construction of the pack and its location had to be optimal in order to allow for the best possible air circulation.

Every nickel-cadmium cell or battery has a specific rated capacity, discharge voltage, and effective resistance. Individual cells are rated at 1.2 volts and voltage for batteries are multiples of the individual cell nominal voltage of 1.2 volts. Sixteen cells connected in series would result in a 19.2-volt battery. As can be seen, however, the discharge voltage will exceed 1.2 volts for some portion of the discharge period (during the takeoff and climb segments). Most manufacturers rate cell capacity by stating a conservative estimate of the amount of capacity that can be discharged from a relatively new, fully charged cell.

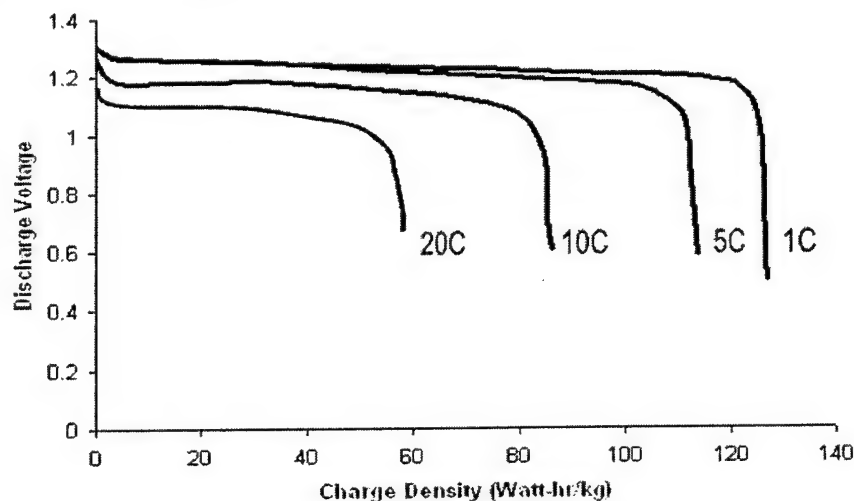


Figure 25 – Typical NiCd Discharge Rates

The graph in Figure 25 shows that when rates of discharge are increased the available capacity becomes more dependent on the discharge rate. At a discharge rate of approximately 15C, the battery efficiency will drop below 80%. When rates of discharge increase, the available capacity decreases as the discharge rate increases. The above trends were also very important for the application in this year's aircraft – working to decrease the C rating would result in higher battery energy available.

Most electric motors available for powering this year's aircraft would require 12-19 Volts input instead of the near 100 Volts that a series pack of high capacity cells would be. A combination parallel-series pack was considered to reduce the voltage and increase the current capabilities, but the difficulties in charging and maintaining balance between the cells eliminated this idea.

The energy requirement for the battery was approximately 15 Watt-hours. The aircraft was sized to use 16 CP-1700SCR cells because they provided the highest energy density, allowing the lightest, least costly battery pack. This pack potential is approximately 18.4 volts under load. Factoring the 40amp maximum current allows 650Watts for takeoff and climb. The Sanyo CP-1700SCR cells were chosen because of their high performance, availability, and suitability for the design.

5.3. Structural Configuration

The maneuvers performed by the aircraft during its mission will produce various loads onto the airframe. Structural sizing had to be performed when designing the airframe components before process of manufacture could begin. Detailed design of the structural configuration of the aircraft defined the shape of these major components and the amount and location of load-bearing material contained within their composite structure.

5.3.1. Wing Structural Design

The wing of the aircraft had to be designed for two critical load conditions – high-G maximum weight maneuver and the maximum weight static tip-test. While in both of these load conditions the maximum stress produced is at the root of the wing, the static tip-test can also cause the wing to fail by shear of the wing tips. Calculations were performed to realistically calculate the normal stress generated at every point along the span of the wing and to allow for appropriate sizing of a load-bearing spar.

Using a number of geometry inputs, it was possible to use an area distribution of the wing to approximate the aerodynamic load distribution across the wingspan. Consequently, this load distribution was used to the spar cap in order to tailor it to handle the aerodynamic load. Given local spar cap thickness, the moment of inertia of the wing could be calculated at any spanwise location. By varying the thickness of the spar cap, it was possible to create a load-bearing structure of lowest weight possible. The optimum variation of number of layers of unidirectional carbon fiber (0.0035 in. thickness per layer) in the spar cap can be seen in Figure 26.

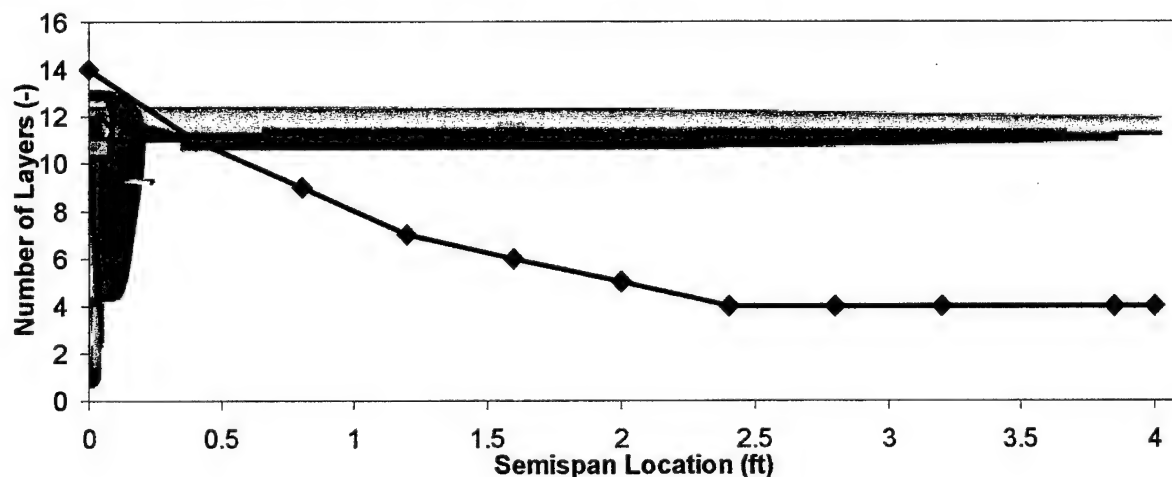


Figure 26 – Number of Layers vs. Semispan Location

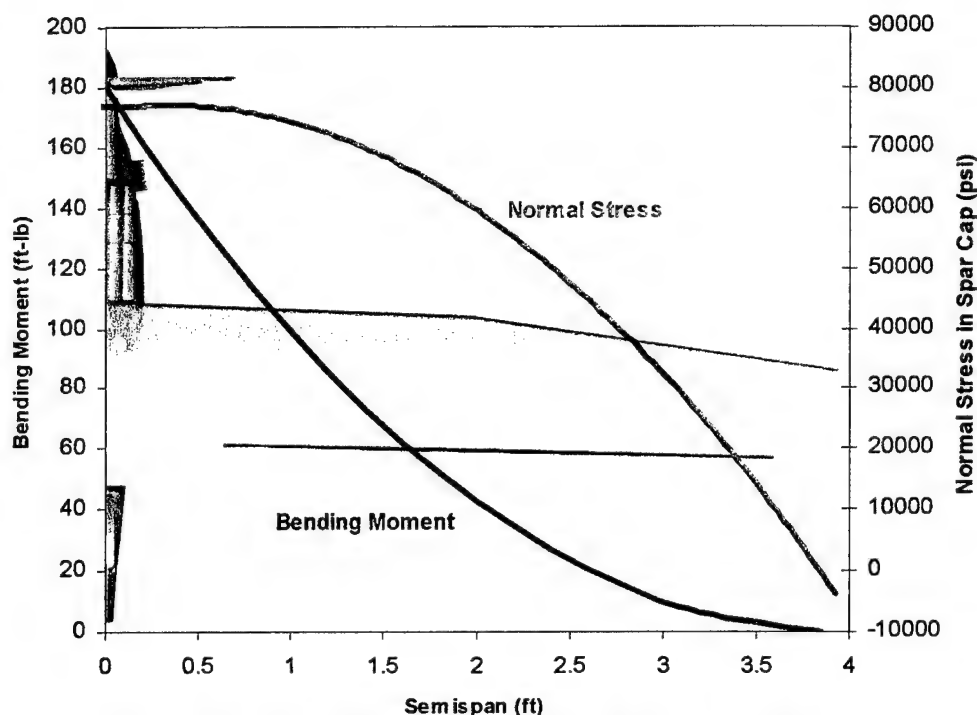


Figure 27 – Bending Moment and Normal Stress vs. Semispan

The bending moment and the resultant normal stresses present in the optimized spar cap structure can be seen in Figure 27. It can be seen that the number of layers in the spar cap says constant at 4 for the outboard 1.5ft of the span. This number was kept constant in order to protect the wing from shear failure during the full-weight tip test, where a concentrated stress is present at the tip.

5.3.2. Wing Joiner Design

An extremely important component that had to be sized before the wing construction could begin was the wing joiner. The wing joiner was conceptually designed as a carbon fiber rod which plugged into two carbon fiber receiver tubes built into the wing core. Besides sizing the joiner to handle the bending stresses of the wing, geometry for the rod had to also be picked. Because both rods and receiver tubes of circular cross-section are much more common and easy to acquire, Cal Poly DBF aircraft have used circular joiners in the past. However, upon performing the calculations shown in Table 21, the advantages of a joiner of a rectangular cross section could easily be observed.

Table 21 – Wing Joiner Geometry Comparison

Wing Joiner - Circular			Wing Joiner - Rectangular		
Weight	16	lb	Weight	16	lb
G Loading	15	-	G Loading	15	-
Wing Force	120	lb	Wing Force	120	lb
Arm	2	ft	Arm	2	ft
Moment	240	ft-lb	Moment	240	ft-lb
Joiner Dia.	0.54	in	Joiner Height	0.50	in
			Joiner Width	0.375	in
I	2.01E-07	ft ³	I	1.88E-07	ft ³
CS Area	0.229	in ²	CS Area	0.1875	in ²
6in rod wt	2.7	oz	6in rod wt	2.2	oz
Stress	186299	psi	Stress	184320	psi

From the table above, it can easily be seen that when sized to the same failure criteria, the rectangular joiner has a lower cross-sectional area, a direct driver of joiner weight, than the circular joiner. The weight of the joiner can be reduced by approximately 25% if using a rectangular cross-section joiner with a manufactured carbon-fiber receiver tube. Although ultimate compressive strength of the joiner material is used, the G-loading used to determine the stresses is higher than that expected in flight, so the joiner is sized with a factor of safety. The loadings and dimensions shown for the rectangular joiner in the table above are the dimensions chosen to be used in the 2004 aircraft.

5.3.3. Wing Structural Verification

In order to validate the method used to manufacture the main wing of the aircraft, a composite plate using composite construction identical to that used in the main wing was made out of white bead foam, Rohacell, carbon fiber and kevlar. The ratio of kevlar and carbon fiber, the main stress-bearing components of the wing construction, was made to equal that found at the root of the main wing. This allowed the simulation of the stress conditions at the most critical location. The plate constructed was secured as a cantilever beam and instrumented with a strain gauge – this setup can be seen in Figure 28.

Weights were attached to the plate, and the values of strain in the top surface of the plate due to bending were recorded at each individual loading condition.

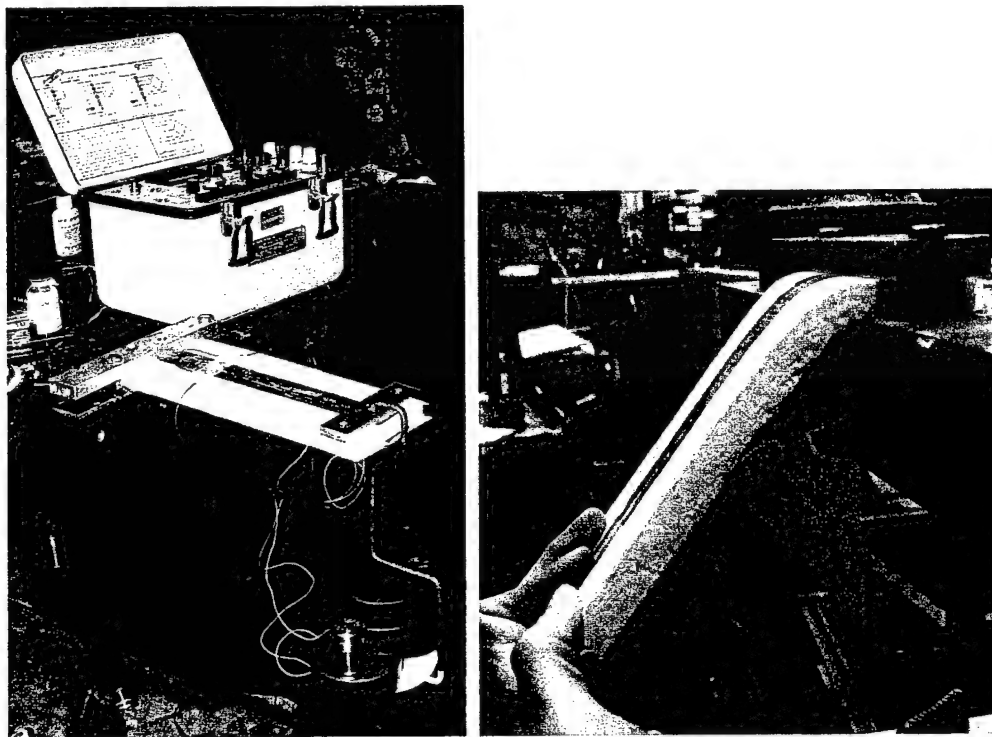


Figure 28 – Instrumented Test Panel Undergoing Destructive Testing (Tests 1 and 2)

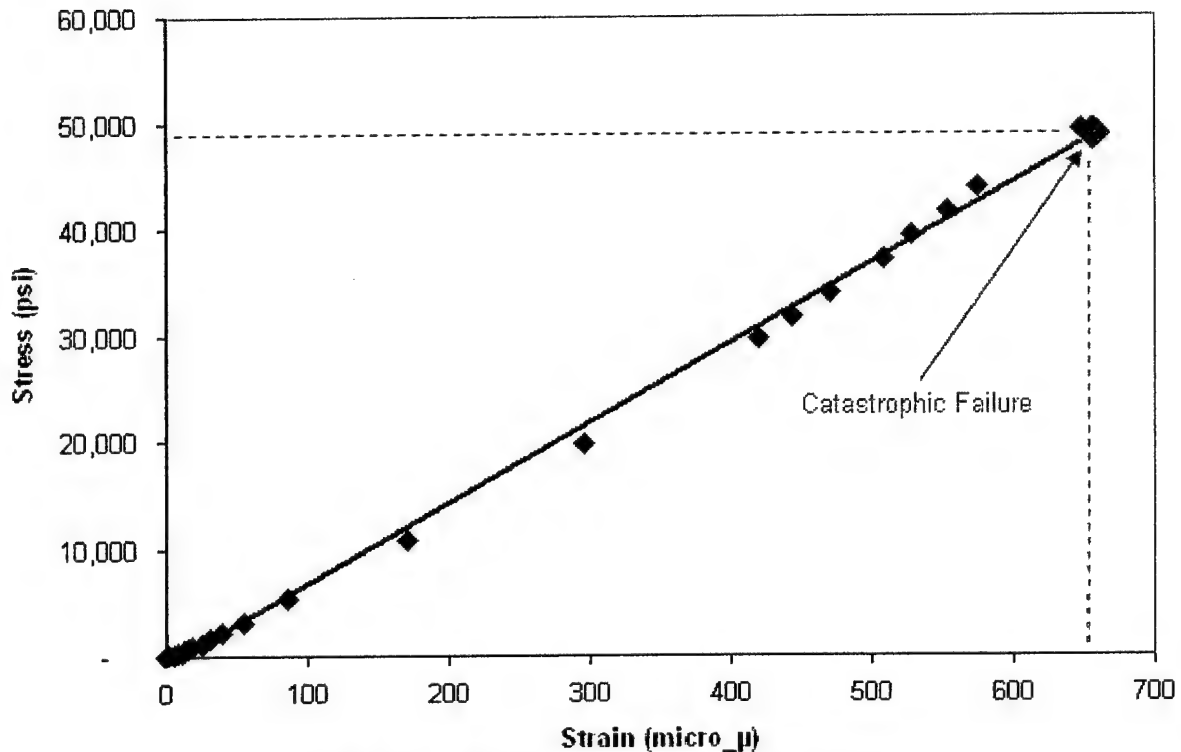


Figure 29 – Destructive Testing of Wing Structure

As can be seen from Figure 28, failure in the plate occurred in the compression surface – the result of buckling and delamination of the fiber and matrix composite skin. Using the data collected via the strain gauges, it was possible to plot a relationship of stress vs. strain for the composite sandwich used to manufacture the wings of the aircraft. This relationship can be seen in Figure 29. From the figure above, it can be seen that the maximum stress that the representative structure of the wing can carry is approximately 50ksi. It is likely that the full-scale wing will be able to handle higher values of stress, both because of the more attention to detail given during its manufacture, and the thicker carbon fiber spar cap being less prone to buckling.

5.3.4. Wing Weight Buildup

The weight of the fully configured wing could be predicted using a simple component weight buildup. These results can be seen in Table 22 below.

Table 22 – Wing Weight/Spar Cap Thickness Calculations

Area			Spar Cap Root Width		
	5.0 ft ²			1	in
Aircraft Weight	16	lbs	Spar Cap Root Area	0.049	in ²
Span	96	in	Skin	1.6	oz/ft ²
Average Chord	7.5	in	Resin Content	0.5	-
Aspect Ratio	12.8	-	Foam	1.2	lb/ft ³
T/c	0.10		Caps	0.4	Oz
Airfoil	0.052		Skins	3.6	Oz
Gs	12	-	Foam	3.6	Oz
Bending Moment	5	Ft*lbs	Misc	2.5	Oz
3.0 oz thickness	0.0035		Joiners	2.2	Oz
max stress	50000psi		Shear Web	1.4	Oz
			Total Weight	0.8	Lb

5.3.5. Keel Structural Design

With the keel being the main load-bearing component of the aircraft, it had to be sized for both the stresses it could see during landings and for the stresses caused by high-speed flight and maneuvering. High positive-G maneuvering and high-speed flight both necessitate a force down on the horizontal tail in order to cancel out the pitch-down moment of the wing. This creates a moment couple between the main wing and the horizontal tail which has to be transferred through the keel. Landing loads create a condition of maximum stress at the main gear attachment point, as the components located far in front and rear of the aircraft are rapidly decelerated. The keel was designed to not excessively deflect during 130fps flight, and to not be damaged in a 15-G landing deceleration.

5.3.6. Main Landing Gear Structural Configuration

The main landing gear is one of the most important components of the aircraft, and it is also the most difficult to repair in case of damage. Because of this, the landing gear of the aircraft was one of the most ruggedly-designed and built components. Being manufactured out of unidirectional carbon-fiber, the landing gear was designed to handle the stress of a 20-g crash landing. The solid model of the landing gear was tested in Cosmos, a finite element analysis software by Structural Research & Analysis Corp.

Although wheel axles would likely space the force application point slightly outwards from that modeled, the simplification is acceptable, considering that such a crash would surely destroy the axles. The structural parameters of the carbon fiber and thermoset matrix composite were obtained from Matweb®. Although not the data for the actual material used in the construction of the main gear, the numbers are representative of those of industry-standard IM class of carbon fiber prepreg materials.

Table 23 – Carbon Fiber Properties

Mechanical Properties	Metric	English
Tensile Strength, Ultimate	2700 MPa	392000 psi
Tensile Modulus	140 GPa	20300 ksi
Flexural Modulus	70 GPa	10200 ksi
Flexural Yield Strength	550 MPa	79800 psi
Poisson's Ratio	0.3	0.3
Shear Strength	70 MPa	10200 psi

Having loaded the model with forces representative a 20-g crash condition, the deflection of the landing gear and the stresses present in the structure could be arrived at. These are shown in Figure 30.

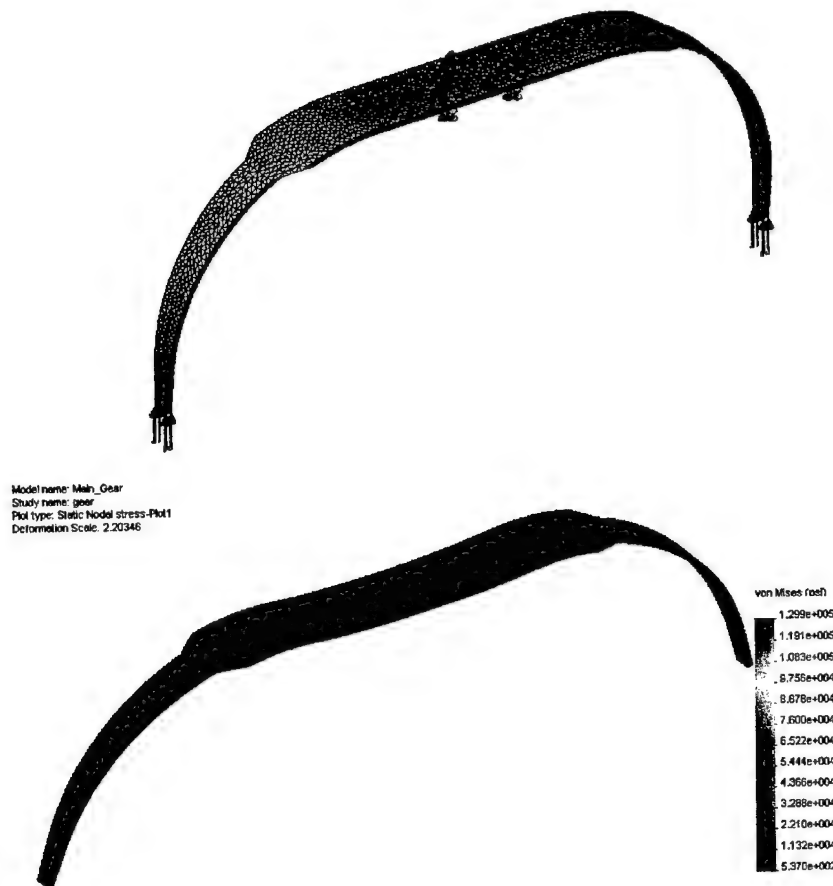


Figure 30 – Meshed Solid Model and Static von Mises Stresses (20G Loading, Maximum Weight)

5.4. Aircraft Performance Characteristics

The point-design performance code is capable of outputting various performance curves for the aircraft. Using the integrated engine/propeller model, it was possible to determine the propulsive power available to the aircraft at every airspeed. From the drag buildup, the drag of the aircraft could also be derived. Using these performance characteristics, a maximum climb rate curve for the aircraft was constructed.

From Figure 31 below, it can be seen that the maximum velocity that can be achieved by this aircraft is in the range of 125 feet per second. The power available was predicted for a 14x14 propeller – aircraft high-speed performance is likely to be less with a prop of a lower pitch/diameter ratio. The maximum climb rate available with this propeller is approximately 55 ft/second, and should increase slightly with a larger diameter, higher thrust propeller. By calculating the parasite and induced drag for the aircraft at various airspeeds, the Lift/Drag ratio could be found. The curve showing the variation of Lift/Drag ratio with respect to velocity can be seen in Figure 32.

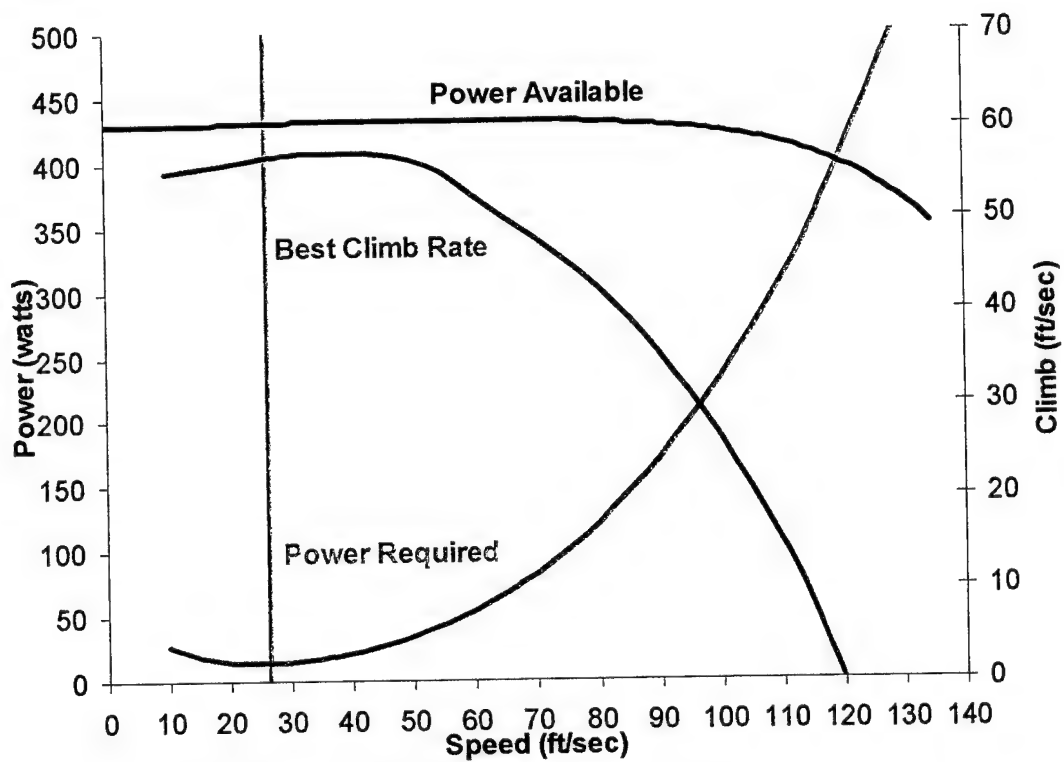


Figure 31 – Power Req'd vs. Power Available, Climb Rates

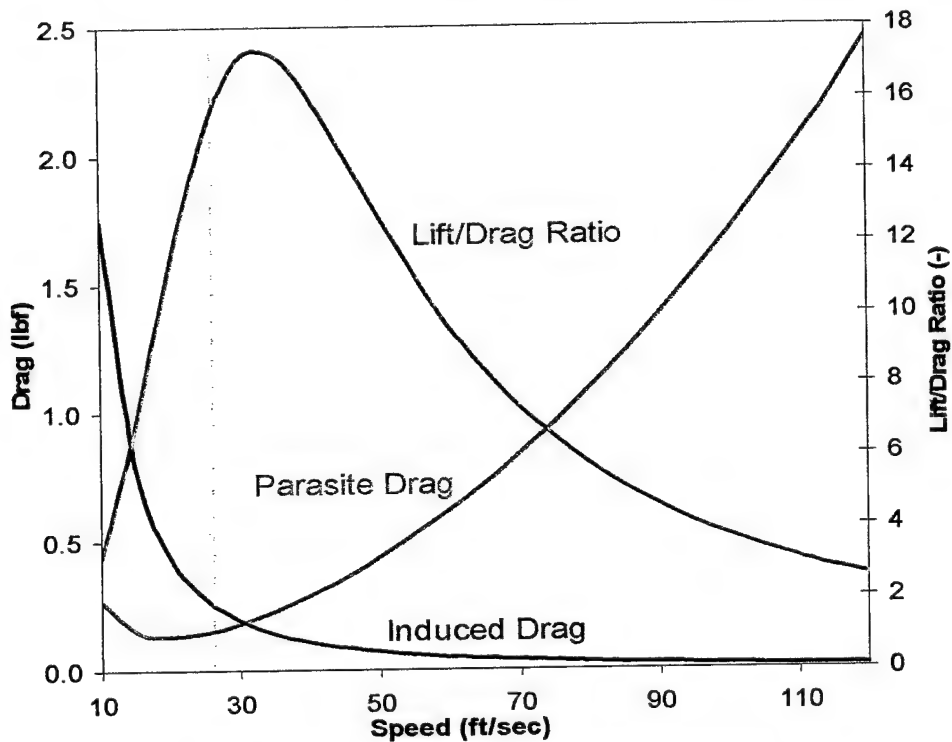


Figure 32 – Drag and Lift/Drag vs. Airspeed

The lift to drag ratio can be seen to peak at quite a low airspeed of 30ft/second. The likely cause is the aircraft's low wing loading and a comparatively "dirty" fuselage. The lift/drag ratio peaks at a value slightly above 16, a believable value for this type of an aircraft.

5.5. Water Tank and Release System Design

Particular requirements which the tank had to be designed to satisfy were present. The tank designed had to drain water and be filled as fast as possible and have a simple yet sturdy water-release mechanism.

In order to be able to quickly fill the tank, the team decided to use a simple one-way valve system. This system consists of a flexible flap attached to the middle of the fill hole, designed to seal itself against the inside of the tank when not pushed upon. The general construction and operation of this system can be seen in Figure 33 below. The water will be transferred into the tank directly from the two 2-liter soda bottles – after experimenting, it has become clear that it is possible to achieve transfer rate of approximately 5 seconds/bottle with this arrangement. By pushing the two bottles into the fill hole as shown in Figure 33, the entire tank can be filled in an extremely short time without the use of complicated ground-based equipment such as a pump.

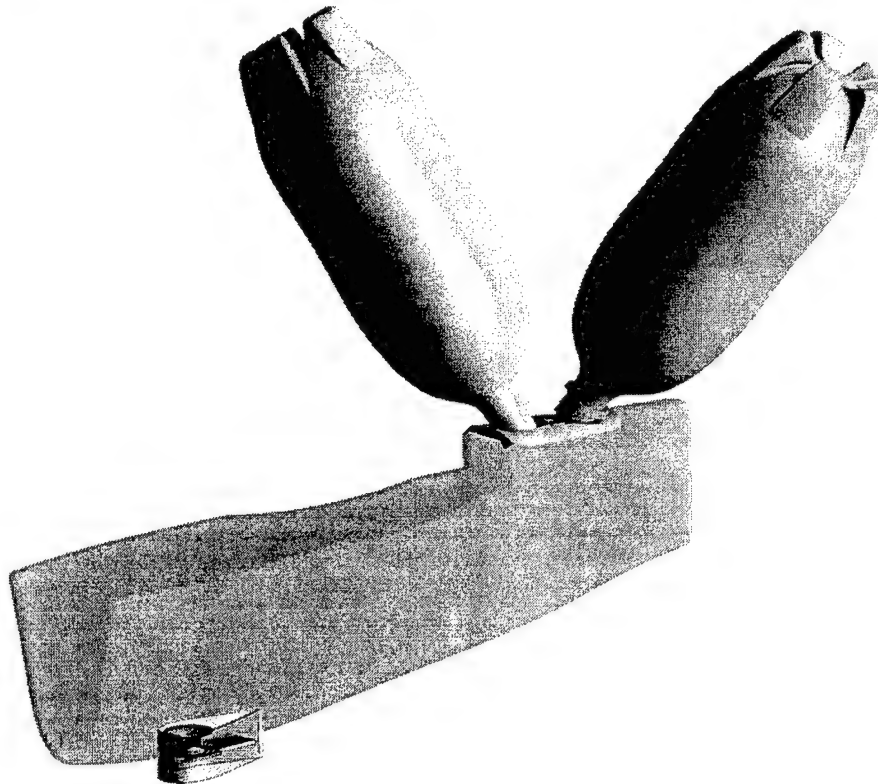


Figure 33 – Water Filling and Release Systems

Using preliminary tests performed on the water tank extraction system, a faired-in convergent-flow nozzle was picked as an optimum method for water extraction. The exit of the nozzle is protected from the oncoming airstream by an airfoil-shaped "wind-blocker", which also contains the release valve, the location of which can also be seen in Figure 33. The valve is actuated via a pull-pull cable running from a servo located above the tank.

5.6. Aircraft Assembly and Storage

The aircraft can fit into its storage container with most components still attached; only the wing and the tails have to be separated. In order to lessen the damage that would be taken in a crash, the wing, the landing gear and the empennage are all attached using nylon bolts that can shear in a crash, reducing the damage taken by the actual airframe components. Main wing is attached with 4 bolts, two of which also secure the main landing gear. The empennage is attached using two nylon bolts which are screwed into threaded connectors located within the vertical tail.

5.7. Center of Gravity Calculation

Using the detailed solid model and the estimated component weights, a center of gravity calculation could be undertaken in order to enable the design team to precisely locate the aircraft components with respect to each other.

Table 24 – Center of Gravity Calculation

Component	Weight (lb)	Arm (in)	Moment (lb-in)
Wing	0.8	15.7	12.56
Empennage	0.39	45	17.55
Keel	0.45	19.6	8.82
Nose Gear	0.38	7	2.66
Main Gear	0.69	18	12.42
Motor and Speed Controller	1.06	4.6	4.876
Batteries	1.39	9.5	13.205
Tank	0.31	15	4.65
Rx + Battery	0.59	40	23.6
Total Moment (lb-in)			100.341
Total Weight (lb)			6.06
CG Location (in)			16.56

5.8. Rated Aircraft Cost

Table 25 – Rated Aircraft Cost

Component	Value	Multiplier	Result	WBS Section
Wing Span	8.3 Ft	8	66.4	WBS 1.0
Max Exposed Chord	0.8 Ft	8	6.4	
Control Surfaces	2 #	3	6	
Max Body Length	4.0 Ft	10	40	WBS 2.0
No Act. Cont. Vert. Surf.	0 #	5	0	WBS 3.0
Act. Cont. Vert. Surf.	1 #	10	10	
Horizontal Surfaces	1 #	10	10	
Servo/Controller	6 #	5	30	WBS 4.0
Propellers	1 #	5	5	WBS 5.0
Engine Number	1 #	5	5	
MFHR TOTAL			178.8	

5.9. Final Aircraft Configuration

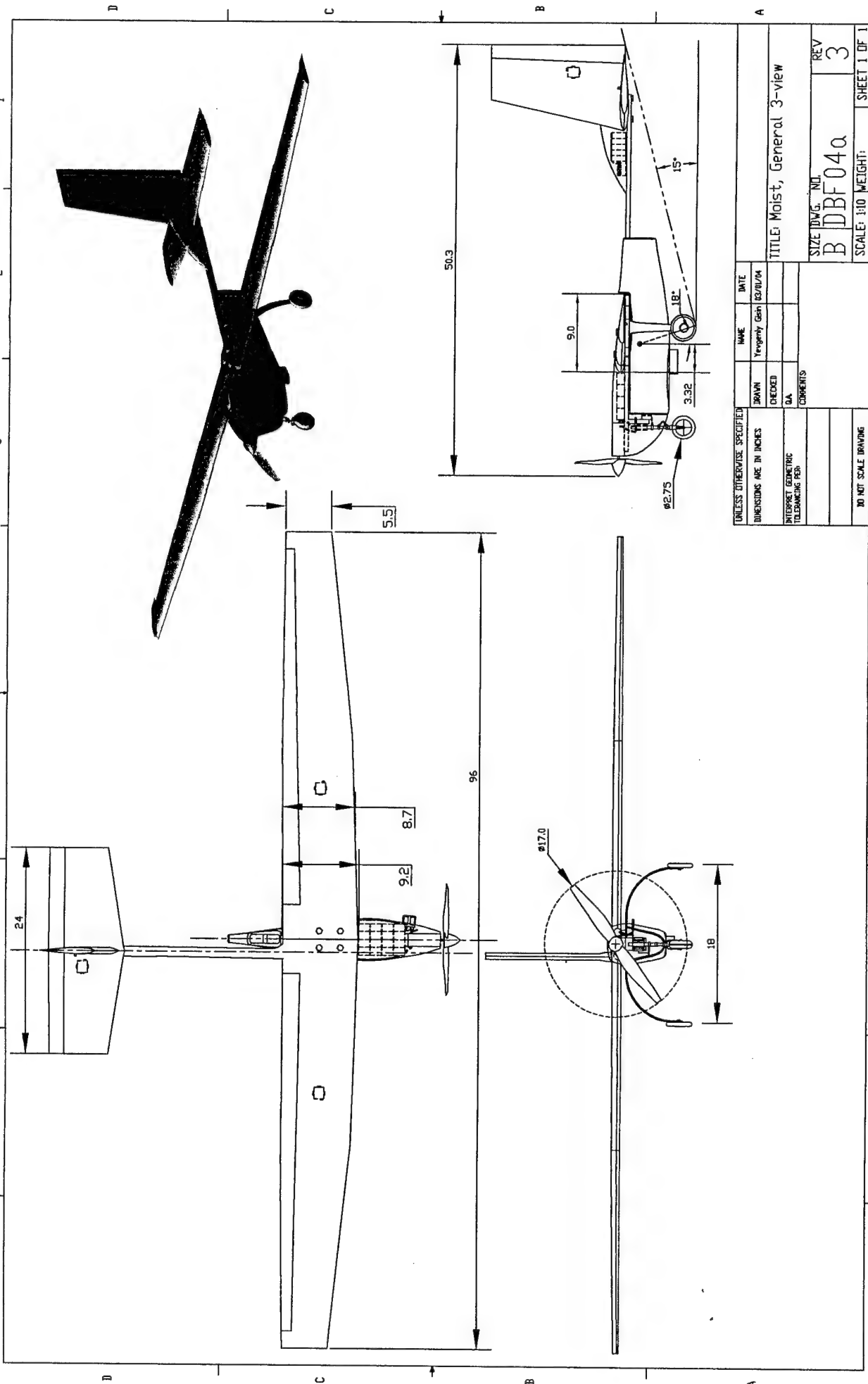
The final aircraft configuration for the 2004 DBF Competition aircraft is presented in Table 26.

Table 26 – Final Configuration

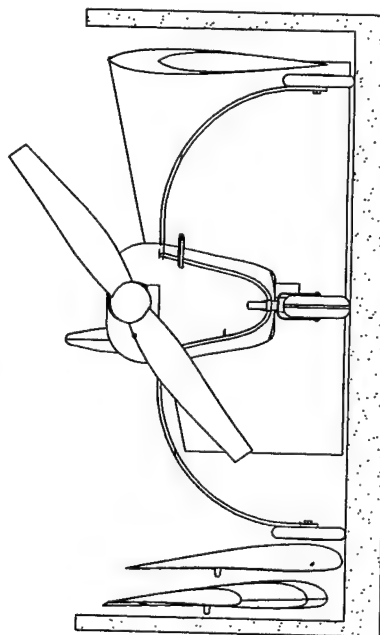
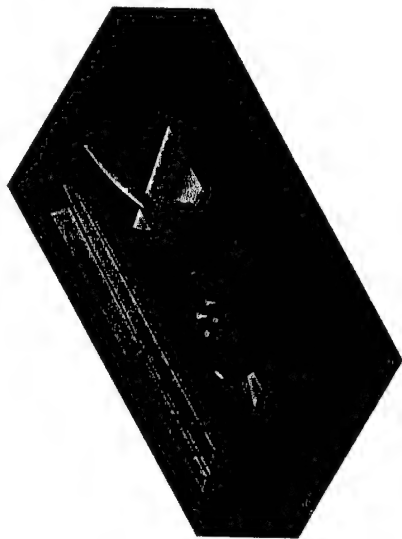
Aircraft Component	Specification
Aircraft Length/Height	53 in/25in
Battery Pack	16 Sanyo CP1700-SCRz cells
Configuration	3 columns of 4
Propulsion	
Motor/Gearbox	Graupner 930-6/Maxon 3.7:1
Speed Controller	Jeti 40
Propeller(s)	APCe – 17x12 payload mission, APCe – 14x14 ferry mission
Wing	
Airfoil-thickness-camber	d9g9-10%-3%
C _L Maximum	1.65
Planform	Modified Schuemann
High-Lift Device Type	Full-span simple flap, 15° deflection
Aspect Ratio	12.8
Area	5ft ²
Aileron Servo Type	Hitec HS-5125
Construction Type	Bead foam-core, Rohacell shear web, carbon-fiber spar cap, kevlar skin
Empennage	
Vertical Tail Area	0.92ft ²
Horizontal Tail Area	1.33ft ²
Vertical Tail C.V.	0.0573
Horizontal Tail C.V.	1.06
Servo Type	Hitec HS-5125
Construction Type	Bead foam-core, balsa shear web, carbon-fiber spar cap, kevlar skin
Landing Gear	
Wheel Diameter	2.5in
Main Gear Type	Carbon-fiber spring arch
Nose Gear Type	Robart 654 Steerable Nose Gear
Nose Gear Servo	Hitec HS-85
Payload System	
Water Volume Carried	4 liters
Radio control	
Receiver	Multiplex IPD 12 channel
Transmitter	Multiplex mc 4000
V _{maximum}	
Maximum Weight	110 ft/sec
Empty	115 ft/sec
V _{stall}	
Maximum Weight	42 ft/sec
Empty	27 ft/sec
Takeoff Distance	
Maximum Weight	130 ft
Empty	80 ft
ROC max	55 ft/sec
L/D max	17
Empty Weight	6.06 lbf
Takeoff Gross Weight	14.86 lbf

5.10. Drawing Package

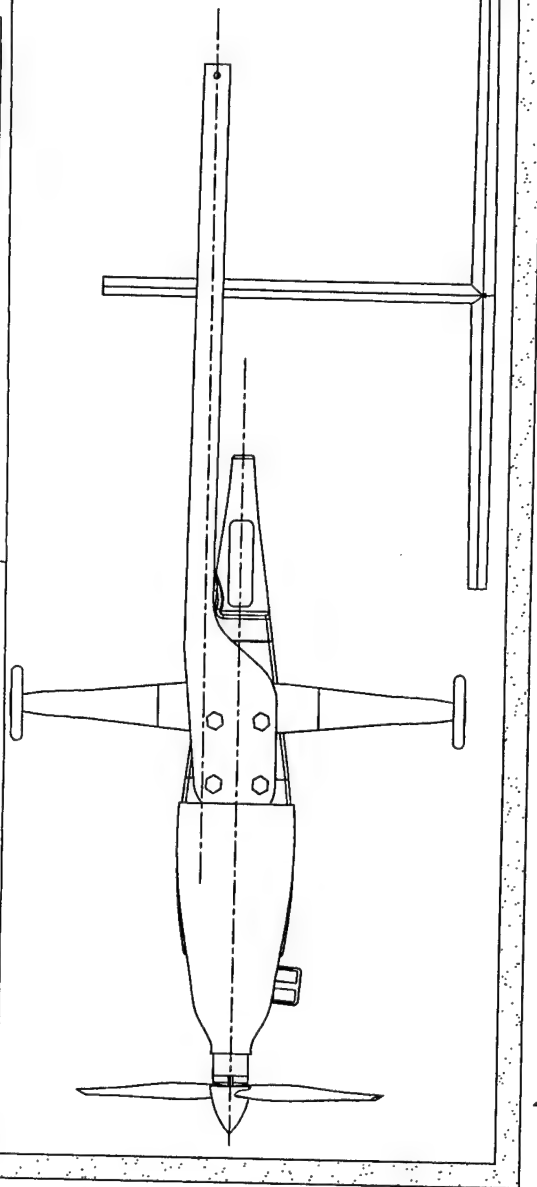
The drawings presented on the following pages include the general 3-view of the aircraft assembled for flight showing all relevant dimensions and a 3-view of the aircraft configured for transport.



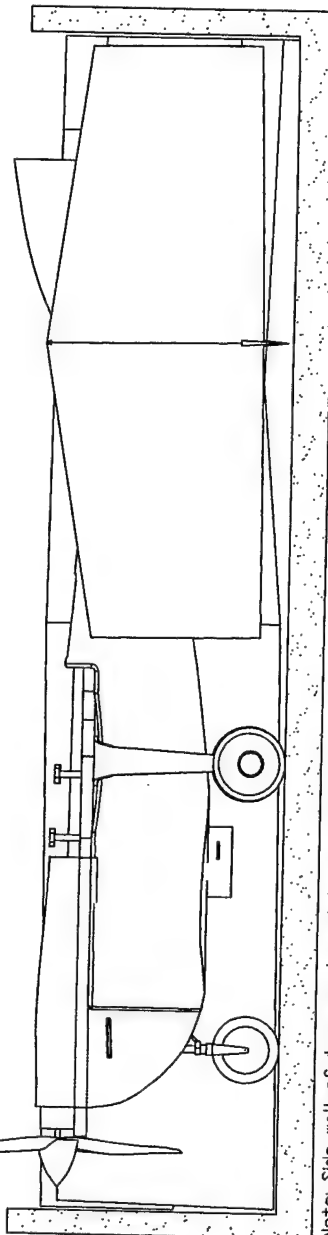
UNLESS OTHERWISE SPECIFIED			
DRAWN	NAME	DATE	
CHECKED	Yegorin Gah	03/01/04	
QA			
COMMENTS			
DIMENSIONS ARE IN INCHES			
INTERPRET GEOMETRIC TOLERANCING PER			
DO NOT SCALE DRAWING			
TITLE: Moist, General 3-view		SIZE DWG. NO.	
		B DBF04a	
		REV	
		3	
SCALE: 1:10 WEIGHT:		SHEET 1 OF 1	



Note: Front wall of transport container removed for clarity.



Note: Side wall of transport container removed for clarity.



Note: Side wall of transport container removed for clarity.

NAME	DATE
Yongyong Gish	03/10/04
DESIGNED	CHECKED
COMMENTS	
TITLE: Moist, configured for transport 3-view	
SIZE	REV
DBF04b	3
SCALE: 1:5 WEIGHT: SHEET 1 OF 1	

6. Manufacturing Plan

The minimalist design of the aircraft had the of benefit simplifying construction, since major components such as the non-load bearing tank could be manufactured independently and then bonded or bolted to the keel, at or near the c.g. With the aircraft being designed to "bolt together", the pieces could all be easily replaced in the event of failure of one of them.

6.1. Figures of Merit

The method of manufacture of the aircraft was chosen using the following figures of merit.

6.1.1. Availability of Materials and Tools

Materials

Various construction materials were considered, from ubiquitous balsa wood to now more available composites like fiberglass and carbon fiber. Boron, though highly desirable for stiffness is too difficult to acquire to make it a viable material. Therefore exotic, difficult to acquire materials would receive a -1, mail order, 2-3 day delivery received a 0, and if the material was locally available it received a 1.

Tools

Computer Numerically Controlled (CNC) machines are very accurate, but require long set up times, and trained operators. CNC operations are most effective in the machining of high-density foam plugs for mould manufacture, or to machine moulds directly. General shop tools would include items such as a band saw, compressor and drill press. Tools that required special machinery (CNC) receive a -1, general shop tools received a 0, and common household tools received a 1.

6.1.2. Skill

Machinery and various fabrication techniques require some training and skill. Fiber reinforced composites are being used more and more frequently. Working with composites requires some initial training, but the skill required for effective composite fabrication is not much than that required for wood working, and many of the same tools are used. Skills that require significant training and/or skills received a -1. Skills that requires little training or skill receive a 0. Skills that require no training or skill received a 1.

6.1.3. Construction Time

Balsa is a readily available and an easy material to work with, therefore construction time is relatively short. Composites generally require days to manufacture a mould (if one is required) and hours to lay-up and cure the part once the mould is finished. Furthermore the time required for vacuum bagging and post cure significantly adds to the construction time of the component. Composites are a heavy investment in time when compared to other materials, but the quality of the part and the ability to easily manufacture a part of complex shape makes it well worth the investment. Construction processes that can be completed in days receive a -1. Construction processes that can be completed in hours receive a 0 and minutes receive a 1.

6.1.4. Reliability

Components on critical systems must be reliable since a failure could jeopardize the mission, even non-critical components may be expensive or difficult to replace in the event of failure. The items that have low mean time between failures received a -1, an average mean time between failures received a 0 and items that have high mean time between failures received 1.

6.1.5. Performance

High component performance is essential due to the nature of the competition. Components had to meet design strength and stiffness requirements for a minimum weight penalty. The components that showed to have below average performance, received a -1. The components that had average performance received a 0 and above average received a 1.

6.1.6. Manufacturing Processes Figure of Merit

Using the merit definitions described above, a figure of merit seen in table 26 was constructed, and manufacturing processes were chosen based on ratings given.

Table 27 – Manufacturing Processes and Materials Considered for Construction

		Availability of Materials/ Machinery	Skill Required	Construction Time	Cost	Reliability	Performance	Total
	Weight Factor	1	1	2	2	4	6	
Wings	Hollow composite	-1	-1	-1	0	1	1	6
	Foam core composite	0	0	1	0	1	1	12
	Foam core balsa covered	1	0	1	1	-1	-1	-5
Water Tank	Lost foam composite	0	0	1	1	0	0	4
	CNC machined mould	-1	-1	-1	-1	1	1	4
	Male plug / Female mould	0	0	0	0	1	1	10
Keel	Balsa	1	0	1	1	-1	-1	-5
	Fiber glass	0	0	0	1	0	0	2
	Bi directional Carbon	0	0	0	0	0	1	6
	Uni directional Carbon	-1	0	0	-1	1	1	7
	Kevlar	0	0	0	0	1	-1	-2
	Metal	0	0	1	1	-1	-1	-6
Landing Gear	Commercially available	1	1	1	1	0	0	6
	Metal	1	-1	1	1	0	0	4
	Unidirectional Carbon	-1	0	0	-1	1	1	7
	Bidirectional Carbon	0	0	0	0	1	1	10

6.2. Manufacturing processes

The manufacturing processes that were chosen using the figure of merit above are described in more detail below.

6.2.1. Keel

In the absence of a fuselage all major components are bonded or bolted directly to the keel – it being the major longitudinal load-bearing component of the aircraft. The keel was manufactured as a unidirectional carbon fiber and Rohacell foam sandwich. Half-inch thick Rohacell foam sheet was cut into the profile of the keel using full-scale technical drawings as a template.

Unidirectional carbon fiber was laid up wet onto the foam with lengthwise fiber orientation, from nose to tail. Bi-directional carbon and Kevlar "sock" were laid up over the carbon to increase torsional rigidity. The sandwich was cured under vacuum in a low temperature oven at 140°F. Because of this being a wet lay-up component, the outmost care was taken to keep the fiber to matrix ratio as high as possible – the value estimated and used in weight buildup was 50/50.

6.2.2. Wing and Tail Surfaces

Wing and tail surfaces were of foam core composite construction. The foam was low-density white bead foam. Spar caps are multi-ply unidirectional carbon tapes with Kevlar wing skins. Because of the low compression strength of white foam, a ½-in thick shear web of Rohacell was placed in the wing core and connected the top and bottom spar caps. Kevlar wing skins were wetted out on Mylar sheets, and wrapped around the wing core. The lay-up was carefully vacuum bagged and cured in a low temperature oven.

Control surfaces are constructed by removing a cutting a quarter inch spanwise groove into the lower skin at the trailing edge. The groove is cut through the foam and up to the upper skin. Therefore the upper skin becomes the hinge for the aileron – being made of kevlar, structural fatigue is unlikely to be the mode of failure. Port and starboard wings are connected at the centerline by a rectangular cross-section carbon fiber joiner tube. The two halves of the joiner tube are bonded directly to the spar caps to transmit bending loads in the wing.

6.2.3. Water Tank

Water tank halves were constructed by wet lay-up of Kevlar into a female mould. Since the tank is a non-load bearing member 3 plies were deemed sufficient. Baffles were fabricated and bonded into the tank halves. The baffles not only minimize sloshing of the fluid but also provide stiffness for the tank while serving as a load path for the mounting points of the tank to the keel. To simplify construction, the exit nozzle of the tank was fabricated as a separate piece and bonded into the tank. The nozzle was given a smoothly convergent shape to minimize head loss to the water flow, and a simple sliding door exit valve controlled by a push pull servo was attached.

Originally, the nozzle was designed to have a small diverging section to aid in the transition of the water from the throat into the free stream air. After further research into the rules of the contest, it was found that the exit of the nozzle must have the maximum diameter of 0.5 inch. This is for the ease of inspection by the contest officials. The removal of the divergent section of the nozzle is not expected to decrease the dump time significantly.

The filler cap was constructed of a combination carbon and Kevlar in such a way that the door could flex about a line through its center (in a clam shell fashion) enabling a fast refill with both bottles at the same time. The return force on the door due to the stiffness of the fibers pushed the cap against the inside of the tank hatch, sealing the tank.

6.2.4. Landing Gear

Landing Gear was constructed by lay up of unidirectional prepreg carbon fiber onto a semicircular male mould. Fibers were compacted by rolling lay-up with a roller, before the mould was vacuum bagged and oven cured.

6.3. Manufacturing Plan

The manufacture of the aircraft had to proceed in an organized manner – in order to achieve this, the team planned out a manufacturing schedule, presented below in Figure 34.

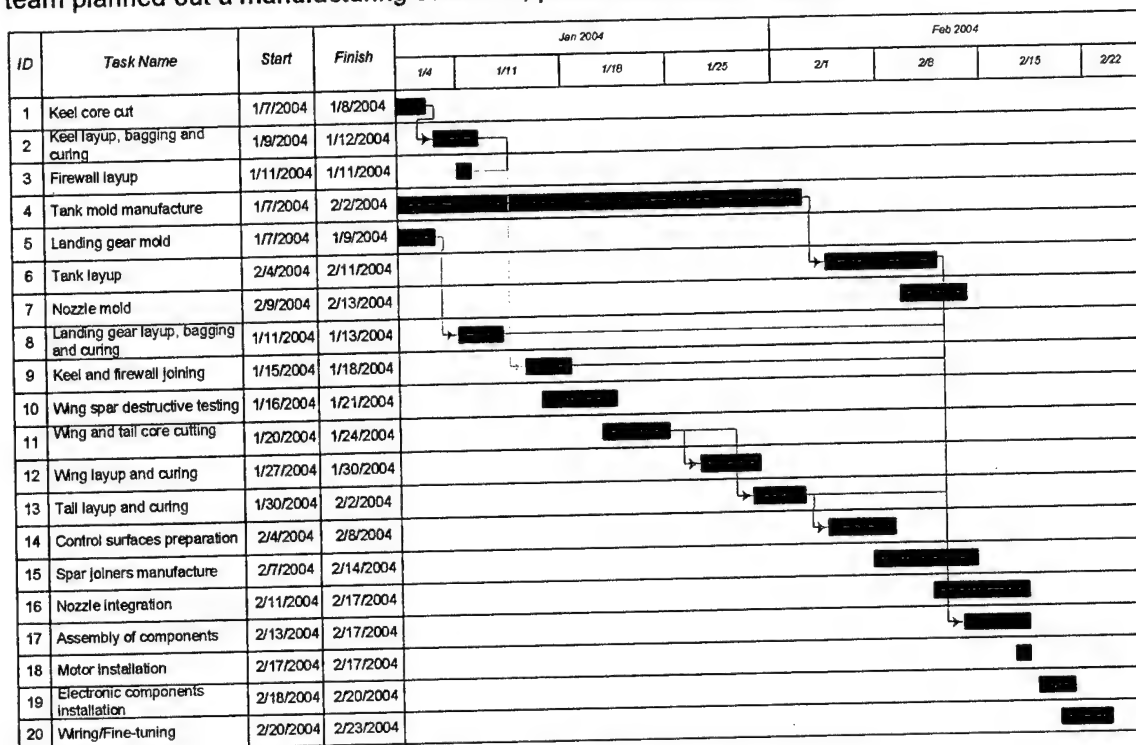


Figure 34 – Manufacturing Schedule

7. Testing

7.1. Testing Objectives

Qualification of aircraft's main components was achieved through individual testing. A thorough test schedule was maintained to provide sufficient time for modifications and improvements. The main components tested for maximum loading were the wing, tail, and keel.

7.1.1. Wings and Tail

Wing shear webs were tested by fabrication of a simple test block shown in Figure 31. The depth of the block being equal to the maximum camber of the wing, thus providing an accurate representation of the expected normal stresses in the shear webs. The clamped block was loaded to failure by addition of weights at the free end. Failure mode, as expected occurred via delamination of the spar cap in compression. Construction of the tail was identical to that of the wing with the difference being in the shear webs. Testing of the tail was therefore done in a similar fashion to the wing.

7.1.2. Keel

Since the keel is of relatively simple construction, the entire component was tested rather than constructing a test sample, thereby saving time and improving test accuracy. Similar to the shear web test sample, the keel was tested in bending and in torsion, however the keel was loaded only to the maximum

expected flight conditions. Test results indicated that the keel had insufficient torsional rigidity. The condition was rectified by the lay up of an additional Kevlar “sock” over the keel.

7.1.3. Tank and Nozzle

The majority of tank testing was done before the completion of the tank moulds using a test tank made using the “lost foam” process. Testing of the production tank indicated a lack of stiffness in the part. The tank was modified by the additional of unidirectional carbon fiber. The use of a tank mould enabled the production of multiple parts that could be used to test exit nozzle configurations and mechanisms; testing continues in this area.

Table 28 – Testing Schedule and Qualifications

Component	Test Date	Qualify
Wing		
Wing Joiners		
Tail		
Keel		
Landing Gear		
Connections		
Water tank		
Release Valve		

7.2. Flight Tests

Visual inspections before and after flight will be conducted in order to evaluate any potential damage of the airframe. Flights will also be video taped to provide accurately timed performance throughout each segment of the flight. Detailed flight performance of the aircraft was gathered using a GPS receiver, solid-state gyroscopes and a Pitot-static probe installed on the aircraft, with data readings gathered at the frequency of 1hz. The system used to collect the data is identical to that used on the *Dragon Eye* UAV and was provided by Jennings Engineering of Los Osos, CA. The instrumented aircraft can be seen in Figure 35 on the next page.

During flight tests, the aircraft started at an altitude of about 600 ft and the motor was turned off. At this point, the aircraft was trimmed for a stable gliding descent, with velocity, heading and altitude changes recorded from test data gathering equipment. With no energy being added to the system by the propulsion system, the Lift/Drag ratio of the aircraft could be calculated from its flight speed and descent rate.

The equation used was: $\frac{L}{D} = \frac{1}{\tan(\alpha)}$, where α is the aircraft glide angle. The data was gathered at three glides of various speeds, collated together and the resulting Lift/Drag vs. airspeed curves compared to those predicted analytically in Figure 36.

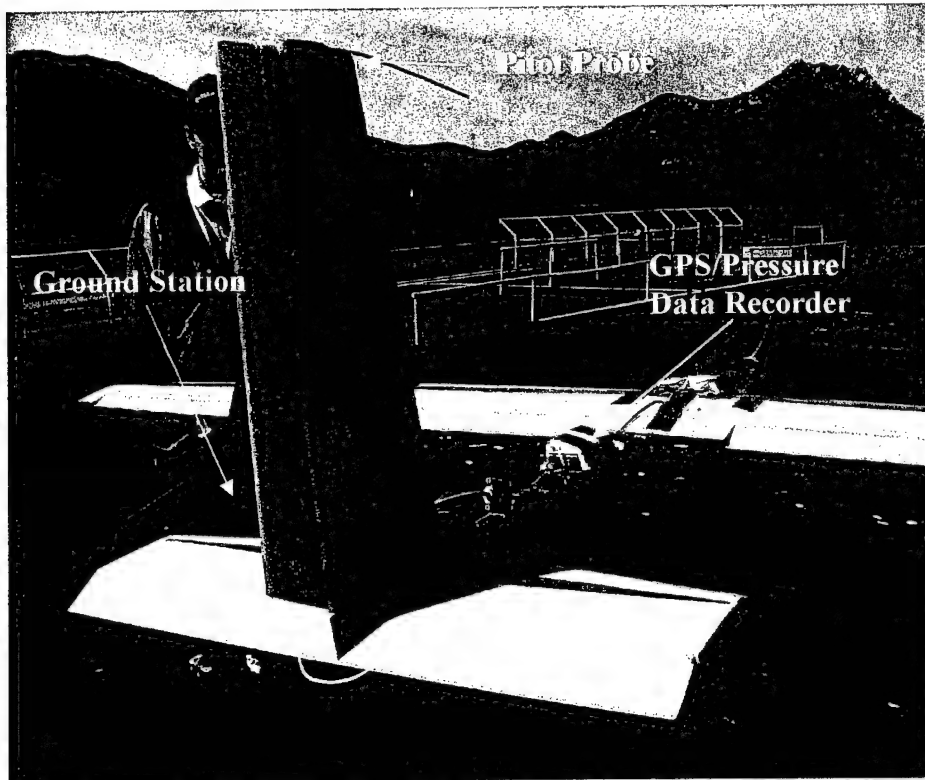


Figure 35 – Instrumented Aircraft Before Flight Test

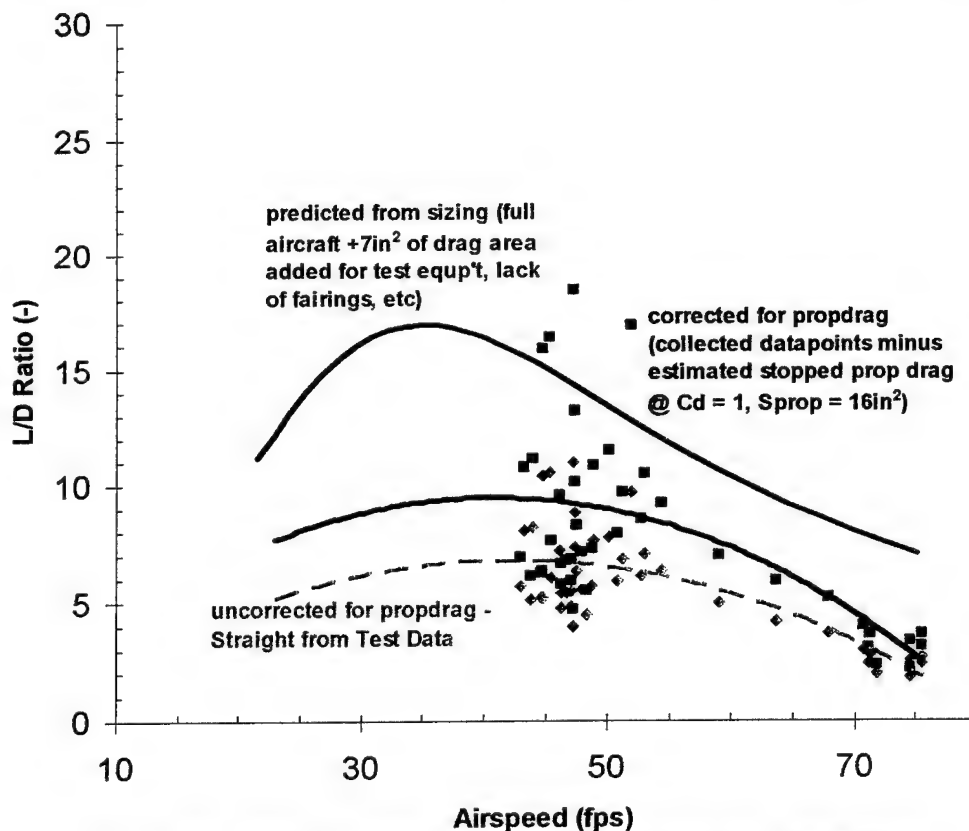


Figure 36 – Flight Test Performance Data Gathered vs. Predicted

A number of explanations can exist for the fact that the gathered test data, even after correction, is still lower than that predicted by the performance code. It is likely that the lack of full fairings on the aircraft affected the drag polar negatively. It is also practically impossible to achieve the optimum flight conditions of the max L/D when controlling an aircraft with a remote control in windy weather.

The pitch stability of the aircraft was noticed to be quite low, to the point of making the aircraft difficult for the pilot to fly. Although this flight characteristic may be beneficial during the low-weight ferry mission, by enabling the aircraft to be more maneuverable, it is not something desirable during heavy-weight flight. A factor that exacerbated the effects of the pitch instability was the tendency of the aircraft to stall abruptly. Since the pitch instability was the result of low ($< 5\%$) static margin, a decision was made to move the payload CG slightly forward in order to achieve a higher static margin during the critical flight regime.

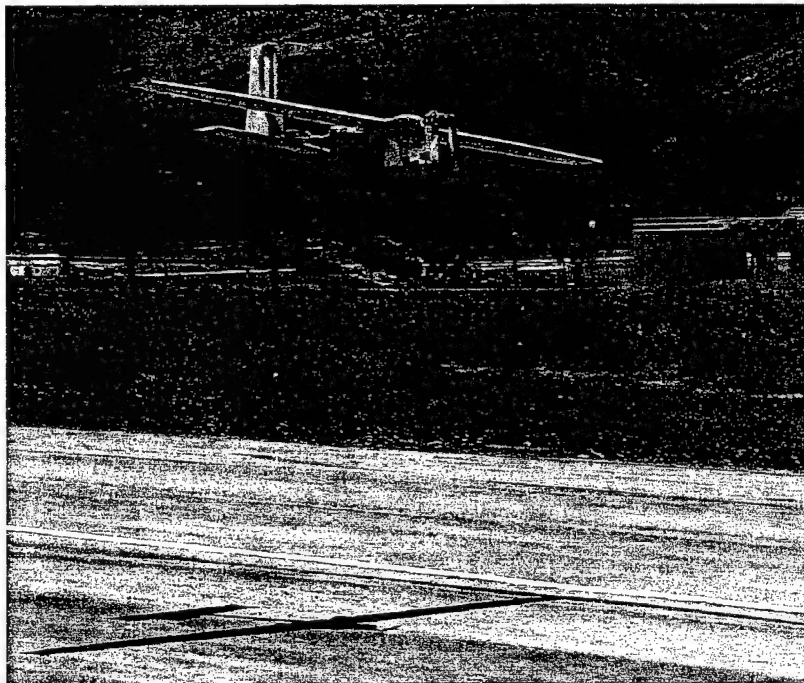


Figure 37 – First Flight

One of the important lessons learned during flight test was unexpected. Upon the second landing of the day, the firewall/nose gear mount part of the keel delaminated at a joint. In Figure 38, the delamination of the carbon fiber under tension can be seen.

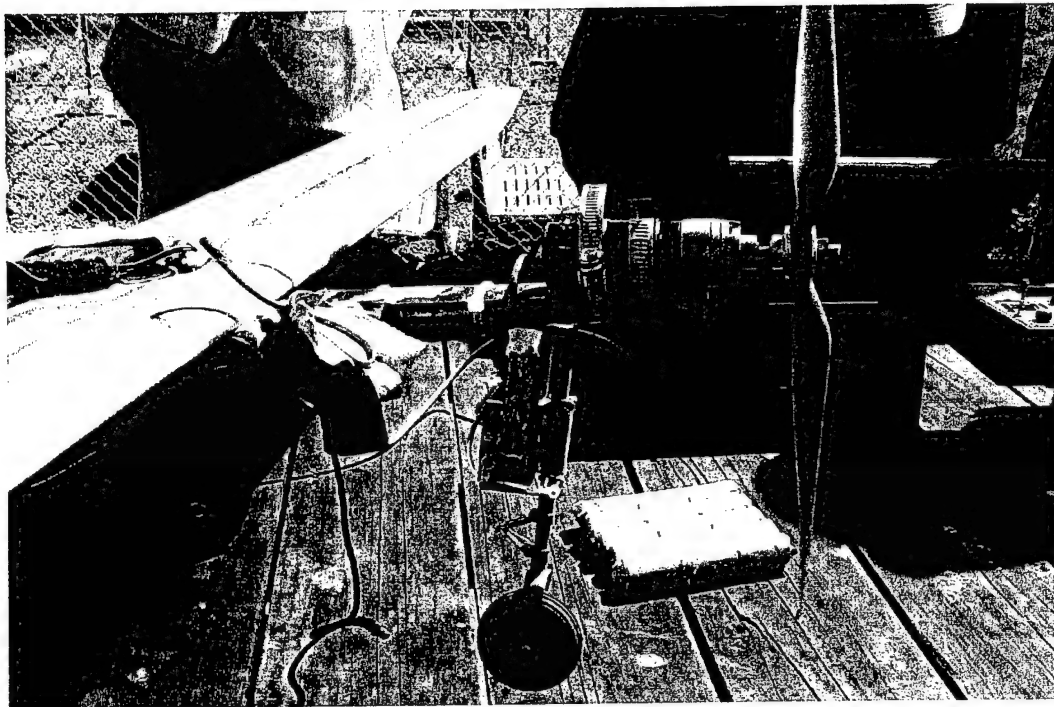


Figure 38 – Deformed Firewall/Landing Gear Mount

This failure demonstrated that the nose gear mount was not attached to the rest of the keel securely enough. This component will have to be re-attached with better use of materials and a more correct design of the joint in order to ensure its strength. The nose gear will also be moved and angled slightly forward in order to both mitigate ground impacts and to also improve the ground handling/landing characteristics of the aircraft.

REFERENCES:

¹ Raymer, Daniel P., *Aircraft Design: a conceptual approach*, AIAA, Inc.

² Shaufele, Roger D., *The Elements of Aircraft Preliminary Design*, Aires Publications, Santa Ana, CA

³ Robert J Boucher, *AstroFlight Electric Motor Handbook*, Los Angeles, California, 1994. ISBN:0-9644065-00

⁴ ibid



Università degli studi di Roma "La Sapienza"

GALILEO V

AIAA / CESSNA / ONR
Student
Design / Build / Fly Competition 2003/04

Design Report



The Flying Centurions

"Non est ad astra mollis e terris via"



Table of Contents

1	Executive Summary	pag 1
1.1	Introduction	pag 1
1.2	Conceptual Design	pag 1
1.3	Preliminary Design	pag 1
1.4	Detail Design	pag 2
1.5	Manufacturing process	pag 2
1.6	Testing Sessions	pag 2
2	Management Summary	pag 3
2.1	Team Organization	pag 3
2.1.1	<i>Organization and "pre-Conceptual" Design</i>	pag 3
2.1.2	<i>Team Management</i>	pag 3
2.1.3	<i>Team Architecture</i>	pag 3
2.1.4	<i>Design Area</i>	pag 4
2.1.5	<i>Building Area</i>	pag 5
2.1.6	<i>Testing Area</i>	pag 5
2.1.7	<i>Report Area</i>	pag 5
2.1.8	<i>Logistic Area</i>	pag 5
2.2	Milestone Chart	pag 5
3	Conceptual Design	pag 7
3.1	Problem Statement	pag 7
3.2	Aircraft configuration	pag 8
3.3	Fuselage/Tank configuration	pag 10
3.4	Wing Configuration	pag 11
3.5	Wing controls	pag 13
3.6	Tail configuration	pag 14
3.7	Motor and Propeller position	pag 15
3.8	Landing gear configuration	pag 15
3.9	Structural Configuration	pag 16
3.10	FOMs Analysis Results	pag 17



4 Preliminary Design	pag 19
4.1 Introduction	pag 19
4.2 First Sizing Trade Studies	pag 19
4.2.1 Main Assumptions	pag 19
4.2.2 Known Parameters	pag 20
4.2.3 Major Design Parameters	pag 21
4.2.4 Fire Fight Mission	pag 21
4.2.5 Construction	pag 22
4.2.6 Analysis Methods	pag 22
4.2.7 Analysis Results	pag 24
4.3 Fine Trade Studies and design Optimisation	pag 24
4.3.1 Aerodynamic Considerations	pag 24
4.3.2 Propulsion Analysis	pag 28
4.3.3 Performances & Flight Mechanics	pag 29
4.3.4 Structural Analysis	pag 35
 5 Detail Design	pag 38
5.1 Introduction	pag 38
5.2 Aerodynamics and surface arrangement	pag 38
5.3 Flight Dynamic and Control	pag 39
5.3.1 Control Surfaces	pag 39
5.3.2 Handling Qualities	pag 41
5.4 Structures	pag 44
5.4.1 Fuselage Structural Details	pag 44
5.4.2 Wing Structural Details	pag 44
5.4.3 Tail Structural Details	pag 44
5.4.4 Landing Gear Structural Details	pag 44
5.4.5 Radome Structural Details	pag 45
5.4.6 Tank Structural Detail	pag 45
5.5 Propulsion System	pag 45
5.6 Final Aircraft Table	pag 46
5.7 Rated Aircraft Cost	pag 46
5.8 Drawing Package	pag 48



6	Manufacturing Plan and Processes	pag 51
6.1	Introduction	pag 51
6.2	Alternative processes investigated	pag 51
6.3	Prototype Manufacturing	pag 52
6.4	Manufacturing Processes Selected	pag 53
6.4.1	<i>Fuselage Manufacturing and Tooling</i>	pag 53
6.4.2	<i>Wing Manufacturing and Tooling</i>	pag 53
6.4.3	<i>Tail and Empennage Manufacturing and Tooling</i>	pag 53
6.4.4	<i>Landing Gear Manufacturing and Tooling</i>	pag 53
6.5	Manufacturing Milestone Chart	pag 53
7	Testing Plan	pag 55
7.1	Structural Tests	pag 55
7.2	Wind Tunnel Tests	pag 56
7.2.1	<i>Propulsion tests</i>	pag 56
7.2.2	<i>Aerodynamic tests</i>	pag 56
7.3	Flight-Tests	pag 58



1. Executive Summary

1.1 Introduction

This report describes, step by step, the path followed in designing and building Galileo V, the aircraft developed by the Flying Centurions team from "La Sapienza" University of Rome for the AIAA/Cessna/ONR Student Design/Build/Fly 2004 Competition. The first step was to analyze the contest rules in order to find out the main parameters useful to meet the mission requirements. We immediately realized that our aircraft had to be able to meet the requirements of both missions, so we tried to optimize it to find the best trade off between cargo capability (mainly for Fire Fight mission takeoff) and speed (for both missions cruise). These two main aircraft qualities were the guidelines of the entire project development.

1.2 Conceptual Design

At the beginning of the design process the whole team was split into 4 groups which were free to incite their fantasy in order to suggest a first project able, in their opinion, to gain the highest score. Logically the main problems were to research for a speedy (and thus light) aircraft but, on the other hand, for a quite slow plane able to carry and to quickly dump the water payload. For this reason various series of figures of merit (FOMs) were introduced in order to narrow the field of possible configurations. The purpose of this conceptual phase was to fix some parameters for next design phases, such as wing, motor and landing gear.

1.3 Preliminary Design

At this point, another splitting was introduced so that more accurate studies were done. The first group (aerodynamics and flight mechanics) had to select the best wing airfoil and all the aircraft components in order to obtain good performances during take off, landing, and dumping phases. For this reason a conventional tail was chosen and it was thought to endow the entire wing span with "flaperons". The second group (structures) attended to the problems inherent with the structural behavior of the aircraft. This group focused its attention mainly to the presence of the water tank: its weight is about half the entire gross aircraft weight. It was taken into account also the problem of the sizing and opening of the dumping valve. The third group (propulsion) attended the propulsive branch of the design; using numerical simulations, the relationship between number of battery cells, actual thrust curve, and propeller dimension was studied.

The work of the three groups during the preliminary design phase was simplified by introducing a self-made optimization program which allowed to deeply investigate parameters like wing span, wing area, tail configuration, fuselage and tank shape, and the number of battery cells; at the same time the effects of a variation of these parameters on the Rated Aircraft Cost (RAC) were studied. The developed program reduced the set of variables which could gain the highest potential score, so the three groups had to select the final values in order to obtain the best performances of the aircraft. At this point it was possible also to draw the first CAD model.



1.4 Detail Design

In the detailed design phase the preliminary sizing of the aircraft was improved: each component and subsystem was deeply analyzed taking into account how every single aspect had to be integrated in the global project. Through the use of a finite elements analysis, structure loads were simulated and, then, the theoretical results were compared with experimental tests performed on the first prototype of the aircraft. It allowed to define the final sizing of the components. Shape, dimension, and position of water tank and valve were accurately designed in order to minimize the dumping time, considering the possibility to perform the 360° turn with a radius as big as possible. Static and dynamic stability were studied as well taking into account the different aircraft attitude required during the two missions. The difference in the MTOW of the two mission configurations really affects the pitching moment. We decided to trim the airplane for "ferry" configuration; in this way no additional drag would reduce the high cruise speed required to obtain the best flight score. The location of servos, receiver, and cables was defined, and the type of propellers, cells, and motor were selected. All this design phase was realized taking into account the problems relative to manufacturing process. At the end it was possible to complete the CAD drawing package of all the components of the aircraft, and also the assembly scheme in order to help us to build the final model.

1.5 Manufacturing process

During the building phase we assembled first a full scale prototype using low cost materials and only after testing its efficiency we built the final aircraft. In this way we were able to judge the validity of our studies, and eventually change the original project in order to gain the best structural behavior for all the components of the aircraft. We also dealt with some problems in the building process because of our limited skills, sometimes producing non-satisfying results.

1.6 Testing Sessions

In this last design phase the main duty was to carry out all the experimental analysis in order to guarantee the reliability needed to complete safely all the missions planned. Various types of specimens were mechanically tested so that the materials needed to manufacture each component were singled out. Basing on the results obtained in the D/B/F 2003 edition we were able to evaluate the loading capabilities of the wing. Just like last year, a 1:2 scale semi-model was used in wind tunnel test to provide the whole aircraft polar drag and important indications on the shape of the aerodynamic fairings between the wing and the fuselage. Furthermore, the propulsive group had to test the motor-propeller set, obtaining thrust and current values at various flight speed. Finally, during the first flights of the aircraft other different tests were planned and carried out in order to have more information about the real behavior of the airplane.



2. Management Summary

2.1 Team organization

2.1.1 *Organization and "pre-Conceptual" Design*

The team for the D/B/F 2004 Edition was first organized at the end of May 2003. At the beginning the number of students involved was huge: about 60 students took part in the first meetings. Following the previous experience in the contest, the first step was to organize the whole team so that we could engage a lot of *new* students, who are the ones who took part in the contest for the first time. Therefore 4 groups were organized in order to begin to take confidence with the rules and the organization. Each group was led by an *old* student and its goal was to propose as many as possible pre-concept projects which could solve all, or in part, the problems inherent to the two compulsory missions.

2.1.2 *Team Management*

At the end of the first phase, the entire team was reorganized in order to realize the most useful possible structure. We knew it is fundamental to coordinate the work of everyone to obtain the best results in the designing phases, so we tried to build the architecture of the team in order to respect the following principles: 1) to clearly identify people who would have the responsibility of leading the team along the design process; in particular, there should be one or more persons, the team managers, able to make decisions, schedule work-packages, assign tasks and check for they are performed; 2) tasks must be shared to specialized groups, each one with its own leader; the latter should play inside his group the same role the team manager plays within the team; 3) the authority should be delegated to the groups' leader who organize their group's work to make specific, *local* decisions, in such a manner that the flow of tasks assignation goes from up to bottom, and problem resolution goes from bottom to up; 4) *global* decisions must be made by the team manager with the help of technical *staff tables*, masters in the subject is being discussed.

2.1.3 *Team Architecture*

Driven by the previous considerations we have located a group of major areas of interest in the project contest: designing / building / testing / flying / documenting. Figure 2.1 shows how we decided to split these areas in other sub-areas and displays the role of anyone in the whole team.

As in the last years, Prof. G. De Matteis is our official advisor and he supported us in more than one occasion: he gave us both technical and logistical advices in order to achieve the best results. This year we have decided to have more than one team manager, with a rotation between the *old* members, due to the complexity of the task; this duty, really consist in directing and coordinating the work of all the students involved, paying attention to the deadlines in the design and manufacturing process. In such a charge of coordinating the teamwork, he was supported by a seniors council, composed by students with previous DBF experiences. At the subsequent level, the team was divided in three main areas, aerodynamics and flight mechanics, structural, and propulsion each leaded by a responsible who coordinate the specific tasks. Some works, concerning multi-subject studies, as the conceptual design stage and the realization of the optimization



algorithm in the preliminary design stage, needed to be carried on by all the groups, together with the team manager.

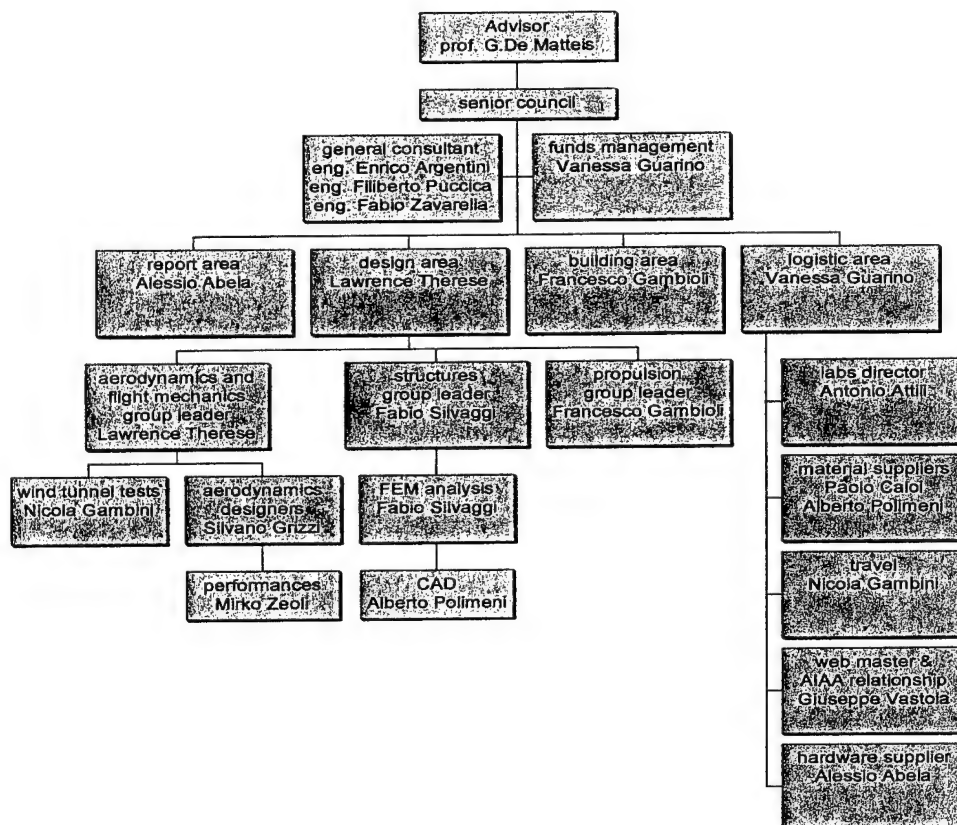


Figure 2.1 Team architectural structure

2.1.4 Design Area

Aerodynamics and Flight Mechanics Group: the targets of this group were the shaping and sizing of the lifting surfaces and evaluating the aerodynamics loads. Furthermore, it had to predict the aircraft performances, stability, and handling qualities, in order best meet the mission requirements. Its work was based on analytical, numerical, and experimental tools. **Structural Group:** this group had the responsibility to size the main structural elements and to choose the suitable materials to be used in the construction. It also had to select the right integration methods, and to supply the building group with the drawings needed for the manufacturing process. The tools adopted were analytical, numerical, and experimental too. **Propulsive Group:** its main target was the selection of the motor-propeller-cells system. With analytical and experimental tools it was possible to narrow the possible combinations to a few solutions which could be tested directly during the prototype flight sessions to reach the final solution.



2.1.5 Building Area

The leader of the building group had to receive the theoretical inputs about the shape and the internal structure of the airplane and to coordinate the manufacturing process that lead to the final plane. He planned building activities and controlled the work of his group. All the students involved in the project gave their contribute to the manufacturing process of the mock-up, the prototype, and the final model because in this way it was possible to teach them what they probably will never learn during the academic courses.

2.1.6 Testing Area

The three main groups engaged in the design process were strictly involved in the testing area too. Really the tests are extremely useful during the design process, giving new information on the right way to proceed. Leaders of the Design Area's groups were also involved in testing activities which are tightly connected to the subjects of their studies.

2.1.7 Report Area

Since the beginning of the organization of the team a report group was formed, with a leader. We feel the report plays an important role in the computing of the overall score. For this reason, since the pre-conceptual phase, each group had to write and support by documents all the work it did and the results it achieved or it thought to achieve. All the papers obtained were collected and the duty of the report group was to organize and revise this information in order to produce an organic review, meeting the requirements of the competition.

2.1.8 Logistic Area

This area was not directly connected to the design or building process, but it had the fundamental duty to supply the entire team with funds, tools, facilities, hardware and software instruments, and any item to improve the configuration sizing, realizing, testing. In particular, we felt the need to identify one person responsible for the management of funds, one person for looking materials and components, two persons for dealing with the laboratories and one person for external relationships and contact to AIAA organization.

2.2 Milestone Chart

A correct time scheduling is an essential issue to meet the requirements of the competition. We identified early in the design process a series of scheduled timings for the major activities we had to perform, and marked some deadlines representing the main milestones we would have to meet along the work. An overall summary of main timings and deadlines is represented in figure 2.2. Many more detailed monthly plans were produced during the work, so to guarantee not to disagree with the dates imposed by AIAA organization.

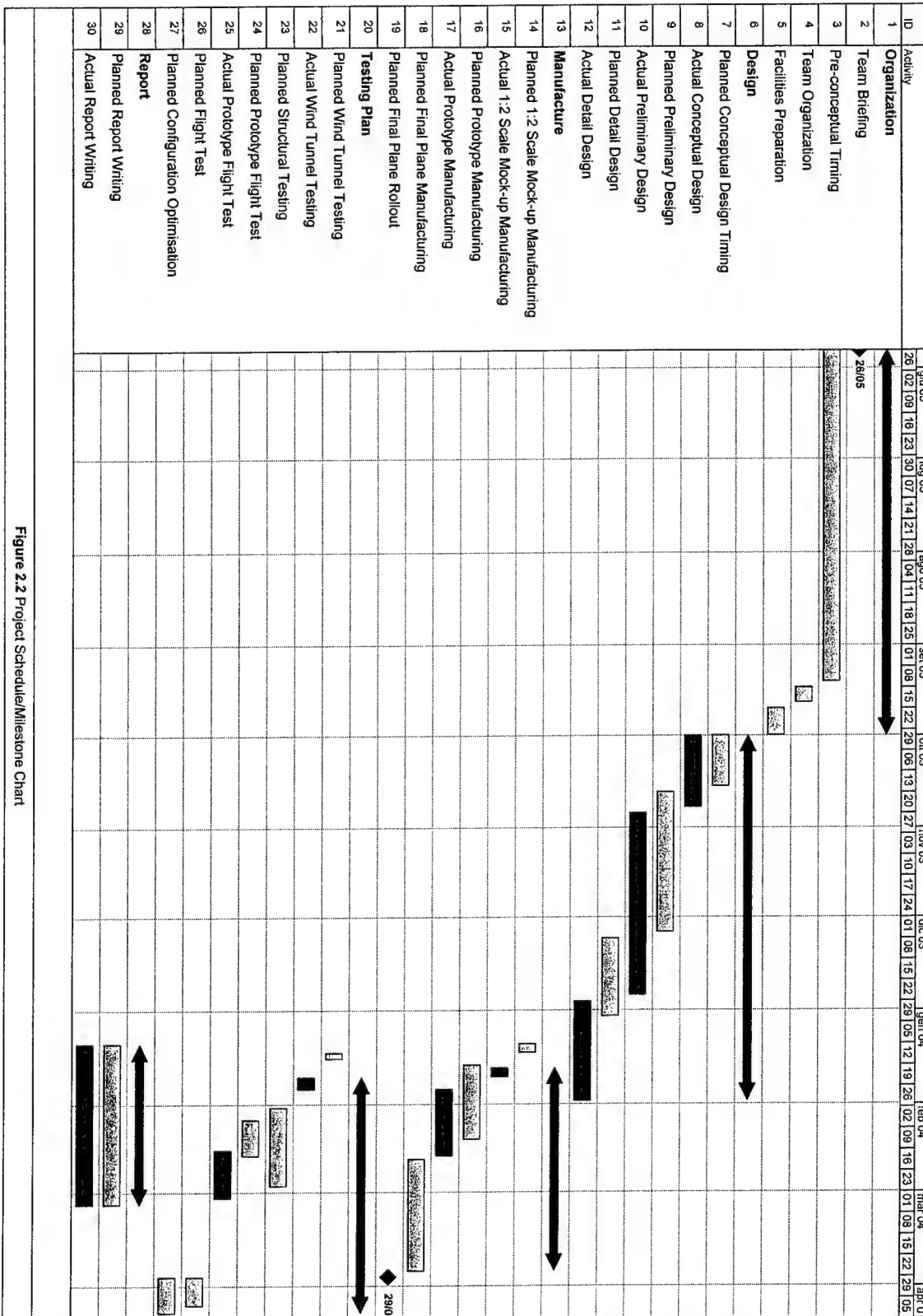


Figure 2.2 Project Schedule/Milestone Chart



3 Conceptual Design

3.1 Problem Statement

The rules analysis leads to the design of an aircraft with the following major characteristics:

- a) Dimensions limited by the case box
- b) Take off run less than 150 ft
- c) Ability to perform both missions
- d) Lowest possible RAC

The first characteristic requests an aircraft composed by "pieces" with limited dimensions, able to fit all together at the same time in the box. The second one requires an accurate analysis of the aerodynamic behaviour and performances. The third and the fourth ones are felt to be the most important. The ability to perform both missions may lead to aircrafts with very different characteristics, while the RAC (which is deeply influenced by many other design parameters and so will be considered in almost all the design process) has a high influence on the final score. Then in the following two sections we describe what the RAC is and analyze the missions in order to define the primary design parameters whose optimization led us to the final configuration.

3.1.1 The Overall Score

The overall score of the DBF contest is a combination of three numbers: the Written Report Score (WRS), the Total Flight Score (TFS) and the Rated Aircraft Cost (RAC), using the formula:

$$\text{Score} = (\text{WRS} * \text{TFS}) / \text{RAC}$$

The best Single Flight Scores (as defined in the next paragraph) from each of two different mission types will be summed to obtain the team's Total Flight Score.

The Rated Aircraft Cost is a function of the complexity and technological costs of design and construction of the entry. It is computed as:

$$\text{RAC} = (300 * \text{MEW} + 1500 * \text{REP} + 20 * \text{MFHR}) / 1000$$

Where MEW is the Manufacturers Empty Weight, defined as the Actual airframe weight in lbs with all flight and propulsion batteries but without any payload; REP is the Rated Engine Power, defined by:

$$\text{REP} = [1 + 0.25 * (\# \text{ engines} - 1)] * \text{Total Battery Weight}$$

and MFHR is Manufacturing Man Hours, estimating the work required to build the airframe and the control system. It takes into account geometrical size of wing and fuselage, the number and type of wing control surfaces (ailerons, flaps, spoilers, flaperons etc.), the empennage configurations (horizontal and vertical surfaces, with or without control), and the number of servos and motor controllers used.

The importance of a low RAC can be understood considering that lowering it, for example, from 10 to 9 the overall score would increase more than 11%.

3.1.2 Multirole Design Problem

The two completely different missions forced us to design a real multirole aircraft able to resolve the conflict between two opposite wingload design requirements.

In the "Fire Fight" mission the aircraft will be filled with up to 4 liters of water, will take-off in 150 ft, reach the upwind pylon, and turn. During the downwind leg, included the 360° turn, it will dump its water load. At the



downwind pylon, it will turn and land. Once stopped, the aircraft will be reloaded, and it will fly another circuit. After the last landing the tank will have to be completely empty. Maximum dump orifice diameter is 0.5 inch. The Single Flight Score for this mission is equal to the weight (in lbs) of the carried water times the mission Difficulty Factor, equal to 2.0, divided by the mission time. In the "Ferry" mission the aircraft will take-off without any payload, complete four complete laps, and land. In each downwind leg, it will have to complete a 360° turn. The Single Flight Score for this mission is equal to the Difficulty Factor, equal to 1.0, divided by the mission time. For a better performance in the first mission, the aircraft has to be able to lift a heavy weight, and fly enough slowly to dump all the water. This would lead to a wing with a large surface, and high C_L ; to win the high aerodynamic drag induced by high C_L and large wing, the aircraft will need a powerful propulsive system. In order to gain the highest score in the second mission, the aircraft will need just to fly as speedy as possible. This would lead to a small and light airplane with a reduced wing surface and a lighter propulsive system. Obviously the aircraft able to win the contest will need to resolve the trade-off between the requirements of the two missions. As a conclusion, the design parameters we will consider, will have to suit the characteristics listed at the beginning of this section, and resolve "The Multirole Problem".

3.1.3 Design Parameters

The main constraint to the aircraft dimensions is due to the volume of the water tank. In the conceptual design we will design an aircraft able to carry the maximum 4 liters load; really preliminary analysis of how the payload would affect the total score, persuaded us to carry the maximum payload permitted allowed. We have investigated different configurations according to the following design parameters: shape, size and location of the water tank, number and location of lifting surfaces, wing planform, tail configuration, propulsive system location and configuration, structural solutions.

3.1.4 Alternative Configuration Concepts

Just like last year, we considered two ways to solve the problem of selecting, among the possible configurations, the one that best suits the design requirements: the first one is to consider at one time all the variables and create a single global decision matrix; the second one is to consider a set of "sub problems", each with a reduced number of variables; the configuration selection goes on in a cascade of solutions of these local problems. Considering our previous positive experiences, we felt this second way more efficient because it permits to point out, by suitable FOMs, the influence of each parameter on a reduced set of design targets.

3.2 Aircraft Configuration

The first and more general sub problem concerned the choice of the number and location of lifting surfaces. The investigated configurations were:

Canard: globally more efficient, due to the absence of trim drag and the higher overall Cl_{max} at take-off compared to the conventional configuration. Therefore it allows, at the same thrust level, a reduction of the wing area, compared with the conventional configuration. However it has a worse longitudinal stability, either for the fore position of the elevator and the difficulty to manage the C.G. position.

Conventional: allows an accurate prediction of performances and flight characteristics, particularly for stability



and flight qualities. Then it requires a faster and easier research and development process, suiting the spirit of the contest. It is used as a term to compare the other concepts.

Flying wing: would give a very low RAC, having no tail, control surfaces and associated servos, with the best surface/wetted area ratio. Also, it usually has a very low drag. On the other hand, its flight and handling qualities are very poor, due to the low number of control surfaces. Another drawback is that we have no reference for the design, which makes difficult to build the vehicle.

To evaluate the configuration which best fits the requirements of the contest we have considered the FOMs in table 3.1, with values in a range 1 (the worst) to 5 (the best), and with adequate weighting factors:

RAC: rated aircraft cost was considered as the main figure of merit for screening the concept, since it directly affects the final score and it is a way to quantify the cost of different solutions. It was therefore heavily weighted.

Missions: this FOM shows how a configuration is able to perform different missions as stated by the rules. This year the aircraft must complete both missions, so this FOM has a high weighting factor.

Drag: a configuration with a low aerodynamic drag needs less power, thus it allows us to reduce the number of cells. This point heavily affects the single flight score, because variations of both the RAC and the flight speed are involved.

Handling qualities: we have also considered stability and maneuverability. An aircraft with good handling qualities allows a more accurate tracking of the desired flight profile, reducing flight time, and, above all, take-off and landing times.

Easy to design and build: the need to design and build the aircraft in a short time with somewhat limited resources, led us to consider this important FOM, even though it is not directly linked to the contest score. This FOM has the second higher weighting factor.

The values assigned to the FOMs for each concept were evaluated in a qualitative way. The RAC is the most important parameter among the FOMs, so we made a first sizing for every configuration to calculate the RAC.

Table 3.1 shows the weighted decision matrix we used to choose the configuration considering the previous FOMs. Even if RAC is the parameter with the greater weight, the winning configuration is not the one with the lowest RAC, that is the canard. It appears that the conventional solution is the best option, as it suits very well the requests of the FOM.

FOMs	Weighting Factors	ALTERNATIVE CONCEPTS		
		Canard	Conventional	Flying wing
RAC	0.30	4	3	3
Missions	0.25	4	5	4
Easy to build	0.15	3	5	1
Drag	0.15	4	3	5
Handling qualities	0.15	2	5	1
Tot	1.00	3.55	4.1	2.95

Table 3.1 Aircraft configuration: weighted decision matrix



3.3 Fuselage/Tank configuration

The layout of the fuselage configuration is deeply linked to the choice of the tank shape. Obviously we would design a fuselage as small as possible, able to contain the tank. The tank has to dump in the shortest time, allowing a higher flight speed on the down-wind leg in order to reduce the flight time. It has also to lead to an efficient fuselage.

The FOMs considered for the analysis of the fuselage/tank configuration are:

- RAC: the fuselage configuration affects the RAC through the structural weight.
- Dump time: the tank shape affects the dumping time.
- Aerodynamic efficiency: measures the global aerodynamic efficiency of the configuration.
- Volume: the ability of the fuselage to contain the 4 liters tank.
- Design ease: some fuselage/tank shapes are more difficult to design and build.

The analyzed solutions were:

- Axial sym: in this configuration the entire fuselage is a single axial-symmetric body. This solution has a good aerodynamic behavior with a low drag.
- Pod-like: this configuration has an axis symmetric section, carrying only payload and propulsive system; tail surfaces are connected to the fuselage by a boom. It is lighter, with a lower RAC. The aerodynamic efficiency is not very good, because the limited length of the fuselage does not allow the realization of fairings in the aft region.
- Lifting body: the lifting force produced by this configuration allows a reduced wing span. This leads to a lower RAC compared to the other configurations. In this configuration the tank has a limited height, probably giving a longer dump time. During the cruise, which represents the larger part of the mission, this configuration has a higher drag; this affects both flight time and propulsive sub-system and therefore the RAC.
- Fin: this airfoil shape, tall and narrow, allows us to have a vertical tank, which probably reduces the dump time. On the other hand the large frontal area generates a higher drag. Moreover, the large lateral area produces unwanted lateral behaviors.

Table 3.2 shows the decision matrix that led to the selection of the axial symmetric configuration.

<i>FOMs</i>	<i>Weighting Factors</i>	Fuselage/Tank shape			
		Axial sym.	Pod-like	Lifting	Fin
RAC	0.25	5	5	3	3
Efficiency	0.25	5	3	2	1
Dump Time	0.20	4	4	2	5
Volume	0.20	5	5	3	4
Building	0.10	5	5	4	4
Tot	1.00	4.8	4.3	2.65	3.2

Table 3.2 Fuselage shape: weighted decision matrix



3.4 Wing Configuration

The third addressed problem was the selection of the shape and location of the wing. The FOMs adopted in this screening are:

RAC: it was considered as a very important FOM, since it is directly related to the final score. The number of surfaces, their extension, and the weight of the required structures all affect this FOM. As a result, RAC was heavily weighted.

Structure: it measures the difficulty of the process of sizing and building a tough and reliable fuselage-wing junction. We did not consider this parameter very critical, so it was given a low weighting factor.

Stability: it quantifies the roll stability contribute; also in this case the weighting factor is low because we can correct the instability with other wing parameter (i.e. dihedral, sweep...). We give to this parameter a fairly high weight due to the meteorological conditions of the contest site.

Aerodynamics: it indicates the aerodynamic efficiency of the wing-fuselage system. Once the wing span is fixed, a lower wing is more sensitive to interference between the boundary layers of wing and fuselage, and therefore requires greater attention in designing appropriated aerodynamic fairings. It was given an intermediate value of the weighting factor because it affects cruise speed and mission time

Tank interference: the interference between the tank and the wing structures. It was given a intermediate weighting factor too.

For the wing, the following solutions were considered:

The high-wing is the solution for the unloading problem. It has good efficiency without fairings if compared to a low-wing. It also provides a positive contribution to the roll-stability. Finally it is easy to connect to the fuselage but not with the gear system.

The mid-wing needs particular solutions to design and build the tank, because the wing structures intersect the volume where the tank is probably located.

The low-wing, compared to the high-wing, has a lower aerodynamic efficiency and a negative contribute to the roll-stability. These problems can be solved introducing supplementary devices (fairings, wing twist, ...) that have a negative effect on the RAC. The low wing can be easily coupled with the landing gear.

The biplane-wing allows to obtain a good aspect ratio with a short wing span, clearing more room (longitudinally) available in the box. Unfortunately, this solution is ruled out by high RAC and low aerodynamic efficiency. Table 3.3 shows the decision matrix that led to the select in the high wing.

FOMs	Weighting Factors	Wing Configurations			
		High wing	Mid-wing	Low wing	Bi-wing
RAC	0,25	5	5	5	3
Tank	0,20	5	3	4	4
Stability	0,20	5	4	3	4
Aerodynamics	0,20	5	4	3	1
Structures	0,15	4	3	5	1
Tot	1,00	4,85	3,9	4	2,7

Table 3.3 Wing configuration: weighted decision matrix



Once a high-wing configuration was adopted, the problem of wing planform was addressed. The proper FOMs for this screening are:

RAC: considering that the RAC depends on wing span and maximum chord, we felt important to find how the planform, keeping unchanged the area, affects this parameter. We gave to this parameter the highest weighting factor because it affects the final score more than the others.

Drag: measures, at given wing area and flight C_L , the aerodynamic drag produced by the wing. It has a double influence on the flight mission. Also, it affects the flight speed and, consequently, the mission time. Moreover, it affects the RAC through the battery consumption. For these reasons it has an high weighting factor.

Construction: this parameter measures the difficulties related to the wing construction, from the point of view of the requested tools, complexity and time of assembling the parts. This is less important than the previous two.

Stall behavior: this FOM measure how the different planforms affect the behavior of the aircraft in incipient stall conditions. The considered effects are the C_l spanwise distribution and the Reynolds's number at the wing tip. We give importance to this FOM because during the water dumping the airplane flies at high angle of attack.

The considered planforms are:

Elliptic wing: this is the best shape from the aerodynamic point of view because the induced drag is minimum. The RAC value is between rectangular and tapered wings and the wing has a quite good stall behavior. The main drawback is the higher complexity in manufacturing.

Rectangular wing: keeping unchanged the area, this solution presents the minimum RAC value. Moreover it can be built very easily independently by the building techniques used. However it has a poor efficiency from the aerodynamic point of view.

Tapered wing: has a quite good aerodynamic efficiency, but lower than the elliptic wing. The building difficulties of this solution are intermediate between those of the other two planforms but the RAC is higher. The stall behavior of this configuration is particularly critical. In fact, considering for example a taper ratio 1:3, which minimizes the induced drag, the Reynolds number decreases from the root to the tip of the wing. Considering the typical sizes of our model, this would lead to a very low tip Re (about 70'000), with a negative effect on airfoil performances (for an elliptic wing this fact is less important because the part of wing with reduced chord has a far smaller surface). Another problem for the wing tip is due to the spanwise C_l distribution of the tapered wing, where C_l grows from the root to the tip. A negative twist angle would solve these problems realizing a good stall behavior. However, this would significantly increase the building complexity. Table 3.4 shows the decision matrix that led us to select the rectangular planform.

FOMs	Weighting Factors	Wing Planform		
		Elliptic	Rectangular	Tapered
RAC	0,30	4	5	2
Drag	0,25	5	3	4
Stall behavior	0,25	4	5	2
Construction	0,20	1	5	3
Tot	1,00	3,65	4,5	2,7

Table 3.4 Wing planform: weighted decision matrix



3.5 Wing controls

We felt important to study the wing controls (ailerons, flap, flaperons) in this section because this would help us in solving "The Multirole Problem", stated as the pivotal topic of the design process.

The FOMs considered were:

RAC: the value of each control multiplier, the number of servos, and the wing area required to produce the same maximum take-off lift were all considered. Hence it has a high weighting factor.

Lateral Control: this FOM takes into account the ability of each configuration to produce a given roll control torque. Considering that all the investigated configuration have similar behavior, the weight of this FOM is not high.

Cruise Drag: it considers the wing aerodynamic drag. As seen above, it affects many others parameters, mainly the cells weight and the flight speed, very important for a high overall score. Then it has a high weighting factor.

Pitch Trim: this FOM takes into account the pitch trim during the takeoff, deeply affected by the considered control configuration. It is important due to the assigned take-off distance.

Structural Strength: the position and size of control surfaces affect the twist torque on the wing and consequently the structural requirements for the needed wing strength.

The considered control configurations are:

Ailerons: they give a low RAC, because in the WBS (Work Breakdown Structure: it is a function that takes into account the building complexity of the aircraft) they have a low multiplier and require just one servo. This configuration requires a lower pitch trim, due to the low C_{M_i} ; it also produces a low twist torque. On the other hand it requires a larger wing area, useless in the Ferry mission.

Flaperons: the RAC value is quite good, the multiplier in the WBS is 1.5, they require two servos, but allow us to build a smaller wing. This would lead to a reduced drag, important in the Ferry mission. But there is a higher twist torque, and the lateral control is quite less efficient.

Ailerons e flaps: is the worst configuration for the RAC-related aspects: multiplier and number of servos. They also require more control surfaces. The other characteristics are similar to the ones of the wing with flaperons, but they give a better lateral control.

The wing with flaperons seems to be the best trade-off between RAC, controllability, and drag, as shown in table 3.5.

FOMs	Weighting Factors	Controls		
		Ailerons	Flaperons	Ailerons+Flaps
RAC:	0,25	5	5	2
Lateral control:	0,15	5	4	5
Cruise Drag:	0,3	2	5	5
Pitch Trim:	0,15	5	4	4
Structural Strength:	0,15	4	3	3
Tot	1	4,1	4,55	3,95

Table 3.5 Wing controls: weighted decision matrix



3.6 Tail configuration

The FOMs considered for the analysis of the tail configurations were:

RAC: the RAC directly affects the overall score, and so the weight of this FOM is high. The tail parameters that influence the RAC are the number of fixed and moving surfaces and the number of servos.

Control moment: this parameter affects the take-off and cruise performances of the aircraft and it is strongly dependent on the tail configuration. It should ensure a high control power at take-off. The importance of this parameter was less important than the one of the RAC.

Construction: this FOM considers the manufacturing easiness and strength to weight ratio. The contribution given to construction is less than RAC and the same of control moment.

Efficiency: the tail should produce a low drag during the cruise. The weight given to this figure is the lowest because the drag produced by the tail is, anyway, little if compared to fuselage and wing ones.

The considered alternatives are:

T-tail: the great advantage of this solution is to be immune from the wake effects of wing and fuselage. The aerodynamic efficiency and the control power are higher than the conventional tail, but lower than the H-tail. The RAC is the same than of the conventional tail. However the construction is penalized: the vertical surface should be strong enough to sustain the linked horizontal one.

V-tail: even if it optimizes the RAC, this solution has lower scores on the other FOMs. It has a low aerodynamic efficiency and control moment, since the equivalent horizontal surface should respect the "1/4 span rule", giving insufficient longitudinal stability and control.

H-tail: this solution, with the two fins acting like winglets, was a way to increase the effective aspect ratio of the horizontal surface. The problem of this configuration is the high RAC value for the presence of many aerodynamic surfaces.

Conventional tail: this configuration has the advantages of a reduced RAC, allows a good control especially during the dumping phase and is the easiest to build. Moreover, our know-how allows an accurate prediction of performances and flight characteristics, especially for stability, flight qualities and control during the take off.

Cross-tail: compared to the conventional tail, this solution would increase the lateral stability, allowing a double size of the vertical surface. As a drawback, the construction is harder.

Table 3.6 shows the results of weighted decision matrix. The winning configuration is the conventional tail.

FOMs	Weighting Factors	Tail Configurations				
		T	V	H	Conv.	Cross
RAC	0,40	4	5	2	4	4
Control Moment	0,25	5	2	5	4	4
Construction	0,25	3	2	3	5	3
Efficiency	0,10	4	2	4	3	3
Tot	1,00	4	3,2	3,2	4,15	3,25

Table 3.6 Tail configuration: weighted decision matrix



3.7 Motor and Propeller position

From past years D/B/F contests, we have always seen that the configuration with one motor and one battery pack is the best in terms of a low weight and RAC. Moreover a tractor propeller is the best trade-off between efficiency and structural complexity.

3.8 Landing gear configuration

The study of the landing gear configuration considered four options, using the following FOMs:

RAC: the structural weight and the number of servos are directly involved in the RAC computation, so it must be considered. Because of the little influence of the landing gear on the RAC, its weighting factor is the lowest.

Aerodynamic efficiency: it measures how each configuration affects the aircraft aerodynamic performances; a further drag reduces the aircraft speed and range, so the weighting factor for this FOM is high.

Reliability: this FOM is very important because a failure of the landing gear during the landing phase would seriously damage the aircraft. The retractable configurations are then disadvantageous, because we cannot be sure that the deploying system would always work safely.

Take off run: it considers the runway length required for take off. If the aircraft exceed the take off distance we loose one flight attempt out of five, hence the weighting factor for this FOM is quite high.

Considered landing gear configurations are:

Fixed fore tricycle: the aerodynamic efficiency is low, due to an additional drag during the cruise flight. On the other hand, it has an excellent reliability and good take off behavior.

Fixed aft tricycle: the aerodynamic efficiency is little better than in the previous one, because the drag and the structural weight are lower. But it requires a longer take off run. Moreover, it's impossible to adjust the airplane direction during take off or landing while the aft wheel is lifted from ground.

Retractable fore tricycle: this configuration improves the aerodynamic behavior if compared to the fixed one. But the RAC is higher, because an additional servo is required to retract the gear and, moreover, the aircraft is heavier. It could have reliability problems.

Retractable aft tricycle: it generally has as benefits and drawbacks as the precedent one. It also is penalized by a longer take off length required.

Table 3.9 shows how the fixed fore tricycle configuration better meets the requests of the selected FOMs.

FOMS	Weighting Factor	Landing gear configuration			
		Fixed Fore Tricycle	Retractable Fore Tricycle	Fixed Aft Tricycle	Retractable Aft Tricycle
Reliability	0,35	5	3	5	3
Take off run	0,30	5	5	3	3
Efficiency	0,25	2	5	3	5
RAC	0,10	4	1	5	2
Tot	1,00	4,15	3,90	3,90	3,40

Table 3.9 Landing gear configuration: weighted decision matrix



3.9 Structural Configuration

We analyze now the different building technologies to implement the main parts of the aircraft: wing, fuselage, tail, and landing gear. The FOM used for each study were:

RAC: it is affected by the volume and the weight of the aircraft, and then it depends on the type of structures used.

Cost: it takes into account the economical resources needed to build the considered component.

Reparability: it measures the ease to recover the mechanical properties of a damaged structure.

Know how: it estimates the experience and the skill needed to use the selected technologies.

Technologies: this FOM looks upon the availability of the tools required to implement the selected building technology (i.e. machines as lathes for the moulds, pressurized vat, vacuum bags, ...).

Strength: it is an estimation of the strength to weight ratio of a considered building technology product.

Obviously, the weighting factors for these FOMs are very different for each structure considered, depending on the distinct functionality that the aircraft parts have; the structural configuration technologies investigated are:

The traditional wooden structure: it is realized with ribs and spars (frames and stringers for the fuselage), it is the cheapest one and requires simple building technologies; however, it is quite difficult to realize, and to repair in case of an accident depending on the damage extent.

Shell structure: it requires the simplest assembling, and allows big advantages reducing the weight and the volume keeping a high strength. However, it needs a great skill and it is very expensive.

Skin + core structure: it means a core of a light material covered with a composite skin. It has a similar strength if compared with the shell but is relatively simpler to build.

Sandwich box: obviously it was considered only for the fuselage. It is a solution with intermediate properties between the traditional configuration and the skin + core; it allows the effortlessness to build and to repair of the first, and the strength of the second. However, this involves a higher complexity in terms of required technologies for the assembling.

Tables 3.10-3.11-3.12-3.13 show that a skin + core solution is the best option for the wing. The landing gear will be realized with composite materials. The sandwich structure meets our requirements for the fuselage while the traditional structure is the best way to build the tail.

FOMs	Weighting Factors	WING STRUCTURE		
		Traditional	Shell	Composite skin + core
Know How	0,20	4	2	5
Technologies	0,20	5	2	4
Costs	0,20	5	1	3
Strength	0,15	3	4	5
Reparability	0,15	1	2	4
RAC	0,10	5	1	3
Tot	1	3,90	2,00	4,05

Table 3.10 Wing structure: weighted decision matrix



<i>FOMs</i>	<i>Weighting Factors</i>	FUSELAGE STRUCTURES			
		Traditional	Shell	Composite skin + core	Sandwich box
Know How	0,25	4	2	5	5
Technologies	0,25	5	2	4	5
Strength	0,25	3	4	4	5
RAC	0,15	4	1	3	4
Cost	0,10	5	1	3	4
Tot	1,00	4,10	2,25	4,00	4,75

Table 3.11 Fuselage structure: weighted decision matrix

<i>FOMs</i>	<i>Weighting Factors</i>	Tail structures		
		Traditional	Shell	Composite skin + core
Know How	0,25	5	2	4
Technologies	0,20	5	1	3
Strength	0,15	4	2	5
Reparability	0,15	3	4	5
RAC	0,15	5	1	3
Cost	0,10	1	2	4
Tot	1,00	4,15	1,95	3,95

Table 3.12 Tail structure: weighted decision matrix

<i>FOMs</i>	<i>Weighting Factors</i>	LANDING GEAR STRUCTURES			
		Aluminum bow	Aluminum single leg	Composite bow	Composite single leg
Strength	0.4	4	3	5	4
RAC	0.3	1	2	4	5
Reparability	0.2	3	2	1	2
Cost	0.1	5	4	1	2
Tot	1	3	2.6	3.5	3.7

Table 3.13 Landing gear configuration: weighted decision matrix

3.10 FOMs Analysis Results

At the end of the conceptual study we found the configuration, through the use of FOMs, we thought could gain an high score. A monoplane was preferred to a biplane (because of the lower RAC and the higher cruise speed), though the latter would have guarantied a better dumping of water payload. To accommodate the tank and to prevent problems during take off and landing, caused by possible wind, a



high wing was chosen, instead of a low or a medium one. In despite of better performances of a H tail, a conventional one was considered the best choice thanks to its lower weight on RAC function. Flaps were thought necessary to take off in Fire Fight configuration and, in addition, they ensure the aircraft to fly slow enough to allow sufficient time for water to be emptied. A single motor design was preferred to a two motors one due to its much lower RAC. At last the economic resources forced us to use low cost materials, which, anyway, during last years experiences, yielded great results.

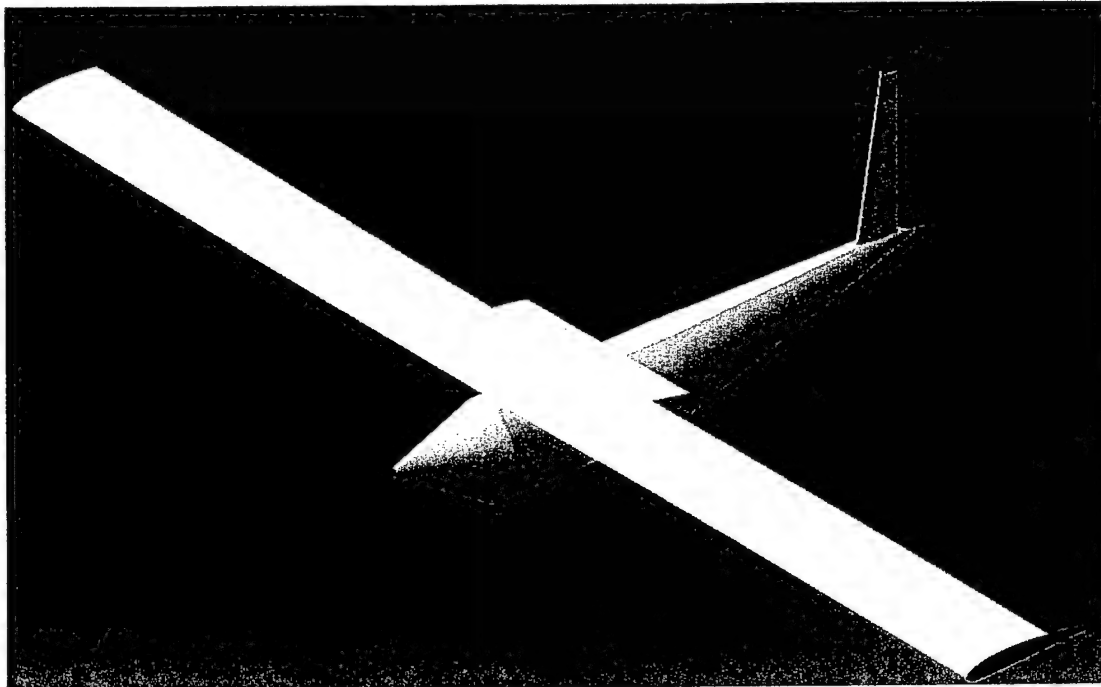


Figure 3.1 Final concept



4 Preliminary Design

4.1 Introduction

Once the configuration and the building technologies were stated, we had to size the components of the whole aircraft in order to best meet the goals of the two missions. For this purpose an optimization method was introduced to select the most performing set of design parameters. At this moment the preliminary study was split into two phases; in the first one we wrote an algorithm that allowed us to obtain a limited range of optimized design variables values. In the second phase the best set of variables was defined by a fine trade study.

4.2 First Sizing Trade Studies

In the first phase of the sizing process, we wrote a Matlab 6.5® program, called Optim 6.0, able to evaluate the effects of the various sets of investigated design variables on the overall score, and to give the optimum configuration, in terms of variable values as output. Yet, a computation with discrete design parameters gives results suffering from intrinsic limits (the iteration steps of each variable have a finite space, while the relative optimum could fall in one of the gaps). More, an algorithm dealing with a problem with a high number of variables, unavoidably introduces approximations and simplifying hypotheses. For these reasons, the results given as output by the optimization program were not considered the unique solution for the configuration sizing problem but just an indication of a reduced range of variation of the considered design variables: each set of parameters, gaining a score within 15% of the maximum, was considered for the subsequent fine trade study.

4.2.1 Main assumptions

To formulate the optimization problem some simplifying hypotheses were introduced:

1. In the optimization algorithm we needed to know the aerodynamic parameters of the whole aircraft. For the sake of simplicity, we chose to link these parameters to the adopted airfoil: once the characteristics of an airfoil and the actual dimensions of a finite wing is known, it is possible to find out the lift, the drag, and the pitching moment of the wing. In addition, we need to sum the contribution of the tail, the fuselage and the landing gear. These contributions can be considered as known parameters in agreement with the following assumptions:
 - the geometry of the horizontal tail (span, chord, planform, and airfoil) was fixed because of its influence on mission requirements we felt critical: increase of take off C_L and the decrease of the cruise C_D . These effects can be easily determined from the wing geometry (chord and airfoil). In fact, chosen the airfoil, from the pitch balance, the angle of attack of the horizontal tail during take off and cruise can be calculated, and so we can evaluate which % of C_L and C_D must be added or subtracted to those developed by the wing. A more accurate study on the parameters of the horizontal tail (airfoil, chord, coupling angle, % of elevator, maximum elevator deflection) would be carried out later.
 - The geometry of the wing, following the conceptual results, was fixed in span, leaving the chord and the flaperons rotation as variables.



- We considered that the effect of vertical tail, fuselage, and landing gear was to increase the total C_D . During the conceptual design, the fuselage shape and dimension were determined together with maximum dimensions of the tail vertical surfaces and landing gear.

Therefore, the variables for the aerodynamic design were reduced to the coefficients of the selected airfoil: C_{lMAX} , C_{mAC} , k e C_{d0} . We identified five low Reynolds (about $10e5$) airfoils of different families. The optimization process analyzed these airfoils and pointed out which family of airfoil best fitted our requirements.

2. For the stability and handling qualities, we considered that the distance between the aerodynamic center of wing and tail is in the range 2.5-3 mean wing chord ($c = 10.23''$).

The relative position between the C.G. and the a.c. of the wing was supposed to be about half an inch, with the C.G. aft.

3. An analytic relation between propulsive configuration and thrust was introduced in the optimization algorithm. We obtained this relation by extrapolating the data of maximum thrust, as a function of the number of cells and of the system motor/propeller/reduction-gear, obtained from a set of analyses performed with the commercial software MotoCalc®. This software uses a database with the characteristics of several electric motors and other components and, for a set motor/cells/reduction/propeller, gives useful data on:

Available thrust at various airspeeds.

Shaft power.

Voltages e currents.

Temperatures reached by the motor and the cells.

Accepted results were to satisfy following constraints:

- Current < 40 A
- Power loss < 100 W
- Discharge time > 5 min

Preliminary analysis allowed us to limit the possible motor-propeller configuration to 15 options, which gave the best results in term of shaft power, efficiency, and cell discharge time (table 4.1). For each configuration the T_{MAX} vs. #cells curve was found. The parameters in the optimization process were the number and type of cells and the motor/propeller set (out of 5 selected).

4. In the conceptual design phase a maximum take-off weight of 9 kg (19.84 lbs) was considered.

4.2.2 Known parameters:

From the conceptual design and the previous statements, the following parameters are known:

- W gross take-off weight: 9 kg (19.84 lb)
- bw wing span: 2.4 m (8 ft)
- bf flaperon halfspan: 1m (3.28 ft)
- bt horizontal tail span: 0.6 m (2 ft) (=25% bw)
- ct: horizontal tail chord: 0.2 m (8")



- μ friction coefficient: 0.03
- C_d : fuselage + vertical tail + landing gear = $0.03 + 0.008 + 0.04 = 0.078$
- Wing planform (selected in the conceptual)

4.2.3 Major Design Parameters

The variables considered in the optimization algorithm were reduced to those shown in table 4.1. For any of them, the table indicates the lower and upper limits of the considered range of variation.

variable	description	Range	
		minimum	Maximum
c	Wing chord	0.2 m (8")	0.3 m (12")
c_f	Flaperon chord	25% c	35% c
Tcell	Type of cells	1300 mA	3000 mA
Ncell	Number of cells	8	24
"motor"	Motor-propeller-reduction set	Graupner ULTRA 930-8, 930-7, 930-6 propeller: 18" to 22"; reduction set: 3.75:1	
Vc	Cruise speed	15 m/s (49 ft/s)	30 m/s (98 ft/s)
Nv	Turn loading factor	1	2
"airfoil"	C _l max, C _m , k, C _{d0}	families: SD, FX, Eppler, NACA 4 digit, CH.	

Table 4.1 First Sizing Trade Studies: Major Design Parameters

4.2.4 Fire Fight mission:

The two missions are characterized by different critical parameters: the Fire Fight mission requires higher T_{MAX} at take-off and a total lower energy consumption with respect to the ferry mission. We decided to optimize the Fire Fight mission, as it provides the main contribute to the total score: with the same time spent to accomplish the two different missions, the score marked by the Fire Fight mission is about 30 times the score of the other one. Once the program has identified a set of configurations that maximizes the mission score, a check on cells energy is performed: OPTIMUM 6.0 chooses the amperage of cells in order to satisfy the energy consumption for the Ferry mission as well. An estimation of required charge is obtained by simulating the Ferry mission with the previously selected parameters. If needed, it raises up the number of cells in order to reach the correct amount of current. The Fire Fight mission consists in flying the race lap, carrying the water payload and dumping it in the downwind leg, twice. The mission can be divided in five different flight phases:

- Take-off run: begins with the aircraft at rest and ends when the take-off speed, that is 1.1 times the stall speed, is reached; the fixed take-off run is the tightest requirement to deal with.
- Climb: it goes from the end of the take-off to an altitude of 20 m (about 65 ft); the analytic model for the maximum rate of climb at the maximum excess power is used to describe this phase.
- Cruise and water dumping: this phase sums up the two straight flight segments (about 2000 ft);
- Turn: sums up the 2 turns at the pylons and the 360° turn in the downwind leg for each lap, in a total of 8 180° turns; the analytic model for the balanced turn with a constant load factor is used.
- Landing: a glide from the cruise altitude to ground and braking from landing speed to zero.



4.2.5 Cost function:

For each set of design variables, the algorithm calculates the RAC and the time spent to perform the standard mission. The target function to be maximized by the optimization tool is:

$$\text{Final Score} = 100 / (\text{Flight Time} \cdot \text{RAC})$$

4.2.6 Analysis Methods

The optimization algorithm, the flow-chart of which is described in figure 4.1, was implemented in the **Optim 6.0** program (written in Matlab 6.5®), which carries out the computations sketched in the figure: various input sets are given and the one that provides the higher overall score is selected. In the **OPTIM 6.0** final version, the program calls the following Matlab® subroutines:

- **TAKEOFF:** from the thrust vs. speed relation, the program integrates, step by step, the motion equations (from zero to the take-off speed) considering the aircraft aerodynamic characteristics, the weight, and the effect of the wheel-runway friction.
- **CLIMB:** the fastest-climb speed is determined analytically, depending on the wing loading and the parameters of the polar curve for the whole aircraft, namely C_{D0} and K . It integrates the aircraft motion equation, from the take-off speed to the climb speed; finds out the time spent to reach this speed, and then the time to reach the cruise altitude of 20 m (65 ft). The flight path angle is found analytically; so that it is possible to have in output the horizontal range flown.
- **CRUISE-DUMP:** finds out the length of the path flown in this condition, subtracting from the sum of straight segments the horizontal length run in take-off and climb. From the cruise speed, it gives the elapsed time. There is a constraint in the downwind leg run time, because of the need to dump all the water.
- **TURN:** uses a balanced turn model with constant speed. From the turn load factor, it finds out the required thrust, C_L and the turn radius, and then the length flown, the time and the energetic consumption.
- **LANDING:** it uses a model of glide descent, with turned-off motor, at the angle of attack of maximum efficiency. It integrates the motion equations from cruise altitude to ground in these conditions and finds out the residual horizontal speed. Then, the motion equations are integrated from this speed to zero speed, considering the braking action of the wheel friction on the runway and of the aerodynamic drag. It gives as output the distance run and the time for the descent and braking phases.

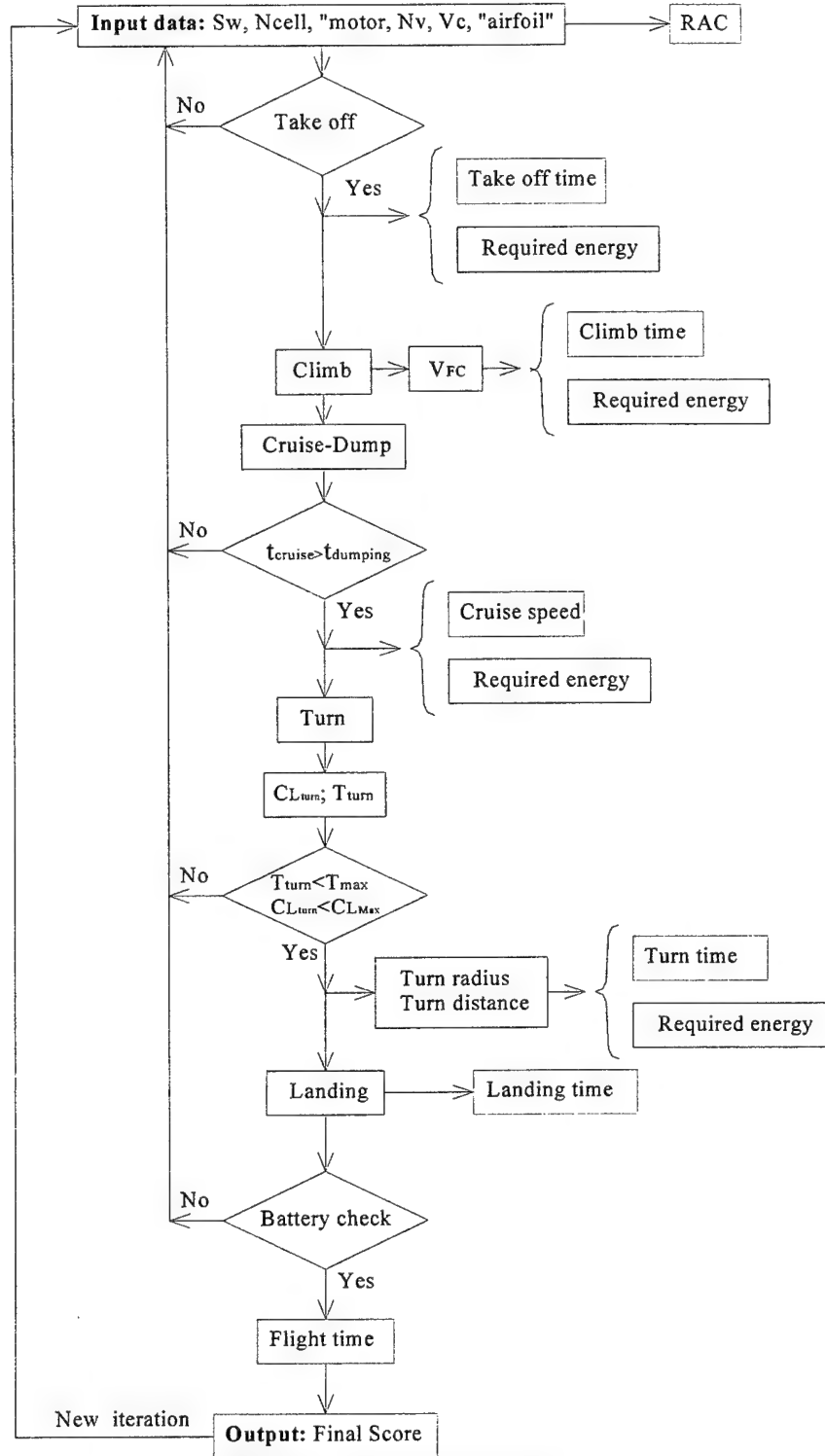


Figure 4.1 Optimization algorithm



The OPTIM 6.0 executes as follows: it takes a set of design variables as input, from which the RAC is calculated, and considering the particular Maximum thrust vs. Speed relation of the selected propulsion system, the TAKEOFF subprogram is run. Then it performs a check on the lifting equation at the end of the runway. If the requirement is not satisfied, the execution stops and a new set of design variables is considered. At this point the elapsed time and the energetic expenditure for take-off are calculated. Next, the CLIMB subprogram is executed, and the time and the energetic spending for this flight phase are found. From the cruise speed it is possible to find the cruise thrust. At this point the program checks if the cruise thrust is lower than the maximum thrust available for the adopted propulsion system. If the requirement is not satisfied, the execution stops and a new set of design variables is considered. Then the CRUISE subprogram is called. It takes as input the time we calculated to be necessary for the entire water dumping and gives as output the cruise speed and the energetic expenditure. In the turn analysis a double check is performed: on the turn thrust, lower than the maximum one, and on the C_L , lower than C_{Lmax} (to be sure that the aircraft does not stall during this maneuver). The TURN subprogram computes the turn time and the energetic expenditure. Next, the LANDING subprogram is executed, giving the same data as output. Now it is possible to perform the "battery check", to verify that energetic demand of the two missions is lower than the battery configuration supply. Finally, the total flight time and the Final Score are calculated.

4.2.7 Analysis Results

The results of the program, when the final score is within 15% of the maximum overall score, indicate, for each design parameter, the following range:

Sw:	from 0.56 to 0.70 m ² (7.1 – 8.1 ft ²)
Tmax:	from 26 to 30 N (5.8 – 6.7 lbf);
Cells #:	from 11 to 17;
Cells type:	from 1700 mA to 2400 mA;
Motor:	Ultra 930-8 12V.
Propeller:	19" to 21";
Airfoil:	SD family;
Vc:	from 20 to 25 m/s (65 – 82 ft/s);
nv:	from 1,4 to 1,7;
Vto:	from 12 to 15 m/s (39 – 49 ft/s);

4.3 Fine Trade Studies and design Optimisation

4.3.1 Aerodynamic Considerations

Wing

The best airfoil in term of overall score belongs to the "SD" family; now there is the problem of choosing the exact airfoil to be used on the aircraft. Out of the nine airfoils analyzed from this family, we disregarded those with a very low $C_{m_{ac}}$, because the double camber on the upper surface makes too hard to build the wing with sufficient accuracy. We also discarded the laminar ones, because the cusp on



the trailing edge causes the same building problems and their efficiency is strictly related to manufacturing tolerances we cannot afford. The other six airfoils are very simple to produce (no sharp trailing edge, no high camber or cusp), and do not have too high moment coefficient (no more than -0.1), condition that our OPTIM 6.0 shows to be particularly penalizing.

In order to take-off in 150 ft with full water tank (4 liters) we need a high camber and high thickness airfoil, but it would increase drag and reduce max efficiency; so we chose a flaperons configuration to raise $C_{l_{max}}$ with moderate augment in cruise drag. We found that the behavior of a flapped wing, as we could expect, is highly affected by the value of the Reynolds number. Therefore, the analytical simulation gave us values to be confirmed by experimental tests and empirical methods. With the flaperon span previously fixed, we calculated a good value for the chord as 30% of the aerodynamic mean chord (26cm, 10.24") for aerodynamic and manufacturing considerations and a travel of about 20° , to keep enough lateral control even with a complete deflection. An estimation of the additional C_m was conducted to test the tightest trim condition on take-off, with all flaperons down and at maximum take off weight (MTOW).

At this point we compared the polar and C_l curves. Once wing surface and geometry, weight and flight speed (and then the whole aircraft C_L) are defined, the cruise airfoil C_l is determined. Comparing the polar for various family SD airfoils, we found out that the difference in the C_d at C_l near the cruise value is quite small, also considering the trim drag. By focusing on the curves with the higher maximum C_l (always taking into account the trim loss), we concluded that the SD 7032 airfoil has superior characteristics. Among these, we selected the "D" variant, for the higher maximum C_l (but only some %) and for the smoother stall. For the wing planform, the rectangular shape was early selected, as the one having the largest surface for a given RAC. Moreover it was undoubtedly the easiest to be manufactured. The wing dimensions, allowing us to take-off safely and with an good cruise efficiency, are 240 cm (7.87 ft) in span (as previously fixed) by a chord of 26 cm (10.23").

Horizontal tail

A NACA 0012 symmetric airfoil was used for the all moving tail; the most efficient configuration, for the requested control moments, has a span of 60 cm (1.97 ft) (25% of the main wing span) and 20 cm (7.87") chord. The aerodynamic characteristics were found with a custom software, developed by us in Excel®; it plots the curves of lift, drag, efficiency and the polar for the single components and for the whole aircraft depending on the aircraft geometry; this software takes into account the interference between the parts regarding the wakes and the induced speeds. To deal with the stall, the program finds the spanwise lift distribution using the Shrenk method. It considers only the linear part of the lift curve, and the related polar, using experimental data to update the curves and foresee the behavior of the non-linear parts.

Vertical tail

A NACA 0012 symmetric airfoil was used for the vertical tail. The sizing came from the following assumptions:

- Control volume of about 0.05.
- Contribution to lateral-directional stability in term of $C_{l,\beta}$ and $C_{n,\beta}$.
- Low aspect ratio to avoid stall even with large sideslip angles.



For the reasons summarized above, the vertical tail has a root chord of 20 cm (7.87"), a tip chord of 15 cm (5.91"), span of 32 cm (12.60"), with an aspect ratio of about 1.8.

The attitude of the fuselage was used as reference. As a result, the cruise is at 0° angle of attack, with the minimum of the fuselage drag. From the efficiency curves it can be seen that, for the design angle of attack, the efficiency of each aircraft component is very near to the maximum, (minimum for the tail because of negative lift) which is a proof of a good design. For the definition of the fuselage shape, stated that axis-symmetric shape minimizes the form-drag, we looked for the best trade-off between shape and cross-section dealing with the need of a manufacturing ease.

We have sketched the fuselage as a wing with very low aspect ratio (0.17) shaped as an inverted asymmetric airfoil. With this considerations we have a positive C_m and a positive zero lift angle.

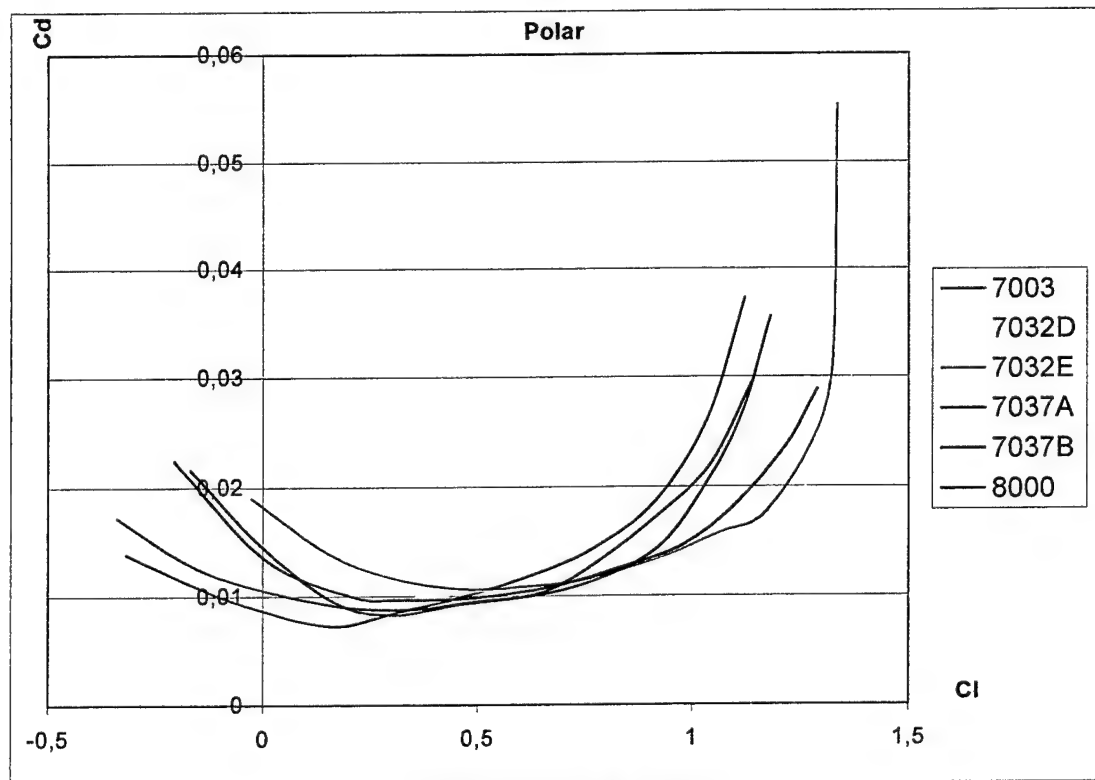


Figure 4.2 SD family polars

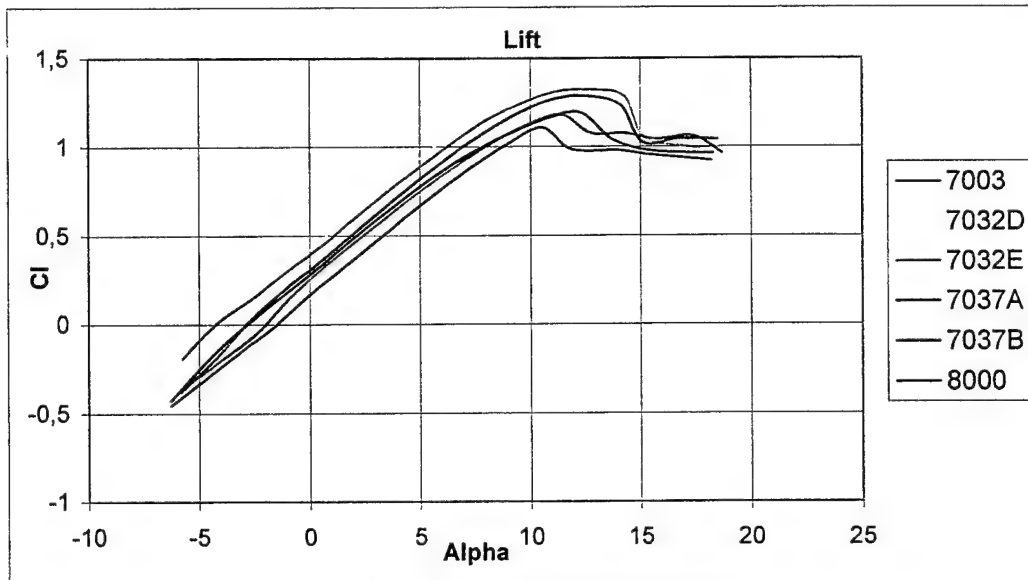


Figure 4.3 SD family lift curves

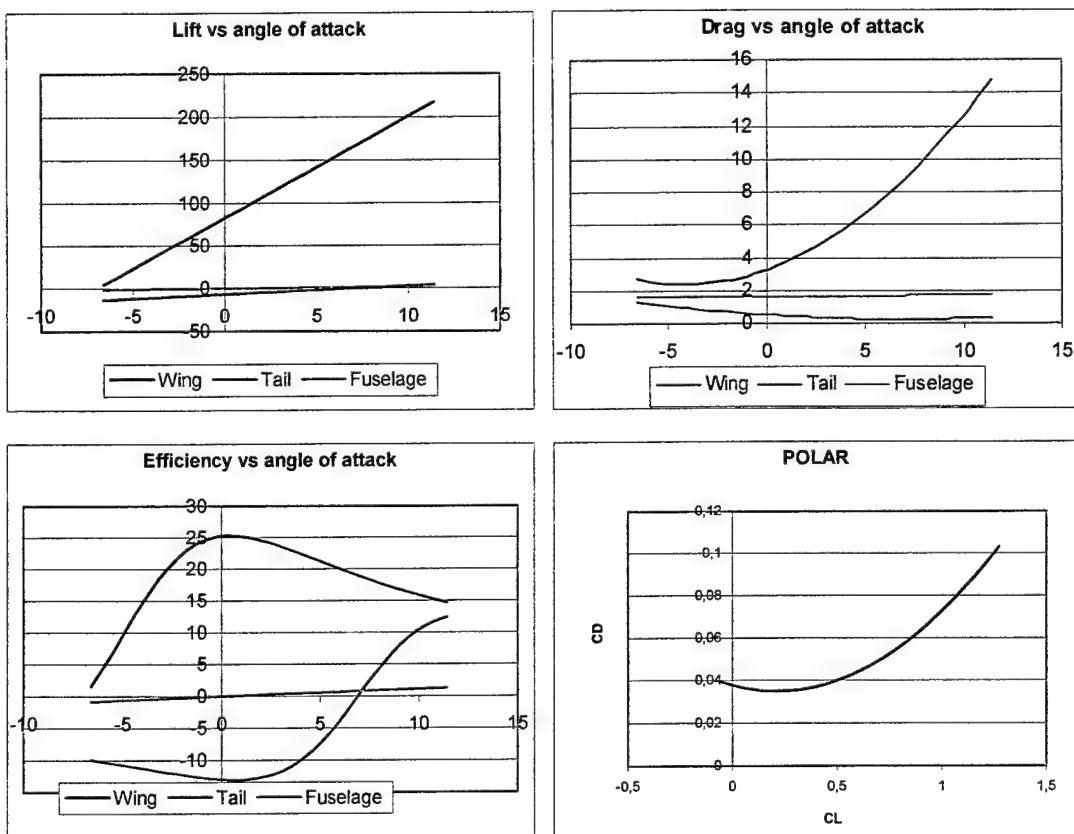


Figure 4.4 Whole aircraft



4.3.2 Propulsion Analysis

The optimization program OPTIM 6.0 showed that we need a thrust of 28-32 N at zero speed. Suitable motors are the three Graupner models: Ultra 930-8 12V, Ultra 930-7 10V, and Ultra 930-6 8V. By using the software Motocalc®, an evaluation of the maximum obtainable speed was carried out for each of the three motors.

The program indicated that the 930-6 motor, with a 17"x10" propeller and a 3.75:1 reduction gear seems to meet the requirements for the optimization. Nevertheless it was discarded because 15 battery cells are required to achieve the thrust needed for take-off, but they give too much tension (18 V instead of the 8 V for which this type of motor was designed).

The configuration 930-7 with the same reduction gear, 18"x12" propeller, and 16 cells has the same problems of overload than the previous one and, moreover, it has a consumption of 2350 mAh calculated for the Ferry mission; since we considered battery cells with an amperage of 2400 mAh, this configuration was rejected for the clear possibility of not completing the mission.

Therefore, the chosen motor was the third possible: the 930-8 with 16 cells, 19"x12" propeller, and reduction gear 3,75:1. This configuration has demonstrated to be the most reliable for both energy consumption and overload tension.

The figure 4.5 shows the motor performance characteristic curves, obtained with Motocalc®.

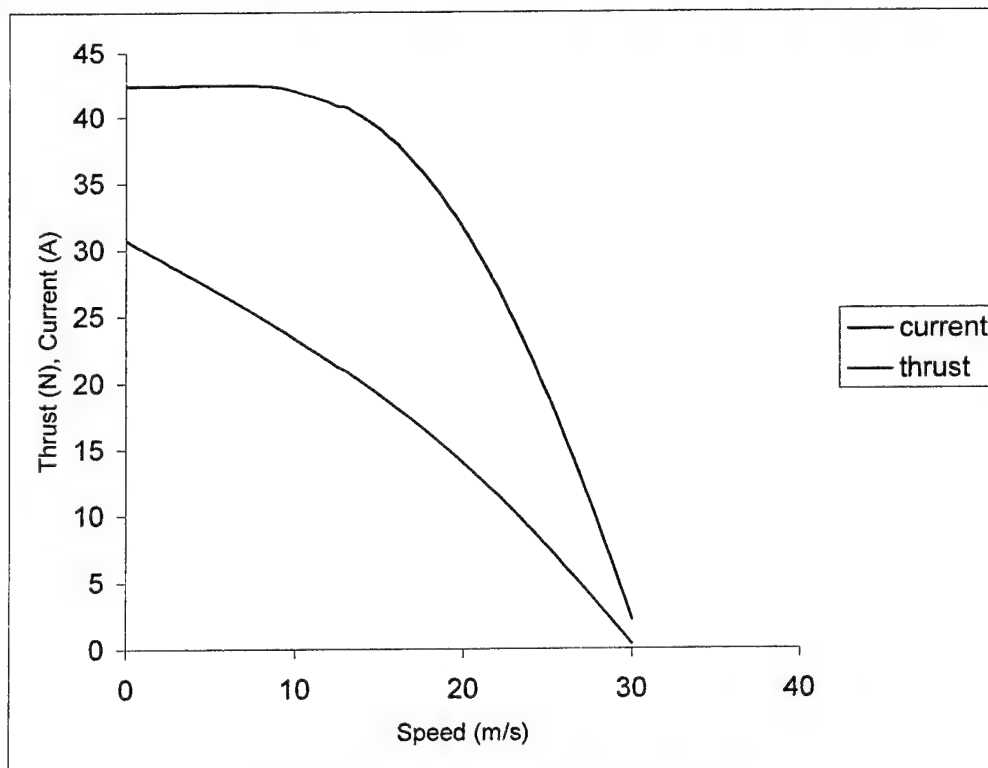


Figure 4.5 Motor thrust and drained current



4.3.3 Performances & Flight mechanics

Steady level flight

The first considered condition was steady level flight at an altitude of 20 m (about 65 ft).

The tail location aft the wing is related to the following considerations:

- Control volume of about 0.5 to have a good C.G. range.
- Contribution to the longitudinal stability of the whole airplane.
- Ability to trim in various flight conditions.

From the aerodynamic analysis we had the polar of the complete aircraft, and from the propulsive analysis, the thrust as a function of the flight speed. Then, considering the balance of forces and pitch moment, we found out a value for the tail arm of 68 cm (26.77") and a cruise speed for the full payload configuration (with a total weight near 9 kg, 19.84 lb) of about 20 m/s (65 ft/s). For this condition we studied the fixed command longitudinal static stability.

From tail deflection and angle of attack, we found the pitch coefficient of the whole aircraft, given the static margin and the tail distance, and considering the contribution of wing, tail and fuselage and the downwash effect on the tail. With an iterative method we found wing and tail angles that would make the aircraft stable and trimmable, that is with $C_{m_0} > 0$ and $C_{m_\alpha} < 0$. It results: wing trim (i_w) 1° ; tail trim (i_t) -2.2° .

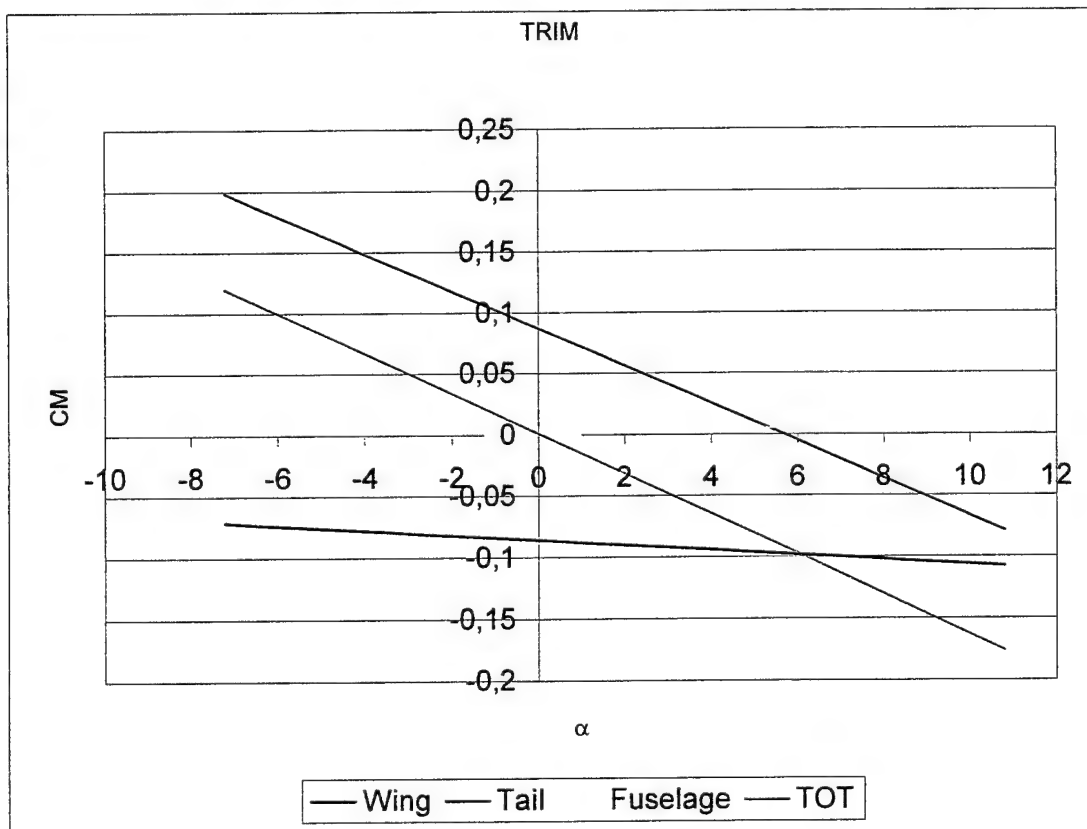


Figure 4.6 Trim analysis



Landing gear

The nose wheel gear configuration has many advantages. Nosewheeled aircraft are less demanding because of the more or less level attitude: they can be taxied faster and straighter. Shallower angle of attack makes for a faster acceleration on take-off. There is less risk of nosing over when landing.

Anyway, some disadvantages have to be taken into account; if there is too much load on the nose wheel:

- It is hard to rotate nose up on take-off through insufficient elevator power.
- The mainwheels lie aft, which makes it hard to counterbalance by rudder the couple caused by a crosswind acting on the fuselage ahead of the mainwheels.

With the above considerations, the final configuration came from the balance of the following constraints:

- To avoid the tendency of the airplane to sit on the tail, the main wheel can be located aft of the perpendicular dropped from the center of gravity to the ground, by an angle of about 15 degrees.
- The wheelbase between the nose wheel and the main wheel can be determined considering the static load on the nose wheel ranging between 25% and 40% of the supposed MTOW.
- The aft position of the main wheel is related to the rotation angle at take-off, to have tail clearance.

The elevator power must be able to counterbalance the effect of the weight and the wing lift, with the main wheel as pivot point. This is another reason to have an all moving tail instead of a simple flap-like elevator.

Thrust and Power

From the propulsive analysis we obtained the maximum Shaft Power, the Available Power and Thrust as functions of the flight speed. The Required Power and Thrust were determined from the aerodynamic parameters. Analyzing the diagram, we have obtained the cruise speed as intersection between the curves, whereas the maximum efficiency speeds were extrapolated.

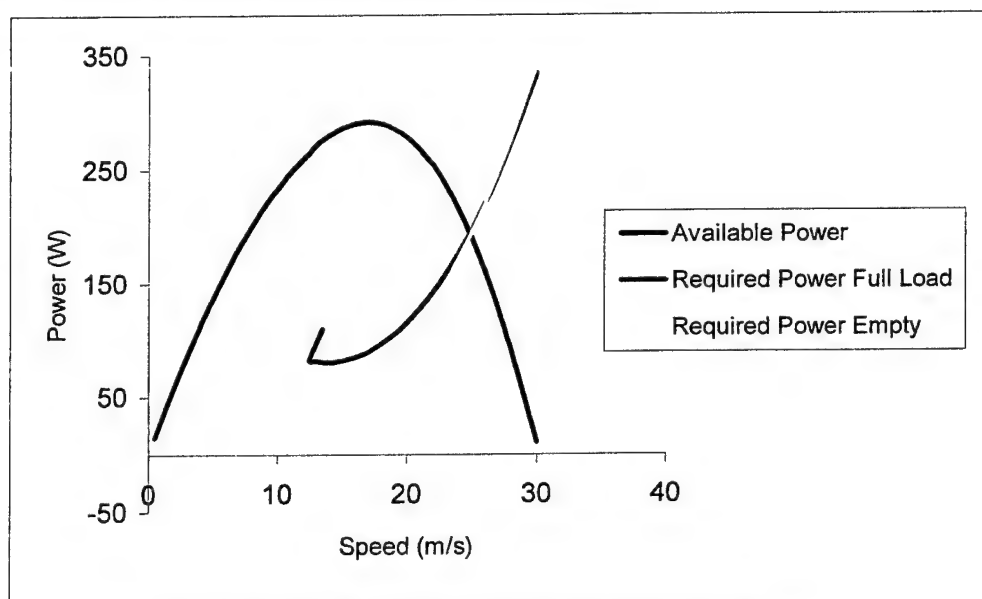


Figure 4.7 Power analysis of loaded and empty configuration.

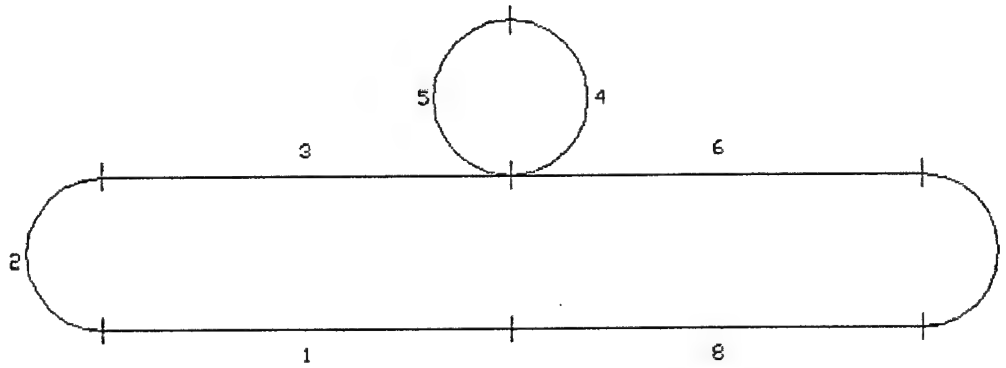


Figure 4.8 Path fractions

To evaluate running times and energy consumption, the circuit has been divided in 8 parts, as sketched in figure 8:

- **Ferry mission**
 - Segments 1 & 8: once take-off+climb and descent+landing respectively.
three times as cruise.
 - Segments 2,4,5 & 7: four times as balanced turns.
 - Segments 3 & 6: four times as cruise.
- **Fire Fight mission**
 - Segments 1 & 8: take-off+climb and descent+landing respectively.
 - Segments 2,4,5 & 7: balanced turns.
 - Segments 3 & 6: both cruise.

Take-off analysis

It was carried out by integrating step by step the motion equation of the vehicle along the take off run:

$$m \frac{\Delta V}{\Delta t} = T - D - \mu(W - L) \Rightarrow \Delta V = \frac{g}{W} [T(V) - \frac{1}{2} \rho V^2 C_D S - \mu(W - \frac{1}{2} \rho V^2 C_L S)] \Delta t$$

where the thrust as a function of speed is the one previously obtained, the aerodynamic forces are known from the selected coefficient of the polar and wing area, and the weight is the one estimated. By choosing a temporal integration step $\Delta t = 0.2s$ it is now possible to calculate the ΔV from the speed. Starting from rest initial conditions, the speed and the distance covered at each step have been calculated:



$$V_{i+1} = V_i + \Delta V(V_i) \quad ; \quad s_{i+1} = s_i + V_i \Delta t + \frac{1}{2} \Delta V \Delta t$$

If the algorithm is stopped when the take off velocity $V_{TO} = 1.1 V_{Stall}$ is reached, it is possible to determine the runway length needed. The consumption during this phase, was obtained from the current intensity as a function of the flight speed and then as a function of time; the consumption in terms of mAh was so calculated through the integral $\int i(t) dt$.

The table below shows the results of this process:

Empty Configuration	Loaded Configuration
$s_{TO} = 9.38 \text{ m (17.26 ft/s);}$	$s_{TO} = 43.02 \text{ m (7.97 ft/s);}$
$V_{TO} = 14.5 \text{ m/s (47.57 ft/s);}$	$V_{TO} = 16 \text{ m/s (52.49 ft/2);}$
$t = 1.8\text{s;}$	$t = 5.6\text{s;}$
$\text{mAh} = 21.41$	$\text{mAh} = 65.06$

Climb: in this phase, the flight speed was given as a constant parameter in order to estimate the performances; through a graphical-analytical approach the Rate of Climb (RC) vs. Speed (V) relation was drawn as from the previous phases we have the required and the available power, the rate of climb is

given by the equation: $RC = V \sin \gamma = \frac{\Pi_a - \Pi_r}{W}$

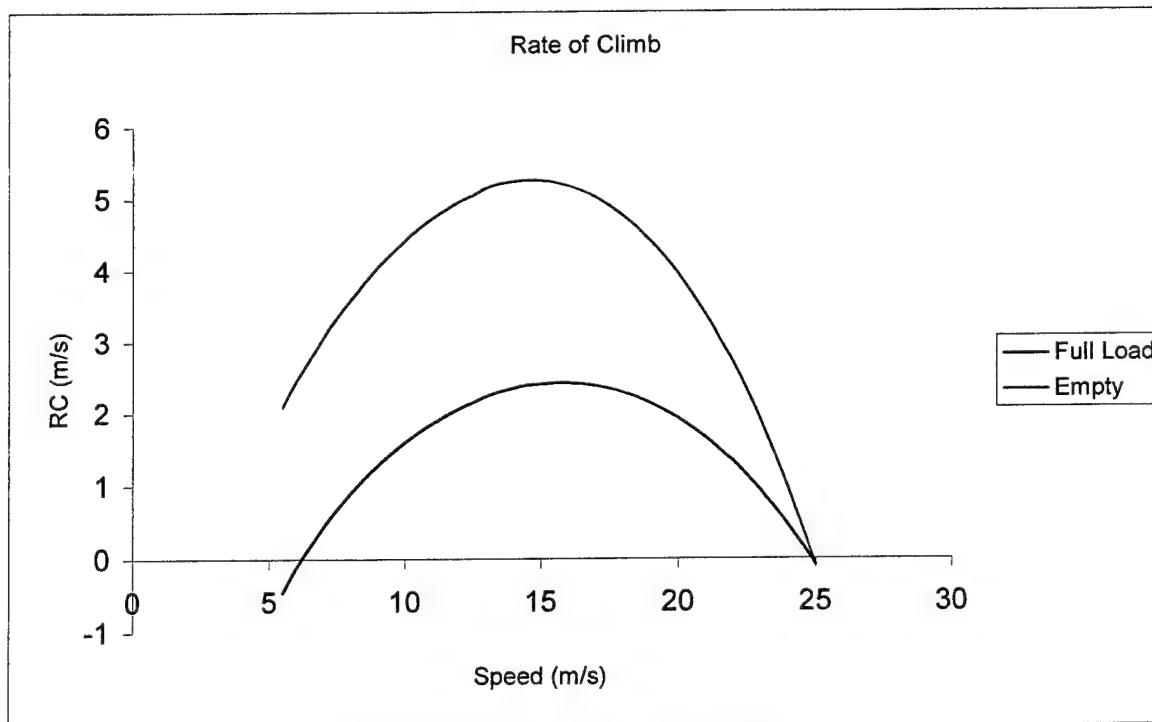


Figure 4.9 Rate of Climb vs. flight speed



We can find the fastest climb speed (V_{FC}), the flight path angle (γ), and the running time (t);

In both the considered conditions (empty and loaded), the fastest climb speed is higher than the stall speed. It is then possible to perform the climb with the maximum excess power. For this condition we easily determined the thrust to weight ratio from the level flight efficiency and the flight path angle. On the other hand, it is impossible to perform the climb at the steepest climb speed, that is, at the maximum flight path angle, because it is lower than the stall speed.

In order to estimate the motor consumption during the climb we multiplied the same given speeds by the elapsed time; in this way the needed current was calculated:

Empty Configuration	Loaded Configuration
Max RC = 5.26 m/s (17.26 ft/s);	Max RC= 2.43 m/s (7.97 ft/s);
V_{FC} = 14.5 m/s (47.57 ft/s);	V_{FC} = 16 m/s (52.49 ft/2);
γ = 21.27°;	γ = 8.73°;
t = 7.25s;	t = 7.87s;
mAh = 80.64	mAh= 82.30

Balanced turn: in this phase the maneuver load factor was assumed to be equal to 1.3 for the loaded configuration and 1.5 for the empty one; from the new equilibrium condition between required and available power the speed, the turning radius (R), and the necessary time were obtained. These are the results for the two configurations, empty and loaded:

Empty Configuration	Loaded Configuration
V = 24.5 m/s (80.38 ft/s)	V = 16 m/s (52.49 ft/s);
R = 73 m (179.56 ft);	R = 37.58 m (172 ft);
t = 9.6 s;	t = 10 s;
mAh = 50.95	mAh =23.68

Cruise: from the thrust curves the cruise speed and the correspondent times and consumptions were obtained:

Empty Configuration	Loaded Configuration
V = 24.5 m/s (ft/s);	V = 15.5 m/s (ft/s);
t = 6.22 s	t = 9.8 s
mAh= 37.00	mAh= 24

Gliding flight: this flight condition was considered because the landing is carried out at zero thrust, to optimize the cell consumption and/or in case of a propulsion system failure. The basic parameters we needed to know are the glide speed V_g and the time needed to descent. These parameters were determined in the case of a glide from the altitude of 20 m (65.62 ft), when the aircraft exits the last turn.

Empty Configuration	Loaded Configuration
V_g = 12.24 m/s (40.16 ft/s);	V_g = 12.24 m/s (40.16 ft/s);
t = 12.5 s	t = 12.5 s
mAh= 37.00	mAh= 24

In gliding flight consumption is zero; A conservative estimation was done, considering it as in the cruise phase.



Analysis of the two missions: the previous data were used in order to calculate times and consumptions; the two mission were schematized as follows:

- Ferry Mission: [1 take-off & climb + 16 turn + 14 cruise + 1 glide & landing]_{load}
- Fire Fight Mission = [2 take-off & climb + 4 turn + 2 cruise]_{load} + [4 turn + 2 cruise + 2 glide & landing]_{empty}. We have supposed an instantaneous water dumping during the first half of the 360° turn on the downwind leg.

Flight Phases	FERRY MISSION		FIRE FIGHT MISSION			
	# Segments	Time (s)	# Segments		Time (s)	
			Loaded	Empty	Loaded	Empty
Take-off run	1	1.8	2	-	5.6	-
Climb	1	7.25	2	-	7.87	-
Cruise	14	6.22	2	2	9.8	6.22
Turn	16	9.6	4	4	10	9.6
Glide	1	12.25	-	2	-	12.25
Landing	1	3	-	2	-	3
Mission time (s)	264.98		164.88			
Charge (mAh)	1472.25		763.24			

Table 4.2 Mission analysis

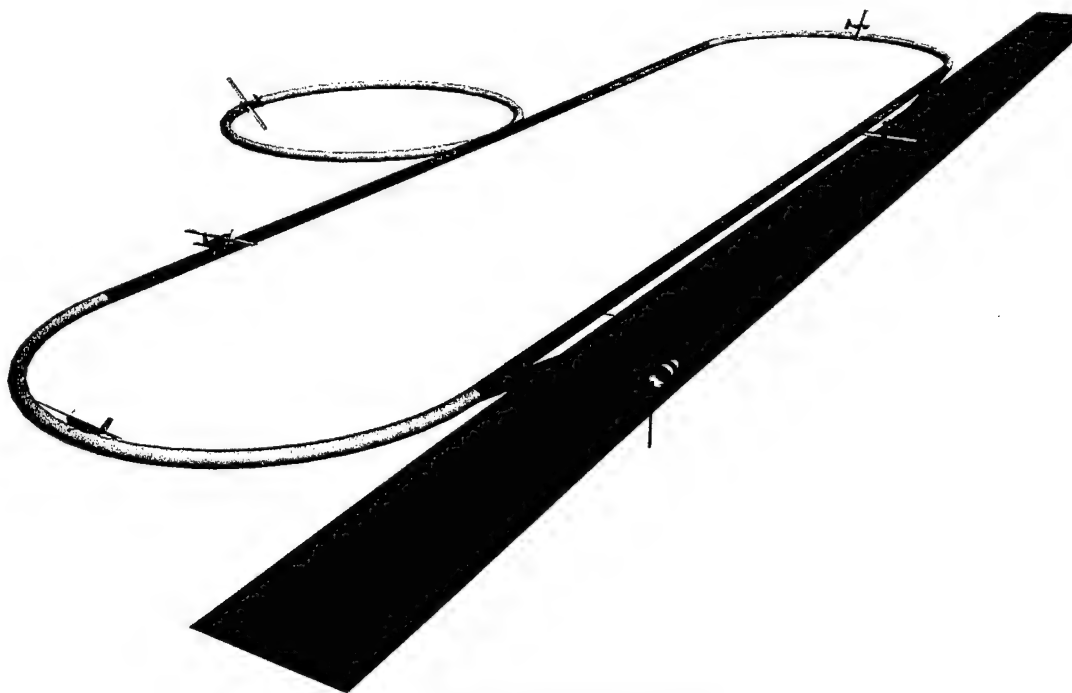


Figure 4.10 Flight path segments



4.3.4 Structural Analysis

We identified four main components of the aircraft: wing, fuselage, tail and landing gear. In order to predict the highest stresses the materials will suffer, the approach we followed was to perform an analytical study of simplified models of the load bearing structures of each single component and a numeric verification of results. The analytical study concerned the sizing of wing and tail spars, the tail boom, plates' thickness of the boxed central section of fuselage and the landing gear strut. The numerical analysis was developed using the MSC Nastran® software and it regarded mainly the composite made components.

Wing structural analysis

The wing is composed by two half wing each with a span of 1.125 m (3.69 ft). The half wings are characterized by a full span flaperon that reduces the chord of the airfoil from 26 cm (10.24") to 18.2 cm (7.16"), while its maximum thickness is 2.8 cm (1.1"). We decided to adopt a single carbon fiber reinforced plastic (CFRP) tube as wing spar because of the reduced volume we can deal with in the wing and for building ease; the tube is drowned in the polystyrene core of the wing in the max thickness region and has an inner diameter of 1.8 cm (0.71"). The spar goes along the whole wing span, enclosed within two edge ribs (tip and root) and realizes the joint with the fuselage by an inner aluminum tube 60 cm long, fixed in the fuselage. The core of the wing is covered with a single layer of glass fiber reinforced plastic (GFRP) manually layered up. The strength of the wing under bending moments induced by lift, structural test verification and gust loads (usual at Wichita) were considered to size the spar thickness. The thickness of the spar tube strong enough to resist the highest bending moments we supposed to lift at a load factor of 3.6 (gust condition) is 1 mm (0.04").

Twist analysis verified that a single ply of glass fiber 0.25 mm thick (0.01"), weighting 80 g/m², is generously resistant. A finite element (FE) analysis confirmed our analytical results; figure 4.12 shows the half wing deformation under structural test load conditions for 8400 elements and 7033 nodes.

Fuselage structural analysis

The fuselage is composed by three main components: radome, central section and tail section; Radome has no structural duty; it has a mere aerodynamic purpose and was obtained from a manual lay up of glass fabric on a polyurethane mould. The motor, cells and controllers housed in the radome are set in structures linked to the fore bulkhead of the fuselage central section. The latter is basically made up of 5 composites plates (nomex honeycomb + carbon skins); it bears the loads transmitted by the half-wings, the tail planes and the landing gear that are coupled to them with cylindrical connectors (wing and tail) or directly bolted on it (gear). The sandwich thickness was analytically determined for the most loaded plates, i.e. the lateral ones where the half-wing joined. There where available nomex core of two different thicknesses, 6 mm (0.24") and 8 mm (0.32"), while for the skins we used one layer of carbon fabric weighting 100g/m².

The tail section consists in the same CFRP beam used for the wing spar that links the tail surfaces with the aft bulkhead of the fuselage. The aerodynamic shape was obtained by polystyrene foam coated with a plastic ply. The whole fuselage was modeled by an FE model developed to check the analytic study. The connections fuselage/tail and fuselage/motor-case have been simulated using DOF spring elements with fixed stiffness.



The resultant model consists of 2262 elements and 1845 knots. Two load conditions were considered: static and dynamic. In the static load condition the aircraft is supposed to be at rest on the ground; in this case the fuselage has been considered fixed to the landing gear constrains. In dynamic load condition, the aerodynamics loads considered are the ones in the worst flight condition (gust with 3.6 load factor); in this case the fuselage has been considered pinned to joint of the wing. The considered loads are:

- the propellers reaction couple;
- the loads (forces and moments) transmitted from the tail;
- the loads (forces and moments) transferred from the wings;
- the motor-group weight;
- the body accelerations due to the worst flight condition.

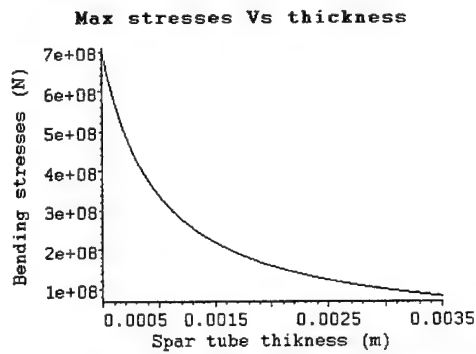
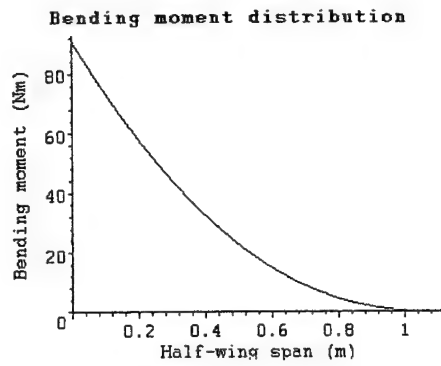
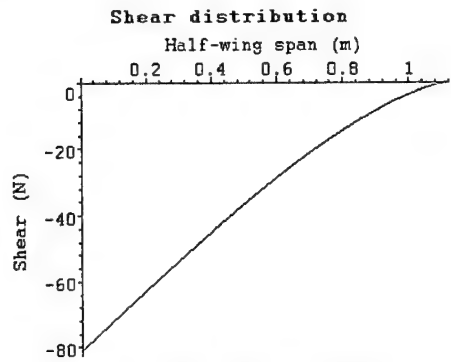
The result of the static analysis showed the most stressed elements and permitted to size them suitably. The 8 mm (0.32") core was elected as the most satisfying for the required strength in the wing connector area. The overall sandwich thickness is 8.6 mm (0.34").

Tail structural analysis

The conventional tail configuration was built assembling the vertical and horizontal wooden structured surfaces to the CFRP tail boom. Each surface is built with balsa ribs and lime stringers and has a single CFRP cylindrical spar that realizes the linkage with the tail boom. Spars sizing was performed on the basis of the maximum bending stresses, transmitted by the tail during the maneuvers: an 8 mm (0.32") diameter, 1 mm (0.04") thick carbon spar was chosen for both the horizontal and the vertical surfaces. The maximum bending stress is lower than 300 MPa (43'511 psi).

Landing gear structural analysis

The landing gear was sized according to maximum bending and shearing stresses we evaluate will be generated during the landing phase. It was modeled as a beam with a know initial warp, bolted on the lateral fuselage plate. An analytic study was performed to investigate the buckling behavior of the landing gear structure. The results of this study, suggested us to laminate 10 layers of Carbon+Kevlar fabric + 2 layers of unidirectional CFRP. A numerical FE analysis verified this decision. The main gear strut has been modeled with 234 elements and 240 nodes FE model. The Hoffman fracture criterion has been used because of non isotropic material property in two principal directions. In order to simulate the ground impact condition, the connection between the landing gear and the wheel has not been considered infinitely rigid, DOF spring elements with appropriate stiffness but have been used. The load conditions considered in the landing gear sizing, are referred to a landing at a vertical speed of 2 m/s (6.6 ft/s), widely in the range of vertical speed found for the gliding flight phase. The maximum stress, produced in the external carbon layers, is nearly 35 MPa (5'076 psi), while the max failure index is under 0.20 value with a safety coefficient of 3.5.



Wing Spar design: shear, bending
moment distribution along the wing
spar and max bending stresses

Figure 4.11 Wing spar analysis.

CLS

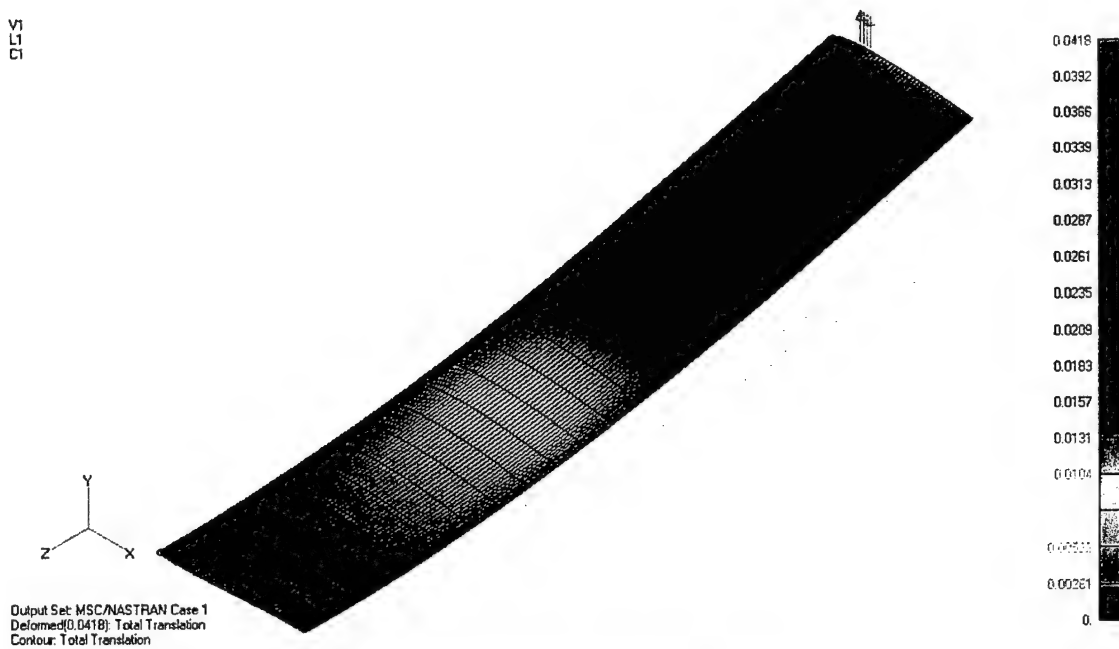


Figure 4.12 Half wing: total translation (m)



5 Detail Design

5.1 Introduction

At the end of the preliminary design stage, we had already sized the main components of our plane. The concept shape was defined as well as the structural and propulsive subsystem. Moreover, we had identified predicted performances in various flight conditions. In the next phase of the design process we had to focus attention on those elements we did not have studied yet, and to evaluate with more accuracy the performances we could not estimate in detail before, such as the dynamic behaviour of the plane. Therefore, we proceeded with the sizing of control surfaces and the analysis of the systems to join the main structural elements; we addressed the problem of the cooling system of the propulsive group and the best way to arrange servos and wires.

5.2 Aerodynamics and surface arrangement

Wing

After the preliminary phase, we already had the main characteristics of the wing and empennage.

Our interest was in refining the study on the flaperons. To achieve this purpose, we have used a code, Xfoil®, that allowed us to obtain results to compare with the semi-empirical data obtained by the procedures illustrated in the texts from Stinton and McCormick.

Results of the Xfoil® simulation:

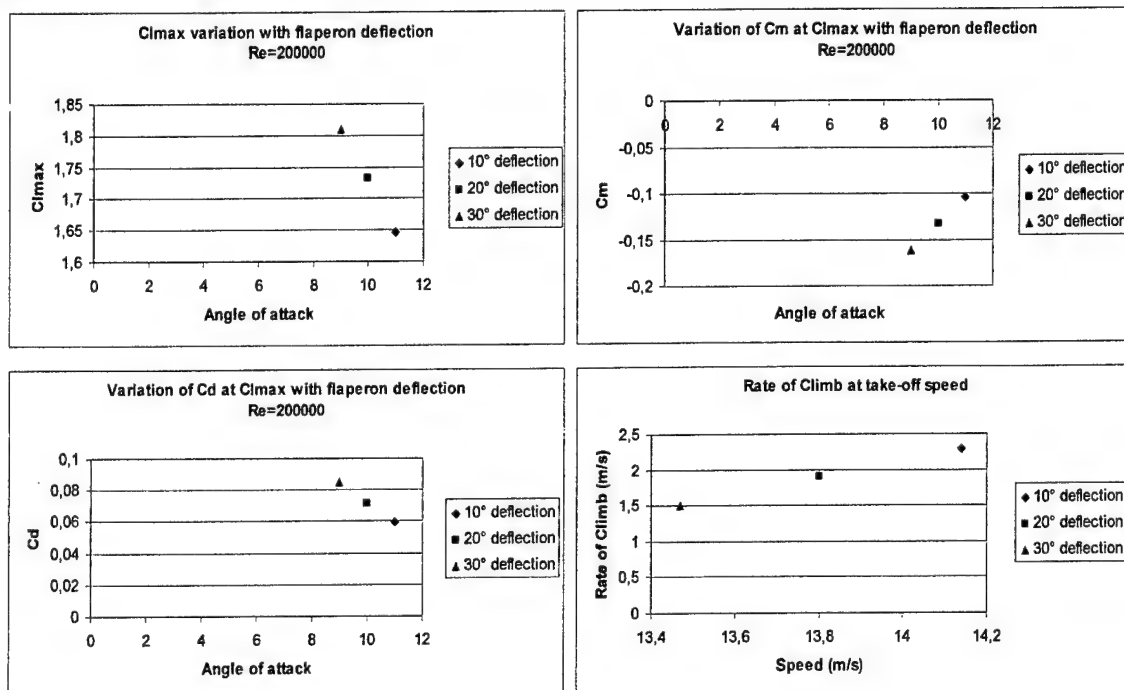


Figure 5.1 Flaperons charts



We have found the flaperons deflection of 30° to be a limit position; during take-off is important to have a good Rate of Climb and, as in the landing phase, enough lateral control, given, in our configuration, by a differential deflection of the same surfaces used for the flaperons.

Horizontal tail

The longitudinal position was determined during the preliminary phase; the tail arm was calculated taking into account stability and C.G. range. The vertical location came from the analysis of the following issues:

- Effect of downwash angle
- Behavior with the wing stalled
- Tail clearance

The result is a relative position, from the top of the fuselage, to the chord, of 2,5 cm (0.98"). The trim angles of the tail and the wing were calculated in the preliminary phase. They are confirmed by this refined study. Moreover, the wing, with an aspect ratio of 9,23, stalls at a shallower angle than the tail which has an aspect ratio of 3; the vertical location and the lower aspect ratio should guarantee, even in disturbed flow, enough control authority to recover, with a pitch-down moment, from a stall.

Spin & fin

The long span of the wing, compared to the length of the plane, gives a ratio of about 2; for this and other reasons we have studied the spin tendency of our plane.

An analysis of the moments of inertia $I_{xx}=A$ and $I_{yy}=B$ indicates a pro-spin inertia couple, being $B/A < 1$. From the Euler equations we have deduced the factor $(1-B/A)$, which is positive; our aircraft can be said to be "wing dominated". A further analysis of the chosen fuselage shape has showed a low body damping, mainly in the rear part, where the rounded tail cone has a damping coefficient related to the squared centre section one, of $1/3.5$. All this issues would lead to adopt the following possible fixes:

- Dorsal and/or ventral strakes
- Position of the vertical tail for a good spin recovery

The ventral strakes meet the need of augmented lateral area aft the C.G., not increasing appreciably the cruise drag. The vertical has been positioned as aft as possible, to have a good value for the control volume, leaving the rudder out of the tail wake. As a rough rule the rudder should have at least $1/3$ of his area outside the wake of the stabilizer. The wake has been sketched as the flow between a 30° line from the trailing edge and a 60° line from the leading edge of the stabilizer.

Our rudder is almost completely out of the tail wake.

5.3 Flight Dynamics and Control

5.3.1 Control Surfaces

We had to size the ailerons and rudder mobile surfaces. For the ground directional control, we introduced a steering nose gear directly linked to the rudder servo. We sized the control surfaces using the procedure suggested by Raymer.



Ailerons: The ailerons use the same surface designed for the flaperons. For this reason, in this phase, we have just verified the aileron control power given the configuration. To do this, we have used the balance between the roll moment produced by the ailerons and the roll damping at steady-state roll rate p_{ss} , of 100 deg/sec with a maximum deflection $\delta_A = 15^\circ$

Rudder: With the fin dimensions already fixed in the preliminary phase, the rudder sizing came from the analysis of a steady sideslip. This requirement is for the design to have adequate roll and yaw power to perform steady sideslip maneuvers. This can become significant during cross-wind landing, when the sideslip angle is the greatest because of low airspeed. To maintain a steady sideslip, the net sideforce, rolling and yawing moment must vanish. In the usual analysis it is assumed that the aileron and rudder are used to maintain a specified sideslip angle. Furthermore, it is usual to assume that the aileron does not generate sideforce, leaving the rudder as the only sideforce generator. Once the rudder deflection is found, the bank angle required to obtain zero sideforce is found. Then, we have checked to see if the required control deflections and bank angle are acceptable.

$$\begin{aligned} C_{Y_\beta} \beta_e + C_{Y_{\delta_R}} \delta_{R_e} + \frac{mg \cos \theta_e \sin \phi_e}{1/2 \rho V^2 S} &= 0 \\ C_{l_\beta} \beta_e + C_{l_{\delta_A}} \delta_{A_e} + C_{l_{\delta_R}} \delta_{R_e} &= 0 \\ C_{n_\beta} \beta_e + C_{n_{\delta_A}} \delta_{A_e} + C_{n_{\delta_R}} \delta_{R_e} &= 0 \end{aligned}$$

We have guessed a lateral wind of about 5 m/s (16 ft/s) and a speed of about 15 m/s (49 ft/s) with a subsequent β_e of about 18° . With the hypothesis that no more than 75% of the roll and yaw control authority be devoted to maintaining steady sideslip and that the bank angle is less than 5° , we have found for the rudder a chord of 11 cm (4.33") and a span of 28 cm (11.02").

The lower side has been cut at an angle of 45° to have a complete tail rotation clearance.

Pitching-moment equation and Trim: The pitch moment, about the center of gravity, has to be equal zero. This moment is the sum of the contributes produced by the various aircraft components: wing, fuselage, tail. For a given flight condition, is possible to calculate the single contributes and check if the sum is zero. If this condition is not met, it is possible to vary the tail lift, changing the tail incidence, so that the moment vanishes. The change of the tail lift produces a change of the total lift of the aircraft, which should balance the weight. Then, the change of the tail lift causes a change of the angle of attack. To solve the problem an iterative method can be used, or better the graphical solution proposed by Raymer: once the angle of attack α and the tail incidence i_H are arbitrarily chosen, we calculate the total pitch moment coefficient:

$$C_{mcg} = C_L (\overline{X_{cg}} - \overline{X_{acw}}) + C_{mw} + C_{mfus} - \eta_h \frac{S_h}{S_w} C_{Lh} (\overline{X_{ach}} - \overline{X_{cg}})$$

where C_{Lh} is the tail contribute, function of the downwash angle and the zero lift angle due to the elevator deflection, found out in the previous elevator sizing. Under the considered hypotheses, it is possible to calculate the total lift coefficient, where the wing and tail lift coefficients are summed, considering the change of the dynamic pressure on the tail. For different angles of attack we calculated the total lift coefficient



and C_{mcg} . For $C_{mcg} = 0$, it is possible to find the trim conditions for different tail deflection angles.

5.3.2. Handling Qualities

At this point we encountered the problem of studying the dynamics stability of the designed aircraft, to predict how the aircraft motion evolves following a perturbation of its equilibrium state. As trim condition we considered a steady state level flight at cruise speed (20 m/s) and full weight (9 kg). The equations of motion were linearized using the theory of little perturbations. In so doing we obtained, as usual, two sets of decoupled equations for longitudinal and lateral dynamics. The linear equations were written in the space-state. So, we could calculate eigenvalues, damping, and therefore, coefficients and natural frequencies and to analyze the stability of the system. Then we studied the response of the system to input of 1 deg for tail (longitudinal dynamics) and for ailerons (lateral dynamics). To follow this procedure we needed to calculate stability and control derivatives (non dimensional and dimensional). To this end, the method proposed by Roskam was used.

$C_{L,\alpha}$	$C_{D,\alpha}$	$C_{M,\alpha}$	$C_{L,q}$	$C_{M,q}$	$C_{L,\dot{\alpha}}$	$C_{M,\dot{\alpha}}$
4.4741	negligible	-1.1088	5.2125	-8.0758	negligible	negligible

Table 5.1 Longitudinal non-dimensional derivatives

C_{L,i_H}	C_{D,i_H}	C_{M,i_H}
0.3432	negligible	-0.89021

Table 5.2 Longitudinal control derivatives

$I_{yy} [kgm^2]$	X_α	M_α	$M_{\dot{\alpha}}$	M_q
0.321768	0.41757	-8.38967	0	-7.94366

Table 5.3 Longitudinal derivatives and moment of inertia about Y body axis

$C_{y,\beta}$	$C_{l,\beta}$	$C_{n,\beta}$	$C_{y,p}$	$C_{l,p}$	$C_{n,p}$	$C_{y,r}$	$C_{l,r}$	$C_{n,r}$
-0.7018	-0.1039	0.1358	-0.1076	-0.2653	-0.0286	0.2879	0.1623	-0.0913

Table 5.4 Lateral-directional non-dimensional derivatives

C_{l,δ_A}	C_{n,δ_A}	C_{y,δ_A}
1.82178	-1.40612	negligible

Table 5.5. Lateral control derivatives

$I_{xx} [kgm^2]$	$I_{zz} [kgm^2]$
0.415106	0.672739

Table 5.6 Moment of inertia about X and Z body axes

Y_β	L_β	N_β	L_p	N_p	L_r	N_r
-0.73263	-5.62509	4.53655	-2.99233	-1.1465	10.54419	-3.65997

Table 5.7 Lateral-directional dimensional derivatives

Once the aerodynamic derivatives and the reference flight condition were calculated, we had the components of the state and control matrices. Then, two simple codes were developed in commercial software Matlab® to calculate eigenvalues, damping coefficients and frequency for the longitudinal (phugoid and short period) and lateral-directional modes (roll, spiral and dutch roll).



Longitudinal dynamics

From table 5.8 we observe that the real part of the eigenvalues is negative, positive damping so that both modes are stable. Furthermore, the results show how the short period damping is nearly ten times that of the phugoid. The same frequencies, calculated with the approximate models (second-order) of phugoid and short period, are respectively: $\omega_{PH} = 0.566$ rad/sec, e $\omega_{SP} = 11.67$ rad/sec.

Mode	Eigenvalue	Damping	Frequency [rad/sec]
Phugoid	$-0.03697 \pm 0.5217i$	0.0707	0.523
Short Period	$-6.32 \pm 14.00i$	0.411	15.4

Table 5.8 Longitudinal modes

These values are quite close to the ones obtained as output of the Matlab® program.

Next we evaluated the response of the plane model to a single nose down impulse command of 1 deg tail deflection. By analyzing figure 5.1, we can deduce that in the first seconds, when the short period is excited, we find the biggest variation of angle of attack and pitch rate. Then, at later time, when the phugoid mode is the dominant one, we can see the biggest variation of airspeed and pitch attitude.

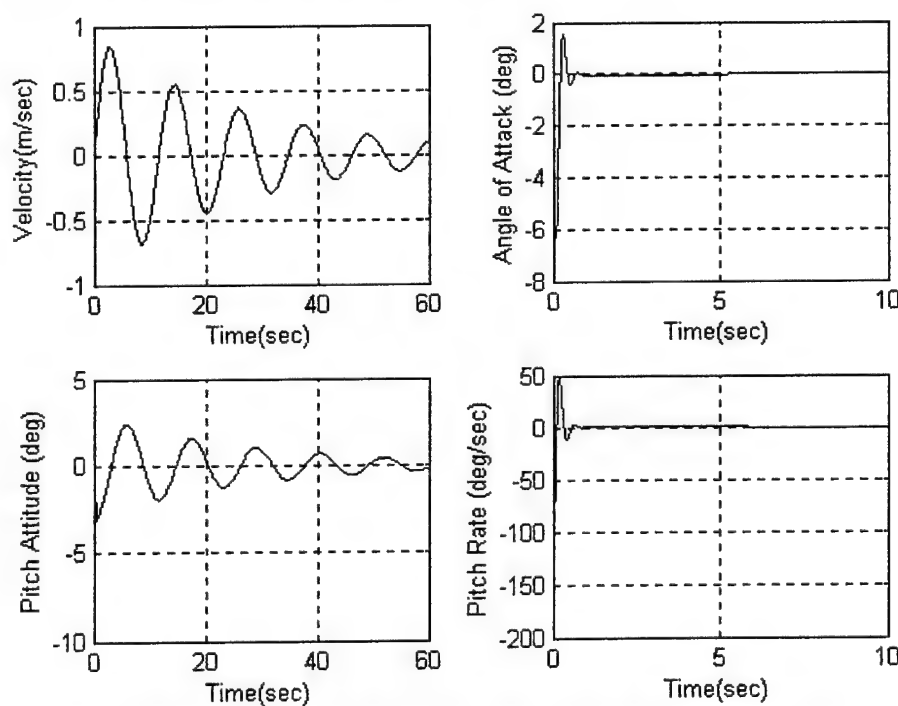


Figure 5.2 Longitudinal response to a 1-deg elevator impulse input



Lateral-directional dynamics:

The Matlab® program gave the eigenvalues, damping coefficients and frequencies shown in table 5.9 for the roll, spiral and dutch roll modes.

Mode	Eigenvalue	Damping	Frequency [rad/sec]
Spiral	0.00202	-1	---
Dutch Roll	$-2.6 \pm 5.84i$	0.407	6.4
Roll	-14.6	1	---

Table 5.9 Lateral-directional modes

Results show a slightly unstable spiral mode. It is associated with a real eigenvalues which mainly represents the variations in roll attitude $\Delta\phi$ and depends mostly on the $C_{l,\beta}$. Anyway, spiral mode is typically associated with a slow dynamic. This is our care, actually: in fact the time constant is low so that the pilot has time to react. The dutch-roll is an oscillatory mode with significant component in the yaw Δr and the roll $\Delta\phi$ variables. Table 5.10 shows that it is stable. The roll mode is associated with a real root and the motion is predominantly in roll rate Δp . Next we analyzed the response to a single 1 deg impulse on the ailerons, positive (i.e.: right aileron upwards).

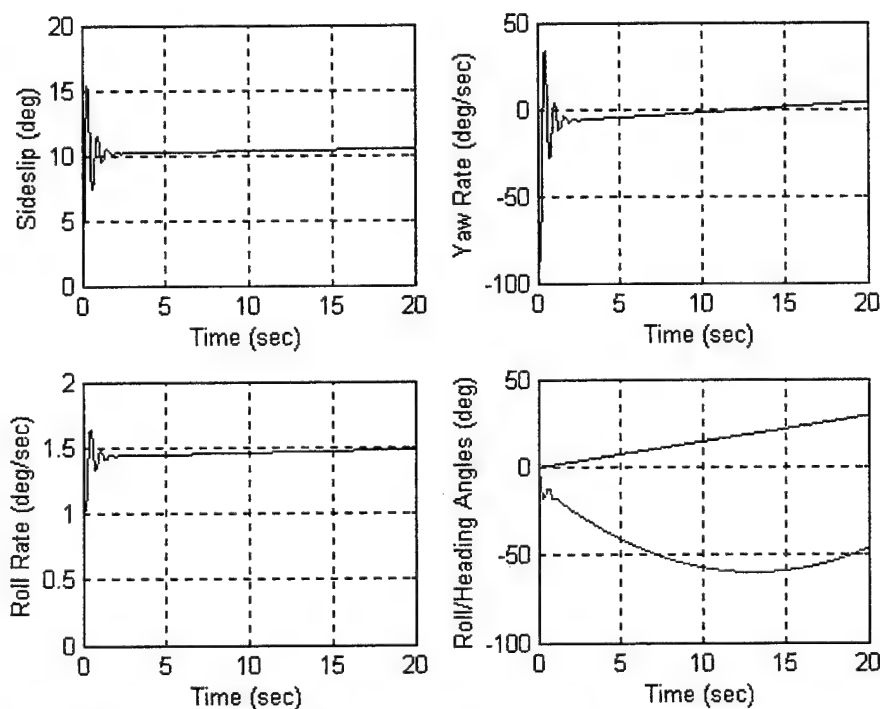


Figure 5.3 Lateral-directional aircraft responses to a 1-deg aileron impulse input



5.4 Structures

Once the main components of the aircraft have been sized, next design phase was to describe their integration and detailed description. Differently from last year, we don't have the constraint to set the airplane in the specified box with the lower amount of components disassembled, in order to minimize the assembly time. However to limit the parts would results in minor structural complexity and weight reduction. This aspect of the design process has been considered as a key goal to deal with.

5.4.1 Fuselage Structural Details

The fuselage is designed caring not to expose sharp angles to the flow of the propeller and with a reduced cross section. Its structural body, the central section, is a volume wide enough to enclose the tank, the receiver and its cells and to contains the joints structures that link to wing, tail, landing gear and radome. It mounts two outward servos that command respectively the nose wheel steer – vertical surface and the tank's orifice open/closed position. Half-wings are prevented to slip from tube thanks to a screw fixed on the aligning CFRP little spar that run from each half-wing mid-span rib to the root rib. The tail section is fixed to the central section of the fuselage by a CFRP tube constrained between the two aft bulkheads. On the front bulkhead an aluminum structure bears the motor and two eight-cells battery packs. A GFRP radome encloses the propulsion system and it is fixed to the central section of the fuselage by two lower and one upper screws.

5.4.2 Wing Structural details

The wing consists in two different parts or half-wings, joining the fuselage. Each half wing is shaped on a polystyrene core and covered with a single ply of GFRP skin. Two lime ribs are placed at the root and tip of each half-wing; This ribs bear a full span tubular CFRP spar that join the male aluminum tube, 0.6 m (23.62") long, of the fuselage. A third balsa rib is placed between the previous ribs allowing to set the half-wing carbon aligning spar. The polystyrene core transmits loads to the composite structures. The flaperon's servos are drowned into the core of the lower face of each half-wing in the mid-span and they are fixed to the wing skin by a lime wood thin plate.

5.4.3 Tail Structural Detail

The Conventional tail, the horizontal and vertical plane, is realized with balsa ribs and lime stringers. Both surfaces have a single CFRP spar tube with a diameter of 8 mm (0.31") and thickness of 1 mm (0.04"), providing bending load resistance and joining the tail boom. This spar allows the whole horizontal stabilizer to spin about. The vertical surface has a second spar tube that is the hinge of the rudder. The fuselage tail section is realized with polystyrene foam covered by a ply of cover. While horizontal tail is all moving thanks to a dedicated servo, the vertical rudder movements are coordinated by a servo with fore landing gear wheel. The disassembled configuration in the box sees only horizontal tail set with fuselage, while vertical is assembled in second time.

5.4.4 Landing Gear Structural Details

The landing gear system is a fore tricycle. The fore leg, made of steel, is jointed with CFRP hinges to the bottom of the fore frame of the fuselage. A servo, fixed in the same frame, is dedicated to move directly



this leg to allow steering the plane while on the ground, and at the same time to govern the moving part of vertical tail during the flight using a tether system. The main gear legs are positioned behind the barycentre of UAV, and are built by a manual lay up of carbon-kevlar fabric and epoxy resin cured at environmental condition and controlled pressure. The linkage with the fuselage is obtained by three bolts on the lateral plates. In the box the landing gear is disassembled by the rest of plane.

5.4.5 Radome Structural Detail

Radome, having only aerodynamic purpose, is made with 2 ply CFRP (120g/m^2). The enclosed volume contains the motor and the cell pack whose support structures are linked with the fore frame of the fuselage. The Radome will lay joined with the rest of the fuselage in the box. A frontal air inlet will supply the right cooling of the motor and cells pack.

5.4.6 Tank Structural Detail

The adopted water tank is the result of evaluating different geometric types under several aspects. To assure complete water dump, the ideal shape of the tank should be a sphere, optimizing the capacity and the outer surface. Otherwise, this shape is difficult to build and to fit in an axial symmetric fuselage, so we looked for a silhouette easy to build but still efficient in dumping the water. After the analytical study we had realized three types of tanks: prismatic with octagonal section; semi-pyramidal with octagonal section; semi-pyramidal with rectangular section. To perform the dump phase in each cruise condition, the orifice is positioned near the lower tanks base, after the C.G. position of the aircraft. We performed dumping tests and recorded times with several pressure and trim conditions. The first one has an average dump time of 40 sec; the second one dumps in 33 sec but has a high building complexity; the last one is easy to realize and complete the dump phase in 31 sec. This one is the selected tank set.

5.5 Propulsion System

The propulsion system had already been fully designed at the end of the preliminary design phase. The propulsive group had selected the proper motor and gear-box. It planned to perform a series of wing tunnel and flight test to choose the propeller and a mission flight profile which would enhance aircraft performances. At this stage of the design the propulsive group considered the various possible cooling systems. It decided a simple frontal air intake would be sufficient to guarantee the proper motor and cells cooling.



5.6 Final Aircraft Table

Geometry		
Length	1.18 m	3.87 ft
Span	2.4 m	7.87 ft
Height	0.62 m	24.4 ft
Wing area	0.62 m ²	6.71 ft ²
Aspect ratio	9.23	
Control volume	0.25	

Weight Statement		
Airframe	2.48 kg	5.47 lb
Propulsion System	1.54 kg	3.39 lb
Control System	0.648 kg	1.43 lb
Payload System	4.15 kg	9.15 lb
Empty Weight	4.67 kg	10.29 lb
Gross Weight	8.82 kg	19.44 lb

Performances			
C _{LMax} clean		1.17	
C _{LMax} flapped		1.49	
L/D Max		12	
Static Margin		0.21	
Rate of Empty	6.2 m/s	20.34 ft/s	
Climb Gross	3 m/s	9.84 ft/s	
Stall Speed Empty	9 m/s	29.53 ft/s	
	Gross	12.51 m/s	41 ft/s
Max Speed Empty	24.5 m/s	80.38 ft/s	
	Gross	23.5 m/s	77.1 ft/s
Takeoff Run Empty	9.24 m	30.32 ft	
	Gross	43 m	141.07 ft

System	
Radio	Futaba FP8 UPS
Servos	Futaba S9402
Battery Configuration	16 cells, serial
Motor	Graupner Ultra 930-8 12 V
Propeller	19" x 12"
Gear Ratio	3.75:1

Table 5.10 Final aircraft table

5.7 Rated Aircraft Cost

In the following table the final aircraft RAC is determined according to the supplied cost model:

$$RAC = (A \cdot MEW + B \cdot REP + C \cdot MFHR) / 1000 = 9.401 \text{ thousand \$}$$



Coefficients calculation

Coefficient	Description			Value	Coefficient	Value	Total	
Manufacturers Empty Weight (MEW)	Empty weight			10.362	Manufacturers Empty Weight Multiplier (A)	\$ 300	3108.45	
	10.362 lb							
Rated Engine Power (REP)	# of motors	Battery weight		2.116	Rated Engine Power Multiplier (B)	\$ 1500	3174	
	1	2.116 lb						
Manufacturing Man Hours (MFHC)	Wing			82.165	155.9	Manufacturing Cost Multiplier (C)	\$ 20/hour	3118
	External surface	# of controls	Control type					
	6.716 sqft	2	flaperon					
	Fuselage			23.748				
	Volumes							
	1.187 cuft							
	Empennages			20				
	# of horizzontal	# of vertical with control						
	1	1						
	Drive system			30				
	# of servoes or controllers							
	6							

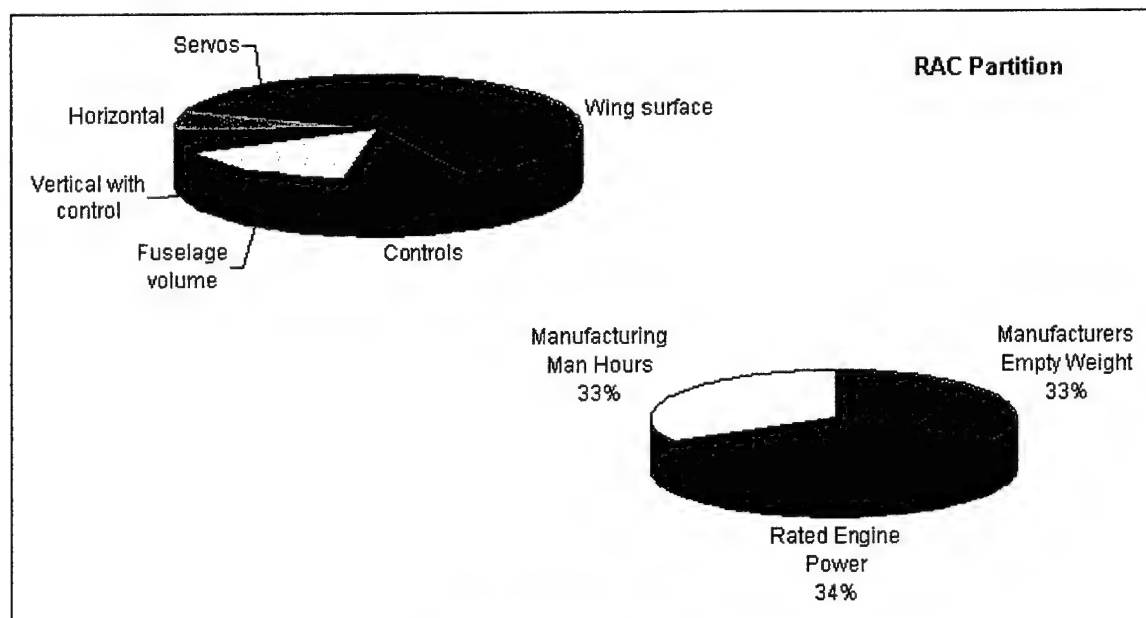


Figure 5.4 Final RAC



6 Manufacturing Plan and Processes

6.1 Introduction

The purpose of the design process should lead to a construction phase well planned, optimized and as short as possible. For this reason a set of figures of merit (FOMs), as in the Conceptual Design Phase, was chosen in order to achieve the best methods for building the model.

6.2 Alternative processes investigated

The extensive use of composite materials allowed us to select between different production procedures for each component. Some techniques lead to excellent surface smoothness but they raise the costs and the skill required; on the other hand, techniques that give rougher surfaces, have lower costs but are easy to use. Therefore, it was necessary to select the optimum processes needed for the construction.

The alternative considered processes were:

- Hand Lay-Up: it provides the roughest results for the composite materials; the costs are quite low, but it causes some faults due to the gaps caused by lack of accuracy in hand-deposited fibers on the preliminary gel coat.
- Polyurethane, wood, or metal moulds: this is not properly a building method, but it was taken into account because it could be part of each construction process concerning composite materials in order to obtain a better result. The moulds give the highest superficial smoothness, in particular the metallic ones, but they are the very expensive.
- Curing cycles in autoclave or oven: the quality of this technique can bring to high performing and structural pieces, due to the optimal pressures and temperatures obtained during the polymerization; the time required for an accurate manufacture is very long, and the temperature must be given gradually in order to avoid material stresses. This is an expensive technique due to the initial cost of the half-processed materials used and the high production discards.
- Foam hand hot wiring: a block of polystyrene foam can be easily cut and modeled using a hot wire. It is a quite cheap technique; it requires a good skill, but our know-how was improved with our previous experience in this contest.
- Lime wood/Plywood Framing: it is the classical way to build the aircraft without spending a lot of money and resources; unfortunately a manufacture made with this process is quite heavy and requires a lot of time; moreover, the stiffness is an important issue, along with strength of the product; sometimes the building tolerances are too high.
- Balsa Sheeting: it guarantees enough smoothness modeling the desired shape; it is used to cover frames but cannot be used in structural components.
- Fiberglass Sheeting: its cost is quite low if compared to other fibers; it is quite fast to lay and it gives good results, even though the elastic module is not properly high.

The considered FOMs were:

- Cost: actually the team members plan to raise themselves the funds necessary for the construction of the aircraft and for traveling to the United States for taking part in the contest. Thus, our budget



was quite low, and then this is one of the most important FOMs. Obviously techniques and materials judged to be too expensive were often discarded, even though sometimes they were a forced choice.

- **Required skill:** this FOM measures the experience necessary to use the selected technology; the previous contests gave us some abilities in building the aircraft in several ways, but we don't have the same skill in all the manufacturing processes.
- **Availability:** it takes into account the difficulty in disposing of materials and facilities.
- **Reliability:** this FOM depends on the strength and stiffness of the component constructed with the selected technology and material.
- **Building time:** this represents the final aim of the whole manufacturing process because a delay in the construction of one single component would produce a bigger delay in the assembly of the complete plane.

All the FOMs listed above were not used in a direct way in a decisional matrix; we preferred to incorporate them as variable parameters driving us in deciding which processes were the most convenient to build each part and subsystem of the plane.

All the manufacturing processes had to be evaluated by comparing them in a quantitative way. First of all, we wrote a matrix in which we could compare the various skills considered; this array gave us the right suggests to proceed. The table 6.1 shows the results.

	Hand Lay-Up	Moulds	Curing cycles	Foam Hot-Wiring	Lime/Plywood Framing	Balsa Sheeting	Fiberglass Sheeting
Fuselage	3	4	5	3	3	3	5
Wing	4	3	4	5	4	3	5
Tail	3	3	3	4	5	4	4
Landing gear	5	3	3	null	null	null	3
Tank	2	3	2	null	3	2	4
Radome	1	5	4	4	null	null	5

Table 6.1 Skill decision matrix

In some cases it's impossible to combine a specific technology with a certain component, according with the results reached at the end of the conceptual design phase; in these situations we have used the string "null". Combining the results here obtained we selected the manufacturing processes to be used.

6.3 Prototype Manufacturing

A full-scale prototype of the aircraft was built. The purpose of this first model was to obtain data and information about the behavior and the handling qualities of the final plane. For several reasons, the material selected to build the whole prototype was wood, in particular plywood and balsa sheets. The fuselage, with an adequate inner volume for the housing of the water tank, is composed of four plates; the tail, the empennage, and the wing are built in a classical way, with ribs, stringers and fabrics.



6.4 Manufacturing Processes Selected

From the analysis of the previously introduced FOMs and skill decision matrix, we have evaluated the manufacturing techniques to be used for each aircraft component and the best ones were so selected.

6.4.1 Fuselage Manufacturing and Tooling

The first duty of the fuselage is the housing of the water tank and, then, allowing a simple way to assembly the coupling systems of the two half-wings, the tail, and the landing gear and withstand the relative transmitted loads. Moreover, the fuselage should have an aerodynamic shape in order to produce the lowest additional drag. For this reason we considered this component as the most important in the manufacturing process. Two prepreg carbon skins were layered in a shaped mould with a core of nomex, then were all cured in autoclave in order to obtain an honeycomb sandwich structure; this composite is an excellent trade-off between flexural stiffness, strength and lightness. The motor support was realized with aluminum. It was hitched to the main structure of the fuselage with screws and glue. The radome was made with GFRP laid inside a chalk mould. The water tank made of ABS (Acrylonitrile-Butadiene-Styrene, a thermoplastic polymer). For single and little parts other various materials, like wood, aluminum, steel, and plastic, were utilized.

6.4.2 Wing Manufacturing and Tooling

The lifting surfaces were built with a polystyrene interior with a manual lay up of a GFRP skin on in order to ensure the needed rigidity. The core was made of polystyrene foam, shaped with the hot-wiring technique. An outer carbon tube was drowned within each entire half-wing, along the maximum thickness axis. For a good coupling, an inner tube, with a length of 1 m, was fixed into the fuselage. The used epoxy resin polymerizes at room temperature in 24 hours. Once layered, each half-wing was wrapped in a plastic sheet, and put inside a mould under controlled pressure. This process has a low cost and the surfaces obtained are quite smooth. At the center of the wings we obtained the little bays for the servos. The flaperons were made with balsa sheets, covered with a Thermo-retractable film, linked to the wing with glued hinges.

6.4.3 Tail and Empennage Manufacturing and Tooling

The tail cone was manufactured as the wing, with a carbon tube sank in the polystyrene core used as main boom. The all-moving horizontal tail was made in the same way as the flaperons. Its rotation was obtained by introducing a little carbon tube that crosses all the ribs. The vertical surfaces were realized in the same way. The fin was fixed to the tail boom with a carbon tube and so the rudder surface.

6.4.4 Landing Gear Manufacturing and Tooling

The main landing gear was made laying up CKFRP (Carbon-Kevlar Fiber Reinforced Plastic) fabric and unidirectional carbon fiber for the outer layers. The double curvature shape was obtained from wooden mould. The gear was then fixed to the external surfaces of the fuselage with screws. The fore gear is composed with a spring fixed to the fuselage just below the motor cradle.

6.5 Manufacturing Milestone Chart

Figure 6.1 shows the Milestone Chart of the schedule followed by our team throughout the manufacturing process. The string "planned" precedes some of the periods listed; this fact is due to the compulsory date of shipping of the present report.; the schedule of the latter periods should be read as just indicative.

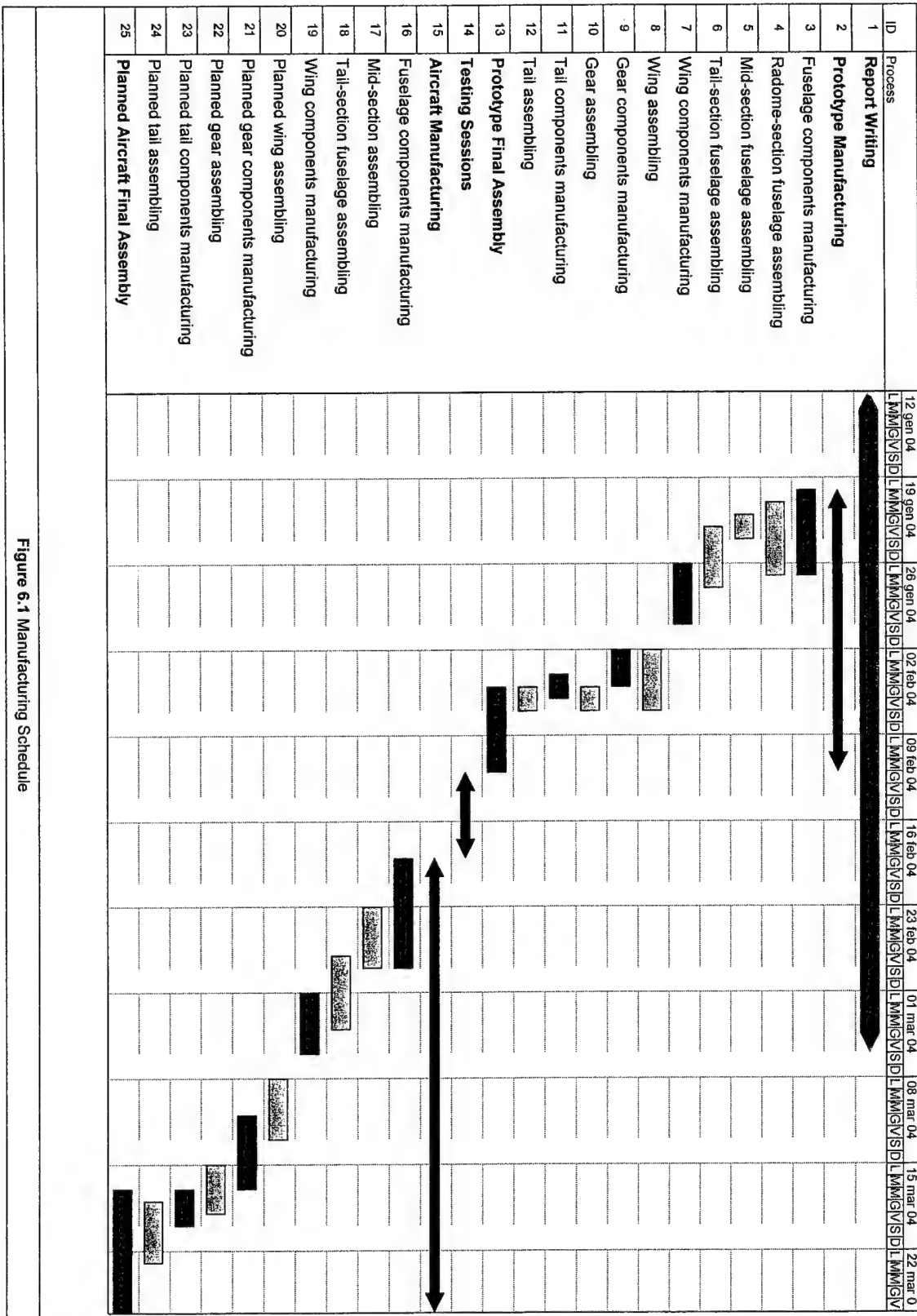


Figure 6.1 Manufacturing Schedule



7 Testing plan

7.1 Structural tests

To evaluate the performances of the actual structure in the operative conditions along with standard specimen tests is important to test the various structural elements of the real plane with the actual load conditions. In particular, we planned to perform experimental analysis on the wing, to establish its load carrying capabilities and its dynamic behavior. We planned also to perform tests on the structural subsystems which are located within the fuselage, such as the bayonet coupling of the wing, tail booms, and the undercarriage. Testing the assembled half-wing had the purpose to obtain the real stiffness and strength with respect to the nominal data obtained with analytical and numerical studies. We have built 3 half wings and fixed an electric strain-gauge (S/G) near the root section, at the point of maximum airfoil thickness (where is the spar), to measure strains on the skin. Then, we have simulated the static inspection condition, i.e. we have fixed the root section of the wing as a cantilever beam and applied to the tip an increasing load. The S/G works like a Wheatstone bridge. It uses the variation of the resistivity of conductor when it is deformed by mechanical stress. We have used a half-bridge configuration to obtain bridge amplification on the signal, to avoid the effects of temperature and of unwished tensile or compressive forces applied on the wing. The S/G was glued by a phenolic resin on the wing upper surface, 8 cm from the root section over the spar location. We managed data acquisition and setting of the device by the HBM software supplied with the SCOUT 55 amplifier. To load the wing we have used weights of different sizes; analysis data for the three specimens are summarized in table 7.1.

Applied load	Wing 1	Wing 2	Wing 3
[kg]	strain[$\mu\text{m/m}$]	strain[$\mu\text{m/m}$]	strain[$\mu\text{m/m}$]
1	67.2	73.2	69.6
2	153.1	139.5	155.1
3	211.2	198.2	198.3
4	242.1	212.4	242.1
5	286.4	248.2	263.2
6	302.7	269.3	277
7	340.5	306.2	304.1
8	Skin failure	345.1	339.8
9		Skin failure	361.4

Table 7.1 Wing static tests

An unexpected result was the difference within the critical loads. Inspecting the number 1 wing failure area, we could notice in the crack region (on the lower surface) that glass fibers were not properly impregnated of resin. So the failure was due to the buckling of those fibers. On the other side Wing 2 broke showing a clear delamination within the fibers and the core. We noticed that this delamination began from servo seat, a point of stress concentration. By plotting the experimental diagram σ - ϵ for the first wing, we deduced a value of the elastic modulus equals 20 GPa, exactly the one we used in the sizing study, averaging the results supplied by standard coupon tests we had performed. This result validates our first impression about the flexural strength



of the buckled wing skin: the offset from nominal behavior of the material is certainly due to local manufacturing faults. The last test validated our conjectures about the method to improve the stiffness of the skin during the manufacturing process: we managed to round off the sharp corners of the servo bay hole on the skin and to improve locally the soaking of the glass fibers. Dynamic tests of the half-wing have been performed to compare natural frequencies and modal shapes obtained experimentally with the ones calculated with numerical FE codes. We could predict the actual wing would show lower frequencies with respect to the ones found by using FEM codes, because of the imperfect manufacturing process and the difficulty of simulating an ideal fixed constraint condition. We have used an impact hammer. An accelerometer (shock limit of 500g) was placed on the hammer's head (PCB 356B18), while the measurement accelerometer (PCB333B30) had a 50g shock limit with a voltage sensitivity of 100 mV/g. The acquisition system was made of a 16 bit National board NI DAQ Card AI 16XE 50, with 16 channels and a scan rate of 20,000 samples per second. To constrain the wing at its root, trying to reproduce its real condition of operation, we clamped the cylindrical spar to a steel support. Along the wing span (1,125 mm) we identified 11 key-points of measure (with a step of 100 mm). Data recording and processing was done by software we developed in LabVIEW®. We have been able to identify the first 3 natural frequencies of the structure. Table 7.2 shows the comparison between experimental and numerical results.

	FEM analysis output	Experimental results
f1	15.02 Hz	9.9 Hz
f2	72.7 Hz	69.17 Hz
f3	138.77 Hz	130.4 Hz

Table 7.2 Natural frequencies comparison

7.2 Wind tunnel tests

7.2.1 *Propulsion test*

The propulsion system was fastened to a dynamometric scale in order to measure the thrust at various air speeds. This was done to obtain an experimental curve of the available thrust (and power) in every flight conditions and to compare it with our Motocalc® results.

During the same test we have obtained the trend of the current consumption in the same speed range.

7.2.2 *Aerodynamic test*

With the same dynamometric scale we have conducted aerodynamic tests with 1:2 scale aircraft semi model in order to obtain the drag polar of the whole airplane, the CL vs α and CM vs α charts.

Both propulsion and aerodynamic experimental results are in good accordance with the numerical simulations carried out in the preliminary and detailed design stage.

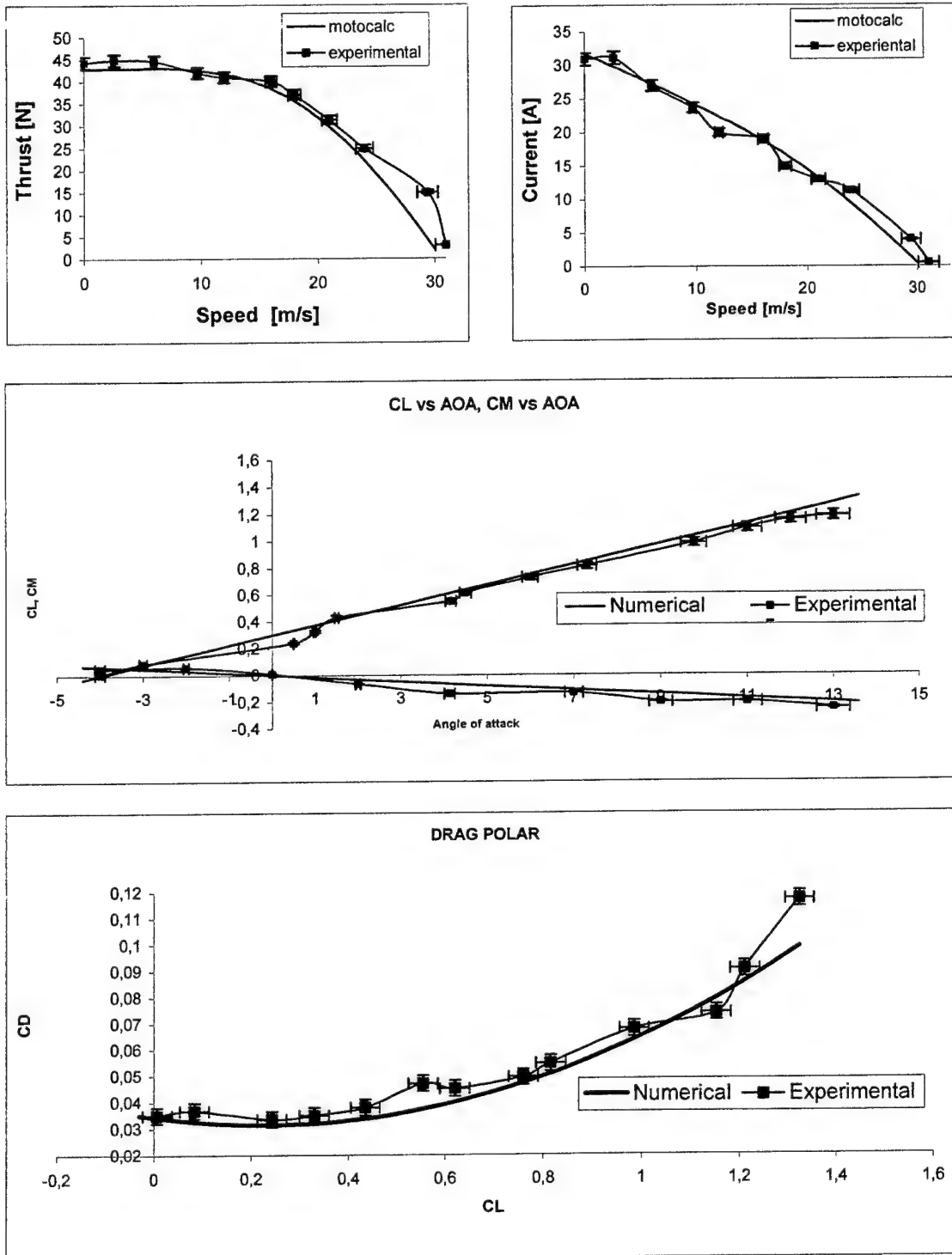


Figure 7.1 Wind tunnel tests



7.3 Flight tests

After the static and dynamic tests on the wing of the airplane we felt useful to arrange a series of flight tests; the experimental data obtained have been a valuable tool to certify our analytical results about performance, flying and handling qualities of aircraft. These tests were performed on a full-scale prototype built with low cost materials, always within safety limits, with the same layout and mass distribution of the designed airplane. For a careful execution of the flight tests, we have developed a pre-flight checklist.

Weight and balance			
-C.G. location in the desired range?			
Static test			
-Airplane lifted at MTOW from the tips w/o structural damage?			
Propulsion system			
Propeller and motor			
-Tighten?			
Wiring			
-Check the polarity			
-Fuse			
Radio transmitter and servos			
-The switch is in the "ON" position?			
-Servos are all linked and working?			
-Check the "FAIL SAFE MODE"			
Control surfaces	Flaperons	Tail	Rudder
-Linkages properly attached?			
Landing gear			
-Properly attached?			
Miscellaneous			
-Verify all components secured to the aircraft			

Table 7.3 Pre-flight check list

The flight test sessions have been carried out on February the 28th and scheduled as listed below:

Full throttle motor testing with the airplane hold motionless.

Low and high-speed taxi tests. These tests will demonstrate aircraft controllability on the ground.

Flights of both mission profiles with time acquisition of the single path segments.

The aim of these tests was to obtain a set of realistic times, together with the water filling time, useful to evaluate our final score and to compare with the calculated analytical values in the preliminary phase.

Flight with a sensor box on board able to record air speed, angle of attack, and heading. In order to accomplish this task, we have built a Pitot tube, a wind vane and purchased a digital compass module. Our university thanks to a thesis developed by two graduating students has provided all the electronics devices and software knowledge.



Electronic devices characteristics

Low pressure differential transducer Honeywell 163PCO1D75. It is an analogical sensor providing in output a tension that is proportional to the pressure difference measured by the pitot tube. It has a range of 0–5" of water, a maximum value of 5 V and an accuracy of 0.5%. By considering a cruise speed of 24 m/s (78.7 ft/s), the relative error is about 0.3 m/s (1 ft/s).

Rotative potentiometer (Vishay Spectrol). It is able to convert the angular rotation of the wind vane into an electric signal.

Compass module (TCM2 Compass Module, Navigation Precision). Through a serial interface it gives the heading value. The software that manages the serial communication with the embedded PC has been previously realized in the thesis studies.

The on board PC acquires and processes the different signals coming from these sensors; it consists of two PC/104 boards, a power supplier board, a CPU board linked via serial with the compass module, and an analogical acquisition board (Diamond Systems MM-32-AT).

A Simulink® model has been implemented to manage data acquired from sensors and to transmit them to a ground station by mean of a radio modem.

The sensor box has been placed in the tank compartment while the pitot tube and the wind vane were mounted under and out of the tip root of the right wing respectively.

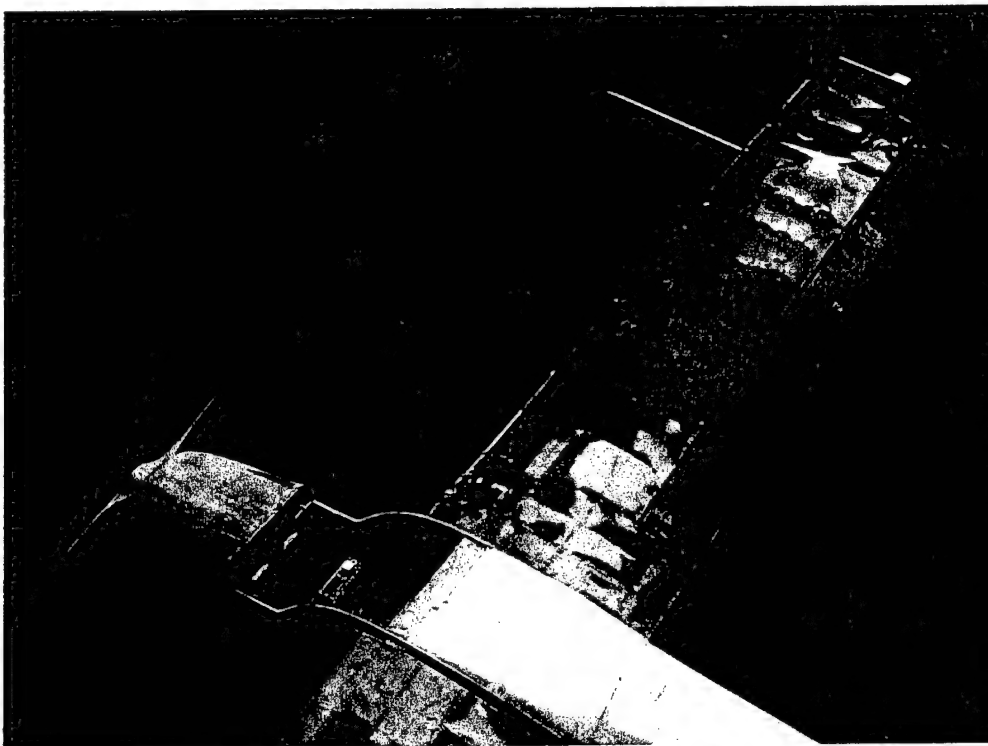


Figure 7.1 Prototype with sensor box, pitot tube and wind vane.

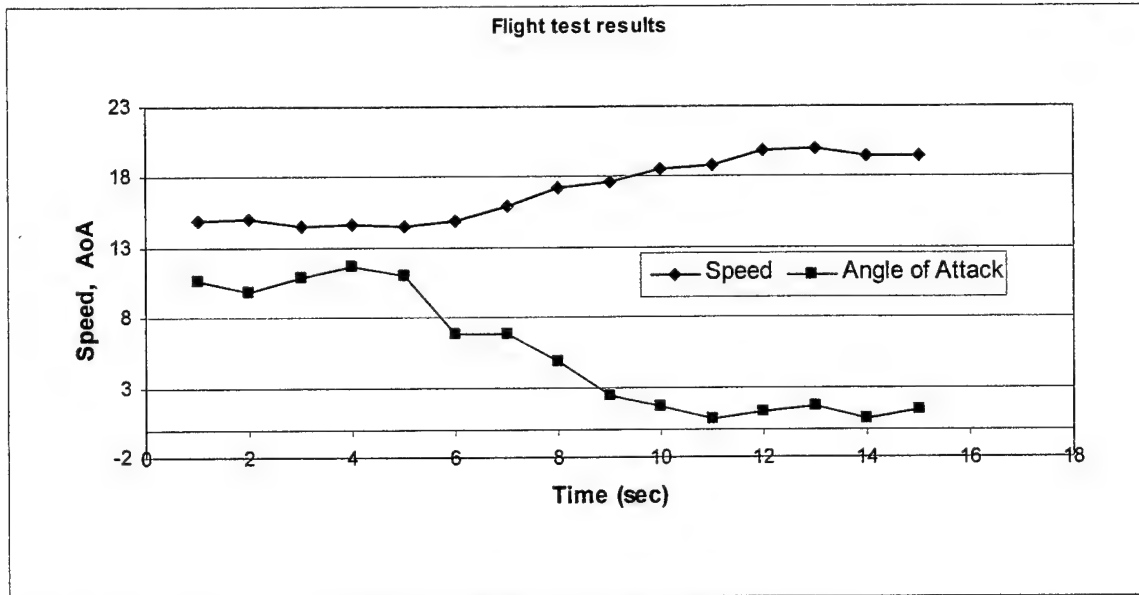


Figure 7.2 Results of the instrumented flight test

In the figure 7.2 are plotted data results from the pitot and the wind vane; they refer to a flight condition simulating the transition from a max C_L flight attitude to a cruise condition.



Figure 7.3 First flight

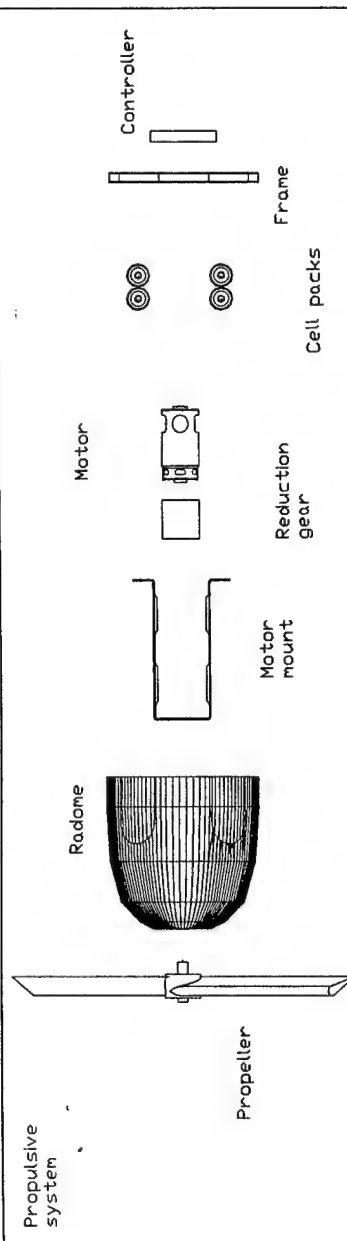
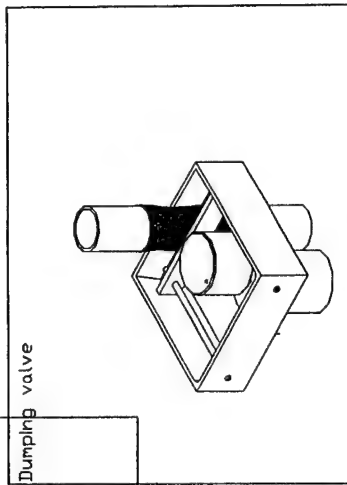
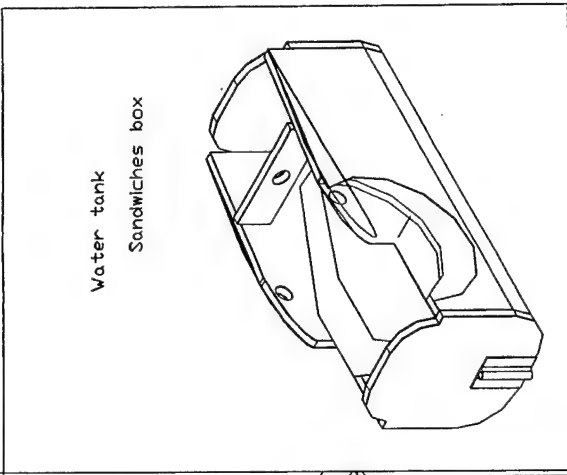
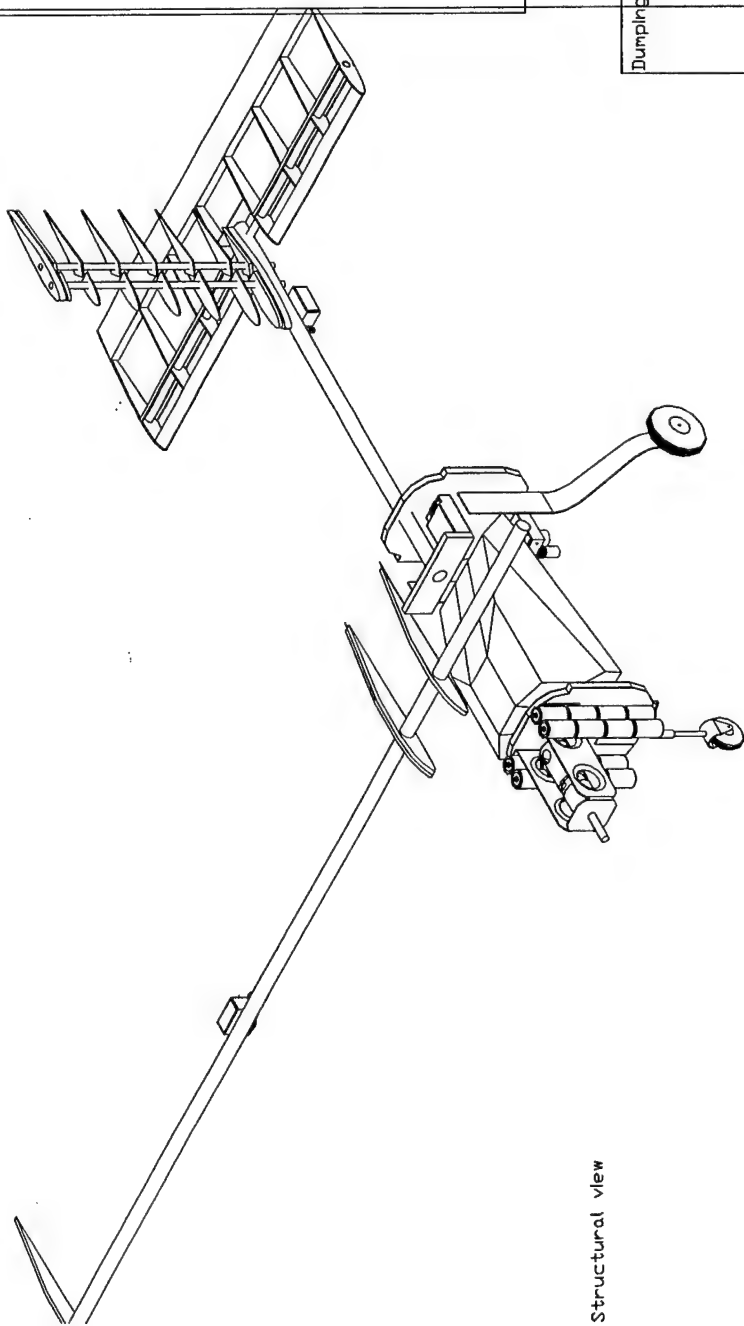


Table. 2	DBF competition 2004
31-1-04	The Flying centurions
	GALILEO V

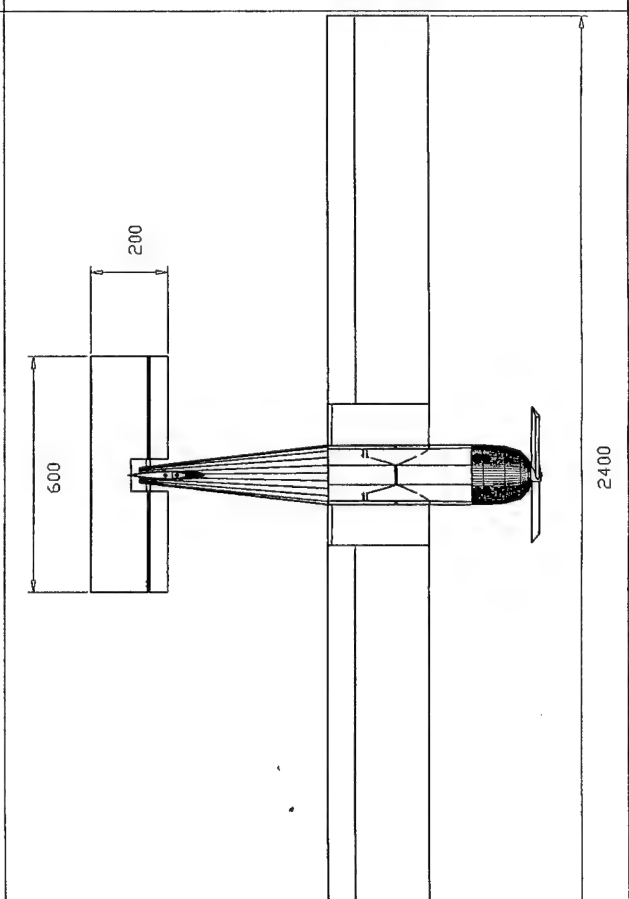
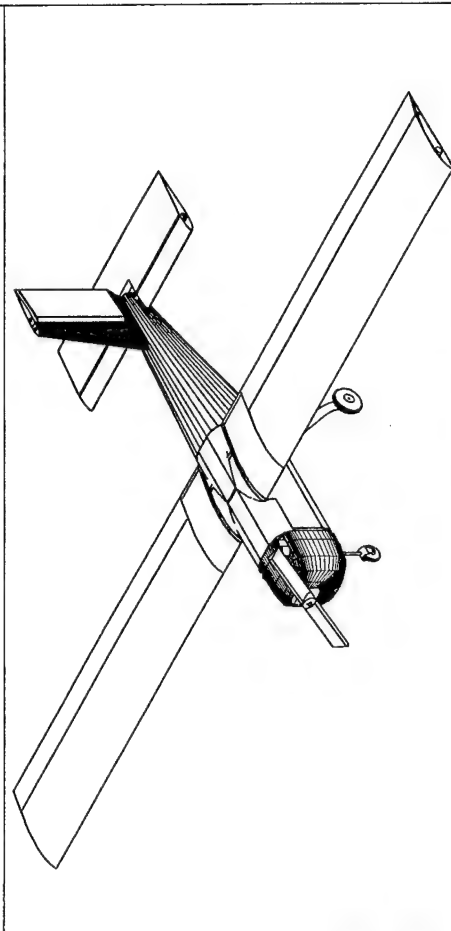
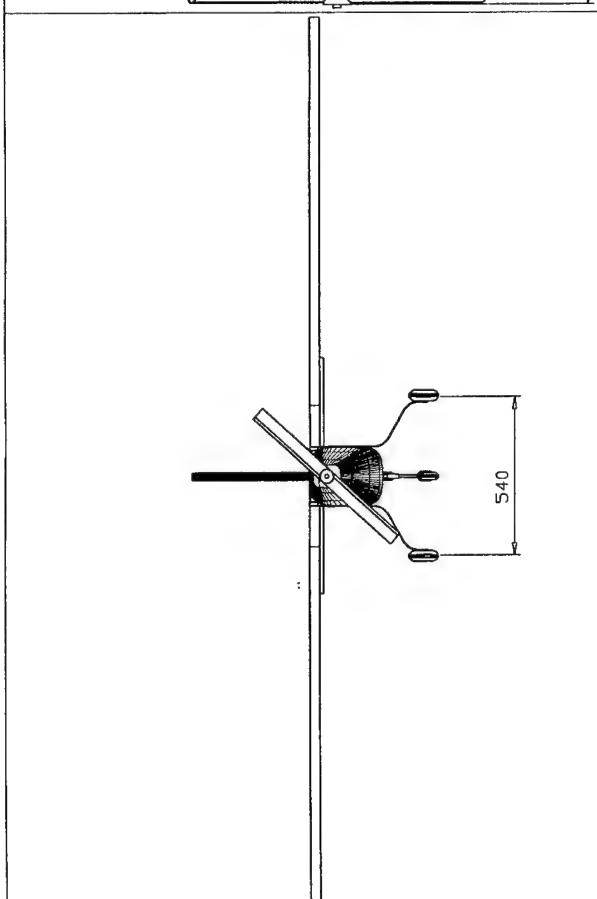
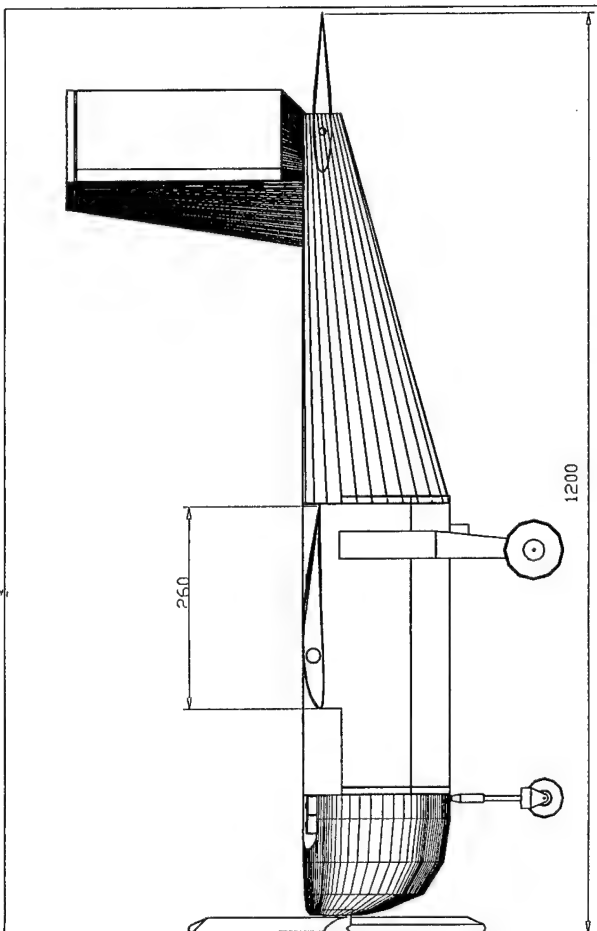
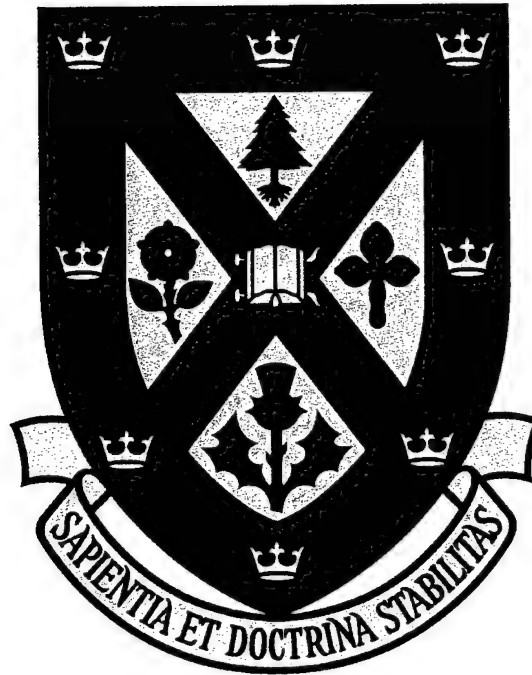


Table. 1	DBF competition 2004
31-1-04	The Flying centurions
GALILEO V	



2004 AIAA DBF Competition Design Report



Queen's University at Kingston "Squirt"

Department of Mechanical Engineering
Department of Engineering Physics

March 8, 2004

Table of Contents:

1.0	Executive Summary	1
2.0	Management Summary	3
2.1	Personnel and Organizational Structure	4
2.2	Scheduling	5
3.0	Conceptual Design	7
3.1	Examined Configurations	8
3.2	Design Screening	9
3.3	Aircraft Configuration	12
4.0	Preliminary Design	16
4.1	Aircraft Sizing	16
4.2	Take Off Gross Weight (TOGW) Estimation	17
4.3	Propulsion System Selection	17
4.4	Airfoil Selection and Wing Area	19
4.5	Wing Area	21
4.6	Aspect Ratio (AR)	22
4.7	Horizontal Stabilizer Sizing	22
4.8	Vertical Stabilizer Sizing	23
4.9	Fuselage Design and Sizing	24
4.11	Drag	27
4.12	Accelerated Stall Characteristics	29
4.13	Take-off Performance	29
4.14	Endurance and Range	31
4.15	Stability	32
4.16	Predicted Performance	33
5.0	Detailed Design	35
5.1	Weights	35
5.2	Payload Fraction	35
5.3	Wing Sizing and Performance	36
5.4	Tail Sizing and Performance	37
5.5	Propulsion	38
5.6	G-Loading	39
5.7	Control Systems	40
5.8	Aircraft Safety	41
5.9	RAC	42
6.0	Manufacturing Plan and Processes	46
6.1	Wing Construction	46
6.2	Fuselage Construction	47
6.3	Tail Construction	48
6.4	Figure of Merit	49
6.5	Evaluation and Selection	50
6.6	Description of Construction Techniques Employed	51
7.0	Testing Plan	56
7.1	Test Objectives	56
7.2	Ground Testing	56
7.3	Flight Testing	58
8.0	References	60

1.0 Executive Summary

The Queen's 2004 entry to AIAA's Cessna/ONR Design/Build/Fly (DBF) competition provides a return to the traditional roots of model aviation and to the strengths of its team members. Though a range of design alternatives were investigated and tested, the final competition aircraft features a very compact and extremely lightweight design with a minimal power system. With a wingspan of 1.22 m (48 in), overall length of 1.29 m (50 in) and an unloaded weight of 2.2 kg (5.1 lbs), "Squirt" will prove to be a very competitive aircraft in this year's competition. Building on the experiences gained during the last two competitions, both built-up and foam construction methods were employed to great success. Powered by only 10 cells, we are confident that Squirt will capture the overall title.

After a disastrous 2003 competition, a decision was made that more flight testing and design optimization was necessary in order to avoid the mistakes made in the past. To this end, design work was begun as soon as the rules were available. After careful review, it was discovered that the majority of the score during this year's competition is contributed by the Fire Fight task, with only approximately 10% contributed by the Ferry mission. Therefore, a design optimized to perform well in the Fire Fight task was deemed necessary in order to ensure a competitive aircraft.

With the aid of a spreadsheet, a comparison of a wide variety of aircraft configurations and sizes was completed. Design alternatives included, monoplanes, tandems, biplanes and flying wings with power systems ranging from 10 cells to 36 cells. Payload ability, expected flight times, and RAC were among the variables considered during this comparison. Based on the competition restraints and scoring, a small tandem design running a minimal battery pack was deemed the optimal configuration as no horizontal tail section is included in the RAC as the rear wing provides stabilizer functionality. The minimal size of the battery pack also helped to reduce the RAC substantially allowing this configuration to score well while only carrying 1 L of water per takeoff.

To this end, a fully functional tandem prototype named "Goliath" was designed, constructed and flown in early November. This prototype was 1.22 m (4') in length with two 0.91 m (36") wings. Goliath tipped the scales at 2.5 kg (5.5 lbs) and featured a power system nearly identical to that employed on Squirt. Though designed using the recommended geometrical factors as detailed in Lennon's Basics of R/C Aviation, the tandem design was found to be extremely unstable in pitch. Though a variety of modifications were made to Goliath throughout the numerous test flights, the configuration was eventually deemed unusable and that a more stable configuration would be needed in order to score well at the competition.

A second design spreadsheet was then produced which provided an increase in the weighting of the stability criterion. After this analysis, Squirt was born. A high-wing monoplane, Squirt was

designed at the same scale as Goliath; however, a lighter and more efficient power system was employed in order to reduce the overall weight of the aircraft while maintaining the level of performance. With a wing area of 0.40 m^2 (624 in^2) maximum takeoff weight was deemed to be 3.6 kg (8 lbs) which would allow Squirt to carry 1.5 L of water per takeoff. In order to provide predictable, stable performance, a conventional horizontal and vertical tail configuration was used. Due to Squirt's small overall dimensions, compliance with the flight box size constraint is easily ensured.

In order to minimize the weight of the airframe, multiple test wings and fuselages were constructed using built-up methods to determine the optimal configuration in terms of strength and weight. As Squirt will never perform a landing fully loaded with water, a minimal tricycle based landing gear system was employed. The optimal configuration resulted in an approximate 130.6 cm^2 (20.25 in^2) fuselage cross-section which provides the basis for a very low-drag airframe.

With a 12×8 APC electric propeller, Squirt is able to generate approximately 410 Watts (0.55 Hp) off of its 10 cell, 2400 mAh pack. An Astroflight FAI-15 motor running a $2.38:1$ gearbox is used in a tractor configuration to provide the necessary thrust. Fully loaded for takeoff, 17.0 N (59 oz.) of thrust are produced with a power loading of 108 Watts / kg (49 W / lb.) and a wing loading of 90 g/dec^2 (30 oz. / ft^2). With the Eppler 197 airfoil employed, this allows for a rapid takeoff without the need for flaps. At full throttle, the battery pack can provide 3.1 minutes of running life which is more than adequate for the predicted 2.5 minute maximum sortie time. Cruising speed is estimated at 26.7 m/s (60 mph) with a top speed of 29.1 m/s (65 mph) and an 11 m/s (23 mph) stall speed fully loaded. With no payload the stall speed reduces to 8 m/s (18 mph) while the power loading increases to 183 W / kg (83 W / lb.) with a wing loading of 553 g/dec^2 (18.8 oz. / ft^2). It should also be noted that during payload jettison, no reduction in flight speed will be necessary.

Having perfected the construction techniques used to produce Squirt and proven the power system during Goliath's campaign, the Queen's Aero Design team is confident that Squirt will prove to be the optimal design for this competition. Relying on a low RAC due to a minimal power system and compact geometry, Squirt should prove to be extremely competitive aircraft throughout the campaign.

2.0 Management Summary

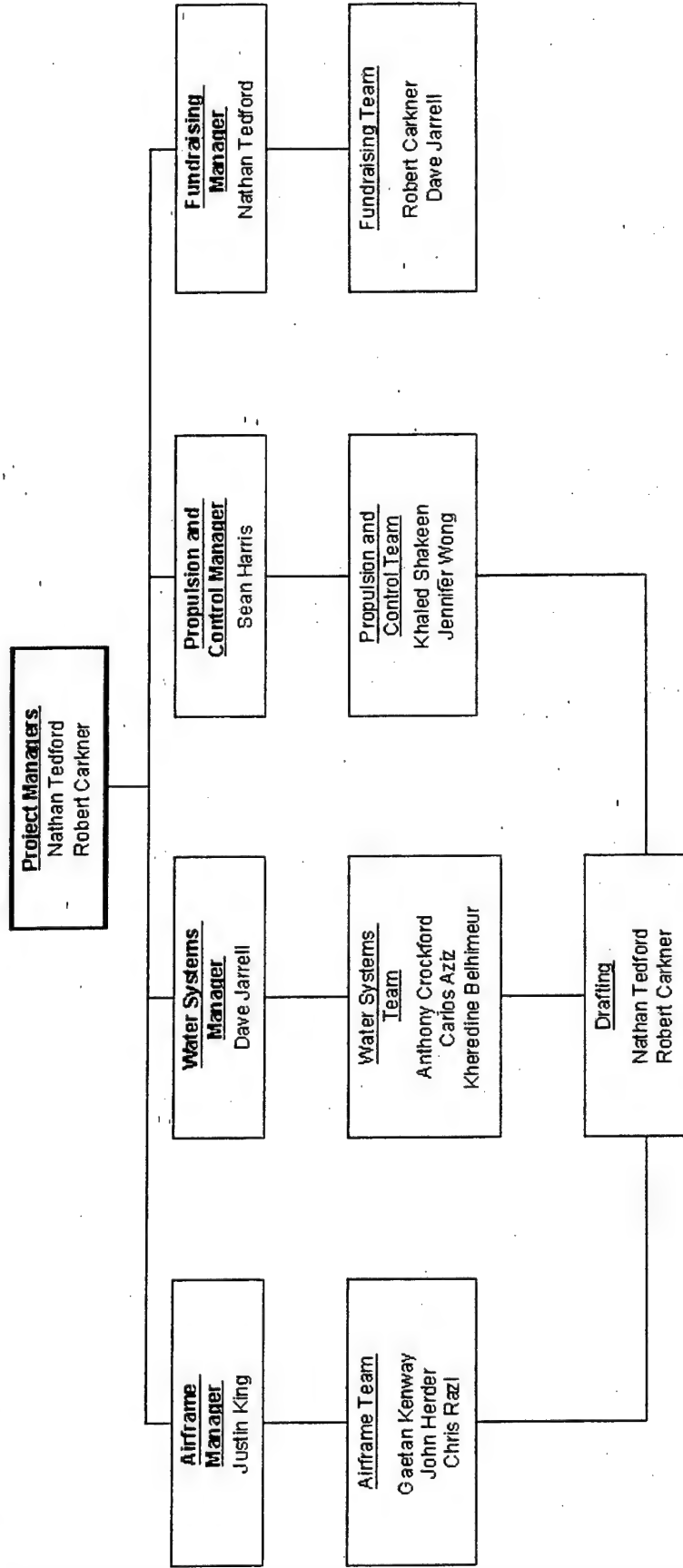


Figure 2.1 – Queen's Aero Design Team 2003-04 Organizational Structure

2.1 Personnel and Organizational Structure

During the initial design phases of the project, large group brainstorming sessions encompassing the entire team were used in order to generate a wide range of design alternatives and solutions to the problems and constraints imposed by the rules. During this time, the basics of aircraft design and operation as well as R/C modeling was taught to the younger members of the team in order to provide them with enough information to become active participants in the discussion. After arriving at a consensus regarding the aircraft design, the team was then split into a number of subgroups to more easily focus on particular areas of importance.

During the design phases for both Goliath and Squirt the organizational structure of the team was based upon a functional matrix model. Design tasks were divided up to fall into one of three subgroups with fundraising and finance added as a fourth group. All team members were expected to be members of at least two of the subgroups. By exposing all members of the team to multiple aspects of the project, each individual member becomes more knowledgeable which leads to increased efficiency during construction. Figure 2.1 shown above provides a visual breakdown of the team's subgroup structure. Note that in the interests of clarity, only the primary subgroup of each member is shown.

The three design subgroups were tasked with the research, development and design of one of the major systems of the aircraft. The fundraising group was responsible for approaching outside companies to secure monetary donations, product discounts, and access to tooling. Rough sketches of each subgroup's efforts were submitted to the drafting team who were responsible for drafting the working drawings of the aircraft into AutoCAD or Solid Edge as required.

During the initial phases of the project, full team meetings were held at two week intervals. The purpose of these meetings was to assemble all the subgroups in one location, facilitating systems integration. Each subgroup leader was expected to give a report on their progress and any problems encountered. Effort was made to ensure that viable solutions to each problem encountered were generated in order to allow the subgroup to continue with design during the following week. These meetings also provided a means of communication between the subgroups and that each component would interface properly with the completed airframe.

Separate from these full team meetings, subgroups were expected to hold design sessions at least once a week. These sessions were scheduled by the respective subgroup manager to ensure that there were no conflicts with any of the subgroup members. One of the project managers would attend these meetings to ensure that component design was progressing in the proper direction. However, it should be noted that the project managers functioned as team members at these meetings, and were not responsible for leading the discussion or design. It

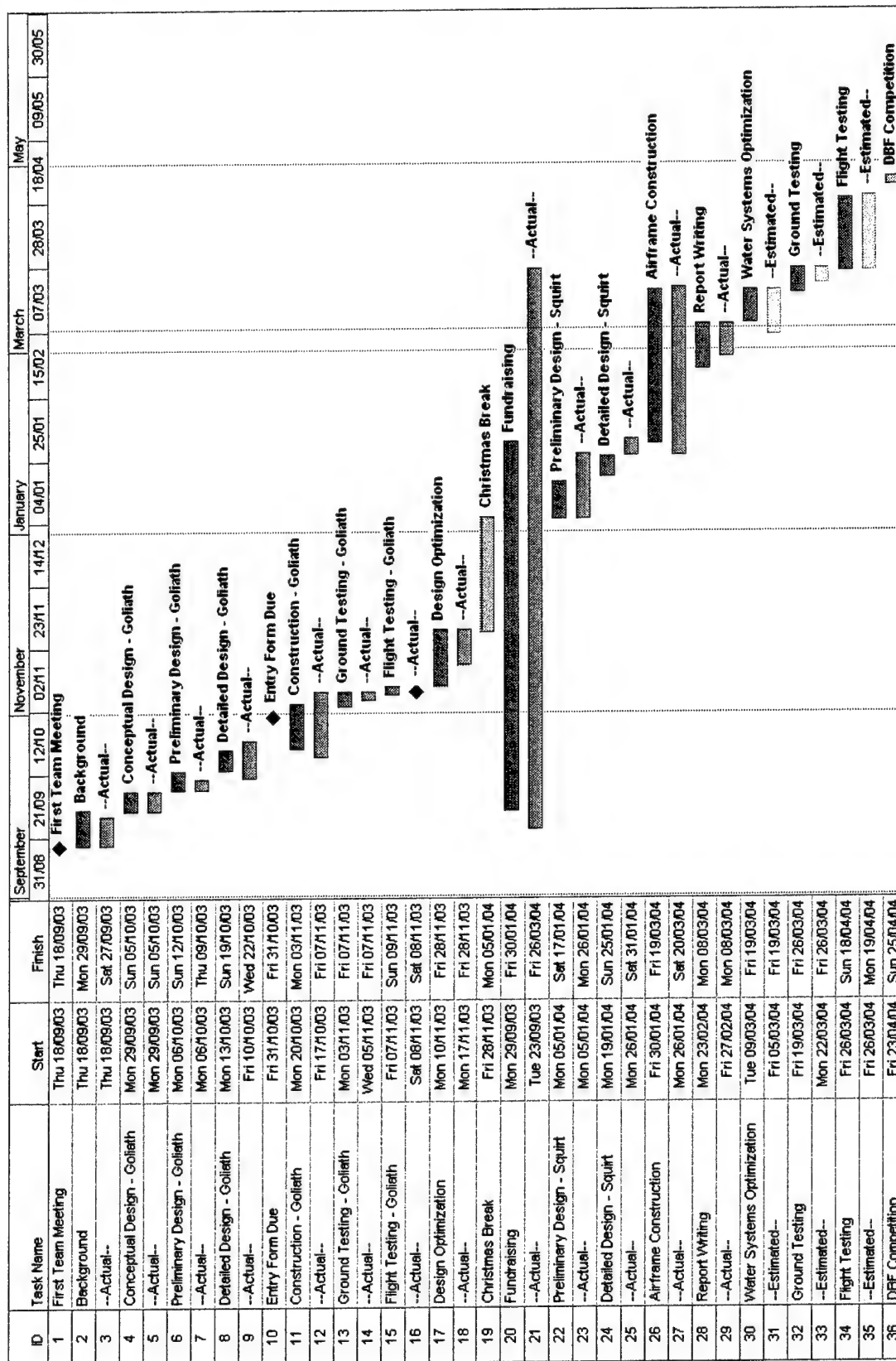
was felt that the final aircraft configuration would benefit by leaving the younger students in charge of the various components, as this would ensure that everyone on the team had a chance to be an active participant in the design process. This process also helped develop some innovative ideas and designs that may not have been conceived of by the veteran members due to varying perspectives. By ensuring that everyone was involved with the design process, the construction of the competition aircraft could be completed in the most efficient manner possible.

After the design of each system had been finalized, the subgroups were disbanded to allow for the construction phase of the project. Shop hours were set by the project managers, with a schedule being given to each member of the team. This allowed individual team members to work around their own schedules and decide when they would be able to devote time to construction. A senior member of the team was present at each building session to help guide the effort and to teach the newer members the construction techniques required. This system ensured that every team member, regardless of prior building experience, was able to contribute to the final assembly of the aircraft.

2.2 Scheduling

To ensure that the project would be completed before the date of the actual competition, a timeline was produced during the team's second general meeting. Based on our veteran member's previous experience in the Design/Build/Fly Competition, the project managers were able to make reasonable assumptions as to the length of time required to complete each stage of the project. As can be seen in the Gantt chart below, most estimates were very close to the actual completion time. Figure 2.2 shows the Gantt chart generated during this meeting and actual completion times of items to date. It should be noted that during the construction of the timeline, slack was included in the projecting deadlines in an effort to prepare for unaccounted difficulties that may occur.

Figure 2.2 – Gantt Chart of 2003 / 2004 Scheduling



3.0 Conceptual Design

The 2004 DBF competition provides two separate mission tasks that must be accomplished by the same aircraft. The "Fire Fight" mission involves heavy lifting and slow flight while the "Ferry" mission involves unloaded high speed flight. These missions have difficulty factors (DF) of 2 and 1 attached to them respectively. The aircraft's total flight score is the sum of the individual flight scores from each mission task. Single flight scores (SFS) can be calculated as follows:

$$\text{Fire Fight SFS} = \frac{2 * (\text{Lbs } H_2O)}{\text{Mission Time}}$$

$$\text{Ferry SFS} = \frac{1}{\text{Mission Time}}$$

Two final factors are then applied to the total flight score in order to calculate a team's final score.

$$\text{Final Score} = \frac{\text{Report Score} * \text{Total Flight Score}}{\text{Rated Aircraft Cost}}$$

Though the report score provides an important scaling factor in the final score calculation, it can largely be ignored during the design of the aircraft. The Rated Aircraft Cost (RAC) cannot. The RAC provides an estimate of the cost of the aircraft based on airframe geometry, weight, battery power, and motor configuration. Therefore, the RAC will vary greatly dependant on the final configuration of the aircraft. A simplified representation of the RAC calculation is:

$$\text{Rated Aircraft Cost, \$ (Thousands)} = (\$300 * MEW + \$1500 * REP + \$20 * MFHR) / 1000$$

Where *MEW* is the Manufacturer's Empty Weight, *REP* is the Rated Engine Power and *MFHR* is the Manufacturing Man Hours estimate. These factors are calculated separately in a later section.

Through the use of an excel spreadsheet, it was discovered early on that no matter the amount of water carried (down to 1/2 liter) the Fire Fight mission provides a much higher percentage of the final flight score than the Ferry mission (assuming similar flight times). This result shows that in order to be competitive at this year's competition, an aircraft must be designed to excel at the Fire Fight mission. It is assumed that any aircraft capable of performing well during the Fire Fight will perform acceptably during the Ferry mission provided enough battery power is available to ensure that it can be completed successfully.

In addition to completing these two missions successfully, the aircraft must also fit (disassembled) into a flight box which is no larger than 48" x 24" x 12". Finally, the aircraft must be capable of taking off with a ground run of less than 150'.

3.1 Examined Configurations

Having determined that an aircraft capable of high-performance during the Fire Fight mission is necessary, a number of possible aircraft configurations were examined in order to determine the optimal design for this task. Brief descriptions of each design follow below.

Flying Wing

A flying wing could be built that would utilize an oversized center section to house the internal water tank. As no tail would be present, an airfoil with a low pitching moment and reflexed trailing edge would be required. An issue that may arise with this configuration is its ability to disassemble and fit into the flight box. Large joints along wing surfaces are typically draggy and quite heavy. The stability of this configuration is also an issue based historical competition results.

Blended Wing

Similar to the flying wing configuration described above, a blended wing configuration would utilize a conventional tail in place of the reflexed airfoil. This allows the main body of the aircraft to decrease in length and also allows a conventional airfoil to be employed. As with the flying wing configuration, issues relating to the fit of the blended wing into the flight box can also be raised.

Biplane

By utilizing a conventional fuselage and tail configuration, the biplane would be the easiest to construct of the designs mentioned thus far. By using two separate wings the total wing area is split which allows a smaller overall wingspan to be used. A potential drawback related to past experiences with biplanes is that the two wings must be mounted extremely accurately to avoid flight instability.

Monoplane

A monoplane resolves the instability issues raised by the biplane configuration, but boasts a larger wingspan and chord which may present difficulty during storage in the flight box. Overall this design is the most stable and predictable of the group.

Canard

By exchanging the aft-tail configuration for a canard, savings can be realized in the RAC as no horizontal tail is present. As with the biplane, splitting the required lift over two surfaces allows the overall geometry of the aircraft to be reduced facilitating fit into the flight box. A disadvantage of this canard configuration is that unlike aft-tail designs, canards are very sensitive to the sizing of their foreplane. Therefore much testing and calculation would be required in order to produce an aircraft stable enough for competition use. Very accurate wing mounting techniques would be necessary as the relative AoA between the foreplane and main wing is also paramount to flight stability.

Tandem

Similar to the canard design, the tandem splits the required lift between two separate wing platforms. However, unlike the canard, the foreplane in this case is equal in span to the main wing (as in a biplane), further decreasing the span of the main wing platform. As the foreplane span is fixed, it reduces the sensitivity of the design on foreplane sizing which provides increased stability over the canard configuration. A lower RAC is also realized as the main wing provides horizontal tail functionality. Very accurate wing mounting techniques would be necessary as the relative AoA between the foreplane and main wing is paramount to flight stability.

3.2 Design Screening

3.2.1 FOM Criteria

Having investigated the above designs, a Figure of Merit (FOM) was developed in order to facilitate the selection of the ideal configuration. The following FOM criteria were used in assessing the viability of each design.

Stability (S)

If an aircraft is difficult to control in the air, it is unlikely that a high flight score can be realized. As past experiences have shown Kansas to have high, unpredictable winds, a plane with predictable responses will greatly aid the pilot. As this is an important criterion but does not directly affect the aircraft's final score, a weighing factor of 2 was applied.

Ease of Manufacture (EOM)

The greatest design in the world is of no use to anyone if it is impossible to manufacture. An aircraft that is easy to manufacture allows more time for testing and design optimization studies to be performed which usually results in a more efficient design when compared to a complex aircraft. However, as no flight testing can be accomplished over the winter months due to inclement weather, it was assumed that the necessary expertise could be developed during the year to build any design accurately. Therefore, this criterion was assigned a weighting factor of 1.

Flight Performance (FP)

This criterion refers to the performance of the aircraft as related to the Fire Fight task. It includes the estimated amount of water carried and time of flight for each configuration. As this directly affects our final score, the flight performance criterion was assigned a weighting factor of 4. It should be stated that each configuration was given the same ranking in the FOM comparison shown in Table 3.1. This is due to the assumption that given adequate time, each configuration could essentially produce similar flight times and possess similar cargo capacities resulting in identical Fire Fight flight scores.

Geometry (GEO)

The geometry of the each configuration is extremely important as it determines the number of "pieces" and aircraft must possess to fit inside the flight box. A large or awkward geometry may require multiple joints and attachment points which would increase the overall structural weight and complexity. As the geometry of the plane does not affect the final score but is an important constraint imposed by the rules, a weighting of 3 was assigned to this criterion.

Weight (WT)

The overall weight of the airframe affects the final score in two distinct ways. Firstly, the RAC is directly proportional to the empty weight of the aircraft via the *MEW* variable. Therefore, decreasing the weight of the airframe decreases the RAC which provides an increase in overall score. Secondly, by minimizing the weight of the airframe for a given wing area, more water can be carried by the aircraft which provides a higher overall flight score in the Fire Fight mission. As this criterion affects the overall score in two distinct manners, it was assigned a weighting factor of 5.

RAC

The Rated Aircraft Cost (RAC) of the final aircraft provides a final scaling factor in determining our final score. As the flight score is divided by the RAC, so to was the sum total of all other factors divided by the RAC in this comparison (See Section 3.2.2 for clarification if needed). Due to this special treatment of the RAC criterion, no additional weighting factor was applied. The preliminary RAC calculation for the six configurations can be viewed in Table 3.4 which is presented at the end of this section.

3.2.2 FOM Comparison

Having outlined the various FOM criteria and their assigned numerical weightings, rankings between 1 and 5 were assigned to each configuration based on each criterion. Larger rankings indicate more preferred options. Total scores were based on the following calculation:

$$Total = (2 S + EOM + 4 FP + 3 GEO + 5 WT) / RAC$$

Table 3.1 – FOM for Design Screening

Aircraft Concept	S (2)	EOM (1)	FP (4)	GEO (3)	WT (5)	RAC (*)	Total
Flying Wing	2	3	3	2	4	7.3	6.16
Blended Wing	3	3	3	1	3	7.9	4.94
Biplane	4	4	3	4	5	6.4	9.53
Monoplane	5	5	3	3	5	5.7	10.70
Canard	4	3	3	4	5	5.8	10.34
Tandem	4	3	3	5	5	5.6	11.25

Based on the FOM, it can be seen that the optimal configuration proves to be a tandem design. To that end, a prototype tandem aircraft (Goliath) was designed and built throughout September and October with ground and flight testing occurring in early November. During flight testing, it was discovered that Goliath was unstable in pitch and after numerous attempts to correct the problem; the design was considered a failure and scrapped. This lead the team back to the conceptual design phase of the project once more.

Though the tandem design was a failure, much valuable information was learned from Goliath and a second FOM was constructed to evaluate the design alternatives left to the team. In every sense this FOM was identical to the one shown in Table 3.1 except that the stability criterion was assigned a weighting of 5. It was decided that the plane must survive flying the course in order to post a score, and therefore stability is perhaps the most important criterion of the six listed. Table

3.2 shows this new FOM with the adjusted rating and rankings for the stability criterion. All other weightings and all rankings remain unchanged.

Table 3.2 – FOM for Second Design Screening

Aircraft Concept	S (5)	EOM (1)	FP (4)	GEO (3)	WT (5)	RAC (*)	Total
Flying Wing	2	3	3	2	4	7.3	6.99
Blended Wing	3	3	3	1	3	7.9	6.08
Biplane	4	4	3	4	5	6.4	11.41
Monoplane	5	5	3	3	5	5.7	13.33
Canard	3	3	3	4	5	5.8	11.55
Tandem	3	3	3	5	5	5.6	12.5

Therefore, with the adjusted stability weighting and rankings, a conventional monoplane design was now shown to be the optimal configuration for this year's DBF competition.

3.3 Aircraft Configuration

3.3.1 Component Configuration

Having decided on a monoplane configuration, further FOM's were used in order to determine the layout of the aircraft. Specific items addressed by this FOM are listed below.

Wing Positioning

Possible wing configurations for a single monoplane are either at the high, mid, or low sections of the fuselage. A high-wing design provides good stability and does not interfere with the water dump, but may interfere with water loading. A mid-wing design provides the best drag profile of the three, but largely interferes with the cargo bay. A low-wing configuration allows an unobstructed cargo bay and easy loading, but may interfere with the water dump mechanism. It is also the least stable configuration of the three.

Tail Configuration

Possible tail configurations investigated were the V-tail, T-Tail, or conventional tail layouts. A V-tail system is very lightweight as it requires only two surfaces. However, it has been known to exhibit control problems during violent flight maneuvers. A conventional tail configuration is also very light, but requires slightly more tail area due to the positioning of the horizontal stabilizer in the wing's downwash. While a T-tail configuration is the most efficient of the three designs, it is also typically much heavier than the other layouts.

Undercarriage Configuration

For the undercarriage of our aircraft, tricycle, bicycle and tail-dragger configurations were examined. A tricycle gear provides the best ground handling and stability of the three, but produces the highest drag. A tail-dragger design has slightly lower drag than the tricycle setup, but has mediocre ground handling characteristics, especially in a strong crosswind. A bicycle gear provides the lowest drag of the three configurations, but at the loss of ground stability and handling.

Engine Number

Though the competition limits the aircraft to the use of electric brushed motors from either Astroflight or Graupner, the number of engines can be varied. A single engine provides the most efficient solution from a systems standpoint, however the cost of large engines are prohibitive and the overall weight of a larger engine may be more than the combined weights of two or more smaller motors. Multiple engine solutions are typically less stable and more difficult to set up than single engine solutions. Any weight savings from a multi-engine setup are also typically offset by the weight of the motor pylons.

Engine Configuration

Both tractor and pusher configurations were examined for suitability on our aircraft. A tractor configuration provides the most stable configuration and places weight forward of the wing which helps to counterbalance the tail. A pusher configuration would need to be placed aft of the cargo bay to avoid interference with the water tank. Therefore, it is likely that ballast would be needed to counterbalance the weight of the engine and the tail behind the wing's center of lift.

3.3.2 FOM Component Comparison

Having outlined the various component configurations above, the same FOM criteria as detailed in Section 3.2 were used to compare the designs with the exception of the geometry (GEO) factor and RAC. As each layout will not affect the fit of the aircraft in the flight box to any significant degree, including the geometry factor would not provide any useful information. Similarly, though slight changes in the RAC occur due to changes in the tail configuration, the overall impact of the tail configuration on the RAC is not significant enough to include it in this analysis.

Table 3.3 – FOM for Alternate Configuration Comparison

		S (5)	EOM (1)	FP (4)	WT (5)	Total
Wing Position	High	5	5	4	5	71
	Mid	4	3	5	4	63
	Low	3	5	4	5	61
Tail Configuration	V-Tail	3	4	4	5	60
	Conventional	5	5	3	5	67
	T-Tail	5	3	5	3	63
Undercarriage Configuration	Tricycle	5	5	3	5	67
	Bicycle	3	3	5	5	63
	Tail-Dragger	4	4	4	5	65
Engine Number	Single	5	5	5	5	75
	Multiple	4	4	4	5	65
Engine Configuration	Tractor	5	5	5	5	75
	Pusher	4	4	5	5	69

Therefore, based on the above FOM, this year's entry to the DBF competition will consist of a high-wing monoplane configuration with a conventional tail design. The undercarriage will feature a tricycle gear configuration while a single engine in a tractor configuration will be used to provide the necessary thrust. This configuration coupled with the experience gained during the construction and testing of Goliath will allow the production of a very stable aircraft capable of performing exceedingly well at both the Fire Fight and Ferry missions.

Figure 3.4 – Conceptual Design RAC Comparison

		Flying Wing	Blended Wing	Biplane	Monoplane	Canard	Tandem
A	Empty Weight Multiplier	300	300	300	300	300	300
B	Rated Engine Power Multiplier	1500	1500	1500	1500	1500	1500
C	Manufacturing Cost Multiplier	20	20	20	20	20	20
MEW	Empty Weight (lbs)	6	6.25	5.5	5	5.5	5.5
REP	Engine Power	1.5	1.5	1.5	1.5	1.5	1.5
	Battery Weight (lb)	1.5	1.5	1.5	1.5	1.5	1.5
	Number of Motors	1	1	1	1	1	1
MFHR	Manufacturing Man Hours	161.65	187.8	125	98.6	95.6	83.6
	1.0 Wings	130	90	40	50	52	40
	Number of Wings	1	1	2	1	2	2
	Wing span (ft)	4	4	3	4	3.5	3
	Wing Chord (ft)	3	2	0.5	1	0.6	0.5
	# ailerons	2	2	2	2	2	2
	# flaperons	0	0	0	0	0	0
	# ailerons + flaps	0	0	0	0	0	0
	# ailerons + spoilers	0	0	0	0	0	0
	# ailerons + flaps + spoilers	0	0	0	0	0	0
	2.0 Fuselage	16.65	52.8	25	3.6	3.6	3.6
	Body length (ft)	3.33	5	5	2	2	2
	Width (ft)	0.5	0.66	0.5	0.3	0.3	0.3
	Height (ft)	0.5	0.8	0.5	0.3	0.3	0.3
	3.0 Empennage	0	20	20	20	10	10
	# vertical surfaces	0	0	0	0	0	0
	# vertical surfaces with Control	0	1	1	1	1	1
	# horizontal surfaces	0	1	1	1	0	0
	4.0 Flight System	15	25	40	25	30	30
	# servos or motor controllers	3	5	8	5	6	6
RAC:		7283	7881	6400	5722	5812	5572

4.0 Preliminary Design

4.1 Aircraft Sizing

As a first set to achieving the maximum final score possible, the overall geometry of the aircraft was first optimized. As the final score is dependant on both the flight score and the RAC of the aircraft, an optimum flight score / RAC combination must exist. To this end, four separate aircraft geometries were proposed in order to investigate the effect of increasing and decreasing the amount of water carried per takeoff. Table 4.1 provides a brief overview of the battery pack weight and water carried per takeoff of each configuration.

Table 4.1 – General Aircraft Specification – Sizing Investigation

Aircraft	Battery Pack Weight (lbs.)	Water Carried per Takeoff (Liters)
1	5	4
2	2.87	2
3	1.42	1
4	1.42	1.5

In order to calculate the final flight score, the RAC of the proposed aircraft geometries were estimated. This estimation can be found in Table 4.2 below.

Table 4.2 – Aircraft RAC – Sizing Investigation

		Aircraft			
		1	2	3	4
MEW	Empty Weight Multiplier (A)	300	300	300	300
	Estimated Empty Weight (lbs)	14	9	5	5
	MEW Total:	4200	2700	1500	1500
REP	Rated Engine Power Multiplier (B)	1500	1500	1500	1500
	Battery Weight (lb)	5	2.87	1.42	1.42
	Number of Motors	1	1	1	1
	REP Total:	7500	4305	2130	2130
MFHR	Manufacturing Cost Multiplier (C)	20	20	20	20
	Number of Wings	1	1	1	1
	Wing span (ft)	8	8	4	4
	Wing Chord (ft)	1	0.8	0.66	1.1
	# ailerons	2	2	2	2
	# flaperons	0	0	0	0
	# ailerons + flaps	0	0	0	0

# ailerons + spoilers	0	0	0	0
# ailerons + flaps + spoilers	0	0	0	0
1.0 Wings - Total	85	69	31.4	49
Body length (ft)	7	6	4	4
Width (ft)	0.66	0.5	0.41	0.41
Height (ft)	0.8	0.5	0.41	0.41
2.0 Fuselage - Total	74	30	13	13
# vertical surfaces	0	0	0	0
# vertical surfaces with Control	1	1	1	1
# horizontal surfaces	1	1	1	1
3.0 Empennage - Total	20	20	20	20
# servos or motor controllers	7	7	6	6
4.0 Flight System - Total	35	35	30	30
MFHR - Total:	4278	3080	1897	2249
RAC:				
	15978	10085	5527	5879

From Table 4.3, it can be seen that the optimal aircraft geometry is that of aircraft 4. Though similar to aircraft 3, by increasing the wing area more water can be carried, which drastically increases the total score. Based on this analysis, Squirt was designed to have a 48" wing span with a low aspect ratio to increase available wing area. A minimal battery pack of between 10 – 16 cells will be used and will allow the aircraft to carry approximately 1.5 L of water per takeoff.

4.2 Take Off Gross Weight (TOGW) Estimation

With the overall geometry of the aircraft set, an accurate estimate of the gross weight of the aircraft could now be performed. Fortunately, the construction of Goliath provided the team with an accurate blueprint regarding the airframe weight of an aircraft this size. Furthermore, almost all systems used on Goliath were recycled for use on Squirt. These systems include the battery pack, motor, speed controller, receiver, receiver pack and servos, and all landing gear. Therefore the final estimate of the empty airframe weight of this year's aircraft was 2.27 kg (5 lbs) including the 10-cell battery pack. Adding the estimated payload of 1.5 L (1.5 kg / 3.3 lbs) of water, a final **TOGW of 3.77 kg (8.3 lbs)** was calculated.

4.3 Propulsion System Selection

4.3.1 Motor Configuration

As stated by the 2004 DBF Competition Rules, only brushed electric motors from the Graupner or Astroflight may be used in this competition. In addition, a fuse must be present in the circuit to limit the continuous current supplied to the motor to 40 amperes or less.

Before a specific motor could be chosen, an estimate of the power required by the motor was conducted. For a smooth surfaced runway, between 40 and 50 Watts / lb. is recommended for takeoff¹. Using 50 Watts / lb. (110 W / kg) as a guideline, approximately 400 Watts of power will be required from the motor system during takeoff.

Criteria used in the motor comparison were weight, motor efficiency, cost, and availability. In addition to current motor offerings from both manufacturers, electric flight message boards were used to find older motor models that had been phased out. After a thorough survey of equipment, four motor / gearbox combinations were chosen that suited the required application: An Astroflight Cobalt-15 with a 3.69:1 Superbox, an Astroflight FAI-15 with a 2:38:1 Hex Gearbox, a Graupner 1300-7 with a 2:1 Power Gear Gearbox, and a Graupner 1300-9 with a 2:1 Power Gear Gearbox.

As initially these motors were being compared for use on the Goliath, the availability and cost criterion were brought to the forefront as the team had not completed fundraising at this time. However, acquisitions of a variety of slightly used Astroflight and Graupner motors had been made by the team throughout the summer in anticipation of the competition. These motors had been advertised for sale on electric flight boards and were acquired from individuals performing brushless conversions. Given the tight timeline for the construction and testing of Goliath and the team's financial situation, it was decided one of the team's existing motors would be employed. This narrowed the selection to between an AstroFlight Cobalt-15, AstroFlight FAI-15 and Graupner 900-8. Due to the insufficient continuous power rating of the 900-8, it was discarded from further consideration.

ElectriCalc, a commercial software package, was then used to compare the two motor / gearbox combinations with different propeller and cell selections. In this manner, detailed information regarding each motor's optimal efficiency, thrust, propeller pitch speed, duration and current draw was tabulated. During this comparison it was found that the FAI-15 performed ideally with a 10 cell, 2400 mAh pack whereas the Cobalt-15 required 16 cells at 1700 mAh. Though the performance of both systems was essentially identical, the FAI-15 system was found to be 85 g (3 oz) lighter. Thus, the FAI-15 motor with a 2.38:1 hex gearbox will propel Squirt on its way to victory.

4.3.2 Battery Selection

The power output of a battery pack is defined as $P = I V$. As the maximum allowable current is restricted to 40 A, a 10 V pack is required to provide the necessary 400 Watts to the motor during takeoff (assuming 100% efficiency). Given that standard NiCad cells typically experience voltage depression under load, a minimum no-load pack voltage of 12 V was selected. At 1.2 Volts per cell, this 12 Volt criterion translates to a **10-cell battery pack**.

With the number of cells now finalized, the capacity of the cells was determined based on expected flight times. As each sortie will require approximately 3 minutes of flight at full throttle, the necessary capacity can be calculated as follows:

$$\text{Capacity} = \text{Flight Time (min.)} * \text{Current Draw (A)} / 60$$

$$\text{Capacity} = 2 \text{ Ah}$$

Therefore, a minimum cell capacity of 2000 mAh is necessary to provide at least 3 minutes of flight at full throttle. From a survey of available NiCad cells, 2400 mAh cells provided the closest match to this requirement while still providing adequate flight time. For our particular application, **Sanyo CP-2400SCR** Sub-C cells with a 4.5 mΩ internal impedance will be used. These cells are readily available at a low cost and provide both high power density and low internal impedance.

4.3.3 Propeller and Gearing Selection

In order to configure an aircraft for optimal flight, the thrust and pitch speed produced by a propeller must be balanced. Typically, recommended pitch speeds for electric aircraft are between 3 and 4 times the stall speed of the aircraft. Approximately values for the loaded and unloaded stall speeds of Squirt are 10.9 m/s (23.1 mph) and 8.3 m/s (17.6 mph) respectively. Combining these two stall speeds with the pitch speed recommendation gives an ideal pitch speed range of between 26.7 m/s (60 mph) and 28.4 m/s (64 mph). Therefore, in order to produce the minimum acceptable loading on the power system, an initial pitch speed of 26.7 m/s (60 mph) was chosen.

Using the ElectriCalc modeling software, the selected cell, motor, gearbox and propeller pitch information was input in order to determine an appropriate propeller diameter. With a predicted current draw of 42 amperes at full throttle, a 12" diameter propeller best satisfies the system requirements. At full throttle, this 12" x 8" propeller produces **17.0 N (3.8 lbf)** of static thrust with a pitch speed of **26.2 m/s (59 mph)**. This provides the aircraft with a thrust to weight ratio of approximately 1:2 while fully loaded.

4.4 Airfoil Selection and Wing Area

4.4.1 Airfoil Selection Criteria

As this year's entry is based around having a highly stable flying configuration, an airfoil with gentle stall characteristics was considered a necessity. Other desirable characteristics were generated and a FOM used to determine the most suitable airfoil. Criteria used for the evaluation are detailed below.

Stall Characteristics

Stall characteristics of an airfoil typically dictate the reaction time available to a pilot after an unexpected occurrence such as a sudden wind gust or temporary loss of control. Airfoils with gentle stall characteristics allow the pilot more time with which to correct the error, hopefully negating a catastrophe. As last year's entry crashed due to the poor stall characteristics of its airfoil this criterion was assigned a weighting of 5.

Maximum C_L

As the maximum allotted takeoff distance is specified to be 45.7 m (150'), the maximum C_L of an airfoil becomes very important. In addition to decreasing the takeoff distance of the aircraft, a higher C_L reduces the amount of power required during climb-out. Due to the fact that if the aircraft cannot takeoff before the aforementioned 150' no score can be registered, this criterion was assigned a weighting factor of 5.

Induced C_D at Expected Cruise AoA

Due to the minimal nature of this year's planned power system, battery power will be at a premium at all times throughout the competition. Therefore, an airfoil with a low induced drag at cruise allows the aircraft to conserve power during most phases of the circuit. Though important in an overall sense, the induced drag of the airfoil is not expected to vastly impact mission performance and as such is assigned a weighting of 2.

Pitching Moment (C_M)

Airfoils that provide a high C_L typically have higher pitching moments than symmetrical or flat-bottomed airfoils. This increased pitching moment requires a larger tail surface to counteract, which increases the induced drag of the aircraft. As increasing the size of the tail surface adversely affects the RAC, this criterion was assigned a weighting of 3.

Ease of Manufacturing

The difficulty in constructing each airfoil must also be taken into consideration. Complex, high lift airfoils usually possess thin trailing edges and concave undersides. These features typically require heavier structures that are more time consuming and complicated to build in order to maintain structural rigidity. Due to the slight increase weight and time required for construction, this criterion was assigned a weighting of 2.

4.4.2 Airfoil Selection FOM

Airfoil lift and drag data were obtained from both the UIUC Summary of Low-Speed Airfoil Data publications and from the SNACK software package. Promising airfoils were chosen and their performance examined with regard to the FOM criteria listed above. Table 4.4 shows the final FOM regarding airfoil selection.

Table 4.4 – Airfoil Selection FOM

Airfoil	Stall Characteristics (5)	Max. C_L (5)	Induced C_D (2)	Pitching Moment (3)	Ease of Manufacture (2)	Total
Clark Y	5	5	4	4	5	80
Eppler 193	5	5	5	5	4	83
Eppler 197	5	5	5	5	5	85

4.5 Wing Area

As the maximum dimension available inside the flight box is 48", it was decided that the wing span should conform to this dimension as closely as possible. The creation of two wing panels that could be connected to provide a wing span larger than 48" was investigated and quickly discarded because of the increase in weight necessary at the attachment point. Therefore, Squirt will use a single wing panel with a 48" span.

For R/C aircraft in general, wing loadings of over 90 g/dec² (30 oz/ft²) are too be avoided if the aircraft is to handle well in flight. However, decreasing the wing loading requires a larger wing platform which produces higher parasitic drag and increases the aspect ratio of a fixed span wing. Therefore a TOGW wing loading of 90 g/dec² (30 oz/ft²) was decided upon which results in a wing area of 0.41 m² (638 in²). From this, the C_L at cruise was determined from the standard lift equation shown below. Three-dimensional effects reducing the overall lift of the wing will be more thoroughly examined later in this section.

$$C_{L_{min}} = \frac{2L}{\eta \rho S_w V_{max}^2}$$

where η is the efficiency of the wing, assumed to be 0.9, and L is the total lift required, equal to the TOGW of 3.8 kg (8.3 lbs.). This equation gives a required airfoil C_L of 0.20 ± 0.1 at the maximum speed of 29 m/s (65 mph) and of 0.24 ± 0.1 at a cruise speed of 26.7 m/s (60 mph).

As valuable time can be lost performing low-G maneuvers, it was desired to have an aircraft capable of performing maneuvers with a G loading of at least 2.5 at cruise speed. Using the

above values, this generates a required maximum C_L of 0.6 ± 0.1 , which is well within the maximum C_L value attainable by each of the airfoils compared in Table 4.4.

The maximum takeoff distance is another of the primary design considerations during airfoil selection. If the C_L of an airfoil is not high enough to allow takeoff within the set distance, high lift devices would need to be incorporated. With the preliminary weight, thrust, and wing area known, and by setting the takeoff distance to 45.7 m (150 ft), a minimum C_L for take off was determined to be 0.4 ± 0.1 , which is again achievable by many airfoils.

Based on the above calculations and the FOM of Table 4.4, the airfoil selected for Squirt was the **Eppler 197**. The Eppler 197 features a C_L of 0.26 and a C_D of 0.0068 at its minimum drag angle of 0° , and a maximum C_L of 1.28 as the angle of attack approaches the critical angle of 11° . A neutral angle of incidence (0 degrees) will be set in order to provide the required lift at cruising speeds.

4.6 Aspect Ratio (AR)

A high aspect ratio reduces the induced drag of the aircraft, and allows for a faster cruise speed for the same power. However, due to the constraints placed on the geometry of the aircraft by the flight box, the wing span has been fixed at 1.2 m (48 in). Therefore, the chord must be set in order to attain the necessary wing area of 0.41 m^2 (638 in^2). This results in an average chord value of 0.33 m (13 in) over the span. Though a tapered platform was considered, the loss of wing area for increased efficiency is not advantageous in this event due to the restricted wing span. Thus a rectangular platform of **0.33 m (13 in)** chord was selected which results in an aspect ratio of **4**. Though an AR this low would normally not be used, decreasing the wing area by reducing the chord is not acceptable as it would reduce the maximum TOGW of the aircraft, impacting the final score.

4.7 Horizontal Stabilizer Sizing

The primary design considerations used to determine the required tail surface dimensions are stability and control authority. The wing is capable of at least a 2.5 g acceleration before stalling, and the Eppler 197 has a moment coefficient of approximately -0.06 for a cruise AoA approximated at 0° . The stabilizer must be capable of overcoming both the pitching moment of the wing and the moment caused by a finite separation between the center of gravity and the center of pressure on the wing (assumed for now to be within 0.0254 m or 1 in. of each other). The tail must then still provide enough torque for control. This leads to the inequality:

$$X_{ach} \frac{1}{2} C_{Lh} \rho S_h V^2 \geq \frac{1}{2} C_M \rho S_w V^2 c + 2.4 X_{acw} W + I \ddot{\theta}$$

From this, the product of the stabilizer maximum lift coefficient, surface area, and distance from the center of gravity ($X_{ach}C_{Lh}S_h$) can be found. In order to minimize its size and reduce drag, the tail is placed as far aft as feasible to give it a large moment arm on which to act. As Squirt's fuselage length can approach 48" due to the flight box restriction it was determined that the length of the fuselage alone would not provide an adequate tail moment arm.

It is common practice to use a stabilizer that is approximately 20 to 22% percent of the wing area and an elevator that is 40% of the stabilizer area. With the slow flight speeds and multiple takeoff and landings in this competition, pitch authority was deemed very important. With no penalty for stabilizer area, an area that is 22% of the wing was preferred. Therefore, a 0.094 m^2 (146 in^2) stabilizer located 0.69 m (27 in.) from the CG would require a C_L of approximately 0.2 ± 0.1 which is easily attainable by many airfoil sections. However, in order to produce the lightest structure possible, a symmetrical $\frac{1}{4}$ " balsa stick stabilizer was chosen over a symmetrical airfoil section. Like symmetrical sections, stick construction also has the desired qualities of low drag due to minimal frontal area and zero pitching moment. The elevators are tied together under one servo which is located in the fuselage providing further weight savings.

The horizontal stabilizer platform is also designed with a taper ratio of 0.5 to reduce its induced drag. An aspect ratio close to 5 was also desired in order to further reduce induced drag. This resulted in a stabilizer with a root chord of 0.25 m (10 in.), a tip chord of 0.13 m (5.5 in.), and a 0.51 m (20 in.) span. Based on this geometry, the horizontal tail aspect ratio was calculated to be 4.8.

4.8 Vertical Stabilizer Sizing

With the use of a conventional tail, the vertical stabilizer could also be constructed of $\frac{1}{4}$ " balsa stick as it does not have to support any vertical loading. For an airplane to be stable in yaw, the Center of Lateral Area should be about 25% back from the center of gravity. In the preliminary AutoCAD design drawings, quick area moment calculations were done to show that the area selected was adequate for yaw control. Common modeling design practice states that the vertical tail area should be approximately 40% of the horizontal tail area used. Thus a vertical fin area of 0.04 m^2 (68 in^2) was employed, resulting in a root chord of 0.25 m (10 in.). The vertical fin was also swept for aesthetics.

4.9 Fuselage Design and Sizing

4.9.1 Fuselage Design Considerations

During the preliminary design stage, several design parameter and sizing trades were considered. While innovative design and construction methods were investigated, they were weighed against ease of manufacture and functionality. During the selection of an appropriate airframe geometry, tradeoffs between simplicity of construction, strength, weight and reduction of drag were considered. The following aspects of performance were considered in designing the fuselage geometry.

Efficiency

The layout chosen for the fuselage should optimize the space required for the airframe structure while also limiting the fuselage's overall size. The internal water tank was the primary constraint considered during the initial design stages.

Manufacturing Ease

The airframe should limit the cost and time required for its construction. As a limited number of facilities are available to the team, the required tooling for each manufacturing method must be considered.

Functionality

The fuselage must function properly as a water-carrying aircraft which requires repeated dumping and loading of the cargo. The design feature which provides access to the water tank must be both rugged and quick to use due to the rushed nature of water loading. Provisions must be made to ensure stable flight in both a loaded and unloaded configuration.

Structural Rigidity

The airframe structure must be sufficiently strong and stiff to account for the substantial payload and the repeated landings that the aircraft will encounter. The structure must also be rigid enough to prevent flexing that could reduce horizontal or vertical stabilizer effectiveness. The type of materials used and the thickness chosen for the primary structural components of the aircraft depended on their ability to withstand this expected loading.

Drag Penalty

The design of the airframe should minimize the amount of parasitic and interference drag created by the fuselage. This will reduce the power required for cruise and increase overall top speed, augmenting motor run time. All junctions between airframe components should be smoothly faired in order to reduce interference drag. Any fuselage upsweep should be less than 15° to prevent separation drag.

4.9.2 Fuselage Sizing

The final design of the fuselage was based heavily on the considerations above, with its overall length dictated by the maximum flight box size, and the required tail moment arm. The internal tank is designed to support a maximum of 1.75 L of water, with flight consideration being given to water volumes between 1.0 L and 1.75 L. The volume required for a water tank this size is approximately 1750 cm^3 (107 in^3) assuming minimal wall thickness. At 0.44 m (17.5 in) in length with a 5.1 cm (2 in) height and 7.6 cm (3 in) width, the rectangular water tank is centered over the wing's $\frac{1}{4}$ chord point (predicted CG location) in order to ensure that the CG will not shift in the loaded and unloaded configurations. The 1.27 cm (0.5 in) dump orifice is also positioned under the wing's $\frac{1}{4}$ chord point to ensure that the CG of the aircraft does not shift during the dumping procedure. In order to accommodate these tank dimensions, the fuselage throughout the center section - which houses the tank - boasts a 0.12 m (4.75 in) width and 0.13 m (5.25 in) height. As stated previously the selected length of the fuselage is 1.2 m (47.5 in) which provides an adequate tail moment arm for the horizontal stabilizer while still conforming to the constraints imposed by the flight box.

The fuselage is based on a rounded geometry which varies down the length as required by the location of the internal tank. The aft section of the fuselage fairs smoothly into the tail and rudder in order to reduce interference drag and increase the tail's efficiency. The wing is also faired into the top of the fuselage to further reduce interference drag. The radio control equipment resides at the rear of the fuselage while the battery compartment is located above the water tank. Sufficient room was included in the battery compartment to allow them to shift over 10 cm (4 in) either forwards or backwards to facilitate the balancing of the plane if required. The propeller is mounted slightly above the centerline of the plane which provides enhanced stability and allows for adequate ground clearance by the propeller.

4.9.3 Water Loading

Access to the water tank is facilitated through the use of a removable hatch present on the upper section of the fuselage immediately in front of the wing. This hatch is secured by 2 small rare earth magnets which allow quick removal between flights. The water loading mechanism can then be inserted directly into the front of the exposed tank, and the tank filled. A rubber stopper with small 0.08 cm (0.03 in) diameter holes through it is also present on the underside of the hatch to ensure both that no water spills during flight and to provide atmospheric venting during dumping.

4.9.4 Water Dumping

The water tank exit orifice is located directly under the $\frac{1}{4}$ chord of the wing in order to ensure that the CG does not shift during the dump procedure. A small rubber cylinder $\frac{1}{4}$ " thick with a 0.5" inner diameter and 1" outer diameter is affixed directly to the underside of the tank and provides an interface with the bottom of the fuselage. A hinged lid is present at the bottom of the fuselage and covers the exit orifice. A retractable pin can then be actuated by an attached servo to allow the release of water. The lid must be manually reset on the ground prior to the next filling of the tank. With a full complement of 1.5 L of water onboard, expected dumping rate through the 1.27 cm (0.5") diameter orifice is 0.25 L / s. Assuming a worst case dump rate of 0.10 L / s in case of inadequate tank ventilation, this converts to 15 seconds of dump time. As the downwind leg of the course will require more than 15 seconds to traverse, the aircraft can remain at cruise velocity during dumping which will help to improve flight times relative to those aircraft that possess large water tanks.

4.9.5 Speed Loader

In order to minimize the loading time required, a specialized water loading device will be utilized. The loader consists of four 2 L pop bottles mounted upside down to a plywood tray. Each bottle is secured from shifting through the use of packing tape and vertical support posts. Prior to the commencement of the flight, each bottle is filled with exactly half of the water required per takeoff through the use of a graduated cylinder. Hinged caps are then affixed to each bottle and the device turned right side up. Flexible tubing is present inside the bottles to provide venting to the atmosphere when the caps are released. A second reservoir is then attached to the bottom of the tray which encompasses the four soda bottle exits. When time starts, the first trigger is pulled which releases the water from two soda bottles into the lower reservoir. As there are handles

present on the tray, this can be accomplished as the ground crew is running towards the plane on the tarmac. By the time the crew reaches the plane, the soda bottles have completely emptied into the lower reservoir. The upper hatch on the aircraft is then removed and the hose from the reservoir inserted into the water tank. A ball valve situated along the hose from the reservoir is then turned and the internal tank filled. Once complete the hatch is replaced and the ground team leaves the tarmac. For the second loading, the procedure is repeated using the remaining full soda bottles.

4.10 Undercarriage Design

The tricycle landing gear design used for Squirt is designed primarily to provide excellent ground handling qualities as Kansas has been known to experience high wind conditions. As landing will only occur with an empty aircraft, the landing gear themselves do not experience heavy impact loading. A main wheel stance of approximately $\frac{1}{4}$ of the wingspan was chosen to prevent upset in high crosswinds. The nose gear is located as far forward on the main fuselage as possible and is positioned 10 cm (4 in) behind the firewall. As the propeller is mounted 12 cm (4.8 in) up the fuselage, the length of the nose and main gear need only be 7.6 cm (3 in) to provide adequate propeller ground clearance. A gear length of 0.10 m (4.1 in) allows slightly less than 15 degrees of rotation and 0.08 m (3 in) of propeller to ground clearance. The main landing gear was positioned 0.045 m (1.8 in) behind the center of gravity so that once the aircraft rotates on takeoff; the wheels remain behind the center of gravity. The nose gear uses a 0.004 m (0.16 in) diameter music wire bent into a dual coil configuration in order to absorb landing impacts. The main gear is a commercially available monocoque aluminum setup designed for 0.40 c.i. models.

Standard vinyl model aircraft wheels 0.057 m (2.25 in) in diameter are used for the main gear and nose gear. Though the vinyl deforms slightly under loading, they provide adequate friction to ensure that the aircraft does not sliding sideways in strong crosswinds. The friction of these wheels also provides good directional control during ground runs.

4.11 Drag

In order to make accurate predictions of the flight speed and acceleration, the drag on the aircraft must be calculated. In this basic estimation, the total drag is taken to be the sum of parasitic drag and the induced drag from the wing. This approximation does not take into account the interference drag caused by the junction of various aircraft components. As interference drag can

be virtually eliminated through the application of proper drag reduction techniques, wing and tail fairings were incorporated into the design and construction of Squirt.

4.11.1 Parasitic Drag Coefficient

Parasitic drag was estimated using the "component build-up" method. A flat-plate skin friction drag coefficient (C_f) for fully developed turbulent flow was calculated for each major component of the aircraft and then multiplied by a "form factor" (k) that estimates losses due to form drag:

$$C_{D\text{Para}} = \sum \left[\frac{k \times C_f \times A_{\text{wetted}}}{S_w} \right]_{\text{component}} \quad C_f = \frac{0.455}{(\log_{10} Re)^{2.56}} \quad Re = \frac{V \times L}{\gamma}$$

Table 4.5 – Parasitic Drag Estimation

Component	$A_{\text{wetted}} (m^2)$	Re (pVL/u)	C_f	Thickness Ratio	Form Factor (k)	$C_{D\text{ Parasitic}}$
Wing	0.805	656831	0.004992	0.0432 (t/c)	1.07	0.010683
Fuselage	0.537	2273646	0.003982	10.0000 (L/De)	1.10	0.005844
Wheels	0.015	113682	0.007140	0.1111 (t/d)	1.13	0.000308
Gear Struts	0.023	94685	0.007435	0.0670 (t/w)	1.80	0.000765
Stabilizer	0.188	397715	0.005503	0.0125 (t/c)	1.02	0.002626
Rudder	0.125	423087	0.005436	0.0064 (t/c)	1.03	0.001732
Total						0.021959

The total parasitic drag coefficient estimate is **0.022**, which seems reasonable for an aircraft of this shape and size. In order to help reduce parasitic drag, Squirt will have a very smooth Mylar skin on all surfaces.

4.11.2 Induced Drag Coefficient

The induced drag coefficient is dependent on a proportionality factor "K" and the square of the C_L for moderate angles of attack. As Squirt utilizes a one piece wing with a 48" span, the aspect ratio is fairly low and hence the induced drag is relatively large. Winglets and endplates were considered as ways to help minimize the induced drag; however these would decrease the available span for the wing itself shrinking the total wing area.

$$e = 1.78(1 - 0.045 \times AR^{0.68}) - 0.64 = 0.945 \quad K = \frac{1}{\pi Ae} = 0.82 \quad C_{D\text{Induced}} = KC_L^2 = 0.027C_L^2$$

4.11.3 Total Drag

The total drag is based on its velocity at which the aircraft travels. While the Reynolds number term in the parasitic drag equation does change with velocity, its effects are negligible for a calculation of this accuracy. The induced drag coefficient does however depend heavily on velocity due to the C_L term. Thus the coefficient of drag at a known airspeed and C_L is given by $C_D = 0.022 + 0.027C_L^2$. The actual drag force experienced by the aircraft is given by $D = 0.5C_D\rho V^2S_w$.

4.12 Accelerated Stall Characteristics

The minimum controlled level turning radius for an airplane is determined by the maximum radial acceleration the wing can sustain before an accelerated stall. The maximum G-load that can be produced by the aircraft is given by the ratio of the maximum lift available from the airfoil to the lift generated in steady level flight. The angle of bank at which the wing can still provide the necessary lift for the airplane is given by:

$$\cos\beta = \frac{C_{L_{cruise}}}{C_{L_{max}}}$$

Thus the **maximum angle of bank is 80°**. The maximum radial acceleration before the onset of an accelerated stall is calculated using the equation:

$$\tan\beta = \frac{a_{stall}}{1 \cdot g}$$

This gives a loading of **5.45g's**. Thus, if the aircraft experiences more than 5.45g lateral acceleration, the maximum lift available from the wing will be exceeded and an accelerated stall will occur.

From this data the minimum radius of turn with no altitude loss is **13m (44 ft)** as given by the equation:

$$R = \frac{V_{cruise}^2}{a_{stall}}$$

4.13 Take-off Performance

Take-off distance is broken into three components: ground roll, rotation distance, and climb-out distance. Rotation distance is assumed to be negligible for an aircraft of this size.

4.13.1 Ground Roll

The ground roll distance (d_g) of the aircraft is given by:

$$d_g = \frac{V_{TO}^2}{2 \cdot a_{mean}}$$

where,

$$M \cdot a_{mean} = \left[T_{mean} - \left(A + B \cdot C_{Lcruise}^2 \right) \frac{1}{4} \rho V_{Mean}^2 S_w - \mu \left(W - C_{Lcruise} \frac{1}{4} \rho V_{Mean}^2 S_w \right) \right]$$

Take-off speed (V_{TO}) is taken as 15% above stall speed:

$$V_{TO} = 1.15 \cdot V_{stall}$$

The C_L and C_D used in this equation are the values at cruise speed, as the plane can be considered in level flight while on the ground with its wing angle of incidence relative to the runway. Static thrust is estimated from the available motor data from ElectriCalc. This yields a ground roll acceleration of **3.66 m/s² (11.99 ft/s²)**. The ground roll is **21.0 m (68.9 ft)**, at TOGW which is well under the 150 ft limit. Empty weight ground roll was calculated to be **12.6 m (41 ft)**. These distances are given assuming a no wind condition.

4.13.2 Climb out Distance

The climb out angle for the aircraft is given by the equation:

$$\tan \vartheta = \frac{T}{W} - \frac{D}{L}$$

A **climb angle of 12°** is achieved. If this rate of climb were held constant so that there is no gain in velocity after lift off, a distance of **47 m (154 ft)** would be needed to reach an altitude of 10 m (32.8 ft). The performance under these assumptions is as expected for a heavily loaded aircraft. To increase the climb rate, the aircraft should be allowed to accelerate to its minimum drag velocity in level flight, at which point the excess power available at this velocity can be used for climb.

4.14 Endurance and Range

4.14.1 Minimum Drag Velocity

As parasitic drag increases with increasing velocity and induced drag decreases, there exists a point of minimum drag. The velocity at which this minimum drag occurs is also where minimum thrust is required, as thrust is equal to drag. The minimum drag velocity is given by:

$$V_{\min \text{ drag}} = \left(\frac{B}{A} \right)^{1/4} \left(\frac{2Mg}{\rho S_w} \right)^{1/2}$$

Where A and B correspond to the parasitic (0.022) and induced drag (0.027) respectively. The minimum drag velocity for Squirt is **13.1 m/s (29.5 mph)** at which only **1.7 N (0.4 lbf)** of thrust are required.

4.14.2 Endurance

The aircraft achieves maximum endurance when flying at its minimum throttle setting. This is achieved at $V_{\min \text{ drag}}$ where the lowest thrust is required. The ElectriCalc commercial software package is used to estimate the endurance of the aircraft with the selected motor and battery arrangement. It was found that $V_{\min \text{ drag}}$ could be achieved with a minimum throttle setting of 37%. At this setting, ElectriCalc estimated a run-time of 34.2 minutes. Due to electrical losses in the wire leads, losses in the speed controller, and difficulty in maintaining $V_{\min \text{ drag}}$, a conservative estimate of 90% of this value was taken. Thus the endurance of Squirt is **30.8 minutes**. Note that this estimate neglects power needed for take-off, climb-out, and landing.

4.14.3 Range

The maximum range characteristics of an electrically powered aircraft differ from those of a gas-powered plane, as motor efficiency drops at increased throttle settings. The maximum range of the aircraft is achieved not at the best lift-to-drag velocity, but at the lowest possible throttle setting—at the endurance throttle setting. To calculate the range, the endurance prediction of 30.8 minutes is multiplied by the endurance velocity of 12.4 m/s (26.3 mph). This method produces a maximum range value of **25.4 km (15.8 miles)**. This assumes a zero wind condition and again neglects the power needed for takeoff, climb, landing and energy loss maneuvers.

4.15 Stability

Static stability is achieved when the forces on the aircraft created by a disturbance to the flight path push the aircraft back in the **direction** of its original state. Dynamic stability is achieved when the dynamic motions of the aircraft are damped, eventually returning the aircraft to its original state. Without the software to perform a dynamic stability analysis to any degree of accuracy, the stability analysis presented here has been limited to static stability.

4.15.1 Longitudinal Stability

The maximum allowable distance between the center of gravity of the aircraft and the location of the $\frac{1}{4}$ chord neutral point of the wing was determined using the following stability criterion:

$$\frac{dC_{M(CoG)}}{dL} = \frac{x}{c} - \eta_H \left(\frac{S_H}{S_W} \right) \left(\frac{l_H}{c} \right) \left(\frac{a_H}{a} \right) \left(1 - \frac{d\epsilon}{d\alpha} \right) + \frac{dC_{Mf}}{dC_L} \leq 0$$

The marginally stable case value of x , the distance from the $\frac{1}{4}$ chord, was found by setting the above inequality to zero and evaluating. This yielded a value of 28.7%, which means that for the aircraft to be longitudinally stable, the center of gravity can be located at no more than 28.7% of the wing chord from the leading edge. The difference between the actual center of gravity and the maximum allowable center of gravity is termed the static margin. With the predicted center of gravity at 25% of the mean aerodynamic chord, a **static margin of 0.04** is achieved. This value is acceptable, but care will have to be taken to ensure a rearward shifting of the CG does not occur during flight.

4.15.2 Lateral-Directional Stability

In order to provide directional stability, the moments about the center of gravity must be such that the derivative of the yawing moment is less than zero. In order to determine the yawing moment derivative about the center of gravity, the pitching moment derivative of the fuselage and vertical fin must be evaluated. The derivative of the pitching moment of the fuselage in the case of Squirt will be negligible because the fuselage areas ahead of and behind the center of gravity are approximately equal. The derivative of the vertical fin pitching moment can be expressed by:

$$\frac{dC_{mfin}}{d\theta} = \left(\frac{dC_{Lfin}}{d\alpha} \right) \left(\frac{S_{fin}}{S_W} \right) \left(\frac{l_H}{c} \right)$$

Where $dC_{L_{fin}}/d\alpha$ is the slope of the lift curve of the vertical fin, S_{fin} is the vertical fin area, S_w is the wing area, l_H is the tail moment arm and c is the mean aerodynamic chord of the wing. The value of the vertical fin pitching moment derivative was evaluated to be 1.3.

$$\frac{dC_{mCG}}{d\theta} = \frac{dC_{mFuselage}}{d\theta} - \frac{dC_{mfin}}{d\theta}$$

This value is subtracted from the fuselage pitching moment derivative to determine stability.

This results in a **lateral-directional pitching moment derivative of -1.3**, meaning the aircraft exerts a restoring force in the direction opposite the disturbance and is hence statically stable.

4.15.3 Roll Stability

Based on the high-wing design of Squirt, no wing dihedral was incorporated. As the high-wing configuration provides a stable platform for the aircraft, it was deemed unnecessary. Previous experience with no dihedral, high-wing aircraft have proven the validity of this assumption.

4.16 Predicted Performance

Tables 4.6 and 4.7 detail the expected mission performance of Squirt in the Fire Fight and Ferry Missions respectively. These predictions are based on the following assumptions.

1. Except during takeoff and landing the aircraft will fly at its cruise velocity (26.7 m/s)
2. Cornering maneuvers will be restricted to 4 g loading on the aircraft. Therefore the expected radius of turn is 18 m.
3. Water dumping will be completed in a sufficiently short time so that no reduction in speed is necessary.

Total Score:

Based on the estimates provided in Tables 4.6 and 4.7, the expected flight score for the Fire Fight mission based on a payload of 1.5 L of water per takeoff is **5.79** whereas the expected flight score for the Ferry mission is **0.41**.

Summing these scores and dividing by the expected RAC of 6.23 (thousand) provides Squirt with a **final score of 0.99** before scaling by the report score.

Table 4.6 – Expected Fire Fight Mission Time

Loading Phase:	Run to Aircraft, Load water, Clear Runway, Arm Aircraft	23 seconds
Takeoff:	Accelerate to V_{TO}	4 seconds
Level Flight:	610 m (2000 ft) straight flight	25 seconds
Cornering:	2 x end turns at 18m radius	4.5 seconds
	1 x 360° turn	4.5 seconds
Landing:	Disarming and Positioning	10 seconds
Loading Phase:	Run to Aircraft, Load water, Clear Runway, Arm Aircraft	23 seconds
Takeoff:	Accelerate to V_{TO}	4 seconds
Level Flight:	610 m (2000 ft) straight flight	25 seconds
Cornering:	2 x end turns at 18m radius	4.5 seconds
	1 x 360° turn	4.5 seconds
Landing:	Final Approach	5 seconds
Total Mission Time:		137 seconds

Table 4.7 – Expected Ferry Mission Time

Takeoff:	Accelerate to V_{TO}	4 seconds
Level Flight:	2440 m (8000 ft) straight flight	100 seconds
Cornering:	8 x end turns at 18m radius	18 seconds
	4 x 360° turn	18 seconds
Landing:	Final Approach	5 seconds
Total Time:		145 seconds

5.0 Detailed Design

The design of any airplane is a highly iterative process, involving many changes to the initial preliminary design before arriving at the final configuration. To accommodate this, a spreadsheet was developed that performed the necessary calculations while only requiring airfoil properties and some aircraft geometry inputs. Drawings of the final aircraft design are presented at the end of this section.

5.1 Weights

An estimate of the components, structure and payload to be carried was tabulated. Airframe structure was calculated based on volume approximations of the materials used in the construction of each part, and by using data obtained from last years aircraft. Care was taken not to underestimate the weight of the aircraft, as all design features require an accurate approximation of this weight in their calculations. A summary of weight is presented below.

Table 5.1 – Aircraft Component Weights

Description	Weight (lbs)	Weight (kg)	Number	Subtotal (lbs)	Subtotal (kg)
Water	3.300	1.497	1	3.300	1.497
Water Tank	0.200	0.091	1	0.200	0.091
Micro Servos	0.063	0.028	6	0.375	0.170
Receiver	0.125	0.057	1	0.125	0.057
Main Gear	0.250	0.113	1	0.250	0.113
Nose Gear	0.150	0.068	1	0.150	0.068
Wing	0.775	0.352	1	0.775	0.352
Tail	0.250	0.113	1	0.250	0.113
Fuselage	0.750	0.340	1	0.750	0.340
Motor	0.560	0.254	1	0.560	0.254
Main Battery Pack	1.420	0.644	1	1.420	0.644
Speed Controller	0.075	0.034	1	0.075	0.034
Propeller	0.125	0.057	1	0.125	0.057
TOGW with Water				8.355	3.790
Empty Flying Weight				5.055	2.202
Airframe Weight				2.175	0.987

5.2 Payload Fraction

Payload fraction is a measure of the payload's contribution to the take-off gross weight of the aircraft. Squirt's payload fraction carrying 1.5 L of water is **0.395**.

5.3 Wing Sizing and Performance

5.3.1 Wing Planform

The dimensions proposed in the preliminary design were further refined in an attempt to increase the accuracy of the wing performance calculations. The wing area was recalculated using the detailed AutoCAD drawings, accounting for the fuselage carry-over and taper. The wing area was finalized at **0.40 m² (624 in²)** with a constant chord of **0.33 m (13 in)** which produces a maximum wing loading of **904 g/dec² (30.8 oz/in²)**.

5.3.2 Aileron Sizing

The ailerons were sized based on historical data for effective control. A 60% semi-span, 16% chord Frise-type ailerons were selected for their high efficiency. Frise-type ailerons function by create drag when deflected upward, helping to yaw the airplane into the turn. A sealed hinge line is used to increase the effectiveness by an additional 15%. Each aileron was therefore assigned an area of **0.019 m² (30 in²)**.

5.3.3 Stall Velocity

An airfoil efficiency factor, η , of 90% was used to relate 2-dimensional airfoil data to a 3-dimensional wing. This value accounts for lift loses at the tip and slight inaccuracies in the airfoil construction. This reduces the maximum coefficient of lift of the Eppler 197 from 1.28 to 1.15. Thus the stalling speed can be calculated by the equation.

$$V_{STALL} = \sqrt{\frac{2Mg}{\eta C_{l_{max}} \rho S_w}}$$

This results in a stall speed of **10.9 m/s (23.1 mph)** fully loaded and **8.3 m/s (17.6 mph)** when empty.

5.3.4 C_L at Cruise and Maximum Velocity

In order to determine maximum velocity and the resulting C_L , several iterations must be done. By iterating between velocity and C_L values, a final cruise and maximum velocity were found. The cruise velocity was taken to be 90% of the maximum velocity.

Table 5.2 - Maximum and Cruise Velocities

	Velocity	Velocity	C_L
V_{CRUISE}	26.7 m/s	60 mph	0.23
V_{MAX}	29.1 m/s	65 mph	0.20

5.3.4 Wing Incidence

With the known cruising velocity, the angle of incidence for the wing was determined. This angle provides the model with the correct lift for level flight at the cruise velocity, taking the aspect ratio (AR) into account.

$$\alpha = \frac{a_0 + 18.24 \times C_{L_{cruise}} (1 + T)}{AR} = 0.3^\circ$$

Where, a_0 = the angle of attack of the wing at $C_{L_{cruise}}$ and T is the planform adjustment factor.

The pitching moment of the wing at the cruise velocity and angle of incidence was calculated to be -7.0 N/m (-495 oz/in).

5.4 Tail Sizing and Performance

5.4.1 Horizontal Stabilizer Platform

The horizontal tail has an area of 0.234 m^2 (146 in^2), which is 23% of the wing area. A tip chord of 0.14 m (5.5 in), a root chord of 0.25 m (10 in) and a span of 0.51 m (20 in) give an aspect ratio of 4.8. Historic guidelines suggest an elevator area of between 30 and 40 percent for effective pitch control. Therefore, an elevator area of 0.036 m^2 (56 in^2) was used, representing 38% of the stabilizer area.

5.4.2 Horizontal Stabilizer Lift

Basic model airplane guide lines suggest that the horizontal tail be placed approximately 2.5 times the mean aerodynamic wing chord from the neutral point of the wing to the neutral point of

the stabilizer. The neutral point of both airfoils is assumed to be at the $\frac{1}{4}$ chord line. This guideline would suggest the use of a 0.81 m (32 in) tail moment arm. However, due to fuselage sizing restrictions imposed by the flight box, the moment arm was reduced to **0.69 m (27 in)**.

With a pitching moment of -7.0 N/m (-495 oz/in) and a tail moment arm of 0.69 m (27 in) the horizontal tail must provide a down force of **9.6 N (33.6 oz)** assuming a 50% stabilizer efficiency. This down force is provided by the negative lift from the stabilizer airfoil, requiring a $C_{l_{stab}} = -0.22$.

5.4.3 Horizontal Stabilizer Incidence

The angle of incidence required for a $\frac{1}{4}$ " stick stabilizer to provide this C_l was calculated to be -2.73° assuming two-dimensional flow. Using the same equation as the wing to account for the effects of an aspect ratio of 4.8, the tail plane incidence thus becomes -3.66° .

The down wash from the wing and its effect on the stabilizer were then taken into account. The horizontal moment arm and the height of the stabilizer from the wing were calculated and their values were used with charts (Figure 2, pg 40, Lennon, Andy; "Basics of RC Model Aircraft Design" ref 10.) to provide the correct tail incidence required. A final tail incidence of -2.4° is used.

5.4.4 Vertical Stabilizer Platform

The vertical stabilizer platform remained unchanged from the preliminary design. The rudder area was set at 45% of the vertical stabilizer which is larger than recommended 40% from historical guidelines, but will provide the pilot with adequate control authority during the highly loaded turns. The resultant rudder area is **0.019 m^2 (29 in^2)**.

5.5 Propulsion

Motor and propeller selection remained unchanged from the preliminary design. A single AstroFlight FAI-15 will provide the aircraft with sufficient power. An AstroFlight hex gearbox with a 2.38:1 gear ratio will turn an APC 12" by 8" electric propeller with an approximate pitch speed of **26 m/s (59 mph)** and provide an approximate 16.9 N (3.8 lbs) of static thrust. At a predicted current draw of **41.3 amps**, full throttle duration of the 10 cell, 2400 mAh battery pack is **3.1 minutes**. The computer radio will limit the current to below 40 amps at full throttle static draw in order to avoid blowing the fuse. Also, due to the propeller unloading in the air, the current draw is typically lower than predicted. As much of the mission sortie is flown at a partial throttle setting, pack duration should be higher than the predicted 3.1 minutes.

5.6 G-Loading

In predicting the maximum g-load the aircraft is capable of handling, the aircraft's structural capabilities were estimated with a calculation of the spar's maximum allowable bending stress.

5.6.1 Structural Loading

A **G-load rating of 4** was assigned as a prediction of the maximum loading the airplane would experience under normal flying conditions while at the maximum TOGW.

For the following calculations, the assumption was made that the wing spar carried all of the wing loading and that the spar would experience heavier loading than any other aircraft part. Thus, the maximum bending stresses the spar can handle will determine the G-load capability of the plane.

The wing manufacturing plan calls for an "I" beam spar to be used, with a carbon laminate for each flange and a vertical grain balsa shear web. Thus, the maximum bending stresses these elements can handle will determine the G-load capability of the plane. As nearly all G-loadings placed on the airframe would be positive, this puts the upper spar into compression and the lower into tension. Thus the number of carbon fiber laminates would be different for each spar flange. From these assumptions, the cross sectional area of these respective materials could be calculated.

The maximum bending moment experience by the wing was calculated using basic force and moment analysis and found to be **63.6 kN/m (363 lbf/in)** at the root, dropping to zero at the wing tip. The second moment of inertia (I_y) was calculated for the area of the carbon fiber cross section. With the known distance to the neutral plane (z), the bending stress could be calculated using the equation:

$$\sigma_x = \frac{M \cdot z}{I_y}$$

The dimensions of the upper spars (stock sizes) were then iterated to achieve a safety factor of approximately 1.5 (to account for lamination defects) with positive 4 G loading. It was found that 1.5 layers of carbon fiber on a 0.013 m (0.5 in) by 0.0064 m (0.25 in) piece of balsa was required for the bottom spar. Because the compressive properties of carbon fiber are much lower than its tensile strength, 2.5 layer of fiber were necessary for the top spar. In order to be sure that the spar did not fail in shear, vertical grain balsa shear webs were used to join the two spar halves together.

5.7 Control Systems

5.7.1 Receiver and Programming

Control of the aircraft is provided by a **Futaba 8 channel PCM** transmitter and receiver with its failsafe programmed as per competition rules. Each control surface has its own servo and receiver channel, allowing programmable mixing to be incorporated. Ailerons are programmed to provide differential control for more up throw than down. Slight rudder application is also programmed to operate in conjunction with the ailerons to provide coordinated turns.

5.7.2 Flight Pack Battery

A five cell, **1100mAh, NiMh** battery pack is used to power the receiver and servos. This pack size is large enough to complete several missions, but will be peak charged again after each ten-minute flight. The **6.0V** system increases power to all servos for a minimal weight gain.

5.7.3 Servo Selection

As weight is at a premium on this design, the decision to employ micro servos was made early on in the design phase. Many micro servos have static load torques capable of moving the flight surfaces, however, most have fragile gear sets that are unable to handle sudden dynamic loads. For this reason, servo selection was restricted to micro servos with metal gear sets. In order to select the proper servo, the load on each control surface must be calculated. The torque on the servo can be calculated with the equation below.

$$T = 8.5 \times 10^6 (C^2 V_{\max}^2 L \sin(S_1) \tan(S_1) / \tan(S_2)) = \text{oz} / \text{in}$$

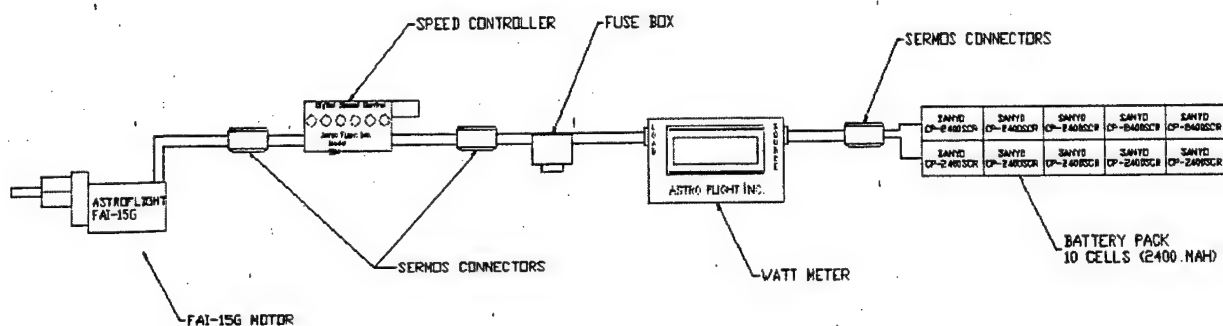
Where T is the torque in oz/in, C is the control surface chord, L is the control surface length, S_1 is the max control surface deflection (assumed to be 20°), and S_2 is the maximum servo deflection from center (30° each way for most servos). The maximum torque on each flight surface was calculated. The aileron servos experienced the highest flight load of all the surfaces with a load of **22.2 N/cm (31 oz/in)** each. After viewing many servos and comparing their torque, weight, speed and price, the **Hitec HS-81MG Standard Micro Servo** was selected. At 6.0V, this servo provides **29.4 N/cm (41.6 oz/in)** at a speed of 0.09s/ 60° in 16.6 g (0.6 oz) package. It was decided to use this servo exclusively throughout the entire aircraft, as the weight savings from using other micro servos were minimal. It also meant that only one type of spare would be needed for the aircraft.

5.8 Aircraft Safety

5.8.1 Fuses

In order to comply with the contest rules, a fuse on the motor power line must be used in order to keep currents below 40 amperes. This also protects the motor and speed controller from drawing too much current if for some reason the propeller should become jammed. The fuse will be removed from the aircraft during loading to disarm the motor.

Figure 5.1 - Squirt's Wiring Diagram



5.9 RAC

The Final RAC of Squirt was calculated as detailed in the competition rules. As the horizontal stabilizer has a span of over 20% the main wing span, it was included as a second wing, which slightly increased the RAC over preliminary estimates. The summation of the MFHR section was completed as follows:

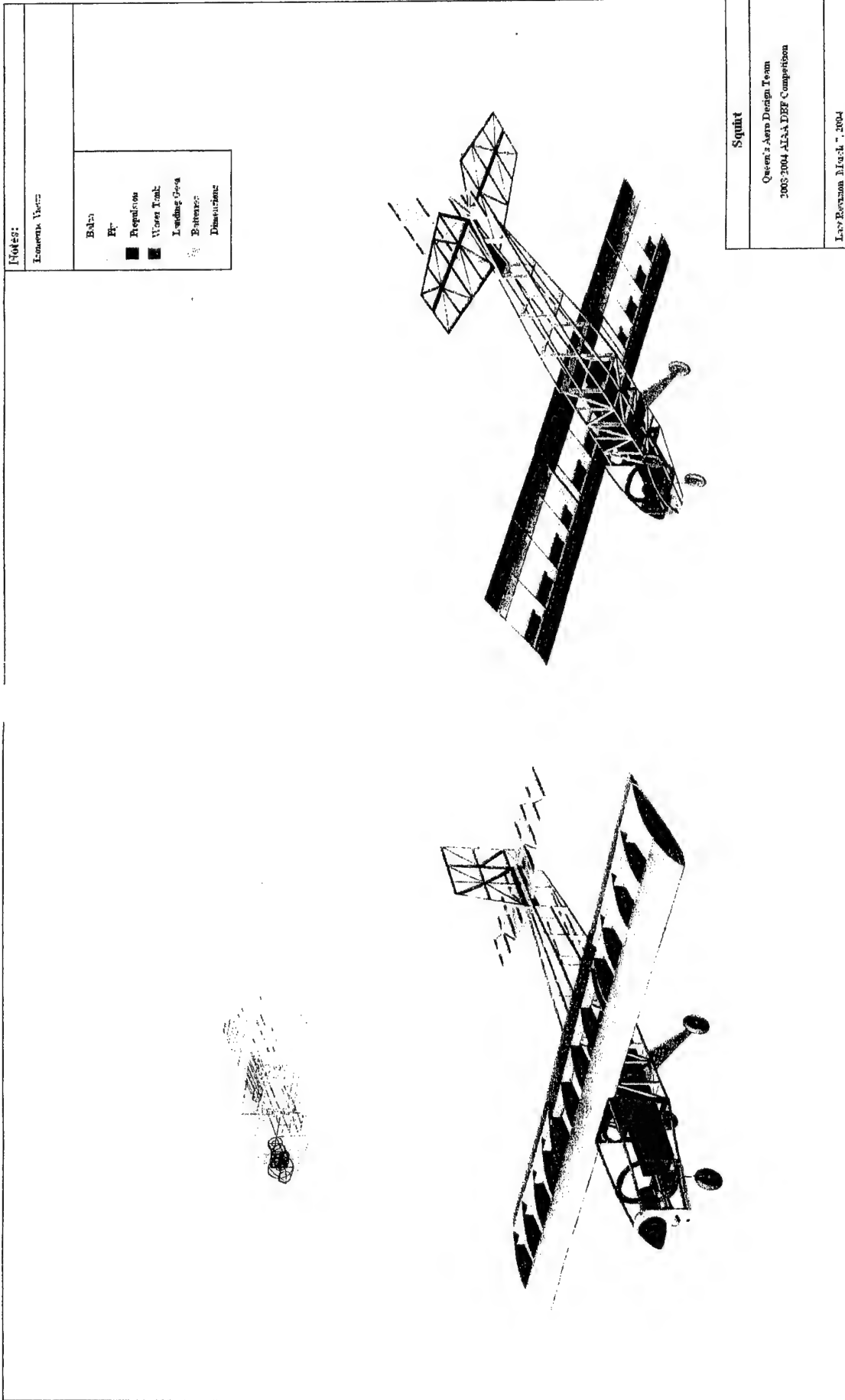
$$MFHR = 20 * (10 * \text{Span} * \text{Chord} + 5 * \text{Ctrl Fn. Multiplier} + 20 * \text{Length} * \text{Width} * \text{Height} + 10 * \# \text{ Vertical Surfaces} + 5 * \# \text{ servos or motor controllers})$$

Table 5.3 – Final RAC of Squirt

MEW	Empty Weight Multiplier (A)	300
	Estimated Empty Weight (lbs)	5.1
	MEW Total:	1530
REP	Rated Engine Power Multiplier (B)	1500
	Battery Weight (lb)	1.42
	Number of Motors	1
	REP Total:	2130
MFHR	Manufacturing Cost Multiplier (C)	20
	Number of Main Wings	1
	Wing span - Main Wing (ft)	4.00
	Wing Chord - Main Wing (ft)	1.10
	Ctrl. Fn. Multiplier - Main Wing	1
	Number of Horizontal Tails	1
	Wing span - Stabilizer (ft)	1.67
	Wing Chord - Stabilizer (ft)	0.90
	Ctrl. Fn. Multiplier - Stabilizer	1
	1.0 Wings - Total	68.9
	Body length (ft)	4.23
	Width (ft)	0.40
	Height (ft)	0.44
	2.0 Fuselage - Total	14.7
	# vertical surfaces	0
	# vertical surfaces with Control	1
	# horizontal surfaces	0
	3.0 Empennage - Total	10
	# servos or motor controllers	7
	4.0 Flight System - Total	35
	MFHR - Total:	2571.8
Squirt's Final RAC:		6231.8

Table 5.4 – Summary of Aircraft Configuration

Item	Imperial	Metric	Item	Imperial	Metric	Item	Imperial	Metric
Propulsion			Horizontal Stabilizer			Performance		
Motor	AstroFlight FAI-15G		Airfoil	1/4" Balsa Stick		CL Max.	1.28	
Speed Controller	Astro 204D		Area	146 in ²	0.094 m ²	L/D Max.	44	
Cells	2 x 5 cell stick pack 2400 mAh capacity		Span	20.0 in	0.508 m	Max. Rate of Climb	23°	
Gearing	2.38:1		Root Chord	10.0 in	0.254 m	V _{max}	65 mph	29.1 m/s
Propeller	12 x 8, APC Electric		Tip Chord	5.5 in	0.140 m	V _{cruise}	60 mph	26.7 m/s
Static Thrust	3.8 lbf	17.0 N	MAC	7.87 in	0.200 m	V _{stall (Loaded)}	23.1 mph	10.9 m/s
Run Time (100%)	3.1 min	3.1 min	Thickness	0.25 in	0.006 m	V _{stall (Unloaded)}	17.6 mph	8.3 m/s
Motor Efficiency	79%		Aspect Ratio	4.8		Takeoff (Gross)	69 ft	21 m
Wing			Taper	Double Taper		Takeoff (Empty)	41 ft	13 m
Airfoil	Eppler 197		Taper Ratio	0.525	0.525	Weight Statement		
Wing Area	624 in ²	0.403m ²	Elevator Area	58 in ²	0.032 m ²	Airframe	2.2 lbs	1 kg
Span	48 in	1.22 m	Elevator Span	9.75 in	0.248 m	Propulsion	2.1 lbs	0.96 kg
Root Chord	13 in	0.330 m	Elevator MAC	3.85 in	0.098 m	Control System	0.58 lbs	0.26 kg
Tip Chord	13 in	0.330 m	Tail Moment Arm	27.0 in	0.686 m	Payload System	0.20 lbs	0.09 kg
MAC	13 in	0.330 m	Vertical Stabilizer			Payload	3.3 lbs	1.5 kg
Wing Thickness	1.75 in	0.044 m	Airfoil	1/4" Balsa Stick		Empty Weight	5.1 lbs	2.2 kg
Aspect Ratio	3.70		Area	68 in ²	0.044 m ²	Gross Weight	8.4 lbs	3.8 kg
Taper	None		Root Chord	10.0 in	0.254 m	Control Systems		
Aileron Area	30 in ²	0.019 m ²	Tip Chord	8.0 in	0.203 m	Radio	Futabu 8-Channel PCM	
Aileron Length	14.4 in	0.36 m	MAC	9.0 in	0.229 m	Servos	Hitec HS-81MG Micro Servos	
Aileron MAC	4.8 in	0.12 m	Height	7.0 in	0.178 m	Receiver Pack	5 Cells @ 1100 mAh NiMH	
Wing Loading (Gross)	30.8 oz/ft ²	904 g/dec ²	Rudder Height	9.0 in	0.229 m	Fuselage		
Wing Loading (Empty)	18.8 oz/ft ²	553 g/dec ²	Rudder MAC	9.0 in	0.229 m	Length	50.7 in	1.29 m
			Rudder Area	29.1 in ²	0.019 m ²	Max Height	5.25 in	0.13 m
						Width	4.75 in	0.12 m



Notes:

—all dimensions given in inches
Drawings simplified for simplicity

Bağış

—15—

Propulsion

Ware1 Tanf:

Landre's Gen

Barrelle?

Conclusions

not

Front

Side

Squirt

Queen's Aero Design Team
2003-2004 AIAA DCF Competition

Lawrence A. J. 2003

6.0 Manufacturing Plan and Processes

Squirt's design can be broken down into three separate components, all of which can employ multiple construction techniques. Various methods of building the wing, fuselage, and tail appendage were analyzed and the best techniques were determined with a figure of merit matrix.

6.1 Wing Construction

6.1.1 Foam and Fiberglass

This technique involves cutting a wing from low density foam using a hot-wire cutting apparatus. The wing cores are then strengthened by the addition of a balsa, spruce or carbon fiber spar. Provision is then made for flap and aileron actuation installation before the entire surface is coated with sufficient fiberglass or carbon cloth to provide the necessary strength. Some advantages of this method are that it can be used to reproduce highly complex airfoils very accurately with little effort as well as being able to provide very strong wing platforms. Typically these wings also have good impact resistance should the aircraft crash. The chief disadvantage of this technique is that the wings produced are typically heavier than those produced with other methods.

6.1.2 Built-up Construction

Built-up construction has been the traditional technique employed by the team, though it has proven to be very time consuming. Ribs are cut into an airfoil shape from thin balsa or aircraft plywood and are then positioned on a jig so that there are 4 to 6 inches between each one. The spars, made of balsa, spruce, carbon fiber, or of some combination, are glued in and a shear web of cross-grained balsa is positioned to form the web of the I-beam structure. Leading and trailing edges are formed by gluing balsa to the front and back of the ribs, and the whole structure is then sanded to ensure a streamlined shape. Thin balsa sheeting is applied from the leading edge back to the spar on both the top and bottom of the wing, forming a strong D-tube structure, which provides adequate strength in torsion. The whole structure is then covered with a thin plastic film to form a smooth airfoil surface. This technique forms a light, rigid structure.

6.1.3 Carbon Fiber Monocoque

This technique is the most technically demanding of the three choices presented. An airfoil is drawn up in a 3-D modeling computer program and is transmitted to a computer controlled milling machine. The machine must then mill two female molds, one for each the top and bottom of the wing, from a temperature stable material. The molds are then prepared and pre-impregnated carbon fiber is laid up into the cavity. The mold is then placed under vacuum in an autoclave and baked at approximately 120 degrees Celsius for three hours. Once cooled, the wing halves are released from their molds and are carefully sanded and glued together. This technique requires very complex and expensive facilities, materials, and expertise; however, it results in a light, strong and durable wing.

6.2 Fuselage Construction

6.2.1 Foam and Fiberglass

A foam block is shaped and hollowed with a hot-wire foam cutter to provide the necessary fuselage profile. After sanding, a thin layer of fiberglass is applied to the exterior. Overall these structures are very tough and have excellent surface finishes. They tend to be very time consuming to build however due to the amount of sanding necessary. Weight is also a concern with these structures due to the sheer amount of material present.

6.2.1 Built-up Construction

This form of construction stretches back to the early days of both full-sized and model aircraft flight. Many thin strips of wood (balsa on model planes) connect several wooden formers to produce the fuselage frame. This frame is then covered by doped paper, silk or a shrinkable plastic film. This method is labor intensive, yet produces a very light structure. Durability is an issue however and this type of structure requires extensive repair after a crash.

6.2.2 Carbon Fiber Monocoque

This technique makes use of expensive composite materials to produce a very strong and lightweight fuselage. A mold of the required fuselage shape is made up of a heat resistant material. Several layers of pre-impregnated carbon fiber are laid up onto the mold, a sheet of thin

structural honeycomb (which acts as a shear web for the carbon) is placed into the lay-up, and then more carbon fiber is laid up on top. The assembly is vacuum bagged and then heated until the epoxy cures. This technique requires access to expensive materials, equipment, and expertise, but can produce excellent results. The chief disadvantage is that it is nearly impossible to repair after a mishap, and joining parts can be difficult. The other difficulty in working with this material is that it requires approximately 7 hours per part, regardless of its size.

6.3 Tail Construction

6.3.1 Foam and Fiberglass

A strong and smooth airfoil can quickly be made by cutting the required shape from medium density foam and then adding a single layer of fiberglass. The fiberglassed surface is then covered by a sheet of thin plastic and the whole assembly is placed in a vacuum until the epoxy has hardened. The plastic sheets can then be peeled away, leaving a perfectly finished tail surface. While this method of construction can result in a perfectly sculpted complex airfoil, it tends to be heavier than the other options available.

6.3.2 Sheet Balsa

By far the easiest way to construct a tail, thick, light sheet balsa can be cut in the required planform shape and then the edges can be rounded with a sanding block. Although the tail does not take a proper streamlined shape, the extra drag is usually accepted for the ease of construction. This method of construction is durable, but is heavy and prone to warping with changes in temperature and humidity.

6.3.3 Built-up Construction

A built-up tail is the lightest, but most fragile option. Construction is very similar to a built-up wing, with a set of evenly spaced ribs joined by a double spar and shear web, and the leading and trailing edges. Sheeting is sometimes extended right to the trailing edge to give a slight increase in torsional stiffness. The chief disadvantage of this design is that it is very time consuming to construct. Also worth considering is that the tiny balsa structure that makes up a built-up surface is vulnerable to damage, especially on a portion of the plane that is often accidentally banged and knocked during storage and transportation.

6.4 Figure of Merit

To choose the best combination of manufacturing processes for Squirt, a qualitative figure of merit was conceived to evaluate each processes merits and weaknesses. Five criteria were selected for the comparison and each construction method was assigned a ranking that illustrates its performance in each category. The separate categories are described in detail below.

Weight

With the marginal power system employed in this year's aircraft, weight is the primary factor to be considered. By reducing the weight of the airframe, more water can be carried resulting in a higher final score. As this is the most important of the criterion considered, it was assigned a weighting of 5.

Strength

Structural failure is expensive and can be dangerous under the wrong conditions. To ensure that the aircraft will be able to withstand the loads experienced in flight and on the ground, structural integrity was chosen as the second criterion in the FOM. As the aircraft must be able to withstand the loading inflicted upon it without damage in order to complete the mission profile, this criterion was also assigned a weighting of 5.

Skill

In order to produce the most lightweight, efficient structures possible, the selected construction technique must either be known to the team or be easy to learn and perfect. Though an important consideration in its own right, it was felt that adequate time was available throughout the year to master whatever construction technique was chosen. Therefore a weighting of 2 was applied to this criterion.

Expense

Among the various construction techniques discussed, there large discrepancy in cost exists. As some techniques use exotic materials or machining, while the more mundane and traditional techniques make use of the builder's individual skill material costs vary greatly. As Squirt was designed with the meager budget of the team in mind, the cheaper option is often worth pursuing due to fiscal necessity. As such, this criterion was assigned a weighting of 4.

Time

The final item considered is the length of time each method requires. As Squirt was designed and built on a 100% volunteer basis, time is not in unlimited supply. All design and construction must be made around the demands of a full engineering course load. Therefore, though an entire year is available for design and construction, time is a very important factor, especially to our veteran members, and thus was assigned a weighting of 3:

6.5 Evaluation and Selection

6.5.1 Analytical Method

Each construction technique was evaluated in terms of each of the five criteria listed above. As before, rankings between 1 and 5 were applied to each technique in each category based on the relative performance of the technique in that category. The total score is simply a sum of the rankings in each category multiplied by that category's weighting factor.

Table 6.5.1 – Construction Technique FOM

	Weight (5)	Strength (5)	Skill (2)	Expense (4)	Time (3)	Total
Wing						
Foam and Fiberglass	3	4	4	4	5	69
Built-up Construction	5	3	5	5	4	82
Carbon Fiber Monocoque	4	5	3	3	4	75
Fuselage						
Foam and Fiberglass	3	4	4	4	4	71
Built-up Construction	5	3	5	5	5	85
Carbon Fiber Monocoque	4	5	3	3	4	75
Tail						
Foam and Fiberglass	3	5	4	3	4	72
Sheet Balsa	4	4	3	4	5	77
Built-up Construction	5	3	5	5	4	82

6.5.2 Selection

The Figure of Merit indicated that built-up construction techniques would be suitable for the flight surfaces (wing and tail) and fuselage. This is primarily due to its extremely light weight, and the fact that most of the team members have previously had experience with it. The methods employed during the construction of these components are described below.

6.6 Description of Construction Techniques Employed

6.6.1 Wing

Once the Figures of Merit indicated that the wing surface would utilize built-up construction techniques, work began with drafting software to produce the set of working drawings necessary for this type of construction. In a built-up surface, be it a wing or a vertical fin, the airfoil shape is created by cutting out pieces of balsa wood with the proper profile, which are subsequently known as 'ribs'. The exact shape of the ribs depends on their spacing along the flight surface. This spacing can range from 10cm (4inches) between ribs as on Squirt's wing, or can be less for the smaller flight surfaces.

The CAD program must produce a set of outlines, which can then be cut from balsa. These outlines are then printed full size and affixed to the balsa sheets. The individual ribs are then cut on a scroll saw and sanded to the correct profile.

While the ribs are being cut, spar preparation is also performed. The spars are made from a laminate of balsa wood and unidirectional carbon fiber. The carbon fiber is applied in a wet lay-up process over the balsa spar and then vacuum bagged for 24 hours. Once removed from the vacuum system, the spars are then trimmed to the correct dimensions and then set aside until required.

Once the ribs have been sanded to the correct profile, they are aligned through the use of leading and trailing edge subspars. These subspars serve to maintain the correct spacing between the ribs and prepare the setup for spar installation. This entire procedure is also completed on a slate table to ensure a completely flat working surface.

With the ribs in place, the bottom spar is glued into its prepared position. The shear webs (the web of the I-beam configuration) are then prepared and glued in their position between the ribs. A rib spacing of 10cm (4 in) becomes important at this stage as balsa is sold in either 7.62cm (3inch) or 10cm (4inch) widths. By spacing the ribs accordingly, time can be saved by not having to trim each shear web. Weight can also be saved at this stage by tapering the shear webs' width to account for the reduced loading conditions at the wing tips.

Once the shear webs have been installed, the top spar is then glued in place. This forms the final section of the wing's I-beam, and the increase in wing rigidity is apparent as soon as it is properly installed. The leading and trailing edges are then glued in place, which serve to increase the torsional rigidity of the unfinished wing until sheeting can be installed. Installation of the necessary servo mounts, hinge points, landing gear mounts and wing dowels can now proceed.

Sheeting is now applied to the leading edge and trailing edge of the wing. 1/16" balsa sheet is glued from the leading edge to the top and bottom spar, producing a "D-tube" wing structure. This structure gives the wing its required torsional rigidity and helps to maintain the wing's proper airfoil profile in flight. The center section of the wing is fully sheeted at this point to ensure a hard mounting surface is present at the fuselage interface.

Once sheeted, the wing is filled and sanded to prepare for covering. Servo motors are installed in their bays at this point and are then wired and tested. The wing is then covered with a self-adhesive heat-shrinkable Mylar, which protects the balsa structure as well as bridging the open bays between ribs. Other than the installation of the control surfaces, covering is the final stage in constructing a built-up flight surface.

6.6.2 Fuselage Construction

The construction of the fuselage uses essentially the same initial techniques as described above. Work is begun with drafting software to determine the optimal location of bulkheads along the fuselage taking into account areas of high stress any taper that may be present. Once complete, the CAD program is used to produce a set of outlines, which can then be cut from balsa or aircraft plywood as appropriate. Typically balsa formers are used except in areas of high stress as they are much lighter than the equivalent plywood former. In Squirt's design only two ply bulkheads are present and are used for the firewall and the nose gear mount. Ply doubling plates are also used for the wing interface to provide the necessary extra strength.

These outlines are then printed full size and affixed to the balsa or ply sheets and are once again cut on a scroll saw. With any plywood bulkheads, material that is not strictly needed for strength is also cut away in order to lighten the structure.

$\frac{1}{4}$ " x $\frac{1}{4}$ " balsa stringers are now created through the use of a balsa stripper and sheets of balsa wood. These stringers run along the length of the fuselage and provide the necessary strength and rigidity to the structure. Once the bulkheads have been cut and sanded to the correct profile, a level surface is used along with a series of jigs to assemble the proper geometry. Once the bulkheads have been located correctly, stringers are ran along the length of the fuselage and glued to the bulkheads where appropriate. At this point ammonia may be applied to the stringers to assist in bending them around any sharp bends or tapers.

Once the stringers are in place, installation of flight systems can begin. The water tank is fitted and interfaced with the necessary bulkheads while provisions are made for water entry and exit. The nose gear and main landing gear are also added at this point. In order to minimize the chances that an impact on landing will cause structural failure, extra trussing is added to the main gear / fuselage interface.

Mounting blocks and fairings are now produced for the wing / fuselage interface and the tail / fuselage interface in order to minimize induced drag. The removable hatch used during water loading also accomplishes the function of the main wing fairing. The fuse box, motor, servos, speed controller and receiver are also installed at this point and the necessary wiring run to and from the receiver. Preliminary motor and control checks are performed at this point to ensure that everything is functioning as expected.

Once all components have been installed and tested, the fuselage is sanded and prepared for covering. A self-adhesive heat-shrinkable Mylar covering is used to protect the balsa structure and bridge the open bays between stringers. Final assembly of the tail and wing can now be completed and the entire aircraft flight tested.

6.6.2 Tail Construction

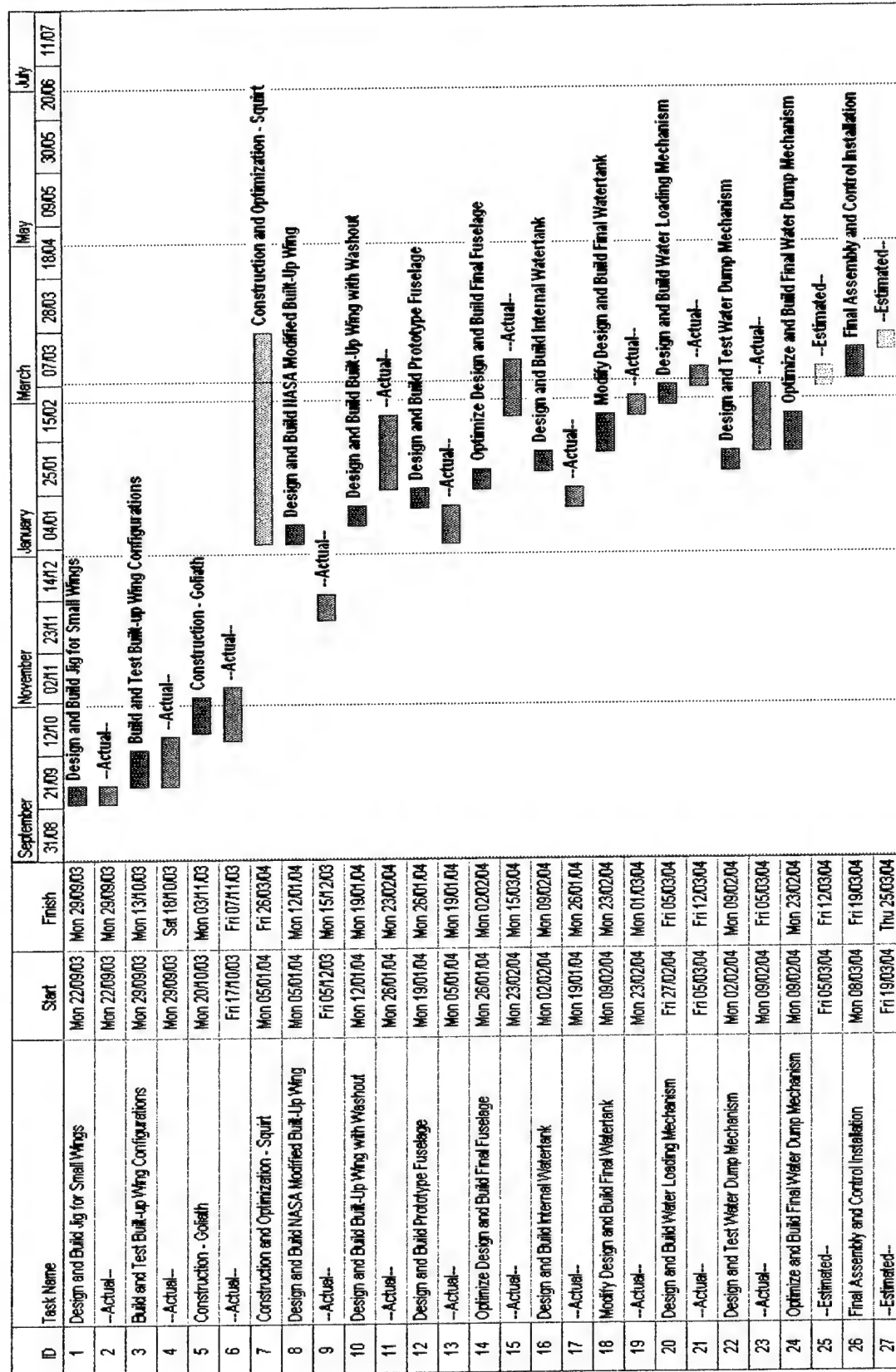
Though typical built-up construction involves the use of airfoil ribs as detailed in the Wing Construction section above, it was decided that this was not feasible for the size of tail required. As the horizontal and vertical stabilizers are quite small, a true built-up section would have proven to be quite heavy and time consuming to construct. Therefore, stick construction was utilized in order to provide the necessary profile and tail areas.

After deciding upon stick construction, work began with drafting software to produce the working drawings necessary to allow for the construction of the two stabilizers. A full-size layout of positioning of each of the $\frac{1}{4}$ " x $\frac{1}{4}$ " balsa sticks was completed with the aid of a CAD program. This template was then plotted and affixed to a slate table to ensure perfectly flat construction. Stringers were then cut to size, sanded and placed directly on top of the drawings in the designed configuration which ensures a high degree of accuracy during construction. Once completed, the stringers were then glued together and the leading edge rounded to reduce drag.

Once the vertical and horizontal stabilizers as well as rudder and elevators had been completed each surface was filled and sanded as necessary in preparation of covering. A self-adhesive heat-shrinkable Mylar covering was used to protect the balsa structure and bridge the open bays between the sticks. An alignment jig was then used in order align the vertical tail with the horizontal section. Once properly aligned, the two sections were glued together. A balsa fairing was then installed at the interface in order to reduce the interference drag generated. A blind nut was also included in this fairing in order to facilitate mounting to the fuselage.

Having completed the main surfaces, the rudder and elevators were attached to the tail through the use of Cyanoacrylate (CA) hinges. A sharp knife blade is used to cut a thin slot into both the tail section and control surface section. The CA hinge is then slid into one section, and glued in place through the use of Thin CA glue. Once affixed, the exposed end of the hinge is then slid into the remaining section and glued in place. Throughout this procedure appropriate clearance must be allotted to allow adequate deflection of the control surface.

Figure 6.1 – Gantt Chart of Manufacturing Timelines



7.0 Testing Plan

7.1 Test Objectives

Though a design may seem to work on paper, ensuring that it functions as expected is the primary objective of any test program. In order to fully test the construction techniques, airfoil, power system and fuselage design of this year's aircraft, a full scale prototype aircraft was proposed as an integral part of our test schedule. Table 7.1 provides a testing schedule along with anticipated test dates.

Table 7.1 – Test Objectives and Schedule

Test	Test Objective	Anticipated Test Dates
Wing Structure Testing	To determine the lightest wing practical for use on the competition aircraft.	September 2003 January / March 2004
Wing Strength Testing and Failure Mode Analysis	To compare the predicted and actual failure strength of a completed wing platform and analyze the resulting failure mode	September 2003
Fuselage Strength Testing	To determine the optimal structural configuration of the fuselage that will withstand in flight loading. To optimize the weight of the fuselage.	September / October 2003 January / March 2004
Water Systems Testing	To ensure that the water loading and dumping mechanism function as designed. To optimize the design of the internal water tank	January / March 2004
Flight Testing	To prove the final power system To compare the actual stability characteristics of the aircraft to predicted data. To provide the pilot opportunity to become acquainted with the aircraft and its handling characteristics.	November / December 2003 March / April 2004

7.2 Ground Testing

Ground testing comprises the first four test items of Table 7.1 and occupies the majority of the testing schedule. Throughout this series of testing programs, each major structural component of the aircraft was tested and refined many times with each iteration bringing the final design closer to the optimal configuration. Multiple full scale test sections of the fuselage, wing

and water tank were built and analyzed for weight, strength and functionality with modifications discussed amongst team members. The construction of "Goliath" also greatly improved the understanding of the interaction of various components and brought to light interface issues that would greatly simplify the construction of Squirt. A summary of the test results from the ground testing schedule proposed in Table 7.1 can be found in Table 7.2. Note that "Goliath" has been included as a separate entry.

Table 7.2 – Ground Testing Results

Test	Result
Wing Structure Testing	Reducing the weight of the wing through either decreasing the total number of ribs, or through including structural cutouts in the ribs is not practical. Weight savings are minimal (< 10 g) and the structural deficits created are large. - A standard built-up wing platform will be used.
Wing Strength Testing and Failure Mode Analysis	The I-beam spar configuration is stronger than predicted by a factor of 1 g (5 lbs for our test wing). - Updated I-beam strength modeling equations. Shear web buckling in the inboard section of the wing was the most common mode of failure. - Shear webs increased in thickness for the inboard 50% of the wing span
Fuselage Strength Testing	Balsa truss configuration too strong and heavy for this application. - Balsa stringers utilized throughout much of the design Fuselage in general heavier than necessary. - Plywood bulkheads replaced with balsa. Plywood doubling plates added where required. Frontal cross section very large and draggy - Components rearranged to reduce width by 0.75" and height by 1.25"
Water Systems Testing	Fiberglass tank too heavy for this application. Also, acetone does not eat foam as well as expected. - Tank design switched to foam from fiberglass to reduce weight Initial tank design required large fuselage cross section - Tank redesigned to integrate with bulkheads and provide structural strength. Allowed reduction in fuselage cross section. Initial water dump mechanisms leaked when tank was loaded. - Dump mechanism redesigned and tested many times. Results in a smaller, lighter and simpler system.
"Goliath"	- Identified Wing interface issue with fuselage - Proved that water tank AND batteries must be present over the predicted CG in order to properly balance aircraft. (Ballast was required rearward of the CG as the batteries had been located forward of the CG) - Increased skill in the use of metallic covering materials - Identified sheeted truss structure employed as overbuilt and unnecessary - Proved the use of cooling vents as an appropriate way to provide cooling to the motor and vent the water tank.

7.3 Flight Testing

In advance of the flight testing program, a flight testing checklist was developed to ensure that the plane would function as planned. The following are a summary of the main items addressed. Note that it is important that these procedures are observed before each flight, not just the first flight of the day.

- Ensure main flight pack, receiver pack and transmitter pack fully charged. Record power input into main pack during charge (mAh)
- Ensure all servo screws tightened securely.
- Ensure all control rods and clevises are attached and secured.
- Ensure propeller is secured tightly to motor with propeller nut.
- Verify neutral of position of servos with radio system.
- Verify proper direction of operation of control surfaces with radio system.
- Ensure proper failsafe setup on radio system in event of loss of contact through the use of the ON/OFF switch.
- Check flight board to ensure that no one else is flying with the same frequency in the vicinity.
- Perform range check to verify proper operation of radio system.
- Check runway for debris and clear as appropriate.

Flight testing results and lessons learned from "Goliath" can be viewed in Table 7.3. Flight testing will commence on Squirt as soon as the weather allows as the runway is currently snow covered.

Table 7.3 – Flight Testing Results

Item	Result
Power System	<p>Fully loaded takeoff distance of 90' recorded off of grass runway.</p> <ul style="list-style-type: none"> - Power system provides adequate thrust for takeoff. <p>Through the use of a Watt Meter, typical battery pack endurance is shown to be slightly over 4 minutes at flight speeds.</p> <ul style="list-style-type: none"> - Acceptable within in the context of the competition. <p>Top speed of aircraft estimated to be 55 mph.</p> <ul style="list-style-type: none"> - Within 5% of the estimated top speed of "Goliath". Power system shown to perform essentially as predicted.
Tandem Stability	<p>Tandem design was unstable in pitch</p> <ul style="list-style-type: none"> - Modifications to the CG, and AoA of both wings were unable to provide a stable flight envelope - Tandem design will not suffice for the competition
Control Surface Authority	<p>Servos found to have necessary torque for providing smooth control functions</p>

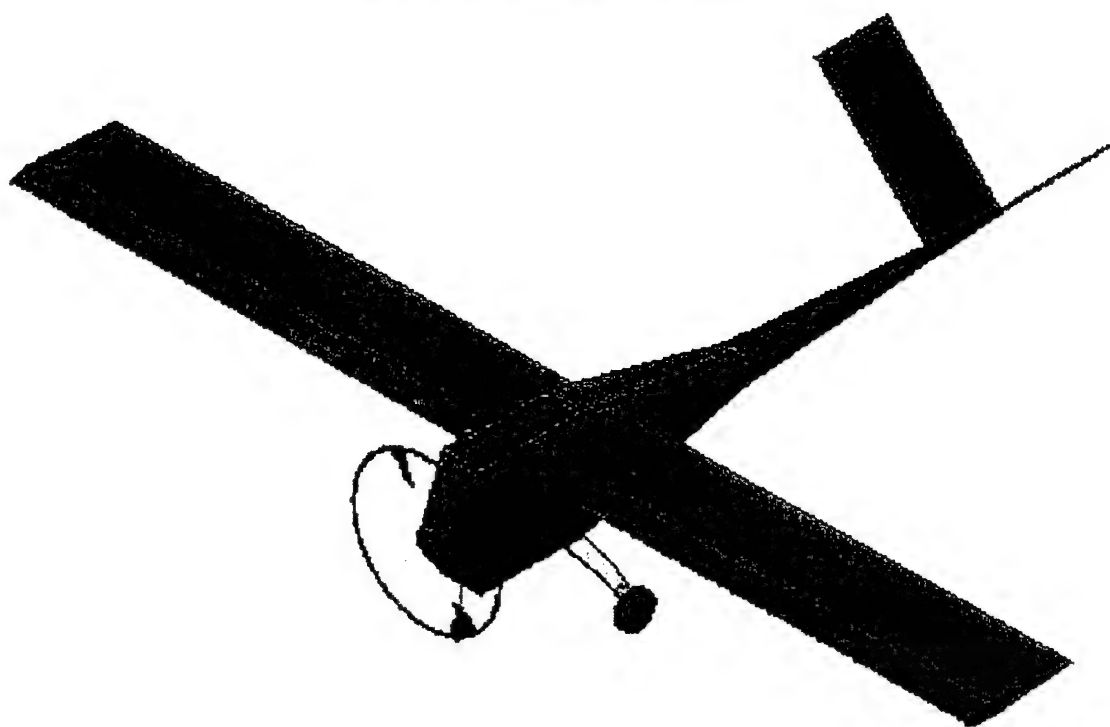
	<ul style="list-style-type: none">- Servos will be incorporated into final design (HS-81MG)Ailerons, elevator and rudder found to possess adequate control surface area and deflection to ensure quick aircraft response to commands.- Relative sizing of control surfaces relative to wing area will remain constant between Squirt and Goliath
Airfoil Selection	<p>Eppler 197 provided gentle enough stall characteristics to allow the pilot to avert many near crashes and return Goliath safely to the ground.</p> <ul style="list-style-type: none">- Airfoil proven. Eppler 197 incorporated into Squirt's design
Pre-Flight checklist	<p>Loss of propeller nut during final flight proves importance of adhering to pre-flight checklist before EVERY flight, not just first flight of the day.</p> <ul style="list-style-type: none">- Stowing garbage bags inside aircraft makes cleanup easier.- Pre-flight checklist procedures revised to ensure mishaps do not happen again.

8.0 References

1. Lennon, Andy. Basics of R/C Model Aircraft Design. Y. DeFrancesco: Ridgefield, CT. 1999.
2. Eppler, Richard. Airfoil Design and Data. Springer-Verlag: Germany. 1990.
3. Foster, Steve. "Undercarriage Design for Queen's Cargo Aircraft." Undergraduate Thesis Project, Department of Mechanical Engineering. March, 1994.
4. Horton, Johanna Lisa. "Cargo Aircraft Stability Analysis." Undergraduate Thesis Project, Department of Mathematics and Engineering. April, 1993.
5. McCormick, Barnes. Aerodynamics, Aeronautics, and Flight Mechanics, second edition. John Wiley & Sons, Inc.: New York. 1995.
6. Munson, Young, and Okiishi. Fundamentals of Fluid Mechanics, second edition. John Wiley & Sons, Inc.: New York. 1994.
7. Raymer, Daniel. Aircraft Design: A Conceptual Approach. AIAA Education Series. American Institute of Aeronautics and Astronautics, Inc.: Washington, D.C. 1989.
8. Abbott, Ira. Theory of Wing Sections. McGraw-Hill Book Company Inc.: Toronto. 1949.

2003-2004 AIAA Foundation Cessna/ONR Student Design Build Fly Competition

DESIGN REPORT



“Turbulence Syndrome”

**Virginia Polytechnic Institute
and State University**

March 2004

TABLE OF CONTENTS

1 Introduction.....	1
1.1 Executive Summary.....	1
1.1.1 Conceptual Design	1
1.1.2 Preliminary Design.....	1
1.1.3 Detailed Design	1
2 Team Management Summary.....	2
3 Conceptual Design	6
3.1 Mission Requirements.....	6
3.1.1 Aircraft Storage and Assembly.....	6
3.1.2 Takeoff and Landing	6
3.1.3 Mission Emphasis.....	6
3.1.4 Aircraft Cost Considerations.....	7
3.2 Aircraft Concept Features and Configurations	7
3.2.1 Figures of Merit.....	7
3.2.1.1 Wing Configuration	7
3.2.1.2 Tail Configuration.....	8
3.2.1.3 Landing Gear.....	9
3.2.1.4 Tank Design	10
3.2.2 Concept Configurations and Decision	11
3.3 Conceptual Design Conclusions.....	14
4 Preliminary Design	15
4.0.1 Standard Values for preliminary calculations	15
4.0.2 Maximum aircraft weight	15
4.1 Wing	16
4.1.1 Wing sizing	16
4.1.2 Wing Structure Concepts	16
4.1.2 Traditional Wing Structure.....	16
4.1.3 Spar Analysis and Testing	17
4.2 Tail.....	19
4.2.1 V-tail Sizing	19
4.2.2 V-tail Structure.....	19
4.3 Payload.....	20
4.3.1 Tank Drain Time Analysis	20
4.3.2 Tank Structure.....	20
4.4 Fuselage.....	23

4.4.1 Fuselage Configuration	23
4.4.2 Fuselage Structural Analysis	23
4.4.3 Tail Boom	24
4.4.4 Tail Boom Analysis	25
4.5 Propulsion.....	27
4.5.1 Motor and Battery Configurations.....	27
4.5.2 Motocalc™ Results.....	28
4.5.3 Final Configurations.....	28
4.6 Stability and Control.....	28
5 Detailed Design.....	29
5.1 Wing	29
5.2 Tail.....	31
5.3 Fuselage.....	31
5.4 Landing Gear	32
5.5 Payload.....	32
5.6 The Propulsion System	33
5.7 RAC	34
5.8 Final Aircraft Configuration.....	35
5.9 Drawing Package	38
6 Manufacturing Plan.....	44
6.1 Manufacturing Processes Investigated	44
6.1.1 Wing Construction	44
6.1.2 Fuselage Construction	45
6.1.3 Empennage Construction.....	46
6.2 Figures of Merit Used	46
6.2.1 RAC	46
6.2.2 Weight.....	46
6.2.3 Performance.....	47
6.2.4 Ease of Construction.....	47
6.2.5 Stability and Control.....	47
6.2.6 Reliability	47
6.2.7 Repair.....	47
6.2.8 Cost of Construction	47
6.3 Selected Processes for Major Component Fabrication	48
6.3.1 Wing.....	48
6.3.2 Fuselage	48
6.3.3 Empennage	49

6.4 Timeline for Manufacture.....	49
7 Testing Plan	51
7.1 Test Objectives and Schedule.....	51
7.2 Detailed Test Objectives and Results	51
7.2.1 Tank Drain Test	51
7.2.2 Oil Flow Visualization Test	52
7.2.3 Wing Structural Test	52
7.2.4 Propulsion System Performance Test	53
7.2.5 Landing Gear Structural Test	53
7.2.6 Wing-Fuselage Interface Structural Test	53
7.2.7 Fuselage	53
7.2.8 Empennage	53
7.2.9 In-Flight Performance Test.....	54
8 References	57

1 Introduction

1.1 Executive Summary

This report is an overview of the design, manufacturing, and testing procedures used in the development of the Virginia Polytechnic Institute and State University (Virginia Tech) entry in the 2004 Design, Build, and Fly competition; Turbulence Syndrome. This aircraft was designed to complete the predefined missions; the Fire Bomber Mission and the Ferry Mission.

1.1.1 Conceptual Design

A traditional three-phase design model was adopted in the development of the aircraft with Figures of Merit (FOM) heavily used for each phase. For the conceptual design phase, both the mission and the general shape of the airplane itself were investigated. The mission analysis also determined that the rated aircraft score was heavily dependent upon the amount of water carried. The majority of conceptual design was spent on general concepts of aircraft. The team split into four conceptual groups and each designed its own ideal aircraft. This served two purposes: it helped the new members become more comfortable with actual aircraft design and helped start the development of several new ideas all at once. These designs will be further investigated in Section 2 of this report. This investigation provided a foundation on which to base the preliminary designs. Each design was rated and put into a spreadsheet to calculate FOM. Finally, a conceptual design was chosen based off the resultant FOMs in the analysis.

1.1.2 Preliminary Design

The preliminary design phase consisted of basic sizing and integration of the initial conceptual design ideas. Since several of the conceptual designs were similar, the final idea of the plane is a blend of these ideas. During this phase, parameters were identified in order to stay within several budgets. These included but were not limited to: power budgets, weight budgets, servo budgets, and ease of manufacturing budgets. These will be discussed in greater detail in Section 3. Each component of the airplane was rated according to these parameters, and the best was selected for use in the aircraft. In addition, missions were modeled in more detail to allow for better understanding of the design parameters.

1.1.3 Detailed Design

The detailed design phase included several methods of analysis that were utilized to define the final aircraft specifications. The methods of analysis were dynamic stability analysis, computational aerodynamics, mission flight simulation, structural analysis and physical experimental testing. The results of this testing were then utilized to finalize the dimensions of the aircraft, system architecture, aircraft performance and selection of the components. The drain time of the tanks was a major area of concern on the flight qualities of the aircraft and the final score. The tank system was optimized to have a low-weight, high flow design that worked reliably.

At the conclusion of the detailed design phase of the Turbulence Syndrome team contest effort, the team had defined the system component selection and final dimensions of the aircraft. With this information, the team was able to calculate the stability and performance of the aircraft. This in-depth design and analysis gave the team confidence that it would accomplish its goals for the 2003-04 Design/Build/Fly Competition.

2 Team Management Summary

The Virginia Tech DBF team consisted of 48 undergraduate students and one graduate student all enrolled in either Aerospace or Mechanical Engineering. To deal with a group this large, an effective organization plan had to be developed in order to utilize everyone's skills and, produce a well-built aircraft on time.

The executive leadership of the team was composed of a program manager, chief engineer, senior graduate consultant (SGC), senior undergraduate consultant (SUC), secretary, treasurer, six function-team leaders and six component-team leaders. The six function-teams were the Aerodynamics and Controls Team, Propulsion and Electronics Team, Aircraft Performance Team, Structures Team, Testing/Integration Team and Manufacturing Team. The six-component teams were Wing Team, Fuselage Team, Landing Gear Team, Drafting Team, Tank Team and Tail Team. An effort was made to organize the internal structure of the team in respect to past years. The result of this new organization structure was shorter completion times for all sub-projects and better communication throughout the team.

The program manager had the primary function of guiding the team through the entire project, from conceptual design to competition. The program manager was responsible for keeping the team on schedule, and integrating the efforts of each team. The first challenge for the program manager was recruiting new team members by raising interest in students of all academic levels. As a result of recruiting efforts, the team size doubled from last year, expanding the team's vision for future competitions. The chief engineer had the task of guiding the team's technical progress and assessing the validity of the results that are produced on an individual basis and in relation to other components.

The function-teams were a method to organize people into their knowledge areas. Once assigned to a function team, the member was assigned to a component team made up of members from the other function teams. The co-mingling of function team members in one component team facilitated cross-team communication. The Drafting Team produced accurate and timely drawings of system components for prototyping and detail design work. The Integration/Testing team performed component testing to determine interoperability of the various systems. The Fuselage Component Team was responsible for determining the structural stability and integrity of the aircraft and designing the internal layout of the fuselage along with integrating the motor and tank compartments. This team also played an integral role in material selection for major structural elements. The Wing Component Team and Tail Component Team designed the wing and tail portions of the aircraft for both aerodynamic and structural criteria. These teams also designed control surfaces to optimize stability and control. Methods of water

deployment and tank placement were determined by the Tank Component Team. The Landing Gear Component Team optimized and constructed a gear system that was able to support the aircraft during takeoff and landing as well as be lightweight.

This organization style distributed the workload evenly, allowing the team to complete the design process in a timely fashion. Figure 2-1 shows the planned and actual timing of major elements of the design process. The planning of these times was based off past years and the ability of the team. Figure 2-2 details the managerial layout and team organization.

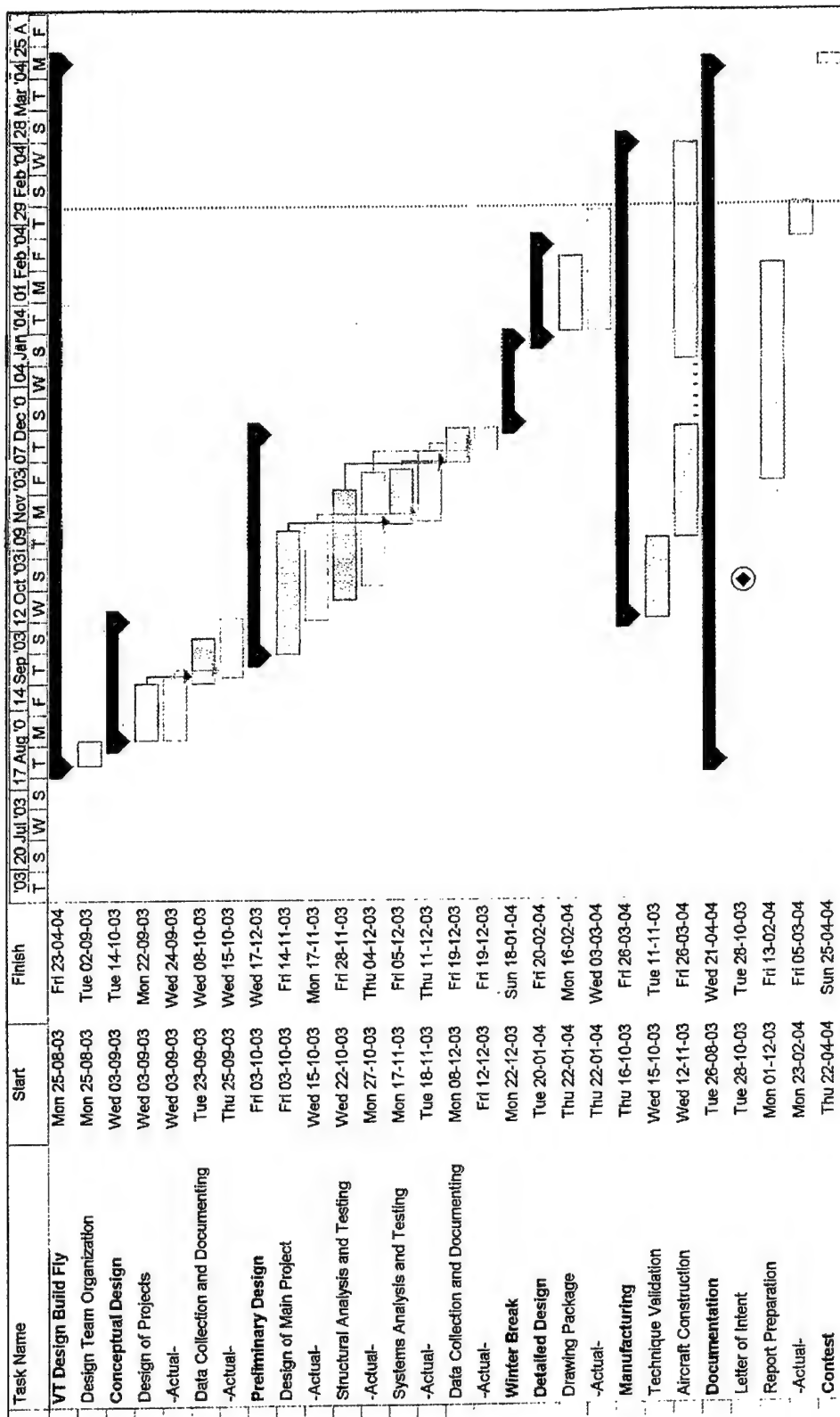


Figure 2-1: Virginia Tech Design/Build/Fly 2003-2004 Schedule

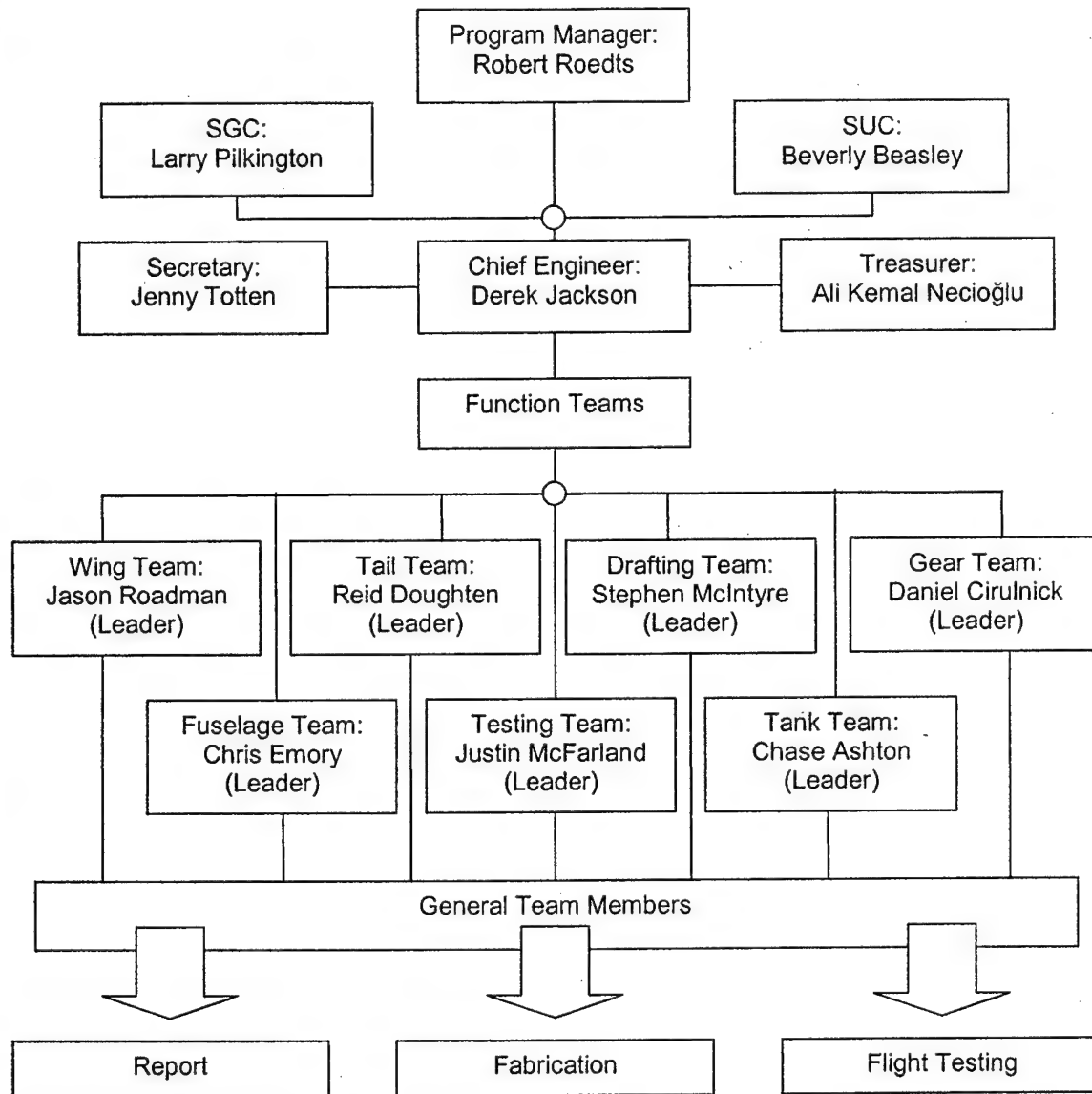


Figure 2-2: Managerial Layout

3 Conceptual Design

The goal of conceptual design was to evaluate the mission requirements, compare configuration features with FOM, construct complete concept configurations, and evaluate the conceptual designs with a decision matrix. One of two missions was chosen as the focus for design, and early approximations of weight and rated aircraft cost (RAC) were determined as concept evaluation criteria.

3.1 Mission Requirements

Two missions were specified under the competition rules: a Fire Bomber Mission and a Ferry Mission. One mission must be chosen for each flight, but both missions may be attempted separately for competition. The sum of the single best flight scores from each mission is the total flight score.

3.1.1 Aircraft Storage and Assembly

The aircraft must be able to fit in a rectangular box with inner dimensions of 1 ft by 2 ft by 4 ft. In contrast to last year's requirements, there is no timed assembly.

3.1.2 Takeoff and Landing

For both missions, the aircraft must be able to takeoff within 150 ft. The aircraft must land on the runway, but the flight score will still be accepted if the aircraft rolls off the runway after landing. The flight score will be zero if the aircraft exceeds the maximum takeoff distance.

3.1.3 Mission Emphasis

With a difficulty level of 2.0, the Fire Bomber Mission heavily affects the total flight score. The mission consists of two sorties; each sortie consists of loading the aircraft, takeoff, and dumping the water on the downwind leg of the flight path. The maximum water capacity is 4 L, which must be loaded from four unpressurized 2-liter soda bottles. The water must be dumped between upwind and downwind turn markers as signaled by the pilot. A single 360° turn must be completed on the downwind leg of each lap. The water tank opening may not exceed 0.5 in. at the exit. Time penalties will be given for inadvertent dumping of water, an incomplete second lap, excessive water spillage during loading, and any unloaded water at final landing. The mission score is determined by the difficulty factor multiplied by pounds of water divided by flight time.

The Ferry Mission has a difficulty level of 1.0. For this mission the unloaded aircraft must complete four laps of the standard flight path, including a 360° turn on each downwind leg. Time penalties are added for any incomplete laps. The mission score is simply the difficulty level divided by the flight time.

The Fire Bomber Mission was chosen for emphasis in conceptual investigations since it imposed the most constraints on final aircraft design.

3.1.4 Aircraft Cost Considerations

RAC greatly affects the final aircraft score. It is determined based on size and complexity of the aircraft design through factors such as empty weight, engine power, and manufacturing hours. An approximate RAC was determined for the conceptual design process; it will be further studied in Section 5.

3.2 Aircraft Concept Features and Configurations

Conceptual aircraft design features, specifically the wings, tail, landing gear, and tank design, were compared based on past experience, academic aerospace engineering background, and comparator aircraft studies. The conceptual features were then incorporated in several possible configurations for final evaluation.

3.2.1 Figures of Merit

Numerical FOMs were used to compare various aircraft features on a scale of 1 (poor) to 5 (excellent). Each feature was evaluated on the basis of RAC, performance, reliability, ease of construction, weight, and stability and control. The importance of each of the six criteria was rated by each function and component team leader to determine a final score.

3.2.1.1 Wing Configuration

Five wing configurations were evaluated on the six chosen criteria for conceptual design: biplane, low-wing, mid-wing, high-wing, and flying wing configurations. The numerical FOMs for wing configuration are given in Table 3-1.

The biplane wing configuration was investigated for its high lift, low speed qualities. However, the RAC and weight penalties incurred were more than enough to disqualify biplane designs. Initial analysis showed that the tail span of the biplane would be greater than 25% of the wingspan, resulting in a third wing penalty for RAC. The biplane would also be more time consuming for construction because of the additional structural members needed to integrate the wings with the fuselage.

Three variations of a conventional mono-wing configuration were studied. The low-wing and mid-wing resulted in the same FOM score. Low-wings and mid-wings are both proven reliable concepts, perform well, and are stable in flight. However, both designs would require significant integration with the fuselage structure where the tanks would be located. A high-wing design impacts the RAC and weight the same as low and mid-wings, but since the wing is located above the vertical center of gravity, it increases the aerodynamic stability of the aircraft. The high-wing also improves performance because it eliminates downwash from the fuselage over the wing. Additionally, the high-wing would ease construction by not interfering with tank placement in the fuselage. As indicated by the FOMs, the high-wing configuration would be the best choice for the above stated reasons.

A flying wing design was also investigated. Flying wings improve the RAC and weight because fewer surfaces are necessary. Flying wings also have higher volumetric capacity for payload storage.

However, as evidenced by past teams, the flying wing is more difficult to balance and problematic at takeoff.

Table 3-1 Wing Configuration FOM

	RAC	Weight	Performance	Construction	S & C	Reliability	TOTAL
<i>Weight</i>	<i>0.16</i>	<i>0.16</i>	<i>0.19</i>	<i>0.15</i>	<i>0.17</i>	<i>0.17</i>	
Biplane	1	2	3	2	4	3	2.54
Low-wing	4	4	5	4	4	4	4.19
Mid-wing	4	4	5	4	4	4	4.19
High-wing	4	4	5	5	5	4	4.51
Flying wing	5	5	4	5	1	2	3.62

3.2.1.2 Tail Configuration

Six tail configurations were evaluated on the six chosen criteria for conceptual design. The six empennage configurations studied: conventional, T-tail, H-tail, V-tail, Y-tail, and inverted V-tail. The results of the tail investigation are given in Table 3-2.

The conventional tail was initially studied because of its proven reliability and ease of construction. It could easily be implemented on almost any design. Given its familiarity, the conventional tail would result in a low RAC and weight. However, the conventional tail was only mediocre in terms of performance and stability when compared to other empennage configurations. Since performance and stability carried the largest weight in the FOMs, the conventional tail was not selected for use on the aircraft.

A T-tail configuration was investigated as another tail option. The T-tail scored fairly well for RAC and weight but was eliminated on the basis of stability and reliability. T-tails are prone to early stall because of downwash from the wing at high angles of attack.

The H-tail was considered as a possible configuration because it was used by the team last year. From this experience, the H-tail was rated high for good reliability and ease of construction. However, the three surfaces composing the H-tail negatively impact RAC, weight, and performance. The H-tail was eliminated mostly because of its weight; the team wanted to keep the tail light for RAC concerns.

V-tails, Y-tails, and inverted V-tails have been shown to have improved stability characteristics over other empennage configurations. The dihedral of the V- and Y-tails give the same stability performance with less total surface area. The reduction of wetted area results in lower drag. With fewer surfaces to manufacture, the V-tails were rated as high as conventional empennage configurations for ease of construction. The need for additional construction eliminated the Y-tail from competition. The inverted V-tail was rated higher than the regular V-tail in stability and control because it had favorable roll reversal characteristics, whereas the regular V-tail had detrimental roll reversal effects. The inverted V-tail

was rated very low for performance because it would be prone to scraping the ground on takeoff. With all factors considered, the upright V-tail was chosen as the final empennage configuration.

Table 3-2 Tail Configuration FOM

	RAC	Wt.	Perf.	Const.	S & C	Reliability	TOTAL
<i>Weight</i>	<i>0.15</i>	<i>0.14</i>	<i>0.19</i>	<i>0.14</i>	<i>0.22</i>	<i>0.17</i>	
Conventional	4	5	4	5	3	5	4.27
T-tail	4	4	3	3	2	2	2.93
H-tail	3	3	3	4	3	5	3.51
V-tail	5	5	5	5	4	4	4.66
Y-tail	3	3	4	3	4	3	3.44
Inverted V-tail	5	5	2	5	5	4	4.31

3.2.1.3 Landing Gear

Two types of landing gear were evaluated, fixed and retractable. The first part of Table 3-3 shows the results of the investigation. The team's previous experience with retractable landing gear coupled with other teams' difficulties with this type of gear at competition ultimately led to its poor ranking. Fixed gear was chosen because it offered fewer failure points.

Four types of fixed landing gear were selected for further investigation: music wire, Marooned-type, aluminum, and custom aluminum. The results of the fixed landing gear investigation are shown in the second part of Table 3-3.

A music wire landing gear had been built by many team members and had proven reliable on smaller scale model aircraft. Their simple construction and ease of repair made them a desirable solution. The high loading applications anticipated would require a heavy gauge wire, and this ultimately disqualified the music wire landing gear because of high weight.

The landing gear used on the 2001-2002 Virginia Tech aircraft, Marooned, was investigated. This gear was of a fixed design utilizing wood, fiberglass, and carbon fiber. While this design worked during competition, fabrication difficulties and integration problems led to the disqualification of this design.

The aluminum gear category encompassed all commercially available landing gear premanufactured from aluminum. Models designed for aircraft weighing up to 15 lbs were available. While the loaded aircraft weighed in excess of this rating, the landing gear would provide an acceptable solution for the unloaded configuration and would work during initial flight testing.

The custom aluminum category encompassed all types of aluminum landing gear fabricated by the team. While less reliable and more difficult to construct than commercially available gear, increased strength made this type of gear desirable. Ultimately the decision to work with commercially available

gear was made. If this design proved inadequate, modifications could be made utilizing a model fabricated by the team.

Table 3-3 Landing Gear FOMs

	RAC	Wt.	Perf.	Const.	S & C	Reliability	TOTAL
<i>Weight</i>	0.12	0.17	0.13	0.19	0.13	0.26	
Fixed	4	4	3	5	2	4	3.66
Retractable	1	2	5	2	4	1	2.50
Music Wire	5	5	3	5	3	3	3.96
Aluminum	4	4	5	5	5	5	4.71
Custom Aluminum	3	3	4	3	5	4	3.65
Marooned	2	2	3	4	2	3	2.77

3.2.1.4 Tank Design

The criteria for tank design concepts were modified to reflect true cost, feasibility, and durability. Three tank ideas were then compared: premanufactured, plastic-molded, and stereolithography. The FOM for tank design is given in Table 3-4.

Premanufactured tanks include motor oil bottles, plastic kitchen containers, and R/C gas tanks. These tanks are readily available, thus giving them a high score for cost and feasibility. The thickness of these tanks, while increasing durability, also increases weight and difficulties with modification. Despite these drawbacks, this tank design would prove most beneficial for the team.

Plastic molded tanks provided better adaptability with the fuselage. These tanks would have to be manufactured entirely by the team, resulting in a low score for construction. However, with the responsibility of manufacturing comes better control over the final weight. The materials for this tank design are inexpensive and easily obtainable, thus rendering it very feasible. The inexperience of the team with this type of construction could potentially affect the durability, which was the ultimate cause for its elimination.

Stereolithography was explored as another option. A stereolithography tank was desirable for its flexibility in design, light weight, and strength. The construction would be easy, needing only a CAD drawing to feed the machine; however cost and lack of available machinery hindered this option's selection for final tank design.

Table 3-4 Tank Design FOM

	Cost	Wt.	Feasibility	Const.	Durability	TOTAL
<i>Weight</i>	0.16	0.19	0.21	0.18	0.26	

Premanufactured	4	2	5	3	5	3.91
Plastic molded	4	4	4	2	3	3.38
Stereolithography	1	4	2	5	5	3.54

3.2.2 Concept Configurations and Decision

As decided by FOMs, the final conceptual design would feature a high-wing, upright V-tail, fixed aluminum landing gear, and modified premanufactured tanks. Given these decisions, the team began assembling the various features into complete conceptual designs. The conceptual design configurations were presented and evaluated by the team with a decision matrix.

One design concept, the Super Stik, featured a long, slender, vertically rectangular fuselage and a rectangular wing. The rectangular fuselage would allow maximum height for draining the water, while the rectangular wing would optimize the lift, area, and RAC. Super Stik's components consisted of one motor, one speed controller, and servos for the rudder, elevators, and ailerons. To reduce the fuselage RAC and more evenly distribute the wing loading, the batteries were mounted in or under the wing. The water tank and fuselage were molded as one structure. The wing was given a high aspect ratio to reduce frontal cross sectional area, allowing low drag and high speeds. In order to fit in the box, the maximum fuselage length was 4 ft, and the empennage section and outer wing sections would be detachable. Super Stik is illustrated in Figure 3-1.

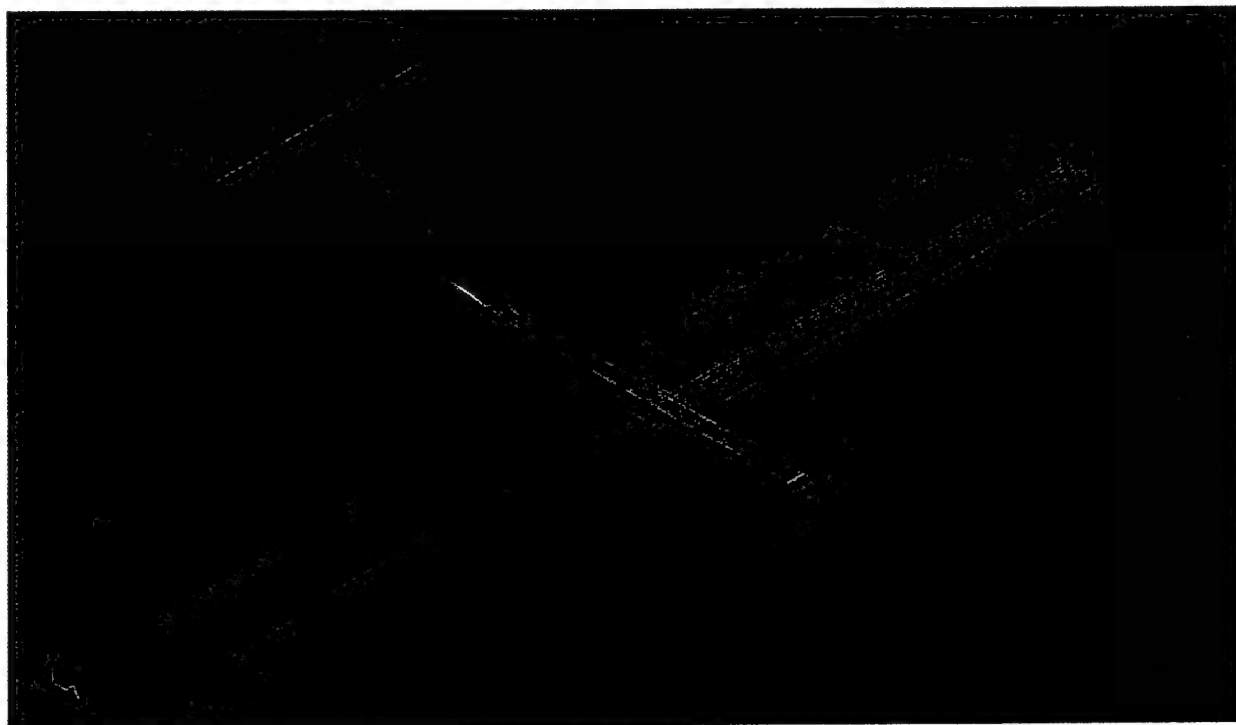


Figure 3-1: Super Stik Concept

Another concept considered was the NDY-2E. This concept would be easy to build. It featured dual engines, a triple tail boom, and the use of the tank as a structural element. The fuselage would be easily modified for maximum aerodynamic efficiency; its structural elements consist of carbon tube stringers with balsa wood for shaping. All electronics would be shielded from water by housing them in wing pods with the motors, which would also serve to distribute the wing loading. A 6-inch aluminum spinner would be used on the nose for ease of construction. The empty weight and RAC were estimated as 16 lbs and 17, respectively. NDY-2E is illustrated in Figure 3-2.

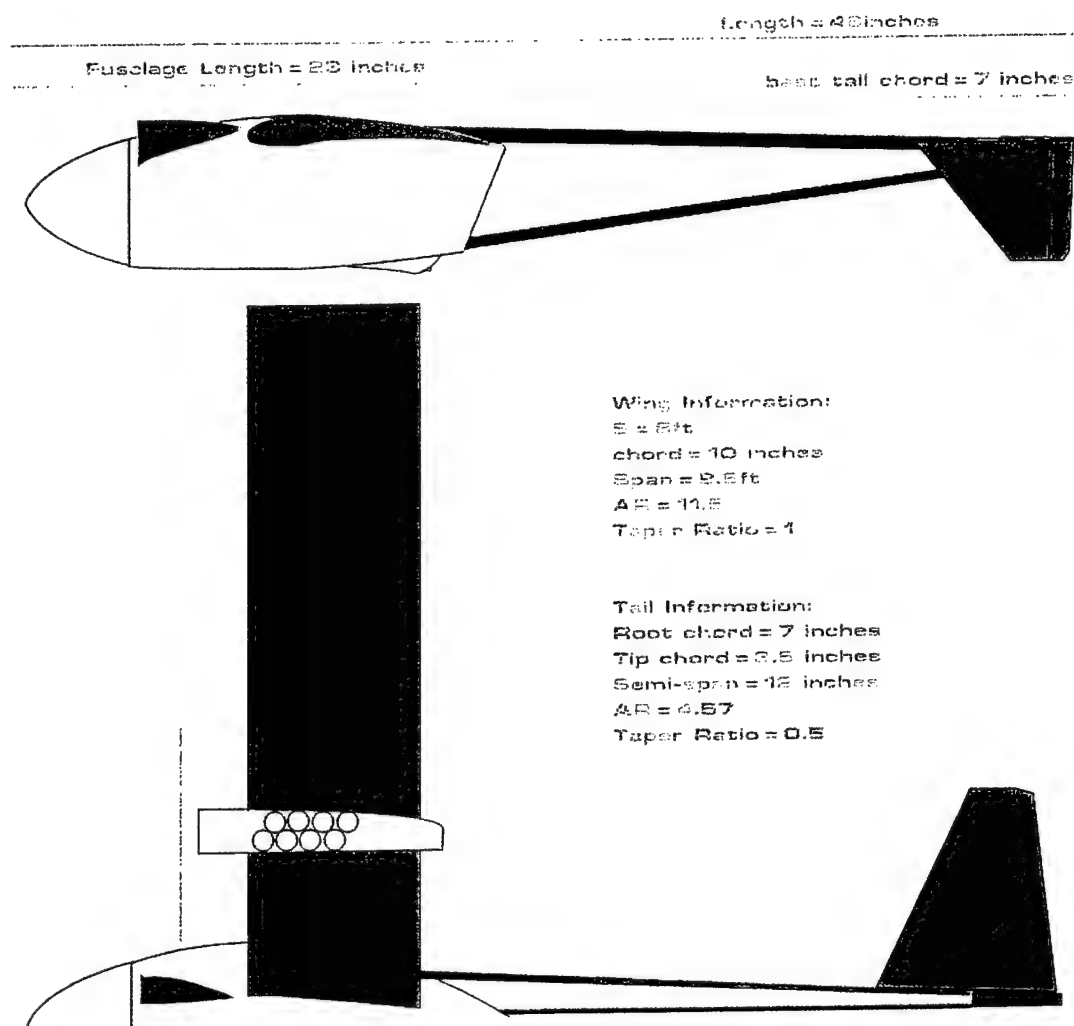


Figure 3-2: NDY-2E Concept

The Kingfisher concept was designed to maximize the height of the tank and minimize drain time. Halving the drain time would nearly double the team's total score. The static drain time of the tank (11 in. high, 4 in. wide, 6 in. long) was estimated as 26 sec. Partitions would be added inside the tank to mitigate sloshing. The total weight would be 28 lbs, with a total length of 6 ft (2 ft fuselage, 3 ft tail boom, and 1 ft tail chord). The frontal area would be 250 in.² for low drag. The wings had an aspect ratio of 5.5 and 13.9 ft² of area. Four degrees of dihedral would be added for increased stability, and the wing loading would be

32.2 oz/ft². Initial sizing of the V-tail resulted in a horizontal area of 3.09 ft² and a vertical area of 1.35 ft² (Raymer). The moment arm from the quarter-chord of the wing to the quarter-chord of the tail would be 3.6 ft, and the V-tails would have an angle of 45° from horizontal for ease of construction. Tricycle landing gear was incorporated into this design. Initial calculations gave an estimated RAC of 16.7 and takeoff distance of 127 ft. The Kingfisher concept is illustrated in Figure 3-3.

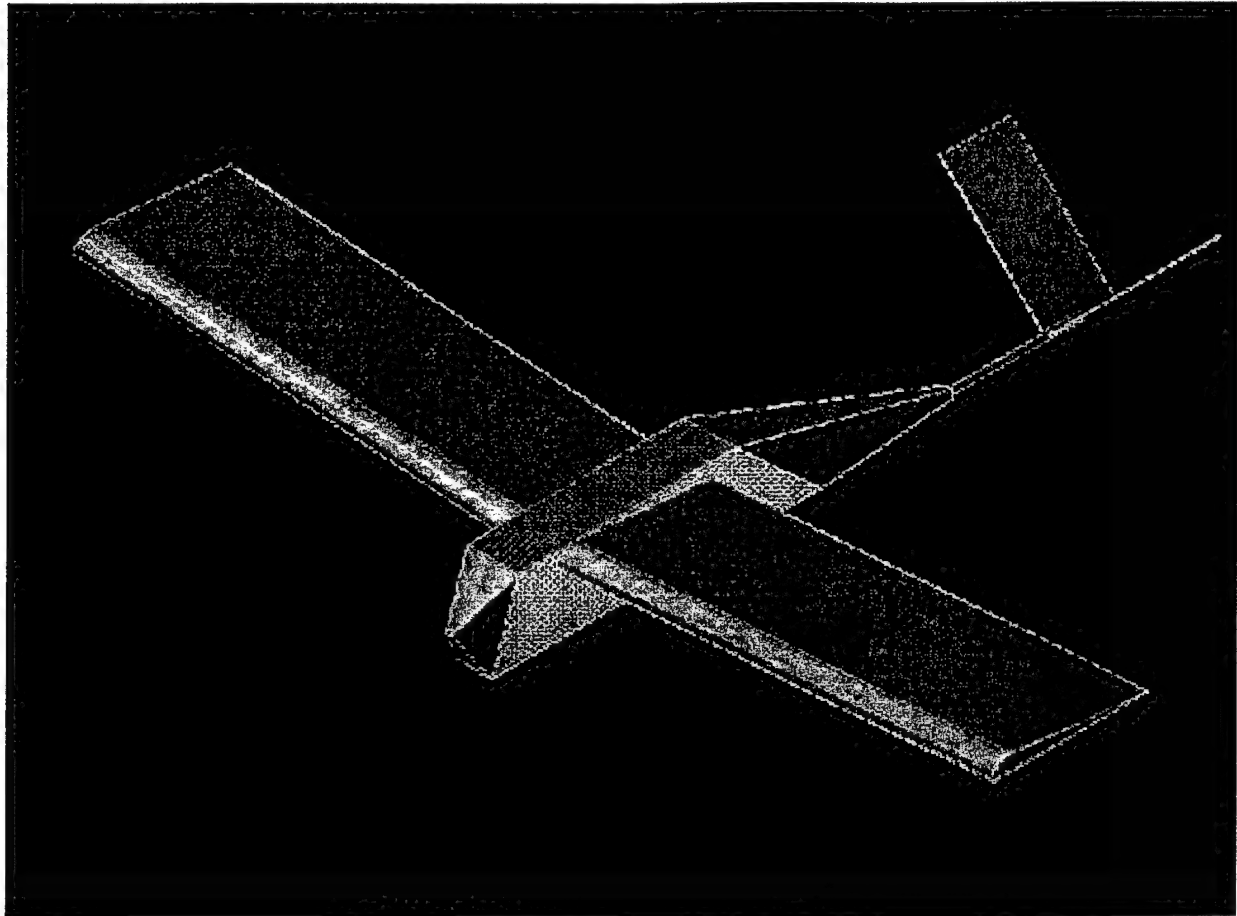


Figure 3-3: Kingfisher Concept

The Otto concept had a predicted takeoff distance of 95 ft. This was due to its huge wing area (9 ft span, 15.5 in. chord). The Otto would have circular ribs framing the fuselage and an 18 in propeller. The total length of the aircraft was 4 ft to ensure that it fit in the box. A 9 in. tall tank would allow fast drain time, and the tank would be positioned under the quarter chord of the wing. The tank would only be 6.5 in. long in order to minimize free surface wave effects. The RAC was estimated as 16.6, and the weight as 28.8 lbs. The Otto is illustrated in Figure 3-4.

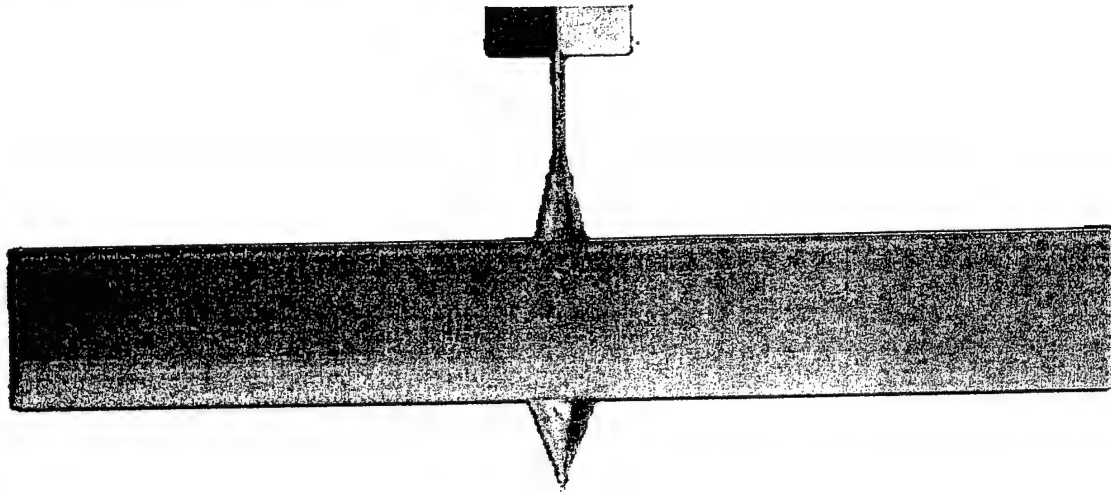


Figure 3-4: The Otto Concept

The configurations discussed above were evaluated in an FOM, Table 3-5. The Otto was eliminated because the tail was not large enough to give adequate stability, and the frontal area was quite large, thus increasing drag. The Super Stik was eliminated because it would have been tail heavy. The NDY-2E was eliminated on the basis of complexity and multiple engines, though it did demonstrate remarkable prospects for aerodynamic performance. Overall, the Kingfisher concept was rated the best. It was deemed a compromise of the best qualities of all concepts considered.

Table 3-5: Concept Configuration FOM

	RAC	Weight	Performance	Construction	S & C	Reliability	TOTAL
<i>Weight</i>	0.17	0.17	0.19	0.15	0.15	0.17	
Super Stik	5	4	3	4	4	3	3.81
NDY-2E	3	3	5	2	5	4	3.70
Kingfisher	4	4	4	4	5	5	4.22
Otto	4	3	2	3	1	3	2.68

3.3 Conceptual Design Conclusions

During conceptual design, the team studied and evaluated the mission requirements to begin designing an airplane for competition. The aircraft should be able to carry and deploy up to 4 L of water, takeoff within 150 ft, and fit in a box of previously specified dimensions, among other requirements. Upon evaluating the mission, the team investigated several concept features for the wing, tail, landing gear, and tank design. The team chose a high-wing, V-tail, fixed aluminum landing gear, and premanufactured tanks. The team incorporated these features into four different conceptual configurations. The team chose Kingfisher as the winning concept, renamed it Turbulence Syndrome, and progressed to preliminary design.

4 Preliminary Design

After the basic configuration for Turbulence Syndrome was chosen, analysis began on a more detailed level of each component. The main components of the aircraft were payload, fuselage, wing, tail, landing gear, propulsion and stability and control. Throughout the analysis, these components were optimized for flight performance and structural integrity while maintaining the lowest possible RAC. Incorporating these results into an iterative process, the basic dimensions of the aircraft and the maximum desired weight were chosen.

Throughout the preliminary design there was a continued focus on completing the mission that would give the most allowable points, the Fire Bomber Mission. There was also an emphasis on the idea of interchangeable parts. If a component were to fail during flight testing, that piece would be replaced easily with no change to the adjoining parts.

4.0.1 Standard Values for preliminary calculations

During parts of the conceptual and a majority of the preliminary design, initial values were used for basic sizing of the wing, tail, fuselage and propulsion. These values were outlined by the Chief Engineer and are listed in Table 4-1.

Table 4-1: Standard Values

Takeoff Velocity, V_{to}	$1.2 \cdot V_{stall}$
Takeoff Distance, S_{to}	150 ft
Coefficient of kinetic friction During ground roll, μ_k	0.005
Wing Drag Coefficient, C_{do}	0.05
Maximum Lift Coefficient, C_{Lmax}	1.2
Static Thrust, T_o	9 lbs
Wing loading, W/S	40 oz/ft ²
Maximum Airspeed, V_{max}	55 mph
Air Density, ρ	0.002 sl/ft ³

4.0.2 Maximum aircraft weight

Before any performance or stability calculations were run, there was a need to determine the maximum gross weight. Using the weights from comparator aircraft and taking into account the weight for 4 L of water, the maximum gross weight was set to a conservative 27 lbs. During the initial weight estimation, the following assumptions from conceptual design were made: 1 motor, 34 battery cells, 1 receiver battery, wing weight of 0.5 lbs/ft² and a tricycle landing gear configuration.

4.1 Wing

From the performance optimization of takeoff distance, the wing was sized to have a 9 ft span and 12 in chord. The airfoil chosen was a Clark Y with a 12% or 1.4 in. maximum thickness based on its aerodynamic qualities.

4.1.1 Wing sizing

The initial sizing of the wing was set by the maximum gross weight and required takeoff distance. The standard values stated in Section 3.0.1 and the maximum weight was input into a MATLAB wing area versus takeoff distance estimation program. The initial sizing returned a wing area of 8 ft². This wing had a corresponding wing loading of 54 oz/ft². For most R/C aircraft the nominal wing loading limit is 40 oz/ft². When the area was calculated for a wing loading of 40 oz/ft², the corresponding area was 10.8 ft². This value was too large and increased the RAC dramatically. After further performance analysis the wing area was chosen to be 9 ft² with a wing loading of 48 oz/ft². This wing loading was acceptable because the wing loading will be reduced after the payload is released. Using this wing area, a rectangular wing was designed with a span of 9 ft and a chord of 1 ft.

4.1.2 Wing Structure Concepts

The driving motivation for the design of the wing was that it could be easily constructed and repaired, lightweight, and simplistic construction, so that there would be less chance for error. Three configurations for the wing structure were examined; hollow-molded, composite foam cored, and traditional built-up spar and ribs. Table 4-2 shows a figure of merit for each design. Once all three were analyzed it was determined that the traditional built-up wing would be the optimal choice. There was prior knowledge of traditional building techniques, and a traditional wing could be developed quickly.

Table 4-2: Wing Design FOM

	Cost	Wt.	Feasibility	Const.	Durability	TOTAL
<i>Weight</i>	<i>0.16</i>	<i>0.19</i>	<i>0.21</i>	<i>0.18</i>	<i>0.26</i>	
Hollow-molded	3	5	2	3	2	3.17
Composite	3	3	3	1	5	3.17
Traditional	4	5	5	5	3	4.32

4.1.2 Traditional Wing Structure

The basic design of the traditional wing consisted of a spar with carbon fiber caps, balsa ribs and sheeting. The critical design parameters were set by the results from the performance analysis and the dimensions of the box that the wing must fit in. From these criteria the spar (Figure 4-1) was designed to have a maximum height of 1.4 in. and be capable of holding the aircraft when lifted at the tips with a 13 lb point load upward at each tip. Due to the large span, the wing needed to be split into three independent

sections so it would fit in the box. The outboard sections measured 37 in. each, and the inboard section measured 46 in.

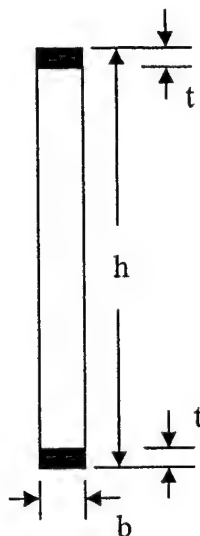


Figure 4-1: Spar layout

4.1.3 Spar Analysis and Testing

The initial design was composed of an end-grain balsa core material with 3 layers of carbon on each die. This structure did not hold up under testing. The center section spar failed when the cap buckled and debonded from the balsa core. To remedy this problem the entire spar was wrapped in fiberglass. With the wrapped spar, the outer section spars failed under a load of 5 lbs instead of the calculated 15 lbs. By inspecting the failure, it was apparent that the spar cap was too thin and the balsa core was not supporting the cap sufficiently.

The first step in modifying the spar design so handle higher loading was to compare the wing with a comparator wing. The Allegra Lite R/C glider, designed by Mark Drela, was examined because it had a similar spar structure. The glider can be launched by winch. A winch launch imparts a massive load on the wings, in excess of 150 lbs, leading to a 1400 lb-in moment at the root. The spar cap was 0.7 in. wide and 0.030 inches thick at the root. Turbulence Syndrome's bending moments were estimated to be around 4200 lb-in, with the original design calling for a spar cap only 0.5 in. wide and 0.024 in. thick. The

solution to this problem was three-fold. A light-plywood core was used so that it could carry the core stress. In addition, the thickness of each cap was increased from 3 layers to 10 layers. Finally the entire spar was wrapped in light fiberglass to keep the caps attached to the core under compressive buckling loads. Analytic computation, using the equations in Table 4-4, was used to confirm the theory. Testing of the new spar confirmed the corrections.

Table 4-3: Spar Dimensions and MATWEB Material Properties

E_{core}	1350 ksi
E_{cap}	3350 ksi
Thickness	0.05 in.
Height _{center}	1.4 in.
Height _{tip}	1.3 in.
Width _{center}	0.5 in.
Width _{tip}	0.25 in.
Load	30 lbs
Span	108 in.
Span _{tip}	37 in.
$\sigma_{coremax}$	4.5 ksi
σ_{capmax}	550000 ksi

Table 4-4: Spar Calculations

$I_{core} = \frac{1}{12} b(h-2t)^3 \frac{E_{core}}{E_{cap}}$ $I_{cap} = 2\left(\frac{1}{12} bt^3 + bt\left(\frac{h}{2}\right)^2\right)$ $I_{tot} = I_{core} + I_{cap}$ $M = \frac{P \times Span}{2}$ $\sigma = \frac{Mh}{2I_{tot}}$ $\delta = \frac{P \times Span^3}{3EI_{tot}}$	Section	$I \text{ (in}^4\text{)}$	$\sigma \text{ (ksi)}$	$\delta \text{ (in)}$
	Center	0.0282	20.1	.833
	Tip	0.0120	30.0	.629
	Total	Na	na	1.46

4.2 Tail

Compared to the other concepts presented for the tail configurations, the V-tail was chosen as the most qualified out of all the choices.

4.2.1 V-tail Sizing

The sizing of the V-tail was based on Raymer's initial sizing method. The vertical area of the tail was calculated using:

$$S_{VT} = c_{VT} b_w S_w / L_{VT} \quad (4.1)$$

where c_{VT} is equal to 0.04, b_w is the wingspan, S_w is the wing area, and L_{VT} is the moment arm from the quarter-chord of the wing to the quarter-chord of the tail. The horizontal area of the tail was calculated using:

$$S_{HT} = c_{HT} \bar{c}_w S_w / L_{HT} \quad (4.2)$$

where c_{HT} is equal to 0.5, c_w is the wing chord, S_w is the wing area, and L_{HT} is the moment arm from the quarter-chord of wing to the quarter-chord of the tail. The values of c_{VT} and c_{HT} were determined from based on data from comparator homebuilt aircraft since these are similar to our aircraft.

These equations were put into an Excel spreadsheet and optimized. In order to prevent the tail from exceeding $\frac{1}{4}$ the span of the wing, a margin of error of 0.6 in. was imposed. The resulting V-tail had a 90° angle between the surfaces, a span of 18.25 in., and a chord of 9.75 in.

4.2.2 V-tail Structure

During the design of the tail structure, there was a focus on keeping the tail as lightweight as possible. The tail must also be capable of fitting inside the box. The design called for separating the tail from the fuselage during transport. Due to these constraints a few iterations of the tail structure were performed.

The initial design consisted of a 3/16 in. plywood flat frame with a balsa truss structure. The tail was glassed at the root to add additional strength. Finally the tail was covered in Monokote. This design experienced minimal bending but excessive torsion during load testing.

In order to increase the structural stiffness of the tail, the balsa truss structure was removed and the amount of plywood in the frame was increased. The frame was widened so that it could accommodate carbon lamination, which would increase the torsional and bending stiffness. After a number of attempts, the bonding of the carbon fiber was unsuccessful. Additionally, this increased the overall weight of the tail.

The final design of the tail structure moved away from the simplistic single sheet plywood frame and focused on traditional built-up model similar to that of the wing. A NACA 0008 airfoil was used for the new tail configuration since it is a symmetric airfoil and can be used for a control surface. Instead of using a traditional single-spar design, two $\frac{1}{4}$ in carbon fiber rods were placed at the $\frac{1}{4}$ chord and just in front of the control surfaces. The ribs were then slid onto the spars. The structure was covered in

Monokote. The carbon fiber rods resisted most of the bending during load testing and, when coupled with balsa ribs, minimal torsion existed. The rods also provided a way of connecting the tail to the tail boom.

4.3 Payload

In order to achieve a maximum flight score, a large emphasis was placed on the tank design to minimize drain time. Other areas of consideration during the design of the tank were the free surface effects and adverse moments caused by sloshing.

4.3.1 Tank Drain Time Analysis

The initial evaluation of the tank involved investigating the natural flow of water. A test scenario of a cylindrical tank with an exit hole diameter of 0.5 in. was investigated. Bernoulli's equation (4.3) was applied from the top of the water surface to the orifice.

$$\frac{P_1}{\rho g} + \frac{u_1^2}{2g} + z_1 = \frac{P_2}{\rho g} + \frac{u_2^2}{2g} + z_2 \quad (4.3)$$

From the results of the analysis it was determined that there was a direct relation between the time to discharge to the height of the tank of

$$Time = C \times \sqrt{height} \quad (4.4)$$

where the constant, C, is related to the volume of the tank. It was also discovered that the time to drain is independent of the shape and size of the cross sectional area of the tank.

4.3.2 Tank Structure

The conceptual design of the water tank structure was chosen to consist of a premanufactured RC gas tank. Upon further analysis of the gas tank, it was deemed that it was too heavy and bulky. The gas tank design was also not conducive to alterations and integration. The large inner surface area also posed a problem with free surface effects. Without the addition of multiple bulkheads or baffles, the single 4 L tank would cause instability while draining.

Instead of using a single gas tank, two smaller water bottles were examined. By separating the water into two separate tanks, the free surface effects were reduced. Two Rubbermaid™ 3092-87 1.9L (Figure 4-2) tea jugs were selected. The fuselage was designed to fit the two tanks. After further investigation, it was discovered that Rubbermaid™ tanks, made of polyethylene, were difficult to seal and leaked profusely. When filled to capacity, the two tanks totaled to 5 L. The tanks proved to be too tall to integrate the drain system into the 12 in. tall fuselage. Due to these problems, an executive decision was made to abandon this configuration and find a better solution.

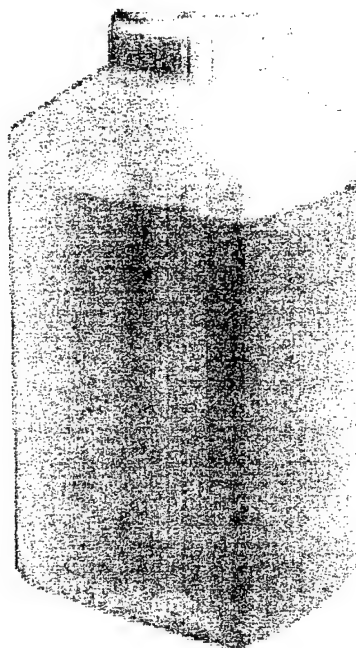


Figure 4-2: Rubbermaid™ 3092-97 1.9 Liter Drink Bottle

An alternate tank system, consisting of four 1-quart Valvoline™ (Figure 4-3) motor oil bottles was investigated. The oil bottles were lightweight, had good drain characteristics, and could be partially molded under heat. They were also easily modified to adapt a drain manifold such that all could be emptied simultaneously.

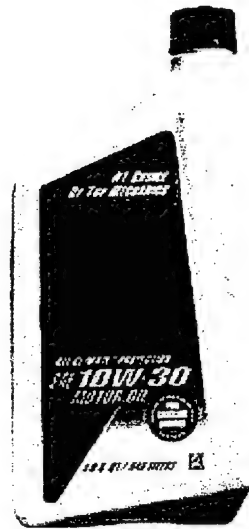


Figure 4-3: 1-quart Valvoline™ Motor Oil Bottle

The rules state that all of the water must drain out of a single 0.5 in. hole. A range of valve types was investigated, from 0.5-in. plumbing ball valves, to $\frac{3}{8}$ -in. garden hose ball valves, to a flood gate style valve. It was found that the flood gate style valve (a hole with a sliding door) was difficult to seal. The PVC plumbing ball valves were not only heavy, but very difficult to turn, and the garden hose valves were not large enough. A solution was found in the form of a 0.5 in. inner diameter ball valve from an automated one hour film developing machine. This valve was very easy to turn, and a mounting plate was built into the case.

A manifold to connect all four oil bottles into one drain was designed. The design was created by the cutting of a wax mold in the desired shape, coating the wax mold with PlastiDIP™ (a brush-on rubber), wrapping the manifold in fiberglass, and then melting the wax out of the cured rubber shell. Plastic zip-ties secured the joints, and silicone grease was applied to further seal the system.

During the development of the remote release system, several configurations were researched: direct servo connection, pulley system, and solenoid valve. The solenoid valve was eliminated because of its weight and excessive power consumption. The pulley system was eliminated due to its complexity and possible specialized servo requirements. The disadvantage to the direct servo connection was that it could put excessive strain on the servo. To overcome this limitation, a high torque servo was needed. A

standard size high torque 90° servo was tested for its ability to successfully open and close the valve and it proved to be more than adequate, however, this servo was too large to fit within the confines of the fuselage. The second servo option was a 180° retract servo. The advantages to this servo are its light weight and small size. The disadvantage is that the motor travels 180° and only 90° of travel are needed.

4.4 Fuselage

The primary objectives of the fuselage were to house the tank and propulsion systems. An additional objective was to create a sturdy mount for the wing and the tail boom. Since the time to drain the water was dictated by the height of the tanks, the fuselage was designed to be tall.

4.4.1 Fuselage Configuration

Two main designs for the fuselage were examined. The first configuration was made up of plywood bulkheads held together by the carbon fiber tubes. It was examined and analyzed due to its easy construction, adaptability to internal and external changes in the structure, and general lightweight design. The other design was a traditionally built-up fuselage. The traditional fuselage offered increased dependability, easy construction, strong mounting points for the tail boom and wing, and easily obtainable parts. The uncertainties associated with the carbon tube and plywood bulkhead design led to an unproven structure for this year's aircraft, but opened an option that could be examined for following years.

The final structure of the fuselage consisted of a continuous plywood center spine with bulkheads in the main fuselage section connecting to side panels. A balsa wood truss structure was extended back from the aft bulkhead to the aft of the center spine. A fiberglass cone was used as a tail boom and was connected aft of the spine. All the parts were assembled with slots and epoxy, and the entire fuselage was covered in Monokote.

4.4.2 Fuselage Structural Analysis

To verify that the fuselage would be able to support the wing at takeoff and landing, a detailed analysis was conducted on the main structure of the fuselage. The profile view of the fuselage can be seen in Figure 4-4. It was shown that the vertical landing load would be carried by two points, the nose gear mount and the main gear mount. The weight of the plane was concentrated at the center of gravity for this simplified model. The condition requiring the largest amount of force occurred during landing with the tanks fully loaded. The estimated load experienced in this situation was a 30 lbs load.

The geometry of the simplified model was a single beam as shown in Figure 4-4, the model was 3/8 in. in thickness. The load was applied 7 in. behind the nose gear.

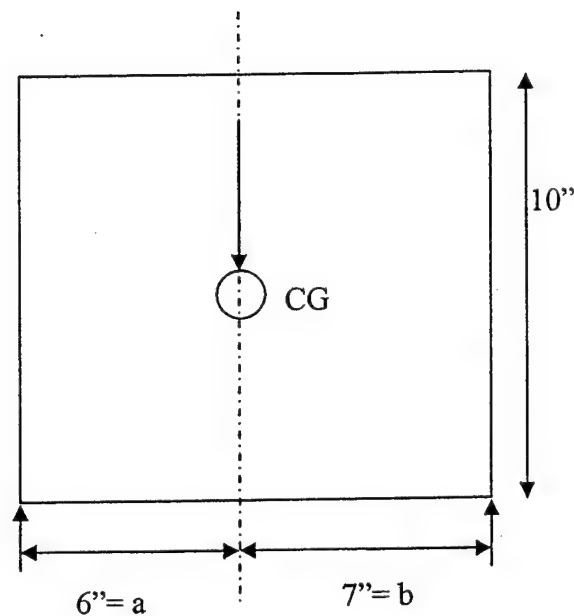


Figure 4-4: Profile View of the Fuselage

Once the dimensions were determined, the analysis was conducted. Equations 4.5-7 below are the results of this analysis:

$$I = \frac{1}{12}bh^3 = \frac{1}{12} \frac{3}{8} 10^3 = 31.25 \text{ in}^4 \quad (4.5)$$

$$M_b = \frac{Pa}{L}(L-a) = \frac{30 \times 6}{13} \times 7 \cong 97 \text{ lb-in} \quad (4.6)$$

$$\sigma_{\max} = \frac{M_b y}{I} = \frac{97 \times 5}{31.25} = 15.52 \text{ psi} \quad (4.7)$$

According to MATWEB, the failure strength of light plywood is about 4500 psi. Therefore it was determined that the designed fuselage would be capable of withstanding a landing up to 300 g's. The Young's Modulus of light plywood is approximately 1350 ksi. Although the structure could withstand a large load, there would be no prior notice at failure due to the value of the Young's Modulus.

4.4.3 Tail Boom

Numerous designs were examined for the tail boom structure. Such concepts were a wood truss structure, a carbon tube, and a fiberglass skin cone. The wood truss structure did not qualify because it would be too fragile and heavy. The carbon tubes were also discarded because they would not be strong enough and would make mounting to the fuselage difficult. The fiberglass cone configuration was chosen

because it possessed the lightweight qualities and strength needed, with easy integration to the main fuselage. These qualities were tested and proven through the manufacturing of a prototype.

4.4.4 Tail Boom Analysis

Although a prototype was manufactured and tested for structural integrity, an analysis was needed to confirm the findings. The cone was analyzed from the attachment point of the cone to the aft fuselage for bending analysis, where the bending moment was the largest. For torsion analysis, the attachment point was examined for twist. For shear analysis, both the fuselage attachment point and the front of the tail attachment point were tested. Carbon strips were placed at equal intervals around the cone. For bending, the cone was analytically split up into the fiberglass cone and the carbon strips. For the vertical bending, the carbon strips were modeled as two beams of differing widths, but had same height at different radii from the center of the circular beam. For the horizontal bending, the carbon strips were modeled as three beams; one in the middle, and two equidistant from the center, all of the same geometry, but the two beams at a 60° angle are assumed to be vertical as seen in Figure 4-5. For torsion, the carbon strips are ignored, and the polar moment of inertia, J , was calculated at each end, then the stress was determined. Twist was also found for the entire tail boom by an iterative method.

The cone skin was assumed to be 0.01 in. thick; the carbon strips were all 0.5 in. wide and 0.05 in. thick, and the length was set at 18 in. long. The load was set to 8 lbs at the tip. The constants, in Table 4-4, were used in the analysis; E and G were for a $\pm 45^\circ$ laminate whereas σ was for a unidirectional laminate. Since it was in torsion, the stress was actually going 45° along the fibers and that determined the failure of fiberglass.

Table 4-4: Values Used for Carbon Analysis (MATWEB)

E_{glass}	2.06×10^6 psi
G_{glass}	1.67×10^6 psi
σ_{glass}	38000 psi
E_{carbon}	3.35×10^7 psi
σ_{carbon}	5.5×10^8 psi

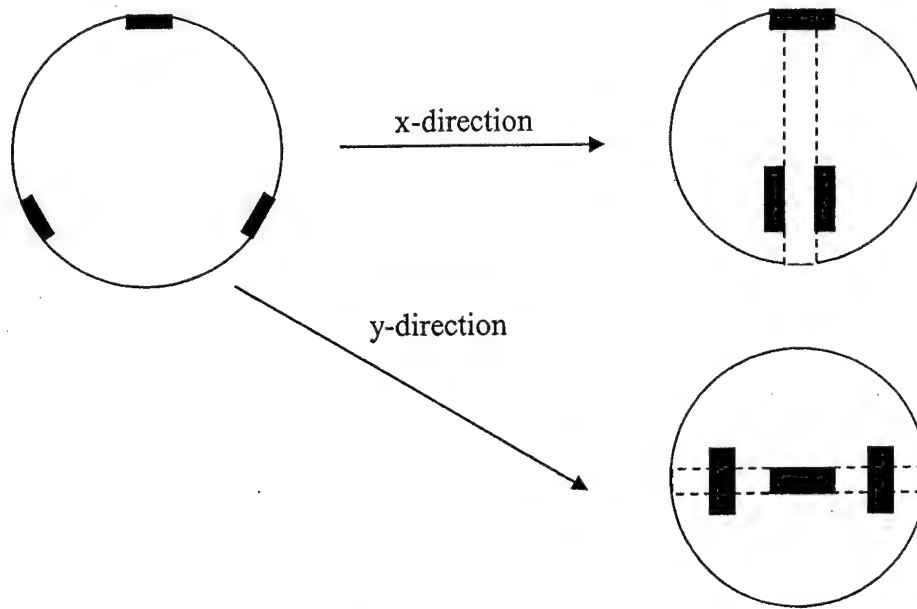


Figure 4-5: Rear View of the Fuselage

The calculations associated with the bending were:

$$I_{cone} = \frac{\pi}{4} (r_o^4 - r_i^4) \frac{E_{carbon}}{E_{glass}} = .178 in^4 \quad (4.8)$$

$$I_{c-x} = \frac{1}{12} b h^3 + b h r_o^2 + 2 \left(\frac{1}{12} h b^3 + b h \left(\frac{r_o}{2} \right)^2 \right) = 0.760 in^4 \quad (4.9)$$

$$I_{c-y} = \frac{1}{12} h b^3 + 2 \left(\frac{1}{12} b h^3 + b h \left(\frac{r_o \sqrt{3}}{2} \right)^2 \right) = 0.759 in^4 \quad (4.10)$$

$$M = PL = 144 lb - in \quad (4.11)$$

$$\sigma_x = \frac{M \frac{r_o}{2}}{I_{cone} + I_{c-x}} = 346 psi \quad (4.12)$$

$$\delta_x = \frac{PL^3}{2E_c (I_{cone} + I_{c-x})} = 4.96 \times 10^{-4} in \quad (4.13)$$

$$\sigma_y = \frac{M \frac{r_o}{2}}{I_{cone} + I_{c-y}} = 346 psi \quad (4.14)$$

$$\delta_y = \frac{PL^3}{2E_c (I_{cone} + I_{c-y})} = 4.96 \times 10^{-4} in \quad (4.15)$$

The calculations associated with the torsion were:

$$J_{fuse} = \frac{\pi}{32}(d_o^4 - d_i^4) = 3.57e - 1in^4 \quad (4.16)$$

$$J_{tip} = \frac{\pi}{32}(d_o^4 - d_i^4) = 4.76e - 4in^4 \quad (4.17)$$

$$\tau_{fuse} = \frac{Tr_o}{J_{fuse}} = 453.78psi \quad (4.18)$$

$$\tau_{tip} = \frac{Tr_o}{J_{tip}} = 37815.13psi \quad (4.19)$$

$$\phi = 1.63^\circ \quad (4.20)$$

4.5 Propulsion

All propulsion analysis was conducted using the R/C motor configuration program Motocalc™. According to earlier analysis, 9 lbs of static thrust was needed for the aircraft to takeoff in 150 ft. In order to ensure there would be enough thrust to takeoff twice fully loaded, 10 lbs of static thrust was set as a minimum.

A minimum cruise speed of 55 miles per hour was chosen to provide a minimum course completion. At this minimum cruise speed, Motocalc™ estimated that the aircraft would need 6.5 lbs of thrust to maintain level flight and a turning radius of 67 ft. Since the exact amount of thrust that this system would produce was unknown, the goal for a 67 ft radius was increased to alleviate the requirements for the system. Consequently, a minimum of 5 lbs of thrust and cruise speed of 55 miles per hour was chosen. Full throttle was designated to complete the minimum in a minimum of 3 minutes and 30 sec.

4.5.1 Motor and Battery Configurations

Numerous motor and battery combinations were narrowed by the elimination of configurations involving three or more motors. The two battery pack - two motor configuration was also ruled out because 2.5 lbs of batteries could not produce enough voltage or sufficient endurance. Also, the need for two speed controllers in this configuration increased the RAC.

A single motor - dual battery pack configuration was chosen. Contest rules dictate the use of nickel cadmium batteries. Two key properties were focused on when searching for batteries: low internal resistance and high power density. The top three batteries matching these specifications were the SR 2500 Max, SR 2000 Max, and Sanyo 2300 SCE.

4.5.2 Motocalc™ Results

The values used in Motocalc™ were: a weight of 23 lbs, wing area of 9 ft², Clark Y airfoil, fixed landing gear, and an Astro 204D speed controller. The known gear boxes from Astro-Flight of direct drive, 1.63:1, 2.75:1, and 3.3:1 ratios were used.

Motocalc™ outputs a primary list of each combination, including thrust, runtime, and climb rate at static thrust. Configurations were sorted by static thrust to eliminate those that did not meet the static thrust criteria. With 50 possible combinations remaining, a set of standards was developed to narrow the list. Configurations were eliminated with: pack voltage 25% over motor rating, less than 4.5 lbs of thrust at cruise, more than 4.5 lbs of batteries, more than 20-in. diameter propeller, less than 10 lbs of static thrust, less than 60 miles per hour top speed, and propeller availability.

After the results from Motocalc™ were obtained, two-motor configurations were eliminated. Every two-motor configuration ran 40% to 65% over their voltage limit and 25% to 40% over the maximum sustained current draw. The two-motor configuration also weighed more than the single-motor configurations.

4.5.3 Final Configurations

After the elimination process, the selection of configurations was narrowed to five. Two of the configurations used an Astro-Flight Cobalt 60 motor and three used Graupner Ultra 3450-7 motors. The configurations are listed in Table 4-5:

Table 4-5: Motor Configurations

Configuration	Motor	Gearbox	Propeller	Batteries	Thrust (lbs)	Speed (mph)	Runtime (min)	% Over Volt
1	Astro	Direct	13x7	SR2000	10.05	56	3:03	21
2	Astro	1.63:1	17x12	SR2000	10.51	64	3:55	11
3	Graupner	2.75:1	18x14	SR2000	11.28	59	4:28	23
4	Graupner	2.75:1	18x14	SR2000	10.80	58	4:41	21
5	Graupner	2.75:1	18x16	SR2000	10.19	61	3:56	19

4.6 Stability and Control

Due to the large wing, it was necessary to have either a large tail or a large moment arm to maintain lateral-directional and pitch stability. In order to keep a low RAC by not excessively extending the fuselage, a large tail was needed. The horizontal projection of the V-Tail could not exceed a total span of 27 in. without being considered a second wing. Taking this into consideration, a compromise was made between tail size and fuselage length. The quarter chord of the tail was placed 42 in. back from the quarter chord of the wing. At this distance 125 in.² of projected vertical area was needed to maintain lateral-directional stability, and 250 in.² of projected horizontal area was needed to maintain longitudinal stability.

The high-wing was chosen during the conceptual design phase so that Turbulence Syndrome would be less sensitive to roll moments and disturbances. Due to this, the ailerons had to be sized appropriately. Aileron sizing was accomplished by using graphs and equations in Raymer. The resulting aileron dimensions are listed in Table 5-2.

Following wing and tail sizing, handling qualities of Turbulence Syndrome were calculated using the Vortex Lattice Codes, Tornado (Melin) and JKayVLM (Jacob Kay). Tornado is a freeware code available to anyone with MATLAB software. Tornado relies on the slope of the camber line for its computation, and is programmed with equations for NACA 4 digit series airfoils. Since the Clark Y airfoil was chosen for the main wing, an advanced version of Tornado was used that allows the user to input alternate camber line slopes. JKayVLM is a software code available to seniors in the Virginia Tech Senior AOE Design Lab that is based on flat plate assumptions.

The first step in calculating the stability and control derivatives was to validate the advanced version of Tornado. Tornado analysis of a Clark Y wind tunnel model (6 in. chord, 37 in. span) was compared to experimental data collected in the Virginia Tech Stability Tunnel. Mediocre validation of Tornado led the team to explore JKayVLM as an additional method of stability analysis. A validation of the JKayVLM code is provided with the reference.

Table 4-6 lists the stability derivatives for Turbulence Syndrome, determined from both Tornado and JKayVLM. These coefficients show that the airplane has a favorable static margin and is stable in most flight conditions. The instability in $C_{l\beta}$ and $C_{n\beta}$ was attributed to choosing the traditional V-tail over the inverted V-tail. To assure that the instability of $C_{l\beta}$ and $C_{n\beta}$ would not pose a threat to the aircraft, a scale model balsa glider was constructed for testing. The model performed exceptionally well in both indoor and outdoor conditions, implying acceptable performance for Turbulence Syndrome.

Table 4-6: Turbulence Syndrome Stability Derivatives

Longitudinal		Lateral Directional	
$C_{L\alpha}$	5.1876	$C_{n\beta}$	-0.05756
$C_{m\alpha}$	-1.5397	$C_{l\beta}$	0.02644
$C_{m\delta e}$	-1.2536	$C_{n\delta r}$	-0.09594
Static Margin	15.9%	$C_{l\delta r}$	0.03311
		$C_{n\delta a}$	-0.0036
		$C_{l\delta a}$	0.3498

5 Detailed Design

5.1 Wing

The wing had a span of 9 ft and a constant chord of 1 ft for a total area of 9 ft² and an aspect ratio of 9. The airfoil used was a Clark Y with a 12%, or 1.4 in., thickness. A traditional built-up spar and rib construction technique was used. The wing had three sections, the center section spanning 46 in. and each outboard section spanning 31 in.

The center section of the wing had a 1.4 in. tall, 0.5 in. wide spar built up from four layers of 0.125 in. light ply and capped top and bottom by ten layers of unidirectional carbon fiber tape. The entire assembly was wrapped with two layers of 0.75 oz/ft² fiberglass cloth. Rib halves were cut on the Laser CAMM, and then glued to the front and rear of the spar with butt joints and tristock gussets. The ribs were placed at 5 in. intervals. Leading edge stock, 0.75 in. tall, was glued to the front of the ribs, and 1.25 in. trailing edge stock was glued to the aft of the ribs. The forward 1.25 in. and aft 1.75 in. of the wing was sheeted, and the top of the ribs were capped with 0.0625 in. balsa.

The middle 5.375 in. of the center section were left open so that the spar could slide down into a slot in the top of the fuselage between the fore and aft tanks. The spar was clamped to the fuselage using hose clamps and a protective strip of Mylar. At the rear of this open section a 1 in. wide, 0.125 in. thick light ply plate spanned the gap between the ribs. Two 6-32 bolts were threaded through this plate and into blocks in the fuselage to secure the aft section of the wing, providing increased torsional rigidity to the wing mount.

The tip sections of the wing were built up in a similar pattern to the center section. Rib halves were butt-joined and gusseted to the spar, LE and TE stock added, and 0.0625 in. sheeting completed the assembly. The major difference was between the center section and the tip sections of the wing spars: the tip spars were only 0.25 in. thick and 1.3 in. tall, but were still capped top and bottom with ten layers of unidirectional carbon fiber tape and wrapped with two layers of 0.75 oz glass cloth. A 6 in. section of each tip spar extended beyond the innermost rib and was fit to a slot in the center section spar. This slot was created during construction of the center section spar by making a 0.25 in. thick, full height plug that was removed after the spar was finished. The gap left between the top of the tip spar and the top of the slot in the center spar was filled with silicon-filled epoxy resin to ensure a tight fit. Short wooden dowels glued to the rear of the innermost rib of the tip sections fit into a hole in the outermost ribs of the center section to transfer torsion loads between the sections. A strip of electrical tape seals the joint and ensures that the tip not pull out of the center section in flight.

Ailerons were built up with short 0.0625 in. balsa ribs, a 0.25 in. by 0.375 in. balsa leading edge, a 0.125 in. balsa trailing edge, and then sheeted with 0.0625 in. balsa. Each aileron spanned 26.75 in., and had a chord of 2.5 in. The ailerons were centered spanwise on the tip sections of the wing starting at 83.3% of the wing chord. Each aileron has a dedicated servo, mounted within the wing tip at the center of the aileron. With independent servos, the ailerons may be used as flaps if needed. The servos were mounted in light ply trays that slid into slotted hardwood rails mounted within the wing structure. A hatch was bonded to the light ply tray, and was secured to the rails with small screws. The entire wing was then covered with Monokote.

Load tests conducted after construction found that the wing deflected 2.675 in. at the center with 26.5 lbs hung from the bottom of the fuselage, and the plane was supported at the tips of the wing. This was 1.2 in. more than predicted, but still well within reasonable limits. Torsional testing found that the wing did not twist a measurable amount with 2 lbs suspended from the trailing edge of the wing tip.

5.2 Tail

The tail was an upright, 90 degree V-tail. Each stabilizer had a span of 17 in. and a chord of 9.75 in., leading to a projected 125 in.² of vertical area and 250 in.² of horizontal area. The quarter-chord of the tail was 42 in. behind the quarter-chord of the wing. The ruddervators had a span of 17 in., a chord of 2.5 in. and were flush with the tips of the stabilizers. The stabilizers were built up using two 0.25 in. carbon fiber tubes as fore and aft spars, 0.0625 in. balsa ribs with a NACA 0008 airfoil, 0.125 in. by 0.1875 in. balsa leading edge and sub-trailing edge, and 0.0625 in. balsa sheeting from the LE to 25% chord and from 50% chord to 75% chord. The ruddervators were built up with 0.125 in. square balsa stock, then sanded to taper to the trailing edge. The stabilizers and ruddervators were covered with Monokote.

The carbon fiber tubes extended from the stabilizers 1 in. and were inserted into fitted blocks that were bonded to the tail cone with epoxy and fiberglass reinforcements. These blocks were faired to tail cone and stabilizers with hollow blue foam pieces that were lightly bonded to the assembly. Each ruddervator had a dedicated servo mounted in the fuselage just aft of a bulkhead (#5, see structural drawing). Control rods were built with a joint just aft of bulkhead #7, in the hollow of the tail cone, to allow the rods to be split for transport.

5.3 Fuselage

The fuselage was built up from seven 0.125 in. light ply formers bonded to either side of a 0.125 in. light ply central spine. Bulkheads #1 through #5 were a rectangular shape, 12 in. tall and 5.375 in. wide, while bulkheads #6 and #7 were circular with 4.625 in. and 4 in. diameters, respectively. The 0.125 in. light ply sides were bonded to bulkheads #1 through #5. A tail cone was molded out of fiberglass with carbon fiber reinforcements and pinned to the aft of the spine over bulkheads #6 and #7. Total length, from spinner backplate to tip of the tail cone, was 63 in.

Bulkhead #1 served as mount for the motor and nose gear, and front of the battery compartment. The motor was clamped to a standard glass-filled nylon engine mount with hose clamps. This mount was then bolted to a box that was designed to break from bulkhead #1 in the case of a propeller strike, saving wear and tear on the motor and gear box. A shelf between bulkheads #1 and #2 supported the batteries in the vertical direction, and straps passed through bulkhead #1 clamped the batteries in place. Rubber matting ensured that the batteries did not slide under the straps.

The forward two tanks were placed between bulkheads #2 and #3 and on either side of the spine. A 0.25 in. wooden dowel was run under the tanks, through the fuselage sides and spine, to hold them in place. The aft two tanks were placed between bulkheads #4 and #5 in a similar manner to the forward tanks. A cutout was made in the spine between the fore and aft tanks so that a manifold and drain valve could be placed within the fuselage. The wing spar fit between bulkheads #3 and #4, and a hardwood block was bonded in place so that the spar could be clamped to the fuselage with hose clamps. A notch was cut in the top of the spine just aft of bulkhead #5 to accept the rear spacer in the wing center section.

This notch was boxed in with 0.125 in. light ply and hardwood blocks were added under the box to accept 6-32 blind-nuts for the wing rear attachment. The main gear was bolted to a pine block bonded to the fuselage behind bulkhead #5 and at the bottom of the spine. Tristock reinforcements were added to this critical joint.

Two 0.25 in. by 0.375 in. hardwood rails were run from the outside of bulkhead #5, at mid height, through bulkhead #6 and tapered to bulkhead #7. Additional 0.5 in. square balsa stringers were run from the corners of bulkhead #5 to the junctions of bulkhead #6 and the spine, and the junctions of bulkhead #6 and the hardwood rails. This provided a smooth transition from rectangular to circular cross sections and torsional rigidity.

A tapered carbon tube was bonded over bulkhead #6 and #7. Hardwood blocks were bonded at the juncture of the spine and the carbon tube, and 0.125 in. holes were drilled to accept brass pins. Matching holes were drilled in the tail cone and the brass pins held the cone in place during flight.

A fairing of hollowed foam and light glass smoothed the transition from the spinner to bulkhead #1. The rest of the fuselage was covered with Monokote.

5.4 Landing Gear

The main gear was a standard model airplane landing gear formed from 0.125 in. aluminum stock. The top of the gear was 4 in. wide and 6 in. long, a little longer than the width of the fuselage. Standard $\frac{5}{32}$ in. axles were used with standard 3 in. model airplane wheels. The main wheels are thin, low profile aluminum wheels with an outer O-ring. Overall, the gear measured 6 in. from the bottom of the wheels to the bottom of the fuselage, and spanned 14 in. wheel-to-wheel. Four 6-32 nylon bolts secured the gear to the pine wood block in the bottom of the fuselage, allowing the gear to shear off in a crash, saving damage to the fuselage. The gear did flex considerably under hard landing loads, but it was considered a replaceable item in the event that it was permanently bent.

The nose gear was a Robart RoboStrut nose unit with a shock absorber built into the strut. The strut mount was adjusted to set a level attitude on taxi. A standard 3 in. wheel was used for the nose gear. Four 6-32 bolts secured the nose gear mounting block to the hardwood block bonded to bulkhead #1. The nose wheel is controlled by a linear actuator system that transmits only the rudder input from the ruddervator servos to the nose wheel, eliminating the need for an extra servo just to control ground steering. Both nose gear and main gear wheels were faired with wheel pants.

5.5 Payload

The four oil quarts, the manifold, and the 0.5-in. ball valve were assembled and tested for leaks. A 180° retract servo was chosen because of its high torque, lightweight, and low power requirements. A 90° arc was cut into the servo control arm to allow for proper throws. The servo was then connected to open and close the ball valve. A bottom plate was made and placed flush with the bottom of the valve. The completed assembly was positioned into the airplane, and the bottom plate was flush with the bottom of the fuselage.

Because drain times varied the aircraft conditions, it was decided to make two interchangeable drain configurations: one with a tube, and one without. Static drain times without a tube averaged about 20 sec. If this drain time proves inadequate, a 10 in. long, 0.5 in. diameter extension tube can be fit around the ball valve. To reduce drag in flight, a push rod was attached to the valve servo in order to retract the tube. Adding the tube to the valve dropped the average drain time to 15 sec.

All four tanks are filled through the back two tanks. One-way flow valves were inserted into the rear tanks to prevent water from back-flowing into the rear tanks, creating a tail heavy condition. The volume of the four oil quarts was slightly larger than 4 L. To allow the tanks to be filled to overflow with 4 L, foam pellets were added to the tanks to fill the extra space. Each of the four tanks had a 90° elbow directed into the airflow to prevent spilling.

5.6 The Propulsion System

The Astro-Flight Cobalt 60 brushed electric motor was chosen because of its high power to weight ratio, its ability to meet the required thrust needs, and its availability. This motor had been used by the Virginia Tech DBF Team for the past three years and had proven to be a powerful and reliable motor. The motor was run through a break-in period in order to lubricate the bearings and to check for defects. It was then mounted to a testing jig and timed to run at maximum efficiency at the expected cruise current level of 30 amps.

SR2000-Max Nickel Cadmium cells were chosen for their medium capacity, lightweight and low internal resistance. The total weight of the battery pack was less than 4 lbs. Prior to assembly of the pack, each cell was tested for capacity and ability to hold a charge. The cells were soldered directly together, end to end, to reduce weight and internal pack resistance. Two battery packs of seventeen cells were constructed and wrapped in the required heat-shrink tubing, then connected in series to form a 34-cell, 40.8 V battery pack. Splitting the battery pack served two purposes: mounted within the fuselage bulkheads, it would not compromise the strength of the structure by notching the spine and a smaller pack allowed for more complete recharging of the batteries by lowering the required voltage and pack resistance. Thirteen gauge stranded copper cable, the optimal size in terms of connector acceptance and low resistance, was used to wire the propulsion system. A 40 amp fuse was placed in series between the battery pack and the motor as per contest rules.

Contest rules required the use of a commercially available, unmodified propeller; availability of a range of high performance propellers was a heavily weighted factor when choosing a final propulsion system. The Fire Bomber Mission, flying with 4 L of water, required a high level of static thrust for takeoff. A high performance, nylon, pattern style, 17x12 propeller was selected. The Ferry Mission required the aircraft to fly the course as fast as possible. Since the aircraft is almost 9 lbs lighter for the Ferry Mission, static thrust requirements are not as high and a higher top speed is desirable. A 16x14 propeller was chosen for this mission. The higher pitch propeller was more efficient at high speeds because it had the ability to accelerate more air per revolution. The smaller diameter propeller offset the increased pitch, allowing similar runtimes as with the 17x12 propeller.

Another consideration was the adverse weather at Cessna Field in Wichita, KS, where high speed winds are often present. Because flying into a strong headwind is similar to flying at high speeds in calm air, it is necessary to move a larger volume of air to produce the same amount of thrust. To overcome potentially adverse weather conditions, the 16x14 propeller may be used for either mission depending on atmospheric conditions at the time of flight.

5.7 RAC

Once the final configuration and specifications for the aircraft had been determined, the RAC was computed using a Microsoft Excel spreadsheet that incorporated the equations set forth in the contest rules. The final RAC was computed as 14.14. The data used to compute the RAC is shown below in Table 5-1.

Table 5-1: Turbulence Syndrome RAC

A	300	Multipliers
B	1500	Multipliers
C	20	Multipliers
# Engines	1	
Battery Weight (lbs)	4	
REP	4	$(1 + .25 * (\# \text{ engines} - 1)) * \text{Battery Weight [lbs]}$
Manufacturers Empty Weight MEW (lbs)	14.83	
Wing Span (ft)	9	
Max Wing Chord (ft)	1	
Wing Area	9	Wing Span * Max Wing Chord
WBS wing area	90	10 * Wing Area
Ailerons = 1	1	Control Function Multiplier
WBS Control Wing Surfaces	5	5 * Control Function Multiplier
WBS Wing	95	WBS Control Wing Surfaces + WBS Wing Area
Max Fuselage Width (ft)	0.46875	
Max Fuselage Length (ft)	5.291666667	
Max Fuselage Height (ft)	1	
WBS Fuselage	49.609375	10 * Max height * Max Width * Max Length
# Non-Active Vertical Surface	0	ex. Winglets
# Vertical Surfaces With Control	0	Enter 0 if V-tail
# Horizontal Surfaces	0	"less than 25% wingspan"
V-Tail (Enter 1)	1	Enter 0 if Conventional
WBS V-Tail	15	V-Tail * 15
WBS Horizontal	0	10 * # Horizontal Surfaces
WBS Vertical	0	$(5 * \# \text{ Non-Active Vertical Surfaces}) + (10 * \# \text{ Active Vertical Surfaces})$
WBS Tail	15	WBS V-Tail + WBS Horizontal + WBS Vertical

# Servos	4	
# Speed Controllers	1	
WBS Flight Systems	25	5 * (# Speed Controllers + # Servos)
MFHR	184.609375	WBS Wing + WBS Fuselage + WBS Tail + WBS Flight Systems
Calc 1	4449	A * Manufacturers Empty Weight
Calc 2	6000	B * Rated Engine Power
Calc 3	3692.1875	C * Manufacturing Man Hours
Calc 4	14141.1875	Calc 1 + Calc 2 + Calc 3
RAC	14.14119	Calc 4 / 1000
	\$14,141.19	

5.8 Final Aircraft Configuration

To fit the plane in the 4 ft, by 2 ft, by 1 ft box, the wing, main landing gear, tail cone, and empennage were removed from the fuselage. The wing was then divided into three sections: a center section 46 in. long, and two outboard sections each 37 in. long. The empennage was removed from the tail cone to further increase packing efficiency. The fuselage was put in the bottom of the box on its side, the empennage and tail cone beside the fuselage, and the three wing sections lay on top of the fuselage.

Table 5-2 below lists Turbulence Syndrome's components with dimensions and details.

Table 5-2: Final Aircraft Specifications

Fuselage

Length	63.5 in.
Height	12 in.
Width	5.625 in.

Wing

CL max	1.2
Airfoil	Clark - Y
Span (b)	9 ft
Chord (C)	1 ft
Aileron Span	26.75 in.
Aileron Chord	2.5 in. (20% C)
Incidence Angle (i)	0°
Inboard Section	46 in.
Outboard Sections	31 in.
Taper Ratio (A)	1
Aspect Ratio	9

Propulsion

Motor	Astro-Flight Cobalt 60
Gear Box	1.63:1
Prop	17x12, 16x14
Cell Type	SR 2000-Max
Cell Number	34 Cells

Tail

Airfoil	NACA 0008
Span (per surface)	18.25 in.
Horizontal Projection	26 in.
Chord	9.75 in.
Ruddervator Chord	2.5 in.
Ruddervator Span	17 in.

Table 5-3 shows the weights of the components in the aircraft. It also shows the balancing of the aircraft:

Table 5-3: Aircraft Weights and Balancing

Part	Weight (oz)	Weight (lb)	Location (in)	Moment (oz-in)
Prop	4	0.25	10	40
Motor	23.1	1.44375	8.375	193.4625
Gearbox	1.88	0.1175	10	18.8
Battery	69	4.3125	5.875	405.375
Nose	6	0.375	6	36
Nose Gear	3.26	0.20375	6	19.56
Rear Gear	12	0.75	-5.625	-67.5
Wing	42.9	2.68125	-1	-42.9
Empty Tank	8.75	0.546875	0	0
Valve+Manifold	3.92	0.245	0	0
Water	140.8	8.8	0	0
Total Fuselage	28.1	1.75625	-2.5	-70.25
Tail Boom	4	0.25	-30	-120
Tail	12	0.75	-44.5	-534
Speed Control	1.92	0.12	8	15.36
Reciever Battery (avg)	4.25	0.265625	6	25.5
Wing Servo	4.72	0.295	0	0
Valve Servo	2	0.125	4	8
Tail Servo	4	0.25	-6	-24
Reciever	1.44	0.09	-6	-8.64
Total	378.04	23.6275		-105.2325

Note: For Location a positive denotes a forward position and a negative number denotes an aft position.

Below in Table 5-4 values such as climb rate, course length, and cruising speed are listed. The left side of Table 5-4 shows values calculated with a full battery charge. The right side of Table 5-4 shows values calculated with power levels at 85% of maximum to simulate the sortie of the mission. Shown in Table 5-5 are the calculated values for the empty speed mission using the 16x14 propeller.

Table 5-4: Payload Mission Performance Characteristics

Payload Mission			
Maximum Takeoff Distance	150 ft	17 x 12 Propeller	
Gross Takeoff Weight	24 lbs		
First Flight:		Second Flight:	
(Full Charge)			
Take off Distance	114 ft	Take off Distance	140 ft
Take off Speed	52 ft/sec	Take off Speed	52 ft/sec
Rate of Climb	13.4 ft/sec	Rate of Climb	10.4 ft/sec
Cruise Altitude	50 ft	Cruise Altitude	50 ft
Time to Climb (50 ft)	3.75 sec	Time to Climb (50 ft)	4.8 sec
Cruise Speed	80 ft/sec	Cruise Speed	73 ft/sec
Turn Radius	75 ft	Turn Radius	90 ft
Approximate Course Distance	2942 ft	Approximate Course Distance	3131 ft
Approximate Course Time	44 sec	Approximate Course Time	49 sec
Total Flight Time ≈ 95 sec = 1.55 min			

Table 5-5: Performance Characteristics of the Empty Speed Mission

Speed Mission	
Maximum Takeoff Distance	150 ft
Gross Takeoff Weight	15 lbs
16 x 14 Propeller	
First Flight:	
(Full Charge)	
Take off Distance	43 ft
Take off Speed	52 ft/sec
Rate of Climb	20 ft/sec
Cruise Altitude	50 ft
Time to Climb (50 ft)	2.5 sec
Cruise Speed	95 ft/sec
Turn Radius	70 ft
Approximate Course Distance (4 Laps)	11519 ft
Approximate Course Time	135 sec
Total Flight Time ≈ 135 sec = 2.25 min	

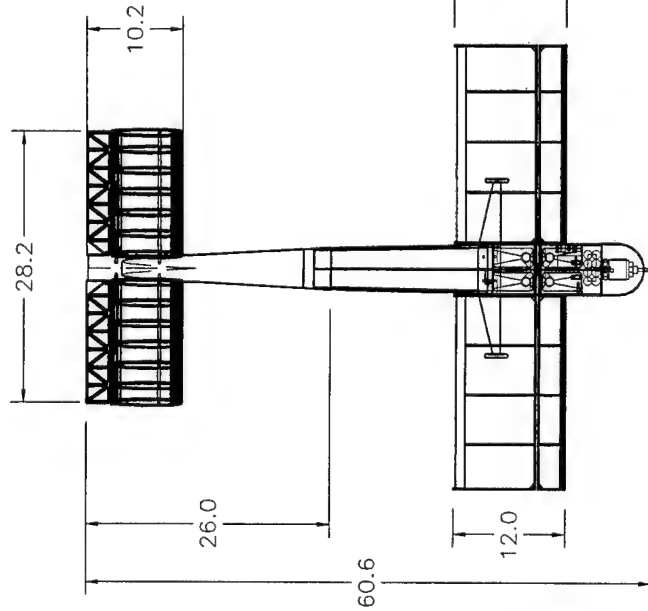
5.9 Drawing Package

The Drafting Team compiled data from the component-teams to produce accurate drawings of the Turbulence Syndrome aircraft. The drawing package consists of a dimensioned 3-view detailed design, an isometric layout of major components and their locations, a drawing of the payload deployment and restraint system, and a 3-view of the fuselage and its structural components.

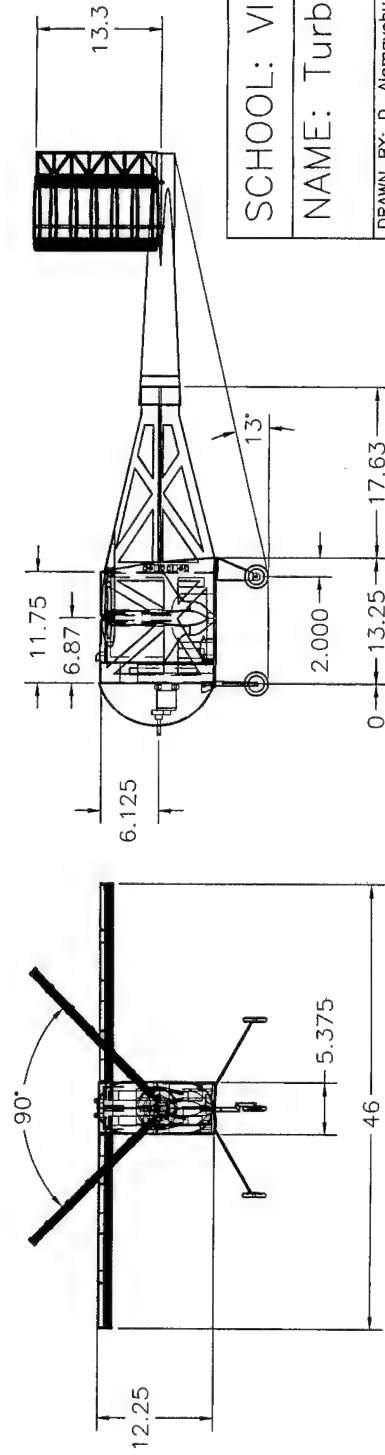
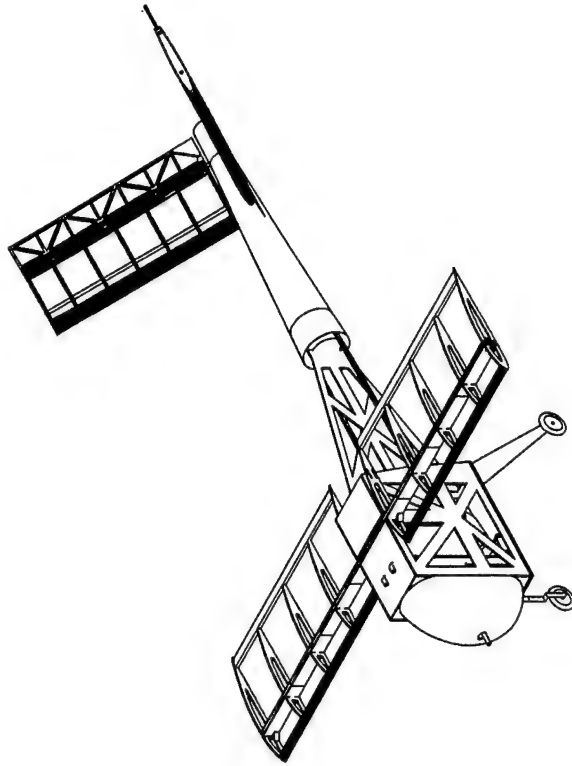
DESCRIPTION:
 DETAILED DRAWING OF INBOARD STRUCTURE
 TOP, FRONT, RIGHT, AND ISOMETRIC VIEWS

DATE:
 02/27/2004

APPROVED



Outboard Wing Section



SCHOOL: VIRGINIA TECH

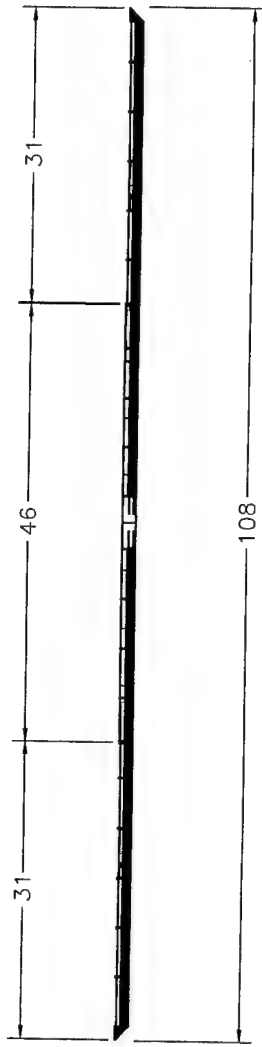
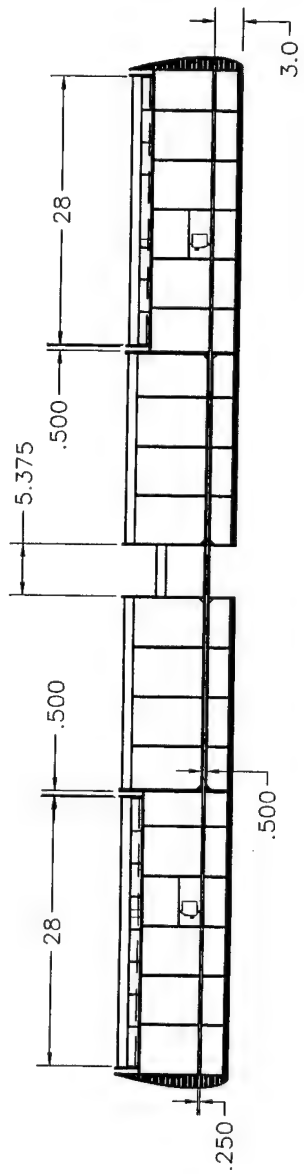
NAME: Turbulence Syndrome

DRAWN BY: D. Alemayehu, C. Ashton, S. McIntyre, L. Pilkington
 CHECKED BY: S.D. McIntyre, J. Roadman, R. Roedts

SCALE: 1"=0.075" DATE: February 27, 2004 SHEET: 1 of 5

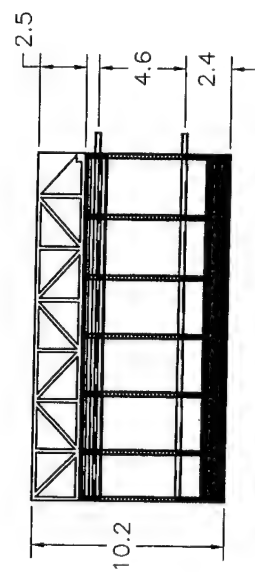
PRODUCED BY AN AUTODESK EDUCATIONAL PRODUCT

DESCRIPTION: DETAILED DRAWING OF WING AND TAIL STRUCTURE: TOP AND FRONT VIEWS	DATE: 02/28/2004	APPROVED
---	---------------------	----------



SCALE: 1" = 0.075"

Note: A Clark-Y Airfoil was used in the wing.



SCALE: 1" = 0.15"

Note: A NACA 0008 Airfoil was used in the V-tail.

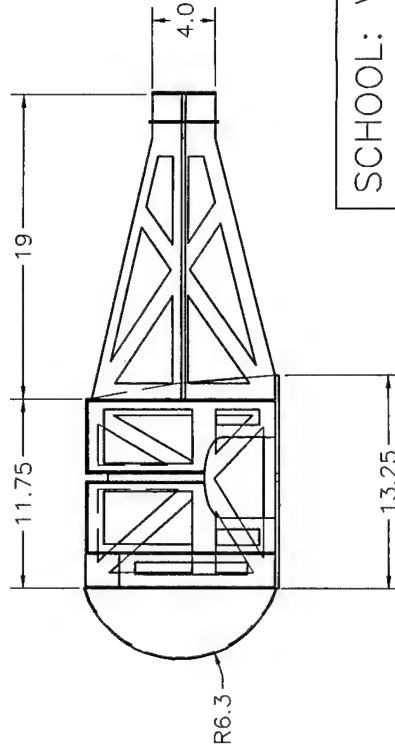
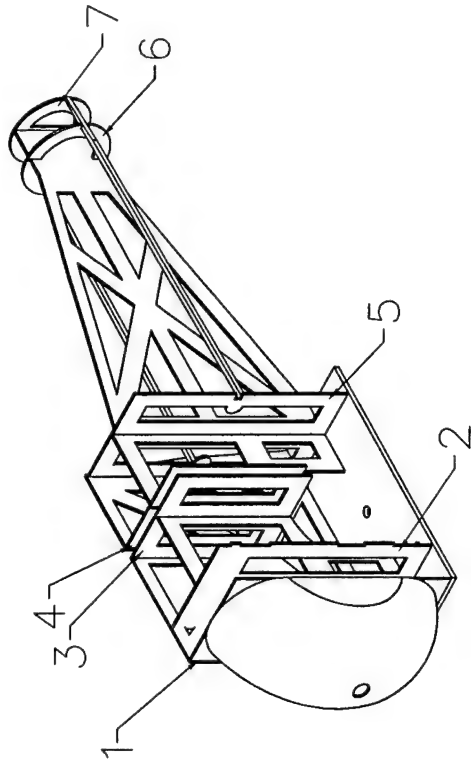
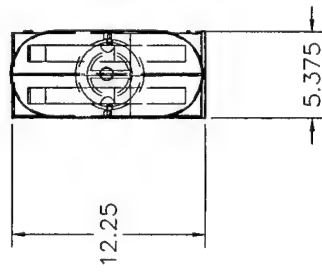
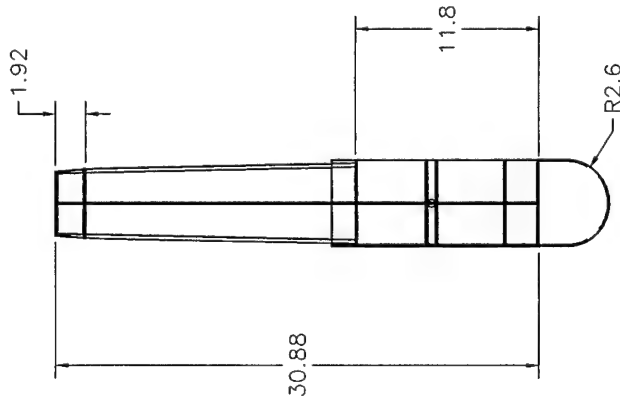
SCHOOL: VIRGINIA TECH

NAME: Turbulence Syndrome

DRAWN BY: D. Almayehu, C. Ashton, S. McIntyre, L. Pilkington
CHECKED BY: S.D. McIntyre, J. Roadman, R. Roedts

SCALE: AS NOTED DATE: February 27, 2004 SHEET: 2 of 5

DESCRIPTION: DETAILED DRAWING OF FUSELAGE STRUCTURE TOP, FRONT, RIGHT, AND ISOMETRIC VIEWS	DATE: 02/27/2004	APPROVED
--	---------------------	----------



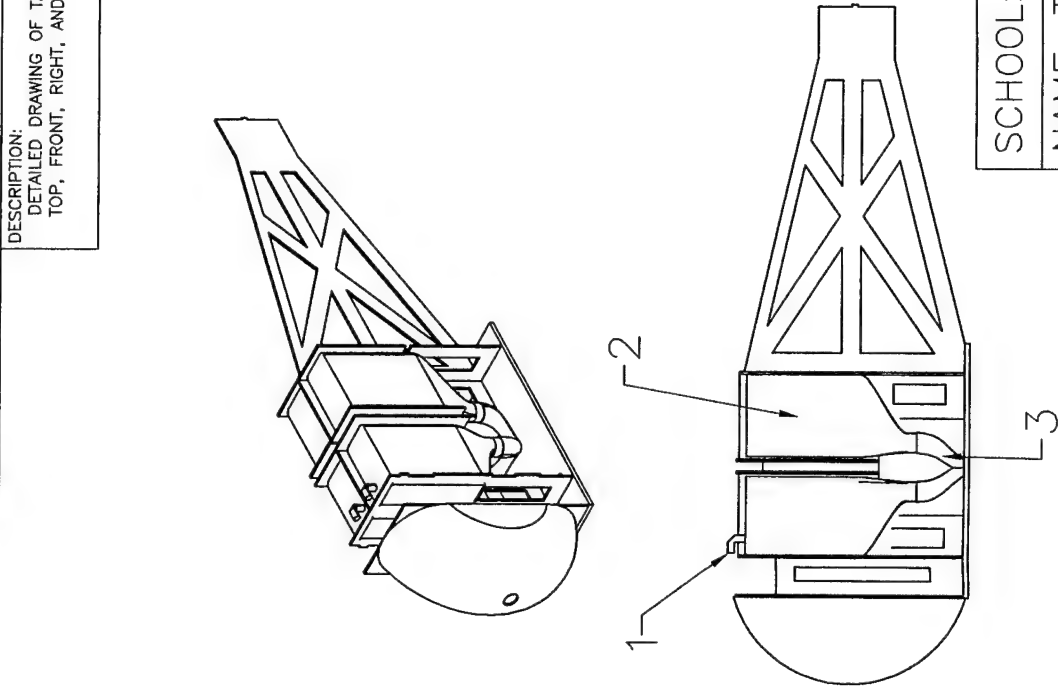
SCHOOL: VIRGINIA TECH
NAME: Turbulence Syndrome
DRAWN BY: D. Alemayehu, C. Ashton, S. McIntyre, L. Pilkington
CHECKED BY: S.D. McIntyre, J. Roadman, R. Roedts
SCALE: 1"=0.125" DATE: February 27, 2004 SHEET: 3 of 5

DESCRIPTION:
DETAILED DRAWING OF TANK LAYOUT
TOP, FRONT, RIGHT, AND ISOMETRIC VIEWS

DATE:

02/28/2004

APPROVED



PART	PART DESCRIPTION
1	2x ONE WAY INPUT WATER VALVE
2	4x WATER TANK
3	MANIFOLD

SCHOOL: VIRGINIA TECH

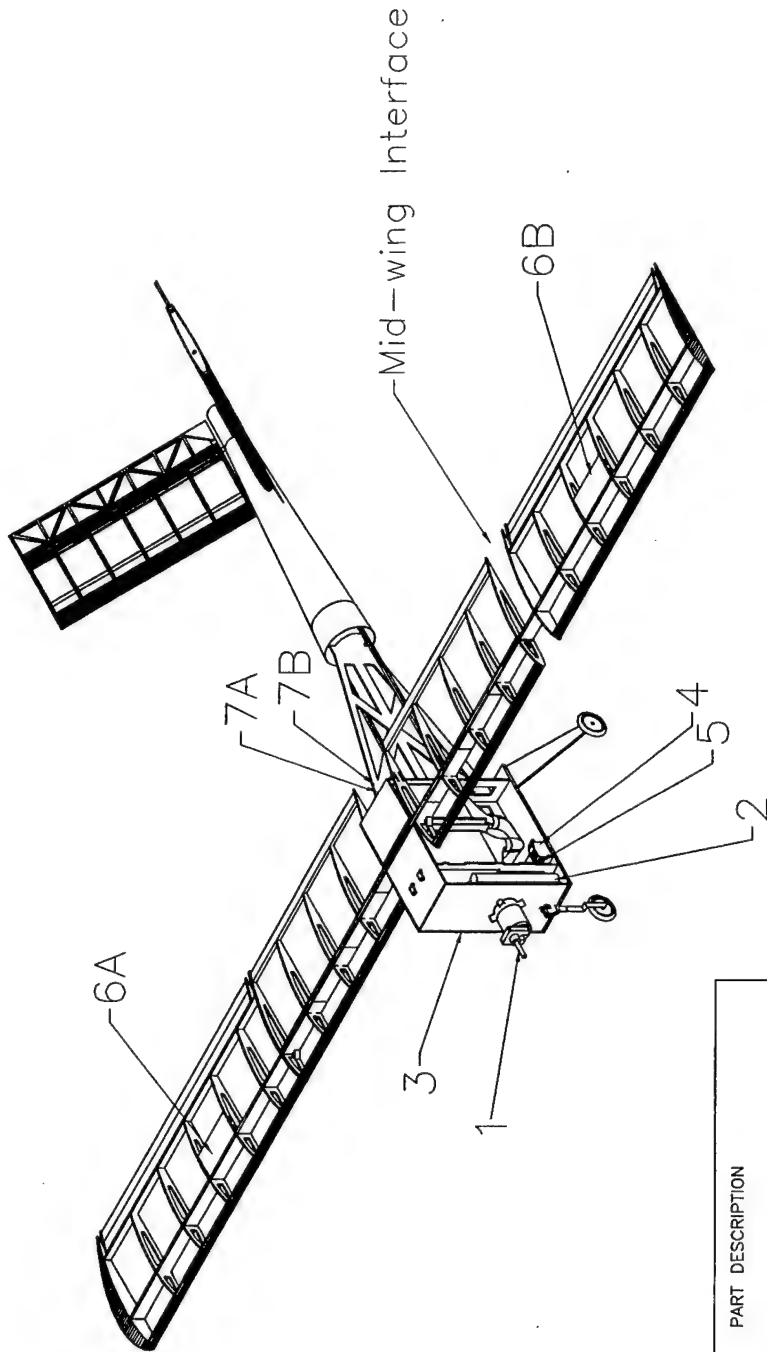
NAME: Turbulence Syndrome

DRAWN BY: D. Alemayehu, C. Ashton, S.D. McIntyre, L. Pilkington

CHECKED BY: S.D. McIntyre, R. Roedts

SCALE: 1" = 0.15' DATE: February 27, 2004 SHEET: 5 of 5

DESCRIPTION: DETAILED DRAWING OF ELECTRONIC PART PLACEMENT	DATE: 02/27/2004	APPROVED
--	---------------------	----------



PART	PART DESCRIPTION
1	ASTROFLIGHT COBALI 60 MOTOR WITH GEARBOX
2	32 CELL SANYO SR2000-MAX FLIGHT BATTERY PACK
3	RECIEVER BATTERY (HIDDEN)
4	FUTABA 7 CHANNEL RECEIVER
5	WATER TANK RELEASE SERVO
6A	RIGHTAILERON SERVO (HIDDEN)
6B	LEFTAILERON SERVO (HIDDEN)
7A	LEFT RUDDERVATOR SERVO (HIDDEN)
7B	RIGHT RUDDERVATOR SERVO (HIDDEN)

SCHOOL: VIRGINIA TECH		
NAME: Turbulence Syndrome		
DRAWN BY: D. Alemayehu, C. Ashton, S. McIntyre, L. Pilkington		
CHECKED BY: S.D. McIntyre, J. Roodman, R. Roedts		
SCALE: NTS	DATE: Febuary 27, 2004	SHEET: 4 of 5

6 Manufacturing Plan

6.1 Manufacturing Processes Investigated

For each major component, a list of available tooling was compiled. Access to a shop with basic woodworking tools including a band saw, scroll saw, drill press, belt sander, and Dremel tool was available. Additionally, the team had access to a computerized laser cutter capable of scoring and cutting two dimensional CAD files out of wood and plastic. Stereolithography and autoclave facilities were investigated on campus, but proved to be prohibitive because of cost and inadequate experience. Given the resources available, a variety of manufacturing processes were investigated.

6.1.1 Wing Construction

Previous team aircraft utilized wings that were relatively heavy, weighing an average of 0.5 lb/ft^2 . Early in the design process, new fabrication techniques were investigated to effectively decrease the overall weight of this year's wing. These techniques included a hollow wing utilizing balsa and composite material sheeting with minimal internal structure, an all composite wing with no internal structure, a foam core wing and then a traditional built-up wing. Additionally, the 4 ft box dimension required that the 9 ft wing be build in three pieces.

Internet investigation on a hollow wing produced very little information about this construction technique and the team did not have the experience necessary. A smaller scale model was fabricated to investigate it further. This model was constructed around a foam core. Fiberglass-coated balsa sheeting formed the wing skin. Carbon strips were added in a spanwise and diagonal fashion to increase bending and torsional strength. The foam was removed from the core of the wing except for small sections of foam at the leading and trailing edges for support. The completed small scale test model of the hollow molded wing produced a wing weighing 0.22 lbs/ft^2 with potential to withstand Turbulence Syndrome's design flight loads. However, it was noticed that the foam crushed relatively easily leading to buckling of the wing skin during loading. Furthermore, this construction method did not produce the desired leading edges.

Composite materials including fiberglass and carbon fiber have very good strength-to-weight characteristics and it was decided to further investigate a construction method exclusively utilizing these materials. Initial research yielded even less information than what was obtained for the hollow molded wing. Only two members of the team had any previous experience with this construction method and previous attempts to build this type of wing were unsuccessful.

A third method of wing construction investigated made use of a foam core with fiberglass skin and carbon fiber reinforcements. This method would prove quick to build and many people on the team had experience building this type of wing. Furthermore, this construction method has been utilized extensively by many teams in years past. However, one main drawback is the increased overall weight associated with this construction method.

The final type of construction method utilized was a traditional spar and rib built-up design. Previous aircraft that capitalized on this method produced extremely strong wings with relatively simple

construction. It was determined that weight savings could be achieved through the use of a composite spar, greater rib spacing and reduction in total sheeting. This construction method also provided for easy repair since parts were easily fabricated and extras could be produced at the same time in case an accident occurred during flight testing.

6.1.2 Fuselage Construction

It was deemed important to reduce the overall weight of the fuselage as well. However, the team had very little experience with any building techniques outside of traditional former and panel construction. Brainstorming yielded a design capitalizing on carbon rods to support formers with minimal outside panels. An entirely composite design making use of an autoclave was also investigated.

The little information that was gathered from other teams as well as university resources suggested that making the autoclaved fuselage would prove time-consuming and expensive. Furthermore, repairs to damage during test flying would be difficult or impossible. Thus, production of several fuselages would be necessary. Additionally, cost and time factors associated with this technique would effectively make changes during the later phases of the design and flight testing impossible.

Figure 6.1 details a construction method replacing much of the outside fuselage panels with lighter and stronger carbon rods. It was decided that further investigation was necessary in order to accurately compare this construction method with others. A test model was built to validate the design. Loading of the model showed that, while bending was not a problem, torsional loading was not carried at all. The epoxy joints were easily broken and the bulkheads twisted with respect to each other around the carbon rods. To add torsional strength, side panels would be necessary. The additional space needed for carbon rods also increased fuselage dimensions and RAC.

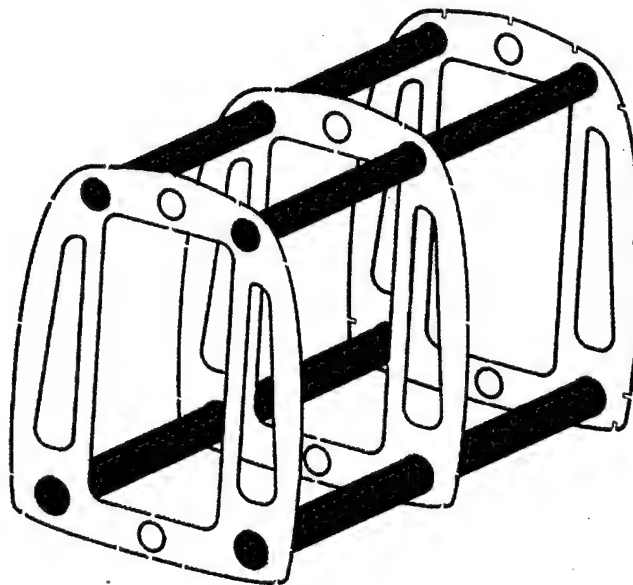


Figure 6-1: Carbon Rod/Bulkhead Design

Many team members are experienced model builders and were very familiar with the traditional construction technique utilizing bulkheads, formers, and side panels. Materials considered included balsa stock, balsa ply, birch ply, and carbon fiber reinforcements. While this construction technique utilized more parts and was the heaviest of the solutions investigated, it promised to be easy to build and repair. Like the wing, extra parts could be created and utilized for fast repairs.

Regardless of the design chosen, fuselage dimensions as well as the box size required that the fuselage be built in two pieces. This constraint became a significant factor when analyzing the designs.

6.1.3 Empennage Construction

While initially not a concern, weight proved to be a major consideration in the tail surfaces as well. Due to aircraft geometry, minimal allowance was given for extra weight this far aft. The entire empennage needed to weight less than 10 oz. Two construction methods were investigated: a flat plate and a built-up rib and spar design. The flat plate would be simpler to construct and easily duplicable for spare parts. Initial construction testing led to problems with torsional strength of the flat plate. Carbon reinforcements were added and lightening holes were cut in the experimental models. Results showed that a flat plate tail would end up well over the 10 oz budget. The team felt confident that a design could be developed utilizing carbon fiber tubes for spars. An experimental test surface was built to validate this design. The single surface weighed less than 3 oz.

6.2 Figures of Merit Used

The FOM categories and weighting, described in Section 2, were used to evaluate the various construction methods. Additionally, two categories comparing ease of repair and cost of construction were added. The addition of these categories was deemed necessary since some of the techniques investigated ranked closely in the original categories. Relative weighting between original categories was kept constant. The repair category was given equal weight as the reliability category. Cost of construction, while a consideration, was the least important factor. It was given a weighting lower than any other category. The detailed breakdown of category weighting can be seen in Table 6-1.

6.2.1 RAC

Any adverse affects on RAC from construction techniques were considered. Some techniques, especially in fuselage construction, required additional space for structural members. This effectively increased RAC by increasing fuselage volume. Weight of components also became a factor in this category.

6.2.2 Weight

Component weight was considered based on its overall contribution to aircraft weight. Initial concerns with total aircraft weight led to weight being a strong consideration. Although weight was a part of the RAC category, its importance to overall aircraft performance justified additional emphasis. The

lightest construction technique was given a 5, the heaviest a 1 and all others ranked relative to these two extremes.

6.2.3 Performance

The performance category took into account the finished product of each construction method. Surface finish, accurate sizing, and geometric accuracies were considered. If duplication of given dimensions or shapes, such as the wing's airfoil, would prove difficult the construction method was ranked accordingly. Tendency of a method to warp or wrinkle also ranked poorly. This category was a measure of how well the construction method could replicate the desired performance parameters.

6.2.4 Ease of Construction

While there are several experienced modelers on the team, ease of construction became a significant factor. The relatively short time allotted for building made it important that the team be confident in their ability to accurately produce a part with the chosen construction method. Techniques with which the team had very little experience ranked low, while successful techniques ranked high. Material availability was another consideration.

6.2.5 Stability and Control

While stability and control was not greatly affected by construction method, techniques were evaluated in this category based on any adverse affects that the technique would cause. Examples of items considered under this category include balancing problems.

6.2.6 Reliability

For the aircraft to meet the strict construction schedule and withstand the rigors of competition, construction techniques needed to be reliable. Any undesirable characteristics in validation models resulted in poor ranking.

6.2.7 Repair

Previous aircraft performance at competition made it necessary to consider the time necessary to repair a component. If an aircraft is damaged during competition, fast repair can help mitigate the effect on the team's performance. Repairs that could be completed in 30 minutes were used as a basis since this time frame would allow the team to receive flight scores even if the aircraft experienced minor damage. Simple repairs would effectively increase the team's performance by returning to flight-ready status faster.

6.2.8 Cost of Construction

While a relatively large amount of money was budgeted for the aircraft, cost of construction was still a consideration. Techniques that utilized excessive amounts of composite materials were ranked low due to their expensive nature. Similarly, if a technique required the team to purchase time to let team members work in a machine shop or other facility, it was also ranked low. This category effectively disqualified the composite wing.

Table 6-1 Manufacturing Process FOM

		RAC	Weight	Perf.	Const.	S & C	Rel.	Repair	Cost	TOTAL
Wing	Weight	0.12	0.12	0.15	0.11	0.13	0.13	0.13	0.11	
	Hollow Mold	4	4	1	2	2	2	1	3	2.31
	Composite	5	5	4	1	3	1	1	1	2.67
	Foam	1	1	4	3	3	4	4	3	2.93
	Rib and Spar	3	3	3	5	3	5	5	5	3.96
Fuselage	Weight	0.14	0.15	0.12	0.13	0.11	0.12	0.12	0.11	
	Traditional	3	1	3	5	3	5	5	5	3.66
	Carbon Tubes	1	4	1	2	2	1	3	3	2.15
	Composite	5	5	5	1	3	2	1	1	2.98
Empennage	Weight	0.11	0.1	0.14	0.11	0.17	0.13	0.13	0.11	
	Flat Plate	3	1	2	2	2	2	3	3	2.25
	Rib and Spar	3	5	3	4	4	3	2	3	3.35

6.3 Selected Processes for Major Component Fabrication

6.3.1 Wing

The traditional rib and spar construction proved the best design for wing construction. The spar was built in three pieces and consisted of a ply core capped with carbon fiber on top and bottom and then wrapped in fiberglass cloth. Carbon was also wrapped around the tips of the inboard spar to reinforce the joint. The outboard spars slipped inside the inboard spars, joining the two panels together. A smaller pin slid into a hole in the inboard section near the trailing edge to keep the two sections from twisting. Ribs were balsa in the center of the wings; tip ribs and ribs at the intersections were plywood. Both leading edge and trailing edge stock were utilized to simplify construction. Torsion was carried through balsa sheeting on the top and bottom of both leading and trailing edges. Between the leading and trailing edge sheeting, strips of balsa wider than the ribs and the same thickness were added as cap strips. These strips created an I-beam rib structure. Servos mounted on plywood panels slid into corresponding slots in the wing for easy removal and maintenance. Ailerons were built with ribs and sheeting. All joints between balsa components were fastened with CA glue; any joints incorporating plywood or fiberglass were bonded using epoxy. The entire wing was lightly sanded before Monokote was applied. Hinging of all control surfaces was done with Monokote after all components had been covered.

6.3.2 Fuselage

Classic built up construction was utilized for the main section of the fuselage. The plywood bulkheads of the main fuselage interlock with a center spine and two side panels. All internal components fastened to the bulkheads. The side panels stop forward of the tail cone attachment point. The tail cone slides over the aft end of the center spine. Side loads in this area, as well as the geometric transition between the main fuselage and the tail cone, were carried by balsa stringers.

6.3.3 Empennage

A built-up construction similar to the wing was utilized for the empennage. Carbon tubes were placed at the quarter-chord and at the trailing edge immediately in front of the control surface hinge. These spars slid into corresponding holes in the rear of the tail cone. The ribs had matching holes and slid over the spars. Sheeting was added to the leading and trailing edges in a similar fashion as the wing. Again, cap strips ran between the leading and trailing sheeting to create an I-beam rib design. The leading edge was balsa stock sanded to fit the airfoil shape. The trailing edge spar had a balsa strip glued the aft side to provide the appropriate surface to hinge the control surfaces. Control surfaces made use of a Warren truss structure and did not utilize any sheeting. Monokote hinges were utilized for the attachment of control surfaces.

6.4 Timeline for Manufacture

Deadlines were set for component construction. Construction times were estimated and doubled in the hope of producing an accurate schedule for construction. Dependencies between component construction were also considered. Using these dependencies and estimated times, intermediate construction deadlines were created working backward from the desired completion date of March 26, 2004. Figure 6-2 shows a construction timeline. Allotted times are shown in red, actual times in olive. Examination of actual construction times shows that, due to problems in finalizing construction techniques, actual construction was delayed in some instances. However, overall progression of construction is right on schedule at the time of report submission.

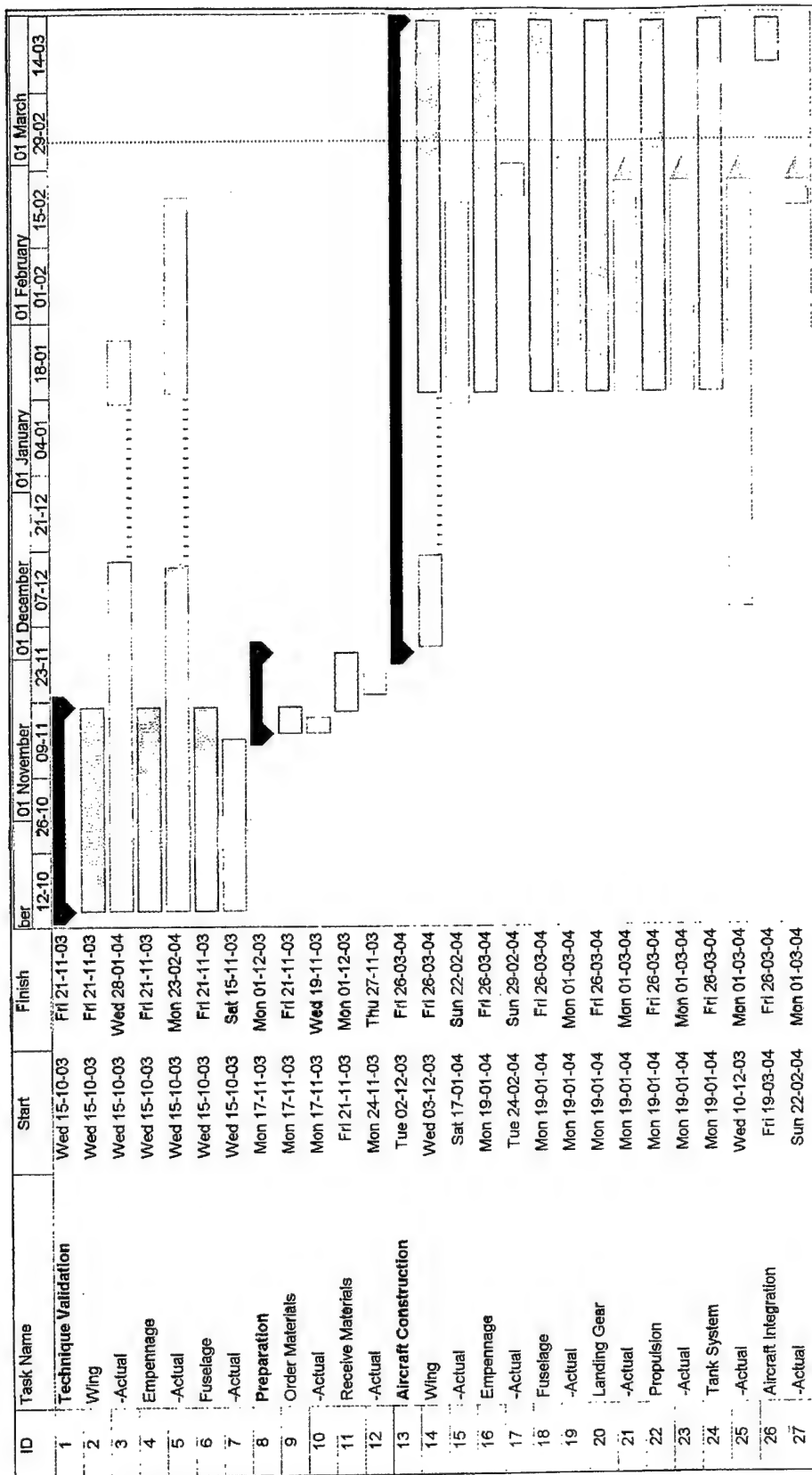


Figure 6-2: Manufacturing Schedule

7 Testing Plan

Aircraft subsystem testing is vital to the validation of all design criteria prior to first flight. While many lessons learned from previous experience are introduced throughout the design process, demonstrating flight-worthy hardware has its own unique challenges. Each system is unique and requires an independent verification that it may meet, exceed, or fail design criteria.

7.1 Test Objectives and Schedule

Many tests were implemented to improve the overall design of the aircraft. Each aircraft component was tested thoroughly in an iterative testing process. Table 7-1 contains the primary goals of the testing procedure and the schedule on which those goals were achieved. A detailed look at each test group is located in Section 7.2.

Table 7-1: Test Summary and Schedule

Test	Primary Objective	Schedule
Tank Drain Test	Develop the optimum tank drainage system for the current mission.	9/03 - 2/04
Oil Flow Visualization Test	Observe flow properties over the chosen airfoil.	1/04
Wing Spar Structural Test	Verify the structural adequacy of the wing's main structural component.	11/03 - 2/04
Propulsion System Performance Test	Confirm that the propulsion system meets the required specifications.	2/04 - 3/04
Landing Gear Structural Test	Ensure that the landing gear will withstand the rigors of competition.	1/04 - 3/04
Wing/Body Structural Test	Verify the structural adequacy of the wing/body components and interconnecting joints.	2/04 - 3/04
In-Flight Performance Test	Validate the performance characteristics of the final aircraft design.	3/04 - 4/04

7.2 Detailed Test Objectives and Results

7.2.1 Tank Drain Test

The goal of this experiment was to develop the relationship that defines the flow patterns from the tank, with a specific goal being to decrease the estimated drain time. The team tested and evaluated the effects of several different draining system features including a two- and four- tank setup, a vortex generator, positive pressure assist and a retractable drain tube.

From the test results, the team was then able to eliminate all the concepts that added complexity to the design without yielding significant benefits and use the remaining results to determine that the main factor involved in decreasing the drain time was the height of the water column. It should be noted that the inclusion of a simple tube on the exit port decreased the time and that the effect of having horizontal sections within a tank trapped the water and significantly increased the drain time.

Table 7-2: Drain Testing With a Volume of 4 L.

Test	1	2	3	4	5	6	7	8	9
Tube Length (in.)	0	0	0	7	11	16	21	8	17
Drain Time (sec)	22	19	21	20.4	12	10.5	15.7	17	14.5

7.2.2 Oil Flow Visualization Test

The objective of the oil flow visualization test was to determine the stall characteristics for the Clark Y airfoil with a taped joint. From the results, it was determined that the taped joints had a positive effect on the stall characteristics by causing turbulent flow at higher angles of attack therefore delaying the advent of stall. Because the tape was beneficial, no other flow modifying devices were needed.

7.2.3 Wing Structural Test

It was assumed that wing would be able to withstand the expected flight loads if it could withstand the tip test performed during technical inspection with a safety factor of 1.3, roughly equivalent to a 3g turn. Initial testing of the balsa core spars with carbon caps showed that the carbon easily delaminated off the core material. All subsequent spars with carbon caps were wrapped with a thin layer of fiberglass to prevent delamination. Secondary testing of the outboard spars led to failure at a 5 lbs tip load. A repeat of the test was conducted before it was discovered that a mistake in the analysis was made. Additionally, it was found that vertical grain balsa cores were not supporting the carbon caps as desired. Testing of a plywood core without carbon was performed. A sample outboard spar made strictly of plywood was found to fail at 12 lbs. The analysis was repeated and a mistake was found. Additional analysis was done for a plywood core, capped in carbon, and wrapped in fiberglass. Individual testing of each component showed that tip loads could be carried with a factor of safety of 1.3. Further load testing was postponed until initial wing construction was completed to allow the ribs to constrain spar twisting. The completed wings were able to withstand standard and inverted tip testing with a 27 lbs load. Deflection was 2.625 in., some of which was observed to be at the wing joints. While it would have been desirable to know how much loading the wing could withstand without failure, non-destructive evaluation was utilized because of timeline constraints.

Early in the construction phase, a test wing was built. While this wing proved to be under-built and flexible, it was a good test bed for experimenting with torsional loads on wings. Loads were placed on the tip of the wing at the trailing edge. Using an incidence meter, a deflection of 1.3°/oz was observed. The wing was covered and the test was repeated yielding a deflection of 0.08°/oz, a full order of magnitude increase in torsional stiffness. While stiffer, it was determined that additional torsional rigidity would be necessary. The balsa sheeting added to the wings produced another full order of magnitude increase in torsional stiffness, bringing the torsional stiffness of the wing to within acceptable limits.

7.2.4 Propulsion System Performance Test

This test was designed to ensure that the static thrust and run time would meet the performance speculations put forth in the design process. The team would then check the resulting data with Motocalc™ predictions and use this to determine if a lower cell capacity could be used to reduce the overall weight while still providing sufficient runtime.

In preparing for this test, we found that both of the available Astro-Flight 60 motors from the previous year were damaged and that some of the cells in the previous year's battery pack had chemically reversed. As such, the battery packs were split up to prevent further cells from reversing, and more testing will be completed following hardware procurement.

7.2.5 Landing Gear Structural Test

The primary objective of this test was to test the resiliency of the landing gear to both plastic deformation and shock absorption.

Upon further research and testing, it was found that no off-the-shelf main gear was available that could resist plastic deformation so the gear will have to be modified. The results of the testing also showed that a Robart™ heavy duty strut would provide a favorable balance of the shock absorption and strength that is required of the nose gear in a tricycle configuration. Lastly, it was determined that a fully loaded landing should be avoided.

7.2.6 Wing-Fuselage Interface Structural Test

This test was done to verify that all the structural components of the wing and fuselage could withstand the load requirements. By testing the wing tip with inverted and non-inverted loads well beyond those produced in the expected flight envelope, it was determined that the integrity of the wing-fuselage interface and the mid-span joints was acceptable. The integrity of each wing junction was shown to improve with the use of tape.

7.2.7 Fuselage

The fuselage was tested as two separate components. The main fuselage was hung from a simulated plywood spar and loaded to 30 lbs successfully. For reasons similar to those used in wing testing, a non-destructive approach to evaluation was taken. Tail cone validation was conducted in a similar manner with an 8 lbs load at the very tip of the cone. Minimal deflection was observed.

7.2.8 Empennage

Empennage validation was conducted similarly to the wing validation. Loading of the flat plate produced a deflection of 1 in. with a 4.5 lbs load placed at $\frac{2}{3}$ of the span at the quarter-chord, equivalent to the maximum aerodynamic loads experienced in flight. While this was acceptable, the flat plate performed poorly in torsion. Additionally, carbon reinforcements proved difficult to laminate to the plywood plate. Testing of the built-up tail surface showed better results with the surface deflecting 1.375

in. with a 4.5 lbs load placed at $\frac{2}{3}$ span at the quarter-chord and less than 1° of deflection when 2 lbs was placed at the tip at $\frac{3}{4}$ chord. The additional bending deflection was determined to be acceptable.

Decreased weight and increased torsional stiffness made this surface a desirable choice.

7.2.9 In-Flight Performance Test

The objective of this test will be to determine the aircraft performance and stability during critical flight conditions and to evaluate the control response of all critical systems. Listed below is the in flight test schedule that will be run upon the completion of Turbulence Syndrome. Prior to each flight a Pre-Flight Checklist (Table 7-3) must be completed. The pre-flight checklist ensures that all steps have been completed to allow a safe and successful flight. During each flight, an In-Flight Data Recordings Sheet (Table 7-4) must be completed. This sheet contains all of the necessary parameters to calculate the basic performance characteristics of the airplane during the given flight. The data collected and analyzed can then be used to enhance the total performance of the aircraft and optimize the aircraft setup and in-flight maneuvers performed in subsequent missions.

1. Sortie 1 – Ground Taxi Test
 - Configure aircraft for the Fire Bomber Mission.
 - Validate V-tail / Nose gear steering system.
 - Check ground stability at a range of speeds.
2. Sortie #2 – First Flight
 - Configure aircraft for the Ferry Mission.
 - Perform basic flight maneuvers; evaluate stability and control.
 - If run time permits, perform advanced maneuvers at pilot's discretion.
3. Sortie #3 – Drain Test
 - Configure aircraft for the Fire Bomber Mission.
 - Perform basic flight maneuvers; evaluate stability and control.
 - Perform a straight and level drain test.
4. Sortie #4 – Full Mission
 - Configure aircraft for the Fire Bomber Mission.
 - Perform Fire Bomber Mission profile.
5. Sortie #5 – Full Mission
 - Configure aircraft for the Ferry Mission.
 - Perform Ferry Mission profile.

Table 7-3: Preflight Checklist

Preflight Checklist					
Flight #	Mission Profile				
Time	Location				
Test	Completed	Additional Info			
Tail surfaces secured					
Tail control lines connected					
Tail boom aligned & secured					
Nose cone secured					
Propeller nut tightened					
Propeller longitudinal load >15lb					
Landing gear secured					
Wing servos connected					
Wing joints taped and secured					
Wing Tip Test					
CG Check Within FWD & AFT Limits		CG Location			
Battery Pack 1 Voltage		Pack #		Voltage	
Battery Pack 2 Voltage		Pack #		Voltage	
Receiver Battery Voltage		Pack #		Voltage	
Transmitter Battery Voltage		Pack #		Voltage	
Electrical connections correct and secured					
All control surfaces working properly					
Valve operating correctly					
Fail Safe Check					

Table 7-4: In-flight Data Recordings Checklist

In-Flight Data Recordings					
Flight #			Mission Profile		
Time			Location		
Lap #		1	2	3	4
Tank Fill	Volume				
	Time				
Power On	Time				
Liftoff	Distance				
	Time				
180 Marker	Crossing Time				
	Altitude				
180 Turn	Start Time				
	Start Distance				
	Radius				
	End Time				
	End Distance				
180 Marker	Crossing Time				
360 Turn	Start Time				
	Start Distance				
	Start Altitude				
	Radius				
	End Time				
	End Distance				
	End Altitude				
180 Marker	Crossing Time				
	Altitude				
180 Turn	Start Time				
	Start Distance				
	Radius				
	End Time				
	End Distance				
180 Marker	Crossing Time				
	Altitude				
Touchdown	Distance				
	Time				
Full Stop	Distance				
	Time				

* All time measurements are relative to the start time of 00:00. All distance measurements are in feet

8 References

1. Bertin, J.J., and Smith, M.L. Aerodynamics for Engineers, Third Edition. 1998 Prentice-Hall, Inc. Upper Saddle River, NJ, pg 286.
2. Drela, Mark. "Xfoil 6.94 Subsonic Airfoil Development System." <http://raphael.mit.edu/xfoil/>, Last updated December 18, 2001.
3. Jacob Kay, W.H. Mason, W. Durham, F. Lutze and A. Benoliel, " Control Power Issues in Conceptual Design: Critical Conditions, Estimation Methodology, Spreadsheet Assessment, Trim and Bibliography," VPI-Aero-200, November 1993.
4. MATWEB. <http://www.matweb.com/index.asp?ckck=1>. Last updated February 28, 2004.
5. Melin, Thomas. Tornado Vortex Lattice Method. Available <http://www.flyg.kth.se/divisions/aero/software/tornado/>.
6. Raymer, Daniel P. Aircraft Design: A Conceptual Approach. 3rd Edition. AIAA: August 1999.
7. Selig, Michael. "UIUC Airfoil Data Site." <http://www.aae.uiuc.edu/m-selig/ads.html>. Last updated December 8, 2002.

2003-2004 CESNA/ONR STUDENT DESIGN-BUILD-FLY COMPETITION

UNIVERSITY OF FLORIDA

SWAMP STUKA

DEPARTMENT OF MECHANICAL AND AEROSPACE ENGINEERING

231 MAE-A, P.O. Box 116250

Gainesville, FL 32611-6250

TEAM MANAGER

MICHELE DI BENEDETTO

ASSISTANT TEAM MANAGER

LEAH KAMLEITER

TEAM LEADERS

JOHN CRANE

DAVE WILSON

ART HOMS

TECHNICAL ADVISOR

DAVID JENKINS, Ph. D

ADMINISTRATIVE ADVISOR

DOLORES KRAUSCHE, Ph. D

Team Manager: Michele Di Benedetto		
Assistant Team Manager: Leah Kamleiter		
Aerodynamics	Structures	Systems
Team Lead: John Crane	Team Lead: Dave Wilson	Team Lead: Art Homs
Charles Nipper	Jessica Allen	Tristan Goldbach
Mike Sytsma	Brooke Hedlund	Laura Dahlene
Chris Rodriguez	Darren Gibson	Tom Cowan
Miguel Palaviccini	Carlos Fernandez	Daniel Klockenkemper
	Fred Leve	

TABLE OF CONTENTS

LIST OF TABLES	III
1 EXECUTIVE SUMMARY	1
2 MANAGEMENT SUMMARY.....	1
2.1 ORGANIZATION OF DESIGN TEAM.....	1
3 CONCEPTUAL DESIGN.....	2
3.1 PROBLEM STATEMENT.....	2
3.2 MISSION SPECIFICATIONS.....	2
3.2.1 <i>Fire Flight Mission</i>	2
3.2.2 <i>Ferry Flight Mission</i>	3
3.2.3 <i>Aircraft Storage</i>	3
3.2.4 <i>Rated Aircraft Cost</i>	3
3.2.5 <i>Take Off</i>	3
3.3 ALTERNATIVE CONFIGURATION CONCEPTS.....	3
3.3.1 <i>Wing Design</i>	4
3.3.1.1 The Rectangular Wing.....	4
3.3.1.2 The Strongly Tapered Wing.....	5
3.3.1.3 The Moderately/Slightly Tapered Wing	6
3.3.1.4 The Elliptical Wing	7
3.3.1.5 Wing Planform Analysis.....	8
3.3.2 <i>Tail Design</i>	8
3.3.2.1 Horizontal Tail.....	9
3.3.2.2 T-Tail.....	10
3.3.2.3 Preliminary Values for T-Tail	10
3.3.2.4 Tail Analysis.....	11
3.3.3 <i>Tank Design</i>	11
3.3.3.1 Custom Made tank with Solenoid Valve	11
3.3.3.2 Pre-made Tank with Flapper	11
3.3.3.3 Tank Analysis	12
3.4 FINAL RANKINGS	12
4 PRELIMINARY DESIGN.....	12
4.1 STRUCTURAL DESIGN.....	12
4.1.1 <i>Design Parameter and Sizing Trades</i>	13
4.1.2 <i>Design optimization and Trade Studies</i>	13

4.1.3	Component Preliminary Design.....	13
4.1.3.1	Bulkheads	13
4.1.3.2	Horizontal Tail and Elevator	14
4.1.3.3	Tank	17
4.1.3.4	Landing Gear	17
4.2	AERODYNAMICS DESIGN.....	17
4.2.1	Design Parameter and Sizing Trades	17
4.2.1.1	Airfoil Selection	17
4.2.1.2	Wing Design	18
4.2.2	Analysis method	19
5	DETAIL DESIGN.....	21
5.1	STRUCTURAL COMPONENT.....	21
5.1.1	Component selection.....	21
5.1.2	Final Design.....	21
5.1.2.1	Bulkhead Detail Design	21
5.1.2.2	Fuselage Detail Design.....	22
5.1.2.3	Horizontal Tail and Elevator Detail Design	22
5.1.2.4	Vertical Tail and Rudder Detail Design.....	24
5.1.2.5	Tank Detail Design	25
5.1.2.6	Landing Gear Detail Design.....	25
5.2	WING COMPONENT	26
5.3	PROPULSION COMPONENT	26
5.4	RATED AIRCRAFT COST.....	27
5.5	FINAL DESIGN	28
5.6	FINAL DESIGN DRAWINGS.....	29
6	MANUFACTURING PLAN AND PROCESS	29
6.1	FUSELAGE MANUFACTURING AND ASSEMBLY	29
6.1.1	Investigated processes.....	29
6.2	WING MANUFACTURING AND ASSEMBLY.....	30
6.2.1	Investigated processes.....	30
6.2.2	Final design process	31
6.3	PROPULSION MANUFACTURING AND ASSEMBLY	32
6.3.1	Investigated processes.....	32
6.3.2	Final design process	33
7	TESTING PLAN	34

7.1	STRUCTURAL TESTING	34
7.1.1	Testing Objectives.....	34
7.2	AERODYNAMIC TESTING.....	34
7.2.1	Testing Objectives.....	34
7.3	PROPULSION TESTING.....	34
7.3.1	Testing Objectives.....	34
7.4	RESULTS	34
7.5	LESSONS LEARNED FOR COMPONENT AND FULL AIRCRAFT	35
8	REFERENCES	ERROR! BOOKMARK NOT DEFINED.

LIST OF TABLES

TABLE 2.1	TEAM ORGANIZATION AND MEMBERS	2
TABLE 3.1	CONCEPTUAL WEIGHT ESTIMATES FOR MAIN COMPONENTS	3
TABLE 3.2	MAJOR DESIGN FACTORS.....	8
TABLE 3.3	FOM FOR FINAL DECISION ON CONCEPTUAL OPTIONS	12
TABLE 4.1	PARAMETERS USED TO DETERMINE HORIZONTAL TAIL	14
TABLE 4.2	PARAMETERS USED TO DETERMINE VERTICAL TAIL.....	17
TABLE 4.3	TORNADO RESULTS.....	19
TABLE 5.1	PROPULSION COMPONENT	27
TABLE 5.2	RATED AIRCRAFT COST.....	27
TABLE 5.3	AIRCRAFT SIZING	28
TABLE 6.1	MILESTONE CHART FOR MANUFACTURING.....	29
TABLE 6.2	FOM FOR FUSELAGE MANUFACTURING PROCESS	30
TABLE 6.3	FOM FOR WING MANUFACTURING	31
TABLE 6.4	FOM FOR ENGINE SELECTION	33
TABLE 6.5	FOM FOR BATTERY SELECTION.....	33
TABLE 7.1	SCHEDULE FOR FUSELAGE TESTING	34

LIST OF FIGURES

FIGURE 3.1	WING WAKE EFFECT ON THE HORIZONTAL TAIL (LENNON 37)	10
FIGURE 4.1	HORIZONTAL AND VERTICAL TAIL PLACEMENT VERTICAL TAIL.....	15
FIGURE 4.2	RUDDER AREA NOT BLANKETED BY HORIZONTAL TAIL.....	16
FIGURE 5.1	DIMENSIONAL DRAWING OF THE HORIZONTAL TAIL IN INCHES	23
FIGURE 5.2	DIMENSIONED DRAWING OF THE VERTICAL TAIL.....	25

1 Executive Summary

The development process for the University of Florida Design Build Fly team included several ideas from the members on paper. These design parameters for the ideas were then put into calculations to see if they were feasible for the required missions. After looking at the calculation results for various designs the thought of how to build these ideas came into play. What design ideas were the easiest to manufacture, lowest cost, and lightest weight were taken into account. Wide ranges of alternative ideas were considered from a bi-wing plane and T-Tail to a simple classic tail dragger airplane. The simplest design, lightest weight and manufacturing ability is what we strived to develop this year.

2 Management Summary

The University of Florida Design-Build-Fly team consists of eighteen members. These aerospace and electrical engineering students are divided into several smaller groups in order to work more effectively together. This team structure is described in greater detail below.

2.1 Organization of design team

First, a team manager was chosen to provide direction for the team. The team manager was responsible for keeping the team on track, making sure everyone was communicating

Next, in order to make the large group more manageable, everyone was dividing between three more focused groups: Aerodynamics, Structures, and Systems. A Team Lead, who was responsible for overseeing that the members of the group completed that aspect of the design, headed each of these groups.

Communication is vital in a large group project such as this; therefore many meeting and discussion times were established. The entire team met bi-weekly to discuss the current status of the project, and to bring everyone up to date on any important findings or design changes. The manager, assistant manager, and team leads met once a week to ensure good communication between each smaller group. In addition, the team leads met with each of their respective groups as they deemed necessary to complete their assignments.

Table 2.1 Team Organization and Members

Team Manager: Michele Di Benedetto		
Assistant Team Manager: Leah Kamleiter		
Aerodynamics	Structures	Systems
Team Lead: John Crane	Team Lead: Dave Wilson	Team Lead: Art Homs
Charles Nipper	Jessica Allen	Tristan Goldbach
Mike Sytsma	Brooke Hedlund	Laura Dahlene
Chris Rodriguez	Darren Gibson	Tom Cowan
Miguel Palaviccini	Carlos Fernandez	Daniel Klockenkemper
	Fred Leve	

Table 2.2 General Milestone Chart

Event	Planned	Actual
Conceptual	December 1, 2003	December 1, 2003
Preliminary	January 1, 2004	February 1, 2004
Detailed	February 1, 2004	February 9, 2004
Building Completed	February 26, 2004	March 4, 2004
Flight Testing	March 1, 2004	Not completed
Report Preparation	February 21, 2004	March 5, 2004

3 Conceptual Design

3.1 Problem Statement

The main goal of the conceptual design was to come up with an aircraft that would fulfill the requirements of the competition while maintaining ease of manufacturing. While several ideas were brought up during this process, the limits of manufacturing equipment and expertise ultimately ruled the design process.

3.2 Mission Specifications

There were several aspects to the mission specifications that were overriding factors in the design of Swamp Stuka. They are outlined in this section.

3.2.1 Fire Flight Mission

The aircraft must lift and dump up to 4L of water. The goal of the team was to carry all 4L for maximum points. The water may only exit through a 0.5" diameter hole, and must be dumped in a single 360° turn.

3.2.2 Ferry Flight Mission

The purpose of this mission is speed. The aircraft must complete 4 laps without any payload.

3.2.3 Aircraft Storage

The aircraft must be stored in a 4' x 2' x 1' box. Thus, either the length of components would need to be monitored, or joints would need to be constructed and considered in a structural analysis.

3.2.4 Rated Aircraft Cost

The rated aircraft cost (RAC) is based on engine power, empty weight, and manufacturing man hours based on surface area. The final score is inversely proportional to the RAC, so keeping the engine, size, and weight down will be crucial to success.

3.2.5 Take Off

Take off distance is confined to 150 ft. Engine power and wing loading must conform to take off requirements.

3.3 Alternative Configuration Concepts

During conceptual design, many aspects of the aircraft were discussed. Conceptual designs for the main components of the aircraft are outlined in this section.

In order to begin the design process, several assumptions had to be made. First, a rough idea of weight had to be determined. These are found on Table 3.1.

Table 3.1 Conceptual Weight Estimates for Main Components

Component	Weight (lb)
Water	8.9
Fuselage	5.0
Motor	2.1
Batteries	5.0
Wings	4.0
Radio	2.0
Miscellaneous	3.0
Total	30.0

Secondly, the cruise speed was assumed to be 30 mph based on team experience. Lastly, the density ratio of the air was estimated to be 0.963 for Wichita, Kansas (alt 1342 ft above sea level)

3.3.1 Wing Design

Several wing planforms were investigated. These were a rectangular wing, a strongly tapered wing, a slightly tapered wing, and an elliptical wing. Their implications to the design process are outlined below.

3.3.1.1 The Rectangular Wing

Pros:

- Easiest type to build.
- Does not stall easily.

Cons:

- Parts of the wing are underemployed, not carrying their fair share of the model's weight. Although the wing chord is constant, the load carried by each chordwise section falls off sharply towards the tips.
- As noted in the section above, the outer parts of the wing do not reach their max possible lift coefficient. Therefore we are using more wing area and wing weight for less lift.
- The drag of the whole wing is higher in comparison to the other planforms.

The following formulas were used to arrive at the design parameters listed below

- $S = bc$
- $AR = \frac{b^2}{S}$
- $Re = KcV$ where $K = 756$ at alt = 1342 ft (Lennon, p. 17)
- Required $C_l = \frac{3519W}{\sigma V^2 S}$ (Lennon, p. 14)
- $C_{d,tot} = C_d + C_{dp} + C_{di}$
- $C_{di} = \frac{0.318C_l^2}{AR}$ (Lennon, p. 23)
- $C_{dp} \approx 0.01$ (Simons, p. 217)
- $PF = \frac{C_l^{1.5}}{C_{d,tot}}$

Design Parameters

- Span, $b = 11$ ft
- Root Chord, $c = 1.2$ ft
- Planform Area, $S = 9.167 \text{ ft}^2$

- Aspect Ratio, $AR = 8.46$
- Wing Loading, $W/S = 33.6 \text{ oz} / \text{ft}^2$
- Reynolds Number, $Re = 354000$
- Required Lift Coefficient at cruise, $C_l = 0.946$
- Selected Airfoil – NACA 7512 mounted at $i = 1 \text{ deg AoA}$
 - $C_l = 0.948$
 - $C_d = 0.011384$
 - $C_m = -0.249$
- $C_{di} = 0.0337$
- $C_{d,tot} = 0.055$
- Power Factor = 16.726

3.3.1.2 The Strongly Tapered Wing

Pros:

- Good for a steady, low speed.
- Approximates an elliptical lift distribution

Cons:

- The tips stall first, resulting in loss of roll control.
- Due to high profile drag and premature stalling at low Re , calculations show that almost all aerodynamic advantages of the tapered wing are lost on small models.

The following formulas were used to arrive at the design parameters listed below

- $C_{mean} = \frac{c(1+\lambda)}{2}$
- $S = bc_{mean}$
- $AR = \frac{b^2}{S}$
- $Re = KcV$ where $K = 756 \text{ in} / \text{mph}$ at alt = 1342 ft (Lennon, p. 17)
- Required $C_l = \frac{3519W}{\sigma V^2 S}$ (Lennon, p. 14)

Design Parameters

- Span, $b = 11 \text{ ft}$
- Root Chord, $c = 1.4 \text{ ft}$

- Taper Ratio, $\lambda = 0.3$
- Mean Chord, $c_{mean} = 0.91 \text{ ft}$
- Root Reynolds Number, $Re = 381000$
- Mean Reynolds Number, $Re = 248000$
- Tip Reynolds Number, $Re = 114000$
- Planform Area, $S = 10.01 \text{ ft}^2$
- Wing Loading, $W/S = 47.95 \text{ oz / ft}^2$
- Required Lift Coefficient at cruise, $C_l = 1.35$

3.3.1.3 The Moderately/Slightly Tapered Wing

Pros:

- A compromise between the heavily tapered and rectangular wing.
- The load distribution is matched more closely to the area.

Cons:

- This planform will cause a relatively small mild tip stall effect but much less than the strongly tapered wing.

The following formulas were used to arrive at the design parameters listed below

- $c_{mean} = \frac{c(1 + \lambda)}{2}$
- $S = bc_{mean}$
- $AR = \frac{b^2}{S}$
- $Re = KcV$ where $K = 756 \text{ in / mph}$ at alt = 1342 ft (Lennon, p. 17)
- Required $C_l = \frac{3519W}{\sigma V^2 S}$ (Lennon, p. 14)

Design Parameters

- Span, $b = 11 \text{ ft}$
- Root Chord, $c = 1.4 \text{ ft}$
- Taper Ratio, $\lambda = 0.3$
- Root Reynolds Number, $Re = 381000$
- Mean Reynolds Number, $Re = 305000$
- Tip Reynolds Number, $Re = 229000$

- Planform Area, $S = 12.32 \text{ ft}^2$
- Wing Loading, $W/S = 38.96 \text{ oz} / \text{ft}^2$
- Required Lift Coefficient at cruise, $C_l = 1.1$

3.3.1.4 The Elliptical Wing

Pros:

- This is the only type of planform that will produce, at all speeds, constant downwash with a load distribution precisely matching the area.
- Best regarded as an ideal to be approached as closely as possible.

Cons:

- Tip stalling low Re at the wingtips, resulting in loss of roll control.
- Some wing positions may reduce the load carrying capacity.

The following formulas were used to arrive at the design parameters listed below

- $S = \frac{\pi}{4}bc$
- $AR = \frac{b^2}{S}$
- $Re = KcV$ where $K = 756 \text{ in} / \text{mph}$ at alt = 1342 ft (Lennon, p. 17)
- Required $C_l = \frac{3519W}{\sigma V^2 S}$ (Lennon, p. 14)
- $C_{d,tot} = C_d + C_{dp} + C_{di}$
- $C_{di} = \frac{0.318C_l^2}{AR}$ (Lennon, p. 23)
- $C_{dp} \approx 0.01$ (Simons, p. 217)
- $PF = \frac{C_l^{1.5}}{C_{d,tot}}$

Design Parameters

- Span, $b = 11 \text{ ft}$
- Root Chord, $c = 1.5 \text{ ft}$
- Planform Area, $S = 12.96 \text{ ft}^2$
- Wing Loading, $W/S = 37.0 \text{ oz} / \text{ft}^2$
- Reynolds Number, $Re = 408000$

- Required Lift Coefficient at cruise, $C_l = 1.04$
- Selected Airfoil – NACA 7512 mounted at $i = 2.5$ deg AoA
 - $C_l = 1.088$
 - $C_d = 0.011021$
 - $C_m = -0.262$
- $C_{di} = 0.0371$
- $C_{d,tot} = 0.0582$
- Power Factor = 18.4

3.3.1.5 Wing Planform Analysis

From the above analysis, a rectangular planform was shown to be the most effective design considering ease of construction. While its power factor was not the highest, it was comparable to the elliptical wing planform designed. The tapered wings, while lighter, required a larger lift coefficient. The lowered Reynolds numbers at the tips could also not easily be compensated for to prevent stalling at the tips.

Table 3.2 Major Design Factors

Planform	C_l	$C_{d,tot}$	Req AoA (deg)	Power Factor
<i>Rectangular</i>	0.948	0.055	3	16.73
<i>Strongly Tapered</i>	1.35	N/A	N/A	N/A
<i>Slightly Tapered</i>	1.1	N/A	N/A	N/A
<i>Elliptical</i>	1.09	0.0582	4.5	18.4

3.3.2 Tail Design

The tail configuration is designed to balance the forces and moments generated by the wing, propeller, and fuselage. The horizontal stabilizer must provide sufficient pitch control for maneuverability and counteract the pitching moment tendency of the aircraft. The vertical stabilizer must provide yaw control while not producing excessive roll coupling. Based on equations found in Lennon, we developed a spreadsheet that relates aircraft data to tail design parameters.

Two designs were considered for the tail surface arrangement. A horizontal tail mounted to the fuselage and a T-tail (horizontal stabilizer mounted on top of the vertical stabilizer).

3.3.2.1 Horizontal Tail

A horizontal tail mounted to the fuselage has reduced efficiency because of it resides near the wake generated by the wing. It is also within the slipstream of the prop. Since a low wing design is being implemented, the stabilizer should be placed as far above the wake centerline as possible. This is limited only by the geometry of the fuselage.

The following equations were used to analyze the two designs

$$M_{net} = W_{total\ weight} * (d1) + M_{wing\ moment} + D_{wing\ drag} * (d2) + T_{thrust} * (d3)$$

$$L_{tail} = M_{net} / TMA$$

d1= horizontal distance CG to .25MAC

d2= vertical distance CG to MAC

d3= vertical distance CG to thrust line

TMA = Tail moment arm (Lennon 38)

$$HTA = 2.5 * MAC * 0.2 * WA / TMA \quad (Lennon\ 33)$$

$$TL = L_{tail} / HTA$$

$$H = C_l * (\% \text{ semi-span from chart}) * 2 * 12 / (100 * \text{Wing Span}) \quad (Lennon\ 38)$$

$$M = M_{0.9} = 0.5 * MAC * 12 - H \quad (Lennon\ 38)$$

$$M = 1.10M_{0.9} \quad (\text{for T-Tail})$$

$$VTA \approx 0.45 * RLA \quad (45\% \text{ rear lateral area})$$

$$RA = 0.25 VTA \quad (\text{rudder area})$$

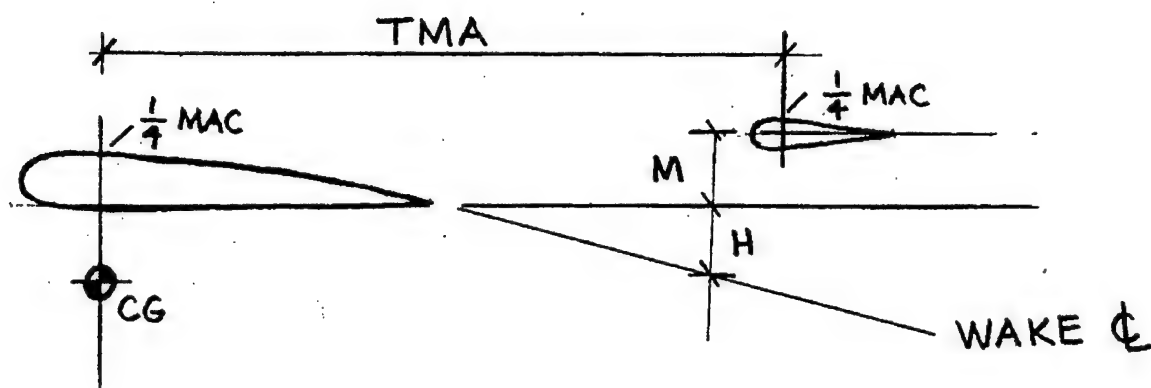


Figure 3.1 Wing Wake effect on the Horizontal Tail (Lennon 37)

M_{net}	= 0.153 lbft
L_{tail}	= 0.044 lb
HTA	= 1.71 sq.ft
TL	= 0.026 lb/sq.ft
H	= 0.047 in
$M_{0.9}$	= 5.95 in
VTA	= 0.61 sq. ft
RA	= 0.18 sq ft

3.3.2.2 T-Tail

A T-tail places the horizontal stabilizer in a position out of the wing wake and possibly above the prop slipstream. This provides excellent control and maximum efficiency, but introduces loading through the vertical stabilizer.

3.3.2.3 Preliminary Values for T-Tail

M_{net}	= 0.153 lbft
L_{tail}	= 0.044 lb
HTA	= 1.54 sq.ft (10% reduction, optimization from efficiency)
TL	= 0.028 lb/sq.ft
H	= 0.047 in
M	= 6.55 in
VTA	= 0.65 sq. ft
RA	= 0.19 sq ft

3.3.2.4 Tail Analysis

From the above analysis, a conventional horizontal configuration was found to be the most effective tail configuration.

3.3.3 Tank Design

Two concepts for the design of the tank were presented during the conceptual design. They were a custom made tank and an existing tank. The benefits and disadvantage of each are described below.

3.3.3.1 Custom Made tank with Solenoid Valve

The idea for the custom built tank was that it would fit entirely in the fuselage. It would be built from carbon fiber (based on the technology the team has). A solenoid valve would control the water flow, and a complicated venturi tube would lower the pressure near the orifice to pull the water out of the tank.

The pros of this idea is that the tank can be made in any size desired. The solenoid valve would guarantee control of the flow, and the venturi tube would aid in speed to empty the tank.

The downside is that solenoid valves are found mostly in AC configurations, and the plane runs on DC voltage. Additionally, the venturi tube increased the drag considerably.

3.3.3.2 Pre-made Tank with Flapper

The ease of manufacturing lead the team to consider a premade tank (ex: soda bottle, etc). Additionally, a toilet bowl flapper with a servo would serve as the flow control. No pressured air would be used to empty the tank.

The advantage to this design is that manufacturing is easy. There is no increased drag associated with this design.

The downside to using this design is the additional burden of making sure the flow is controlled. Additionally, the tank can only come in certain sizes.

3.3.3.3 Tank Analysis

The team chose to use a premade tank due to manufacturing issues. Additionally, an appropriate solenoid valve could not be located. Thus, a flapper will be used.

3.4 Final Rankings

The ideas presented in this section are summarized in Table 3.3 with their figures of merit. The final airplane will have a rectangular wing, horizontal tail, and a premade tank with a flapper to control the flow.

Table 3.3 FOM For Final Decision on Conceptual Options

Option	Benefit	Construction	Weight	Total
<u>Wing Design</u>				
Rectangular	0	1	0	1
Strongly Tapered	0	-1	0	-1
Moderately Tapered	0	0	0	0
Elliptical	1	-1	0	0
<u>Tail Design</u>				
Horizontal	0	1	1	2
T-Tail	1	-1	0	0
<u>Tank Design</u>				
Custom Made	1	-1	0	0
Premade	0	0	1	1
<u>Tank Flow Control</u>				
Solenoid Valve	1	-1	-1	-1
Flapper	0	0	1	1

4 Preliminary Design

This section outlines the preliminary design for the structure and aerodynamic designs.

4.1 Structural Design

In the preliminary design of the fuselage the two parameters that mattered the most was structural rigidity and the total weight of the aircraft. Each of the parameters had to be optimized to create the most efficient aircraft possible.

4.1.1 Design Parameter and Sizing Trades

The weight of the aircraft had to be as small as possible, but this would cause the aircraft to be weaker then could be allowed. If the aircraft were built up too much, it would be too heavy to lift with the given engine and battery constraints. As the tank increased in size, the beam of the aircraft had to be expanded. If a cylinder was used with a seven-inch diameter, the fuselage had to be increased to at least seven inches in diameter to match the tank supports.

Once the tank was decided the wing was found to need about a sixteen-inch chord. This necessitated that the fuselage be able to support a wing of this size.

4.1.2 Design optimization and Trade Studies

The first trade study conducted for the fuselage was to determine the basic shape. The two choices were a rectangular or square cross-section, and the second was a circular or elliptical shape.

For ease of manufacturing, the rectangular shape was easily more practical then the elliptical shape. Bulkheads could be cut out using a table saw and then sanded to the correct sizing. An elliptical shape would require the use of either a hand-held scroll saw or a 12-in band saw, but with either tool the need for training would be increased for those who had never used the machines before.

For aerodynamics the circular cross section would cause less drag than that of the rectangular shape. However, by tapering the cross-section at the front and rear of the aircraft the parasite drag could be reduced and by incorporating fairings for any protrusions including the propeller assembly the blunt body drag could be reduced.

The second trade study was on different material that would be used during construction. There were three main ideas: carbon fiber for most of the aircraft with some balsa and fir used to help maintain the shape, a mostly fir aircraft, and an almost completely balsa aircraft.

An aircraft that was made of carbon fiber could be very light when compared with an aircraft of similar size made from conventional material

4.1.3 Component Preliminary Design

4.1.3.1 Bulkheads

Fir was originally chosen for the material for the bulkheads. This was to allow the bulkheads to help the sides act as an I-beam in handling the bending moment caused by the loading of the horizontal tale and elevator.

4.1.3.2 Horizontal Tail and Elevator

The horizontal stabilizer was located and sized to provide the necessary stability for the airplane in flight. The primary purpose of the tail is to counter the moments produced by the wing. The elevator is the control surface that will control the pitching moment.

To minimize the interference caused by the wake of the wing the vertical placement of the tail is important. It must be placed higher than the wake of the wing during straight and level flight. This is shown in Figure 4.1.

The tail will be located at the rear of the six-foot fuselage, which produces a tail moment arm of 44 in (measured from the quarter chord of the wing to the quarter chord of the tail.) The tail area is proportional to the wing area, by the relationship given in Eq. 1.

$$HTA = (2.5 \times MAC \times 20\% \times WA) / TMA \quad (\text{Eq. 1})$$

Table 4.1 Parameters used to Determine Horizontal Tail

TMA	Tail-moment arm	44	in
WA	Wing area	1728	in ²
MAC	Wing's mean aerodynamic chord	16	in
HTA	Horizontal tail area	314.2	in ²

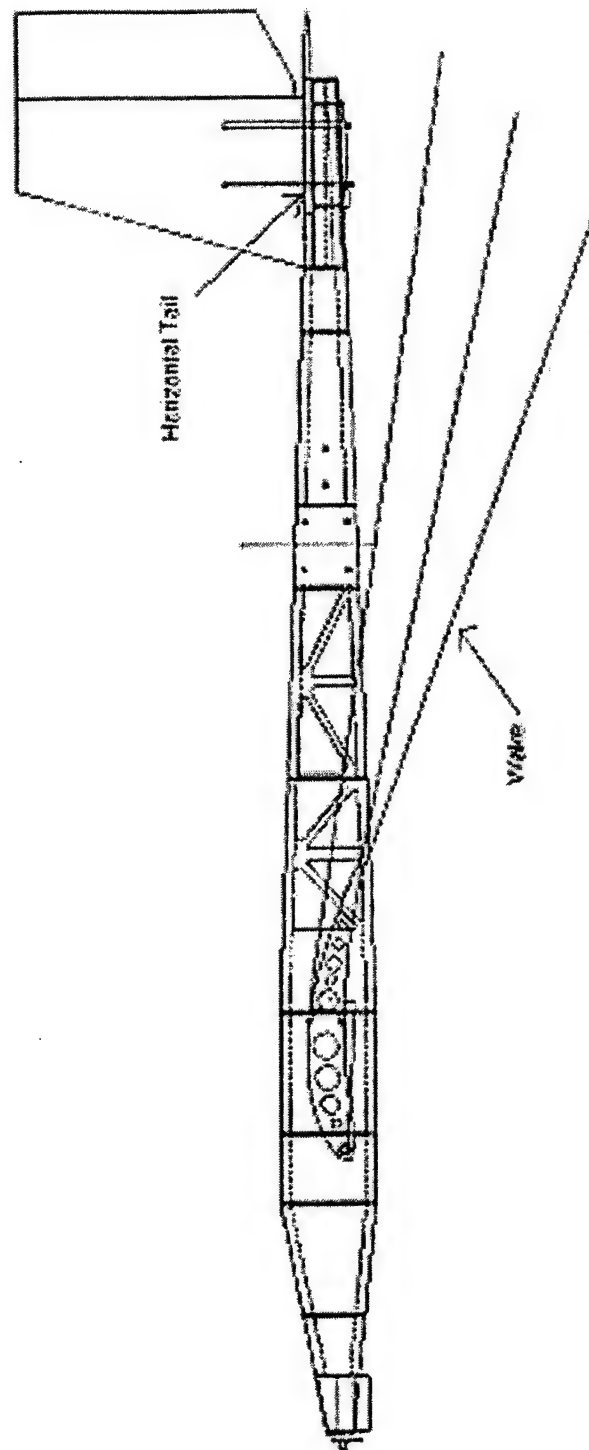


Figure 4.1 Horizontal and Vertical Tail Placement Vertical Tail

The vertical stabilizer has also been located and sized to provide the necessary stability for the airplane in flight. The vertical tail's control surface, the rudder, is used for yaw control, meaning that it can turn the nose of the aircraft to the right or left.

The location of the vertical tail will be approximately the same as that of the horizontal tail, only above and slightly forward. It is moved forward in order to create a larger percentage of the rudder area which is unblanketed. As a rule, at least 1/3 of the rudder should be out of the wake. This is shown in Figure 4.2.

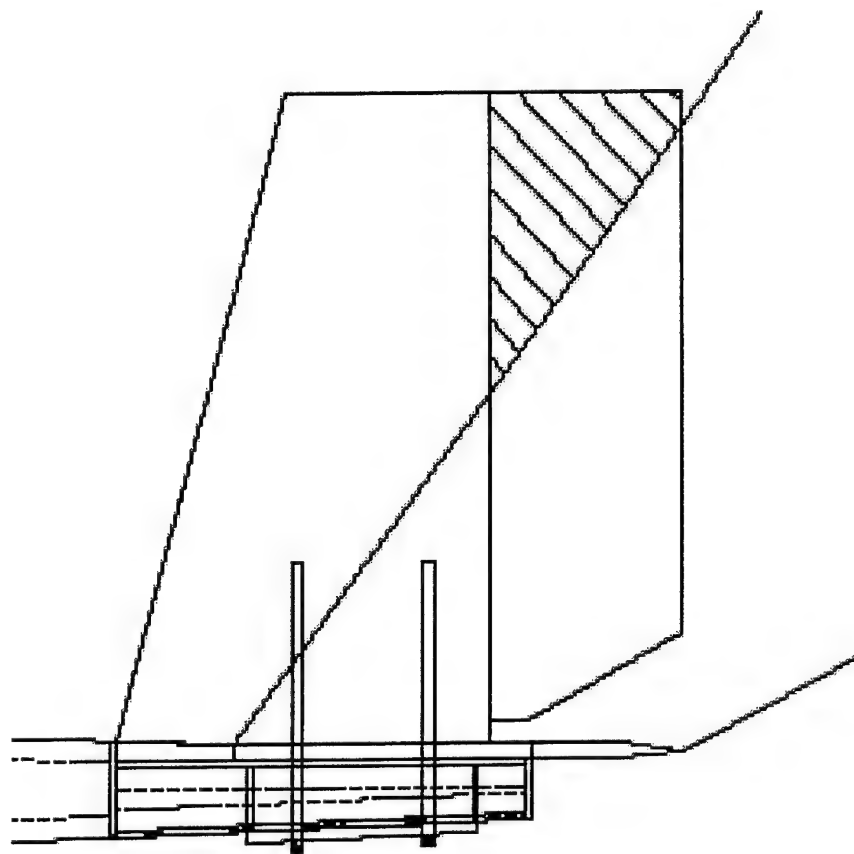


Figure 4.2 Rudder Area not Blanketed by Horizontal Tail

The total area of the vertical tail was determined using Eq. 2. As shown in the table, the necessary vertical tail area is approximately 170 in². The tail as drawn right now has an area of approximately 160 in².

$$VTA = (c_{VT} \times b_W \times WA) / TMA \quad (Eq. 2)$$

Table 4.2 Parameters used to Determine Vertical Tail

C_{VT}	vertical tail volume coefficient	0.04	--
B_w	wing span	108	in
WA	wing area	1728	in ²
TMA	tail-moment arm	44	in
VTA	vertical tail area	169.7	in ²

4.1.3.3 Tank

Two different types of plastic containers were investigated. One was a thick plastic jug like those used for gasoline containers. The pros were that it was easy to machine, but its thickness also made it heavier.

A second plastic container made of thinner plastic container was eventually chosen due to its lightness, symmetry, and lack of handle. While not as easy to machine as the first plastic, it was still possible.

4.1.3.4 Landing Gear

A fixed landing gear approach was chosen because it is less complicated and less expensive. The bicycle and quadricycle landing gear configurations require a flat takeoff and landing so they were disregarded due to the great change in weight of the plane in the during the competition. The multi-bogey is the heaviest landing gear and this configuration was disregarded because of weight requirements. The tricycle gear was looked into but, it was still heavier than the tail dragger. The single main was also looked into but it still was heavier than the tail dragger configuration. The terrible turn stability is the main problem with the tail dragger configuration. Connecting the rear landing gear to the rudder control surface will help to alleviate this problem. Finally the tail dragger configuration was chosen based on the following reasons: its simplicity, light weight, ability to land at higher angles of attack, and its predetermined angle of attack during takeoff that provides higher lift and larger amount of propeller clearance.

4.2 Aerodynamics Design

4.2.1 Design Parameter and Sizing Trades

4.2.1.1 Airfoil Selection

It was seen that the most efficient design would imitate a heavy-lift plane, as this would minimize RAC while maximizing payload capacity. Thus heavy-lift airfoils were investigated. According to Selig, et. al. [3,4], the best heavy-lift airfoils are

- FX 63-137

- M06-13-128
- FX 74-CL5-140 MOD
- CH 10-48-13
- S1223
- S1223 RTL
- S1210
- E423

Of these, the airfoils that were optimal in the Reynolds number region (see Wing Design) of interest were the S1223, S1223 RTL, and E423. While the Selig airfoils provided slightly better aerodynamic performance, the Eppler airfoil had easier manufacturing capability, so it was selected as the airfoil of choice.

4.2.1.2 Wing Design

The Rectangular Wing:

The following formulas were used to arrive at the design parameters listed below

- $S = bc$
- $AR = \frac{b^2}{S}$
- $Re = KcV$ where $K = 756$ at alt = 1342 ft (Lennon, p. 17)
- Required $C_l = \frac{3519W}{\sigma V^2 S}$ (Lennon, p. 14)
- $C_{d,tot} = C_d + C_{dp} + C_{di}$
- $C_{di} = \frac{0.318C_l^2}{AR}$ (Lennon, p. 23)
- $C_{dp} \approx 0.01$ (Simons, p. 217)

Design Parameters

- Span, $b = 9$ ft
- Root Chord, $c = 1.34$ ft
- Planform Area, $S = 12.06$ ft²
- Aspect Ratio, $AR = 6.72$
- Wing Loading, $W/S = 26.5$ oz / ft²

- Reynolds Number, $Re = 365000$
- Required Lift Coefficient at cruise, $Cl = 0.748$
- Selected Airfoil – E423 mounted at $i = 4$ deg AoA
 - $Cl = 0.748$
 - $Cd = 0.0142$
 - $Cm = -0.298$
- $C_{di} = 0.0265$
- $C_{d,tot} = 0.0507$

4.2.2 Analysis method

Computational Fluid Dynamics, CFD, was used for the preliminary analysis of the wing properties. Xfoil by Drela at MIT allows for very fast analysis of an airfoil's 2-D properties. The Xfoil program uses vortex lattice theory to predict lift, drag, and twisting moments for an airfoil under certain flight conditions. Xfoil is also useful because it has a viscous iteration method, which can help predict where the flow will detach under a flight condition. However, a 2-D analysis would probably give insufficient data for the aircraft analysis, and at very least would not give the necessary information to calculate center of gravity and static margin.

A very extensive search found Tornado, a GPL'd program that was simple to use and provided ample information on a design. The Tornado program runs in Matlab and included with it several wing designs for existing aircraft. The Cessna 172 Skylane example was calculated in Tornado under standard flight conditions and then compared against data found on Cessna's website. The program's units were converted to English by changing the density of air in a configuration file. The results for the aircraft flying at:

- 190 ft/s
- 8000' or $\rho = .0019$ sl/ft³
- 80% power X 160BHP X 550 ftlb/s/hp / 190 ft/s = 370 lbs thrust

Table 4.3 Tornado Results

Cessna Website	Dry Weight	1600	
	Lift		Drag
Tornado(alfa=0)	-254		3.5
1	450		4.27
2	1155		31.2
3	1860		77.55
4	2569		142

It can be easily seen that the results from Tornado are sufficient to calculate ballpark figures for aircraft design. However, it fails to take into account several important forces and effects.

- Includes no provision for fuselage drag and lift, this can account for a major part of the Thrust/drag discrepancy
- Does not account for propeller wash or variable air stream velocity
- Does not account for parasite drag, also does not account for laminar/turbulent flow regimes. This is important for calculating the overall drag of the wing.
- Assumes flow over wing stays attached until last 10% of chord, according to documentation
- Assumes wings are all 'thin airfoils.' Uses an airfoil's MCL to calculate flow properties.

Nevertheless, Tornado is a valuable tool for determining many forces acting on the wings and control surfaces. It also allows for control surfaces and deflections. The Tornado data can thus be used to calculate many aerodynamic forces acting on a craft, one must only be careful in interpreting its results. Furthermore, Tornado may be used to find stability derivatives around a certain state (e.g. $\alpha = 0$).

The preliminary design of the wing called for a rectangular planform with a chord of 16" and a span of 9'. The Tornado program was not initially able to utilize any airfoil other than NACA 4 digit. The creator of Tornado, Thomas Merlin, was contacted for help modifying the program to accept mean camber line files output from Xfoil. This modification allowed us to calculate aircraft with different airfoils.

Data was calculated for the DBF craft assuming the following variables.

- Span = 9'. Chord = 1.334'
- $\rho = .0022 \text{ sl/ft}^3$
- $V_{\text{stall}} = 44 \text{ ft/s}$
- Camber from Eppler 423 airfoil

The Tornado analysis outputs important information about the aircraft.

- Overall forces and moments
- Overall force and moment coefficients
- Pictures indicating chord loading and span loading
- A chart indicating span loading
- A chart indicating local Cl
- A central difference expansion about a state

The overall forces are primarily useful in finding the lift and induced drag created by a wing. The moments are useful from a stability point of view. Furthermore, the tail surfaces may be designed to create a neutral moment around a point. The span loading chart is very useful as it may be integrated to

determine the moment distribution along the span of the wing. The moment and shear loading charts may be used to design the wing beam. The chart indicating local Cl along the span of the wing is extremely useful in determining how a stall will propagate along a wing surface.

The central difference expansion about a state can be extremely useful from a stability and controls point of view. Many calculations regarding the stability of an aircraft require that the effects of small perturbations around a state be known. The Tornado program takes a beginning state and calculates for solutions around that state. Tornado then linearly interpolates to find the stability derivatives. An especially useful facet of this calculation is that it includes derivatives specifically for elevator and rudder deflections.

5 Detail Design

This section outlines the structural, aerodynamic and propulsion final design.

5.1 Structural Component

5.1.1 Component selection

As described in the trade studies done during the preliminary design, the fuselage was to be made mostly with conventional material. Balsa plywood was used for the sides of the aircraft and the bulkheads. This material would best be suited to take the loading expected on the sides, being mostly the bending moment caused by the horizontal tail and elevator. Since this was to be a non-aerobatic aircraft the bending moment caused by the vertical tail would be minimal in comparison and was neglected. If a single layer of balsa were used, it would have to have been placed with the grain running the length of the fuselage. While this configuration would be optimal in a compressive load situation, the balsa so weak in the longitudinal direction that it would crack down the grain during actual loading situations. The plywood has the feature of having the grains of its plies set at a 90° angle with respect to each other, allowing the cross grain stiffness to help strengthen the grain of the outer sheets.

5.1.2 Final Design

5.1.2.1 Bulkhead Detail Design

The bulkheads were designed with the central portion being omitted since the stresses will be greatest at the outer edges of the bulkhead. This omission also lightened the entire bulkhead system by over fifty percent when compared with the preliminary bulkheads. To increase the surface area for the adhesive during construction balsa triangle stock was added to the sides of the bulkhead that would come in contact with the sides of the aircraft.

5.1.2.2 Fuselage Detail Design

The sides of the aircraft were designed to be as light as possible while still being able to handle the loading of the tail structures. This was accomplished by using a separating the fuselage into two sections: the front fuselage containing the wing box and tank, the second would contain the tail structure. Each of the two sections would have a single sheet of 1/8-inch plywood for siding. Cutting a truss structure in the front section of the fuselage with each beam being 1/2-inch thick lightened the sides. This lightening method saved 1/10 of a pound for the fuselage, or a 20% reduction in weight for the sides.

The skin on the top and bottom of the fuselage used 1/16-inch balsa. This material was selected since the loading would only incur a minimal amount of shear during banked turns.

5.1.2.3 Horizontal Tail and Elevator Detail Design

As described in the preliminary design section, the area of the horizontal tail was calculated to be 314.2 in². Figure 3 shows a dimensioned drawing of the tail that is within 2% of the reference area. The selected geometry and dimensions yield an actual area of 318.3 in², and an aspect ratio of 4.07.

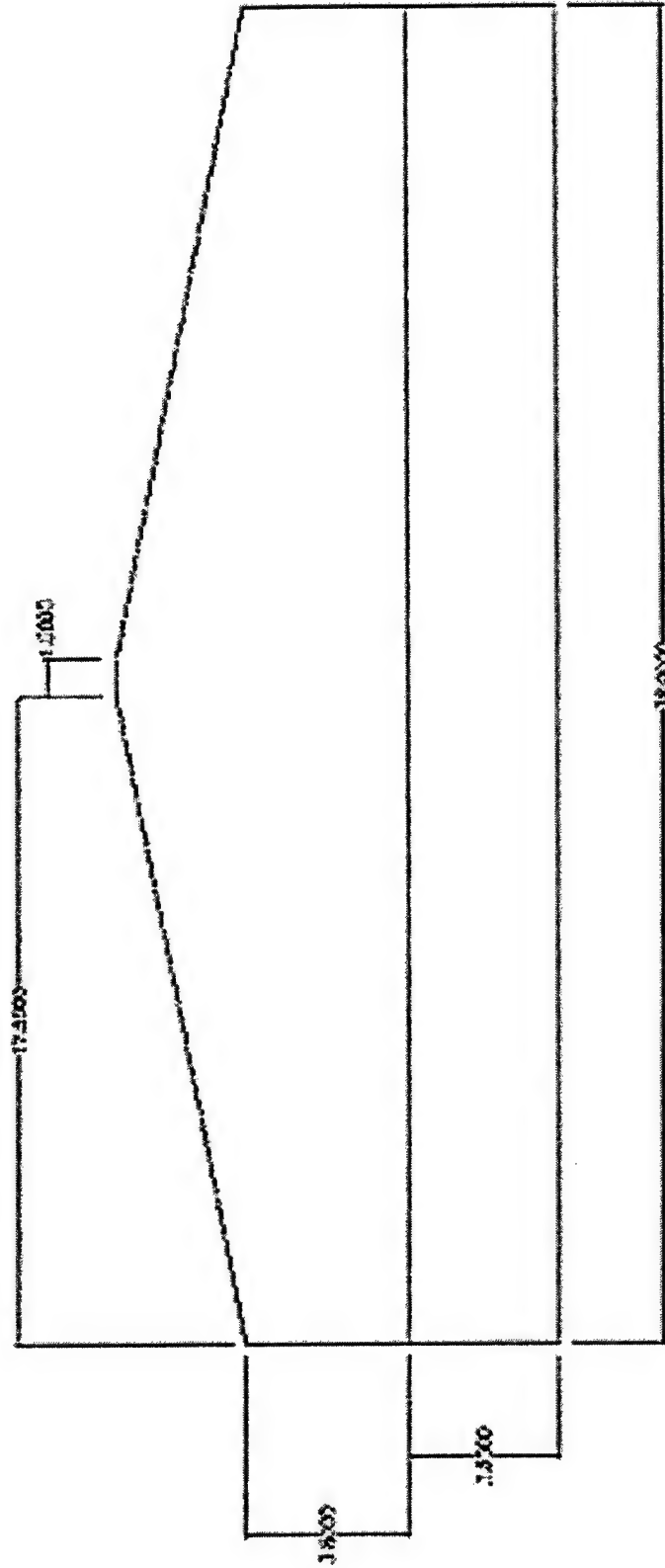


Figure 5.1 Dimensional Drawing of the Horizontal Tail in inches

Ideally, the airplane's tail would have its own airfoil, and in effect, be a mini-wing. In addition, because it is required to provide lift both up and down, a symmetric airfoil is recommended. But, for the purposes of an RC aircraft, that is complicated and unnecessary. This plane's tail will therefore be made out of a flat balsa sheet, which at least satisfies the symmetry requirement. The flat sheet will be less effective aerodynamically than an airfoil, but the aerodynamic benefit is not enough to justify the extra complexity in manufacturing.

The next element of the horizontal tail to be considered is the elevator. The larger the elevator area with respect to the total tail area, the more effective the elevator will be. Typically, the elevator chord will be 25-50% of the tail chord, and the area will be 30-40% of the horizontal tail area. Knowing that the area is 318.4 in^2 and the average chord is 8.8 in, a chord of 3.5 in, which is 40% of the 8.8 in tail chord, is chosen. The elevator sizing can also be seen in Figure 3.

An elevator deflection of 25° , both up and down, should be sufficient.

5.1.2.4 Vertical Tail and Rudder Detail Design

For a low-speed aircraft, the vertical tail sweep should be 20° or less, as there is no need to worry about reaching a Critical Mach Number. The sweep for this aircraft tail was chosen to be 14.5° . The dimensions of the tail are shown in Figure 5.1.

Next, the rudder must be designed. Rudders are typically 25-50% of the tail area, so for an area of 160 in^2 , a 40% rudder would be 64 in^2 . The actual area of this plane's rudder is 61.5 in^2 . The bottom of the rudder is notched to allow the elevator room to deflect.

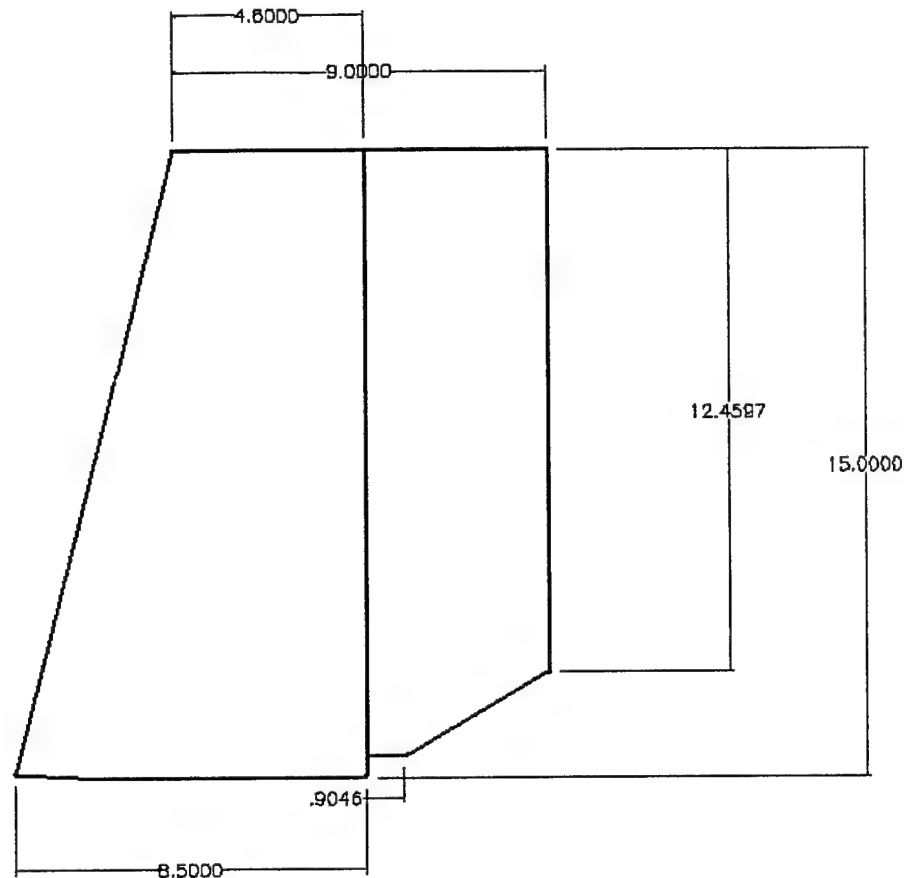


Figure 5.2 Dimensioned Drawing of the Vertical Tail

5.1.2.5 Tank Detail Design

The tank was constructed from a prefabricated plastic cylindrical container. A conical end piece was constructed to maintain laminar flow as much as possible, with a final exit orifice of 0.485 inches. A rubber flapper connected to a servo serves as the flow control device.

The tank rests between the wing support rods and is supported by two Kevlar straps connected to the wing rods.

5.1.2.6 Landing Gear Detail Design

The front landing gear is a single piece of 2024 aluminum bent into a strut. The bend is at 45-degree angle with respect to the horizontal for maximum strength in both directions. There will be a 2ft clearance between the wheels and the landing will be just shy of a foot off the ground. The height of the front gear was chosen to account for the 14in propeller and the clearance needed for it. With an impulsive force of about 60lb worst case scenario would give $M = 16\text{lb} \cdot 9.5 \cdot \sin(45) = 107.5$. This bending moment would

produce a $\sigma = \frac{Mc}{I} = 27.53\text{ksi}$. This is appreciable seeing that the strength of this aluminum is 50ksi. This is even more appreciable with the added tension springs added.

The back landing gear was chosen to be around 2in high to get an acceptable tip-over angle. There was needed a way to make the back landing gear bend as the rudder did for control and steering purposes during takeoff. A wooden slot was designed to accommodate for this where one side was attached to the rod holding the wheel and the other attached to the spring wire from the rudder.

5.2 Wing Component

The wing was split into two pieces to allow for sizes that would fit in the constraint box. The outboard section would be supported by a channel beam with sizings that would provide strength to support point loads at the wing tips, simulating the true test of supporting the aircraft on its wingtips at the competition. The beam was modeled using isotropic beam theory.

A circular carbon fiber tube with sufficient diameter and wall thickness to support the high bending moments on the inboard wing would support the inboard section. A rod was chosen over a channel or I beam based on ease of fuselage construction and commercial availability of the tubes. Carbon fiber was chosen because of its high strength to weight ratio when compared to aluminum. The carbon fiber tube would also act as the joining mechanism of the inboard and outboard sections. The tubes are sold with fiberglass sockets manufactured to allow a sliding fit over the tubes. The wing joint was placed such that a portion of the tube would stick out of the inboard section and allow the outboard section to slide over it. The sockets would attach to the inboard and outboard sections while the carbon fiber tube could be removed from both sections to allow easy placement in the box constraint.

Most of the ribs were constructed out of balsa, but ribs in critical locations (such as the inboard – outboard joint, the inboard-fuselage joint, and the outboard socket ends) were built using light-ply for added strength.

5.3 Propulsion Component

The motor selected was the Astroflight 40 Cobalt Geared Motor p/n 640G with a 14x8 propeller. Powering the motor are CP1700SCR battery cells with 1700mAh capacity. We used 21 cells for the motor for a max supply of 25.2 volts. The speed controller is a 60 amp speed control from Astroflight with a McMaster-Carr Blade-Style Low-Voltage Fuse Maxi 32VDC

Table 5.1 Propulsion Component

Motor	Astroflight 40 Cobalt Geared Motor p/n 640G
Propeller	14x8 APC
Batteries	21 CP1700SCR battery cells, 1700maH capacity (25.2 volts)
Speed Control	Astroflight 60 amp speed control
Fuse	McMaster-Carr Blade-Style Low-Voltage Fuse Maxi, 32 VDC

5.4 Rated Aircraft Cost

Table 5.2 Rated Aircraft Cost

<u>RATED AIRCRAFT COST</u>	
<u>MEW</u>	10.89 lb x \$300
<u>REP</u>	5 lbs x \$1500
<u>MFHR</u>	224.93 x \$20/hr
WBS 1 Wing	128 hr
WBS 2 Fuselage	51.93 hr
WBS 3 Vertical Tail	10 hr
WBS 3 Horizontal Tail	10hr
WBS 4 Servos	25 hr
<u>Total</u>	\$11011.93

5.5 Final Design

Table 5.3 Aircraft Sizing

Geometry	
Wing Span	108 in
Wing Area	1736.64 in ²
Aspect Ratio	6.72 in
Length Fuselage	73.25 in
Height Fuselage	10 in
Control Volume	
Rudder	58.5 in ³
Elevator	108 in ³
Performance	
CL max	.748
L/D Max	14
Max Rate of Climb	19 ft/sec
Stall Speed	44 ft/sec
Max Speed	30 miles/hr
Take-off field length	
Empty	75 ft
Gross weight	120 ft
Weight	
Airframe	98 oz
Propulsion System	58 oz
Control System	16 oz
Payload System	2.24 oz
Payload	128 oz
Empty Weight	174.24 oz
Gross Weight	302.24 oz
System	
Radio used	9-channel PCM
Number of Servos	5
Battery Configuration	21 cells movable for cg balancing
Motor	Astroflight 40 Colbalt Geared
Propeller	14 in
Gear Ratio	1.7:1

5.6 *Final Design Drawings*

Refer to Appendix A.

6 **Manufacturing Plan and Process**

Table 6.1 Milestone Chart for Manufacturing

Milestone	Predicted Date of Completion	Actual Date of Completion
Final design completion	Dec. 31	Jan 20
Start Construction	Jan. 5	Jan 15
Finish front fuselage	Feb. 15	Mar. 4
Finish aft fuselage	Feb. 23	Feb. 27
Finish wing	Feb. 24	Mar. 2
Finish tail pieces	Feb. 25	Feb. 27
Skin airplane	Feb. 26	Mar. 4

6.1 *Fuselage Manufacturing and Assembly*

6.1.1 **Investigated processes**

The first process investigated for building the fuselage was a truss system with each piece cut out of 1/8-inch balsa stock. The design of the structure was sound, but the manufacturing of the trusses was too complicated. Each piece needed to have the ends sanded to fit exactly, and with the taper that was designed into the fuselage this was found to be very exacting.

The second process was the plywood side, which was the procedure used for the actual construction. In this process each side had its outline cut out of a sheet of plywood. All features were then placed on the sheet and manufactured. To keep both sides symmetric to each other, the sides would be temporarily joined together back to back. This method would place each feature at the same point with respect to the waterline and fuselage station. Using this method eliminated any joints in the sides of the fuselage due to the single piece construction. However the 1/8-inch plywood sheet costs more than the balsa stock of the truss system.

When deciding on which process to use for the manufacturing of the fuselage, the FOM considered were: time, training, weight, strength, and joint system as seen in table 6.1.

Table 6.2 FOM for Fuselage Manufacturing Process

	Time	Training	Weight	Strength	Joint System	Cost	Total
Weighting	1	1	2	2	1	2	
Truss System	-1	0	0	0	-1	1	0
Single Piece	1	1	1	0	1	0	5

During construction of the vertical and horizontal stabilizers and their respective control surfaces a truss system was used. This was allowable since the control surfaces were a 2-D truss system and could be constructed using 3/8-inch balsa stock.

6.2 Wing Manufacturing and Assembly

6.2.1 Investigated processes

Monococque Wing Construction

This method utilizes CNC milling to produce precise wing tools out of high-density foam. The wing tools could then be used to construct wings out of fiberglass or carbon fiber composites. The method allows the construction of very complex design shapes with relative ease. It is, however, costly, as the cost for high-density foam and carbon fiber composites is high. This method also places unnecessary weight at the wing tips with respect to the light loading there.

Foam Wing Construction

A template is constructed of the desired airfoil shape. The template is then attached to a block of foam of the desired wing length and cut using a hot wire. This method effectively produced wings in a matter of hours with accurate results. These wings, however, were inherently weak and heavy.

Traditional Wing Construction

A template is made of the desired airfoil shape and used to cut out balsa ribs. The ribs are connected with two spars constructed of spruce and shear webs made of balsa. The spars and shear webs are arranged to form a channel beam for ease of construction. The entire body is then coated with a heat-treated elastic film to form a stressed skin. This method produces a very light, strong wing, but at the cost of construction time, as it is very labor intensive.

Table 6.3 FOM for Wing Manufacturing

Process	Construction	Cost	Weight	Strength	Total
Monococque	0	-1	0	1	0
Balsa Wing	-1	1	1	1	2
Foam Wing	1	1	-1	-1	0

6.2.2 Final design process

E423 airfoil templates were shaped from aluminum scrap and used to construct ribs from both balsa and light-ply. The outboard spars were constructed of spruce while the inboard spar was made of a carbon-fiber tube. A leading edge piece was sanded to shape from stock balsa leading edge. A trailing edge piece was built using stock balsa trailing edge. Both the leading and trailing edge pieces were notched at the same places span wise for rib placement.

A wing jig was constructed using two half-inch aluminum rods placed on top of angled aluminum constructed such that its edged produced a flat plane on which to place the rods. Alignment holes of the diameter of the aluminum rods were drilled into the ribs with a custom made hole-saw. The ribs were placed on the jig and spaced using the notches in the trailing and leading edges and glued to each using thick CA (all gluing, unless otherwise specified was with thick CA). Half-inch triangle stock was then used to further strengthen the trailing edge joint.

The spruce spars were then glued into the top and bottom slots cut into the ribs. Shear webs were then glued in between ribs to the back of the spars to form a channel beam. The inboard half the wing was then sheeted using 1/16" balsa to form a closed D-cell. The entire outboard wing section was then covered with micafilm.

The wings constructed above formed the outboard wing section. The inboard wing section was built by first gluing the carbon fiber tube sockets into the fuselage using long-curing epoxy. Ribs were then placed over them and glued to the socket using long-curing epoxy. The leading edge and trailing edge pieces were glued, as noted previously. The "wing stubs" were then sheeted using 1/16" balsa again forming a closed D-cell. The stubs were also coated using micafilm.

The joining mechanism of the wing stubs and outboard wing sections is the carbon fiber tubes. The tubes stick out of the wing stubs six inches and provide an area to slide the outboard wing sections on. The outboard wings were slid on and the sockets were then glued using long-curing epoxy to the ribs and leading edge piece. Gluing the sockets in place allows for a good fit while ensuring that they will be removable to fit inside the box.

6.3 *Propulsion Manufacturing and Assembly*

The main goal of the propulsions system is to provide enough thrust to the aircraft for its flight purposes while minimizing the system's total weight. It must also be noticed that, for safety concerns, the propulsions system is relatively commercial in nature

Hence the extent of manufacturing the propulsions system is not much more than a mounting bracket for the motor itself within the front of the plane. Assembly of the propulsions system is the main emphasis of the team's work and where most of our time went during the production phase of the project. Wiring was of the utmost importance. The electrical systems needed to be as minimal as possible, and could not interfere with the plane's main function. The wiring and power would be placed in the aircraft only after major construction was completed. Since the systems would consist of considerable mass it would help to stabilize the center of gravity.

6.3.1 *Investigated processes*

The approach that our team took to the propulsions systems was to first select an engine and then allows all other components to fall in place. Since this approach meant many decisions would have to be made quickly later on in the design process, our team set out to make catalogs of possible candidates for all devices peripheral to the engine. Once the electrical motor was chosen, our catalogs would allow us to make quick decisions about all other components to the system.

The motor that powers this aircraft had to be carefully chosen to match its purpose and limit inconveniences later on in the process of making this aircraft flight worthy.

First priority was choosing to use a multiple or single engine design for the airplane. This decision was made very early in the competition because it was necessary to allow the other teams to continue with their work without having to worry about changing from a fuselage mounted single engine designed to a wing mounted multiple engine

Four main choices for engine were considered. The candidates were the Cobalt 40 Gearbox, Cobalt 40 Superbox, Cobalt 60 Superbox and Cobalt 90 Superbox. These were the only motors that could actually supply the desired thrust for this airplane in a single engine configuration. The Gearbox and Superbox versions of the engines were chosen to limit the drain of the batteries and maximize our flight time.

Table 6.4 FOM for Engine Selection

Criteria	640G	640S	660S	690S
<i>Weight</i>	+1	+1	0	-1
<i>Power Consumption</i>	+1	+1	0	-1
<i>Power Output</i>	-1	-1	0	+1
<i>Availability</i>	+1	-1	+1	+1
<i>Flexibility</i>	+1	+1	0	-1
<i>Price</i>	+1	+1	0	-1
Total	4	3	1	-2

From this decision we were able to begin looking for the secondary devices to accompany the engine. The only component of considerable mention was the battery pack and it was narrowed down to two possibilities. The two apparent choices were the CP1700SCR fast recharge cell and the KR1800SCE high capacity cell. Both of these cells could provide the needed amp hours for the aircraft to maintain flight for the maximum flight period allotted by the contest.

Table 6.5 FOM for Battery Selection

Criteria	640G	640S
<i>Weight</i>	0	0
<i>Convenience(charge rate)</i>	+1	0
<i>Availability</i>	+1	0
<i>Price</i>	0	+1
Total	2	1

6.3.2 Final design process

Since overall weight, as well as balance, is of such great importance, the Astroflight Cobalt 40 motor was used. As the Cobalt 40 weighs only 17 ounces, this provided critical weight savings at an extremity of the plane's fuselage.

For batteries, Sanyo CP1700SCR cells were chosen, as possess desirable electrical discharge characteristics within reasonable cell dimensions. Twenty-one cells will be used to power the motor and various electrical systems on the plane.

While many propeller choices were available, the 14x8 propeller was chosen, as it provided a much greater amount of thrust than smaller propellers, while still within acceptable electrical power consumption.

7 Testing Plan

Table 7.1 Schedule for Fuselage Testing

Testing	Estimated Time of Completion
Propulsion Static Testing	March 1
Landing Gear Drop Test	March 16
C.G. Location	March 16
Propulsion Dynamic Testing	March 16
Wing Testing	March 16

7.1 Structural Testing

7.1.1 Testing Objectives

The objective for the structural testing is to verify the capability of the design to deal with the loading caused by the wings, tail surfaces, tank, and batteries. Producing small prototypes of the fuselage system and testing them with loadings comparable to those that would be experienced during flight could allow the objectives to be reached. Also using the finite element program built into Mechanical Desktop 6 would allow the predicted stress in the aircraft to be seen.

The test performed on the tank was a static test to find the amount of time it took to empty the tank. Initial construction gave a time of 45 seconds. Further refining of the end piece gave a time of 35 seconds.

7.2 Aerodynamic Testing

7.2.1 Testing Objectives

Testing objectives for aerodynamic testing include roll and pitch stability and wing twist.

7.3 Propulsion Testing

7.3.1 Testing Objectives

Static testing included using a sting balance to produce static thrust results with various propeller configurations. Dynamic testing objectives include finding how much thrust is needed to get off the ground with a full payload. These results may require a change in the motor configuration.

7.4 Results

At the time of this paper due to first year involvement and not knowing how long the actual building time would take the plane has not flown yet.

7.5 *Lessons Learned for Component and Full aircraft*

Lessons going to be learned from dynamic and static testing of propulsion components is the static testing results are not always similar to those found when flying.

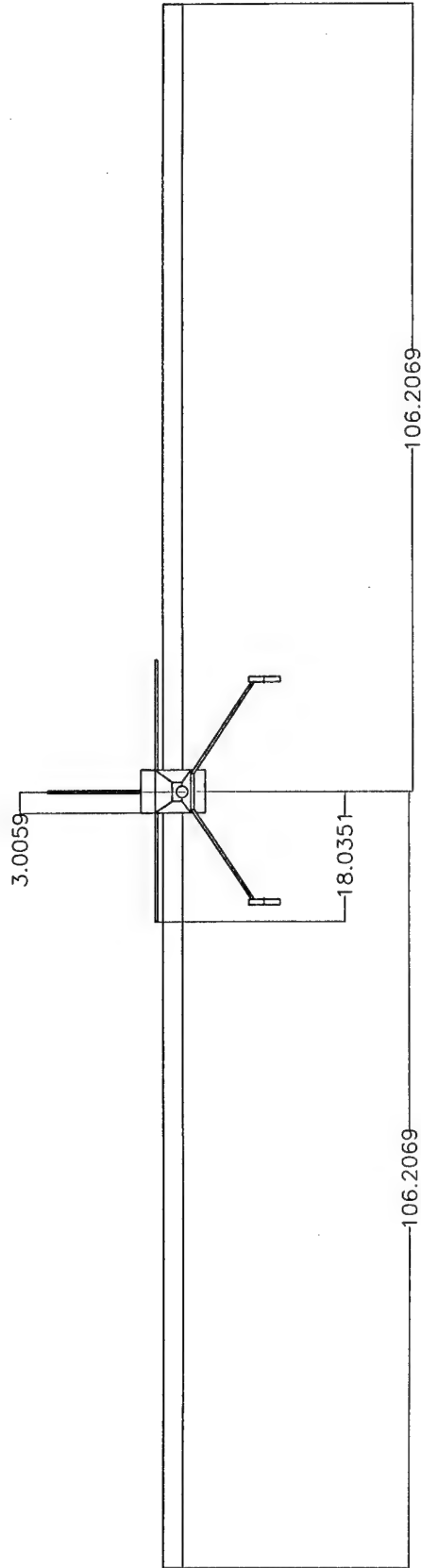
8 REFERENCES

1. Lennon, A. "Basics of R/C Model Aircraft Design," Air Age, Inc., Ridgefield, CT.
2. Simons, M., "Model Aircraft Aerodynamics," Special Interest Model Books, Ltd., Poole, UK.
3. Selig, M., Guglielmo, J., Broeren, A., Giguère, P., "Summary of Low-Speed Airfoil Data – Vol. 1", SoarTech Publications, Virginia Beach, VA.
4. Selig, Lyon, Giguère, Ninham, Guglielmo, "Summary of Low-Speed Airfoil Data – Vol. 2", SoarTech Publications, Virginia Beach, VA.
5. Anderson, John D., "Introduction to Flight", McGraw Hill, Boston, 2000.
6. Lennon, Andy, "The Basics of R/C Model Aircraft Design", Motorbooks International, 1996.
7. Raymer, Daniel P., "Aircraft Design: A Conceptual Approach", American Institute of Aeronautics and Astronautics, Reston, VA, 1999.
8. Daniel P. Raymer (1989). *Aircraft design: a conceptual approach* American Institute of Aeronautics and Astronautics Inc., Washington, D.C
9. Hibbeler, R.C. (1998). *Engineering Mechanics: Statics Eight Edition* Prentice-Hill Inc., Upper Saddle River, New Jersey
10. AutoDesk's Mechanical Desktop 6

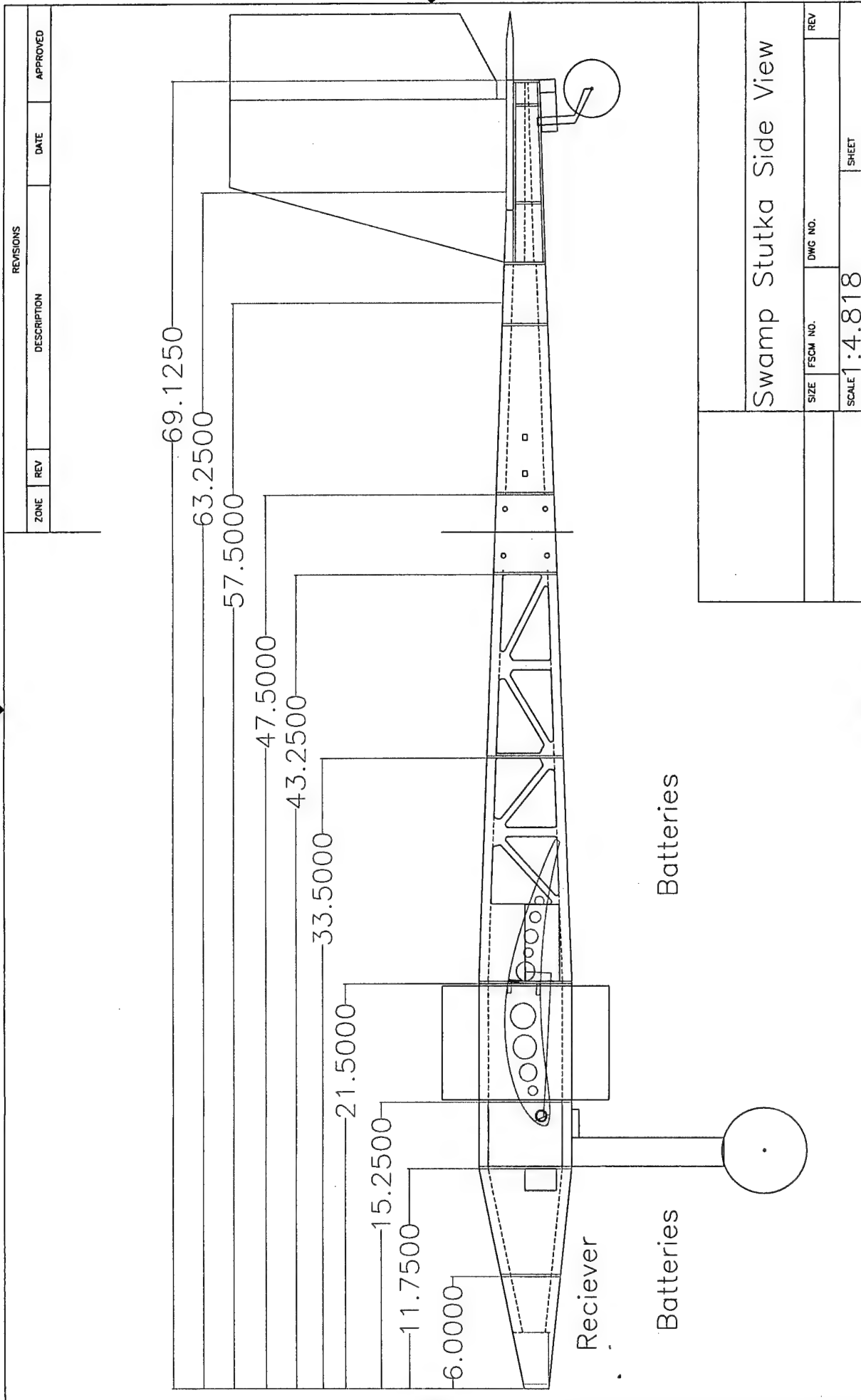
9 APPENDIX A: 3 View Drawing



REVISIONS			
ZONE	REV	DESCRIPTION	DATE
APPROVED			



Swamp Stutka Front View			
SIZE	FSCM NO.	DWG NO.	REV
SCALE 1:16.43			SHEET



REVISIONS			
ZONE	REV	DESCRIPTION	DATE
			APPROVED

Swamp Stutka Side View

SIZE	FSCM NO.	DWG NO.	REV
SCALE 1:4.818		SHEET	



		Swamp Stuka Top View			
	SIZE	FSCM NO.	DWG NO.	REV	
	SCALE 1:122			SHEET	

2003/2004 American Institute of
Aeronautics and Astronautics Student
Design, Build Fly Competition: The Fire
Bomber

“Yeager Bomber”
Design Report

By
AIAA “Pegasus” Of Western Michigan University
‘04 team

Table of Context

1.0 Executive Summary	1
1.1 Overview of the Design Process	1
1.2 Overview of the Manufacturing and Testing	1
2.0 Management Summary	3
2.1 Yeager Bomber Team Structure	3
2.2 Timeline of the Design, Manufacturing and Testing of the Yeager Bomber	5
3.0 Conceptual Design	7
3.1 General Mission Requirements	7
3.1.1 General Airplane Requirements	7
3.1.2 Fire Bomber	7
3.1.3 Ferry Mission	8
3.1.4 Rated Aircraft Cost (RAC)	8
3.2 Aircraft Configuration	8
3.3 Tail Configuration	9
3.4 Fuselage Configuration	9
3.5 Payload Configuration	10
3.6 Propulsion Configuration	11
3.7 Landing Gear Configuration	12
4.0 Preliminary Design	13
4.1 Overview of Yeager Bomber Mission Modeling and Optimization Approach	13
4.1.1 Computer Modeling	13
4.1.2 Modeling through Experimentation	13
4.1.3 Optimization	13
4.2 Initial Take-off Analyze and Weight Estimate	14
4.2.1 Weight Estimate	14
4.2.2 Initial Take-off Analyze	15
4.3 Aerodynamics Team	16
4.3.1 Wing Design and Sizing	16
4.3.2 Tail Sizing	19
4.3.3 Fuselage Design	20
4.4 Payload Design and Optimization	22
4.5 Propulsions Team	23
4.5.1 Power Required	23
4.5.2 Motor Selection	24
4.5.3 Propeller Selection	25
4.5.4 Battery Selection	27
4.5.5 Servo Selection	28
4.5.6 Speed Control Selection	29
4.5.7 Connectors Selection	31
4.6 Landing Gear Team	31

4.6.1	Main Gear Design	32
4.6.2	Wheel Selection	33
5.0	Detailed Design	35
5.1	Final Architecture	35
5.1.1	Main Wing Design	35
5.1.2	Tail Design, Sizing and Control	36
5.1.3	Fuselage Structure	39
5.1.4	Payload Architecture	40
5.1.5	Propulsion System	41
5.1.6	Electrical System	41
5.2	Final Aircraft Specifications	42
5.2.1	Final Geometry Table	42
5.2.2	Final Rated Aircraft Cost	43
5.2.3	Drawing Package	43
5.3	Final Aircraft Predicted Performance	47
5.3.1	Take off Performance	47
5.3.2	Rate of Climb	49
5.3.3	Stability Margin and Trim	50
5.3.4	Roll Rate	51
5.3.5	Final Mission Prediction	52
6.0	Manufacturing Plan	53
7.0	Test Plan	56
7.1	Component Testing	56
7.2	Flight Testing	56
7.3	Lessons Learned	58
	Reference	59

List of Tables and Figures

Figure 1: Management Structure	4
Figure 2: Total Project Gant Chart	6
Table 1: General Configuration Design Matrix	8
Table 2: Tail Configuration Design Matrix	9
Table 3: Fuselage Configuration Design Matrix	10
Table 4: Payload Materials Design Matrix	10
Table 5: Payload Position Design Matrix	11
Table 6: Propulsions Configuration Design Matrix	11
Table 7: Figure Weight Estimate Table	15
Table 8: Airfoil Data Table	17
Figure 3: CL vs. Alpha for the 4312 Wing (10 deg. flap deflection) graph	18
Table 9: Airfoil Selection Matrix	19
Table 10: Aircraft Characteristics Table	19
Table 11: Summary of Tail Surfaces Area Table	20
Table 12: Yeager Bomber Weight Balance	21
Figure 4: Algor 7.0 Results	22
Figure 5: Power Require Vs. Velocity Graph	24
Table 13: Motor Selection Matrix	24
Figure 6: Propeller Efficiency Vs. Propeller Advance Ratio Graph	26
Figure 7: Propeller Efficiency Vs. Velocity Graph	27
Table 14: Battery Selection Matrix	28
Figure 8: Stick Force Vs. Speed Graph	29
Table 15: Speed Control Data Table	30
Table 16: Speed Control Selection Matrix	30
Table 17: Summary of Landing Gear Dimensions Table	33
Table 18: Wheel Selection Matrix	33
Figure 9: Wing Schematic	36
Table 19: Tail Dimension Summary Table	37
Figure 10: Payload Schematic	40
Figure 11: Circuit Diagram of Yeager Bomber	41
Table 20: Yeager Bomber Basic Information Table	42
Table 21: Final Rated Aircraft Cost Table	43
Figure 10: Side View of the Yeager Bomber	44
Figure 11: Top View of the Yeager Bomber	45
Figure 12: Front View of the Yeager Bomber	46
Figure 13: Take-off Height Vs. Take-off Distance Graph	47
Figure 14: Ground Speed Vs. Take-off Distance Graph	48
Figure 15: Acceleration Vs. Take-off Distance Graph	48
Figure 16: Velocity Vs. Rate of Climb Graph	50
Table 22: Yeager Bomber Predict Score Table	52
Table 23: Fuselage Material Selection Matrix	54
Table 24: Tail Material Selection Matrix	54

Figure 18: Manufacturing Gant Chart	55
Table 25: Component Testing Table	56
Table 26: Flight Testing Table	57
Table 27: Pre-Flight Check List	57

1.0 Executive Summary

This report is a total summary of the design process taken by the American Institute of Aeronautics and Astronautics "Pegasus" of Western Michigan University for the Student Design, Build, Fly Competition. The plane and design team name is the Yeager Bomber. This is to pay respect to our inspiration the famous test pilot Chuck Yeager. The bomber part is in reference to the mission, a fire bomber.

1.1 Overview of the Design Process

The design process has three major phases, the conceptual design phase, the preliminary design phase and the detailed design phase. Each one of these phases has a significant part in the design and optimization of the design. To improve design and project management the design team was broke down into four sub-teams: landing gear, aerodynamics, payload, and propulsions.

The conceptual design phase dealt primarily with definition of the problem and the total aircraft configuration. From the analysis of the problem it was decided that both missions would be designed for with the emphasis on the fire bomber mission. There were six different configurations that were examined in this phase: total aircraft, tail, fuselage, payload, propulsion, and landing gear. The Yeager Bomber than was designed to have a high wing, tricycle landing gear, and a T-Tail. Also, the design of the payload system took many phases, ending with a bath tub plug like device as the final design.

The preliminary design phase was primarily used for modeling of the design rather than design optimization. There were two primary types of modeling done. Most of the design was modeled in computer programs, providing quick and accurate models. Experimental modeling was the other type utilized. This was done on critical components that would greatly increase the Yeager Bomber's performance. The tests done were propeller efficiency, connector efficiency, payload release mechanism testing and wheel selection testing. This data led the way for model optimization allowing for the Yeager Bomber to be built faster, lighter and stronger.

The final dimensions and architecture was determined in the detailed design phase. All of the components were given final sizes. Also a check was done to confirm that all of the components would fit together during the manufacturing phase. Also, every material needed and how they will be attached was decide at in this phase. In addition to the final architecture and dimensions, a final mission performance modeling was done. It was found that the Yeager Bomber would reach all expectations and should receive a 2.5 score for the fire bomber mission.

1.2 Overview of the Manufacturing and Testing

The manufacturing process required a few key skills that the design team did posses. The primary material used in the aircraft construction is carbon fiber. A great understanding of how to work with the material was gained throughout the fuselage design and construction. The tail was constructed of balsa wood. This process is not as time consuming and works well for the tail. An industry mentor, Duncan Aviation, allow the Yeager Bomber team to use their facility to bend the landing gear. Overall the manufacturing process took 2 months to complete.

The testing of components was done during the manufacturing time. Two different propeller tests, a payload test, and landing gear test were all preformed. The advantage to doing these tests to the production model is to confirm that they were accurately modeled in the design phase as well as to make sure performance will be optimum. It was found that all parts would perform as expected.

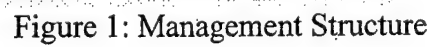
2.0 Management Summary

Team Yeager Bomber is made up of fourteen highly motivated aeronautical engineering students and one electrical engineering student. It is very important to have good team management and clear lines of communication with a group this large.

2.1 Yeager Bomber Team Structure

The mission statement of the Yeager Bomber team is to develop professional engineers; with this in mind the team was broken down into three different levels and four different engineering teams: the landing gear team, the payload team, the propulsions team and the aerodynamics team. The landing gear team was comprised mostly of freshmen and sophomores. The landing gear is a great beginning problem and starts to expose the underclassmen to the design process. This team is closely supervised by the upperclassmen. The landing gear team is responsible for designing the landing gear and picking out the wheels that will be used. The next level of engineering comprised of the payload team and the propulsions team. Both of these teams have a few sophomores but mostly juniors and seniors. These teams, with their understanding of the design process, really start to apply the different concepts learned in their engineering classes. The payload team designed the water tank and release mechanism for the airplane. The propulsions team was responsible for selection and testing of the motor and propeller used for the airplane. They also selected the radio controller as well as the servos needed for the airplane. The final team is the aerodynamics team. This team is responsible for the aerodynamics, control systems and structural analysis of the airplane. Because of the in-depth skills needed for this team, it is comprised only of seniors.

The Yeager Bomber team also has an administrative team. The administrative team is composed of six members. These members do their administrative duties in addition to helping with the design and manufacturing of the airplane. The president is responsible for the entire project. He makes discussions that pertain to the whole group as well as set the schedule for the project. The Yeager Bomber team has two vice-presidents. The vice-president of the organization is in charge of all the administrative aspects of the team and the vice-president of the project is similar to a project manager for the engineering teams. The treasurer of team Yeager Bomber is responsible for procuring all the funds need to build the airplane as well as travel to the competition site. The Public Relations Officer does the recruiting of new members. The final member of the administrative team is the secretary. He makes the arrangements to travel as well as help with any other administrative task that arise during the course of the year. Please refer to figure 1 for a table of the team structure.



2.2 Timeline for the design, manufacturing and testing of the Yeager Bomber

Before the design process started, the President, with the help of his upper cabinet members, made a list of milestone and goals to help team Yeager Bomber stay on task. This helped the team figure out what milestones need to be reached before others. The design of the water tank needed to be almost final before the design of the fuselage could take form. The size of the wing needed to be established before the size of the tail could be decided. This schedule ensured that the team focused on different milestones and goals at the right time. All of the design milestones were reached. A similar schedule was also made for the manufacturing and testing phases of the process. A ghant chart of the total project is including in figure 2.

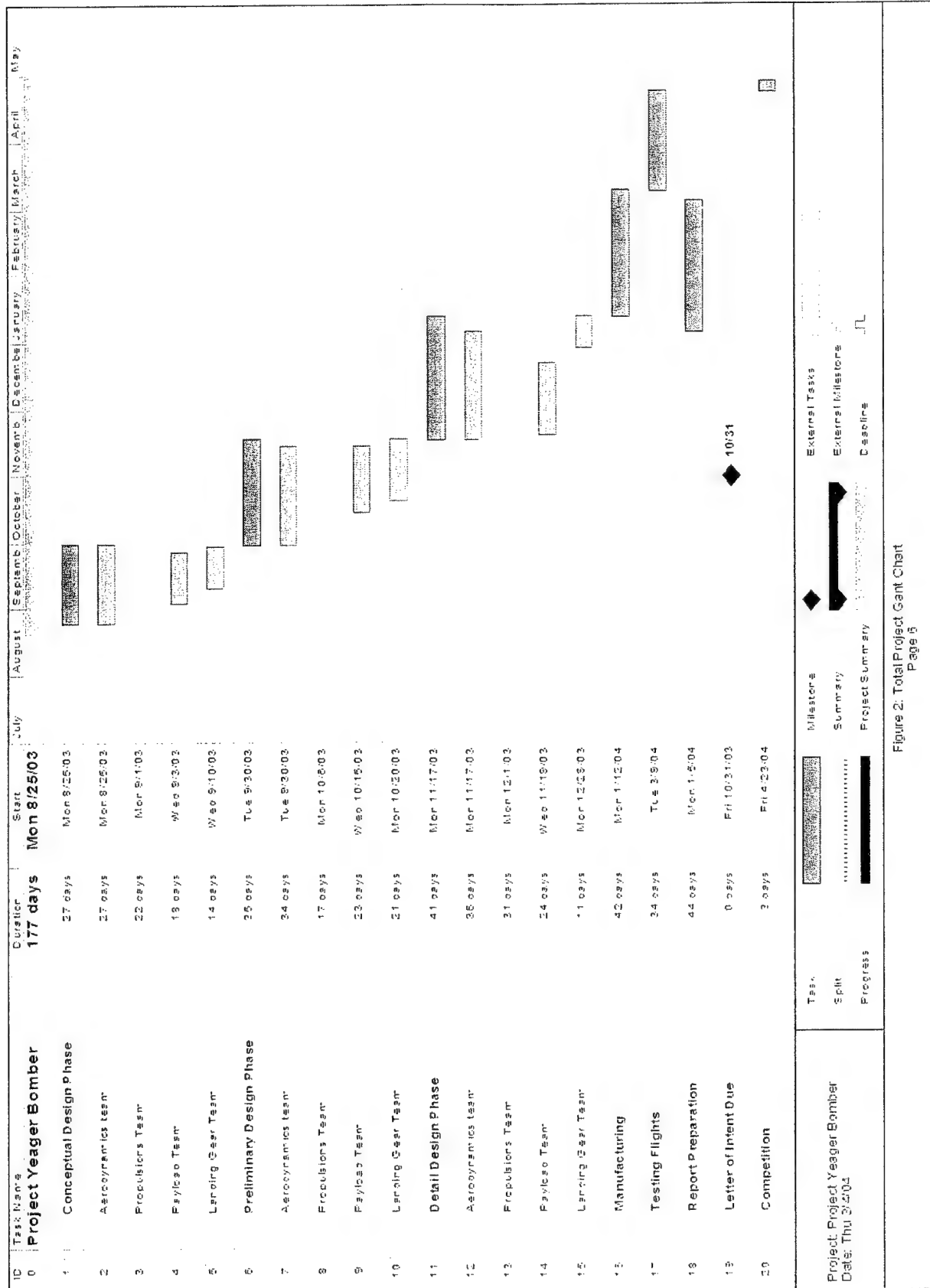


Figure 2: Total Project Gantt Chart
Page 6

3.0 Conceptual Design

Team Yeager Bomber decided that both missions would be taken into consideration during the design process. The emphasis would be on the Fire Bomber Mission because it would score the most points. However, the Ferry Mission is a great proof of concept mission and was also taken into consideration during this phase of the design process. The conceptual design phase was primarily used to determine basic configurations of the Yeager Bomber design. The mission requirements were used heavily to determine the different configurations of the Yeager Bomber.

3.1 Mission Requirements

To make a great aircraft, a thorough understanding of the requirements for both the airplane and the mission are needed. Through an understanding of those requirements, design goals can then be set. It is through meeting those goals that a great design is then achieved.

3.1.1 General Airplane Requirements

There are two general airplane requirements: size constraint and take-off distance. The constraint set on the size is that it must be able to fit into a four foot by two foot by one foot box. The plane may be disassembled to fit into the box. This will greatly affect the size of the fuselage and wing as those are the two largest components of the aircraft. Also the connection mechanisms need to put the piece together will cause extra structural analysis to confirm that they will not break. The second major airplane requirement is take-off distance. The take-off distance is limited to 150 ft or less for the sortie to be qualified for the competition. The airplane will take off twice for every trial. This makes the 150 ft mark critical in deciding both wing area and the thrust needed. Both of these requirements need to be met in order to place in this competition.

3.1.2 Fire Bomber Mission

This mission has the airplane carry and drop a maximum of four liters of water. This mission is a simulation of a fire bomber dumping suppressant on a fire. The water needs to be dropped down wind of the judges. The time will start when the aircraft is being loaded with four liters of water. Then the airplane will take-off and perform a 360 degree turn as it goes around the course. After that the water will be deployed down wind of the judges. The aircraft will then land and be reloaded. It will do this iteration twice for one trial. The total time needs to be within ten minutes. This mission was given a difficulty factor of two. Also the weight of the water will be factor into the competition score. The more water weight carried the better.

3.1.3 Ferry Mission

This mission has the airplane perform three laps of the course fully loaded with water. During each lap the airplane must complete three 360 degree turns in the opposite direction of travel. This mission is a simulation of carrying fire suppressant to a fire site without dumping it. This mission has a difficulty factor of 1 with no bounces of water weight carried.

3.1.4 Rated Aircraft Cost (RAC)

The airplane will also be judged on a scaled rated aircraft cost. This cost is an estimate of how much the airplane would cost if it were to be manufactured. The RAC is inversely proportional to the score for the competition. Therefore, the RAC needs to be minimized in order to maximize the competition score. The RAC cost is more important than the amount of water to be carried because it affects the total scores, not just the trial score.

3.2 Aircraft Configuration

There were four configurations that were examined during the conceptual design phase. Those four configurations are Conventional, Canard, Bi-plane, and Flying Wing. These four configurations were evaluated by four figures of merit (FOM). The first was eases of construction. It is critical that the Yeager Bomber be easy to construct since the design team, not a manufacturing team, will be constructing it. The next figure of merit is take-off distance. If the airplane can not take off in a 150 feet, that sortie will not count. Deployment of the payload is another important FOM. It is important from a stability and control stand point that the payload be dropped with minimal change to the center of gravity. The final FOM is the total airplane's rated aircraft cost. It is important to have a low rated aircraft cost to do well in the competition. The table below is the design matrix:

	Eases of Construction	Take-off	Deployment of Payload	RAC	Total
Weight Factor	0.2	0.3	0.2	0.3	
Conventional	4	5	4	3	4
Canard	3	1	4	3	2.6
Bi-Plane	2	4	3	1	2.5
Flying Wing	3	3	4	2	2.9

Table 1: General Configuration Design Matrix

When evaluated by the FOM, the conventional configuration was significantly better than the other choices.

The conventional configuration has three choices for wing placement: high, mid and low wing. This choice is not as significant as the total configuration choice. When making this choice, characteristics of the all three choices were examined and a discussion was made. The mid wing is hard to attach to fuselage and also give no clear advantage. This is why it was ruled out. The low would be easily attached to the fuselage. The primary advantage of the low wing is for retractable landing gear, but because our design will have fixed gear this is not an

advantage. Also the low wing placement would most likely adversely affect the deployment of the water. The high wing was chosen because it could be easily attached to the fuselage and it would not negatively affect the deployment of the water. The high wing also is more protected from any ground debris that would be kicked up during take-off and landing.

3.2 Tail Configuration

There were four different tail considered for the Yeager Bomber: Conventional Tail, T-Tail, +/- Tail and V-Tail. Each of these has their own unique qualities that they would bring to the design. To further evaluate them a design matrix was created:

	Manufacturing Time (15%)	Cost (15%)	Weight (35%)	Control (35%)	Total
V - Tail	0	2.5	2.5	0	1.25
T - Tail	4	2.5	3	3	3.775
+ - Tail	0	2.5	2.5	2.5	2.125
Conventional Tail	5	2.5	2.5	2.5	2.875
	0 = High	0 = High	0 = High	5 = High	
	5 = Low	5 = Low	5 = Low	0 = Low	

Table 2: Tail Configuration Design Matrix

In manufacturing time, the conventional tail was ranked the highest because it is the simplest and most common. All of the types are equal in cost because all would be made from the same materials. The T - Tail was ranked the highest in weight because a small size difference is awarded due to the use of a T - Tail. This size difference is awarded due to an end plating effect that occurs due to the horizontal being on top of the vertical tail. The T - Tail was also ranked highest in control because it will be located away from the downwash effect of the wing. The T-Tail was chosen because it would add the most desired qualities to the design.

3.4 Fuselage Configuration

As with all fuselage design, the fuselage is designed around the payload. This year the mission is to drop 4 liters of water. The fuselage team worked closely with payload team when deciding the material for the tank, the tank size and the tank orientation. After the payload team finalized the tank and release mechanism, the fuselage design was started.

The primary constraint on the fuselage was that its dimensions were sufficient to hold the 6 inch diameter and 10 inch long tank. Second constraints consisted of fitting in the 4 foot by 2 foot by 1 foot box, with enough room to hold other key components such as motor batteries, etc. Three initial designs were made to comply with those constraints: a carbon fiber design, a built up balsa wood design, and a combination design. The carbon fiber design was examined because carbon fiber can be molded to any shape and it has great strength. The built up balsa wood design was analyzed primarily for its easy of construction and repair if needed. The combination of these two designs was analyzed to see if their qualities could be combined to get a better design. Each of those designs was then judged based on the following figures of merit:

Weight, Easy of Construction, Strength and Durability and RAC. The following table shows the results of that analyze:

	Weight	Strength and Durability	Easy of Construction	RAC	Total
Weight	0.2	0.4	0.2	0.2	1
Carbon Fiber	4	5	2	3	3.8
Balsa Wood	5	2	4	3	3.2
Combination	4	3	3	3	3.2

Table 3: Fuselage Configuration Design Matrix

The Carbon Fiber design was chosen for further evaluations. This was primarily due to the large amount of strength the carbon fiber provides for the fuselage.

3.5 Payload Configuration

Five materials for construction of the payload mechanism were analyzed in a design matrix. The criterion of the matrix is the weight of the material, the reliability of the final product, the durability of the final product, and the time required to manufacture. Table 4 is the design matrix for the payload material selection.

	Weight	Reliability	Durability	Manufacturing	Total
Weight Factor	0.25	0.5	0.2	0.05	1
Plastic Bag	5	2	0	1	2.3
Plexiglas	1	4	4	3	3.2
Custom Fiberglass	2	4.5	4	2	3.65
Modified Storage Jar	4	4	3	4	3.8
PVC	0	5	5	4.5	3.725

Table 4: Payload Materials Design Matrix

The highest material was PVC, but upon presenting this data to the total design team it was decided that PVC was much too heavy to use. Therefore it was decided to use the modified food storage jar as the base of the payload mechanism.

After discussion with the pilot and the aerodynamic team it was decided the sloshing of the water in the tank must be kept to a minimum. A decision was reached that some sort of dampening system had to be incorporated in the design. A brainstorming session came up with the idea to put open ended plastic cylinders into the main payload section to dampen waves. The cylinders would create a chamber effect that would limit water movement in the payload device.

	Profile	CG Shift	Filling	Total
Weight Factor	0.4	0.5	0.1	1
Lengthwise	5	3.5	4	4.15
Wing wise	1	2.5	3	1.95
Vertical	3	2.5	5	2.95

Table 5: Payload Position Design Matrix

This design matrix was used to decide the orientation of the cylindrical section of the payload. The factors of profile, potential of center of gravity shift, and ease of filling were analyzed. The lengthwise orientation was the best in all three categories and was chosen.

Release Mechanism:

Two ideas have been formulated for use for the release valve. The main idea is to use a device similar to a drain plug that will simply be lifted by a servo. The secondary plan is to use a commercially available check valve that will be forced open by a servo. The drain plug idea is being pursued the most because of its low weight and small overall size. The secondary plan is being formulated because of the risk of the plug not being water tight.

The plug design is basically a one half inch hole in the bottom of the plane that is filled with a piece of rubber; on the inside of the tank is a rubber washer to help seal the tank. Initial tests show that the washer doesn't seal well. Axle grease was applied to the washer and was quite successful in eliminating leaks.

The leakage prompted the idea for a new design that would only use the rubber piece. Instead of just being a guide, the rubber would actually serve as a cork. This design is still being formulated.

3.6 Propulsions Configuration

	Weight	RAC	Cost	Total
Weight Factor	0.25	0.5	0.25	1
Tractor Type	5	5	5	5
Pusher Type	5	5	3	4.5
Dual Motors	2	2	1	1.75

Table 6: Propulsions Configuration Design Matrix

Three main types of engine choices were used in the preliminary design phase of the aircraft. To decide between them, we used factors of weight, Rated Aircraft Cost (RAC) and actual cost of the motors, and produced a design matrix. This design matrix is shown above in Table 6. Each factor is described below:

Weight: Motor weight had a weighting of 25%. This was an important factor because total aircraft weight was an issue due to the oversized payload of the mission. However, it was not as important as the RAC, and therefore carried a lower weighting. Dual Motors scored the lowest because the weight of both motors would greatly exceed the weight of a larger, individual one.

RAC: Rated Aircraft Cost had a weighting of 50%. This was the most important factor due to the high penalty of an extra engine on the RAC. The Tractor and Pusher Type motors both scored higher because of this RAC advantage.

Cost: Motor cost had a weight of 25%. Actual cost of the motor was a factor due to the limited budget we had to work with. Purchasing an additional motor would require additional fund

raising that we could put to use in other aspects of the aircraft. Due to the complexity of a pusher type, and the additional cost of purchasing the dual motors, the tractor type scored the highest.

Conclusion: After analyzing the design matrix; it was decided that a high powered tractor type motor would be the best design.

3.7 Landing Gear Configuration

The first step in choosing the landing gear for the Yeager-Bomber was to decide on an initial design. Two options were discussed, a tail dragger landing gear and a tricycle landing gear. The tricycle landing gear was chosen for many reasons. Due to the competition's objective, a tail dragger design might interfere with water being dropped from the belly of the fuselage. Any interference with the back wheel could cause drag on the aircraft. The tricycle gear was the best choice for our goal with less chance of interfering with the mission and best conservation of space and power. Retractable landing gear was considered but ruled out due to the need for more servos and power. Also, a retractable landing gear would require extra space for storage inside the fuselage, requiring a larger fuselage to house both the cargo and the landing gear.

4.0 Preliminary Design

The preliminary Design phase focuses on a more detailed understanding of the mission requirements. This was done through computer modeling and experimentation. After a good understanding was gained the design can then be optimized. It is through this optimization that a better and more specific design can be obtained.

4.1 Overview of Yeager Bomber Mission Modeling and Optimization Approach

After initial ideas and concept are found it is important to model the designs in an efficient and accurate way. It is through the modeling the design that the best optimization can occur. The best way to model something is to actually build it and test it. However, this is a very cost intensive way. Another excellent way to model the Yeager Bomber is through computer modeling. This is a more cost effective way to make a model. Both of these methods were used to model the Yeager Bomber and its different components.

4.1.1 Computer Modeling

Team Yeager Bomber took advantage of a few different computer programs when analyzing the airplane. It is important to utilize different programs that have different specialties. The computer programs that were used are: MathCad, Sub 3-D, Algor 7.0 and Auto CAD. MathCad was the primary program used for most modeling. MathCad is a program that solves complex mathematical equations. The main advantage of this program is it allows for quick iterations of different equations. MathCad programs were written for roll rate, rate of climb, take-off analyze, etc. The results of those programs are in the sections that follow. Another program used was Sub 3-D. Sub 3-D is a program that analyzes different aerofoil shapes for primary aerodynamic coefficients. Sub 3-D helped determine the aerofoil selected for the wing as well as what the primary aerodynamic coefficients would be for the Yeager Bomber. Sub 3-D results are in section 4.3.1. All of the finite element analyze (FEA) was done utilizing Algor 7.0, a structural analysis program. The results of the FEA of the fuselage are in section 4.3.3. Pro Engineering was used to draw the Yeager Bomber. Drawings with Auto CAD are in our drawing package in section 5.2.3.

4.1.2 Modeling through Experimentation

In order to achieve accurate results on some components, experimental modeling is required. These experiments were conducted to choose which component or configuration to use and which is the best performing. Team Yeager Bomber performed four experiments to gain a better understanding of the designs to be used. The four different experiments were a landing gear wheel experiment, a payload release mechanism experiment, a connector experiment, and a propeller/motor experiment. These experiments allowed for a greater understanding of the components and how they could be designed for optimal performance.

4.1.3 Optimization

With the creation of accurate models the design can be systematically optimized. After the experimentation was carried out, the design teams made the best decision for the aircrafts wheels, connector, and propeller. A better understanding of the payload device was gained through experimental testing and significant design improvements were incorporated. The computer models also gave enormous amounts of information. That information was then used to reduce size and weight of the total design.

4.2 Initial Take-off Analyze and Weight Estimate

One of the major design requirements is to take-off 150 ft. This is where team Yeager Bomber started its modeling and analysis. Wing loading and wing area were determined by this analysis. To accurately model take-off an accurate design weight is needed. This was the first step taken.

4.2.1 Weight Estimate

Team Yeager Bomber used last year's plane as a primary bench mark for this year's airplane. Despite the different objectives, the planes will be very similar because they are both cargo missions. To gain a better understanding of the weight of the aircraft and where it was located each component from the Western Flyer was weighed. The Western Flyer was broken into eight main components: wing, fuselage, tail, tail boom, engine, propeller, batteries and landing gear. With these weights know weight estimates were made for the Yeager Bomber. Components, such as the fuselage weight was decrease because team Yeager Bomber should be able to manufactures those components lighter. Three more components were added to those eight for the total weight estimate. Those components were payload, payload device and nose gear. Estimates were done on those by using knowledge of the material that will be used for those components. The table below shows all components and the total weight being 33.5 lbs.

Component	Weight(lb)
Wing	9.161
Engine	2.1
prop	0.2
Back Landing Gear	1.25
Nose Gear	1
Tail	1.25
Tail Beam	0.1
Payload Device	1.5
Fuselage	3
battery pack	5
Payload	9

Total weight (lb) 33.561

Table 7: Figure Weight Estimate Table

4.2.2 Initial Take-off Analyze

If the Yeager Bomber did not take-off in 150 ft the mission would not count for total score, thus it was critical that the Yeager Bomber achieved take off before this distance. The first step that was taken was making some initial estimates on how much thrust, lift coefficient, aspect ratio, aircraft efficiency and drag coefficient. These values were gained from the Western Flyer, the primary bench mark, and also from the Zephyr, Utah State's 2003 entry the secondary bench mark. Both of these benchmarks were used to prevent any bias data taken from the Western Flyer, being that many of the members who designed the Yeager Bomber also designed the Western Flyer. The next step that was taken was finding the stall speed while varying the wing loading. This was done by the writing of a MathCad program. The following equation was utilized.

$$V_{\text{stall}}(h, WS) := \sqrt{\frac{WS \cdot 2}{\rho(h) \cdot Cl_{\text{max}}}}$$

After the stall speed was calculated an accurate model for the ground roll was created. This was done using equations found in Daniel Raymer's *Aircraft Design: A Conceptual Approach*. These equations are found on page 565. To find ground roll to take-off constants need to be found, K_t and K_a .

$$K_t := \left(\frac{T}{W} \right) - \mu \quad K_a(h, WS) := \frac{\rho(h)}{2 \cdot WS} \cdot \left(\mu \cdot Cl - C_{do} - \frac{1}{\pi \cdot AR \cdot \epsilon} \cdot Cl^2 \right)$$

$$K_t = 0.199 \quad K_a(1, 1) = -4.479 \times 10^{-4} \frac{\text{lb}}{\text{ft}^3}$$

From these constants where then entered into the ground roll equation.

$$Sg(h, WS) := \left(\frac{1}{2 \cdot g \cdot Ka(h, WS)} \right) \cdot \ln \left[\frac{Kt + Ka(h, WS) \cdot (V_{stall}(h, WS) \cdot 1.1)^2}{Kt + Ka(h, WS) \cdot \left(0 \cdot \frac{ft}{sec} \right)^2} \right]$$

With these equations the Wing loading (WS) was then able to be solved for. This was done assuming the ground roll would be 130 ft assuming the transition would take 20 ft. Transition would require a more in-depth program that will be looked at later. After wing loading was found total wing area would then be solved for. It was found to approximately 10 ft².

Given

$$Sg(h, WS) = 130 \text{ ft}$$

$$\text{WingLoading}(h, WS) := \text{Find}(WS)$$

$$\text{WingLoading} \left(0, 2.8 \cdot \frac{\text{lbf}}{\text{ft}^2} \right) = \frac{\text{lbf}}{\text{ft}^2}$$

$$Sw := \frac{W}{\text{WingLoading} \left(0, 2.8 \cdot \frac{\text{lbf}}{\text{ft}^2} \right)} \quad Sw = \text{in}^2$$

Now that the basic wing loading, wing area and weights are know a more in-depth model of the Yeager Bomber can be created. A more in-depth model will confirm or disprove the assumptions made with this initial analysis. Hence, the design process is iterative.

4.3 Aerodynamics Team

The aerodynamics team is responsible for designing the wing, tail and fuselage of the airplane. This is a large responsibility. The aerodynamics team is comprised of the senior level engineers for that reason. The aerodynamics team utilizes most of the data obtained in the initial take-off analyze and weight estimates. It is the modeling below that will prove or disprove those assumptions.

4.3.1 Wing Design and Sizing

Airfoil Selection

The airfoil of the wing is one of the main factors in aircraft design, as it directly affects lift, drag, and the overall performance. Depending on the mission profile, an airfoil should be chosen that would optimize the flight characteristics while meeting the requirements of the mission profile. The team decided that the primary consideration in the airfoil selection was the maximum lift coefficient. This decision was made based on the mission profile, Figures of Merit, and short take-off and landing capability. The team desired the aircraft to be capable of carrying the maximum payload while flying at the predicted airspeeds, which were moderately low. To meet these constraints, two factors were taken into account: wing area and lift coefficient.

As the lift coefficient of the wing increases, less surface area is required. A smaller wing would decrease the weight of the aircraft and lower the manufacturing cost. A wing with a low lift coefficient, however, would decrease the induced drag. After considering the advantages of each design, the team decided to use a high-lifting wing.

The aerodynamics team researched data of multiple airfoils from *Theory of Wing Sections* (see Table 8). In addition to the lift coefficient, the geometry of the profile was also taken into consideration, as it would affect the manufacturability of the airfoil. After examining the characteristics of each, the team then reduced the selection to three possible airfoils: NACA 4312, 4412, and 4415.

Airfoil	C_{lmax}	C_{l0}	C_{d0}	AOA at C_{lmax} (deg.)
23012	1.2	0.2	0.01	12
4312	1.5	0.4	0.012	13
4415	1.3	0.4	0.012	12
2415	1.2	0.2	0.01	13
2412	1.2	0.2	0.01	14
4412	1.4	0.4	0.011	12
65-012	1	0.0	0.009	12
747A-415	1.2	0.2	0.011	16
663-418	1.3	0.2	0.011	17
0012-64	1.2	0.2	0.01	12

Table 8: Airfoil Data Table

Platform design

In addition to the knowledge and experience gained during last year's DBF competition, the AIAA Pegasus team also had the resources used during that endeavor. The wing used in the previous year was well designed and built. It had a 4312 airfoil, which was one of the viable choices determined by the aerodynamics team. As the wing was completely removable from the fuselage, the option to use it for this year's design competition was considered. An analysis was done to determine exactly which airfoil would be most efficient and to verify whether or not any advantage could be gained by using last year's design.

Three models of the existing wing, one for each airfoil profile, were created in Sub-3D. This enabled the engineers to hold everything constant and see how the aerodynamic characteristics varied due to each particular airfoil (see Figure 3). It could be seen on the data plots that the wing with the 4312 airfoil had a slightly higher lift coefficient than the other two. It was also noticed that there appeared to be no substantial difference between the drag coefficients.

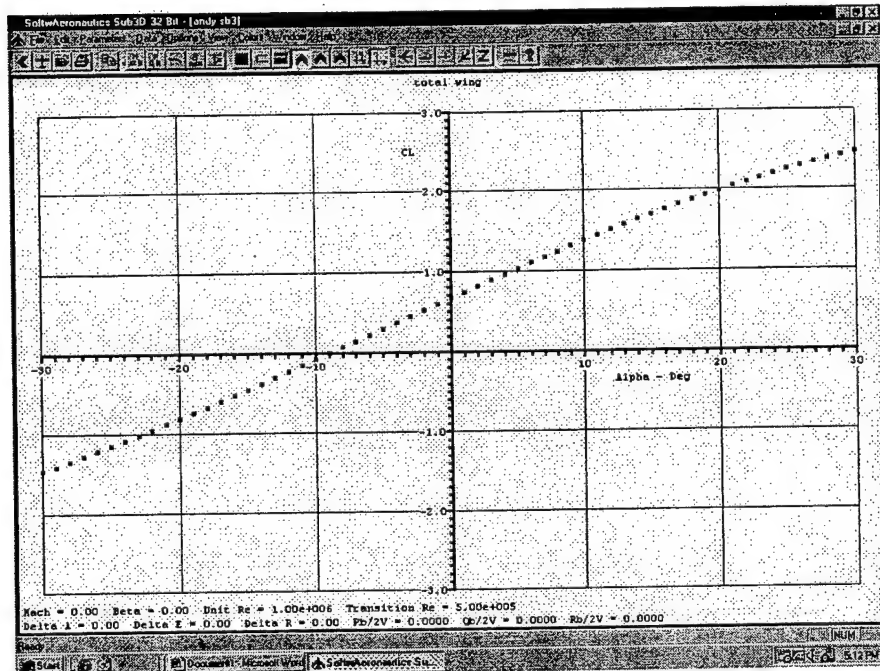


Figure 3: CL vs. Alpha for the 4312 Wing (10 deg. flap deflection)

With the data obtained from the Sub-3D analysis, a MathCad program was written to determine the take-off distance needed. As before, the existing wing's geometry was used. The equation used for this calculation, from Aircraft Design, is given as:

$$S_G := \left(\frac{1}{2 \cdot g \cdot K_A} \right) \cdot \ln \left[\frac{K_T + K_A \cdot (V_f)^2}{K_T + K_A \cdot (V_i)^2} \right]$$

Where:

$$K_T := \frac{T}{W} - \mu$$

$$K_A := \frac{\rho}{2 \cdot \frac{W}{S}} \cdot \left(\mu \cdot C_l - C_{D0} - \frac{1}{\pi \cdot AR \cdot \epsilon} \cdot C_l^2 \right)$$

V_i = Initial velocity

V_f = Final Velocity ($1.1 \cdot V_{stall}$)

From the MathCad program, it was found that any of the three wing designs would be able to take-off within the required 150 feet. However, a 4312 was able to lift-off in the shortest distance (127 feet). This was considered to be highly desirable, as it would allow for a larger margin for unknown errors such as wind shears, tail wind, and ground resistance.

In order to finalize the airfoil selection, the team created a design matrix that took into account the manufacturing, take-off distance, and total lift of the wing (see Table 9).

Airfoil	Manufacturability	Take-Off	Lift	Total
4312	3	3	3	9
4412	1	1	2	4
4415	1	1	0	2

Table 9: Airfoil Selection Matrix

According to the matrix, a 4312 was the optimal choice. The aerodynamic performance of the airfoil was either greater or equal to the other two. Another tremendous advantage to a 4312 is that the wing from the previous year could be used. Aside from exploring certain modifications to the wing, the aerodynamics team was then able to manage its time and focus on other features of the aircraft. A summary of the characteristics of this wing is in the table below, with the lift and drag calculated at cruise conditions.

Aircraft Characteristics	
Lift	60 lbf
Drag	.834 lbf
Stability Margin	4.5 inches

Table 10: Aircraft Characteristics Table

4.3.2 Tail Sizing

The sizing was done using the Tail Volume Coefficient method.

$$c_{vt} = \frac{L_{vt} \cdot S_{vt}}{b_w \cdot S_w} \quad c_{ht} = \frac{L_{ht} \cdot S_{ht}}{C_w \cdot S_w}$$

From table 6.4 on page number 112 of *Aircraft Design: A Conceptual Approach* by Daniel P. Raymer standard C_{vt} and C_{ht} values were obtained. These values are for a Military Cargo/Bomber aircraft.

$$c_{vt} := 0.08$$

$$c_{ht} := 1.00$$

It was then concluded that the main constraint set on the tail was due to the rated aircraft cost. It stated that, in order to prevent the horizontal stabilizer from being counted as a second wing, the horizontal stabilizer must have an area less than 25% of the wings total area. Also due to the constraint of being in the 4 ft by 2 ft by 2 ft the shortest distance is need. To comply with these two constraints the 25% of the total wing area was set as the area of the horizontal stabilizer 25% of the total wing area is:

$$S_w := 10.66 \text{ ft}^2 \quad St_{\max} := .25 \cdot S_w \quad St_{\max} = 2.665 \text{ ft}^2$$

Due to the use of a T - Tail design we can reduce this area by 5%. This will help reduce drag and the total weight of the aircraft. So:

$$St_{\text{tail}} := .95 \cdot St_{\max}$$

$$St_{\text{tail}} := 2.532 \text{ ft}^2$$

Using the St_{tail} found into the Tail Volume Coefficient Equation for the horizontal stabilizer it is possible to obtain the length from the aircraft C.G. to the horizontal stabilizer aerodynamic center (ac).

$$C_w := 11.65n \quad L_{ht} := \frac{c_{ht} \cdot C_w \cdot S_w}{St_{tail}} \quad L_{ht} := 4.088 \text{ ft}$$

This length is then used in the vertical stabilizer equation gives the area of the vertical stabilizer.

$$b_w := \frac{S_w}{C_w} \quad S_{vt} := \frac{c_{vt} \cdot b_w \cdot S_w}{L_{ht}} \quad \text{where } L_{vt} \text{ is approximately } L_{ht} \quad S_{vt} := 2.291 \text{ ft}^2$$

Below is a table that summarizes the tail sizing:

Summary of Tail Surface Area

Distance from CG to Tail	4.088 ft
Area of Horizontal	2.532 ft ²
Area of Vertical	2.291 ft ²

Table 11: Summary of Tail Surfaces Area Table

4.3.3 Fuselage Design

The primary mission of the fuselage is to carry the tank. Therefore, the body of the tank was sized to hold the tank. It was decided that the tank would be at quarter chord of the wing to allow minimal displacement of the center of gravity while loaded, unloaded and dumping. The other two constraints were the motor placement and the tail boom connection. The motor needs a 3.5 in square area at the front of the airplane to allow for mounting. This then blended back to a 7 in by 9 in cross sectional area to hold for the tank. The tank area then tapered up to a 1.5 in square area for the tail boom connection. This allowed for the maximum aerodynamics with room for all of the major components. The final design constraint was the airplane had to fit into a 4 ft by 2 ft by 1 ft box. For that reason, the length of the fuselage was locked at 42 in this allowed for it to fit into the box with room to spare.

After the basic dimensions were established, a weight balance analysis was done to determine the stability characteristic of the airplane. The following table shows the weight balance.

Component	Weight(lb)	(-) is behind CG Distance from CG (in)	Total Moment (lb*in)
Wing	9.161	-3	-27.483
Engine	2.1	19	39.9
prop	0.2	23.75	4.75
Back Landing Gear	1.25	-4	-5
Nose Gear	1	16	16
Tail	1.25	-49.056	-61.32
Tail Beam	0.1	-37.5	-3.75
Payload Device	1.5	0	0
Fuselage	3	-1	-3
battery pack	5	7.9	39.5
Payload	9	0	0
Total weight (lb)	33.561	Total Moment (lb*in) (longitudinal)	-0.403

Table 12: Yeager Bomber Weight Balance

A slight nose down moment was left to help with the stability of the aircraft. The nose down moment will help bring an airplane out of stall. Also if there are manufacturing defects or inaccurate estimates the position of the batteries will be variable to make sure that we maintain a slightly negative moment.

A similar weight balance was done for the vertical plane. It was found that our design was very top heavy with our high wing construction. In order to make this moment less our engine was moved up one inch to allow for a better thrust line through the airplane. Our advisor was confident that would be enough because the vertical balance is not as critical as the longitudinal.

The final analysis done was a finite element analysis of the structure of the Yeager Bomber. The advantage of the carbon fiber/ honeycomb sandwich skin is that it is the only structural component of the airplane simplifying analysis. The design need to be able to withstand the loads of flying, landing and the point load of the tail bomb entering the fuselage. In addition to those requirements no point deflections would be allowed because that would alter the aerodynamic qualities of the fuselage. The figure below shows that the maximum deflections will be in the tail area. Those deflections are extremely small allowing for a huge structural safety factor of the aircraft.

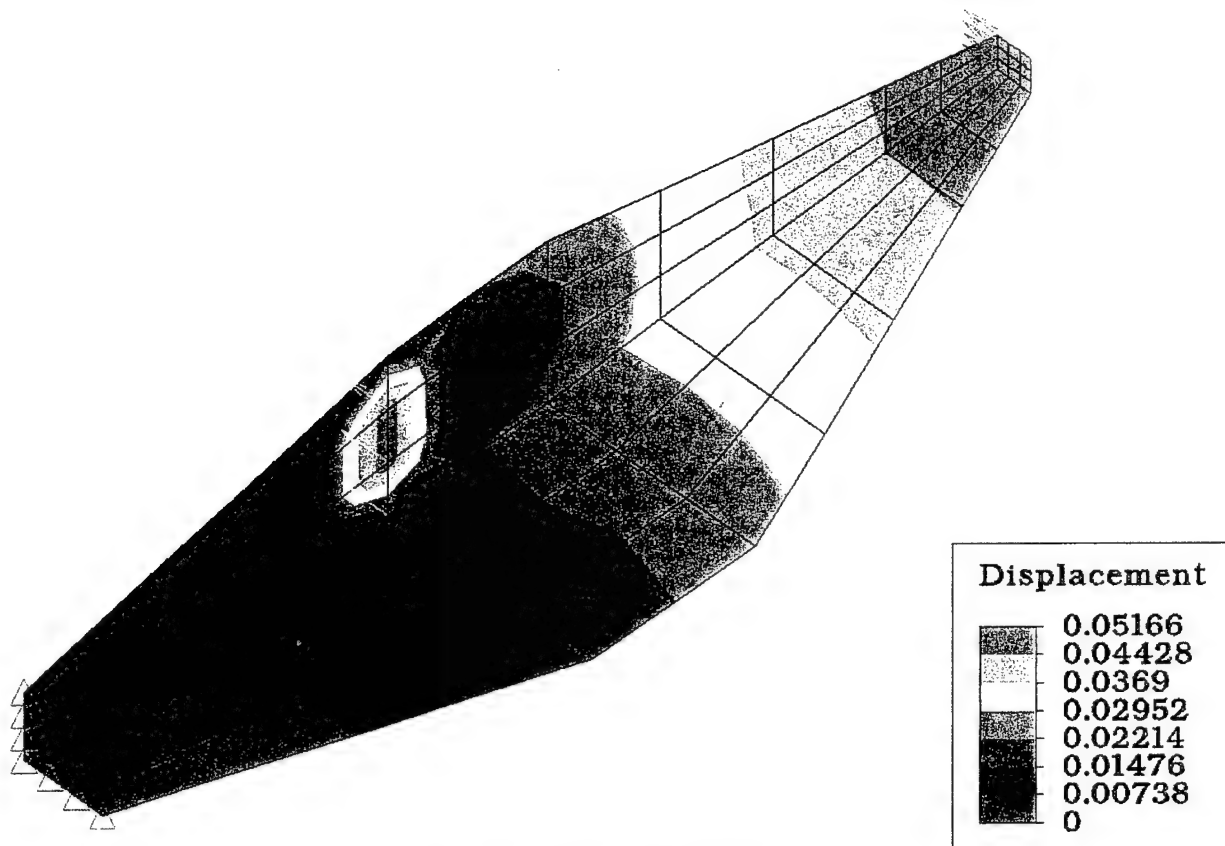


Figure 4: Algor 7.0 Results

4.4 Payload Design and Optimization

The design of the payload mechanism has progressed during three main stages of testing and design. The first tests that were conducted focused on the dynamics of the flow problem. A one-half inch hole was drilled into a bottle cap and used to simulate the exit hole of the plane for testing. The first test with the cap on a two-liter bottle show very clearly the need for an air inlet, no flow occurred without the air hole. Gradual enlargement of the air inlet showed that a one-quarter inch hole was the approximate minimum needed to create the maximum flow rate. The estimated time for four liters of water to flow out was determined by emptying one bottle and multiplying by two. The time that was determined was 30 seconds.

The next step was to design a valve system that could be remotely controlled. After much deliberation the three main ideas devised where to create a kink in a hose, to use a door-type valve, or to use a bathtub stopper design. After considering factors like manufacturing feasibility, reliability, and weight, the bathtub stopper design prevailed. Testing began on the valve design by affixing a rubber stopper that was just under $\frac{1}{2}$ inch to a metal rod along with a rubber skirting to make the seal. This design proved to be quite leaky. The application of axle grease onto the skirt proved to seal moderately well, but needed to be reapplied more than was acceptable. Further deliberation brought about the idea of just plugging the hole with the rubber stopper alone. Earlier fears of jamming were quelled with a few tests. The new plug made a

perfect seal with much less pressure than the skirt required. It was shown that the plug would not jam with the pressure required to seal the valve in many separate tests.

After the valve workings were decided upon, a mechanism was needed to raise and lower it. Two main ideas came up in this area, a crank and connecting rod, and direct lifting from above the tank. This debate was settled with a trip to the hobby shop where a rubber boot was discovered that would seal perfectly in the case of direct lifting.

The container used to hold the four liters of water was stumbled upon by accident. Initial thoughts of fabricating a tank from scratch proved to be unreliable or overly heavy. One gallon (3.78 L) storage containers were found at a local store. The containers (tanks) proved to be very sturdy and quite light. The tanks were drilled with ½ in. holes for drainage and other holes were made for filling and for access of the lifting rod. The extra volume needed to bring the tanks up to four liters is to be accomplished in the filling tube.

Another area of concern for the team was sloshing of water causing loss of control during payload release. The idea of separate chambers to reduce sloshing was formulated and implemented into the payload tank. The chambering effect was created by inserting vertical plastic cylinders into the tank that extend almost top to bottom of the tank. The overall effect is that of eight large chambers and 15 smaller chambers between the main ones. This makes sloshing occur very locally and reduces the overall shift of water mass without hindering downward flow.

4.5 Propulsions Team

The propulsions team is responsible for the selection of the motors, servos, batteries and the controlling devices. Even though this team is selecting store bought parts it is still very critical to the overall design process. It would be detrimental if they choose the wrong product. Last year the wrong batteries were selected costing flight time. It is important that that mistake is not repeated. To ensure that it does not; all parts were put through extensive design matrixes with figures of merit that pertain to those parts.

4.5.1 Power Required

In order to determine which engine would be used on the airplane, power required needed to be determined first. Power required was calculated at sea level with

$$Pr(V, w) := C_{do} \cdot 0.5 \cdot \rho \cdot V^3 \cdot S_w + \frac{2 \cdot (n \cdot w)^2}{\pi \cdot AR \cdot \epsilon \cdot \rho \cdot S_w \cdot V}$$

where $C_{do} = 0.04$, $S_w = 11.66 \text{ ft}^2$, $AR = 11.309$, $n = 1$, and $\epsilon = 0.7$. Using the maximum weight of the aircraft and minimum weight, which are 35 lbf and 25 lbf respectively, and varying the airspeed gave the power required graph seen below.

Power Required (hp) vs. Velocity (mph)

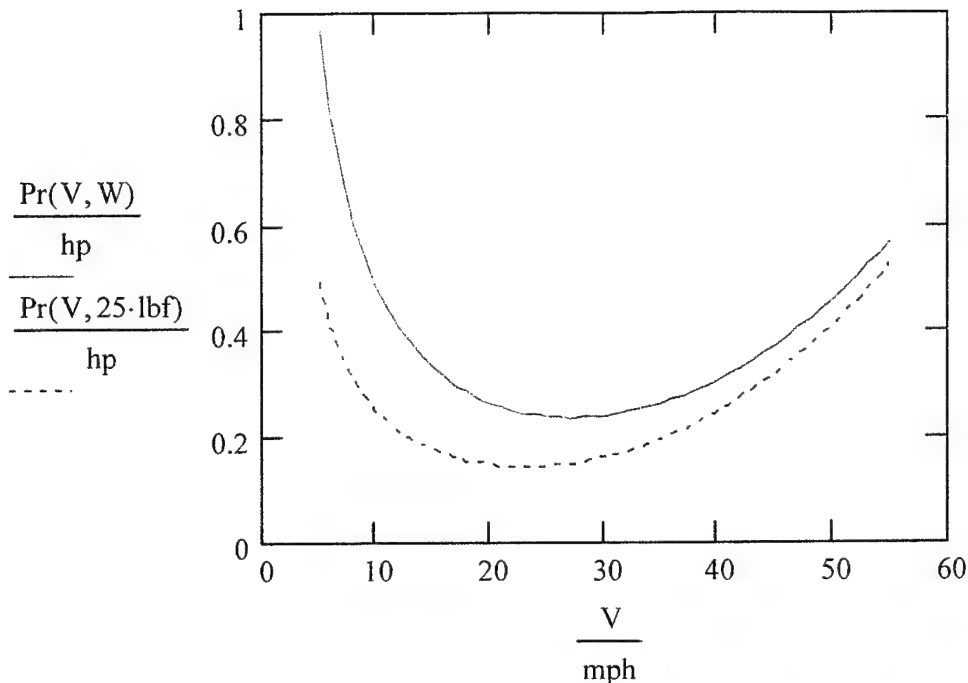


Figure 5: Power Require Vs. Velocity Graph

This information made it convincing that this aircraft required the largest of the engines available for the competition. With the efficiency of the propeller selected being 0.37 and the maximum continuous power available from the motor being 1.609 hp, the power available was computed to be 0.476 hp using a correction factor of 0.8.

4.5.2 Motor Selection

	Cost	Max Thrust	Max Power	Excess Thrust	Weight	Total
Cobalt-90	5	5	3	5	1	3.8
Cobalt-60	3	3	3	1	3	2.4
Weight	0.1	0.2	0.2	0.3	0.2	1

Table 13: Motor Selection Matrix

Motor Selection was based on 5 basic characteristics: Cost, Maximum Thrust, Maximum power, Excess Thrust, and Weight. These criteria were put into a design matrix in table 13. The criteria for each are outlined below:

Cost: Cost was determined to carry a 10% weight, as it is a factor in the decision process. The Colbalt-90, although more expensive, was purchased last year, which reduced the out of pocket cost to purchase a motor.

Max Thrust: Max Thrust was determined to carry a 20% weight. The maximum thrust provided by the motor is essential for the plane to get off the ground, especially during take-off. It was found that the Cobalt-90 will provide more thrust than the Cobalt-60. However, the Cobalt-60 was still found to be adequate to get the plane off the ground according to Astroflight's Technical Specs.

Max Power: Max Power was determined to carry a 20% weight. The two motors were selected because their maximum power available was 1200 watts. The Power Required equations determined that our plane would require between 700 and 900 watts, depending on prop efficiency and actual plane weight. Because of the high power requirements, all the other possible motors were excluded. So, while both the Cobalt-60 and 90 have the same max power, it was the main factor used to exclude the other motor possibilities.

Excess Thrust: Excess Thrust was determined to carry a weight of 30%. This is one of the most important factors in motor selection. While max power was required to select the possible motors to choose from, excess thrust is critical in ensuring the plane will get off the ground. Due to the significant weight associated with the payload, and weight of the aircraft in general, it was determined that the Cobalt-60 would barely provide the thrust required to lift off. This left little room for error in case of uncontrollable circumstances, such as bad weather or strong winds. Therefore, the excess thrust available from the Cobalt-90 was given a higher weighting.

Weight: Weight was determined to carry a 20% weight. The motor weight has several impacts on plane design, such as tail size, landing gear size, payload positioning, and other factors that could impact the positioning of the center of gravity and the aerodynamic center of the plane. Because of all these factors, and the fact that the Cobalt-60 is 12 grams lighter, it was given a higher weighting.

The Cobalt-90 has highest score. Further research into these two motors showed that the higher thrust of the Cobalt-90 proved to be the most important factor in motor selection. Furthermore, it was decided that the plane could be designed around the weight of the motor, which reduced the significance of the weight characteristic. The motor should be the Cobalt-90.

4.5.3 Propeller Selection

The 24 X 10 propeller used in the Western Flyer was used for this experiment. The 24 X 10 should give the Yeager Bomber the required thrust of 9 lbf to take-off in 150 ft. This experiment will prove that and give a better understanding of the propeller. Propeller efficiency is the primary reason for development this experiment. This was due to the number of problems that were related to this issue in the Western Flyer. The propeller efficiency is a function of thrust, air stream velocity, and power to the propeller. One of the many uses of the wind tunnel (ADWT) is to provide a way to test the propeller at various airspeeds. The experimental setup consisted of not only the portion of the apparatus that was built, but also the instrumentation, power source, balance, and wind tunnel itself. The power source and ADWT control computer were the 2 input sources for the experiments. The ADWT is used to input changes in speed of wind tunnel and angles of attack. The ADWT recorded the wind tunnels characteristics of velocity and dynamic pressure as well as the apparatus's angle of attack including all of the

forces acting on the 6-axis Aerolab balance. The data was recorded using integrated volt-meters and amp-meters and the propeller's rpms were recorded using a photocell rpm sensor.

EXPERIMENTAL PROCEDURE:

The first step of the experimental runs was zeroing all the equipment. This is important because, zeroing the equipment is necessary due to temperature differences that may occur during a given period of time. The propeller efficiency testing will be done at 8 different wind tunnel speeds. The speeds being tested are 5-40% of the maximum of velocity of the wind tunnel increasing at 5% increments. At each of the speeds, the propeller was run at 4 different RPM's. Before the propeller was run, the tunnel was tested at those 8 airspeeds to determine a "zero" value with which to compare the data. This data would account for the weight of the apparatus.

RESULTS:

The data that was taken was collected and graphed into 5 individual graphs. The 5 being overall propeller efficiency, overall propeller efficiency grouped by run, Propeller efficiency vs. Velocity, Propeller thrust given input voltage, and Propeller thrust vs. Velocity. However, one of the most important data aspects that were concluded from the graph was when the wind tunnel was run above 20% of the max velocity of the wind tunnel. The propeller no longer produced thrust. Below are is the overall propeller efficiency vs. propeller advanced ratio and the overall propeller efficiency vs. velocity. These are the graphs when read properly tell us that the best efficiency is 37%. The velocity graph tells us that efficiency is going to occur between 15-25 feet per second.

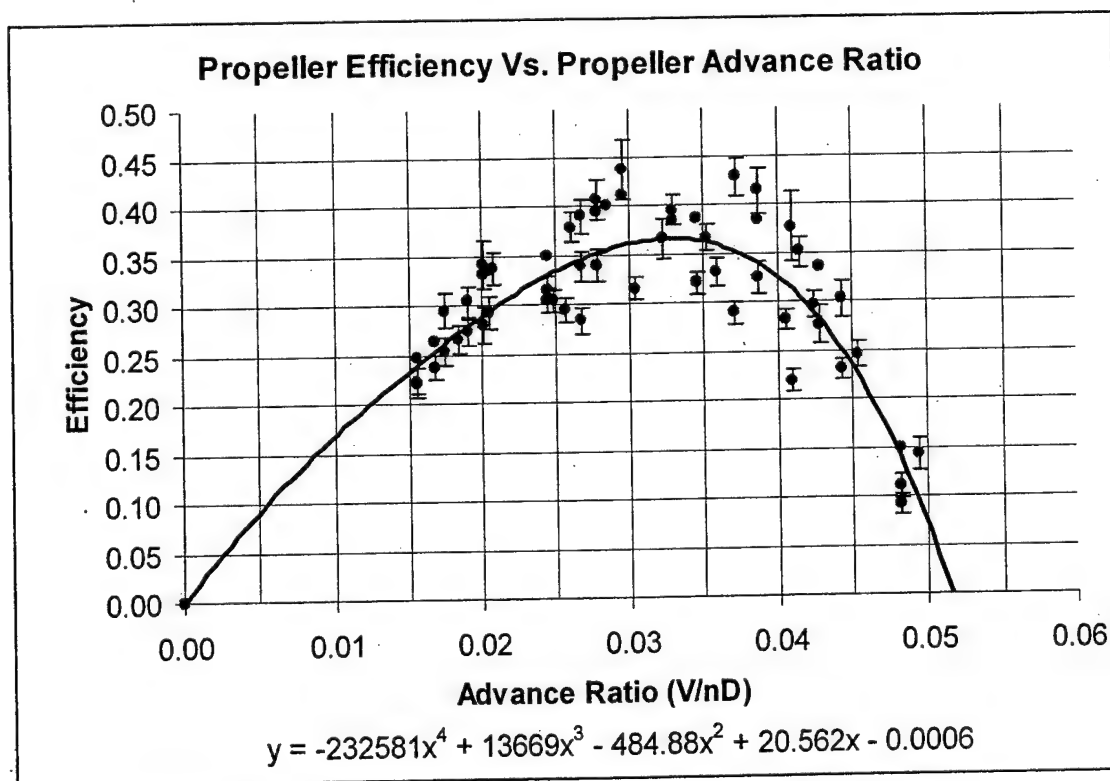


Figure 6: Propeller Efficiency Vs. Propeller Advance Ratio Graph

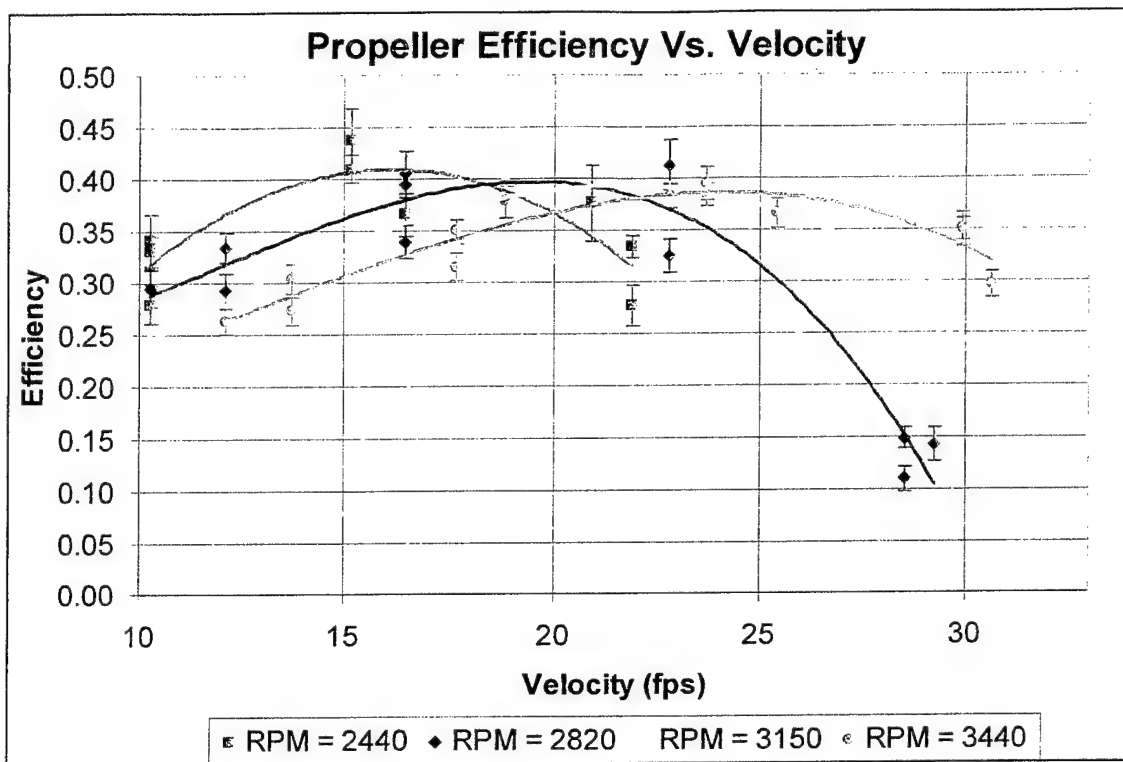


Figure 7: Propeller Efficiency Vs. Velocity Graph

ANALYSIS:

One of the many important things of the results of these graphs that was found was that the maximum efficiency was somewhere around 37%, whereas the efficiency of a propeller is 80 to 85%. Some of the factors that reduced its overall maximum efficiency were rough surface, square propeller tip and a very thick trailing edge. Many other useful relationships derived from one of the graphs were RPM and incoming air velocity. The knowledge gained from this experiment helped to create a more realistic model of the propeller. Despite the bad efficiency the 24 x 10 propeller will still be used because it will give the require take-off thrust of 9 lbf.

4.5.4 Batteries Selection

Battery cell selection was based on five basic characteristics: cost, capacity, charge time, internal resistance and weight. The criteria for each are outlined below:

Cost: Cost was determined to carry 10% weight, as it is a factor in the decision process. However, the current plan is to have the batteries donated by Battery Outlet and therefore should not significantly sway the total in either direction.

Capacity: Capacity was determined to carry a weight of 20%. The capacity of the battery is going to have a large impact on the duration of flight for the plane. Higher capacity cells will last longer than lower capacity cells. The KR-CH is a C-size cell, and will carry a higher

capacity than the other two which are sub-c size cells. However, the KR-2300SCE is a higher capacity model than the CP-2400SCR and thus carries a larger weight.

Charge Time: Charge time was determined to carry a 10% weight. This will be an important factor if we are to be able to efficiently test the plane, with 48 hours charge times (as found in the KR-CH) causing long delays, and 14 hours charge times (found in the CP-2400SCR and KE-2300SCE) allowing for daily flight if necessary.

Internal Resistance: Internal Resistance was determined to carry a weight of 30%. This is one of the two most important factors in battery cell selection. The internal resistance defines the amount of current that the cells are capable of producing. Since we are operating a motor that requires a high current, the cell with the lowest internal resistance was chosen to have the highest value (CP-2400SCR).

Weight: Weight was determined to carry a 30% weight. This was the second most important factor in cell design, as the packs are required to meet a specified weight of five pounds. Furthermore, being able to build a pack of less than five pounds lowers the RAC of the plane, which leads to a better score in the competition. For example, the rules define the RAC of one pound of battery weight to be \$1500. Therefore, the lower the battery pack weight the less the aircraft will cost and the higher our score at competition. The KR-2300SCE is the lightest of the 3 cells, with the CP-2400SCR following behind at only 2 grams heavier, and the KR-CH weighing in at 10 grams more than the CP-2400SCR.

	Cost	Capacity	Charge Time	Internal Resistance	Weight	Total
Weight Factor	0.1	0.2	0.1	0.3	0.3	1
KR-CH	1	5	1	1	1	1.8
CP-2400SCR	1	3	3	5	4	3.7
KR-2300SCR	1	4	3	3	5	3.6

Table 14: Battery Selection Matrix

Results: Multiplying each score by the appropriate weighting gives the CP-2400SCR the highest score, with the KR-2300SCR following closely behind. Further research into these two cells showed that the higher milliamp-hour rating of the CP-2400SCR and the lower internal resistance proved more valuable than the 2 gram weight advantage of the KR-2300SCE.

Conclusion: The battery packs should contain the Sanyo CP-2400SCR cells.

4.5.5 Servo Selection

To determine what servos would be needed for the aircraft, the stick fixed and stick free forces needed to be calculated. These were calculated in Mathcad, and the resulting stability margins for stick fixed and stick free were 3.789 in and 1.899 in, respectively. The free stick force was then graphed against the speed of the aircraft and produced the following graph.

Stick Force (lbf) Vs. Speed (mph)

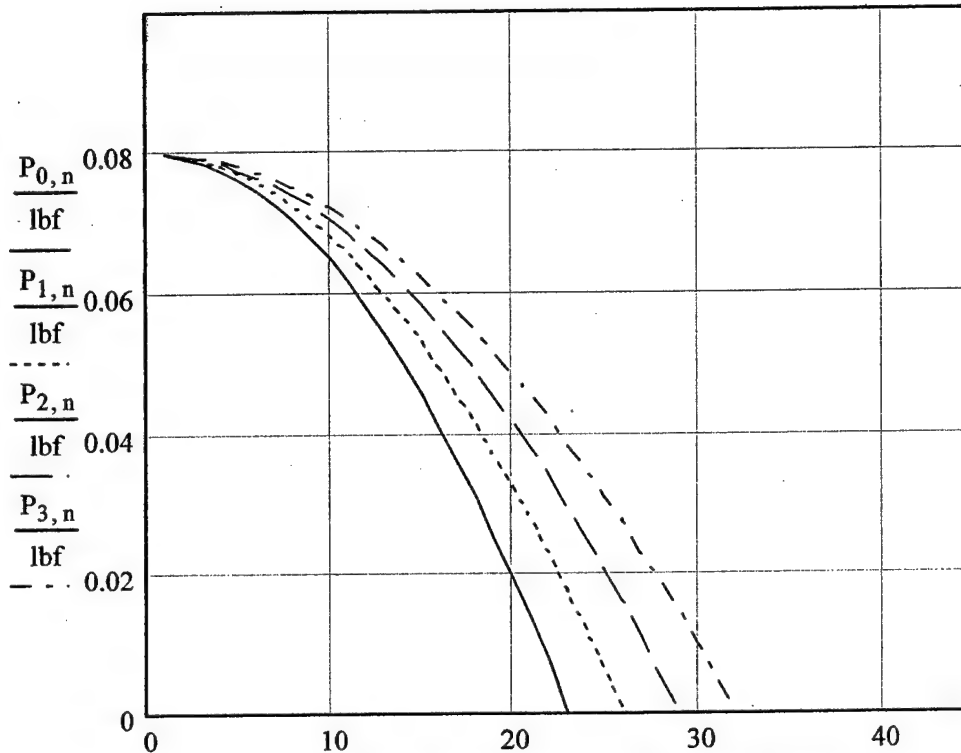


Figure 8: Stick Force Vs. Speed Graph

This graph proved that the highest stick force needed on the aircraft's control surfaces was 0.08 lbf. Since the payload deployment device needed a higher force than 0.08 lbf, it became the new force that governed the servo selection. Any servo that was chosen for the payload device would be suitable for the control surfaces. All of the servos were chosen the same to provide consistency in the aircraft.

4.5.6 Speed Control Selection

To meet the performance requirements of the mission, it was calculated that the model would require approximately 200 to 400 watts to fly. Using the expected prop efficiency and motor parameters, it was calculated that our motor would need to handle about 1200 watts continuously. Based on that requirement and the electric motor characteristics, it was decided that our speed control should be able to handle a 36 cell battery pack and about 30 amps, including a margin of safety.

Model	cost	max V	max I	BEC	opto	brakes	weight
A.F. 204D	\$89.95	45 V	60 A	No	Yes	No	35 g
Jeti 450	\$57.90	37.5 V	45 A	No	No	No	24.8 g
Jeti 60	\$82.90	37.5 V	60 A	No	No	Yes	39 g

Table 15: Speed Control Data Table

Cost – 5%: The price of speed control was determined to rather insignificant.

Max V – 40%: The maximum voltage rating was determined to be extremely important to the success of our mission. If the maximum voltage rating were to be exceeded, it could result in speed control failure and total loss of power or a worse catastrophic failure.

Max I – 40%: Just like the maximum voltage, the maximum current rating was decided to be equally important. The speed control must be able to deliver the required power without exceeding its design parameters.

BEC – 0%: It was decided to keep the propulsion and flight system control batteries separate, so a battery eliminator circuit was not a requirement of the speed control.

Optical Isolation – 10%: It was decided that optical isolation would help prevent the power system from causing interference to the flight control system. This is important to maintaining positive control and there was deemed important, but not nearly as important as the max current or voltage rating.

Brakes – 0%: Having a speed control with brake capabilities is not helpful to the flight performance.

Weight – 5%: Although weight is a very important consideration in the flight characteristics, because all the speed controls weigh very little, only a small consideration was given.

Model	cost	max V	max I	BEC	opto	brakes	weight	TOTAL
A.F. 204D	3	5	5	1	5	1	4	4.17
Jeti 450	5	1	1	1	1	1	5	1.4
Jeti 60	4	1	5	1	1	1	3	2.85
	.05	.4	.4	0	.1	0	.05	

Table 16: Speed Control Selection Matrix

Result:

The clear winner is the Astro Flight 204 D Speed Control.

4.5.7 Connectors Selection

In order to accurately determine the best connectors for the airplane, and experiment needs to be run to determine exactly which connectors have the lowest resistance values. This experiment will provide information on approximately how much voltage loss we will have in the plane, and whether or not we can build the pack with fewer cells.

Connector Experiment Analysis

Procedure:

1. Design a circuit with a 6V voltage source in series with the connector being tested, along with an additional resistor of approximately 6 ohms to draw a current of 1 amp through the connector.
2. Use a digital multi-meter to measure the voltage across the standard connector, and record observations.
3. Repeat for the Sermos and Deans Ultra connectors.

Theory:

In theory, there is zero loss of voltage between the battery and the motor. However, since wires and connectors must be used to take the power from the batteries and deliver it to the motor, it is know this is not the case. Therefore, analysis of the internal workings of the circuit is required if the actual voltage across the motor is to be found. By measuring the voltage drop across each resistor the current can be found. The voltage is divided by the current (theoretically 2 amps) to find the internal resistance of each connector. This resistance is estimated to be in the range of milliohms, but only experimentation will tell for sure.

Data and Results:

Standard servo connector:	$12 \text{ mV} / 1 \text{ A} = 0.012 \text{ Ohms}$
Sermos connector:	$1 \text{ mV} / 1 \text{ A} = 0.001 \text{ Ohms}$
Deans Ultra connector:	$0.15 \text{ mV} / 1 \text{ A} = 0.00015 \text{ Ohms}$

Using the power supply to provide 6 volts, and using (6) 1 Ohm resistors allowed us to provide a current of approximately 1 amp. The resistances are shown above, with the Deans Ultra connector yielding the lowest internal resistance, 98.75% lower than the standard connector.

From experimentation, it was determined that the best resistor in terms of internal resistance was the Deans Ultra connector. The low internal resistance will provide a lower voltage drop when we apply the high currents required by the motor.

4.6 Landing Gear Team

The landing gear is a key component of the airplane. If the landing gear does not have a low coefficient of friction the plane will not be able to take-off in time. The landing gear is comprised of two main components: the landing gear and the wheels. The wheels will be selected from those available on the market. However, the main gear will need to be designed to handle the weight and impact of the Yeager Bomber.

4.6.1 Main Gear

The design of the main gear was done through a structural analysis of the forces that are going to be applied to it. Dimensions such as over-all height, wheel width, and the location of the landing gear on the fuselage were predetermined by the aerodynamics team. From those rough dimensions a free body diagram was draw. The total force on the landing gear was 35 lbs and then a safety factor of 2 was used for an impact loading that might occur. The stress equations were taken from R.C. Hibbeler's Mechanics of Materials. Below are the calculations and results:

Moment on Landing Gear wheels

$$y(t) := \frac{t \cdot 3.5 \cdot 5.75 + t \cdot 8.06 \cdot 2}{(t \cdot 5.5) + t \cdot 8.06}$$

$$I_{yy}(t) := \frac{1}{12} \cdot t \cdot 8.06^3 + t \cdot 8.06 (y(t) - 2) + \left(\frac{1}{12} \cdot 3.5 \cdot t^3 \right) + t \cdot 3.5 (5.75 - y(t))$$

$$M_y := 35 \cdot 7.5 \quad \sigma_y := 37000 \quad z := 4$$

$$\sigma(t) := \frac{M_y \cdot z}{I_{yy}(t)}$$

Given

$$\sigma(t) = \sigma_y$$

$$\text{Thickness}(t) := \text{Find}(t)$$

$$\text{Thickness}(.01) = 4.743 \times 10^{-4} \quad \frac{1}{8} = 0.125$$

Sizing for upper plate

$$\sigma_{cf} := 10 \quad A(w) := 7 \cdot w$$

$$p := 70 \quad \sigma(w) := \frac{p}{A(w)}$$

Given

$$\sigma(w) = \sigma_{cf}$$

$$\text{Width}(w) := \text{Find}(w)$$

$$\text{Width}(.01) = 1$$

Below is a table summarizing the information obtained in this section:

Width of plate connecting to Fuselage	1 in.
Width of plate connecting to Base	1 in.
Thickness of Plates	1/8 in.
Diameter Brace Tube	1/2 in.
Position of Tube from bottom (Wheel Base)	1 in.
Length of Tube	14 in.

Table 17: Summary of Landing Gear Dimensions Table

Based on the calculations, the above values are sufficient for the performance of the aircraft in terms of take-off and landing. They will hold the weight of the aircraft, as well as withstand the force impact upon landing.

4.6.2 Wheel Selection

An experiment was decided to be the best way to model the wheels. The experiment was done to determine the best wheels as far as rolling ability and the smallest friction coefficient.

Wheel Selection Experiment:

Procedure:

Three wheels were examined in this experiment. One choice was the wheels from the Western Flyer (rubber wheel, 4.5 inch diameter). The second was the same model and style, but one inch smaller diameter. The third was a different style wheel, still 4.5 inches, but with a foam wheel. All choices had plastic cores, and the new wheel had a metal inner casing.

A testing device was built. This device had the following was a 3-by-1 foot wood piece, attaching a landing gear base towards one end of the board. Then a long, thin metal strip (bent in the middle) for the nose gear. A rollerblade wheel was added to the front nosepiece with a bolt attaching it between the metal ends. Then each different set of wheels to be tested was attached to the back landing gear.

In order to ensure the same results, the same inclined plane was used in all the tests. This consisted of a 5-foot piece of wood about 3 feet in width set at an angle of about 30 degrees. Each set of wheels down was sent down the incline and recorded the distance it rolled. There were three trials for each set.

Results:

Wheel Type	Distance (feet)* – Trial 1	Distance (feet)* – Trial 2
Du-Bro (new)	38.5	38.4
Large Wheel (4.5")	30.7	48.5
Small Wheel (3.5")	26.1	NA

*The above results are an average of the three test runs.

Table 18: Wheel Selection Matrix

Conclusion:

After the tests were completed, we concluded that the best choice for wheels would be the larger (4.5") old wheels used on last years plane. To be sure we were making the right decision; we inserted the information from our test into a design matrix and calculated the values. Again, we found the best wheels were the large old wheels with the new inserts.

5.0 Detail Design

The final stage before manufacturing is the detail design phase. This phase is putting together all the different components of the Yeager Bomber. One of the goals of this design phase is that everything is known for the manufacturing process. Also this phase acts as a last chance to optimize the design and also model it to confirm that it will behave the way it is designed too.

5.1 Final Architecture

The final architecture is the specifics of the Yeager Bomber. It is a detailed explanation of every component on the Yeager Bomber. It is the realization of all equations and general concepts discussed in the conceptual design phase.

5.1.1 Main Wing Design

As stated earlier, the existing wing had rather excellent performance. The wing was comprised of three connecting sections: a rectangular centerpiece that sat on the fuselage, and two detachable outer sections. The advantage of having the wing disassemble into three components was that it was able to fit inside the required 4ft. X 2ft. X 1ft. box, while still having a large wing area.

The two outer sections were tapered at the leading edge to reduce the effects of the wingtip vortices. This would increase the efficiency of the wing and also reduce the weight. The wing also utilized flaperons. Instead of having two control surfaces on each wing, the flaperon served as both the flap and aileron. This meant fewer servos were needed.

With a wing area of 10.66 square feet, the aircraft had a calculated take-off distance of 150 feet. As this was well under the required distance, the team discussed the idea of reducing the wing area by cutting off a portion of the wing tip. This would help reduce the weight and cost of the aircraft. However, the necessary tools for this to be done with any great precision were unavailable. The team also weighed the risk of permanently damaging the wing through such a process. The decision was then made that the wing would not be modified. The dimensions of the wing are given below:

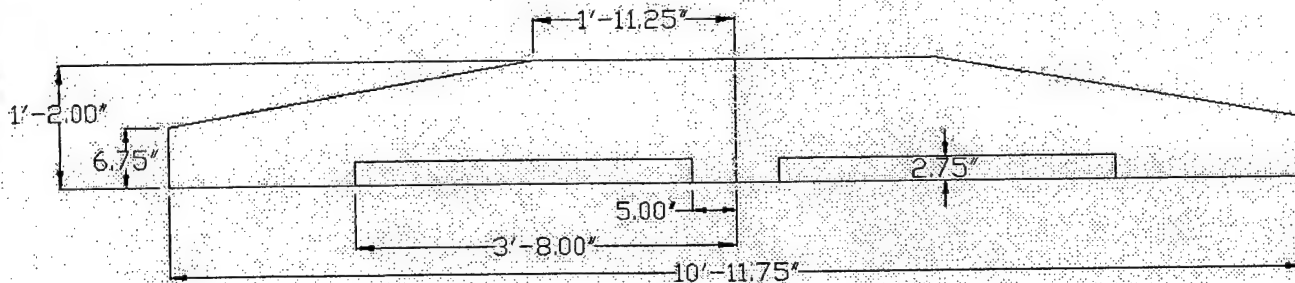


Figure 9: Wing Schematic

5.1.2 Tail Design, Sizing and Control

Sizing:

Analysis with the Sub-3D program shows that to create the good lift coefficient with a deflection of the elevator an aspect ratio of 3.75 is desirable. It also showed that the elevator should be approximately 30 percent of the horizontal stabilizer chord.

$$AR_h := 3.75 \quad C_h := \sqrt{\frac{St_{tail}}{AR_h}} \quad b_h := AR_h \cdot C_h$$

The horizontal stabilizer will have zero sweep and zero taper so the chord and span will be:

$$C_h := .822\text{-ft} \quad C_h = 9.864\text{in} \quad b_h := 3.081\text{-ft} \quad b_h = 36.972\text{in}$$

The chord of the horizontal stabilizer will be the tip chord of the vertical stabilizer. The vertical stabilizer will have a taper in the front and, due to space constraints, will be only 21 inches tall. Therefore, the vertical stabilizer dimensions will be:

$$C_{vt} := C_h \quad h_v := 21\text{-in}$$

$$S_{vt} = C_{vt} \cdot h_v + \frac{1}{2} \cdot (C_{vr} - C_{vt}) \cdot h_v$$

Therefore,

$$C_{vr} := \frac{2 \cdot (S_{vt} - C_{vt} \cdot h_v)}{h_v} + C_{vt} \quad C_{vr} := 21.556\text{in}$$

As mentioned before the control surfaces will be thirty percent of the chord. For the elevator:

$$C_e := .3 \cdot C_h \quad \text{Elevator chord length} \quad C_e := .246\text{ft} \quad C_e = 2.952\text{in}$$

The elevator will span the entire length of the horizontal stabilizer.

$$b_e := C_h \quad \text{Elevator span} \quad b_e := 3.081\text{-ft} \quad b_e = 36.972\text{in} \quad S_e := C_e \cdot b_e \quad \text{Elevator Area} \quad S_e := .76\text{-ft}^2 \quad S_e = 109.44\text{in}^2$$

For the vertical stabilizer:

$$mac_v := \frac{C_{vt} + C_{vr}}{2} \quad \text{Mean aerodynamic chord of the vertical stabilizer.}$$

The rudder must be cut off a little under the full height of the vertical stabilizer to allow for elevator deflection.

$$h_r := h_v - \sin(30\text{-deg}) \cdot C_e \quad h_r := 1.627\text{ft} \quad h_r = 19.524\text{in}$$

The mean aerodynamic chord of the rudder will be thirty percent of the vertical stabilizer mean aerodynamic chord.

$$C_r := .3 \cdot \text{mac}_v \quad C_r := .393\text{ft} \quad C_r = 4.716\text{in}$$

The rudder will have a taper ratio equal to the taper ratio of the tail.

$$C_{rt} := .3 \cdot C_{vt} \quad \text{Chord of the rudder at the top} \quad C_{rr} := .3 \cdot C_{vr} \quad \text{Chord of the rudder at the bottom}$$

$$S_r := C_r \cdot h_r \quad S_r := .639\text{ft}^2 \quad S_r = 92.016\text{in}^2$$

Below is a summary of the tail sizing:

	(ft)	(in)
Chord of the horizontal stabilizer	0.822	9.86
Span of the horizontal stabilizer	3.081	36.975
Chord of elevator	0.246	0.2958
Span of the elevator	3.081	36.975
Area of elevator	.76 ft ²	109 in ²
Height of the vertical stabilizer	1.75	21
Top chord of vertical stabilizer	0.822	9.86
Bottom chord of vertical stabilizer	1.796	21.5
MAC of vertical stabilizer	1.309	15.7
Height of rudder	1.627	19.521
MAC of rudder	0.393	4.712
Area of rudder	.639 ft ²	91.9 in ²

Table 19: Tail Dimension Summary Table

Controls:

Now that the tail is dimensioned it is necessary to find out if the control surfaces will be able to produce a strong enough moment to lift the nose wheel off the ground for the initial take-off role. Initial fuselage design has put the main gear four inches behind the center of gravity. To initialize the take-off role it is necessary to make the weight on the nose gear equal to zero. This means that the entire thirty five pound weight of the aircraft will be on the main gear. This creates a moment about the main gear equal to the total aircraft weight times the distance. Also assume that the lift created by the wing is equal to zero.

$$\Sigma M = M_{cg} - M_t = 0 \quad M_{cg} := 35\text{-lbf} \cdot 4\text{-in} \quad M_{cg} := 140\text{-lb-in} \quad M_t = M_{cg} \quad \text{To initialize take-off role}$$

Using Sub-3D it was found that the horizontal stabilizer could produce a $CL_{max} = 1.3$ with a thirty degree deflection of the elevator. Through previous calculations it was determined that the approximate stall speed of the aircraft will be 25 mph. Using this data it is possible to determine the maximum lift force of the aircraft at take-off speed.

$$X_t := L_{ht} - 4 \text{ in} \quad \text{Distance for horizontal stabilizer aerodynamic center to main gear}$$

$$CL_{tmax} := 1.3 \quad \text{Maximum tail lift coefficient for 30 degree elevator deflection}$$

$$q_{st} = \frac{1}{2} \cdot \rho_{sl} \cdot V_{st}^2 \quad \text{Equation for dynamic pressure at stall speed and sea level.}$$

$$q_{st} := \frac{1}{2} \cdot .00238 \frac{\text{slug}}{\text{ft}^3} \cdot \left(25 \frac{\text{mi}}{\text{hr}} \right)^2$$

$$q_{st} := 51.475 \frac{\text{lb}}{\text{ft} \cdot \text{sec}^2}$$

$$St_{tail} := 2.532 \text{ ft}^2 \quad \text{Area of the horizontal stabilizer}$$

$$L_{tmax} := CL_{tmax} \cdot q_{st} \cdot St_{tail} \quad L_{tmax} := 5.266 \text{ lbf}$$

$$M_{tmax} := L_{tmax} \cdot X_t \quad M_{tmax} := 237.232 \text{ lbf} \cdot \text{in}$$

This shows that the maximum moment that the designed horizontal stabilizer with the corresponding elevator can create is plenty big enough to lift the nose wheel off the ground at stall speed. Considering the design of the aircraft fuselage it may be interesting to know what the minimum CLmax would be for the tail. This will give a bare minimum elevator deflection for when the aircraft is actually being built.

$$M_{tmin} := M_{cg} \quad L_{tmin} := \frac{M_{tmin}}{X_t} \quad CL_{tmin} := \frac{L_{tmin}}{q_{st} \cdot St_{tail}} \quad CL_{tmin} := .767$$

For safety, this number will be multiplied by 1.25, this guarantees that the number will be accurate even if some minor design changes take place.

$$CL_{tsafe} := CL_{tmin} \cdot 1.25 \quad CL_{tsafe} := .959$$

Minimum adjusted CL that the horizontal stabilizer must create to rotate the aircraft at stall speed.

The second part of tail control surface analysis is on the vertical stabilizer. The vertical stabilizer must be large enough to maintain stability if the aircraft is in a side slip.

$l_b := 42\text{-in}$ Length of fuselage

$d_b := 7\text{-in}$ Diameter of circle having the same cross sectional area as the thickest point on the fuselage.

$$CL_{b\beta} := 2 \cdot \frac{1}{\text{rad}} \cdot \left[1 - 1.76 \left(\frac{l_b}{d_b} \right)^{\left(\frac{-3}{2} \right)} \right]$$

$CL_{b\beta} := 1.76$ Lift curve slope of the fuselage

$$CN_{b\beta} := CL_{b\beta} \cdot \frac{-11\text{-in}}{b_w} \quad CN_{b\beta} := -0.147$$

$\eta_t := 1$ $a_v := .1 \cdot \frac{1}{\text{deg}}$ Lift curve slope of the vertical stabilizer

$$\epsilon_\beta := 0 \quad CN_{v\beta} := \eta_t \cdot c_{vt} \cdot a_v \cdot (1 - \epsilon_\beta)$$

$CN_{v\beta} := .458$ Yawing moment coefficient of vertical stabilizer

$$CN_{\text{total}} := CN_{v\beta} + CN_{b\beta} \quad CN_{\text{total}} := .311$$

Having a CN total of .311 proves that the aircraft has enough yaw stability.

5.1.3 Fuselage Structure

The entire fuselage is a carbon fiber exoskeleton. This provides excellent strength and durability to the aircraft. This also requires no entire supporting elements to the fuselage which saves weight. Two layers of carbon fiber were used on the outside and one to sandwich in the core material. The carbon fiber sheets were laid at forty-five degree angles from one another to give it the optimum strength. The honeycomb is the lightest core material available. This is why it was used over 90% of the aircraft. After consulting Duncan Aviation's Structural Engineer Tim Walker, it was decided that an end grain balsa wood core would be used for extra strength in certain areas. Those areas are the landing gear mount, engine mount and tail mount areas. The landing gear mount area was decided for the end grain balsa wood because it would allow for better dispersion of the impact of landing than the honeycomb. The engine mount area would also use end grain balsa wood because of vibrations caused by the engine. The last area, the tail mount area, was decided to add extra strength due to the moment on the tail boom from the tail.

The only compromises to the carbon fiber exoskeleton are ventilation and access ports. There will be four ventilation ports and two access ports. The four ventilation ports are to make sure the engine and batteries do not over heat. They will be located on the front and either side of the engine. The fourth will be located in the behind the batteries to help draw air through the

entire front section of the airplane. The two access ports will both be located on the top of the Yeager Bomber. The main access port will be covered by the wing when fully assembled. This will allow for any changes to be made to the water tank and the tail mount system. A smaller access port will be located above the batteries. This will allow for changing of the batteries and any other electrical problems. This access port will also double as an additional ventilation port for the batteries.

In conclusion the fuselage will be a very strong and reliable system. It will provide the primary structure of the aircraft with the carbon fiber exoskeleton. This exoskeleton will provide enormous strength and good protection in the event of a crash. The fuselage was also has ventilation and access ports to allow for a cooling of the engine and batteries and a quick change for components that might fail.

5.1.4 Payload Architecture

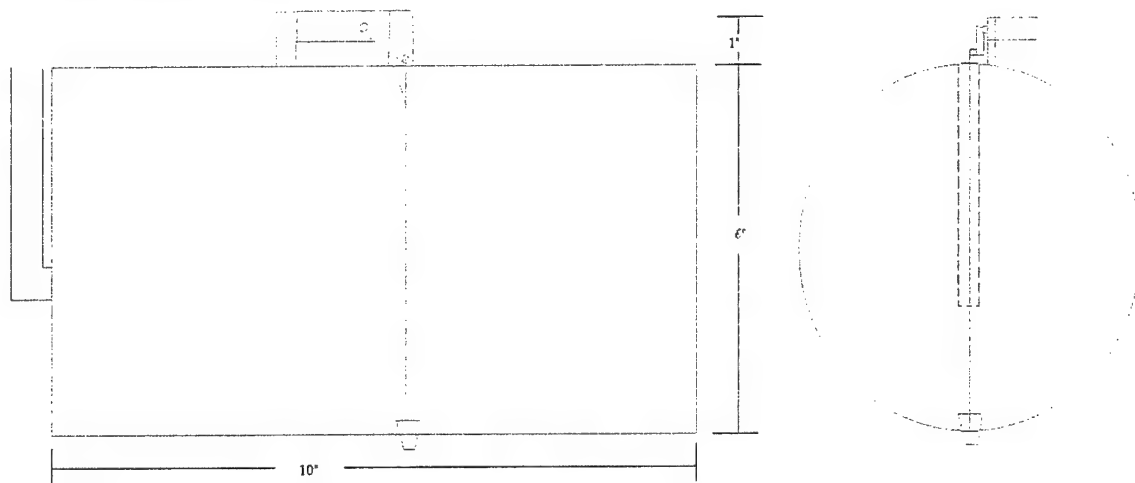


Figure 10: Payload Schematic

The payload mechanism (Figure 1) consists of three main systems. The first system is the tank. The tank is drawn in red in Figure 1 and is the primary containment for the water. The tank has a volume of 3.78 L, just shy of the full 4 L specified.

The second system is the fill system which is drawn in blue in Figure 1. The fill tube serves three purposes. First and most importantly, it is for the filling of the tank. Its second function is to provide air flow into the tank during emptying. Lastly it helps to make up the .22 L of water that the main tank is lacking.

The third and most important system is the valve system, shown in green in Figure 1. The valve system consists of one miniature high-output servo, Plexiglas mounting brackets, a metal connecting rod and a rubber plug. The operation of the valve is quite simple. To open the drain hole the servo rotates and lifts the connecting rod. This in turn lifts the rubber plug free from the exit hole. To close the hole the process is reversed and the plug is pushed back into place.

5.1.5 Propulsion System

In the area of propulsions, several factors contributed highly to the design of the aircraft. Previous experience with the DBF competition suggested that having enough power is critical to the success of the design. Other experience proved that a more complicated design would require more manufacturing hours and would cause more trouble when it was time to begin testing. So, using this knowledge, and adding design matrices for alternatives, this plane is being designed around a tractor type motor design using a Cobalt-90 Astroflight motor. These specifications will provide enough power to achieve the mission objectives, and will also be the simplest in manufacturing.

5.1.6 Electrical System

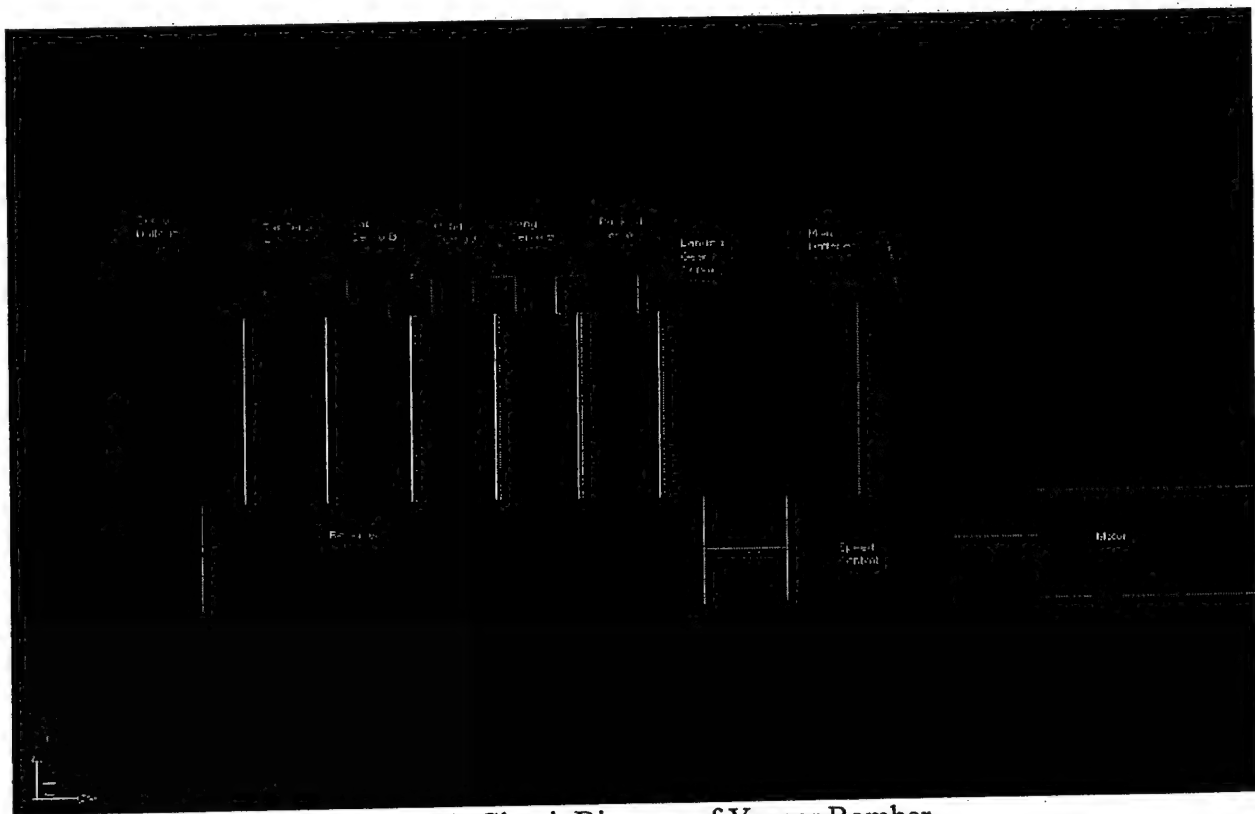


Figure 11: Circuit Diagram of Yeager Bomber

In the area of electronics, the previous DBF competitions played a large part in the design. These competitions showed that our battery packs and cell selection had to be based on the requirements of the motor. Also, the connectors were found to cause significant voltage drops through the aircraft. There was also some concern about the compatibility between the motor and the rest of the electronics. So, using all this information, the decision was made to use an Astroflight Speed Controller, a controller-compatible receiver (based on the pilot's specifications), high-torque servos, a Sanyo CP-2400SCR battery cell, Deans Ultra connectors, and short, carefully installed wire where possible.

5.2 Final Aircraft Specification

All of the specification in a comprehensive sections listing out all of the geometry and systems of the Yeager Bomber.

5.2.1 Final Geometry Table

Yeager Bomber Basic Information Sheet

Geometry

Length	72.5 in	C ₀	14 in	Horizontal Tail	
Boom Length	30 in	C _t	6.75 in	AR	3.75
Body Length	42.4 in	Airfoil	4312	Chord	9.762 in
					36.609
Span	131.75 in	Tail Area		Span	in
Height	20 in	Vertical	2.201 ft ²	Tail airfoil	0009
Wing Area	10.66 ft ²	horizontal	2.482 ft ²		
Aspect Ratio	11.477				

Performance

CL _{max}	1.8		
L/D max			
Max ROC (loaded)	210 ft/min		
Max ROC (unloaded)	440 ft/min		
Stall Speed	40.95 ft/sec	27.3 mph	
Max Speed	51.33 ft/sec	35 mph	
Take Off Length			
Gross Weight	150 ft	V rotation	30.26 ft/sec
Empty Weight	74 ft	V lof	44.104 ft/sec

Weight (lb)

Wing	9.161
Engine	2.1
prop	0.2
Back Landing Gear	1.25
Nose Gear	1
Tail	1.25
Tail Beam	0.1
Payload Device	1.5
Fuselage	3
battery pack	5
Payload	9
Empty Weight	24.561
Gross Weight	33.561

Systems

Radio	Futaba	
Servos	3: JR-Z590M	3: JR-NES-537
Batteries	Cp-2400SCR	
Motor	Cobalt 90	
Propeller	24 x 10	
Connectors	Dean's	

Table 20: Yeager Bomber Basic Information Table

5.2.2 Final Rated Aircraft Cost

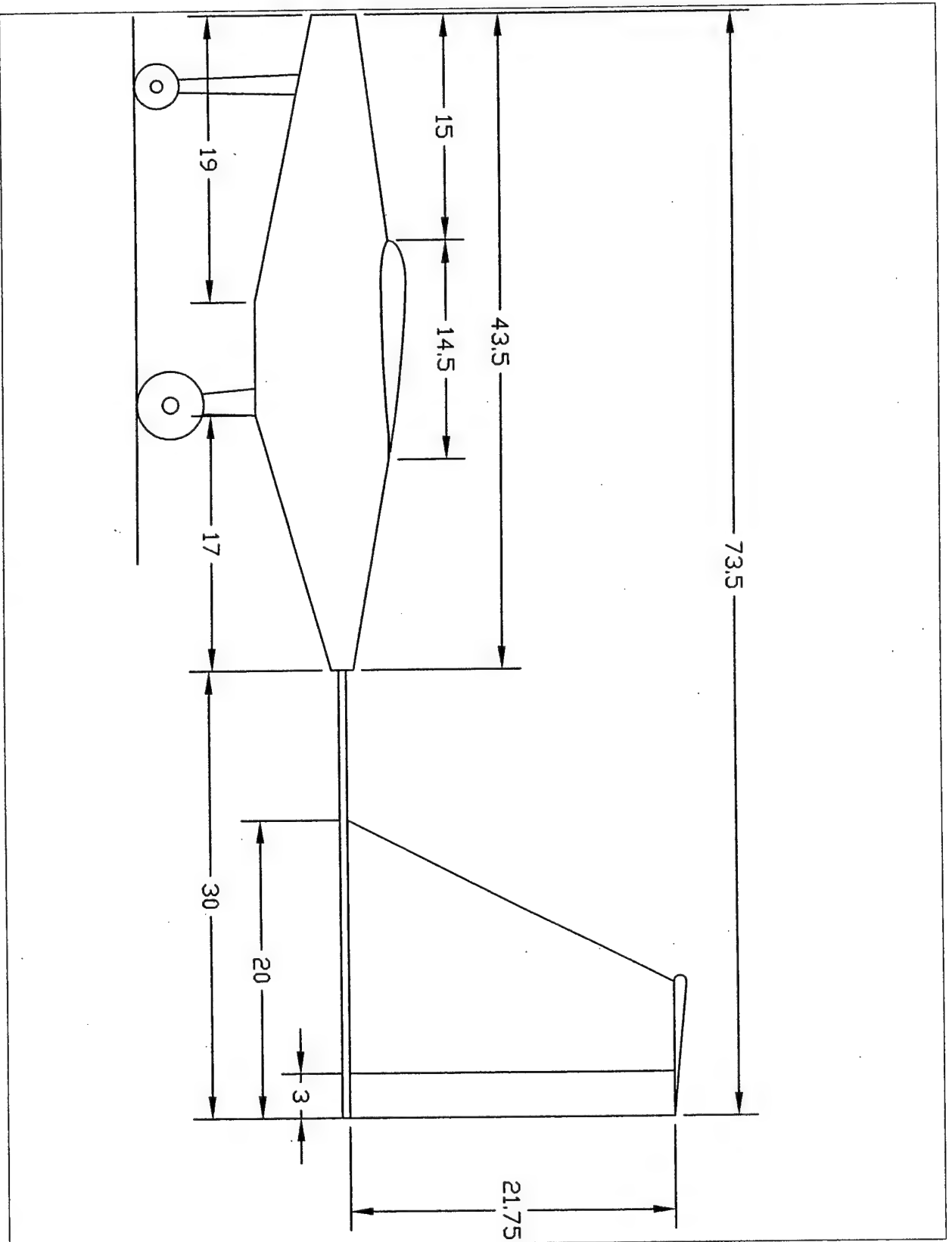
AIAA "Pegasus" of WMU Rated Aircraft Cost

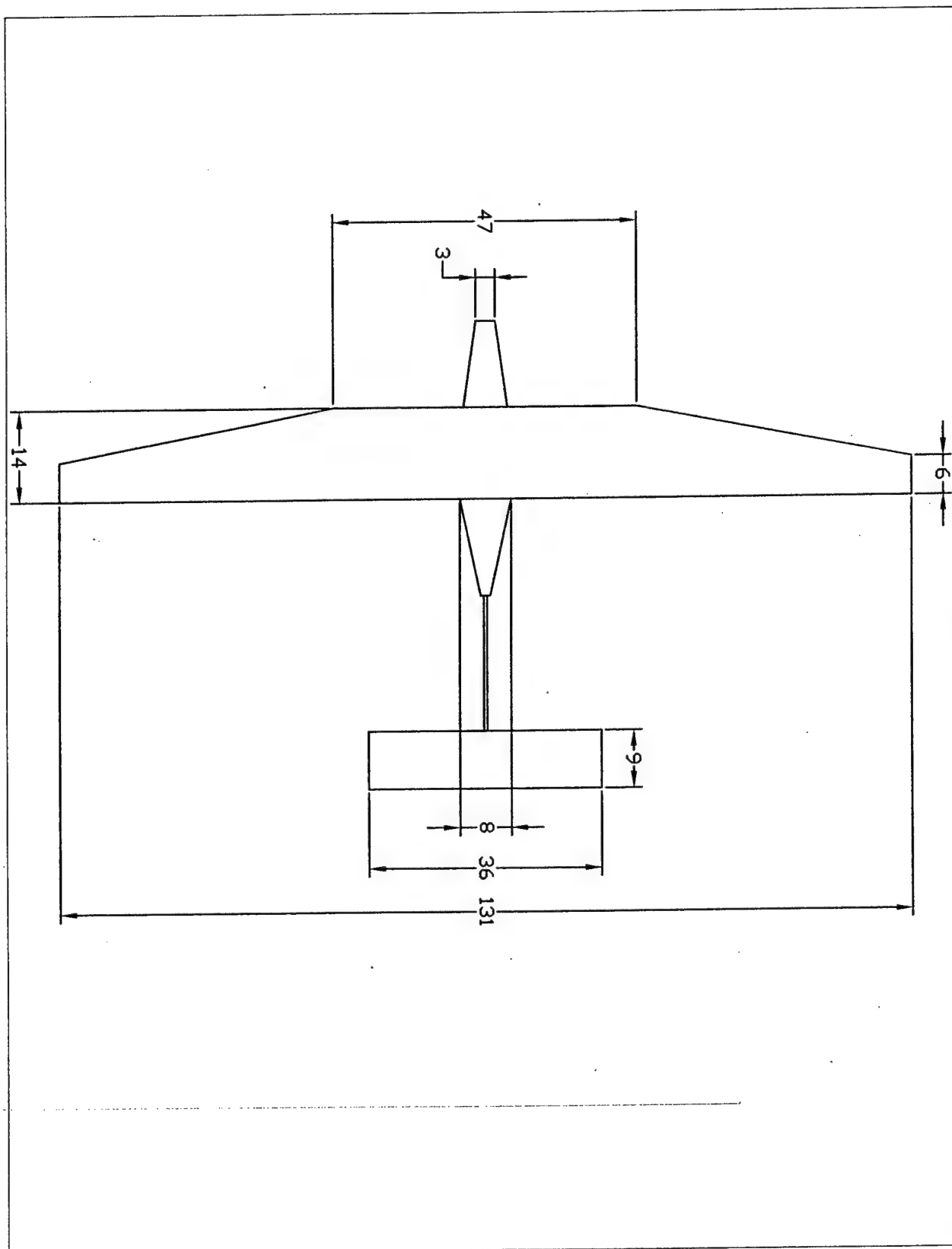
Manufacturing Empty Weight Multiplier	\$ 300.00
Rated Engine Power Multiplier	\$ 1,500.00
Manufacturing Cost Multiplier	\$ 20.00
Manufacturers Empty Weight (lbs)	24.6
Rated Engine Power	5
Manufacturing Man Hours	
WBS #1 (wings)	135.59028
WBS #2 (Fuselage)	46.990472
WBS#3 (Empennage)	20
WBS#4 (Flight Systems)	35
Total	237.58075
TOTAL RAC	\$ 19.63

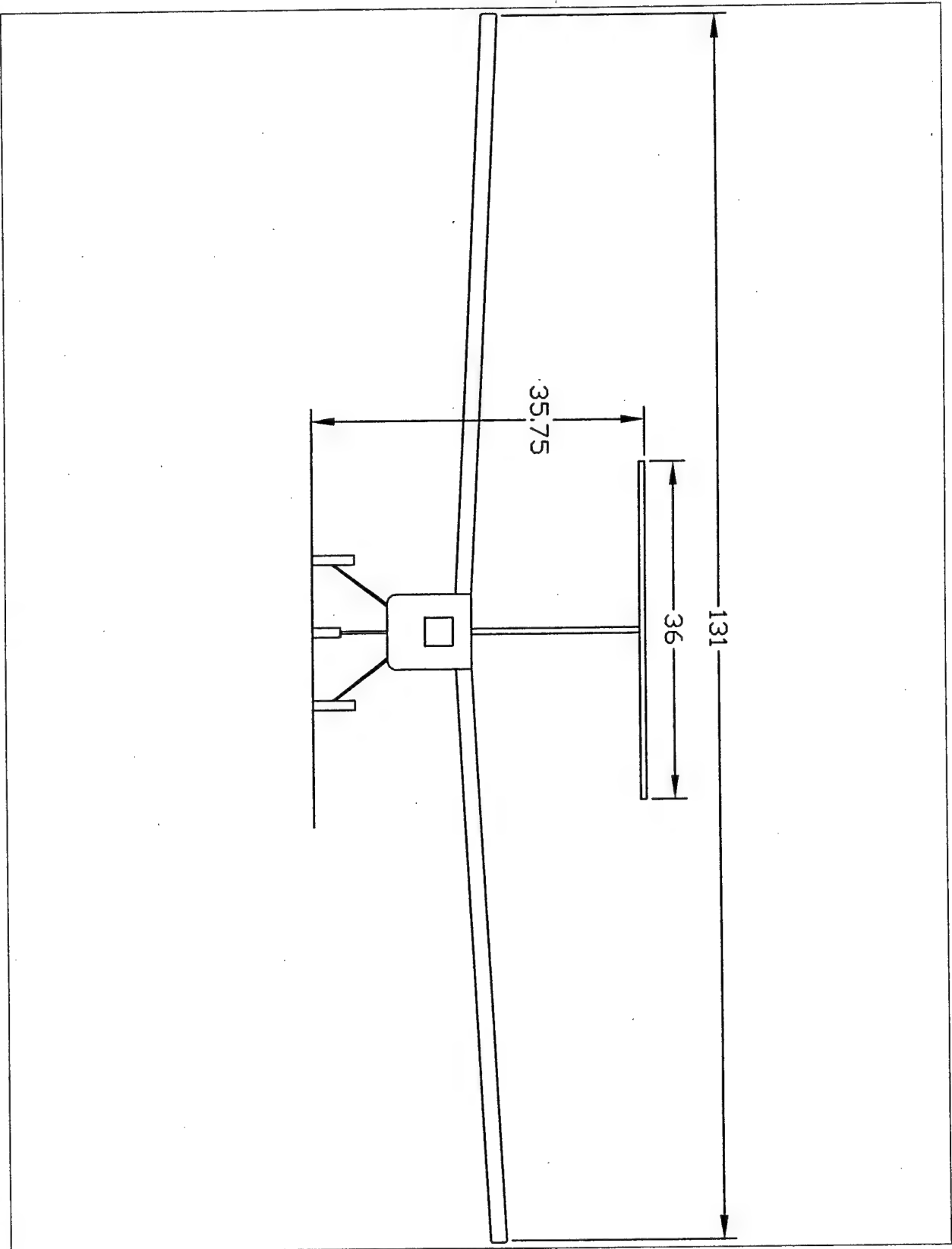
Table 21: Final Rated Aircraft Cost Table

5.2.3 Drawing Package

The following are the schematics of the entire airplane when full assembled.







5.3 Final Aircraft Predicted Performance

The final aircraft performance predicts how the aircraft will behave. This ensures that the Yeager Bomber meets all of the mission requirements. Also this will help the Pilot fly the airplane because he has a better understanding of how it will behave.

5.3.1 Take off Performance

The take-off of the airplane is one of the key performance factors. If the airplane can not take-off in the 150 ft the flight will not count for the score. Therefore, after the initial take-off analysis, a more in-depth study was then performed. Two separate MathCAD programs were written to evaluate the take-off performance. The first was an extension of the program written for the initial take-off analysis. Added to this program was rotation and transition on top of the ground roll. The second program was an in-depth study of the flight profile especially at take-off. Take-off#2 modeled the lift, acceleration and rate of climb of the Yeager Bomber. Take-off#2 yielded the following results:

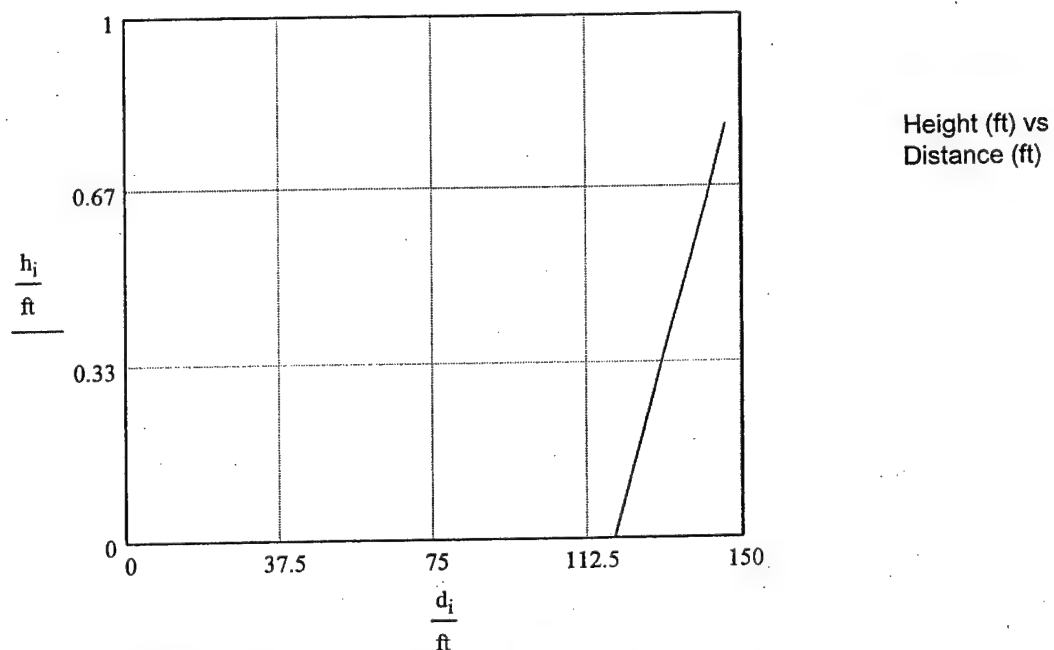


Figure 13: Take-off Height Vs. Take-off Distance Graph

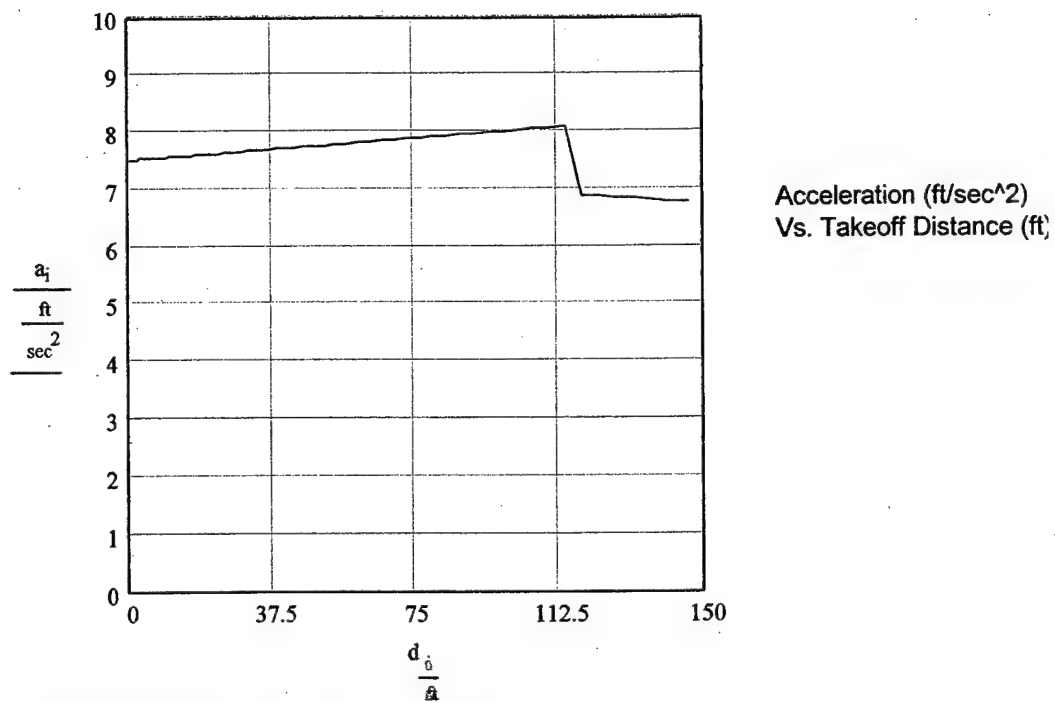
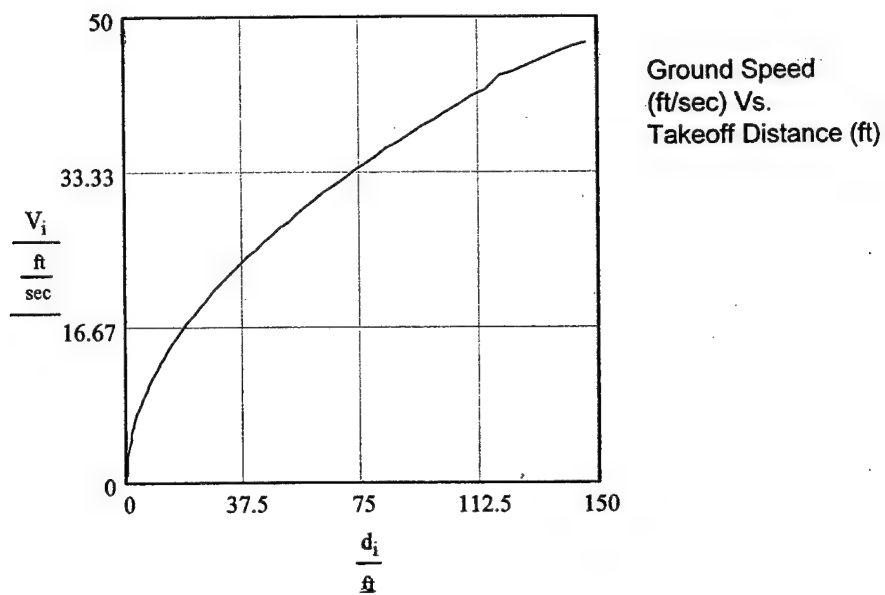


Figure 14: Ground Speed Vs. Take-off Distance Graph
Figure 15: Acceleration Vs. Take-off Distance Graph

From these graphs valuable data can be obtained. The first graph tells us the Yeager Bomber will reach 1 ft in 150 ft. This means take-off will occur on time. The next two graphs support this. The Ground Speed Vs. Take-off distance confirms that $1.2 \cdot \text{stall speed}$, 44 ft/sec, occurs. This is a critical speed to reach during take-off so that a stall does not occur while climbing to the cruise altitude. The final graph, Acceleration Vs. Take-off Distance, gives a good idea of where rotation will start. This is at 112 ft where the acceleration dramatic is reduced as aerodynamic drag starts to effect the Yeager Bomber. Another important fact obtained from this program is that take-off will occur in approximately 8 seconds.

The take-off#1 iterates through the following take-off equation. These equations are from Raymer's Aircraft Design book.

$$S_g(h, WS) := \left(\frac{1}{2 \cdot g \cdot K_a(h, WS)} \right) \cdot \ln \left[\frac{K_t + K_a(h, WS) \cdot (V_{\text{stall}}(h, WS) \cdot 1.1)^2}{K_t + K_a(h, WS) \cdot \left(0 \cdot \frac{\text{ft}}{\text{sec}} \right)^2} \right]$$

$$S_r(h, WS) := 1.1 \cdot \text{sec} \cdot V_{\text{stall}}(h, WS) \cdot .5$$

$$S_{tt}(h, WS) := \sqrt{R(h, WS)^2 - (R(h, WS) - .5\text{ft})^2}$$

$$\text{BFL}(h, WS) := S_g(h, WS) + S_{tt}(h, WS) + S_r(h, WS)$$

It is from these equations that the Balanced Field length turns out to be 10 ft longer to reach a height of 1 ft. By breaking the take-off into three segments, ground roll, rotation and transition, a better comparison of the two programs can be obtained. Both programs agree of the rotation and transition segments. The variation occurs with the ground roll. Because the Yeager Bomber needs to be off the ground at 150 ft and not at 1 ft take-off#1 was revalued with just the round roll and rotation. This puts the Yeager Bomber off the ground at 142 ft.

In conclusion, two different methods of obtain take-off distance were examined for the Yeager Bomber. They differed by 10 ft. However, both programs concluded that the Yeager Bomber would be off the ground at 150 ft. Therefore, the Yeager Bomber will satisfy the take off distance for the competition.

5.3.2 Rate of Climb

Rate of climb was computed using the three important weights which are 25 lbf, 30 lbf, and 35 lbf. The rate of climb was then graphed versus the velocity to produce the following graph.

ROC (ft/min) at the three critical weights vs. Velocity (mph)

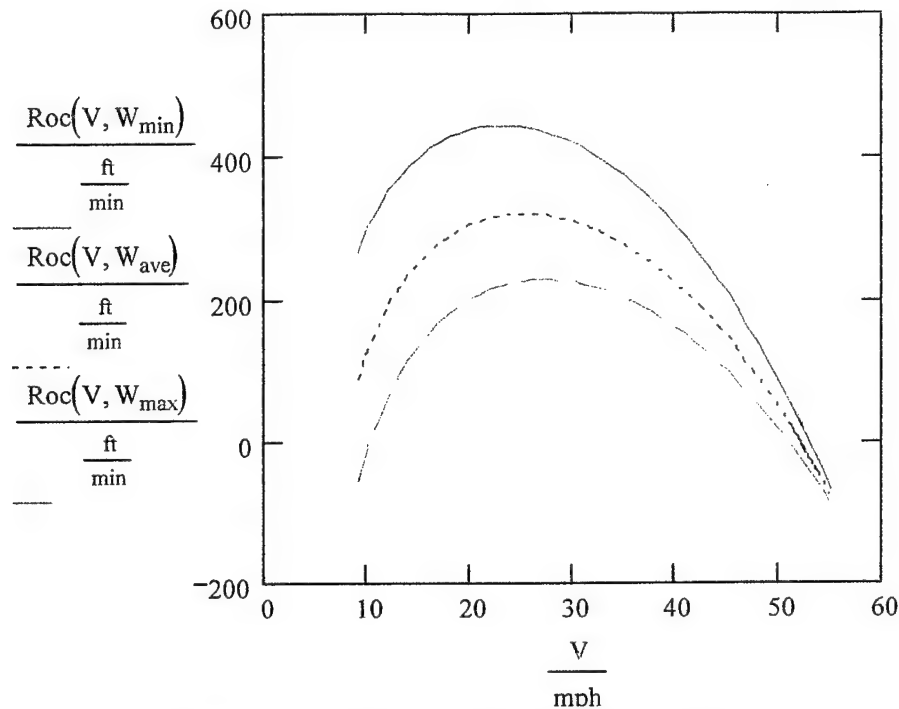


Figure 16: Velocity Vs. Rate of Climb Graph

5.3.3 Stability Margin and Trim

When the fuselage was being designed, it was decided that mounting the payload horizontally, thus allowing more sloshing of the water in flight, was more beneficial, due to the advantage in aerodynamics, than mounting the payload vertically which would have reduced the amount of water movement. This early decision is what dictated the decision to design the aircraft with a fairly high stability margin. These calculations merely verified that the design was stable enough to allow for minor payload shifting.

The high stability margin was also chosen due to the manner of the mission. With the dropping of the payload in mid flight and the position of payload system it was thought that a high stability margin would be beneficial to the design.

Using equations from *Aerodynamics Aeronautics and Flight Mechanics* by Barnes W. McCormick, the change in stability was analyzed. First the neutral point was estimated,

$$h_n := \frac{a_w \cdot h_{nw} + a_t \cdot \eta_t \cdot \frac{St}{S_w} \cdot h_l \cdot (1 - \epsilon \alpha)}{a_w + a_t \cdot \eta_t \cdot \frac{St}{S_w} \cdot (1 - \epsilon \alpha)}$$

This estimated number was then used in the following equation to obtain the aircraft stability margin,

$$\text{Stat} := (\text{hn} - \text{h0})$$

h0 was set at 0.3 so the equation resulted in:

$$\text{Stat} = 0.44$$

$$\text{Stat} \cdot \text{MAC} = 5.127 \text{in}$$

These equations were used in a MathCAD program to determine the non-dimensional stability margin. The non-dimensional number was then multiplied by the wing mean aerodynamic chord to produce the 5.127 inches.

Using the information above, trim flight conditions were estimated for several different weights and velocities. Then the lift created by the tail was analyzed using:

$$\text{CL}(\alpha, \text{it}) := \text{at} \cdot [\alpha \cdot (1 - \epsilon\alpha) - \text{it}]$$

The results showed that the lift coefficient for the tail hovered around zero in all situations. The aircraft was designed to have a neutral tail and these calculations verified that the completed design still maintained a neutral tail.

5.3.4 Roll Rate

When examining the stability and control of the aircraft, the rolling rate was analyzed. The roll rate, defined as P, needed to be sufficient enough to allow the pilot to maintain control while at low speeds. According to *Aerodynamics, Aeronautics, and Flight Mechanics* by McCormick (page 519), the total rolling moment of the wing can be expressed as:

$$L := -q \cdot a_0 \cdot \tau \cdot \delta_a \cdot \int_{y_1}^{y_2} c \cdot y \, dy$$

The limits of integration represent the distances from the inboard and outboard edge of the flaperon to the mid-span. These distances were then non-dimensional with respect the half span. The rolling moment could then be expressed in non-dimensional form.

$$x_1 := \frac{y_1}{\frac{b}{2}} \quad x_2 := \frac{y_2}{\frac{b}{2}} \quad C_l := \frac{-1}{4} \cdot a_0 \cdot \tau \cdot \delta_a \cdot A \cdot \int_{x_1}^{x_2} \left(\frac{c}{b} \right) \cdot x \, dx$$

The 2-D lift curve slope of the flaperons was corrected for the downwash effect due to the wingtip vortices. If a non-dimensional form of the roll rate is defined as P_{bar} and the wing has a linear taper, the rolling moment coefficient can then be rewritten as:

$$C_l := \frac{-a_0 \cdot P_{bar}}{12} \cdot \frac{(1 + 3\lambda)}{(1 + \lambda)} \quad \text{assuming that} \quad P_{bar} := \frac{P \cdot b}{2 \cdot V}$$

The roll rate can then be calculated for a given flaperon deflection and airspeed. The roll rate during take-off needed to be determined, since the airspeed will be lowest and the controllability critical. The flaperon deflection was set to 10 degrees and the airspeed set to $1.2 \cdot V_{stall}$, which is the usual take-off velocity. At this deflection and airspeed, the aircraft had a calculated roll rate of 14.06 degrees/second. The FAR Part 23 Regulations require a minimum roll rate of 12 degrees/second at this velocity. The aircraft, therefore, will have good controllability during take-off.

5.3.5 Final Mission Prediction

Since a very accurate model of our plane has been established, a predicted score can be calculated. In order to do this accurately the flight was broken into six different components. Then a predicted time for each of those was calculated for each section. 20% of the total time was added for unforeseen effects such as adverse wind condition. The cruise for the fire bomber mission was set at 35 mph and the ferry was set at 40 mph. This difference is due to the difference in weight. Also the water weight was entered in as 8 lbs when calculating the total score.

	Fire Bomber	Ferry
Loading	20	na
Take-off	8	6
Climb	30	15
Cruise	40	136
Maneuvering	24	96
Descent	30	15
Landing	8	6
Second Sortie	160	na
Total Time (sec)	320	274
Plus 20%	384	328.8
Total Score	2.5	0.182481752

Table 22: Yeager Bomber Predict Score Table

6.0 Manufacturing Plan

A wide range of options were available to select from for manufacturing the airplane. Among the list was a balsa wood frame construction, a fiber reinforced foam, a plywood balsa wood composite, and a carbon honeycomb composite. Each of these had advantages and disadvantages that needed to be explored. The factors investigated are: Availability of Materials and Supplies (AMS), Skill Required to Build (SRB), Cost to Build (CTB), Material Strength and Durability (MSD), Time Required to Build (TRB), and Estimated Weight of Part (EWP).

In order to explore the manufacturing options FOM tables were devised. These tables were useful to help uncover unforeseen problems during the manufacturing process. For example, one method may be low cost and quick to fabricate, but would lack in durability and may lead to strength problems down the road. Many of these qualities seem obvious when selecting materials and construction methods, however it is a step that needs to be taken to ensure the fabrication is completed within budget, on time, and within dimension tolerances. In order to complete the FOM table, values were set to each factor for analysis.

AMS:

+2	Adequate access to tools and materials required
+1	Adequate access to tools or materials
+0	Not sufficient access to tools and materials

SRB:

+2	More than two people available with required skill
+1	Two or less people available with required skill
+0	Zero people available with required skill

CTB:

+2	Free of charge or easily payable
+1	Within budget but expensive
+0	Not within budget

MSD:

+5	Reusable after a crash
+1	Functional but will need replacement after a crash
+0	Hard to function with, too delicate

TRB:

+2	Twenty man hours or less required
+1	Twenty to fifty man hours required

+0	Over fifty man hours required
----	-------------------------------

EWP:

+2	Low impact on RAC
+1	Sustainable impact on RAC
+0	Unsustainable impact on RAC

Fuselage FOM:

Material / Method	AMS	SKB	CTB	MSD	TRB	EWP	Total
Balsa Wood frame and Skin	2	1	2	1	1	1	8
Fiber reinforced Foam	2	1	2	1	1	1	8
Plywood frame and Balsa Skin	2	1	2	1	1	1	8
Carbon Fiber Honeycomb Composite	2	2	1	5	0	1	11

Table 23: Fuselage Material Selection Matrix

From Table 23, a carbon fiber construction was selected. This plane is planned to perform many flight tests, each involving some risk of a crash. If a crash was to occur during the test phase and the fuselage needed to be replaced or repaired it would put the program immediately behind schedule. Since it is affordable to have replacement components for the rest of the plane it will be far quicker to simply replace the parts that are broken onto the same fuselage, rather than build another plane from the bottom up. In addition to favoring carbon's strengths, many members of the team have previous knowledge of constructing parts with carbon fiber and honeycomb. This is a major advantage for the team to ensure the fuselage is at proper dimensions and is fabricated in the allotted time.

Wing FOM:

A FOM table for the wing is not provided. Earlier in the design phase it was chosen, due to time and cost, to use a carbon fiber wing that was already made and available to use for the project. This wing was built for the 2003 AIAA DBF competition. Knowing this a FOM table for the wing would be redundant.

Tail FOM:

Material / Method	AMS	SKB	CTB	MSD	TRB	EWP	Total
Balsa Wood frame and Skin	2	2	2	1	2	2	11
Fiber reinforced Foam	2	1	1	1	1	2	8
Plywood frame and Balsa Skin	2	2	2	1	2	0	9
Carbon Fiber Honeycomb Composite	2	2	1	5	0	0	10

Table 24: Tail Material Selection Matrix

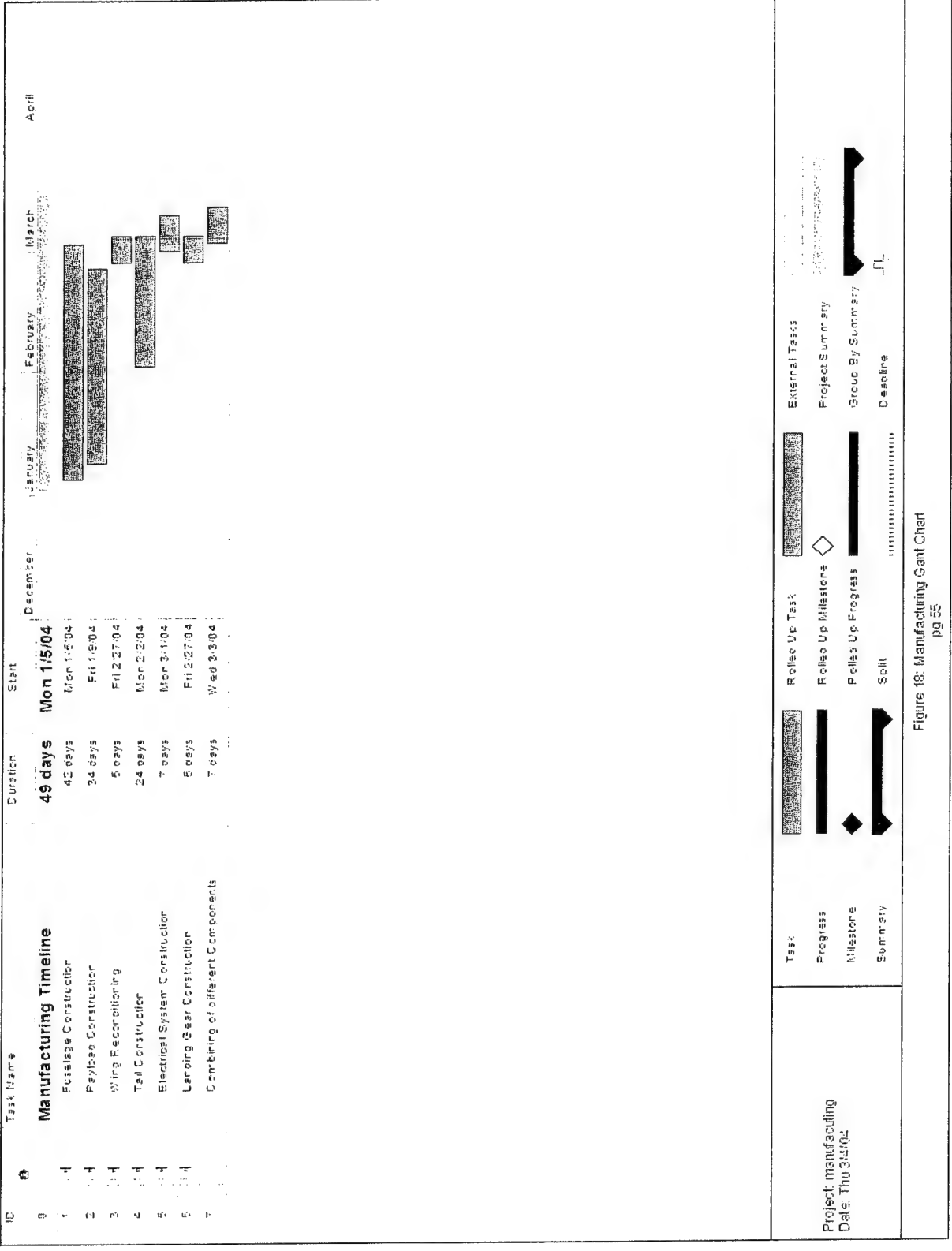


Figure 18: Manufacturing Gant Chart
pg 55

7.0 Test Plan

7.1 Component Testing

It is important to test analytical methods by actual testing the device. Through these test a better understanding of the different component is gained and therefore a better prediction of how the plane will fly. There are three different component tests that will be done to confirm our calculations. Also these tests will prove our design of the components before they are integrated into the plane. Those tests are listed in Table 25.

Component	Objective
Propeller Testing	To find the most efficient prop that will give the thrust needed
Landing Gear Test	To confirm that our landing gear can handle the impacts of landing as well as confirm the roll friction coefficient
Payload Test	To confirm the payload can hold and release 4 liters of water

Table 25: Component Testing Table

7.2 Flight Testing

The success and optimization of any design occurs during flight testing. This is the only way to analyze all of the different components and how they interact together. The flight testing will take place in two major portions. The first is the static testing of the airplane and the second is the dynamic testing. It is important to have a good plan for the testing. A good plan will make sure that if there is a failure it is able to be fixed without destroying the airplane. A wing tip test should be done before flying because if the structure can not withstand being held by the wings it will certainly crash in flight. Table 26 lists both the static and dynamic parts of the flight test. These tests will be done in order and if one fails it will be corrected and passed before moving to the next step in the process. Table 27 is a preflight check list that will be performed before all Dynamic Flight Test.

Static Test	Objective
Unloaded	
Wing Tip Test	Confirm structural Soundness of design
Inverted Wing Tip Test	Confirm structural Soundness of design
Loaded	
Wing Tip Test	Confirm structural Soundness of design
Inverted Wing Tip Test	Confirm structural Soundness of design
Control Surfaces Check	Makes sure the plane will go where it is suppose to
Payload Release Check	Makes sure that the water will go out when we tell it

Dynamic Flight Test	Objective
Flight Test One	Proof of Concept
Proof of Concept (Unloaded)	Does it fly? Do the controls handle the way the pilot wants?
Proof of Concept (loaded)	Does it fly? Do the controls handle the way the pilot wants?
	Does the water dump out?
Flight Test Two	Aircraft Performance
Take-off Distance	
Landing Distance	
Maximum Speed	
Water Dumping Time	
Turning radius/roll rate	
CL testing	
Flight Test Three	Mission Sorties
Fire Bomber	
Transport	

Table 26: Flight Testing Table

Preflight Check List

General Aircraft

Wing Tip Test	go	no go
unloaded	go	no go
loaded	go	no go
Fail Safe Check	go	no go

Control Surfaces

Elevator	go	no go
Rudder	go	no go
Nose Gear	go	no go
Flaperons	go	no go

Payload

No leak when loaded	go	no go
Deploys Water	go	no go
Reseals for second sortie	go	no go

Final

(Visual Inspections to verify all components are working)	go	no go
---	----	-------

Flight Test	go	no go
--------------------	-----------	--------------

Table 27: Pre-Flight Check List

7.3 Lessons Learned

Propeller Testing:

Calculations showed that a 24 X 10 propeller was needed. To decide which propeller brand name was going to perform the best three different 24 X 10 propellers were tested. The Test was done comparatively for the three test where static thrust and thrust at 28 ft/sec were taken. The three propellers selected were a one-piece composite APC propeller, a regular wood Zinger and a sport wood Zinger. From the wind tunnel testing all of the propellers performed the same. They all produced 7 lbf at static and 3.5 with 28 ft/sec incoming velocity. Since there was no performance differences the lightest propeller was chosen. That propeller was the regular wood Zinger.

Payload Test Results:

The payload device was tested a multitude of times. The first round of test was done without the servo. This was done to make sure the device would work properly. The release mechanism did drain and reseal properly. The next test done was with the servo moving the plug. This revealed a few different facts. The drain time was found to be 42 seconds. The dumping will hopefully take just one leg of the loop for dumping. Also a problem was found, a leak when resealing. The leak was extremely minimal; a drop of petroleum gel was used to stop the leak and make resealing happen. The final test done was a shake test. This was done to see if the anti-sloshing barriers worked. They did work but not as well as expected. In conclusion the payload device works very well.

Landing Gear Test:

Impact loading is hard to approximate due to the large number of variables, especially when it is a landing aircraft. To give a realistic approximation a static load of 85 lbf was applied to our landing gear. This is more than twice the weight of the aircraft and should give a safe approximation. After the load was applied there was no noticeable deflection in our landing gear. The only change was the rubber coated foam wheels did slightly compress. This test proved that the landing gear is safe.

References:

- Abbot, I.H. and A.E. Von Doenhoff. *Theory of Wing Sections*. Dover, NY 1959.
- Hibbeler, R.C. *Mechanics of Materials*. Prenticed Hall. Upper Saddle River, NJ 2000
- McCormick, Barnes W. *Aerodynamics, Aeronautics, and Flight Mechanic*. Danvers, MA 1995.
- Raymer, Daniel P. *Aircraft Design: A Conceptual Approach*. AIAA. Reston, VA. 1999.
- Schmidt, Louis V. *Introduction to Aircraft Flight Dynamics*. AIAA. Reston, VA. 1998.
- Torenbeek, Egbert. *Synthesis of Sub-sonic Airplane Design*. Netherlands. 1982.
- Walker, Tim. Personal Interview. Structural Engineer at Duncan Aviation. December 17, 2003.

2003/2004 AIAA Foundation

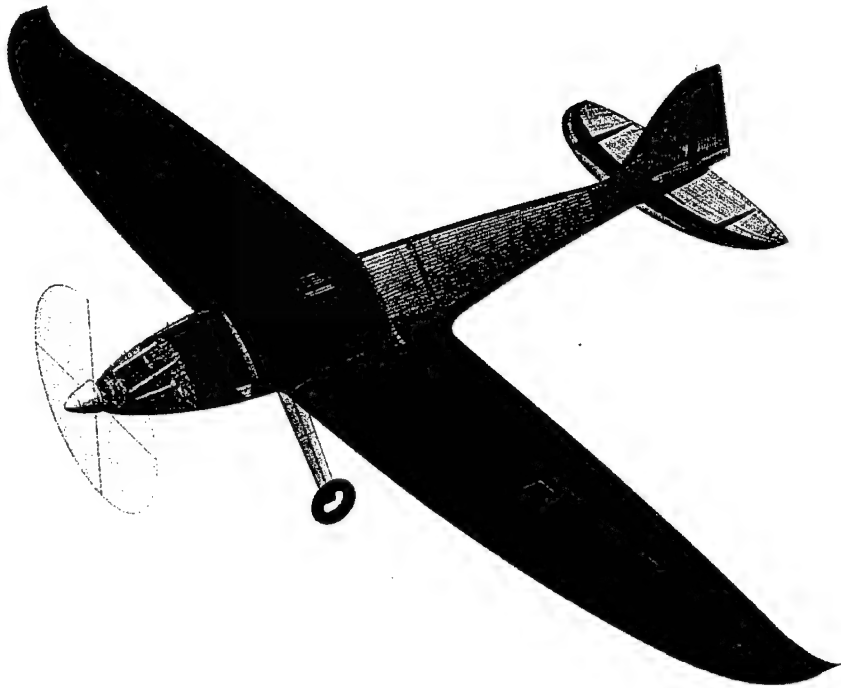
Cessna/ONR Student Design/Build/Fly Competition

DESIGN REPORT
MARCH 9, 2004



Department of Aerospace Engineering

Mississippi State University



"PHYXIUS"

TABLE OF CONTENTS

1. EXECUTIVE SUMMARY	1
1.1 Conceptual Design	1
1.1.1 Conceptual Design Alternatives	1
1.1.2 Conceptual Design Results	1
1.2 Preliminary Design	2
1.2.1 Preliminary Results	2
1.3 Detail Design	3
1.4 Manufacturing	4
1.5 Flight Testing	4
2. MANAGEMENT SUMMARY	5
2.1 Organization of the Team	5
2.2 Assignment Areas	5
2.3 Milestone Timeline	5
3. CONCEPTUAL DESIGN	9
3.1 Mission Requirements	9
3.2 Conceptual Design Concepts	10
3.2.1 Airframe (Fuselage) Configuration	10
3.2.2 Wing Design	11
3.2.3 Empennage Configuration	11
3.2.4 Engine Configuration	12
3.2.5 Landing Gear Configuration	12
3.3 Figures of Merit	13
3.3.1 Description of the Figures of Merits	13
3.3.2 Scoring of Design Concepts	14
3.4 Rated Aircraft Cost Factors	15
3.5 Conceptual Design Selection	16
3.6 Conceptual Design Summary	16
4. PRELIMINARY DESIGN	17
4.1 Design Parameters and Sizing Trades	17
4.1.1 Payload System	17
4.1.2 Airfoil Selection	17
4.1.2.1 Horizontal Stabilizer Airfoil Selection	19
4.1.3 Propulsion Configuration	20
4.1.4 Thrust Loading and Wing Loading Study	20
4.1.5 Structural Analysis of the Spar	21
4.1.6 Engine Selection	22
4.1.7 Available Thrust Model at Speed	24
4.1.7.1 Wind Tunnel Results	25
4.1.8 Sizing of the Horizontal Tail	26
4.1.9 Longitudinal Control	28
4.1.10 Longitudinal Dynamic Analysis	29
4.1.11 Sizing of the Vertical Tail	29
4.1.12 Lateral/Directional Dynamic Analysis	31
4.2 Structural Material Considerations	31
4.2.1 Research	31
4.2.2 Materials	32
4.3 Flight Performance	32
4.3.1 Performance Data	32
4.4 Optimization Code	34
4.5 Estimated Mission Times	36
4.6 Summary of Preliminary Results	37
5. DETAIL DESIGN	38
5.1 Weights and Balance Sheet	38
5.2 Component Selection	38

5.3 Systems Architecture	39
5.3.1 Wing	39
5.3.2 Fuselage	40
5.3.3 Empennage	41
5.3.4 Landing Gear	41
5.3.5 Engine Mount	42
5.3.6 Payload Deployment	42
5.4 Payload System	42
5.5 Rated Aircraft Cost	43
5.6 Drawing Package	45
6. MANUFACTURING PLAN	50
6.1 Construction Methods Investigated	50
6.2 Construction Materials Investigated	50
6.3 Figures of Merit	51
6.4 Results	51
6.5 Manufacturing Timeline	53
7. FLIGHT TESTING PLAN	54
7.1 Objective	54
7.2 Schedules and Check Lists	54
7.3 Results	55

1. EXECUTIVE SUMMARY

This report documents the efforts of a select group of aerospace engineering students at Mississippi State University (MSU) to design, fabricate, and flight test Phyxius, an electrically powered unmanned aerial vehicle (UAV). Optimized for stability and balanced performance with a takeoff distance of less than 150 ft, Phyxius represents a balanced design that carries a maximum of 4 L of water to be deployed during flight. Phyxius can be disassembled and stored in a box measuring 4ft x 2 ft x 1 ft.

1.1 Conceptual Design

During the first meeting, members were assigned to one or more of six major groups. The groups include Aerodynamics, Flight Mechanics, Flight-Testing, Weights and Balance, Propulsion, and Structures. During the early team meetings, members were given the opportunity to submit an individual design that would meet the requirements specified in the rules of the Cessna/ONR Design/Build/Fly (DBF) Competition for 2004. After all conceptual ideas were presented; the groups were instructed to meet each week, separate from the team meetings, to discuss how their group was affected by the conceptual ideas and how to improve on each idea.

1.1.1 Conceptual Design Alternatives

The concepts, presented by the groups, were categorized as canard or conventional tail airframe design. The canard configuration was considered for its takeoff capabilities. The conventional design was considered for its stability and recognized success. Traditionally, Mississippi State's team has chosen to go with this concept. The idea, in the past, has been to build a conventional airframe around the mission profiles

The two design concepts were expanded into a total of twelve conceptual designs that differed in airframe configuration, wing placement, and empennage configuration. A more detailed description of each conceptual design appears later in this report.

1.1.2 Conceptual Design Results

Based on the Figures of Merit placed on each design, the conceptual designs were narrowed from twelve to four designs for further consideration. In the end, the final configuration chosen was a tail-dragging conventional fuselage incorporating a conventional tail with a low-mounted elliptical wing. The propulsion system chosen was a single Graupner motor with a Frudenthaler propeller.

1.2 Preliminary Design

During the preliminary design phase, the groups communicated and shared information to determine the size of Phyxius. The UAV was to be optimized for performance; utilizing information from the Aerodynamics, Propulsion, and Structures group. The rated aircraft cost (RAC) was selected as the objective function. Using the available information, thrust-to-weight ratio and wing loading were selected as design variables with take-off as the constraint. If the take-off velocity was less than the stall speed, the RAC was assigned a value of zero. Also, side constraints were placed on the design variables based on the storage box dimensions. Once the dimensions of the wing were calculated from the optimization program, the Flight Mechanics group sized the empennage to produce a UAV with a positive static margin and good stability characteristics. The constraints placed on the Flight Mechanics group were that the fuselage length must be less than 48 in.; the horizontal tail span must be less than 24 in. but greater than 12 in., and the vertical tail span must be less than 12 in.

1.2.1 Preliminary Results

The results from the wing sizing showed that the optimum design coincided with the take-off constraint. In 2001, the first year that Mississippi State University participated in the DBF competition, the design point was chosen close to this constraint. However, the manufactured weight was 5 lb greater than its predicted value, and that difference caused undesirable take-off and climb performance. This year, the design point was chosen such that the best design was away from the side constraint but still possessed a high score.

To acquire accurate data for the propulsion system, the Graupner Ultra 3300-5 engine with gear reduction and a 16x13 propeller were analyzed both statically and dynamically in the MSU low-speed wind tunnel. The results of the wind tunnel testing on the motor and propeller showed a static thrust of 11 lb with a pitch speed of 85 mph.

The final airframe was designed for completing both missions. The payload placement coincided with the empty weight center of gravity. The design was estimated at a weight of approximately 16 lb and was predicted to attain a RAC of 12.9. The sizing and the performance data of Phyxius are presented in Table 1.1 and Table 1.2.

Table 1.1 Preliminary Component Sizing

Preliminary Component Sizing	
Fuselage Length (ft)	4
Wing Span (ft)	7
Wing Chord (ft)	1
Wing Aspect Ratio	7
Horizontal Tail Span (ft)	2
Horizontal Tail Chord (ft)	0.75
Vertical Tail Span (ft)	2
Vertical Tail Chord (ft)	0.75
Engine	Graupner Ultra 3300-05
Gear Box	2:1
Propeller Selection (in)	16x10
RAC (Predicted)	10

Table 1.2 Preliminary Performance Results

Preliminary Performance Results		
	Loaded	Unloaded
$C_{L,max}$	1.2	1.2
$(L/D)_{max}$	15	15
Stall Speed (mph)	35	25
Maximum Rate of Climb (ft/min)	1100	2600
Neutral Point Location (% of Chord)	40	
CG Location (% of Chord)	30	
Take-Off Distance (ft)	130	50
Maximum Speed (mph)	60	80
RAC	12.9	

1.3 Detail Design

The purpose of the detailed design was to select components for Phyxius and to model the aircraft in a graphics program that would indicate UAV size and configuration, storage configuration of disassembled parts, and payload location and deployment. Using the "Analysis" section of the graphics program, a detail of the component weight and location was collected, and the center of gravity was determined. Using this information, a RAC table was constructed. A detailed description of the construction of the aircraft was completed. This description includes the wing, fuselage, empennage, and landing gear. A detailed description of the payload deployment is also developed.

1.4 Manufacturing

The construction of the UAV was considered from the beginning of the design phase. There were many methods of construction suggested by the team members, ranging from off-the-shelf (OTC) components to a completely molded design. The team concluded that the construction of the UAV must not be time consuming, and must offer an overall low material weight. Based on these Figures of Merit, the team decided to construct the UAV using a molded composite design based on computer numerical control (CNC) machined molds.

1.5 Flight Testing

Phyxius I was to be built based on the detailed design. A second UAV, Phyxius II, was to be built with lessons learned from flight-testing of Phyxius I. Flight-testing would allow the team to analyze performance based on actual mission flights. A group leader was selected from the experienced pilots. The flight-testing leader presented a schedule of flights, detailing the timeline of missions to be performed. The group leader was assigned a group of students to help analyze and present the results from flight-testing. The results and analysis were to be used in the modification of the second and third set of parts ordered for Phyxius II. The third set of parts was considered the contingency plan and would be used for necessary improvements or repairs on either plane.

Flight-testing has been carefully planned and executed. Pre-flight briefings have been scheduled before each proposed flight. These briefings will allow the students to gain perspective from actual flight-testing personnel. Any problems encountered during flight-testing will be reported to the team and resolved accordingly.

2. MANAGEMENT SUMMARY

The 2003 Mississippi State University DBF team consists entirely of aerospace engineering students. This year's team is large but contains an even spread of underclassmen and veterans of previous Design/Build/Fly (DBF) teams. With 7 seniors, 16 veterans, and a total of 25 students, the group was organized according to experience and skills.

2.1 Organization of the Team

During the first meeting, a chief engineer and a project manager were nominated and elected by team members. With a team of 25 students, mostly underclassmen, it was decided that leadership would have to be shared. Using the experience of 16 veterans and the skills of four R/C pilots, the team was broken into four groups: Aerodynamics, Flight Mechanics, Propulsion, and Structures. Each of the groups would have a veteran group leader. This would provide each group some experience from previous DBF teams and also the skills related to building and piloting remotely controlled airplanes. In addition, a group composed of pilots was put in charge of construction and flight-testing. Also, several groups were created to help with administrative activities. The organization of the team is presented in Table 2.1.

2.2 Assignment Areas

Each group was assigned the task of contributing to the design and construction of Phyxius. Also, on a weekly basis, other tasks were assigned to ensure timely satisfaction of goals. Group leaders were responsible for distributing workload among the respective group members and providing a status report to the entire team. Each group contributed to the overall design and the major decisions. The team as a whole voted on necessary improvements or changes. Table 2.2 illustrates individual involvement in each process. A maximum rating of 5 is given to those who contributed the most to a given task.

2.3 Milestone Timeline

An initial timeline was set to ensure that work was done on a consistent basis. The team held weekly meetings, and the chief engineer and project manager met with the faculty advisor on a weekly basis to ensure that the schedule was maintained. However, further delays were encountered in construction due to miscommunication between the Structures group and the Construction groups. Figure 2.3 shows the milestones and respective timelines.

Table 2.1 Team Organization and Responsibilities

Chief Engineer: David Bodkin Project Manager: Jordan Haines Faculty Advisor: Dr. Robert King		
Group	Members	Responsibilities
Finance and Accounting	Jordan Haines (GL), David Bodkin, Mark VanZwoll, Cedric Gould	Maintaining and tracking of funds and the purchasing of materials.
Public Relations	Angela Spence (GL), Nikki King, Vanessa Aubuchon	Generating press releases to the university and soliciting funds.
Documentation	Amar Amin (GL), Allen Hammack	Taking notes during meetings and collecting any material deemed necessary for documentation.
Aerodynamics	Mark VanZwoll (GL), Amar Amin, Nikki King, Christopher Eigenheer	Analysis of UAV components and the interaction of the components with the airflow around them
Construction	Cedric Gould (GL), Jordan Haines, Christopher Eigenheer	Scheduling of manufacturing and supervising the construction of the UAV
Flight Mechanics	Alex Szymanski (GL), Travis Klima, Ryan Smith, Nathan Alday, Scott Smith	Sizing the UAV specifications based on stability and control issues.
Flight Testing	Cedric Gould (GL), Mark VanZwoll, William Lott	Developing a flight testing plan and obtaining an airfield to perform flight testing.
Weights and Balance	Joshua Jacobs (GL), Vanessa Aubuchon	To know at all times the weight of the aircraft and its various parts, and the location of the center of gravity.
Propulsion and Systems	Cedric Gould (GL), Jennifer Esper, Adrienne Bottom, Christopher Holloman, Robert DiGiacomo	Researching the subject of thrust models for electric engines and experimental testing of potential motor/propeller combinations.
Structures and Design	Brent Buckner (GL), William Lott, Mark Harris, Brandon Lasseigne, Chris Cureton	Taking the sizing of the UAV and developing the structure that would carry the loads.

GL – Group Leader

Table 2.2 Involvement of Each Member

	Nathan Alday	Amar Amin	Vanessa Aubuchen	David Bodkin	Adrienne Bottom	Brent Buckner	Chris Cureton	Robert DiGiacomo	Christopher Eigenheer	Jennifer Esper	Cedric Gould	Jordan Haines	Allen Hammack	Mark Harris	Christopher Holloman	Joshua Jacobs	Nikki King	Travis Klima	Brandon Lasseigne	William Lott	Scott Smith	Ryan Smith	Angela Spence	Alexander Szymanski	Mark VanZwoll
Finance & Accounting:																									
	Budget	0	0	0	4	0	0	0	0	0	0	5	0	0	0	0	0	0	0	0	0	0	0	0	
Purchasing		0	0	0	4	0	0	0	0	0	0	5	0	0	0	0	0	0	0	1	0	0	0	0	
Manufacturing:																									
	Wing Assembly	2	0	3	4	3	1	2	3	4	1	5	2	2	1	3	2	0	3	2	4	2	3	2	3
	Fuselage Assembly	1	0	3	4	2	1	0	3	5	0	5	2	2	1	4	4	1	1	2	4	2	0	2	3
	Horizontal and Vertical Tail	1	0	3	4	3	1	2	3	5	0	5	3	0	1	4	1	0	3	1	2	2	3	0	4
	Systems Integration	0	0	0	4	0	5	0	3	5	0	3	1	0	1	5	1	3	1	0	2	2	0	3	0
Report:																									
Executive & Management	1	5	0	4	0	0	0	0	0	0	0	0	0	0	0	0	0	0	0	0	0	0	0	0	
Conceptual Design	1	5	2	0	0	0	2	0	0	0	0	0	3	0	0	3	1	0	0	2	0	0	0	5	
Preliminary Design	1	5	2	0	0	0	2	0	0	0	0	0	3	0	0	1	1	0	0	3	0	0	0	5	
Detail Design	1	5	2	0	0	2	1	0	3	0	0	0	3	0	0	0	0	0	0	2	0	0	0	5	
Manufacturing Plan	1	5	2	0	0	0	0	0	2	0	2	5	3	0	0	0	0	0	1	4	0	0	0	0	
Flight Testing:																									
Pilot	0	0	0	0	0	0	0	0	0	0	4	0	0	0	0	0	0	0	0	5	0	0	0	0	
Ground Crew	0	0	0	0	0	1	0	1	0	0	5	0	0	0	0	2	0	0	1	1	0	0	0	0	
Propulsion:																									
Thrust Model	0	0	0	0	0	0	0	1	0	2	5	0	0	1	5	0	0	0	0	0	0	0	0	0	
Motor/Propeller Testing	0	0	0	0	4	1	0	1	1	0	5	0	0	1	5	0	0	0	0	0	0	0	0	0	
Performance:																									
Sizing and Optimization	0	0	0	4	0	0	0	0	0	0	0	0	0	0	0	0	0	1	0	2	2	0	0	5	
CG and Neutral Point Analysis	1	0	1	4	0	0	0	0	0	0	0	0	0	0	0	3	0	1	0	0	2	0	0	5	
CAD:																									
Components	0	0	0	5	0	1	0	0	0	0	0	0	0	0	0	0	0	0	0	0	0	0	0	0	
Engine Mounts	0	0	0	5	0	1	0	0	0	0	0	0	0	0	0	0	0	0	0	0	0	0	0	0	
Wing	0	0	0	5	0	0	0	0	0	0	0	0	0	0	0	0	0	0	0	0	0	0	0	0	
Fuselage	0	0	0	5	0	0	0	0	0	0	3	0	0	0	0	0	0	0	0	0	0	0	0	0	
Horizontal and Vertical Tail	0	0	0	5	0	0	0	0	0	0	0	0	0	0	0	0	0	0	0	0	0	0	0	0	
Stability & Control:																									
Horizontal and Vertical Tail Sizing	2	0	0	4	0	0	0	1	0	0	0	0	0	0	0	0	0	3	0	1	2	0	5	0	
Servo Selection	0	0	0	4	0	0	0	1	0	0	0	0	0	0	0	0	0	0	0	1	0	0	5	5	
Control Surface Sizing	1	0	0	4	0	0	0	1	0	0	0	0	0	0	0	0	0	3	0	3	2	0	5	1	
Administration:																									
Scheduling	0	0	0	5	0	0	0	0	0	0	0	3	0	0	0	0	0	0	0	1	0	4	0	0	
Soliciting Funds	0	0	0	4	0	0	0	0	0	0	2	3	0	0	0	0	0	0	0	0	0	5	0	0	
Documentation	0	5	0	5	0	0	0	0	0	0	0	3	0	0	0	0	2	0	0	0	0	4	0	0	

Table 2.3 Timeline and Milestone of Major Events

Task	Start	Finish	Sep 03	Oct 03	Nov 03	Dec 03	Jan 04	Feb 04	Mar 04	Apr 04
Conceptual Design										
Planned	01-Sep	24-Sep								
Actual	01-Sep	15-Oct								
Propulsion Model and Testing										
Planned	16-Sep	11-Dec								
Actual	16-Sep	25-Feb								
Submission of Entry Form										
Performance and Sizing										
Planned	23-Sep	01-Dec								
Actual	23-Sep	01-Dec								
Obtain Half Funding										
Planned	24-Sep	01-Dec								
Actual	15-Nov	12-Dec								
Detailed Design										
Planned	15-Oct	12-Dec								
Actual	22-Oct	12-Dec								
Manufacturing										
Planned	12-Jan	15-Feb								
Actual	12-Jan	03-Mar								
Flight Testing										
Planned	03-Feb	28-Feb								
Actual	28-Feb	March								
Report										
Planned	12-Jan	27-Feb								
Actual	12-Jan	07-Mar								
Submission of Report										
Design/Build/Fly Competition										
		23-25-Apr								

3. CONCEPTUAL DESIGN

The conceptual design phase of the UAV focuses on defining the rough layout of the UAV. Each group was given the challenge of presenting a conceptual idea that meets the mission requirements of the competition. Also, team members were given the opportunity to present individual ideas. After applying the Figures of Merit to the alternative design concepts, the final conceptual design for Phyxius emerged. The selection for the conceptual design represents a configuration that will accomplish the mission requirements with minimum penalty in rated aircraft cost (RAC).

3.1 Mission Requirements

The UAV was designed to complete two mission profiles. Each profile is given a difficulty factor based on the complexity of the mission. The higher the difficulty factor, the better the team's score. Competing teams will be allowed five flight attempts, choosing any of the two mission profiles, and will be judged on the best single flight attempt from two separate mission profiles. Adding to the complexity of the design, the UAV must fit inside a rectangular box with dimensions of 2 ft x 1 ft x 4 ft. Each mission profile will be timed based on completion.

All mission profiles share common characteristics. The UAV must takeoff in a distance of 150 ft and must carry a water tank. The flight profile consists of a closed-traffic pattern with the direction of travel determined based on the wind conditions. The upwind and downwind legs measure 1,000 ft with no specified distances for the base and crosswind legs. The contest director determines the altitude for the pattern during the competition. From past experience with this competition, the altitude ranges from 100 ft to 200 ft above the ground.

The "ferry" is the least difficult mission. The UAV must take-off, complete four laps/patterns, and land. On all downwind legs, the UAV must complete a 360-degree turn opposite of the base and final turns. The aircraft will have no water payload in this mission.

The "firefight" is the most difficult mission. The aircraft will begin the mission empty. The mission will consist of two sorties. For the first sortie, the aircraft will be loaded with water. Then it must take-off and dump its water load during the downwind leg, and land. For the second sortie, the aircraft will be reloaded with water and the dumping mission is repeated. The maximum water capacity for all aircraft will be four liters. The teams will load the aircraft during the mission from four plastic 2-liter "soda" bottles. The teams may use gravity or a "pumped loading." The bottles may not be pressurized to assist loading. On all downwind legs, the UAV must complete a 360-degree turn opposite of the base and final turns. The water may only be dumped during the downwind leg. Therefore, the aircraft must fly slowly enough to allow for dumping of the entire water carried onboard. The maximum dump orifice diameter is 0.5 in.

3.2 Conceptual Design Concepts

Members of the DBF team presented a total of twelve conceptual designs. Upon examination of each concept, it was determined that four major features defined each of the design concepts presented: airframe configuration, wing design, and empennage configuration. Design suggestions from the entire team resulted in the concepts defined in Table 3.1.

Table 3.1 Concept Descriptions

Concept Number	Airframe	Wing	Empennage
1	Conventional	Low AR	V-Tail
2	Conventional	High AR	V-Tail
3	Conventional	Low AR	H-Tail
4	Conventional	High AR	H-Tail
5	Conventional	Low AR	Conventional
6	Conventional	High AR	Conventional
7	Canard	Low AR	V-Tail
8	Canard	High AR	V-Tail
9	Canard	Low AR	H-Tail
10	Canard	High AR	H-Tail
11	Canard	Low AR	Conventional
12	Canard	High AR	Conventional

3.2.1 Airframe (Fuselage) Configuration

The conventional airframe was chosen for its stable reputation as well as its ease of analysis and construction. Being able to analyze data on a well-known structure would allow for more trust in theoretical results. Traditionally, Mississippi State University has chosen this configuration. Since attending the competition for the past three years, this airframe has been a consensus for the majority of universities attending this competition.

The canard airframe was chosen for its effective take-off capacity. The essential design of the lifting-canard was to provide lift during flight. If some of the lift from the canard was used during take-off in conjunction with the lift from the wings, the ground roll would be less than that of the conventional airframes. Using the canard would allow more freedom in areas that would have to be compromised for short take-off with the other designs such as storage box constraints. The canard would be comparable in weight to the conventional UAV.

3.2.2 Wing Design

The design of a wing depends largely on the aspect ratio. For this design, aspect ratios of eight or less were considered low, and aspect ratios higher than eight were considered high. High-aspect-ratio wings have the advantage of creating less induced drag. However, due to the extra inertia, roll damping, and tendency to tip stall, high-aspect-ratio wings do not perform or handle as well as low-aspect-ratio wings. Also, a high-aspect-ratio wing would be difficult to design considering the design constraints associated with the size of the storage box.

Tapered wings were briefly discussed and dismissed. Although there was quite an advantage to tapering the wings, the skill and time required to design, analyze, and build a tapered wing outweighed the advantage. The basic rectangular wing that was proven effective in the past was easily analyzed and manufactured. For stability reasons, a rectangular wing with no dihedral would be placed on bottom of the fuselage.

Elliptical wings were discussed in great detail. Elliptical wings provide a greater advantage over rectangular and tapered wings. The elliptical planform was noted for its difficulty in construction. However, this type of wing greatly increases the span-wise efficiency factor, e . This efficiency factor for an elliptical wing is very close to the maximum value, 1, which is desired in any planform shape of a wing.

3.2.3 Empennage Configuration

The empennage is used for stability and control. Therefore, it is important for the airflow over the empennage to remain attached. The canard, tail surface ahead of the wing, would allow for less wing or propulsion flow interference. It would also lessen the nose-down pitching moment caused by high-lift devices by producing lift that adds to the wing lift. However, canards can be destabilizing if the center of gravity (CG) is not properly located.

The "V"-tail has less wetted area compared to conventional tails. Less wetted area equates to a lower RAC number. However, it is less efficient in pitch inputs and requires radio mixing.

The "H" tail has a large wetted area compared to conventional tails. A large wetted area is less efficient in the RAC but is simple in design. An "H" tail allows for more rudder control for the large wind gusts at the competition site.

Two types of configurations were investigated for the horizontal stabilizers. The first was a conventional configuration with the elevator mounted to a fixed stabilizer. The second configuration was a fully-flying-horizontal-tail with the entire horizontal tail acting as the control surface. This fully-flying-

horizontal-tail idea was adopted because of its reduction in both drag and manufacturing time. This configuration would also aid the reparability issue. For example, if the empennage on Phyxius was damaged, another horizontal stabilizer could replace the damaged piece, thus making the repair process easier.

3.2.4 Engine Configuration

Even though not listed in Table 3.1, two engine configurations (i.e., tractor and pusher) were analyzed with tractor configuration chosen for Phyxius. A pusher propeller design was rejected because the configuration would involve mixing the pusher propeller with a tail-dragger configuration. Also, the UAV would disrupt the airflow seen by the propeller and thus reduce its efficiency. A tractor propeller was selected because most propellers available are made for this kind of operation and it does not face any of the problems faced by the pusher. The next decision was how many motors would be needed. Obviously, the more motors on the plane the greater the weight. It would be in the team's best interest to reduce the weight as much as possible. Also, conversing with the optimization group revealed that a single motor would reduce the RAC score. Therefore, a single engine, tractor propeller configuration was chosen.

3.2.5 Landing Gear Configuration

Two landing gear configurations were considered; tricycle and tail-dragger. A tail-dragger aircraft would reduce the RAC of the aircraft. A tail-dragger configuration would incorporate a main landing gear and a tail wheel for ground control. The tricycle gear was eliminated because it involved a main gear and a nose wheel. In past competitions, the nose wheel has been a heavy structure that increased the RAC score.

3.3 Figures of Merit

Figures of Merit were chosen to identify how each concept compares to the others in the overall selection. Figures of Merit were decided based on the RAC, mission profiles, and other scoring qualities and were weighted according to how important each factor was to the overall score. The weights were assigned a value from 1 to 5, with 5 being the highest. The Figures of Merit for RAC has a large value because it is vital to the total score and is negative because it would count against the total score. The Figures of Merit and the weight factors are detailed in Table 3.2.

Table 3.2 Figures of Merit and Weighted Values

Figures of Merit	Weight Factor	Mission Feature
Performance and Handling	3	Handling qualities of UAV, ease of piloting on closed course
Speed	4	Time to complete entire airborne portion of mission
Take-off Performance	5	Ease of take-off within a 150 ft distance
Repairability	1	Ease of repair upon structural damage
Simplicity	3	Simplicity of design, structure and components
Center of Gravity (CG)	3	Necessity to control CG location
Rated Aircraft Cost	-4	Rated Aircraft Cost

3.3.1 Description of the Figures of Merits

Performance and handling is given a weight of 3. It is important for the UAV to be easily controllable in flight. Although the pilot must feel comfortable with the UAV, he does not need a UAV so stable that performance is compromised. The team decided with the advice of the pilot, that the UAV must be stable, but not to compromise other Figures of Merit with the perfection of this one. The pilot states that he will be comfortable with having to "work" the UAV somewhat.

Since the missions are timed, speed is a necessity and was given a weight of 4. In order to maximize speed, the weight, drag, and propulsion must be considered. The weight of the UAV must be kept as low as possible for speed and RAC. The drag produced by the UAV and its payload must also be minimized. This means optimizing the placement and shape of the payload container to obtain the best aerodynamic shape for the vehicle.

Because take-off must be within 150 ft, or the flight is void, take-off performance became our most important Figure of Merit, hence, given a weight of 5. The plane will have to be light enough and

generate enough lift for this parameter to be successful. A design consideration with this parameter is the induced drag during take-off. Because the UAV is operating at relatively low speeds, the induced drag will be high.

Repairability was given a low weight factor of one. The reasoning behind this is that the UAV will be designed around the other parameters first and crash worthiness will have to be compromised. The idea is to build a second UAV and have parts for a third. If the UAV is compromised in flight and is lost, there will be the option of replacing parts or the entire UAV. This provides the ability to design for RAC and simplicity.

The last quality, RAC, was considered to be an important design criterion. The objective in any competition is to win, and to win, the overall score must be greater than the opponents. The RAC is a penalty in the overall score. The higher the RAC, the lower the overall score will be. This is why the weight factor is negative. It acted as a penalty in the ranking of the design concepts.

3.3.2 Scoring of Design Concepts

Based on the Figures of Merits discussed, each design concept was evaluated by receiving a score of five (excellent) to one (poor). The scores from these Figures of Merit were multiplied by their corresponding weight factor and summed to obtain the overall score for each concept as

$$TOTAL = \sum_{i=1}^7 s_i \cdot WF_i \quad (3.1)$$

where,

s is the score of each figure of merit for each conceptual design, and
WF is the weighting factor of each figure of merit.

The score of each design concept is shown in Table 3.3. The top 4 configurations were chosen for further evaluation prior to selecting the final design concept for Phyxius.

Table 3.3 Scoring of Design Concepts

Concept	Take-Off	Performance	Speed	RAC	Repairability	Simplicity	CG	TOTAL	Action
1	5	3	8	-4	3	6	3	32	FC
2	5	3	4	-4	3	6	3	28	E
3	5	6	8	-8	2	6	3	30	E
4	10	6	4	-8	2	6	3	31	E
5	5	6	8	-4	3	6	6	38	FC
6	5	3	4	-8	3	6	6	27	E
7	10	3	4	-8	2	6	3	28	E
8	10	6	8	-8	2	6	3	35	FC
9	10	3	4	-4	2	6	3	32	E
10	10	3	4	-4	2	6	3	32	E
11	10	6	8	-8	2	6	3	35	FC
12	10	6	4	-8	2	6	3	31	E

E - Eliminate

FC - Further Consideration

3.4 Rated Aircraft Cost Factors

Rather than discussing individual designs, we will describe the effect of different types of components. These effects are presented in Table 3.4.

Table 3.4 Rated Aircraft Cost Factors

Component	Type	Effect on RAC
Fuselage	Conventional	Longer than the other type, so costs more. Added length required additional structural weight.
	Canard	More "wing" area but less empennage; about same RAC as conventional except, additional cost expected due to weight.
Wing	High AR	Higher cost per square foot due to cost formula Greater structural weight
	Low AR	Lower cost per square foot Reduced structural weight
Tail	V	Slightly reduced cost from formulas
	H	Slightly higher RAC cost due to increased control area.
	Canard	Increased cost due to necessity to score as a wing.

3.5 Conceptual Design Selection

The end of the conceptual design phase saw four configurations to elaborate on for further discussion. The canard was eliminated from further consideration because of the stability issues and experience with seeing canards in the past competitions. Although it was known that a correctly designed canard would show the desirable features, the concern with little canard experience overwhelms the possibilities. Other factors that led to this decision were stability and control issues. The conventional UAV has qualities desirable in a payload carrying UAV. Furthermore, Concept 1 was eliminated because of the V-tail configuration. It was noted that the V-tail would reduce the RAC by having fewer control surfaces. The concern with little V-tail experience lowers the possibilities for this configuration similar to the canard. Therefore, the conceptual design chosen to be considered for preliminary analysis was Concept 5.

3.6 Conceptual Design Summary

Based on the Figures of Merit placed on each design, the twelve conceptual designs were narrowed to four designs left for further consideration. In the end, the final configuration chosen was a conventional fuselage incorporating a conventional tail with an elliptical low wing and a tail-dragging landing gear set-up. The propulsion system chosen was a single Graupner motor with an AeroNaut Frudenthaler propeller.

4. PRELIMINARY DESIGN

4.1 Design Parameters and Sizing Trades

In the preliminary design phase, we had to consider many variables such as engine type, propeller size, wing area, chord length, airfoil sections, and aspect ratio to name a few. There are many combinations of these variables that will produce a flying UAV. We decided to optimize our UAV design from a performance standpoint, utilizing information from the Aerodynamics group, Propulsion group, and Structures group. Once the dimensions of the wing were calculated from the optimization program, the Flight Mechanics group sized the tail and the fuselage dimensions to produce a UAV with a positive static margin and good handling characteristics. Once the sizing of the UAV was completed, a more detailed performance analysis was conducted. This included investigations into maximum lift-to-drag ratio, maximum rate-of-climb, power available and power required, and estimated duration for each mission.

4.1.1 Payload System

The original design for the water-loading manifold was modeled after the refueling device used by NASCAR teams during pit stops. This device consists of a tank that holds the fuel, a neck that guides the fuel into the car, and a vent tube that allows the fuel to flow out of the device and into the car quickly and smoothly. The initial manifold is constructed using 1½ in. PVC pipe, two 1½ in. T-fittings, one 1½ in. sanitary fitting, one 1½ in. ball valve, a wooden dowel, and metal tubing. This manifold was built to hold one two-liter bottle. The metal tubing was used to construct a vent, which allows air to flow in as the water flows out of the two-liter bottles and manifold. The mass flow rate from the tank was optimized by adjusting the diameter of the vent tube. The first vent tube was ¼ in. copper tubing. When tested, the water bottlenecked out of the two-liter bottle and manifold. The vent tube diameter was then increased to ½ in. copper tubing allowing more air to flow into the bottle. When tested, the two-liter bottle emptied in 11 seconds. The water flowed smoothly but was restricted by the size of the ventilation tube. A third ventilation tube was constructed of 3/8 in. aluminum tubing. When tested, the bottle and manifold emptied in 6 seconds.

4.1.2 Airfoil Selection

The selection of the wing airfoil for Phyxius was a daunting task due to the multi-mission nature of the contest. An airfoil conducive to heavy lifting is desired for the firefighting mission, while an airfoil more suited for speed is preferred for the ferry mission. The Aerodynamics group needed to find an airfoil that would perform both missions well. X-Foil⁷ was utilized in the comparison of possible airfoil sections. After calculating the required range of C_L values to fly both missions, the Aerodynamics group selected seven airfoils and directly compared them. The aerodynamic data from these two airfoils were plotted in Figures 4.1 and 4.2.

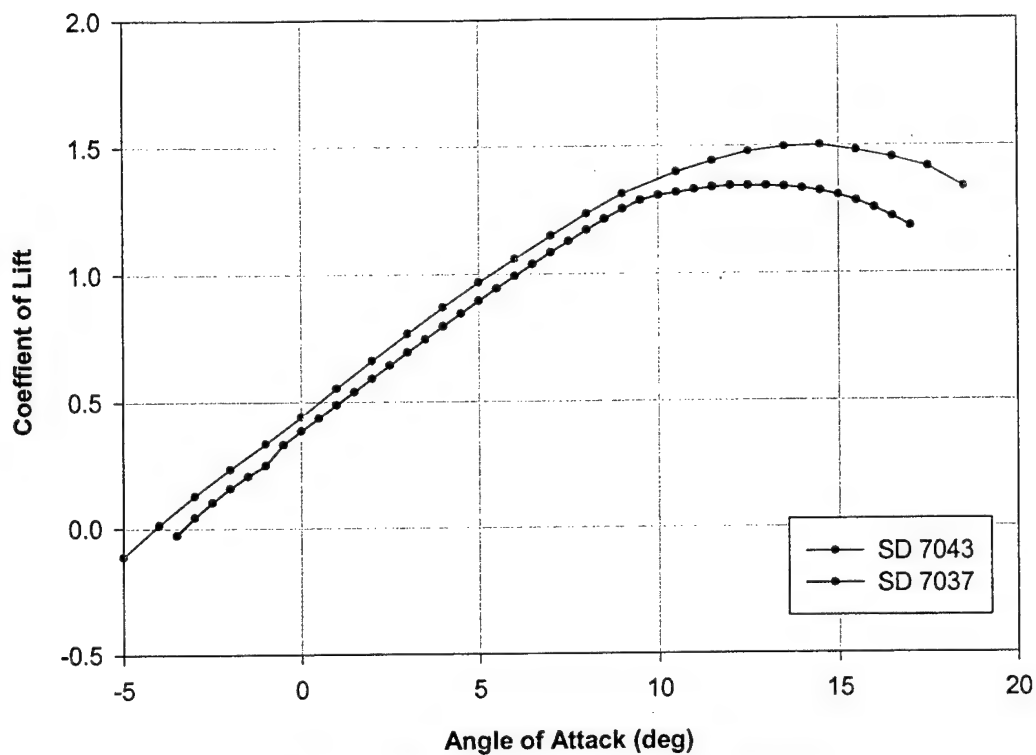


Figure 4.1 Lift Coefficient vs. Angle of Attack

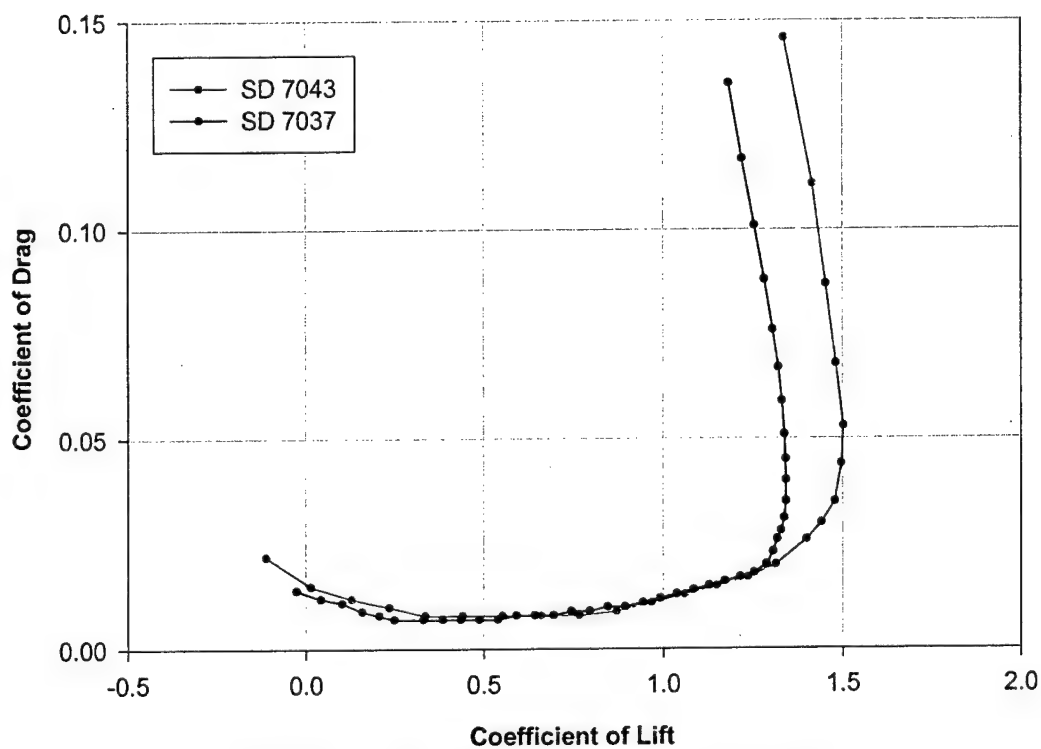


Figure 4.2 Drag Coefficient vs. Lift Coefficient

The drag polar comparison of these seven selected airfoils allowed the group to make a final airfoil decision. The SD 7037 and SD 7043 produced the greatest lift-curve slope as shown Figure 4.1. These airfoils also exhibit comparatively good drag characteristics for the amount of lift they produce. The SD 7043 was chosen over the SD 7037 because its lift curve dropped more gradually and remained slightly higher as angle of attack was increased, producing a gentler stall.

4.1.2.1 Horizontal Stabilizer Airfoil Selection

The choice of the wing airfoil provided the Aerodynamics group the necessary guidelines for the selection of an appropriate airfoil for horizontal stabilizer. The variation of pitching moment coefficient versus angle of attack was plotted for each of the two candidate airfoils. Interestingly, the SD 7043 selected has a C_M value lower than the other proposed airfoils as shown in Figure 4.5. The SD 7037 produces the proper C_L and C_M values to counter the C_M of the wing, and we chose this airfoil for the horizontal tail. The pitching moment coefficient plot is shown in Figure 4.3.

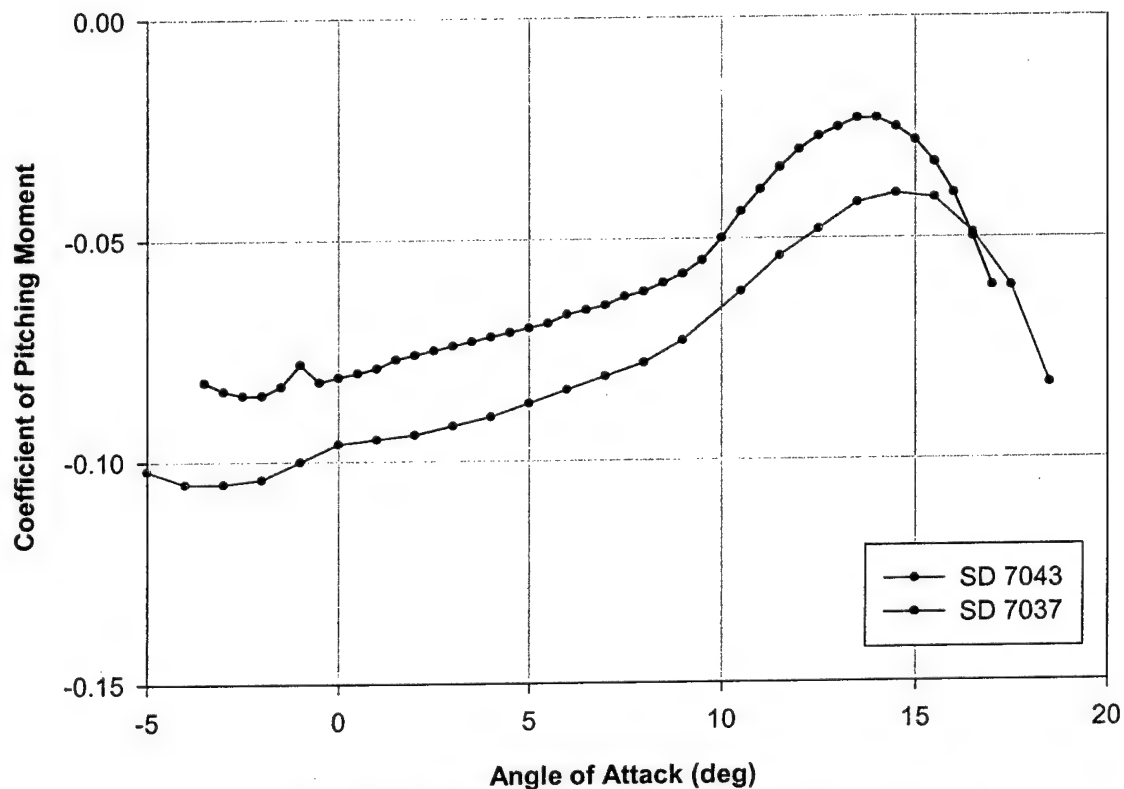


Figure 4.3 Pitching Moment Coefficient vs. Angle of Attack

4.1.3 Propulsion Configuration

Due to the nature of the preliminary design, only a tractor engine configuration was determined to be practical. Next, we had to decide on the number of motors to use. Many small motors could equal the weight of one large motor, as well as possibly having a greater overall propulsive efficiency. However, further discussion revealed that a single motor would minimize the RAC score. Thus, a single engine with tractor propeller configuration was chosen.

4.1.4 Thrust Loading and Wing Loading Study

In order to determine the size of engine that would be needed to achieve the take-off roll of 150 ft, we performed a study on the effect of wing- and thrust-loading on the take-off roll. Assuming that the aerodynamic drag force is much smaller than thrust, and that thrust was constant for the entire take-off roll, the equation for take-off is simplified as a function of both wing- and thrust-loading.

$$\text{Take - Off Roll} = \frac{1}{2g} \cdot \frac{1}{\frac{T}{W} - \mu} \cdot \frac{2}{\rho C_{L_{\max}}} \cdot \frac{W}{S} \quad (4.1)$$

where,

g is acceleration due to gravity,

T is the thrust,

W is the weight,

S is the wing platform area,

ρ is the air density, and

μ is the coefficient of friction for the runway surface

The results from Equation 4.1 are presented in Figure 4.4. Since this plot is an approximation of the actual takeoff distance, we chose a take-off distance of 130 ft instead of 150 feet for a margin of safety of 15 %. This will allow a factor of safety. For a take-off distance of 130 ft and a wing loading around 3.25lb/ft² the minimum thrust loading needed to take-off must be greater than 0.4, which means that the amount of thrust required must be slightly less than half the weight of the UAV.

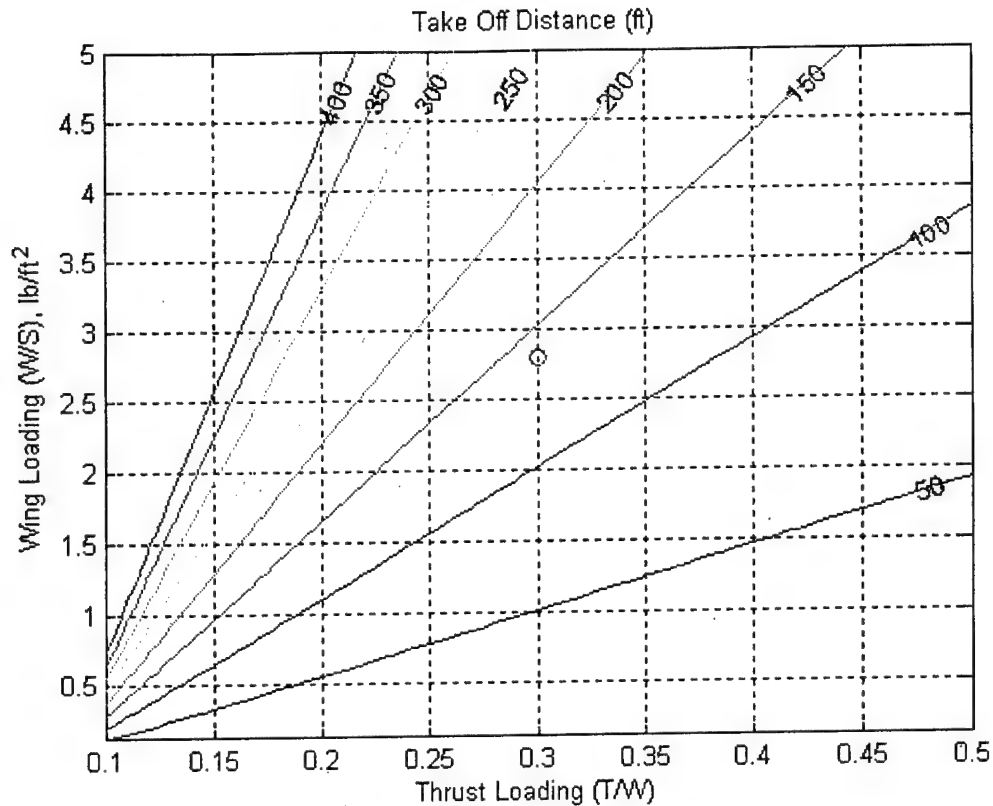


Figure 4.4 Contour Plot for Take-Off Distance

4.1.5 Structural Analysis of the Spar

We examined three designs for the main spar modeled as a cantilever beam. The tip-loading test that will be performed during technical inspection presented the most critical loading condition resulting in a maximum deflection obtained as:

$$y = \frac{-pL^3}{3EI} \quad (4.2)$$

where,

p is the load,

L is the length of the beam,

E is the Young's Modulus, and

I is the area moment of inertia

The chosen spar utilized unidirectional carbon strips at the quarter chord of the wing. A strip in the upper and lower wing surfaces changed from 2.5 in. at the root to 0.5 in. at the tip. Using Equation 4.2 showed a maximum deflection of 0.75 in. for a 30 lb load at the tip.

4.1.6 Engine Selection

There are two brands of engines that are legal for DBF competitions, Graupner and AstroFlight. A Graupner electric motor was chosen because AstroFlight motors have proven to be too inefficient in past entries. The thrust needed was based on the take-off roll analysis which showed that the thrust loading must be greater than 0.4 to achieve lift-off before 130 ft. For a single-engine, 16-lb UAV (fully loaded), many engine-gearbox-propeller combinations could achieve the necessary amount of thrust. To narrow the list of prospective candidates, additional factors were added, namely pitch speed, input voltage, efficiency, and availability. The only engines that could produce that amount of thrust and fit the additional criteria are the Ultra 3300-5, 3300-6, and 3300-7 with a gear reduction ratio of 2:1. Using *MotoCalc* and *P-Calc* software, a series of propeller and motor combinations were considered.

MotoCalc and *P-Calc* are both programs for choosing and predicting the performance of an electric model UAV power system based on the characteristics of the motor, battery, gearbox, propeller, and speed control. With *MotoCalc*, a range for the number of battery cells, gear ratio, propeller diameter, and propeller pitch can be specified to produce a table of predictions for each combination. *P-Calc* was used to cross-reference and validate *MotoCalc*'s calculations, as well as some in-house developed prediction worksheets.

Initial results indicated an Ultra 3300-5 motor would be the best choice since it allowed for higher pitch speed, ample thrust to take-off, as well as a lower input voltage (meaning fewer battery cells). The results of the *MotoCalc* analysis are shown in Figure 4.5. A *MotoCalc* analysis was also performed on the Ultra 3300-6 for the sake of comparison. The results from this analysis are shown in Figure 4.6.

Each of these charts is composed of three data series: static thrust, maximum speed, and static run time. Static thrust is a measurement of the thrust created by the motor and propeller on a stand at 100% throttle at zero velocity. Maximum speed was the top speed that the plane could reach given the UAV model in *Motocalc*. Finally, static run time is the amount of time the motor can run at 100% throttle on a test stand.

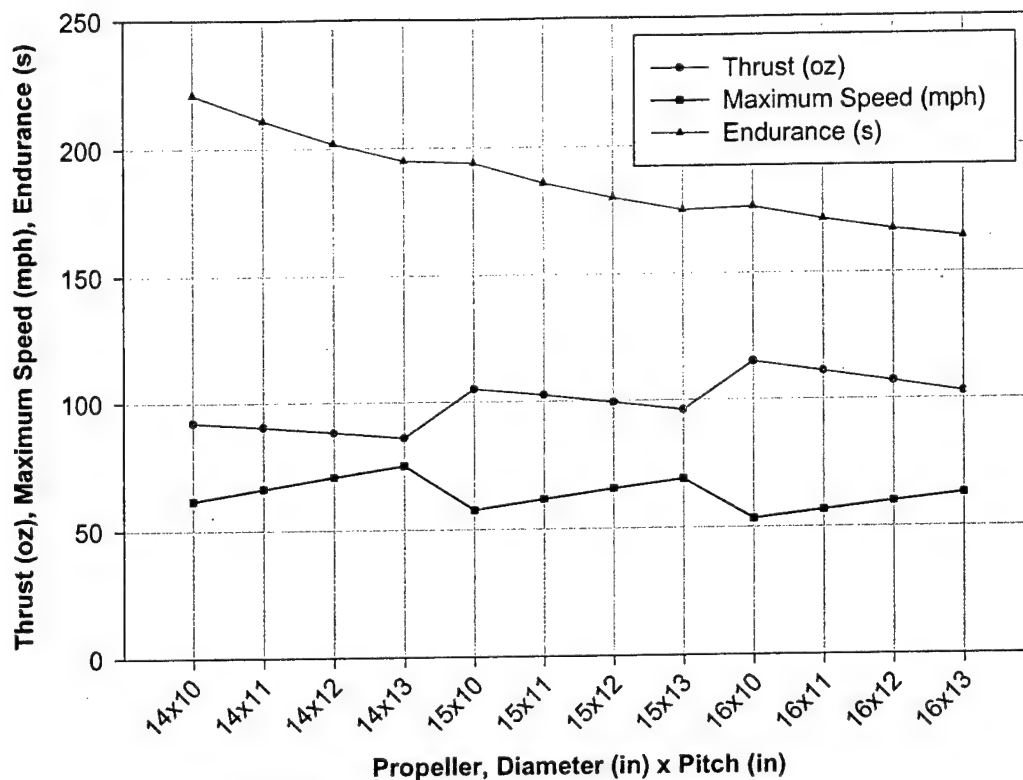


Figure 4.5 Motocalc Analysis of the Graupner 3300-5

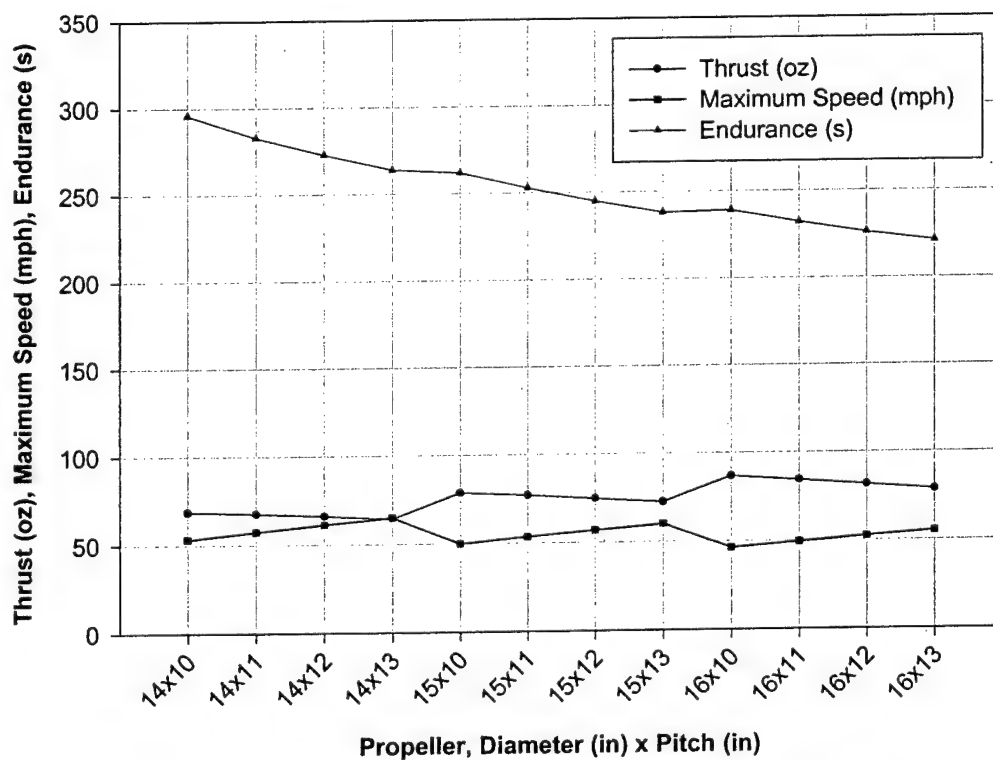


Figure 4.6 Motocalc Analysis of the Graupner 3300-6

Examining the charts revealed that a Graupner Ultra 3300-5 produces more thrust, longer run time, and a higher top speed. With the given results, it was decided that a Frudenthaler 16x13 carbon-folding prop would offer a sufficient runtime, excess thrust, and a high enough maximum speed for both missions. Motor performance for this configuration is shown in Table 4.1.

Table 4.1 Ultra 3300-5 Motor Performance

Static Performance	Propeller	16x13
	Current (A)	43.9
	Input Power (W)	822.8
	Electrical Efficiency (%)	63.3
	Input Power Loading (W/lb)	54.7
	Output Power Loading (W/lb)	34.6
	Propeller RPM	5118
Performance at 65 mph	Thrust (lb)	6.43
	Current (A)	38
	Electrical Efficiency (%)	71.9
	Thrust (lb)	3.1
	Time (min:sec)	3:10

It is important to note that the amperage, though slightly more than the 40 A limit mandated by the rules of competition, is within allowable design tolerance of the *Maxi Slow Blow* 40 A fuse. Another quantity of interest is the input power loading, which is about 54.7 W/lb. A common rule of thumb among industry is that an input power loading of 55-W/lb is necessary for an aerobatic UAV. Because the input power loading for Phyxius is at 55 W/lb, superb flight performance is expected. The last quantity of interest is the endurance at 65-mph. A rough estimate of the flight lap distance is around 4000 ft, including a few 360-degrees turns, which equates to 42 s per lap. Four laps at 42 s a piece equates to 2 minutes and 48 seconds total time. Therefore, the UAV should have excess duration.

For the competition this year, Sanyo 2000 mAh batteries were chosen. It was determined that 18 cells weighed less than 5 lb and would provide the most thrust and top speed. The speed controller chosen for the competition was an AstroFlight 204D. This speed controller can handle the current and has worked well in the past.

4.1.7 Available Thrust Model at Speed

The thrust available from the engine was approximated by the observing the engine's characteristics. With a given engine/propeller selection, the engine will have its highest thrust, $T_{\max, \text{static}}$, when the UAV is not moving. When the free stream velocity is equal to the velocity of the propeller, V_{\max_eng} , thrust will

be zero. From this relationship, the thrust available from the engine was assumed to be linear with velocity and was dependant on the number of engines and engine/propeller selection. This assumption, while not exact, resulted in an error of less than 5 % for engine/propeller cases evaluated by the previous MSU DBF teams. In addition, this error was on the side of caution, as the actual thrust curve is concave downward. The linear relationship can be expressed as

$$T_{avail} = N_{engines} \left(T_{static} - \frac{T_{static}}{V_{max,eng}} V \right) \quad (4.3)$$

Table 4.2 Ultra 3300-6 Motor Performance

Static Performance	Propeller	14x15
	Current (A)	39.6
	Input Power (W)	677.3
	Electrical Efficiency (%)	70.0
	Input Power Loading (W/lb)	84.77
	Output Power Loading (W/lb)	59.3
	Propeller RPM	5643
	Thrust (lb)	7.99
Performance at 80 mph	Current (A)	17
	Electrical Efficiency (%)	74.1
	Thrust (lb)	3.07
	Time (min:sec)	2:52

4.1.7.1 Wind Tunnel Results

In order to get accurate performance numbers for this UAV, the Graupner Ultra 3300-5 engine geared at 2:1 turning a 16x13 AeroNaut-Frudenthaler carbon folding propeller was tested in the Mississippi State University wind tunnel. The goal of the experiment was to obtain dynamic properties of the engine/propeller combination at full power. The velocity was varied from 0 to 80 mph while collecting data from the thrust load cell, and these values were compared to *MotoCalc* and the thrust available estimate described in the previous estimate.

As shown in Figure 4.7, the *MotoCalc* data over predicted the experimental data collected from the wind tunnel. The thrust available estimate, however, under predicted the experimental data. The conclusion was to use the experimental data in the optimization program because it is better to use what is actually available than to over predict the value for thrust. The two reasons why *MotoCalc* may have over predicted were that the engine used in *MotoCalc*'s analysis may not have the exact timing as the actual engine obtained may not take into consideration the propeller stall near static conditions.

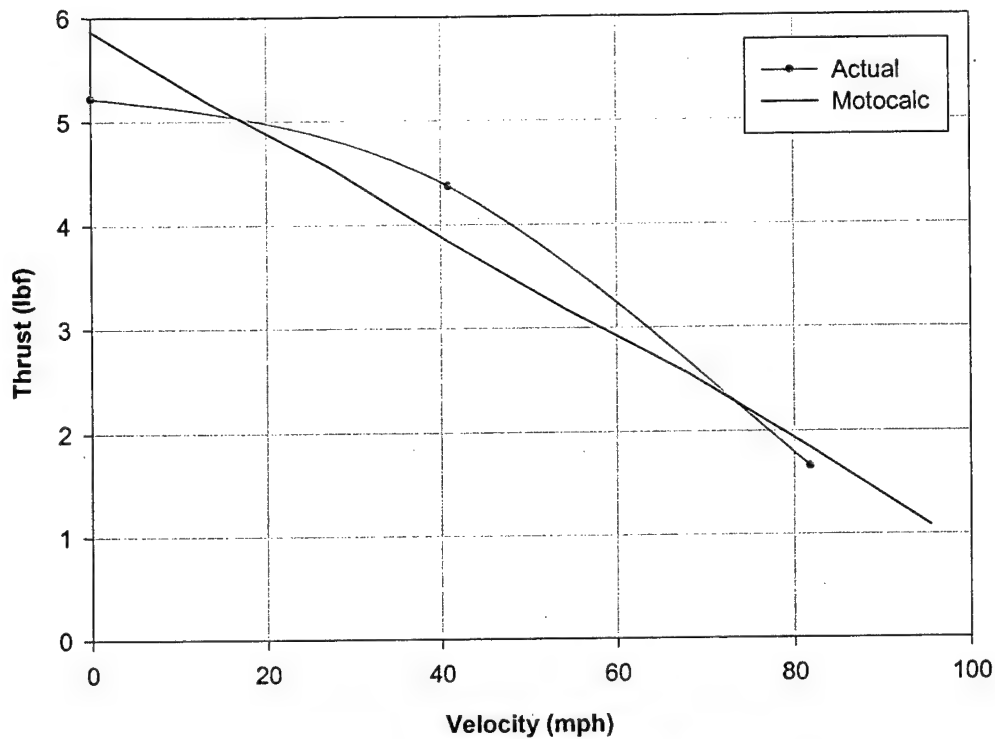


Figure 4.7 Thrust Loading vs. Velocity

4.1.8 Sizing of the Horizontal Tail

Once the dimensions of the wing were calculated, the tail was sized to produce a UAV with good static and dynamic stability characteristics. In order for the UAV to be longitudinally stable, the partial derivative of pitching moment with respect to angle of attack must be less than zero.

$$C_{m_\alpha} = \frac{\partial C_m}{\partial \alpha} < 0 \quad (4.4)$$

In order for the aircraft to trim about the pitch axis, the coefficient of pitching moment at an angle of attack of zero must be greater than zero.

$$C_{m_0} = C_{m_{\alpha=0}} > 0 \quad (4.5)$$

From these inequalities a force and moment balance was performed with each component of the UAV. The moment coefficient expressions are

$$C_{m_\alpha} = C_{m_{\alpha, \text{wing}}} + C_{m_{\alpha, \text{fuselage}}} + C_{m_{\alpha, \text{tail}}} \quad (4.6)$$

$$C_{m_0} = C_{m_{0,wing}} + C_{m_{0,fuselage}} + C_{m_{0,tail}} \quad (4.7)$$

The individual terms in these equations were solved with the help of computational fluid dynamics, and equations from Nelson³.

Table 4.3 Moment Coefficients with Respect to Angle of Attack

Component	C_{m_α} Contribution
Wing	0.207
Tail	-0.83
Fuselage	0.257

The individual terms for Equation 4.4 - 4.6 were composed of sizing parameters such as the incidences of the wing and tail, the surface area of the horizontal tail, the CG for the UAV, and the moment arm from the aerodynamic center of the wing to the aerodynamic center of the horizontal tail. These parameters were varied to produce an aircraft with a positive static margin and a surface area less than or equal to 25 % of the surface area of the wing. The results for the coefficient of pitching moment curves with varying angle of attack are presented in Figure 4.8. The results from the sizing are presented in Table 4.4.

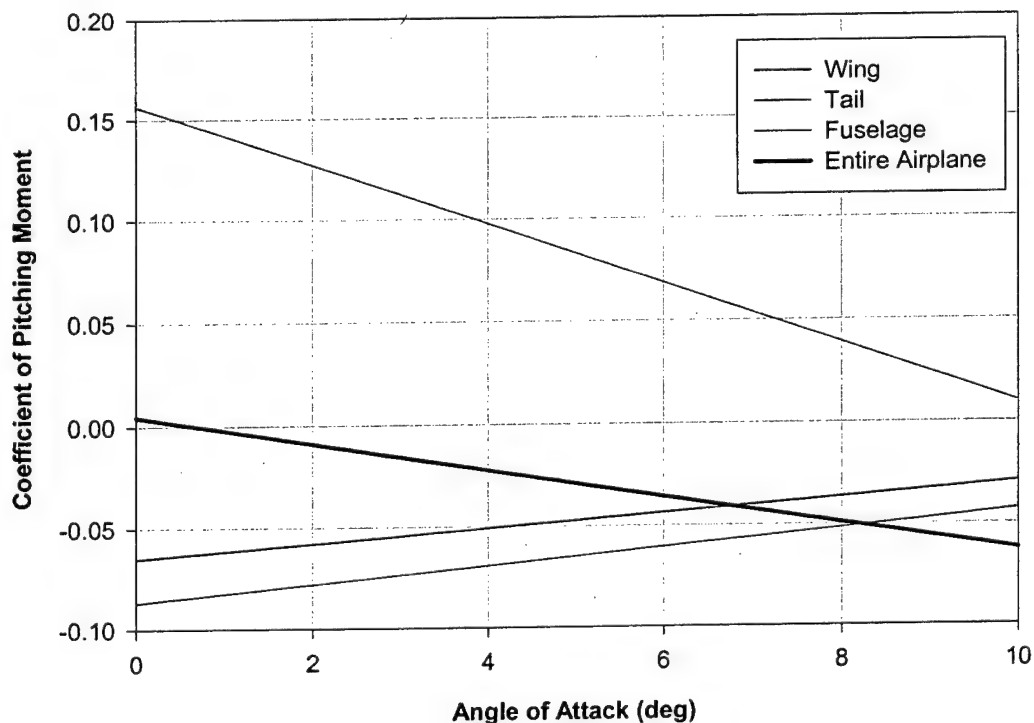


Figure 4.8 Longitudinal Stability Characteristics

Table 4.4 Longitudinal Stability Information

Tail Moment Arm (in)	26.77
Incidence of Wing (deg)	1.0
Incidence of Tail (deg)	-1.5
Span of Horizontal Tail (deg)	20.5
Chord of Horizontal Tail (in)	6.6
Center of Gravity (X_{cg}/c)	0.305
Full Trim Condition (deg)	3.403
Static Margin (%)	13.66
Neutral Point (C_{np}/c)	0.39

4.1.9 Longitudinal Control

In previous years, a two-piece horizontal tail and elevator was used. This year a fully-flying tail was chosen over the conventional tail. By reducing external control rods and gaps between the control surfaces the total drag should be decreased. The flying tail should also reduce production time. As it can be seen in Figure 4.9, the aircraft can be trimmed to ± 16 degrees angle of attack. This can be achieved with a deflection of ± 5 degrees.

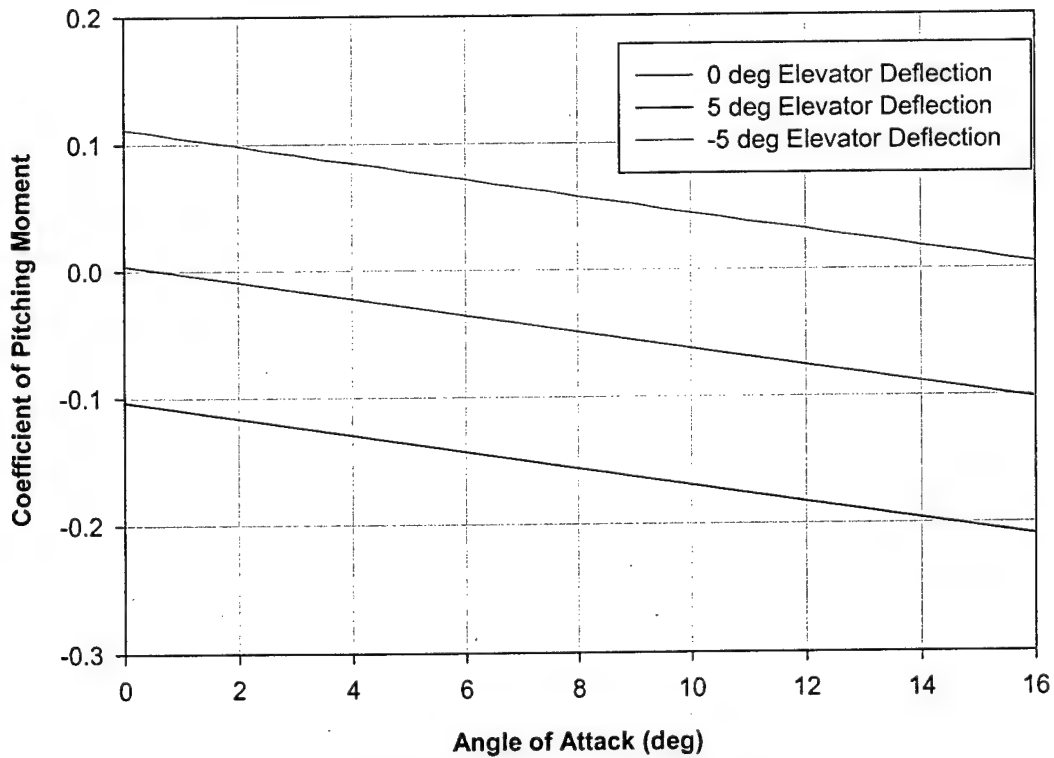


Figure 4.9 Longitudinal Control

4.1.10 Longitudinal Dynamic Analysis

Using Nelson³, the equations of the longitudinal dynamic equations were analyzed to determine the time period and the damping values for the short period and phugoid modes. The analysis was deemed necessary due to the unconventional lifting body fuselage.

Table 4.5 Longitudinal Dynamic Characteristics

Short Period (Loaded)	
Eigenvalues	$-12.615 \pm 9.325i$
Damping Ratio	0.802
Time Period (s)	0.398
Phugoid (Loaded)	
Eigenvalues	$-0.031 \pm 0.279i$
Damping Ratio	0.103
Time Period (s)	18.951

The eigenvalues remain negative, hence the UAV is stable, for both the loaded and unloaded cases. The target damping ratio for the short period was 0.707, and as it can be seen in Table 4.5 the actual value is within an acceptable error of level one handling qualities according to Table 4.5.

Table 4.6 Damping Value for Short-period Mode

Level	Minimum	Maximum
1	0.35	1.3
2	0.25	2.0
3	0.15	N/A

Table 4.6 values are taken from Nelson³ for aircraft that requires rapid maneuvering. The phugoid eigenvalues also remain stable for both loaded and unloaded cases, and the damping ratio is within tolerable limits due to the long time period.

4.1.11 Sizing of the Vertical Tail

Raymer⁵ and Nelson³ recommend a value for the stability coefficient between 0.05 and 0.1. Using the exact expression for $C_{n\beta}$ found in Nelson, the span and the cord of the vertical stabilizer were varied to produce positive stability while allowing it to fit inside the box. The results are plotted in the Figure 4.10.

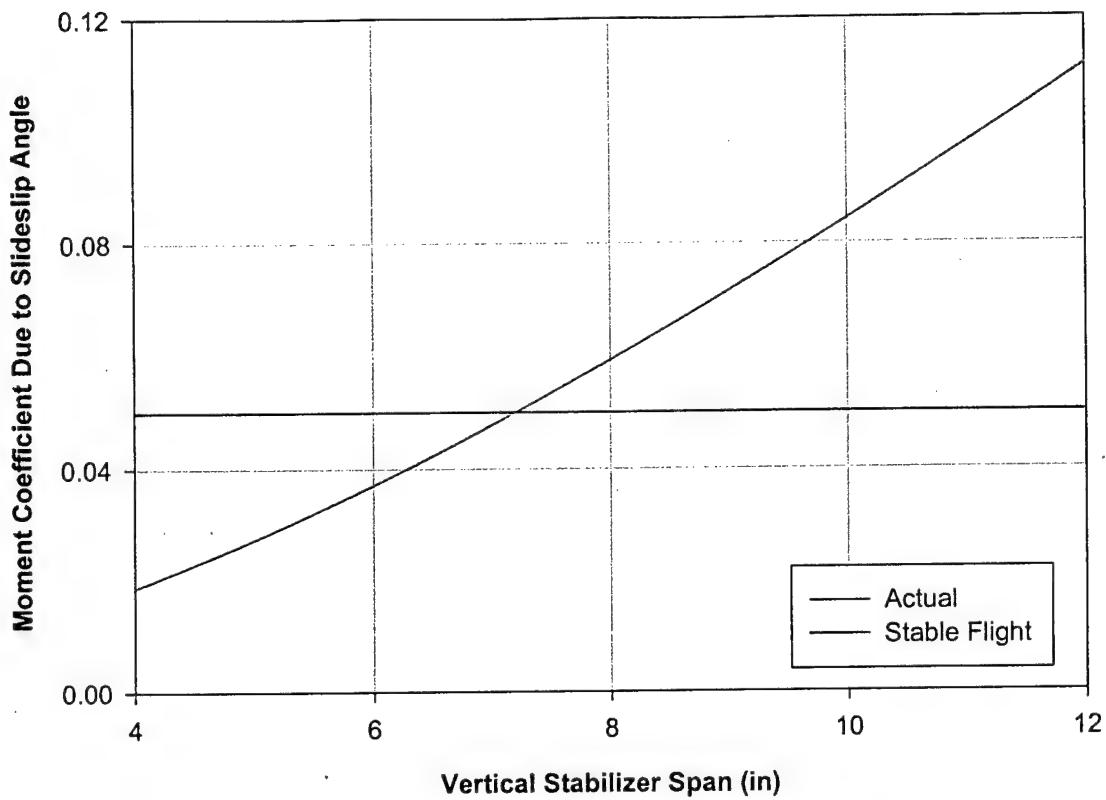


Figure 4.10 Analysis of Vertical Stabilizer Size

The decision was made to reduce the size of the vertical stabilizer from previous years. The target value for $C_{n\beta}$ was chosen to be 0.079. This action should decrease the parasitic drag and allow the tail to remain attached in the box, while still maintaining acceptable lateral directional stability.

Table 4.7 Directional Stability Information

Tail Moment Arm (in)	26.77
Span of Vertical Tail (in)	7.3
Chord of Vertical Tail (in)	10

4.1.12 Lateral/Directional Dynamic Analysis

The lateral directional dynamic modes of the aircraft were analyzed to determine the time period and the stability of the aircraft.

Table 4.8 Lateral-Directional Modes

Dutch Roll	
Eigenvalues	$-20.99 \pm 44.347i$
Damping Ratio	0.4
Time Period	0.12 s
Roll	
Eigenvalues	$-46.514 \pm 0i$
Damping Ratio	1.0
Time Period	0.023 s
Spiral	
Eigenvalues	$-0.042 \pm 0i$
Damping Ratio	1.0
Time Period	23.615 s

From the data given in Table 4.8 it can be seen that the entire lateral directional mode is negative, meaning the modes are stable. The spiral mode is very close to the origin but it is within acceptable values for visual flight.

4.2 Structural Material Considerations

4.2.1 Research

After the Figures of Merits were assigned, the team decided to investigate the possibility of an all-composite aircraft. The process almost certainly demands the use of molds to obtain the desired shape. Since molds are to be machined, the team designed a very streamlined airplane. The curvature of the airplane naturally results in a very difficult structure to analyze; therefore, most of the structural design is modeled after existing composite planes already in production. The Structures group visited several RC air shows to inspect the various designs and configurations. The main points were the type and number of layers of fiberglass found in the skin, the type and placement of carbon in the structure, and the internal bracing used. In most cases the skin of the aircraft is the primary structure. Only a few bulkheads were used at key locations, such as spar crossovers, landing gear attachment points, motor mounts, and wing roots.

4.2.2 Materials

Coupons of various types of material were made to test the material properties and to evaluate lay up technique. The two materials used in these coupons were carbon and fiberglass. The carbon was more porous, yet it had high rigidity. The fiberglass was not as rigid but it was far more durable. When the fiberglass samples were crushed the fibers remained intact, the carbon samples however, broke into many pieces. From crashworthiness standpoint, the fiberglass could be repaired more easily. The carbon was also very porous, which meant that it would be unwise to use it for the tank skin. The fiberglass was also very easy to use in tight bends and corners, where the carbon would begin to bridge over these obstacles. It was decided that the skin should be constructed of multiple layers of a lightweight fiberglass and the structural members inside should be made of carbon due to its higher rigidity.

Different laminating techniques were also investigated for use in fuselage structure. These techniques involve using other materials as the desired structural shape and applying the carbon over them. The materials used were honeycomb sheets, foam, balsa, and Rohacell. The foam allowed for an easy material to cut to shape and was used for bulkheads and formers. The Rohacell provided a firm surface in flat sheets but was not appropriate in larger structures. The Rohacell was used within the skin lay up to increase buckling resilience in areas that do not have much structure.

4.3 Flight Performance

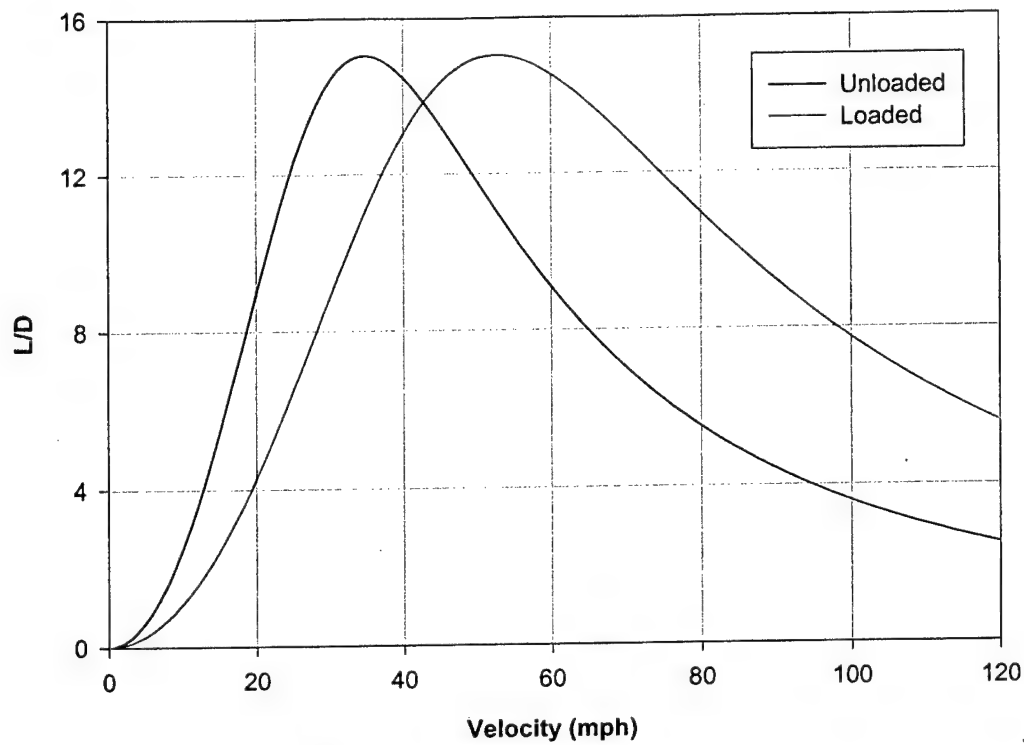
4.3.1 Performance Data

Before analyzing the steady flight performance of the UAV, the geometry of the UAV along with relevant weights must be reviewed.

Table 4.9 Sizing for Performance Calculations

Loaded Weight (lb)	16.5
Unloaded Weight (lb)	7.7
Span (in)	84
Chord (in)	11.8
Surface Area (ft ²)	5.4
Aspect Ratio	9
Oswald Efficiency Factor (Assumed)	0.95
Zero Lift C _D	0.03

The performance numbers of interest to the team were the lift-to-drag ratio, power required, power available, and rate of climb for velocities ranging from 0 to 80 mph. Figures 4.11-4.13 illustrate the results of the performance analysis.



$(L/D)_{\max} = 15$ for Loaded and Unloaded

Figure 4.11 Lift-to-Drag Performance at SSL

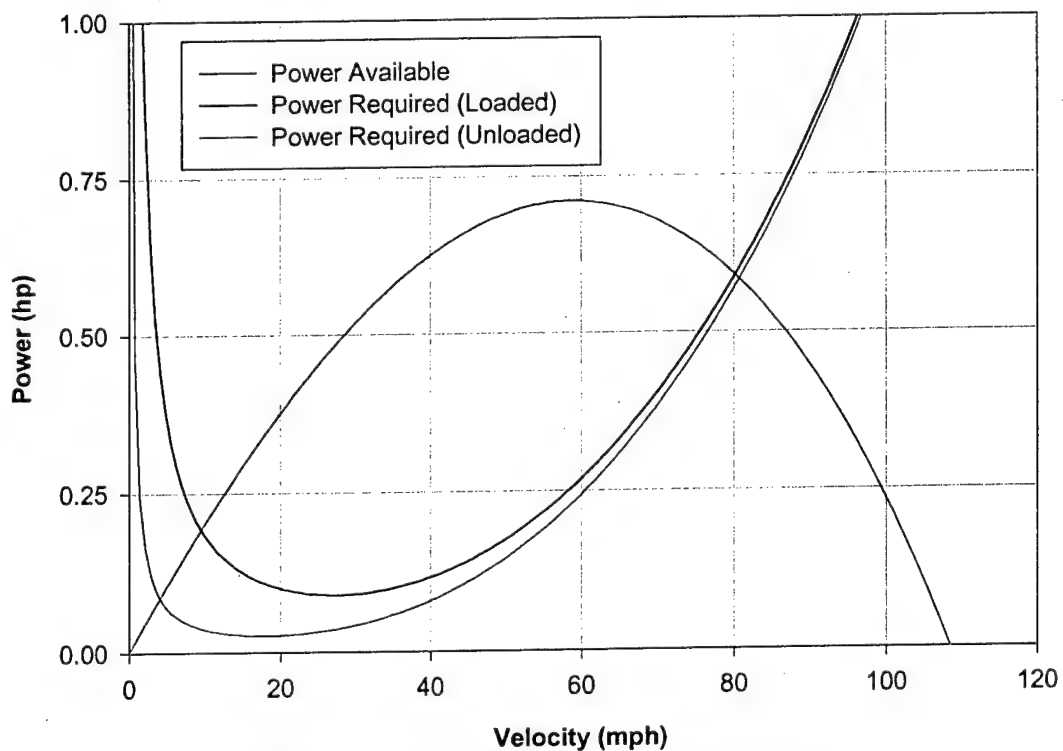
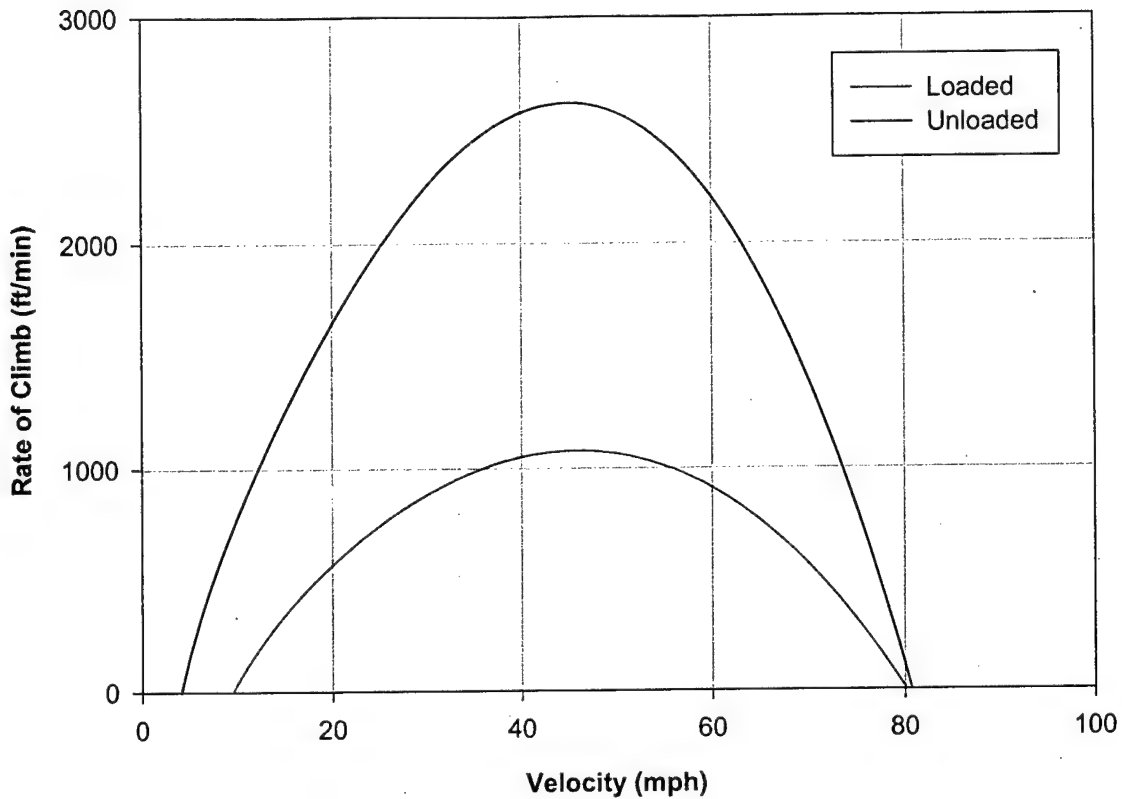


Figure 4.12 Power Available/Required at SSL



Loaded $RoC_{max} = 1003.6 \text{ ft/min @ } 47.9 \text{ mph}$
 Unloaded $RoC_{max} = 2612.9 \text{ ft/min @ } 45.9 \text{ mph}$

Figure 4.13 Rate of Climb Performance at SSL

4.4 Optimization Code

The optimization code was written using MathCAD. The code optimized the thrust to weight ratio and the wing loading. These two optimized values were plotted against one another for five different conditions of flight. The five conditions were cruise, turn, climb, take-off, and landing. The relationship between the thrust-to-weight ratio and wing loading is given below.

$$TW = \frac{q}{\alpha} \left[\frac{C_{D_0}}{WS} + k \left(\frac{n\beta}{q} \right)^2 WS \right] \quad (4.8)$$

Where,

WS is the wing loading
 TW is the thrust-to-weight ratio
 k is the inverse of the quantity of $\pi \cdot AR \cdot e$
 q is the dynamic pressure
 n is the load factor, and
 α and β are constants

Figure 4.14 shows the graphical representation of the relationship between the thrust-to-weight ratio and wing loading. After this plot was generated, a point was chosen in the design space. The feasible design space in Figure 4.14 is to the left of the take-off constraint, to the right of the cruise constraint, and above the turn constraint.

The important constraint to team Phyxius was the turning radius. Since each downwind leg involved a 360-degree turn, the team wanted to optimize the turning radius. Figure 4.15 shows the turning radius as a function of velocity.

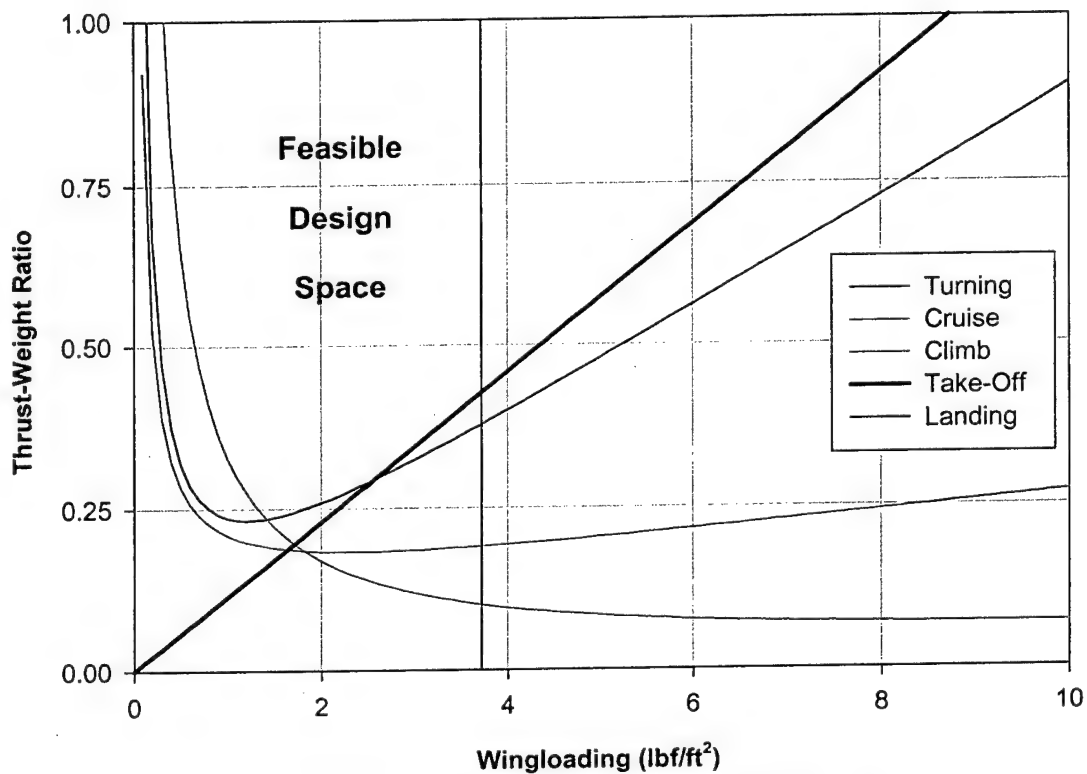


Figure 4.14 Wing Loading vs Thrust-to-Weight Ratio

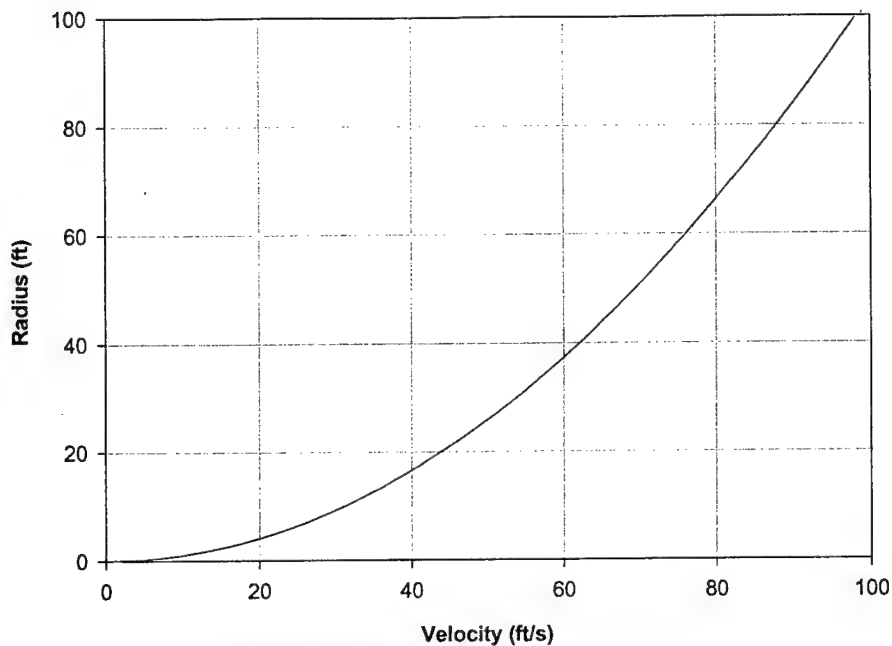


Figure 4.15 Turn Radius Performance

4.5 Estimated Mission Durations

The mission durations were estimated with the assumption that the UAV was flying at a speed of 60 mph and light and variable winds. The durations for take-off/climb and descending/landing were estimated. The times to complete the 360-degree turns were estimated by finding the circumference of the turning radius and multiplying that number by 60 mph. Time was allotted for turns around the pylon. The results are presented in Table 4.10.

Table 4.10 Mission Times

Mission 1		Time to Complete (min:sec)
Take-off and Climb to Pylon		0:10
3.5 Laps, No Payload, 4 360-deg Turns		2:00
Landing		0:15
Total Time for Mission 1		2:25
Mission 2		
Take-off and Climb to Pylon		0:15
0.5 Lap, Release Water, 1 360-deg Turn		0:20
Landing		0:15
Reload Water Tanks		0:10
Take-off and Climb to Pylon		0:15
0.5 Laps, Release Water, 1 360-deg Turn		0:20
Landing		0:15
Total Time for Mission 2		1:50

4.6 Summary of Preliminary Results

The sizing of the UAV was done using performance equations constrained by RAC and storage box dimensions. The results from the sizing show a stable UAV with a positive static margin and a short takeoff roll of less than 150 ft. Tables 4.11 and 4.12 present a summary of the sizing numbers and the performance values of the UAV.

Table 4.11 Directional Stability Characteristics

Sizing Results for Phyxius	
Wing (SD 7043)	
Span (in)	84
Chord (in)	11.8
Aerodynamic Center (% of Chord)	26
CG (% of Chord)	30.5
Neutral Point (% of Chord)	45
Surface Area (ft ²)	5.4
Incidence (deg)	1.5
Aspect Ratio	9
Fuselage Length (in)	
	47.2
Empennage (NACA 0009)	
Horizontal Tail Span (in)	20.5
Horizontal Tail Chord (in)	6.48
Vertical Tail Span (in)	6.48
Vertical Tail Chord at Root (in)	10.2
Incidence (deg)	-1.0
Tail Moment Arm (in)	26.77

Table 4.12 Performance Values

	Unloaded	Loaded
$C_{L,max}$	1.2	1.2
$(L/D)_{max}$	15	15
RoC max (ft/min)	2612.9	1003.6
Stall Speed (mph)	24.3	35.6
Maximum Speed (mph)	75	55
Take-Off Distance (ft)	130	45

5. DETAIL DESIGN

5.1 Weights and Balance Sheet

Table 5.1 Weights and Balances

	Distance from Nose (in)	Weight (lb)	Moment (in-lb)
Empennage w/ Servos	41.33	0.428	17.689
Wing w/ Servos	15.46	2.55	172.87
Fuselage w/ Servo	17.97	9.62	19.19
Main Landing Gear w/ Mount, Wheels, & Brakes	11.32	0.3	3.4
Tail Landing Gear w/ Mount, Wheels, & Servo	46	0.1	4.6
Motor	3.23	1.125	3.634
Motor Batteries	12.58	2.3	28.93
Receiver	9.3	0.10	0.93
Receiver Battery	9.3	0.25	2.325
Total Weight (lb)		16.423	
Aerodynamic Center of the Wing (% of Chord)		25.9	
Neutral Point (% of Chord)		45	
Location from Nose of CG (in)		13.88	

5.2 Component Selection

Table 5.2 Component Selection

Component	Selected Part	Comments
Motor (1)	Graupner Ultra 3300-5	Selected by preliminary design optimization
Speed Control (1)	Astro Flight 204D	Appropriately sized for selected motor It can handle the current and has worked well in the past
Battery Packs (2)	SR 2000 mAh 18 cells	Offer best available energy density in a moderate-resistance cell
Servos	Hitec HS-85, HS-225	Offer both high speed and high torque
Main Landing Gear	Graphtech AeroWorks Edge CLG-112	Relatively light, properly sized for payload deployment
Tail Wheel	Graphtech CTW-301	Single wheel at empennage for steering
Propellers	AeroNaut CAM Frudenthaler 16x10, 16x13	Selected through <i>Motocalc</i> analysis and wind-tunnel testing.

5.3 Systems Architecture

5.3.1 Wing

Phyxius is a low-wing UAV that incorporates removable wings. The wing is composed of two outboard sections with a carbon fiber tube carried through. These outboard sections contain a tube joiner that aligns the wing and supports the spar caps. The fuselage also contains a tube joiner that transfers loads from the spar to the fuselage and tank. A 44 in. x $\frac{3}{4}$ in. carbon tube fits into the joiners to attach the wings to the fuselage. The wings are laterally held in place via bolted tabs extending from the wing root into the fuselage.

Each outboard section contains an aileron. The aileron is controlled using a Hi-Tech mini digital servo. The transmitter that controls the servo is also programmed to incorporate flaperons to assist in take-off. The servo is accessible through removable hatches on the bottom surface of the wing.

The internal structure of the wing was constructed of light ply, balsa, carbon fiber, fiberglass; and Kevlar. The main wing was designed to be hollow with the majority of the structure integrated into the skin during lay up. The skin is composed of 5 layers of 2 oz fiberglass in a [0/45/90/45/0] orientation to carry all torsional loads. The spar caps consist of a layer of unidirectional carbon fiber that varies in width from 2.5 in. at the root to 1 in. at the tip and is centered over the quarter chord on the top and bottom surfaces to carry bending loads. To provide a carry through structure, a $\frac{3}{4}$ in. carbon fiber tube is used. A receiver tube butts against the root of the wing and extends 17.5 in. into the wing at the quarter chord of the root. This tube is glued to the top and bottom surfaces and is positioned by ribs at each end. In the chord-wise direction are several 1 in. strips of carbon fiber to strengthen and hold the form of the wings. The root edge of the wing is formed by a piece of 1/8 in. thick lite ply to provide a flat surface to butt against the fuselage. Balsa is used to support the areas around the aileron and provide form.

The skin on the wings is thicker than the fuselage skin since they have greater loads to bear. The skin is composed of 5 layers of 2 oz fiberglass with an alternating weave orientation. In some areas a sixth layer of fiberglass is used for extra support, such as the cutout area for the ailerons and the root. A strip of unidirectional carbon was set into the wing skin lay-up in order to gain flexural rigidity against lift forces. The carbon is set between the second and third layers of the fiberglass, to help prevent delamination. The unidirectional carbon is oriented just above the wing joiner, at about the quarter chord line, and extends from the root tapering off toward the tip.

The root of the wing is capped with aircraft grade plywood similar to its mating surface on the fuselage. The tube joiner passes through this plate and extends half the distance of the wing terminating in a rib constructed of foam. This rib has the shape of the airfoil section at that wing station. The tube

joiner and the foam rib are glued to the inside of the upper and lower surface of the wing skins. The trailing edge of the wing is cut out for the control surfaces and framed in with balsa. The cutout section, used as the control surface, is also framed in with balsa and attached to the wing with hinges.

5.3.2 Fuselage

For most aircraft, the fuselage must be designed around the payload. The payload for Phyxius, a tank containing a maximum of 4 L of water, was a major design condition. Like the wing, the skin is designed to carry bending loads. The skin is composed of four layers of 2 oz fiberglass in a [0/45/45/0] orientation. Since the tank is hard shelled, it is used as a structural member. The tank is composed of the same material and orientation as the skin and is connected to the spar and landing gear structure. Bulkheads and formers were used to connect the tank and skin of the fuselage. These members were composed of carbon fiber sheets with a core of 1/4 in. thick pink foam. Three bulkheads, one at each end of the tank and one in the tail, attach internal structure to the skin as well as hold form. The formers, which are bulkheads with a hole cut out, support the tank in the vertical and lateral directions.

The fuselage skin is composed of four layers of 2 oz fiberglass with Rohacell strips set into the center of the lay up. The Rohacell is used in the rear of the fuselage to increase the rigidity of the tail. The configuration of the layers is symmetric to avoid possible cross coupling associated with the weave layering. The weave of the second layer is rotated 45 deg from the first. In the tail, the Rohacell strips are laid down; next the third layer is put down with no rotational offset with respect to the second. The fourth layer is however offset from the third by 45 deg, thus the layers are symmetric about the Rohacell. The wing joiner is a carbon tube, which slides into a sleeve, also a carbon tube. The sleeve extends through the fuselage, from wing root to wing root. The belly pan skin of the fuselage also has four layers of 2 oz fiberglass constructed on a 45 deg. bias throughout. Carbon strips, made of 3 oz cross weave are run under the area of the bulkheads to distribute the loads the bulkheads will impart upon the skin.

Structural members constructed of a carbon-foam-carbon sandwich are used in key places in throughout the fuselage. There are bulkheads located in front and rear of the tank. These bulkheads are bonded to the tank face and to the skin. The front bulkhead serves as an attachment point for the motor mount. The motor mount is an aluminum bracket bolted and glued to the front face of the first bulkhead. The second bulkhead, affixed to the rear of the tank, also holds a portion of the batteries and the servo used to operate the dumping valve. The third bulkhead is located in the tail and serves as a mounting location for the pivot mechanism used to operate the fully flying tail. The next type of structure made of the carbon-foam sandwich is the former. These formers are used around the tank, filling the quarter inch gap between the tank and the skin. They are the same thickness as the bulkheads yet only as wide as the gap. Encircling the tank, they form a cage supporting the loading in this area.

The landing gear and the wing joiner attach to a brace constructed of aircraft grade plywood. The brace is a frame in the shape of an "H", and it is fixed to the underside of the tank as well as the lower skin. The landing gear is affixed to the middle plate using nylon bolts, and the wing joiner tube passes through holes in the two upright portions. The tube joiner then passes through another thinner plywood plate, which caps the end of the wing root where the outer wing separates. The landing gear is a carbon strut, which is bolted onto the cross member of the frame. Nylon screws were used to allow the gear to break off in the event of a crash, rather than cause further damage to the internal structure.

5.3.3 Empennage

Even though the empennage is not a major load-bearing structure, care was taken to transfer the loads to the fuselage without sacrificing additional weight or structural integrity. Due to the shape of the aircraft the vertical stabilizer was molded into the fuselage skins allowing for a continuous piece. A balsa structure was used to support the vertical stabilizer and rudder.

The horizontal stabilizer's skin and spar are the same as the main wing. The main difference is a 1/8 in. carbon dowel is used to control the movement of the fully flying tail. This dowel is located at 50 % of horizontal stabilizer's root chord.

The horizontal stabilizer is constructed in the same manner as the wing. There is a strip of unidirectional carbon running the full length. Being a fully flying tail, its tube joiner is also its pivot point. There is a structure acting as a spar for the vertical stabilizer, which also supports the mechanism used to rotate the stabilizer.

5.3.4 Landing Gear

Landing gear was researched and analyzed. The landing gear is a vital component, which must comply with the storage box and payload requirements. The gear must be able to disassemble from the UAV easily for storage and also be light in weight but structurally sound for landings with both payloads.

The landing gear configuration consisted of a main gear and a tail gear. The landing gear was purchased off-the-shelf from TNT Landing Gear. The main gear was a composite structure made by Graphtech. It is sufficiently wide to allow the deployment mission to be carried out and strong enough for the heaviest loaded landings. The width from the right to left wheel is 20 in. and the height is 6 ¾ in. The tail gear is an "L" shaped wire connected to the rudder to enable steering. The main gear is attached using two bolts.

5.3.5 Engine Mount

The motor mount was machined out of Aluminum to be lightweight and strong. It was also designed to be disassembled for removal of the motor. Countersunk bolts in the back of the first bulkhead attaches the motor mount to the fuselage structure.

5.3.6 Payload Deployment

A simple servo system is used for payload deployment. The servo rotates a cylindrical valve 90 deg. to align the incoming air-hole and the outgoing water hole. A hose connected to the air hole connects to the root of the leading edge to provide a vent for the tank. The water exit of the valve is connected to a nylon tube that hangs out of the bottom of the fuselage.

5.4 Payload System

During the competition, two 2-liter bottles will be emptied into the airplane. A manifold that will accommodate two 2-liter bottles was built to shorten the loading time. This manifold was constructed much like the first with an extra hole for the second bottle to mount in. Each bottle uses a separate vent tube constructed of the 3/8 in. aluminum tubing used in the third preliminary test. When tested, the system consistently emptied in 4 s. This time was confirmed by repeating the test several times. The designers determined that the 1½ in. diameter exit for the manifold was too big for the airplane. This was adjusted using 1 in. PVC pipe and a 1 in. ball valve. The original competition manifold was modified by reducing the pipe diameter below the 1½ in. sanitary fitting. The manifold was elongated by increasing the column from 12 to 48 in. This new design was tested and produced an emptying time of 3 s.

5.5 Rated Aircraft Cost

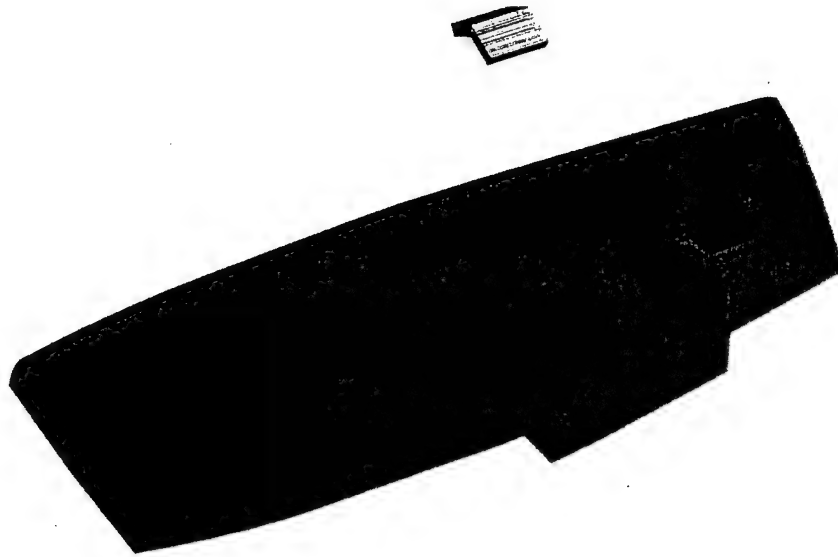
Table 5.3 Rated Aircraft Cost Worksheet

	Measurement	Scale	Hourage	Cost
Manufactured Empty Weight (lb)	7.7	300		2310
Number of Engines	1			
Battery Weight (lb)	2.3			
Rated Engine Power	2.3	1500		3450
Manufacturing Hours				
Wing Span (ft)	7	10	70	
Wing Chord (ft)	1			
Wing Control Surfaces	2	1.5	3	
Fuselage Length (ft)	4	20	24.06	
Fuselage Height (ft)	0.36			
Fuselage Width (ft)	0.83			
Vertical Surface Active Control	2	10	20	
Horizontal Surface	1	10	10	
Servos and Motor Controllers	6	5	30	
Number of Engines	1	5	5	
Propellers	1	5	5	
Total MFHR		10	167.06	7141.11
Total RAC				12.9011

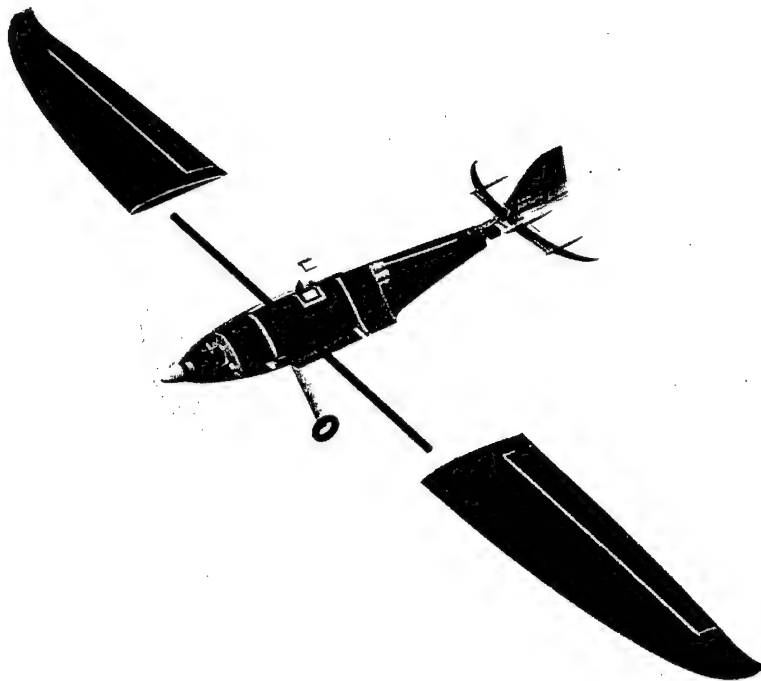
Table 5.4 Geometry Data for the Sized UAV

Geometry		
Length (in)	47.2	
Span (in)	84	
Height (in)	11	
Wing Area (in ²)	780	
Performance		
	Unloaded	Loaded
CL max	1.2	1.2
L/D max	15	15
RoC max (ft/min)	2612.9	1006.3
Stall Speed (mph)	24.3	35.6
Maximum Speed (mph)	75	55
Take Off Distance (ft)	45	130
Weight Statement		
Airframe (lb)	3.3	
Propulsion System (lb)	3.5	
Control System (lb)	0.5	
Payload System (lb)	0.2	
Payload (lb)	8.5	
Empty Weight (lb)	8	
Gross Weight (lb)	16.5	
Systems		
Radio Used	Futaba 9ZAP WC2	
Servos Used	Hitec HS-85, HS-225	
Battery Used	SR 2000 mAh - 18 cells	
Battery Configuration	1 x Rectangular Pack Arrangement (3x4) 1 x Rectangular Pack Arrangement (2x3)	
Motor	Graupner 3300-5	
Propeller	AeroNaut CAM Frudenthaler 16x10, 16x13	
Gear Ratio	2:1	

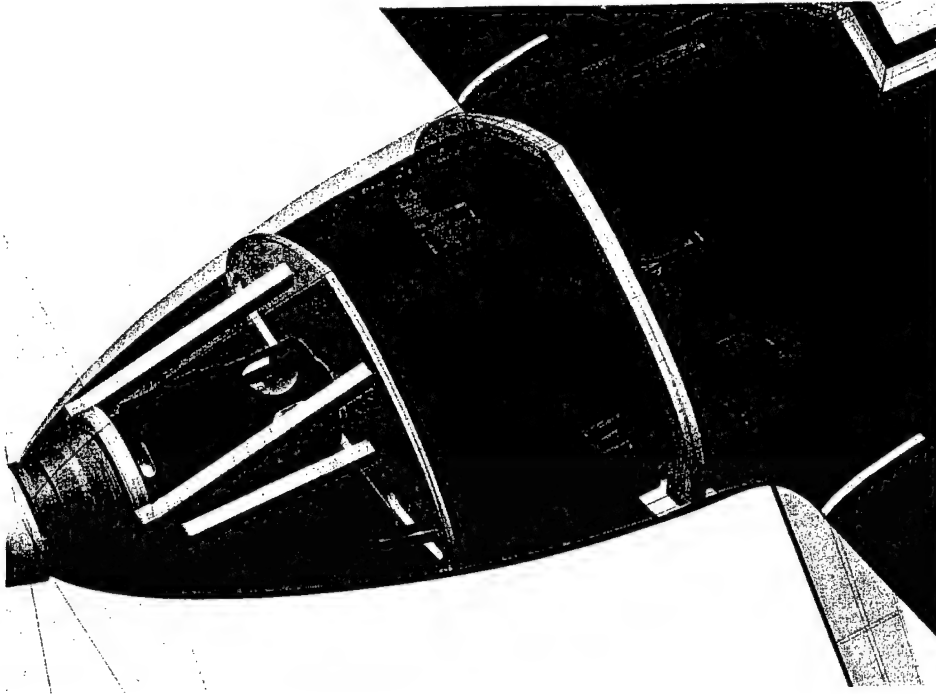
5.6 Drawing Package



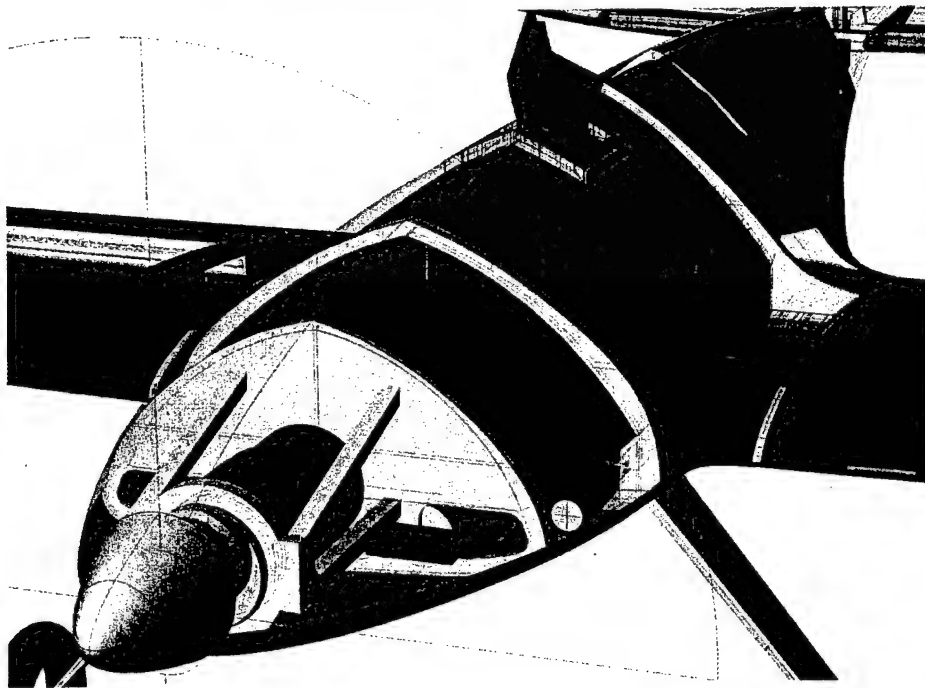
Payload System



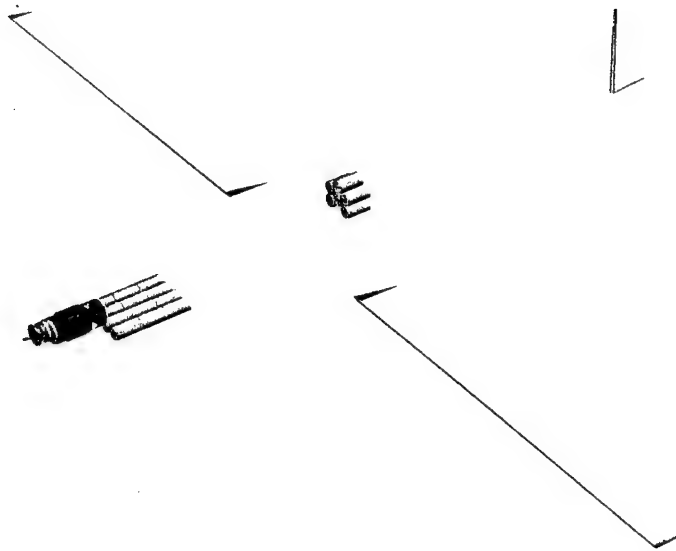
Structural Model



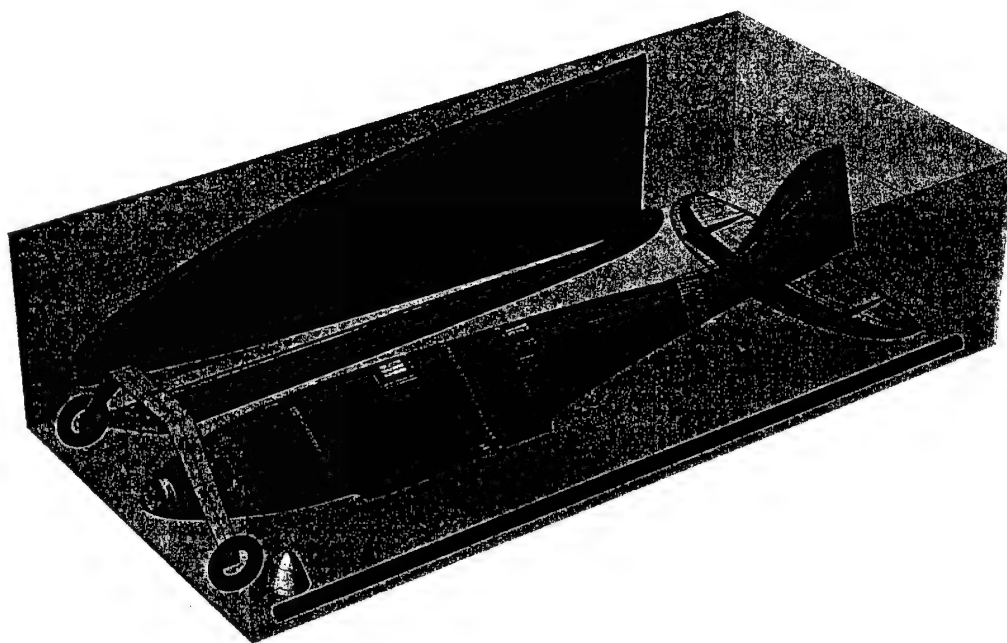
Propulsion System and Battery Placement



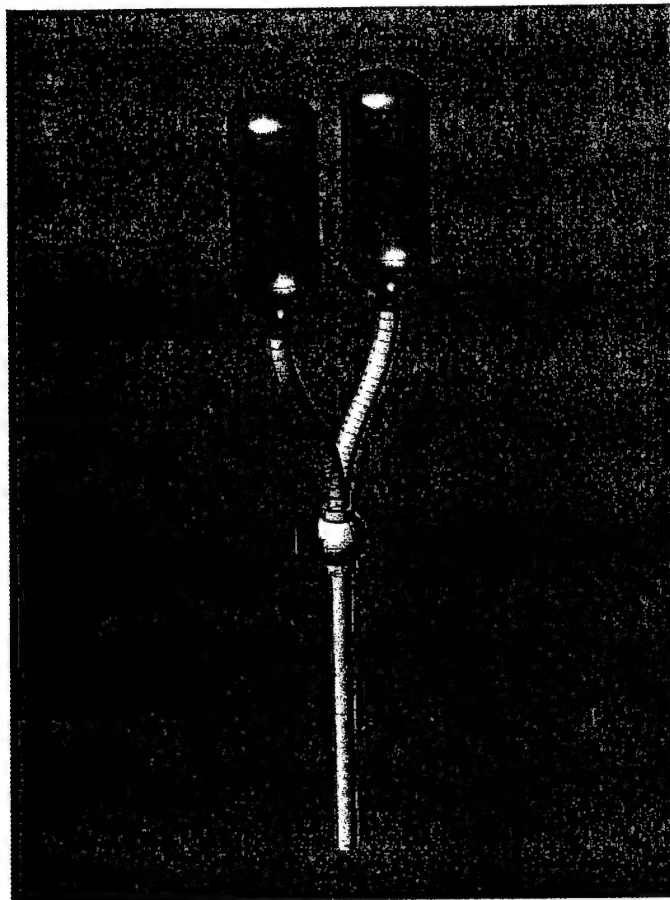
Propulsion System and Payload System



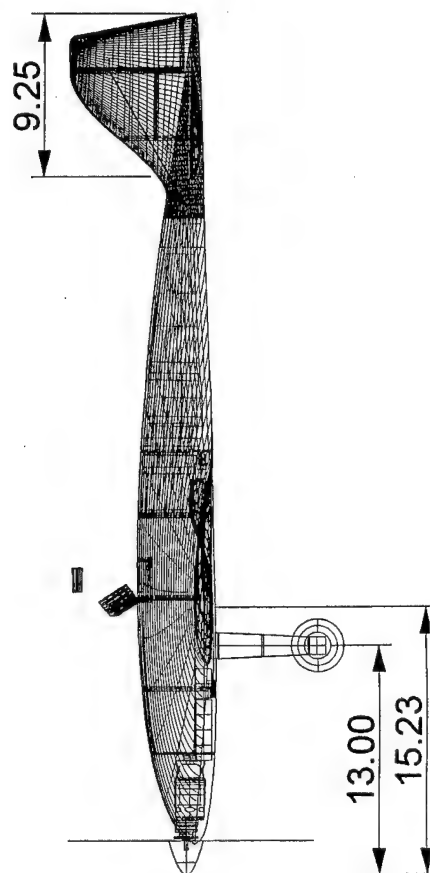
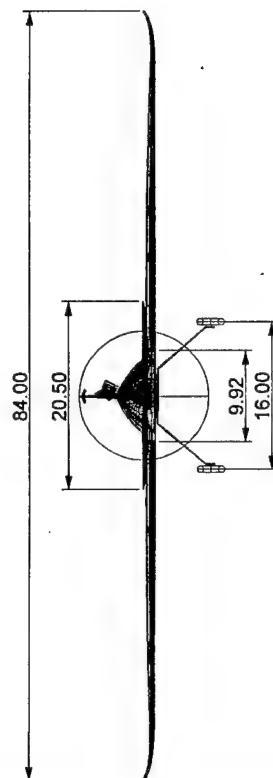
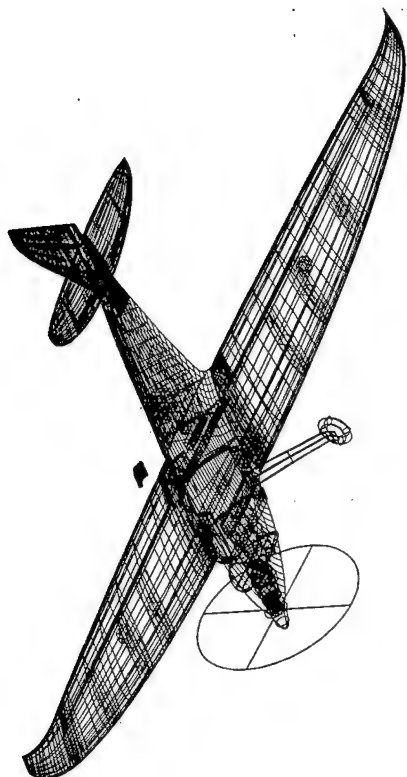
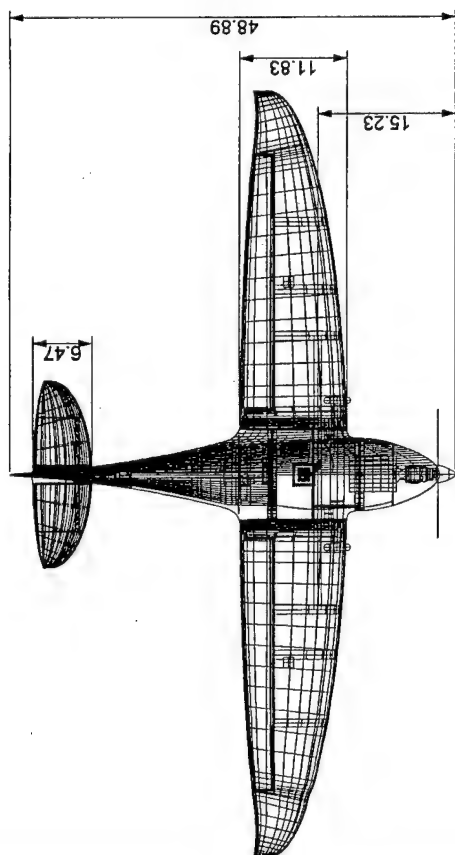
Battery Configuration



Phyxius in the 4'x2'x1' Box



Manifold Assembly



6. MANUFACTURING PLAN

Developing a manufacturing plan requires analysis of options and a manufacturing schedule. Several methods of construction were investigated and analyzed. From these methods, the team applied Figures of Merit to decide which would most benefit the design. A schedule was developed to guide construction and modification of major and minor components of the UAV.

6.1 Construction Methods Investigated

Table 6.1 Construction Methods Investigated

Method	Description
Off-the-shelf (OTS)	Components that can be purchased from hobby stores (only applicable to certain structures).
Moldless	Refers to solid-core structures in which skins (if any) are applied directly to the underlying core.
Built-up	Refers to structures that are assembled from individual components that may be either hand- or machine-cut. Skins, if any, simply conform to the underlying structure.
Molded	Internal structures may be built-up or solid-core, but skins are pre-molded to exact shapes before assembly to structure.

6.2 Construction Materials Investigated

Table 6.2 Construction Materials Investigated

Materials	Skill	Description
Advanced Composites	4	Refers to glass-epoxy, Kevlar-epoxy, and carbon-epoxy. Skills associated may include: composite layouts, mold construction, and vacuum bagging techniques.
Foam	3	Includes low- and high-density EPS, as well as 1-lb white foam. Skills associated may include: template construction and hot wire cutting.
Metal	2	Refers to aluminum construction. Skills associated may include: cutting, bending, and drilling.
Wood	1	Includes balsa, light-ply, aircraft plywood, and hardwoods such as spruce and basswood. Skills associated may include: gluing, cutting, and sanding.

6.3 Figures of Merit

The Figures of Merit applied to the manufacturing plan were developed based mostly on the skills and time of team members. The important factors affecting the plan were decided by the team and voted on.

Availability of the product is important in two ways. If the product is completely inaccessible, it gets a very low score. However, if the product is accessible but the time to receive is prolonged, it may still receive a low score. A good example of this is anything ordered from AstroFlight.

The skill level of the team members is also a driving force in the decision to choose a construction method. This year's team had several members who felt comfortable with composite construction. Due to composites' greater strength and possible weight savings, it was chosen as the main manufacturing method.

The time required to complete component construction is also a vital part of the analysis on the manufacturing options. Obviously, no matter the cost of other merits, time is of great importance. While composite manufacturing requires large tooling times, once the molds are finished skins can be fabricated in a matter of hours.

Repairability is considered for selected components. The plane, as a whole, is not built for repairability. Therefore, spare parts and components will be bought and manufactured so that in the event of a rough landing or crash the damaged section can simply be replaced.

Cost is always an issue in building an aircraft. The manufacturing plan considered cost from the beginning. Spending a lot of money in one place may assure cutbacks in other places. Considering the need to take 25 students to competition this year, cost was a major consideration of the plan in manufacturing. However, the cost for the composite fabric and epoxy was offset by generous donation from Advance Technologies of Starkville, MS.

6.4 Results

The results of the analysis and scoring are detailed in Table 6.3. A score of one is the worst and five, the best. The milestone chart can be found in Figure 6.1. One may notice from the milestone chart that much less time is given to the construction of the second plane. This assumption is based on modifications and lessons learned during the original construction.

Table 6.3 Selection of Major Component Construction Methods and Materials

Description			Figures of Merit					
Structure	Method	Material	Availability	Skill Level	Time Required	Repairability	Cost	Results
			2	4	5	1	3	
Fuselage (internal)	built-up	wood	4	3	3	2	3	46
		adv. comp.	3	4	4	3	4	57
Fuselage (skin)	molded	adv. comp.	4	3	4	4	4	56
	built-up	wood	4	4	2	3	3	46
Wing (spar)	built-up	wood	4	3	3	4	3	48
	molded	adv. comp.	4	4	2	3	3	46
	OTS	metal	2	3	4	3	1	42
Wing (other internals)	built-up	wood	3	3	3	3	3	45
		foam	3	4	4	1	5	58
		adv. comp.	4	3	2	3	3	42
Wing (skins)	built-up	wood	3	3	3	4	3	46
	molded	adv. comp.	4	3	4	3	4	55
Empennage (internals)	built-up	wood	3	3	3	3	3	45
		foam	5	3	4	1	5	58
		adv. comp.	4	4	3	3	4	54
Empennage (skins)	built-up	Wood	3	3	3	5	3	47
	molded	adv. comp.	4	4	4	3	3	56
Landing Gear	OTS	metal	3	4	4	3	3	54
		adv. comp.	4	4	4	4	2	54
	built-up	metal	4	2	2	3	3	38
Wing joiner	OTS	metal	3	3	2	3	4	43
		adv. comp.	5	4	5	2	3	62
	built-up	metal	4	3	2	3	3	42
		adv. comp.	3	2	2	3	2	33
		wood	5	4	3	3	4	56

6.5 Manufacturing Timeline

Task Name	Start	Finish	Dec	Jan	Feb	Mar	Apr
Phyxius I	01/09/04	03/13/04					
Fuselage Assembly							
Planned	01/16/04	02/15/04					
Actual	01/23/04	02/06/04					
Wing Joiner							
Planned	01/13/04	02/10/04					
Actual	01/15/04	01/29/04					
Wing Spar Assembly							
Planned	02/01/04	02/10/04					
Actual	01/13/04	01/20/04					
Empennage Internals							
Planned	01/16/04	01/23/04					
Actual	01/22/04	01/24/04					
Empennage Skins							
Planned	01/23/04	01/25/04					
Actual	01/24/04	01/31/04					
Landing Gear							
Integration							
Planned	02/04/04	02/11/04					
Actual	02/03/04	02/21/04					
Final Assembly							
Planned	2/15/04	02/28/04					
Actual	02/15/04	02/27/04					
Phyxius II (Predicted)	03/15/04	04/15/04					

Figure 6.1 Milestone Chart of Major Event

7. FLIGHT TESTING PLAN

7.1 Objective

The objective of flight-testing is to familiarize the pilot with the UAV and to simulate competition missions for score optimization. A schedule was developed to complete the testing needed to modify Phyxius II. The structure of the schedule will allow the team to find the problem areas and make necessary adjustments in a timely fashion. Results from each test would be recorded and analyzed for further improvements the UAV's performance.

7.2 Schedules and Check Lists

Due to the limited amount of time available to accomplish certain milestones, it was decided to break-up flight-testing into four segments. The first three segments would consist of four flights each, while the last segment would continue until competition. Those segments of testing are intended to familiarize the pilot with the UAV. Slow speed and stall characteristics, power-off glide, and a simulated competition flights would give the pilot familiarization with UAV handling abilities and mission profiles. The last test segment is intended to simulate competition missions for increased individual flight scores.

Table 7.1 Flight-Testing Scheduled Tasks

Segment	Flight Test Tasks
1	Slow Speed and Stall Characteristics
2	Power-off Glide
3	Simulate Competition Missions
4	Simulate Competition Missions to Increase Score

Several considerations were noted during a meeting with Dr. Tom Edwards and Mr. Calvin Walker of the Mississippi State University Raspet Flight Research Laboratory. Before flight-testing at the airport, a certificate of authority was required to waive FAA Part 91 requirements for the UAV, and proper authorities working at the airport must to be notified. Because of the short duration of the flights, the airport board found not reason to issue Notices to Airmen (NOTAM's) during flight-testing days. A pre-flight briefing was needed before each test to ensure facility requirements were followed. Some of these requirements were that communication must be made with other aircraft in the pattern, that flight-testing would occur only when visual flight rules were issued, and that a Raspet employee would monitor the tests.

7.3 Results

As of the 9th of March, the construction of Phyxius I was not completed. Therefore, flight-testing was not done prior to the deadline of this report paper. However, the flight-testing of Phyxius I will be completed shortly. While in flight, it is important to stay inside the guidelines for the V-n diagram. The diagram displays the load factor as a function of velocity. The V-n diagram determines whether stall or structural failure will occur at a particular load factor and velocity. The V-n diagram for Phyxius is shown below.

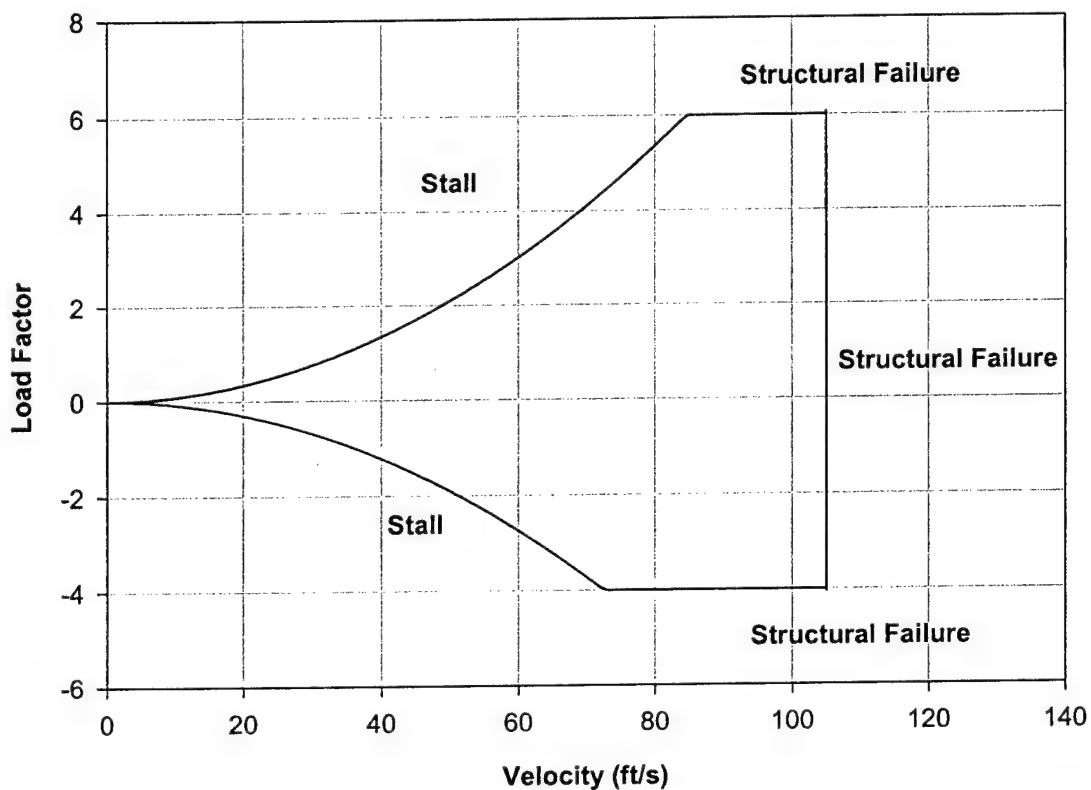


Figure 7.1 V-n Diagram for Phyxius

REFERENCES

1. Anderson, John D. Introduction to Flight. 4th Edition. WCB/McGraw-Hill, New York. 2000.
2. Bruhn, E.F. Analysis and Design of Flight Vehicle Structures. Jacobs Publishing, Inc. Indiana. 1973.
3. Nelson, R.C. Flight Stability and Automatic Control. 2nd Edition. WCB/McGraw-Hill, New York. 1998.
4. NASG (*Nihon univ. Aero Student Group*). College of Science & Technology Nihon University. 11 November 2000. <http://www.nasg.com/index-e.html>.
5. Raymer, Daniel P. Aircraft Design: A Conceptual Approach. 2nd Edition. American Institute of Aeronautics and Astronautics, Washington, D.C. 1992.
6. Vinh, Nguyen X. Flight Mechanics of High-Performance Aircraft. 4th Series. Cambridge University Press, New York. 1993.
7. XFOIL. Massachusetts Institute of Technology. 11 December 2000. <http://raphael.mit.edu/xfoil/>.

**2003/2004 AIAA Cessna/ONR/
Student Design Build Fly Competition**

ENGINEuity – IGI
University of California Los Angeles
March 2004

1. Executive Summary

This report depicts the design, manufacturing, and testing processes of UCLA ENGINuity's entry in the 2004 Cessna ONR Design/Build/Fly Competition. The two mission types are the Fire Flight (with a water payload, heavy lift) and Ferry (with no payload, fast flight). Scoring for the competition is dependent on flight times and mission difficulty, as well as Rated Aircraft Cost (RAC) and report scores. The focus of the team was to create a design for optimal performance while keeping the RAC as low as possible.

1.1 The Design Process

The design process began by analyzing the rules for this year's competition. Every aspect of each mission was broken down until each team member had an understanding of what was required. Also, the RAC formula was thoroughly examined so that it would be clear which aspects of design weighed heavily towards determining the final aircraft score. This was followed by brainstorming conceptual designs in accordance with what the competition entailed, focusing especially on aspects which were considered to potentially yield significant advantages over other teams.

The many different configurations were narrowed down by applying figures of merit (FOM) and the top designs were then chosen for computational analysis with software support. With this analysis completed, a final preliminary design was determined. Using this model, a platform was established so that analysis of the physical structures within the plane could begin. Different materials were researched for their potential uses in different parts of the plane. Using FOM based on availability, manufacturability, time, and economic considerations, materials and their specific applications were decided upon.

With the conceptual design complete, structural tests were performed both physically and by use of software support to ensure that significant weight bearing structures would not fail under the greatest expected loads. All properties of the plane were tabulated according to the chosen materials and specifications. Final analysis of the plane was done using as few approximations as possible so that accurate projections could be made about flight characteristics.

1.2 Design Alternatives Investigated

There were a countless number of designs to choose from when considering all the possible combinations of different design options for each component of the plane. Starting with the back, a conventional tail was compared to the T-tail and V-tail configuration. Focus was then drawn to wing selection, noting differences between a rectangular or swept wing, as well as flying wing or

by-wing planes. Next, the placement of the wing was considered (low, middle, or high on the fuselage) and with this, the main landing gear set up. Both retracts and fixed gear were considered by comparing weight savings with drag effects. For the actual propulsion system, a multiple-motor setup was looked at but quickly noted as too costly when considering the RAC while not showing any significant advantages in performance. Batteries were chosen according to the powerplant, but preliminary judgment suggested the maximum amount of batteries would be best for maximum power. However, it was noted that such battery weight would weigh heavily in RAC considerations.

When considering the actual structure of the plane, materials had to be chosen to best fit our needs. Of those considered were foam, balsa wood (for sheeting as well as structural rigidity), plywood, aluminum, monokote sheeting, composites and fiber glass. The central goal here was to choose a structural system with adequate strength but one which weighed as little as possible. This was important not only for the RAC, but for our planes speed performance and hence our final flight scores.

Another area of great design interest was the actual water tank. Initial sketches included a tank running lengthwise through the plane's fuselage, or a tank balanced around the center of gravity bloating the side panels outward. Neither configuration was found to provide adequate dumping time, so attempts were made to maximize the available hydrostatic force. Radical ideas were considered such as pivoting the entire tank around the center of gravity to hang vertically during dump off, or flying the plane at a sharp angle to tilt the tank. However, they did not seem practical from a manufacturing or control standpoint. Therefore, efforts were put into researching a retractable nozzle, deployable from the bottom of the tank to increase the available hydrostatic force during dumping of the payload.

1.3 Highlights of the development process

Although the Fire Flight is designated as the heavy lift, slow flight portion of the competition, it seemed a fast time here was very important in scoring better than other teams. A focal point of this goal was dumping the water as fast as possible so as not to lose any speed in slowing down for adequate drainage. The retractable nozzle seemed to reduce this time by a few seconds in the analysis; however, when considering the excess weight of the nozzle and supporting structures, as well as the difficulty of controls and effects on RAC, a fixed deployment point was chosen. In doing so, the tank was modeled to extrude out from under the fuselage, using the added height to increase the hydrostatic force. An air inlet was also designed to open simultaneously with the outlet nozzle, thus adding a slight boost.

To account for this added front plate area, a stream line approach was taken in every aspect of the plane. The tank cross section itself will be airfoiled, as well as the protruding landing gear (fixed gear was chosen to reduce weight). The wheels themselves will have covers for increased drag reduction, and the overall form of the plane will be similar to a symmetric airfoil, teardrop shape. Essentially, the focus was determined to be the production of a plane with very low weight and high power, so that by minimizing all drag considerations lap times would be reduced drastically, even with a heavy payload.

In keeping with the motto of a light weight plane, a structural setup was designed relying heavily on high strength, low density composite spars. Thorough analysis was performed using Cosmos Works to ensure that there would be no failure, especially at the high stress joints.

2. Management Summary

It was decided early on that the most efficient way to go about the design of this UAV was to split the team into three sub-groups, each focusing on a specific task: propulsion, structures, and aerodynamics. Each of these groups had an assigned manager to ensure that specific duties were delegated and taken care of in a timely fashion.

The propulsion group had the responsibility of choosing an appropriate configuration to power the UAV. Optimization was necessary to find the most efficient combination amongst a variety of motor, battery, and propeller options. Not only was the selection a part of their task, but the accompanying analysis and testing as well.

The structures group was assigned to design appropriate structures for the entire aircraft. Important tradeoffs were considered between strength and weight, as well as applicability in light of RAC and flight times. Their tasks included material selection as well as finite element testing for significant load bearing structures. Considerations were also made for the actual manufacturing of selected parts.

The aerodynamics group was in charge of considering advantages and disadvantages of various aircraft configurations. Research was required to fully understand the applicability of each combination for a UAV with a significant payload, as well as a requirement to achieve high speeds. Accompanying these decisions was the necessary stability analysis to determine flight characteristics for any selected design, as well as flow testing using software packages for real life simulations.

Although distinct in description, the groups were required to consult with one another regularly because so many characteristics of the design process were linked together. The factor that tied all in considerations was the effect of each design on RAC and predicted flight performance, and the tradeoffs between each with any change in design. To ensure a coherent and complete design process, group managers would first meet together before breaking off with their respective teams. If necessary, a second brief meeting could also be held between managers before leaving so that teams would know which direction to take before the next group meeting. The graph that follows illustrates the team breakdown.

Group	UCLA #1: <i>Enginuity</i> - IGI		
Lead Engineer	Robert Lane		
Sub-Groups	<i>Propulsion</i>	<i>Structures</i>	<i>Aerodynamics</i>
Manager	Raffi Kojayan	Carla Giron	Robert Lane
Members	Dominick Vicente	Yung Hsin Christian Lopez Underclassmen	Josh Highman Will Lin
Responsibilities	Configurations and analysis of motor, battery and prop	Selection, analysis, and Finite Element Modeling of key structural components	Consideration of various aircraft configurations, as well as flow and stability analysis

Figure 2.1. Team structure

3. Conceptual Summary

3.1. Mission Requirements

Scoring is solely dependant on Report Score, Mission Flight Score, and Rated Aircraft Cost. Assembly time will not be considered for scoring purposes. For Mission Flight score, the score is inversely proportional to time, so that the best score correlates with the shortest mission time. There are certain guidelines within the competition. The aircraft must fit in a 4' x 2' x 1' box in its disassembled state. The airplane cannot weigh more than 55 lbs due to AMA limitations. Over the counter nicad batteries must be used to power an over the counter Graupner or Astroflight electric motor. Also, the battery weight cannot be greater than 5 lbs.

3.2. Alternate Aircraft Configuration Possibilities.

To determine the proper aircraft configuration a wide variety of aircraft were researched and tradeoffs recognized. The search was narrowed based on figures of merit chart that awarded one point to those airplane configurations that are used most widely in remote control flight and zero for those configurations that are unlikely to be found in remote control flight. The chart was assembled as follows

Aircraft configuration	RC likelihood
Canard	0
Biplane	0
Blended wing body	0
Conventional tube-wing-tail	1
Delta winged	0
Tube body blended to wing	1
Two tubes and wing	1

Table 3.2.1. Different aircraft configurations and related figure of merit

From this chart it can be deduced that more conventional airplane configurations must be considered for UAV flight. Further analysis to narrow down the search considered airplane functionality. One point was awarded if the airplane type fit the function specified. The total points were added up and then the maximum points would dictate the configuration.

	High max velocity	Heavy lifter	Total points
Pylon racer	1	0	1
Cargo airplane	0	1	1
Fire bomber	0	1	1
glider	0	0	0

Table 3.2.2. Functional airplanes and related figure of merits

From this chart it must be concluded that a cross between a racing and lifting airplane configuration must be found to achieve maximum success.

Tail configuration was another point of interest. During flight maximum control was desired and thus a conventional tail or t-tail was decided upon. The t-tail is a good arrangement because it does not feel the effects of downwash like a conventional tail. However, the t-tail has added structural considerations which increase the weight and complexity of the airplane. For RC flight the downwash can be considered small enough that it is more far more desirable to go with a conventional tail configuration.

Wing shape was also a major factor in the airplane configuration. Sweep-back is not applicable for subsonic purposes unless it is desirable to move back the aerodynamic center of the aircraft. However, this will probably not be the case. The other consideration is to maximize the wing lift distribution. An elliptical wing plan form will give the airplane a maximum elliptical lift distribution. However, the elliptical shape is too difficult to manufacture and thus will not be chosen. Lift distribution can also be maximized by tapering the wing, but also has manufacturing complexities. The lift distribution discrepancy of remote controlled aircraft with tapered wings compared to rectangular wing is small and therefore the rectangular wing will be chosen for the final configuration.

From research into different aircraft configurations it was decided that "IGI" be a tubed body with a rectangular wing and conventional tail.

3.3. Numerical Figures of Merit (FOM) used for Screening

FOM were used to analyze two key components of the airplane structure: wing area and wing span (thus determining chord length). As these values were varied, the resulting effects were noted on flight times for both missions, as well as the Rated Aircraft Cost (RAC). Using a scoring method similar to that implemented in the final judging of the competition, a Final Merit Rating (FMR) was given to each configuration.

3.3.1 Qualifying Takeoff Distance (QTD)

Any flight that requires more than the allotted 150 ft for a successful takeoff will be disqualified. For this reason, if a configuration results in an estimated takeoff distance greater than 150 ft, a QTD value of 0 will be assigned, thus negating that configuration. On the other hand, because the advantage of shorter takeoff distances will be apparent in overall flight times, and thus mission scores, it would be unnecessary and inaccurate to account for this effect twice. Therefore, a simple qualifying score of 1 will be given for any configuration resulting in a takeoff distance less than 150 ft.

$$\text{QTD} = 0 \text{ if distance is greater than 150 ft} \quad (3.3.1a)$$

$$\text{QTD} = 1 \text{ if distance is less than 150 ft} \quad (3.3.1b)$$

3.3.2 Fire Flight Score (FFS)

The FFS was calculated based on the appropriate scoring equation illustrated in the rules for this years competition. The score has a difficulty factor coefficient of 2.0 and is inversely proportional to mission flight time. Because water weight is constant with all configurations, it was not considered in this scoring:

$$\text{FFS} = 2.0 / \text{estimated mission time} \quad (3.3.2)$$

3.3.3 Ferry Score (FS)

Again using the rules as a guideline, the FS is simply dependant on the difficulty factor coefficient (in this case, 1.0) and flight time:

$$\text{FS} = 1.0 / \text{estimated mission time} \quad (3.3.3)$$

3.3.4 Rated Aircraft Cost (RAC)

The equation for calculating this FOM comes directly from the competition rules. It is simply a way of quantitatively scoring the overall design of the plane, rewarding simpler designs with higher scores:

$$\text{RAC} = (300 * \text{MEW} + 1500 * \text{REP} + 20 * \text{MFHR}) / 1000 \quad (3.3.4)$$

Here MEW represents the Manufacturers Empty Weight. This includes all components of the airplane but not the payload. REP stands for Rated Engine Power and is defined as follows:

$$\text{REP} = [1 + (0.25 * (\# \text{ engines} - 1))] * \text{total battery weight} \quad (3.3.5)$$

Lastly, MFHR stands for Manufacturing Man Hours, and is defined as the sum of four sets of Work Breakdown Structure (WBS) hours:

$$\text{MFHR} = \text{WBS1} + \text{WBS2} + \text{WBS3} + \text{WBS4} \quad (3.3.6)$$

$$\text{WBS1} = 10 \text{ hr/ft}^2 * (\text{wing span} * \text{chord} * \# \text{ of wings}) + 5\text{hr} * \text{CFM} \quad (3.3.6 \text{ a})$$

$$\text{WBS2} = 20 \text{ hr/ft}^3 * (\text{body length} * \text{width} * \text{height}) \quad (3.3.6 \text{ b})$$

$$\begin{aligned} \text{WBS3} = & 5\text{hr} * (\# \text{ vertical surfaces with no active control}) + \\ & 10\text{hr} * (\# \text{ vertical surfaces with active control} + \# \text{ horizontal surfaces}) \end{aligned} \quad (3.3.6 \text{ c})$$

$$\text{WBS4} = 5\text{hr} * (\# \text{ servos/controllers}) \quad (3.3.6)$$

Note in equation 3.3.6a CFM stands for Control Function Multiplier and is a coefficient ranging from 1.0 to 3.0, depending on the configuration of control surfaces chosen. Because variations in this parameter would only effect the RAC by about 1.5% of the projected value, it was not significant in deciding the actual control surface configuration. Instead, an optimal configuration will be chosen according to the airplane's flight requirements, and the score will then depend on this control surface choice. Therefore, a constant value of 1.5 (correlating to flaperons) was assigned for preliminary RAC calculations.

3.3.5 Final Merit Rating (FMR)

The FMR calculation simply mimicked the overall score calculation in the competition by summing the mission flight scores and dividing by the overall RAC:

$$\text{FMR} = (\text{FFS} + \text{FS}) / \text{RAC} \quad (3.3.7)$$

3.4. Mission Modeling and Analysis

3.4.1. Total Aircraft Weight.

To estimate an initial weight for the UAV appropriate components were selected that would fulfill the design requirements. These components are all selected according to their respective

effectiveness to their respective application. Equations for calculating structural weights of R/C aircraft are unreliable compared to actual estimates of the structures being used. Therefore structural weights for the main wing, fuselage, landing gear, and empennage were estimated based on the materials used in each of these sections respectively

Main Wing Weight. The weight of the main wing was estimated by calculating the weight of the respective ribs and struts. For an initial estimate carbon fiber composite was used as the material for the main wing with each rib having a thickness of 1/8 of an inch. An average density of carbon fiber composite and high density balsa was calculated and used to find the weight of the struts. Each of the struts was estimated to be 1/8 inch by 1/8 of an inch cross-section and an overall length of six feet. For initial estimates an over constrained structure of ten ribs and six struts would be considered and then optimized in later calculations.

Fuselage Weight. In the same manner as the wing the fuselage weight was calculated using and over constrained structure with eight ribs each 1/8 of an inch thick and having six struts with cross-sections the same as the wing struts running through the length of the fuselage. The cross-sections of the ribs were all estimated at four inches by four inches. The length of the fuselage was estimated to be four feet. The weight break down is as follows

Component	Weight
Motor	32 – 34 oz
Batteries	3 - 5 lbs
Servos	1.3 oz/ servo
Receiver	3 oz
Water	9 lbs
Landing gear	1-1.5 lbs
Wing structure	2-4lbs
Tail structure	1-1.5 lbs
Fuselage structure	2 - 5 lbs
Total estimated weight	20.76 – 28.88 lb

Total estimated average weight will be around 25 lbs.

Landing Gear Weight. The landing gear weight was estimated using typical R/C aircraft

3.4.2. Parasitic Drag.

Parasite drag was calculated by using the Component Build-up method from Raymer. The totaled parasite drag coefficient is defined by the following equation:

$$(C_{D_0})_{subsonic} = \frac{\sum (C_{fc} FF_c Q_c S_{wet_c})}{S_{ref}} + C_{D_{misc}} + C_{D_{L\&P}} \quad (3.4.1)$$

C_{fc} is the flat plate skin friction coefficient and depends on the Reynolds number. Since the Reynolds number changes with velocity the cruise velocity was used in calculating the parasite drag. FF_c is the component form factor and it estimates the pressure drag due to viscous separation. Q_c is the interference effects on the component drag. $C_{D_{misc}}$ is the miscellaneous drag from the landing gear other protrusions. Finally $CD_{L\&P}$ is the leakage and protuberance drag and it is estimated at 3% of the of parasite drag. Leakage and protuberance drag is the drag that occurs when air is sucked through holes and gaps in the aircraft from high pressure to low pressure zones.

C_{fc} is defined by equations according to laminar or turbulent conditions. For Laminar conditions C_{fc} is defined as

$$C_f = 1.328 / \sqrt{R} \quad (3.4.2)$$

and for turbulent conditions C_{fc} is defined as

$$C_f = \frac{0.455}{(\log_{10} R)^{2.58} (1 + 0.144 M^2)^{0.65}} \quad (3.4.3)$$

Where R is the Reynolds number and M is the Mach number. For the turbulent case the Mach number can be neglected because R/C aircraft fly well below the Mach number. To evaluate C_f 20% laminar and 80% turbulent conditions will be considered since for RC aircraft most of the flow is turbulent due to the propeller.

Form factor is calculated according to the type of protrusion into the airflow. Raymer defines the FF for the wing and tail as

$$FF = \left[1 + \frac{0.6}{(x/c)_m} \left(\frac{t}{c} \right) + 100 \left(\frac{t}{c} \right)^4 \right] \left[1.34 M^{0.18} (\cos \Lambda_m)^{0.28} \right] \quad (3.4.4)$$

Where "t/c" is defined as thickness divided by chord, "(x/c)_m" is defined as the chord wise location of the maximum thickness of the airfoil, and Λ_m is the sweep angle of the maximum-thickness line. The fuselage the form factor is defined as

$$FF = \left(1 + \frac{60}{f^3} + \frac{f}{400} \right) \quad (3.4.5)$$

Finally for the tank protrusion FF may be defined as

$$FF = 1 + (0.35 / f) \quad (3.4.6)$$

where in all cases "f" is defined as

$$f = \frac{l}{d} = \frac{l}{\sqrt{(4\pi)A_{\max}}} \quad (2.4.7)$$

Interference effects of components, "Q", were approximated to be 1.0 except for the tank protrusion which was approximated to be about 1.5 because it is causing significant drag because it will significantly be blocking the airflow. The wetted surface area is the total surface area of the component exposed to the air.

A variety of initial sizing for the fuselage, wing, tail, landing gear, and tank protrusion were used and values for C_{do} were calculated for each case. To find the drag coefficient of the landing gear and wheels we used values for Drag of dynamic pressure listed in Raymer for the components. Since "IGI" will have fixed landing gear the tires will have a fairing on them to decrease drag. Fairings are essential for decreasing drag. Weight considerations for added fairings are not a concern since streamlined structures will be made of fiberglass. A wheel and tire with no fairing has a D/q value equal to 0.25, where as with the added fairing D/q reduces to 0.13. Drag coefficients for the landing gear are calculated by taking D/q and dividing it by the reference area. The miscellaneous drag coefficient added to the drag coefficient for each of the components gives a total parasite drag. This parasite drag coefficient is multiplied by the correction factor for leakage and protuberances to get the leakage and protuberance drag coefficient. Adding up these drag coefficients gives the total parasite drag coefficient.

3.4.3. Induced Drag.

To estimate the induced drag coefficient an Oswald efficiency factor must be determined. To calculate the Oswald efficiency factor a realistic approximation will be used from Raymer for a straight wing and is defined as

$$e = 1.78(1 - 0.045A^{0.68}) - 0.64 \quad (3.4.8)$$

The coefficient of induced drag is defined from McCormick (1995) as

$$C_{D_i} = \frac{C_L^2}{\pi A e} \quad (3.4.9)$$

With a higher aspect ratio the Oswald efficiency factor is approximated to one making the denominator larger and thus the drag coefficient smaller as expected.

3.4.4. Thrust Considerations.

In considering motor selection we consulted McCormick. The follow equations are used to calculate thrust

$$J = \frac{V}{nD} \quad (3.4.10)$$

"J", the advance ratio, is used to find the efficiency of the wing, " η ", which is then used to find the Thrust produced by the propeller, which is defined as

$$T = \frac{\eta P}{V} \quad (3.4.11)$$

Maximum thrust will come from power of the motor as well as efficiency for the propeller. The efficiency of the propeller will be assumed to be maximum in the range of 0.75-0.8 which is a range taken from historical data for aircraft.

3.4.5. Takeoff.

Wheels of the UAV must be off the runway before the 150 foot mark. For takeoff the aircraft takeoff distance is determined by the distance at which the wheels must be off the runway and is defined as

$$S_G = \frac{mV_{L/O}^2}{2[T - D - \mu(W - L)]_{0.707V_{L/O}}} \quad (3.4.12)$$

The bracket portion in the denominator denotes the average acceleration of the aircraft from zero velocity to lift-off velocity. The lift-off velocity is 1.1 times the stall velocity. The stall velocity is directly related to the wing loading and maximum lift coefficient. To minimize takeoff distance the acceleration must be increased and the lift-off velocity must be decreased.

The takeoff time is simply the lift-off velocity over the average acceleration of the aircraft which was defined earlier.

3.4.6. Climb.

Rate of climb is important to the mission in order to reach steady level flight and attain maximum cruise speed. The rate of climb "R/C" is defined in McCormick as

$$R/C = \frac{V(T - D)}{W} \quad (3.4.13)$$

McCormick defines the time to climb from sea level to the desired altitude as

$$t = \frac{h_{abs}}{(R/C)_0} \ln \frac{1}{1 - h/h_{abs}} \quad (3.4.14)$$

The required power is defined by McCormick as

$$(T - D)V = W \frac{dh}{dt} + \frac{d}{dt} \left(\frac{1}{2} \frac{W}{g} V^2 \right) \quad (3.4.15)$$

"TV" is the available power which is determined by the engine and "DV" is the required power. The difference of the two gives the excess power for the climb.

3.4.7. Steady Level Flight.

In this phase of the mission the goal is to attain the fastest time with the least amount of energy dissipated by the motor. The optimum speed for propeller-driven aircraft is defined in McCormick as

$$V_{opt} = \left[\frac{4}{\pi e A \rho_o^2} \frac{(W/S)^2}{\sigma^2 (f/s)} \right]^{1/4} \quad (3.4.16)$$

"f" is an approximation of the flat plate area of the aircraft and σ is the ratio of air mass density to sea level density, which is for our case approximately equal to one. The time of steady-level flight can be calculated by multiplying the distance of steady level flight by this optimum cruise velocity. The overall distance of steady level flight is a function that is dependent on both the rate of climb and descent.

The energy required for steady level flight can be determined by a simple energy balance

$$E = Wh + \frac{1}{2} \frac{W}{g} V^2 \quad (3.4.17)$$

3.4.8. Turning.

A high turn rate is essential for the 180 and 360 degree turns that must be made during the flight. The turn rate is defined in terms of the centripetal acceleration which in turn is dependent on the velocity of the aircraft as well as the turn radius.

$$\dot{\psi} = a / V \quad (3.4.18)$$

$$a = \frac{V^2}{R} \quad (3.4.19)$$

$$R = \frac{2W}{\rho S C_L g \sin \phi} \quad (3.4.20)$$

A higher turning rate is determined by the centripetal acceleration and in turn the size of the turn radius. Essentially the governing factors for a higher turn rate are the bank angle, " ϕ ", and the

velocity of the aircraft as well as the sizing of the aircraft. Another important factor to consider during turning is the bank angle that will stall the inner wing. The bank angle that will create a one-wing stall is defined by Raymer as

$$\phi_{stall} = \cos^{-1} \left(\left(\frac{V_{inner}}{V_{cg}} - 1 \right) \left(\frac{-2R}{b} \right) \right) \quad (3.4.18)$$

" V_{inner} " will be the stall velocity of the aircraft.

3.4.9. Descent. For descent the aircraft will land within the runway limits and therefore there are three aspects of descent that are of interest: air distance, transition distance, and the ground distance which are all defined from McCormick as

$$S_A = \frac{SH}{\theta_D} + \frac{V_A^2 \theta_D}{0.4g} \quad (3.4.19)$$

$$S_{TRAN} = 2V_A \quad (3.4.20)$$

$$S_G = \frac{V_A^2}{2a} \quad (3.4.21)$$

From these equations it can be seen that the main factor is the approach speed which must be optimized for the ground distance. To determine the time to land the aircraft it will be assumed that the approach velocity will be constant with no flaps and thus time in the air and transition zone will be simply

$$t = \frac{S_A + S_{TRAN}}{V_A} \quad (3.4.22)$$

and time for the ground portion will be

$$t = \frac{V_f - V_A}{a} \quad (3.4.23)$$

" a " is the deceleration due to drag and friction with the ground. If breaks are considered for the UAV then the coefficient of friction on dry concrete will be 0.4, which is a value taken from Raymer for this case. Energy for the landing is not as important since the engine will not be put in reverse thrust. If breaks are implemented then they will be connected to a separate energy source.

3.5. Results.

For results from conceptual analysis a wing area and wing span must be selected. A program to determine the optimal wing area and wing span was used. The program inputs will be the wing span and wing area and the outputs will produce approximated FBT and HSFT. The outputs will determine the initial wing geometry. The lift coefficient will be evaluated for a NACA 4409 airfoil for initial estimates. The following table is a selection of wing geometries that give the UAV adequate lift and fulfill the mission requirements.

$S_w(\text{ft}^2)$	$b \text{ (ft)}$	$S/W \text{ (oz/in}^2\text{)}$	V_{stall}	$C_{D_Takeoff/landing}$ $\alpha=15^\circ$	C_{D_climb} $\alpha=10^\circ$	Max Takeoff distance	FBT (min)	HSFT (min)
6	6	0.46	48.36	0.24	0.21	140.36	2.71	2.89
7	6	0.40	44.77	0.27	0.23	124.37	2.64	2.78
7	7	0.40	44.77	0.22	0.19	121.00	2.74	3.00
7	8	0.40	44.77	0.19	0.17	112.93	2.85	3.23
8	6	0.35	41.88	0.29	0.25	112.61	2.61	2.70
8	7	0.35	41.88	0.24	0.21	104.99	2.68	2.90
8	8	0.35	41.88	0.21	0.18	100.57	2.77	3.11
9	6	0.30	39.48	0.32	0.27	103.71	2.59	2.64
9	7	0.30	39.48	0.26	0.22	95.61	2.64	2.83
9	8	0.30	39.48	0.22	0.19	91.00	2.72	3.02

Figure 3.5.1. Initial wing sizing

3.6. Conclusions.

The results in the data table are approximated results based on approximate fuselage sizing and tail sizing. The program used the equations discussed earlier to find the total time for both missions. Based on these results the optimum wing sizing is the 9 square foot wing area with a 6 foot wing span. The lower aspect ratio wing gives faster times for both missions because the aspect ratio is in the denominator for equation (3.4.17) during cruise. However, the aspect ratio wing gives the highest drag coefficient and the longest takeoff distance. To make up for this the wing is larger and the wing loading is smaller and thus the takeoff distance is sufficient.

4. Preliminary Design

The conceptual design phase analyzed different wing sizes and geometries that would meet the mission requirements and then the optimum wing size and geometry was used based on the results. Based on this wing geometry the tail and fuselage sizing will be determined through programs that compute aerodynamic algorithms. The empennage and fuselage size will be optimized to give a static margin around 10%. The water tank will be determined and drainage time will be analyzed based on an algorithm based program and from this an optimal water tank shape and size will be determined. After the sizing has been completed a more intricate analysis on Drag will be performed using CFD methods through COSMOS Flowworks. These drag calculations will then be iterated into the equations for performance discussed in the conceptual design

4.1. Design Parameters and Sizing Trades.

4.1.1. Airfoil Design.

For selection of the airfoil a program called design foil was used to calculate polar curves. It was determined that NACA four-digit airfoils fit the needs of the UAV design and thus a four digit airfoil must be selected. From analysis of the range of airfoils that could be used to give the aircraft sufficient lift during takeoff and steady level flight it was determined that NACA 4409 would be the correct airfoil for the missions. The NACA 4409 has enough camber to allow the aircraft to fly with a zero degree wing incidence at steady level flight thus decreasing the drag from a flat plate area. The airfoil polar curves were generated by DesignFoil below:

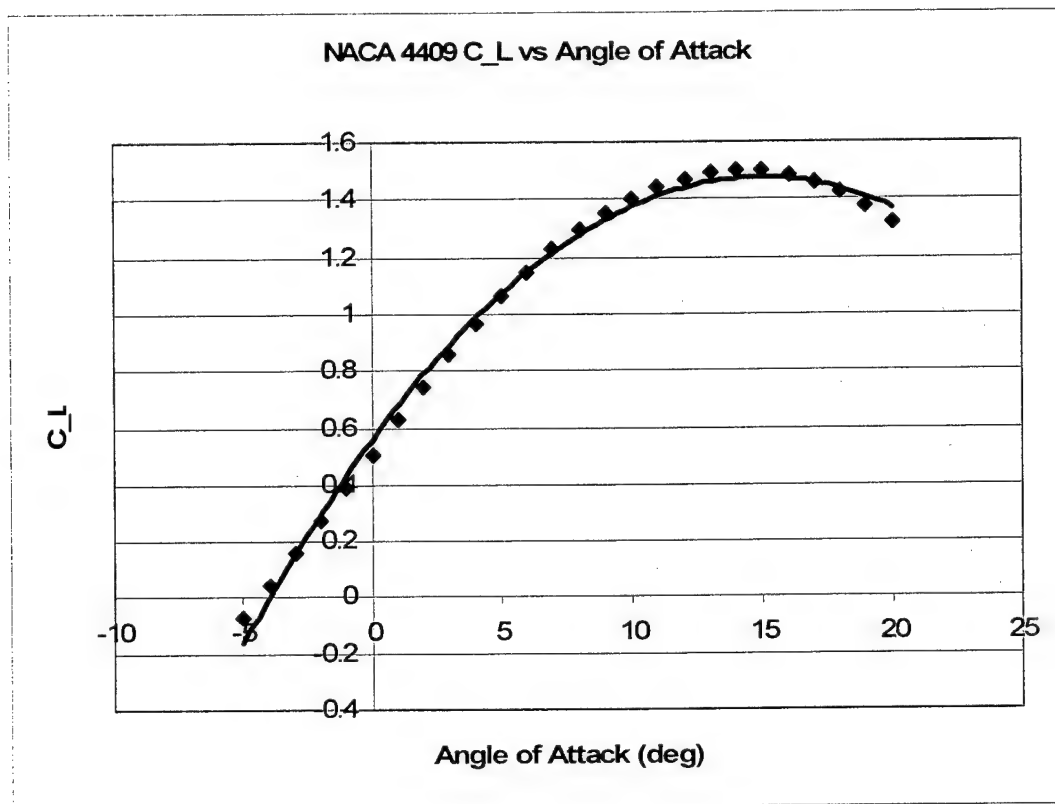


Figure 4.1.1. Polar curve for NACA 4409 airfoil

4.1.2. Estimating Maximum Lift Coefficient.

For initial estimates the maximum lift coefficient for the wing will be based on the NACA 4409 airfoil. However, the maximum lift coefficient of the airfoil is not equal to the max lift coefficient of the wing. The actual maximum lift coefficient of the wing is slightly smaller than the max lift coefficient of the airfoil. Raymer approximates the max coefficient of the airfoil to be around 90%. And thus the maximum lift coefficient will be about 1.35. According to the results at the end of the preliminary design an airfoil will be selected that will give the optimal lift to drag ratios.

4.1.3. Wing Area and Wing Span.

From analysis of wing sizing it was concluded that a 9 square foot area and 6 foot wing span would be optimum for the competition. This configuration gave the lowest mission times. However, since it is an approximation critical trading issues must be considered. From understanding equation (3.4.9) a lower aspect ratio wing will have more drag than a high aspect ratio wing. On takeoff and landing it would be optimal to have a large aspect ratio to reduce takeoff distance. However, at cruise the optimum velocity equation, equation (3.4.16), shows that the lower aspect ratio wing will create a higher optimum cruise velocity. This concept is easily understandable by

looking at gliders compared to sport flying airplanes. Because the most important factor is time of the mission it is concluded that a low aspect ratio would be implemented in the design.

With this low aspect ratio, however, there must be enough wing area to decrease the wing loading and thus decrease takeoff distance. From the table it can be seen that the larger wing area gives better times, because takeoff distance decreases and thus the aircraft will reach the optimum cruise velocity faster. Wing spans exceeding eight feet were not considered, because the wing pieces would not be able to fit in the box constraint without making out of more than two pieces. This needlessly complicates the task.

4.1.3.1 Down Wash from the wing.

It is important to know the effects of the downwash, w , because it causes some kind of deflection of flow downward at the tail, which will reduce the angle of attack. This vertical flow will effect stability calculations and thus must be analyzed. The angle at which this deflection of air towards the tail occurs is denoted as ϵ , and is defined in McCormick as

$$\epsilon = \frac{w}{V} = \epsilon_\alpha \alpha \quad (4.1.1)$$

ϵ_α is equal to the rate of change of ϵ with α , angle of attack, and this rate is useful for calculating longitudinal static stability, which will be discussed in detail later. To find w the Biot-Savart law must be implemented because a vortex line is in consideration. McCormick defines the w as

$$w = k \frac{\gamma}{4\pi h} (\cos \alpha + \cos \beta) \quad (4.1.2)$$

In this equation the height, 'h', is the height of the tail above the centerline where ' α ' and ' β ' are the angles that the tail ac makes with the ends of the circulation line considered.

4.1.4. Static Stability Analysis.

4.1.4.1. Fuselage and Empennage Sizing.

For initial sizing of the fuselage front plate area was kept to a minimum. It was assumed that all the batteries would be stored in the forward section of the fuselage. This means that a minimum area of about four square inches would be the front plate area after storage of these components were taken into considerations. The other governing factor for fuselage length was the empennage which is determined based on the moment arm of the tail aerodynamic center with the aerodynamic center of the wing. Having a short moment arm even though it decreases the RAC makes the tail surface area much bigger to make up for stability. Having a larger tail causes

more drag. However, with a longer moment arm and thus smaller tail, the RAC is larger because of the longer length of the fuselage. Making the fuselage longer than four feet also requires a detachable emennage. The joint will need to be strengthened and thus an added weight must be considered as one of the trade-offs for the longer fuselage. A compromise must be made that will give the airplane more than adequate stability while also keeping the RAC down to a minimum.

To determine the optimum tail sizing for the UAV design a program called DBF_Hstab was written based on algorithms from the static stability analysis presented in McCormick. The optimum design will decrease the flight time while keeping the RAC to a minimum. The main factors for the longitudinal stability were the location of the neutral point, the tail sizing, and the incidence angle of the tail which are defined in McCormick as

$$\text{Neutral Point} = \frac{h_{nw} + h_t \eta_t \frac{S_t}{S} \frac{a_t}{a_w} (1 - \varepsilon_\alpha)}{1 + \eta_t \frac{S_t}{S} \frac{a_t}{a_w} (1 - \varepsilon_\alpha)} \quad (4.1.3)$$

$$\text{Area of Horizontal Stabilizer} = \frac{V_H l_t}{Sc} \quad (4.1.4)$$

$$\text{Incidence of Horizontal Stabilizer} = - \frac{C_{Mac} C_{L\alpha} + C_{M\alpha} C_L}{C_{L\alpha} C_{Mi} - C_{M\alpha} C_{Li}} \quad (4.1.5)$$

In the equation for the neutral point the downwash is one of the determining factors. If it is too large then the neutral point will be placed in front of the leading edge of the wing. This would mean that the center of gravity for a 10% static margin would have to be somewhere near the nose of the aircraft. Having the center of gravity be forward on the fuselage is desirable to prevent the airplane from pitching up, but having the center of gravity be too far forward is undesirable because it will cause a damping moment that is too large and may cause the airplane to become unstable.

The incidence of the horizontal stabilizer with respect to the tail center line was determined by summing the lift coefficients for the aircraft up and then solving for the angle of attack which was substituted into a moment balance equation and then the moment of the aircraft was set equal to zero for stability. In this manner the incidence was determined.

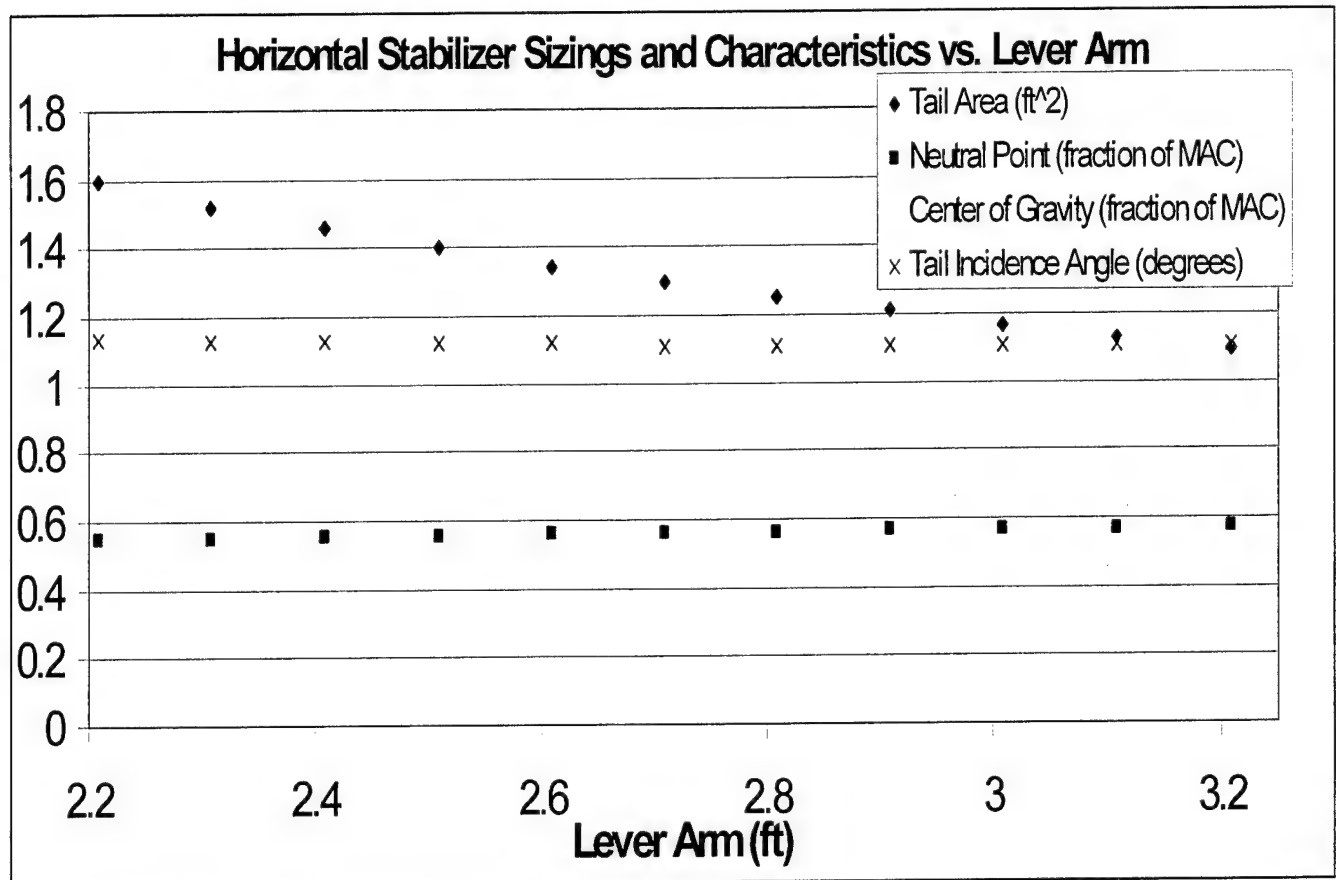


Figure 4.1.1. Longitudinal stability

In the same manner as the horizontal tail, the vertical tail area was determined by summing up all the directional (yaw) moments of the airplane and finding an adequate surface area that would meet zero yaw stability. A program was written based on algorithms taken from McCormick that found the vertical tail span and surface area. The program summed up the yawing moments due to the different components of the aircraft and then the vertical tail surface contribution to yawing was determined and the resulting area was calculated.

Lateral stability of the aircraft was also a consideration in the static stability analysis for the UAV. The two main contributions to lateral stability are wing placement and dihedral.

4.1.3.2. Wing placement on the fuselage and wing Dihedral.

McCormick says that a negative value of the rate of change of rolling moment with sideslip angle, $C_{l\beta}$, is important to the handling qualities of the aircraft. $C_{l\beta}$ is effected by the wing placement and the dihedral of the wing and is defined respectively as

$$\text{Low-wing } \Delta C_{l\beta} = 0.00016 / \text{deg} \quad (4.1.6)$$

$$C_{l\beta} = -\frac{\alpha}{6} \left(\frac{1+2\lambda}{1+\lambda} \right) \Gamma \quad (4.1.7)$$

The dihedral effects on the lateral stability of the aircraft are considerable compared to the low-wing configuration. The resulting lateral moment coefficient is negative. It was decided to go with a small dihedral angle, because if the dihedral is too large then the moment will be too high. This large stabilizing moment will actually spin the aircraft if it is high enough and cause much difficulty for control of the aircraft.

4.1.5. Control Analysis.

For control of the airplane to perform a maneuver there will be ailerons for lateral control, an elevator for pitch, and a rudder for yaw. The sizing of these different control surfaces will each be analyzed and then determined based on historical data. Stick forces will not be considered, because servo torque ratings are well above the loads that the control surfaces will feel. In the detail design a dynamic stability analysis will be performed. If any instabilities are found then the control surfaces and stabilizers will be resized.

4.1.5.1. Elevator Sizing.

The elevator will be the conventional surface that extends along the span of the horizontal stabilizer. The chord of the elevator will be 35 % of the chord of the horizontal stabilizer which is a value taken from typical RC aircraft that will give adequate control. The elevator will not need an aerodynamic balance, because the servo torque is large enough to handle control surface loads. This conclusion was made based on research of typical UAV aircraft operating at similar speeds and control requirements.

4.1.5.2. Aileron Sizing.

The ailerons sizing will be determined based on historical guideline for aileron sizing discussed in Ramer. For "IGI" the aileron will be 50% to 80% the span of the wing. The chord of the aileron will be from 15% to 20% of the wing chord. It is better to have the ailerons closer to the tips to give more control of the aircraft. Therefore the Aileron will be 50% of the span with 20% of the chord of the wing.

4.1.5.3. Rudder Sizing.

Like the elevator the rudder will run along the entire span of the vertical stabilizer and the chord percentage will be from 30%

4.1.6. Motor Selection.

The motor will be selected based on the optimal propeller-motor combination that will give a high thrust number while keeping the amp draw down to a specified rating. It is important that the motor-propeller combination gives the aircraft a high max velocity, while also giving enough thrust to lift-off within the specified take-off distance. MOTOCALC 7.08, an RC motor analysis program was implemented and the Astroflight 90 direct drive and gear box were compared to see which one could operate at higher velocities. The direct drive allowed the aircraft to reach a max velocity of 73 mph, while the gear box only allowed the aircraft to reach a max velocity of 41 mph. Based on this analysis it was decided to go with the Astroflight 90 direct drive motor.

4.1.7. Propeller Diameter and Pitch.

The Astroflight online store offers differing propeller sizes for different rpms and power settings. All of the suggested propeller sizes will be considered for later analysis.

4.1.8. Battery Weight.

The battery weight will range from 3 lbs to 5 lbs based, because of the necessary voltage for the high power setting of the Astroflight 90 engine. Different combinations of battery amperage settings with battery weights will be analyzed and the optimum combination will be chosen.

4.1.9. Landing Gear Selection

Due to initial design considerations, it had been decided that a tail-dragger set up would be used for the landing gear. This would increase the angle of attack during take off dramatically, thus reducing the time required to lift off. Also, such a configuration would allow for more prop clearance due to the tilt angle of the plane. With that decided, considerations had to be made for fixed or retractable gear, with or without brakes. Factors taken into consideration to help make this decision included drag, weight, cost, and landing distance. According to the matrix shown below, it was decided to go with a fixed landing gear set up that included brakes.

		Drag	Weight	Landing	Cost	TOTAL
weighing factor		3	3	2	1	
Fixed gear	brakes	0	2	0	2	8
	no brakes	0	2	1	1	9
Retractable gear	brakes	1	0	0	0	3
	no brakes	1	0	1	0	4

Figure 4.1.2. Landing gear figure of merit

4.1.10. Loading Factor during turning.

A very important design parameter to consider for the structure of the aircraft is the ultimate loading on the wing during turning. Depending on the maximum bank angle during a steady turn this load factor is defined as

$$n = \sqrt{\left(\frac{\psi V}{g}\right)^2 + 1} \quad (4.1.8)$$

The ultimate load of the aircraft is always larger than this turning load and can be estimated with a 1.5 margin of safety. The ultimate load is estimated for a sustained turn at a differing bank angles and speeds falls within the range of 6-9 g's.

4.1.11. Water Tank Sizing.

To analyze the drainage time for the water tank an unsteady control volume analysis was used. A program was written called DBF_tanktime based on the continuity equation which is defined in Munson as

$$\frac{\delta}{\delta t} \int_{cv} \rho dV + \int_{cs} \rho \underline{w} \cdot \underline{n} dA = 0 \quad (4.1.9)$$

After separating and integrating the time to drain for a tank given both width and depth as functions of heights the drainage time can be determined. Time for the tank to drain is defined as

$$t_{drainage} = \int_0^h \frac{x(h)w(h) + h \left[\frac{dx(h)}{dh} w(h) + x(h) \frac{dw(h)}{dh} \right]}{A_h \sqrt{2gh}} dh \quad (4.1.10)$$

In the above equation $x(h)$ is the length, $w(h)$ is the depth, and h is the height of the tank. A_h is the area out of which the water drains from. Inputs would have symmetrical tanks both in the fuselage span direction and length direction. To minimize the drain time one must maximize the height at which the water drains. Therefore, it is best to have the majority of the water volume up high in tank and a drainage tube extending from the center of the bottom of the tank downward a certain distance. It was found that the longer the drainage tube the faster the water drains. However, the analysis does consider the friction within the tube. From experiments it was found that the tube did not drain as fast as theoretical predictions because of this friction. Therefore a compromise was made and a tube height of 12 inches was selected as the drainage tube. The

configuration of the tank sizing that gave a drainage time of around 12 seconds is sized up in the figure below.

4.1.12. Aircraft drag.

From determining the optimum sizing for the aircraft it is now possible to iterate these sizing into the drag equations discussed in the conceptual analysis section and find a more accurate result for the component build up drag.

Another consideration that must be made is the drag from the cylinder. The C_D for the cylinder was estimated to be 1.1 taken from Munson. This coefficient gives a drag of 0.544 lbs, which correlates to 81.5 oz-in of torque acting at the pivot. This was found by modeling the cylinder as a cantilever beam with a distributed force acting across it. The resultant moment is large enough so that a high-torque servo is required for reliable performance.

4.1.13. Performance.

4.1.13.1. Takeoff.

More accurate takeoff distances were determined by iteration of optimized drag and thrust with the decided airplane sizing into the performance equations. The takeoff distance is well within the required distance, because the wing loading was so low.

4.1.13.2. Accelerated Climb.

In the accelerated climb regime of the flight mission there are several aspects that must be considered: Best rate of climb, best angle of climb, and a rate of climb that will allow the UAV to reach maximum velocity as quickly as possible. The best Rate of climb will get the aircraft to the steady level flight regime the quickest. However, it will also incur drag penalties that will reduce mission time. The best angle of time is only sought after if the aircraft must clear high obstacles as quickly as possible. Again this is not sought after for the mission at hand, because the aircraft will incur horizontal velocity penalties and thus give the lowest mission time. Therefore a rate of climb and angle of climb that is optimum for the aircraft to reach maximum horizontal velocity is of the most important. The optimum rate of climb and climb angle are determined by graphical analysis through plotting the rate of climb vs horizontal velocity which is shown on the following page.

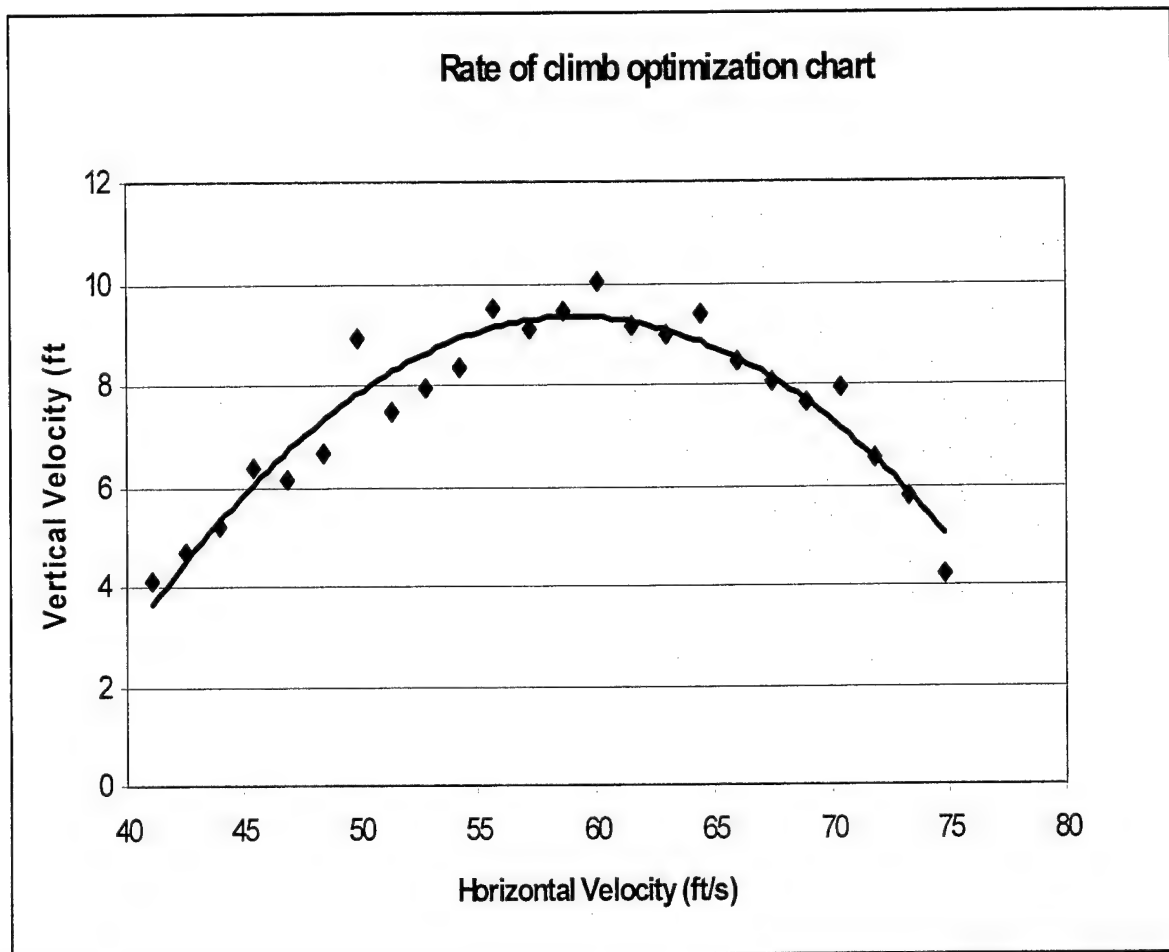


Figure 4.1.3. Rate of climb optimization

From analyzing this graph the optimum rate of climb will be around six ft/sec which will allow the aircraft to accelerate to a maximum 75 ft/ second. This is important for mission times.

4.1.13.3. Steady Level Flight.

For conceptual analysis the optimum speed equation was implemented for steady level flight to determine the optimum wing geometry. Now that the geometry has been optimized an analysis to find the maximum speed of the aircraft was implemented. Maximum speed during steady level flight takes place when the thrust curve intersects with the drag curve. Better drag calculations based on a narrower range for the sizing of the aircraft as well as better thrust numbers based on conceptual analysis coupled with motocalc program gave accurate thrust and drag curves. The maximum velocity was determined by intersection point of the two curves in the following plot

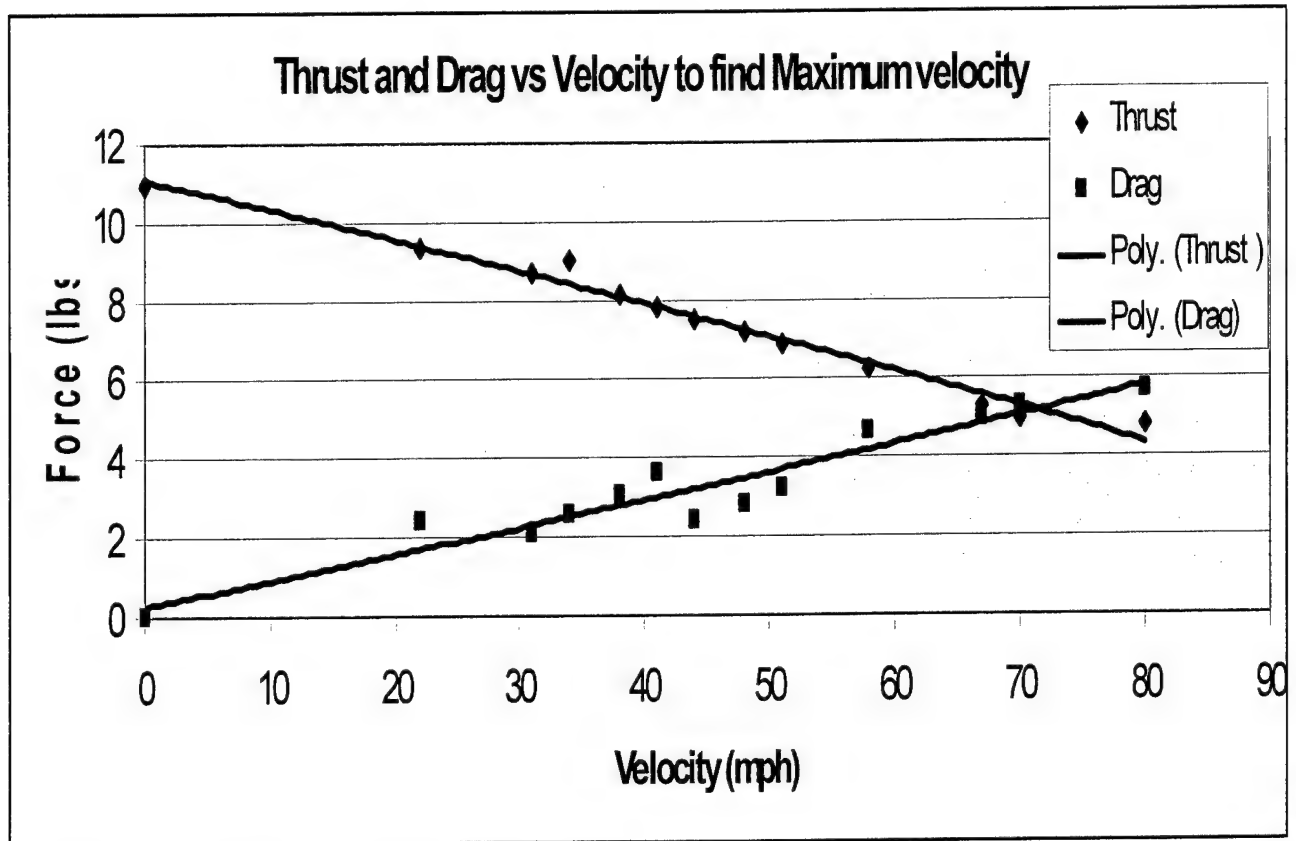


Figure 4.1.4. Maximum Velocity determination

The graph shows that the maximum velocity is around 72 mph.

4.1.13.4. Turning.

During the downwind segment of the fire-bomber flight the entire gallon of water must be drained. Earlier in the preliminary analysis it was discussed that radius size of the turn will be increased to give the airplane more time to drain the water. By doing this IGI does not have to have any flaps to slow down the aircraft. On this leg of the mission the turn time will need to be about four to five seconds long in order for the entire gallon to drain. From optimized sizing of the aircraft the bank angle and turn radius for this time will need to be 140 foot radius which gives a bank angle of about 30 degrees.

4.1.13.5. Descent and Landing.

The main issue with Descent and Landing is whether or not breaks are required. The aircraft has been designed for high cruise speeds, which means that on descent the aircraft will be coming at high approach speeds. The resulting landing distance will be too long. To shorten landing distance either breaks or spoilers may be considered. Spoilers are not practical, because they increase weight more than breaks while also adding to the complexity of the aircraft wing structure. The breaks, however, are an independent structure and less heavy as well. For this reason since the landing distance is so long breaks will be added to the wheels which will increase acceleration by a factor of

4.2. Optimization techniques and results.

The sizing for the aircraft will be determined based on the analysis discussed in this section. Iterative results will be used to find the horizontal and vertical stabilizer sizing based on statically stable conditions. Also control surfaces will be initially sized based on historical data and altered later according to performance optimization restrictions.

4.2.1. Aircraft Sizing Parameter.

Design Parameter	Value
Wing Area (S_w) ft^2	9
Wing Span (b) ft	6
Horizontal Stabilizer Area (S_h) ft^2	1.6
Horizontal Stabilizer Span (b_h) ft	1.5
Vertical Stabilizer Area (S_v) ft^2	.8
Vertical Stabilizer Span (b_v) ft	0.8
Elevator Chord (% of Horizontal Stabilizer chord)	30
Elevator Span (b_e) ft	1.5
Rudder Chord (% of the Vertical Stabilizer chord)	30
Rudder Span (b_r) ft	0.8
Aileron Chord (% of wing chord)	20
Aileron Span (b_a) (% of wing span)	50
Wing Dihedral (Γ)	2
Wing Placement on Fuselage	Low
Number of motors	1
Motor	Astroflight 691
Propeller Diameter x Pitch (in)	14x10,15x10,16x10

Figure 4.2.1. Optimized aircraft sizing table

4.2.2. Aerodynamic and Stability Characteristics.

The following are stability and aerodynamic characteristics of "IGI"

Characteristic	Value
Maximum Lift Coefficient	1.35
Drag Coefficient at Takeoff	0.323353
Drag Coefficient at Climb	0.2761
Maximum Takeoff Distance (FBS)	132.7046
Maximum Takeoff Distance (HSFS)	124.5842
Static Margin	10%
Yaw Stability Derivative	.05

Figure 4.2.2. Aerodynamic and stability characteristics table

4.2.3. Performance of "IGI".

Performance Parameters	Value
RAC	
Time FBT	2.373979
Time HSFT	2.275037

Figure 4.2.3. Performance Optimization

4.3. Conclusions.

From analysis of different sizing and optimization techniques the performance parameters indicate a reduction in time which means an optimized aircraft is taking form. In the detail analysis the Calculation errors will be corrected and data will be iterated to find better optimized results for "IGI".

5. Detail Design

5.1. Main Wing.

The rectangular wing with a low aspect ratio is key to reaching a maximum velocity. Improvements upon the wing must be considered. Analysis into the effects of a blended wing portion into the fuselage, the effects of wing plates, and also the effects of twist will be explored and considered.

5.1.1. Blended Wing Portion.

Analysis on the effects of blending a portion of the wing by reducing the total wetted area of the aircraft. This effects the drag of the aircraft. Also, the blended wing effects the drag by eliminating the interference drag effects from the joint of the wing and fuselage.

5.1.2. Wing End Plates.

Wing plates effect the wing by increasing the effective aspect ratio by the following relation defined in Raymer as

$$A_{effective} = A(1 + 1.9h / b) \quad (5.1.1)$$

Increasing the effective aspect ratios by adding end plates on wings that already have high aspect ratios barely affects the aspect ratio. However, low aspect ratio wings will be affected much more. For "IGI" it is beneficial to add endplates because induced drag effects will be felt by the effective aspect ratio making the induced drag smaller, while still giving us a high maximum velocity. Adding wing plates, however, does raise the aircraft cost slightly since it is a vertical surface. Therefore, plates will be added to the wing. The endplate size will be chosen based on structural reliability, because the wing tips will experience a lifting force from the flow cross-over at the tips of the wing.

5.1.3. Twist and washout.

Twist on a wing is used to prevent the wing tips from stalling while also making the lift distribution closer to the ideal elliptical lift distribution. For making turns that reduce the inner wing velocity to V_{stall} having a twist would be beneficial. Twist however is very difficult to manufacture and for this reason will not be implemented in the design.

5.2. Airfoil Refinement.

The NACA 4409 airfoil was initially chosen because it gives enough camber to allow the aircraft to fly without any wing incidence angle. However, after further analysis it is seen that the NACA 4409 gives slightly too much lift and therefore can be reduced in maximum thickness. The allowable thickness for the airfoil depends on the servo placement within the wing. The allowable thickness was calculated to be 1.4 inches. This means that a NACA 4408 airfoil can be used, which will have lift and drag characteristics that are virtually the same as the NACA 4409.

5.3. Drag Refinements.

With optimized results of the final sizing of the aircraft drag calculations based on the conceptual analysis was once again iterated. CFD was also implemented by using COSMOS Flowworks to study the pressure distribution across an object. This analysis is limited, however, because of limited computing power. COSMOS meshes the object to be tested in a flow and then it solves the flow characteristics of each fluid cell. To analyze a large structure like the wing the mesh would need to solve around 900,000 cells, which would take more than a week to solve. Therefore, only analysis of structures that have less than 200,000 fluid cells were considered for special drag analysis. The resulting drags calculated through using this program will be iterated into the drag equations defined earlier and a new more accurate drag will be calculated.

5.3.1. Cylinder drag.

The cylinder drag calculates the flow across the cylinder which was previously estimated to be about 0.544 lbs. This estimate was based off of historical data taken from Munson. COSMOS analyzed the flow past the cylinder during deployment period as shown below

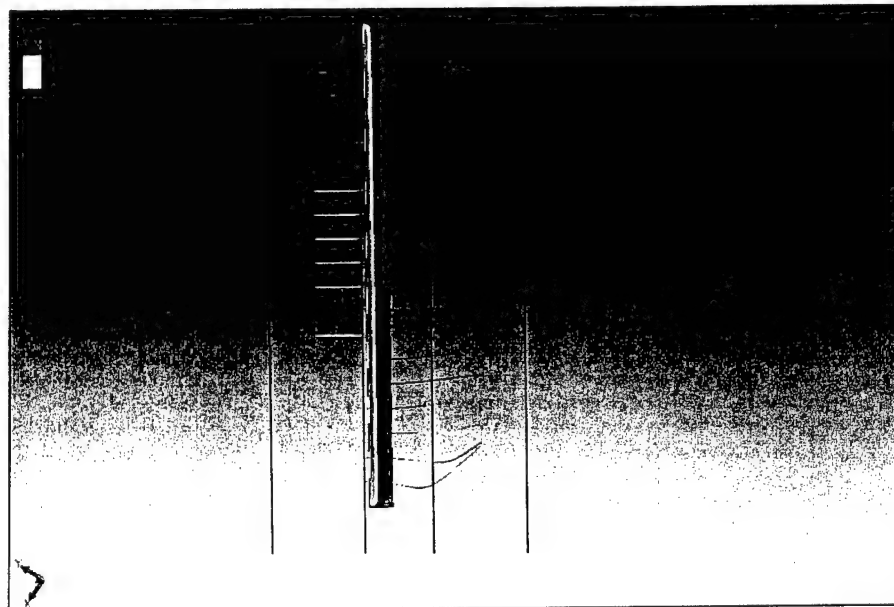


Figure 5.3.1. Cylinder drag during cruise conditions using COSMOS FlowWorks

COSMOS FlowWorks calculated resulting forces on the cylinder to be

Force [lbf]	
x-component of force [lbf]	0.349
y-component of force [lbf]	-0.00187
z-component of force [lbf]	0.00038

Figure 5.3.2. Force on cylinder

The x-component is the drag on the cylinder. This drag is more accurate than the previous approximation for the cylinder. The torque on the joint due to a distributed load with the resultant force acting on the center of the cylinder is calculated to be 49.97 oz-in, which is almost half as large as the previous estimation. Even though the cylinder will not need a high torque servo to rotate the wheel, the weather conditions could be unfavorable and thus a high torque servo will be used to ensure mission success.

5.3.2. Landing Gear Drag.

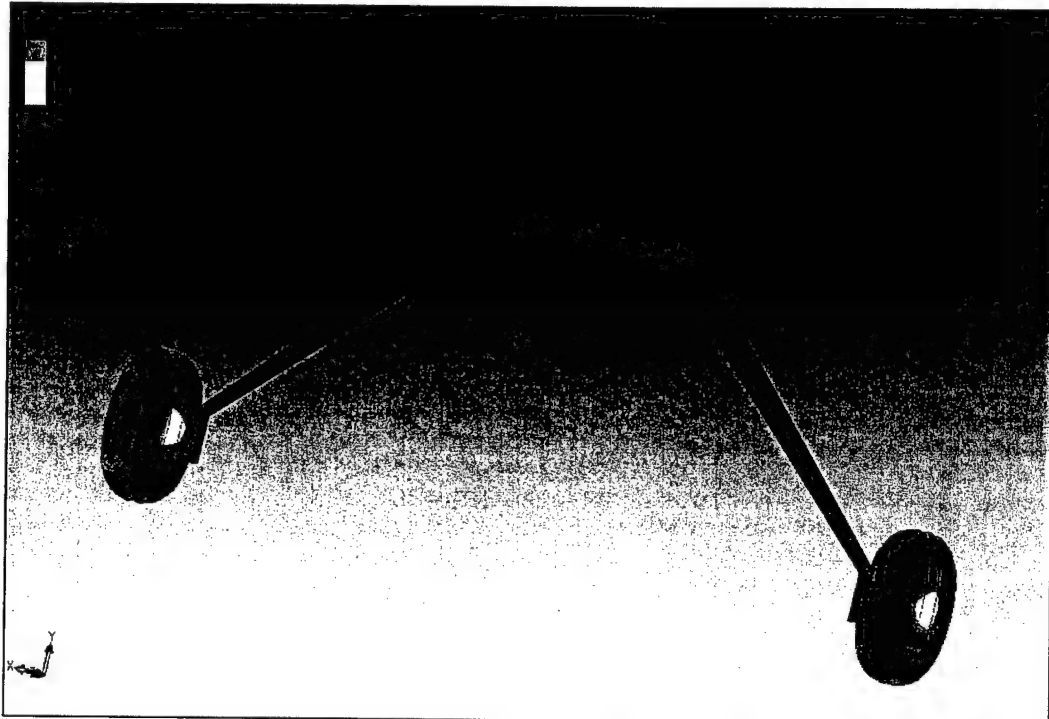


Figure 5.3.3. Landing gear COSMOS Flowworks analysis for drag without fairings

Force [lbf]	
x-component of force [lbf]	0.00712
y-component of force [lbf]	0.0118
z-component of force [lbf]	0.29

Figure 5.3.4. Forces on the landing gear without fairings

The z-component is the Drag on the landing gear. When the landing gear has fairings as in the following figure

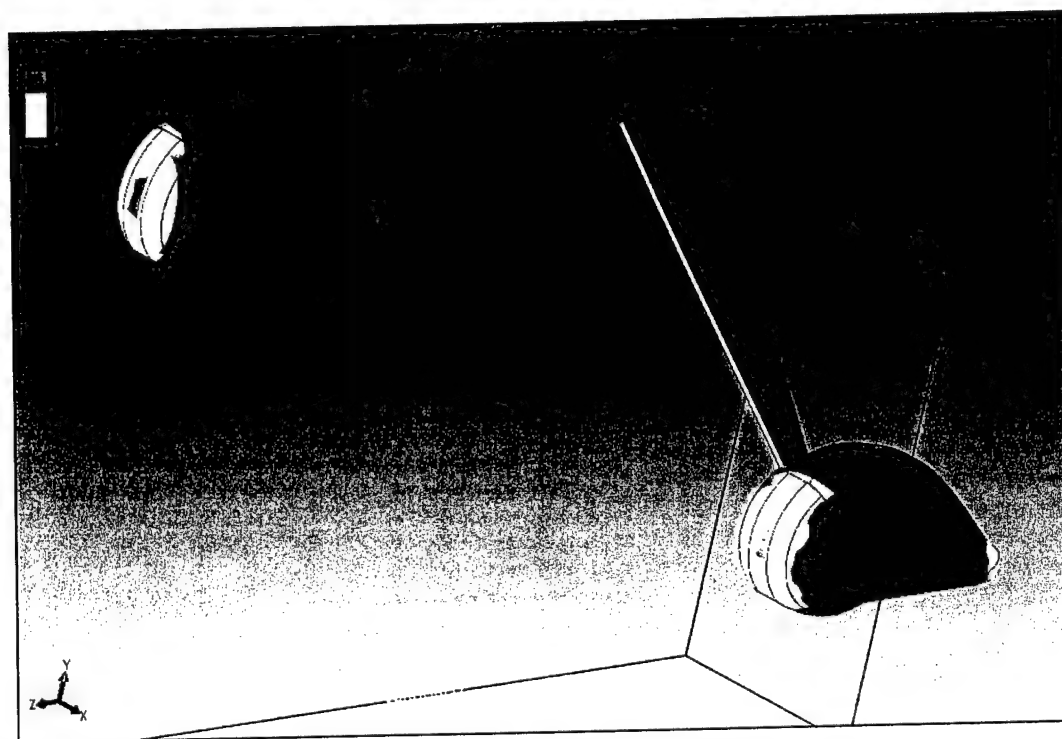


Figure 5.3.5. COSMOS FlowWorks analysis on landing gear with fairings

Force [lbf]	
x-component of force [lbf]	0.000514
y-component of force [lbf]	0.1231
z-component of force [lbf]	0.167

Figure 5.3.6. Forces on the landing gear with fairings

When the landing gear has fairings it is amazing to not that the drag is cut in half. Also, there is a lift component to the fairings due to the airfoil. Fairings are a good improvement and helpful to the mission success.

5.4. Propulsion optimization.

One of the first considerations in propulsion systems was the specific motor configuration for the plane. This was the selection between a single motor or multiple motors, and with the multiple motor configuration, an independent or shared battery source. When considering each option, the focus was tradeoff between performance and RAC. It was found that a multi-motor design with individual battery packs showed no advantage over a shared battery source design. With this shared battery configuration, there was a significant increase in power when compared to a single motor, thus translating into higher speeds and shorter lap times.

However, weight and RAC disadvantages were of even greater importance. With multiple motors, not only is the weight of the additional motor significant, but the corresponding support structure, which must be strong (and relatively heavy) to handle the new source of thrust. This additional weight is also detrimental when considering RAC, as reflected through the MEW score. Also, the additional motors add to the REP score, which has a coefficient multiplier of 1500. Therefore, it was decided to focus future propulsion research and design with a single motor in mind.

5.4.1. Motor Selection.

Knowing that a single motor would be used to drive a relatively heavy plane (preliminary weight estimations ranged between 20 to 28 lbs), immediate focus was on finding a powerful motor, in terms of torque and thrust. This was important for takeoff considerations (getting off within the 150 ft limitation) as well as the top speed of the airplane. This limited the search to Astroflight 60 or 90 series motors and Graupner 800 or 900 series motors. However, it was immediately seen using MotoCalc that with otherwise equivalent arrangements, Graupner motors could not match the thrust or efficiency ratings of Astroflight motors. This and the reliable history of Astroflight motors helped to further narrow the search for an appropriate motor.

The four motors remaining for consideration were the Astroflight 60 or 90, as well as the 2.75:1 geared versions of these motors. More thorough analysis was done with MotoCalc for each of these, varying key parameters such as propeller pitch and diameter, battery amperage rating, and battery weight, according to manufacturer's suggestions for optimal performance. It was found that, while the geared motors displayed an incredible amount of thrust, there was a significant reduction in projected top speed when compared to the direct drive motors. This increase in acceleration but decrease in velocity was seen to balance out in the Fire Flight mission, due to

two acceleration periods and minimal time at top speed. However, there was a serious disadvantage when looking at the Ferry mission, in which the majority of flight would be at or near maximum velocity. Therefore, the motor was decided to be a direct drive Astroflight.

The final consideration was between a 60 or 90 series motor. The data tables already produced were further analyzed: thrust and efficiency for both motors were found to be very similar. Of course, the 60 series weighs about 10 oz less than the 90, thus reducing the RAC. However, most configurations with the 60 series were projected to draw more than the allowable 40 amps from the motor. Adjustments in prop diameter and pitch were required to compensate for this fault. Doing so resulted in an efficiency and top speed loss of 5% and 14% respectively, when compared to similar Cobalt 90 projections. These performance values were found to be more important than the additional 10 oz weight (translating to an additional 0.188 RAC points), by considering the reduction in flight time for the Fire Flight and especially the Ferry mission.

5.4.2. Battery and Prop Selection.

With the motor selected according to a general analysis of all parameters, a more in-depth approach was taken for finding the optimal battery and propeller package based on specific variables. These areas of interest were battery rating, battery weight (or number of cells), propeller diameter, and propeller pitch.

The battery rating determines the projected lifetime of the battery cells. It was important to find batteries that would not die out given our flight estimation times. However, overshooting this time by a significant amount would indicate that there was excess energy not being utilized, and therefore acting as dead weight. For this purpose, batteries of 1700 mAh, 1900 mAh, and 2400 mAh were considered.

For each of the battery ratings, configurations ranging from four to five pounds were considered. Lower battery weight was a very important consideration in RAC because, as mentioned earlier, it affects both MEW and REP scores. However, lower weight implies less cells, which correlates to less power driving the motor. There was also a significant reduction in predicted top speed when using less batteries. This correlates to increased flight times, which must be weighted against any advantages gained from decreased RAC when considering the final score.

Propeller diameter and propeller pitch were varied through the full range of manufacturer's suggested optimal combinations. It was found immediately that pitch values of seven inches resulted in very low speeds without significant increases in thrust or power. Therefore, detailed tests were taken for 15 and 16 inch props with 10 inch pitch. Each test was noted for motor

current draw, projected battery life, thrust, and top speed. Both current draw and battery life were considered limiting factors in the decision. Because motor amperage is set to a maximum by the competition rules, any configuration drawing more than the 40 amps was given a "0", disqualifying it altogether. This was because accurate motor performance could not be projected. So as not to throw out potentially ideal models due to calculation limitations, a zero was only given when amperage draws where 43 or greater, signifying a relatively large discrepancy in performance when compared to the very close predicted values among test configurations. Similarly, projected mission times have been calculated so that any configuration with less battery life than required for the mission is also discredited with a "0" score.

For those combinations that were valid, thrust and maximum velocity were used to predict mission scores for both FFS and FS. These, combined with the effect of battery weight on RAC, were used to calculate a TFM (if either of the aforementioned limiting factors were zero, the TFM was shaded with gray to depict an invalid score). Note these calculations are only for the purpose of battery and prop selection. Although the RAC might not be exact, the relative change due to a one-pound increase is accurate, so that comparison amongst different scores is relevant in this study.

The table shows that a four-pound set of 1700 mAh results in the highest TFM. The actual score is the same for both propellers. However, due to excessive current draw, the 16 inch prop is not a viable option. Therefore, a 15 inch prop will be used with the battery package described above.

Battery Rating (mAh)	1700		1900		2400	
Battery Weight (lbf)	4	5	4	5	4	5
Current	1	0	1	0	1	1
Battery Life	1	0	1	1	1	1
Top Speed (ft/s)	98	108	87	101	81	92
Takeoff Thrust (oz)	170	187	150	176	130	158
RAC	13.5	15.3	13.5	15.3	13.5	15.3
FFS	0.84	0.86	0.81	0.85	0.79	0.82
FS	0.43	0.46	0.40	0.44	0.38	0.42
TFM	9.41	8.63	8.96	8.43	8.67	8.10

Figure 5.4.1. Propulsion test 15x10 prop

Battery Rating (mAh)	1700		1900		2400	
Battery Weight (lbf)	4	5	4	5	4	5
Current	0	0	1	0	1	0
Battery Life	1	0	1	1	1	1
Top Speed	98	108	87	101	81	92
Thrust	190	177	162	181	146	171
RAC	13.5	15.3	13.5	15.3	13.5	15.3
FFS	0.84	0.86	0.81	0.84	0.79	0.82
FS	0.43	0.46	0.40	0.44	0.39	0.42
TFM	9.41	8.63	8.96	8.37	8.74	8.10

Figure 5.4.2. 16x10 prop

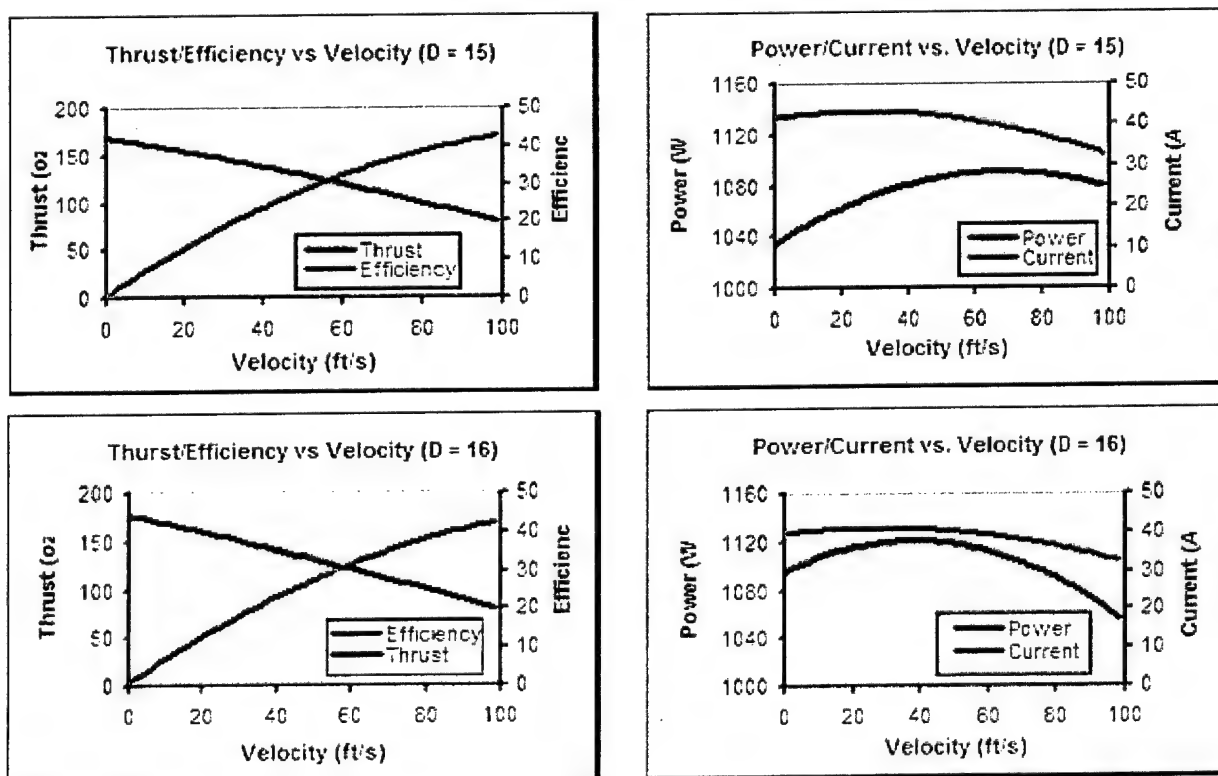


Figure 5.4.3. Motor performance for 15 and 16 inch diameter prop

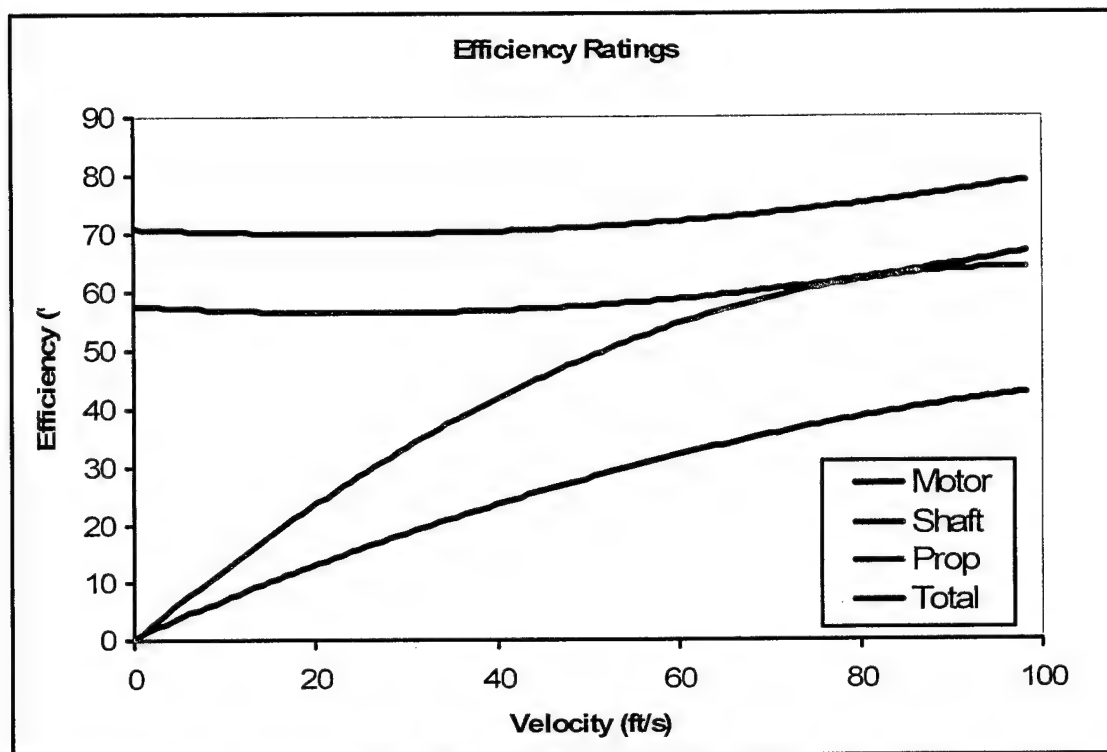


Figure 5.4.4. Efficiency for 15x10

5.5. Wing Joint Analysis.

To better support the ribbed wing structure, main wing supports were selected both at the leading edge and trailing edge. The otherwise hollowed out wing will have a female plug at both ends of the wing, with the male insert attached firmly to the fuselage. To actually fasten the wing, two nylon bolts will be screwed through each edge, for a total of four per wing. This design is also advantageous in situations where the aircraft might land wing-first. The nylon bolt design should allow the bolts to break in shear stress, so that the wings would disengage from the fuselage with minimal damage in case of a very awkward landing or complete crash.

The wings were designed not only for the estimated 25 to 28 pounds of lift, but also to withstand the estimated 7.5g acceleration during tight turns. For this reason, the leading edge screws bolt in horizontally through the vertical mount, while the trailing edge screws bolt in vertically through the horizontal mount. The male plug itself will be balsa with thin plywood doublers, providing ample strength with minimal weight. Although this assembly may seem a bit complicated, it was noted early on that assembly time was not a factor in scoring this year. For that reason, relatively time-consuming attachments were accepted as design possibilities.

Model name: leading edge wing piece
 Study name: def
 Plot type: Static Model stress - Plot1
 Deformation Scale: 1404.74

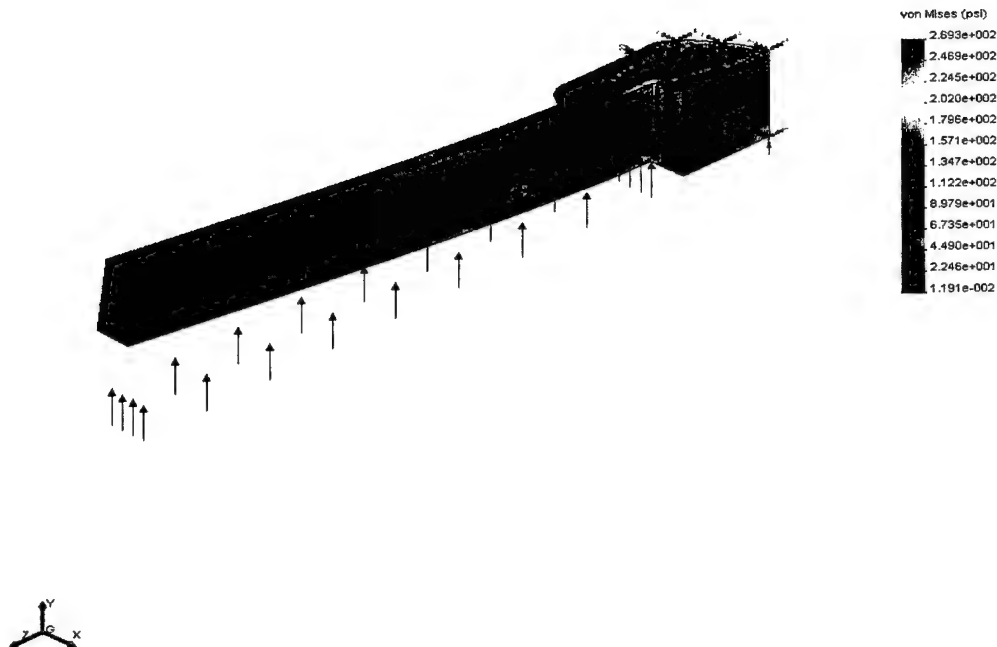


Figure 5.5.1. stress distribution for wing joint

5.6. Water Deployment System.

It had been found that an extendable hose leading from the water outlet would greatly decrease the drainage time. To accommodate this mechanism, it was decided that a high torque servo should be placed close enough to the joint to translate adequate force for the pushing/pulling of the hose. The servo is connected with a pushrod to a small circular bracket sliding along the hose; the hose itself pivots from the nozzle base. Thus, the entire joint can be modeled as a four-bar mechanism with one sliding joint. Due to this degree of freedom, small adjustments could be made easily (such as varying pushrod length) if found necessary during flight testing.

By looking at the configuration, it was found that the same servo could simultaneously open the water valve, so that the water would start to drain just as the hose becomes vertical. This is simply a direct connection from the second control arm of the servo horn to the valve control arm: as modeled, a 90° rotation in the servo would completely open or close the valve with a direct pushrod linkage.

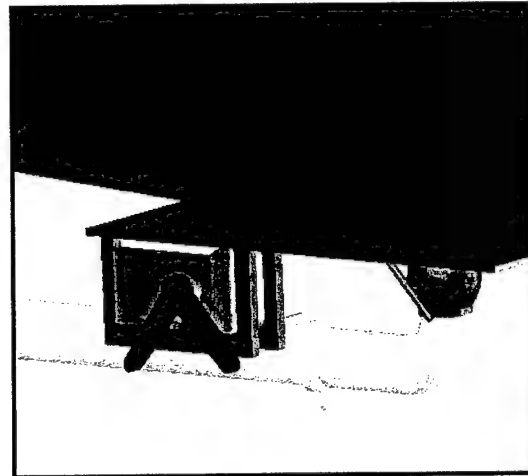
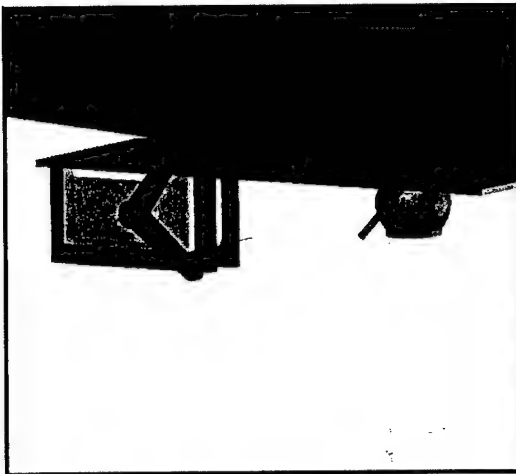


Figure 5.6.1. Water deployment system

5.7. Final Aircraft Specifications. After iterative analysis for optimal performance predictions the final aircraft specifications are as follows

Geometry	Value
Length (ft)	4
Span (ft)	6
Height (ft)	7.25
Wing Area (ft ²)	9
Aspect Ratio	4
Horizontal Stabilizer Area (ft ²)	1.6
Horizontal Stabilizer Sweep (ft)	33
Horizontal Stabilizer Span (ft)	1.5
Elevator Span (ft)	1.5
Elevator Chord (ft)	.36
Vertical Stabilizer Area (ft ²)	0.5
Vertical Stabilizer Sweep (deg)	33
Vertical Stabilizer Span (ft)	0.8
Rudder Span (ft)	0.8
Rudder Chord (ft)	0.24
Aileron Span (ft)	1.5
Aileron Chord (ft)	0.25
Main Wing Airfoil	NACA 4408
Horizontal/Vertical Tail Airfoil	NACA 0009

Table 5.7.1. Geometry Statement

Weight Statement	Value
Airframe (lbf)	8.7
Propulsion System (lbf)	6
Control System (lbf)	0.52
Payload (lbf)	9
Manufacturers Empty Weight (lbf)	15.22
Gross Weight (lbf)	24.22

Table 5.7.2. Weight Statement

Systems	Value
Radio	Futaba 9CA/CH
Servos	4xFutaba S3004, 1xFutaba S3801
Speed controller	AstroFlight Model 204
Battery Configuration	40xSanyo CP-1700 SCR - mAhr
Motor	Astroflight 691
Gear Ratio	1:1
Propeller	15x10
Brakes	Custom
Landing gear	Custom

Table 5.7.3. Systems Statement

5.8. Rated Aircraft Cost Calculation.

$$\text{RAC \$ (Thousands)} = (A * \text{MEW} + B * \text{REP} + C * \text{MFHR}) / 1000$$

A = \$300

B = \$1500

C = \$20 per
hour

RAC =	13.96433
bw	4
wingspan	6
chord	1.5
length	4
width	0.5
height	0.604167

MEW = Manufacturers empty weight	15.27
REP = (.25 * (# engines - 1)) * battery weight	4
MFHR = summation of WBS	169.1667
WBS 1	95
10h/ft2 * wingspan * chord * # wings	90
5h * 1 (for ailerons)	5
WBS 2	24.16667
20 h/ft3 * length * width * height	1.208333
WBS 3	25
5h per vertical surface with no control	5
10h per vertical surface with control	10
10h per horizontal surface with control	10
WBS 4 5h per servo or motor controller	25

Figure 5.8.1. RAC

5.9. Final Aircraft Performance Analysis.

The changes in drag, thrust, weight, and lift are iterated into the performance program to give new performance data. A simple dynamic stability calculation was done to test for longitudinal dynamic stability.

5.9.1. Dynamic Stability.

Calculating Dynamic stability is a difficult task and much of the analysis done for "IGI" was theoretical resulting in very approximate answers. Analysis was based on McCormick's analysis and because of complexity reasons longitudinal modes were only considered during takeoff and cruise conditions. The longitudinal modes of "IGI" are summed up in the following table

Longitudinal Modes				
Short	σ	w_n	ζ	Doubling time
Takeoff	-1.6503+/-1.0356	1.95	.847	.859
Cruise	-4.0056+/-1.694i	4.3439	.922	.752
Phugoid				
Takeoff	-.0994+/- .7886i	.794	.125	6.973
Cruise	-0.0144+/- .6355i	.637	.022	30.66

Table 5.9.1. Longitudinal modes for certain conditions and resulting stability characteristics

5.10. Predicted Performance.

The predicted performance of the aircraft for the FBM and the HSFM are given in table 5.10.1. The FBM and HSFM have a flight score of

Aircraft Performance		FBM	HSFM
Takeoff	Distance	103.14	95.3
Landing	Distance	136.8	114.4
Flight	Time	1.98	2.1
	Flight Score	1.01	0.476
Total Score		1.48	

Figure 5.10.1. Performance statement

6. Manufacturing Plan

The airplane will be broken up into three segments of structural sub-sections: wing, fuselage, and empennage. Each section was looked at independently, noting that certain materials may be more applicable in different aspects of the design. The focus with wing design was to build a long-spanning weight supporting structure. The fuselage, on the other hand, dealt with issues of focused strength and reinforcement considerations, such as landing gear mounting and payload tank support. Finally, the empennage had to support relatively small loads, so that structural rigidity was not as grave a concern.

Decisions for the exact structural make up of each of the aforementioned sections were based on the following criteria:

Cost: With a limited budget, cost was an important deciding factor for different processes. This was especially notable due to the wide range of costs applicable for different structural options.

Manufacturability: This takes into consideration both the complexity of tooling as well as team member's experience with specific processes. Scores were given according to the availability of any necessary equipment, team members' ability to use the machinery, as well as the ease of learning the new process.

Time: While some options seemed very appealing, time constraints had to be taken into consideration. This could correlate to excess time required for manufacturing or time considerations in acquiring materials.

Strenght/Weight: As with every aspect of this design, this tradeoff was an important consideration with every structural choice. The effect of additional weight is noted in flight performance as well as RAC, so that careful consideration was required when choosing heavy materials for strong structural support.

Due to a donation of a large supply of carbon fiber composites, cost for this otherwise expensive option was not a great issue. Balsa is also relatively inexpensive. Foam requires tooling which the team did not posses, so that there was an unavoidable one-time cost in manufacturing that had to be considered for foam purchases.

The team had extensive experience with balsa and woodworking, and only a few members had experience with foam carving. Although nobody possessed any experience with carbon fiber construction (use of the auto-clave and water-jet cutting), there were instructors available to us that were willing to help. However, due to the limited machinery, time was an important consideration.

		Cost	Manufacturability	Time	Weight	Total
weight factor		1	2	2	3	
Wing Section						
Foam Core with Composite Sheeting		1	1	1	1	8
Foam Core with I-beam		0	0	1	0	4
Regular Balsa buildup		2	2	2	1	8
Carbon Fiber Buildup		2	1	1	2	9
Empennage						
Foam Core		1	1	1	1	8
Balsa Wood		2	2	2	1	13
Carbon Fiber		2	0	1	2	10
Fuselage						
Hollowed Foam		1	0	1	1	6
Balsa/Plywood Buildup		2	2	1	1	11
Carbon Fiber Buildup		2	0	0	2	8
Combination Buildup		2	1	1	2	12

Figure 6.1. Manufacturing Figure of Merits

7. Testing

7.1. Test Objectives and schedules.

A series of tests were performed to determine reliability and performance. The following table are the tests that have been performed

Test	Objective	Date
Wing Spar Test	Determine the loading for a balsa plywood doubler	1/22
Airfoil Rib Stress Test	Determine yield of composite rib	1/29-2/05
Water Drainage Test	Determine real times of water drainage statically	2/15
Landing Gear Test	Determine loading for aluminum landing gear	2/15
Motor and Battery Test	Determine optimum combination of battery with selected motor	2/25

Figure 7.1. Table of tests and schedules

7.2. Flight Checklist.

A Flight checklist was created to ensure that the UAV will be ready for flight. The checklist is as follows

Checklist	Description	
CG location	Location < 0.5 of chord?	
Control surfaces securely linked and level with stabilizer	All linkages fastened and do servos work?	
Wing tip test	Withstand 30 lb load when hoisted from wing tips?	
Water drainage tube leakage?	Is the joint leaking water?	
Fail Safe	Tx off, elevator full up, flaperons/rudder full right, throttle off, payload in place?	
Miscellaneous	Is every surface component fastened and working?	

Figure 7.2. Checklist

REFERENCES

Raymer, Daniel P., (1999), Aircraft Design: A Conceptual Approach 3rd ed., AIAA, Virginia.

McCormick, Barnes W., (1995), Aerodynamics Aeronautics and Flight Mechanics 2nd ed., Wiley, NJ.

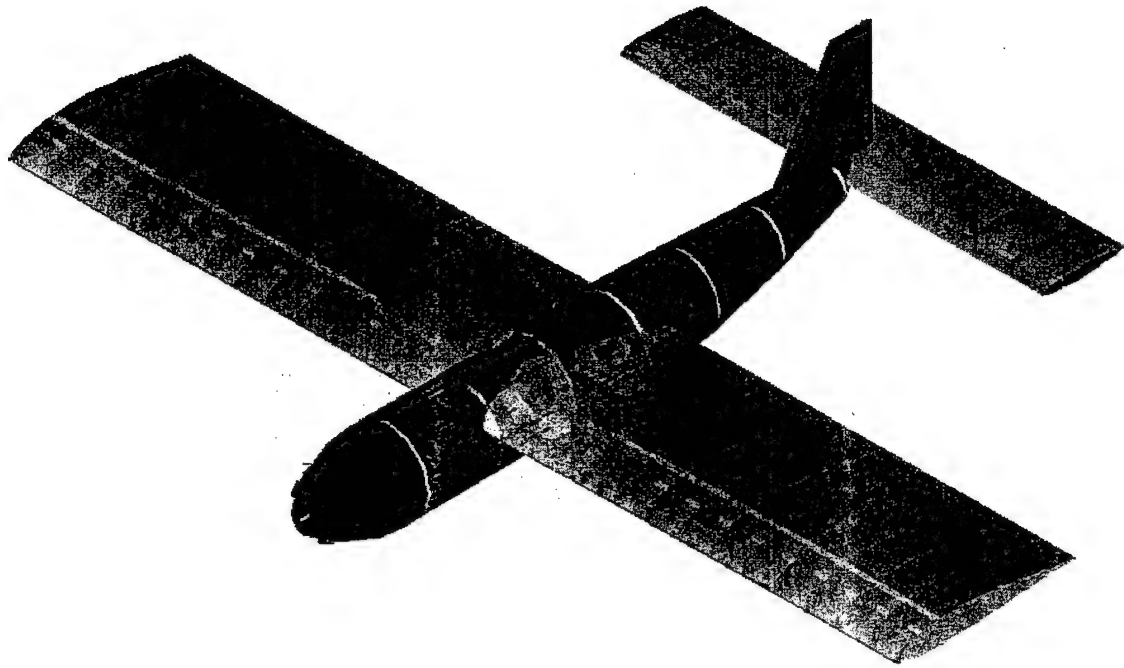
Munson, Bruce R., (2002), Fundamentals of Fluid Mechanics fourth ed., Wiley, New York.

Sun, C.T., (1998), Mechanics of Aircraft Structures, Wiley, New York.

Craig, Roy R. Jr., (2000), Mechanics of Materials, Wiley, New York.

2003/2004 AIAA Foundation Cessna/ONR Student Design Build Fly Competition

DESIGN REPORT



**“Kamikaze”
Clarkson University
March 2004**

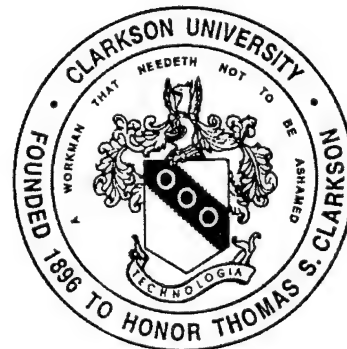


Table of Contents:

<u>Section:</u>	<u>Page:</u>
1.0 Executive Summary_____	4
1.1 Design Development Summary_____	4
1.2 Range of Design Alternatives Investigated_____	4
1.3 Major Areas in the Development Process for the Final Configuration_____	6
2.0 Design Team Configuration_____	6
2.1 Scheduling_____	7
3.0 Conceptual Design_____	10
3.1 Mission Profile_____	10
3.1.1 Mission Specifications for a Fire Bomber UAV_____	10
3.1.2 Mission Specifications for a Ferry UAV_____	10
3.2 Configurations Considered_____	10
3.2.1 Wing Considerations_____	11
3.2.1.1 Wing Placement_____	11
3.2.1.2 Planform Shape_____	11
3.2.1.3 Winglets_____	11
3.2.1.4 Wing Control Surfaces_____	12
3.2.2 Tail Configurations_____	12
3.2.3 Fuselage Configuration_____	13
3.2.3.1 Number of Fuselages_____	13
3.2.3.2 Types of Fuselages_____	13
3.2.3.3 Boomed -Vs- Conventional Fuselage_____	13
3.2.3.4 Open versus Closed Fuselage_____	14
3.2.4 Propulsion_____	14
3.2.4.1 Number of Motors/ Propulsive Devices_____	14
3.2.4.2 Type of Propulsive Device_____	14
3.2.4.3 Propulsion Integration_____	15
3.2.5 Landing Gear Configurations_____	15
3.2.6 Payload Placement and Deployment_____	15
3.3 Preliminary Rated Aircraft Costs for Each Candidate Design_____	16
4.0 Preliminary Design_____	18
4.1 Design Parameters and Sizing Trades_____	18
4.1.1 Wing_____	18
4.1.2 Fuselage Components and Payload_____	18
4.1.3 Aircraft Length and Empennage Size_____	18
4.1.4 Motor Specifications_____	18
4.1.5 Propeller Dimensions_____	18
4.1.6 Battery and Cells_____	19
4.2 Mission Model Analysis_____	19
4.2.1 Overview (things used)_____	19
4.2.2 Weight_____	19

4.2.3 Lift/Drag Calculations	20
4.2.4 Stability/Control	22
4.2.5 Propeller Analysis	24
4.2.6 Turn Analysis	25
4.3 Optimization Trade	26
4.3.1 Design Parameters	26
4.3.2 Mission Parameters	27
4.4 Conclusions	27
5.0 Detail Design	28
5.1 Configuration detail design	28
5.2 Structural Component Selection	28
5.2.1 Fuselage	28
5.2.2 Wing	28
5.2.3 Empennage	29
5.3 Secondary Component selection	29
5.3.1 Propulsion and Controls	29
5.3.2 Payload	29
6.0 Manufacturing Plan	35
6.1 Figures of Merit	35
6.1.1 Availability of Materials	35
6.1.2 Cost	35
6.1.3 Time	35
6.1.4 Weight	35
6.1.5 Staff	35
6.2 Weighted Objective Tables	36
6.3 Manufacturing Processes Investigated	37
6.3.1 Wings	37
6.3.2 Fuselage	37
6.3.3 Payload	38
6.3.4 Tail	38
6.4 Manufacturing Milestone	38
7.0 Testing Plan	39
7.1 Test Objectives and Schedule	39
7.2 Pre-flight and Test Flight Checklists	40
7.3 Test results	42

1.0 Executive Summary

This report is an overview of the design development process through completion used by the Clarkson University DBF team for the 2003-2004 AIAA founded DBF competition hosted in Wichita, KS. Within this document are all the decisions, thoughts, and problems that occurred, and were dealt, with during the development of the "Kamikaze" from paper to the finished product. This year's competition required that the aircraft be capable of completing one of two missions: Fire Bomber and/or Ferry.

1.1 Design Development Summary

In the conceptual design phase, it was first decided that the "Fire Bomber" mission should be chosen as the main baseline mission for the aircraft. Having a difficulty multiplier of two, this would aid in boosting the flight score. With this mission in mind, the team met and brainstormed about 25 different conceptual designs and part configurations. After much discussion, the number of reasonable and appropriate designs was reduced to four. These four designs were then heavily scrutinized by multiple figures of merit broken into aircraft component categories; for example, wing, empennage, and power plant considerations.

Next, the preliminary design phase began and multiple aircraft components were selected and their sizes and characteristics refined. To do this, a computer script was written to aid with the calculations. From this code, it was easy to visualize the trends and optimization points that would be necessary for a successful aircraft design. The major areas where the code was implemented were in the analysis of: expected flight performance at various flight speeds, stability and control characteristics, propeller and motor selection, and the rated costs of any modifications. Another major component of the preliminary design phase was the usage of wind tunnels in determining efficient configurations which lead to major modifications of the initially chosen design.

Having refined the design using the optimal values from the preliminary design phase, the detailed design phase began. Within this phase, specific parts of the aircraft were designed and then assembled as a whole. One major consideration was that of payload integration. Also, the ability of the payload container to empty of water within reasonable time ranges was investigated and the introduction of a ram air system was tested. Considering the mission that was chosen, this was a crucial step within the detailed design phase. Moreover, any slight part modifications were made at this time as well.

In the end after various testing throughout the different phases on aerodynamic, performance, structural and stability ramifications a final product remained. The overall geometry of the aircraft aided in the ease of assembly of the aircraft from the box and high performance.

1.2 Range of Design Alternatives Investigated

As listed above, the team initially came up with twenty five different configurations to be considered during the conceptual design phase. These designs differed in motor placement, wing/empennage configurations and fuselage configurations. Propulsions ideas that were presented were ducted fans vs. conventional propeller (tractor or pusher) as well as the possibility of multiple motors. As for overall aircraft configurations, there were ideas presented for joined wings, oblique wings, forward swept wings, etc. As for the fuselage: twin fuselages, a single fuselage, a single boom and a twin boom were all discussed and reviewed. In the end, four designs were left. The first represented the "standard configuration" that is exhibited by most aircraft. By this, the aircraft had a single fuselage, a mid wing, and a standard tail. The next design was the same as the first with the exception that the fuselage would be a lifting surface as well. The third design was a twin fuselage aircraft that somewhat resembled the P-38 Lightning and the final design closely resembled the British "Spitfire" except that it had a tail boom instead

of tapered fuselage. In the end, based on design considerations and rated aircraft costs, it was decided that the "Spitfire" idea would best serve the team for this year's competition.

1.3 Major Areas in the Development Process for the Final Configuration

The major hurdle in the development process was that of the payload and the fact that as the water was being dumped the aircraft weight would decrease by approximately 50%. When designing the aircraft the stability and control and performance would be greatly affected by this. Therefore, with this consideration in mind, it was decided that the center of gravity of the payload be placed to exactly meet the center of gravity of the aircraft.

Also, it was initially decided in the conceptual design phase, that a single boom be used instead of a full length fuselage. Through wind tunnel testing, it was discovered that although the boom would be significantly lighter, the performance of the aircraft would be greatly inhibited by the drag on the rear of the fuselage section and that would lead to lower flight scores. Since the goal of the competition is to obtain as high a score as possible, this modification was quickly made.

Another major consideration was that of battery and motor performance during flight. Due, once again, to the type of mission selected, the aircraft would be relatively heavy which would add more strain to the motor. Since the motor will need to be run at higher power levels to combat this, the drainage rate of the batteries would be increased. Therefore, dry run tests of just the batteries and the motor were done to give the team an idea of what the expected performance of the batteries should be. This consideration greatly influenced the configuration of the aircraft since Wichita is notorious for high wind speeds.

Finally, the way that the aircraft would behave in flight was studied. To make things as easy on the pilot as possible, the performance and stability and control analyses were done with this in mind. These studies provided guidelines on propeller selection, control surface type selections, aspect ratios, empennage sizing, and power requirements.

Having studied these various issues, an overall aircraft geometry was refined and selected that would exhibit strong performance characteristics and complete the mission successfully.

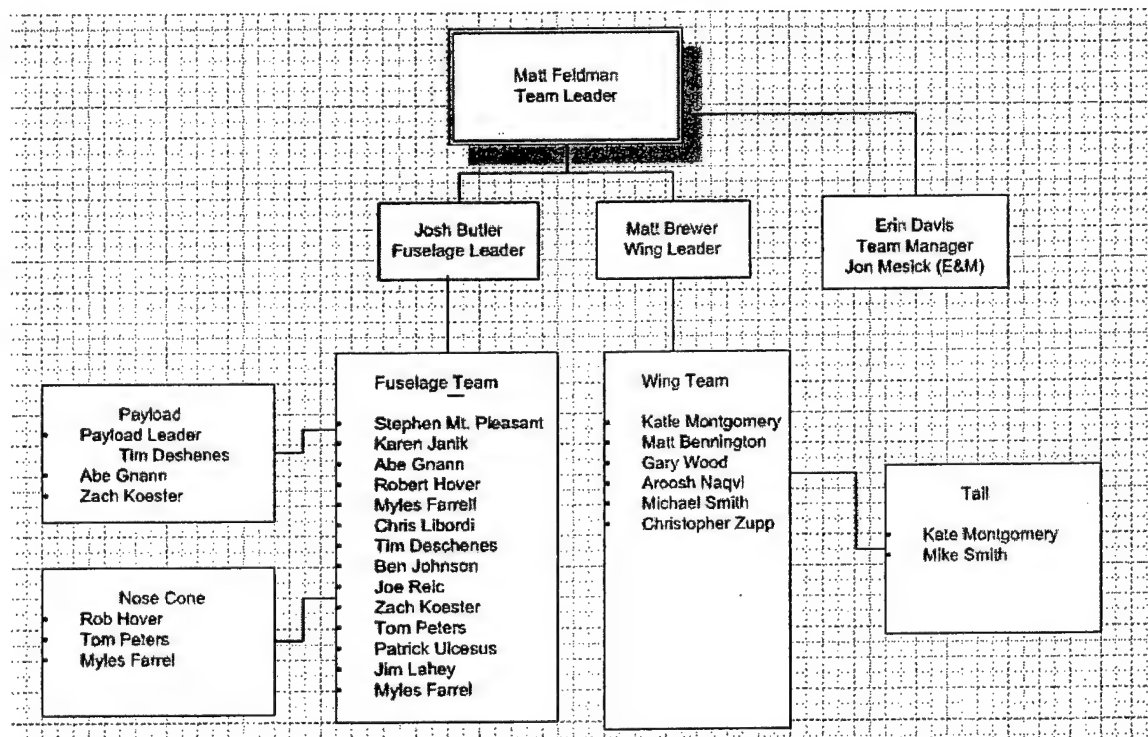
2.0 Design Team Configuration

This year's team consists of twenty four members. A team manager, from the Engineering and Management School, has been added to the team to help maintain the budget, aid in team activities and form the team schedules, and help with the design report.

All members had the option to help in the design process and calculations. All ideas were listened to and those who wished to learn how to do the calculations were welcome. When building had begun, the base group of twenty four people broke up into two groups; fuselage and wing. Each member of the team had the choice of which team they would like to participate with. The teams followed their own schedule, and the team leader formatted their build sessions and how the team would perform and break up from there. Fuselage and wing then broke into smaller groups. The fuselage team leader designated certain individuals to work on payload and the nose cone. The team leader of wing also designated certain people to work on the tail of the aircraft. Each team leader kept a log in sheet and those who showed up to build at the build sessions logged in. The team leader then based his decision of those who would be attending completion from who came to the most build session and applied the most effort to the team.

The design report was given to groups of two to three people, with an older member in each group so that under classmen could learn how to write the report. Anyone that was interested in writing the report was welcome to help.

Figure 2.1



2.1 Scheduling

This year the team decided to make a change in the scheduling. It was decided to have the majority of our building done by February. It was essential that the schedule was realized by all team members so as to stay on schedule. At the beginning of the semester the team leaders planned out the dates and steps that would be taken to build the aircraft to assure that it is complete by February. This would allow for the team to perform more testing and obtain flight time before competition. All the dates and scheduling desires were placed into a timeline.

ID	Task Name	Start	Finish	Predecessors	1 '03	Sep 7 '03	Sep 14 '03	Sep 21 '03	Sep 28 '03	Oct 5 '03	Oct 12 '03	Oct 19 '03	Oct 26 '03	Nov 2 '03
1	Design and Calculations	Thu 9/4/03	Wed 9/17/03		T	F	S	S	M	T	F	F	S	S
2	CAD Designs	Thu 9/18/03	Thu 10/9/03	1	T	F	S	S	M	T	F	F	S	S
3	Work on report	Sat 10/18/03	Wed 3/3/04											
4	Management Summary	Sat 11/1/03	Sat 2/28/04											
5	Conceptual Design	Sat 11/1/03	Wed 11/26/03											
6	Preliminary Design	Thu 1/1/04	Wed 1/28/04											
7	Detail Design	Wed 1/29/04	Sat 2/2/04											
8	Manufacturing Processes	Sat 10/18/03	Sat 2/28/04											
9	Testing	Sat 2/28/04	Wed 3/3/04											
10	Executive Summary	Wed 3/3/04	Wed 3/3/04											
11	Wing	Sat 10/18/03	Sat 2/28/04											
12	Cut out ribs for wing and horizontal tail	Sat 10/18/03	Sat 10/25/03											
13	Sand all ribs	Sat 10/19/03	Sat 10/25/03											
14	Mount ribs on spars	Sat 10/18/03	Sat 10/25/03											
15	Use pieces to make flap, elevators, rudder	Sat 10/18/03	Sat 10/25/03											
16	Glue leading edge and sand	Sat 10/25/03	Sat 11/1/03											
17	Sheet up to 1/4 cord	Sat 10/25/03	Sat 11/1/03											
18	Sheet wing	Sat 10/25/03	Sat 11/1/03											
19	Make Servo Mounts	Sat 10/25/03	Sat 11/1/03											
20	Drill holes for control rods	Sat 10/25/03	Sat 11/1/03											
21	Covering the wing	Wed 2/18/04	Sat 2/28/04											
22	Mounting Servos	Sat 2/28/04	Sat 2/28/04											
23	Attach flap, elevator and rudders	Sat 2/28/04	Sat 2/28/04											
24	Fuselage	Sat 10/18/03	Wed 3/10/04											
25	Cut bulkhead	Sat 10/18/03	Sat 10/25/03											
26	Construct bulkhead with stringers to length	Sat 10/18/03	Sat 10/25/03											
27	Assemble bulkheads to stringers and set payload	Sat 10/18/03	Sat 10/25/03											
28	Set the 5 rear bulkheads to the spine	Sat 10/18/03	Sat 10/25/03											
29	Mount engine spacer to the fire wall	Sat 10/25/03	Sat 11/1/03											
30	Mount engine onto spacer	Sat 10/25/03	Sat 11/1/03											
31	Start wing box construction	Sat 10/25/03	Sat 11/1/03											
32	Construct wing box	Sat 11/1/03	Sat 11/8/03											
33	Assign team for nose cone	Sat 10/25/03	Sat 11/1/03											
34	Make air foil with foam	Sat 11/1/03	Sat 11/8/03											
35	Payload deployment and battery placement	Sat 11/1/03	Wed 2/25/04											
36	Landing Gear	Wed 3/3/04	Sat 3/6/04											
37	Engine Speed Controls	Sat 3/6/04	Sat 3/6/04											
38	Receiver	Sat 3/6/04	Sat 3/6/04											
39	Monokote	Sat 3/6/04	Wed 3/10/04											

Project: (New) DBF Timeline
Date: Mon 3/6/04

Task

Split

Progress

Milestone

Summary

Project Summary

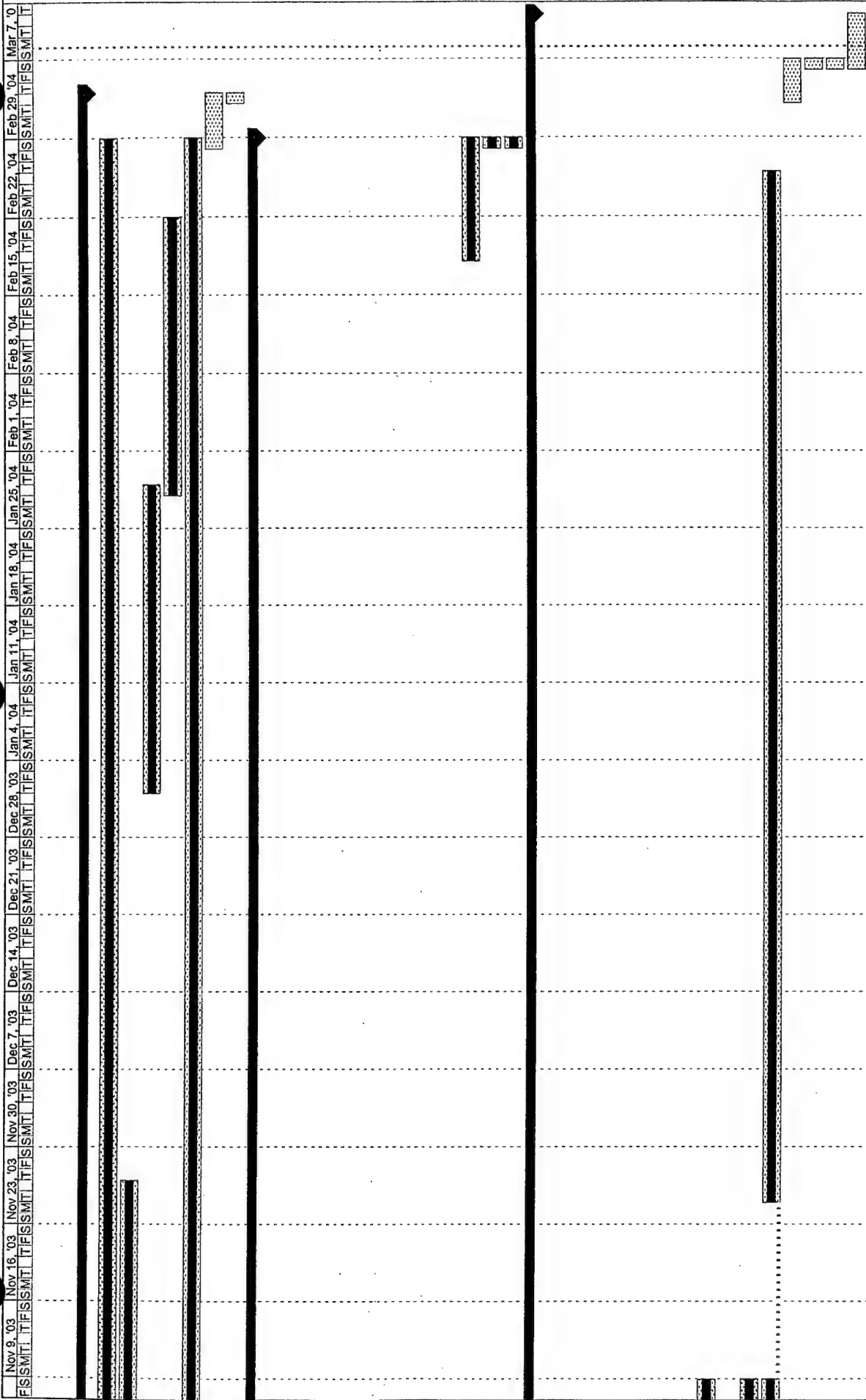
External Tasks

External Milestone

Deadline

Page

1



Task	Milestone	External Tasks
Split	Summary	External Milestone
Progress	Project Summary	Deadline

Project: (New) DBF Timeline
Date: Mon 3/8/04

3.0 Conceptual Design

This year the aircraft mission profile was to complete one, or both, of two possible missions that were each assigned a multiplier based on their degree of difficulty. These missions required the aircraft to carry/deploy a water payload and/or fly laps as quickly as possible. The first conceptual decision made was to complete mission A. This decision was based strictly on the merit of the high difficulty multiplier. After exploring the design requirements for both missions, it was decided that mission B would also be attainable without insurmountable design complications. The decision to proceed with mission A provided a guideline to the conceptual designs considered, and had a heavy hand in narrowing the design possibilities.

3.1 Mission Profile

3.1.1 Mission Specifications for a Fire Bomber UAV

Payload: A water payload not to exceed 4 liters.

Range: 2 laps around a designated course with a payload.

Cruise Speed: 35 MPH

Take-off/Land: Balanced field length of 150'

Power plant: Astroflight Cobalt 90 Electric Motor, 40 Amp fuse, maximum of 5 pounds of batteries.

3.1.2 Mission Specifications for a Ferry UAV

Payload: None.

Range: 4 laps around a designated course.

Cruise Speed: 45 MPH

Take-off/Land: Balanced field length of 150'

Power plant: Astroflight Cobalt 90 Electric Motor, 40 Amp fuse, maximum of 5 pounds of batteries.

3.2 Configurations Considered

With payload and speed being the governing design factors on the aircraft, reducing weight during construction and streamlining of the design were the top priorities as various configurations were considered. Since the aircraft had no aerobatic flying requirements, design requirements such as long tail moments for better tracking and precise control were immediately discarded. Hence, all unneeded sections of the aircraft could be done away with to conserve weight, reduce drag and mass.

3.2.1 Wing Considerations

3.2.1.1 Wing Placement

A major consideration was where the wing was to be placed. The three suggested configurations were a high wing, a mid-wing, and a low-wing. Various aspects of each are displayed in Table 3.1.

Table 3.1: FOM Chart for Wing Placement

Wing Placement	Stability	Ease of Construction	Sturdiness of Gear	Total
High	8	8	7	31
Mid	7	6	5	23
Low	5	7	8	26

As seen above, the end result was that a high wing placement would be ideal based upon the constraints listed above. For high wing aircraft with wing mounted landing gear, weight is an issue since more structure is required due to the necessary length of the landing gear struts. To combat this weight problem, a sub-decision was made that the landing gear be mounted on the fuselage instead; therefore, this is the reason for the high score that can be seen in Table 3.1 for gear sturdiness.

3.2.1.2 Planform Shape

The shapes considered were an ideal elliptical planform, swept, tapered, and constant chord. The advantages and disadvantages are displayed in Table 3.2.

Table 3.2: FOM Chart for Wing Planform

Wing Planform	Stability	Ease of Construction	Aerodynamic Performance	Total
Elliptical	6	3	10	19
Tapered	6	7	9	22
Swept	8	5	5	18
Constant chord	7	10	6	23

The tapered planform was decided upon because of its consummate balance between simplicity of construction and stability, while still maintaining an excellent capacity for aerodynamic performance.

3.2.1.3 Winglets

The usage of winglets was considered to increase the aerodynamic aspect ratio, which, in effect, increases the performance by decreasing the induced drag on the aircraft. After careful consideration, it was found that the performances increases were not comparable to the increase in RAC (5 hr. /Vertical Surface).

3.2.1.4 Wing Control Surfaces

Various types of wing control surfaces were considered based on their ability to increase takeoff and landing performance and maneuverability without sacrificing cruise speed. These options were explored in Table 3.3.

Table 3.3: FOM Chart for Wing Flaps

Control Surfaces	Takeoff/Landing Perf.	RAC	Ease of Construction	Total
Flaps + Ailerons	10	1	5	16
Ailerons	1	10	10	21
Flaperons	10	5	10	25

Flaperons were chosen due to the combination of simple construction and excellent takeoff and landing performance.

3.2.2 Tail Configurations

The types of configurations considered were t-tails, v-tails, double vertical tails, or a conventional tail. Each type was evaluated in Table 3.4.

Table 3.4: FOM Chart for Tail Configuration

Tail Configuration	Stability	Ease of Construction	Additional RAC	Interference during Payload deployment	Total
T-tail	6	5	10	9	30
V-tail	3	4	10	9	26
Double inverted verticals	10	7	5	9	31
Conventional	7	7	10	9	33

The conventional tail was chosen for its ease of construction, stability, and extremely low cost.

3.2.3 Fuselage Configuration

3.2.3.1 Number of Fuselages

A single fuselage vs. a dual fuselage was discussed. Advantages and disadvantages for each were evaluated using Table 3.5.

Table 3.5: FOM Chart for Number of Fuselages

Number of Fuselages	Ease of Construction	Weight	Payload capabilities	Aerodynamic Performance	Total
Single	8	8	7	8	31
Double	6	4	9	5	24

The mission requirements called for a single payload package. A double fuselage would add to the complexity of the design due to running tubing for water drainage from both fuselages to the exit. Also, the double fuselage would increase the rated aircraft cost significantly in addition to doubling the weight. The single fuselage was therefore the obvious choice.

3.2.3.2 Types of Fuselages

The types discussed were blended wing bodies, lifting bodies, and a standard configuration. Advantages and Disadvantages are as shown in Table 3.6.

Table 3.6: FOM Chart for Fuselage Type

Fuselage Type	Ease of Construction	Aerodynamic Performance	Stability	Total
Blended Wing Body	3	8	1	12
Lifting Body	5	6	3	14
Standard Configuration	8	3	9	20

The most practical design for the stability and construction needs was the standard fuselage. Though it suffered in the performance category, it is still most suited to the necessary missions based on stability.

3.2.3.3 Boomed -Vs- Conventional Fuselage

Tail booms were considered for their reduction of weight and skin friction drag. The advantages and disadvantages were weighted and evaluated using Table 3.7.

Table 3.7: FOM Chart for Boom Configuration

Booms	Weight	Stability	Aerodynamic Performance	Ease of Construction	Total
Single	8	6	8	7	35
Double	5	8	6	6	28
None	3	7	7	6	31

As discussed earlier, the single tail boom was selected as the most practical design. As a light weight way to attach the tail, the single boom cuts unnecessary weight and construction time.

3.2.3.4 Open versus Closed Fuselage

An open fuselage was considered to cool the batteries as well as reduce weight. A closed fuselage was considered to reduce the drag on the payload and the amount of skin friction due to the increased exposure of surface area. It quickly became clear that the reduction in drag on the closed fuselage was far more effective than the small weight increase generated by the open fuselage. Therefore, the closed design was chosen.

3.2.4 Propulsion

A major conceptual design consideration is the question of propulsion. Should the aircraft have multiple motors? What type of motor should be chosen? Propeller or ducted fan? How should the propulsive device be integrated into the aircraft geometry? These questions were considered and FOM's made in this section.

3.2.4.1 Number of Motors/ Propulsive Devices

The usage of one or two motors was debated. The advantages and disadvantages for each were found and inserted into Table 3.8 to decide which would be used.

Table 3.8: FOM Chart for Number of Motors

Number of Motors	Weight	Power	Ease of Construction	Total
Single	8	4	6	20
Double	4	7	5	16

The single motor was chosen because it was capable of meeting the necessary power needs, and drastically reduced the weight of the aircraft.

3.2.4.2 Type of Propulsive Device

The usage of a conventional prop configuration vs. a ducted fan was considered. The advantages and disadvantages for each were put into Table 3.9.

Table 3.9: FOM for Ducted Fan

Ducted Fan	Aerodynamic Performance	Weight	Battery Power Needs	Ease of Construction	Thrust	Total
Ducted Fan	8	5	2	5	6	26
Conventional Propeller	6	7	8	8	8	37

The conventional propeller was selected due to the exorbitant battery-power cost of a ducted fan, as well as the added unnecessary weight of a ducted fan.

3.2.4.3 Propulsion Integration

How the propulsive device was to be integrated was considered as well as whether a pusher or a tractor propeller should be used, if not both. The characteristic differences were evaluated using Table 3.10.

Table 3.10: FOM Chart for Propulsive Integration

Propulsive Integration	Aerodynamic Performance	Weight	Cooling	Ease of Construction	Total
Wing Root	7	6	6	6	25
Inside Fuselage	8	8	7	8	31
Tail Mounted	5	5	8	7	25
Wing Tips	7	6	8	5	26
Outside Fuselage	8	7	8	4	27

The decision was made to house the propulsive device within the fuselage for the significant reduction in drag that this option offers, as well as its low weight requirement.

3.2.5 Landing Gear Configurations

The types of landing gear considered were the tail dragger and the tricycle landing gear with a controllable nose wheel. Both configurations were also considered using retractable landing gear and fixed landing gear. The benefits and disadvantages of these designs were explored in table 3.11.

Table 3.11: FOM Chart for Landing Gear

Wing Planform	Weight	Ease of Construction	Takeoff Performance for a High Wing	Total
Retractable Dragger	5	3	5	13
Tail Dragger	7	7	5	19
Retractable Tricycle	3	3	10	16
Tricycle	7	7	10	24

The tricycle landing gear was chosen due to its takeoff performance for a high wing aircraft.

3.2.6 Payload Placement and Deployment

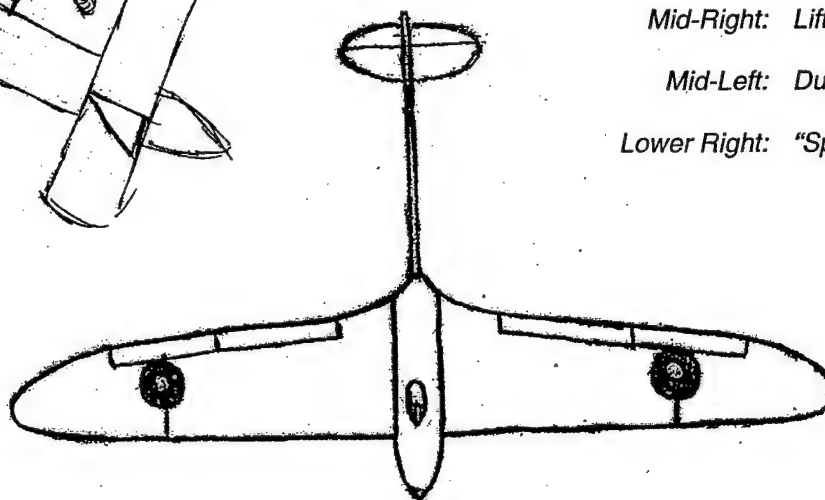
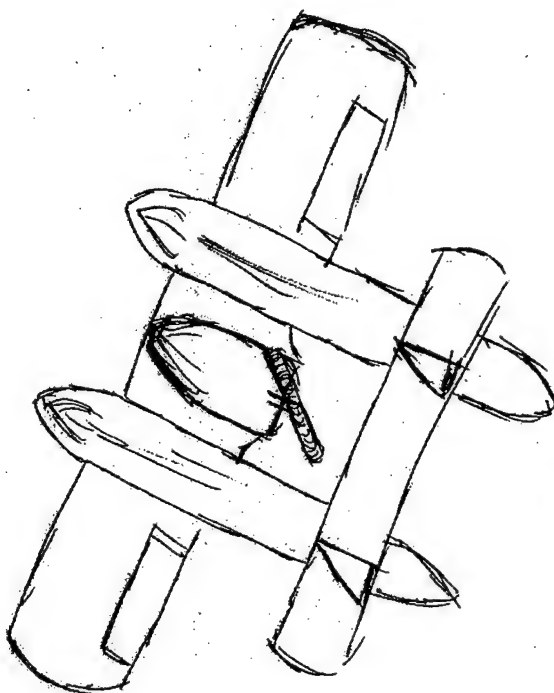
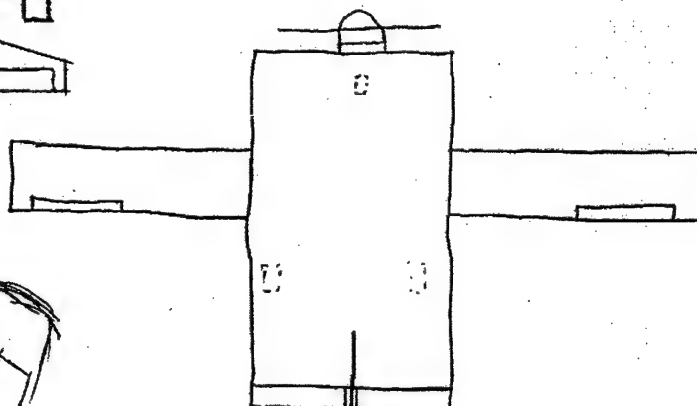
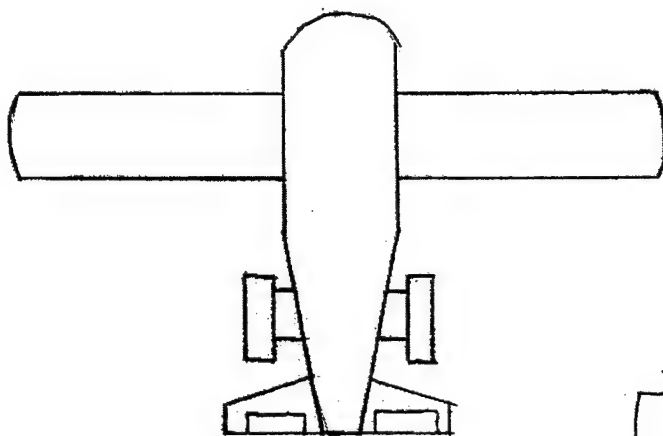
It was decided that the payload be placed at the center of gravity of the aircraft for stability and control. Two types of deployment were discussed. The usage of a ram air system vs. no deployment assistance was considered for the water discharge. The ram air system would need tubing that would increase parasite drag and weight, but offered a faster deployment. No deployment assistance would lead to less drag and reduced weight, but higher flight times would be required since the aircraft would have to cruise at a slower speed to fully discharge the water.

3.3 Preliminary Rated Aircraft Costs for Each Candidate Design

Listed below are the different rated aircraft costs of the top four conceptual designs as well as a picture of each.

Table 3.12: Rated aircraft costs

Standard			Lifting		
Category		Penalty (\$)	Category		Penalty (\$)
Weight	12.00	3600.00	Weight	12.00	3600.00
REP	5.00	7500.00	REP	5.00	7500.00
Wing Area	11.50	2300.00	Wing Area	11.50	2300.00
Flaperons	2.00	60.00	Flaperons	2.00	60.00
Fuselage Volume	1.78	711.11	Fuselage Volume	2.67	1066.67
Vertical Surface	1.00	200.00	Vertical Surface	1.00	200.00
Horizontal Surface	1.00	200.00	Horizontal Surface	1.00	200.00
Servos	5.00	500.00	Servos	5.00	500.00
Total (\$)		15071.11	Total (\$)		15426.67
Dual Fuse			Spitfire		
Category		Penalty (\$)	Category		Penalty (\$)
Weight	12.00	3600.00	Weight	12.00	3600.00
REP	5.00	7500.00	REP	5.00	7500.00
Wing Area	11.50	2300.00	Wing Area	11.50	2300.00
Flaperons	2.00	60.00	Flaperons	2.00	60.00
Fuselage Volume	3.56	1422.22	Fuselage Volume	0.89	355.56
Vertical Surface	2.00	400.00	Vertical Surface	1.00	200.00
Horizontal Surface	1.00	200.00	Horizontal Surface	1.00	200.00
Servos	5.00	500.00	Servos	5.00	500.00
Total (\$)		15982.22	Total (\$)		14715.56



Design Concepts

Upper Left: Standard

Mid-Right: Lifting Body

Mid-Left: Dual Fuselage

Lower Right: "Spitfire"

4.0 Preliminary Design

The basis of the preliminary design was to determine different characteristics of the plane including weight, size, payload, placement of payload, and other physical characteristics to help optimize the plane. The major areas of concern were the aspect ratio, wing and wing box strength, and the weight.

4.1 Design Parameters and Sizing Trades

Based on the ideas proposed in the conceptual design phase, the optimal design parameters and sizes were chosen and revised to increase performance and the overall score of the design. These design parameters are listed in the paragraphs below.

4.1.1 Wing

The initial wing design was based on wing loading from the fuselage. After wing loading was analyzed, the necessary area of the wing was then calculated and from there the wing-span and chord length was found. To minimize the aircraft cost, flaperons were chosen over flaps and ailerons because of the cost effectiveness. The wings were to then be connected into a wing box built off of the fuselage. For added support, the wings were connected using two aluminum dowel rods.

4.1.2 Fuselage Components and Payload

The fuselage components were chosen based on the load carried. The main spine of the fuselage was chosen to be of carbon fiber due to its strength at a low weight. Aluminum rods were used as stringers to give added support for the payload in addition to the spine. Laminated wooden bulkheads were used to hold the stringers and spine together and to aid in the resistance of torsional shear. The volume of the fuselage was maximized for payload but minimized for cost efficiency. Opportunity costs of both the payload and cost were considered and the size of the plane was determined.

4.1.3 Aircraft Length and Empennage Size

The aircraft length was designed knowing that it had to fit in the aircraft storage box and had to maximize the volume of the payload. As the length of the aircraft increases, the aircraft cost also increases so the length was designed based on these components. The main concern with designing of the empennage is stability of the plane. A longer horizontal surface was chosen for the added stability, but since it was longer than a quarter of the wing span it is now considered another wing. Even though this increases the aircraft cost it is compromised with the added stability of the plane.

4.1.4 Motor Specifications

The selection of a motor was based on weight of motor, number of motors to use, power output, and electric current drawn from the batteries. Increasing the weight of the motor would give a higher power output, but at the same time increase aircraft cost. Adding more motors to the plane would also give a higher power output and increased weight, but increase the aircraft cost substantially. The motor selected was based on these conclusions and cost effectiveness.

4.1.5 Propeller Dimensions

For best overall propulsive efficiency, a larger diameter propeller should be used, but ground clearance and compressibility effects limit the use of a larger diameter propeller. Since the

plane will be flying at lower airspeeds, a propeller with a lower pitch-to-diameter ratio was chosen because it should have a greater propulsive efficiency.

4.1.6 Battery and Cells

The weight of the batteries carried has a direct effect on the aircraft cost and the power output by the motor. The more batteries that are carried, the higher the power output and the higher the aircraft cost is going to be. Taking into consideration that the plane will be flying at lower air speeds, there will be some optimum point between the battery weight and power output that will maximize performance and cost efficiency.

4.2 Mission Model Analysis

The preliminary design phase focused on the creation and implementation of computer programs to analyze the different elements of flight including lift, drag, turning, and weight of aircraft. The programs used equations to help optimize the overall performance of the plane. This made it possible to analyze different parameters of the aircraft to attain the best overall score.

4.2.1 Overview (things used)

The amount of water carried as a payload was an initial determination. Once the weight from the payload was determined, the necessary motor type as well as the propeller diameter and pitch were chosen. Once the estimated mission time was calculated, the number of battery cells was determined. With the average velocity of the plane, the airfoil shape and wing area were determined for the necessary lift. The wing was also designed to carry the load of the fuselage plus the payload. When the time to run the obstacle was calculated, the use of a ram-air system was added to the payload deployment. A computer program was developed to do most of these calculations.

4.2.2 Weight

The first consideration that comes to mind when you think about weight is the weight of the payload. For the fire bomber mission, a team can carry up to four liters of water, where each liter of water is roughly about 2 pounds per liter so depending on how much water the team wants to carry all depends on how the fuselage is going to be built around it. Another thing to consider is the motor and batteries. The motor used is an Astro-90 cobalt motor which weighs approximately 1.9 pounds. The batteries used are nickel cadmium 2400 max which weighs approximately 1.25 pounds per pack. The predicted wing weight was calculated based on the size and area of the wing. The wing weight will increase accordingly with an increase in wing span, area, and design load. The rest of the components of the aircraft are represented in Table 4.1. The overall weight for the plane was projected around 14.3-25.7 pounds.

Table 4.1 Components of the aircraft versus its projected weight

Component	Project Weight (lbs)
Power Plant	5 ~ 7
Control	.25 ~ 1
Landing Gear	.4 ~ .8
Wing	1.25 ~ 2.50

Horizontal Tail	.2 ~ .6
Vertical Tail	.2 ~ .4
Fuselage	3 ~ 5
Payload	4 ~ 8

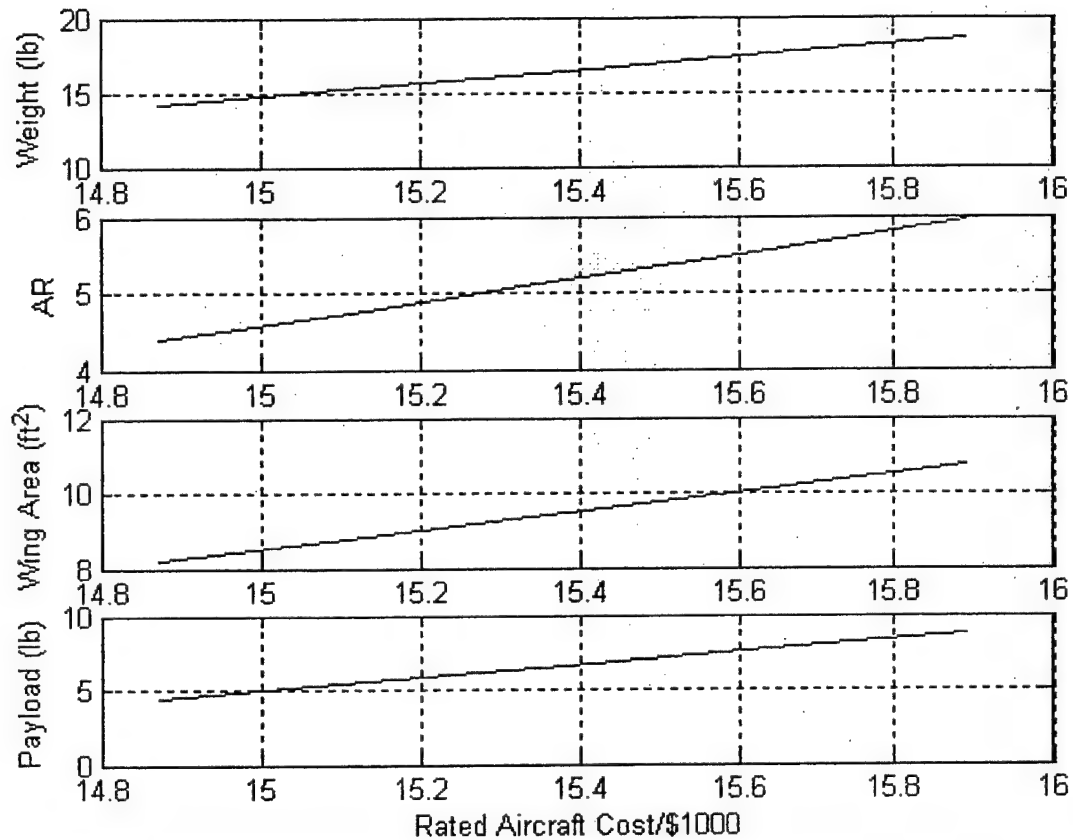


Figure 4.1 Weight and other components of the aircraft versus cost of the aircraft

The trends in Figure 4.1 show that as payload, wing area, aspect ratio and weight increase, the cost of the aircraft will also increase. These trends were plotted using the script based on the specified weights in Table 4.1 and other aircraft analysis equations.

4.2.3 Lift/Drag Calculations

The lift and drag calculations were based on the different ranges of the weights projected in Table 4.1. These projected weights were then put into the script along with lift and drag equations. The relationships are shown in Figure 4.2

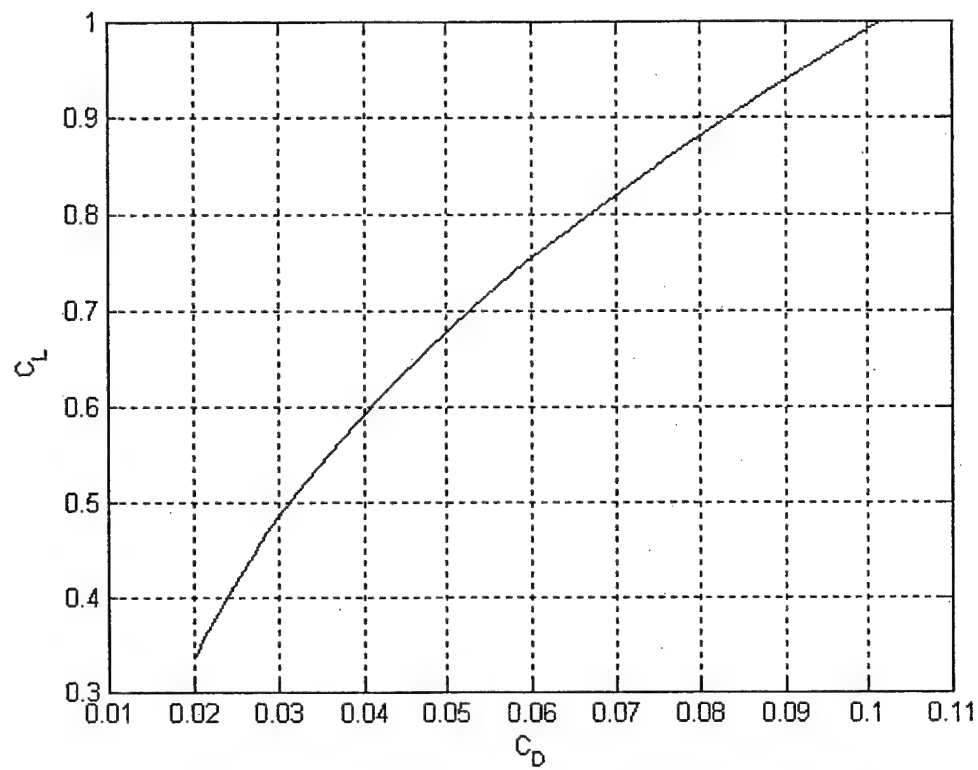


Figure 4.2 Coefficient of Lift versus Coefficient of Drag

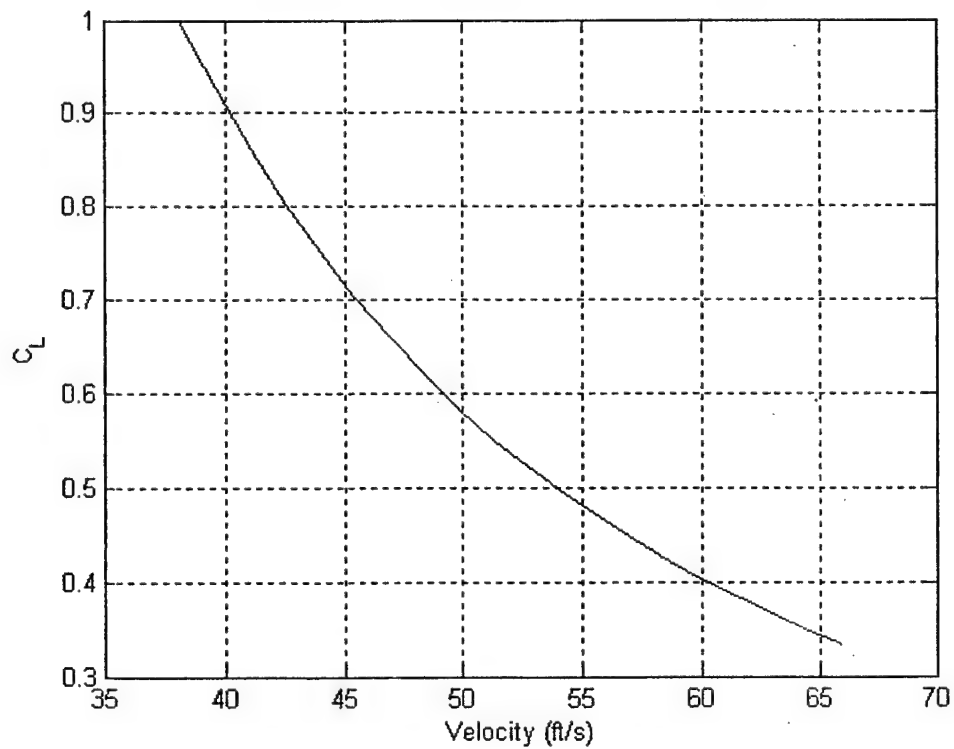


Figure 4.3 Velocity versus Coefficient of Lift

These graphs represent the trends of C_D and C_L versus each other and versus velocity over time based on the specified weights given in Table 4.1. The table shown below is of different airfoil designs that were considered for the wing of the aircraft. The Eppler 197 design was chosen due to the fact that at low air speeds this airfoil is very efficient.

Table 4.2 Different airfoils and their specifications considered for the aircraft

Airfoil	C_{Lmax}	AOA° @ C_{Lmax}	C_D @ C_{Lmax}	Stall Behavior
NACA 2412	1.1	12	0.015	Gentle
NACA 0012	0.9	12	0.014	Moderate
NACA 6412	1.4	12	0.025	Gentle
NACA 64-412	1.3	12	0.010	Abrupt
E197	1.17	10	0.015	Gentle
E68	1.0	12	0.030	Abrupt
E214	1.2	10	0.030	Moderate
E211	1.1	12	0.035	Abrupt
E205	1.2	13	0.030	Moderate
E222	1.1	12	0.030	Moderate
E230	0.8	8	0.020	Moderate

4.2.4 Stability/Control

With the above information, the next step was calculating the stability and control characteristics of the aircraft. Figure 4.4 shows the overall pitching moment coefficient of the aircraft based upon the different aircraft components. It can be seen that the overall airplane is stable.

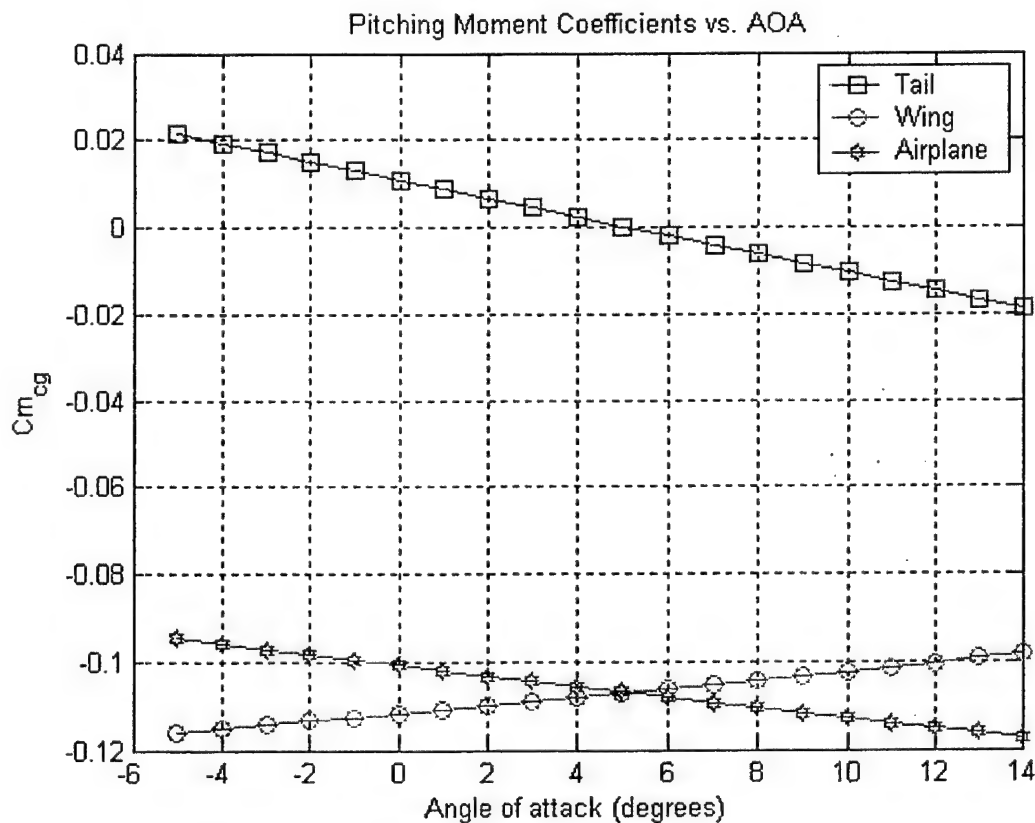


Figure 4.4: Cm_{cg} vs.. AOA

Figure 4.5 is a visualization of the different pitching moments based upon different elevator deflections.

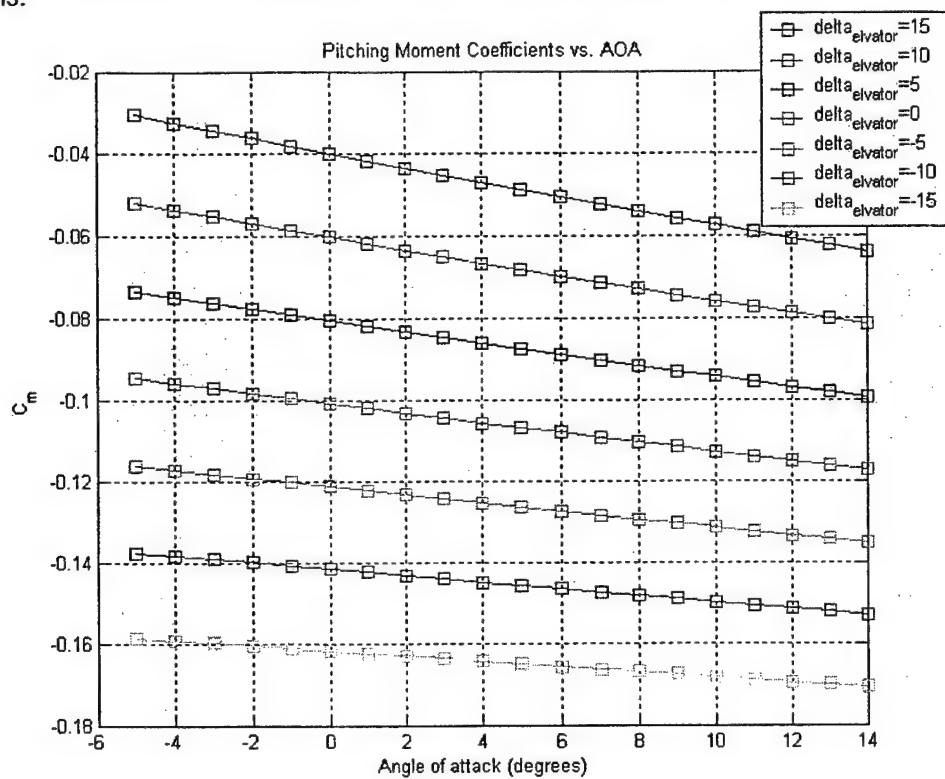


Figure 4.5: Pitching moment coefficient vs. AOA at various elevator deflections

As shown below, the yaw moment characteristics of the aircraft due to different sideslip angles can be seen. Although the plot is of a curve, rather than a usual linear line, the plane is still stable.

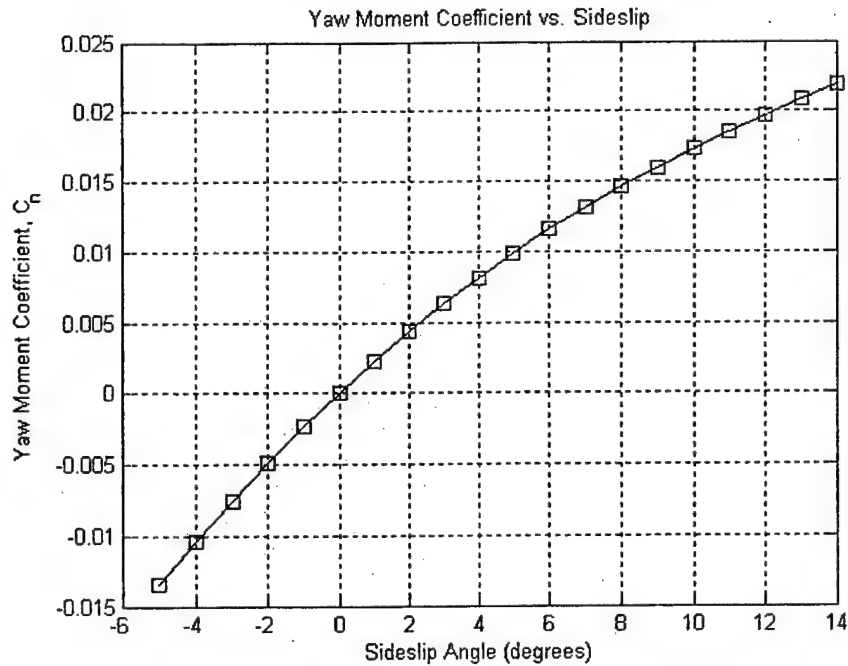


Figure 4.6: Yaw moment coefficient vs. sideslip

4.2.5 Propeller Analysis

In order to guarantee that the most efficient propeller be selected, the computer program was used to aid in the selection. Figure 4.7 shows the different analyses done for the propeller.

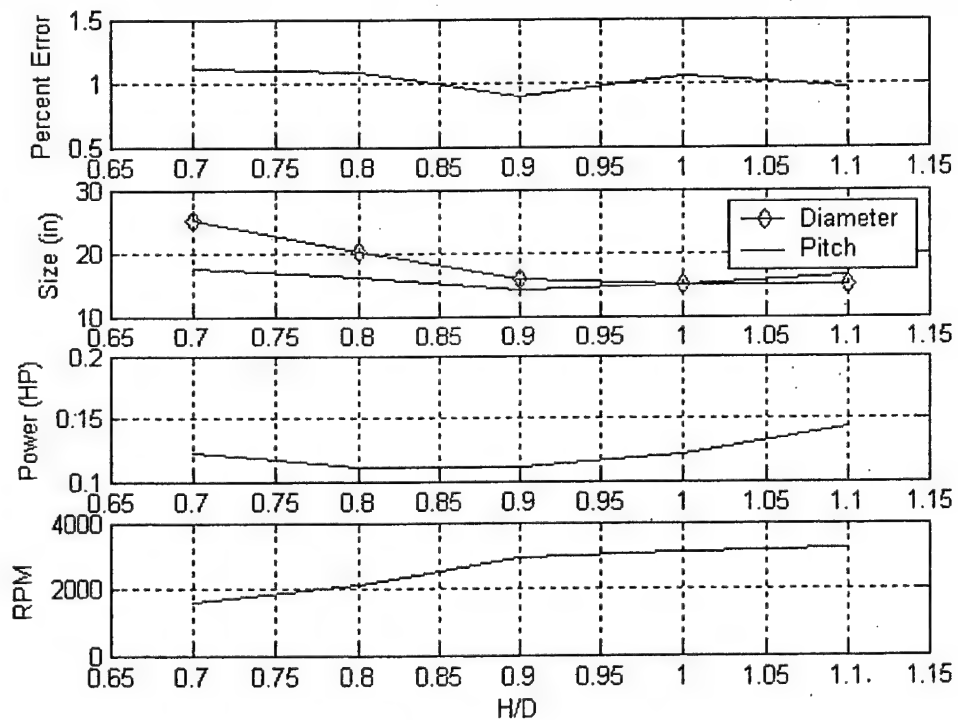


Figure 4.7: Propeller analysis curves

As a result of these comparisons, the selected propeller was a 16X14. This was chosen due to its high RPM values with the lowest possible power requirement.

4.2.6 Turn Analysis

Turn analysis is important because it shows how fast an aircraft can maneuver during a turn at different turn radii. The graph of Figure 4.8 shows that at slower velocities the higher the turn radius is going to be.

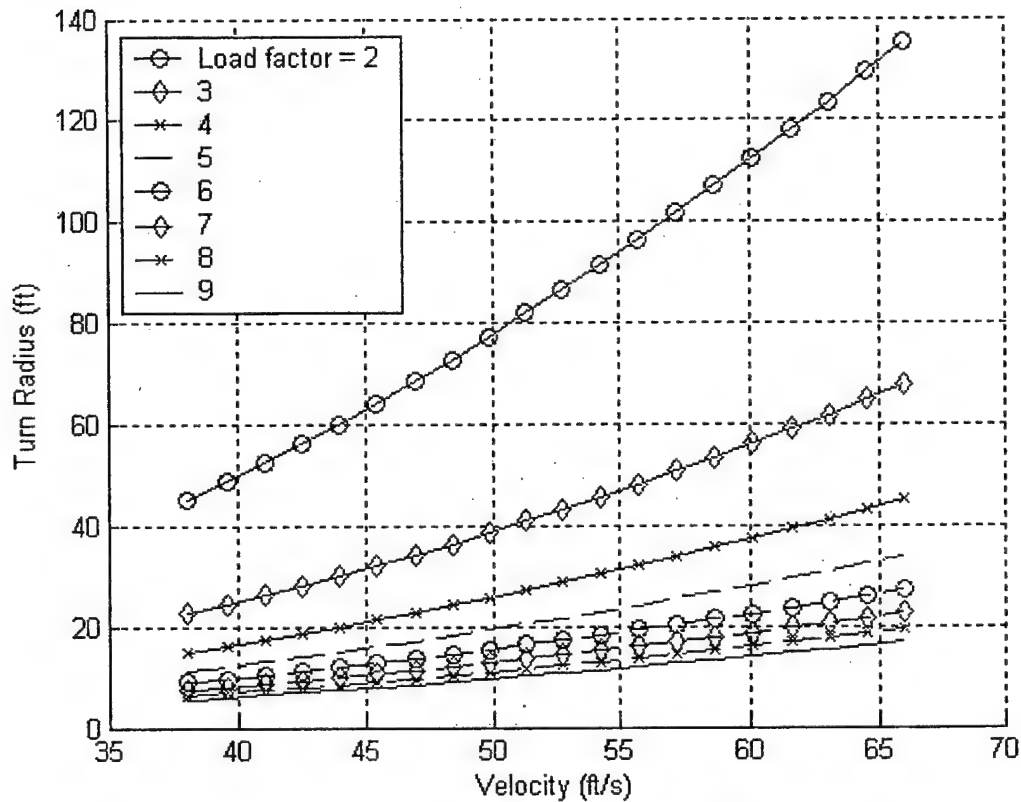


Figure 4.8 Velocity versus Turn Radius

As shown in Figure 4.8, the larger the load factor, the tighter the turn. This is reaffirmed using a load case example of $n=5$ in Figure 4.9. This specific load was the one that was selected based upon its maneuverability characteristics without too much added weight.

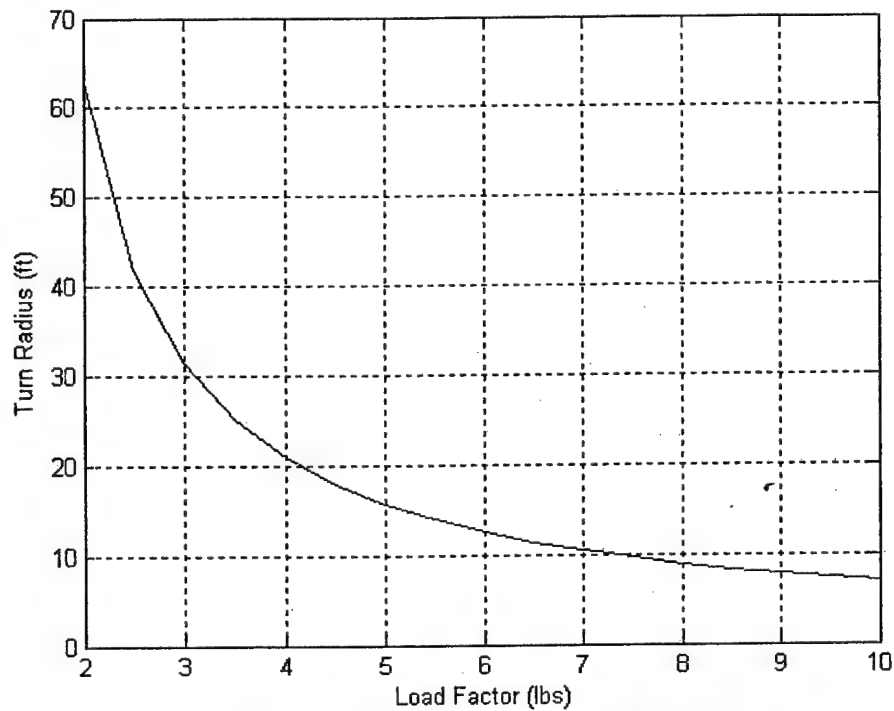


Figure 4.9 Load Factor versus Turn Radius

4.3 Optimization Trade

Having run the designed program, and viewing its results as shown above, numerous decisions were made and optimization points were sorted. These results and decisions were used to guarantee that the aircraft would achieve the highest flight score possible.

4.3.1 Design Parameters

For maximum effectiveness, Table 4.3 shows an optimized range of the design parameter sizes that lead to the lowest RAC but still have enhanced performance abilities.

Table 4.3: Optimized parameter sizes

Design Parameter	Value Selected
Wingspan (b), ft	7-8
Wing Area (S_w), ft^2	8.5-10.5
Vertical Tail Span (bv), ft	.6-.9
Vertical Tail Area (S_v), ft^2	.14-.2
Horizontal Tail Span (bht)	3.0-3.75
Horizontal Tail Area (S_{ht}) ft^2	1.6-1.8
Turning Load Factor (n), g	5
Battery Weight (W_b) lb	5
Propeller Pitch and Diameter	16 x 14
Flight Speed (V) mph	45
Rated Aircraft Cost, k\$	15.8

4.3.2 Mission Parameters

Table 4.4 shows the predicted mission performance at a 45 mph flight speed which was selected to be optimal flight speed.

Table 4.4: Predicted mission performance

Performance Parameters	Approximate Value
RAC (k\$)	15.8
Flight Time (min)	1.9

4.4 Conclusions

The overall results of the preliminary design phase was used to verify initial assumptions made in the conceptual design phase such as wing placement, tail type and control surface choices. From the computer program that was implemented to assist in performing the preliminary analysis, specific optimization points were easily seen and can now be applied to the detailed aircraft design.

5.0 Detail Design

After completing preliminary design it was necessary to size and select both primary and secondary components. By comparing previously collected data, a motor size was selected, along with primary building materials. Methods of component construction were weighed and investigated along with component make up. Finally a mockup fuselage was constructed in order to gauge internal component meshing.

5.1 Configuration detail design

The final configuration resembled a commercial cargo plane similar to the C-130. In order to compensate for fluid payload, a high mounted wing provided increased stability. To lessen the complexity of servo linkage, minimize the RAC, and provide more control, flaperons were installed. Although, the tail may appear somewhat large, it was needed to conform to a similar aspect ratio of the wing and provided sufficient stability. In addition, the fuselage was built to accommodate a large payload with as much streamlining as possible while still being able to fit the aircraft components intact in the required sized transport box.

5.2 Structural Component Selection

5.2.1 Fuselage

Due to high drag coefficients resulting from the fuselage in past years, a new approach was taken in the fuselage design. The 2001 fuselage consisted of fiberglass and basswood as its major construction components, which resulted in a total weight of 9 pounds. The 2002 fuselage, although weighing less than the previous year still had significant aerodynamics shortcomings. This year, the nose cone, constructed out of fiberglass, was designed similar to commercial transport aircraft. In the conceptual design process, a single boom tail was determined to be sufficient, but in detailed design it became apparent that a tapered fuselage should be employed to merge with the horizontal tail and provide a more streamlined body. In order to provide increased fuselage rigidity, the bulkheads were constructed out of 1/4" plywood rings which were connected together with a series of hollow aluminum stringers and one carbon fiber spine. With this type of construction the sheeting did not play a primary role in holding the fuselage together, making manufacturing of such fuselage much easier than last year. This fuselage design provided a cavity for the bladder without the necessity of a floor which decreased the overall fuselage weight. Instead of previous attempts of sheeting with fiberglass which produced unacceptable fuselage weight, 1/16" balsa wood was selected to sheet this year's design.

5.2.2 Wing

To keep the wing light and simple, a regular balsa spar and rib method of construction augmented with a carbon fiber plug-in spar wing joiner was selected. R/C aircraft in the 20lb category regularly employ 3/32" balsa ribs and were therefore chosen. Last year, a central carbon fiber spar was employed but this greatly decreased the strength of each rib and created difficulties in construction. Instead, each rib was notched on the top and bottom and a 1/4" square balsa strip was fastened as the wing spar. The sheeting needed was determined to be 1/8" balsa in order to support the structural wing loading.

To ensure a fit into the 4' long box, the maximum wingspan for a single piece wing was limited to 4 feet. For this reason, the wing was designed in 2 halves that employ a plug-in spar to join them. A dual rod method was designed to attach the wing to the fuselage. This consists of a carbon fiber tube in the leading edge and an aluminum tube similar to the ones used in the fuselage to fasten at the trailing edge of the wing. This method is a tried and tested method employed regularly on most R/C aircraft.

5.2.3 Empennage

Last year, the 25% wing area rule was followed, but this provided insufficient stability for the size of the aircraft. To improve on this, a larger horizontal tail was incorporated. This only slightly increased the RAC and so was a reasonable improvement on design. Without the restriction of the 25% rule, a larger tail with a similar aspect ratio to the main wing was incorporated. This component was constructed in the same manner as the main wing. A single vertical tail design was employed similar to the vertical tails found on conventional cargo planes. This was constructed out of a 1/4" square balsa frame and sheeted with 1/16" balsa.

5.3 Secondary Component selection

5.3.1 Propulsion and Controls

As a result of a relatively large aircraft weight of 16 pounds, a larger motor was required for the 2001 plane. The Astroflight Cobalt 90, weighing 32 ounces, was eventually decided upon. With an estimated aircraft weight of 9 pounds for the current design, the Astroflight Cobalt 60, with overall weight 22 ounces, was selected for propulsion. This motor requires fewer cells, 32 as compared to 36. Additionally, the motor requires fewer amps, 2.5 as compared to 3.0; and can attain a higher top speed of 347(rpm/volt) as compared to 256(rpm/volt). Due to previous mounting difficulties, a Great Planes 60-120 motor mount was purchased for reliable configuration.

Radio selected for this year's aircraft was a top of the line JR PCM-10X. This provided the aircraft and the pilot with nearly infinite degrees of flexibility and precision and will be able to handle any sort of competition design it is used to control. As the model is not a precision, high performance pattern aircraft, standard ball bearing brushless JR 517 servos were once again selected for this year's plane because of previous outstanding performance, reliability, and cost effectiveness. A Hobbico CS-35 mini servo was selected for operation of the payload valve.

5.3.2 Payload

Since the given fuselage was chosen in order to accommodate a cylindrical bladder, soda bottles seemed like an ideal component. To decrease the adverse effects of the water shifting during maneuver, a system of straw barriers was installed throughout the bladder. Using gravity to increase performance of payload deployment, the obvious placement of the release valve was on the bottom of the fuselage. In order to prevent an unwanted internal moment, the valve was placed in line with the calculated center of gravity of the airplane. Since testing times of the water deployment, constricted by the 1/2" diameter exit rule, exceeded calculated downwind flight time, a positive pressure assist system was introduced. Constructed of two half inch tubes protruding from the top of the fuselage, this system provided adequate support in deployment of the water in wind tunnel testing.

Table 5.1 Aircraft Specifications

Performance	
CL max(clean)	1.1
L/D max	10.533
Max Rate of Climb	ft/min
Stall Speed	25 ft/s
Max Speed	66.01 ft/s
T/o length (empty)	70 ft
T/o length (gross)	110 ft

Wing Geometry	
Length	4.85 ft
Span	7 ft
Height	1.5 ft
Wing Area	10.06 ft ²
Aspect Ratio	5.57
Flaperon Area Per Side	0.21 ft ²
Chord	1.44 ft

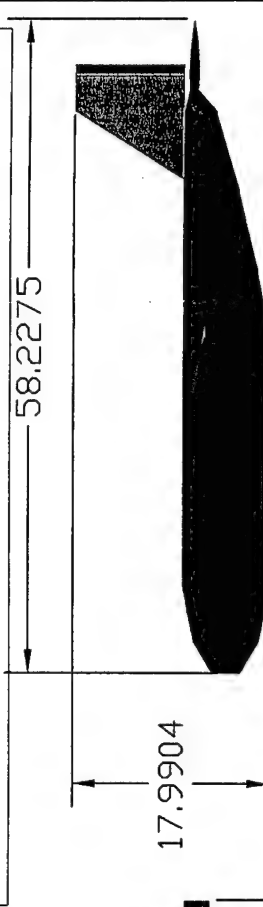
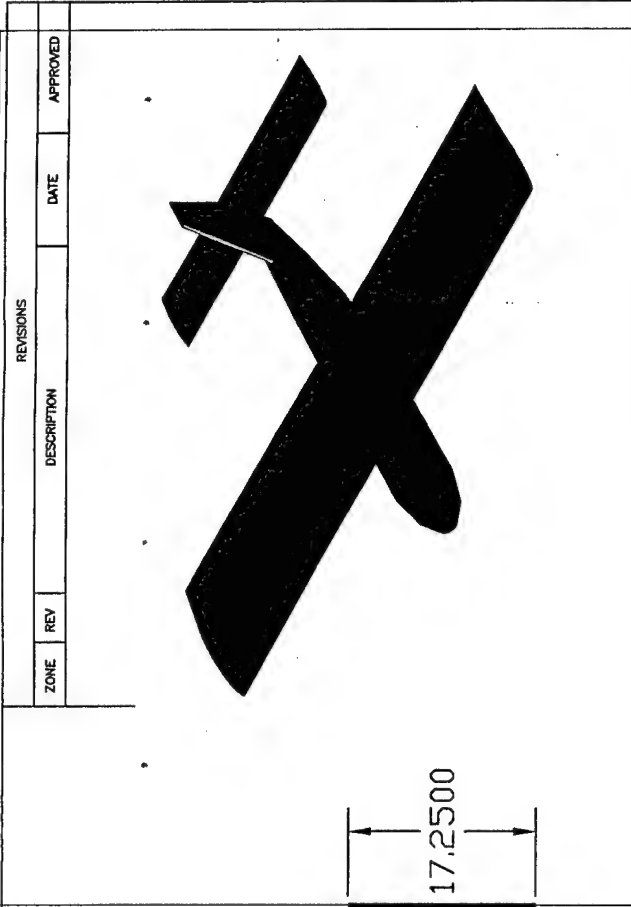
Weight Statement	
Airframe	6.42 lbs
Propulsion System	6.97 lbs
Control System	.75 lbs
Payload System	.252 lbs
Payload	5.97 lbs
Empty Weight	14.392 lbs
Gross Weight	20.362 lbs

Systems	
Radio Used	JR PCM-10x
Servos Used	JR 517 & HOBBICO CS-35
Battery Config	32X2400mAh SANYO CP-2400SCR NiCad
Motor	AstroFlight Cobalt 60
Propeller	15x8
Gear Ratio	Direct Drive

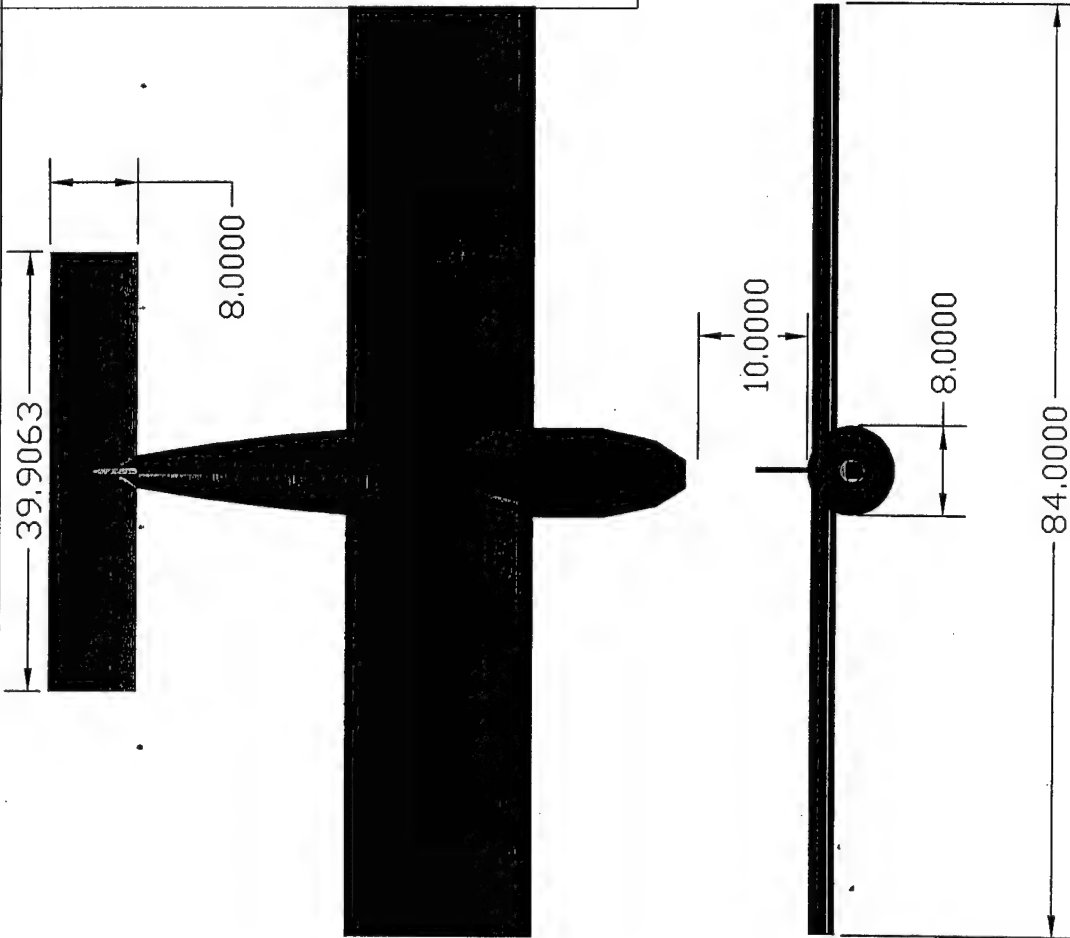
Table 5.2 RAC of aircraft

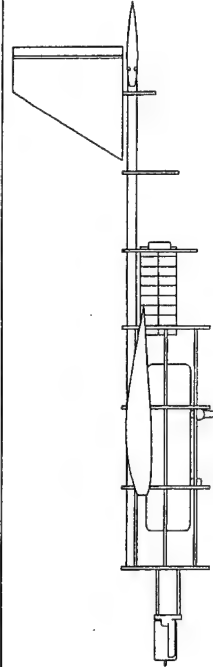
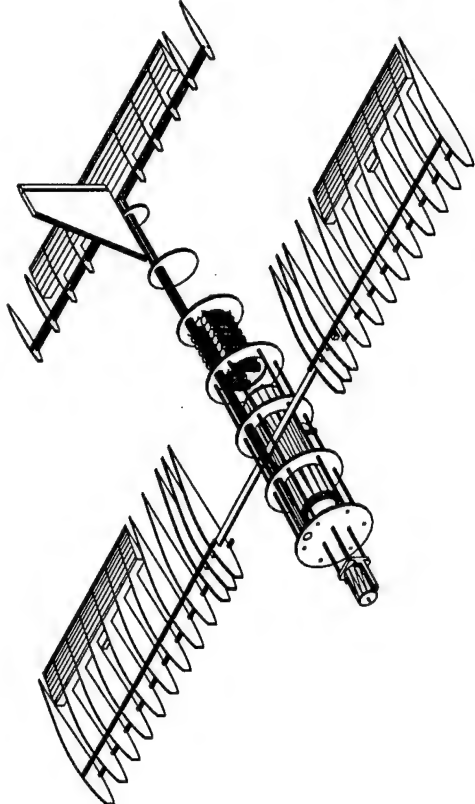
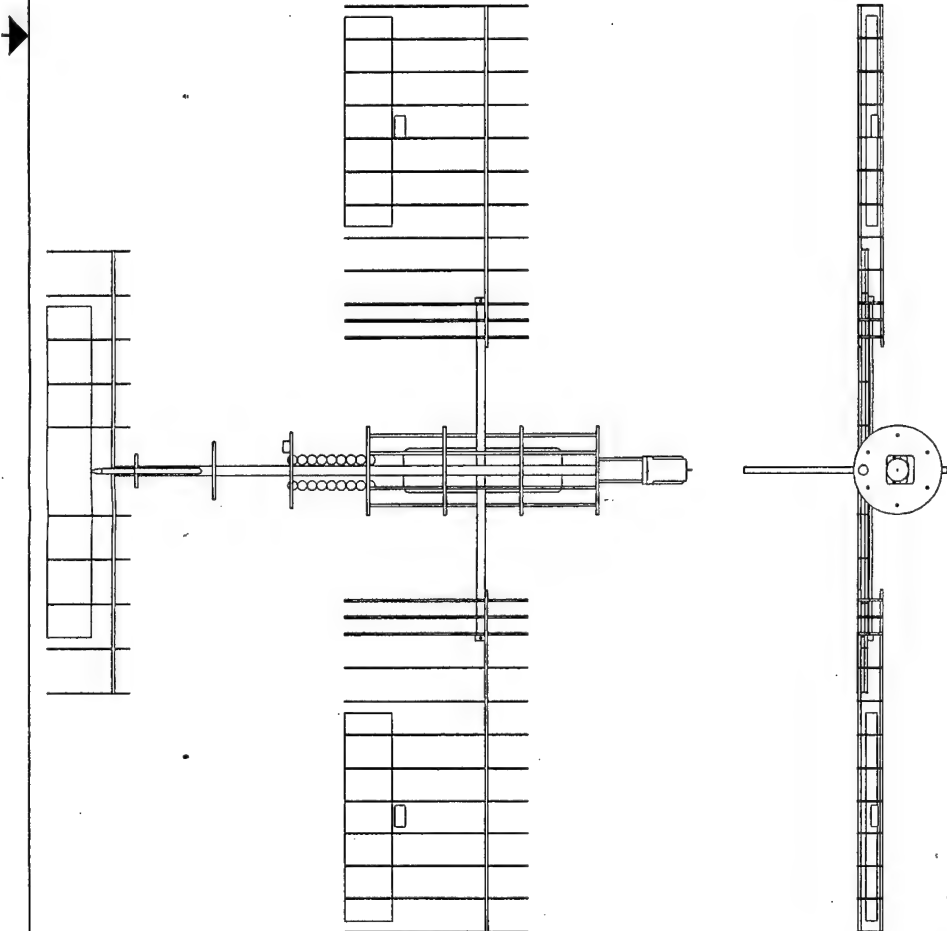
Category		Penalty
MEW	14.00	\$ 4,200.00
REP	5.00	\$ 7,500.00
Wing Area 1	11.50	\$ 2,300.00
Wing Area 2	2.22	\$ 444.44
Fuselage Volume	1.78	\$ 711.11
Vertical Surface	1.00	\$ 200.00
Flaperons	2.00	\$ 300.00
Ailerons	1.00	\$ 100.00
Servos	6.00	\$ 600.00
Total		\$ 16.36

REVISIONS			
ZONE	REV	DESCRIPTION	DATE
			APPROVED



Overall Config & Dimensions			
Clarkson University '03-04			
DBF			
Drawn By:	SIZE	FSCM NO.	DWG NO.
TJP			
SCALE		SHEET	

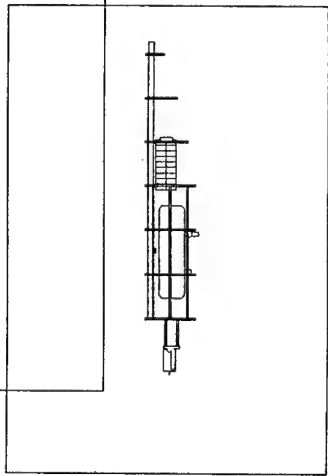
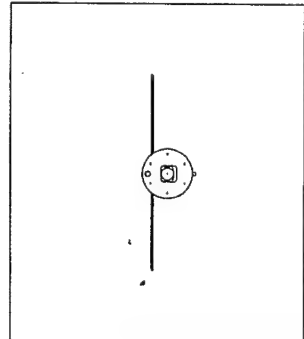
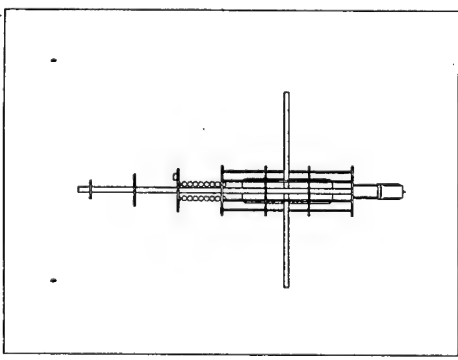
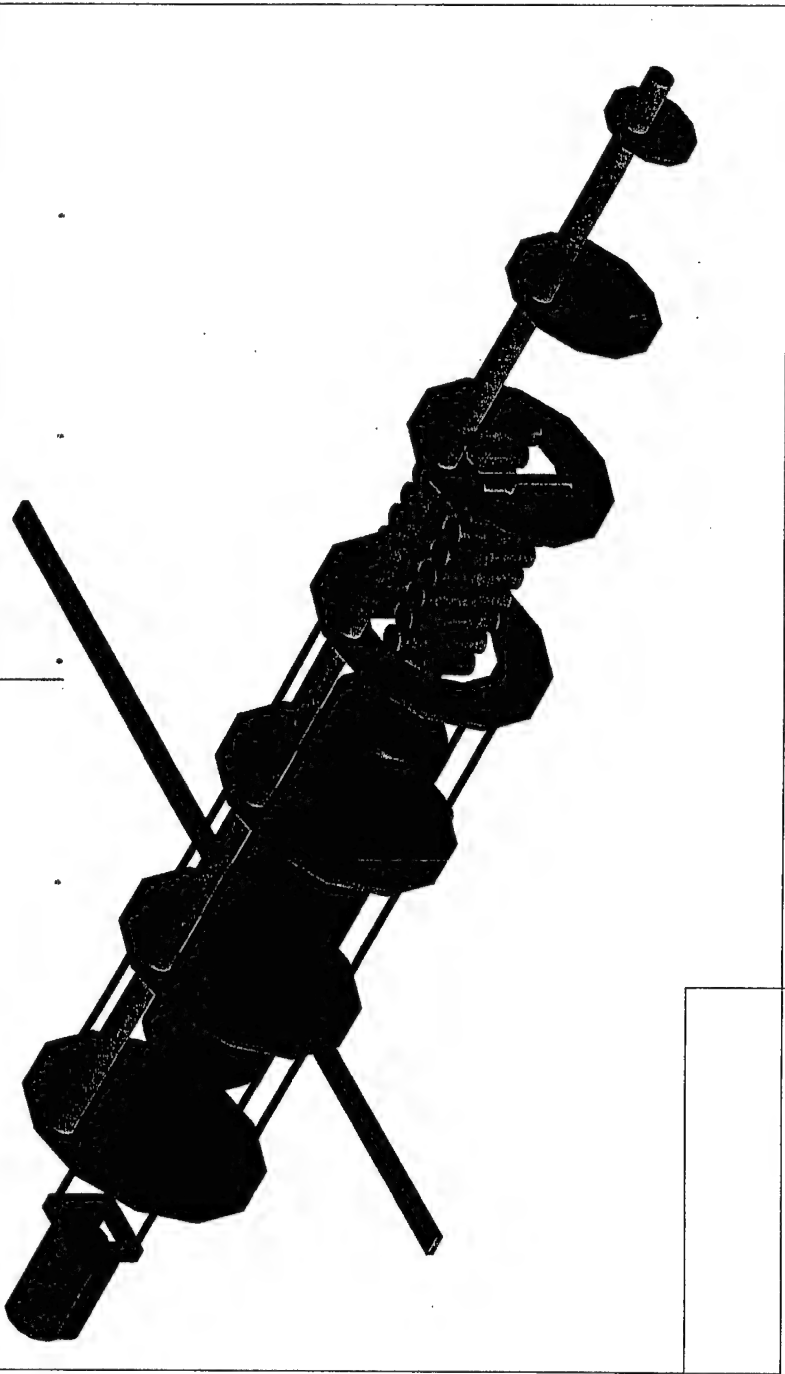




Structural Drawing		Clarkson University '03-04	
Drawn By:	TJP	SIZE	DBF
		FSCM NO.	DWG NO.
		REV	SHEET

REVISIONS			
ZONE	REV	DATE	APPROVED

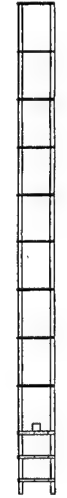
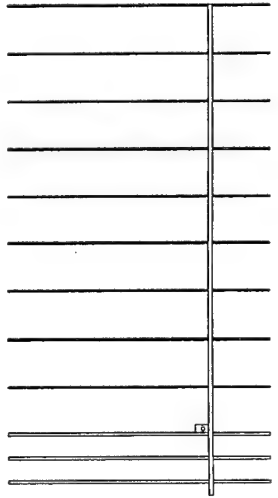
REVISIONS			
ZONE	REV	DESCRIPTION	DATE
			APPROVED



Fuselage Components		Clarkson University '03-04	
DBF		REV	
Drawn By:	SIZE	TSCM NO.	DWG NO.
TJP	SCALE	SHEET	



REVISIONS			
ZONE	REV	DESCRIPTION	DATE
			APPROVED



Wing Structure Components	
Clarkson University '03-04	
DBF	
Drawn By:	SIZE
TJP	FSCM NO.
	DWG NO.
	REV
	SCALE
	SHEET

6.0 Manufacturing Plan

A key concern when designing the aircraft was that the aircraft must be manufactured in a reasonable amount of time so that there would be time for redesign if necessary. In order for this to occur, the materials used were carefully planned out as well as the time allotted for each main aspect of the manufacturing. To stay on schedule a manufacturing milestone chart was created and figures of merit were taken into consideration in order to make a manufacturing plan that fit the announced objectives.

6.1 Figures of Merit

A list of Figures of Merit (FOM) was created and reviewed while making the manufacturing plan. The FOM served as a way to score the possible decisions, without bias, in correlation with the manufacturing of the aircraft. The FOM that were used were availability of materials, cost, time, weight, and staff.

6.1.1 Availability of Materials

One of the most important factors in keeping with a set manufacturing schedule is the availability of materials. If the materials are not present, then the manufacturing procedure falls behind, and cannot begin again until those materials are available. If the materials were not available the procedure received a score of 1. If the materials were attainable, but they were not received in a short period of time, the procedure received a score of 5. If the materials were easily attainable, the procedure received a score of 10.

6.1.2 Cost

One key factor in the manufacturing process that may be overlooked is the cost. It is very important to stay within budget, and if there isn't money available, the procedures cannot take place. If the procedure was too expensive and didn't seem viable in correlation with the budget a score of 1 was given. If the procedure seemed costly, but was within the means of the budget a score of 5 was given. If the procedure was within budget and inexpensive a score of 10 was given.

6.1.3 Time

A time period of 5 months was scheduled for building and testing the aircraft. If a certain procedure was going to take longer than 4 weeks a score of 1 was given. If the procedure was going to take between 2 to 4 weeks a score of 5 was given. If the procedure was going to be completed within a week or less was given a score of 10.

6.1.4 Weight

The weight of the overall aircraft stems from the weight of the aircraft components. This was an important factor in the manufacturing process. The procedures were scored from the ones containing the heaviest components up to the ones containing the lightest components, 1,5,10.

6.1.5 Staff

The manufacturing process cannot be completed without people to work on the assigned processes. Some manufacturing processes involve more people than other processes. A score of 1 was given for those procedures where more than 8 people were needed to complete the task. A score of 5 was given for those tasks that involve 4 to 8 people and a score of 10 was given to those procedures that required less than 4 people for a given task.

6.2 Weighted Objective Tables

Each FOM in the list was used to create a weighted objectives table that was used in the decision making process for the manufacturing schedule. The tables are shown below for the list of five FOM.

	Availability of Materials	Cutting/Sanding/Gluing	Payload	Fiberglassing	Monokote Application	Foam-Hot Wiring	Balsa/Plywood Framing	Servos	Control Surfaces
Number of People		10	3	3	2	3	10	2	2
FOM score		10	5	5	10	5	10	10	10

Figure 6.2.1: Availability of Materials in a weighted objectives table

	Cost	Cutting/Sanding/Gluing	Payload	Fiberglassing	Monokote Application	Foam-Hot Wiring	Balsa/Plywood Framing	Servos	Control Surfaces
Number of People		10	3	3	2	3	10	2	2
FOM score		10	10	5	10	10	10	10	10

Figure 6.2.2: Cost in a weighted objectives table

	Time	Cutting/Sanding/Gluing	Payload	Fiberglassing	Monokote Application	Foam-Hot Wiring	Balsa/Plywood Framing	Servos	Control Surfaces
Number of People		10	3	3	2	3	10	2	2
FOM score		5	1	1	10	5	5	10	5

Figure 6.2.3: Time in a weighted objectives table

	Weight	Cutting/Sanding/Gluing	Payload	Fiberglassing	Monokote Application	Foam-Hot Wiring	Balsa/Plywood Framing	Servos	Control Surfaces
Number of People		10	3	3	2	3	10	2	2
FOM score		10	1	5	10	5	10	5	10

Figure 6.2.4: Weight in a weighted objectives table

	Staff	Cutting/Sanding/Gluing	Payload	Fiberglassing	Monokote Application	Foam-Hot Wiring	Balsa/Plywood Framing	Servos	Control Surfaces
Number of People		10	3	3	2	3	10	2	2
FOM score		1	10	10	10	10	1	10	10

Figure 6.2.5: Staff in a weighted objectives table

6.3 Manufacturing Processes Investigated

The manufacturing process took place in Clarkson's University's Center for Advanced Materials Processing Student Project Lab. The plane was manufactured out of balsa, foam, carbon fiber, and fiberglass. The material selections for the various aircraft components were analyzed and the final selections for material were settled on at the end of the detailed design.

6.3.1 Wings

The wing was constructed from a balsa frame. The initial option for the wing spar was carbon fiber. This spar was tested and analyzed against a balsa spar. It was found that the carbon fiber spar was stiffer and harder to work with. The balsa spar was lighter, easier to manufacture, and less costly than the carbon fiber spar, so the balsa spar was chosen and used.

6.3.2 Fuselage

The fuselage was constructed from wood bulkheads and balsa stringers. The spine for the fuselage was evaluated from analyzing wood versus carbon fiber. The wood spine resulted in ease of manufacturing while the carbon fiber provides stiffness for the aircraft. It was decided that a carbon fiber spar would be used. When constructing the nose cone, fiberglass versus balsa was compared. The fiberglass resulted in being smooth and light weight. Foam was also used as a material selection on the fuselage. A foam wing box was constructed because it was easier to shape than balsa and it improved aerodynamics and weight.

6.3.3 Payload

A bladder versus a plastic container was considered for a holding compartment for the payload. The bladder provided shape forming yet it was hard to guarantee full water deployment. The plastic container was stiff, light, and easier to empty, so the plastic container was chosen.

6.3.4 Tail

The horizontal tail was constructed from a balsa wood frame. The ribs were constructed from 3/32" balsa and it was sheeted with 1/16" balsa. The vertical tail was constructed from 1/4" balsa rods and covered with 1/16" balsa sheeting.

6.4 Manufacturing Milestone

An important aspect of the manufacturing plan was a detailed schedule that gave certain deadlines for particular processes. A milestone chart was produced with the planned time that was allotted, and on the same chart is the actual time that the processes took. It is clear on the milestone chart the time frame for the production and the actual completion time.

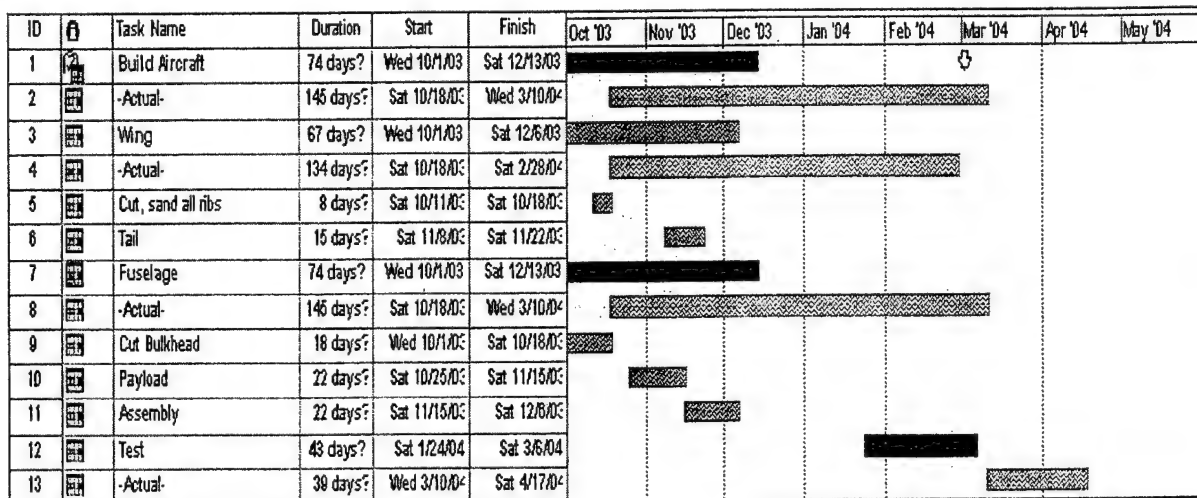


Figure 6.4.1: Manufacturing Milestone Chart

7.0 Testing Plan

As with any design, flight testing is an integral part of the design process. This is an opportunity to collect quantitative data to be compared with expected performance estimates. The following testing plan is for certain aircraft components and the entire package itself. Having used tests of individual components, more efficient design details were able to be implemented.

7.1 Test Objectives and Schedule

A list of test objectives and the relevant dates on which those tests were to be performed can be seen in Table 7.1.

Table 7.1: Test objectives and schedule

Test	Purpose	Dates
Component wind tunnel testing	Refine component profiles and reduce overall drag force.	10/1-11/15
Payload Deployment	Ensure timely water deployment and test ram air system.	1/20-1/27
Wing Structure	Confirm that wing structure has sufficient strength to withstand wing loadings during flight conditions.	1/10-2/1
Weight and balance	Determine that the aircraft cg is within allowable limits.	2/1-2/6
Propulsion and electrical systems	Test battery capacity, ability to cool properly, and overall electrical system components.	1/27-2/12
Empty Flights	Demonstrate capabilities of actual flight.	3/1-4/1
Loaded Flights	Demonstrate the ability to meet the requirements of the Fire Bomber mission.	4/1-4/20

7.2 Pre-flight and Test Flight Checklists

Prior to any flight there are a series of checks that must be performed to ensure that the aircraft is in a suitable flight condition (Table 7.2). The reasons that this was determined to be necessary were: that the aircraft must be reassembled for each flight, to ensure that no damage was incurred during transport, and that all electrical and control components are in working condition.

Table 7.2: Pre-flight Checklist

Pre-Flight Check List Items		
Battery charge	Are the battery packs fully charged?	
Fuse Check	Is the fuse intact?	
Servo Connections	Is every servo connected?	
Wing Joint Security	Is the wing firmly attached?	
Horizontal Tail Security	Is the horizontal stabilizer firmly attached?	
Vertical Tail Security	Is the vertical stabilizer firmly attached?	
Control Surface Joints	Are all control surface joints in good condition?	
	Moving freely?	
Control Corrective Adjustments	Are all control surfaces deflecting to desired positions?	
	Correct directions?	
Motor Mount Security	Is the motor firmly attached?	
Propeller Integrity/Balance	Is the propeller cracked? Is it balanced?	
Fail Safes	Correct deflection with Tx off?	
Landing Gear	Secure?	
	Aligned?	
Payload	Is the payload secure?	
	Water tight?	
	Is the aircraft still balanced?	
Surface Integrity	Are there any holes in the skin?	
	If so, were they repaired?	
Radio	Any interference at 100' with antenna detached?	

To obtain the flight characteristics while the aircraft was airborne a separate list was created (Table 7.3). As listed, these categories are a direct measure of flight characteristic qualities during ground tests, taxi tests, empty flight and loaded flight. The tests were divided as such since these represent the logical progression of tests that were/will be done post aircraft completion.

Table 7.3: Flight Tests and Categories

Flight Tests		
Static Thrust →Battery drainage time at 100% power →Battery drainage time at 60% power →Thrust measurements at 30% throttle →Thrust measurements at 60% throttle →Thrust measurements at 100% throttle Comments:	Acquired Data	
		(s)
		(s)
		(lb)
		(lb)
		(lb)
Taxi Test →Adequate directional control? Comments:		
	Yes/No	
Empty Flight →Takeoff distance →Time to climb to cruise altitude →Stable? →Flight time at 60% throttle →Flight time at 100% throttle Comments:		
		(ft)
		(s)
	Yes/No	
		(s)
		(s)
Loaded Flight →Takeoff distance →Time to climb to cruise altitude →Stable? →Flight time at 60% throttle →Flight time at 100% throttle →Payload deployment time Comments:		
		(ft)
		(s)
	Yes/No	
		(s)
		(s)
		(s)

7.3 Test results

Having performed the tests as stated previously, the following results were obtained and conclusions drawn.

Table 7.4 Results and Conclusions

Test	Results and Conclusions
Component wind tunnel testing	It was found that although a boom tail would decrease total aircraft weight, the drag penalty for a squared back would severely inhibit flight performance. Therefore it was decided that a conventional fuselage was more desirable.
Payload Deployment	Although the water escaped from the 1/2" hole within 30 seconds, having used a "ram-air" system lowered that time to around 20 seconds which would lead to faster downwind legs, therefore shorter flight times and increased score.
Wing structure	Having tested the wing with first the loaded weight of the aircraft (20 lbs) and then double, it was decided that a carbon fiber joiner tube was required for additional stiffness than balsa could provide.
Weight and Balance	After performing a tip test at the 1/4 chord, it was found that the aircraft's cg was within design parameters.
Propulsion and Electrical Systems	After running the motor with a 15x8 propeller at various power settings, it was decided that the optimal cruise setting would be between 60-70% throttle for maximum battery performance.



Georgia Institute of Technology
2003-2004 AIAA Design, Build, Fly Competition
Table of Contents

EXECUTIVE SUMMARY	1
DEVELOPMENT SUMMARY	1
RANGE OF ALTERNATIVES INVESTIGATED.....	2
MANAGEMENT SUMMARY	5
TEAM STRUCTURE	5
PROJECT DEVELOPMENT	5
COMMUNICATION AND INFORMATION MANAGEMENT.....	5
CONCEPTUAL DESIGN	8
PROBLEM STATEMENT	8
<i>Scoring Structure:</i>	10
RAC ANALYSIS	10
AIRCRAFT CONFIGURATIONS INVESTIGATED	11
<i>Vertical Wing Placement</i>	12
<i>Number of Lifting Surfaces</i>	12
<i>Vertical Thrust Line Location</i>	12
<i>Landing Gear</i>	12
<i>Empennage Type</i>	12
<i>Number of Motors</i>	12
<i>Longitudinal Thrust Orientation</i>	13
DESIGN SPACE SCREENING	13
CONFIGURATION SELECTION	14
PRELIMINARY DESIGN	19
ANALYSIS METHOD SUMMARY	19
DESIGN PARAMETERS AND SIZING TRADES INVESTIGATED.....	20
<i>Wing Loading and Wing Area</i>	20
<i>Aspect Ratio and Planform Design</i>	21
<i>Airfoil Selection</i>	22
<i>Fuselage and Payload Sizing</i>	23
PROPULSION SYSTEM.....	26
PROPULSION SYSTEM DESIGN TRADES	27
<i>Empennage Sizing</i>	27
SYSTEM OPTIMIZATION	28
PROPULSION SYSTEM OPTIMIZATION ROUTINE.....	28

<i>Motor Selection</i>	29
<i>Propeller Selection</i>	29
<i>Battery Selection</i>	29
<i>Other Notes and Interpretations</i>	29
RESULTS OF THE OPTIMIZATION STUDIES	30
<i>Predicted Performance</i>	30
STORAGE REQUIREMENT	31
DETAIL DESIGN	33
SYSTEMS ARCHITECTURE	33
<i>Structural:</i>	33
<i>Mechanical</i>	33
<i>Electrical:</i>	34
<i>Electromechanical:</i>	34
<i>Pneumatic:</i>	35
COMPONENT SELECTION	35
<i>Airframe Material Selection:</i>	35
<i>Component Material Selection:</i>	36
<i>Pneumatic Systems Selection:</i>	36
GEOMETRY DATA	37
WEIGHT AND BALANCE DATA	39
SYSTEM DATA	39
MANUFACTURING PLAN	47
WINGS	49
EMPENNAGE	49
FUSELAGE	49
LANDING GEAR	51
DEPLOYMENT MECHANISM AND INLET PORT	51
MANUFACTURING SCHEDULES	52
TEST PLAN	53
STATIC TESTS: DRAIN TESTS	53
STATIC TESTS: MOTOR TESTS	54
STATIC AND DYNAMIC TESTS: PROPELLER TESTS	54
DYNAMIC TESTS: FLIGHT TESTING	54
LESSONS LEARNED	54
REFERENCES	58

This report summarizes the major developments of Georgia Institute of Technology's entry into the 2003-2004 American Institute of Aeronautics and Astronautics' Design, Build, Fly (DBF) student design competition. This annual event is organized by the Office of Naval Research and Cessna Aircraft Company and is sanctioned by the Academy of Model Aeronautics. Though a new rule set is released every year, the nature of this annual competition involves designing and building an unmanned aerial vehicle to carry a specified payload for a specified mission. The total score for a school's entry is based on three components: a written report score, a manufacturer's rated aircraft cost, and a mission flight score.

Development Summary

Documentation of the development of Georgia Tech's DBF contest entry in this report follows the traditional design sequence as outlined in the contest rules. During the project however, all of the design phases overlapped to some degree. For example, the aircraft sizing and performance studies that are traditionally considered a Preliminary Design task, supported the configuration studies that are traditionally a Conceptual Design task. Configuration studies were performed with consideration of material selection and component options, even though these studies are traditionally considered Detail Design tasks. Each phase was a continuous process involving many intricate studies that supported the overall design efforts. It would not be feasible to show detailed documentation of all these studies, and the reader is therefore encouraged to bear in mind that this document is merely a summary of the developments of the contest entry.

The flowchart in Figure 1 illustrates Georgia Tech's DBF development process. Team management recognized that small UAVs that are built for a very short service life have some unique design challenges. Data gathering, education, and accumulation of practical experience, represented by "Information Gathering" in the figure, was therefore emphasized during the project to support analysis capabilities. The analysis methods used to manipulate this information were learned from academic studies and are represented by "Information Processing." Similarly, "Logical Interpretation" represents the cumulative assessment of experience acquired in the research and development areas.

Conceptual Design was interpreted as the specification of the relative orientation of the major components and assemblies of the aircraft. The decision for the most appropriate arrangement would be derived from many sources. Some of these included analysis and interpretation of the contest rules, evaluation of construction options, skills and capability assessment, and research into performance trends. The process for handling the highly complex selection criteria was roughly modeled after Integrated Product and Process Development (IPPD). This process involved defining the feasible design space, identifying selection criteria, screening the design space against these selection criteria, and making final quantitative evaluations of the remaining candidates.

Once the configuration was selected, the vehicle needed to be appropriately sized. This design phase is summarized in the Preliminary Design section of this report. A more detailed analysis of the mission

was conducted during this phase in order to clearly define the performance requirements in terms of weight, cruise airspeed, takeoff distance, and other such metrics. These requirements were the framework for the development architecture and gave focus to the team's design efforts. This ongoing process was supported not only by detailed sizing trade studies, but also by empirical data gathered by the team from assorted tests and experimentations. These tests and experiments are summarized in the Test Plan section of this report. Optimization of the system's parameters came from careful interpretation of deterministic and probabilistic studies conducted by the team.

The final decisions for vehicle parameters are summarized in the Detail Design section of this report and include vehicle geometry and performance predictions. Preparation for manufacturing involved selecting appropriate components and materials and designing the details of components and subassemblies necessary for the aircraft's functions. The final selections for the propulsion system, electrical and pneumatic components, and airframe construction materials are documented in the Detail Design and Manufacturing Plan sections of this report.

Major Developments in the Design

The final aircraft configuration selected was a fixed low-wing, aft-tail aircraft with non-retractable tricycle landing gear and a single tractor-fan propulsion system. The first prototype aircraft flew on October 29, 2003 and various prototype components have continued to be tested in flight up to the time of this report. A detailed study indicated that carrying a full payload of 4 liters would be most likely to produce the highest score. Testing and experimentation with drain tubes validated theories that drain times for the payload dump could be reduced by installing a long, deployable drain tube to the underside of the aircraft. Lower drain times for maximum payload directly translated into higher points for payload weight carried and increased Total Flight Score with minimal incremental impact to aircraft costs.

Revisions to the design lead to the final geometry of the wing and the final selection of the propulsion system. Nearly all other components were dependent on these critical design objectives, and production of new prototypes validated design studies. The final aircraft geometry includes a 53 inch long fuselage, a 77 inch wingspan, and 5.6 ft² of wing area. Propulsion system optimization studies resulted in the choice of a Graupner Ultra 930-8 motor with an APC 16x12 propeller used for the Fire Bomber mission and a Mejzlik 16x14 propeller used for Ferry Mission. Battery pack design included 14 cells of 1700mAh cells wired in series to deliver 16.8 V to the motor. The final RAC of the aircraft is \$7.62 in thousands. Total Flight Score is estimated at 16.0 with missions times recorded in minutes. With a normalized report score of 100, the Total Score is estimated at 209.9.

Range of Alternatives Investigated

The competitive nature of the project pushed the team to explore all feasible options that had the potential for competitive advantage. Wing designs that the team investigated ranged from straight to swept planform, low-wing to high-wing placement, and from single to multiple lifting surfaces. Various geometries of the fuselage were considered, including twin fuselages and wing-body configurations. A range of stability and control devices were considered. Propulsion systems were considered in fore and

aft as well as multiple installations. Various propeller configuration options were also considered, including tractor fans, pusher fans, and ducted fans. Additionally, tricycle, tail-dragger, and bicycle landing gear were evaluated.

The ranges for propulsion systems included motors from the Graupner and AstroFlight families. Corresponding propellers ranged from 10 to 20 inches in diameter, and 4 to 18 inches in pitch. In essence, the team weighed alternatives that ranged from the lightest and fastest options to the heaviest and slowest. The range of parameters was screened for the ratio of estimated Flight Score against the corresponding Rated Aircraft Cost (RAC) to give a single output metric for the entire system: Total Score. The compliance of the Georgia Tech's entry to the specifications in the RFP is given below in Table 1.

Table 1: Compliance Matrix

RFP SPECIFICATIONS		Georgia Tech Contest Entry
	Constraint Summary	Response
Team	All team members must be full time students.	Compliant in full
	At least 1/3 of the team must be underclassmen.	70.83% of team is comprised of underclassmen
General	No rotary wing or lighter-than-air vehicles	Fixed wing configuration employed
	No payload internal to the wing	Payload is internal to fuselage
	Must be unmodified Graupner or AstroFlight motor	Unmodified Graupner motor chosen in design
	Propeller must be commercially produced	Unmodified Mejzlik propeller selected
	Motors must be limited to 40A by specified fuse	Requisite 40 Amp used inline from + battery terminal
	Must use "over the counter" NiCad cells	Sanyo Cadnica batteries selected
	Maximum battery pack weight is 5.00lbs	Battery weight 1.7 lbs
	Aircraft and pilot must be AMA legal	Compliant in full
Safety	Must submit completed and signed RAC	To be presented on April 23, 2004 at contest site
	Verify structural integrity	Structure integrity tested and verified
	Aircraft must employ requisite radio fail safe	Digital receiver programmed to specifications
	Fuse must be accessible from outside of vehicle	Compliant in full
Mission Profile	Aircraft must pass upright and inverted wing tip tests	Aircraft designed to withstand 12g flight load and qualifies tip test
	Aircraft must fit inside a 1x2x4 ft box	All aircraft components fit inside requisite area
	Payload capacity can not exceed 4 liters	Payload tank designed and manufactured to 4 liters
	Maximum dump orifice is 0.5 inches	Dump orifice designed and manufactured to .5"
Report	Payload does not leak from aircraft	Valve shows no signs of leakage when connected to oversized tank
	Report must not exceed 60 pages, TOC and cover page are extra	Report length 53, plus 5 page drawing package, and 2 page TOC
	Report pages must be 8.5x11 inch except drawing pkg; 3-view must be on 11x17 inch paper	3-view on 11x17, 1 drawing package page 11x17, all others 8.5x11
	All figures must be either 1/2 or full page.	Compliant in full
	Text must be 1.5 space, 10pt, Arial font w 1 in. margins, Tables and Figures also 10pt Arial	Compliant in full

Proper management of personnel was essential to project success. This management included delegating tasks to appropriately skilled team members, enforcing deadlines, coordinating resource acquisition, and adapting quickly to new developments. Team organization emphasized large groups early in the project when analysis benefited from the experience of older members and the unbiased judgment of new members. Movement through the design process led to a dispersion of the team members from large groups to small groups and individual effort. Coordination between groups ensured focus on project goals and was greatly facilitated by regular meetings and other group communication.

Team Structure

The 2003-2004 Georgia Tech DBF team consisted of twenty-four students: seventeen underclassmen, six seniors, and one graduate student. Six students from the 2002-2003 DBF team became the Project Leaders shown in Table 2. These students were responsible for delegating tasks, setting deadlines, and managing resources. Project Leaders were also responsible for identifying project task needs and forming task groups. Each task group was assigned a Task-Group Leader that was also a Project Leader. This person was individually responsible for the task-group's obligations. Task-Group members were selected on a voluntary basis to encourage personal interests and dedication to the project. Project objectives not requiring group effort were not assigned a Task-Leader and were completed by smaller groups and individuals.

Project Development

The timeline of major developments during the course of the project is given in the Figure 2. Progress in research and development areas was presented weekly to the entire team. The team would discuss progress, assess results, and develop new directives. Project Leaders would set and enforce deadlines as necessary to ensure project success. The "planned" project bands shown in Figure 2 were continuously updated as necessary to adapt to new developments. The "actual" project bands therefore show the divergence from the desired order of developments.

Communication and Information Management

Project Leaders knew that communication among the group was not only useful, but because of the interrelationships between tasks, it was also crucial to project success. Weekly meetings by themselves would not have been sufficient to maintain the pace of the project if team management did not supplement communication by other means. A team website was maintained at www.dbf.gatech.edu, and was used to post announcements, share files, and record team progress. Contact information, including phone numbers, e-mail addresses, and web messaging identification was disseminated among the group. Additionally, office space was provided by the faculty and staff of Georgia Tech for 24 hour access to a central location for meetings and posting information.

Analysis:	Project Leaders:												Senior			Junior			Sophomore			Freshman		
	R Thomas	K Diggs	E Matthews	J Pitoniak	B Poole	D Sullivan	Z Zurita	M Baumgardner	M Daskilewicz	J Oubre	D Prestifillipo	A Rao	A Sachan	J Bateman	A Dekle	C Featherly	T Gales	J Kirkwood	D Teuscher	W Wisler	R Fields	J Hopkins	M Peterson	M Wronka
Problem Analysis																								
Sensitivity Analysis																								
Research																								
Configuration Selection																								
Sizing Trade Studies																								
Sizing Optimization																								
Mission Analysis																								
Structural Analysis																								
Performance Predictions																								
Component Selection																								
Propulsion Selection																								
Empirical Data Analysis																								
Loading																								
Unloading																								
Fuselage																								
Wings																								
Empennage																								
Landing Gear																								
Aircraft Assembly																								
Loading																								
Unloading																								
Wind Tunnel Testing																								
Static Propulsion Testing																								
Flight Testing																								
Loading																								
Unloading																								
Documentation and Reporting																								
Compilation and Review																								
CAD Drawings																								

Table 2: Personnel Assignment Areas

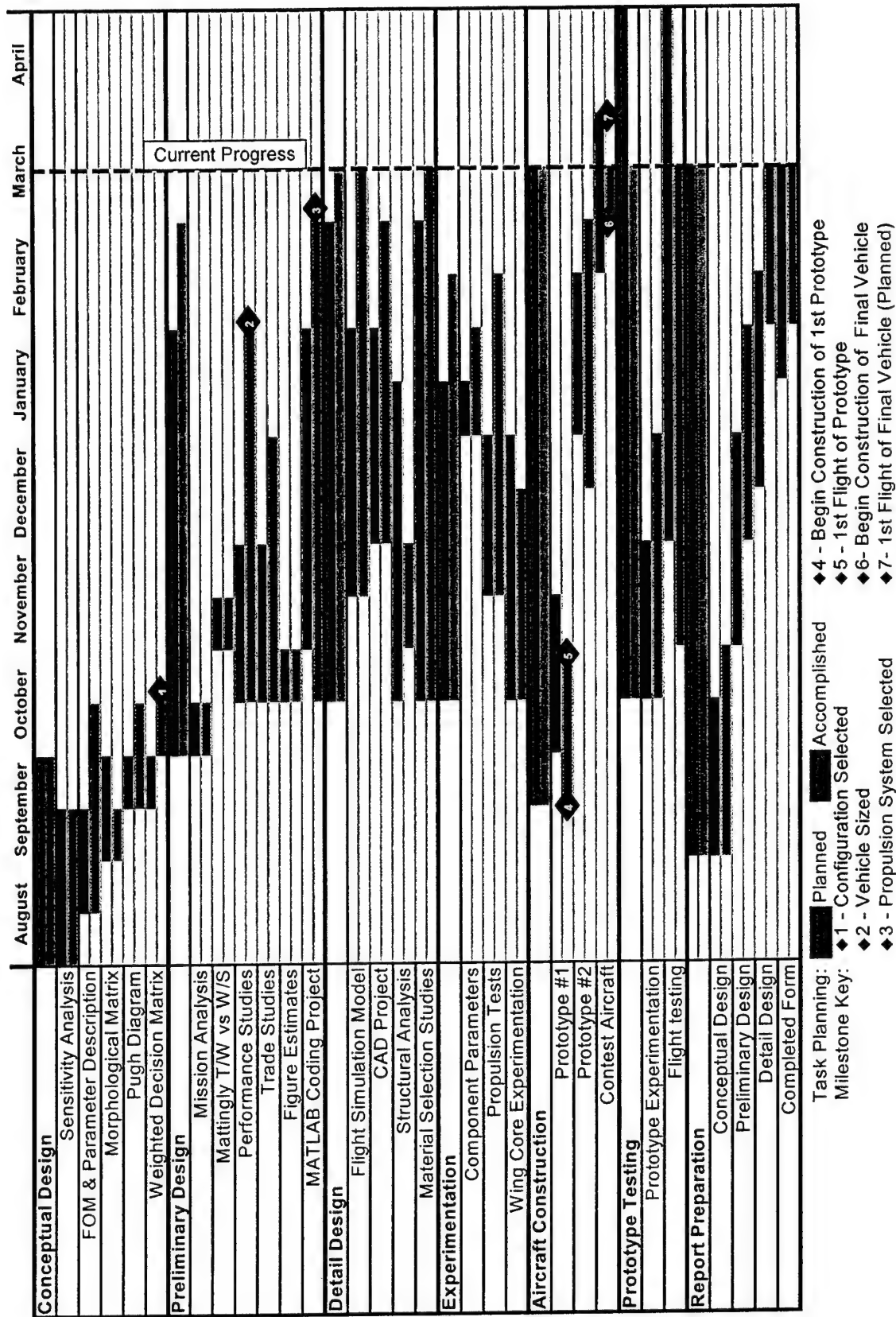


Figure 2: Project Development Gantt Chart

CONCEPTUAL DESIGN

The goal of Conceptual Design was to select the most appropriate aircraft configuration for the given Request for Proposal (RFP). Aircraft "configuration" was defined as the relative orientation of the major components of the aircraft, including lifting and control surfaces, propulsion system, payload, and landing gear. Each component arrangement investigated had implications relating to aerodynamics, structures, and mechanics. The down-selection criteria were based on problem statement interpretations of the RFP and perceived implementation difficulty vs. merit. These criteria were used to systematically rank competing configurations and select the most appropriate configuration for the given RFP

Problem Statement

The key elements of the mission requirements specified by the RFP were summarized in part by a mission profile (Figure 3 and Table 3 through Table 5). Further elements consisted of RFP-dictated constraints, and contest administration rulings on team questions. Together, these elements defined a constrained problem for which the overall objective was to achieve a simultaneous Flight Score and RAC that would maximize the Total Score within the team's available resources. An additional constraint not shown below for the aircraft that had particular significance during Conceptual Design was that the configuration had to be able to be packaged in a 1x2x4 foot box.

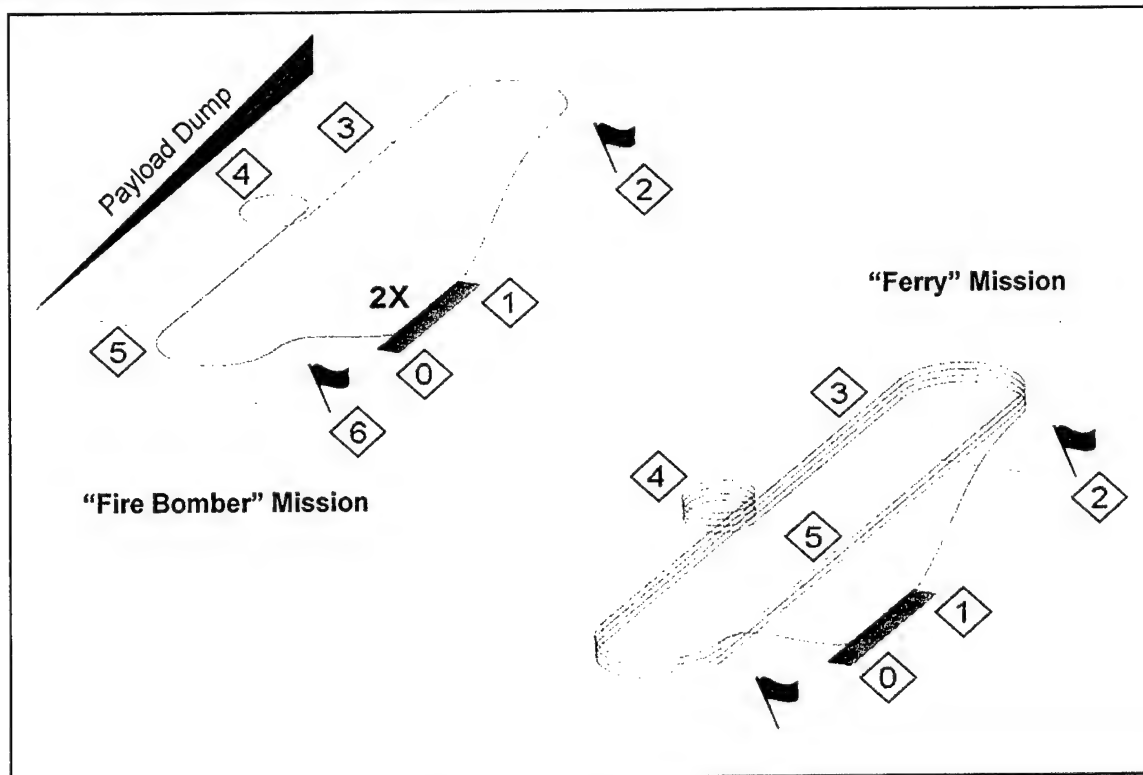


Figure 3: Course Layouts

Table 3: "Fire Bomber" Mission Profile by Phases

PHASE	DESCRIPTION
0-1	Takeoff ground roll at maximum power without taxi. Field elevation pressure altitude 2000 feet and temperature 100°F. Ground roll is 140 of 150 foot maximum to rotation on wet, hard surface ($V_{TO} = 1.2 \cdot V_{STALL}$).
1-2	Climb to minimum safe operating altitude (10 to 50 feet) at maximum power. Continue to first flag located 500 feet from starting point.
2-3	After cleared of the upwind flag, initiate minimum radius 180° turn at maximum power. Bank angle +60°.
3-5	Establish level cruise flight at maximum power. Begin payload dump once clear of the downwind flag. Terminate dump before reaching the downwind flag.
4	Initiate minimum radius 360° turn in opposite direction of pattern anywhere along downwind leg. Bank angle +60°.
5-6	Reduce power and begin descent through base and final approach paths. Turn to base and final not initiated until cleared of the downwind flag, 500 feet from starting point.
6-0	Complete landing approach after 1 st lap to stop at starting point. Reload aircraft and repeat 1 through 6. After the 2 nd lap, complete landing approach and touch down before the starting point and roll to full stop anywhere after the starting point.

Table 4: "Ferry" Mission Profile by Phases

PHASE	DESCRIPTION
0-1	Takeoff ground roll at maximum power without taxi. Field elevation pressure altitude 2000 feet and temperature 100°F. Ground roll is 140 foot. to rotation on wet, hard surface ($V_{TO} = 1.2 \cdot V_{STALL}$).
1-2	Climb to minimum safe operating altitude (10 to 50 feet) at maximum power. Continue to first flag at 500 feet from starting point.
2-3	After cleared of the upwind flag, initiate minimum radius 180° turn at maximum power. Bank angle +60°.
3-5	Establish level cruise flight at maximum power. 180° turns not initiated until cleared of the flags, 500 feet in either direction from starting point. Repeat pattern until 4 laps are completed.
4	Initiate minimum radius 360° turn in opposite direction of pattern for each downwind leg. Bank angle +60°.
5-0	After the 4 th lap of the pattern, complete landing approach and touch down before the starting point and roll to full stop anywhere after the starting point.

Table 5: Performance Requirements/Constraints

	PERFORMANCE ITEM	REQUIREMENT
C.1	Payload	0-4 liters; to be dumped during flight
C.2	Takeoff Distance ^A	150 feet
C.3	Landing Distance ^B	500 feet
C.4	Sustained g Load ^C	$n \leq 12$
C.5	Flight Score	Maximize Flight Score against RAC to maximize Total Score

NOTES:

A. Including 1.5 second rotation, wheels must be clear of the ground at 150 feet from starting point.

B. Maximum allowed; includes complete approach path, through touchdown to full stop.

C. Load factor is figured at sea level for aircraft gross weight plus payload weight.

Scoring Structure:: The team examined the scoring equations to look for factors that would influence the design. The team's Total Flight Score (TFS) is given by:

$$TFS = (DF * Lbs\ Water / Best\ Mission\ Time)_{Fire\ Bomber} + (DF / Best\ Mission\ Time)_{Ferry} \quad (1)$$

DF here is the mission difficulty factor. The DF for Fire Bomber is 2, and the DF for Ferry is 1. Total score can be calculated as:

$$Total\ Score = \frac{Written\ Report\ Score * Total\ Flight\ Score}{Rated\ Aircraft\ Cost} \quad (2)$$

These equations would be used in later studies to determine the impact of design decisions on Total Score.

RAC Analysis

A study was performed to determine the cost each aircraft component contributed to RAC and quantify the tradeoffs between Flight Score and RAC. The Pareto Principle which states that 80% of a system's variability is typically determined by 20% of the system variables, suggested that only a few of the RAC factors were very influential to the response of Total Score. Screening the design space of feasible vehicles could be greatly simplified if the range of options was reduced to a smaller set of most influential factors. In order to accomplish this, a designed experiment was developed, to vary the fourteen input factors for RAC using Design of Experiments (DOE) methodology. The calculation of RAC based on these parameters was specified by the contest rules, and was entered into a MS Excel spreadsheet, along with a range of values for each parameter (Table 6).

Table 6: Design of Experiments Parameter Ranges

#	INPUT	LOW	HIGH	#	INPUT (CONTINUED)	LOW	HIGH
1	Empty Weight (lbs)	5	20	8	Max Fuselage Width (ft)	.25	1
2	# Motors	1	2	9	Max Fuselage Length (ft)	2	6
3	Battery Weight (lbs)	1	5	10	V Surfaces, No Active Control	0	2
4	Wing Span (ft)	2	8	11	V Surfaces, Active Control	0	2
5	Wing Chord (ft)	.25	1.5	12	H Surfaces < 25% Span	0	2
6	# Control Surfaces	1	3	13	Servos/Motor Controllers	3	8
7	Max Fuselage Height (ft)	.25	1	14	# Propellers/Fans	1	2

The team used the DOE with the statistical analysis tool JMP to compute the prediction profile for the fourteen input variables. This prediction profile indicated the sensitivity Total Score to inputs for specific conditions. The Pareto Plot in Figure 4 shows the relative contribution of various inputs to total variability of the Total Score for the input ranges given in Table 6. From this plot it can be seen that battery weight and empty weight are by far the most influential parameters affecting RAC. The team knew that configurations that favored low battery and aircraft weight should be favored, and that other options, such as number of control surfaces and number of servos, would not be as influential to RAC. Such knowledge was particularly important to the team for Conceptual Design since specific parameter values for RAC calculations were not yet known. Between the prediction profile and the Pareto Plot, the team could identify configurations with the potential for favorable RAC's without calculating the exact RAC of each configuration.

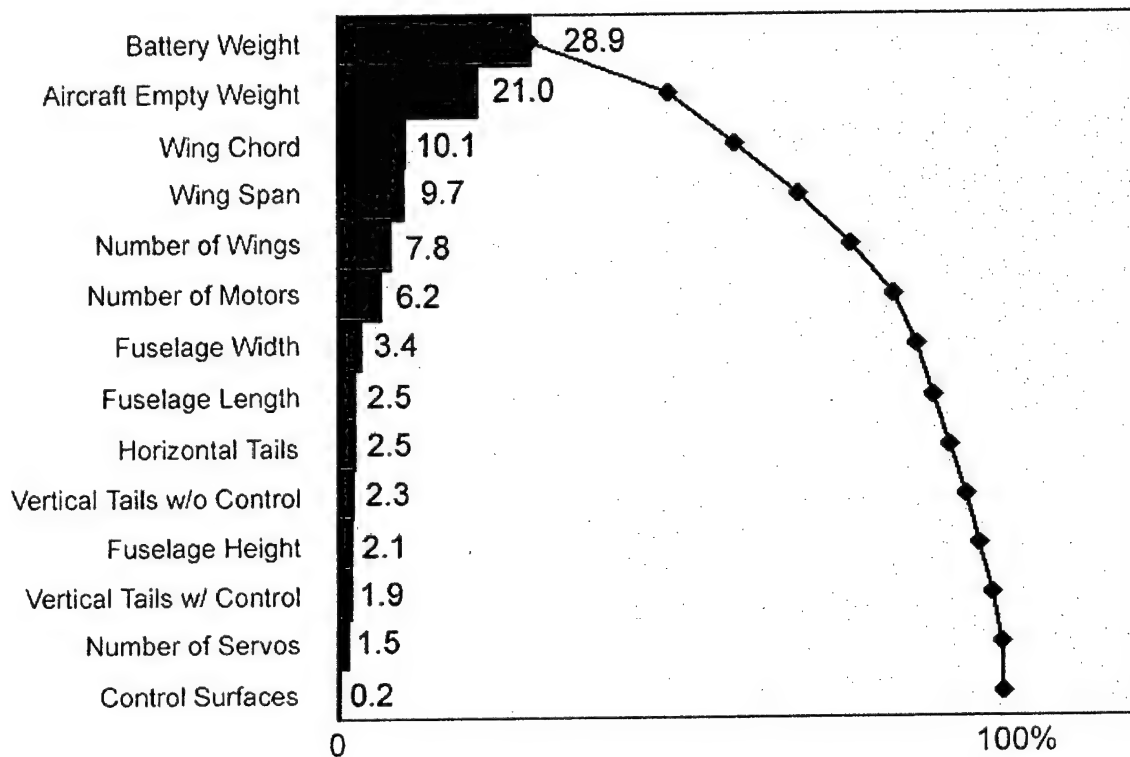


Figure 4: Pareto Plot for Rated Aircraft Cost

Aircraft Configurations Investigated

The team did not want to overlook any configuration that had the potential to offer a competitive advantage over competing concepts. Towards this end, the team undertook a comprehensive enumeration of possible aircraft configurations. Seven component categories were chosen to represent the characteristics of the aircraft configuration. These categories were the following:

Vertical Wing Placement: The placement of the wing was categorized as being either high, mid, or low assuming conventional placement of stabilization surfaces and thrust lines. The vertical placement of the wing has structural, aerodynamic, and logistic implications about the aircraft. For example, low-wing configurations represent short landing gear, favorable takeoff distance due to additional ground effect, and payload being supported underneath by the wing spar. High-wing configurations offer favorable dynamic stability but these configurations were thought to incur a penalty in structural weight due to the placement of the landing gear. Mid-wing aircraft were thought to have greater maneuverability.

Number of Lifting Surfaces: This category was intended to represent options for the number of primary lifting planes, not including stabilization surfaces. A biplane for example would have two lifting planes. This category did not, however, exclude the possibility of lifting planes that were also used for stabilization. Therefore, the area of the feasible design space represented by "2" in the morphological matrix included conventional biplanes as well as unconventional configurations such as box-wing/joined-wing designs.

Vertical Thrust Line Location: The vertical placement of the thrust line was a major design consideration for the relative orientation of the components of the aircraft. Particularly, the vertical placement of the thrust line relative to the drag of the aircraft affects trimmed conditions and pitching moments. Some configurations raised propeller clearance issues. For example, tractor propellers with tail-dragger landing gear had the possibility of tipping forward when stopping quickly, causing the propeller to strike the ground. For high-wing configurations with tractor propellers the landing gear to be either excessively long or mounted on the fuselage in order to achieve adequate propeller clearance. This category was therefore created to capture such configurations.

Landing Gear: The configuration of the landing gear had structural implications as well as ground handling implications. Tail dragger configurations were considered to have a greater risk of poor ground handling than tricycle gear. Bicycle landing gear was included to represent a lightweight option with a penalty in ground handling.

Empennage Type: This morphological category was created to reflect the addition of small, auxiliary stabilization planes that would control the aircraft about the pitching and yawing axes. Arguments related to this category included discussion of RAC, installed weight, wetted area and other drag penalties, installation complexity, and appropriate control authority. For example, the end-plate effect of T-tails was preferred over conventional tails. However conventional tails were thought to have lower structural weight and simpler installation.

Number of Motors: Aircraft possessing single or twin motors were also represented in the morphological matrix. Basic motor theory suggests that fewer motors are preferred, so multiple motor configurations greater than two motors were not considered. Lateral thrust orientation was implicit in some two-motor configurations. The possibility of eliminating vertical surfaces and using differential thrust for longitudinal stability was discussed.

Longitudinal Thrust Orientation: The vertical and lateral thrust lines identified, along with the longitudinal placement of the propulsion system. This category was intended to capture the longitudinal location of the thrust line with respect to the center of gravity (CG). For example, single motor configurations with the motor mounted in the aft region of the aircraft oriented the thrust behind the CG and thus, broadly speaking, were considered inherently unstable with respect to propulsion. Tractor fans, in which the CG trailed the thrust location, were considered inherently stable. Thus, the two were differentiated in this category.

Design Space Screening

The team desired a systematic method to define the Figures of Merit that would be used to rank different configurations, as well as a method of determining how each FOM should be weighted to reflect its importance toward achieving a high Total Score. Such a method was found in "Quality Function Deployment" methodology (Cohen, 1995), which utilizes a "House of Quality" (HoQ) matrix to show relations between a product's features and the needs the product is intended to fulfill.

Aircraft needs were interpreted from the mission analysis and became the "Desired Qualities" in the House of Quality (HoQ) shown in Figure 5. The set of "Quality Characteristics/Configuration Variables" represent numerical metrics affecting Total Score. The relationship between each Desired Quality and each Quality Characteristic/Configuration Variable was examined and assigned a value of "strongly linked," "moderately linked," or "weakly/possibly linked". For example a link exists between the need to dump payload in flight and the number of servos. Such relations were recorded in the colored "Impact Relations" field of the HoQ. The results showed that some needs responded similarly to the set of Configuration Variables and were grouped together as shown in Figure 5. These groups were called the "Figures of Merit" (FOMs) for Conceptual Design and are described in Table 7. It should be noted that the Impact Relations field in the HoQ does not distinguish between positive and negative impacts, but only the relative magnitude of an existing relationship.

Each FOM was assigned an "Influence" value based on how strong its overall relation was to the Configuration Variables. These values were specified as 0, 3, or 9 based on a qualitative assessment of the magnitude of the FOM's relative influence. A separate group was formed for those needs that were found to be only very slightly impacted by the Configuration Variables and labeled "Not Considered." These needs had little significance in Conceptual Design, but would be reexamined in Preliminary and Detail Design and are therefore shown. Similarly, the Thrust Orientation response was found to have very little influence on the needs, and was thus discarded. However for completeness, it is also shown. The requirement "Aircraft Must Be Contest Legal" was fulfilled by only including contest-legal configurations in the Morphological Matrix. Rotorcraft and lighter-than-air craft were not included, and thus this requirement did not need further consideration in the Conceptual Design phase.

The triangular field in the HoQ was used to record the tradeoffs and benefits between the different Quality Characteristics / Configuration Variables. This information was helpful in determining how the trades of one component influenced another. Also shown are the "Directions of Improvement" for each

Quality Characteristic, with a 0 indicating the cases for which the team believed the optimum value was neither the maximum nor minimum. For example, it was believed that an optimal wing area existed that was neither the smallest nor the largest in the feasible design space.

The HoQ suggests that the Speed FOM is greatly influenced by the propulsion system and the size of the aircraft. Stability and Control are both affected by the type and number of control surfaces. RAC is most affected by battery weight and aircraft empty weight, (as shown in Figure 4) and feasibility was affected by factors including estimated costs, and the team's ability to design, analyze, and construct a given configuration.

Table 7: Figures of Merit

FOM	POLARITY / DESCRIPTION	WEIGHT	RELATED MISSION FEATURE
Speed	INCREASE by:	9	Directly enhances Total Flight Score
	DECREASE Frontal Area		
	INCREASE Available Thrust		
	DECREASE Surface Intersections		
	DECREASE Volume/Wetted Area		
Stability	INCREASE by:	3	Improves probability of mission success
	INCREASE Static Margin		
	INCREASE Size		
	Improve Gust Response		
	Improve Ground Stability		
RAC	DECREASE by:	9	Lower RAC translates directly to higher Total Score
	DECREASE Battery Weight		
	DECREASE Aircraft Empty Weight		
	DECREASE # of Motors		
	DECREASE # of Control Surfaces		
Control	INCREASE by:	3	Enhances flight times and ensures mission success
	INCREASE Number of Control		
	INCREASE Number of Servos		
Feasibility	INCREASE by:	9	Supports delivery of proven concepts for mission success
	Use Inexpensive Components		
	Use Easily-Manufactured Configurations		

Configuration Selection

After accounting for the exclusions noted above, the morphological matrix (Table 8) contained six categories, allowing for 1,134 unique configurations. Individual configurations were specified by choosing one option from each category. This list of configurations was screened manually to exclude those with readily apparent poor feasibility. For example, a tail-dragger with no empennage would not be a sensible combination. Other configurations were excluded when strong similarities existed between two configurations, such as two designs varying only by tail type. In short, only the configurations necessary to adequately describe the design space were considered.

Trades/Benefits Key:

- + As one quality improves, the other also improves.
- As one quality improves, the other becomes worse.
- o Relationship between qualities is perceived, but not clearly defined.
- () No perceived relation between qualities.

Direction of Improvement Key:

- ↑ More is better
- ↓ Less is better
- o The right amount is best
- () Non-Directional Metric

		Direction of Improvement														Desired Qualities Aircraft must:	FOM INFLUENCE	Figures of Merit
		↑	↓	↓	↓	↓	↓	↓	0	0	0	0						
		Weight of Payload Carried	Fire Bomber Mission Time	Ferry Mission Time	Fuselage Volume	Propulsion System Weight	Empty Weight	Wing Area	# of Control Surfaces	# of Servos	# of Lifting Planes	Vertical Wing Placement	Thrust Line Location	Landing Gear Configuration	Empennage Type	# of Motors	Tractor/Pusher (Not Considered)	INFLUENCE
Speed	9	Complete missions quickly	■	●	●	◆	■	■	■	◆	■	■	■	◆	◆	●	■	9
	3	Take off in 150 feet	●			■	●	●	■		■	◆				■		3
Control	3	Turn in both directions							●	■	◆				■			3
	3	Sustain adverse wind/weather	◆			■	■	●	■			■	■		■		◆	3
Stability	3	Fly, Land without sustaining damage	■			■	●	●	■			■	■	■	■		◆	3
	9	Have suitable RAC for Flight Score	●	●	■	●	■	■	■	◆	●			◆	■	●		9
Feasibility	9	Be repaired easily if damage occurs					◆	◆	■	■	■			◆	■			3
		Fit team's budget				●	◆	◆	◆	■	■			◆	◆	●		9
		Fit team's skill level				◆	◆	■	■	■	■			◆	■	■		3
Not Considered (0)		Fly 1 mile with payload, 2 miles empty	●	■	■	●	■				◆					■		1
		Carry Payload	●	■	●	■	◆	■								■		1
		Dump payload in flight	■	■	◆	■			◆									0
		Be refilled quickly between flights	●	◆					◆									0
		Be contest legal			◆	■	■											0

Impact Relations Key:

- The quality characteristic and the desired quality are strongly linked.
- The quality characteristic and the desired quality are moderately linked.
- ◆ The quality characteristic and the desired quality are weakly or possibly linked.
- () No relation is perceived between the quality characteristic and the desired quality.

Figure 5: House of Quality for Conceptual Design

Table 8: Morphological Matrix

CATEGORY	MORPHS			
Vertical Wing Placement	High	Mid	Low	
Number of Lifting Surfaces	1	2	3	
Thrust Line Location	Above CG	Inline with CG	Below CG	
Landing Gear	Tricycle	Tail-Dragger	Bicycle	
Empennage	Standard Canard	T Cruciform	V Twin	Inverted-V None
Number of Motors	1	2		

This design space was further screened by eliminating those configurations which were thought to be significantly worse than a selected baseline configuration. The baseline configuration was chosen to represent a typical UAV of a similar service category. This process is represented by the partial Pugh Evaluation Matrix of Figure 6. Each configuration in the matrix was evaluated for each of the FOMs as "better than" (+), "worse than" (-), or "the same as" (0) the baseline configuration. This evaluation process was intentionally superficial as it only served as a method for coarse screening of options. The sum of each rating was tabulated at the right to indicate the relative magnitude of favorability or un-favorability. Any configuration not meeting the team's cutoff margins was discarded and not investigated further.

Configurations:	Figures of Merit:	Speed	Stability	RAC	Control	Feasibility	Sum +s	Sum -s	Sum 0s	Continue?
High Wing; 1 Wing; High Thrust; Tricycle; Standard; Single Engine		0	0	0	0	0	0	5		Yes
Low Wing; 1 Wing; Mid Thrust; Bicycle; T Tail; Single Engine		+	-	0	-	-	1	3	1	No
Mid Wing; 2 Wings; Mid Thrust; Tail Dragger; Standard; Twin Engine		+	0	-	-	-	1	3	1	No
High Wing; 2 Wings; Low Thrust; Bicycle; V Tail; Single Engine		0	+	-	-	-	1	3	1	No
High Wing; 1 Wing; Low Thrust; Tricycle; Standard; Twin Engine		+	0	-	+	-	2	2	1	Yes
High Wing; 3 Wings; High Thrust; Tail Dragger; V Tail; Single Engine		0	+	0	-	-	1	2	2	No
High Wing; 3 Wings; Low Thrust; Tail Dragger; Standard; Twin Engine		+	+	-	-	-	2	3	0	No
High Wing; 2 Wings; Low Thrust; Bicycle; Twin; Single Engine		0	+	-	-	-	1	3	1	No
High Wing; 3 Wings; Low Thrust; Bicycle; Cruciform; Twin Engine		+	+	-	-	-	2	3	0	No
High Wing; 1 Wing; Mid Thrust; Tricycle; Twin; Single Engine		0	0	0	0	0	0	0	5	Yes
Low Wing; 2 Wings; High Thrust; Tail Dragger; Standard; Twin Engine		+	0	-	-	-	1	3	1	No
Mid Wing; 1 Wing; Mid Thrust; Tricycle; Twin; Single Engine		0	-	0	0	0	0	1	4	No
High Wing; 1 Wing; Low Thrust; Tricycle; Cruciform; Twin Engine		+	0	-	+	-	2	2	1	Yes
High Wing; 1 Wing; High Thrust; Bicycle; Inverted V; Twin Engine		+	+	-	-	-	2	3	0	No
High Wing; 2 Wings; High Thrust; Tricycle; Twin; Twin Engine		0	+	-	0	-	1	2	2	No
Mid Wing; 2 Wings; Low Thrust; Bicycle; Cruciform; Twin Engine		+	0	-	-	-	1	3	1	No
Low Wing; 2 Wings; High Thrust; Tricycle; Twin; Twin Engine		0	0	-	0	-	0	2	3	No
High Wing; 2 Wings; High Thrust; Bicycle; Twin; Single Engine		0	+	-	-	-	1	3	1	No

Figure 6: Pugh Evaluation Matrix

There were 30 configurations that passed the Pugh evaluation. The next level of investigation involved a similar evaluation process but pursued in much greater detail. It was at this level that the team

applied broad trade studies, researched material selection and manufacturing capabilities, and conducted rudimentary performance calculations. Again, the configurations were evaluated as per the FOMs, but this time they were assigned a score, ranging from 1 to 10, that reflected the favorability of that configuration to the FOM. A score of 10 would indicate a highly favorable relationship between the configuration and the FOM. The assigned scores in each field were multiplied by the FOM weight, and the resulting scores were summed for the configuration's overall score. These overall scores are shown at the far right in Figure 8: Weighted Decision Matrix. This figure has been rearranged by total score to rank the competing configurations. The highest scoring configuration was a low-wing monoplane with a high thrust line, tricycle landing gear, standard empennage and a single motor, and is illustrated in Figure 7

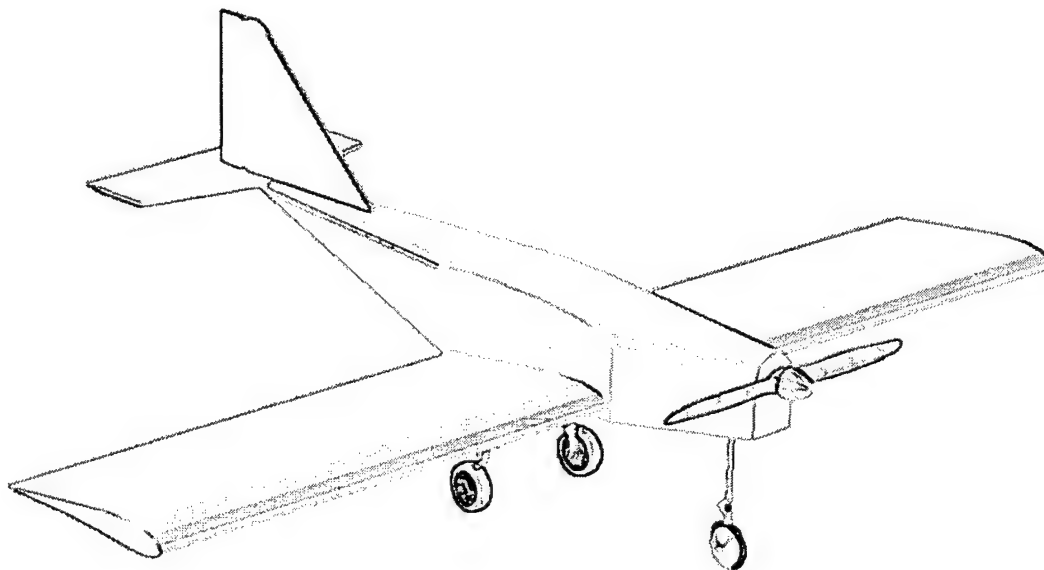


Figure 7: Selected Configuration

Configurations	Weight:	Figures of Merit					Total
		Speed	Stability	RAC	Control	Feasibility	
		9	3	9	3	9	
Low Wing; 1 Wing; High Thrust; Tricycle; Standard; Single Engine		6	5	5	6	7	195
Low Wing; 1 Wing; Mid Thrust; Tricycle; Standard; Single Engine		6	5	5	6	6	186
High Wing; 1 Wing; Mid Thrust; Tricycle; Standard; Single Engine		6	5	5	5	6	183
High Wing; 1 Wing; High Thrust; Tricycle; Standard; Single Engine		6	5	5	5	6	183
Low Wing; 1 Wing; Low Thrust; Tricycle; Standard; Single Engine		6	4	5	6	5	174
High Wing; 1 Wing; Low Thrust; Tricycle; Standard; Single Engine		6	5	5	5	5	174
Low Wing; 1 Wing; High Thrust; Tricycle; Inverted V; Single Engine		6	5	6	4	3	162
Low Wing; 1 Wing; Mid Thrust; Tricycle; Inverted V; Single Engine		6	5	6	4	3	162
High Wing; 1 Wing; Mid Thrust; Tricycle; Inverted V; Single Engine		6	6	6	3	3	162
Low Wing; 1 Wing; Low Thrust; Tricycle; Inverted V; Single Engine		6	5	6	4	3	162
High Wing; 1 Wing; High Thrust; Tricycle; Inverted V; Single Engine		6	6	6	3	3	162
High Wing; 1 Wing; Low Thrust; Tricycle; Inverted V; Single Engine		6	6	6	3	3	162
Low Wing; 1 Wing; High Thrust; Tail Dragger; Standard; Single Engine		6	4	5	4	4	159
Low Wing; 1 Wing; Mid Thrust; Tail Dragger; Standard; Single Engine		6	4	5	4	4	159
High Wing; 1 Wing; High Thrust; Tail Dragger; Standard; Single Engine		6	5	5	3	4	159
High Wing; 1 Wing; Mid Thrust; Tail Dragger; Standard; Single Engine		6	5	5	3	4	159
Low Wing; 1 Wing; High Thrust; Tricycle; V Tail; Single Engine		6	4	6	4	3	159
Low Wing; 1 Wing; Mid Thrust; Tricycle; V Tail; Single Engine		6	4	6	4	3	159
High Wing; 1 Wing; Low Thrust; Tail Dragger; Standard; Single Engine		6	5	5	3	4	159
Low Wing; 1 Wing; Low Thrust; Tail Dragger; Standard; Single Engine		6	4	5	4	4	159
High Wing; 1 Wing; Mid Thrust; Tricycle; V Tail; Single Engine		6	5	6	3	3	159
Low Wing; 1 Wing; Low Thrust; Tricycle; V Tail; Single Engine		6	4	6	4	3	159
High Wing; 1 Wing; High Thrust; Tricycle; V Tail; Single Engine		6	5	6	3	3	159
High Wing; 1 Wing; Low Thrust; Tricycle; V Tail; Single Engine		6	5	6	3	3	159
Low Wing; 1 Wing; High Thrust; Tail Dragger; V Tail; Single Engine		7	4	6	2	2	153
Low Wing; 1 Wing; Mid Thrust; Tail Dragger; V Tail; Single Engine		7	4	6	2	2	153
High Wing; 1 Wing; Mid Thrust; Tail Dragger; V Tail; Single Engine		7	5	6	1	2	153
Low Wing; 1 Wing; Low Thrust; Tail Dragger; V Tail; Single Engine		7	4	6	2	2	153
High Wing; 1 Wing; High Thrust; Tail Dragger; V Tail; Single Engine		7	5	6	1	2	153
High Wing; 1 Wing; Low Thrust; Tail Dragger; V Tail; Single Engine		7	5	6	1	2	153

Figure 8: Weighted Decision Matrix

Sizing the chosen configuration was the main objective of Preliminary Design. Early sizing studies qualified the aircraft for storage in the 1x2x4 foot box. Later analysis involved sizing trades with respect to the defined mission requirements, and evaluation of design decisions with respect to their impact on Total Score. The supporting analyses for these trades and design decisions became the framework for the vehicle performance analysis code which would be used to optimize final vehicle parameters.

Alls sizing studies were directed to optimizing the overall output metric for the system: Total Score. More specifically, the ratio of Total Flight Score to RAC governed Total Score. Large geometries and large propulsion systems that favored mission success paid penalties in RAC, smaller systems that would carry the same payload ran the risk of inadequate performance, but had the potential for higher Total Score. The fundamental task of vehicle sizing was accurate definition of the intricacies of the involved interrelationships.

Analysis Method Summary

The configuration selection process described in Conceptual Design (page 8) could not have been executed without translation of mission requirements into vehicle requirements. For vehicle sizing, the mission requirements were reduced to generate specific performance requirements. Using these performance requirements the team was able to define a preliminary geometry for the vehicle using regression analysis of empirical thrust- and wing-loading data for other UAVs. The interrelationship of vehicle geometry with vehicle performance was roughly defined by the thrust-to-weight vs. wing loading across a range of reasonable estimates of airspeed, and is discussed on page 20.

As relationships of vehicle geometry and vehicle performance were defined, the team studied the details of sizing trades and how they affected RAC and Flight Score, and subsequently, Total Score. These trade studies would compose the majority of the team's work throughout the project and involved primarily wing sizing and propulsion system selection.

The fuselage geometry was generated from the payload volume requirement and appropriate empennage placement. Streamlining the fuselage reduced drag and allowed for the installation of subsystems, and thus other requirements of the fuselage had little impact on fuselage sizing studies. The fuselage definition is discussed on page 23 of this report.

Similarly, the size and placement of the empennage was primarily governed by the size of the wing. A wing definition would have a corresponding empennage definition that would provide sufficient stability and control while minimizing drag. Empennage sizing is discussed on page 27 of this report.

As sizing of the wing and propulsion systems were the most important objectives of overall vehicle sizing, the team developed an optimization routine for coupled propulsion system sizing and wing sizing the objective of which was maximization of Total Score. This routine involved propulsion system optimization using a mission performance analysis based on preliminary vehicle design definition. Vehicle design definition was updated for each locally optimum design specification of the propulsion system. Given the initial vehicle wing definition, drag profiles were calculated, and the propulsion system

optimization routine calculated the smallest, lightest components (i.e. those yielding lowest RAC) that were able to satisfy the required takeoff conditions. Final interpretation check for alternatives would complete the design space screening. This optimization routine is described on page 28 of this report.

Design Parameters and Sizing Trades Investigated

Wing Loading and Wing Area: The primary sizing parameters investigated for the wing were the wing area, planform shape, aspect ratio, and airfoil. As described previously, the interrelationship of vehicle geometry with vehicle performance was roughly defined by a plot of the thrust-to-weight vs. wing loading. The team was able to determine initial parameters with empirical data from UAVs of similar payload and mission requirements. The form of the so-called “master equation” that was used was:

$$\frac{T}{W_{TO}} = \frac{\beta}{\alpha} \left\{ \frac{qS}{\beta W_{TO}} \left[K_1 \left(\frac{n\beta W_{TO}}{q S} \right)^2 + K_2 \left(\frac{n\beta W_{TO}}{q S} \right) + C_{D_0} + \frac{R}{qS} \right] + \frac{1}{V} \frac{d}{dt} \left(h + \frac{\dot{V}^2}{2g_0} \right) \right\} \quad (3)$$

where T/W_{TO} is the thrust-to-weight ratio, W_{TO}/S is the wing loading, β is the mission segment weight fraction, α is the thrust lapse, K_1 is the induced drag factor, K_2 is the drag offset due to camber, n is the load factor, C_{D_0} is the zero-lift drag coefficient, q is the dynamic pressure, R is the additional drag due to flaps or landing gear, h is the altitude, and g_0 is the acceleration due to gravity.

A plot could be generated for each of the flight conditions associated with the mission segments shown in Figure 3: Course Layouts. In this form, this so-called “master equation” can be used to map point-performance constraints on a design plot as a visualization tool for investigation of the design space. For the simplified DBF case, its only requirements are a weight specification, a thrust lapse profile, a parabolic drag polar, and a flight condition definition. The only true constraint on the design space is the takeoff requirement, and this constraint is shown with various cruise conditions in Figure 9: Constraint Diagram.

Some of the UAV empirical data suggested that a reasonable approximation for airspeed was 60 mph. The 60 mph plot in Figure 9 intersects the takeoff constraint at a wing loading of 2 lbs/ft², however this convention is most likely more appropriate for a commercial or military UAV, and the team questioned whether such a modest wing loading was appropriate for a competition aircraft. It was suggested that this point be used for the “empty” condition of the Ferry Mission, and the T/W value for something closer to 3 lbs/ft² be used for the Fire Bomber mission.

At this point for the preliminary vehicle definition, the team had a design T/W and W/S . From the empirical UAV data the team could estimate a weight component breakdown and thus total weight. These weights were 8.0 lbs and 16.8 lbs with full payload. Dividing the weight with full payload by the chosen wing loading of 3 lbs/ft² gave a wing area of 5.6 ft².

These figures were only used as the initial starting point and would later be revised in the optimization routine (page 28). Higher wing loadings were favored in some discussions because of the lower vehicle RAC and better gust response. In opposition, higher wing loadings increase takeoff distance and thus

power required. The RAC sensitivity to the propulsion system suggested that additional RAC benefits due to smaller wing areas could be cancelled by greater required propulsion system size.

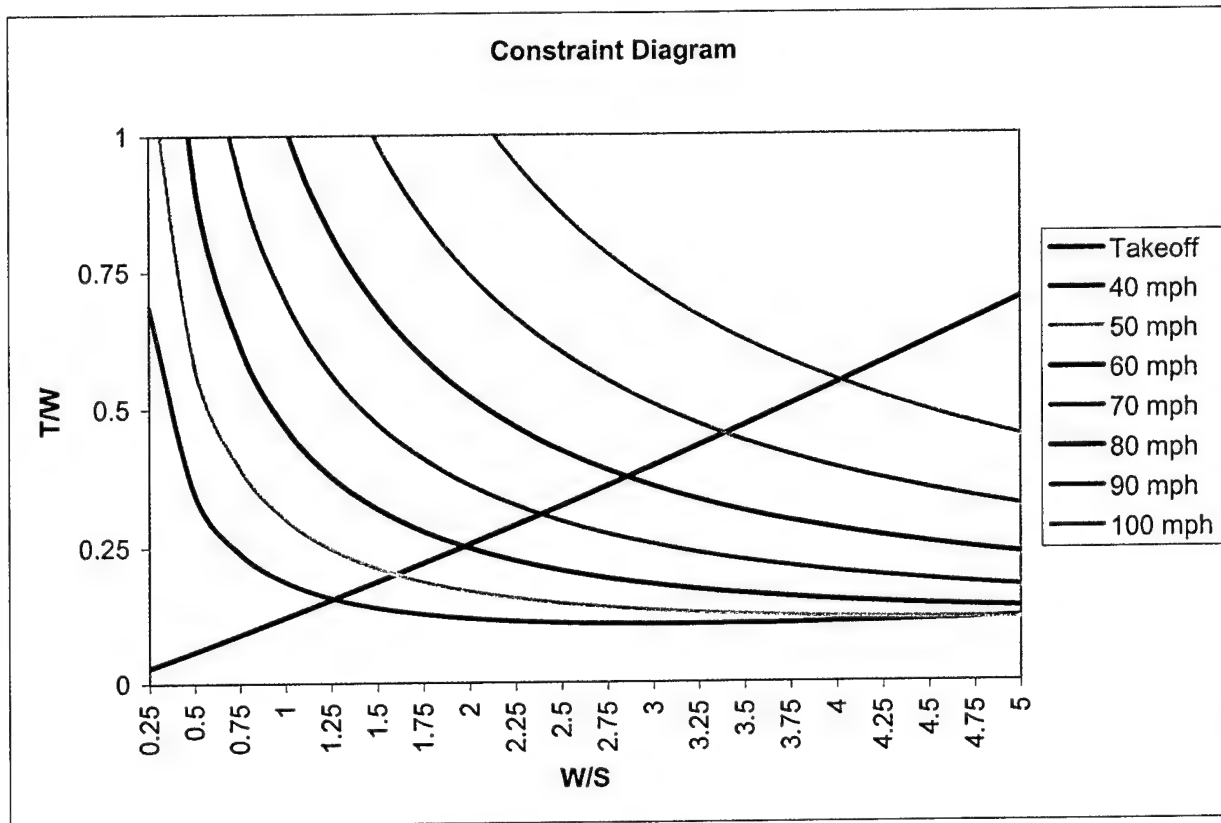


Figure 9: Constraint Diagram.

Aspect Ratio and Planform Design: The 2003-2004 DFB RAC structure did reflect differences for high or low aspect ratios for wings with fixed area. The team favored higher aspect ratios for drag reduction and greater roll stability. Higher aspect ratios also had the potential to reduce takeoff distances. However, such wings would be penalized by the higher density required to support the fully loaded weight during wingtip load tests during the DBF technical inspection and during flight. There were therefore strength arguments in favor of lower aspect ratios.

Structural analysis established a design maximum load factor of 12. The maximum continuous spar that can be fit inside the 1x2x4 foot box would be approximately 53 inches. For an estimated empty weight of 8lbs, the spar would have to support at least 96 lbs of weight in three-point loading. Assuming a 7075 T6 Aluminum wing spar of common 0.032 inch wall thickness, the minimum acceptable moment of inertia for a round structural tube was used to determine a diameter of 0.75 inches. With a small buffer for wing material above and below the tube, the team's minimum allowable wing thickness would be 1.0 inch.

This requirement had implications about the aspect ratio and airfoil selection. The team did not want to exceed 4 feet per wing panel in order for the aircraft to be packaged easily in a 1x2x4 foot box. This

constraint placed an absolute upper limit for aspect ratio of 11.4. For 5.6 ft² of wing area, the resulting chord for a rectangular planform was just under 6 inches. With a minimum allowable thickness of 1.0 inch as described, the minimum thickness-to-chord ratio would be 0.166. This conclusion did not leave many options for attractive airfoils.

Following similar arguments through several iterations, the team settled on an aspect ratio of 6.57 neglecting the fuselage carry-through area. This ratio was felt to offer a near-optimal balance of performance and structure. Assuming a rectangular planform, the wingspan was at 72.5 and chord length was 10.5 for 5.6 ft² of wing area. The new minimum allowed thickness-to-chord ratio was then 0.095.

Although rectangular planform designs offer the best lift per dollar of RAC, they do not have favorable load distributions but were predicted to have better stall characteristics. The Oswald efficiency factor for the described wing of 0.90 could be improved by taper, washout, or alternate wingtip airfoil. Research showed that a 0.45 taper ratio (Raymer p.63) would most closely approximate an elliptical lift distribution for a "straight" taper. However, implementing such a planform was found to increase RAC by approximately \$200 for fixed wing area. It was also predicted to have a much greater probability of tip stalls that could lead to total mission failure. Further research (Simons) found that the increased viscous effects at low Reynolds numbers may reduce the effectiveness of a tapered wing. A final taper ratio of 0.91 in coordination with 3° of washout was determined to be optimal for the system.

While an elliptical planform is the most aerodynamically efficient design, construction difficulties raised feasibility issues, and led the team to consider other planforms. Rectangular planforms were known to be less efficient, but offered the greatest ease of construction and have inherent stability characteristics. A tapered planform would approximate an elliptical lift distribution, however RAC accounts for only the maximum wing chord, thus tapered planforms are not cost-effective.

Airfoil Selection: Planform geometry, estimated cruise velocity, and estimated weight would only give the team a rough approximation of the performance of the wing. Further definition came from the airfoil selection, which was used to update the performance profile of the aircraft and later, revise the selection of propulsive components. Selection trades included lift-to-drag ratios for various conditions and relationships between lift at angles of attack and pitching moments. Other considerations were maximum stall angle, stall characteristics, and the potential for flow separation bubbles.

Using the UIUC Airfoil Database, several potential airfoils were identified which satisfied the minimum thickness-to-chord ratio requirement. These airfoils were screened to remove those with a maximum lift coefficient below a minimum acceptable value of 1.1. From the estimated cruise velocity and total aircraft weight for the Fire Bomber mission, the required lift coefficient was calculated to be 0.42. The drag coefficients of the selected airfoils were compared at this cruise lift coefficient to determine the airfoil with the least possible drag. Drag coefficients which corresponded to lower aircraft weights were also investigated to ensure that the chosen airfoil would be satisfactory at off-design configurations. Finally, after ensuring that basic stability margins would be satisfied, the Selig/Donovan 6060 was chosen.

Fuselage and Payload Sizing: The DBF contest rules specify 0 to 4 liters of payload for the Fire Bomber mission. Although fuselage dimensions were scored in the RAC, the team could not simply assume maximum payload and minimize corresponding fuselage size. It was not known if there was a smaller payload, and thus smaller vehicle, that could fly faster and obtain a higher Total Flight Score. Again relating to the single output metric for the entire system, Total Score, the team had to determine the optimal payload volume for the Fire Bomber mission such that both missions would maximize Total Flight Score and minimize RAC. This critically important study would facilitate the determination of not only fuselage size, but also overall vehicle size.

An analysis was developed that held certain aircraft parameters constant and defined others to be proportional to the amount of payload carried. This allowed the team to estimate RAC as a function of only the amount of payload carried. For the purposes of this study, Total Score was fixed with a normalized report score to observe the Flight Score's response to the only remaining unaccounted variable: flight speed. The analysis was therefore set up to calculate the necessary change in flight speed to achieve an equivalent change in payload carried. The corresponding calculations were done in MATLAB and produced the graph of flight speed required vs. payload carried to achieve a fixed Total Score shown in Figure 10: Payload Volume Optimization. A brief description of the inputs to the program is given in Table 9.

Table 9: Constant Inputs for Optimal Payload Capacity Analysis

CONSTANT INPUT	VALUE	NOTES
Fire Bomber Course Length	5256 ft	Based on 2 laps with 50 ft radius for all turns
Ferry Course Length	10512 ft	Based on 4 laps with 50 ft radius for all turns
Density of Water	62.4 lb/ft ³	Standard temperature and pressure
Planar Wing Density	0.344 lb/ft ²	Extrapolation form empirical data
Linear Fuselage Density	0.269 lb/ft	Extrapolation form empirical data
Propulsion System Weight	3.16 lb	Extrapolation form empirical data
Other Fixed Weight	1.63 lb	Includes servos, landing gear, empennage, subsystems
Fuselage Width	5.00 in	RAC considers only fuselage volume: width and height were held constant, while length was varied. Similarly, wing chord was held constant and wingspan was varied.
Fuselage Height	5.00 in	
Wing Chord	12 in	
Wing Loading	2.80 lb/ft ²	Estimated from previous DBF entries
Number of Servos	7	2x Flaperon, 2x Emp., Payload, Brake, Speed Control
Control Type	n/a	Flaperons, horizontal tail, vertical tail with control.

From these inputs, the remaining parameters affecting RAC were calculated as follows (with payload volume as the only independent variable):

Fuselage Length was calculated by assuming a 4 foot fuselage for an aircraft carrying 4 liters of payload and subtracting the reduction in payload from the Fuselage Volume.

$$Fuselage\ Volume = 48in \times 5in \times 5in - (4\ liters - Payload\ Volume) \quad (4)$$

Equation 4 assumes that overall fuselage dimensions consist of a fixed volume for the aircraft systems plus the payload volume. The 5 x 5 inch cross section was believed to provide sufficient fuselage volume to house all necessary components.

Wingspan was calculated as:

$$Span = \frac{Fuselage\ Length \times \rho_{Fuselage,Linear} + W_{Propulsion} + W_{Other} + Payload\ Volume \times \rho_{H_2O}}{Wing\ Loading - \rho_{Wing,Planar}} \quad (5)$$

Equation 5 uses the wing loading specified in Table 9 (2.80 lb/ft²), together with the total weight of the aircraft to compute the wing span. The weight of the wing is accounted for by subtracting the planar wing density from the wing loading. From this, wing area (a factor of RAC) was calculated as the product of wingspan and wing chord.

Empty Weight was calculated as the sum of the fuselage weight, wing weight, and fixed weight, as shown in Equation 6:

$$W_E = (Fuselage\ Length \times \rho_{Fuselage,Linear}) + (Wing\ Area \times \rho_{Wing,Planar}) + W_{Propulsion} + W_{Other} \quad (6)$$

Flight Speed could finally be calculated by using the above equations as inputs to RAC (calculated using the given equations in the RFP). A baseline flight speed of 60 mph for an aircraft that carries 4 liters of payload was used to calculate a baseline Total Score of 204.54. The MATLAB code computed the necessary flight speed to achieve the same Total Score for other (smaller) payload capacities and plotted the necessary flight speed vs. the amount of payload carried. The results are shown in Figure 10: Payload Volume Optimization. From the results, the team debated whether an aircraft could be built to fly the required speed while carrying the specified amount of payload. Small payload capacities were seen to require very large flight speeds, which were generally felt to be unattainable. Payload volumes greater than 3 liters could not definitively be dismissed. The team reasoned that the required velocities may or may not be attainable, but that significantly higher velocities were less possible, and thus a decision was made to carry the maximum allowed payload of 4 liters.

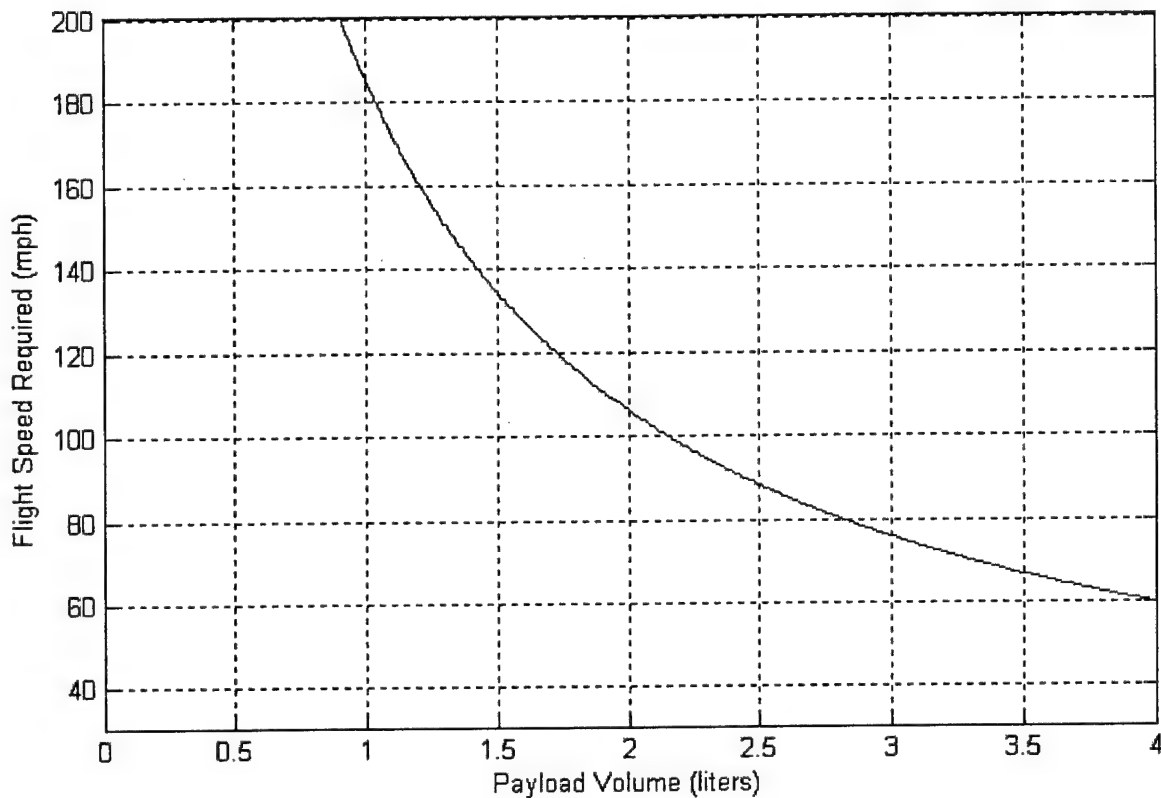


Figure 10: Payload Volume Optimization

It must be noted that the time required to drain the payload had the potential to place an upper limit on the flight speed. The payload must be completely drained through a 0.5 inch orifice over a distance of 1314 feet assuming a 50 feet radius 360° turn. An extremely fast aircraft may complete the 1314 foot downwind leg before the payload has completely drained. This constraint was of great concern. However experiments conducted simultaneously with the above analysis showed that the upper limit on velocity could be made closer to 80mph with an appropriate draining mechanism. Since this speed was significantly higher than the predicted cruise velocity, this constraint was alleviated and the conclusions that the aircraft would carry 4 liters of payload from the above analysis were upheld. Having established the weight of the payload, the team could make preliminary estimates of the overall size and weight of the aircraft.

The next step in sizing the fuselage was to determine the cross sectional area. A streamlined fuselage of low cross-sectional area would minimize form drag, but the resulting long payload bay could potentially jeopardize stability and control because of larger payload shifting. Figure 11: Possible CG Shift for Different Payload Bays shows the results of an analysis that was done to determine the maximum CG shift for differently shaped payload bays. From the figure it can be seen that extremely long payload bays had the potential for substantial CG shifts.

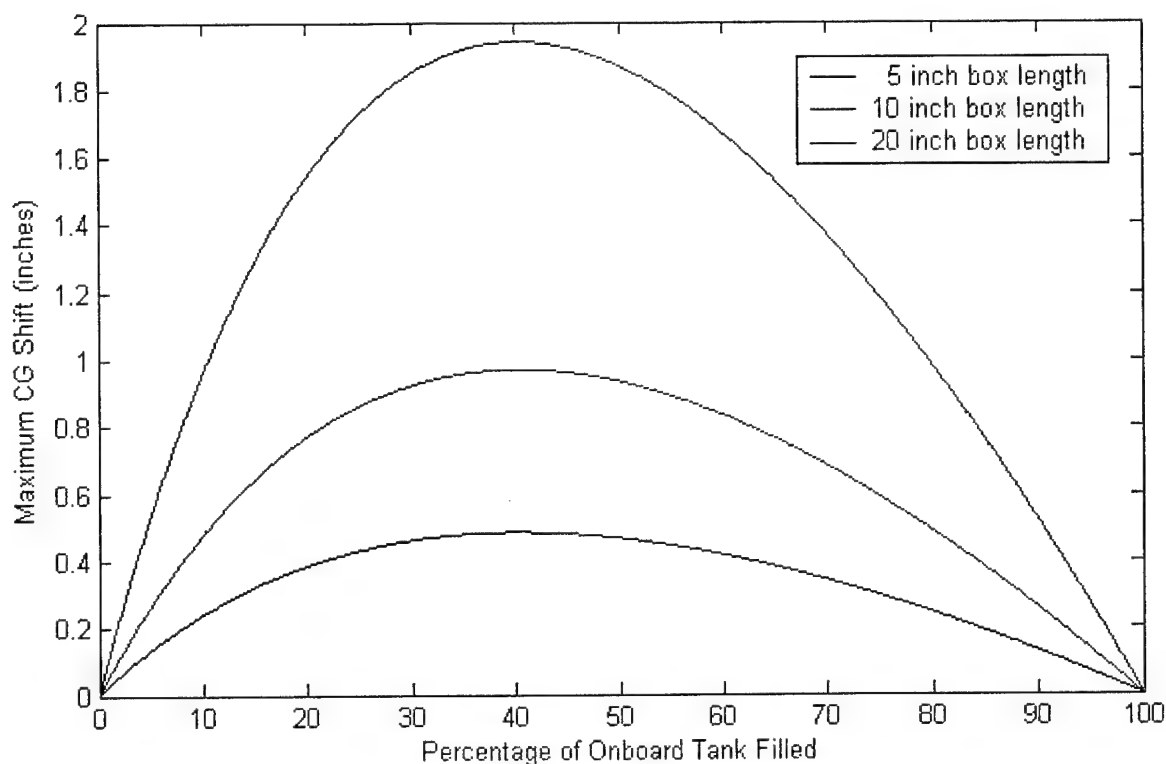


Figure 11: Possible CG Shift for Different Payload Bays

This conclusion led the team to favor payload bays, and consequently fuselages, with larger cross-sectional areas. Arrangement of components in various fuselage volumes helped the team determine an appropriate payload length and cross-sectional area of 12.5 and 20 respectively, for a total of 250 cubic inches, or 4.01 liters. The maximum CG shift for such a bay was approximately 1 inch for extreme conditions, and was anticipated to be within the aircraft's stability margin. Furthermore, this value could be reduced by initiating the 360° turn towards the end of the 1000 foot downwind leg, when the payload bay is almost empty. The fuselage near the payload bay was consequently chosen to have a 5 x 5.5 inch maximum cross section for at least 10 inches of its length, which was believed to be sufficient to house the payload bay and allow room for other internal components.

The final fuselage parameter considered in Preliminary Design was the overall fuselage length. This dimension is discussed in the Empennage Sizing section which starts on the next page.

Propulsion System

The primary parameters for defining the propulsion system were the battery weight, motor, and propeller. Battery weight was found to be the single most influential component of calculating RAC, and optimization studies were done to reduce the weight as much as possible while providing enough power to complete both missions. While the battery pack determines the total available power, the motor, gearbox (if used), and propeller determine the efficiency by which this available power can be converted

into power for flight. This power, along with the aircraft's drag profile, directly leads to the achieved aircraft airspeed. The propulsion system was thus found to be highly influential on both RAC and Flight Score, and as such it was given great attention in the Preliminary Design phase.

Propulsion System Design Trades

It was fairly clear that the most efficient propulsion system capable of completing both missions would yield the best ratio of Total Flight Score to RAC. For a given power output, any propulsion system that was less efficient would require a larger battery capacity to overcome system losses, and would thus be heavier, yielding a higher RAC. Although additional cells added to the battery pack could increase the power output of the propulsion system, the RAC penalty would counter the increase in Flight Score. This tradeoff was calculated for the prototype aircraft to require a 0.35 mph increase per additional ounce of propulsion weight. Otherwise, the additional weight would increase RAC over Total Flight Score, and Total Score would be lower (although the aircraft would be flying faster).

It was predicted that propulsion system optimization could be achieved by modeling the interaction effects of the primary influencing factors. The model would compare vehicle performance with the contest scoring structure; the single output metric to optimize being Total Score. Furthermore, by fitting the modeling and simulation environment to empirical data instead of raw theory, the team could minimize the possibility of erroneous simplifications and overlooked influencing factors. In this way, inconsistencies between theoretical and actual performance would not become problematic as long as trends and interrelationships could be represented accurately.

It follows that the sizing of the propulsion system and the selection of propulsive components were not independent. Determining thrust involved integrating motor performance and propeller performance.

Flight speed (and subsequently determination of flight scores) and RAC were dependent upon the battery weight, which was a function of motor performance for the duration of the flight. The optimization routine described below integrated these relationships for determination of the propulsive components most likely to yield the highest Total Score.

An early sizing iteration, based on the previous year's DBF entry, yielded a prototype aircraft capable of completing the 2003-2004 missions. Because of the success of this early prototype aircraft, the team used the prototype wing definition as a starting point for the propulsion system sizing/optimization routines. This allowed reasonable aircraft geometry (and therefore, drag) estimates to be made before the wing sizing discussed above was finalized.

Empennage Sizing: The team recognized that tail sizing was a tradeoff between stability and drag. The larger and further aft the design of the empennage, the greater the stability. However, these conditions were at the expense of increased RAC and skin friction.

The final wing definition established the tail volume requirements for adequate stability and control. These were 0.599 for the horizontal tail, and 0.0425 for the vertical tail. The team did not want the horizontal tail to exceed 25% of the wing span because of the jump in associated RAC. The RAC impact for fuselage length however was very small. The team therefore maximized the distance of the quarter-

chord of the wing the quarter-chord of the empennage and then correspondingly sized the tail. The resulting geometry is given in the Detail Design section of this report.

System Optimization

Total system optimization was an ongoing process that included nearly every study that the team had conducted over the course of the project. No single design study was isolated in such a way that it was not influenced by the other components of the aircraft. As previously mentioned in the Analysis Methods Summary on page 19 of this report, the primary sizing efforts were the wing definition and the propulsion system selection. Other related trade studies, such as weight component breakdowns and stability calculations, would supplement these two primary sizing efforts. The team started with the preliminary vehicle definition and would continually revise parameters and exhaust options until the definition converged to that described in this document.

The team used many different analysis tools throughout the course of this process. One of the most valuable was the team's first flying prototype. With installed telemetry equipment, the team was able to gather critically valuable performance metrics for the wing and propulsion system. Construction of this prototype was delayed until the vehicle definition began to converge. Periodically, the updated definition would be implemented on the prototype and new information would be processed.

For each update, the team would pair the wing and propulsion system definition with the recorded performance to calibrate optimization studies. The wing sizing was conducted as described on page 20 of this document, and the corresponding propulsion system optimization is presented below.

Propulsion System Optimization Routine

The output performance of individually-selected propulsion system components was weighted against the flight performance of the defined prototype vehicle to determine the Flight Score, RAC, and subsequent Total Score. By calculating the scores for all reasonable combinations for propulsive components, the team could catalog the highest scoring propulsion systems and interpret the results to make decisions about final component selection. Therefore, it was critical for the team to be able to accurately document the flight performance for a comparatively sized aircraft.

Airspeed and RPM data were paired in the recorded telemetry data. By equating thrust with drag during steady-state operation, the team could identify the total drag of the vehicle at multiple velocities in coordination with propeller thrust lapse information. The combined information provided a three dimensional plot of the drag profile for payload weights ranging from 0 to 9 lbs. This drag profile of the vehicle shows total drag as a function of velocity. Drag being a force, and velocity being a distance per time, any point along the line defines the power requirement for that set of conditions. Plots such as these could accurately define much of the feasible design space by varying payload weight and throttle settings during flight tests.

From these plots, the power output of a specific combination of motor, propeller, and battery could be traced to the equilibrium cruise velocity of the defined vehicle. More importantly, the RAC, Flight Score, and Total Score can be associated with combinations of specific propulsive components. Competing

alternatives were ranked against each other by calculating these output metrics for *all* combinations, and the highest scoring combinations would then be interpreted and evaluated by the team for final selection.

Motor Selection: Each propulsion system alternative included a combination of motor, propeller, and battery that was optimized to each other for mission success. There was an optimal motor loading for each voltage increment in which local efficiency was maximized. By incrementing the input voltage to the next step the maximum efficiency point is redefined, and by continuing in this manner, the maximum efficiency output power can be paired with an input voltage for the entire operating range of that candidate motor. The routine continues by completing the same pairing for each candidate motor.

Propeller Selection: After the maximum efficiency condition of the motor was defined, the propeller was selected to maximize cruise velocity precisely to this point of maximum motor efficiency. It is important to note here the power consumption for cruise was assumed to be much greater than that needed for takeoff in either mission because of the duration of each segment. Sizing of the propulsion system under this assumption was based on the cruise condition and then checked for qualification of the takeoff requirement. Matching power outputs in this manner meant maximizing the thrust at cruise. In essence, this assertion meant choosing the largest pitch available for each diameter within a researched catalog of commercially available propellers. Further enforcing the assertion was the fact that propellers of larger pitch-to-diameter (P/D) ratios typically have higher efficiencies. Of the propellers in the researched catalog, P/D ratios higher than 1.0 were not found to be commercially available.

It is important to note that the optimization routine emphasizes the equality of power between the motor and propeller. There was no coded pairing of motor RPM or torque to propeller RPM or torque until the final interpretation of the results. The frictional losses due to the use of a gearbox were neglected, as was the availability of commercially available gear boxes. The argument was that frictional losses were small and uniform and the use of a belt drive would allow a continuous range of "gear" ratios.

It is also important to note that figuring propeller performance was based only on diameter and pitch. The team discussed options for propellers of different planforms and surface textures during interpretation of the final results.

Battery Selection: The single most sensitive component to RAC was the weight of the battery. It was critical that the optimization routine be able to predict the weight of the battery in its computation of Total Score. Early iterations assumed a fixed battery weight of 2.7lbs (based on historical data). Within each iteration following the selection of the motor's operating voltage, the weight of the battery was revised based on (1) the duration necessary to complete the mission (cell capacity) and (2) the operating voltage selected (number of cells). In each iteration the aircraft weight was updated accordingly, as well as the equilibrium cruise velocity, until the new aircraft weight was within 1 ounce of the previous aircraft weight. At this point, the loop was exited, and the next increment for motor operating voltage was selected and the process repeated.

Other Notes and Interpretations: It can be noted that there exists a maximum overall motor efficiency in addition to the "maximum efficiency" from each voltage. The team discussed the possibility that a single

choice for motor based on maximum overall efficiency would not be sufficient for motor selection because of the possibility that (1) the overall output would not be sufficient for the aircraft to complete the mission, or (2) the higher RAC associated with larger energy requirements would counter the increase in Flight Score to produce a lower Total Score. A plot of the power output versus increase in battery weight was integrated into the design iteration in order to account for the ratio of increase in RAC versus the increase in Flight Score.

Results of the Optimization Studies

The optimization studies lead to the geometry and performance predictions that are tabled on page 37 in the Detail Design section of this report. The predicted flight performance is described below.

Predicted Performance: The predicted cruise velocity was 58 mph for the fully loaded condition and 66 mph when empty. Using an estimated 2630 feet for the distance around one lap, the team estimated a flight time of 1.14 minutes on the Fire Bomber mission and 1.8 minutes on the Ferry mission. These times correspond to a Total Flight Score of approximately 16.0. Using the predicted RAC for the optimized aircraft of 7.55 and a normalized report score of 100, the team's Total Score is predicted to be approximately 212.28.

The predicted take off distance for the optimized aircraft is 83 feet without payload and 120 feet for the first lap with payload in the Fire Bomber mission. The team predicted that the loss of battery power during the first lap would increase the takeoff distance for the second lap to approximately 140 feet. These distances assume 10 degrees of flaps.

The cruise C_L for the fully loaded aircraft was estimated to be 0.4240 at an angle of attack of 4° . The empty vehicle had an estimated C_L of .3272 at 2.6 degrees angle of attack. The vehicle is estimated to have a total C_D of .0561 while fully loaded and .0545 when empty. Stability and control coefficient estimates are given in Table 10 The moment coefficient contributions of all the components of the sized aircraft are given in Figure 12

Table 10: Stability and Control Coefficients

$C_{L\alpha}$	$C_{m\alpha}$	$C_{l\beta}$	$C_{n\beta}$	$C_{m\delta e}$	$C_{n\delta r}$	$C_{l\delta a}$
4.31	-0.035	-0.017	0.124	-1.105	-.059	0.430

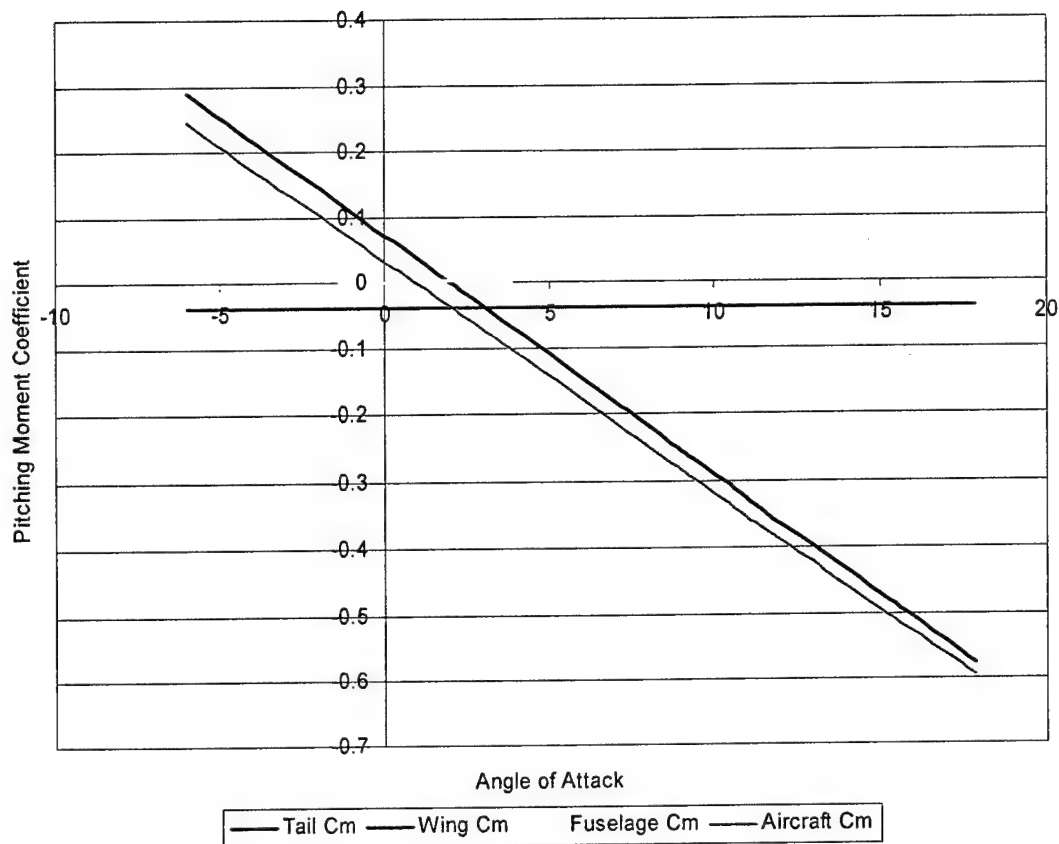


Figure 12: Moment Coefficient

Storage Requirement

One of the few constraints imposed by the contest rules on the design of the aircraft was that all components must all fit inside a 1x2x4 foot box. Component selection, material selection, and component sizing were not done without consideration to this constraint. The final planned arrangement inside this box is shown in Figure 13.

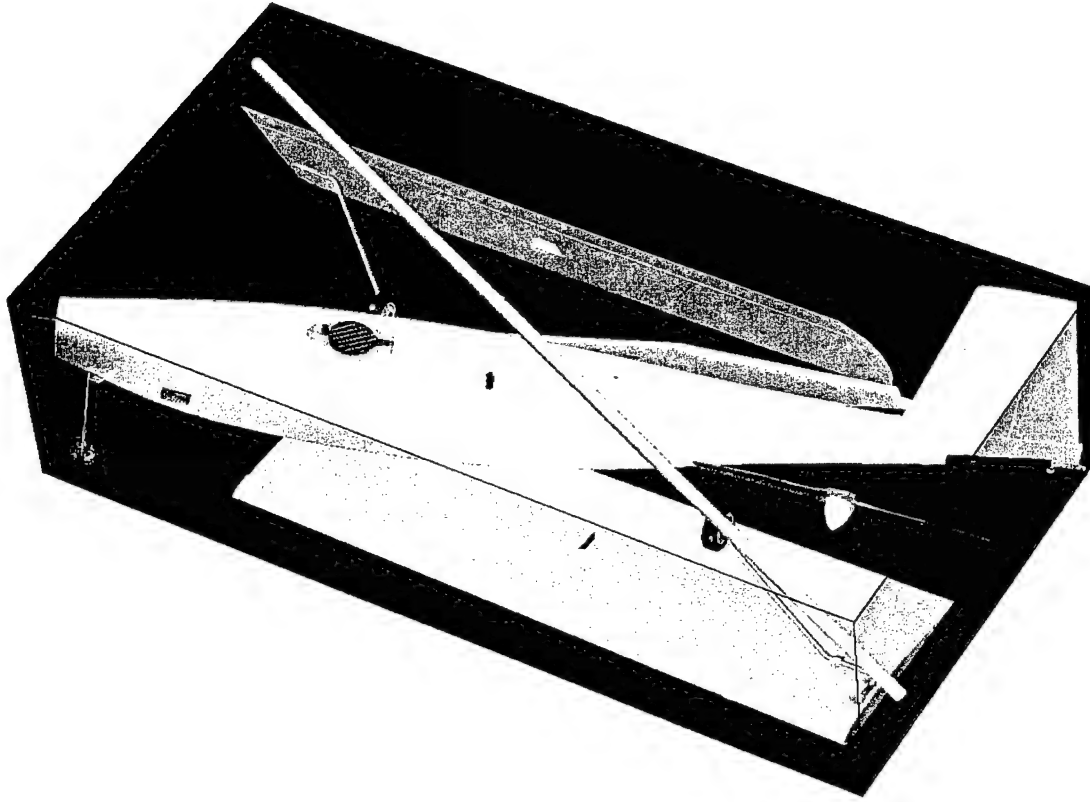


Figure 13: Aircraft in Stowed Configuration

The team interpreted Detail Design to be the integration of all elements of the aircraft definition necessary to manufacture the team's design. The results of interpretations from previously described analyses that lead to the final geometry, material selection, and component selection are thus summarized in this section of the report. The systems architecture includes structural, mechanical, electrical, electromechanical, and pneumatic systems. Also provided in this section of the report are images taken from the CAD rendering of the team's entry. The program IRONCAD was used not only to generate the CAD renderings, but also as a tool to figure weights and balance, available volumes, and component arrangement. The culmination of these efforts was the final expected performance and associated Flight Score that the team expects to achieve at the competition in April 2004. These performance predictions were given in Preliminary Design on page 30.

Systems Architecture

Structural: The main structural elements of the aircraft include the fuselage and airframe, wings and spar tube, empennage, and landing gear. The fuselage was designed to be nearly true monocoque; combining the streamlined-shape requirement with the structural requirement. At the time of writing, three fuselage prototypes had been produced, and there were plans for a fourth to be made before the competition. Each fuselage was constructed of different fiberglass weaves to evaluate the difference in strengths and weights. The fourth fuselage will be constructed similarly to the third, and is described in the Manufacturing Plan (page 47) of this report. The inside of the fuselage features lightweight internal frames that bound the payload bay and provide structure for the installation of the aircraft's subsystems.

The wings of the aircraft were designed to be installed from the outside of the aircraft, and are not an integrated structural member of the airframe. They are mounted on a round, $\frac{3}{4}$ inch 6061 T6 aluminum spar tube that supports the weight of the aircraft and its payload. A single $\frac{1}{4}$ -20x $\frac{1}{2}$ inch nylon bolt through an extension of the payload bay floor plate retains the wing on the spar tube.

The empennage was designed to be mounted securely to the aircraft, yet capable of removal for storage in the 1x2x4 foot box. The vertical fin and rudder, which give a total airframe height of less than 12 inches, is permanently mounted to the fuselage. Small dowels penetrate the fin through the fuselage to give rigidity to the glue joint. The horizontal stabilizer and elevator however are detachable. A small wing saddle positions the assembly to the fuselage, and two $\frac{1}{4}$ -20x1 inch nylon bolts retain the assembly securely from below. These components can thus be easily replaced if damaged in flight.

Mechanical: The mechanical systems of the aircraft include the nose gear steering mechanism, linkages, payload inlet port, and payload dump system. The nose gear steering mechanism came from a commercially purchased DuBro #153, $\frac{5}{32}$ inch nose gear kit. There were two types of linkages installed on the aircraft: The two flaperon linkages and the linkages to the brake valve and deployment valve were short pieces of 2-56 threaded rod with Sullivan Gold-N-Clevises and retaining clips. The threaded rods were treated with Loc-Tite thread lock. The elevator and rudder and nose gear linkages were Sullivan Flex Cable, which could be routed around irregular shapes.

The payload system includes an inlet port, a check valve, and a payload deployment mechanism. The inlet port is used to load the water payload into the aircraft. It features a spring-loaded retaining clip that protrudes above the surface of the aircraft. The lid on the port is also spring-loaded, such that when the retaining clip is pulled back, the lid springs open to expose the payload bay.

During flight, when the payload is being dumped, a check valve mounted at the rear of the payload bay vents air inside to replace the receding water. Many check valves were investigated, and the final decision was to use a valve from a snorkel tube donated to the team by a diver's supply shop. The check valve features a large surface area and extremely low cracking pressure (less than 0.5 psi).

The deployment mechanism is located on the lower surface of the payload bay near the aft end. It was positioned such that with a slight nose up attitude of the aircraft, the payload would concentrate near the drain hole through the deployment mechanism. The design of the mechanism is very similar to a ball valve. The Delrin barrel supports the drain tube and is exposed on either side of the 6061 T6 aluminum mounting block, which allows small ball links to be mounted on the exposed sides and connect the pneumatic cylinders that actuate the mechanism.

Electrical: The electrical system of the aircraft is composed of the receiver, receiver battery, gyros, and propulsion battery. The receiver and receiver battery were placed behind the payload bay in the rear of the fuselage. The 600 mAh Kokam 4.8V (four cells) nickel-cadmium receiver pack and Futaba 1024 9 channel PCM receiver were chosen because they were much smaller than most alternatives and helped reduce overall weight. Their combined weight is only 4.475 ounces.

A small, adjustable rate gyro was installed inline to each flaperon servo as well as the rudder servo. Each gyro weighs 0.4 ounces and was considered worth the penalty in weight. The central leading argument in favor of the gyros was that the gyros would counter the dangers of the neutral stability condition caused by the wing having no dihedral.

The propulsion battery is composed of 14 cells of Sanyo 1700 SCR nickel-cadmium cells. The battery pack is located directly under the wing tube spar to reduce the necessary structure to support its weight. The space between the floor of the payload bay and the lower fuselage panel allows several inches fore and aft to shift the battery and adjust the CG to the $\frac{1}{4}$ chord of the wing. The battery is secured by a combination of Velcro strips and small pieces of foam that keep the battery from shifting in flight.

Electromechanical: The propulsion motor and installed servos make up the electromechanical system. The propulsion motor is mounted in the forward extreme of the fuselage to a $\frac{1}{4}$ inch birch plywood mounting plate. The motor shaft protrudes through the plate without any need for an extension. A propeller adaptor is mounted to this shaft to accept the propeller.

Each wing panel contains a flaperon control servo located half way between the root and tip. This location minimizes the loss of control authority caused by the extremely long control surface flexing under load. The rudder and elevator each have one dedicated servo, and the brake valve and payload deployment valve employ one servo each. In total, six servos were chosen to be installed in the vehicle.

Pneumatic: The pneumatic system includes the deployment actuators, brakes, valves, and accompanying air distribution network. There were two pneumatic cylinders (linear actuators) installed in the aircraft to provide the necessary torque to lower and raise the payload deployment tube. These cylinders were mounted to a small frame that was designed to be loaded in shear across the face of the fiberglass frame. A shearing glue joint was predicted to be stronger than one loaded otherwise. Each $\frac{3}{8}$ inch (bore diameter) cylinder produces 11 lbs of force at 100 psi, for a total force of over 22 lbs of force pushing against this frame. Further frame support comes from the elevator and rudder servos, which are mounted to this frame on one side, and the payload bay floor on the other side. Consequently, the case of each servo could be under stress and support some of the load from the cylinders.

A reasonable configuration estimate showed that the additional RAC for an extra (brake) servo would be \$100. The equivalent decrease in flight time for each mission in order to maintain the same Flight Score was only one second. This equivalency showed that if brakes do not result in a decrease in flight times by at least 1 second, the decision to add brakes would only decrease Total Score. Flight tests with the prototypes showed that brakes significantly reduced the landing ground roll and brought the aircraft to a complete stop approximately 6 seconds faster than without brakes, and so brakes were implemented into the final design.

A single 5.75 cubic inch air tank was used to supply the necessary air pressure to actuate the deployment tube and brakes. Beginning at 120psi, one deployment and retraction of the drain tube reduces the pressure by 15psi, and one normal braking reduces the pressure 8 psi, leaving 97 psi for the second half of the Fire Bomber mission. The minimum allowable pressure in the tank was 46 psi.

Component Selection

The final selection for system components is summarized in Table 14 on page 39. The motor, propeller, and propulsion battery selections were a function of the design optimization routine as described in the Preliminary Design section of this report. The four JR DS8231 servos chosen for the primary control surfaces were chosen to provide adequate control authority for a minimum penalty in current drawn and overall weight. The two JR DS3421 servos used in the pneumatics did not have significant torque requirements, and thus were chosen for their small size and low current draw.

The remaining components of the aircraft not shown in Table 14 were constructed by the team during the course of the project. Translation from theoretical design to installed component required material selection studies. The material selection process involved (1) identifying structural requirements, (2) researching candidate materials and their requisite manufacturing processes, (3) identifying the material availability and cost, and (4) evaluating each option for the most appropriate selection. The results of the material selection processes are described below.

Airframe Material Selection: The team chose to construct the fuselage from composite materials for their structural qualities and manufacturability. The S-glass grade of fiberglass was selected over other composite fabrics because of its lower cost (per square yard) and strength: it was considered more rigid

than Kevlar, but less susceptible to damage due to flexing than carbon fiber. Experimentation with test fuselage sections lead to the choice of 9 oz/yd² and 3 oz/yd² S-glass for the construction of the fuselage.

The entire fuselage was not constructed from fiberglass. Inside the fuselage, the payload bay is bounded by $\frac{1}{8}$ inch C-grade balsa, which is layered on one side by 3 oz/yd² S-glass. The fiberglass waterproofed the balsa and provided additional strength. At the rear of the payload bay, the floor of the compartment was replaced with $\frac{1}{4}$ inch birch plywood to support the loads on the payload deployment mechanism. Additionally, the aft section of the fuselage was wrapped around a $\frac{1}{4}$ inch balsa block which supported the installation of the empennage to the fuselage.

The wings of the aircraft were constructed of expanded polystyrene with $\frac{1}{32}$ inch balsa sheeting. The leading edge and the hinge line were capped with $\frac{1}{4}$ inch balsa strips before finishing. The tip of each wing panel is capped in $\frac{1}{8}$ inch balsa, and the root of each is capped with $\frac{1}{4}$ inch balsa. A phenolic paper wing tube was installed in each panel at the quarter chord along the entire span. Each wing panel was finished in poly-vinyl, adhesive-backed heat shrink covering. The Ultracote brand of covering was preferred over alternatives considered.

Component Material Selection: There were two primary mechanical components fabricated by the team: the inlet port and the payload deployment mechanism (as illustrated in the Drawing Package beginning on 42). The inlet port body was CNC machined from a $\frac{3}{8}$ inch plate of Delrin. The lid was cut from a 0.080 inch plate of carbon fiber. The carbon fiber plate was chosen primarily for its superior strength-to-weight ratio over alternate materials. There were concerns that a weak material would flex between the hinge pin and retaining pin; allowing water to leak around the O-ring. This O-ring, that seals the mechanism, was stamped from adhesive-backed foam. RTV silicone was used to seal the inlet port against the top of the fuselage in addition to the five 6-32 bolts penetrating the frame.

The deployment mechanism consisted of a Teflon-impregnated Delrin rotating barrel and 7075 T6 aluminum housing. Delrin was chosen in both the inlet port and deployment mechanism because of its strength and density (0.0509 lb/in³ for Delrin, compared to 0.702 lb/in³ for Aluminum). Delrin also does not require lubricant while cutting (like metals), and cuts cleanly (unlike many plastics such as Nylon). It was also found to be reasonably priced and readily available. The two components were machined to have a 0.005" gap between them at room temperature. However, due to the different coefficients of expansion for the aluminum and Delrin, this gap would fluctuate for various conditions. The two components were therefore made watertight by a thin coating of petroleum-based lubricant. The vertical water column pressing on each component is only about 4 inches tall, and experimentation up to the time of this report shows that neither mechanism leaks water at static conditions.

Pneumatic Systems Selection: The deployment mechanism and brake system are pneumatically operated. Robart #165 pneumatic cylinders were chosen over servos for the deployment system because of greater ratio of force produced for the penalty in weight. A servo capable of producing 240 in-oz of torque weighs 4.60 ounces with the linkage installed. Comparatively, two $\frac{3}{8}$ inch bore Robart #165 cylinders with a 1.25 inch stroke weigh 1.68 ounces with linkages. The valve, micro servo, and necessary

tubing needed to actuate the cylinder bring the total weight to 3.21 ounces, and produce over 350 in-oz of torque (with a 1 inch arm) at 100psi. The #111 control valve used for the deployment mechanism was manufactured by Spring Air Products, and the JR341 micro servo used was manufactured by JR. Both components were purchased commercially.

The brake system installed in the aircraft was also pneumatic. (Pneumatic brakes have been shown to have a greater weight advantage over other options.) The wheels, brakes, and brake valve selected for installation were purchased commercially from Trim Aircraft of Australia.

The 5.7 in³ air tank used to supply air to the pneumatic system was also purchased commercially from Spring Air Products. This tank was chosen over other options because it was the smallest, lightest tank available that still supplied sufficient air for the two missions. The air tubing supplied from Spring Air Products was composed of an unknown plastic, and quickly showed permanent deformation after being stretched over pressure fittings. At pressures greater than 120psi, this tubing would sometimes fail to stay attached to the pressure fittings. After researching the issue, it was found that similar tubing was prone to leaking and tearing over time. Although the life cycle of the aircraft was to be very short, the tubing was replaced with ether-based tubing from McMaster Carr Industrial Supply Co. with a higher Shore-A durometer rating.

Geometry Data and Performance Data

The primary geometry of the vehicle is shown in the 3-view of the aircraft, Figure 15, on page 42. The external dimensions of the fuselage, wing, empennage, and landing gear are given in Table 11, Table 12, and Table 13. The wing tube spar, which is 53 inches long, fits diagonally in the 1x2x4 foot box when disassembled. When assembled, this tube penetrates 24 inches (66%) into each wing panel. Final Predicted Performance is given in Table 12.

Table 11: Geometry Data

WING		HORIZONTAL TAIL	VERTICAL TAIL
Span (panel)	36.25 in.	9.68 in.	10.00 in.
Span (total)	77.50 in.	19 ³ / ₈ in.	10.00 in.
Chord –Root	11.56 in.	9.75 in.	9.25 in.
Chord –Tip	10.52 in.	6.25 in.	5.00 in.
Airfoil	Selig/Donovan 6060	NACA0007	NACA0007
Thickness	11.25%	7%	7%
Washout	3°	0°	0°
Control Volume	—	0.599	0.0425
Aspect Ratio	6.57	2.42	1.40
Planform Area	5.56 ft ²	1.076 ft ²	0.495 ft ²
% Control Surface	20.00%	31.25%	37.71%

FUSELAGE		OVERALL DIMENSIONS	
Length	52.75 in.	Length	57.00 in.
Width (max)	5.00 in.	Width	77.50 in.
Height (max)	5.50 in.	Height	21.40 in.
LANDING GEAR		EMPENNAGE	
Wheel Base	13.8625 in.	¼ Wing to ¼ Horiz	35.0625 in.
Spread	23.75 in.	¼ Wing to ¼ Vertical	35.0625 in.

Table 12: Performance Data

		At Gross Weight / Fire Bomber	At Empty Weight / Ferry Mission
WING PERFORMANCE DATA			
	CL Cruise	0.4340	0.3272
	CL Maximum	1.117	1.117
	Lift/Drag Maximum	12.2	10.4
	Wing Loading	2.88 lbs/ft ²	1.30 lbs/ft ²
	Stall AOA	11°	11°
	Reynolds Number at Cruise	≈ 520,000	≈ 650,000
PROPULSION SYSTEM PERFORMANCE DATA*			
	Maximum Static Power	760 W	740 W
	Static Thrust	6.9 lbs	6.7 lbs
	Current Drawn at Static	35.2 A	32.6 A
	Maximum Cruise Power	620 W	550 W
	Cruise Thrust (average)	2.07 lbs	2.01 lbs
	Current Drawn at Cruise	35.6 A	32.0 A
	Battery Capacity Consumed	805 mAh	1230 mAh
VEHICLE PERFORMANCE DATA			
	Maximum Velocity	58.0 mph	66.0 mph
	Stall Airspeed – Flaps Retracted	36.4 mph	24.6 mph
	Stall Airspeed – Flaps Deployed	31.2 mph	20.9 mph
	Takeoff Distance	140 ft (max)	83 ft
	Maximum Rate of Climb	120 ft/min	370 ft/min
	Maximum Load Factor	3.49	10.66
	Maximum Bank Angle	73.4 °	84.6 °

* APC 16x12 used for Fire Bomber Mission, Mejlzik 16x14 used for Ferry Mission

Weight and Balance Data

System weights and moments are shown in Table 13 below. The reference datum was taken from the tip of the spinner. For adequate stability, it was determined that the aircraft weight should be balanced on the wing quarter-chord. The payload bay was also balanced about this point to eliminate a shift in CG after payload deployment. All other components are firmly secured in their respective locations to prevent weight shifting in flight.

Table 13: Weight and Balance Data

COMPONENT	WEIGHT	MOMENT
Fuselage	18.00 oz	378.00 in-oz
Wings	19.75 oz	362.81 in-oz
Empennage	3.42 oz	178.30 in-oz
Landing Gear	13.83 oz	217.98 in-oz
Propulsion without Batteries	17.75 oz	98.69 in-oz
Propulsion Batteries	27.25 oz	384.63 in-oz
Control System	11.51 oz	269.54 in-oz
Pneumatic System	2.94 oz	36.34 in-oz
Payload System	8.42 oz	210.07 in-oz
Payload	140.80 oz	2448.51 in-oz
EMPTY WEIGHT	GROSS WEIGHT	CG LOCATION FROM DATUM
122.85 oz	263.65 oz	17.39 in

For abrupt rotation at takeoff, the lateral distance between the CG and the main gear was minimized. Fifteen degrees between the CG location and the main gear axel was considered standard, and the contest entry features seven degrees for this angle. This angle was found to provide a sufficient amount of weight on the nose gear to provide adequate ground handling.

System Data

The system data for the aircraft is given below in Table 14

Table 14: System Data

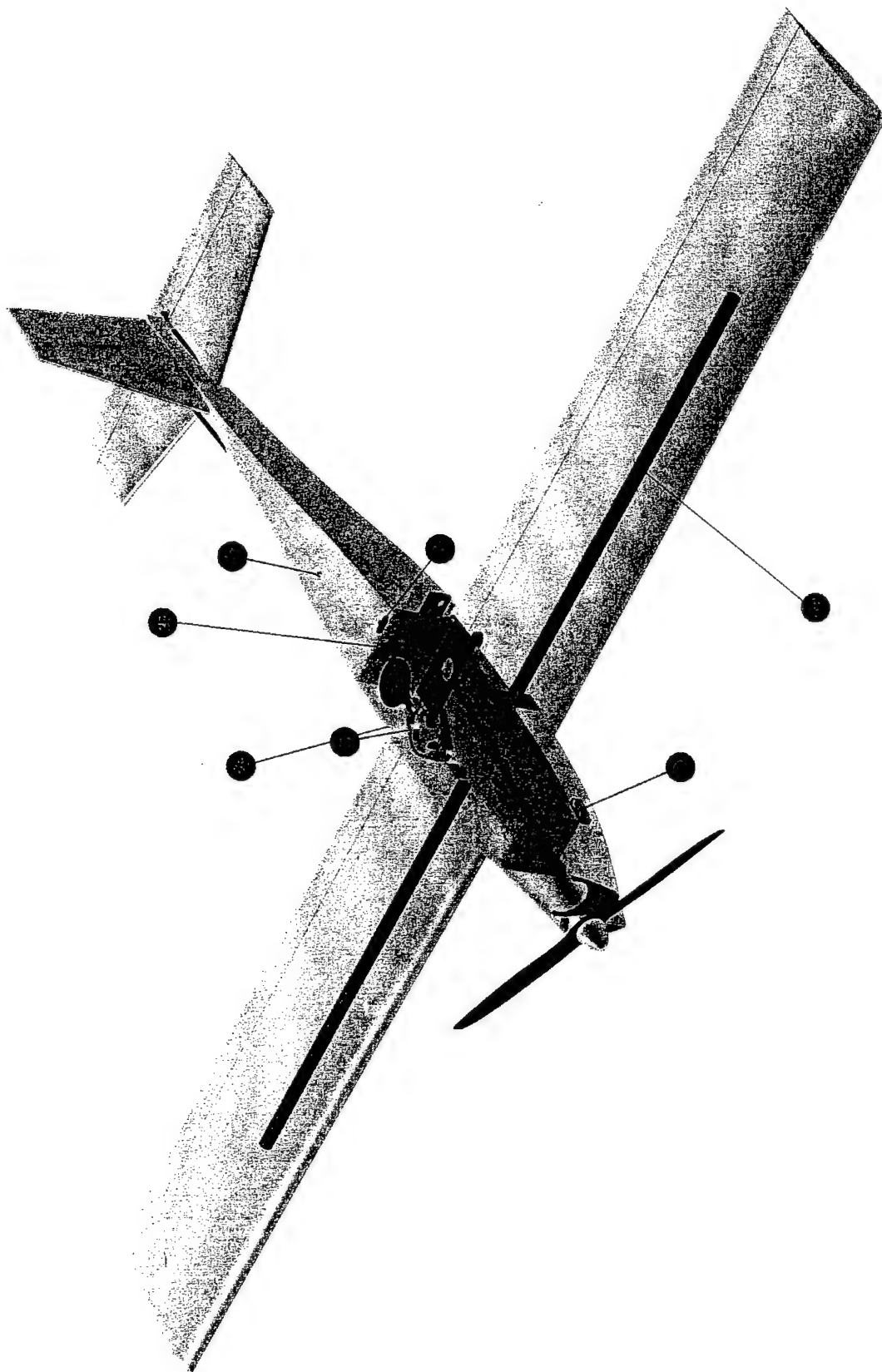
Transmitter Used	Futaba 9Z
Receiver Used	Futaba 1024 9 channel PCM
Servos Used	
Flaperon (x2)	JR DS8231
Elevator	JR DS8231
Rudder / Nose Gear	JR DS8231
Payload Deployment	JR DS3421

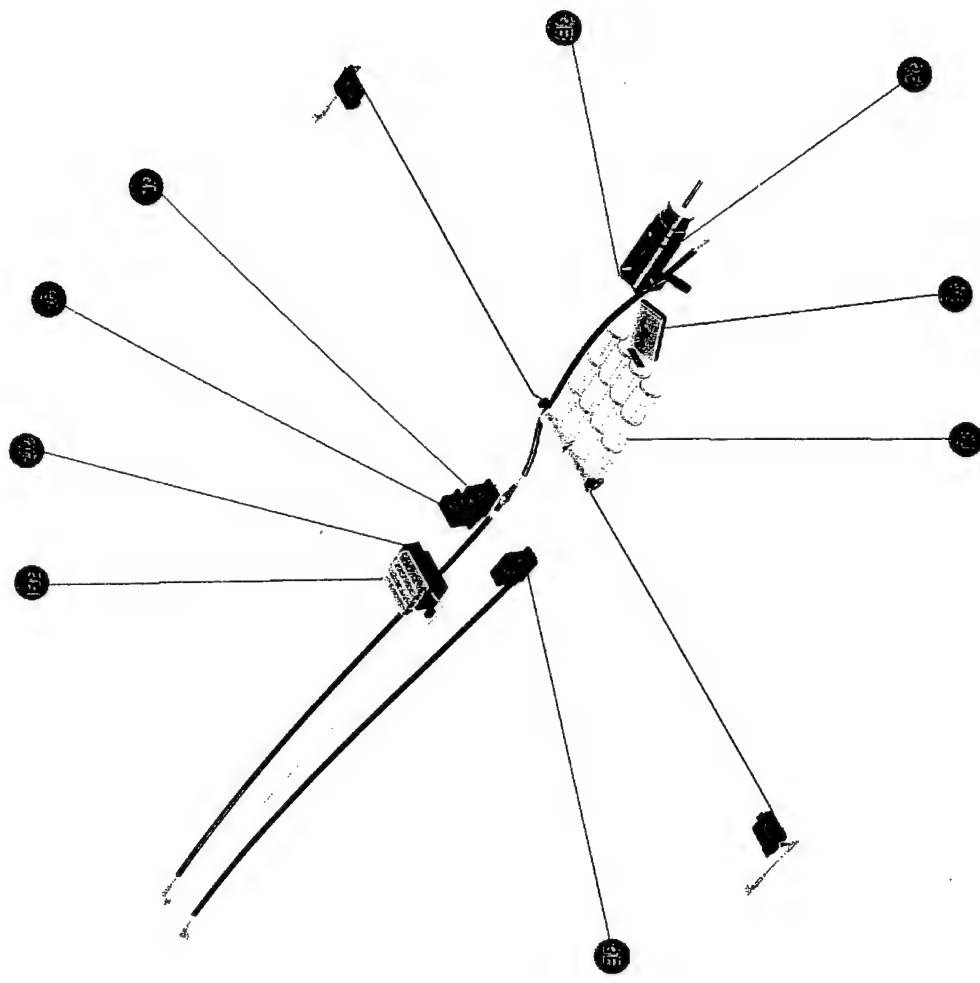
	Brakes	JR DS3421
Receiver Battery		
	# Cells	4
	Capacity per Cell	600 mAh
Propulsion Battery		
	# Cells	14
	Capacity per Cell	1700 mAh
Motor		Graupner Ultra 930-8
Gearbox		Aveox 3.7:1 Lightened
Propeller		
	Fire Bomber	APC 16x12
	Ferry	Mejzlik 16x14
Speed Control		Astro Flight #204
Gyro (x3)		Hobbico Multipurpose

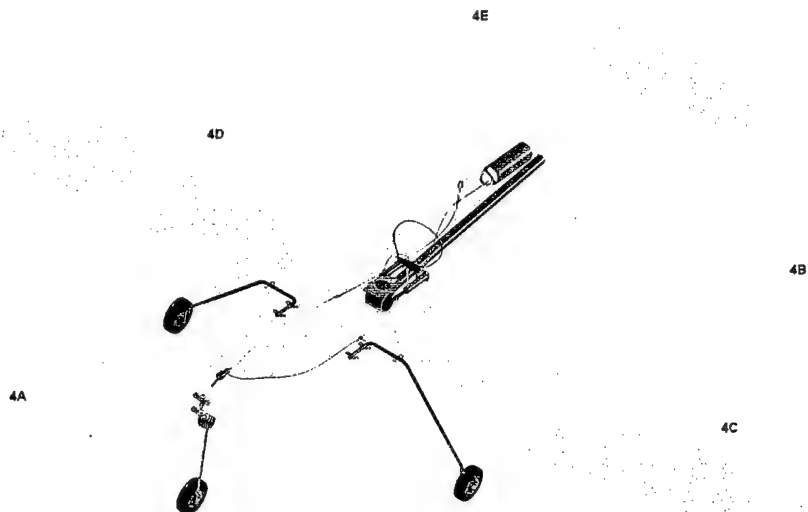
Georgia Tech - DBF 2003/2004 **Rated Aircraft Cost**

Description	Inputs Value Unit	Weight Multiplier	Total Weight	Cost per Pound	Component RAC
Manufacturer's Empty Weight (MEW)					
Empty Weight	7.68 lbs	1	7.678	\$300.00	\$2,303.44
Rated Engine Power (REP)					
Number of Motors	1 -	-	0		
Battery Weight	1.660 lbs	1	1.66	\$1,500.00	\$2,490.00
Description	Inputs Value Unit	Hour Multiplier	Number of Hours	Cost per Hour	Component RAC
Manufacturing Man Hours (MFHR)					
WBS 1.0 Wing			69.39	\$20.00	\$1,387.85
Total Wing Area	6.1892 ft ²	10	61.89		
Span	6.46 feet				
Max Exposed Chord	0.96 feet				
Number of Wings	1				
Total Control Function	1.5 -	5	7.50		
Ailerons?	no -	1			
Flapperons?	yes -	1.5			
Aileron/Flap Combination?	no -	2			
Aileron/Spoiler Combination?	no -	2			
Aileron/Flap/Spoiler Combination?	no -	3			
WBS 2.0 Fuselage			16.87	\$20.00	\$337.38
Total Fuselage Volume	0.84 ft ³	20	16.87		
Body Max Length	4.42 feet				
Body Max Width	0.42 feet				
Body Max Height	0.46 feet				
WBS 3.0 Empennage			20	\$20.00	\$400.00
Number of Vertical Surfaces with no Active Control	0 -	5	0		
Number of Vertical Surfaces with Active Control	1 -	10	10		
Number of Horizontal Surfaces	1 -	10	10		
WBS 4.0 Flight Systems			35	\$20.00	\$700.00
Number of Servos/Controllers	7 -	5	35		
Rated Aircraft Cost, \$ (Thousands) =					\$7.62

Figure 14: RAC Worksheet



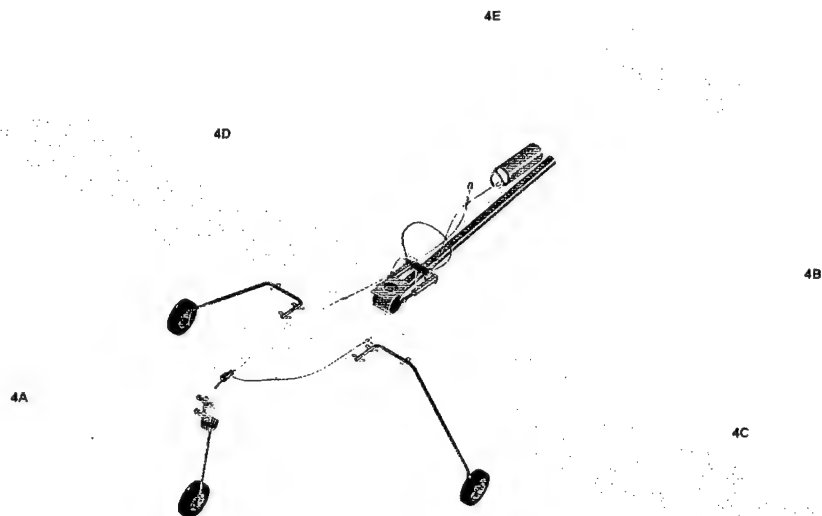




PAGE 4

Component Index					
Page	Pointer	Description	Page	Pointer	Description
Aircraft Exterior - Page 1			Flight Control System - Page 3		
1		Spinner Nut	3	3E	Elevator Servo, JR DS8231
1		Propeller: Mejzlik 16x14	3	3F	Rudder Servo, JR DS8231
1		40 Ampere "Slow Blow" Fuse	3		Rudder Gyro, Hobbico
1		On/Off Switch	3	3C	Futaba 1024 PCM Receiver
1		Fiberglass Fuselage	3	3H	Receiver Battery, 4.8V, 600mAh
1		Horizontal Stabilizer	1		On/Off Switch
1		Vertical Stabilizer	3		Flaperon Gyro, Hobbico (x2)
1,4		Pneumatics Fill Valve	Pneumatic Systems - Page 4		
1		Wing Panels: Left, Right	4	4A	Brake Valve
1		Inlet Port	3	3B	Brake Servo, JR DS3241
Airframe Components - Page 2			4	4B	Deployment Valve, Robart
2		Nose Gear Plate	3	3L	Deployment Servo, JR DS3421
2		Payload Bay Frame	4		Tubing: Tank, Up, Down, Brake
2		Spar Tube, 7075 T6 Al .75"ODx0.032WT	1,4		Pneumatics Fill Valve
2		Cylinder Mount	4	4C	Actuator Cylinder, Robart #165 (x2)
2		Check Valve	4		T-Fittings
2		Payload, 4 liters water	4		Brake, Trim Aircraft for 2.6" Left
Propulsion System - Page 3			4		Brake, Trim Aircraft for 2.6" Right
3	3A	Graupner Ultra 930-8	4	4E	Tank, 5.7cu-in
3	3C	Speed Controller Astro #204	Deployment System - Page 4		
3	3D	Propulsion Battery Pack	4	4D	Deployment Assembly
1		40 Ampere "Slow Blow" Fuse	4		Deployment Tube (shown retracted)
Linkage Assemblies - Page 3			Landing Gear - Page 4		
3		Flaperon Linkage, Right	4		Nose Strut and Support Housing
3		Flaperon Linkage, Left	4		Main Strut, Right
3		Rudder & Nose gear Linkage	4		Main Strut, Left
3		Elevator Linkage	4		Nose Wheel, 2.4"
3		Brake Valve Linkage	4		Gear Retaining Straps (x6)
3		Deployment Valve Linkage			

NOTE: Only key components have been given pointers



PAGE 4

Component Index					
Page	Pointer	Description	Page	Pointer	Description
Aircraft Exterior - Page 1			Flight Control System - Page 3		
1		Spinner Nut	3	3E	Elevator Servo, JR DS8231
1		Propeller: Mejzlik 16x14	3	3F	Rudder Servo, JR DS8231
1		40 Ampere "Slow Blow" Fuse	3		Rudder Gyro, Hobbico
1		On/Off Switch	3	3G	Futaba 1024 PCM Receiver
1		Fiberglass Fuselage	3	3H	Receiver Battery, 4.8V, 600mAh
1		Horizontal Stabilizer	1		On/Off Switch
1		Vertical Stabilizer	3		Flaperon Gyro, Hobbico (x2)
1,4		Pneumatics Fill Valve	Pneumatic Systems - Page 4		
1		Wing Panels: Left, Right	4	4A	Brake Valve
1		Inlet Port	3	3B	Brake Servo, JR DS3241
Airframe Components - Page 2			4	4B	Deployment Valve, Robart
2		Nose Gear Plate	3	3I	Deployment Servo, JR DS3421
2		Payload Bay Frame	4		Tubing: Tank, Up, Down, Brake
2		Spar Tube, 7075 T6 Al .75"ODx0.032WT	1,4		Pneumatics Fill Valve
2		Cylinder Mount	4	4C	Actuator Cylinder, Robart #165 (x2)
2		Check Valve	4		T-Fittings
2		Payload, 4 liters water	4		Brake, Trim Aircraft for 2.6" Left
Propulsion System - Page 3			4		Brake, Trim Aircraft for 2.6" Right
3	3A	Graupner Ultra 930-8	4	4E	Tank, 5.7cu-in
3	3C	Speed Controller Astro #204	Deployment System - Page 4		
3	3D	Propulsion Battery Pack	4	4D	Deployment Assembly
1		40 Ampere "Slow Blow" Fuse	4		Deployment Tube (shown retracted)
Linkage Assemblies - Page 3			Landing Gear - Page 4		
3		Flaperon Linkage, Right	4		Nose Strut and Support Housing
3		Flaperon Linkage, Left	4		Main Strut, Right
3		Rudder & Nose gear Linkage	4		Main Strut, Left
3		Elevator Linkage	4		Nose Wheel, 2.4"
3		Brake Valve Linkage	4		Gear Retaining Straps (x6)
3		Deployment Valve Linkage			

NOTE: Only key components have been given pointers

MANUFACTURING PLAN

The chart shown in Figure 17 represents the manufacturing process selection for the major components and assemblies of the aircraft. For each process, there are five Figures of Merit (FOM's) that evaluate the processes' feasibility for manufacture. For each FOM, there were factors governing the team's ability to conduct a process and produce quality results. These factors were grouped into two categories. "Acquisition Factors" included constraints that were beyond the direct control of the team, and "Constraint Factors" included constraining factors that the team could control. Both categories are shown in Figure 16 on the next page and are described below:

Tools and Equipment (AF) – Reflected the availability of the tools and equipment necessary for the process.

Material Availability (AF) – Reflected the availability of the consumable materials necessary for the process.

Expertise Availability (AF) – Reflected the availability of expertise for consultation; including the existence of known experts and their availability to help.

Associated Risk (AF) – Reflected the variability of geometric and qualitative specifications for produced products.

Budget Constraints (CF) – Reflected the capabilities of the team to allocate funds to a process.

Skills Required (CF) – Reflected the available skills of team members for a process; included experience and education as shown below in Table 15: Skills Matrix.

Table 15: Skills Matrix

Number of People with...	Hot Wire Foam Cutting	Fiberglass Lay-up	Machining - Lathe	Machining - Mill	Machining - CNC	Sanding/ Finishing	Covering - Polyvinyl	Covering - Polycarbonate	Balsa Sheeting	Balsa Framing	Woodworking	Hand Tooling
Expert Skills	4	1	0	0	0	1	0	0	1	1	2	4
Advanced Skills	3	0	2	1	2	3	1	0	1	0	3	5
Intermediate Skills	3	2	3	4	0	2	0	3	2	3	5	4
Basic Skills	5	1	0	0	0	1	1	0	0	0	5	3
Total Skilled Workers:	15	4	5	5	2	7	2	3	4	4	15	16

Scheduling Timelines (CF) – Reflected the logistical constraints of scheduling the start, duration, and completion of processes. Personnel scheduling and project deadlines were included.

Process Dangers (CF) – Included the risk of exposure to harmful chemicals, dangerous machinery, and sharp objects. Countering the weight of this category was the availability of safety equipment and training.

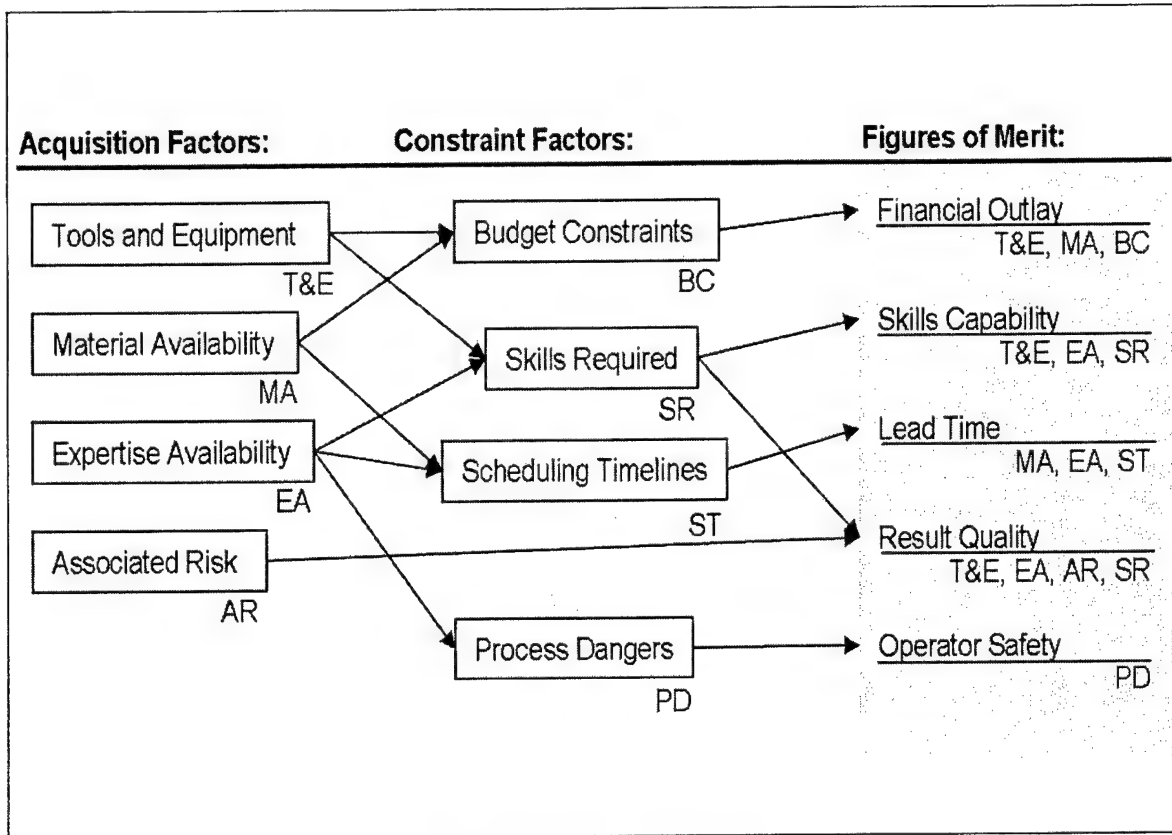


Figure 16: FOM Build-Up

It is important to note that the build-up of each FOM as shown has a slightly different meaning for each process considered in the chart. For example, "Tools and Equipment" is shown as part "Financial Outlay," "Skills Capability," and "Result Quality." Tools and equipment will require some financial outlay in order to either acquire necessary tools and equipment or maintain the function of those tools and equipment. In order to operate the tools and equipment, certain skills are required. Also, a specific type of tool used may provide a higher-quality part than others. Each of the FOM's is affected by more than one constraint as well. For example, "Financial Outlay" is affected by the "Tools and Equipment," "Materials Availability," and "Budget Constraint" criteria.

Furthermore, each criterion under each FOM takes on specific meaning for each process considered. For example, the "Tooling and Equipment" considered for vacuum bagging wings (e.g. vacuum pump, vacuum bags, sealer, etc...) would not be the same as that considered for milling the deployment mechanism (e.g. a milling machine, end mills, micrometer, etc...).

The result of the evaluation of each factor for a process is a bar representing the favorability of that process to the team as it relates to that factor. The intensity of each process's bars is summed to show the process's cumulative favorability for that component or assembly. For each FOM, the team has specified a minimum cutoff for the acceptability of the process. If any process does not meet the minimum level of acceptability, then the process is not considered a feasible option. This level of acceptability is shown in Figure 17 as a dashed line. The cumulative score above this acceptance level is given a quality

score based on its magnitude. The quality scores for each process are summed at the right of the chart for a total quality score that is used to compare all processes that have met the minimum acceptance level for each FOM.

Wings

The wings of the final design are foam core, balsa sheeted with polyvinyl heat shrink covering. This process was selected because it allowed quality results to be produced inexpensively, in a short period of time, by team members with little experience or training.

Construction of the wing began with the foam core. Two airfoil templates were used on either end of a block of foam to cut each wing panel individually (as was necessary due to the wing taper and twist). A $\frac{3}{4}$ inch hole was cut (again using a hot wire) through the entire span of the wing core for the installation of the wing tube. A phenolic wing tube was fit to this hole and glued in place to add strength to the core and provide a smooth guide for the wing spar. The control surfaces were then cut off at 20% of the chord, finished with $\frac{1}{4}$ inch balsa stock, and reattached to the wing with "CA" type hinges. Birch plywood mounts for the landing gear were mounted directly to the phenolic tube near the wing root, and servo pockets were cut at mid-span with a hole drilled through the span to the pocket for the servo leads. Servo mounting blocks were also glued directly to the phenolic wing tube. Balsa sheeting was then applied to the outside of the foam wing core using polyurethane glue and placed in a vacuum bag overnight. Polyvinyl heat shrink covering applied was applied over the balsa sheeting, which yielded superior surface qualities.

Empennage

Although similar to the wing, the empennage construction process chosen was different than that chosen for the wing. There were several contributing factors to the decision to use an alternate construction. The team predicted that the worst loads applied to the empennage would most likely be in transportation and handling, rather than in flight. The small empennage thickness suggested an alternate material selection for greater probability of survival. The decision to use a thin polycarbonate film applied directly to a foam core, therefore dictated the process involved in empennage construction..

Fuselage

The process selected for the construction of the fuselage was a "disintegrating plug." This process involved shaping a large block of Styrofoam to specific geometry at stations along its length in order to accurately match the intended shape. Several layers of lightweight fiberglass were applied to the outside of the foam with epoxy. After the epoxy cured, access hatches were cut, and the foam removed; leaving a hollow, lightweight shell. Bulkheads and payload bay formers were installed to complete the construction of the fuselage.

The entire process could be completed in three days with accurate geometry, sufficient strength, and favorable surface finish. The tools and equipment required to complete the process were scissors, mixing cups, and other such simple devices. The skills required to produce acceptable results were rudimentary, and the materials required were simple, easily obtainable, and cheap.

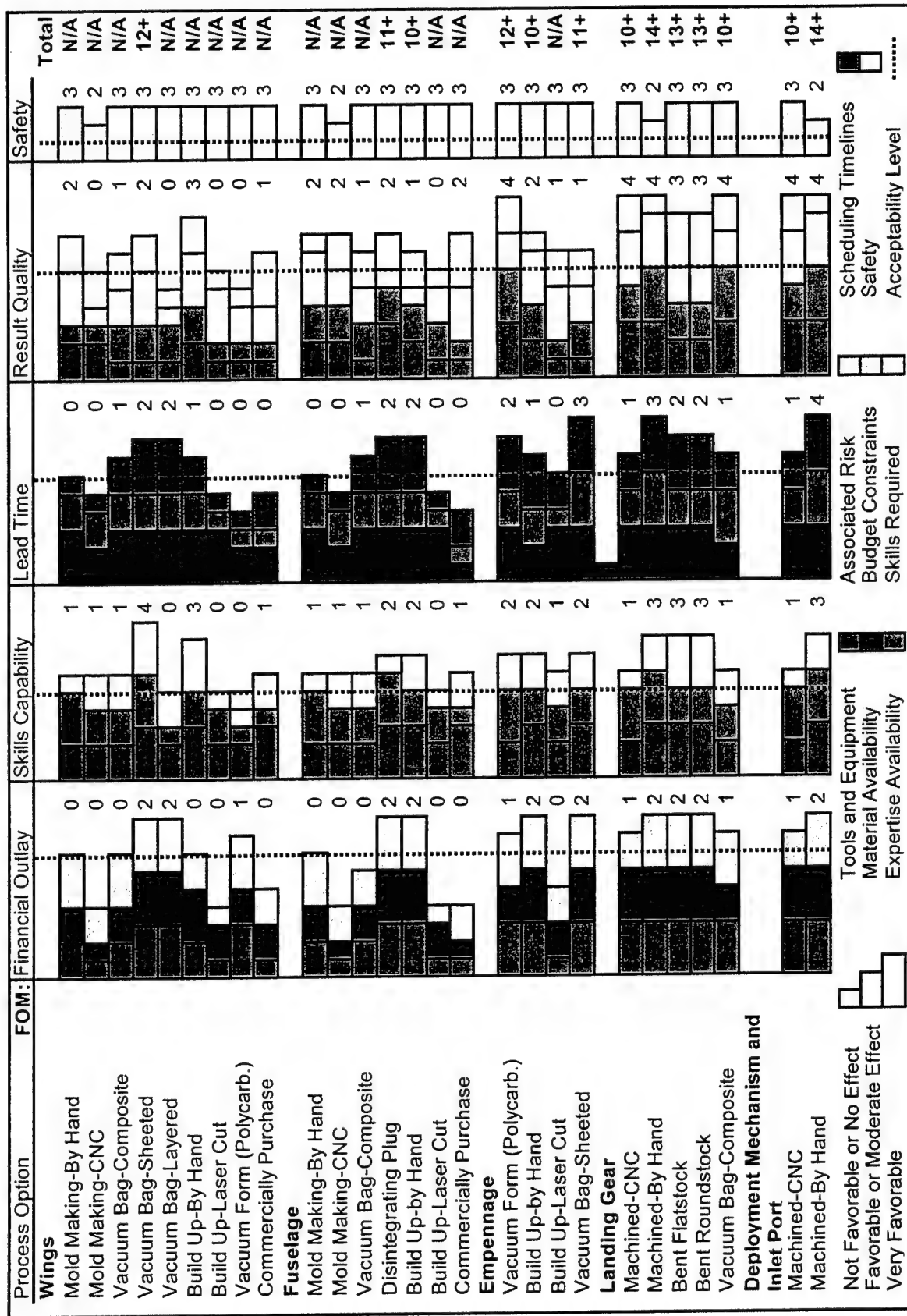


Figure 17: Process Selection Chart

The foam plug used to give the fuselage its shape was cut from the front view, side view, and top view generated from CAD geometry. These dimensions were traced on a rectangular block of expanded polystyrene. A hotwire cutting system was used to trim the block along the lines drawn on the block. This shape was then smoothed with various grits of sandpaper until the desired shape was achieved.

Before laying the fiberglass over the foam shape, pieces of balsa were added as reinforcement to areas that would be under high stress such as in the tail and around the wing spar. Both the top and bottom surfaces were covered with one layer of 9 oz S-glass fiberglass cloth and one layer of 3 oz S-glass cloth, with some sanding between layers. The external surface was sanded and polished before removing the foam from the interior.

Physical extraction of the foam, although laborious, proved to be the most appropriate method. Sharp, penetrating tools were used on the core of the shape, and a much more gentle wire brush was used near the inside of the cured fiberglass. The average weight of the 3 fuselages produced at the time of this report was approximately 15.7 ounces.

Landing Gear

The landing gear design and selection was an excellent example of the interplay of manufacturing capabilities and intended design. After discussing many options, the team decided to use stainless steel rods for the main gear, and a commercially purchased nose strut for the nose gear. The ends of the main struts were turned in a lathe to accept the wheels and brakes. Then a tool specially made to bend small gauge wire was purchased to accurately shape the 1/4 inch stainless steel rods. After some practice, the team was able to produce acceptable results in a timely manner.

Deployment Mechanism and Inlet Port

These two payload system components were designed with consideration to the milling and lathing capabilities of the team. The entire design of the payload system was dependent on not only access to a mill and lathe, but availability of the machines and proper training. These two components were designed to such that they would be stronger than necessary to complete the mission, such that the probability of failure and subsequent rework would be low. Team management felt that scheduling time for training and manufacturing was worth the investment in time and money because of the component's tremendous importance to the function of the aircraft and the future capabilities of the team.

The tight tolerances that the team required for the parts further reinforced the decision to use machining equipment for manufacturing. The payload deployment valve design required that a rotating barrel inside a sleeve had to be manufactured tight enough not to leak, but not so tight that it was difficult to move with pneumatic cylinders.

The decision to use a CNC mill to produce the inlet port was made after consulting a machinist with the team's CAD drawings. Due to the complexity of the part, it was estimated that nearly three days of working time would be needed to produce one part by a team member. Furthermore, there was a high probability of human error ruining the part; leading to delays and further expense. After configuring the

CAD drawing to the necessary CNC file, the entire process took less than three hours from set up to completion.

Manufacturing Schedules

Construction efforts had to be scheduled carefully to ensure timely delivery of the designed components and assemblies. Many of the components of the aircraft were modular, and thus updates to the design did not require a complete overhaul of an existing vehicle. Below in Figure 18, the major components and assemblies involved in the 2003-2004 contest entry are shown with their planned and actual schedules. The "Bottle Manifold" shown under Loading Components was a device used to load the payload into the aircraft quickly.

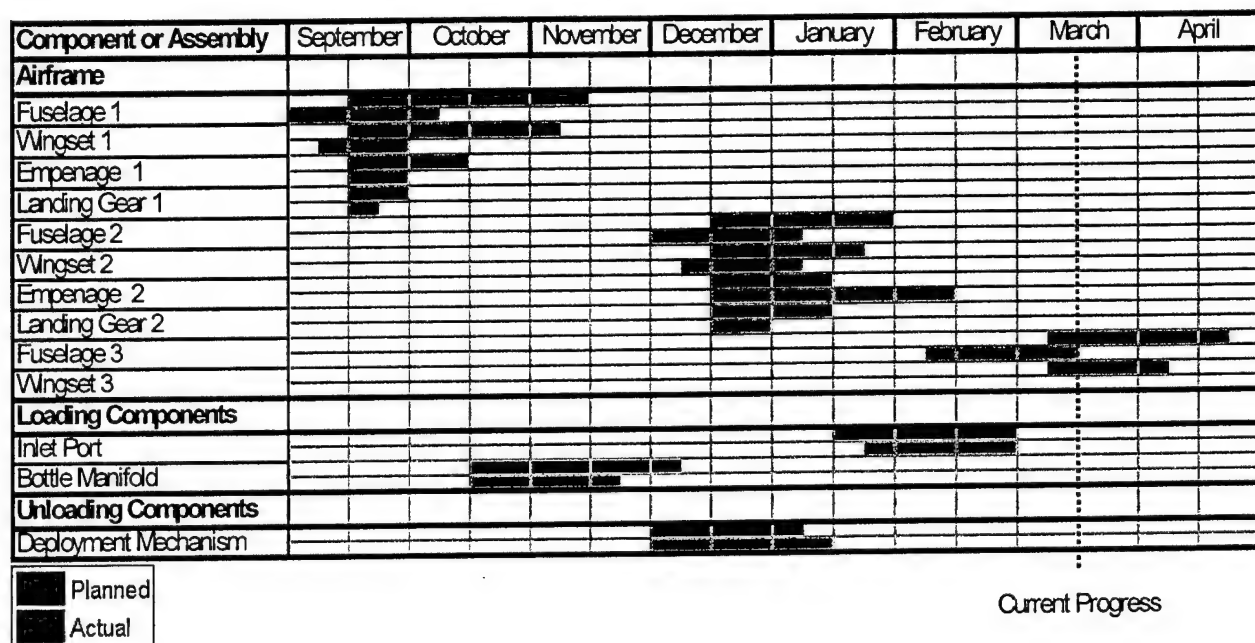


Figure 18: Manufacturing Gantt Chart

Predicted performance for complex systems was often thought better handled by interpretation of empirical data rather than more deterministic methods. Not only were tests conducted to validate designs, but they were also conducted proactively to gather empirical data that would be used to make critical design decisions. This section of the design report summarizes the tests conducted that influenced Georgia Tech's 2003-2004 DBF entry. Major tests and experimentations are summarized in Figure 21 at the end of this section.

Static Tests: Drain Tests

During Conceptual Design, the team discussed the constraint of dumping the entire payload on the downwind leg of the "Fire Bomber" mission between the turn markers. Assuming a 50 foot radius turn, the aircraft would have approximately 1314 feet from which to dump 4 liters of water through a 0.5 inch orifice. The team could determine the maximum allowable airspeed to fly if the dump time could be estimated. Therefore, the team decided to experiment with dumping 4 liters from a container through a 0.5 inch orifice.

The first test involved dumping the water through a $\frac{1}{2}$ inch hole from an un-vented 4 liter container. The average dump time for 4 trials was 92 seconds. Given a distance of 1314 feet as described, the aircraft would have a maximum allowable airspeed of approximately 9.7 mph. Clearly, this speed indicates that either less than 4 liters of payload should be carried, or other means for draining faster needed to be explored. The team then experimented with venting the container and allowing air to flow inside to replace the draining water. Small holes of increasing size from $\frac{1}{8}$ inch to $\frac{3}{4}$ inch in $\frac{1}{32}$ inch increments were drilled for the venting until the team saw significant diminishing returns on drain time reduction. Test results showed that an orifice of $\frac{5}{16}$ inch in diameter would reduce drain times to 31.3 seconds, and subsequently the aircraft would then be able to fly a maximum of 29 mph.

The second series of tests for drain times spurred from the idea that the drain times could be further reduced if the vertical water column height was increased. The team did not want to increase the fuselage height, as this height was scored in the RAC, but would attach a long tube to the valve mechanism that would create a long vertical water column and potentially reduce drain times. There were 5 tube diameters tested (1.00, 0.875, 0.75, 0.625, and 0.50 inches) each of which was tested five times at various decrements in length. Each tube was initially 36 inches long and trimmed in 6 inches until the total length was 6 inches. The average drain time for the five trials at each length was documented and plotted for comparison.

The final decision for tube geometry was 0.75 inches in diameter (with a 0.5 inch orifice at the end) and 18 inches in length below the bottom of the payload bay. Drain times for this tube average 10.3 seconds, allowing a maximum airspeed of 87 mph.

Static Tests: Motor Tests

As discussed in Preliminary Design, the design sequence called for extensive use of modeling and simulation environments for the various components of the aircraft. In addition to manufacturer's published information, the team documented the performance of candidate motors using empirical data gathered from the team's dynamometer. Test objectives included documentation of the current drawn and RPM for input voltages and torques. Input power vs. output power was used to figure motor efficiency. The data collected was used to accurately reproduce the conversion of electrical power to physical power for each candidate motor.

Static and Dynamic Tests: Propeller Tests

Modeling and simulation of candidate propellers was also critical to the design sequence. Using a simple strain gauge, 27 candidate propellers were run at static conditions in order to record RPM and thrust. A cantilever arm mounted to the motor was used to record the input torque. Static thrust data were used to arrange the relative magnitudes of thrust lapse profiles for all candidate propellers. These thrust lapse profiles were fit from wind tunnel data collected for 8 of the candidate propellers. Once all the data was collected, the information was extrapolated to figure the performance of propellers not investigated. This information was used to determine the optimal propeller candidates for the selected motor as described previously in the Preliminary Design section of this report.

Dynamic Tests: Flight Testing

Before the project began, team management recognized that flight testing would be the single most important series of tests conducted. Project plans called for an early prototype, and first flights were conducted in October 2003 (Figure 2: Project Development Gantt Chart). The team also recognized that flight testing without proper data gathering equipment would be strictly qualitative. Telemetry equipment was purchased commercially that was installed onboard the aircraft. The equipment was lightweight, small, and would otherwise not interfere with the performance of the aircraft. A sample rate of 25 Hertz recorded airspeed, propeller RPM, voltage and current to the motor, voltage and current to the receiver, motor temperature, propulsion battery temperature, vertical (z-axis) acceleration, and longitudinal (x-axis) acceleration.

Takeoff performance and cruise performance were evaluated for various aircraft configurations, including various wing designs, motor and propeller selections, and various wing loadings. The team also standardized the preflight, flight line, and post flight checks conducted to help prevent against accidents. This check list is provided in Figure 19.

Lessons Learned

Component testing, including motor testing, static and dynamic propeller testing and drain tube testing, was a critical component of the design optimization plan. The early plans to gather empirical data neglected to recognize that tests and experimentation are in themselves complicated projects. Simply having the component itself was not sufficient for testing it. Test equipment, schedule control, and

Probably the most critical tests conducted were the flight tests of the various prototype and final vehicle components. More experienced team members emphasized the importance of early flight testing. Early prototyping and flight testing proved tremendously informative to the team. Knowing the relative magnitude of the various performance metrics gave the team starting points for design iterations, and adjustments to the prototype aircraft showed the output response for changes to input metrics. The Georgia Tech DBF team considers the tests and experiments conducted as the most educational and enjoyable part of the design project and will use the lessons learned in these activities for future projects.

Preflight Checklist					
Propulsion battery	<input type="checkbox"/>	verify charged	Propeller	<input type="checkbox"/>	correct size, secure
Voltage	<input type="checkbox"/>	verify security	Center of gravity	<input type="checkbox"/>	verify location
Installation	<input type="checkbox"/>	disarmed	Receiver	<input type="checkbox"/>	off
Connection	<input type="checkbox"/>	on	Transmitter	<input type="checkbox"/>	off
Transmitter	<input type="checkbox"/>	on	Receiver battery	<input type="checkbox"/>	verify charged
Receiver	<input type="checkbox"/>	set neutral			
Flapperon switch	<input type="checkbox"/>	check neutral, level	Flightline Checklist		
Flapperons	<input type="checkbox"/>	set/verify	Transmitter	<input type="checkbox"/>	on
Trims			Receiver	<input type="checkbox"/>	on
Wings			Elevator	<input type="checkbox"/>	correct movement
Retaining Screws	<input type="checkbox"/>	tight	Rudder	<input type="checkbox"/>	correct movement
Hinges	<input type="checkbox"/>	tug for security	Ailerons	<input type="checkbox"/>	correct movement
Clevises	<input type="checkbox"/>	secure	Flaps	<input type="checkbox"/>	correct movement
Control horns	<input type="checkbox"/>	secure	Dual rates	<input type="checkbox"/>	correct volume
Position	<input type="checkbox"/>	verify neutral	Propulsion battery	<input type="checkbox"/>	arm
Elevator			40 Amp fuse	<input type="checkbox"/>	Install
Installation	<input type="checkbox"/>	verify security	Throttle	<input type="checkbox"/>	10%
Clevises	<input type="checkbox"/>	secure	Brakes	<input type="checkbox"/>	check
Control horns	<input type="checkbox"/>	secure	<i>Ground crew hold aircraft</i>		
Position	<input type="checkbox"/>	verify neutral	Throttle	<input type="checkbox"/>	0-100-0%
Rudder			Range	<input type="checkbox"/>	check
Installation	<input type="checkbox"/>	verify security	Fail safes	<input type="checkbox"/>	verify
Clevises	<input type="checkbox"/>	secure			
Control horns	<input type="checkbox"/>	secure	Postflight Checklist		
Position	<input type="checkbox"/>	verify neutral	40 Amp fuse	<input type="checkbox"/>	remove
Wheel retaining collars	<input type="checkbox"/>	secure	Receiver	<input type="checkbox"/>	off
Air tank	<input type="checkbox"/>	charged to 120psi	Transmitter	<input type="checkbox"/>	off

55

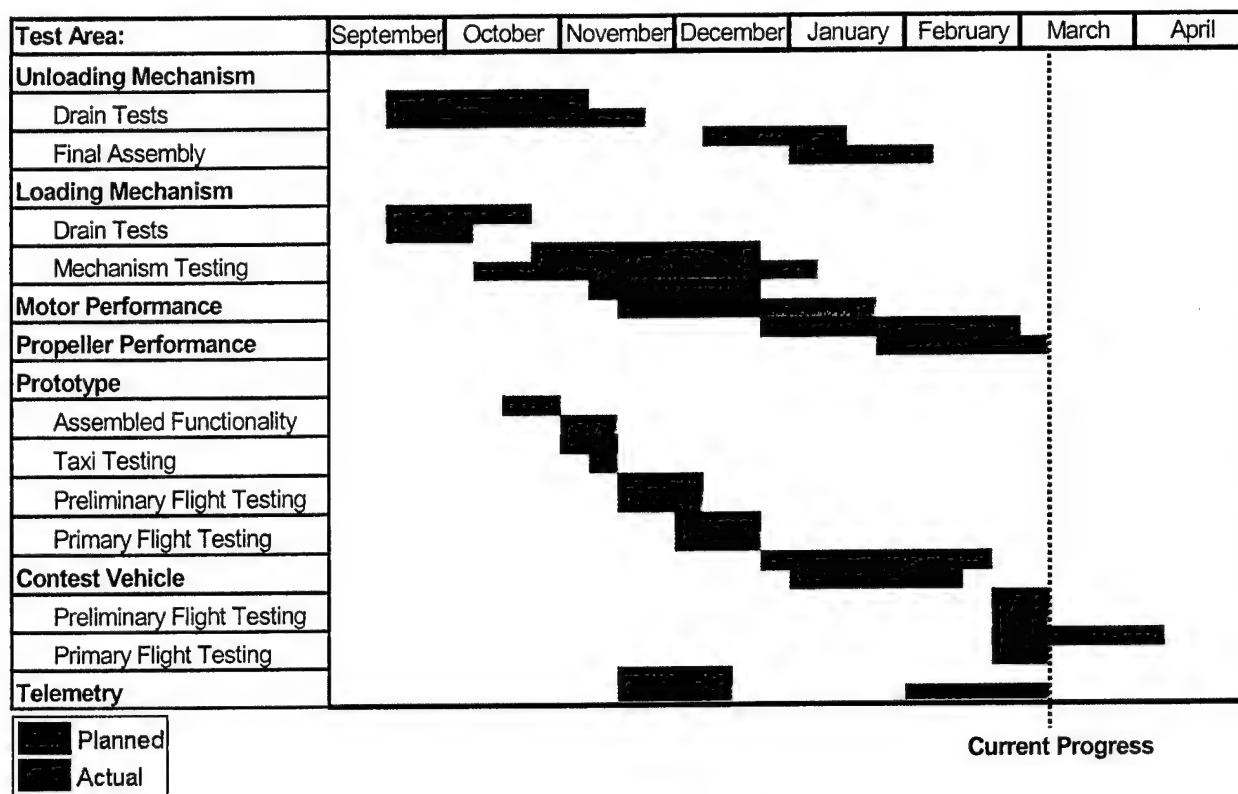


Figure 20: Testing Timeline

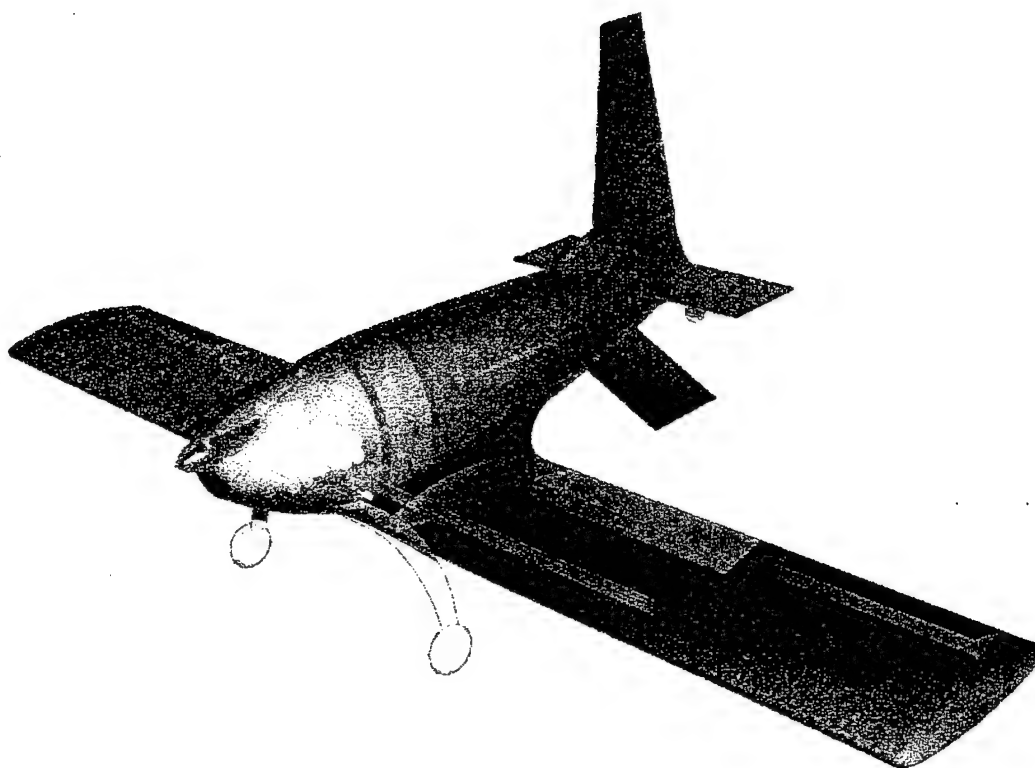
Prototype Aircraft	
Assembled Functionality	
verify configuration assumptions	<input checked="" type="checkbox"/> No major conflicts
identify major assembly or functional problem areas	<input checked="" type="checkbox"/> Assembly proved easy/functional
Taxi Test	
qualitatively assess aircraft ground handling	<input checked="" type="checkbox"/> Ground handling very stable
qualitatively assess the gear strength and function	<input checked="" type="checkbox"/> Landing gear appropriate for task
Preliminary Flight Testing	
establish flight, adjust balance and trim, return safely	<input checked="" type="checkbox"/> Completed
assess handling qualities and adjust control volumes	<input checked="" type="checkbox"/> Completed
Primary Flight Testing	
record performance using installed telemetry equipment	<input checked="" type="checkbox"/> Metrics successfully recorded
measure takeoff distance and cruise airspeed	<input checked="" type="checkbox"/> Takeoff and cruise conditions tested
evaluate performance and make necessary adjustments	<input checked="" type="checkbox"/> Data used in design sequence
Contest Vehicle	
Preliminary Flight Testing	
establish flight, adjust balance and trim, return safely	<input type="checkbox"/> To be completed March, 2004
Primary Flight Testing	
verify adherence to intended design	<input type="checkbox"/> To be completed March, 2004
Telemetry	
Calibration	
fabricate instruments and conduct calibration	<input checked="" type="checkbox"/> Calibrated, and installed
Installation	
verify repeatability and check for low-variance output	<input checked="" type="checkbox"/> Completed for all channels
Motor Performance	
Stall Test	
measure stall current of selected motors	<input checked="" type="checkbox"/> Completed for candidate motors
No-Load Test	
record voltage constant and hysteresis effect for motors	<input checked="" type="checkbox"/> Completed for candidate motors
Dynamic Loading Test	
record performance profile for voltage and load range	<input checked="" type="checkbox"/> Completed for candidate motors
Propeller Performance	
Propeller Geometry	
record pitch, thickness, and hub distance at 12 stations	<input checked="" type="checkbox"/> Completed for selected propellers
Static Test	
record torque, RPM, and thrust	<input checked="" type="checkbox"/> Completed for selected propellers
Dynamic Test	
record thrust lapse profile for selected RPMs	<input checked="" type="checkbox"/> Completed for propeller sub-set
Loading Mechanism	
2-Liter Drain Test	
record drain time for 2-liter soda bottles	<input checked="" type="checkbox"/> Data recorded and used in design
study feasibility of enhancement	<input checked="" type="checkbox"/> Data recorded and used in design
Assembled Functionality	
record 4 liter drain time for various apparatuses	<input type="checkbox"/> Currently in process
assess viability of mechanism to final assembly	<input type="checkbox"/> To be completed March, 2004
Unloading Mechanism	
Drain Test	
experiment with mechanism construction	<input checked="" type="checkbox"/> Data recorded and used in design
Assembled Functionality	
record final performance	<input checked="" type="checkbox"/> Performs requisite function
Rapid Prototyping	
Empennage and Wing	
experiment with various wing constructions	<input checked="" type="checkbox"/> Completed, and used in design
assess strength and finished qualities	<input checked="" type="checkbox"/> Completed

Figure 21: Test Checklist

REFERENCES

1. Cohen, Lou. Quality Function Deployment. Reading, MA: Addison-Wesley, 1995.
2. Etkin, Bernard. Dynamics of Flight. New York, NY: John Wiley & Sons, 1982.
3. Pugh, Stuart. Total Design. Reading, MA: Addison-Wesley, 1991
4. Hoerner, Sigward F. Fluid-Dynamic Drag. Bakersfield, CA: Hoerner Fluid Dynamics, 1965.
5. Lenon, Andy. Basics of R/C Model Aircraft Design. Redfield, CT: Air Age, Inc., 1999.
6. Mattingly, Jack D., and William H Heiser, and Daniel H. Daley. Aircraft Engine Design. Reston, VA:
7. American Institute of Aeronautics and Astronautics, Inc., 1999.
8. Raymer, Daniel P., J. S. Przemieniecki, ed. Aircraft Design: A Conceptual Approach 3rd Ed. Reston,
9. VA: American Institute of Aeronautics and Astronautics, Inc., 1999.
10. Simons, Martin. Model Aircraft Aerodynamics 4th Ed. Swanley, Eng.: Nexus Special Interests, 1999.
11. UIUC Airfoil Wind Tunnel Data on the Web. <<http://www.aae.uiuc.edu/m-selig/pd.html>> Last update: 4/6/98

**2003/2004 AIAA
Cessna/ONR Student Design/Build/Fly
Competition**



**"Paani Hawaii Jahaz" or "Water-Air-Craft"
California State Polytechnic University, Pomona
Aerospace Engineering Department
March 2004**

1. Executive Summary	4
1.1. Overview of Conceptual Design Phase.....	4
1.1.1. Conceptual Design Ideas	4
1.1.2. Conceptual Design Calculations for RAC and Visualization Techniques	5
1.1.3. Results of Conceptual Design Phase.....	5
1.2. Overview of Preliminary Design Phase.....	5
1.2.1. Preliminary Design Considerations	5
1.2.2. Preliminary Design Results	6
1.3. Overview of Detailed Design Phase	6
1.3.1. Detailed Design Considerations	6
1.3.2. Detailed Design Results	6
1.4. Overview of Manufacturing Phase	6
1.4.1. Manufacturing Phase Considerations	7
1.4.2. Manufacturing Phase Conclusions.....	7
1.5. Testing Phase	7
2. Management Summary	8
2.1. Personal Upkeep and Team Architecture	8
2.1.1. Project Manager	9
2.1.2. Aerodynamics Team	9
2.1.3. Propulsion Team	9
2.1.4. Structures Team	9
2.1.5. Team Leaders	9
2.2. Supplementary Positions	9
2.2.1. Drawing/Drafting Team	10
2.2.2. Web Design Position	10
2.2.3. Travel and Logistics Team	10
2.3. Management Timeline.....	10
2.4. Personal Assignment Areas.....	12
3. Conceptual Design	13
3.1. Problem Statement.....	13
3.2. Mission Requirements	13
3.2.1. Aircraft Sizing and Assembly.....	14
3.2.2. Takeoff Distance Rate	14
3.2.3. Fire Fight Mission	14
3.2.4. Ferry Mission	14
3.3. Assumptions.....	15
3.3.1. Estimated Take-off Weight	15
3.3.2. Estimated Cruising Speed	15
3.3.3. Rated Aircraft Cost (RAC)	15
3.3.4. Figure of Merits (FOM)	16
3.3.5. Propulsion.....	16
3.3.6. Design Configuration	16
3.3.7. Landing Gear Configuration	17
3.3.8. Wing Configuration	18
3.3.9. Estimated Total Score	19
3.4. Conclusion for Conceptual Design Phase.....	21
4. Preliminary Design	22
4.1. Internal Configuration.....	22
4.2. Assembly Configuration.....	22
4.2.1. Wing Assembly Configuration	23
4.2.2. Landing Gear Assembly Configuration	23
4.2.3. Empennage Assembly Configuration	23
4.2.4. Fuselage Assembly Configuration	23
4.3. Preliminary Fuselage Design	23
4.3.1. Fuselage Preliminary Rendering	24

4.4.	Wing	25
4.4.1.	Airfoil Configuration.....	25
4.4.2.	Airfoil Velocity.....	26
4.4.3.	Airfoil Pressure Distribution.....	27
4.4.4.	Wing Planform Shape.....	29
4.4.5.	Wing Configuration Summary.....	29
4.5.	Tail Configuration	30
4.6.	Preliminary Propulsion System Configuration	30
4.6.1.	Propulsion System Gearing Configuration.....	30
4.6.2.	Preliminary Propulsion System Conclusions.....	31
5.	Detailed Design	32
5.1.	Rated Aircraft Cost	33
5.2.	Detailed Aircraft Drawing	33
6.	Manufacturing Plan	38
6.1.	Major Components	38
6.2.	Materials	38
6.3.	Figures of Merit	38
6.3.1.	Skill Levels.....	38
6.3.2.	Material Availability.....	38
6.3.3.	Material Cost.....	38
6.3.4.	Time Required.....	39
6.3.5.	Strength to Weight Ratio.....	39
6.4.	Manufacturing Schedule	41
6.5.	Manufacturing Process	42
6.5.1.	Design of Fuselage Mold.....	42
6.5.2.	Construction of a Male Fuselage Plug.....	42
6.5.3.	Construction of Female Fuselage.....	43
6.5.4.	Construction of Foam Core Wings.....	43
6.5.5.	Vertical and Horizontal Surfaces.....	44
6.5.6.	Landing Gear.....	44
6.5.7.	Bulkheads and Firewall.....	44
6.5.8.	Electronic Components and Water Dropping System.....	44
6.6.	Conclusion of Manufacturing Phase	45
7.	Overview of Flight Testing	46
7.1.	Component and Materials Testing	46
7.2.	Static and Ground Testing	46
7.3.	Flight and Dynamic Testing	46
8.	References	48

1. Executive Summary

This report summarizes the development of an unmanned flight vehicle by the team at California State Polytechnic University, Pomona for the 2003-2004 Cessna/ONR Student Design/Build Fly Competition. The team's entry is called "Paani Hawaii Jahaz, and will be flown in the April 23-25, 2004 competition at the Cessna Pawnee East Field in Wichita, Kansas. The Design Build Fly contest involves students designing, fabricating, and demonstrating the flight capabilities of an unmanned aerial vehicle that is electric powered and radio controlled and that which can best meet the specified mission profile. Two different missions are specified, with one being more difficult than the other. Both missions involve the vehicle taking off in maximum horizontal distance of 150 feet, flying either a 2 or 4 lap course, completing a 360-degree turn inside that course, landing and repeating the process. The first mission, called the "Fire Bomber" mission, or Mission A, involves carrying up to 4 liters of water on each lap and flying 2 laps. The second mission is called the "Ferry" mission, or Mission B, and involves flying 4 laps with no water. The goal of the contest is to maximize the total score, which can be done by excelling in three areas. One is to maximize the performance of the airplane, thus achieving a high flight score. Second, the report score needs to be maximized by developing an effective report that documents the design, fabrication and testing process. Finally, the Rated Aircraft Cost (RAC) needs to be minimized by achieving the lowest calculated cost capable within the design of the airplane.

1.1. Overview of Conceptual Design Phase

In the Conceptual Design Phase, detailed analysis and computer experimentation were used to investigate potential optimum designs. The most optimum design for the contest would consist of a vehicle that best balanced the tradeoffs associated among lowest RAC, highest maximum speed and most amount of water that can be carried. The Fire Bomber mission was given a higher priority in design, as its weighting factor is twice that of the Ferry mission. The vehicle's initial design was dictated by the above 3 goals. As a result, for the first mission, the vehicle needs to be large enough to carry an appreciable payload of water, have a high top speed by using a powerful motor, have a low drag design, and be light in weight and small in size to create a low RAC. For the second mission, only 2 tradeoffs needed to be balanced, those of speed and RAC.

1.1.1. Conceptual Design Ideas

We started by evaluating the 3 basic aircraft configurations: conventional wing and tail, blended wing body, and finally the flying wing. These basic configurations were evaluated on their ability to best balance the 3 mission goals. The ability to carry the water payload and drop it was also evaluated for all 3 designs. Using these criteria, we utilized computer design software such as Adynamic, Excel, and Mechanical Desktop to determine the pertinence of each configuration to these mission requirements.

1.1.2. Conceptual Design Calculations for RAC and Visualization Techniques

The conceptual design centered on spreadsheets for varying design considerations, hand layouts and drawings for visualization purposes. We also took advantage of Adynamic's Computational Fluid Dynamics (CFD) editor for drag estimations, VisualFoil for airfoil selection and lift considerations and Mechanical Desktop for design analysis. An Excel spreadsheet was set up to allow us to calculate the RAC values for different configurations of designs and allowed us to see how specific design elements changed the RAC value. Whenever we evaluated more than one different design configuration, we assigned a Figure of Merit (FOM) to it. This allowed for qualitative configuration comparison to see how it affected the RAC.

1.1.3. Results of Conceptual Design Phase

The first two mission investigations indicated that the fire bomber mission would always result in a higher score. As a result, the fire bomber mission was given higher priority in design considerations. The aircraft we found to be the most appropriate was a conventional tail or T-tail plane with high or low wings and a puller motor configuration. The wings would have to be split into two parts in order to fit into the assembly box and we chose a tail dragger configuration for the landing gear.

1.2. Overview of Preliminary Design Phase

In the Preliminary Design Phase, analyses of previously selected designs, and further analysis were used to investigate the optimum final design. Assembly of the aircraft was further investigated; insuring components of the aircraft would easily fit into the 4X2X1 foot box. Wing design was considered next, with a rectangular wing planform being chosen for purpose of simplicity in construction and modeling. An airfoil was selected to accurately match the aircraft requirements of high speed, low drag and heavy lifting. A SD6060 airfoil was ultimately chosen to fit the aircraft constraints. Drag and performance of the preferred configuration were evaluated. Power plant and structural analyses were also performed.

1.2.1. Preliminary Design Considerations

Numerous assembly and construction methods were considered for each design configuration. Design considerations for the wing consisted of three different airfoils that fit the mission configurations. The fuselage configuration was evaluated on the basis of cost, weight and complexity. The tail considerations were between conventional and T-tail. The Power plant configurations considered included brushed motors from Graupner and Astroflight and different combinations of gear ratios, propellers, and battery pack sizes.

1.2.2. Preliminary Design Results

Final decisions were made on the assembly methods and the configurations of the wings, fuselage, and tail. Estimation of the performance gave suitable results to proceed into the detail design. A final groundwork for aircraft design was laid down. A curved, "fish" like airframe that features a gradually tapering cross-section was chosen to lower base drag on the airframe. A low drag, high lift airfoil was chosen, along with a power plant and propeller choice.

1.3. Overview of Detailed Design Phase

A final design was decided on for the aircraft configuration. To do this, a performance evaluation was carried out. Component selection and system layout was also completed. A Final Rated Aircraft Cost was determined, which was similar to what was predicted during the conceptual and preliminary design phase due to the use of fewer batteries than anticipated.

1.3.1. Detailed Design Considerations

Aircraft sizing was finalized, and performance goals were either met or succeeded. An electric motor and battery choice and configuration were finalized. Material choices were finalized, and proof of concept models were constructed. A review of the final aircraft configuration was conducted to insure the aircraft design was of credible and sensible design. Radios, servos and other related equipment was also investigated and chosen for the design. A water dropping system was similarly investigated.

1.3.2. Detailed Design Results

The detailed design resulted from extensive work during the Conceptual and Preliminary Design. Aircraft design and performance figures were calculated and finalized. The airplane was evaluated to be stable during take off, flight and landing. Take-off distances and water dropping performance characteristics were also calculated and defined. Also a manufacturing plan and schedule were created and evaluated.

1.4. Overview of Manufacturing Phase

The manufacturing phase consisted of schedule management, materials choices, materials testing and final vehicle configurations. Materials that were considered for vehicle construction for major components included carbon fiber, fiberglass, kevlar, balsa wood, spruce, monokote, aluminum, and plastic, and steel. The materials were rated for each component by using Figures of Merit (FOM).

1.4.1. Manufacturing Phase Considerations

The final vehicle was constructed primarily from composite materials. This resulted in a strong, stiff and lightweight vehicle structure. Composites materials also offered significant vehicle protection over that of standard materials in terms of crash protection and withstanding damage. A review of the final vehicle construction was conducted, and parts and materials were requisitioned for eventual construction for the flight vehicle.

1.4.2. Manufacturing Phase Conclusions

Manufacturing was conducted during the 1st quarter of 2004. The fuselage was constructed first, then the wings as they were most mission critical. Furthermore, most of the vehicle was constructed in house, with only the necessary items such as batteries, motor, radio and accessories and landing gear being commercially produced items. Final vehicle, electrical and propulsive integration happened over the late part of march and early April. First flight was expected to be April 3, 2004.

1.5. Testing Phase

Numerous component and subcomponent tests were conducted. One of the primary tests was that of the water release system. Times obtained from this dictated much of the aircraft speed over the course. Various material and structure tests were also conducted, insuring that materials would hold up to flight and landing loads. The aircraft was also flight tested, to insure controllability and verify calculated values.

2. Management Summary

The initial Design Build Fly team meeting had a turnout 22 people: 1 faculty advisor, and 12 Juniors, 5 Sophomores and 3 Freshman. It was held in late September 2003, and covered the rules of the competition, mission parameters, and expectations for each member. Purvi Dave was selected as Project Manager. Subsequently, three sub teams - Aerodynamic, Propulsion and Structures were created. More sub teams were considered, but was decided against due to advice from previous years participants that a significant drop off in member participation would occur. Three teams provided an effective work breakup of the design and testing of the airplane. The Aerodynamics team would be in charge of Aeronautical aspects of the vehicle. The Propulsion team would be in charge of all the propulsive and electrical aspects of the aircraft. Finally, the Structures team was responsible for structure design and construction. Individuals were free to choose which team to be on.

2.1. Personal Upkeep and Team Architecture

Over the course of the design phase, significant dropouts on all 3 teams occurred. Persons left for varied reasons with the greatest being apathy of interest, grades and scheduling conflicts. Efforts were attempted to retain as many persons as possible, but largely unsuccessful. By Jan 1st, 2004 the team had stabilized to a core group of 6 people, of 4 Juniors, 1 Sophomore and 1 Freshman. Figure 2.1 illustrates the team architecture and shows team affiliations.

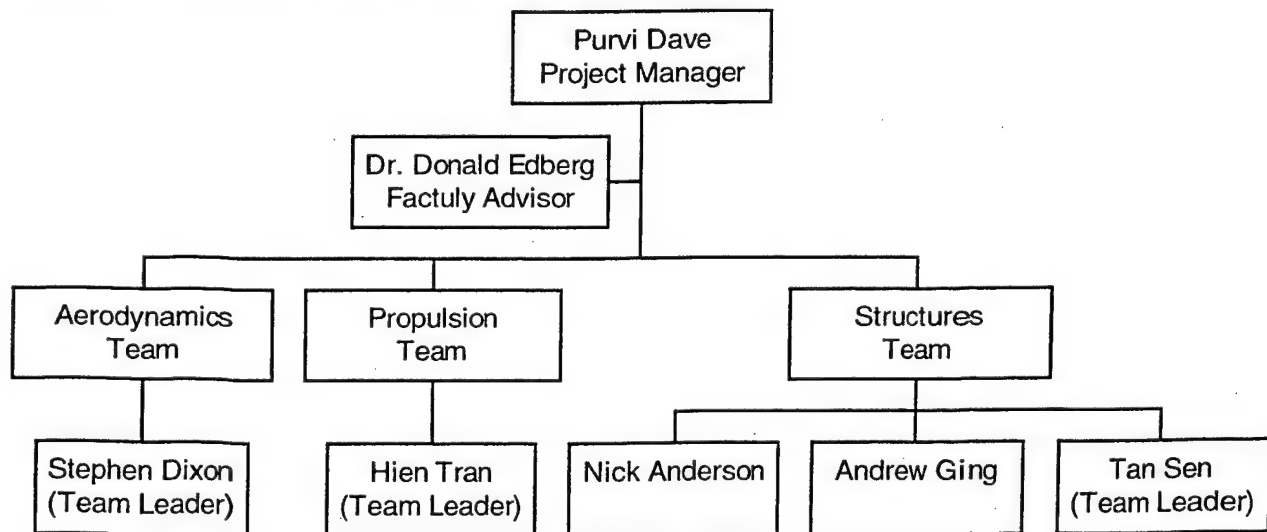


Figure 2-1 Team Architecture

2.1.1. Project Manager

The project manager was in charge of the entire Design Build Fly effort, schedule management and team upkeep. The project manager also acted as the lead fundraising contact, treasurer and organizer of design meetings and construction meetings.

2.1.2. Aerodynamics Team

The Aerodynamics team was responsible for all aerodynamic aspects of the airplane, throughout design, construction and flight-testing, along with establishing stability and performance expectations.

2.1.3. Propulsion Team

The propulsion team was responsible for all propulsive and power aspects of the vehicle. Further responsibilities included dynamic testing of the propulsion system and generation of power curves regarding motor performance.

2.1.4. Structures Team

The structures team was responsible for structural design and fabrication of the flight vehicle. Further responsibilities included evaluations of different materials, along with strength testing and modeling of aircraft structures. The structures team was in charge of manufacturing the flight vehicle, and final vehicle integration. The structures team was also in charge of flight-testing and assessment of the final completed flight vehicle.

2.1.5. Team Leaders

Team leaders were responsible for the individual leadership of their respective teams. Responsibilities included leading test and evaluation sessions for specific design issues, fabrication of vehicle parts, if applicable and being accountable for their specific teams area of responsibility.

2.2. Supplementary Positions

A number of supplementary teams and positions, non-related to specified design architecture were also present.

2.2.1. Drawing/Drafting Team

The Drawing/Drafting was responsible for developing and rendering the final vehicle configuration into CAD drawings. Responsibilities also included supplementing figures, tables graphs and the drawing package for the report.

2.2.2. Web Design Position

The Web Design position was responsible for developing, implementing and maintaining a website for the Design Build Fly Team. Responsibilities included creating and updating a dynamic website, web based calendar for team meetings, a picture gallery, and a page displaying the sponsors for the team. The Web Design position was also in charge of all promotional aspects of the team, for both public and peer review, and sponsorship awareness. The page is located at <http://www.calpolydbf.com>

2.2.3. Travel and Logistics Team

The Travel and Logistics team was responsible for arranging the travel and logistical aspects of the final fly-off. Responsibilities included planning team itineraries according to the most opportune schedule and price, contacting applicable travel companies for educational and group discounts, and purchasing arrangements. The travel and logistics team was also in charge of requesting money from different administrative funds within the university for group travel reimbursement. Travel and logistics also designed, built and coordinated shipping of the flight vehicle and support equipment.

2.3. Management Timeline

A timeline was developed at the start of the project. The timeline continually evolved throughout the design process, as differing ideas emerged on design and manufacturing. The Conceptual Design Phase lasted from September to the end of November. The Preliminary Design Phase lasted from December to January, and the Detailed Design Phase lasted from January to February. A graphical view of the timeline is contained in Figure 2.3. Green lines indicate predicated schedule, purple lines indicate actual schedule.

Timeline	September	October	November	December	January	February	March	April
Team Creation								
Conceptual Design Phase								
Design Matrix								
Design Analysis								
Mission Analysis								
Cost Analysis								
Preliminary Design Phase								
Proof of Concept Testing								
Vehicle Sizing								
Performance Analysis								
RAC Analysis								
Real Cost Analysis								
Vehicle Construction								
Preliminary Design Review								
Detailed Design Phase								
Fuselage Molding Samples								
Wing Lay Up Testing								
Honeycomb Lay Up								
Motor Testing								
Ground/Mockup Testing								
Final Design Review								
Manufacturing Phase								
Fuselage Lay Up								
Wing Lay Up								
Control Surfaces Lay Up								
Control Intergration								
Propulsion Intergration								
Overall Vehicle Intergration								
Flight Vehicle Testing								
Contest Logistical Support								
Design Report								

2.4. Personal Assignment Areas

Figure 2.4 list number of design personnel and assignment areas. This figure summarizes the major design phases and each member's contribution to those phases. A rating of 5 indicates 100% of design time devoted to a given phase and a rating of 0 indicates no involvement.

	Purvi Dave	Stephen Dixon	Hien Tran	Tan Sen	Nick Anderson	Andrew Ging	Alberto Santiago
3. Conceptual Design							
3.1 Mission Objectives	5	0	0	3	5	0	0
3.2 Aircraft Requirements	3	5	1	4	5	2	0
3.3 Mission Analysis and Modeling	1	5	1	0	2	0	0
3.3.1 Drag and Aircraft weight	1	5	1	0	0	0	0
3.3.2 Takeoff, Landing	0	5	1	0	0	0	0
3.3.3 Descend and Steady-level Flight	0	5	0	0	0	0	0
4. Preliminary Design							
4.1 Investigate Design Parameter and Trade-offs	2	4	3	4	4	4	0
4.2 Review and Develop Optimal Figures	3	3	3	3	2	3	0
4.2.1 Weight, Lift, Drag, Thrust Approximation	2	5	3	3	2	4	0
4.2.2 Stability Calculations	0	0	0	0	0	0	5
4.2.3 Takeoff, Landing, Turning, Flight analysis	0	5	3	3	2	4	0
5. Final Design							
5.1 Component Selection	2	5	4	4	5	4	0
5.1.1 Wing (Airfoil, Flaps, ailerons, etc.)	0	5	2	3	5	3	0
5.1.2 Propulsion (Motor, Battery, Prop)	1	0	3	0	2	5	0
5.1.3 Structural Design	0	4	3	5	5	4	0
5.1.4 Water Tank Configuration	2	4	3	4	4	0	0
5.2 Final Aircraft Geometry/Weight and Balance	3	5	4	4	5	5	0
6. Manufacturing							
6.1 Manufacturing Process Selection	3	4	2	4	5	4	0
6.2 Detail Manufacturing Plan	4	4	3	4	5	4	0
7. Drafting Package	0	5	0	0	0	0	0

Figure 2.4

3. Conceptual Design

The conceptual design phase was an analysis of the mission requirements and specific design considerations, which would result in the most competitive design for both mission types. A number of alternative designs tailored to each mission were also evaluated and considered for their individual figures of merits. Alternative designs considerations included the use of non-conventional vehicle designs and alternative static stability devices. Concurrently, tradeoffs between the size of the vehicle's fuselage, wingspan and power plant were primarily investigated.

3.1. Problem Statement

The performance of an aircraft in the competition is based on the total score. The total score consists of three important criteria - written report score, flight score and rated aircraft cost (RAC). Total Score of the competition is calculated as follows:

$$\text{Total Score} = \frac{\text{Total Flight Score} \times \text{Report Score}}{\text{Rated Aircraft Cost}}$$

3.2. Mission Requirements

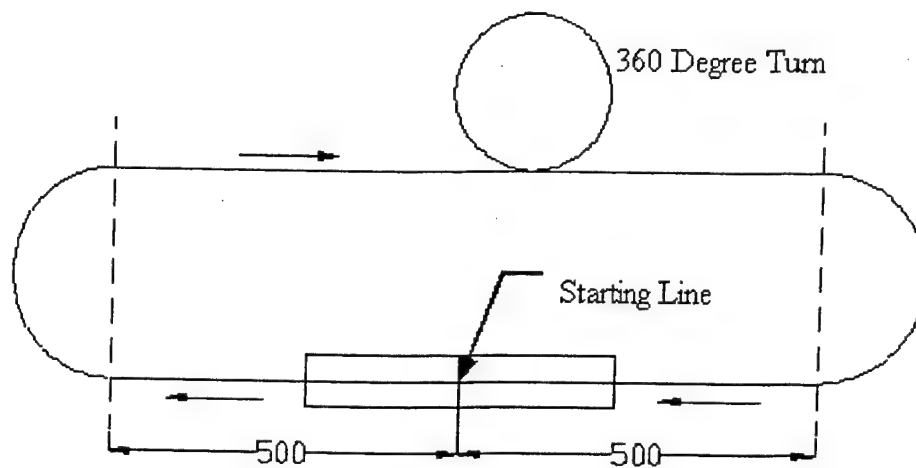
The two possible competition missions were stated to be "Fire Fight" and "Ferry". Each mission had a different degree of difficulty factor. Each mission flown would be scored differently. The Fire Fight mission was evaluated as follows:

$$\text{Mission Score} = \frac{\text{Difficulty Factor (2)} \times \text{Pounds Water Dropped}}{\text{Mission Time}}$$

And the Ferry mission was:

$$\text{Mission Score} = \frac{\text{Difficulty Factor (1)}}{\text{Mission Time}}$$

As illustrated in Figure 3.2, the missions would be flown on a specified course to compete toward **Total Flight Score**.



Course Layout
Shown to Scale

Figure 3.2

3.2.1. Aircraft Sizing and Assembly

Mission requirements stated that the aircraft must fully fit into a 4' x 2 x 1' box. This dictated major conceptual design concerns as to how the flight vehicle would fit into this box, and still meet the required mission parameters.

3.2.2. Takeoff Distance Rate

For each mission, there is a maximum takeoff distance of 150 feet. If this distance is not met, the mission will not be counted as an official mission.

3.2.3. Fire Fight Mission

For this mission, the aircraft must take off with a payload of water, complete a specified lap while dropping the water, land, reload, takeoff, complete a specified lap while dropping the water and land. The water must be dumped during the downwind leg, and exit through an orifice that is no larger than .5 inches. The maximum amount of water that can be carried is 4 liters but there is no minimum requirement for the amount of water carried.

3.2.4. Ferry Mission

For this mission, the aircraft must take off with no water payload; fly 4 complete laps and land.

3.3. Assumptions

To get a logical idea of the total score many assumptions were made. The assumptions were based on the calculations and some experienced students. The basic assumptions in the beginning of the designing stage included of estimated take off weight, estimated cruising speed, initial size configuration, RAC values , propulsion estimations and a study of trade-offs between two mission flights.

3.3.1. Estimated Take-off Weight

The estimated take-off weight of the aircraft included the weight of the battery, engine weight and the weight of the structure. The maximum battery weight possible was 5 pounds. Assuming to use all 5 pounds of the battery, the structure weight from last year's knowledge was taken to be 6 pounds and the weight of the engine was approximately assumed to be 2 pounds. Therefore, the total estimated aircraft take-off weight without any payload was 13 pounds. Going through more analysis, helped in reduction of the battery weight from 5 pounds to 3 pounds, Thereby, giving the final value of empty take-off weight to be 11 lbs. Including the payload of a maximum 4 liters (~9 pounds) of water gave the maximum take-off weight to be approximately 20 pounds.

3.3.2. Estimated Cruising Speed

The cruising speed value was based on the estimation of the power available from the motor to be used and the prop size. The estimation used was 100ft/s, also based on the experience from last year's participation in the competition using a similar motor, aircraft size and prop diameter.

3.3.3. Rated Aircraft Cost (RAC)

The rated aircraft cost was one of the most important factors that contributed to the total score in the competition. Since it was also a factor that can be manipulated and controlled, there were different possible RAC values that could be used for higher score. It was learned during the conceptual stage that lower the RAC, higher the total score would be. The governing equation for the RAC is

$$\text{RAC}, \$ = (A * \text{MEW} + B * \text{REP} + C * \text{MFHR}) / 1000$$

Where A = \$300

B = \$1500

C = \$20/hour

MEW = Manufacturers Cost Multiplier

REP = Rated Engine Power

MFHR = Manufacturing Man Hours

3.3.4. Figure of Merits (FOM)

For Conceptual Design evaluating purposes, a Figure of Merit was assigned to each different characteristic for a particular design configuration. A value of 0 was assigned if a particular characteristic was not applicable to that specific design. A value of 1 was assigned if the design characteristic was not well suited, a value of 2 if the characteristic was acceptable and a value of 3 if the characteristic was good for the design characteristic.

3.3.5. Propulsion

In the conceptual phase, 2 possible propulsive systems for the aircraft were considered; propeller and ducted fan. Single units were only considered, as the added cost, weight and complexity for systems containing more than 1 motor was immediately deemed to be not worth it. Figure 3.3.4 illustrates the different figure of merits for designs considered:

Figure of Merit (FOM) Motor Configuration						
Configuration	Capability	Weight	Complexity	Cost	RAC	Average
Propeller Puller	3	3	3	2	3	2.8
Propeller Pusher	3	3	2	2	3	2.6
Ducted Fan	2	2	1	2	3	2

Figure 3.3.4

The puller configuration would be suitable for most design configurations, and was used as the standard to evaluate other configurations. The pusher configuration created problems during rotation for takeoff, along with shifting the aircrafts CG too far aft. The ducted fan configuration was considered but the difficulty of placing the unit was high, along with the extra weight needed from the duct traveling the length of the unit and the associated ducting. The ducted fan was also a compromise between that of a propeller and turbojet for this size aircraft, and hence was a less efficient propulsive source than either a straight propeller or turbojet.

3.3.6. Design Configuration

4 different overall vehicle design configurations were considered; conventional, conventional with t-tail, conventional with h-tail, flying wing and biplane. Figure 3.3.5 illustrates their relative figure of merits:

Figure of Merit (FOM) Basic Design Configuration						
Configuration	Capability	Weight	Complexity	Cost	RAC	Average
Conventional	2	2	2	3	3	2.4
Conventional T-Tail	3	2	2	3	3	2.6
Conventional H-Tail	2	1	2	2	2	1.8
Flying Wing	2	3	2	3	3	2.6
Biplane	1	1	1	1	1	1

Figure 3.3.5

- 1.1 **Conventional:** Comparing this configuration to the above configurations of bi-plane and flying wing configurations, this configuration provides better performance. However more this design has more structural complexity than that of a flying wing. Taking into account the above factors, this configuration was given a FOM of 2.4.
- 1.2 **Conventional with T-tail:** The conventional T-tail design in the aircraft keeps the tail clear of the fuselage and wing wake. But there was a difficulty factor involved for mounting the horizontal surface of the tail to the vertical T-tail section. However the horizontal surfaces could be smaller in size, as they were more effective than that of conventional or h-tail. Therefore, this design configuration was given a FOM of 2.6.
- 1.3 **Conventional with H-Tail:** The twin fins in the conventional H-tail design was considered vulnerable to damage. The two vertical surfaces for the added to higher RAC, which in turn lowers the total score. As a result of the above criteria, this configuration was given a FOM of 1.8.
- 1.4 **Flying wing:** The flying wing configuration for the aircraft contributed to the design was favorable for a number of aircraft performance characteristics, those being less drag, less weight and higher lift. This in turn contributed to a smaller RAC. A drawback of this configuration was its static instability in the yawing axis. As a result, a flying wing is substantially more difficult to control versus that of a conventional design. However it excelled in other key areas, subsequently a FOM of 2.6 was assigned to this configuration.
- 1.5 **Bi-plane:** This configuration of the aircraft is effective only when the wingspan for an aircraft is constrained. The drawback of this configuration is the large amount of drag caused between the two wings. Considering the above factors, this configuration was given a FOM of 1.

3.3.7. Landing Gear Configuration

During the conceptual design phase 4 possibly landing gear designs were considered; bicycle with pogo tips, tricycle gear configuration, tail dragger configuration and landing skids. Figure 3.3.6 illustrates the relative Figure of Merits for each configuration:

Figure of Merit (FOM) Gear Configuration						
Configuration	Capability	Weight	Complexity	Cost	RAC	Average
Tricycle	3	2	2	2	2	2.2
Tail Dragger	3	3	2	3	3	2.8
Bicycle	2	1	1	3	2	1.8
Skids	1	3	3	2	3	2.4

Figure 3.3.6

The tricycle configuration would be suitable for most design configurations, however the addition of a forward landing gear would add drag, weight and complexity to the aircraft. Also the forward nose gear would need an additional servo for taxing purposes. Therefore the tricycle gear was not rated as highly as others. The tail dragger configuration would be suitable for most design configurations, and the need for only 2 large main wheels saved drag, weight and complexity. The tail dragger can be steered by connecting the rudder to the tail wheel, thus eliminating 1 extra servo needed for the tricycle configuration. The bicycle with pogo tips were not well suited for this aircraft, as this design is primarily for aircraft with larger wing aspect ratios, and the addition of pogo landing gear on the wings would add weight and complexity, especially if they were jettisoned after takeoff. However the bicycle configuration would result in less drag during flight as the wheels do not need to protrude from the fuselage as much as other configurations, and drop away pogo wheels would reduce drag and weight further. Skids were evaluated for their simplicity, low cost and reliability. However, takeoff issues dictated that this design was unfeasible, however simple and practical during landing.

3.3.8. Wing Configuration

During the conceptual design phase, 3 configurations of wing placement were evaluated; high wing placement, mid wing placement and low wing placement. Figure 3.5.7 illustrates their relative figure of merits:

Figure of Merit (FOM) Wing Configuration						
Configuration	Capability	Weight	Complexity	Cost	RAC	Average
High Wing	3	2	3	3	3	2.8
Low Wing	3	2	3	3	3	2.8
Mid Wing	2	2	2	3	3	2.4

Figure 3.5.7

The high wing design would be suitable for all most designs. High wing placement results in a more stable aircraft, easier attachment and higher lift. However, high wing placement necessitates the use of tricycle landing gear, and creates more drag than a low or mid wing placement. Low wing placement would be less suitable for most designs because of the issue of stability. However the low wing design would result in lower drag aircraft and hence a speedier plane. Also a low wing would allow a tail dragger

configuration which had the highest figure of merit in section 3.5.5 . Mid wing design would comprise a tradeoff between that of high and low wing and as a result has a lower figure of merit than that of a high or low configuration. However mid wing would still necessitate the use of tricycle landing gear. \

3.3.9. Estimated Total Score

Mission	A - Fire Fight	B - Ferry
Difficulty Factor	2.0	1
Total Laps	2	4
# of 180° turns/lap	2	2
Total # of 180° turns	4	8
# of 360° turns/lap	1	1
Total # of 360° turns	2	4
Payload	3 L H ₂ O	None
Particular Task	Drop up to 4 liters of water during the downwind leg of the course	Complete 4 laps as fast as possible.

Figure 3.3.9

Total Score predications in figure 3.3.9 were made based on the three types of missions using the assumed flight speeds and estimated RAC. Results are in Figure 3.6 through 3.9 below.

Mission A	2 laps / 4- 180° turns/ 2-360° turns		
Total Mission	Distance (ft)	Velocity (ft/s)	Time of Flight (s)
Take-off	150	42	14
Climb	150	60	8
180° turn	174	75	5
Straight Cruise	1000	88	15
360° turn	348	78	6
180° turn	174	75	5
Descent	150	50	8
Landing	150	42	10
Taxi	50	10	10
Restock	0	0	45
Take-off	150	42	14
Climb	150	60	8
180° turn	174	75	5
Straight Cruise	1000	88	15
360° turn	348	78	6
180° turn	174	75	5
Descent	150	50	8
Landing	150	42	10
Total Distance (ft)	4592		
Total Flight Time (secs)			207

Table 3.7

Mission B	2 laps / 4- 180° turns/ 2-360° turns		
Total Mission	Distance (ft)	Velocity (ft/s)	Time of Flight (s)
Take-off	150	42	14
Climb	150	60	8
180° turn	174	75	5
Straight Cruise	1000	88	15
360° turn	348	78	6
180° turn	174	75	5
Straight Cruise	1000	88	15
180° turn	174	75	5
360° turn	348	78	6
180° turn	174	75	5
Straight Cruise	1000	88	15
180° turn	174	75	5
360° turn	348	78	6
180° turn	174	75	5
Straight Cruise	1000	88	15
180° turn	174	75	5
Total Distance (ft)	6562		
Total Flight Time (sec)			135

Table 3.8

Total Score	
Total Time Mission A (min)	3.45
Total Time Mission B (min)	2.25
Difficulty Factor A	2
Difficulty Factor B	1
lbs water carried	7
Total Mission Score A	4.05
Total Mission Score B	0.444

Table 3.9

Mission Score for the A mission is many times larger than the Mission Score for the B mission, so Mission A holds a greater precedence for aircraft configuration and maximizing the mission score for A.

3.4. Conclusion for Conceptual Design Phase

The FOM during this phase helped to narrow down the options that could be used for the designing of the aircraft. The following conclusions were drawn from the analysis in this phase

Tail Configuration: Conventional tail with Ventral Fins

Aircraft Configuration: Conventional aircraft design

Missions: Mission A and B

Landing gear: Tail dragger

Propeller: Propeller with puller configuration

Wing: Low-wing

4. Preliminary Design

The preliminary design was based on the conceptual design ideas for the aircraft. The aim of this stage was to further develop a design that meets all the mission objectives. The major factors of this stage was to select the best airfoil, designing the most advantageous wing planform, and devise the most beneficial shape for the fuselage. Along with these factors the aircraft must still be able to fit in the assembly box, and be reassembled for flight in a short period of time. Design configurations were formulated around these factors.

4.1. Internal Configuration

Defining the internal configuration began with shaping the fuselage to hold a 3-4 liter water tank. As the flight score of the fire fight mission is determined by amount of water carried and the flight time, the shape and size of the fuselage was greatly influenced by the shape and volume of the water tank. Both the water tank and motor will run along transverse axis through the center of gravity (CG). This will ensure that there will be no CG travel after deployment of the payload. Other components such batteries, receiver, servos, speed control, landing gears, wing and empennage were also considered to assure no CG displacement after payload deployment.

Different configuration diagrams of the aircraft were drawn and evaluated.

A optimum configuration for the components and payload carried within the fuselage was created. It is as follows; the CG of the payload/water tank is placed on the CG of the fuselage. The low wing studied in the CDR was set under the payload with the quarter chord precisely over the CG. Motor placement put the thrust line directly through the CG. Batteries, receiver, and the speed control were placed in between the payload and the motor.

An Landing gear location was added to ensure structural support to the wing and fuselage. Some preliminary bulkheads were added for structure including the motor mount bulkhead. A horizontal and vertical stabilizer, with ventral fins was then added to the approximate size to stabilize the aircraft without increasing the RAC. The diagram was set as the target for the preliminary design and was employed in creating the optimal aircraft. Along with deciding the location of the internal components, each component was weighted to ensure there was no extreme nose-heavy or tail-heavy situation.

4.2. Assembly Configuration

All design configurations centered on being able to fit into the designated box. Without this, the plane would not be flight legal, and to assure a total maximum score, flying must be completed. A method of assembly was hence investigated and subsequently constructed for the chosen design configuration.

4.2.1. Wing Assembly Configuration

The span of the wing is 7 feet, much too long for the box. So, a two part plug-in type of wing would be considered necessary for construction. The plug-in type configuration would make it for easy assembly. A single spar would run the entire length of the wing. 2 shorter spars would run $\frac{2}{3}$ and $\frac{1}{3}$ respectively, each terminating in a false rib contained within the wing to adequately transfer loads to the strong skin of the wing.

4.2.2. Landing Gear Assembly Configuration

The main concern for the landing gear was to have clearance for the propeller and the ventral fins. Concurrently, the main landing gears must have a wide enough stance to distribute the force during landing. Evaluating different landing gear choices in the CDR lead to selecting a tail dragger landing gear configuration as the preferred design.

Retractable landing gear were considered, however when evaluated for design simplicity and RAC cost effectiveness, they were found to be much too complex and would greatly raise the RAC. Hence they were immediately discarded for design purposes. The solution was to use a plug-in type that would plug into the fuselage, and be securely fastened.

4.2.3. Empennage Assembly Configuration

The horizontal stabilizer and ventral fins would be built into the tail of the fuselage to assure adequate strength and reliability. The vertical stabilizer however must be made detachable to fit within the confines of the box. A plug in joint, with point attachment fasteners was considered, and judged to be adequate for design and flight purposes.

4.2.4. Fuselage Assembly Configuration

The length of the fuselage had to be less than 4 feet, unless a plug in or telescoping fuselage arrangement was used. This was judged to be too time cumbersome and complex, so a fuselage with an overall length of less than 4 feet was constrained in the design.

4.3. Preliminary Fuselage Design

A preliminary sketch of the fuselage was created in mechanical desktop. The illustration in the program gave the team an idea of the overall volume. The chosen fuselage shape gave the aircraft an ideal aerodynamic shape to serve the mission objectives, carrying a large payload at high speed. A number of trade studies resulted in the fuselage's final shape being chosen. Figure 4.3 describes these results.

Fuselage Design Configuration					
	Complexity	Aerodynamic	Weight	Strength	Average
Built up w/ straight sides	3	1	3	1	2.00
Built up w/ curved sides	1	2	2	2	1.75
Monocoque w/ straight sides	3	2	2	2	2.00
Monocoque w/ curved sides	2	3	2	3	2.50
Blended Wing and Body	2	3	2	2	2.25

Figure 4.3

Both built up and monocoque designs for the fuselage were considered, as was a blended wing and body shape. Both built up design configurations were judged to not have a high enough strength to weight ratio for our purposes, although they did have less complexity than a monocoque design. The built up configuration was also more applicable to be used on straight sided fuselages, unless a heavy fairing was carried to result in the curved shape. The blended wing and body configuration was deemed acceptable for strength to weight, complexity and aerodynamic aspects, but unknown flight qualities and stability throughout all axis prevented its usage. Monocoque was deemed to be the best configuration for the fuselage. Figures of Merit indicated that a monocoque fuselage with curved sides would result in a higher score, as the aerodynamical aspects were better, and flight loads would be better transferred through the curved composite structures than a straight sided design would.

4.3.1. Fuselage Preliminary Rendering

After the fuselage configuration was selected, a simple shape was drawn up that best fit the internal components carried and resulted in a clean, outer aerodynamic shell. Small wing stubs were also added to fuselages sides, to limit complexity in attaching the wing. Figure 4.3.1 gives a graphical representation of this complete configuration.

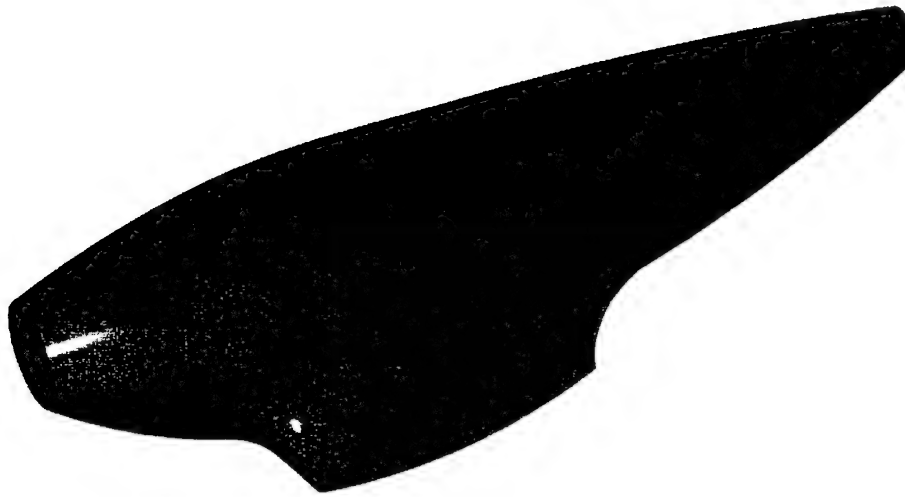


Figure 4.3.1

4.4. Wing

The CDR indicated that having a low or high wing would result in a design with optimum characteristics for both missions. However a low wing would result in less drag, and a faster airplane, at the cost of less stability than a high wing design. A low wing design was however chosen because it better fit the mission suitability requirements.

Also by having a low wing configuration, the design centered on blending the structure of wing attachment in with the structure of landing gear and fuselage to produce a strong unit. The wing's quarter chord will be run through the CG of the aircraft.

4.4.1. Airfoil Configuration

Four different airfoils were considered and investigated to meet with missions' objectives. The four airfoils were Eppler197, Eppler205, SD6060 and RG15. Figure 4.4.1 illustrates the Coefficient of Lift versus Angle of Attack for each airfoil.

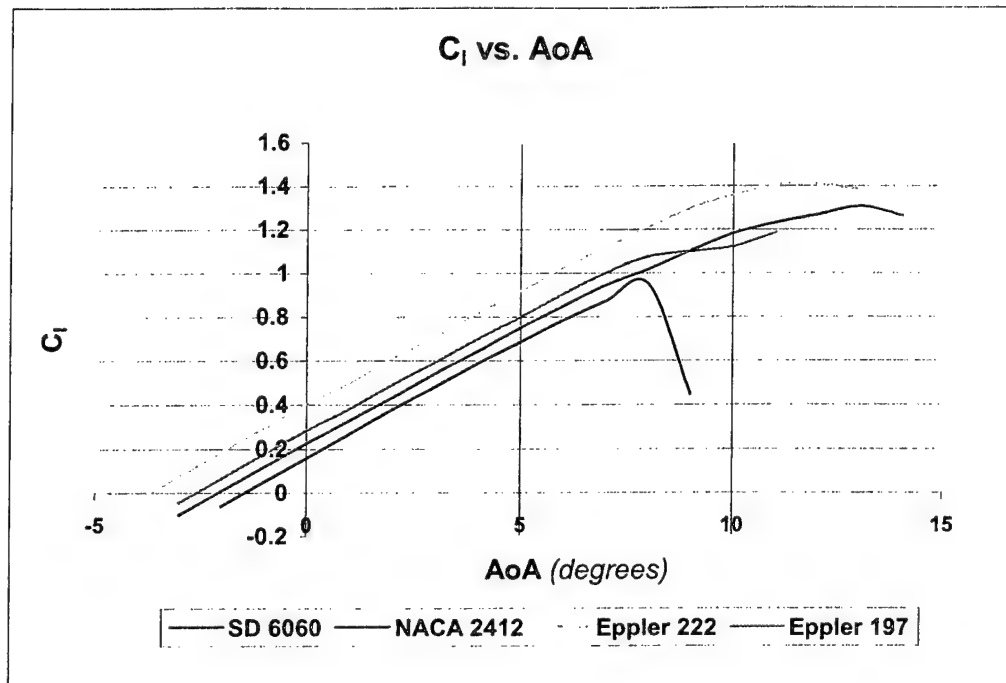


Figure 4.4.1

After evaluating the Coefficient of Lift versus Angle of Attack it was apparent that the Eppler series airfoils created the most lift. The SD6060 however had the least drag. The NACA 2412 was an approximation between the 2 different series. However, the SD6060 was further evaluated because of its low drag characteristics and was found to have adequate lift for takeoff and level and banked flight.

4.4.2. Airfoil Velocity

After choosing the airfoil, the SD6060 was further investigated to insure that it would meet all performance and flight characteristic goals. Hanley Innovation's VisualFoil was used to compute and graphically display airflow and pressure characteristics of the airfoil during flight. The SD6060 has excellent airflow characteristics, being laminar flow throughout most of its profile. Figure 4.4.2 illustrates the airflow surface velocity of the SD6060 airfoil at 0 AOA.

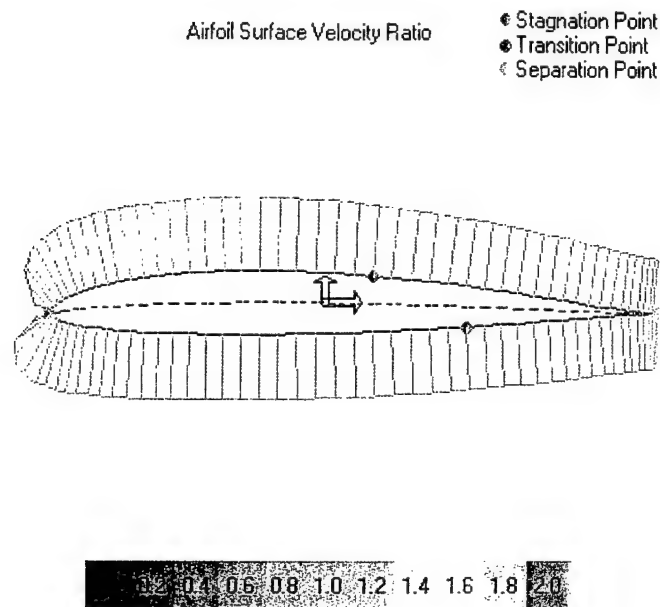


Figure 4.4.2

Figure 4.4.2.1 displays the velocity ratio versus the Chord Position over the entire airfoil.

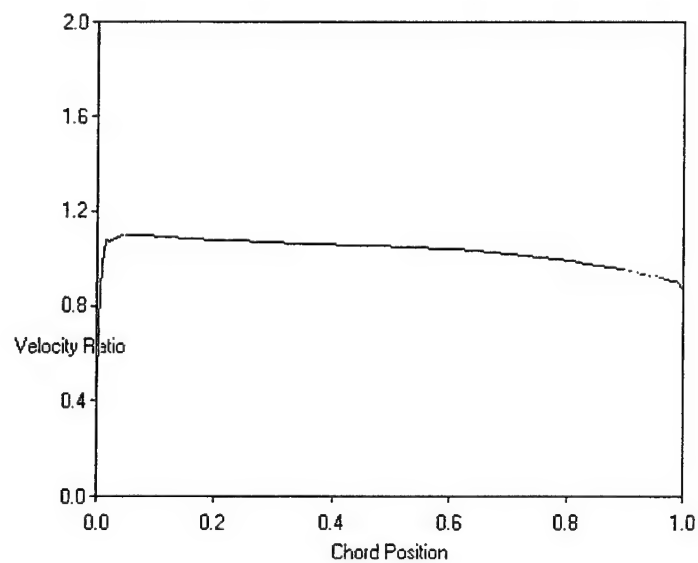


Figure 4.4.2.1

4.4.3. Airfoil Pressure Distribution

Furthermore, the pressure encountered by the airfoil was investigated to insure that drag was indeed as low as predicated. Pressure drag is a large component of the overall airfoil drag, and hence was selected

for further study to insure optimum characteristics. Figure 4.4.2 illustrates the pressure distribution over airfoil.

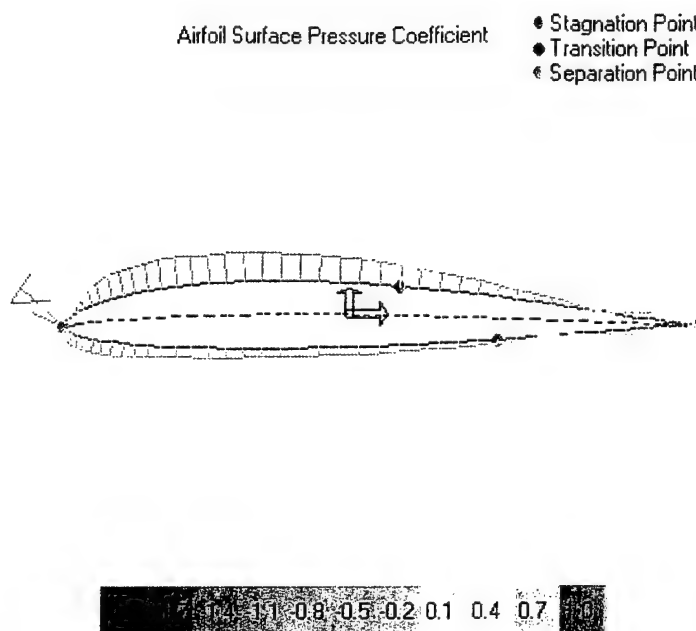


Figure 4.4.2

Figure 4.4.3.1 displays the velocity ratio versus the Chord Position over the entire airfoil.

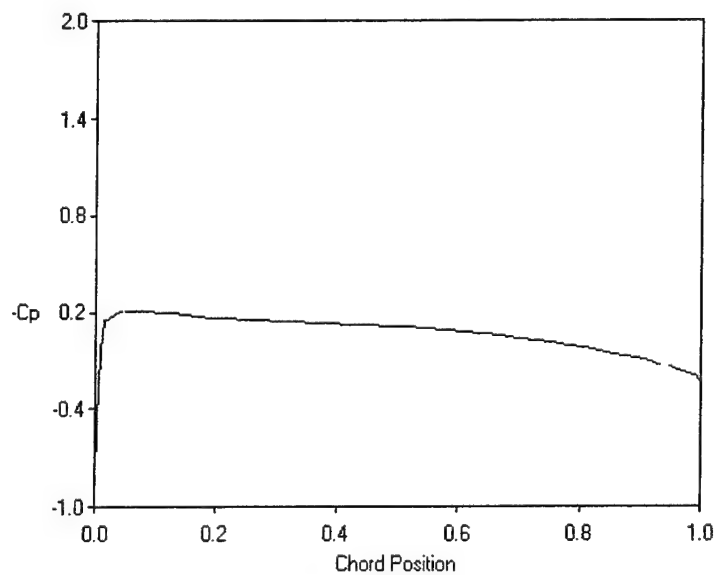


Figure 4.4.3.1

Figure 4.4.3.2 illustrates the lift versus drag for the SD6060 airfoil.

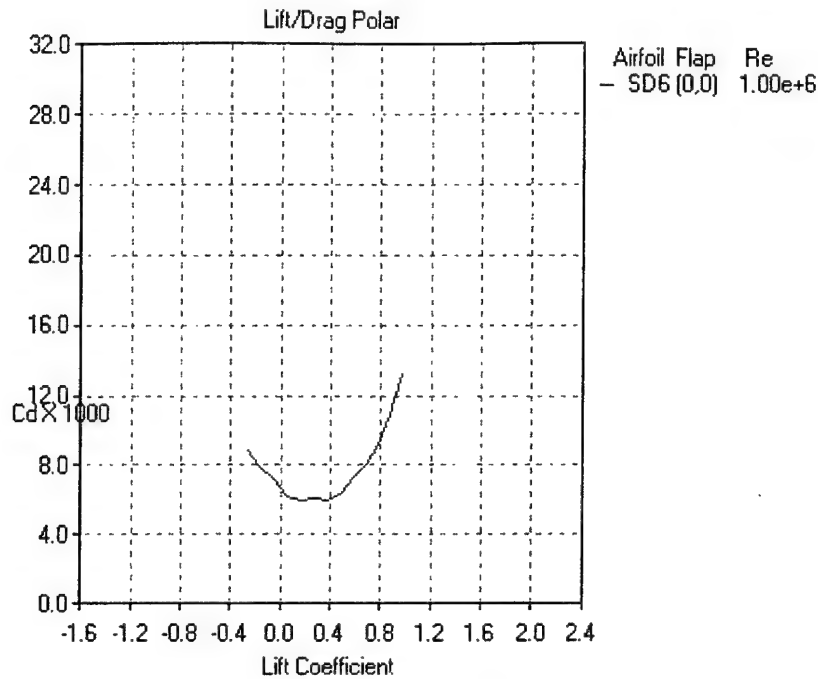


Figure 4.4.3.2

4.4.4. Wing Planform Shape

3 different wing planform shapes were evaluated. Figure 4.4.3 shows their relative figure of merits.

	Wing Planform				Average
	Drag	Weight	Complexity	Cost	
Rectangular	1	1	3	3	2
Tapered	2	2	2	2	2
Elliptical	3	2	1	1	1.75

Figure 4.4.3

A rectangular wing planform was decided upon due to simplicity of design, construction and modeling aspects.

4.4.5. Wing Configuration Summary

Rectangular plan form	
Planform area	7 ft ²
Wing span	7 ft
Chord Length	1 ft
Aspect Ratio	7

Figure 4.4.4

4.5. Tail Configuration

The particular tail design was made due to simplicity and strength. In earlier design, a conventional tail was considered. However, the tail volume coefficient was too low, more surface area was needed for stabilization of the aircraft. As a result, ventral fins were brought into the design, hence increasing the value of tail volume coefficient to meet stability and ratio requirements. Figure 4.5 illustrates the preliminary tail configuration with ventral fins.



Figure 4.5

4.6. Preliminary Propulsion System Configuration

Onsite consultation was held with Astroflight Incorporated staff at their design facility. We originally concluded that an Astroflight 60 or 90 would be required for the power levels we needed to adequately take off and fly.

4.6.1. Propulsion System Gearing Configuration

A gearbox was initially investigated, as this would allow for a larger prop, which would be more efficient than a smaller prop. However, after detailed calculations, and utilizing P Calc, it was determined that this

setup would require too large of a propeller to produce the thrust needed for takeoff in a short distance. An excessive number of NiCad cells would have been required to provide the necessary power to run the aircraft at the speeds desired while still keeping the diameter of the propeller down. Other alternatives would have been to find a gearbox with a lesser ratio, preferably from 1.5:1 to 2:1, or to eliminate the gearbox altogether and use the Cobalt 60 direct-drive.

Several factors went into making this decision. The "Superbox" recommended for the Astro Cobalt 60 motor weighs 2.5 ounces, which increases the Rated Aircraft Cost slightly, making direct-drive favorable. Additionally, a smaller gear ratio for the Cobalt 60 motor is no longer as readily available as the Superbox, and an ideal motor-propeller-battery pack setup was determined to be feasible for our R/C airplane.

From these possibilities an Astroflight Cobalt 60 direct-drive motor with an 14X8 APC or Bolly brand propeller was selected. Using 24 Sanyo SCR 2400 mAh Zapped NiCad cells would satisfy power requirements for this combination.

4.6.2. Preliminary Propulsion System Conclusions

Figure 4.7.2 illustrates the final preliminary propulsion system configuration.

Motor Configuration			
Motor	Astroflight Cobalt 60	Type of batteries	Sanyo SCR 2400 mAh Zapped NiCad
Prop	Bolly Carbon 14x 8	Max Motor Power	691 Watts
Speed Control	Astro 60 Amp	Max Load	30 amps
Number of batteries	24	Motor Weight	22 oz

Figure 4.6.2

5. Detailed Design

The Detailed Design Report was required before any manufacturing of flight vehicle parts could begin. Figure 5 illustrates the completed design.

Geometry			Weight Statement	
Length	3.33 ft		Airframe Weight	5.5 lbs.
Wingspan	7.00 ft		Radio Control System	1.3 lbs.
Height	1.00 ft		Motor Weight	1.2 lbs
Wing Area	7 ft ²		Payload Weight	7 lbs
Aspect Area	7		Battery Weight	3.0lbs
			Gross Weight	19.6 lbs
Control Volume			Power and Control Systems	
Performances				
C _{Lmax}	1.62		Radio	Futaba 9CA
(L/D) _{max}	15.4		Servos	6 HS-635 HB Hitec-High torque
R/C _{max}	26.35 ft/s		Battery Configuration	24 Sanyo SCR 2400 mAh Zapped NiCad
Take-off Distance:	Empty	Gross	Motor	Cobalt 60 Direct Drive
	46.2 ft	140 ft		
V _{max}	103 ft/s		Propeller	Bolly Carbon 14 x 8
V _{stall}	39.1 ft/s		Gear Ratio	1:1

Figure 5

5.1. Rated Aircraft Cost

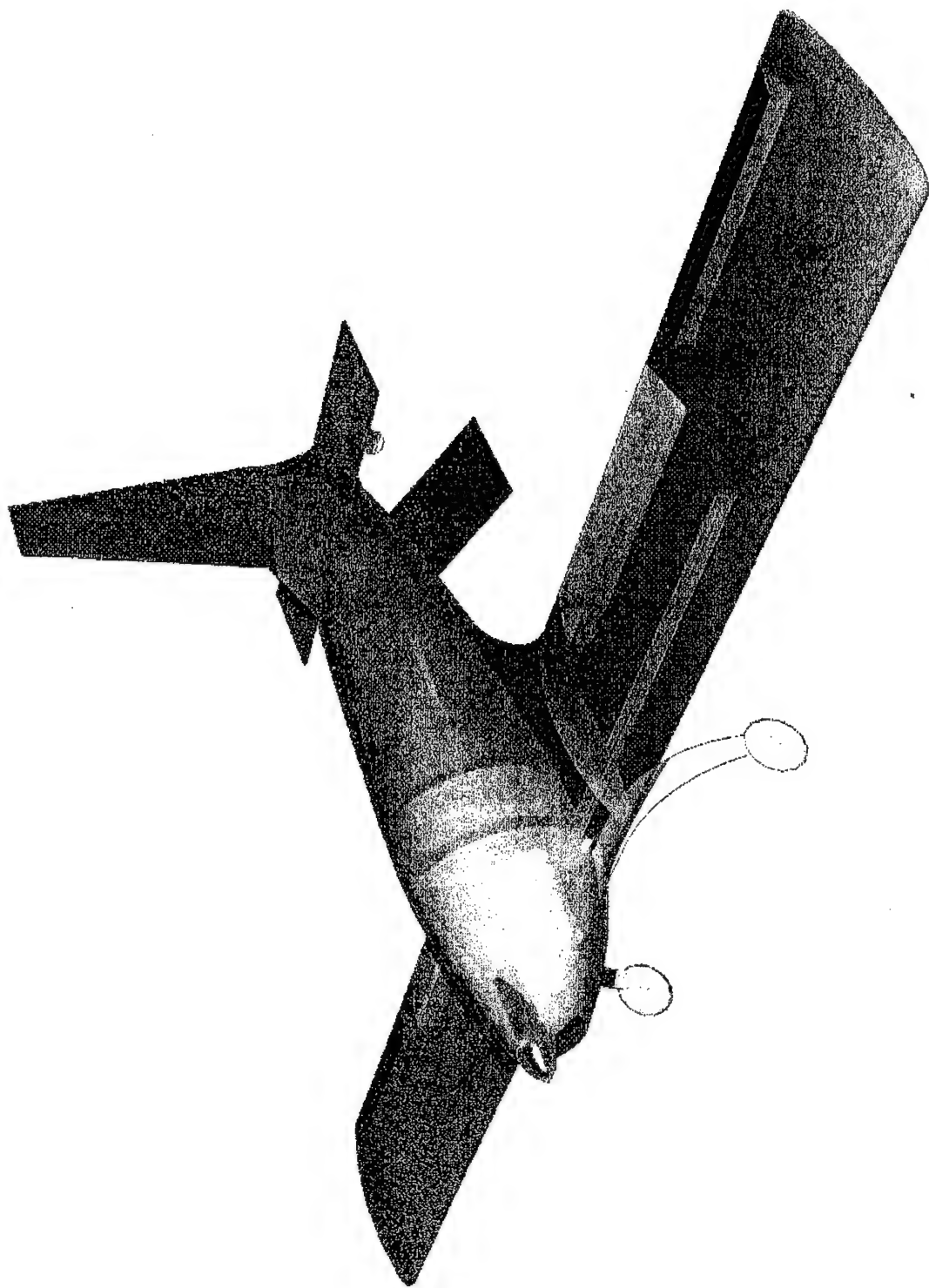
Final RAC is calculated to be 11.188. Figure 5.1 illustrates the final RAC as defined in the official rules.

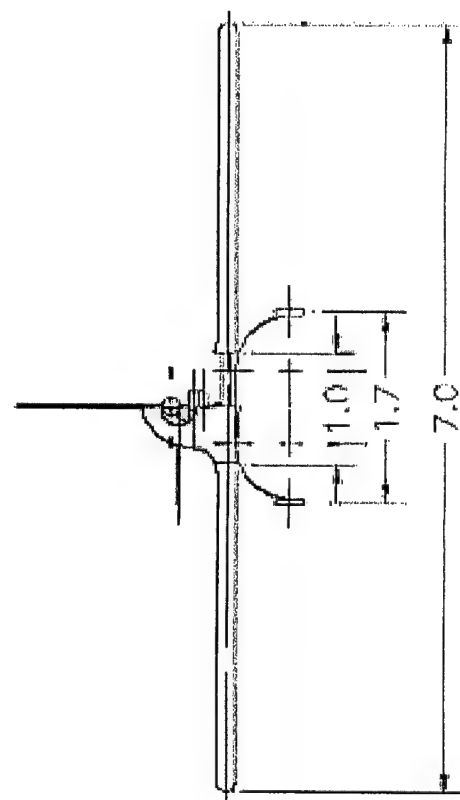
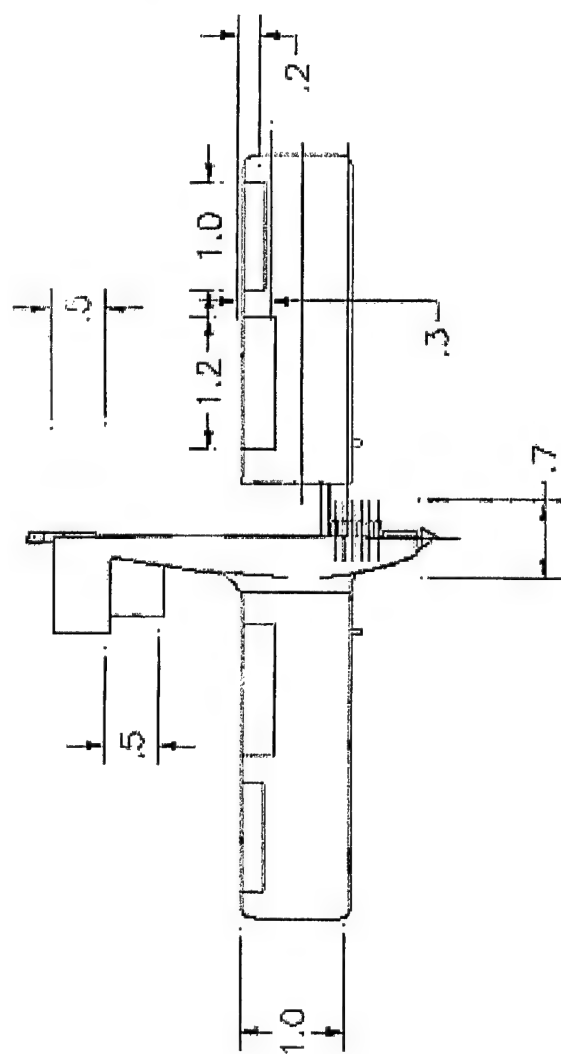
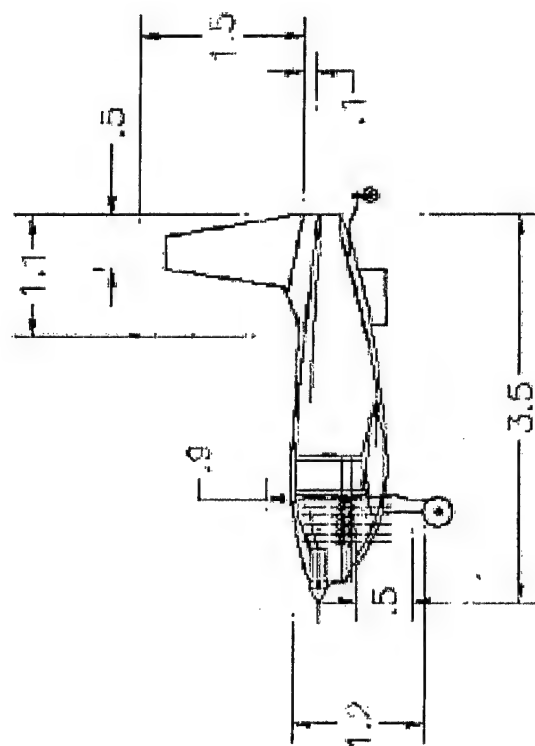
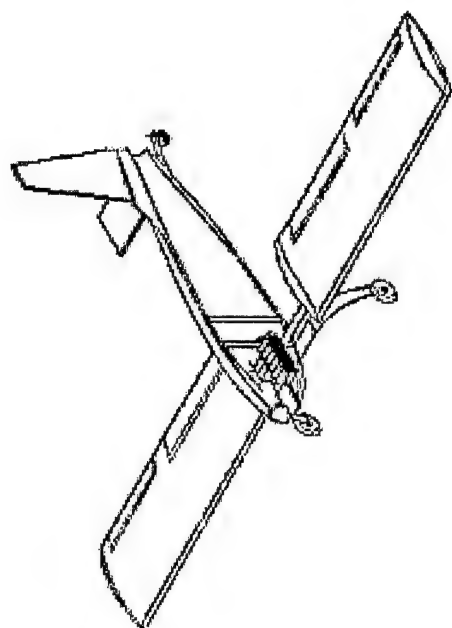
	RAC		11.188
MEW	Value	Cost	Multiplier
Total Weight	11	3300	\$ 300
REP	Value	Cost	Multiplier
(1+.25*(# engines-1)) x Total Battery Weight (lb)	3.2	4800	\$ 1500
MFHR	Value	Cost	Multiplier
Σ WBS hours	154.4	3088	\$ 20 / hr
MFHR - WBS	Value	Hours	Multiplier
1.0 Wings			
wing span (ft) x chord (ft) x number of wings	7	48	10 hr/ft ² Wing Span
ailerons + flaps	2	10	5 hr/control function multiplier
2.0 Fuselage			
Max length (ft) x Max Width (ft) x Max Height (ft)	2.64	26.4	10 hr/ft ³ max length
3.0 Empennage			
# of vertical-ac	1	10	10 hr/vertical-active control
# of vertical	2	10	5 hr/ vertical- non active control
of horizontal	1	10	10 hr/ horizontal surface
4.0 Flight Systems			
# of servos/control	8	40	5 hr/servo

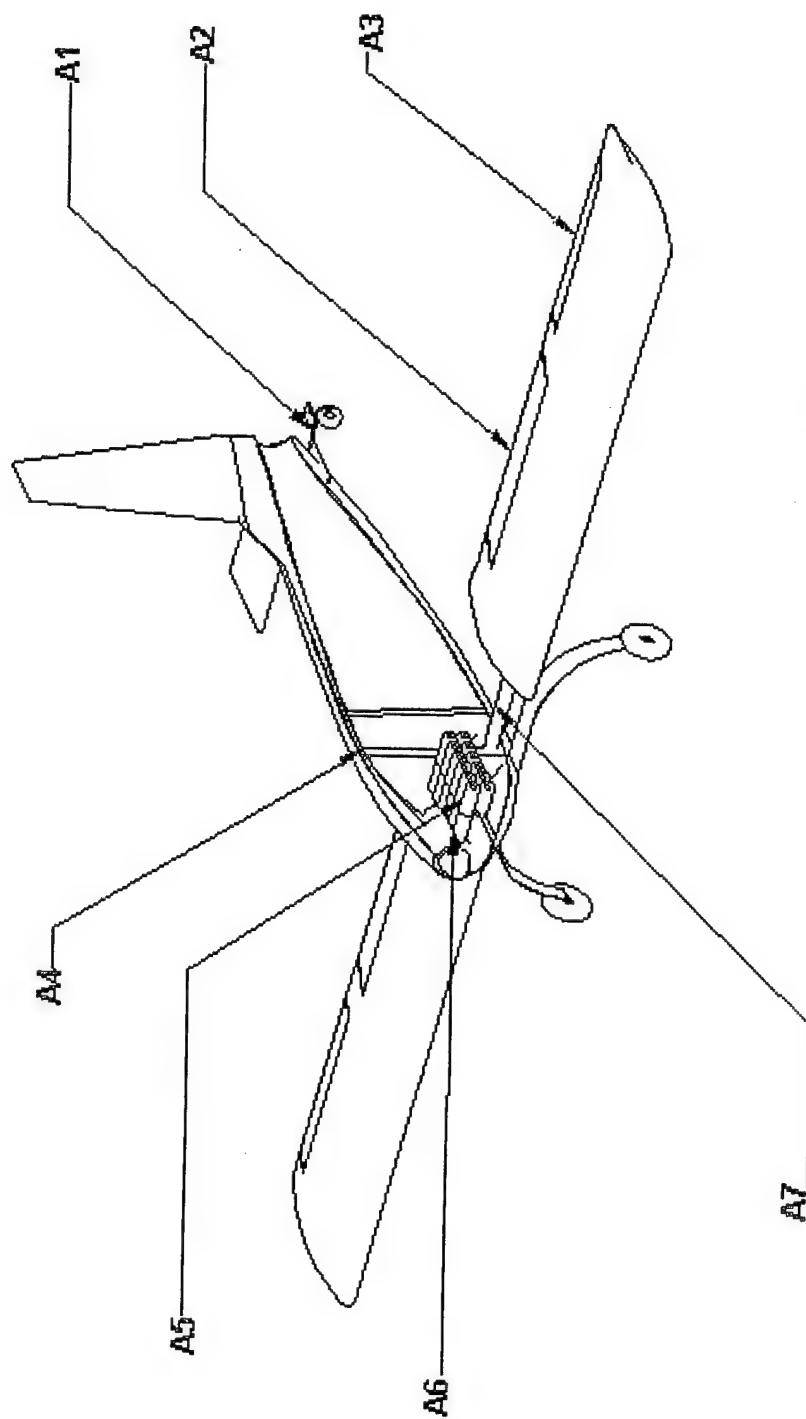
Figure 5.1

5.2. Detailed Aircraft Drawing

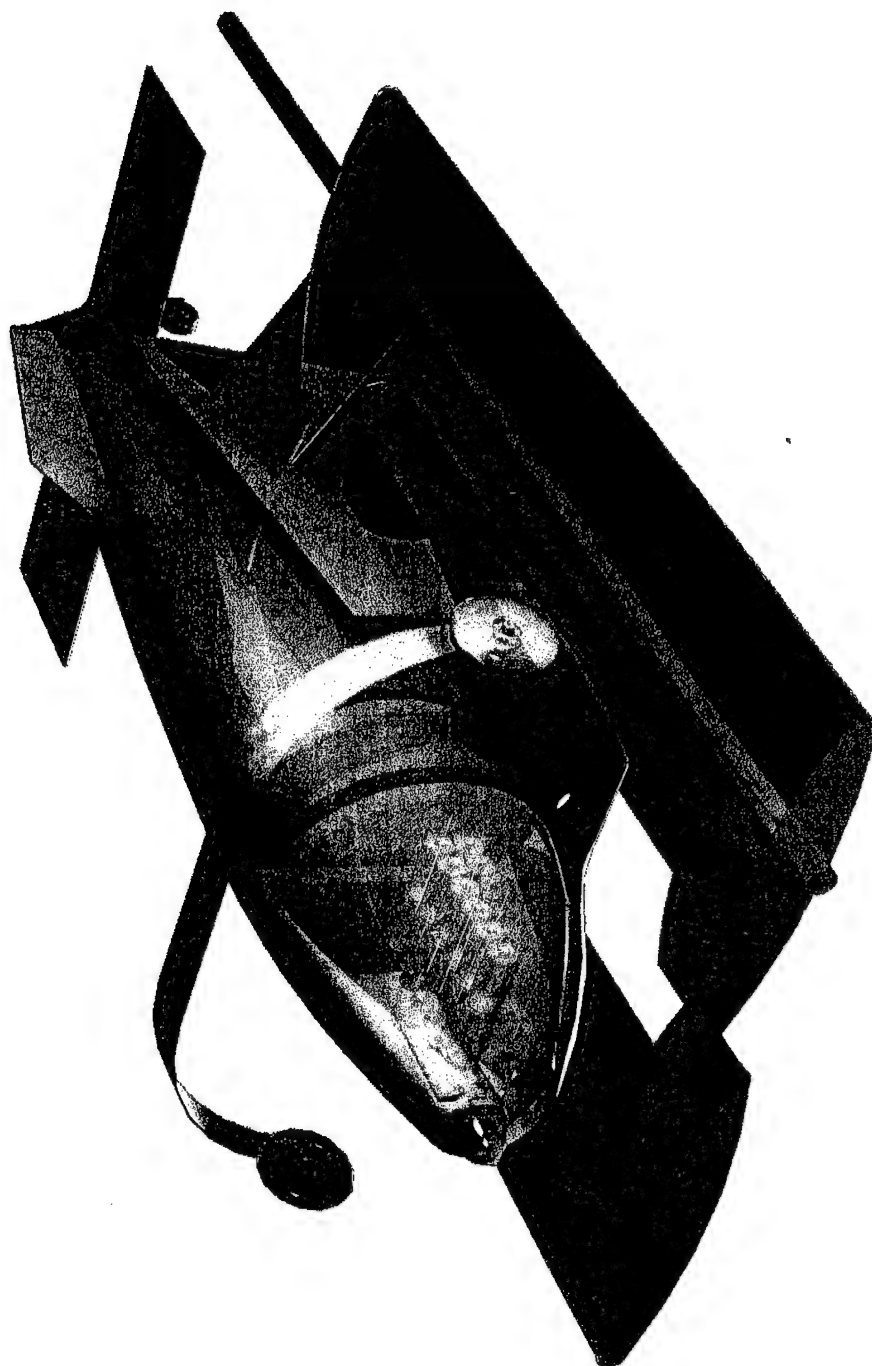
Attached is the drawing package for the completed design.







- A1: Tail Landing Gear
- A2: Flaps
- A3: Ailerons
- A4: Payload Tank
- A5: Batteries (24)
- A6: Electric Motor
- A7: Main Spar



6. Manufacturing Plan

Major flight vehicle manufacturing processes were decided upon by evaluating the possible material selections for each component. Each process was rated on a number scale in which high numbers were desirable characteristics and low numbers were undesirable characteristics. After the evaluation a manufacturing schedule was created.

6.1. Major Components

Major flight vehicle components were defined as the parts of the aircraft that needed to be fabricated by the group. Parts that were constructed by the team were the fuselage, wings, tail, horizontal stabilizers, ventral fins, bulkheads and other related flight structures.

6.2. Materials

Materials that were considered vehicle construction for major components included carbon fiber, fiberglass, aramid, balsa wood, spruce, monokote, aluminum, and plastic, and steel. The materials were rated for each component by using Figures of Merit (FOM).

6.3. Figures of Merit

Figures of Merit (FOM) were used to evaluate the different materials for relative strength, stiffness weight, price and ease of use. Figure 6.3 illustrates the various material choices that are possible.

6.3.1. Skill Levels

A scale ranging from 1-5 was used to express skills need to manufacture a specific component, with 5 being the easiest to manufacture and 1 being the hardest to manufacture.

6.3.2. Material Availability

A scale ranging from 1-5 was used to evaluate the availability of specific materials. A 5 was used when the material was easy to acquire and a 1 was used when then material was difficult to acquire.

6.3.3. Material Cost

A scale ranging from 1-5 was used to evaluate the cost of specific materials. A 5 was used when the material was least expensive per unit area, and 1 used when the material was most expensive per unit area.

6.3.4. Time Required

A scale ranging from 1-5 was used to evaluate the cost of specific materials. A 5 was used when the material was least time intensive to make, and 1 used when the material was the most time intensive to make.

6.3.5. Strength to Weight Ratio

A scale ranging from 1-5 was used to evaluate the strength to weight ratio of specific materials. A 5 was used when the material had the highest strength to weight ratio, and 1 used when the material had the lowest strength to weight ratio.

Aircraft Section	Material	Cost	Availability	Skill	Strength/Weight	Const. Time	Average
Fuselage Skin	Balsa sheet	3	5	2	3	3	3.2
	Carbon Fiber	3	5	3	5	4	4.0
	Kevlar	2	4	4	5	4	3.8
	Flex-core/Carbon Fiber	2	4	1	2	2	2.2
	Fiberglass	3	4	3	4	4	3.6
	Monokote	3	5	4	3	4	3.8
Airframe	End grain balsa	3	5	3	2	2	3
	Honeycomb/Carbon	2	4	5	5	4	4
	Plywood	3	5	3	3	2	3.2
	Coremat	1	3	3	4	3	2.8
	Baltek mat	2	4	3	4	3	3.2
	PVC Foam	3	5	4	3	3	3.6
Wing Skin	Monokote	3	5	4	3	4	3.8
	Carbon Fiber	3	5	5	5	4	4.4
	Fiberglass	3	4	3	4	4	3.6
	Balsa sheet	3	5	2	3	3	3.2
Wing Structure	Balsa	3	5	3	2	2	3
	Honeycomb/carbon	2	4	3	4	3	3.2
	Plywood	3	5	2	2	3	3
	Foam-core	3	5	3	4	4	3.8
Vertical Surface	Balsa/Sheet	3	5	2	4	3	3.4
	Balsa/Monokote	3	5	4	4	3	3.8
	Honeycomb/Carbon	3	4	5	5	4	4.2
Horizontal Surfaces	Balsa/Sheet	3	5	2	4	3	3.4
	Balsa/Monokote	3	5	4	4	3	3.8
	Honeycomb/Carbon	3	4	5	5	4	4.2
Water Tank	Manufactured Plastic	2	4	5	2	2	3
	Built in Carbon	3	2	3	5	4	3.4
Landing Gear	Carbon Fiber	2	4	4	5	3	3.6
	Carbon/Kevlar	2	3	4	3	3	3
	Manufactured Carbon	1	5	5	4	4	3.8
	Aluminum	3	5	4	3	4	3.8
	Steel	3	5	5	1	4	3.6
	Titanium	1	2	3	4	2	2.4
Wheels	Plastic	3	4	5	4	4	4
	Rubber	3	5	5	5	4	4.4

Figure 6.3

6.4. Manufacturing Schedule

The structures team was in charge of creating a schedule for manufacturing the completed design of the flight vehicle. Figure 6.4 provides a schedule of activity for proof of concept tests, support equipment construction and flight vehicle manufacturing

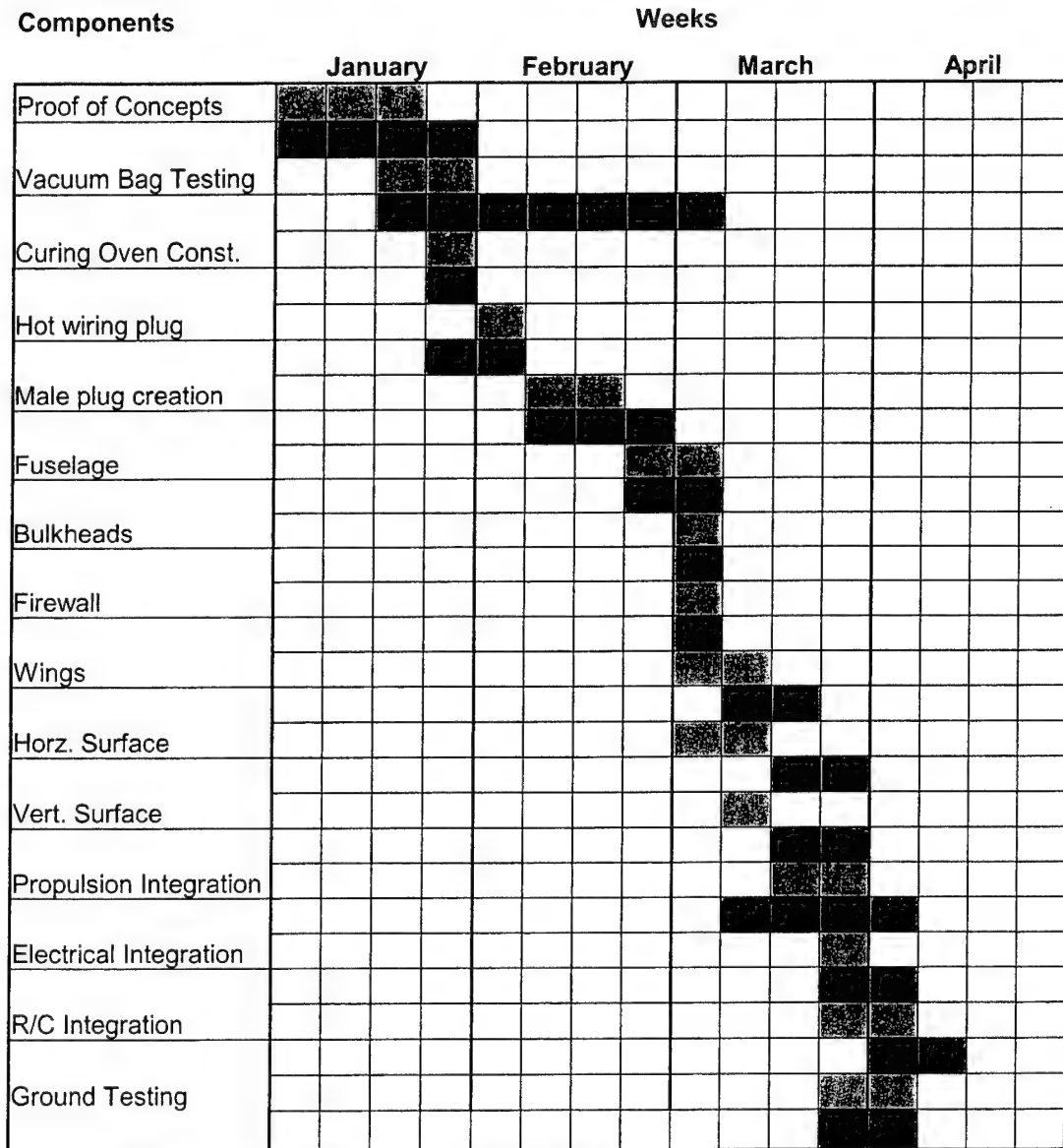


Figure 6.4

6.5. Manufacturing Process

Manufacturing and fabrication took place at the Advanced Vehicle Development at Cal Poly Pomona. The room was shared with other design groups and senior projects, but proved more than adequate for manufacturing purposes. Safety was maintained throughout the manufacturing process by use of proper safety gear as defined by the warning labels on items, and the use of Material Safety Data Sheets (MSDS) for specific materials.

Material choices as defined above lead to different manufacturing processes. The use of widespread composite structures necessitated the need for a vacuum bagging set up, along with a curing oven. The vacuum bagging was used to improve overall laminate strength, by insuring the plies of material were compacted together, and that excess epoxy resin was removed from the part to insure the proper resin to fiber ratio was achieved for all components. All flight vehicle parts were vacuum bagged during lay up and curing.

A curing oven was constructed to allow for all parts to be heated during the cure. This speed up cure time, improved overall strength of the completed part, and raised the Glass Transition Temp (GRT) of the completed component. The maximum temperature allowed for the epoxy resin was 180 F, however parts were only cured to 160 F. Parts containing pink foam (such as wing cores and the fuselage lay-up) were not heated significantly (besides natural exotherming from the epoxy) as the pink foam would expand at different temperatures and affect the completed components size and shape.

6.5.1. Design of Fuselage Mold

During the CDR, PDR and DDR phases we intended to create the fuselage by using a female mold. This involved creating a full size plug of the fuselage, laying-up a female mold off of this plug, and then creating male parts. However once construction of the plug started we realized we would not have enough time to create a female mold, and then male parts. We considered the tradeoffs between a female mold, male mold and lost foam method, and decided a male mold would best fit our intended application and time requirements. A female mold would have simply taken too long, and we would have invested too much time, materials and money into a product that was intended to create multiple copies of the same part, when we only need one, or at most 2.

6.5.2. Construction of a Male Fuselage Plug

Four 4' x 4' x 2" sheets of 1.5 PCF pink housing insulation foam were epoxied together to create one large block of foam. This was subsequently cut in half to allow for a backup fuselage plug to be created in case of problems with the first plug. The block was then assembled on a stand, and hot wired to the correct shape, by way of 4 total cuts. The hotwired foam block was then sanded with a random orbit sander to the required profile. Once the correct profile was obtained, the pink foam was covered by a

thick layer of standard wall spackle. Once sanded this created a hard smooth layer over the entire surface. This layer was then covered in a layer of high solids liquid primer to insure maximum smoothness and evenness over the entire fuselage. At this point the fuselage plug was waxed repeatedly with a high temperature mold release wax, and buffed between each layer of wax. A final layer of Poly Vinyl Alcohol (PVA) was applied to insure smooth release.

6.5.3. Construction of Female Fuselage

Once the male plug was created, a female composite fuselage was molded off this plug. A parting board was used to insure accurate lines on the mold part, along with a flat flange to allow for the two halves to attach. All fabric going onto the mold was "pre-bagged". In essence the material was saturated with epoxy, then vacuum bagged for 20 minutes to insure resin removal from the cloth. Then the fabric was placed onto the fuselage, and bagged again to insure maximum laminate strength and adhesion between plies.

6.5.3.1 Materials of Female Fuselage

The main structural component of the fuselage consisted of a solid matrix of Carbon Fiber and Epoxy. Aeropoxy PR2032 and PH3660 resin was used throughout the process for excellent wet out characteristics, low viscosity, excellent final strength and toughness properties, and has the ability to heat cure. Carbon Fiber was used throughout the fuselage for its excellent stiffness and strength to weight ratios. The double radius curves of the fuselage dictated that a flexible carbon fabric be chosen, so 3K 2x2 Twill 4.8 oz carbon fiber was used.

The bottom section of the fuselage was constructed of a layer of 3k 2x2 twill 4.8 oz carbon, then a layer of Plain Weave 4.9 oz Kevlar®¹ (Aramid) fabric, and a third layer of 3k 2x2 twill 4.8 oz carbon. This resulted in an extremely stiff, strong, tough and lightweight sandwich structure. The Kevlar®¹ fabric was used because of its excellent toughness, abrasion and ballistic resistance properties and vibration dampening characteristics. This sandwich structure resulted in a lower fuselage half that is extremely crash worthy, negating the need for a second, backup airframe to be constructed.

The top section of the fuselage was constructed of 2 layers of 3k 2x2 twill 4.8 oz carbon. This resulted in a stiff, strong and lightweight structure. Kevlar® was not used here, because the top half of the fuselage would not encounter the same loads as the bottom half would.

6.5.4. Construction of Foam Core Wings

Pre-cut SD6060 wing cores were obtained from a local vendor. The wings were then laid up with 3k 2x2 twill 4.8 oz carbon and Aeropoxy resin and vacuum bagged. Woven Dracon Peel Ply was used to insure maximum resin removal from the wings. A false rib was embedded in the wing at 1/3 and 2/3 of the wingspan. A .50 inch carbon fiber rod was then slid into precut core hole up to the false rib, with a .50" ID

¹ "Kevlar® is a registered trademark of E.I. du Pont De Nemours and Company."

carbon fiber tubing completing the rest of the spar length. Access slots were cut into the skin for servos, along with the control surfaces at the back of the wing.

6.5.5. Vertical and Horizontal Surfaces

Vertical and Horizontal surfaces were constructed of .25 " thick HRH-10 3 PCF Nomex, Phenolic coated, standard cell honeycomb with a skin of 3k 2x2 twill 4.8 oz carbon was added to each side, bagged at 10 in Hg/ 5 PSI to limit dimpling of the fabric into the honeycomb cells. The carbon fabric was also pre-bagged to limit resin collection inside the cells.

6.5.6. Landing Gear

The main landing gear was bought from Graphtec RC for time and construction reasons.

6.5.7. Bulkheads and Firewall

Bulkheads were constructed of .25 " thick HRH-10 3 PCF Nomex, Phenolic coated, standard cell honeycomb with a skin of 3k 2x2 twill 4.8 oz carbon added to each side. Bulkheads were then cut to shape to fit into the highly contoured fuselage, and bonded with a hand lay-up of resin and carbon. The firewall was constructed of .25 " thick HRH-10 3 PCF Nomex Phenolic standard cell honeycomb with a skin of 3k 2x2 twill 4.8 oz carbon and 2 layers of Plain Weave 4.9 oz Kevlar®¹ fabric. The kevlar was added to add additional impact resistance for the honeycomb laminate and dampen vibrations from the motor. The kevlar would also serve as to stop the motor from breaking through the firewall in case of crash.

6.5.8. Electronic Components and Water Dropping System

Batteries were mounted as far forward as possible for CG reasons and to limit the power loss from wiring. The receiver was mounted near the rear of the fuselage, to limit EMI interference from the speed controller and propulsion system. A external antenna was also needed as carbon fiber is conductive and blocks radio signals extremely well. Servos were tested before installation to insure proper operation. The water drop valve was placed into the bottom of the tank. A simple ball valve was used to open a .50" inch diameter exit orifice. The fuse was mounted in line with the battery wiring, attached to the side of the airframe in an easy to reach spot, in case replacement was needed.

^{1 2} "Kevlar® is a registered trademark of E.I. du Pont De Nemours and Company."

6.6. Conclusion of Manufacturing Phase

Installation of the electronic components and water dropping system marked the end of the manufacturing phase. The propulsion system and batteries were integrated into the completed structure, and were subsequently powered up to verify continuity throughout the system.

7. Overview of Flight Testing

3 methods of testing were carried out on the for the vehicle, both during design, construction and test flying.

7.1. Component and Materials Testing

Testing of various materials was conducted prior to manufacturing. Materials tested included shear, tensile and yield strength data on many of the materials expected for use in the plane. Furthermore, individual component testing was conducted once parts were constructed. This insured components constructed would withstand normal flight stress. A emphasis on testing to destruction was made on some parts, to adequately gauge how and at what stress components would fail.

7.2. Static and Ground Testing

Once the aircraft was into the integration stage, various ground and static tests were conducted to insure proper operation and reliability of the overall vehicle. Motor performance when mounted in the airframe was a key test, along with battery performance. Control systems operations was also verified, and the radio fail safe checklist fulfilled.

7.3. Flight and Dynamic Testing

Once the vehicle was in the flight stage, specific tests and performance goals were evaluated on the aircraft. After insuring proper take off and climb to altitude characteristics, aircraft speed over the drop leg was measured. Furthermore landing and takeoff characteristics were verified further, and the payload release system was verified to work during flight and drop within the predicted time. Figures 7.3.1, 7.3.2 and 7.3.3 illustrate pre, during and post flight testing checklists.

Preflight Inspection Checklist	
Checked	Process
	1. Assemble Aircraft Structure
	2. Inspect Aircraft Structure
	3. Inspect Electrical System
	4. Inspect Propulsion System
	5. Measure Total Voltage
	6. Verify Electrical Continuity
	7. Verify Drop System Operation
	8. Final Structural Verification Tests
	9. Verify Radio Range Check/Fail Safe
	10. Verify Control Surfaces Operation
	11. Static Propulsion Test
	12. Taxi Test

Figure 7.3.1

During Flight Performance Checklist	
Rating	Checklist
	1. Taxi Performance
	2. Take-Off Performance
	3. Low Speed Stall Characteristics
	4. Climbing Performance
	5. Cruising Performance
	6. Maximum Speed Performance
	7. Maximum Altitude
	8. Dropping Performance
	9. Descent Characteristics
	10. Operating Endurance
	11. Descent Characteristics
	12. Landing Performance

Figure 7.3.2

Post Flight Checklist	
Checked	Checklist
	1. Safe Aircraft
	2. Measure Battery Characteristics
	3. Measure Battery Temperature
	4. Measure Motor Temperature
	5. Verify Aircraft Structural Performance
	6. Un-assemble Aircraft Structure

Figure 7.3.3

8. References

1. Anderson, John. Fundamentals of Aerodynamics. New York: McGraw-Hill, 1991
2. Boucher, Bob Electric Motor Handbook, Marina Del Ray, Astroflight, 1994



University of California
San Diego

Design Report

Submitted March 10, 2004

Rain of Terror

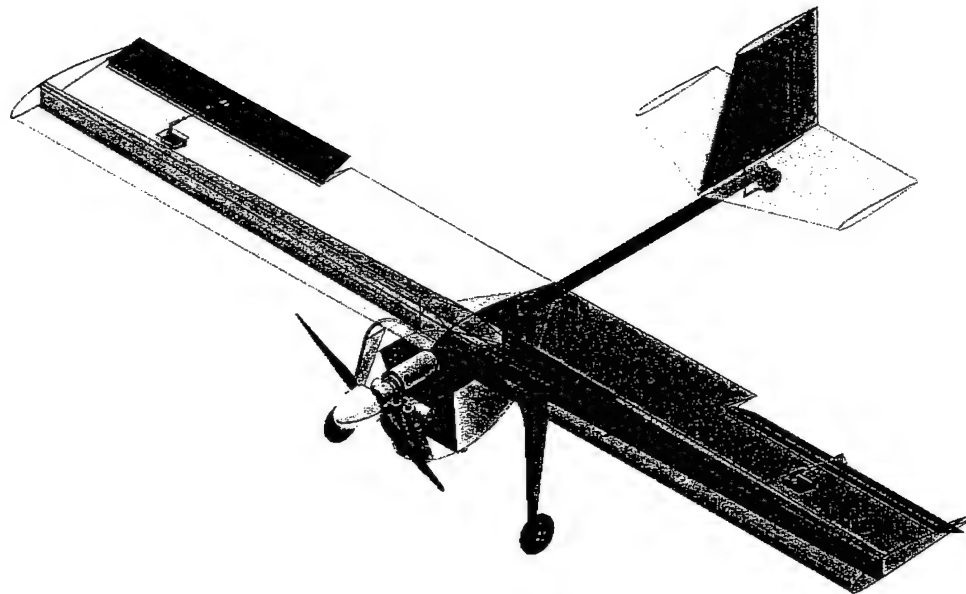


Table of Contents

1.0	Executive Summary	1
1.1	Conceptual Design	1
1.2	Preliminary Design	2
1.3	Detail Design	2
2.0	Management Summary	4
2.1	Architecture of Design Team	4
2.2	Aerodynamics	5
2.3	Structures	5
2.4	Propulsion	6
2.5	Task Scheduling	6
3.0	Conceptual Design	8
3.1	Competition Parameters and Aircraft Configuration	8
3.1.1	Aircraft Requirements	8
3.1.2	Mission Profiles	9
3.1.3	Rated Aircraft Cost	10
3.2	Aerodynamics	11
3.2.1	Aircraft Configurations	11
3.2.2	Wing Placement	12
3.2.3	Wing Shape	13
3.2.4	Tail Design	14
3.3	Structures	15
3.3.1	Wing and Tail Structures	15
3.3.2	Wing Spar	16
3.3.3	Fuselage Structure	16
3.3.4	Water Deployment System (WDS)	17
3.3.5	Landing Gear	18
3.4	Propulsion	19
3.5	Final Aircraft Configuration	20
3.5.1	Figure of Merit for Final Ranking Charts	21
4.0	Preliminary Design	22
4.1	Aerodynamics	22
4.1.1	Wingspan	22

4.1.2	Wing Chord Length.....	23
4.1.3	Airfoil Selection.....	23
4.1.4	Tail Design.....	24
4.1.5	Fuselage Shape.....	26
4.2	Structures.....	26
4.2.1	Factor of Safety.....	27
4.2.2	Wing Structure.....	27
4.2.3	Wing Joiner/Central Platform.....	28
4.2.4	Tail Configuration.....	29
4.2.5	Fuselage Structure.....	30
4.2.6	Aircraft Weight and Center of Gravity.....	31
4.2.7	Water Deployment System (WDS).....	31
4.2.8	Motor Mount.....	32
4.2.9	Landing Gear.....	33
4.3	Propulsion.....	33
4.4	Final Aircraft Configuration.....	34
5.0	Detailed Design.....	35
5.1	Aerodynamics.....	35
5.1.1	Mission Profile and Flight Performance.....	35
5.1.2	Takeoff Distance.....	36
5.1.3	Stability and Control.....	36
5.1.4	Control Surface Sizing.....	37
5.2	Structures.....	37
5.2.1	Wing Structure.....	37
5.2.2	Tail Configuration.....	38
5.2.3	Fuselage Structure.....	39
5.2.4	Water Deployment System (WDS).....	40
5.3	Propulsion.....	41
5.4	Final Aircraft Configuration.....	41
5.5	Final Aircraft Configuration Calculations.....	42
5.6	Rated Aircraft Cost.....	43
5.7	Detailed Drawings.....	44
6.0	Manufacturing Plan.....	60
6.1	Wings.....	61
6.2	Spar.....	61

6.3	Hardpoint.....	59
6.4	Platform.....	59
6.5	Skin & Fuselage.....	59
6.6	Motor Mount.....	59
6.7	Landing Gear.....	59
7.0	Research and Testing Plan.....	51
7.1	Objectives.....	51
7.2	Schedules.....	51
7.3	Testing Procedures.....	51
7.4	Check-lists.....	52
7.5	Results.....	53
	7.5.1 Airfoil Results.....	53
	7.5.2 Motor Testing Results.....	53
7.6	Water Release Testing.....	53
7.7	Valve Testing.....	54
7.8	Wind Tunnel Testing.....	58
7.9	Lessons Learned.....	58
8.0	References.....	59

List of Figures

Figure 2.1:	Rain of Terror Design Personnel.....	4
Figure 2.2:	Rain of Terror Team Milestone Chart.....	7
Figure 3.1:	Fire Fighter Mission Profile.....	9
Figure 3.2:	Ferry Mission Profile.....	10
Figure 4.1:	RAC Score v Surface Area and Aspect Ratio.....	22
Figure 4.2:	Drag Polar, CL v alpha, and Cd v alpha Curves for S4083 Airfoil.....	24
Figure 4.3:	Drag Polar, CL v alpha, and Cd v alpha Curves for NACA0009 Airfoil.....	25
Figure 4.4:	Drag Polar, CL v alpha, and Cd v alpha Curves for NACA 0035.....	26
Figure 4.5:	Distributed and point loads.....	27
Figure 4.6:	Illustration of spanwise profile of the spar.....	28
Figure 4.7:	Central Platform.....	29
Figure 4.8:	Tail Boom Load Model.....	30
Figure 4.9:	Internal Structure of Fuselage.....	31
Figure 4.10:	Cylindrical Valve.....	32
Figure 4.11:	Bottle Cap Vacuum Release Valve.....	32
Figure 4.12:	Motor Mount.....	33
Figure 4.13:	Main Landing Gear Placements.....	33
Figure 5.1:	von Mises Stress and Displacement of Spar.....	38
Figure 5.2:	Tail Configuration.....	39
Figure 5.3:	Structural Component Integration.....	39
Figure 5.4:	von Mises Stress and Displacement of Platform.....	40
Figure 5.5:	WDS Valve Mechanisms.....	41
Figure 5.6:	Force Balance on Door.....	40
Figure 7.1:	Research and Testing Schedule Task.....	51
Figure 7.2:	Testing Checklist.....	52
Figure 7.3:	Pre-Flight Checklist.....	52
Figure 7.4:	Post-Flight Checklist.....	53
Figure 7.5:	Airfoil Data.....	53
Figure 7.6:	Graupner Motor Data.....	53
Figure 7.7:	Time Vs. Water Released Without the Hose.....	54
Figure 7.8:	The Design Valves Tested.....	54
Figure 7.9:	"Modified" Valve Used in Final Design.....	55
Figure 7.10:	The Wind Tunnel Setup with Model.....	56
Figure 7.11:	30% Scaled Fuselage and Partial Wing Model of Final Design.....	56
Figure 7.12:	30% Scaled Model with Cowling.....	56

Figure 7.13:	Wind Tunnel Results at Pressure Hole 6.....	57
Figure 7.14:	Lift Coefficient of the Fuselage with the Cowling Versus Angle of Attack.....	58

List of Tables

Table 2.1:	Rain of Terror Members' Skills and Contributions.....	5
Table 3.1:	Figures of Merit for Wing Configurations.....	12
Table 3.2:	Figures of Merit for Wing Placement.....	13
Table 3.3:	Figures of Merit for Wing Shape.....	14
Table 3.4:	Figures of Merit for Tail Sections.....	14
Table 3.5:	Figures of Merit for Wing and Tail Structure.....	15
Table 3.6:	Figures of Merit for Wing Spar.....	16
Table 3.7:	Figures of Merit for Fuselage Structure.....	17
Table 3.8:	Figures of Merit for Water Deployment System.....	18
Table 3.9:	Figure of Merit for Landing Gear Configurations.....	18
Table 3.10:	Figure of Merit for Propulsion.....	19
Table 3.11:	Aerodynamic Figures of Merit Chart.....	21
Table 3.12:	Structural Figures of Merit Chart.....	21
Table 3.13:	Propulsion Figures of Merit Chart.....	21
Table 4.1:	FOM of Cross Section Selection for Tail Beam.....	29
Table 4.2:	Graupner Motor 3300 series.....	34
Table 5.1:	Evaluation of the mission times and flight modes.....	35
Table 5.2:	Final Aircraft Configuration Calculations.....	42
Table 6.1:	Fabrication processes and their estimated relative costs.....	49

1.0 Executive Summary

This report outlines the steps taken by the student members of the American Institute for Aeronautics and Astronautics (AIAA) at the University of California, San Diego, (UCSD) to design and construct an unmanned remote aircraft to compete in the 2003/2004 Design/Build/Fly (DBF) competition. The objective of the competition was to design an aircraft that operates at optimum performance while meeting all competition and mission requirements set forth by the Cessna/ONR DBF Committee. This aircraft must be able to complete two missions. The first mission (fire fight mission) calls for the aircraft to deploy four liter of water and complete a 360 degree turn during the "downwind" stretch of the course twice with a touchdown between laps in order to refill the water tank. During the second mission (ferry mission), the aircraft must take-off, complete four laps, and land. On all laps flown for this mission, the aircraft must complete a 360 degree turn in the direction opposite of the base and final turns on the downwind leg of each lap.

1.1 Conceptual Design

The conceptual design phase began by first analyzing the competition rules and requirements. The rules stipulated that the aircraft must complete two possible missions. Once the mission objectives were understood the team was divided into three technical groups: aerodynamics, structures, and propulsion. Each group produced figures of merit to represent mission objectives for each component of the aircraft that fell within their technical area. Concepts and ideas were studied in terms of feasibility, adherence to contest and mission requirements, conformance with all technical areas, and scoring potential.

The aerodynamic group sought an aircraft configuration that had an optimal Rated Aircraft Cost (RAC), low manufacturing cost, stability, and aerodynamic efficiency. During the conceptual design, various aircraft configurations were considered: the bi-plane, canard, conventional, and flying wing. Moreover, the aerodynamic group was responsible for the general shape and placement of the wing in regards to the fuselage along with researching various tail designs.

Ensuring the structural integrity of the aircraft was a crucial part of the structural conceptual design process. The structures group took into consideration ease of manufacture, RAC, strength, and weight savings when deciding upon the structural components of the aircraft. Various design concepts for the fuselage, wing, and tail structures along with the Water Deployment System (WDS) and landing gears were discussed.

The propulsion group examined motor and battery combinations to find the optimal configuration, which maximizes thrust while minimizing the rated engine power. Four motor/battery configurations were considered in regards to their effects on the RAC, battery and motor weight, thrust, and current draw.

The conceptual design phase produced a primary aircraft configuration consisting of a conventional monoplane with a rectangular high-wing and T-tail with a WDS that released the payload from the bottom of the fuselage.

In search of the most efficient method by which to deploy the water payload two alternative designs were seriously considered: the first involved a hose that could be rolled on a spool internal to the

fuselage, during payload deployment the hose would be released and fall, and the second design involved a using a venture to speed the flow going over the water exit in order to create low pressure over the water exit holes, increasing the flow rate.

1.2 Preliminary Design

With a complete conceptual aircraft configuration, the preliminary design phase determined the design parameters, and trade studies were done to optimize the parameters.

The aerodynamic group performed trade studies to determine the wingspan, chord length, airfoil, and tail area that would optimize the design. Three wingspan configurations were considered along with various chord lengths and tail dimensions. Moreover, the aerodynamic group discussed and researched numerous airfoils before coming to a decision.

The structural preliminary design included determining the wing, tail, and fuselage structures, along with the motor mount and landing gear configurations. The aircraft's weight, applied loads and location of the center of gravity affected the overall structural design and fuselage layout. The structural group built a prototype of the selected WDS in order to determine the minimum amount of force required to propel the payload from the bottom of the fuselage.

From the information gained by the aerodynamic and structural groups, propulsion requirements were determined by utilizing the stipulated maximum take off distance and aircraft weight. The minimum required thrust to complete the missions was calculated, and the optimum propulsion system configuration was found.

The preliminary design determined the sizing of the wing and tail geometry, primary structure dimensions, and propulsion configuration. The wingspan and chord length were calculated to be eight feet and 12 inches, respectively. The S4083 airfoil was selected for the wing, while the NACA0009 was chosen for the tail. The most efficient shape for the spar was found to take the shape of an I-beam with a chord-wise linear taper. The fuselage was shaped after a NACA0035 airfoil and constructed in three parts/modules, which provides adequate aerodynamic streamlines that reduced drag and gave ample room for the payload. The aircraft's takeoff weight was estimated to be approximately 19.8 pounds and the center of gravity was determined to be 2.5 inches behind the leading edge of the wing. An 18 inch diameter propeller with a 16 inch pitch powered by the Graupner 3300-7 motor and 18 Sanyo 1300 mAh cells compose the propulsion system.

1.3 Detail Design

With the information gained from the preliminary design phase, a foundation was provided for finalizing component and system architecture selection.

The aerodynamics group analyzed the mission. The total theoretical flight scores and RAC costs were calculated determining the desired flight mode and predicted possible scoring potential. Take off distance and aircraft stability were also calculated for optimization.

The structural group finalized the component integration and architecture of the structural design. Local strength requirements were established through finite element analysis to be implemented during manufacturing and incorporated into the engineering drawings. The boom mounting and wing joining details were determined and incorporated into the final design.

The propulsion system was finalized and static tests were performed in order to ensure optimal performance. Wire routing and servo placement for control surface movement was determined and updated into the drawings.

The final configuration of the airplane was a high-wing, conventional t-tail with a pulling motor configuration. The high-wing configuration required no dihedral for stability. The rectangular wing geometry included a span of 8 feet, a chord of 10 inches for an aspect ratio of 9.6. The main wing used the S4083 airfoil and the T-tail is comprised of the NACA0009 airfoil for both the vertical and horizontal stabilizers. The semi-monocoque fuselage housed the payload that is deployed using a servo controlled cylindrical tapered valve; gravity and an increased pressure differential, caused by the placement of a hole at the top of the water tank, were utilized to expel the water from the aircraft. A carbon fiber central platform absorbs loads and connects the payload, boom and empennage, wings, and motor mount. All structural members are composed of fiberglass, carbon fiber, and plywood. With known materials and component sizes, the CG was calculated to be placed 0.0625 inches in front of the quarter chord. An 18 inch diameter propeller with a 16 inch pitch powered by the Graupner 3300-7 motor and 18 Sanyo 1300 mAh cells compose the propulsion system.

The results of the three design phases produced an aircraft that completes the required mission with the highest scoring potential.

2.0 Management Summary

2.1 Architecture of Design Team

The Rain of Terror (ROT) Team consists of nine undergraduate and one graduate UCSD students studying aerospace engineering. Before work commenced, three technical groups were formed: aerodynamics, structures, and propulsion (Figure 2.1). A project manager supervised each technical group, delegating specific tasks in the areas of interest to each of their group members. In so doing, the project managers were responsible for directing and managing their groups' progress in their specialized areas. Skills and contributions of team members are listed in Figure 2.2. A project manager monitored the performance and advancement of the overall team; making sure each group had all the necessary information to complete their assigned tasks. Together the project manager and the lead engineering students kept the team on task and assured the efficient progress and development of the project.

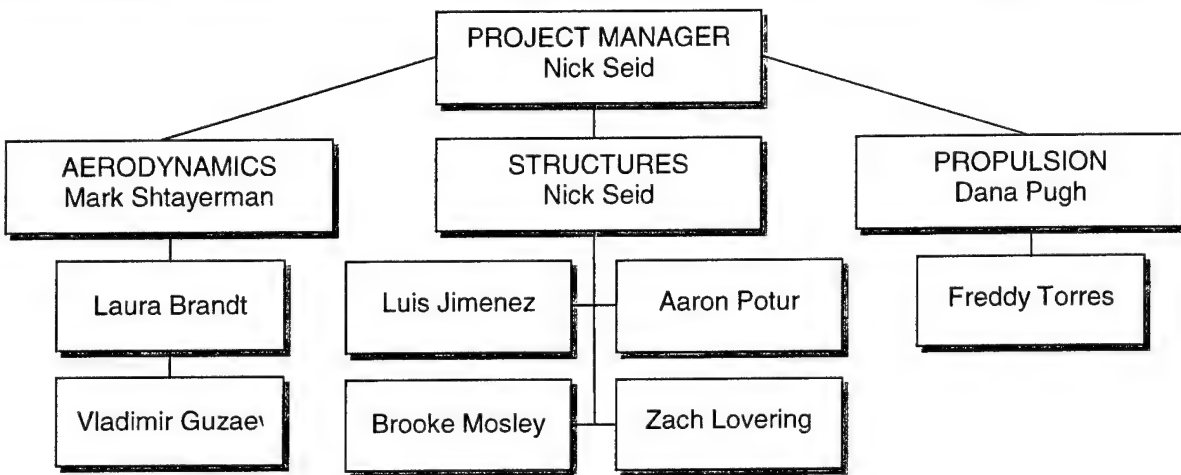


Figure 2.1 Rain of Terror Design Personnel

The consolidation of each groups' efforts into one solid finalized design took a great deal of collaboration and compromise. Since the design concepts of one group places restraints on the other groups, weekly meetings were set up to discuss the integration of the different modules. During these weekly meetings, compatibility issues were resolved, new ideas were generated, and updated assignments were given. This management style allowed for a reliable, secure, and steadfast design process, while considering all aspects of aerodynamics, structures, and propulsion.

Team Members	Major	Year	Auto Desk Inventor	AutoCAD	MSC Patron	Technical Writing	Machining	Fabrication
Laura Brandt	AE	SR	X	X	X	X		X
Vladimir Guzaev	AE	JR		X				X
Luis Jimenez	AE	SR	X	X	X			X
Zach Lovering	AE	FR	X	X				X
Brooke Mosley	AE	JR	X	X				X
Aaron Potur	AE	SR	X	X	X			X
Dana Pugh	AE	SR	X	X	X	X		X
Mark Schlocker	ME	GR	X	X	X			X
Nic Seid	AE	SR	X	X	X	X	X	X
Mark Shtayerman	AE	GR	X	X	X	X	X	X
Freddy Torres	AE	SO		X	X	X	X	X

Table 2.1 Rain of Terror Members' Skills and Contributions

2.2 Aerodynamics

The aerodynamic group was responsible for the shape of the aircraft. The group's primary focus was the analysis of forces acting on the body of the aircraft. These forces were a result of the relative motion between the body and the air (relative wind). In order to accomplish this goal, the aerodynamic group generated a static stability model, based on initial weight estimations, to determine the aircraft lift requirements. Figures of merit and competition regulations were taken into account while performing lift surface sizing. Airfoil selection along with wing, tail, and control surface sizing were conducted with the information gathered from this model. Control surface deflection and servo sizing were also studied using this model to determine control stability and maneuverability. Further aircraft configurations were examined to optimize take off distance, lift-to-drag (L/D) ratio, cruise, and velocity.

During weekly meetings, the structures and propulsion groups conveyed their estimates concerning aircraft weight, sizing, and power requirements, giving rise to the production of updated lift requirements and the refinement of aerodynamic components.

2.3 Structures

The structural group was accountable for determining the structural requirements to support the loads applied on the aircraft; these requirements consisted of designing the component configuration of the aircraft, selection of the materials, and the manufacturing techniques needed to produce the aircraft. Various design considerations for the Water Deployment System (WDS), landing gear, and wing joiner were evaluated in regards to figures of merit and competition regulations in order to obtain an optimum

design. The group's analysis focused heavily on hand calculations and CAD modeling to implement their design ideas. Information was exchanged during the weekly meetings with the aerodynamic and propulsion groups, which aided in the decision of the primary structural components of the fuselage, wing, tail, landing gear, WDS, and other aircraft related components.

2.4 Propulsion

The propulsion group was primarily responsible for providing enough energy and thrust to complete the mission profiles. The group was responsible for analyzing different types of motor, propeller, and battery combinations that would provide the most thrust with an efficient Rated Aircraft Cost (RAC). Figures of Merit (FOM) and competition regulations greatly impacted the propulsion group's criteria. The competition guidelines limited the propulsion group's selection of technical equipment: motors, batteries, and propeller selection. Analytical and experimental means were developed to achieve the best combination of the propulsion systems' three main components in order to create an efficient and stable aircraft. Every change in the aerodynamics or structure of the aircraft called for an adjustment in the propulsion system, which called for collaboration and compromise between the groups during the weekly meetings.

2.5 Task Scheduling

In order to meet the deadline a project milestone chart was created. Following this guideline allowed for a quick and efficient design and manufacturing process. Between mid-September and early October, the team set a tentative schedule of completion dates of each phase of the aircraft development. The chart below (Figure 2.2) depicts the intended and actual dates of completion of eight milestones: design team assembly, conceptual design, preliminary design, detail design, design review, report, aircraft construction, and aircraft testing:

- +! Assembly of Design Team: The returning 2002-03 DBF members collaborated on how many new members the project would need to compete in this year's competition. During the first week of classes, a meeting was held and a new team began to form. The final team had 8 members.
- +! Conceptual Design: During the conceptual design phase mission requirements were defined, alternative configuration concepts were discussed, and a final design was constructed.
- +! Preliminary: With the completion of the conceptual design, an investigation into design parameters was initiated.
- +! Detail Design: The detail design process was composed of component and system architecture selection.
- +! Design Review: A presentation of the aircraft's detailed designs, plans for fabrication, and a cost break down to Faculty Advisor.
- +! Report: The process of the conceptual, preliminary, and detail designed phases were recorded in order to maintain an organized and efficient project progression.

- ±! Construction: The manufacturing process was the most time consuming and lengthy. Therefore, a substantial amount of time was devoted to this phase of the aircraft development.
- ±! Flight Testing: Having completed construction, test flights were undergone to ensure flyability, structural integrity, and stability. A sufficient amount of time was given to the flight test in order to give our pilot enough time to become comfortable with the aircraft and to fix any problems encountered.

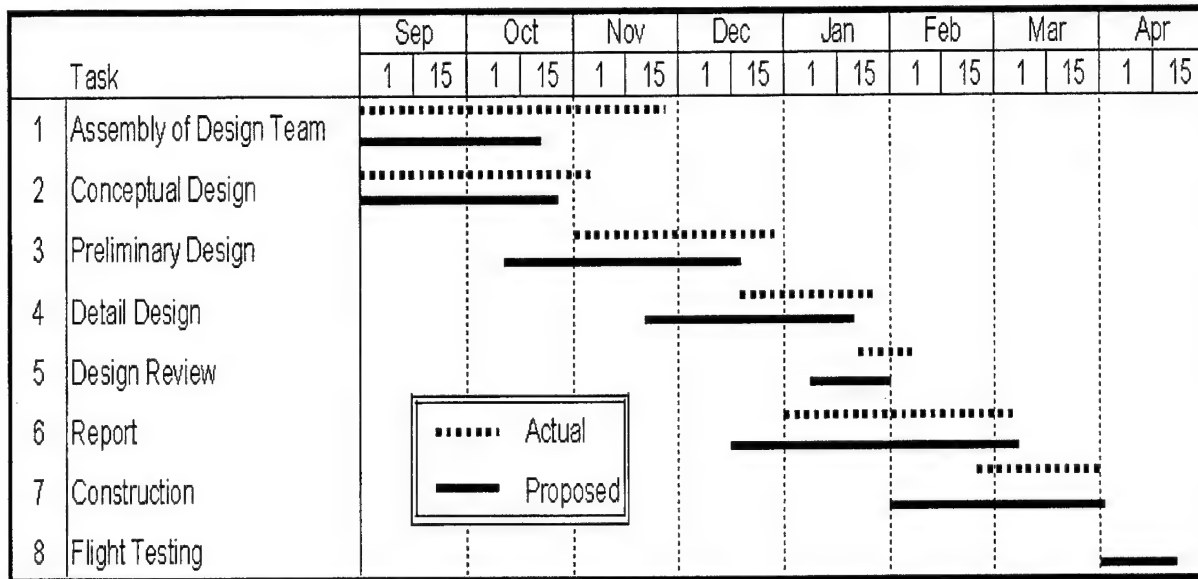


Figure 2.2 Rain of Terror Team Milestone Chart

3.0 Conceptual Design

Four factors dominated the design of the aircraft: competition requirements, aerodynamic effects, structural integrity, and propulsion systems. The competition rules, mission profiles, and Rated Aircraft Cost (RAC) guided the conceptual design phase. The aircraft was considered within three technical areas: aerodynamics, structures, and propulsion. During the conceptual design, the aerodynamic group considered various aircraft configurations, wing shapes, and tail designs while also determining the placement of the wing in regards to the fuselage. The structural group focused on ensuring the structural integrity of the aircraft. They analyzed numerous design possibilities for the fuselage, wing, and tail structures along with the Water Deployment System (WDS) and landing gear. The propulsion group examined four motors and battery combinations to find the optimal propulsion configuration. Within each group, ideas were generated, concepts were collaborated, and compromises were made in order to optimize the design and fulfill mission requirements in order to achieve the best possible score.

3.1 Competition Parameters and Aircraft Configuration

The conceptual design phase commenced with a study of the competition requirements. Within each technical area, a focus was placed on the parameters set by the competition. These constraints affected the aircraft weight and size and in turn affected the RAC.

3.1.1 Aircraft Requirements

The Cessna/ONR Student Design/Build/Fly Competition Committee provided guidelines for the overall size and weight of the aircraft. The contest rules dictated that the unassembled aircraft must fit in to a 2-ft wide by 1-foot high by 4-ft long box. Using solid modeling analysis, maximum dimensions were determined by placing each component into a 3-D model of the box. These dimensions limited the ultimate aircraft size. Dimensions were estimated so that the maximum wing length was four feet, the maximum fuselage height was under one foot and width less than two feet, and the vertical tail size was less than one foot tall. Moreover, the competition required the aircraft to be less than 55 pounds, which limits the choice of component selection.

3.1.2 Mission Profiles

The aircraft must complete two missions. During each lap of the sortie, the aircraft must complete a 360 degree turn on the downwind leg of each lap flown.

- A. Fire Fight; Difficulty Factor 2.0. The aircraft takes off with its payload (water), releases the payload at the downwind leg, and return to land; it is then reloaded, takes off, releases its' payload again, and returns for its final landing (Figure 3.1). The maximum allowable water capacity is four liters.

B.

Phase	Description
1	Take-off and climb to altitude
2	Turn 180 degrees (Begin Releasing Payload at end of Turn)
3a	Fly to center of field
3b	Complete a 360 degree turn
3c	Fly to end of field
4	Turn 180 degrees (Stop Releasing Payload at beginning of Turn)
5	Return to Runway and Land
6	Reload
7	Take-off and climb to altitude
8	Turn 180 degrees (Begin Releasing Payload at end of Turn)
9a	Fly to center of field
9b	Complete a 360 degree turn
9c	Fly to end of field
10	Turn 180 degrees (Stop Releasing Payload at beginning of Turn)
11	Return to Runway and Land

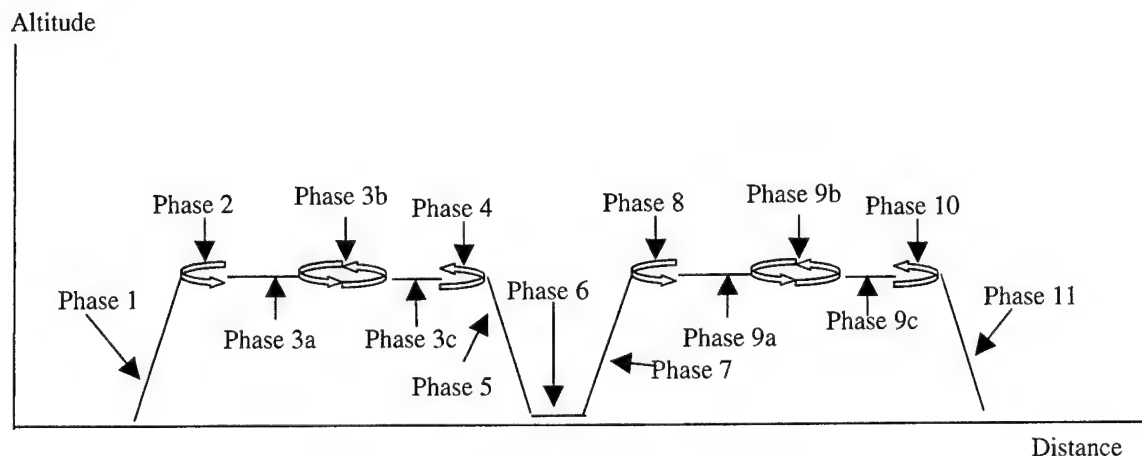


Figure 3.1 Fire Fighter Mission Profile.

- C. Ferry; Difficulty Factor 1.0. The aircraft is required to take-off, complete four laps and land. During each lap the aircraft must complete a 360 degree turn in the direction opposite of the base on the downwind transition (Figure 3.2).

Phase	Description
-------	-------------

1	Take-off and climb to altitude
2	Complete Four Laps Consisting of: a. Turn 180 degrees at upwind end of field b. Fly to center of field c. Complete a 360 degree turn d. Fly to downwind end of field e. Turn 180 degrees and fly towards upwind end of field
3	Return to Runway and Land

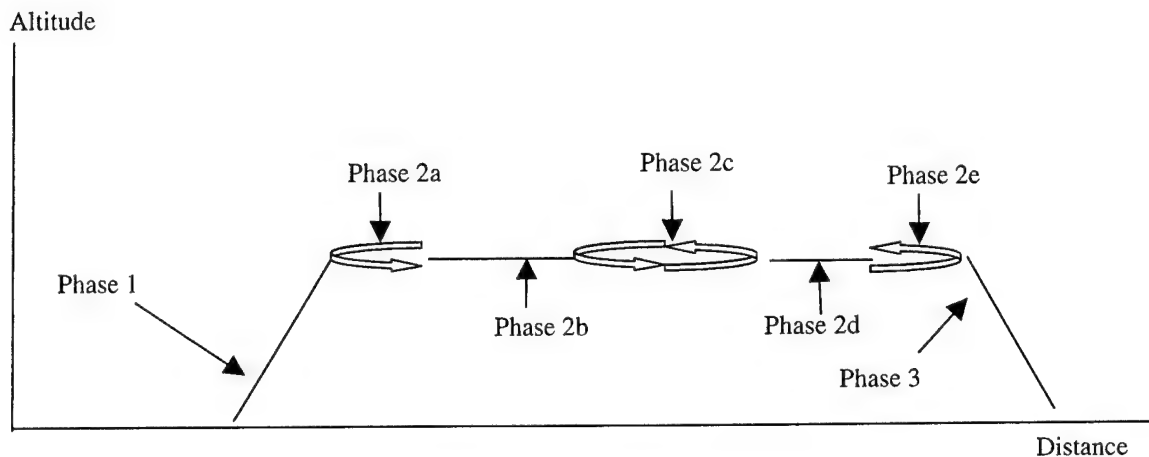


Figure 3.2 Ferry Mission Profile.

An evaluation of several different components was undergone in order to determine the mission that offered the optimum scoring potential. This was done in order to select the mission that the aircraft would be designed around. Because of the different degrees of difficulty, each mission offered a different scoring potential. For instance, mission A required the aircraft to overcome extra weight because of the four liters of water carried in its WDS; while mission B required the aircraft to fly three additional laps. Furthermore, the power requirements for mission A were substantially higher due to the fact that the aircraft must experience two take-offs. Through a complex analysis of comparing the aircraft configurations required by each mission, scoring potential, and RAC, it was found that mission A (fire fight) provided the best opportunity for obtaining points. Therefore, the team decided to design the aircraft around mission A and used mission B as the fall back mission.

3.1.3 Rated Aircraft Cost

The RAC was a mathematical cost function relating all of the aircraft design parameters. The battery and aircraft weight, numbers of wings, size and span, number of servos and control surfaces, fuselage length and tail size all contributed to the RAC. The Rated Aircraft Cost was defined by the following equation:

$$\text{RAC} = (\$300 \cdot \text{MEW} + \$1500 \cdot \text{REP} + \$20 \cdot \text{MFHR}) / 1000$$

÷! MEW = Manufactures Empty Weight. (Actual airframe weight without batteries or payload)

÷! REP = Rated Engine Power. (Defined as $(.25 \cdot (\# \text{ Engines}) - 1) \cdot \text{Total Battery Weight}$)

÷! MFHR = Manufacturing Man Hours. This parameter was the sum of the following:

1. Wing span multiplied by chord length: 10 hr/ft^2 .
2. Fuselage length x Width x Height: 20 hr/ft^3
3. Each vertical surface with active control: 10 hr/surface
4. Each vertical surface with no active control: 5 hr/surface
5. Horizontal stabilizer, no more than 25% of the greatest span: 10 hr/surface
6. Flight systems: 5 hr/servo or motor controller

In order to achieve a high competition score, the RAC must be minimized. Therefore, the wingspan and chord length, fuselage size, and propulsion systems were limited.

3.2 Aerodynamics

The aerodynamics primary components were assessed after the design parameters of the missions were established and the mission with the maximum score potential was chosen. By evaluating past team experiences and the competition guidelines, suitable Figures of Merit (FOM) were established for initial aerodynamic analysis. For each aircraft component, alternative configuration concepts were placed in FOM matrices. The FOM's considered were: RAC, ease of manufacture, stability, and aerodynamic efficiency.

- +! RAC effects: Since RAC is the heavily influences the final score, the RAC changes need to be evaluated for each design change.
- +! Weight: Any weight changes associated with a specific configuration will affect flight characteristics and battery requirements thus increasing RAC score.
- +! Ease of Manufacture: Manufacturing takes materials, time, and resources, a limiting factor.
- +! Stability: Any configurations that will render the aircraft unstable will be heavily penalized because of the increased risk of loss of control and possible destruction of the aircraft. Therefore, this FOM was most heavily weighted because any loss of stability may result in failure to meet mission requirements
- +! Aerodynamic Efficiency: The aerodynamic efficiency accounts for lift, drag and performance of the aircraft, which is responsible for flight time.

The FOMs were compared using a comparative system consisting of +, 0, and – (good, satisfactory, and unsatisfactory, respectively). The RAC, Weight, Ease of Manufacture, and Aerodynamic Efficiency were all given a weight of one, while the stability of the aircraft was given a weight of two because of its overall effect on the mission.

3.2.1 Aircraft Configuration

Various aircraft shapes were researched, including: bi-wing, canard, conventional, and a flying wing. These aircraft shapes were compared in the FOM matrix in Table 3.1. This FOM matrix exposed the advantages and disadvantages of each design concept. The following are the descriptions of each design:

- ÷! Bi-plane: A bi-plane generates extra lift, however, it also generally weighs more, includes more work hours, and the servos associated with a second wing greatly increases RAC score.
- ÷! Canard: A canard has built-in anti-stall characteristics. However, it requires additional thrust to take off because the main wing cannot reach its maximum angle of attack.
- ÷! Conventional: A conventional aircraft has a standard fuselage, tail, and wings, along with well-documented flying capabilities.
- ÷! Flying wing: A flying wing has great weight saving advantages; however, the lack of tail surfaces renders the plane unstable. This concept was easily eliminated.

	Figures of Merit (x weighting)					Decision
	Ease of Manu-facture (x1)	RAC effects (x1)	Stability (x2)	Weight savings (x1)	Sum of Ratings	
(R) – Rejected						
(S) – Selected						
Bi-Plane	-	-	0	-	-3	R
Canard	-	-	+	-	-1	R
Conventional	0	0	0	0	0	S
Flying Wing	-	+	-	+	-1	R

Table 3.1 Figures of Merit for Wing Configurations

Given the relative ease of manufacture, stability, and proven performance, the conventional configuration was chosen, having an RAC of 8.2. The bi-plane had a weight penalty of 2.5 lbs and RAC of 9.3 due to additional wing and extra battery weight to power the plane. Canard design was rejected because of the slight penalty in RAC (0.2) and increased runway distance due to stability characteristics. The flying wing was abandoned, because it was found a highly risky design because of stability, even though the RAC was 7.0.

3.2.2 Wing Placement

Once the shape of the aircraft was decided, the wing placement relative to the fuselage was taken into consideration. High, mid, and low wings with dihedrals were considered and evaluated using the FOM in Table 3.2.

- ÷! High: A high wing has better roll stability because of the placement of center of gravity in relation to the wing. While the high wing does not interfere with the payload deployment mechanisms, it does, however, require the use of large landing gear.
- ÷! Mid: A mid wing is very difficult to construct. This is because they require a transfer of loads through the middle of the fuselage, which would require strengthening the structure and hence adding weight. Furthermore, blending the fuselage body to the wing, to reduce drag, will be very difficult because of the nature of the payload and relative size of the fuselage to the wing thickness.

⚡ Low: A low wing will require dihedral for roll stability. Furthermore, the landing gear is smaller, lighter, and easier to attach and manufacture. Therefore, the landing gear is relatively small in comparison to the landing gear required for a high wing and, thus, lower weight and drag. However the wing spar will interfere with the WDS thus increasing the complexity of the aircraft.

	Figures of Merit (x weighting)					Decision
	Ease of Manufacture (x1)	RAC effects (x1)	Stability (x2)	Weight savings (x1)	Sum of Ratings	
(R) – Rejected						
(S) – Selected						
High	+	0	0	0	+1	S
Mid	-	-	0	-	-3	R
Low with Dihedral	-	0	0	0	-1	R

Table 3.2 Figures of Merit for Wing Placement

The mid and low wing placements were discarded because of the difficulty to manufacture, resulting in larger RAC scores. Due to the ease of manufacture, stability, weight savings, and the RAC effects, an upper wing configuration seemed ideal. The high wing placement allowed for one central structure that combined all dynamic loads during aircraft operation. Additionally, with the superstructure of the aircraft being above the payload, the water release valve mechanism and servo can be easily installed over the CG of the plane, thus providing stability during the deployment of the payload.

3.2.3 Wing Shape

With high wing aircraft in mind, several designs for the wing shape were taken into consideration: elliptical, rectangular, tapered and swept wings. When comparing these different wing designs an additional FOM was included, aerodynamic efficiency (Table 3.3).

⚡ Elliptical: An elliptical wing has the highest efficiency factor, thereby, having the lowest drag.

However, the elliptical wing has a complex shape, which is difficult to manufacture.

⚡ Rectangular: A rectangular wing is the easiest to manufacture and has the lowest RAC score per wing area. However, the efficiency factor is low and, therefore, the drag is high.

⚡ Taper: A taper wing is more efficient than the rectangular wing; however, a larger root cord is required to achieve the same wing area thus increasing the RAC.

⚡ Sweep: A sweep wing provides efficiency benefits at high speeds. However, the aircraft will not experience the benefits of the sweep due to being a low speed. Furthermore, manufacturing a sweep wing has significant difficulties, the wing joiner and spar are very difficult to manufacture.

	Figures of Merit (x weighting)						Decision
	Ease of Manufacture (x1)	RAC effects (x1)	Stability (x2)	Weight savings (x1)	Aerodynamic Efficiency (x1)	Sum of Ratings	
(R) – Rejected							
(S) – Selected							
Elliptical	-	-	0	0	+	-1	R
Rectangular	+	0	0	0	0	+1	S
Tapered	0	-	0	0	+	0	R
Swept	-	-	+	0	-	-1	R

Table 3.3 Figures of Merit for Wing Shape

A rectangular wing was chosen because of the ease of manufacture and the RAC score. This was because, an elliptical wing was almost impossible to manufacture without the proper machinery, while a tapered wing was only 4% more efficient than a rectangular wing given an aspect ratio of 10 (Abbot 17). The tapered wing was also disregarded because it had a higher RAC by 0.1. The swept wing was eliminated because of the difficulty in manufacture and lack of efficiency benefits.

3.2.4 Tail Design

In order to stabilize the aircraft in the pitch and yaw directions, designs for a tail section were considered: V tail, H tail, and T tail. A tail was crucial for the stability of the aircraft. Therefore, the stability FOM was considered the most substantial when it came to selection (Table 3.4).

- ⚡ V tail: This tail provides stability; however, it is difficult to manufacture compared to other designs.
- ⚡ H tail: This design is ideal for twin fuselage planes, because it provides additional stiffness to the structure; however, extra controlled vertical surface and extra weight must be considered.
- ⚡ T tail: This is a conventional tail section design that is highly stable and easy to manufacture.

	Figures of Merit (x weighting)					Decision
	Ease of Manufacture (x1)	RAC effects (x1)	Stability (x2)	Weight savings (x1)	Sum of Ratings	
(R) – Rejected						
(S) – Selected						
V – Tail	-	+	0	0	0	R
H – Tail	0	-	0	-	-2	R
T – Tail	+	0	0	0	+1	S

Table 3.4 Figures of Merit for Tail Sections

A T-tail was selected, because it proved stability and ease of manufacture. A V-tail design was rejected because of the increased complexity of manufacturing, despite the fact that it had a lower RAC (0.15). The H-tail design was discarded because of the penalty of 0.21 in RAC and considered unnecessary since our configuration has only one fuselage body.

3.3 Structures

Ensuring the structural integrity of the aircraft was a crucial part of the design process. Therefore, the structural conceptual design phase began with setting up FOM to ensure a high-quality aircraft. The FOM for the fuselage, wing, and tail structures along with the payload delivery mechanism and landing gear configuration were ease of manufacture, RAC, strength, and weight savings.

- ÷! Ease of Manufacture: This FOM deals with the manufacturing feasibility and difficulty level. This FOM is important because time, materials and resources are limited.
- ÷! RAC Effects: The RAC is an important aspect of the overall score.
- ÷! Strength: Each component is evaluated in terms of how well it will behave given general loading conditions. The wings and tail are often subjected to harsh handling conditions and must therefore be able to withstand heavy loads at maximum g-loading. Additionally, the wings must survive 2.5 g loading of the plane. Therefore, this FOM was heavily weighted because if the structure fails then the mission may be lost.
- ÷! Weight Savings: Any weight change associated with a specific configuration will affect flight characteristics. A low weight aircraft is desirable because weight affects the amount of lift, thrust required, and overall RAC. Therefore, this FOM was also heavily weighted because of its effects on the overall mission.
- ÷! Durability: The aircraft must repeatedly be able to withstand heavy loads.

The structural FOMs were similarly compared using a comparative system consisting of +, 0, and - (good, satisfactory, and unsatisfactory, respectively). The Ease of Manufacture, RAC, and Durability were all given a weight of one, while Strength and Weight Savings were given a weight of two because of their overall effect on the mission.

3.3.1 Wing and Tail Structures

The wing and tail structural design required strength, rigidity, and durability. Three different ideas were considered for the internal structure of the wing and tail: white foam core, blue foam core, and balsa.

	Figure of Merit (x weighting)						Decision
	Ease of Manufacture (x1)	RAC Effects (x1)	Strength (x2)	Durability (x1)	Weight Savings (x2)	Sum of Ratings	
(R) - Rejected							
(S) - Selected							
White Foam Core	+	+	-	-	+	1	S
Blue Foam Core	+	0	0	-	0	0	R
Balsa Frame	-	-	+	+	-	-1	R

Table 3.5 Figures of Merit for Wing and Tail Structure

White foam core was selected for both the wing and tail sections because of the ease of manufacture, RAC, and weight. Compared to white foam, a balsa wood structure seemed impractical. The

manufacturability of a balsa frame structure is very complex and time consuming; the RAC, strength, weight, and durability costs are also high. Furthermore, white foam is less dense and lighter than blue foam, yielding weight savings and a lower RAC value. White foam is less durable and weaker than blue foam. However, for the predicted loads these components undergo, the white foam sufficed.

3.3.2 Wing Spar

The aircrafts spar must be able to withstand two loading scenarios:

- ±! A wingtip test: Assumed to simulate a $\pm 2.5g$ point load.
- ±! Aerodynamic loads: during flight at the aircrafts maximum loaded weight. Loads assumed to be a maximum of 5g's.

Spars can be very difficult to make properly, therefore manufacturing needs were analyzed carefully. An FOM chart was created in attempt to quantify the options considered. The following are FOM's necessary for an effective analysis (Table 3.6).

- ±! I-Beam: Works well in bending of one axis, and fairly in the other. Is not good for torsional loads.
- ±! Box Beam: Work well in two axis and fairly with torsional loads.
- ±! Cylindrical Tube: Bending is the same in two axis and works well with torsional loads.

	Figure of Merit (x weighting)						Decision
	Ease of Manufacture (x1)	RAC Effects (x1)	Strength (x2)	Durability (x1)	Weight Savings (x2)	Sum of Ratings	
(R) - Rejected							
(S) - Selected							
I-Beam spar	+	+	0	0	+	+4	S
Box Beam	0	0	0	0	0	0	R
Cylindrical Tube	-	0	+	+	0	+2	R

Table 3.6 Figures of Merit for Wing and Spar

The I-Beam was selected because of its overall high ranking in Ease of Manufacture, RAC, and Weight Savings. The Box Beam and Cylindrical Tube designs were discarded because they did not rank as well as the I-Beam.

3.3.3 Fuselage Structure

The initial conceptual phase of the fuselage structure was centered on the carrying and delivering of the payload. Therefore, an additional FOM was considered, storage capacity. The aircraft must be able to house the payload, batteries, and flight control servos. Two concepts concerning the fuselage dominated the conceptual design phase: a semi-monocoque fuselage and a thin keel fuselage.

- ±! Semi-monocoque fuselage: This design would house the payload and release it using a cylindrical valve at the bottom of the fuselage.
- ±! Carbon Fiber Fuselage: A thin keel would connect the wings, boom, motor and payload to one structural member.

	Figure of Merit (x weighting)							Decision
	Ease of Manufacture (x1)	RAC Effects (x1)	Strength (x2)	Weight Savings (x2)	Storage Capability (x1)	Durability (x1)	Sum of Ratings	
(R) - Rejected								
(S) - Selected								
Semi-Monocoque	+	+	0	+	+	0	+5	S
Thin Keel	0	-	0	-	0	+	-2	R

Table 3.7 Figures of Merit for Fuselage Structure

The semi-monocoque fuselage structure proved to be the better design. The keel design was heavy and difficult to fabricate. In contrast, the conventional semi-monocoque design provided a balance between the strength, weight and manufacturability. Also, this type of fuselage provided storage room for batteries and motor controller while the keel design does not inherently have extra space.

3.3.4 Water Deployment System

The Fire Fight mission required that the aircraft release water from the fuselage on two occasions during its flight via radio-control. The aircraft consists of an internal tank from which the water was released. Three valve mechanisms were considered for deploying the water. A brief description of the three valve mechanisms is outlined below.

- ÷! Cylindrical Valve: This concept entailed having the water flow out of the tank through a valve which moves a small cylinder from the path of the water, allowing it to exit the tank.
- ÷! Gate Valve: Another idea was to have the valve move a small gate out of the water's path, allowing the water to exit through the space left void by the gate.
- ÷! Ball Valve: This idea requires that the flow of water be prevented by placing a small ball in its path of travel. The amount of water allowed to flow out is determined by how much the ball is removed from the water's exit path.

Each Water Deployment System (WDS) valve concept was considered using the structural figures of merit (Table 3.7); however, additional figures of merit were also utilized: reliability, required servos, and testing data.

- ÷! Reliability: Reliability was the most important design criterion for the AWD. The water must be released flawlessly every time. Therefore, this FOM was weighed twice as much as the others.
- ÷! Servos Required: Additional servos are expensive and add complexity to the design. It was desirable to keep the number of servos to a minimum and keep the design simple in order to keep the weight and RAC low.

Figure of Merit (x weighting)

(R) – Rejected (S) – Selected	Ease of Manufacture (x1)	RAC Effects (x1)	Strength (x2)	Weight Savings (x2)	Reliability (x2)	Servos Required (x1)	Sum of Ratings	Decision
Cylindrical Valve	0	+	0	0	+	+	+4	S
Gate Valve	+	0	0	0	-	+	-1	R
Ball Valve	-	-	-	0	+	-	-3	R

Fig. 3.8 Figures of Merit for Water Deployment System

The cylindrical valve WDS method was selected because of its overall high ranking in RAC, Reliability and Servos Required (requires only one servo). The Gate and Ball Valves were rejected because of there low rankings and the fact that the cylindrical valve ranked so high.

3.3.5 Landing Gear

Three landing gear configurations were studied in the conceptual phase of the design: tricycle, tail wheel and quad.

- ±! Tricycle design: The tricycle design has one strut and tire under the nose of the aircraft and two other struts and tire configurations under each wing.
- ±! Tail Wheel (tail dragger): A tail wheel design is comprised of a strut and tire being placed under each wing and a wheel under the tail boom. This design allows for a wider wheel base and ground directional control.
- ±! Quad: A quad configuration is composed of four tires under the fuselage. This design is unstable at landing and increases weight and drag.

(R) - Rejected (S) - Selected	Figure of Merit (x weighting)						Decision
	Ease of Manufacture (x1)	RAC Effects (x1)	Strength (x2)	Durability (x1)	Weight Savings (x2)	Sum of Ratings	
Tricycle	+	0	0	0	0	+1	R
Tail Wheel	+	0	0	0	+	+3	S
Quad	0	0	0	0	-	-2	R

Table 3.9 Figure of Merit for Landing Gear Configurations

The tail dragger configuration was selected because of the ease of manufacture and weight. The quad landing gear was rejected because of its weight and ease of manufacture. The tricycle landing gear was a possibility; however, it posed problems with the WDS which is addressed in the preliminary design.

3.4 Propulsion

The goal of the propulsion conceptual design phase was to maximize thrust while minimizing rated engine power (REP). The FOM considered were: RAC, battery and motor weight, thrust, and motor current draw.

- ±! RAC: The RAC is a substantial part of the overall score and was therefore, weighted very heavily by the propulsion group.
- ±! Battery Weight: The Battery weight greatly affects the RAC and flight performance and was therefore, weighed heavily.
- ±! Motor Weight: The motor weight is also important to minimize because each addition of a motor directly adds to the manufacture's empty weight (MEW) and REP.
- ±! Thrust: Thrust is important because it is the force required to overcome the drag. Therefore, the thrust was considered a main priority and received a heavy weight
- ±! Current Draw: Motor current draw is imperative to not draw too much power and thus burning up the fuse or the engine thus causing a plane crash.

The structural FOMs were similarly compared using a comparative system consisting of +, 0, and - (good, satisfactory, and unsatisfactory, respectively). The Motor Weight and Current Draw were given a weight of one, while the Battery Weight and Thrust were given a weight of two because of their overall effect on the mission. Because of the large effect, the propulsion system had on the RAC score, the RAC was weighed as three.

Four motor battery configurations were analyzed to optimize performance: 1 motor/1 (1.5 pound) battery pack, 1 motor / 1 (2 pound) battery pack, 2 motors / 1 (2.5 pound) battery pack, and 2 motors / 2 (1 pound) battery packs.

	Figures of Merit (x weight)						Decision
	RAC (x3)	Thrust (x2)	Current Draw (x1)	Motor Weight (x1)	Battery Weight (x2)	Sum of Rating	
1 Motor / 1 (1.5lbs) Battery Pack	+	-	+	+	+	+5	S
1 Motor / 1 (2 lbs) Large Battery Pack	+	0	0	+	0	+4	R
2 Motors / 2 (1lbs) Battery Packs	-	+	+	-	0	-1	R
2 Motors / 1 (2.5lbs) Large Battery Pack	0	0	-	-	0	-2	R

Table 3.10 Propulsion FOM

The setups with two motors received low RAC scores (over 9.5). The RAC is penalized for multiple motors and additional motor weight. Therefore, the systems with more than one motor were discarded.

As seen in Table 3.9, the single motor propulsion systems give favorable RAC values (8.1 and 8.8 respectively for 1.5 pound and 2 pound battery packs), low current draw, low motor weight, and reduced battery weight. From previous experience and competitions, a 1.5 pound battery pack is estimated to be the most efficient and to provide the power required to fulfill the mission. However, in

order to formally decide between the two remaining systems, the thrust must be calculated. This calculation was performed in the preliminary and detail sections.

3.5 Final Aircraft Configuration

With the collaboration of concepts from the aerodynamic, structural, and propulsion technical groups, a final aircraft configuration was produced. The final design had a conventional configuration with a rectangular high white foam wing and T-tail. The fuselage structure was a carbon fiber configuration and a tail dragger configuration was chosen for the landing gear. The propulsion system was comprised of a single motor with a 1.5 pound battery pack.

3.5.1 Figures of Merit for Final Ranking Charts

Aerodynamic FOM Chart

Decision	Sum of Ratings	Aerodynamic Efficiency (x1)	Weight savings (x1)	Stability (x2)	RAC effects (x1)	Ease of Manufacture (x1)	(R) – Rejected (S) – Selected
R	-3	-	-	0	-	-	Bi-Plane
R	-1	-	-	+	-	-	Canard
S	0	-	0	0	0	0	Conventional
R	-1	-	+	-	+	-	Flying Wing
S	+1	-	0	0	0	+	High
R	-3	-	-	0	-	-	Mid
R	-1	-	0	0	0	-	Low with Dihedral
R	-1	+	0	0	-	-	Elliptical
S	+1	0	0	0	0	+	Rectangular
R	0	+	0	0	-	0	Tapered
R	-1	-	0	+	-	-	Swept

Table 3.11 Aerodynamic Figures of Merit Chart

Structural FOM Chart

Decision	Sum of Ratings	Durability (x1)	Storage Capability (x1)	Weight savings (x1)	Strength (x2)	RAC effects (x1)	Ease of Manufacture (x1)	I – Rejected (S) – Selected
S	1	-	-	+	-	+	+	White Foam Core
R	0	-	-	0	0	0	+	Blue Foam Core
R	-1	+	-	-	+	-	-	Balsa Frame
S	+4	0	-	+	0	+	+	I-Beam spar
R	0	0	-	0	0	0	0	Box Beam
R	+2	+	-	0	+	0	-	Cylindrical Tube
S	+5	0	+	+	0	+	+	Semi-Monocoque
R	-2	+	0	-	0	-	0	Thin Keel
R	+1	0	-	0	0	0	+	Tricycle
S	+3	0	-	+	0	0	+	Tail Wheel
R	-2	0	-	-	0	0	0	Quad

Table 3.12 Structural Figures of Merit Chart

Propulsion FOM Chart

Decision	Sum of Rating	Battery Weight (x2)	Motor Weight (x1)	Current Draw (x1)	Thrust (x2)	RAC (x3)	(R) – Rejected (S) – Selection
S	+5	+	+	+	-	+	1 Motor / 1 (1.5lbs) Battery Pack
R	+4	0	+	0	0	+	1 Motor / 1 (2 lbs) Large Battery Pack
R	-1	0	-	+	+	-	2 Motors / 2 (1lbs) Battery Packs
R	-2	0	-	-	0	0	2 Motors / 1 (2.5lbs) Large Battery Pack

Table 3.13 Propulsion Figures of Merit Chart

4.0 Preliminary Design

With a completed general aircraft configuration, the preliminary design phase focused on design parameters and trade studies. The aerodynamic group performed trade studies to determine the wingspan, chord length, airfoil, and tail area that would optimize the design. While, the structural group determined the configuration of the wing, tail, and fuselage, along with the motor mount and landing gear. The Water Deployment System (WDS) was designed and components chosen to perform at maximum efficiency. Moreover, the propulsion group calculated the optimum propulsion system configuration by determining the minimum thrust required to complete the missions.

4.1 Aerodynamics

Once the conceptual design phase was completed, the parameters obtained by the generated primary aircraft configuration were used in the preliminary design phase to further narrow and refine the design. Trade studies were conducted to determine the wingspan, chord length, airfoil, and tail area that would optimize the design.

4.1.1 Wingspan

During the conceptual phase, the wingspan was limited by the competition rule that the aircraft must fit into a 4x2x1 foot box. Therefore, each wing section length was limited to maximum of 4 feet. Furthermore, the competition rules stipulated that the maximum take off distance was 150 feet. In order to minimize thrust and still take off within the required distance, a large wingspan was desired. Optimizing software was written in MATLAB to determine the range for the best wingspan as a function of RAC. The program determined that the optimal wing area of 8 ft² and a wingspan range of 7 to 9 ft minimized the RAC for the aircraft of 19.8 lbs.

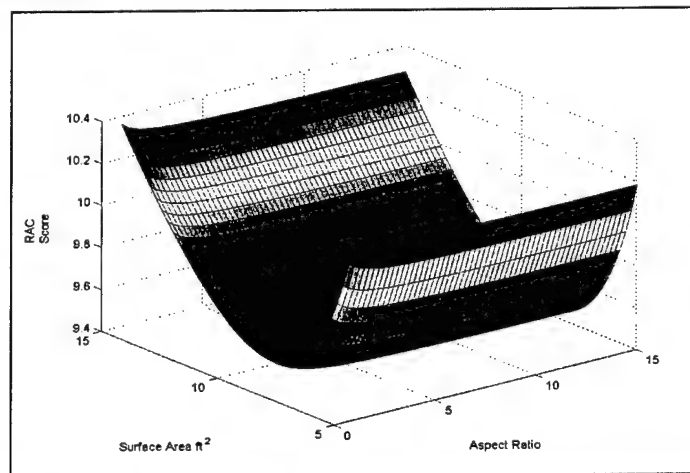


Figure 4.1 RAC Score v Surface Area and Aspect Ratio

4.1.2 Wing Chord Length

Provided a fixed wing area of 8 ft^2 the most aerodynamically efficient wing would have a very large aspect ratio (Figure 4.1). However, the span is limited to the box dimension of 4 foot sections. To simplify the manufacturability of the wings, two equal sections were considered thus limiting the span of the aircraft to 8ft with the chord length of 12 inches.

4.1.3 Airfoil Selection

In order to optimize the takeoff distance and maximize the lift to drag ratio of the wing, numerous airfoils were considered. Profili software was used as a tool to narrow the airfoil selection. Using this software, theoretical coefficients of lift and drag for the Reynolds number of 250,000 and 500,000 were calculated for 50 airfoils. In order to verify computer generated theoretical calculations, a comparison was done with actual wind tunnel results from research performed by Michel Selig. Calculations were performed to determine the total take off distance and the lift to drag ratio. The selection of the airfoil was a process of reducing the take off distance and optimizing the lift to drag ratio, thereby minimizing required thrust.

Remaining airfoils were of the class of medium high lift with fairly low drag with lift coefficient of 1.3 to 1.6 and of parasitic drag of 0.005 to 0.010. An airfoil was sought that provided a high lift to drag ratio (for the whole plane), a low stall speed and a fairly high cruise speed to be able to minimize power at takeoff and achieve the fastest time. Airfoils such as SD7062, GOE-769, E580, and S4083 were considered. S4083 was determined the best compromise between the high cruise speed (52.3) and low stall speed (39.6 ft/s) with a high lift to drag ratio of 15.3. Other airfoils provided lower stall speed but also lower lift to drag ratios meaning that the overall drag would be higher.

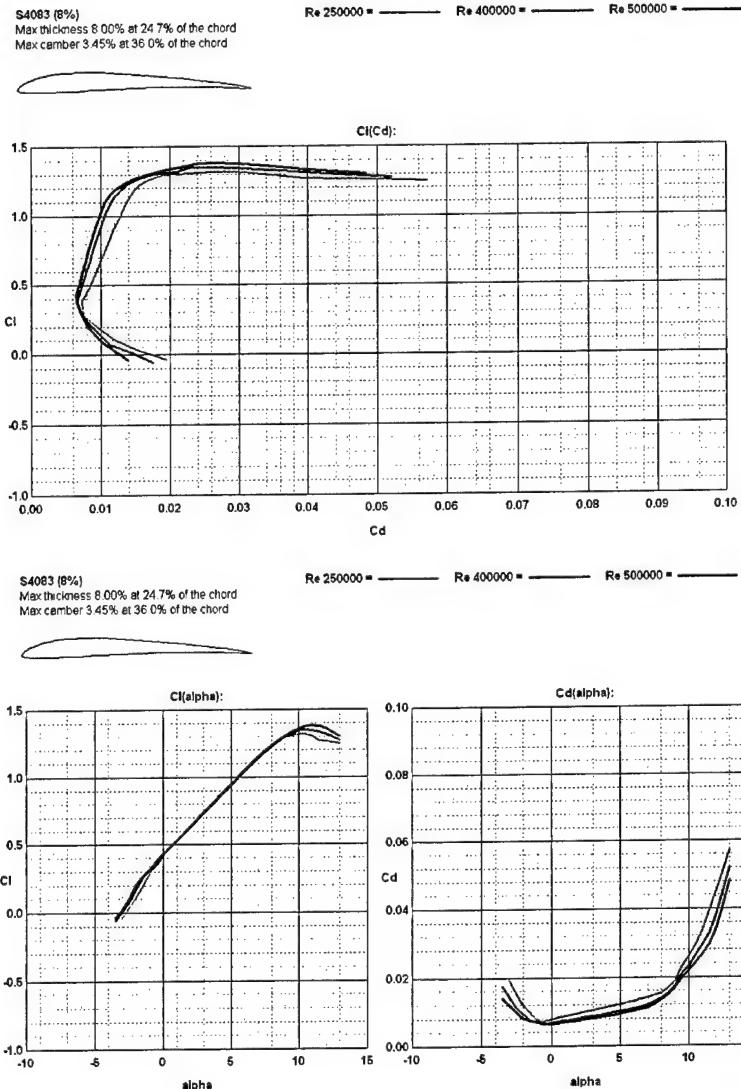


Figure 4.2 Drag Polar, CL v alpha, and Cd v alpha Curves for S4083 Airfoil

4.1.4 Tail Design

Once the wing dimensions were calculated and the airfoil was selected, calculations were performed to obtain the desired dimensions for the tail. This factor limited the height of the vertical stabilizer to 10 inches and the horizontal stabilizer to 22 inches. This coincides with the competition rules, which stipulates that the horizontal stabilizer cannot exceed a quarter of the wingspan.

In order to optimize the tail effectiveness, a boom 42 inches long was used. Numerous symmetric airfoil designs were made available. However, the NACA 0009 airfoil was immediately selected for the horizontal stabilizer because of its reduced drag and it produces zero lift at cruise (Figure 4.3). This selection improved the theoretical stability characteristics.

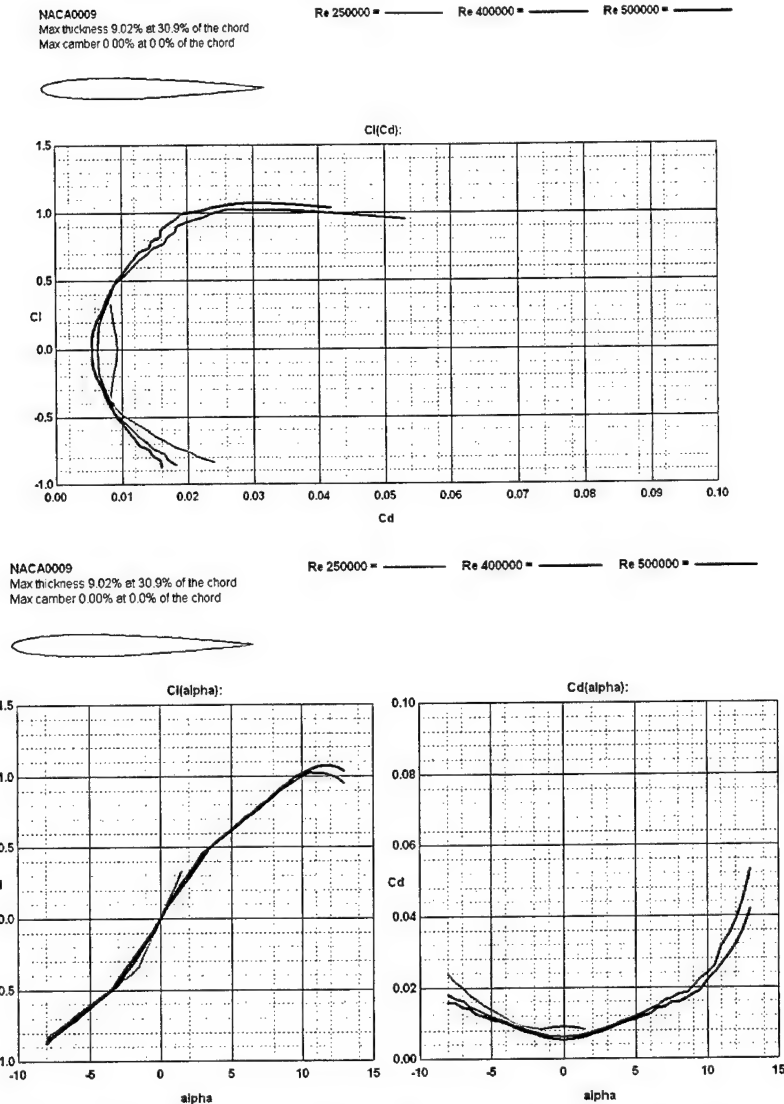


Figure 4.3 Drag Polar, CL v alpha, and Cd v alpha Curves for NACA0009 Airfoil

The stability of the aircraft was further enhanced, by optimizing the tail section area. The area was calculated with the following formulas. The volume coefficients of 0.55 and 0.031 were used for the horizontal and vertical stabilizers, respectively.

$$\text{Area}_{\text{HorizontalStabilizer}} = (\text{Coefficient}_{\text{HorizontalVolume}}) * (\text{MAC}_{\text{MainWing}}) * (\text{Area}_{\text{MainWing}}) / (\text{Arm}_{\text{HorizontalStabilizer}})$$

$$\text{Area}_{\text{VerticalStabilizer}} = (\text{Coefficient}_{\text{VerticalVolume}}) * (\text{Span}_{\text{MainWing}}) * (\text{Area}_{\text{MainWing}}) / (\text{Arm}_{\text{VerticalStabilizer}})$$

Using these empirical equations, the horizontal stabilizer and vertical stabilizer areas were calculated to be 219 inches squared and 99.5 inches squared, respectively.

The mean aerodynamic chord (MAC) for each tail section was determined using the vertical stabilizer's height, horizontal stabilizer's span, and the respective surface areas. Using a taper ratio of 0.85 (Raymer 85), an 8 inch tip chord and 11.9 inch root chord were calculated for both the horizontal and vertical stabilizers.

4.1.5 Fuselage Shape

Various shapes were considered for the fuselage. It needed to be aerodynamically efficient while being able to hold the payload. Therefore, the fuselage is shaped after a NACA0035 airfoil and constructed in three parts/modules. This airfoil is symmetric and has a thickness to chord ratio of 35 percent of the fuselage, which provides adequate aerodynamic streamlines that reduce drag and gives ample room for the payload. The Drag Polar, CL v α , and Cd v α are shown in Figure 4.4.

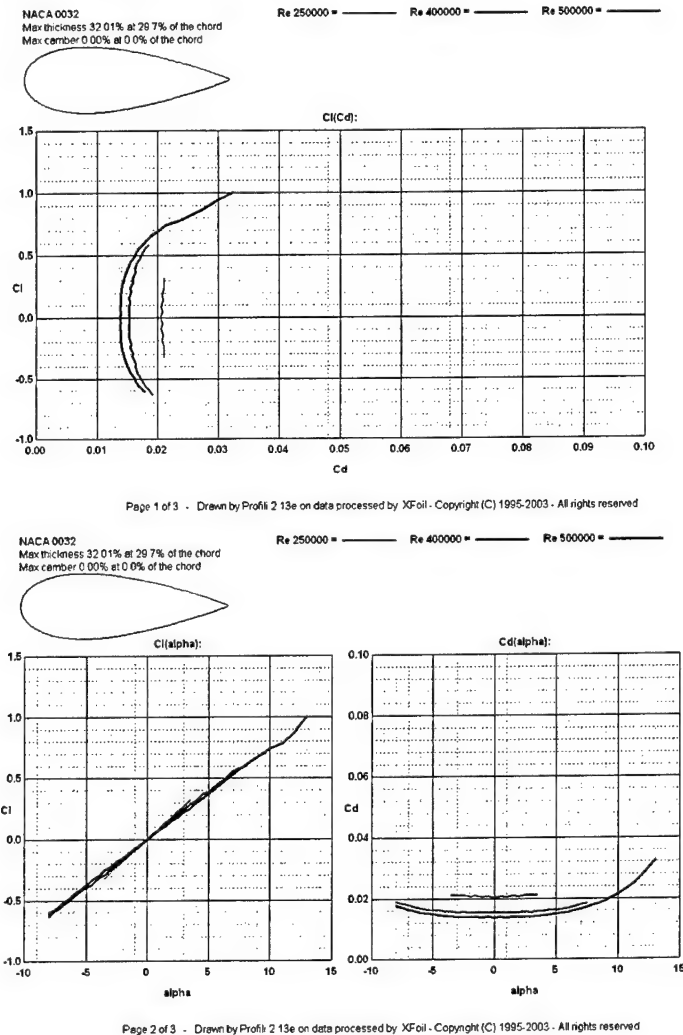


Figure 4.4 Drag Polar, CL v α , and Cd v α Curves for NACA0035 Airfoil

4.2 Structures

During the conceptual design phase the mission parameters and FOM were used to create a basic structure of the aircraft. In the preliminary design more focus was placed on the aircraft's structural requirements:

- ÷! Feasibility of primary structure locations.
- ÷! Load paths of primary structural components.
- ÷! Materials selection for said components.

- ! Sizing of components with a safety factor of 1.25 for yield and 1.5 for ultimate.
- ! Practicality of structural weight to lift available.
- ! Survivability of structure in respect to impact loads from hard landings.
- ! Manufacturability, maintenance and life cycle cost were estimated.
- ! Fit into the shipping container described in the mission profile.

Trade studies were conducted on these design requirements. These studies provided the necessary tools to investigate structural alternatives in location, applied loads, material selection, sizing, and weight of each component. They also played a part in deciding on the overall assembly of the aircraft. Estimates for the aircraft weight and center of gravity were determined. The information gained from these studies produced an aircraft structure that was sound and efficient.

4.2.1 Factor of Safety

The preliminary analysis used factors of safety to produce initial sizing. The analysis conducted to determine the aircraft's structural components optimal thicknesses were subject to factors of safety of 1.25 for yield and 1.5 for ultimate. If sizes were deemed to thin for practical purpose a margin of safety was added in the detailed design.

4.2.2 Wing Structure

The wing structure consists of two main portions, the spar and skin. Since the spar mainly resists bending and skin torsion, these two structural elements were individually analyzed.

The two loading cases determined the tapered shape of the spar: distributed aerodynamic loading and a point load applied at the tip during the wing test. The distributed load was analyzed using Shrenks approximation. These two cases generate different bending moments, as seen in Figure 4.5.

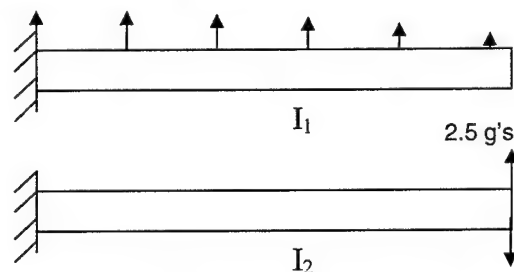


Figure 4.5 Distributed and point loads.

The incorporation of these resulted in the tapered pattern shown in Figure 4.6. The spanwise taper of the spar gives a better strength to weight ratio for the given loading cases. During the preliminary analysis of the spar structure, the bending moment due to the point load of the landing gear was considered to be insignificant compared to the bending moment of the distributed load; therefore, it is not considered separately.

The preliminary thickness needed for the composite spar was calculated by modeling the minimum thickness needed for the spar while retaining a factor of safety of 1.5 is 0.0045 inches for the top and bottom layer.

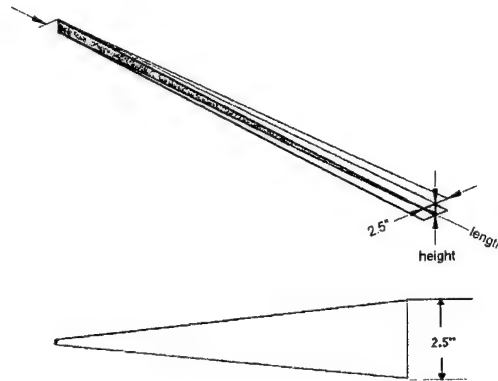


Figure 4.6 Illustration of spanwise profile of the spar.

The primary requirement of the skin is to provide the smooth surface designed by the aerodynamics group and also serve as a platform for the control surfaces. The skin also needs to be as light as possible for overall aircraft performance, while still transferring the torsional loads to the wing joiner. A fiberglass resin matrix was chosen to build the skin. This would give a hard and smooth aerodynamic surface, has an acceptable strength to weight ratio, and is easy to manufacture to the shape of the airfoil.

The wing skin was analyzed using a MATLAB script. The worst case aerodynamic loading was assumed in sizing the thickness of the skin. The wing skin was considered a closed single cell web in torsion. The shape of the actual airfoil was used in the analysis. The preliminary thickness required with a factor of safety of 2.0 is 0.025 inches. The preliminary thickness being very small requires that a larger thickness be used so that the skin can be manufactured accurately. This will increase the factor of safety and should not have a great effect on the final weight of the wing.

4.2.3 Wing Joiner/Central Platform

The central platform is the main load bearing component of the structure, acting as the wing joiner, supports the payload, and attaches the motor mount to the structure. The platform is found at the root of the wing where it experiences both torsion and bending loads; therefore, both types of loading were analyzed.

Once the wing span and configuration was determined, it became necessary that the central platform be used as the method by which the wings attach to the fuselage. The central platform is shaped (Figure 4.7) so that the wings can simply be attached to a hard point in the wing. Its length reaches into the span and four bolts fasten each wing to the fuselage.

Since the central platform is the main structural link between the wings, payload bay, and motor, strength is a major issue. The platform was first thought to be constructed of carbon-foam-carbon sandwich structure. However if the payload hold began to leak in flight, the foam may become wet

and the structure fail. Therefore, a single carbon laminate was used for precaution. The critical thickness of the platform was determined by modeling the platform as a flat plate. By applying point loads when considering the wings, landing gear, and tail boom a laminate thickness of 0.096 inches was found. Loads that were not considered in the calculation were the torque caused by the motor and empennage. These will be considered in a Finite Element Model (FEA) done during the Detailed Design.

The spar which is made of carbon fiber will be adhered to a hard-point to ensure complete transfer of loads to the central platform.

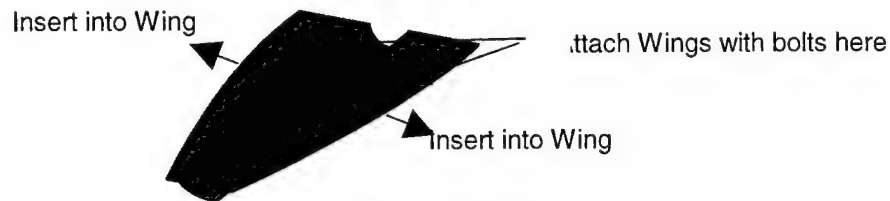


Figure 4.7 Central Platform

4.2.4 Tail Configuration

The primary purpose of the tail is to act as a platform for control surfaces and enhance stability. Three load paths were assumed critical in the design: boom, vertical and horizontal stabilizer. As shown in Figure 4.8, loads were transferred from the stabilizers causing bending and torsion, which were the main forces acting on the boom. The loads applied to these stabilizers were similar to the main wing loads and, therefore, were modeled in a similar fashion.

Two designs were considered for the boom, a truss and a beam. Due to manufacturing limitations, the truss was deemed too complicated and unreliable. Therefore, a beam design was chosen. Several beam cross-sections were considered: square and solid, square and hollow, circular and solid, and circular and hollow. These cross sections were analyzed using the figures of merit: ease of manufacture, plane bending to weight ratio, out of plane bending to weight ratio, torsion to weight ratio, and durability (Table 4.1). The FOMs were compared using a comparative system consisting of +, 0, and - (good, satisfactory, and unsatisfactory, respectively). The ease of manufacture and durability were given a weight of one, while the "plane bending to weight ratio", "out of plane bending to weight ratio", and "torsion to weight ratio" were given a weight of two because of their overall effect on the aircrafts performance.

Figure of Merit (x weighting)							
(R) – Rejected (S) – Selected	Ease of Manufacture (x1)	Plane Bending to Weight Ratio (x2)	Out of Plane Bending to Weight Ratio (x2)	Torsion to Weight ratio (x2)	Durability (x1)	Sum of Ratings	Decision
	+	+	-	-	+	0	R
	+	+	-	0	0	+1	R
	-	-	+	+	+	+2	R
	-	0	+	+	0	+3	S

Table 4.1 FOM of Cross Section Selection for Tail Beam.

After the analysis was complete, the circular hollow tube design was considered the most efficient because of its weight and ability to handle the predicted loads. With forces acting in different directions, a circular tube is desirable because it has uniform behavior. The hollow configuration was chosen instead of the solid configuration in order to lighten the aircraft structure and move the inertial mass away from the neutral axis. The radius arm of the cross section is responsible for the ability of the hollow tube to take torsion loads without weight penalty associated with the solid tube. This produced greater bending and torsion stiffness in reference to a minimized cross sectional area.

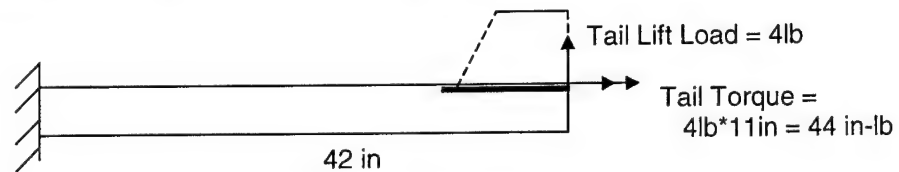


Figure 4.8 Tail Boom Load Model.

Due to availability of material, a boom with an outside diameter of 0.5 inches was selected, while the inner diameter was found through calculations. Using Figure 4.8, two trade studies were performed in order to determine the inner diameter of the boom. The first trade study investigated bending. The boom was modeled as a cantilever beam with a 4 pound point load 42 inches from the quarter chord. By analyzing the stresses through the cross section of the loaded member, the minimum inner cross sectional diameter was found to be 0.4966 inches. The second trade study focused on torsion loads. The torsion of the boom was modeled as a 4 pound side load located at the top of the rudder 11 inches away from the tail boom. By studying the torque applied at the tail, the resulting minimum required inner diameter was found to be 0.4985 inches. Since the inner diameter found in the first case study is smaller than that found in the second, it is deemed the critical inner diameter.

Trade studies conducted on model aircraft tail structures led to the selection of a single vertical and bottom mounted horizontal stabilizer. The studies showed that most tail structures do not contain a spar and are usually comprised of a foam core with fiberglass skin. However, performance aircraft increased bending stiffness by adding a small amount of carbon fiber tow to the top and bottom of the quarter chord. Due to the nature of the competition, the performance aircraft tail structure was selected. The skin thicknesses of the stabilizers were determined by the same modeling as the main wing. The required thickness was calculated to be 0.015 inches of +/- 45 degree fiber glass.

4.2.5 Fuselage Structure

The fuselage is considered the primary load bearing structure, housing the payload, batteries, central platform, tail boom, and motor mount. The main component that is loaded is the central platform, which is used as a wing joiner, payload support, and motor mount attachment. The internal structure of the fuselage is shown in Figure 4.9.

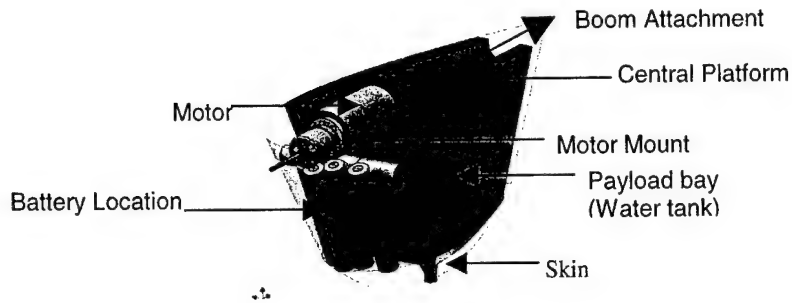


Figure 4.9 Internal Structure of Fuselage

All of the loads from the motor, boom, wings, landing gear servo, and payload will be transferred through the single platform.

The skin of the fuselage was initially to be made as a sandwich structure to save weight, however such thin sheets of carbon can be porous so a single carbon laminate was decided upon. The only section of the payload volume that may deform critically under the weight of water is the face that is perpendicular to the wingspan. Therefore, this face will be modeled as a flat plat and analyzed during the Detailed Design.

4.2.6 Aircraft Weight and Center of Gravity

After the fuselage platform components were initially sized, Autodesk Inventor was used to create a solid model. By inputting the material properties of each element into this computer-generated model, the mass and its specific center of gravity for each component were determined.

The estimated empty weight of the aircraft was 9.5 pounds. This value does not include the 8.8 pounds of water payload and 1.5 pounds of battery. The fully loaded aircraft weight was estimated to be 19.8 pounds and the center of gravity was found to be approximately 0.10 inches in front of the quarter cord.

Much attention was focused on the change in center of gravity during payload release. For this reason the center of gravity for the payload was placed under the center of gravity for the empty weighted aircraft. If the payload's center of gravity were to shift before or aft the empty weighted aircraft, the pilot would need to trim the control surfaces which take energy from the system reducing its efficiency.

4.2.7 Water Deployment System (WDS)

During the conceptual design phase it was decided that a circular valve would be used. However, during the preliminary design phase testing was done in order to verify this decision. Several valve designs (gate valve, ball valve, and cylindrical valve) were considered for payload delivery. Some were tested to evaluate their effectiveness and reliability. Because our final score depends partially on the time that it takes to deliver the payload, the chosen valve must open quickly. Flight time can also be penalized heavily if any water is released after a certain point in the mission; therefore, this valve must also close quickly and effectively.

Through testing (See Research and Testing Plan), a cylindrical valve was determined to be the most effective. It was concluded that the valve would have a tapered cylinder with a matching tapered receptacle (Figure 4.10). A spring was added to draw the two tapered pieces closer together, providing a good seal.

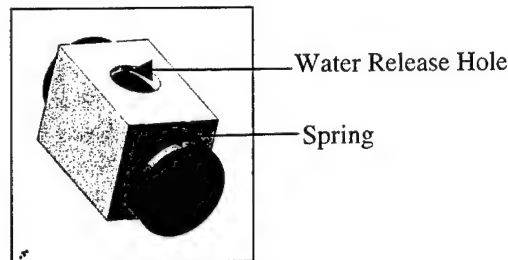


Figure 4.10 Cylindrical Valve

When water begins to flow out of the payload chamber a vacuum will be created unless the volume lost is replaced with another fluid. To offset this affect, a hatch will be opened synchronous with the tapered cylinder valve to allow air to fill the void. This hatch should be aligned with the onset of air to assist the outflow of water by creating a small amount of dynamic pressure.

The mission profile requires that the aircraft's payload be refilled during the mission. The time that it takes to fill the water tank is part of the flight score. To speedily refill the water tank two holes atop the fuselage will accept a fitting made from a two liter soda bottle cap. The same dilemma of a vacuum being created exists for emptying the soda bottles as does the water tank. While rules specify that the two liter soda bottle can not be modified, the bottle cap may. A tube with a single one way valve should reach the height of the bottle in its refill position (Figure 4.11). This should relieve the negative pressure caused by the outflow of water. Water pumps are being considered to assist in the refill process.

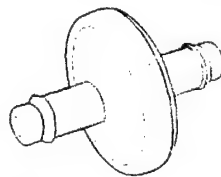


Figure 4.11 Bottle Cap Vacuum Release Valve

4.2.8 Motor Mount

A trade study was preformed taking into account the thrust and landing loads that were transferred to the primary structure. It was found that these loads should be transferred through carbon mounting plate in order to assure the durability of the aircraft. The motor is attached to a pre-impregnated Kevlar motor mount and the motor mount is then attached to the central platform as seen in Figure 4.12. The material was chosen for its thermodynamic properties and resistance to shear from load bearing holes in its structure. It is also believed that the mount is an aircraft saving device due to its ability to fail at high impact loads. This quality would theoretically save the motor in the event of a low speed nose impact.

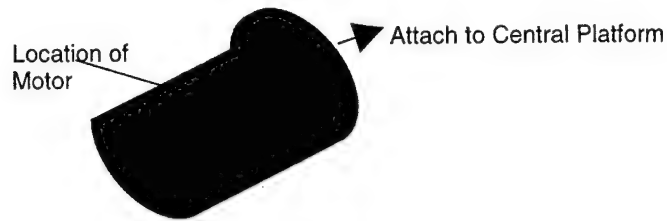


Figure 4.12 Motor Mount

4.2.9 Landing Gear

During conceptual design a tail dragging landing assembly was selected. Selecting this type of landing gear configuration is critical for refilling of the water tank. While the payload is being refilled, air in the payload bay must escape. Using a tail dragger allows for the nose of the aircraft to be pitched upwards, allowing of the air to escape. If there is any air trapped in the payload bay, the total desired volume of water will not fit.

The main landing gear was designed to mount between the wing and the central platform (Figure 4.13). This design was chosen for its simplicity and for structural integrity. Mounting the landing gear on the wings was also considered. However, aircraft with wing mounted landing gear often have problems with structural integrity during landing. When experiencing a hard landing which exceeds the designed load factor, the wings may break due to impact and the aircraft may be unable to complete the mission.

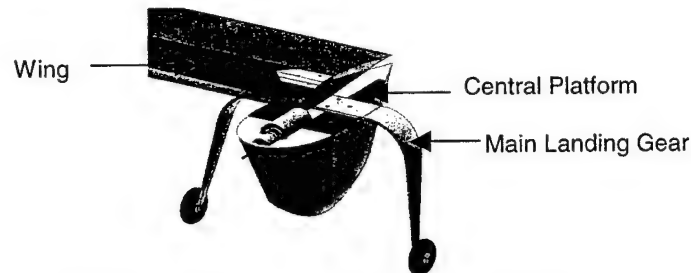


Figure 4.13 Main Landing Gear Placements

When analyzing the landing gear, a five g-loading profile was assumed because the wind gusts at the location of competition are known to rise to 30 miles per hour. The landing gear was modeled as a flat plate and showed that the gear be made of 10 plies of carbon fiber at zero degrees. In the Detailed design this number is verified with a finite element model.

4.3 Propulsion

During the preliminary design, the minimum required thrust to complete the missions was calculated and the optimum propulsion system configuration was found. Since, takeoff requires the most power throughout the mission; it was used to establish the minimum required thrust. The required thrust of 5.7 pounds was calculated using the aircraft weight and wing geometry combined with the maximum takeoff distance. It was imperative to find a propulsion system configuration that would provide a minimum of 5.7 pounds of thrust and draw less than 40 amps of current, which was stipulated by competition guidelines. A gear box is used to lower current draw and allow for a larger propeller to achieve the required thrust.

In the conceptual design, the propulsion system was determined to have a single motor with an approximate 1.5 pound battery pack. According to competition rules a Graupner or Astro motor must be used. From past experience and success, a motor from the Graupner 3300 series was chosen. These motors are known to be reliable and demonstrate high performance.

The Graupner 3300 series offer motors with different numbers of windings, which allow peak efficiencies at different voltages. MotorCalc software was used to determine the best combination of propeller geometry, battery cells, and engine windings. Each configuration's pitch speed, flight time, and current were calculated. Some of the chosen configurations are found in Table 4.2.

Motor and Battery Configuration							
# of Winding	Gear Ratio	# of cells	Pitch Speed (mph)	Flight Time	Propeller Geometry	Thrust (oz)	Current (Amps)
5	2.5:1	16	71.9	1:53	16x16	92	41.2
5	2.5:1	16	52.1	1:43	18x12	127	45.6
6	2.5:1	16	57.9	2:05	18x16	95	37.4
6	2.5:1	18	65.8	2:02	17x16	98	38.2
6	2.5:1	18	62.0	1:52	18x16	109	42.2
7	2:1	16	57.9	2:37	17x16	75.6	29.9
7	2:1	18	57.3	2:10	18x16	93	36.1

Table 4.2 Graupner Motor 3300 series

The optimum propulsion system for this competition has high static thrust, high pitch speed, long flight time, and minimal battery weight while abiding by competition regulations. Gear ratio, propeller diameter and pitch and number of cells are optimized to get the desired values of thrust, flight time and pitch speed. Large diameter propeller provides large static thrust yet low pitch speed. Gearing is used to achieve highest efficiency for the propeller thus increasing flight time. By analyzing the MotorCalc results (Table 4.2), the Graupner 3300-7 motor with a two to one gearbox coupled with 18 Sanyo 1300 mAh cells and 18x16 inch propeller was chosen to achieve the desired thrust of 5.8 pounds resulting in a pitch speed of 57.3 mph. This configuration offered a reasonably high static thrust, high pitch speed, and sufficient flight time while drawing less than 40 Amps; therefore, offering the optimum performance.

4.4 Final Aircraft Configuration

At the conclusion of the preliminary design, the design parameters and sizing trades had all been investigated and the final aircraft component selection and systems architecture was ready to be selected. The preliminary design determined the sizing of the wing and tail geometry, primary structure dimensions, and propulsion configuration. The wingspan and chord length were calculated to be 8 feet and 12 inches, respectively. The S4083 airfoil was selected for the wing, while the NACA0009 was chosen for the tail. The most efficient shape for the spar was found to have a spanwise taper. The aircraft's takeoff weight was found to be approximately 19.8 pounds and the center of gravity was determined to be 1.5 inches behind the leading edge of the wing. An 18 inch diameter propeller with a 16 inch pitch, Graupner 3300-7 motor, and 18 Sanyo 1300 cells compose the propulsion system.

5.0 Detailed Design

With the information gained from the preliminary design phase, a foundation was laid for finalizing component and system architecture selection. The aerodynamics group calculated final wing and tail geometry while the structures group finalized the design of the spar, central platform, and payload bay. The structures group also conducted a detailed analysis of the internal architecture of the fuselage and the propulsion group determined the propeller, motor, and battery cell optimal configuration.

5.1 Aerodynamics

Based on the design parameters and sizing trades investigated during the preliminary design phase, performance characteristics were determined and modified to achieve the mission specifications.

5.1.1 Mission Profile and Flight Performance

The aerodynamic detailed design focused on the mission profiles, which were outlined in the conceptual design phase. In order to optimize the final time and flight score, and hence, the final score, each mission was analyzed for both conventional and performance flight modes:

- ➦ Conventional mode: The conventional mode focuses on flight efficiency, minimizing the number of batteries used.
- ➦ Performance mode: The performance mode was dominated by the concept of maximizing airspeed in order to minimize flight time.

In order to calculate flight time, each mission was profiled by the aircraft's cruise speed, maximum velocity, turn rate, and climb rate, which were determined from the wing geometry, weight, and thrust. Performing numerous calculations (Raymer 27-110), the cruise and maximum velocities were found to be 57.1 and 84.0 feet per second, respectively. Similarly the turn and climb rates were calculated to be 76.8 degrees per second and 14.2 feet per second, respectively. Each mission flight time was then calculated from these numbers.

The estimated flight times and resulting scores are found in Table 5.1. All of the missions were evaluated with no wind conditions at Standard Temperature and Pressure (STP) and all flight scores included an estimated one-minute assembly time.

Mission (x difficulty factor)	Mission Profiling Matrix				
	Conventional		Performance		Escore
	Time (min : sec)	Flight Score	Time	Flight Score	
Fire Fight (2x)	2:16	7.820	2:03	8.786	.966
Ferry (1x)	2:09	0.467	1:41	0.597	.13

Table 5.1 Evaluation of the mission times and flight modes

The two mission flight scores were compared in both conventional and performance modes. In each case, water drop flight scores received the highest flight score. Therefore, this proves the initial assumption that the mission with the most difficulty offered higher scoring potential was correct. This is true whether the aircraft flies in conventional or performance mode.

As shown in Table 5.1, each mission's flight score increased while flying in performance mode. The Fire Fight mission's flight score increased over 10% with the implementation of high performance maneuvering. While not to the same degree as the Fire Fight mission, the Ferry mission flight score also increase while flying in performance mode. Therefore, it was deemed that the performance mode increases the flight score. However, this does not automatically mean that the performance mode will optimize the final score.

The RACs of the two different flight modes were calculated for both missions. While the performance mode reduced flight time, it also required high battery capacitance and weight, thereby penalizing the RAC. The conventional flight and performance modes yielded RACs of 8.02 and 8.332, respectively. However, although the RAC yielded by the conventional flight mode is better than that yielded by the performance mode, the final scores received by these modes with RAC effects were determined to be 96.8 and 105.3, respectively. Therefore, it was determined that high performance mode would increase the overall final score.

5.1.2 Takeoff Distance

Calculations were preformed to determine the aircrafts takeoff distance. Using an estimated stall speed of 44.1 feet per second, the takeoff speed was found to be 48.5 feet per second. For low Reynolds numbers, (250,000 based on mean chord), induced drag is neglected. Therefore, by integrating the ground acceleration (Raymer 565) into Newton's second law, the takeoff distance was found. In order to account for the ground roll, the takeoff distance was increased by 10 percent. A ground-roll distance of 134.7 feet was achieved with an estimated 6.0 pounds of thrust calculated by the propulsion group.

5.1.3 Stability and Control

An aircraft's stability is defined by its ability to return to equilibrium after experiencing a small perturbation. Static stability is a prerequisite for dynamic stability. Pitch stability corrects pitch deflections through a relationship between the main wing and the horizontal stabilizer. For an aircraft to be considered stable the calculated static margin is required to be between 0.25-0.35 of the chord. Yet this will provide an extremely stable aircraft which will require a lot of control effort to turn. Since this competition is performance oriented, a relaxed stability margin of 0.10-0.15 was selected. This relationship determined aerodynamic center to be 1.5 inches behind the center of gravity. Therefore, the airplane proves to be stable, yet maneuverable, as required for the competition. Roll stability was achieved by implementing the high wing design.

Dynamic stability necessitated the placement of the payload cg at the cg of the aircraft, thus restricting the cg movement to a minimum. Furthermore, the restriction of placement of the total cg of the aircraft on the quarter cord provided that the pitching moment of the aircraft would not change during water release portion of the flight.

5.1.4 Control Surface Sizing

To achieve good control characteristics of the aircraft proper control surface sizing is imperative. Using historical guidelines, aileron chord was selected to be 0.2 of the cord or 2 inches and the aileron span to be 0.54 of the cord or 26 inches (Raymer 126-128). Rudder was found to be 9in high and 5in wide fulfilling the guidelines of 90% vertical tail span and 50% chord. Lastly, the guidelines for the elevator are 90% of the span and up to 30% of the chord. The actual size of the elevator was found to be 22in in span and 3 inches in chord. The extension of the elevator span was done to simplify the manufacturability of the tail section.

Pitch stability corrects pitch deflections through a relationship between the main wing and the horizontal stabilizer. For an aircraft to be considered stable the calculated static margin is required to be between 0.15-0.20 of the chord. This relationship, determined by the positions of the center of gravity and the aerodynamic center, was found to be 1.5 inches. Therefore, the airplane proves to be stable, yet maneuverable, as required for the competition. Roll stability was achieved by implementing the high wing design.

5.2 Structures

The structural detailed design focused on the component and systems architecture selection. Integrating and sizing dimensions in order to obtain a proper aircraft load distribution dominated this phase. The main parameter was meeting the competition requirement that the aircraft fit within a 4x2x1 foot container.

5.2.1 Wing Structure

The two load carrying components of the wing are the spar and skin. For analysis, the spar was modeled as a cantilever beam, while the skin was modeled as a shear web. The foam, not being directly in the load path, was not separately modeled.

The spar is designed to transfer the bending forces applied to the wing onto the central platform. The loading of the spar was broken into two cases, a distributed load approximating the maximum aerodynamic loading during flight and a point load representing the load seen during the judge's wing test. This load is taken into separate consideration since the wing will deflect differently than it will during natural distributed aerodynamic loading. MSC-Patran was used to create a finite element model (Figure 5.1). After much iteration an optimal laminate was chosen. Four layers of uni-directional carbon were used in the vertical section of the I-beam, and three layers for each top and bottom horizontal section.

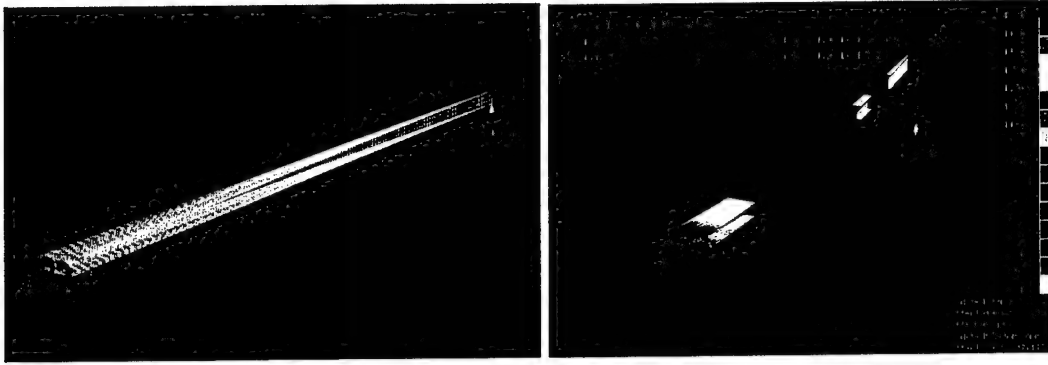


Figure 5.1 von Mises Stress and Displacement of Spar

The wing skin thickness required for a factor of safety of 1.5 was too small to be manufactured properly. Using MATLAB script, the actual manufactured thickness of 0.01 inches was found, which is two plies of fiber glass.

5.2.2 Tail Configuration

The structural detailed design of the tail section was focused on the component integration of the fuselage, boom, tail and sizing dimensions (Figure 5.2). The boom is designed to attach to the central platform which is the key load carrying component in the fuselage.

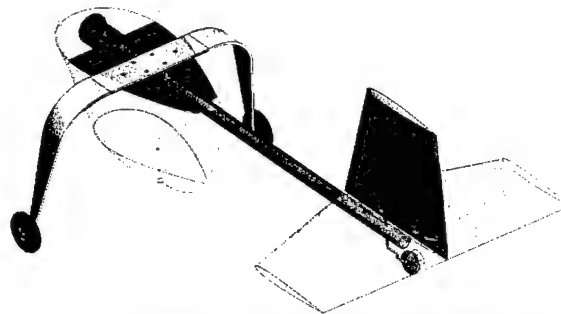


Figure 5.2 Integrated Tail Assembly.

A boom was designed with a 0.5 inch outer diameter and a 0.4966 inch inner diameter. However, a pre-made shaft was selected because of the complexity of manufacturing one from carbon fiber. Unfortunately, a shaft with these dimensions could not be obtained. Therefore, a 0.9 inch shaft with an inner diameter of 0.8 was chosen. The geometry of the boom was verified by applying the estimated loads to the model discussed in the preliminary design. The resulting factor of safety is order of magnitudes greater than that required.

In order to attach the empennage to the boom, analysis was conducted to see how many screws it would take to ensure that the tail stay attached. It was deemed that three bolts were necessary. The horizontal was sandwiched between the vertical and boom. In order to ensure a secure fit, the boom was attached to a hardpoint found in the vertical tail (Figure 5.2). The hardpoint was adhered to the foam and skin of the vertical using cavicol.

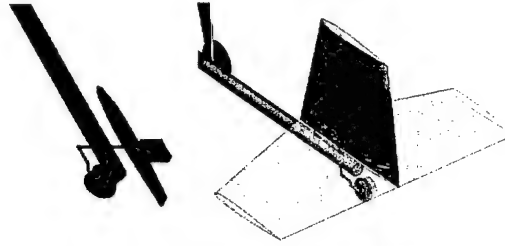


Figure 5.2 Tail Configuration.

While deciding on how the tail should attach to the boom, concerns were addressed about the possibility of a crash damaging the structure. Therefore, nylon screws that shear in the event of a crash were selected in order to absorb damaging kinetic energy.

Two servos were used to power the control surfaces; one was used for the rudder and the other for the elevator. They are connected to the batteries via a wire harnesses also designed to shear.

5.2.3 Fuselage Structure

The detail design of the fuselage focuses on the placement of the CG and the dimensioning of its internal components. The placement of the aircrafts internal components must be placed with precision and accuracy. However, the internal components of the fuselage must also be able to withstand the applied loads. Within the fuselage, the main internal load bearing structure is the central platform. The integration of all aircraft components are found in Figure 5.3.

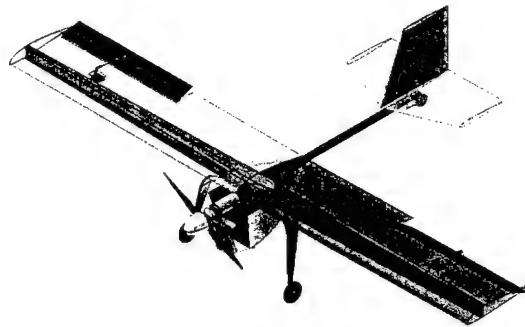


Figure 5.3 Structural Component Integration

There is ample room for the placement of the batteries, receiver and WDS within the fuselage because of the shape which selected in the conceptual design phase. With the receiver and WDS locations fixed, the CG was able to be placed on the quarter chord by locating the 1.35 lb battery pack in approximately 7.5 inches in front of the quarter chord. However, if the actual CG location is inconsistent with the theoretical location due to liberties taken in manufacturing, the batteries can be adjusted shifting the CG closer to its proper location. Due to the placement of the WDS, the CG remains at the same location before and after the payload drop.

As described in the preliminary structural design, the central platform is to absorb all dynamic loads. Because the platform will be exposed to water, this component must not allow water to leak. Therefore a sandwich structure made of carbon-foam-carbon will not be used; instead a single thicker

laminate will be used. In order to verify the thicknesses found during preliminary design, a model of the platform was generated with MSC-Patran software (Figure 5.4). The model, however conservative, encompasses the loads generated during a high speed jerk pull up maneuver (approximately 5g's). By applying the proper loads to this model and a factor of safety of 1.5, an iterative process determined the desired material thickness to be six layers of carbon fiber, approximately 0.078 inches thick. The model experiences a maximum stress of 1.3×10^4 psi at the location of the bolt holes (Figure 5.4).



Figure 5.4 von Mises Stress and Displacement of Platform

As discussed in the preliminary design, the fuselage/water tank is also made of carbon fiber. During modeling, a wall thickness of four plies of carbon laminate was determined. In order to reduce the number of plies, tension bars were integrated to the fuselage at points of highest stress. This lowered the number of plies necessary for the water tank walls to three plies of carbon laminate.

5.2.4 Water Deployment System (WDS)

The water deployment system consists of three major components, the servo controller, cowling and tapered cylindrical valve (Figure 5.5). From the closed position the valve must turn 90 degrees to fully open. From wind tunnel testing, the cowling must rotate approximately 15 degrees to allow the pressure to be minimized. Therefore, the rods', located on the servo arm, orientations must differ in order to achieve the different rotations necessary for each mechanism.

The servo controller rotates the servo-arm which activates the cowling and valve simultaneously via small diameter threaded rods. An additional arm is attached to each mechanism and accepts the threaded rod via threaded receptacles which are allowed to rotate within the mechanism arm. This configuration will allow each mechanism to be "fine tuned".

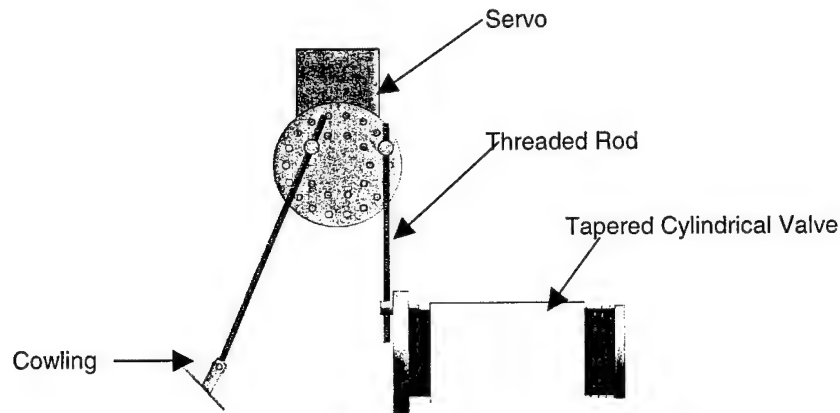


Figure 5.5 WDS Valve Mechanisms

5.3 Propulsion

The final propulsion system was selected from comparing both actual and analytical results. There were discrepancies in the dynamometer results and those calculated using MotorCalc software. The MotorCalc efficiency of the Graupner 3300-7 motor was 67% for the configuration chosen, while the dynamometer efficiency results were over 85%. With the actual efficiency being higher, the thrust output is expected to increase. The mission profiling provided the overall usage of power during mission. For the firefighting mission the Sanyo 1300SCR will provide more than sufficient power for the mission. The energy stored in the batteries is barely sufficient to complete the ferry mission.

5.4 Final Aircraft Configuration

The final configuration was an aircraft with a high-wing, and a moderate aspect ratio of 9.60. Additionally the wings contained no sweep or taper because of the increased cost with negligible increase in performance. The aircraft had good gliding capabilities because of high 15.32 lift to drag ratio. The fuselage was shaped like a tapered and swept wing giving a minimal drag penalty. The tail section was a conventional T-tail with span of 22 inches and height of 11 inches. The landing gear was a tail dragger configuration with the main wheels 2.48 inches behind the CG with an aircraft ground clearance of approximately 1.88 inches. These dimensions were considered necessary so the fuselage does not scrape should a hard impact landing occur. The propulsion system is made up of a Graupner 3300-7 motor, 18x16 propeller, and 18 Sanyo cells. The aircraft breaks down into four individual modules when placed in shipping mode: two wings, fuselage and tail boom.

5.5 Final Aircraft Configuration Calculations (Table 5.2)

Geometry

Aircraft Length	47.6 in
Aircraft Span	96 in
Aircraft Height	19.5 in
Main Wing Configuration	High Mono-Wing
Main Wing Airfoil	S4083
Main Wing Area	960 in ²
Taper Ratio	1
Aspect Ratio	9.60
Main Wing Control Area	90 in ² per wing
Horizontal Stabilizer Area	218.9 in ²
Vertical Stabilizer Area	99.5 in ²
Tail Airfoil	NACA 0009
Horizontal Stabilizer Control Area	66 in ²
Vertical Stabilizer Control Area	45 in ²

Performance

CL max (actual)	1.151
L/D max (actual)	15.32
Maximum Rate of Climb	14.43 ft/sec
Stall Speed	44.1 ft/sec
Takeoff Speed	48.5 ft/sec
Cruise Speed	57.1 ft/sec
Maximum Speed	84.0 ft/sec
Takeoff Distance Loaded (Ground Roll)	149 ft
Takeoff Distance Unloaded (Ground Roll)	74 ft

Weight Statement

Airframe Weight	9.04 lbs
Manufacturer's Empty Weight	10.39 lbs
Payload (4 Liters of Water)	8.80 lbs
Battery Weight	1.35 lbs
Motor Weight	1.90 lbs
Control System	0.75 lbs
Takeoff Gross Weight	19.19 lbs

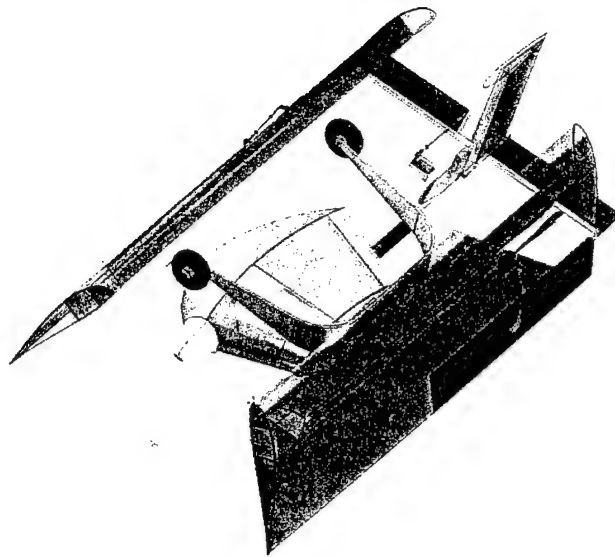
Systems

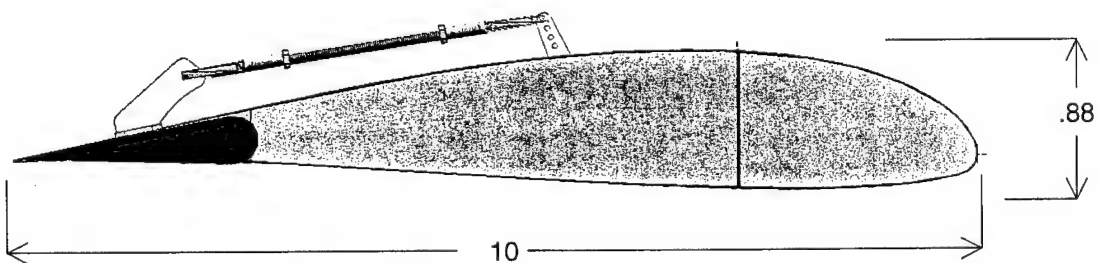
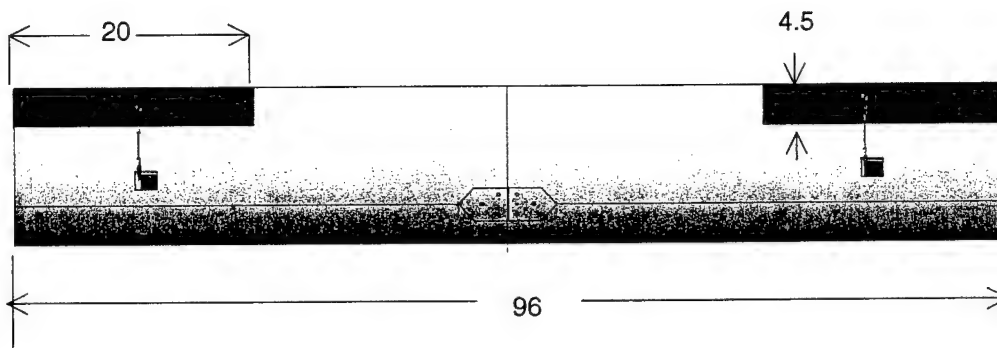
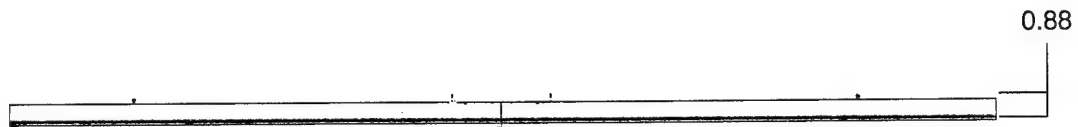
Motor	1 x Graupner 3300-7
Propeller	18x16 thin carbon prop
Gear-ratio	(2:1)
Batteries	Sanyo 1300 (18 cells)
Servos	HS-225MG (2), HS-545BB (2)
Receiver	HPD-07RB (PCM)
Handset	Prism 7X (PCM)

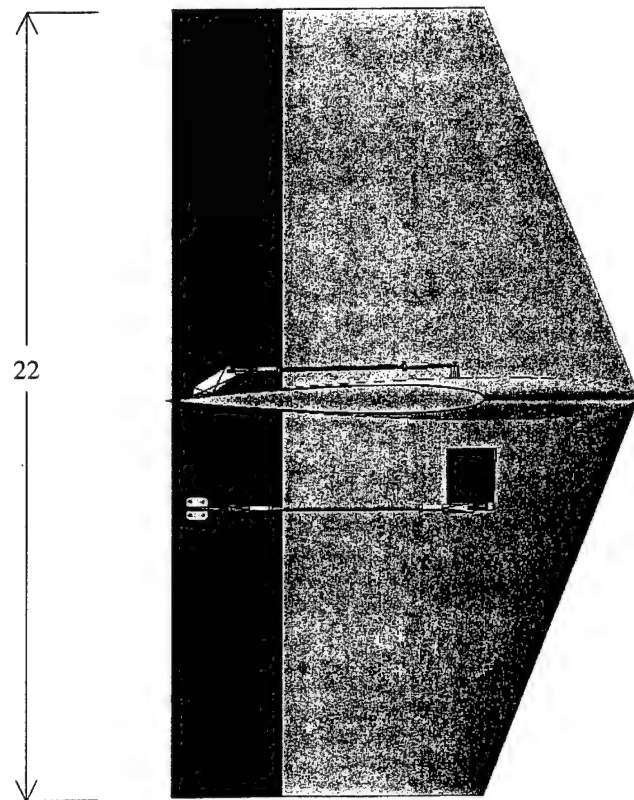
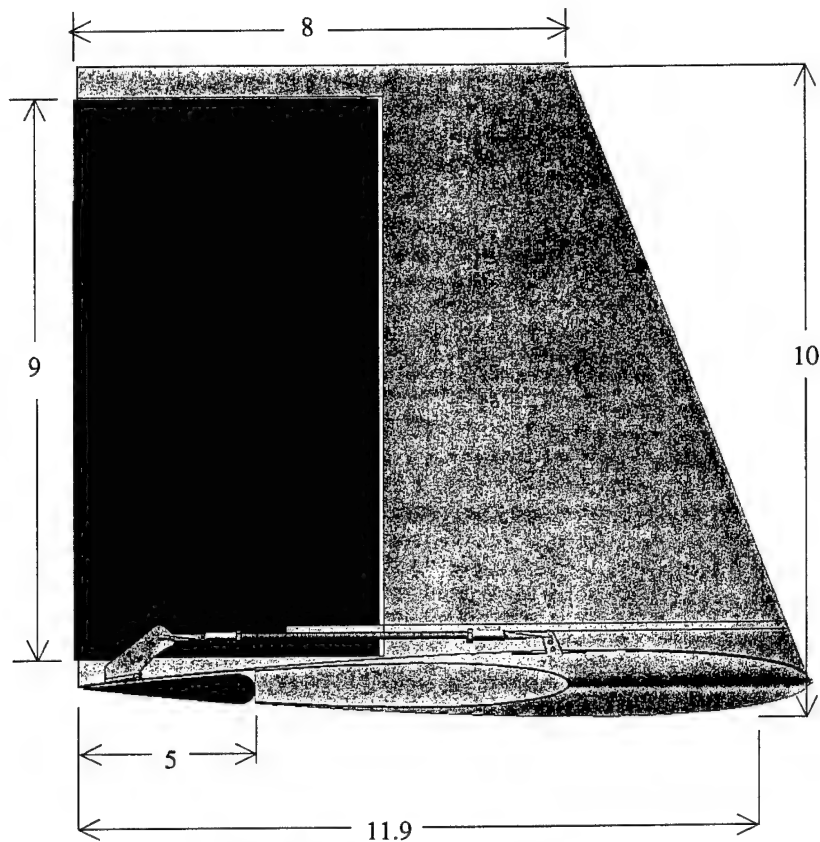
5.6 Rated Aircraft Cost

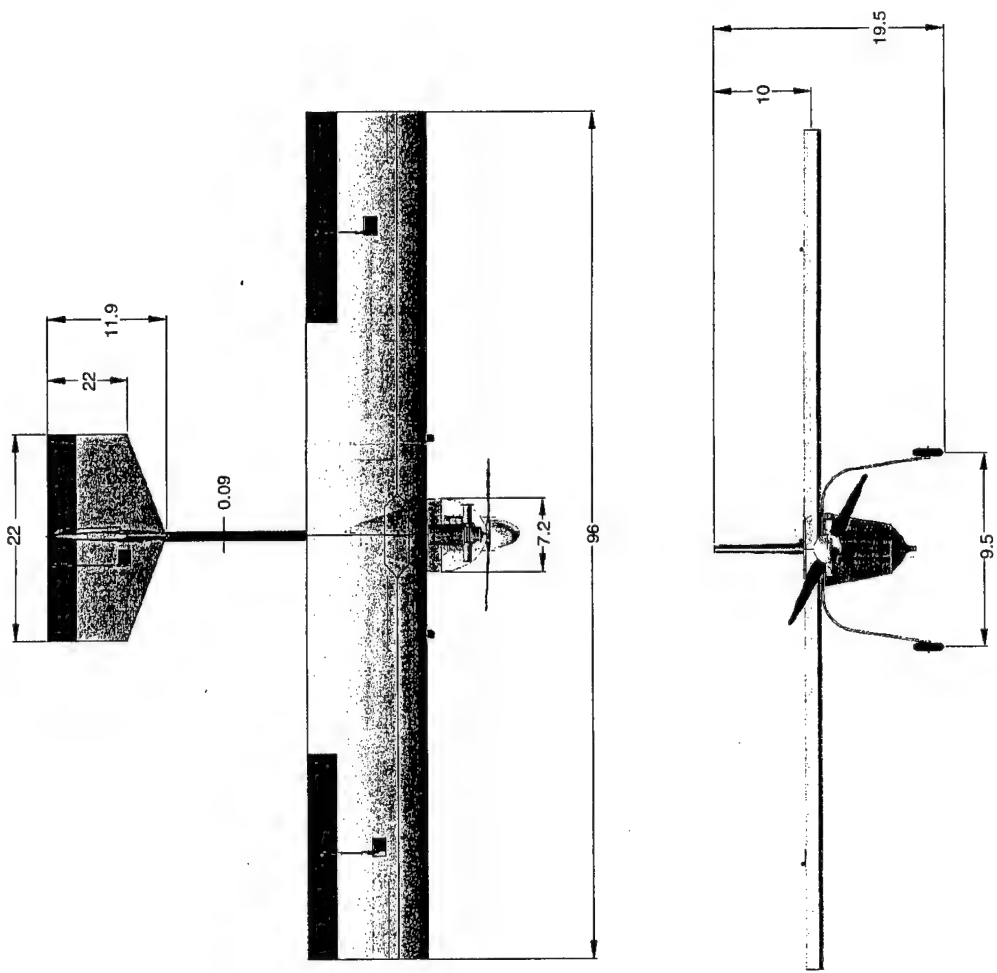
Coefficient	Item	Cost Per Unit	Value		Total MFHR
	Empty Weight		10.39	lbs	
A	A * MEW		3116	\$	
	# of Engines		1.00	#	
	Battery Weight		1.50	lbs	
B	B * REP		2247		
WBS 1.0	Wing Span		7.50	ft	
	Max Chord		1.00	ft	
	Wing Span * Max Chord	10	7.50	ft^2	75
	Ailerons	5	1.00		5
	Flaperons	7.5			0
	Ailerons + Flaps	10			0
	Ailerons + Spoilers	10			0
	Ailerons + Flaps + Spoilers	15			0
	WBS 1.0 Total				80
WBS 2.0	Fuselage Length		5.00	ft	
	Fuselage Width		0.40	ft	
	Fuselage Height		0.83	ft	
	L * W * H	20	1.67	ft^3	33.33333
	WBS 2.0 Total				33.33333
WBS 3.0	Vertical Surface w/o control	5	0.00	#	0
	Vertical Surface w control	10	1.00	#	10
	Horizontal Surface <25%	10	1.00	#	10
	WBS 3.0 Total				20
WBS 4.0	# Servos / Motor Controller	5	7.00	#	35
	WBS 4.0 Total				35
	MFHR Total				168.3333
C	C * MFHR		3366.667		
	TOTAL RAC		8.729		

5.7 Detailed Drawings

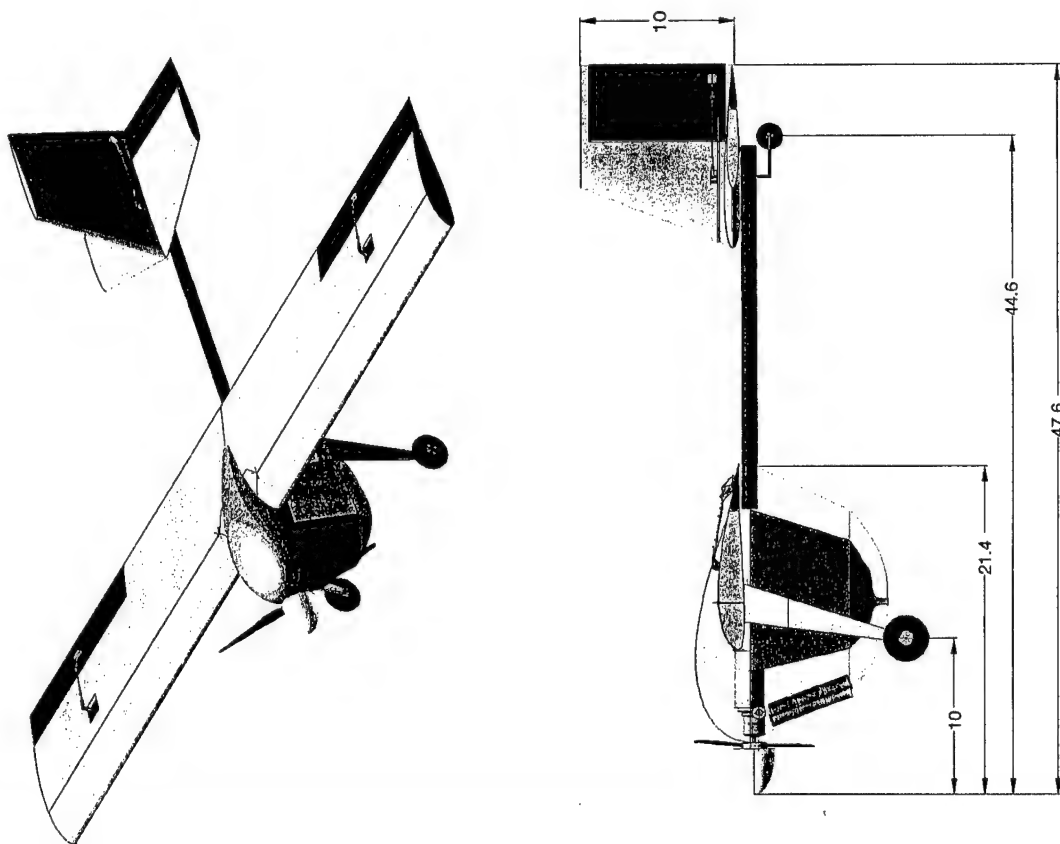








Note: All dimension are in inches.



6.0 Manufacturing Plan

Most of the aircraft is made of carbon fiber or fiberglass and epoxy resin. The techniques to manufacture each individual part vary in order to create the shapes with the level of precision required.

Depending on the requirements for each part, the most efficient fabrication method is selected to give the level of precision needed and minimize the cost, time, materials, and tooling. An estimation of the relative costs of each manufacturing technique is shown in Table (6.1) below.

	Material Use	Training	Difficulty	Tools/ Equip- ment	Tooling	Time	Total
Hot Wire	0	1	2	1	1	1	6
Vacuum Bag	0	1	0	1	0	2	4
Mold	2	0	0	2	2	2	8
LaserCamm	1	1	0	2	0	1	4
Autoclave	0	1	1	2	0	2	6

Table 6.1 Fabrication processes and their estimated relative costs

Some parts require more precise dimensions than others, therefore the technique with the lowest cost that can still deliver the accuracy required for the part to be useful is selected.

6.1 Wings

The most critical property of the wings is the airfoil designed by the aerodynamics group. The wings must accurately portray the shape of the chosen airfoil or the aircraft would not perform as expected.

Templates of the airfoil were cut using a LaserCamm and a hot wire was used to cut the wings. This method was inexpensive and readily available. Space for the spar and hardpoint were cut out and the foam sanded. Small pockets cut were cut lengthwise to hold servos and brake wires. Bi-directional fiberglass was bonded to the top and bottom of the wings to provide the torsional stiffness. Painted mylar enclosed the wing and then the assembly cured in a vacuum bag.

6.2 Spar

The spar must fit inside the wing and connect to the wing sleeve. The critical dimension of the spar is the thickness and is ultimately determined by the number of layers of unidirectional carbon used. A section from the wing cores was cut for the spar.

First the vertical piece of spar will be adhered to the hardpoint. After the carbon fiber vertical spar was cured was sanded to shape, and then adhered to the wing foam cores that have a section cut for these pieces. The horizontal section of the spar was applied to the wing foam cores then vacuum packed and allowed to cure. Some cavicol was used where the horizontal spar piece should be attached to the vertical section to ensure continuity between the two. After curing, this component was sanded to fit the wing profile and prepped for fiberglass skin.

6.3 Hardpoint

The hardpoint is a crucial piece that transfers wing loads to the fuselage via the spar. To ensure that this piece fits the exact profile of the wing cross-section it will be milled using a 4-axis CNC mill. To ensure that all the wing loads are transferred to the hardpoint, the spar has been adhered to the hardpoint during its construction. Four countersunk holes are drilled into the hardpoint so that the bolts that will hold the wings to the fuselage do not protrude into the oncoming airstream.

6.4 Platform

The platform will experience many types of loading and must be constructed carefully. A mold is made from a flat plate with a round bar running down the center. The mold is covered in release wax so that the piece can be removed after construction. Carbon fiber is laid over the mold, on top of the carbon fiber is an absorbent which will draw excess epoxy out of the part. All this is vacuum bagged and left to cure.

6.5 Skin & Fuselage

The purpose of the skin is to provide additional structural stiffness, house the payload and streamline the fuselage. To produce the designed fuselage accurately plugs will be made with pieces of foam. The foam will be cut using a 3-axis CNC mill. The foam will be treated with a gel coat to obtain a smooth finish, then covered with release wax. After the plug is prepped for usage fiberglass or carbon fiber will cover the plug and all is set in a vacuum bag allowing curing. Once cured, the excess areas were trimmed and sanded. The fuselage is then adhered to the platform using epoxy mixed with cavacil and micro balloons.

6.6 Motor-mount

The fabrication method for the motor-mount was determined to be the vacuum bag because the tight dimensions obtained through creating a mold was not needed for the motor-mount to be functional. Therefore the vacuum bag was the method with the smallest cost. A piece of circuit board was cut to the required size. A thin layer of foam was made using a hot wire. Unidirectional carbon fiber was laid on the foam, followed by bi-directional carbon. The carbon foam sandwich structure was vacuum packed and cured. A small mold, a tube just larger than the motor was used to create the motor mount which will cradle the motor. The mold is covered with release wax then covered in a carbon-foam-carbon structure. After its construction, a flat panel is adhered perpendicular to the cradle where the motor is bolted.

6.7 Landing Gear

The landing gear must withstand impact loads and be symmetrical so that the aircraft rolls down the runway straight. These requirements mean that precise and durable parts are needed, negating the importance of low cost fabrication techniques. Therefore, it was decided to make the landing gear with a mold and autoclave. A mold was created by rolling a piece of aluminum to size. Preimpregnated unidirectional carbon fiber was placed in the mold and placed in an autoclave for curing. Then the part was trimmed to size and holes were later drilled for mounting to the aircraft and wheel attachment.

7.0 Research and Testing Plan

Most of the aircraft is made of carbon fiber or fiberglass and epoxy resin. The techniques to manufacture each individual part vary in order to create the shapes with the level of precision required.

Depending on the requirements for each part, the most efficient fabrication method is selected to give the level of precision needed and minimize the cost, time, materials

7.1 Objectives

The purpose of testing confirms or denies a function of a design configuration or design component in the aircraft. The research and testing plan objectives were to gain insight into the drag and lift values of the airfoil types, determine the optimum motor and battery configuration, and the effect of changing the release mechanisms of the payload. Water release tests, wind tunnel testing, and valve testing confirmed or denied if the design used would be sufficient and efficient in the overall final design. These tests allowed the design to achieve maximum development of that particular component or design configuration in turn achieving the best performing aircraft.

7.2 Schedules

A research and testing schedule was organized. Due to the abundant data from Michael Selig's research (Selig) airfoil wind tunnel testing was deemed unnecessary for airfoil selection; however, wind tunnel tests were performed in order to optimize the WDS.

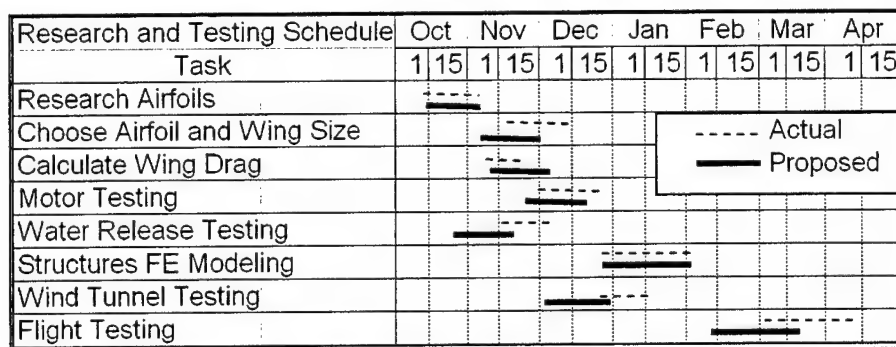


Figure 7.1 Research and Testing Schedule Task

7.3 Testing Procedures

The landing gear is tested for static load bearing ability, as well as for its dynamic properties. The rear landing gear is secured in a cantilever position and 20 pounds of weight is attached to the end of the landing gear. This test is to ensure that the part will be able to hold the entire weight of the airplane. Next, the impact performance of the landing gear is tested by tying the test weight to the end of the landing gear with a string, and the load dropped from a small distance. This will simulate the landing impact of the aircraft on the landing gear. If the landing gear bounces too strongly, damping will be needed to keep the airplane from bouncing back into the air while trying to land.

The structural proof test of the spar is conducted in a similar fashion. This test is to learn whether the spar will withstand the loading being placed on it, as well as to find the deflection of the spar under point loading at the tip of the wing.

The first step of flight testing is to recreate the judges' wing test. The aircraft is lifted by the wing tips for a short period of time. This step is important for safety. Next, the motor is throttled up to full speed while holding the aircraft tail. A series of very simple and gentle maneuvers are performed to check for the general stability of the aircraft. After the flight worthiness and stability have been established, the airplane is then put through some more advanced maneuvers. It is important to know how the aircraft will handle.

7.4 Check-lists

Testing, assembly, pre-flight and post-flight checklists were developed to track testing milestones and ensure safety of flight and personnel.

Testing Checklist

X	Wind tunnel testing
X	Water release testing
	Flight testing
X	Static motor testing
	Dynamic motor testing
X	Structures testing

Figure 7.2 Testing Checklist

Pre-Flight Checklist

	Ensure all batteries are fully charged: motor, receiver and controller
	Check electrical connections and wires for integrity and abrasion
	Inspect fuselage, wings and tail for obvious damage
	Ensure boom and is installed properly
	Inspect landing gear for attachment rigidity
	Ensure wheels spin freely
	Check all flight controls respond to given commands
	Check propeller for cracks, dents and dings
	Check forward fuselage area near motor for FOD
	Ensure payload valve secure
	Install fuse and check for correct rating
	Start and rev motor; listen for unusual vibrations

Figure 7.3 Pre-Flight Checklist

Post-Flight Checklist

	Check wing attachment points for damage
	Inspect wings for structural integrity and skin for ripples
	Inspect motor mount and firewall for cracks or delaminations
	Inspect motor connecting bolts for tightness
	Check motor, motor speed control and battery pack for overheating damage
	Ensure vertical and horizontal tail sections are firmly attached and no loosening has occurred
	Check electrical connections for abrasion or overheating
	Check fuse is not blown
	Inspect propeller for cracks, dents or dings

Figure 7.4 Post-Flight Checklist

7.5 Results

7.5.1 Airfoil Results

The results from the airfoil data are shown in Figure 7.5.

Airfoil Data				
Airfoil	Cl	Cdo	Wing L/Dmax	Aircraft Drag [lb]
S4083	1.3	0.008	14.7	1.82
E214	1.3	0.01	13.6	2.00
E423	1.95	0.017	13.1	2.64
S1210	1.8	0.015	12.9	2.45
S1223	2.1	0.02	11.7	2.91

Reynolds number 300,000

Figure 7.5 Airfoil Data

The difference in drag values between the S4083, the chosen airfoil for the Rain of Terror, and the S1223 is 1.09 pounds. This 60% increase in drag is substantial because it would require additional thrust. In attempts to keep the battery weight low, the choice of the S4083 airfoil was prudent because less thrust is required, which corresponds to less battery weight.

7.5.2 Motor Testing Results

Static testing was performed on a dynamometer and data collected using Labview software. A relevant portion of the Graupner Ultra 3300-5 motor data is shown below.

Graupner Ultra 3300-5 (5-winding) Motor Data				
	# Cells	Volts	Motor RPM	Motor Eff [%]
MotorCalc Data	18	18	7955	52.5
Test Data	18	18	5700	87.0

Figure 7.8 Graupner Motor Data

It was clear that actual static testing must be performed to validate MotorCalc software results.

7.6 Water Release Testing

The water release testing consisted of a bucket with a hole, a scale, and a timer. The bucket was filled with water, weighed, and the water was released with the timer running. The bucket was reweighed to determine the amount of water that was released. The water release testing was done without a tube and then with a four foot two inch long tube. The time it took to release the water was plotted against the amount of water released, Figure 7.9.

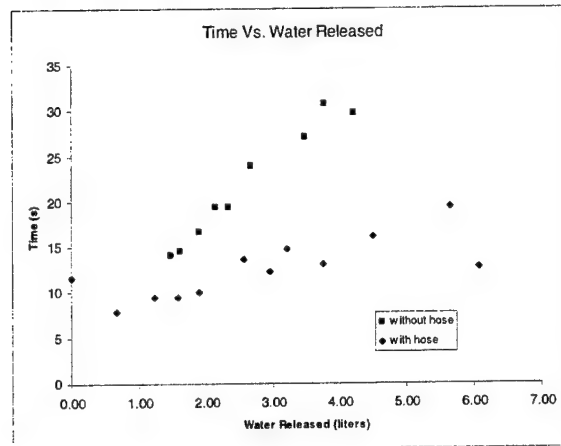


Figure 7.7 Time Vs. Water Released Without the Hose

The results confirmed that the design component of a tube attached to the fuselage would have more effective time to release the water. The benefit of having a long hose dangling from the fuselage was increased water flow rate due to increased height difference from the water source to exit. This device has been deemed illegal for safety reasons; the hose must not drag on ground after landing. To raise the hose after payload release. This would cause the need for more batteries, motors and servos, resulting in an increase in the RAC by 0.35. The aircraft design was configured without a tube attached as a result.

7.7 Valve Testing

During the conceptual design phase various methods for releasing the payload were considered: sliding gate valve and "off the shelf" ball valve, and a cylindrical valve. Figure 7.10 show the gate valve and the ball valve. Determining how the water is released and how it is integrated into the aircraft system were important factors in the decision process. Each valve had its advantages and disadvantages for the aircraft performance.

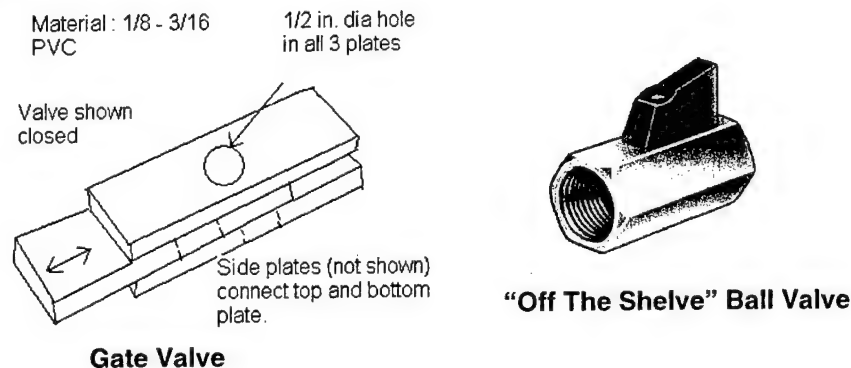


Figure 7.8 The Design Valves Tested

During the preliminary design, each gate valve was acquired and tested to determine the most effective and sufficient design. The release knobs were tested to see how smooth it turned and how much force would be required to turn the knobs. The gate valve design included a flat plate with a one half inch hole,

which could slide in and out of a sleeve that housed an o-ring in order to assure no water leaked when it was in its closed position. However, the gate valve needed complicated mechanisms to open the valve causing the valve to be of larger dimensions. These necessary dimensions failed to fit in the designated valve space on the aircraft. The “off the shelf” ball valve design was bulky in size, and therefore, weighed heavier than the gate valve. A problem that came up when testing the “off the shelf” valve was that large amounts of torque was required to open it. Both suggested valves had problems either with weight or size.

A modified cylindrical valve was then tested. This modified valve was press fit into a receptacle, both which were machined from a Teflon. Teflon was used for its low coefficient of friction. Overall this design mechanically worked with the efficient material of Teflon. This “modified” designed valve and its device to operate it fit well in the designated space. However, this “modified” design also required more torque to open the valve than the servos provided. After more modification and design thought to reduce the amount of torque needed to operate this design while keeping its effectiveness and ease of manufacture, a tapered cylinder was created with a matched tapered receptacle. A spring was used in order to draw the two tapered pieces closer together, providing a good seal. Yet, vacuum grease added to aid the seal of the two tapers. The “modified” valve is in Figure 7.11 below.

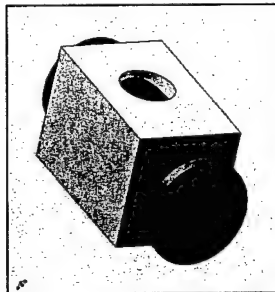


Figure 7.9 “Modified” Valve Used in Final Design

In conclusion for the release mechanism, the “modified” valve proved to be the most effective and a sufficient design for the Reign of Terror’s water release mechanism.

7.8 Wind Tunnel Testing

The wind tunnel located at the UCSD Engineering Building II, room 107 (Figure 7.12) was used to determine if the cowling was beneficial to help release the water from the fuselage and determine if the fuselage shape provides extra lift. The speed of the water release is crucial for the mission’s success and was the main inspiration for wind tunnel testing.

A .3 scaled model of the aircraft was created and tested. The model was mounted in the small wind tunnel testing space as shown in the Figure 7.12. The model was rotated at the mount left and right to change the angle of attack during testing. The pressure readings were taken from holes drilled along the top and bottom of the model, and the tubes were attached to the wind tunnel pressure reader.

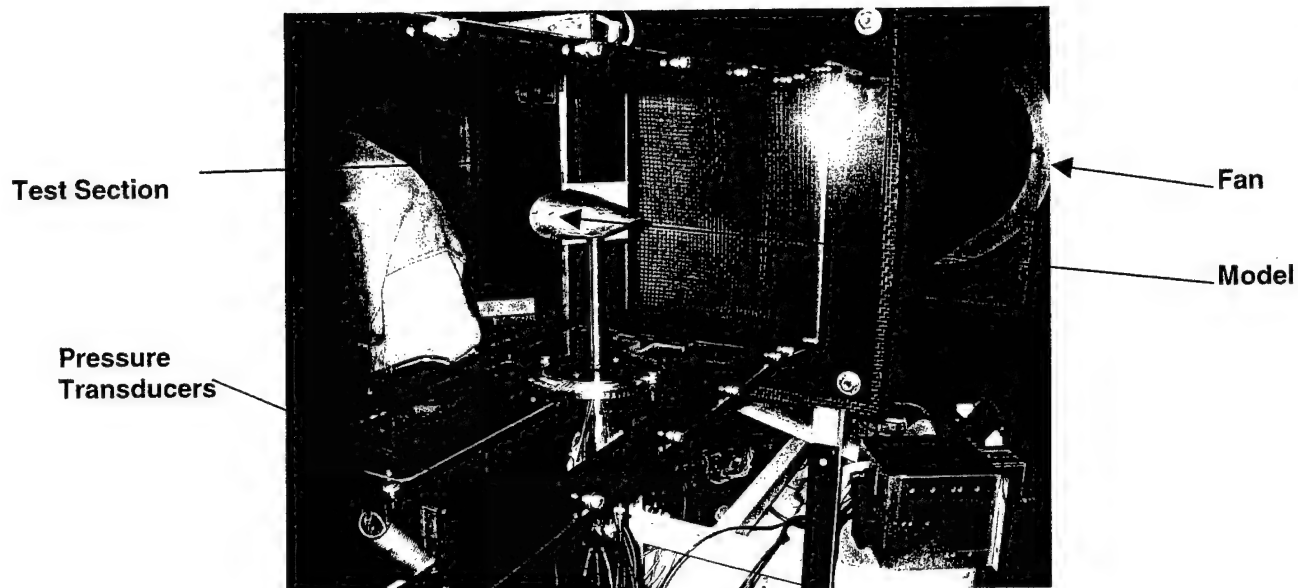


Figure 7.10 The Wind Tunnel Setup With Model

There were two tests: without the cowling and with the cowling. The pressure readings were taken at angles of attack of -10 , -5 , 0 , 5 , and 10 degrees at a range of velocities of zero to 150 mph with 10 degree increments.

The first experiment, analyzed the airflow over the model without cowling as seen in Figure 7.13.

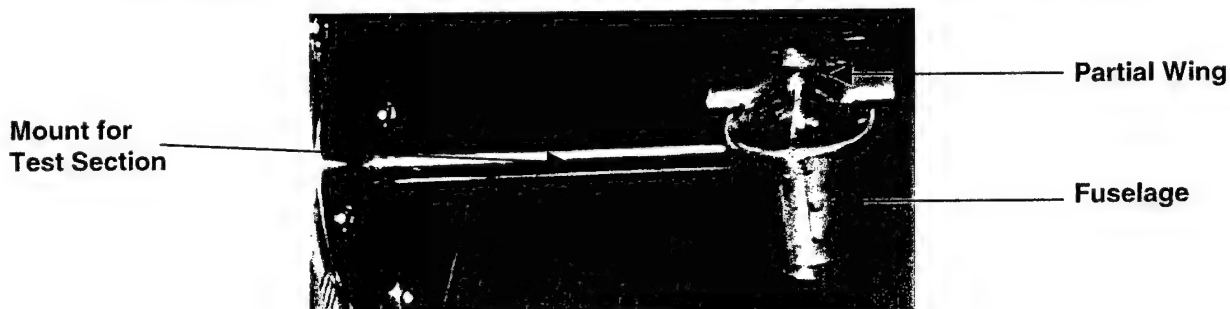


Figure 7.11 30% Scaled Fuselage and Partial Wing Model of Final Design

The second test had the same .3 scaled model, but included a cowling located 2.5 inches from the leading edge of the fuselage, which is on the very bottom of the structure, Figure 7.14.



Figure 7.12 30% Scaled Model with Cowling

The pressure readings for the two experiments were converted to coefficients of pressure for comparison and plotted in Figure 7.15.

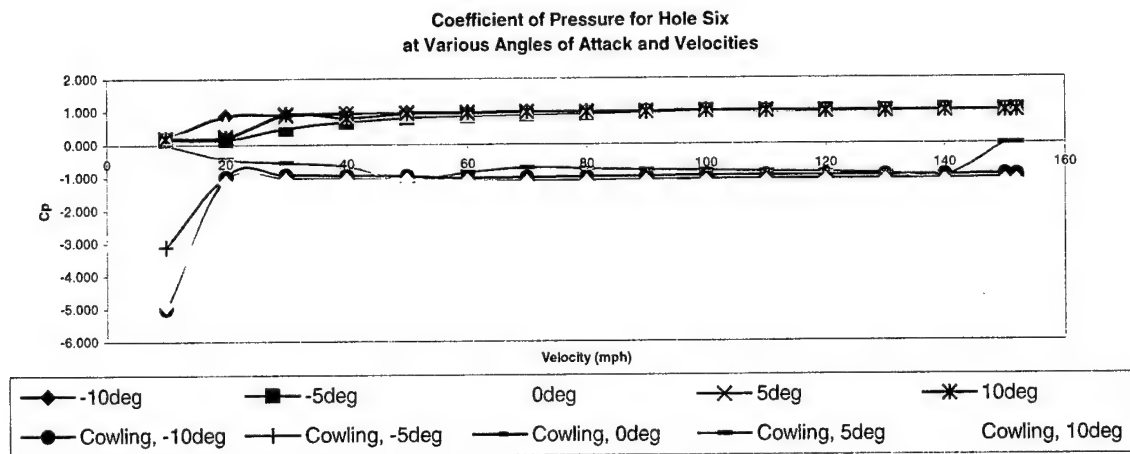


Figure 7.13 Wind Tunnel Results at Pressure Hole 6

The data showed that there was a pressure differences when using the cowling. The coefficients of pressure became negative with the cowling, causing a vacuum like reaction at the cowling's location. This result is beneficial in releasing the water from the payload bay. From the results, it was concluded that the addition of a cowling to the fuselage, in front of the hole where the water is released, will increase the water flow through the hole and reduce the time to completely release the water, thus, improving the mission flight time.

From the coefficients of pressure, the normal force coefficient was determined using the trapezoidal rule to integrate across the fuselage body. From the normal force coefficient the coefficient of lift was determine from by the relationship:

$$L > N \cos(\beta) . A \sin(\beta) \text{ where } \beta = \text{angle of attack (radians)}$$

The data for the axial force was undetermined because the wind tunnel was not equipped to take data along the axial length of the fuselage. The lift calculated was plotted against each angle of attack tested, Figure 7.16.

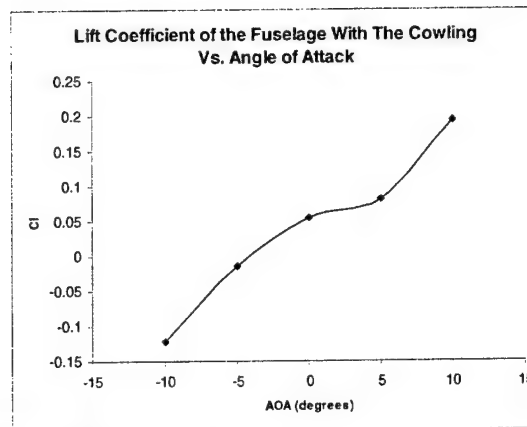


Figure 7.14 Lift Coefficient of the Fuselage with the Cowling Versus Angle of Attack

The results showed that as the angle of attack was increased, the fuselage produces more lift. The fuselage shape has been confirmed to be a sufficient design in wind tunnel testing, and thus, accepted as the final design of the fuselage.

7.9 Lessons Learned

The airfoil data and resulting calculations for the total drag on the aircraft varied. Choosing an airfoil because of its high coefficient of lift (C_l) value is not always the best choice. Comparing the S4083 and S1223 airfoils, it is clear that the latter C_l is much higher. However, the additional drag associated with the S1223 airfoil creates more than a pound of additional drag.

The main lesson learned from the motor testing was the actual test data varied greatly from MotorCalc software calculations. In the case of the Graupner Ultra 3300-5 motor, the motor speed and efficiency with 18 volts is grossly in error. MotorCalc predicts a motor speed of 7955-rpm and 52.5% efficiency while actual static test data gave 5700-rpm and 87% efficiency. Results from the actual test data were used in determining the best motor-battery configuration.

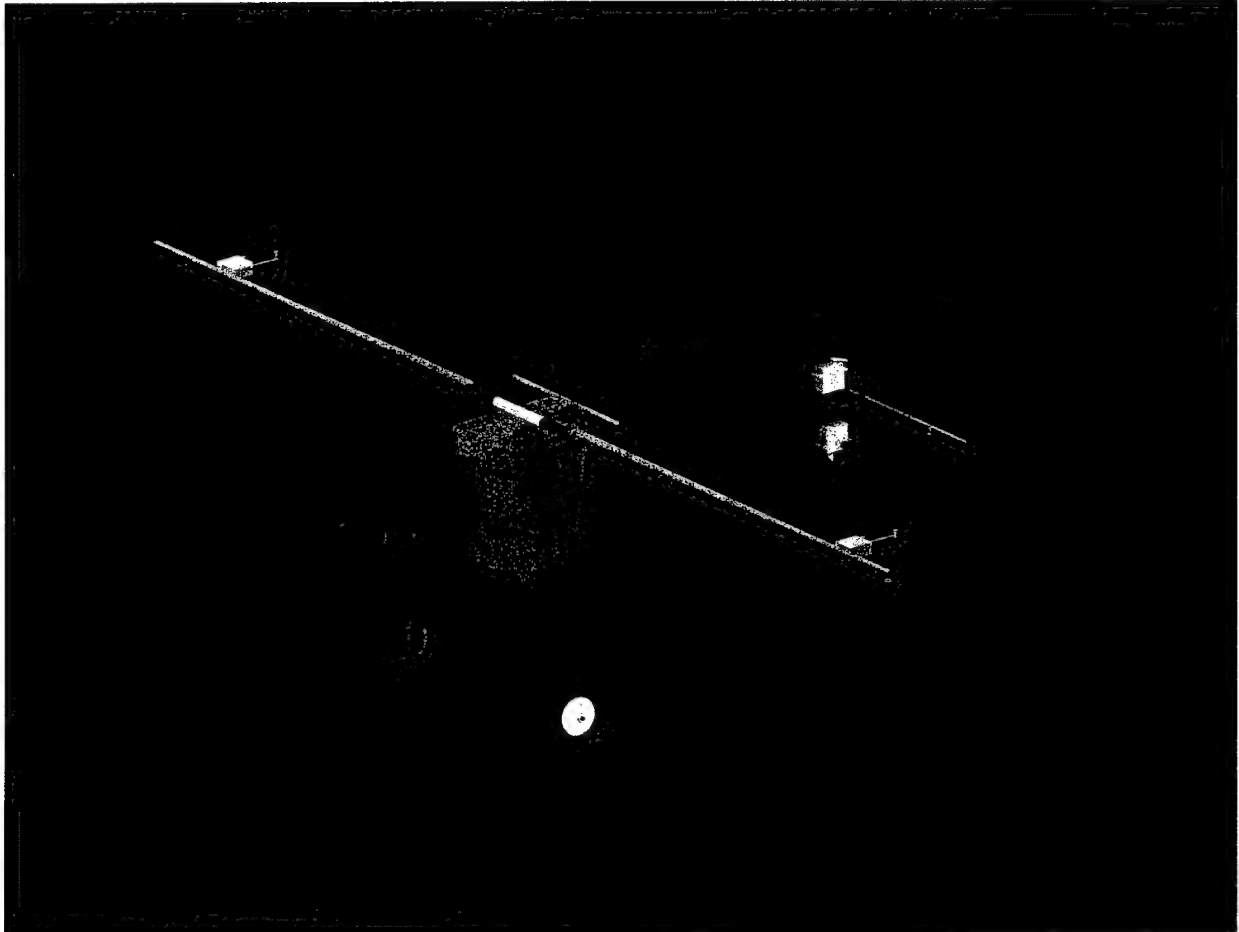
The valve testing proved that a cylindrical valve works better than gate and ball valves; and a taper cylindrical valve works better than a cylindrical valve. These tests also demonstrated that the payload is released faster with a cowling than without a cowling. This shows that the speed of the aircraft has a negative effect on the release of the fluid. Therefore, by blocking the air flow, a vacuum is created and the fluid is pulled out.

8.0 References

1. Abbot I.H., Theory of Wing Sections, Dover Publications Inc, 1949.
2. Nelson, R., Flight Stability and Automatic Control, McGraw Hill, 1989.
3. Nocolia, L..M., Fundamentals of Aircraft Design, METS Inc, 1984.
4. Peery, D.P., Aircraft Structures, McGraw-Hill Inc., 1982.
5. Raymer, D.P., Aircraft Design: A Conceptual Approach, AIAA Education Series, 1989.
6. McMaster-Carr Supply Company. Copyrighted 2004. <http://www.mcmaster.com/> Accessed: February 2, 2004.

2003/2004 AIAA

Cessna/ONR Student Design/Build/Fly Competition



Washington State University
Spirit of Procrastination

Table of Contents

1. Executive Summary	5
1.1. Overview of Design Development.....	5
1.2. Highlights of Development Process	5
1.3. Tools Used	5
1.4. Results of Conceptual Design.....	6
1.6. Results of Preliminary Design	6
1.7. Results of Detail Design.....	6
1.8. Results of Manufacturing Plan	6
1.9. Results of Testing Plan	6
2. Management Summary	7
2.1. Breakdown of Design Team.....	7
2.1.1. <i>Project Manager</i>	8
2.1.2. <i>Assistant Project Manager</i>	8
2.1.3. <i>Purchasing / Fundraising</i>	8
2.1.4. <i>Manufacturing Team</i>	8
2.1.5. <i>Design Report Manager</i>	8
2.1.6. <i>Structures Team</i>	8
2.1.7. <i>Mission Modeling Team</i>	8
2.1.8. <i>Flight Crew</i>	8
2.1.9 <i>Aerodynamics Team</i>	8
2.2. Planning and Scheduling	9
2.3. Milestone Chart	9
3. Conceptual Design	9
3.1. Mission Requirements	9
3.1.1. <i>General Requirements</i>	10
3.1.2. <i>General Mission Requirements</i>	10
3.1.3. <i>Fire Bomber Mission</i>	10
3.1.4. <i>Ferry Mission</i>	11
3.1.5. <i>RAC – Rated Aircraft Cost</i>	11
3.2. Configurations Studied.....	11
3.2.1. <i>Airframe Configuration</i>	11
3.2.2. <i>Fuselage Geometry</i>	12
3.2.3. <i>Landing Gear Configuration</i>	14
3.2.4. <i>Propulsion Configuration</i>	15
3.2.5. <i>Wing Configuration</i>	16

3.2.6. Tail Configuration.....	17
3.3. Conclusions.....	17
4. Preliminary Design.....	18
4.1. Mission Modeling and Optimization Analysis.....	18
4.1.1. Mission Modeling and Optimization Overview.....	18
4.1.2. Aircraft Drag Model.....	19
4.1.3. Aircraft Maximum Lift Coefficient.....	19
4.1.4. Propulsion System Model.....	19
4.1.5. Gross Weight Model.....	20
4.1.7. Dynamics of Flight Model.....	21
4.1.8. Takeoff and Climb.....	21
4.1.9. Level Flight.....	21
4.1.10. Turning.....	21
4.1.11. Descent and Landing.....	22
4.1.12. Water Bombing.....	22
4.2. Aircraft Configuration for Mission Model.....	23
4.2.1. Wings.....	23
4.2.2. Fuselage.....	24
4.2.3. Empennage and Stability.....	24
4.2.4. Propulsion system.....	25
4.3. Optimization Results.....	25
4.3.1. Predicted Mission Performance for Optimized Aircraft.....	25
4.4. Conclusions.....	27
5. Detail Design.....	28
5.1. Basic Requirements.....	28
5.2. Component Design and Selection.....	29
5.2.1. Airfoil Selection.....	30
5.2.2. Empennage System and Stability.....	33
5.2.3. Control System.....	33
5.2.4. The Propulsion System.....	34
5.2.5. The Fuselage System.....	35
5.2.6. Wing to Fuselage Platform.....	35
5.2.7. Water Release System.....	35
5.2.8. Landing Gear System.....	35
5.2.9. Water Loading System.....	36
5.3. Final Aircraft Specifications.....	36
5.3.1. Drawing Package.....	37

5.3.2. Rated Aircraft Cost Calculation	40
5.4. Final Aircraft Performance Analysis.....	40
5.4.1. Predicted Performance	40
6. Manufacturing Plan	42
6.1. Manufacturing Processes and Component Selection.....	42
6.1.1. Wings	42
6.1.2. Fuselage	43
6.1.3 Landing Gear	43
6.1.4. Empennage	44
6.1.5. Payload Loading System	44
6.2. Processes Selected for Manufacture of Major Components	45
6.3.1. Wings	45
6.3.2. Fuselage	45
6.3.3. Landing Gear	46
6.3.4. Empennage	46
6.3.5. Electronic Components.....	46
6.3.6. Payload Deployment System	47
6.3.7. Motor Cooling System	47
6.3.8. Wing to Fuselage Interface and Water Tank	47
6.4. Manufacturing Dependencies	48
6.5. Manufacturing Milestones	48
7. Testing Plan	50
7.1. Test Objectives and Schedules	50
7.2. Flight Testing Checklists	50
7.3. Summary of Test Results and Lessons Learned.....	52
8. References	53

1. Executive Summary

The following summarizes Washington State University's entry, the Spirit of Procrastination, into the 2003-2004 Design/Build/Fly competition. The goal of our team was to achieve the maximum score possible. This is accomplished by minimizing the RAC (rated aircraft cost), while maximizing the flight score. The flights consist of a fire bomber mission, where 2 laps are flown and two loads of water are dumped, and a speed mission, where 4 laps are flown. The paper score must be maximized to perform well in the competition.

1.1. Overview of Design Development

During the conceptual design phase of the development process, analytic approximations were made and figures of merit (FOM) created to decide aspects of our aircraft design. These were based on mission requirements, and qualities we decided were important to the aircraft performing well at the competition. After many aspects of our aircrafts design had been narrowed down in the conceptual design, we progressed to the preliminary design by developing a Matlab routine called WaSoO to iterate thousands of combinations of aircraft parameters. The program used equations for modeling all aspects of the aircraft's flight from takeoff to landing. Some important observations were made when reviewing the results from the optimization program. We found that having a low RAC far outweighed the benefit of having a large, powerful propulsion system designed to make the aircraft fly as fast as possible. It also showed that the smaller and lighter the aircraft, the better the final score would be. Throughout the rest of the preliminary design, calculations were made to determine exact sizes and loads the aircraft would encounter. In the detailed design, final decisions were made concerning the final size and geometry of the aircraft. In the manufacturing process, we determined the best method to manufacture parts and the best materials to construct them out of.

1.2. Highlights of Development Process

The conceptual design of the development process effectively narrowed down aspects of the design for our aircraft. Figures of merit were used to make decisions and discuss alternatives for different parameters in the aircrafts design. The code for the WaSoO program was developed over the course of a semester, which allowed it to accurately model the flight of the aircraft. Aspects of the propulsion system were considered, and low speed airfoil data for choosing airfoils for the wing, fuselage and empennage were studied.

1.3. Tools Used

In the design of the Spirit of Procrastination, we used and are implementing software programs for design as well as analysis and optimization. The design of the plane was created primarily with the use of Pro Engineer Wildfire because of the programs ability to draw in 3-Dimensional aspects and

analyze volumetric shapes. This program allows the user to define electrical components and controls to simulate the actual components and aid in the wiring of the actual plane.

Matlab was used as a development environment for the mission simulation code since it has the ability to print charts and parse scripts. This was very useful in coming up with values for the design of the fuselage, wings, stabilizers and spar. It also provided speeds in corners, straight runs and landing and take-off speeds as well as angles of attack. In the construction of many of the components a CNC router will be used. To get the router to create the parts MasterCAM will be used to convert the ProEngineer drawings to NC code compatible with the router's controller.

1.4. Results of Conceptual Design

The conceptual design narrowed our design down to some specific configurations. The plane was decided to be traditional fuselage configuration with a tractor propeller, a high wing with high aspect ratio, a tall and narrow fuselage, fixed tail dragger landing gear, and an inverted T shape tail.

1.6. Results of Preliminary Design

A computer program was written to compare to model the entire Fire Bomber mission, which was the most critical mission to optimize the aircraft for.

1.7. Results of Detail Design

The detailed design specified the size and geometry for all the aircrafts components. The detailed design also made performance estimations for the aircraft with the size and geometry that was decided upon.

1.8. Results of Manufacturing Plan

The manufacturing plan specified the method of manufacture and material selection (or brand and model) for all the components of the aircraft. Descriptions were made outlining the manufacturing processes for each component.

1.9. Results of Testing Plan

Our testing plan is a thorough checklist for all aspects of flight testing of the aircraft. In addition to flight testing, bench testing of the propulsion system was done and the results were compared to the results of how the team modeled the propulsion system.

2. Management Summary

Design work for the Spirit of Procrastination started in September with only 4 members, the 4 that went to last year's DBF. The AIAA - WSU student chapter President, Zak Valentine, took over as Project Manager for the 2003-04 DBF Team. The chapter's Vice-President, Peter Wiseman took over as Assistant Project Manager. At the beginning of the fall semester, the chapter gained 5 new members. Unfortunately, those members did not stay on for spring semester. Late in the semester, the chapter gained three new members. During the spring semester, a pizza party was announced and fliers posted, and an additional three members were recruited. The team consists of a total of 10 members. This can be broken down to one graduate student, four seniors, two juniors, and three freshmen.

2.1. Breakdown of Design Team

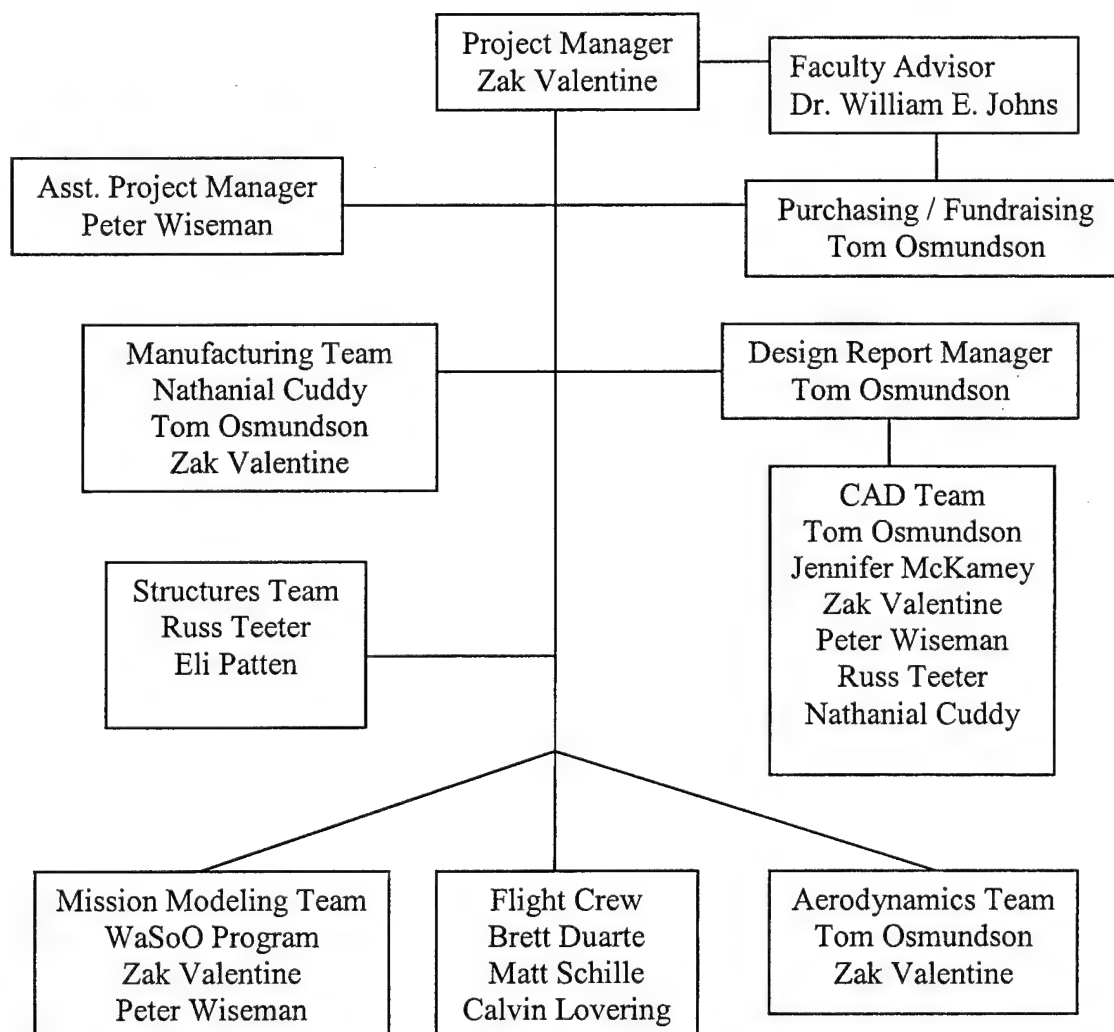


Figure 2.1

2.1.1. Project Manager

The project manager leads the meetings and is responsible for schedule management. The project manager also approves purchase requests. Major decisions made must go through the project manager for approval.

2.1.2. Assistant Project Manager

The assistant project manager acts as the project manager during the absence of the. The assistant is involved in all projects.

2.1.3. Purchasing / Fundraising

The purchasing and fundraising officer keeps track of all purchase orders and organizes all travel arrangements. The officer is also responsible for all fundraising activities.

2.1.4. Manufacturing Team

The manufacturing team is responsible for making all decisions concerning manufacturing processes and materials selection. This includes the construction of many of the airplanes components.

2.1.5. Design Report Manager

The design report manager organizes and delegates the writing of the design report. The design report manager holds the master copy of the paper and all CAD drawings.

2.1.6. Structures Team

The structures team is responsible for modeling, analyzing, and evaluating structural members and specifying parameters related to construction.

2.1.7. Mission Modeling Team

The modeling team is responsible for the complete dynamic modeling of the aircraft for the missions specified in the competition rules.

2.1.8. Flight Crew

The flight crew is responsible for all aspects of flight testing. The crew is also consulted regarding design considerations.

2.1.9 Aerodynamics Team

The aerodynamics team is responsible for investigating designs, analyzing and optimizing fuselage, wing and empennage profiles and configurations. The team is also responsible for calculating static and dynamic stability.

2.2. Planning and Scheduling

Early in the design process, the team defined major design milestones and the dates by which projects/tasks should be achieved. Changes to the schedule and announcements are made at weekly meetings or announced over the team e-mail list.

2.3. Milestone Chart

Task Name	Start	Finish	Aug	Sep	Oct	Nov	Dec	Jan	Feb	Mar	Apr
WSU Design Build Fly	14-Aug	20-Apr									
Conceptual Design Preparation	14-Aug	31-Oct									
<i>Actual</i>	1-Sep	31-Oct									
Data Collection and Documentation	14-Aug	20-Apr									
<i>Actual</i>	14-Aug	20-Apr									
Primary Design Phase	1-Nov	1-Jan									
Optimization Program Preparation	1-Nov	15-Mar									
<i>Actual</i>	1-Nov	15-Mar									
Power Plant Analysis and Testing	1-Jan	1-Feb									
<i>Actual</i>	14-Jan	23-Feb									
Data Collection and Documentation	14-Aug	20-Apr									
<i>Actual</i>	14-Aug	20-Aug									
Detailed Design	1-Mar	20-Apr									
Refinement and Stability Analysis	1-Mar	14-Apr									
<i>Actual</i>	1-Mar	14-Apr									
Structural Analysis and Testing	1-Dec	14-Mar									
<i>Actual</i>	2-Feb	14-Mar									
Drawing Package	1-Jan	1-Mar									
<i>Actual</i>	1-Jan	3-Mar									
Manufacturing	1-Mar	20-Apr									
Component/Aircraft Construction	1-Mar	20-Apr									
Flight Evaluation	1-Apr	20-Apr									
Documentation	14-Aug	20-Apr									
Report Preparation	1-Dec	4-Mar									
<i>Actual</i>	1-Jan	4-Mar									
Contest	23-Apr	26-Apr									

Table 2.3

3. Conceptual Design

The goal of the conceptual design was to investigate the requirements for the two missions and the requirements for the competition. Then consider alternatives for different aircraft configurations, evaluate the alternatives, and choose the best configuration. In the preliminary and detail design, the configuration will be further evaluated.

3.1. Mission Requirements

To win the competition, you must get the maximum total score. The total score is based on report score, total flight score, and rated aircraft cost (RAC), shown in the equation below.

$$\text{Total Score} = (\text{Total Flight Score} \times \text{Report Score}) / \text{Rated Aircraft Cost}$$

The report score was arbitrarily fixed at 85 to simplify calculations. The two other factors, total flight score and rated aircraft cost would be the main focus during our conceptual design.

3.1.1. General Requirements

General requirements for the aircraft are numerous and include the following: Must be any configuration other than rotary wing or lighter than air. The payload must be carried in the fuselage. For blended-wing configurations, it is defined as the inner 9 inches of the semi-span. Must be propeller driven and electric powered with or without gear reduction. Motors must be Graupner or Astro Flight brushed motors. A commercially produced propeller must be used. Motors are limited to 40 amps by means of a blade type fuse. Batteries must be over the counter NiCad and must not be more than 5 lbf. The receiver must be on a separate battery pack. The aircraft and pilot must be AMA legal and the gross takeoff weight 55 lbf or less. Teams must supply a copy of the rated aircraft cost signed by their faculty advisor.

Additionally, the aircraft will be subject to a safety inspection. The inspection will verify all payloads are fastened and secured. The propeller and structural attachments will be inspected. A radio range check will be performed, verify all controls move properly and verify the fail safe works properly. The payload system will be inspected for integrity. The wing system will be inspected using a wing tip lift test and an inverted wing tip lift test at the max payload capacity. The aircraft must have a propulsion system fuse to disarm the motor accessible from outside the aircraft.

3.1.2. General Mission Requirements

In addition to general rules and safety requirements, there are requirements specific to the flight missions. Each team will be given 5 flight attempts and the best of the bomber missions and the best of the speed missions will be added together into a total flight score. General requirements for the missions include fitting (disassembled) into a 2 foot wide by 1 foot deep by 4 foot long box. Aircraft must take off in 150 feet or less. Landing must begin on the runway to obtain a score for the flight. All payloads must be secured using mechanical means. Maximum mission time is limited to 10 minutes.

3.1.3. Fire Bomber Mission

The fire bomber mission will be given a difficulty factor of 2. Aircraft will be loaded, takeoff, dump water on the downwind leg, and return to land. The plane will be reloaded, takeoff, dump on the downwind leg, and return to land. The maximum water capacity will be 4 liters. Water must be loaded from 2 liter soda bottles. Teams may use gravity or pumped loading, but not pressurized soda bottles. A 360 degree turn must be performed on the downwind leg of each lap. Water may only be dumped on the downwind leg of a lap. Maximum dump orifice diameter is 0.500 inch. Pilot must call out "dump on" and "dump off". Early or late dumping, and excessive water spillage will be penalized. The fire bomber flight score will be based on the following equation:

$$\text{Difficulty Factor} * \text{Lbf of Water} / \text{Mission Time} = \text{Fire Bomber Flight Score}$$

3.1.4. Ferry Mission

The ferry mission, also referred to as the speed mission in this document, will have a difficulty factor of 1. The aircraft will takeoff, complete four laps, and land. The aircraft will not carry water during the flight. All laps flown must complete a 360 degree turn on the downwind leg. The speed mission flight score will be based on the following equation:

$$\text{Difficulty Factor} / \text{Mission Time} = \text{Speed Mission Flight Score}$$

3.1.5. RAC – Rated Aircraft Cost

The rated aircraft cost is based on many parameters. These parameters include empty takeoff weight, total battery weight, wing span, wing chord, ailerons and/or flaps and/or spoilers, fuselage length, width, and height, vertical surfaces with or without control, horizontal surfaces, and the number of servos and motor controllers.

3.2. Configurations Studied

3.2.1. Airframe Configuration

Airframe Configuration	Low Weight	Simple To Build	Low RAC	High Speed	Easy to Fly	
Weight	0.2	0.1	0.3	0.3	0.1	Value
Biplane	50	60	50	60	70	56
Canard	80	50	90	70	90	78
Flying Wing	70	50	30	90	20	57
Traditional	90	90	90	80	80	86

Table 3.2.1.

Our team decided to compare four different airframe configurations to conceptualize the layout of the Spirit of Procrastination. Those considered were the biplane, canard, flying wing and traditional. We chose to compare these four since the group was not familiar with any other layouts, and knew that documentation about each format would be readily available to us. Five qualities (columns) were created that the team felt would have the most influence on the decision. These were: low weight, simple to build, low RAC, high speed and easy to fly. Speed and low RAC were given the most weight (30%) since these factors directly influence the final score. Low weight was valued at 20% since a heavier design will influence all of the scoring factors. Simplicity of construction and easy to fly were given the lowest weight (10%), since the teams building and flying skills have matured greatly since last years design.

The biplane was the first possibility considered. It is a much heavier design since two wings need to be supported, is more complicated, would have a high RAC, and would fly slower than a traditional plane. These downsides are reflected in its low score of 56.

The canard faired quite well in every category except simple to build and speed. The canard would be harder for our team to construct because our team has never built or flown a canard aircraft before. The speed was penalized since the more efficient main wing would be in the wake of the less efficient nose wing, possibly creating more total drag than for a conventional layout.

The flying wing was quickly excluded due to a higher RAC. It was found that an increase in width of the fuselage (fixed at 18 inches for Flying Wing) accounted for 14.8% of the RAC per foot for a given design. This negates the supposed advantage of removing the vertical and horizontal control surfaces. Flying wings are also known for their poor stability, so a large flyability penalty was given.

The traditional layout was chosen over all the other designs since it fared well across all categories. This configuration would be lightweight, simple to build, have a low RAC, fly fast and be fairly easy to fly. This conclusion is based on its overall score of 86, which wins over the runner up, the canard, by only 8 points.

3.2.2. Fuselage Geometry

Fuselage H x W x L	Simple to Build	Flyability	Low RAC	High Speed	Water Effects	
Weight	0.1	0.2	0.1	0.3	0.3	Value
Blended Wing Body	30	60	20	90	60	62
Tall x Narrow x Medium	80	70	80	70	100	81
Short x Wide x Medium	80	50	40	70	20	49
Short x Narrow x Long	80	60	80	90	50	70
Tall x Wide x Short	60	60	60	50	80	63

Table 3.2.2.

Our team came up with 5 different fuselage shapes for our Spirit of Procrastination. We considered a blended wing/body, a tall, narrow, medium length fuselage, a short wide medium length fuselage, a short narrow and long length fuselage, and a tall wide and short length fuselage. We produced five different benefit categories our fuselage should have. These were simple to build, flyability, low RAC, high speed, and water effects. Speed and water effects were given the most weight (30% each) because these factors directly influence the score. Flyability was weighted at 20% because if a particular setup makes for an unstable platform for the water load, it will be difficult to fly and more difficult to fly quickly. Simple to build and RAC were weighted lowest (10% each). The simplicity of construction was weighted lower because our fabrication skills have increased greatly over the past year. The RAC was included in our quality categories because of the effect the fuselage shape has on the RAC and ultimately, the final score.

The blended wing/body (or flying wing) was first considered. With complex curves to blend the fuselage and the wing it would be difficult to fabricate. From previous experience, we knew that flying wings could be difficult to fly. The fact that the fuselage is blended into the body means the fuselage width

would be fixed at 18 inches and would result in a high RAC. With the smooth transitions from wing to fuselage, the aircraft would have low drag resulting in high speed. These factors resulted in a score of 62.

The tall height, narrow width, medium length fuselage was considered next. It would have a traditional, easy to construct shape, and traditional flying characteristics. It would result in a low RAC because of all fuselage dimensions, width has the highest penalty. Height raises the RAC more than length by a small amount. Having a tall and narrow fuselage resulted in average frontal area, an average amount of drag, and an average speed. The water effects were the best of all fuselages because the shape would result in good flow out of a single orifice. A tall water tank would result in greater hydrostatic pressure resulting in higher water flow. Overall this fuselage setup resulted in a score of 81.

We next considered a short height, wide, medium length fuselage. We decided it would be an easy shape to construct, but would have unstable flying characteristics due to CG changes with the water in the tank. Because it is wide, it would raise the RAC considerably. It would have the same frontal area as the tall narrow fuselage and about the same drag, resulting in average speed. The water effects are poor because the water tank would have little hydrostatic pressure to empty the tank. These factors resulted in a score of 49.

Our next candidate was the short height, narrow width, long length fuselage. This shape resembles a sailplane fuselage. It would have a traditional shape making it easy to construct but possibly difficult to fly with CG changes from the long water tank. This configuration achieves the same volume as other designs by increasing the dimension where it affects RAC the least, in length. Because it has a small height and width, it has the least frontal area of all the fuselages, resulting in the least drag and the highest potential speed. Of all the categories, the one it performed worst in was water effects. Being long and narrow makes it hard to distribute the water out a single orifice. Having a short height also means having less hydrostatic pressure to drain the water tank. The end result is a score of 70.

The last configuration we considered was a tall height, wide width, and short length. This configuration might be more difficult to construct because everything has to be packed into a ball instead of being more spread out. The team predicted it would fly like any traditional aircraft. The RAC would be high because the fuselage is wide where it hurts RAC the most and is short length where RAC is affected the least. Being wide and tall, there is a lot of frontal area resulting in the most drag, making a slow aircraft. It did do well in water effects where the tank shape and have good hydrostatic pressure result in an easy to drain tank. The end result of this configuration is a score of 63.

The best configuration for the fuselage was the tall height, narrow width, medium length fuselage with a score of 81 points.

3.2.3. Landing Gear Configuration

Landing Gear: Configuration	Low Drag	Light Weight	Low Cost	Time Req.	Gnd Ctrl.	Crash Resist.	
Weight:	0.2	0.2	0.1	0.1	0.3	0.1	Value
Tricycle	50	65	65	70	70	60	63.5
Tail Dragger	70	80	80	90	80	100	81
Outrigger	70	90	60	60	20	50	55
Tricycle Retract	90	30	30	30	70	50	56
Tail Dragger Retract	90	50	50	40	80	80	69

Table 3.2.3.

The landing gear is one of the many important systems in an aircraft. With three fundamentally different landing gear configurations available, a decision matrix had to be developed to help the team decide which system would best suit our initial requirements. The three landing systems consist of the tail dragger, outrigger, and tricycle configurations. The tail dragger is a system which uses three wheels placed such that two wheels sit towards the front of the aircraft, and the third wheel sits at the rear of the airplane under the tail. The tricycle gear also has three wheels, but in a different configuration such that two of the wheels are placed slightly behind the center of gravity and the third is placed in the front in the airplane. The tail dragger system has been used in many different airplanes in the history of flight, but most modern airplanes use tricycle gear instead. The tail dragger gear has its distinct advantages and disadvantages when it comes to landing and taking off. On the ground the angle of attack is high, which lets the aircraft take off without having to rotate like on a tricycle gear aircraft. During landing with a tail dragger, the pilot must be careful with pitch control to avoid bouncing and a possible forward flip. The advantages of a tail dragger include the fact that the tail wheel may be tied into the rudder, which reduces a servo and the weight of a heavy wheel in the nose. Another advantage is rough terrain. This was the primary reason the team converted our trainer aircraft from tricycle to tail dragger.

The tricycle system is the most common landing gear used on modern aircraft. Tricycle gear is popular due to the fact that most modern airplanes use a low wing configuration the tricycle gear can be easily integrated into the structure of the aircraft which saves weight. The taking off and landing for tricycle gear is straight forward when compared to the tail dragger due to the fact that taking off and landing in tricycle gear occur in level situations. One disadvantage of the tricycle gear is that an additional servo must be used to control the nose wheel.

For the outrigger gear, there is one main wheel forward of the CG. There is also a tail wheel and two small wheels at each wing tip. The disadvantage is that the plane starts and stops leaning to one side slightly, giving it poor ground control. The advantage is there is only one large wheel in the airstream.

Also considered was retractable tricycle gear and retractable tail dragger gear. It was decided that the increase in weight, complexity, cost, and crash resistance did not outweigh the lower drag. The result was the fixed tail dragger configuration which earned a score of 81.

3.2.4. Propulsion Configuration

Propulsion Configuration	Efficiency	Takeoff Thrust	Top Speed	Simple to Build	
Weight	0.1	0.3	0.4	0.2	Value
Propeller Pusher	90	90	80	50	78
Propeller Tractor	70	90	80	100	86
Ducted Fan	60	20	100	75	67
Ducted Propeller	60	50	90	60	69

Table 3.2.4.

The decision of the propulsion system was between 4 different basic layouts, Pusher, Tractor, Ducted Fan or Ducted Propeller. The ducted fan or propeller could be in either Pusher or Tractor configuration. Efficiency, takeoff thrust, and high top airspeed were the factors most influenced by this decision. Speed was given a weight of 40%, while takeoff thrust was given a 30% weight. Simple to build was given a 20% weight, and efficiency a 10% weight. Speed was given the highest weight since it directly affects the flight score.

The propeller driven pusher obtained the 2nd highest score. This is due to its tendency to increase efficiency of the airplane by not producing a wake that reduces efficiency of the main wing. However, we gave it a low score for simple to build since such a configuration requires either a canard fuselage or two motors.

The propeller driven tractor had a lower efficiency, but was simpler to build, giving it the high score of 86. It had the same speed and thrust as a pusher configuration.

The ducted fan and propeller were determined to provide the highest flight velocity due to their higher rotation speed, but the thrust from these units would be much lower and the airplane may not be able to takeoff within 150ft. Also, their efficiency suffers due to their smaller size. The result was the tractor propeller configuration which earned a score of 86.

3.2.5. Wing Configuration

Wing Configuration	Strength to Weight	Stability	High Efficiency	Easy to Build	
Weight	0.2	0.3	0.2	0.1	Value
High wing	70	100	100	70	71
Mid wing	50	80	90	60	58
Low wing	90	60	80	90	61
High Aspect Ratio (>7)	60	100	100	60	68
Med Aspect Ratio (5-7)	80	80	80	70	63
Low Aspect Ratio (<5)	100	60	60	80	58

Table 3.2.5.

Based on the decision matrix model for wing configurations and aspect ratios, the factor rankings indicated that a high wing, high aspect ratio design best suit the team's capabilities and requirements (High Wing=71, High Aspect Ratio=68). This result was based on four design factors that were deemed critical to performance of the aircraft: strength to weight ratio, stability, high efficiency, and easy to build. Stability, was weighted the most important, and was assigned weight of 0.3. Strength to weight and high efficiency were equally weighted with a weight of 0.2. Easy to build was given a weight of 0.1.

In terms of wing configuration, the high wing configuration was ranked second in the strength to weight, first in Stability, first in efficiency, and second in easy to build. The high wing configuration had the highest aerodynamic efficiency given the average operational speeds the team decided to operate in, which ranges in the slow speed aircraft category given its scale. Additionally, the high wing configuration, through practice, was easiest to control with less risk for spinning or other flight failures from pilot error. During flight, the design has natural stability due to its geometry, was less affected by ground effect, thus producing less of a tendency to float upon landing.

The other wing configurations ultimately proved less favorable in the decision matrix. The low wing configuration would have been most favorable in the weight to strength factor along with its ease of manufacturability, because the landing gear would have easily been incorporated into the low-wing design by placing the gears underneath the wing. However, in terms of flight control, the low-wing configuration was less stable. The thrust line could potentially be above the aircraft's CG, and the wing could require dihedral to better handle crosswind landing situations. While the mid-wing configuration would have decidedly performed in between high wing and low wing configurations in terms of stability and efficiency, the configuration would have fared poorly with strength to weight and easy to build. The mid-wing would have the risk of running the wing spar through the water, and as a result the ability to construct a quality design of this configuration would have been difficult.

Meanwhile, the decision for a high aspect ratio design as optimal came as a result of ideal performance factors. The high aspect ratio design was decidedly optimal over other ratio options in terms of stability and high efficiency.

3.2.6. Tail Configuration

Tail: Configuration	In Clean Air	Stall Rec./Stab.	High Str.	Low Wt.	Time Req.	Fit In Box	
Weight:	0.15	0.2	0.15	0.2	0.3		Value
Vertical T shape	90	80	60	50	70		69.5
Inverted T shape	80	60	80	70	70		71
Vertical V shape	80	70	60	70	60		67
Short H shape	50	50	50	50	90		62

Table 3.2.6.

To determine the ideal configuration for the empennage, an FOM was created consisting of the different options and their scores in different categories. For the configuration of the tail, we considered four designs: the vertical T shape, the inverted T shape, the vertical V shape, and the short H shape. Each of these four configurations was then rated in five categories, which were weighted according to importance. In clean air dealt with how much drag the tail configuration would generate and how much control surface was in the turbulence of the wings. Stall recovery and stability was concerned with the ability of the tail configuration to recover from a stall or spin and enable stable flight. High strength and low weight considered the structural integrity of the configuration versus how much it would weigh. Time required dealt with how quickly the tail could be built and assembled. Fit in box dealt with how easily the tail could fit into the box used for transporting the plane.

The calculations of the scores showed that the inverted T shape tail configuration would be the best option, with a score of 71. A close second was the inverted T shape.

3.3. Conclusions

In summary, the Spirit of Procrastination shall have the following basic configuration:

- Tractor prop, traditional planform fuselage configuration
- High wing, high aspect ratio
- Tall, narrow fuselage
- Fixed tail dragger landing gear
- Inverted T empennage

4. Preliminary Design

4.1. Mission Modeling and Optimization Analysis

4.1.1. Mission Modeling and Optimization Overview

The majority of time spent developing the Spirit of Procrastination was time spent modeling the Fire Bomber mission. An analysis of the mission scoring system showed that the Ferry mission accounted for a small fraction of the overall score, so a detailed simulation code was developed in Matlab to model the entire Fire Bomber mission. The optimization program was named WSU Spirit of Optimization (WaSoO). Figure 4.2.1 shows the optimization code flow chart.

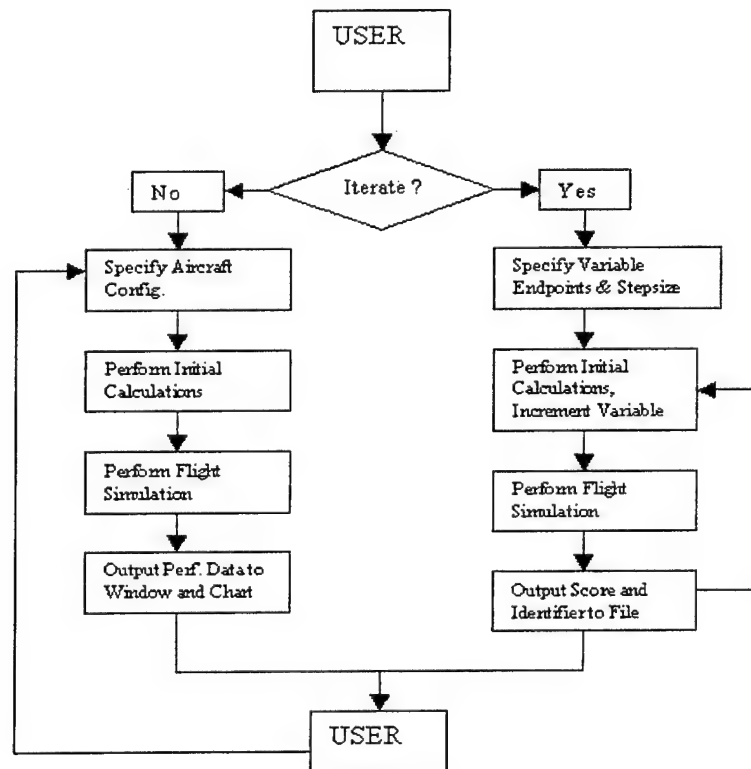


Figure 4.1.1 Optimization Code Flow Chart

The flight simulation portion of the code was run over 112,000 times, each time a single variable was changed and the flight score recorded to a file, along with a unique identifier so the score could be analyzed further. Seven variables deemed most important during the conceptual design were chosen for the analysis; propeller pitch and diameter, motor, number of battery cells, wing area, flaps and fuselage

diameter. This number provided a good compromise between computation time and ranges of configurations.

4.1.2. Aircraft Drag Model

To estimate total aircraft drag, a reference area method was used. Wing area, S_{ref} , was first calculated. For each additional component, a planform area was calculated. The ratio S_{comp}/S_{ref} was used to calculate the percentage that each component contributed to the total drag of the aircraft. Drag coefficients were found by calculating the Reynolds number for each component at an assumed average speed of 50 mph, and using appropriate empirical data. The total of these coefficients make up the C_{Dmin} component of the following formula:

$$C_D = C_{Dmin} + 1/(\pi AR.90)(C_L - C_{Lmin})^2$$

The flight simulation portion of the code simulated flight by varying angle of attack of the aircraft for different flight regimes. For the Eppler 205 used in the simulation, the response between angle of attack and C_L and C_{Lmin} is the lift coefficient at 0 degrees AOA. Thus all components of the equation for C_D were known and the drag was calculated for the aircraft for any given moment during flight simulation.

4.1.3. Aircraft Maximum Lift Coefficient

To keep WaSoO simple, the AOA was not to increase high enough to stall the wing, since stall was not modeled by the program. For the Eppler 205, this corresponded to a C_{lmax} of 1.1 and a maximum AOA of 8 degrees.

4.1.4. Propulsion System Model

Modeling of the power system proved to be the most difficult, yet possibly most important part of the optimization process. The propeller was modeled using rotating wing theory and an empirically determined power formula. The power for the static condition was approximated as follows:

$$P_{abs} = C_p D^4 P RPM^3$$

P_{abs} = power absorbed by propeller

C_p = propeller constant, 1.11 for APC fiberglass propellers

D = diameter of propeller in ft.

P = pitch of propeller in ft.

RPM = speed of propeller in kRPM

An empirical formula was found for static thrust, but was proven to be too inaccurate during static testing, so an equation based on rotating wing theory was derived. The equation is as follows:

$$Thrust = nb \cdot ch \cdot r \cdot 1/2 \cdot \rho \cdot asv^2 \cdot (C_l \cdot \cos(\tan^{-1}(V_x / V_p)) - C_d \cdot \sin(\tan^{-1}(V_x / V_p)))$$

nb = number of blades

ch = chord

r = radius of propeller

ρ = density

asv = accelerated stream velocity

C_l = propeller coefficient of lift, Clark-Y

C_d = propeller coefficient of drag, Clark-Y

V_x = forward velocity

V_p = propeller speed at 75% radius

This thrust relationship allowed us to model the unloading of the propeller during flight, as well as during static conditions. Energy consumption could then be modeled with reasonably accuracy, and a suitable battery choice be made.

4.1.5. Gross Weight Model

Gross weight estimations were based on breaking down the aircraft into individual components or systems. Weight estimates were made for components that were required to operate the aircraft. A matrix of weights was used to determine the weight for any of the 12 motors modeled. A similar table was produced for the battery cells. The total weight of the propulsion system was calculated by choosing a motor, number of cells and cell type, and then summing these values. The weight of a 4inch spinner, an AstroFlight 204D ESC, and a 24x24 propeller were added to create a conservative estimate. The payload of 4 liters of water was determined to weigh 8.8185 lbm. The landing gear parts (two wheels and a tail wheel assembly) were weighed and found to be 3.3 oz. The landing gear strut was approximated to be 2.7oz. The radio gear weights were measured: The Rx battery was 2.2 oz (5 HR-4U800 cells), the Rx 1.5 oz, and Servos 2.1oz. Wing weight was estimated based on the density of the 2003 competition aircraft wing, which was approximately 6 oz/ft of span. Fuselage weight was based on the surface area of the fuselage and the weight of the Kevlar and foam sandwich per square inch.

4.1.7. Dynamics of Flight Model

The dynamic simulation of the aircrafts flight was key in understand both the flight and structure requirements of the aircraft. The simulation focused on the fundamental dynamic forces to derive the velocity and position. The dynamic elements were then applied to a variety of equations to simulate the many aspects over the entire flight. The derived elements allowed us to begin the structural analysis with both the dimensions and forces known. The model used had 3 degrees of freedom, a pitching axis, a forward axis and a vertical axis motion.

4.1.8. Takeoff and Climb

The takeoff was simulation focused around the elements of stall speed and thrust of the aircraft. The two keys of the takeoff are when the aircraft leaves the ground and its rate of climb. By rule the aircraft must leave the ground in no more then 150ft, so all configurations not able to complete this requirement were disregarded. The stall speed and thrust had the largest effect on the takeoff performance of the aircraft. The stall speed of the aircraft was calculated using the calculated lift/drag and predicted weight. The thrust of the aircraft was directly related to the propulsion elements; motor, gearbox, propeller, and batteries. Propulsion equations used allowed the calculation of thrust continual through the takeoff period. When the accumulated velocity was greater then the stall velocity the aircraft took off and was valid if distance travel was less then 150ft. The rate of climb is based on high positive angle of attack and maximum thrust. The lift/drag equation calculated the instantaneous forces throughout the climb to derive the corresponding height. The rate of climb allowed the calculating the height entering the first turn, and an arbitrary minimum height of 100ft acted as the requirement for aircraft consideration.

4.1.9. Level Flight

The level flight simulation of the aircraft focused on the angle of attack. The key to the level flight is maintaining the lift so it equals the weight of the aircraft at any time. The difficulty is the fact that lift changes with speed and in level flight the aircraft is accelerating. The angle must change accordingly, and with water dumping over most of the flight the weight is changing which is difficult to simulate. The important aspect of maintaining angles of attack is that it limits the maximum velocity which is critical in predicting the time to complete the level flight segments of the course.

4.1.10. Turning

The turning simulation of the aircraft focused on banking angle and calculating turn radius. The banking angle is important due the fact that if it is too high the aircraft is unable to maintain level flight, so a force balance equation is required to maximize the banking angle for the tightest turn possible. The banking directly effects lift by lowering the vertical lift, which must not go below the weight of the aircraft to complete a level turn. Another important aspect is the radius at which the aircraft makes the turn in. If

the turn radius is too small the velocity is reduced, but if the turn radius is too large time is lost because there is more distance to travel then required. A force balance equation along the fuselage axis was developed to maintain a constant turn velocity. With the radius and velocity known the gravitational loading could be calculating and applied to the structural calculation for flight components. The calculation of the control volume of the elevator is based on the tightest turn required in the flight.

4.1.11. Descent and Landing

The descent and landing are similar to the takeoff and climb but with no thrust being produced by the aircraft. With the thrust reduced to zero in the beginning of the third turn the height in which the aircraft must descend is reduced to height less then 100ft. With only 300ft to travel before the aircraft must land it is important to reduce the height and speed. During the descent the velocity is decreasing so ideally the speed at touch down is bit higher than the stall velocity to minimize ground role. The simulation calculates the AOA necessary to descend on a linear path that intercepts the runway 300 ft. before the center of the course. When the aircraft touch the runway the focus is on the drag component and the friction from the wheels. The rate at the descending is directly applied to structural calculation required for landing components of the overall structure.

4.1.12. Water Bombing

Toricelli's Law was used to determine the time required to release the payload. This allowed us to model the drain time as a function of the height of the tank. Toricelli's law is as follows:

$$\frac{dV}{dt} = -cA_e \sqrt{2(P/\rho + gh)}$$

$$\frac{dV}{dt} = \text{Tank Draining Rate}$$

c = Contraction Coefficient

A_e = Area of Exit Orifice

h = Height of Tank

g = Gravity

P =Gauge pressure at tank vent, if any.

This equation was used in the optimization code to determine if the aircraft configuration would drain in the distance between turn 1 and turn 3. If not, the tank configuration was rejected, and a new configuration was tried. If the tank inlet is aligned with the air stream, a small gauge pressure is created. This pressure was found to improve drain time by approximately 2 seconds for a 12 inch tall tank. Overall drain tank was approximately 15 seconds for a vented 12 inch tall tank. This was short enough to fully

drain the tank during the draining period at full flight speed. The contraction coefficient was minimized by using a 5th order polynomial to generate a smooth contraction from the tank ellipse to the orifice.

4.2. Aircraft Configuration for Mission Model

4.2.1. Wings

4.2.1.1 Wing Planform

Wing area was chosen as the primary wing dimension to alter during the optimization program run. The airfoil was fixed as an Eppler 205, since the 2003 DBF team was familiar with its characteristics. Aspect ratio was fixed at 7, since a good compromise between efficiency, roll rate and strength occurs near this point. Since wing area affects RAC and nearly every other aspect of flight, it was a crucial variable to analyze. Wing area was related to wing span by the fixed aspect ratio. The wing span was allowed to vary from 5 to 8 ft in 1/2 ft increments. The weight of the wing was estimated to be 6oz/ft of span, based on the 2003 aircraft. Flaps were assumed to increase the Cl by 50% and were toggled on and off. The additional weight of the servo and mechanism were factored into the analysis.

4.2.1.2. Wing Spar Design

The spar for the wing of our plane had to be able to withstand the greatest forces that were going to be exerted during flight. It also had to be stiff enough so that lift would not be lost due to bending of the wing. From the WaSoO program, it was determined that the weight of the aircraft would be approximately 16 lbs. and would undergo a maximum of 4.8 g's while in flight, with a factor of safety of 2.0. The wing also had to have a span of 36 inches for one wing, a maximum deflection at the wing tip of 0.5 inches, and weigh less than four ounces per foot. From the design of the airfoil, it was determined that the wing spar could be no taller than 0.875 inches, and would have to be able to slide onto an aluminum tube to attach it to the fuselage.

Two basic designs were considered for the spar. The first was just to use a carbon tube and the other was to use a strip of balsa wood for the center and two strips of uni-directional carbon fiber laminated onto the top and bottom, all encased in a carbon fiber sleeve. To determine the deflection at the end, the weight was assumed to be equally distributed along the wing, and then the geometry and material properties were used with the equations for bending. It was soon determined that a carbon tube with the size and weight restriction we set would not be satisfactory for the amount of deflection we wanted.

The parameters for the other design had several variables: the height, the thickness of the bottom carbon (with the thickness on the top being twice as much since it would be loaded in compression), the width of the spar and the amount of taper, since it would not need to be as strong toward the tip and weight could be saved. Since the width was not going to be constant along the length of the wing, neither

would the moment of inertia and so standard deflection tables could not be used. Therefore, the equation of moment had to be determined and integrated twice and the constants calculated using the initial conditions of no angle or deflection at the base of the wing. Since this came to be a long and ugly equation, a Matlab routine was used for integration and analysis. Once the equation for bending was found, code was written that would calculate the amount of deflection at the end given a range for all four variables. More than a thousand combinations were tested and all of the ones that had a deflection between 0.4 and 0.5 inches and didn't fail with the maximum force and factor of safety applied to it were saved in a matrix. The ranges of the dimensions were reduced to be in a more desirable range and the program returned a total of about 15 possible combinations. Since the spar had to have an interface where it would go from a rectangular design to circular so that it could slide onto the aluminum tube in the fuselage, we decided we should choose dimensions that would be mostly square at the base of the spar to better adapt to a circle. This left two possibilities and then the lightest one was chosen.

The interface between the carbon tube and the balsa also had to be designed. Since the tube interface had to be strong enough to counteract the moment created by the lift on the wing there would be a couple force applied to it. It was assumed that the couple would be created by equal and opposite triangular loading on the top and bottom of the tube. The maximum force applied at the end of the tube would depend on the distance into the wing that the tube went and needed to be small enough that the carbon sleeve supporting the force would not shear. The magnitude of acceptable force was calculated using the material properties and dimensions of the sleeve and a factor of safety of 2.0.

4.2.2. Fuselage

To simplify WaSoO, the fuselage was approximated as an ellipsoid with a circular cross section. The cross sectional diameter was allowed to vary from 5 to 12 inches in 1 inch increments. The volume of the water tank was related to the height of the fuselage by assuming the water tank was a vertically positioned cylinder that would fit within the fuselage cross section at its largest point. This was used to determine if a small, low drag aircraft with a small payload would score the same or better than a large aircraft with the maximum payload. It was found that the largest fuselages generated the highest score since they had the highest capacity, regardless of drag and RAC penalty. The length of the fuselage was set to make fitting in the box easy. The total length was set at 48 inches, which minimized RAC, had adequate length for reasonably sized control surfaces, and fit in the box.

4.2.3. Empennage and Stability

When designing the empennage, several other aspects were considered. These included overall aircraft length, tail angle of incidence, control volume ratio, vertical tail area, TMA (tail moment arm) and Tail MAC. It was decided that the overall aircraft length should be no longer than 4 feet so that it could best fit into the carrying box. It was also decided it should be no shorter than 4 feet to ensure stability

without enormous horizontal and vertical tail surfaces. The center of gravity of the plane will lie at the 25% MAC of the main wing, and the neutral point of the aircraft is at a distance of 42% of the chord from the front edge of the wing. The differences in the position of these forces would create a moment. To overcome this, the horizontal stabilizer will need to be set at angle so that it will be able to produce a force that will balance the moment from the wing and allow the aircraft to fly level. The moment coefficient, the TMA, and the coefficient of lift were determined at our average airspeed velocity and then used to determine that the angle of incidence for the horizontal stabilizers needed to be negative 1.68 degrees from the horizontal.

To determine the design of our horizontal stabilizers, we had to determine how much stability and control was needed. To do this we used the tail volume ratio and decided we wanted it to be at least 0.5 based on historical data, so that it would be stable enough and yet still allow for adequate maneuverability. To calculate the control volume ratio, we multiplied the tail area over the wing area by the tail moment arm (the distance from the center of gravity for the wing to the center of gravity of the horizontal stabilizer) over the wing chord. With a total horizontal stabilizer area of 136.7 square inches and a chord of 7.5 inches, the control volume ratio came to be 0.528.

We designed the vertical tail area to just be half of the total area of the horizontal stabilizers. This means the area of the vertical tail was set to be 68.35 square inches. The MAC of the horizontal stabilizer was determined to be 7.5 inches with a sweep of 15 degrees. The tail moment arm, which is described in the above paragraph, was calculated to be 27.8 inches.

4.2.4. Propulsion System

The propulsion system was broken into 4 variables, propeller diameter and pitch, number of battery cells, and motor type. Propeller diameter was varied from 11 to 24 inches, and propeller pitch was varied from 6 to 24 inches, each in 2 inch increments. Batteries were varied from 18 to 40 cells in 2 cell increments. Twelve motor/gearbox combinations were compared from the AstroFlight and Graupner motor lines. Unlikely combinations and unavailable propeller sizes were eliminated by WaSoO to reduce computation time. A peak current of 45A was set in the program to prevent selecting designs that would blow fuses and damage the motor.

4.3. Optimization Results

4.3.1. Predicted Mission Performance for Optimized Aircraft

After running the program through 112,000 combinations of aircraft configurations, a list of the best 50 designs were made. It was observed that the top configurations all had the same theme. The

program minimized the number of batter cells and the size of the motor. This resulted in choices that had static current levels up to 45A, which was the maximum limit chosen. The best design had the configuration listed in Table 4.3.1a.

WaSoO Output: Best Configuration	
SCORE =	WING_AREA_SQUARE_FT =
83.51	5.14
FLIGHT_SCORE =	FLAP_EQUIPPED =
8.36	0.00
RAC =	WATER_DRAIN_TIME_S =
8.33	15.50
FLIGHT_TIME_S =	ENERGY_CONSUMED_MAH =
55.80	281.44
STATIC_THRUST_OZ =	TURN_1_VELOCITY_MPH =
137.29	62.87
STATIC_PITCH_SPEED_MPH =	TURN_1_BANKANGLE_DEG =
62.64	70.00
STATIC_RPM =	TURN_1_LIFT_LBS =
3006.80	52.31
PEAK_CURRENT_A =	TURN_1_RADIUS_FT =
44.00	87.45
TOTAL_WEIGHT_OZ =	TURN_1_FORCE_G =
260.47	3.21
THRUST_WEIGHT_RATIO =	TURN_2_VELOCITY_MPH =
0.53	72.74
WING_LOADING_OZ_PER_SQUARE_FT =	TURN_2_BANKANGLE_DEG =
50.65	75.00
MAX_LIFT_DRAG_RATIO =	TURN_2_LIFT_LBS =
14.49	70.02
STALL_VELOCITY_MPH =	TURN_2_RADIUS_FT =
35.07	85.08
MAX_RATE_OF_CLIMB_FT_PER_MIN =	TURN_2_FORCE_G =
1285.70	4.30
MOTOR =	TURN_3_VELOCITY_MPH =
ASTRO40SB	75.68
PROP_DIAMETER_IN =	TURN_3_BANKANGLE_DEG =
24.00	76.00
PROP_PITCH_IN =	TURN_3_LIFT_LBS =
22.00	75.80
NUMBER_OF_CELLS =	TURN_3_RADIUS_FT =
20.00	84.66
WING_SPAN =	TURN_3_FORCE_G =
6.00	4.66

Table 4.3.1.

A visual representation was used to ensure that the simulation was performing correctly. Figure 4.3.1b. is a plot from WaSoO of the Bomber mission. Turns are represented by horizontal dashes at 100 ft. The chart illustrates how the thrust degrades with flight speed. Current was integrated in the code to determine energy consumed. Takeoff distance was 105 ft. as verified on a similar chart.

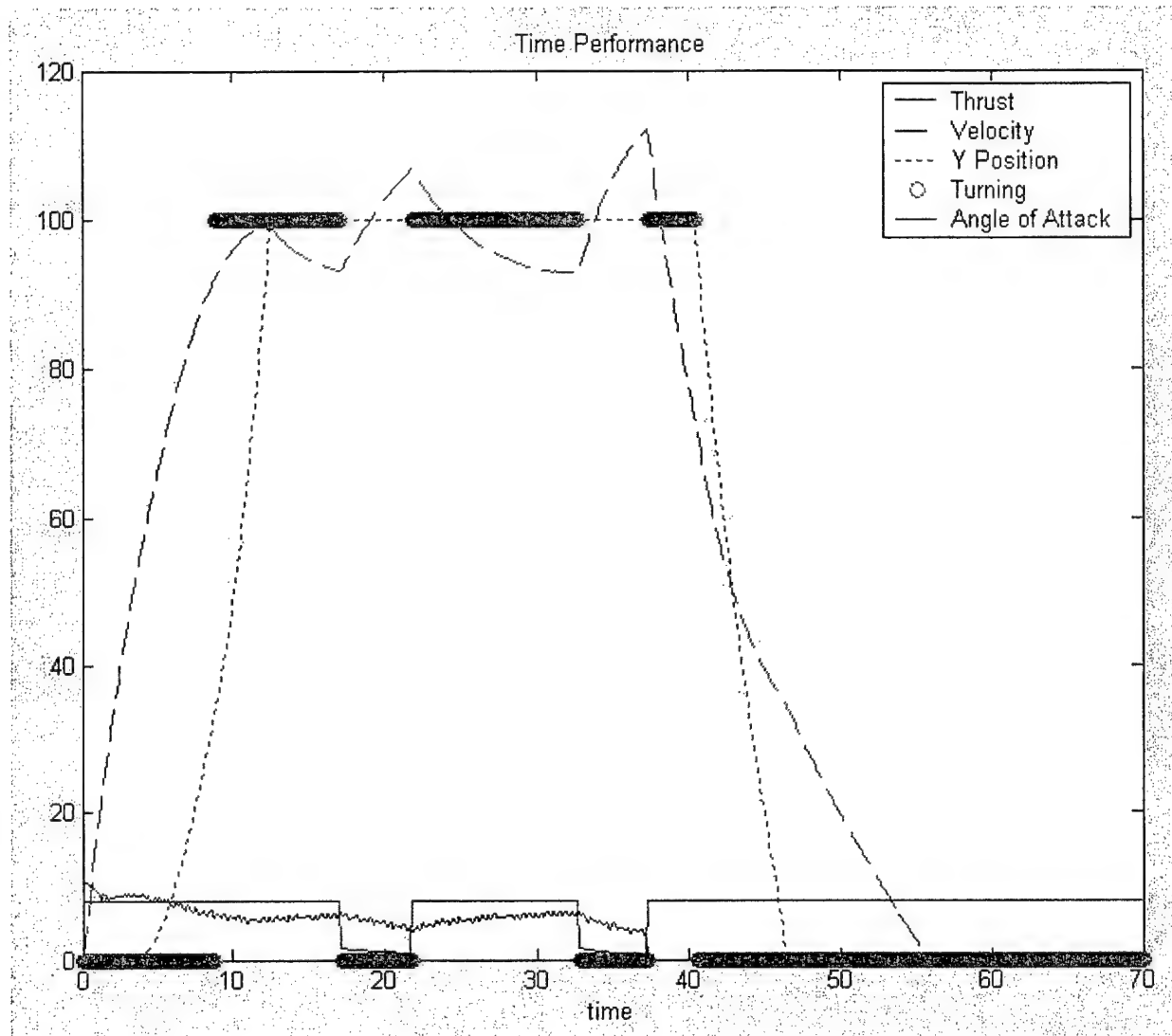


Figure 4.3.1.

4.4. Conclusions

The aircraft configuration from the preliminary design phase made sense to the team. The propulsion configuration minimizes weight, and the fuselage design minimizes RAC and water drain time. It was found that the optimum design carries the maximum water possible. The results of the simulation were estimated to be within 15% of actual values for the real aircraft, based on thrust measurements made on our test stand. Values are optimistic since perfect conditions and perfect pilot maneuvering are assumed. The real aircraft must include safety factors to prevent the aircraft from failing the mission.

5. Detail Design

In the preliminary design, we determined the design parameters to maximize the overall score. This is accomplished by minimizing the rated aircraft cost while maximizing the flight score, primarily the fire bomber flight score. We used a Matlab routine to perform thousands of iterations of design parameters to optimize the specifications of the aircraft to result in the highest possible score. Another simplified Matlab routine was made to be able to quickly determine the overall score from different design parameters, but lacking the complex equations the first program used, making changes easy. We also manually used a program called Motocalc to compare results from our Matlab routine and some of our actual testing. Motocalc would consistently underestimate amperage, RPM and thrust for a particular battery motor and prop combination.

5.1. Basic Requirements

The final design has basic requirements that must be met to meet competition rules and be a competitive design. For our final design, our aircraft must meet our goals for the aircraft specifications. These goals were determined after finishing the preliminary design. These aspects are listed in table 5.1 below.

Engineering Requirements	Required	Goal
Mission Goals		
RAC	None	< 8.5
Gross Weight (lbf)	55	< 18
Battery Weight (lbf)	5	< 2.5
Takeoff Distance (ft)	150	< 135
Flight Time, bomber mission (Min)	10	< 2
Flight Time, speed mission (Min)	10	< 2.5
Dissassembled dimensions (ft)	2 x 1 x 4	2 x 1 x 4
Strength		
Positive load (g)	2.5	7.5
Negative Load (g)	2.5	3.75
Flight Performance		
Stall Speed (mph)	None	30-35
Top speed (mph)	None	65-75

Table 5.1.1.

For the RAC requirement, we wanted our design to have an RAC under 8.5. It was determined that to place well in the competition, a low RAC is needed. Last year, the top three aircraft all had RAC's under 8.5. This was also reflected in the way the overall score made a big jump between the fourth place team and the third place team. Our WaSoO program also verified that for a maximum overall score, a low RAC was needed.

For the Gross weight requirement, it was determined if the plane was to fly with good performance on a small propulsion system (with a low RAC), the plane needed to be very light. Therefore,

our goal was to stay under 18 lbf. Also for a low RAC, a low battery weight was needed. It was determined that to stay under an RAC of 8.5, a battery pack under 2.5 lbf was needed.

For takeoff distance, we felt there was no need for having a shorter than required takeoff run. A short takeoff run (low stall speed) means we have a wing that is too large and will affect high speed performance. We did want to make sure that we could takeoff in the required distance, in case some other variable made our takeoff run slightly longer than expected. Therefore, we set our takeoff distance goal to 135 feet. From calculations made in the preliminary design, this takeoff distance corresponds to a stall speed of 30 to 35 mph.

For mission flight times, we calculated that for a reasonable flight score, a bomber mission time under 2 minutes and a speed mission under 2 minute 30 second was required. The bomber mission also requires that the aircraft be loaded with water twice during the mission. We estimated the time to load the aircraft with water and make it ready for flight was 15 seconds. Doing this twice doubles the time to 30 seconds. This means the bomber mission needs to have an actual in flight time of less than 1 minute 30 second. A 2 minute 30 second speed mission corresponds to an average flight speed of 54 mph. A 1 minute 30 second bomber mission flight time corresponds to an average flight speed of 45 mph. We felt that these goals should be attainable with the propulsion systems investigated in the preliminary design. Considering that the average includes accelerating from takeoff and decelerating to slow speed for landing, we estimated the top speed for the aircraft to be approximately 65 to 75 mph.

Competition requirements mandate that the aircraft be able to fit inside a 1 ft by 2 ft by 4 ft box. Throughout our design process, we must be aware that all parts must fit in the box. We must ensure that no parts are made so big that fitting them in the box will be difficult or impossible.

From our preliminary design, we estimated the flight loads for the aircraft in a turn to be about 5 g. Adding in a factor of safety of 1.5, our aircraft must be designed to withstand 7.5 g. Since we must pass an inverted wing tip lift test, which simulates 2.5 g, with a factor of safety of 1.5 added in, our aircraft must withstand a 3.75 g inverted.

5.2. Component Design and Selection

Part of our optimization program did not calculate certain parameters because it would make the optimization program too complex. These were analyzed in detail separately. These are separated into different systems. These are the wing system, empennage system, control system, propulsion system, fuselage system, wing to fuselage interface system, water release system, landing gear system and water loading system.

5.2.1. Airfoil Selection

The airfoil we selected was the SD7032. This was based on giving us the required stall characteristics, low drag, and highest lift coefficient of airfoils with similar drag. The SG6042 gave a higher lift coefficient, but it had a very sharp stall, which we determined to be unacceptable. Over two dozen airfoils were investigated with data in the Reynolds number range we were operating in.

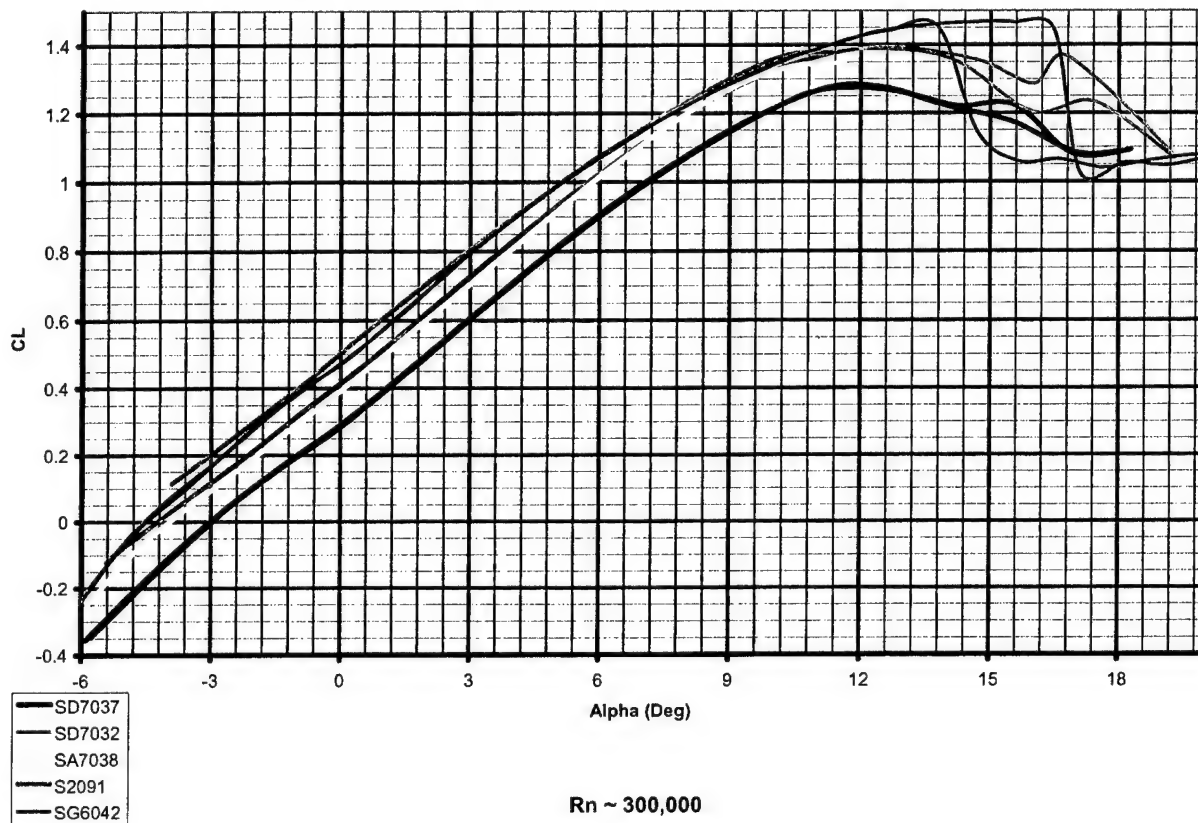


Figure 5.2.1a.

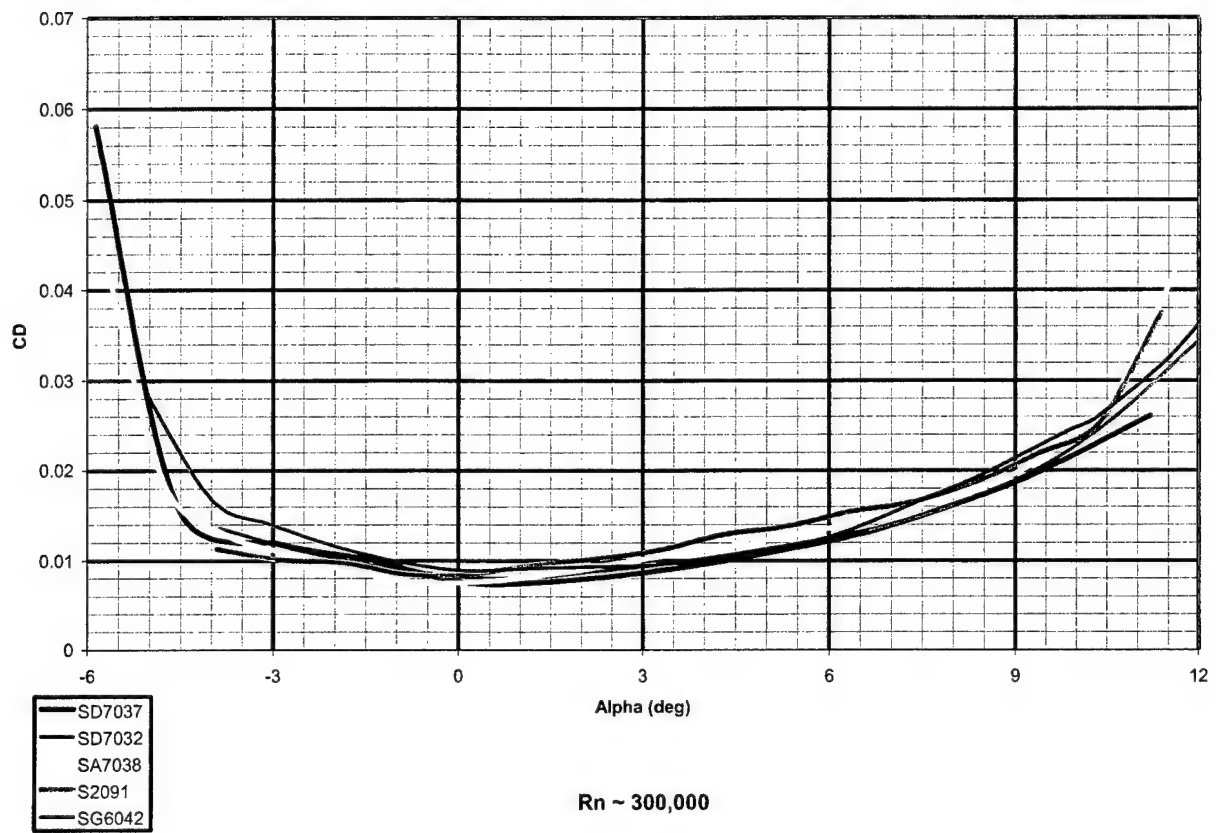


Figure 5.2.1b.

	Area	Full Length	75% span	75%span
16 lbf	No Flap	20% Flaperons	30% Slotted	30% Fowler
Stall	1.2	1.5	2	2.4
25	1201.15	960.9216	878.3424	788.256
30	834.133	667.3066667	609.96	547.4
35	612.833	490.2661224	448.133878	402.171429
40	469.2	375.36	343.1025	307.9125
	Servo, Wing Area, and ctrl surf RAC MFHR			
Stall	No Flap	20% Flaperons	30% Slotted	30% Fowler
25	93.4133	84.23066667	80.996	74.74
30	67.9259	63.84074074	62.35833333	58.0138889
35	52.5578	51.5462585	51.1204082	47.9285714
40	42.5833	43.56666667	43.8265625	41.3828125
	End RAC Result			
Stall	No Flap	20% Flaperons	30% Slotted	30% Fowler
25	7.69	7.5	7.44	7.31
30	7.18	7.09	7.06	6.98
35	6.87	6.85	6.84	6.78
40	6.67	6.69	6.69	6.65

Table 5.2.1.

It was determined by using Table 5.2.1. and other considerations that it was not worth the effort to incorporate flaps into our wing system. Flaps would decrease our wing area required for the stall speed required, resulting in smaller faster wing. Once the flaps are retracted, the wing has a lower lift coefficient and a higher stall speed. This means in high g turns, we will be close to or experiencing high speed stalls. A stall in such a turn could result in loss of control and a crash. At best, you will recover and have lost significant time during the mission. Also, with a wing operating at such a high lift coefficient, the wing will be outside of its "drag bucket" and will experience increased drag equal to or greater than a larger wing operating at a lower lift coefficient. Incorporating flaps would not significantly lower RAC due to the added servos and control surface multipliers. Finally, flaps would be an added complexity to the entire aircraft and would add weight near the weight you would save from reducing wing area.

5.2.1.1. Spar Setup

It was determined that the 36 inch wing spar should be 0.75 inches in height, have a carbon thickness of 0.022 inches on the bottom and 0.045 inches on the top, and would be tapered from a width of 0.75 inches at the base to 0.375 inches at the tip. The outer diameter of the carbon tube would be 0.683 inches and be embedded 3.0 inches into the spar. These dimensions would allow for a deflection of 0.446 inches under maximum loading and would weigh a total of 2.578 ounces, or about 0.859 ounces per foot.

5.2.1.2. Aileron System

The aileron system needs to provide good roll control for maneuvering the aircraft in high speed turns and during low speed takeoff and landing situations. The sizing for the ailerons was determined by the forces needed in high and low speed situations. The control system (aileron servo) needs to be sized correctly to deal with the loads experienced by the ailerons plus a safety margin. It was calculated that the aileron size would need to be of 2.9 inch chord for 12 inches of the outer span, resulting in 36 square inches per aileron. For the wing area we are using this fits with the historic size of ailerons for aircraft.

5.2.2. Empennage System and Stability

To minimize RAC, the length of the fuselage is minimized. A consequence of having a shorter fuselage is requiring larger empennage control surfaces. It was determined that if the fuselage, which needs to be tall for the water tank to drain fast enough, could be made into an airfoil shape and there would be sufficient lateral area where little or no additional vertical surface area would be needed. This was verified with a simple proof of concept model carved out of foam and flight tested.

The configuration of our empennage was determined to be an inverted T. This was based on spin resistance and simplicity of construction. The shape of the horizontal stabilizers was determined to be moderate aspect ratio of with a tapered planform. The horizontal surface is to be of 136.7 square inches, and the vertical tail surface is quite large because the fuselage extends to form the tail.

Elevator size and loading was determined to be 35% of the horizontal stabilizer, resulting in an elevator area of 48 square inches. The vertical stabilizer is molded with the rest of the fuselage as the same piece. Rudder control surface size and loads were determined to be half the elevator area, at 24 square inches.

5.2.3. Control System

The control system was optimized by estimating control surface loads and specifying servos with the required capability (plus safety factor), while having as few servos as possible, and finding servos that will perform their task reliably. One aspect that plagued last years aircraft was having a simple, well routed, and reliable wiring system for the aircraft. This year, our aircraft will use as few electrical connections as possible by making a custom wiring harness. The aileron and empennage control surface loads determined by the equation:

$$\text{Torque (oz-in)} = 8.5E-6 * (\text{Surface chord (cm)})^2 * \text{Speed (MPH)}^2 * \text{Length (cm)} (\text{ctrl surf. degrees}) * \tan (\text{ctrl surf degrees}) / \tan (\text{servo degrees})$$

From this equation, we were able to determine how much torque would be necessary to deflect each of our control surfaces. The load on a servo is based upon the control surface size, being its chord and length, as well as its deflection and the maximum aircraft speed.

After calculating that the aircraft would be flying at most 80mph with a control surface deflection of about 35 degrees, we came to the conclusion that we would need roughly 37 oz-in of torque for each 12 inch by 2.9 inch aileron, 43 oz-in of torque for the 21 inch by 1.9 inch rudder, and 74 oz-in for the 16 inch by 3 inch elevator. We added a factor of safety of 2 to the required torque output, which brings our required torque to 74 oz-in for each aileron, 86 oz-in for the rudder, and 148 oz-in for the elevator. With that specification, a decision for the brand and model of servos could be specified. A servo and a connection to the control surface needed to be made. It was determined the best combination of low drag, reliability, low complexity, and light weight resulted in having the servos placed below the surface of the plane with short external linkages using standard servo linkage parts.

The maximum servo loads for ailerons were determined to be about 148 oz-in. A solution to controlling these surfaces while having low RAC (low servo count), reliability, low drag and light weight was determined. To control the ailerons, one servo is placed in each wing. It was determined that the reliability of the aileron system would be compromised by having a long, complex linkage connect both ailerons to a single servo. There are also few servos that could meet the loading demands and remain light weight. The connection to the control surface is made by using standard servo linkages.

After determining the number of servos and the loads required for the servos, we determined how many cells and what capacity our receiver battery needed to be. It was determined to use a 5 cell receiver battery because of better servo performance at 6 volts and reliability if a cell were to fail (short only). It was determined that the cells needed to handle a worst case servo and receiver load of 2 amps for a theoretical situation where 5 flight attempts were made, each lasting at most 5 minutes. This would require a cell capacity of 0.833 Ah. From this, the brand and model cells for the receiver battery pack could be determined.

5.2.4. The Propulsion System

The propulsion system was optimized using the WaSoO program, which went through 112,000 of iterations of motor, gearbox, battery, prop combinations. The best motor, gearbox, propeller, and battery setups were determined to be an Astro Flight Cobalt 40 motor with a superbox using a Bolly brand 24x24 prop running on a custom battery pack of twenty Sanyo CP-1300SCR cells. From the WaSoO program, it was determined that the above setup maximized flight score by balancing performance with light weight low RAC. We verified the accuracy of the results from WaSoO by bench testing a similar propulsion system setup and comparing to the data WaSoO put out. We tested an Astro Flight Cobalt 40 with a

superbox and connected our batteries from last year, twenty-four SR 2400 Max cells. We then put a 16x16 prop on and put the combination on our test bench.

Cobalt 40 Superbox, 24 cells, 16x16 APC prop		
28 February 2004.		
Parameter	WaSoO	Test Bench Results
Amps	24	33
RPM	5000	4900
Thrust (oz)	70	84

Table 5.2.4.

Our results showed that the WaSoO program underestimated amperage by 27% and thrust by 16%, but accurately modeled RPM within 2%. This error can be fixed by modifying parameters in how the program models thrust, which is one parameter that determines current in the program.

5.2.5. The Fuselage System

With the fuselage shape determined to be tall and narrow, it was decided the fuselage would be an airfoil design when looked at from above, and rectangular from the side. The airfoil design was determined to be a NACA 63A010. Having the fuselage be rectangular in the side view allows the rear of the fuselage to possibly perform the task of a vertical stabilizer. If the vertical stabilizer can be eliminated from the design, the RAC can be reduced. The fuselage will attach to a wing to fuselage interface platform. On this platform, the water tank will be attached. The fuselage needs only to support the weight of the filled tank when it is on the ground.

5.2.6. Wing to Fuselage Platform

The wing to fuselage platform consists of a plate that with an aluminum tube attached to connect both wings together. On the plate are holes for bolts to pass through to attach the platform to the fuselage. To keep the wing from rotating about the spar, two stabilizer pins will be built into the wing assembly and are inserted into holes in the wing to fuselage platform.

5.2.7. Water Release System

The water release system works by having a ball valve actuated by a servo. Linkage is set up between the valve and the servo. The valve is attached to the tank fits through a hole in the bottom of the fuselage to release water.

5.2.8. Landing Gear System

Landing gear is attached to a mounting plate inside the bottom of the fuselage, one inch from the bottom of the outer surface. It was determined that the landing gear should be 18 inches wide (25% of the wingspan) to provide adequate ground stability. The landing gear also was sized to provide 2 inches of clearance for a 24" propeller when the aircraft is level in flight attitude. It was determined that the landing

gear be 7 inches tall from the mounting plate to where the wheel meets the ground. It is also determined that the landing gear needed to be low drag and stiff to provide good landing characteristics with little bounce. It was decided that the cross section of the landing gear would have an airfoil profile to provide low drag.

5.2.9. Water Loading System

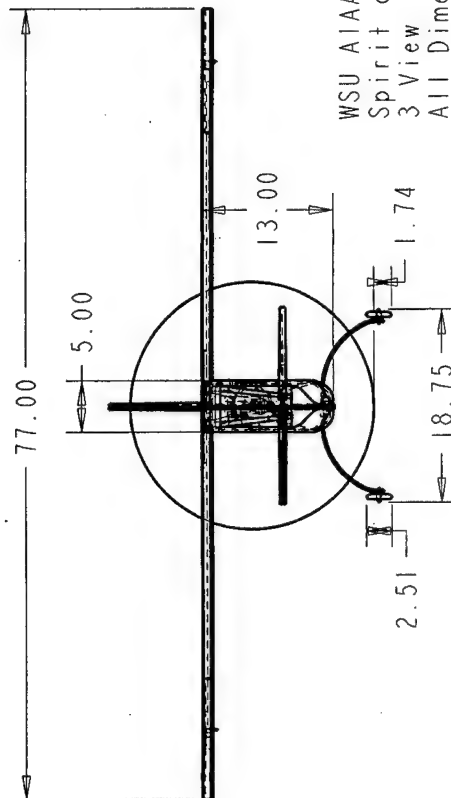
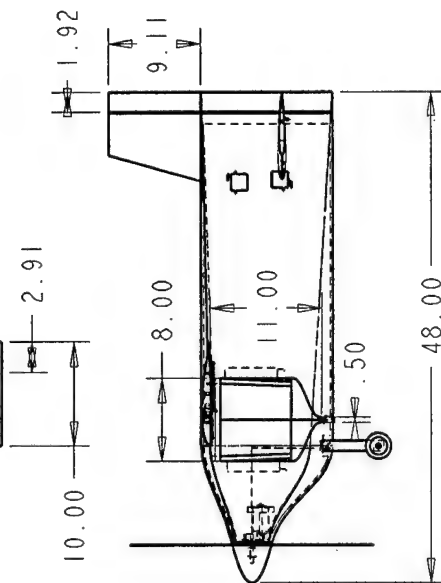
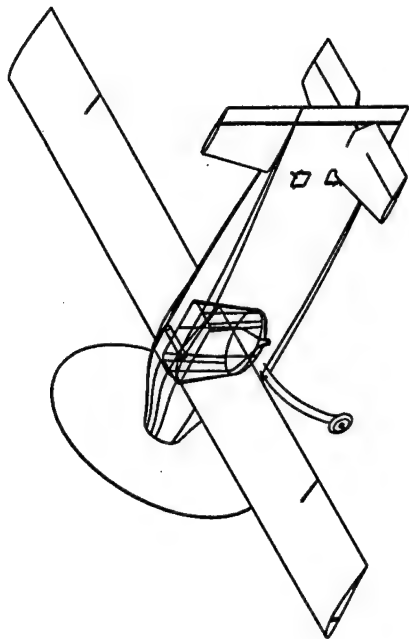
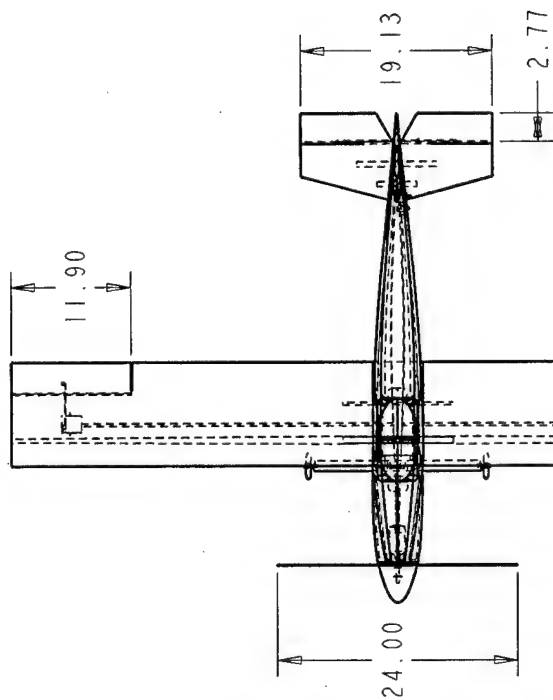
The water loading system consists of a manifold that two 2 liter bottles can screw into. There are water passages that converge to a ball valve. Vent tubes will run into the soda bottles to prevent chugging.

5.3. Final Aircraft Specifications

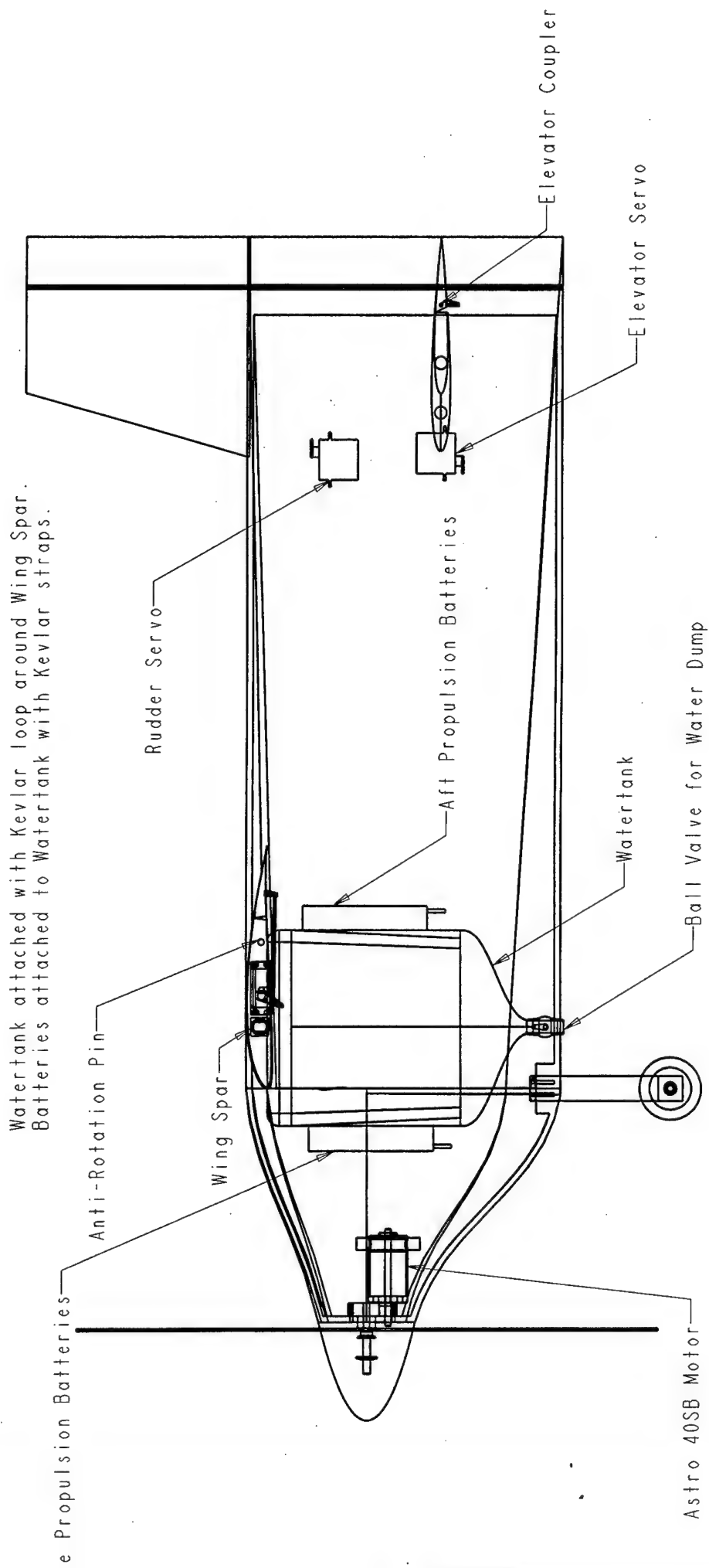
Geometry:		Weight Statement:	
Length (inches)	48	Airframe (lb.)	4
Wing Span (inches)	72	Propulsion System (lb)	2.915
Height (inches)	13	Control System (lb)	0.5
Wing Area (square inches)	720	Payload System (lb)	0.25
Aspect Ratio	7.2	Payload (lb)	8.8
Horizontal Stabilizer Volume, (in ³)	147	Empty Weight (lb)	7.665
Elevator Volume, (in ³)	48	Gross Weight (lb)	16.465
Vertical Stabilizer Volume, (in ³)	156	System:	
Rudder Volume, (in ³)	24	Radio	JR 8103 PCM
Ailerons Volume, (in ³)	72	Servos	5
Performance:		Battery Configuration	20 cells Sanyo CP1300SCR
CL max	1.4	Motor	Astro Flight Cobalt 40 Superbox
L/D max	14	Propeller (nominal)	24 x 22
Max. Rate of Climb (ft./min.)	1200	Gear Ratio	3.31:1
Stall Speed (MPH)	35		
Max. Speed (MPH)	80		
Take-off dist. (Empty Weight)	77		
Take-off dist. (Gross Weight)	106		

Table 5.3.1.

5.3.1. Drawing Package



WSU ATAA
 Spirit of Procrastinatio
 3 View
 All Dimensions in inches



WSU AIAA
 Spirit of Procrastination
 Part Assembly Front View

5.3.2. Rated Aircraft Cost Calculation

Aircraft Cost Model		
RAC	\$7.89	
A	\$300.00	
B	\$1,500.00	
C (\$/hour)	20	
MEW (lb)	9.205	
REP (lb)	1.54	
MFHR (hours)	141.1111111	
Input Parameters		
propulsion battery (lb)	1.54	
airframe weight (lb)	7.665	
wing area (ft^2)	5	
# of wings	1	
control function multiplier	1	
fuselage length (ft)	4	
fuselage width (ft)	0.42	
fuselage height (ft)	1.08	
vert. surface	0	
vert. surface w/control	1	
horiz. surface	1	
# of servos and motor ctrl.	6	
# of engines	1	
MFHR (Manufacturing Man Hours)		
variable name	variable discription	hours
WBS wing	10*(wing area * number of wings) + 5 * control_function_multiplier	55
WBS fuselage	20 * (body length * width * height)	36.11
WBS empenage	5 * vertical surface w/no control + 10 * vert surf w/control +10*horiz surf	20
WBS flight systems	5 * servo or motor controller	30
MFHR Total		141.1

Table 5.3.2.

5.4. Final Aircraft Performance Analysis

5.4.1. Predicted Performance

With the final details of the aircraft determined, the final setup was run one last time in the WaSoO program.

Aircraft Performance	Bomber Mission	Speed Mission
Takeoff Distance (Ft)	105	77
Takeoff Time (Seconds)	3.6	3
Landing Distance (Ft)	300	300
Landing Time (Seconds)	3.6	3
Rate of Climb (Ft/Min)	1200	1550
Turn G's	4.8	4.6
Turn Radius (Ft)	87	87
Stall Speed, Empty (MPH)	27	27
Stall Speed, Gross (MPH)	35	35
Cruise (Avg) Speed (MPH)	60	65
CL Max	1.2	1.2
L/D Max	14	14
L/D Cruise	8	8
Flight Time	114	120
Flight Score	8.3	0.33

Table 5.4.1.

6. Manufacturing Plan

By using figures of merit and some calculations, we were able to determine the manufacturing methods for all of our components. For each component, a material and a construction method were selected. Next, we came up with a plan for how to construct each component.

6.1. Manufacturing Processes and Component Selection

Our figures of merit were set up with qualities on the top row, with weights for each quality on the next row (all weights adding up to 1), and on the left a column with different construction options. There are figures of merit for all major components. These include: the wings, fuselage, landing gear, and empennage. We based the different figures of merit on five qualities; fast construction, low skill level, strength-to-weight ratio, low cost and smooth surface.

Fast construction is a primary concern for our team because of the limited time available for construction. Low skill level is another quality that we wanted. Strength to weight was another primary concern. We need to keep our weight down so that for a given propulsion system, we achieve a higher speed and shorter takeoff. A small propulsion system means low RAC, and low RAC is needed to be competitive in the competition. Low cost is another quality we were concerned with because of our limited budget. The last quality was a smooth surface. A smoother more accurate surface produces a cleaner aircraft with less drag. All of the factors of merit are weighted differently for each component because each component has specific needs.

6.1.1. Wings

Wings	Fast Const.	Low Skill Level	Strength To Wt.	Low Cost	Smooth Surface	
Weight:	0.3	0.1	0.3	0.1	0.2	Value
Negative Mold	30	50	80	30	100	61
Positive Mold	40	10	70	20	60	48
Foam Core	100	90	75	70	80	84.5
Lost Foam Core	80	10	50	70	60	59
Balsa Built Up	60	30	65	30	60	55.5

Table 6.1.1a.

For our wings, we concluded the best construction method for our wings was the simplest, a foam core wing. It is light, fast, easy to make, cheap, and results in an accurate wing profile. For a material, we selected Kevlar. Kevlar has roughly three times the strength-to-weight ratio as fiberglass and is cheaper than carbon fiber.

Composite Materials	Workability	Stiffness	Strength To Wt.	Low Cost	Toughness	
Weight:	0.2	0.2	0.3	0.1	0.2	Value
E-glass	90	60	60	100	70	72
Kevlar	80	75	90	60	100	84
Carbon Fiber	80	100	100	40	60	82
S-glass	90	70	70	80	80	77

Table 6.1.1b.

From Table 6.1.1b., we concluded that Kevlar is better for general purpose use. There are situations where stiffness and strength to weight is of greater importance. In those situations, carbon fiber is the material of choice.

6.1.2. Fuselage

Fuselage	Fast Const.	Low Skill Level	Strength to Wt.	Low Cost	Smooth Surface	
Weight:	0.3	0.2	0.3	0.1	0.1	Value
Negative Mold	60	50	70	60	90	64
Positive Mold	60	50	70	60	50	60
Foam Core	50	70	70	80	50	63
Lost Foam Core	30	60	50	40	50	45
Balsa Built Up	20	40	50	30	40	36

Table 6.1.2.

For the fuselage, we decided the best method of manufacturing was a negative mold. It requires a bit more skill and time than other methods, but it produces a light, low cost fuselage with a great surface finish. A foam core was second, but we decided that the more accurate and smoother profile produced by the negative mold would result in a slightly faster plane.

6.1.3 Landing Gear

Landing Gear	Fast Const.	Low Skill Level	Stiffness to Wt.	Low Cost	Smooth Surface	
Weight:	0.2	0.2	0.4	0.1	0.1	Value
Aluminum	80	80	70	80	80	76
Titanium	80	80	60	60	80	70
Carbon fiber	60	70	90	70	70	76
Steel	90	80	40	90	10	60
Magnesium	80	80	80	60	80	78

Table 6.1.3.

For the landing gear, we decided the best material was magnesium. Compared to aluminum and titanium, for the same stiffness member, the magnesium section was lighter. This was because of the

larger cross section gave a better moment of inertia for the section. A close second was aluminum and carbon fiber. We decided that although magnesium landing gear was easier to make, if we had enough time, carbon fiber gear would be better because of the strength to weight ratio.

6.1.4. Empennage

Empennage	Fast Const.	Low Skill Level	High Str.	Low Wt.	Low Cost	Smooth Surface	
Weight:	0.3	0.2		0.3	0.1	0.1	Value
Negative Mold	50	50		70	70	90	62
Construction	40	70		70	60	60	59
Foam Core	90	90		90	90	75	88.5
Lost Foam Core	70	70		70	60	70	69

Table 6.1.4.

For the empennage, we decided the best method was foam core. There was no sense in taking all the time in making mold for parts that would weigh the same or more than a foam core part. Foam core is quick, easy, and cheap.

6.1.5. Payload Loading System

Charging Unit	Fast Construction	Low Skill Level	Manuverability	Low Cost	Ease Of Use	
Weight:	0.2	0.1	0.3	0.1	0.3	Value
Gravity/Hose	50	60	90	60	30	58
Bleeder/Gravity	40	50	90	50	30	54
Manifold/Gravity	30	40	90	40	50	56
Manifold/Pump Air	30	40	90	40	80	65

Table 6.1.5.

The payload loading system is composed of 5 items; a valve, manifold and holder, air pump and lines, and the operator. The system is designed so that one person can effectively deliver the payload to the plane easily and efficiently. To make this system worth the effort and the trouble the design needed to be effective in lowering the loading time. To do so an air pump was added to the bleeder tubes to deliver a charge of air to the 2 liter bottles the instant the water valve is opened. To be able to release the water and charge the tank at the same the operator will open the water valve and turn on the switch for the air at the same time. With this system the estimated time saved on a gravity charge is 3 seconds. This will be a 38% decrease in time needed to load the plane and drop our time from 8.6 seconds to 5.6 seconds for the loading of the water. To keep the plane from burping the payload a float valve will be used inside the payload tank.

6.2. Processes Selected for Manufacture of Major Components

In the past we have found that manufacturing parts is a bit more complicated than one might first realize. To alleviate the amount of problems during the manufacturing process, we consulted many sources on manufacturing methods for our different aircraft components. After consulting those sources, we have devised a manufacturing process for each component.

6.3.1. Wings

The wings are to be made using a vacuum bag over a Dow building foam core (with balsa or ply end caps) with 1.7oz Kevlar covering the outside. Inside the core is the wing spar. The foam core is cut by using a hot wire and airfoil profile templates. The space for the wing spar is also hot wired out. The wing spar is made from a hollow round section of carbon fiber at the root end, transitioning to a rectangular section the rest of the span. The tube end will have inserted an aluminum 2024-T3 .750" diameter .035" wall 11" long tube connecting the two wings with the wing to fuselage interface. A small screw will keep the wings from sliding out and two wood dowels in the aft section of the wing profile to keep the wing from twisting. The carbon fiber tube will be the first 3" of the spar, made from .750" ID .045" wall tube. Then it will transition to a rectangular section spar. The rectangular section will be of vertically oriented grain light competition grade balsa, transitioning from .750" wide at the round tube transition to .375" near the wing tip (we will need to build a taper jig for table saw), and sealed so it doesn't soak up epoxy like a sponge. There will be a .045" thick unidirectional carbon fiber cap strip on top and .022" thick strip on the bottom. The spar will be wrapped with a carbon fiber braided sock, then it will be vacuum bagged. To bind the layers we will use shell epoxy, which is a mixture of Epon 862 and Epicure 3234.

6.3.2. Fuselage

The fuselage will be constructed using a female mold in tooling foam, waxed, and a composite lay-up made and vacuum bagged to the mold. From the firewall to the vertical stabilizer, the fuselage will be constructed from two halves, left and right. It will be a sandwich lay-up consisting of 3 layers. The outside layer will be 1.7oz Kevlar. The next layer will be building foam cut .250" thick and thermoformed to the mold profile before lay-up. The inside layer is another layer of 1.7 oz Kevlar. In strategic locations, strips of uni-directional carbon fiber and end-grain balsa will be placed between the Kevlar and foam on the inside and outside. Binding the layers again is shell epoxy. Then on top of the inside layer (top layer while in the mold) a perforated peel ply is laid down with a breather layer on top of it. Then the stretchable nylon vacuum bag is put over the mold and vacuum is pulled. At the front, the firewall core will be made of light plywood, .250" thick, instead of building foam. The top of the fuselage will be open for the wing to fuselage interface plate to bolt on and to slide in the water tank, which is suspended from the wing to fuselage interface plate. Where screw attachments are made, building foam will be substituted with end

grain balsa or light plywood. The front of motor will mount to the firewall. The firewall will be directly behind the propeller spinner.

6.3.3. Landing Gear

The landing gear is made by hotwiring a long flat section of high-density foam into a low drag profile. The foam is then thermoformed around a mold to pre-bend it in the correct geometry. Then, strips of uni-directional carbon fiber are laid on the top and bottom. Finally, a carbon fiber braided sleeve is put around it and the combination is wetted out with shell epoxy. It is then vacuum bagged around the mold. Where holes are made, foam is substituted with end grain balsa, and fabric is stretched around where holes are made. Wheel pants are made as a single layer of 1.7oz Kevlar in a negative mold with right and left halves. One half goes around the end of the landing gear where the wheel attaches, the other half attaches to it covering most of the wheel

The wheels we used are Williams Brothers vintage 3-1/8" wheels. They have a narrow profile and allow the wheel pants to be narrow.

6.3.4. Empennage

The vertical stabilizer is molded with the right and left fuselage halves, and construction of it is explained in the fuselage section. Inside the fuselage servo control linkages are run and the tail wheel bracket is mounted on the end of the fuselage. The horizontal stabilizer is constructed of building foam hotwired to a NACA 0009 profile. It is then covered with a layer of 1.7 oz Kevlar. A cutout is made in the foam for a hollow .500" ID .033" wall carbon tube spar. An aluminum tube .500" OD and .035" wall is used to link both horizontal stabilizer halves through the tail boom. The rudder and elevator will be hinged using Robart brand hinges.

6.3.5. Electronic Components

The radio gear selected was based on the transmitter we are using to control the aircraft (JR 8103 PCM). We decided to use our existing JR 9 channel PCM receiver with a custom wiring harness made to run through the plane to connect all the servos to the receiver. The only connections are at the servo (in case one needs replacement) at the receiver. This way there are not multiple servo extension wires with connections to come loose. The receiver antenna is routed along the outside of the aircraft to avoid interference from servo wires and shielding from carbon fiber components. Four servos (rudder/tailwheel, aileron, elevator, and water) and an electronic speed control make up the control outputs. After calculating the torque required in the detailed design, we found the ailerons, rudder, and elevator required 74 oz-in, 86 oz-in, 148 oz-in of torque respectively. The servos selected were chosen by many various attributes. The aircraft demanded that the servos not only have sufficient torque, but

holding power, high speed, low power drain, low weight and small size, high strength of components, high reliability, as well as low cost. We opted to use the Hitec HS-5645MG Digital Servo.

The Hitec servo applies up to 168oz/in of torque at 6 volts. Operating at 4.8 volts it supplies a torque of 143oz/in, which is sufficient for each of our surfaces. The speed varies again depending on voltage from .15-.18 seconds at 60 degrees. This speed allows our surfaces to move rapidly as soon as input from the transmitter is executed. Although this servo has large amounts of torque, speed, and holding power it only draws approximately 8.8-9.1 milliamps at idle and 400-500 milliamps when load is applied. The gears are made from a combination of 3 metal gears and 1 resin gear using dual ball bearings for smoothness. Another factor taken into consideration was the weight and the cost. The servo weighs only 2.1 ounces and is small enough to work in almost any location.

With these attributes it is apparent this servo will not only match our needs but exceed in almost all of them. This servo should supply a reliable control output for the aircrafts control surfaces.

We chose a 5 cell 800 mAh Sanyo NiMH cells for our receiver battery to save on weight and increase the voltage to the servos can operate at higher torque levels. Also, if a cell does go bad (short), the other four cells provide the performance of a normal receiver battery.

6.3.6. Payload Deployment System

Our water deployment system consists of a high-torque servo and linkage to a commercial PVC ball valve that has been trimmed and lightened. The valve is epoxied to the water tank as is the servo mounting plate. The system is simple, throw a non-proportional switch on the transmitter and the servo actuates the valve. The water payload deployment is made using a .500" ID PVC ball valve. The linkage to the servo is made using standard servo linkage parts.

6.3.7. Motor Cooling System

The electric motor, since it will be running near its maximum current rating, will be very close to the melting temperature of the insulation over the windings. To provide a margin of safety, a lightweight aluminum heat sink will be milled out of 1100 Aluminum and wrapped around the motor and secured with screws holding the heat sink around the motor much like a clamp. Paste used for between computer microprocessors and their heat sinks is used to increase the conduction between the motor and the heat sink.

6.3.8. Wing to Fuselage Interface and Water Tank

The wing to fuselage interface is a platform that lies on top of the fuselage and bolts to the fuselage. The water tank is suspended from this platform, and the wings plug into the side of this

platform. Also in this platform are the aileron servo(s) for the wings. The platform contains the tube of 2024-T3 .750" OD .035" wall tube that is 11" long connecting the two wings to the fuselage.

6.4. Manufacturing Dependencies

During the process of building the plane, certain parts need to be finished before others can begin construction. The table below outlines the production sequence.

Step	Process	Dependencies	Est MFG time (Man-hrs)
A	Construct and wax fuselage mold		20
B	Construct water tank mold		10
C	Fabricate water deployment system		8
D	Fabricate landing gear		20
E	Fabricate motor heat sink		2
F	Hot wire foam wing core		3
G	Hot wire foam horizontal stabilizer		3
H	Construct wing spar		12
I	Thermoform foam in fuselage mold	A	6
J	Lay-up fuselage	J, A	20
K	Lay-up water tank	B	10
L	Construct wing to fuselage interface	M	20
M	Assemble & vacuum bag wing and spar	H,F	8
N	Install propulsion system	J,E	1
O	Vacuum bag horizontal stabilizer	G	4
P	Install electronics, batteries, and servos	L, N, O, M	4
Q	Install landing gear	J	1
	Total Man hours		152

Table 6.4.

6.5. Manufacturing Milestones

Below is a chart showing our manufacturing schedule. The bars in dark grey show the planned schedule. The bars in light grey show the actual event.

Task	Feb 04'	Mar 04'	Apr 04'
Dates	1 to 7	8 to 14	15 to 21
Propulsion testing	actual		
Order and receive materials			
actual			

Build aircraft	
Construct and wax fuselage mold	
actual	
Construct water tank mold	
actual	
Fabricate water deployment system	
actual	
Fabricate landing gear	
actual	
Fabricate motor heat sink	
actual	
Hot wire foam wing core	
actual	
Hot wire foam horizontal stabilizer	
actual	
Construct wing spar	
actual	
Thermoform foam in fuselage mold	
actual	
Lay-up fuselage	
actual	
Lay-up water tank	
actual	
Construct wing to fuselage interface	
actual	
Assem. & vac. bag wing and spar	
actual	
Install propulsion system	
actual	
Install propeller and spinner	
actual	
Vacuum bag horizontal stabilizer	
actual	
Install elect., batteries, and servos	
actual	
Install landing gear	
actual	
Flight Testing	
actual	

Table 6.5.

7. Testing Plan

Testing is critical to the manufacture of an aircraft. Questionable analytical data and calculations can be verified with real world results. Testing can show weaknesses, design flaws, and oversights. Testing can also be used as a method for optimization to find the best combination for the aircraft.

7.1. Test Objectives and Schedules

The objective of our tests is to verify calculations made. The first test will be a static propulsion system test. Given a particular propulsion system setup, data is recorded for thrust, current, and propeller rpm. This is compared to data from the WaSoO program. In Table 5.3, we saw that WaSoO underestimated current and thrust. From this data, changes to how WaSoO models thrust and current will be made. The second test will be the flight test. Checklists for the flight and testing can be found in the tables below.

7.2. Flight Testing Checklists

Pre-Flight Checklist

	1. Remove Fuselage from packing crate
	2. Remove wings from packing crate
	3. Slide wings onto wing tube and fasten the wings securely
	4. Pull on wings to ensure they are on
	5. Remove empennage from packing crate and assemble it
	6. Fasten empennage to the aircraft
	7. Remove landing gear from the packing crate
	8. Fasten the landing gear to the plane
	9. Connect all servo extensions within the plane to the receiver
	10. Connect the power plant to the electrical systems
	11. Fill water tank depending on flight plan, make sure water inlet is closed off tightly and check for leaks
	12. Test C.G. of the plane both using both the pitch and roll axis
	13. Turn on the transmitter
	14. Turn on the receiver
	15. Check servo response
	16. Range test the transmitter (50 feet away from plane with antenna down)
	17. Check all moving parts and connections for secure fit

Pre Flight Testing

Day 1: In Shop (Preliminary Testing)

	1. Ground Testing of maiden voyage
	2. Check all removable components to ensure that they are fastened properly to the aircraft (including the tank)
	3. Visually check all electrical connections
	4. Visually check connections of all moveable parts
	5. Turn on radio and receiver and make sure a signal is being sent
	6. Test servos with radio to check for servo reversing, movement of control surfaces and estimate the amount of throw the surfaces will need
	7. Range test the radio and receiver (50 feet between radio and receiver with the antenna of the transmitter down)
	8. Test PCM abilities of the receiver to check fail safe
	9. Test engine to ensure optimum efficiency (static propulsion test)
	10. Stand 100 feet away from the plane and make sure the pilot can differentiate between the top and bottom of the aircraft
	11. Test water charge system to make sure operational by dumping water.

Day 2: At Field (Ground Testing)

	1. Check all removable components to ensure that they are fastened properly to the aircraft (including the tank)
	2. Visually check all electrical connections
	3. Visually check connections of all moveable parts
	4. Turn on radio and receiver and make sure a signal is being sent
	5. Test servos with radio to check for servo reversing, movement of control surfaces and estimate the amount of throw the surfaces will need
	6. Test PCM abilities of the receiver to check fail safe
	7. Test engine to ensure optimum efficiency (static propulsion test)

Day 2: At Field (Waterworks Testing)

	1. Fill the tank with water
	2. Make sure water inlet is sealed properly and check for leaks
	3. Release water on the ground to make sure the plumbing works

Day 2: At Field (In-Flight Testing)

	1. Taxi down the runway and test steering capabilities
	2. Taxi down the runway at full thrust and test high speed taxi
	3. Take off and measure distance the plane needs to become airborne
	4. Trim the aircraft so that it flies straight
	5. Take the plane to a sufficient height, set the engine at idle, and test the stall capabilities
	6. Bank aircraft at various pitches at 0% power, test for tip-stalling
	7. Land aircraft and measure the distance and speed required for landing (touch-and-go may be required)

Day 3: At Field (Going through the paces)

	1. Give full power to the engines and pull up so that the airplane is flying almost vertical and test vertical stall
	2. Test tight turning radius of the plane and check for stall speed while in the turn
	3. Test in flight water release capabilities within the flight path
	4. Simulation of entire DBF competition

7.3. Summary of Test Results and Lessons Learned

It was found accidentally during material experimentation that DOW insulation can be thermoformed to nearly any desired shape using a heat gun or oven. This discovery lead the team to designing the fuselage based on this thermoforming procedure, which will provide the lightest and strongest structure we are capable of producing.

An AstroFlight Cobalt 40 motor was overheated during static testing. The cause was running the motor for over 1 minute near its manufacturer maximum rated current, which was approximately 33A. Future static testing will be to simulate short duration power bursts, such as takeoff and acceleration, and will be limited to 15 seconds.

8. References

Selig, Michael S., et, al. "Summary of Low-Speed Airfoil Data." Volume 1. 1995. SoarTech. Virginia Beach, VA

Davisson, Buddy. "High Wing vs. Low Wing: Which one is Better?" Plane and Pilot. Feb 2002. 17 Sept 2002. <<http://www.planeandpilotmag.com/content/pastissues/2002/feb/highwing.html>>

"Aircraft Spruce and Specialty Co." Catalog. 2001-02

RC Universe. Message Boards: various threads with various authors. <<http://www.rcuniverse.com>>



CASE

CASE WESTERN RESERVE UNIVERSITY



CELEBRATING THE EVOLUTION OF FLIGHT
1903 TO 2003 ... AND BEYOND

CASE WESTERN RESERVE UNIVERSITY

2004 A.I.A.A. DESIGN / BUILD / FLY COMPETITION

Documentation for the Design and Manufacturing of:

FLYING NEMO

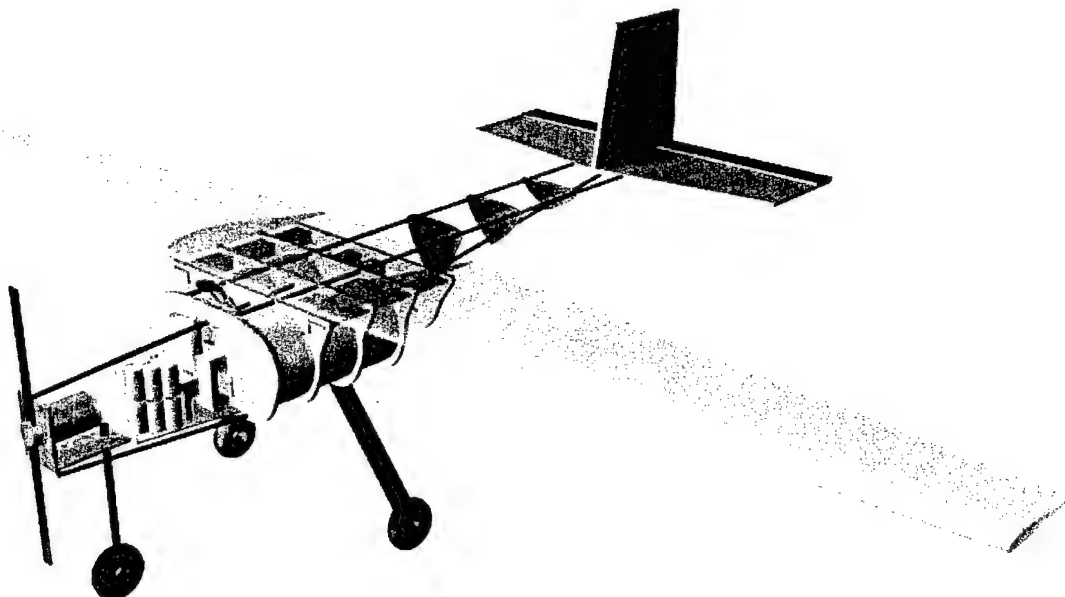


TABLE OF CONTENTS

1	EXECUTIVE SUMMARY	4
1.1	SUMMARY OF THE FINAL DESIGN.....	4
2	MANAGEMENT SUMMARY	6
3	CONCEPTUAL DESIGN	8
3.2	DESIGN PARAMETERS	8
3.3	MISSION PARAMETERS	8
3.4	CONCEPT GENERATION AND SELECTION	10
3.4.1	<i>Fuselage</i>	10
3.4.2	<i>Tail Configurations</i>	12
3.4.3	<i>Wing Configurations</i>	14
4	PRELIMINARY DESIGN	15
4.1	FUSELAGE ANALYSIS	15
4.2	WATER STORAGE SYSTEM ANALYSIS	20
4.3	WING ANALYSIS	20
4.4	TAIL ANALYSIS	21
4.5	LANDING GEAR	21
4.6	PROPULSION AND ENERGY	23
4.7	BATTERIES.....	25
5	DETAIL DESIGN	26
5.1	WATER STORAGE SYSTEM	26
5.2	FUSELAGE	27
5.3	WINGS.....	31
5.4	TAIL SECTION.....	34
5.5	FINAL AIRCRAFT CONFIGURATION AND DRAWING PACKAGE.....	35
6	MANUFACTURING PLAN AND PROCESS	40
6.1	FUSELAGE MANUFACTURING PLAN AND PROCESS	40
6.2	TAIL MANUFACTURING PLAN AND PROCESS.....	40
6.3	LANDING GEAR MANUFACTURING PLAN AND PROCESS	41
6.4	WATER STORAGE SYSTEM MANUFACTURING PLAN AND PROCESS	41
6.5	SYSTEMS INTEGRATION AND ELECTRONICS ASSEMBLY	42
6.6	WING CONSTRUCTION	42
7	TESTING PLAN	44

8	RATED AIRCRAFT COST	45
9	REFERENCES	46

1 EXECUTIVE SUMMARY

This report outlines the methods used by Case Western Reserve University to construct the *Flying Nemo* model airplane for the 2004 AIAA Design / Build / Fly competition. The information given in this report provides an overview of the design intent from concept to manufacture.

The objective of the project was to design and fabricate an unmanned, electric powered, radio controlled aircraft that is affordable, yet powerful enough to achieve the performance required to complete the three missions defined for the competition. The missions are, (1) General Mission, (2) Ferry and (3) Fire Fight.

1.1 Summary of the Final Design

The focus of the fuselage design was the water storage system which consists of two 2-litre bottles placed side by side in the fuselage. As such, the fuselage bulkheads were designed and built to contain the water storage system, leading to the creation of a rectangular fuselage when seen from the front of the aircraft. Several pieces of aluminum micro-tubing were placed along the entire length of the main section of the fuselage, creating connections with the tail and motor mount. The width of the fuselage was also extended to provide space to hold the L-shaped aluminum bars that were used as connection points for the wings. Shrink wrap mylar coverings, which provide an aerodynamic and waterproof covering, were chosen for the fuselage skin. In addition, shrink wrap mylar is also very easy to repair. The final fuselage design was selected based on factors such as manufacturability, accommodation of payload, weight, durability, rated aircraft cost, aerodynamic streamlined structure, conservation of space, ability to mount wings, and environmental concerns.

The final wing design was chosen based on the intent of having a light, strong wing that was easy to attach to the fuselage and its ability to be stored in the six foot length box. The design chosen was a one piece fiberglass wing built around a foam interior (which could be melted out providing a high strength to weight ratio). The wings begin with a 12" chord and taper to 6". A NACA 2412 airfoil was chosen because of its versatility and past success. In addition, a basic airfoil is sufficient when working with an aircraft of less than ten feet in length. Ailerons were built into the wing on both sides to give optimal flight control. The aileron servos were mounted inside the wing.

The design chosen for the tail was a two servo standard tail with two active control surfaces. This design was chosen as it has proven to be effective in the past with similar mission requirements. Furthermore, it allowed for easier manufacturing and had an equal or lower related aircraft cost compared to other tail designs that were considered.

The main landing gear is placed between the second and third last bulkheads, resulting in a position that is a few inches behind the center of mass of the aircraft. The front landing gear was placed on a plywood plate with the motor mount. The main gear is 3/16" thick to support the weight of the plane and provides a 7" clearance from the ground so that a 15 by 10 propeller can be used. The landing gear is made of T-6 aluminum and is supported by 2" wheels. The thickness of the landing gear struts, material selection and wheel sizes were based on the requirements to support the weight of the aircraft.

The propeller chosen for the propulsion system was based on using 24 N2400 SC RC batteries. These were chosen because they fit the Astroflight 40 geared (#640) motor. The batteries are arranged in a pack that sits just behind the motor mount in an otherwise empty area of the plane. Several different propellers were considered but a 15 by 10 prop was chosen because of its power.

The water storage system consists of tubing from each bottle connecting to a single tube at the top and bottom of the tanks allowing water to enter and exit the tanks. Another piece of tubing is fitted over the entrance to direct air flow during flight to maintain a positive pressure in the tanks. A servo controlled slider acts as a valve for the exit tube.

2 MANAGEMENT SUMMARY

Due to the number of people making up the team this year, it was decided that the team could be run by one coordinator whose main responsibility would be to assign tasks, mediate between differing design concepts, and to ensure that all competition deadlines and rules were met. Weekly meetings were scheduled during the University provost hour on Tuesdays. Later on in the year when construction started, meetings would be held sporadically.

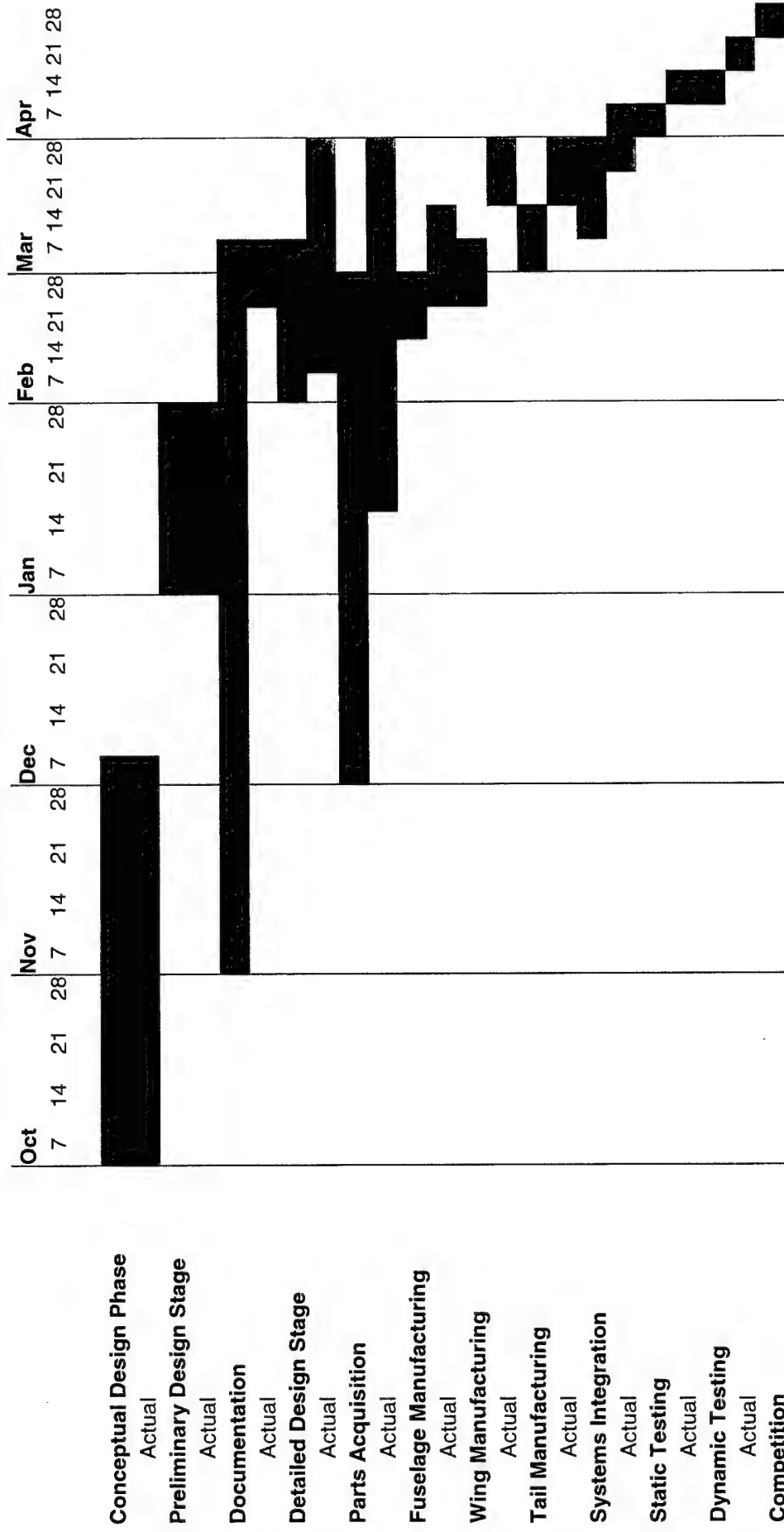
Major design components of the plane were handed out as tasks for some of the group members to complete. An average of two people worked together on each of the major design components (fuselage, wings, tail, water storage system, propulsion, electronics, and landing gear). Those working on the construction of Flying Nemo were in charge of either fabricating their own portion of the plane design or showing someone else how to complete it. Table (1) lists the assignment of personnel to their specific tasks throughout the year. Table (2) lists a timeline of predicted and actual time of completion for the varying design components of Flying Nemo.

Table 1: Assignment of Personnel

Name	Assignment Areas
Eric Braun (Project Coordinator)	Fuselage Design, Fuselage Construction, Team Coordination, Assignment of Individual Tasks, Parts Acquisition, Documentation, Documentation editing, Finances
Dan Haylett	Wing design, Tail design, Electronics and Propulsion design, Documentation
Elizabeth Vermeersch	Wing design, Wing Construction, Documentation
Lori Southard	Landing Gear design, Landing Gear construction
Rachel Divizie	Construction
Chris Roberts	Electronics and Control System Construction
Petrina Ee	Construction
Brian Taylor	Landing Gear design, Documentation, Construction

Table 2: Timeline of Flying Nemo Design and Construction

2004 DBF Project Timeline (Projected and Actual Time of Completion)



3 CONCEPTUAL DESIGN

The first step in the design process was the conceptual design phase. Each idea generated was evaluated to determine the advantages and disadvantages in itself and when integrated into the aircraft. The mission requirements were used as the design parameters and the concept that best fulfilled the design parameters was selected as the final aircraft configuration.

3.2 Design Parameters

The overall goal of the project was to build an aircraft that was able to perform the prescribed mission requirements while operating within a specified set of constraints. The first step in achieving this goal was the conceptual design phase. With the mission requirements and design constraints in mind, the advantages and disadvantages of different aircraft configurations were analyzed and compared. Various configurations were eliminated until an optimal configuration was found. Additional analysis was then carried out on the selected configuration during the development phase.

3.3 Mission Parameters

The mission requirements were divided into three main areas. These were the General Constraints, the Fire Flight (high lift/ low speed flight), and Ferry (high speed flight). The details of each requirement were given as follows

- **General Constraints** (overall aircraft parameters and governing mission rules)
 - The disassembled aircraft must be able to fit in a (2 x 1 x 4)ft box
 - The maximum take off distance is 150 ft (take off is defined as the wheels being off the runway)
 - The aircraft must initially land on the runway for any flight score to be obtained
 - Any payload must be secured mechanically
 - One of the prescribed missions must be selected for each flight
- **Fire Flight**
 - All aircraft will begin the mission empty
 - The aircraft will be loaded, take off, drop it's payload during the downwind leg, return to land, then be reloaded for a repeat performance
 - The maximum allowable volume of water that may be held is 4 liters
 - All aircraft must be loaded using gravity or pumped loading from four two liter soda bottles

- For each lap, the aircraft must complete a 360° turn in the direction opposite of the base and a final turn on the downwind leg of each lap
- The maximum “dump orifice” diameter is .5 inches
- Water may only be dumped on the downwind leg of the flight which is between the upwind and downwind turn markers, and during the dump time, the pilot must call “Dump On” and “Dump Off”
- Water weight will be determined by the starting and ending weight of ground based storage tanks which will be taken when entering and leaving the flight box
- **Ferry**
 - Aircraft must take off, complete four laps, and land with no water payload
 - For each lap, the aircraft must complete a 360° turn in the direction opposite of the base and a final turn on the downwind leg of each lap
 - The final score for this area is given as $1/(\text{Mission Time})$

The possible penalties, which were to be imposed if certain requirements or constraints were not met, were given as follows:

- Water that is dumped early, late, or during the landing, will result in a three minute time penalty for each occurrence
- Excessive water spillage during loading will incur a 1-min time penalty per infraction. The flight line judge will notify the team of the penalty at the time of the infraction. Gross and/or deliberate spillage will disqualify the flight but will count as one of the teams’ flight attempts.
- Three minute time penalties will result if the aircraft is not empty upon the final landing.
- Three minute time penalties will be imposed if the second lap is not completed (incompletion consists of a lap that is not attempted, or not completing the 360 degree turn)

3.4 Concept Generation and Selection

The following section describes the various concepts that were considered and the methods used to determine the final configuration that met the requirements of the mission requirements.

3.4.1 Fuselage

This section of the report describes the methodology used to determine the conceptual fuselage design. Free hand sketches were made to provide a means to visualize the fuselage with a water containment unit that could hold four liters of water. Because the fuselage had to be designed to hold the water, ideas for the water storage system were considered along with the fuselage design. Although dimensioning of the parts were minimal during the preliminary design phase, estimates of the overall size of the fuselage could be determined based on the water storage system. For example, two 2-liter bottles placed side by side surrounded by bulkheads would require a fuselage that was approximately ten inches wide, five inches high and twelve inches long. Finally, a Pugh screening and scoring matrix was used to aid the selection of the best design.

Concept Selection

Since it was decided that the fuselage was the most important aspect of the aircraft because it was directly related to the water storage system, it was in the best interest of the team to finalize the design of the fuselage first before finalizing the designs for the rest of the aircraft. As such, we narrowed down our ideas to the following conceptual designs listed below.

1. Two side by side 2-liter bottles surrounded by equally spaced bulkheads.
2. One 4-liter bottle surrounded by equally spaced bulkheads.
3. Two 2-liter bottles, one in front of the other, surrounded by equally spaced bulkheads
4. Four 1-liter bottles placed inside a fuselage where the bulkheads would be placed to stabilize the bottles

The next step in the design process was to determine which of the four preliminary ideas would be the best. A Pugh screening matrix was used to aid in the selection process. A list of the design criteria used in the screening matrix is shown in Table 3. The following is a list of the criteria use, these criteria are also known as 'numerical figures of merit' (FOM's).

- 1) Manufacturability (Simple or difficult)
- 2) Accommodation of payload (Structurally sound or flimsy)
- 3) Durability (Ability to complete 360° turns and land safely)
- 4) Conservation of space (Ability to fit into a 2'x1'x4' box)
- 5) Ability to mount wings (Would the bottles be in the way of possible mounting locations?)
- 6) Movement of water (Will the center of mass be affected during acceleration?)

Table 3: Pugh Screening Matrix

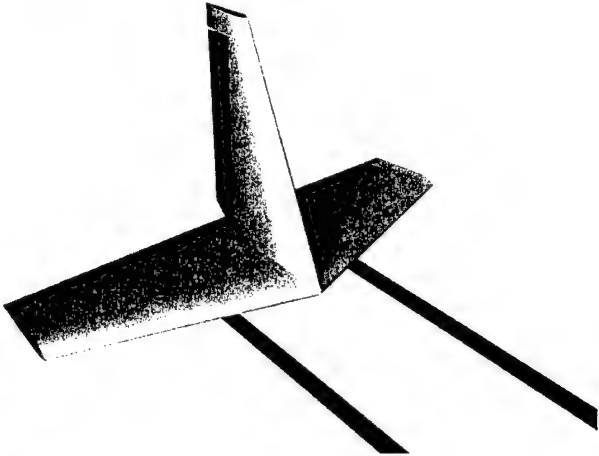
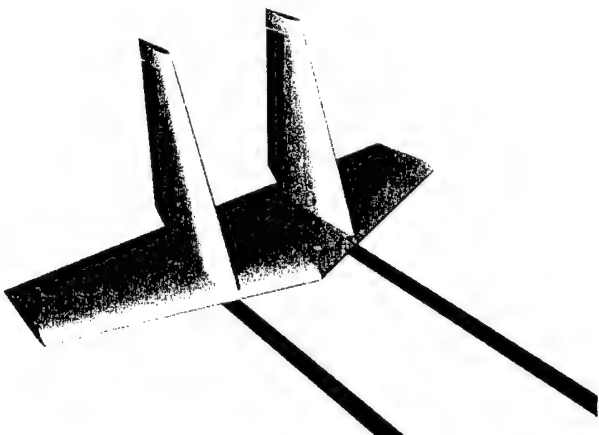
Criteria	1	2	3	4
Manufacturability	+	+	0	-
Accommodation of payload	+	+	0	0
Durability	+	+	0	0
Conservation of space	+	+	0	+
Ability to mount wings	0	0	0	+
Movement of water	0	-	0	+
Totals:	4	3	0	2

Using the data in the above screening matrix, it was apparent that two 2-liter bottles placed side by side surrounded equally by spaced bulkheads was the best design concept. Using one 4-liter bottle was also a feasible idea, however, it was decided that the movement of water would be critical to the performance of the plane. In addition, it would also be fairly difficult to find 4-liter bottles that would be light enough to mount inside a model aircraft.

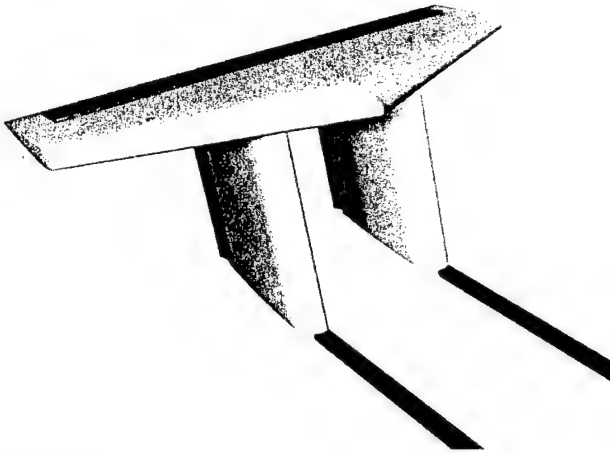
With an estimate of both the weight and size of the fuselage, the material to be used for the bulkheads could be discussed. The possibilities were narrowed down to either a light weight, durable plywood or an aluminum alloy. While aluminum would certainly be stronger, it would also be much more difficult to machine. Furthermore, there were also concerns of the difficulty of integrating other parts into the aluminum structure. Therefore, we decided to use a durable form of plywood based on the ease of machinability as well as our past experiences with using it.

3.4.2 Tail Configurations

Four different tail configurations were considered for the use on the aircraft. The factors that were used to choose the best configuration included effectiveness, ease of manufacturing, and the resulting contribution to the RAC. An effective tail provides sufficient stability to the aircraft for a given distance from the cg of the plane in yaw and pitch. There are many different styles of tails that have been used in aviation history and the successes and failures of a particular tail design were considered in the selection of a tail configuration. The four tail configurations that were applicable for this aircraft are shown below.

Design A 	Configuration <ul style="list-style-type: none">• Standard tail Remarks <ul style="list-style-type: none">• Proven design• 2 servos• Two active control surfaces• Low horizontal stabilizer• 30 RAC hours
Design B 	Configuration <ul style="list-style-type: none">• 2-vertical stabilizers Remarks <ul style="list-style-type: none">• 2 servos• Three active control surfaces• Low horizontal stabilizer• 40 RAC hours

Design C



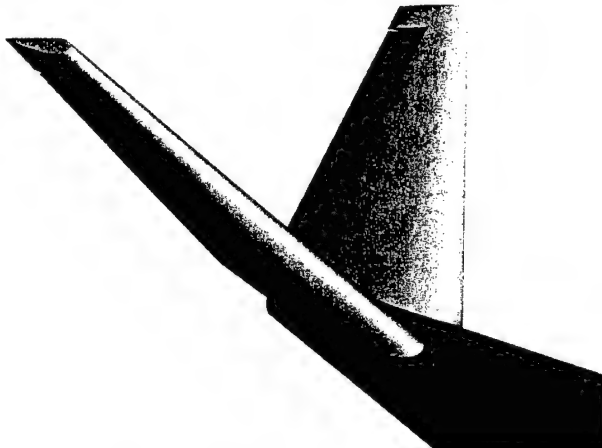
Configuration

- T-type 2-vertical stabilizers

Remarks

- 2 servos
- Not structurally robust
- Three active control surfaces
- High horizontal stabilizer
- 40 RAC hours

Design D



Configuration

- V-type

Remarks

- 2 servos
- Not structurally robust
- One active control surface
- 25 RAC hours

These different configurations exhibit a wide range of performance characteristics. Some provide more stability than others. One consequence of high stability is usually more mass in the back and more resistance to quick turns, reducing the aircraft's maneuverability. Our goal this year is to create a robust-stable plane, as such, maneuverability was less of a concern. The designs shown above have many good aspects and negative aspects and similar to the fuselage selection process, a matrix was created to aid the team in determining the optimum design.

Table 4: Tail Configuration Decision Matrix

Consideration	A	B	C	D
Stability	1	1	1	0
Manufacturability	1	0	0	-1
Drag	0	-1	-1	0
RAC	0	-1	-1	1
TOTAL	2	-1	-1	0

A, B, and C are all very stable designs, and B and C might be slightly more stable. However, we have not mastered the complexities of the V-tail, we assigned D a 0. The Manufacturability of A is the easiest because the support structure of the stabilizers would be easily bound together. The V-tail requires angled sections which would be difficult to implement on the double-tube style boom. Drag is mostly caused by more frontal area, and B and C have the most. In terms of RAC, the main problem with B and C is the extra vertical surface. The V-tail is the lowest, but the sum of the scores for each configuration tells us that A is the best design based on the criterion set forth. The traditional design has proven its robust performance throughout aviation history and will provide the aircraft the stability required to ensure safe flights.

3.4.3 Wing Configurations

The wing should be light, strong, and easy to attach to the fuselage. In addition, it needs to fit into the storage container. Also, construction techniques, strength, weight, durability, rated aircraft cost, and ease of construction needed consideration. Two different wing construction processes were considered. The first one considered was a traditional wooden buildup of the wings. The other method considered was the use of blue foam core wings (<http://www.favonius.com/soaring/foams/foams.htm>). The use of a wooden wing over the use of a reinforced foam wing leads to several more possibilities of problems occurring, such as greater fragility, a much longer build time, and less ease of repair. Obviously, it then made sense to use a reinforced blue foam wing. The wing would then be covered with an epoxy-soaked fiberglass cloth to give it strength. Later, it could be covered with monokote to give a smooth finish.

4 PRELIMINARY DESIGN

The preliminary design process started after the selection of the best design as determined from the conceptual design phase. Based on the chosen options, a detailed analysis was carried out on the various aircraft sections. The analysis was required to size the aircraft, its components and systems. The analysis also comprised of a search into commercial materials and parts that were available in the market that were compatible to the design and requirements of the aircraft.

4.1 Fuselage Analysis

After a fuselage design was selected, the next step was to make more specific specifications, begin dimensioning, and begin choosing materials. The analysis of the fuselage was important because it was the center of the design. In addition, the design of the fuselage also determines the design parameters of many other components of the aircraft.

There were a number of specifications that were required for the fuselage of this aircraft. The specifications are listed below and are separated into the demanded specifications and desired specifications. The demanded specifications were needed and cannot be altered, while the desired specifications are not, but in some cases could be satisfied partially.

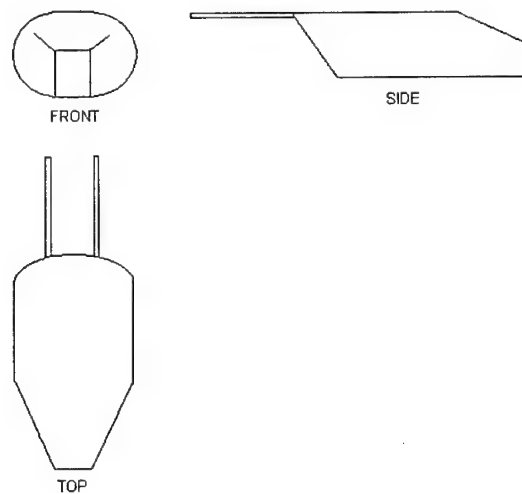


Figure 1: Fuselage Schematic

Demanded specifications (non-negotiable):

- Size – all components of the aircraft (including the wings) must fit into a 2x4x1 ft. box.
- Must withstand dynamic loads of landing without failure of any structural part.
- Must contain a bladder system capable of carrying water.

- House batteries, motor, and other avionic devices
- Must be able to take-off, fly 4 laps, and land. On the downwind leg of each lap, the plane must complete a 360 degree turn in the direction opposite of the base and final turns.

Desired specifications (negotiable):

- Functional Performance
 - Lightweight design
 - Durable – fuselage should remain intact after hard landing
 - Aerodynamic fuselage with low air drag minimizing energy consumption
 - High strength fuselage that maintains structural integrity during flight
 - Ability fly in adverse weather conditions – wind, rain, cold & hot temperatures
 - Detachable tail to fit in box with all components
- Manufacturing
 - Easy to assemble/construct
 - Modular Construction – aircraft built in sections making it easier to connect/disconnect for plane to meet size specifications
 - Quality control – high quality of construction with a minimal amount of defects
- Cost
 - Low material and manufacturing costs
 - Low amount of man-hours spent on construction (man-hours contribute to overall estimated cost for the competition)

To achieve the required performance these qualitative specifications must be translated into quantitative specifications so that they may be realized in a practical manner:

Quantitative Specifications:

Units of Measurement: English Standard System

- Weight: pounds (lbs) → Lightweight
- Length, Width, Height: Inches (in) → Fit in box
- Frontal Area: Square Inches (in^2) → Reduce drag
- Time: Hours (hrs) → Ease of manufacturing
- Money: Dollars (\$) → Reduce aircraft cost

Possible Materials:

- Fiber Glass, aluminum, styrofoam, balsa wood, plywood (various sizes in thickness)

Fasteners:

- Mechanical Screws (various sizes), duct tape
- Adhesives: Super glue and/or Epoxy

Qualitative Specifications:

- Detachable tail section
- Number of Man Hours: Min: 10 hrs.; Max: 100 hrs.
- Quality Control: Due to print specifications (ex. tolerances)
- Durability: Based on materials that will be later chosen
- Costs: Within \$500 budget given by Design Build Fly Team
- Bulkheads (separation distance): Min: 2 in.; Max: 4 in
- Modular: Must fit in a box dimensioned (12 X 48 X 24 in)
- Coefficient of Drag (dimensionless): Min: 0.1; Max: 0.5
- Weight of fuselage (without package): Min: 5 lbs.; Max: 10 lbs.
(The target weight of the entire aircraft with all components including wings, landing gear, batteries, and motors, but without the package, given by the Design Build Fly team is 15 lbs.)
- Length: Min: 36 in.; Max: 48 in

Analysis Models

After the basic framework and layout of the fuselage was decided, and the quantitative specifications were considered, an analysis was carried out to ensure that the design specifications were met. The types of analysis carried out were:

- the total bending stress of the structure and consider landing loadings
- the stresses in the wing connection
- the drag of the fuselage

A side view of the front-half of the fuselage is shown in Figure 2. The maximum load that the fuselage would be required to undertake would be the landing loads (as there can be a substantial increase in the dynamic stresses during a rough landing). Most of the stresses had to be transferred to the main landing gear because the center-of-gravity of the aircraft is located

near them. However, because some of the load is taken by the nose gear, it creates a bending moment that the fuselage had to bear.

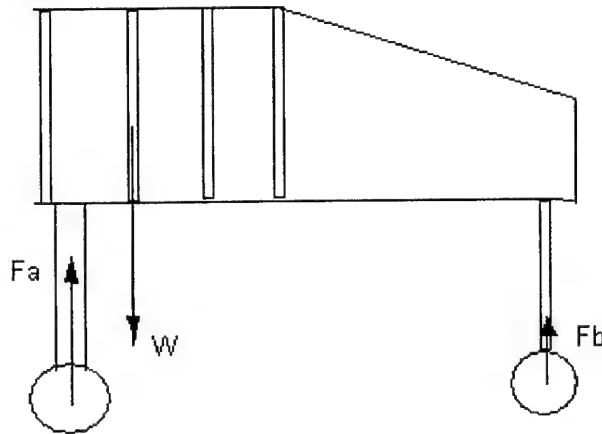


Figure 2: Side-view with Loads

With the setup of the fuselage shown in Figure 3, the bending stresses will manifest themselves as normal stresses in the aluminum spars: compression on the top and tension on the bottom. The eccentricity of the main landing gear and the center of gravity is about 2 inches. The distance from the CG to the front landing gear is about 10 inches. This means that the force F_a is 83% of the weight of the plane W . With this arrangement the maximum moment which occurs on the cross-section at the CG is $M=0.83*W*2$ in*lbs. Using the dimensions of the aircraft and the thicknesses of the spars, the normal stresses in the spars barely reach 1 ksi using 4 times the static weight of the aircraft. With the yield stress of aluminum being around 40 ksi, it was determined that this fuselage would be able to withstand the stresses of landing.

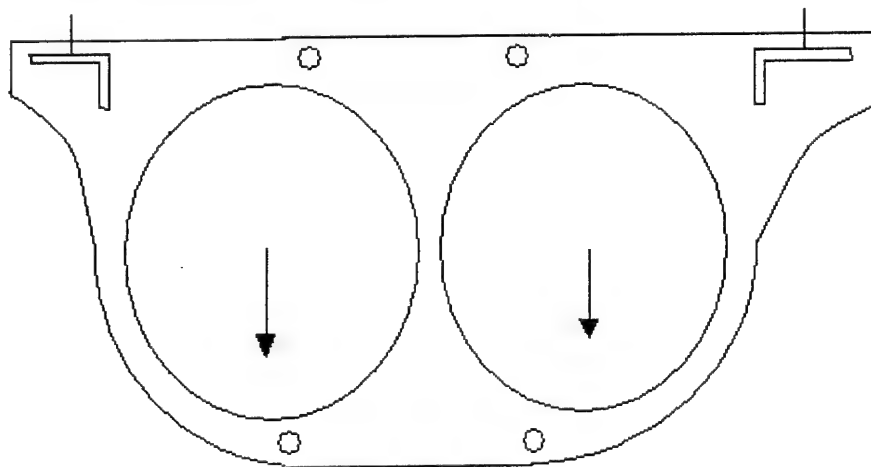


Figure 3: Bulkhead Schematic

Another crucial area in the aircraft which would experience large loads is the connection between the wing and fuselage. It was decided that angled aluminum bars mounted in the bulkhead corners would be used to bear the load of the wing. The L-shaped grooves cut into the bulkhead in Figure (3) provide a snug fit for the angled aluminum bars to sit into. Aligned with the holes cut in the bulkhead and the aluminum bars provide points to bolt down the wing. The wing would be secured at four points, evenly distributing the weight of the aircraft by four. A free-body diagram of a section of angle aluminum between two bulkheads is shown in Figure 4.

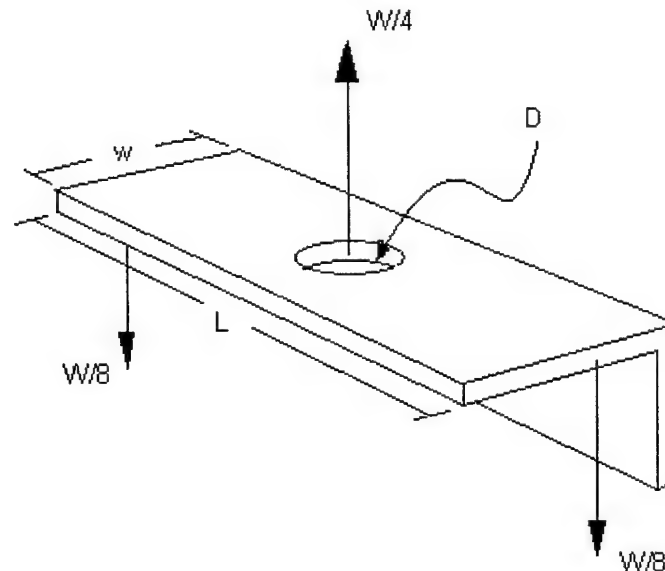


Figure 4: Wing Connection Free-Body Diagram

The maximum moment occurs at the center of this section where the hole is cut. The nominal maximum stress is then calculated using the bending moment stress equation,

$$s = \frac{My}{I}$$

where M is the moment, y is the distance from the centroid to the top, and I is the area moment of inertia of the cross-section. This however must be multiplied by a stress concentration factor because of the hole. The factor depends on the ratio of D/w and is used to determine D . Using the maximum nominal stress and a safety factor of 3, a stress concentration factor can be obtained and D was determined to be $\frac{1}{4}$ ".

An ideal fuselage should cause minimal drag. Drag can be split into two categories, skin friction and pressure drag. Skin friction can be reduced by having a fuselage with minimal surface area. Pressure drag is harder to reduce but plays a much bigger role. The formula for the drag force is:

$$D = \frac{1}{2} C_d \rho A V^2$$

where C_d is the coefficient of drag and depends on the shape of the body, ρ is the density of the air, A is the maximum frontal, cross-sectional area of the fuselage, and V is the velocity of the plane. The two parameters in this equation that we can control are the area, A , and the C_d . The area should be the smallest possible value. For this aircraft, the size of the fuselage was reduced by sizing it to the shape of the bottles and providing the minimum clearance required between the bottles and the outside of the plane for the spars. This resulted in a fuselage that had an elliptical shape of high eccentricity and a coefficient of drag of approximately 0.32.

4.2 Water Storage System Analysis

The most important aspect of the water storage system analysis was to find a solution to balance the center of mass of the water with the rest of the aircraft. Because the aircraft was required to fly with the water storage system both filled and empty, the amount of water present in the plane should not change the center of mass. With this condition present, the center of mass had to be placed in line with the quarter chord of the wing as that would be the location of the center of mass of the entire aircraft. The total weight of the 4-liter water system when filled will be 8.8 pounds.

4.3 Wing Analysis

The wing must support the total weight of the aircraft when picked up by the wingtips from both the top and bottom, so a wing that will not bend easily is needed. The wing must also be as light as possible. The design that achieves both of these objectives is a solid, one-piece fiberglass wing. A solid fiberglass wing can take much more force than could ever be supplied by the approximate 20 pound weight of the plane.

Looking at the various airfoils available, it was decided that the best airfoil for our purposes would be the versatile NACA 2412 airfoil with a wing dihedral of five degrees to add stability to the aircraft. Ideally, the dihedral should allow for the aircraft to be very maneuverable without the use of ailerons. However, since aileron construction is required, it was decided that the servos controlling them will be flush mounted in the wing. The control wires to the receiver will be the only part of the ailerons that need to be connected during aircraft assembly. This setup would require 2 ailerons and 2 servos, increasing the RAC by 16, giving a total wing RAC of 76 hours.

To determine the final wing geometry, the wing was modeled as an ellipse. Using an aspect ratio of 7.6 and the limits of the storage box to determine a dimensional starting point, the final design was selected by entering various wingspans and corresponding chord lengths into a spreadsheet. This spreadsheet took into account the mass of the plane (including the changing mass of the wing) and the expected energy output of a set of battery cells. From that spreadsheet, we determined the final configuration of the wing, which is listed in section 5.3.

4.4 Tail Analysis

With the traditional tail configuration selected, the dimensions and placement of the tail had to be determined. Because many different dimensions could be varied in the design of the tail, the design of the tail is a very subjective process. In the analysis of this aircraft, the vertical and horizontal tail volume coefficient method was used. The horizontal stabilizer's volume coefficient for a stable aircraft is 0.692 (Navion), and for the vertical stabilizer it is 0.040. The formulas for the horizontal and vertical stabilizer volume coefficients respectively are:

$$V_H = \frac{S_H L_H}{S_w m.a.c}$$
$$V_V = \frac{S_V L_V}{S_w b}$$

where S_H is the horizontal stabilizer area which is to be determined, L_H is the distance between the tail's $\frac{1}{4}$ chord and the plane's CG which is determined by the box constraint, S_w is the wing area, and m.a.c. is the mean aerodynamic chord. Solving for S_H gives the area required to determine the span and chord. The second equation is for the vertical stabilizer's volume coefficient and S_V is the vertical stabilizer's area, L_V is the distance from the $\frac{1}{4}$ chord to the CG of the plane, and b is the wing span. Solving for S_V gives the value required to determine the dimensions for the vertical stabilizer.

4.5 Landing Gear

Several criteria were used in designing and selecting an appropriate set of landing gear. The landing gear for this aircraft had to satisfy the following requirements:

- Support the weight of the plane with loading due to water (up to a very safe 30 pounds)
- Be able to negotiate unexpected possible changes in the center of mass due to differences in a water-filled take off vs. an empty landing
- Be able to deal with possible unexpected dynamic loading either in flight or during landing

It was determined that the main landing gear should be placed slightly behind the center of mass of the plane so that the gear would almost directly support the weight of the plane without any moments due to the center of mass.

When considering the design of any landing gear, there are five main dimensions that must be taken into account and these are illustrated in Figure 5.

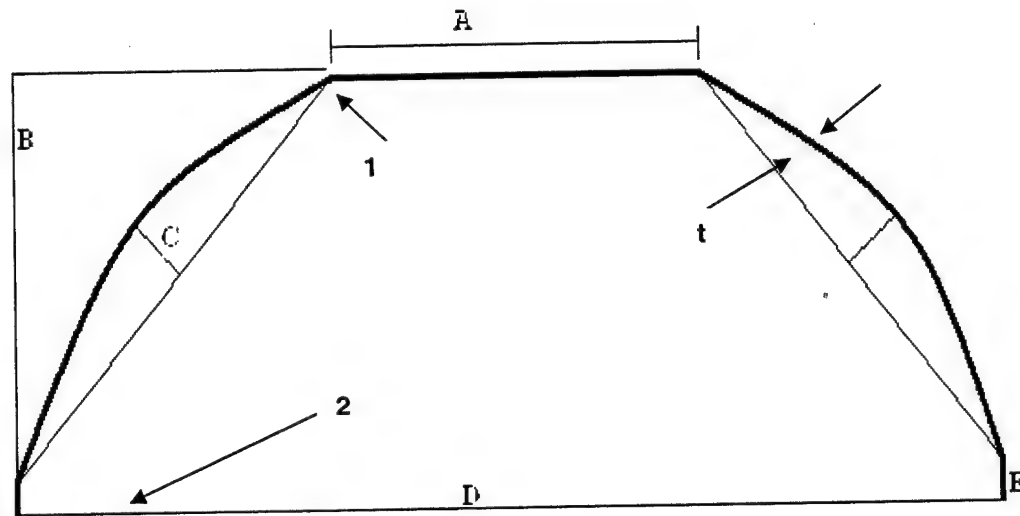


Figure 5: Main Landing Gear Analysis

Dimension C was thought to be an important dimension. Because points 1 and 2 are points of intersection between different segments of the landing gear, they are locations where there will be high stress concentrations. At any point, larger curvature (smaller radius of curvature) causes a higher stress concentration. Therefore, at points 1 and 2, the curvature needs to be minimized to lower the stress concentration. Because of this fact, it was thought that dimension C should be maximized to lower the curvature at points 1 and 2.

Dimension A was taken to be the width of the plane. Dimension B is governed by the length of the propeller and the elastic bending of the plane upon landing such that neither the plane nor the propeller ever touches the ground. Dimension D needed to be optimized such that it stabilizes the plane without landing gear failure.

The thickness t was determined based on the following two formulae:

$$\tau = \frac{3}{2} \left(\frac{V}{A} \right) = \frac{3}{2} \left(\frac{V}{tw} \right)$$

$$\sigma = \frac{K_t M t}{2I}$$

where τ is the shear stress, V is the shear force (taken to be three times the weight to account for dynamic loading), A is the cross sectional area of the beam, σ is the normal stress, K_t is the factor used to account for the curvature at point 1, M is the moment induced by the weight, t is the thickness, and I is the moment of inertia. Based on these equations, it was determined that the thickness that the optimal thickness would be (3/16)in.

4.6 Propulsion and Energy

The propeller was determined by the number of batteries, the type of motor and the rpm that the aircraft was to operate at. Table 5 shows data taken from the Astroflight website and applies to the 40 geared cobalt (640S) motor:

Table 5: Shows prop sizes for various configurations

Battery	Prop	Amps	Watts	Rpm
20 NiCad's	16 x 10	25 amps	550 watts	5,200 rpm
20 NiCad's	18 x 10	32 amps	700 watts	4,500 rpm
24 NiCad's	15 x 10	25 amps	625 watts	6,400 rpm
24 NiCad's	16 x 10	29 amps	750 watts	6,000 rpm

Because we were using 24 cells, a higher ground clearance would be required for the 15x10 prop. However, the power usage of 625 W rather than 750 W would provide more battery time.

An Excel program was developed to test different parameters of propulsion and energy. With this program, we were able to make changes in total airplane weight, total number of batteries, and propeller type. The following tables show the estimated weight, battery configuration, energy stored, and energy needed in the plane.

Table 6: Estimated Component Weights

Masses (kg)	mass	#	mass*#	lbs
Wing	2	1	2	4.40924
Wing connection L-bars/bolts	0.1	2	0.2	0.440924
Vertical stabilizer(s)	0.2	1	0.2	0.440924
Horizontal stabilizer(s)	0.3	1	0.3	0.661386
Nose cone	0.08	1	0.08	0.17637
Fuselage bulkheads	0.1	5	0.5	1.10231
Main Fuselage spars	0.07	4	0.28	0.617294
2nd Fuselage spars	0.03	4	0.12	0.264554
Fuselage skin	0.08	1	0.08	0.17637
Landing gear (main)	0.5	1	0.5	1.10231
Landing gear (front)	0.1	1	0.1	0.220462
Tank (unloaded)	0.1	1	0.1	0.220462
Servos	0.02	5	0.1	0.220462
Receiver	0.01	1	0.01	0.022046
Speed controller	0.01	1	0.01	0.022046
Avionics battery	0.1	1	0.1	0.220462
Main batteries	1.392	1	1.392	3.068831
Pushrods	0.05	1	0.05	0.110231
Monokote	0.05	1	0.05	0.110231
mass of water (per m ³)	1000	0.004	4	8.81848
Total mass (unloaded)	6.172			13.60691
Total mass (loaded)	10.172			22.42539

Table 7: Output Parameters

Output Parameters	value	units
Loaded cruise velocity	41.65489	m/s
Loaded cruise power	1419.143	W
Loaded cruise time	0.960271	s
Unloaded cruise velocity	32.44709	m/s
Unloaded cruise power	670.7422	W
Unloaded cruise time	1.232776	s
Loaded takeoff power	14088.99	W
Loaded takeoff time	1.440407	s
Reload time	20	s
Total mission time	47.26691	s
Energy needed	44967.05	J

Table 8: Energy Calculations

Energy Stored	value	units
Cell energy per volt	2.4	Ah
Cell voltage	1.2	V
Cell energy	10368	J
Cell mass	0.058	kg
# of cells	24	-
Total energy	248832	J
Total mass	1.392	kg
motor efficiency	0.7	-
propeller efficiency	0.5	-
Usable energy	87091.2	J

Much of this information is negligible for the preliminary design. However, since the usable energy was greater than the energy needed, the number of batteries, the weight of the plane, the propeller, and the wing all appeared to be plausible selections to be used in the design of the plane.

4.7 Batteries

It was decided that a pack of 24 N2400 SC RC batteries would be used for the aircraft. With each battery weighting 58 grams, a pack of twenty-four would weigh approximately 3 lbs. These batteries were chosen because of their compatibility wit the Astroflight 40 geared (640S) motor. Only one motor would be used in the aircraft and the batteries would be located forward of the water bottles and behind the motor in order to bring the CG forward in the plane.

5 DETAIL DESIGN

On completion of the preliminary design of the various components of the aircraft, the final configuration of Flying Nemo could be completed. This includes the integration of more detailed components, such as the placement of electronics.

5.1 Water Storage System

The water storage system is built around two 2-liter bottles placed side by side. Water will be poured into the bottles from a tube at the top of the fuselage that connects to both bottles. When the system is filled, another piece of tubing will be fitted across the opening which will direct the in-flight airflow into the storage system, creating a positive pressure which will aid the volumetric flow rate of the water when it is drained during flight. The water drain will be the specified 1/2 inch diameter tube, and it will be connected to both bottoms of the bottles. Figure (6) shows the water storage system design.

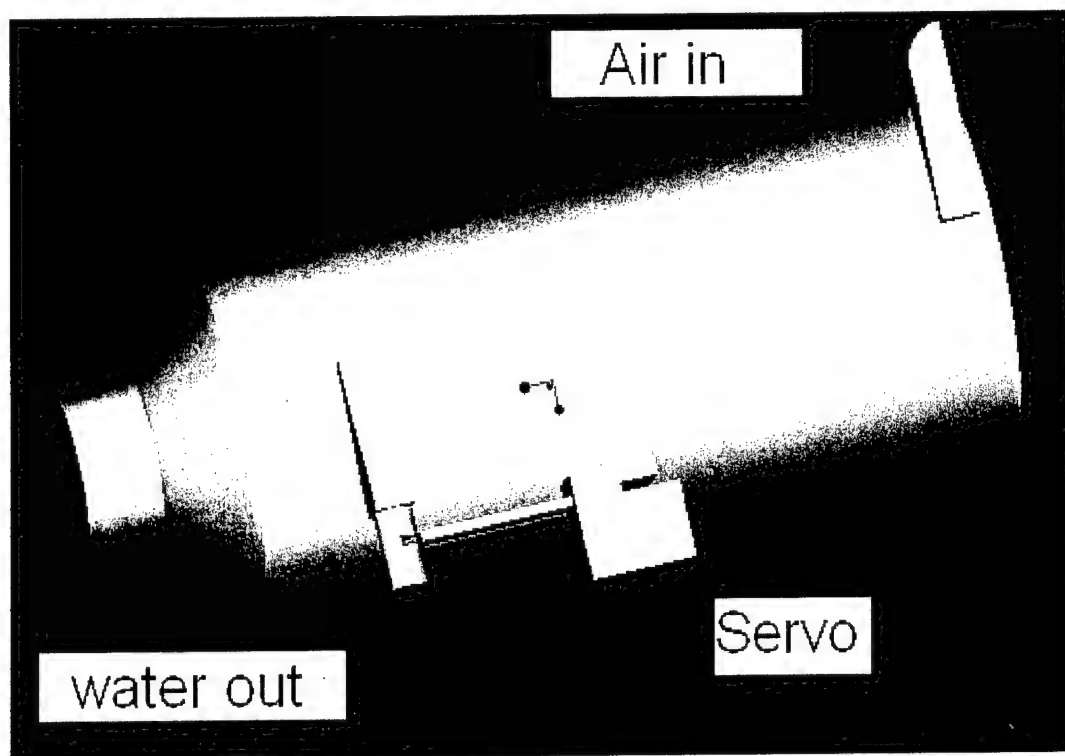


Figure 6: Water Storage System

To open and close the bottom drain, a servo connected to a small sliding plate acting as a cover for the tube will be used to open and close the system.

5.2 Fuselage

The fuselage was designed using a traditional bulkhead skeleton with quarter-inch diameter aluminum micro tubing running the entire length along the top section for both alignment and reinforcement purposes. These tubes extend outwards behind the fuselage in order to connect to the tail section. A similar pair of micro tubing was used for the same purposes on the bottom of the fuselage, only these tubes extend in front of the fuselage to mount the motor onto. The ability to work with the lengths of these tubes made the process of attaining a correct center of gravity much easier as the moments of the tail and motor could be adjusted several times before final placement. The fuselage was designed using *Pro/Engineer 2001*, and the skeleton with component placement is depicted below.

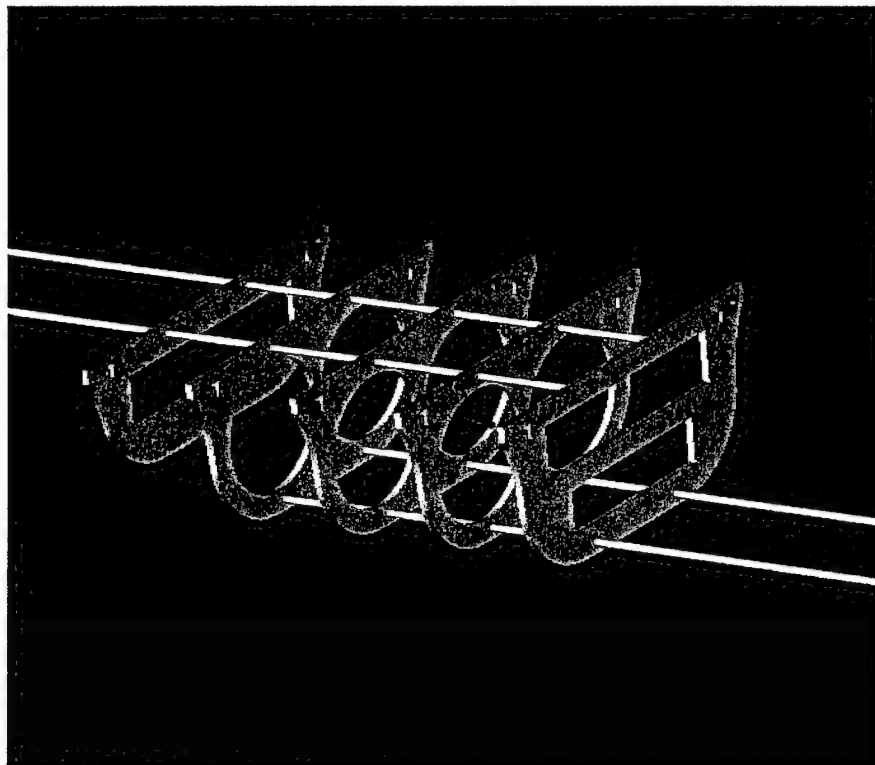


Figure 7: Fuselage skeleton

The material chosen for the bulkheads was 3/16 inch thick birch plywood. All of the bulkheads were cut from 6 inch by 12 inch blanks. First, the bulkheads were designed on *Pro/Engineer 2001* and assembled together in a three dimensional image which provided a visualization of what was being created. Figure (7) shows three different bulkhead designs. The middle sections are bulkheads used to surround the 2-liter bottles. On the ends of the bottles, there are bulkheads that have a horizontal strip across them to hold the bottles in place. The rear bulkhead was tapered up in order to decrease the turbulent airflow heading towards the tail. When the number

and type of bulkheads were agreed upon, the *Pro/Engineer 2001* designs were copied onto the program *Mastercam 9.1*. In *Mastercam 9.1*, the 6" by 12" blanks were designed to be cut by a 1/8 inch end mill. The approximate time for a blank to be cut out by the program was 7 minutes. Figure 8 shows the design of a bulkhead meant to contain the 2-liter bottles. The dimensions on it are roughly the same as the rest of the bulkhead designs.

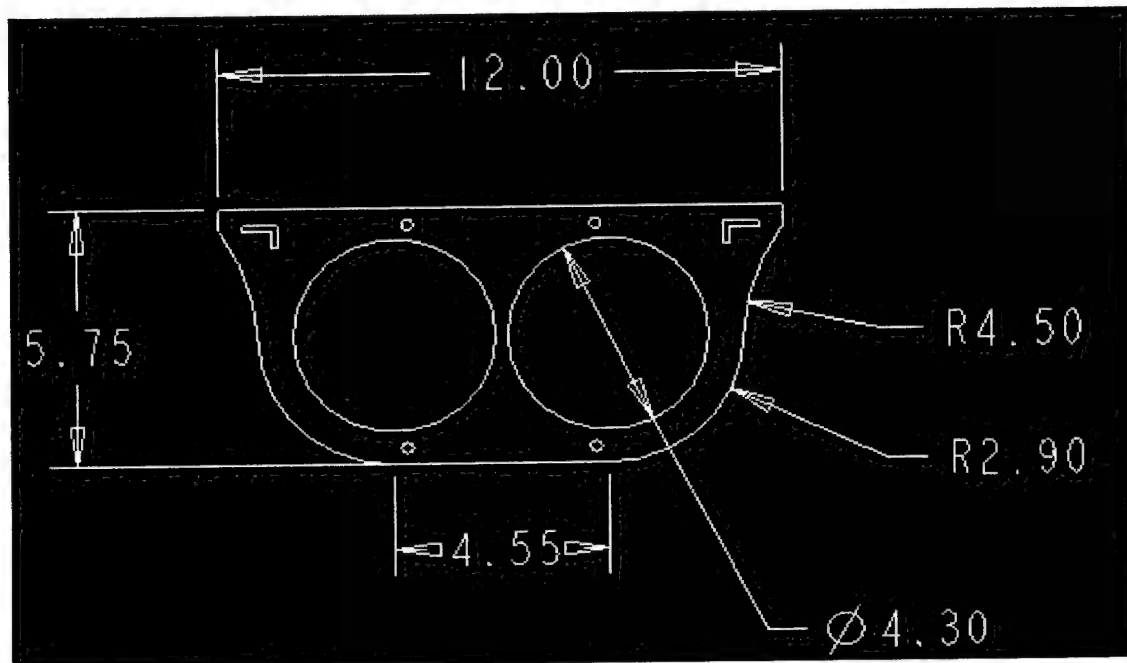


Figure 8: Bulkhead Dimensioned Piece (In Inches)

The diameter of a 2-liter bottle was measured to be 4.3 inches. The bulkhead pieces meant to fit around the bottles had two 4.3 inch holes cut into them, leaving zero tolerance for the fit. After the pieces were manufactured, a press fit tolerance was created by using sanding around the inside edge of the holes. This technique allowed for the tightest press fit possible, which makes movement of the bottles in two directions nearly impossible. Fitting the other bulkheads at the ends of the bottles stopped movement in the last direction.

Decomposition into subsystems

Several subsystems fit into the fuselage and these subsystems are the tail attachment, landing gear mounting, battery mounting, motor mounting, water storage system integration, control and electrical integration, and the mounting of the wing.

The two bottom aluminum micro tubes extend out 12 inches in order to mount the motor. The actual motor mount will sit on a wood plate set between the micro tubing. A third aluminum tube will connect to the top of the motor mount to reduce the moment on the first two tubes. The wood

plate will extend behind the motor mount so the front landing gear can also be attached. With this design no bulkheads will have to be used, thus reducing weight and frontal area. Small balsa bulkheads may be incorporated for the monokote finish, however. Figure 9 shows the integration of the motor mount with the front of the fuselage.

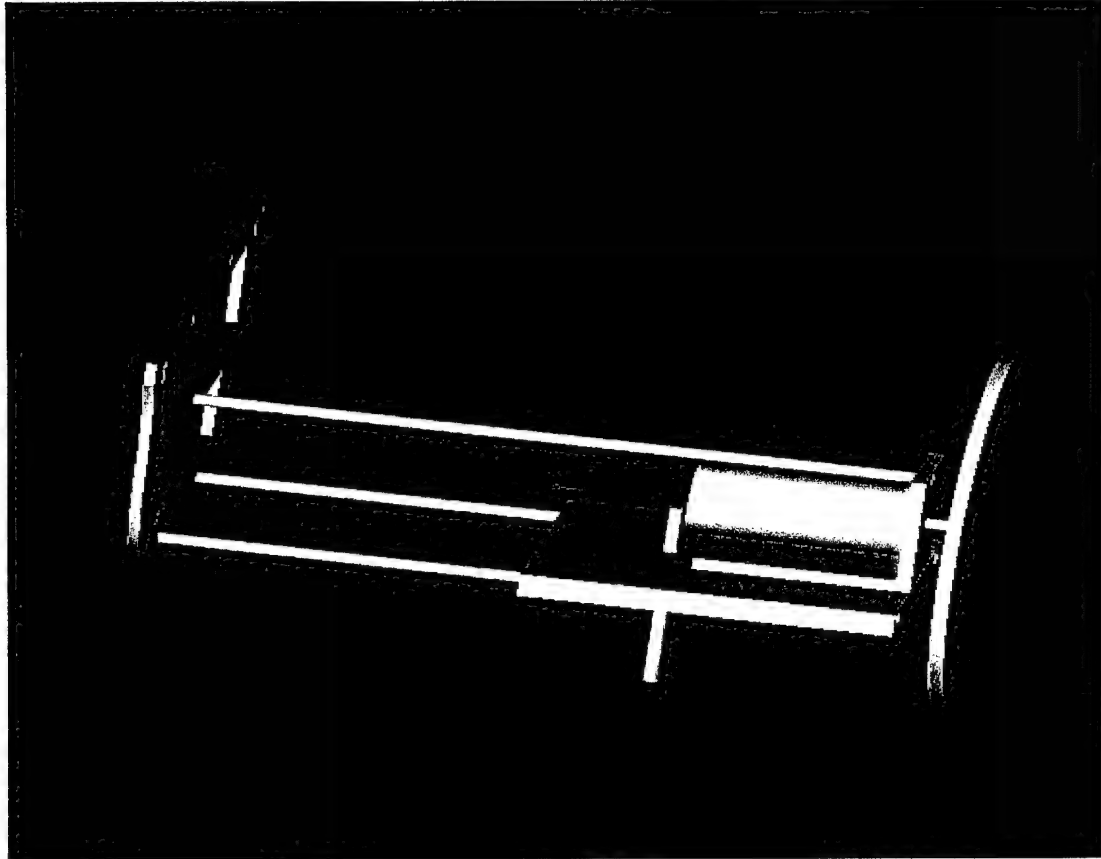


Figure 9: Motor Integration

Another plywood plate was placed between the second and third last bulkheads to mount the main landing gear onto. The landing gear has a chord length of two inches, leaving an inch left on the plate to drill a hole for the water drainage system to fit through. This subsystem is depicted in Figure (10).

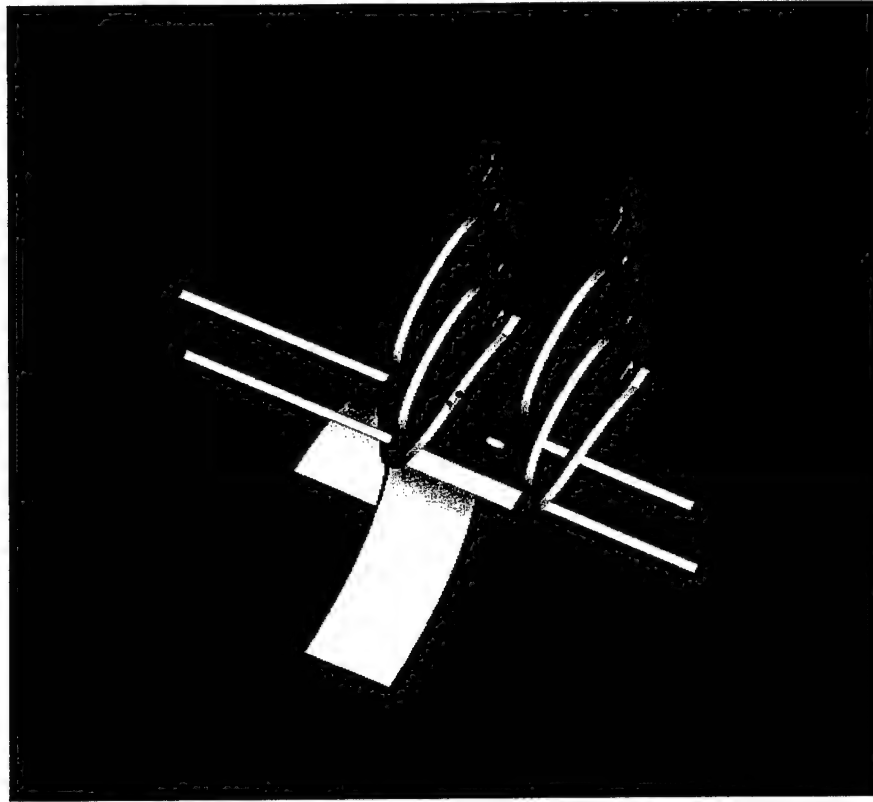


Figure 10: Main Landing Gear Integration

The two top pieces of aluminum tubing extend behind the fuselage to attach to the tail. This provides a good deal of stability for the tail mounting. It also works well with the design of the tail. The tail will be one of the last pieces of the plane to be assembled since it has a large moment. The length of the tubing from the fuselage can be adjusted before final placement as needed.

The area between the first bulkhead and the motor mount is a perfect place to mount the battery pack. The battery pack can simply sit on top of the two bottom aluminum tubes, and it can be secured to the front bulkhead. After mounting the batteries, the rest of the electronics can be placed on top of the battery pack or on top of the bottles in the fuselage.

The last major piece to be assembled to the fuselage is the wing. The wing will be attached by bolts than run through it to L-shaped 1/8 inch thick aluminum bars that run along the edges of the bulkheads. The L-shaped bars also give extra stability for the fuselage. Figure (11) shows the placement of the wing.

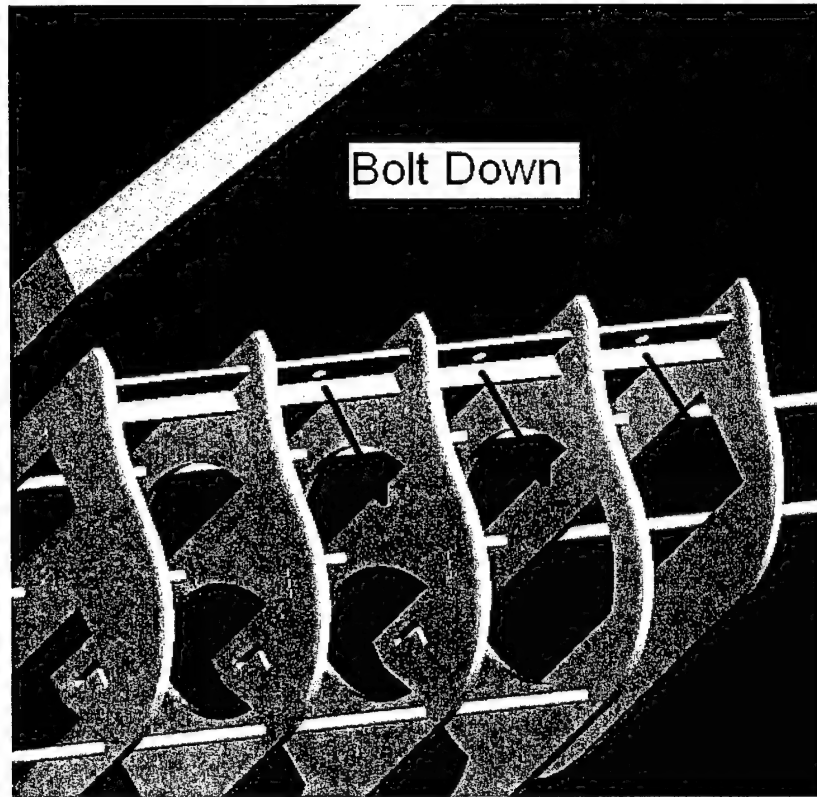


Figure 11: Wing Placement

5.3 Wings

The final wing design consisted of a wingspan of 6 feet, a root chord of 12 inches, and a tip chord of 6 inches on a NACA 2412 airfoil. The trailing and leading edges were equally tapered to accommodate the changing chord length, and an aerodynamic twist of 2 degrees was added to accommodate downwash. Figure (12) shows a chord view of the innermost and outermost sections of the wing, Figure (13) shows the portion of the wing that sticks out from the fuselage, and Figure (14) shows the part of the wing spanning across the top of the fuselage. These drawings were created in this fashion in order to wire cut the Styrofoam interior, which had to be cut in five pieces.

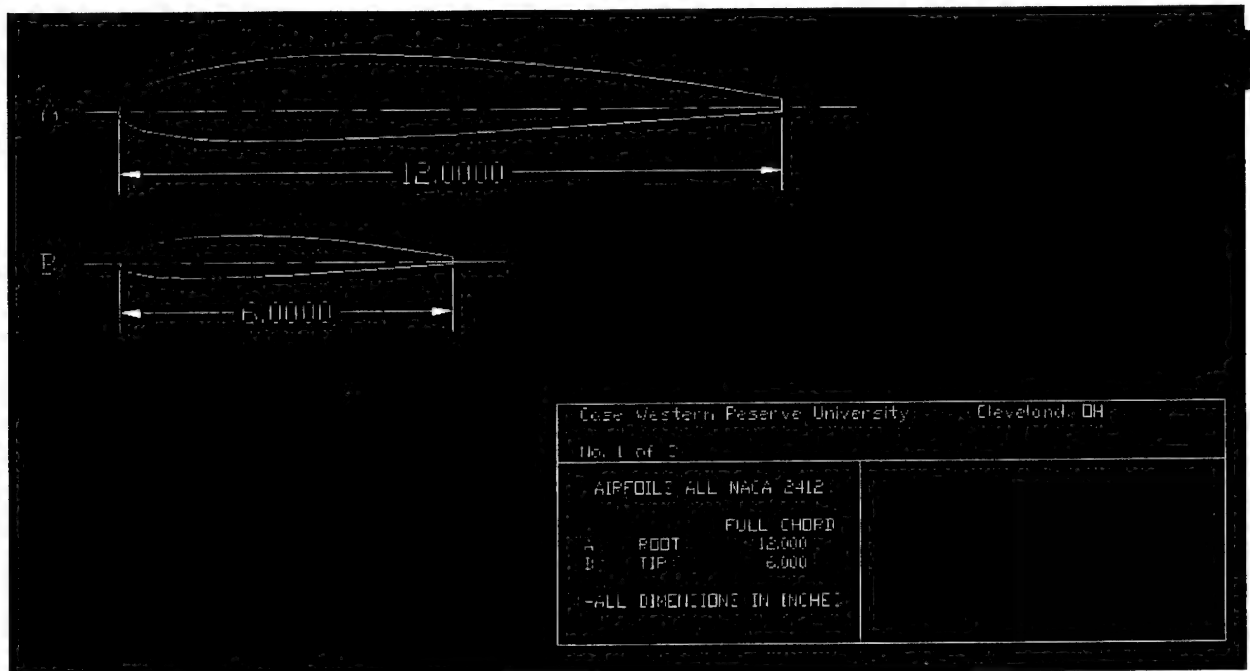


Figure 12: Chord View of Wing

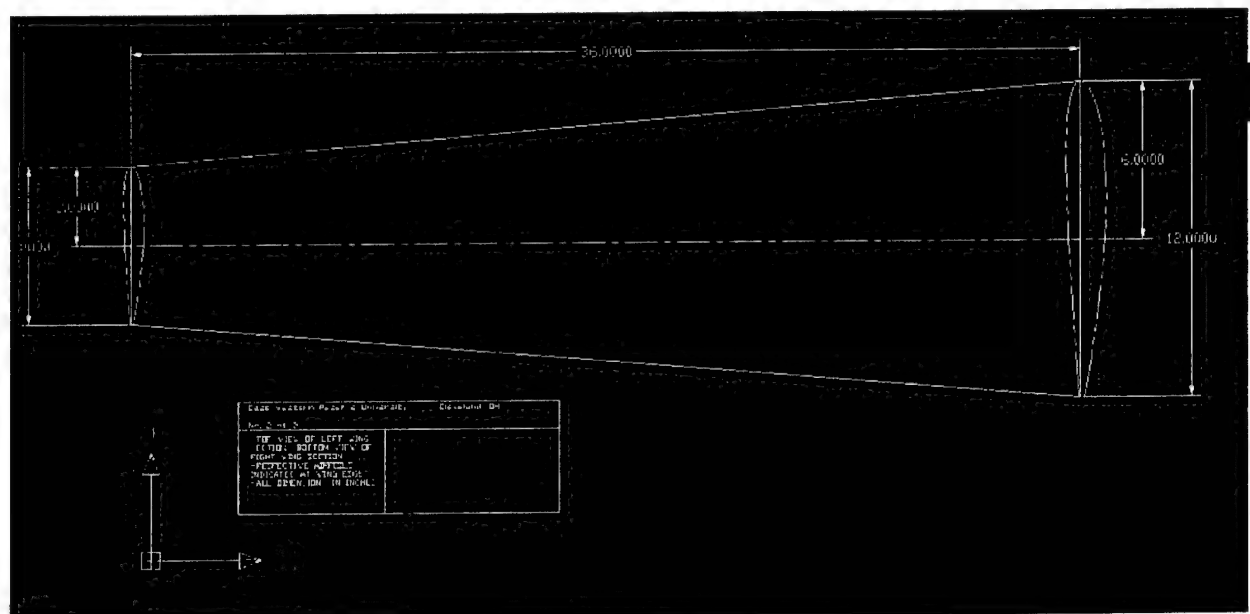


Figure 13: Outer Wingspan

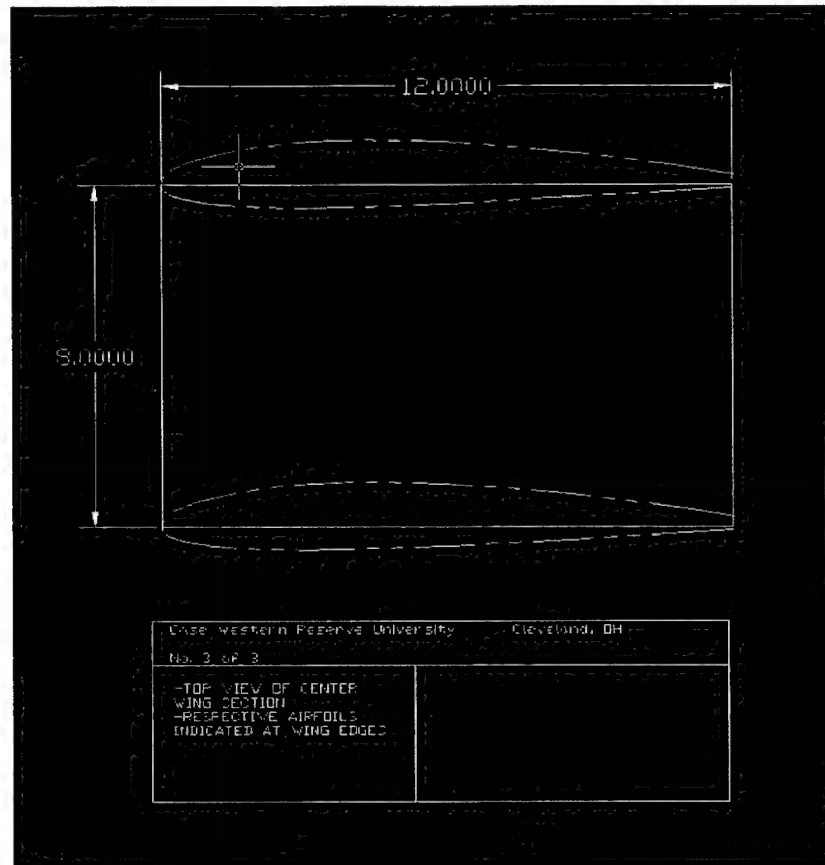


Figure 14: Inner Wingspan

After wing construction, several holes will be drilled in for bolts to connect from the wing to the fuselage.

Another table was made in Excel to analyze particular specifications for the wing. Using the NACA 2412 coefficient of lift as well as other basic parameters, the following data was obtained:

Table 9: Wing Specifications

Input Parameters	value	units
Total Coeff. of drag	0.302075	-
Coeff of ind. Drag	0.002075	-
Coeff of Drag	0.3	-
Coeff. of lift	0.18	-
Wing efficiency	0.7	-
Span	2.13	m
Chord length	0.3	m
Aspect Ratio	7.1	-
Frontal area	0.13	m ²
Top wing area	0.639	m ²

5.4 Tail Section

The tail will be far enough away from the CG of the aircraft to aid in achieving stable flight. We were limited however by the constraint of the box that the plane must fit in. The total distance from the CG to the $\frac{1}{4}$ chord of the vertical and horizontal stabilizer is 30 inches. Using this value and a known volume coefficient gave us areas for the vertical and horizontal stabilizers. They are $S_V = 64 \text{ in}^2$ and $S_H = 120 \text{ in}^2$. With the area set we then picked a mean chord for these airfoils that looked reasonable, which then set our span for the stabilizers. The final dimensions for the stabilizers were:

Vertical Stabilizer

- Root chord = 9 in
- Tip chord = 7 in
- Span = 8 in
- NACA 0012

Horizontal Stabilizer

- Root chord = 9 in
- Tip chords = 7 in
- Total span = 15 in
- NACA 0012

The rudder and elevator will be 2 inches wide and extend the length of the stabilizer. The elevator will be held in place by four hinges mounted in the horizontal stabilizer, and the rudder will be held by three. The rudder's pushrod will extend from the fuselage to a control horn on the rudder then another pushrod will then extend from the rudder to the front wheel.

The tail will be supported by two $\frac{1}{4}$ inch aluminum tubes that extend from the top plane of the fuselage. There will also be an angle $\frac{1}{4}$ inch tube that will run to the bottom of the fuselage. We will prevent buckling with balsa bulkheads suspended between the three spars. A drawing showing the tail dimensions is shown below in Figure (15):

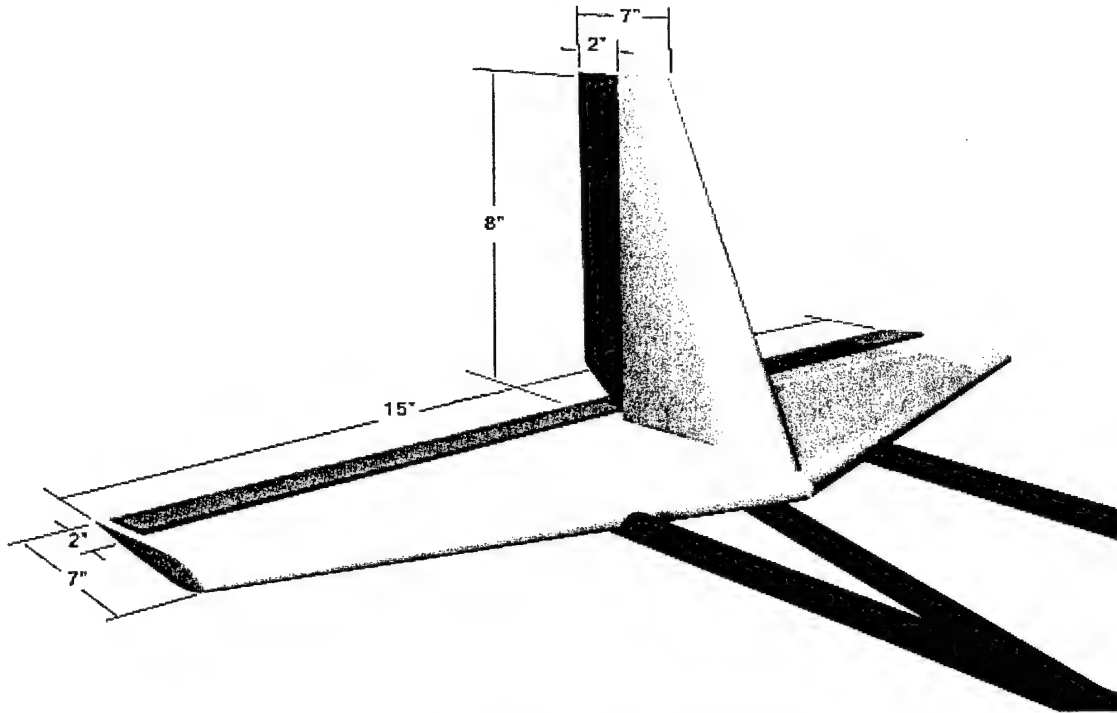


Figure 15: Tail Dimensions

5.5 Final Aircraft Configuration and Drawing Package

The final design of the aircraft will comprise of a small, wide fuselage of approximately 4 feet in length with a NACA 2412 airfoil for the wing, which spans 7 feet. The tail is a standard design with a 15 inch span and a 9 inch maximum chord. The aircraft will be supported with a landing gear that provides approximately 7 inches of clearance from the ground. This inflated height is due to the large size of the propeller being used. Below is a summary of the final aircraft configuration.

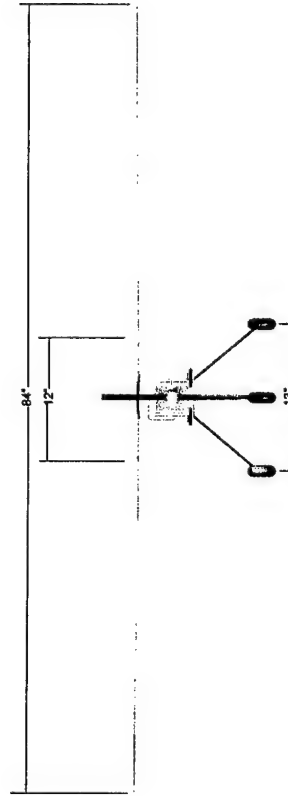
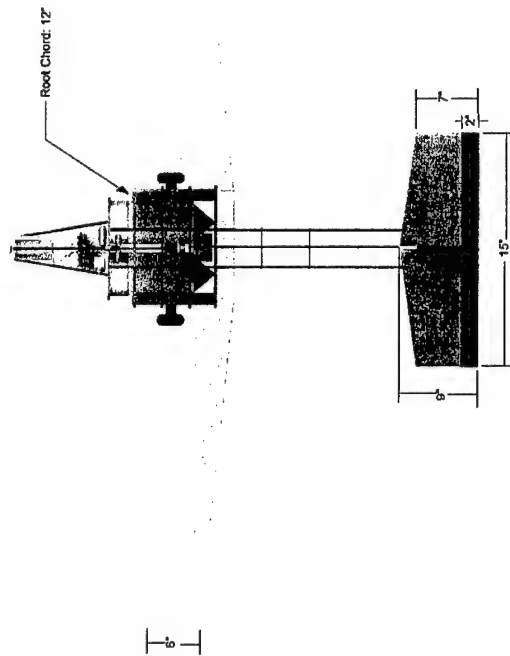
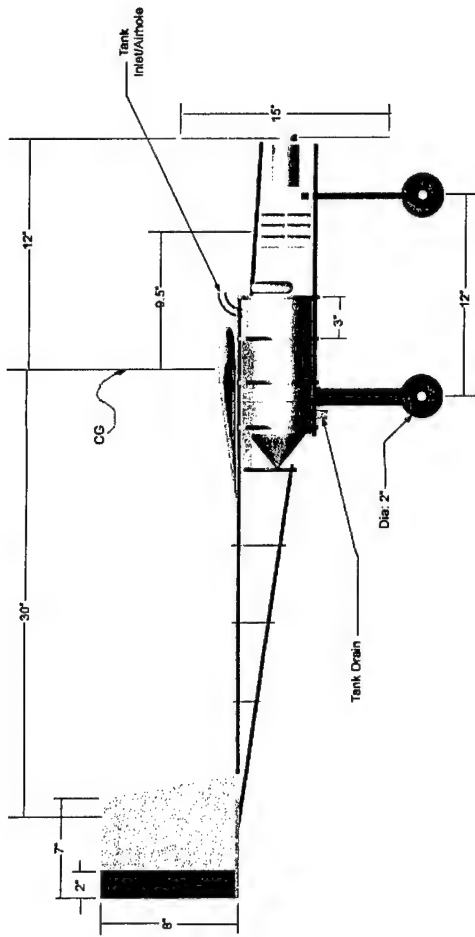
Table 10: Aircraft Configuration

Description	Specification
Fuselage	
Maximum Length	48 in
Maximum Width	12 in
Wing	
Airfoil	NACA 2412
Span	84 in
Chord	12 in
Area	5.5 sq ft
Tail	
Span	15 in
Cord	9 in
Systems	
Servos	5

Battery Configuration	24 N2400 SC RC NiCd Pack
Motor	Astroflight 40 geared (#640)
Propeller	15 X 10
Gear Ratio	3:1
Total Aircraft	
Maximum weight without payload	13.6 lb
Weight with payload	22.4 lb
Rated Aircraft Cost	12.07

The drawing package consists of one 3-view drawing of the plane on a 17 by 11 inch page. This page has not been bound with the rest of the report because of the size difference. The other three drawings in the package are on standard size paper and bound in this document since they show slightly less detail.

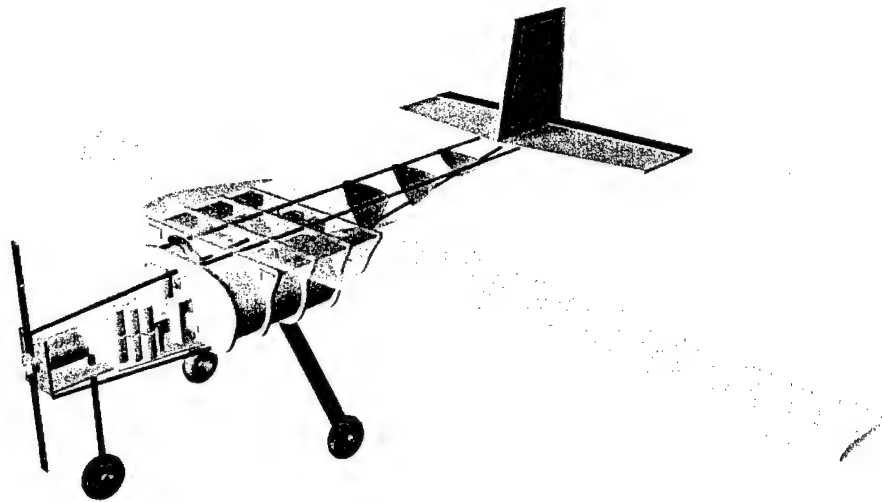
Drawing (1) is a 3-view drawing of the plane from each side. Drawing (2) is an isometric three dimensional view of Flying Nemo. Drawing (3) shows the plane stored in the 4 by 2 by 1 box. Finally, Drawing (4) shows two close-up shots of the front and rear of the plane.



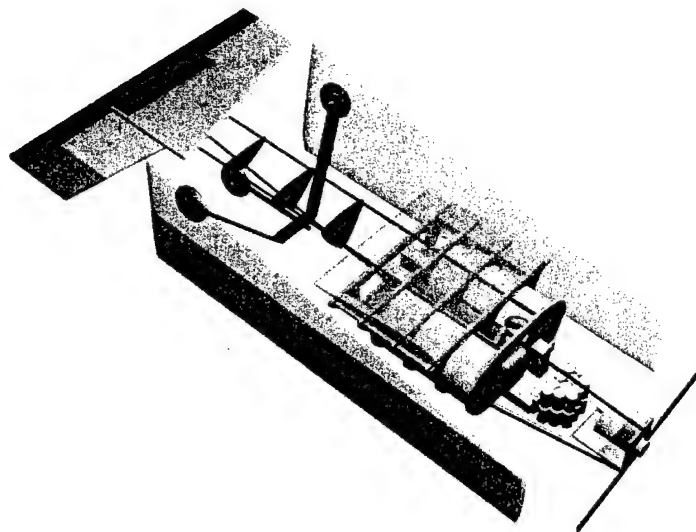
Flying Nemo Orthographic Projections Case Western Reserve University DBF Competition 2004

- *All dimensions in inches
- *Plane in flying configuration
- *Monokote removed for clarity

Drawing 1

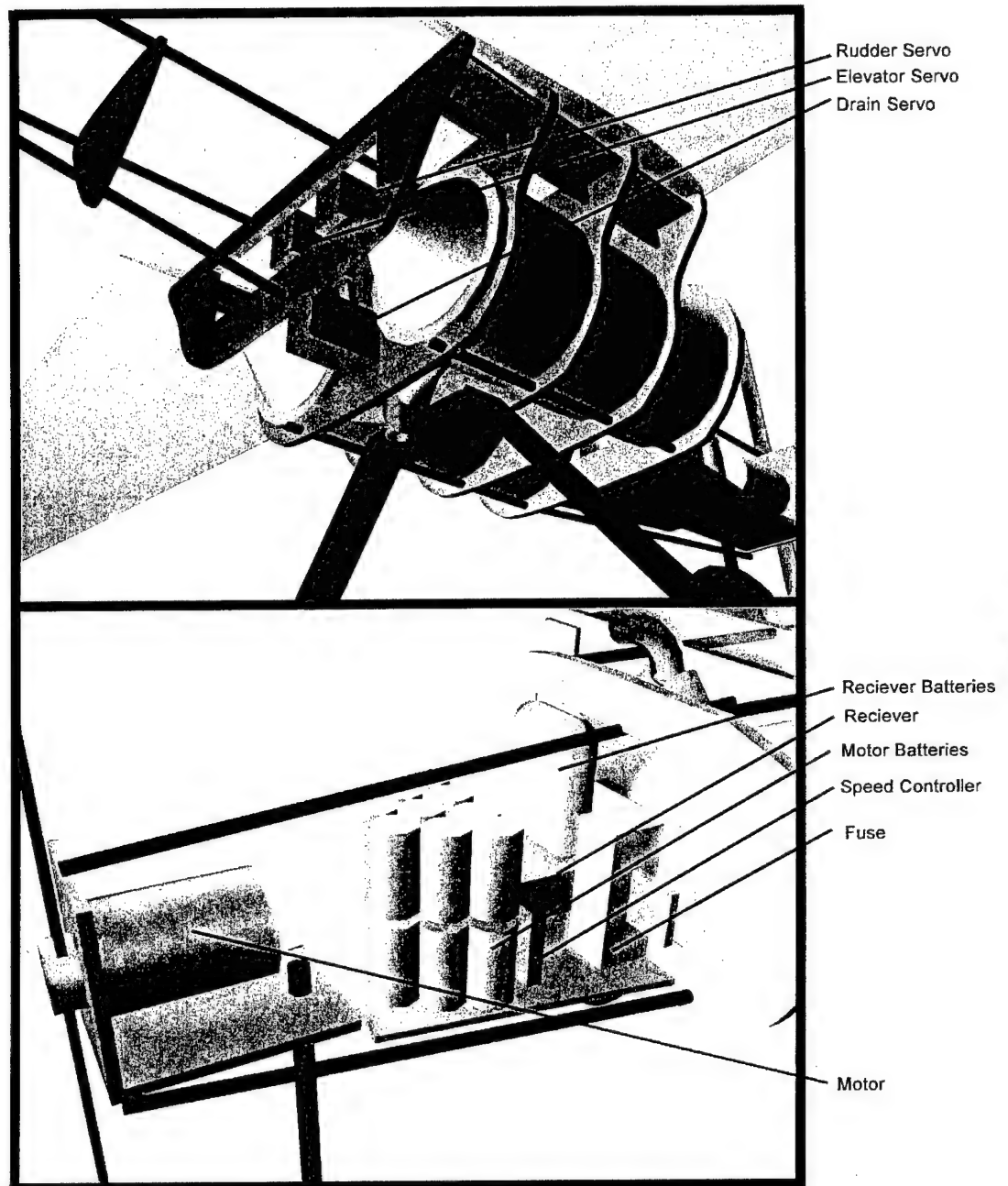


Drawing 2: Isometric View



Drawing 3: Box View

Electronics and Avionics



Drawing 4: Detailed Views

6 MANUFACTURING PLAN AND PROCESS

Before fabrication of the aircraft, a manufacturing plan had to be formulated based on the preliminary and detailed design of the various parts of the aircraft. The following sections describe the plans that were discussed for the production of the aircraft.

6.1 Fuselage Manufacturing Plan and Process

The first few steps of building the fuselage were decided because of the design that is being worked with. First, all of the material for the skeleton of the plane were ordered or manufactured. Next, all of these components were assembled to check for accuracy of fit. After that, they were permanently assembled with industrial grade superglue and fasteners.

Plywood plates were then added to the aluminum micro tubing in the fuselage. That made it possible for placement of the motor mount and landing gear. Once the lengths of the separations between the wing and motor and the fuselage were determined, the aluminum tubes could be cut and the tail and motor could be assembled in the fuselage. Also, the L-bars for the wing connection were assembled.

Those steps made up the majority of the fuselage assembly. When the water storage system, electronics, and wings are integrated, monokote can be applied to the fuselage to give a streamlined shape to Flying Nemo.

6.2 Tail Manufacturing Plan and Process

Because of the traditional configuration, the conservative surface areas of the tail would stick out of the 1'x2'x4' box volume. This meant that a removable vertical stabilizer was needed which complicated the construction of the tail.

The construction began by drawing some NACA 0012 airfoils on the computer and printing the airfoils out to be cut on balsa sheet. The balsa airfoils were held together by wooden dowels making the horizontal and vertical stabilizers. The wooden dowels of the horizontal stabilizers were rigidly attached to the two spars that extend out of the fuselage. The sections between the two aluminum spars were connected by a more rigid slab of wood. Holes were drilled to provide bolting points for the horizontal stabilizer. The final assembly was covered with monokote. Figure 15 shows the tail structure note that the number of airfoils and spars is not accurate.

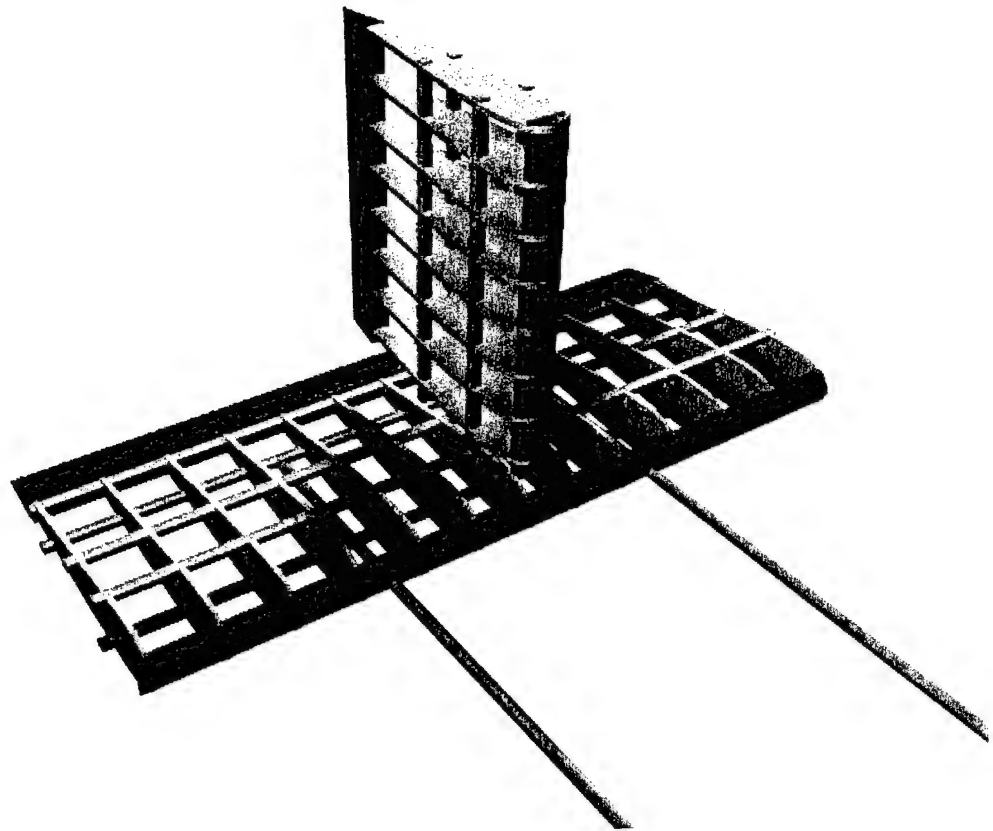


Figure 15: Tail Structure

6.3 Landing Gear Manufacturing Plan and Process

The main gears required simple machining. Two holes were cut on the top of the main gear to provide attachment points for the connection to the bottom of the plywood mount in the fuselage. Two screws were inserted from the fuselage where the main gear can be quickly attached. The two inch wheels were taken from our current inventory. The nose gear was placed on the piece of plywood in the front and connected to a servo enabling it to be steered.

6.4 Water Storage System Manufacturing Plan and Process

The two 2-liter bottles will be placed inside the bulkheads of the plane and secured. When they are secured, holes will be cut in the bottles, and a series of tubes will connect the bottles to a main inlet and exit tube on the top and bottom of the fuselage. After that, the servo for the water drain can be installed and the piece to redirect airflow on the top tube and be manufactured.

6.5 Systems Integration and Electronics Assembly

After the bulkheads of the fuselage were in place, controls lines for the steering were run in the aircraft. Small holes were cut into the bulkheads enabled the steering to be connected to the tail controls, reducing the use of one less servo. After the tail, wings, and motor were integrated with the fuselage, the tail, electronics, and landing gear control lines were installed and configured on the aircraft.

The electronic components were assembled and tested outside of the aircraft prior to installation. The tests were required to ensure all components were functioning before installation.

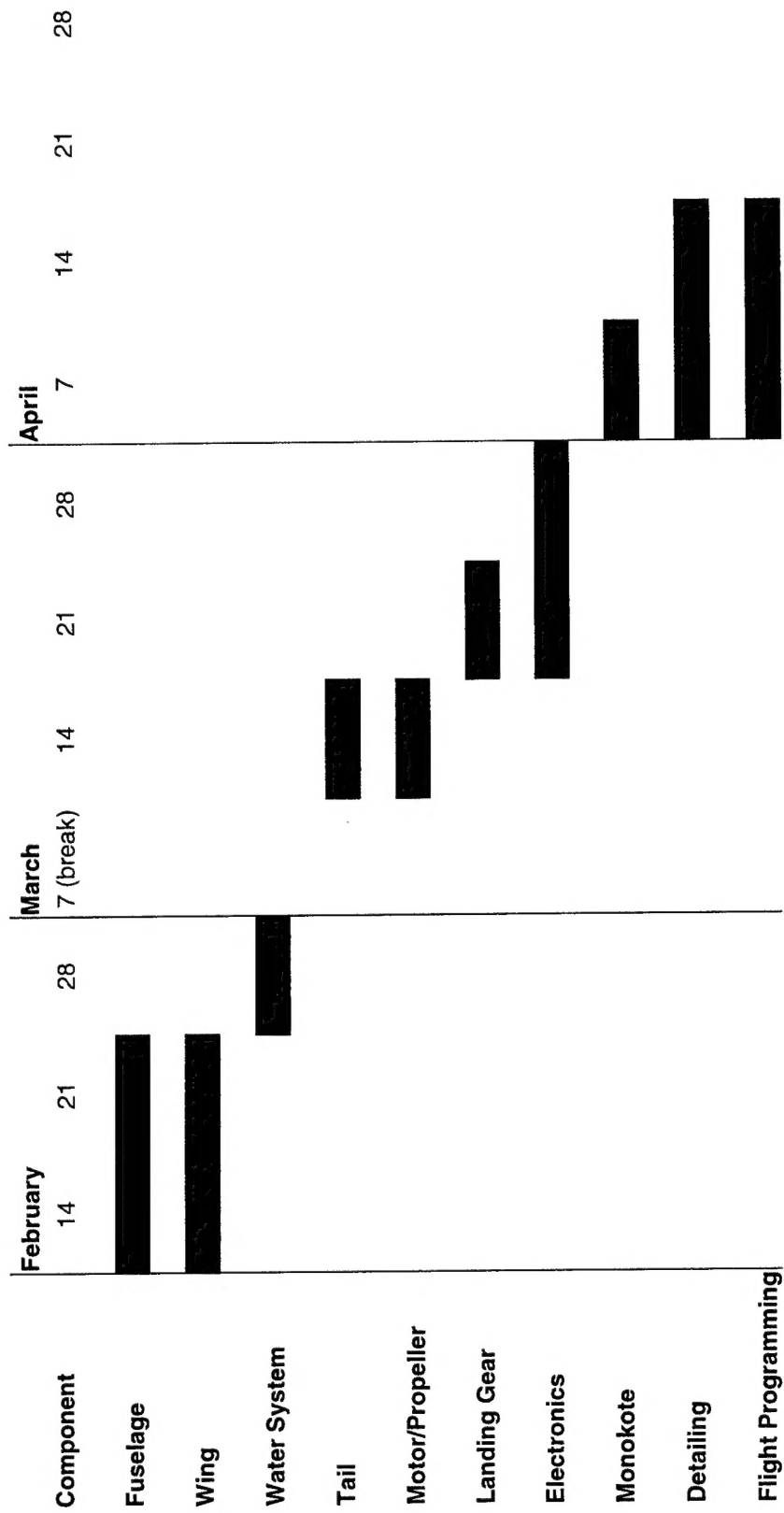
6.6 Wing Construction

The foam model of our wing was sent to us in 5 pieces. First, because of its surface texture, the parts could be taped together into one solid piece. Next, a fiberglass cloth was layered around the styrofoam until a solid fiberglass shell was created. Once it dried, we checked for strength and added on fiberglass until the wing was strong enough to withstand a large bending pressure applied by hand.

After the shell was created, a space was cut for the ailerons. Servos were mounted in the Styrofoam underneath the wing, and a connection line was run from the servos to the ailerons. The ailerons were made by attaching two pieces of thin plywood to a wooden dowel to give the shape of the wing that had been cut out. Finally, the ailerons and wing were covered with monokote, providing a smooth surface for the structure.

Obviously, different components of the plane depend on one another, and there must be some structure to the order of construction. The fuselage and wings can be built independent of each other. After that, the water storage system must be built before the wing is place on the fuselage. Next, the tail and motor can be placed. Finally, the electronics and landing gear can be added on before the plane is covered in monokote. On the next page, Table (11) estimates the times of construction for the different components.

Table 11: Detailed Construction Timeline



7 TESTING PLAN

Due to our construction schedule and Cleveland area weather, we intend to start testing in early April. Before testing the flight capabilities of the aircraft, several static tests will be conducted. The first test will be to check for the center of mass of the aircraft and make the required adjustments by redistributing the variable weights in the aircraft. This is followed by testing the electronics and control systems. Finally, a regular and inverted wing tip tests will be conducted to ensure that the plane will be able to enter the competition.

After all of these tests are completed, the plane will be ready for flight testing. However, before flying the aircraft, a ground run will be conducted by 'driving' the aircraft around the lab. This provides an opportunity to check the stability of the aircraft before flight and allows us to gauge the power requirements for take off.

All flight tests will be conducted on a farm owned by Case Western Reserve University. The farm has a strip of level road that will be used as a runway. The flight tests would allow the team to observe the aircraft's performance in flight and make adjustments to the aircraft as necessary.

8 RATED AIRCRAFT COST

The following table calculates the related aircraft cost for Flying Nemo.

Table 12: Related Aircraft Cost

	Value	Total	Cost (\$)
MEW	13.6	4080	4080
REP		4650	4650
Engines	1		
Battery Weight	3.1		
MFHR		167.2	3344
Wingspan	7	70	
Maximum Chord	1		
Control Surfaces	1	5	
Fuselage Volume	2.36	47.2	
Vertical Surfaces	0	0	
Vert. Control Surfaces	1	10	
Horiz. Control Surfaces	1	10	
Servos/Controllers	5	25	
TOTAL RAC			12.07

9 REFERENCES

Anderson, John D. "Fundamentals of Aerodynamics," Third Edition, 2001, McGraw-Hill Companies, Inc. New York, NY.

Çengel, Yunus A. and Robert Turner. Fundamentals of Thermal-Fluid Sciences. Boston: WCB McGraw-Hill, 2000.

Hill, Philip and Carl Peterson. Mechanics and Thermodynamics of Propulsion. 2nd Ed. Redding, Mass.: Addison-Wesley Publishing Company, 1992.

Gere, James M. and Stephen P. Timoshenko. Mechanics of Materials. 4th Ed. Boston: PWS Publishing Company, 1997.

Juvinall, Marshek. "Fundamentals of Machine Component Design," Third Edition, 2000, John Wiley & Sons, Inc.